AD A066569

DDC FILE COPY

10

DDC
REPRODUCED
MAR 29 1979
C

MINUTES OF THE EIGHTEENTH EXPLOSIVES SAFETY SEMINAR

VOLUME II

LEVEL III
No 66-68



This document has been approved for public release and sale; its distribution is unlimited.

EL TROPICANO MOTOR HOTEL
SAN ANTONIO, TEXAS

12-14 SEPTEMBER 1978

SPONSORED BY

DEPARTMENT OF DEFENSE EXPLOSIVES SAFETY BOARD

ALEXANDRIA, VA

79 03 29 05

(6)

MINUTES OF THE

EIGHTEENTH EXPLOSIVES SAFETY SEMINAR

Volume II

Held at

El Tropicano Motor Hotel

San Antonio, Texas,

12-14 September 1978.

Sponsored by

Department of Defense Explosives Safety Board

Alexandria, Virginia

(11) 14 Sep 78

(12) 953 p.

APPROVED FOR PUBLIC RELEASE; DISTRIBUTION UNLIMITED

034 850

79 05 29 00

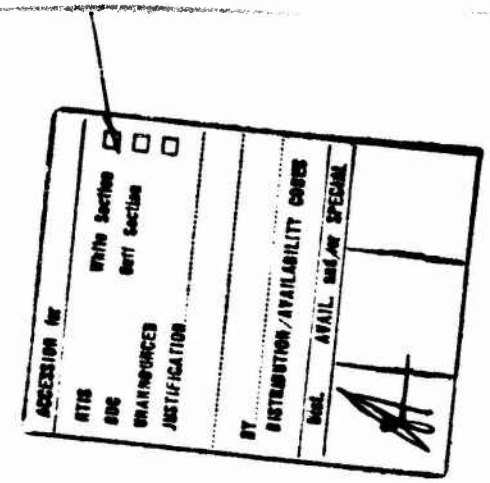

TABLE OF CONTENTS

VOLUME II

SESSION - RISK ANALYSIS & PREDICTION I
Moderator - Mr. John Atkins

DATA FOR RISK ASSESSMENT OF ACCIDENTAL EXPLOSIONS IN PROPELLANT GROUND HANDLING AND TRANSPORT SYSTEMS..... 927
Mr. Van B. Parr and Ms. Patricia K. Moseley

WORKBOOK FOR ESTIMATING EFFECTS OF ACCIDENTAL EXPLOSIONS IN PROPELLANT GROUND HANDLING AND TRANSPORT SYSTEMS..... 953
W.E. Baker, J.J. Kulesz, R.E. Ricker, P.S. Westine, V.B. Parr, L.M. Vargas, and P.K. Moseley

SPECIAL CONSIDERATIONS FOR SPACE TRANSPORTATION SYSTEMS PROCESSING AT KENNEDY SPACE CENTER..... 989
Mr. John R. Atkins

SESSION - FIRES AND EXPLOSIONS
Moderator - Mr. Ray Myers

RADFORD ARMY AMMUNITION PLANT NITROGLYCERIN EXPLOSION..... 1003
LTC Thurman Watts, USA

THE ACCIDENT WHICH OCCURRED AT THE PONT-DE-BUIS GUN-POWDER FACTORY ON 7TH AUGUST 1975..... 1089
Mr. Jean Quinchon

EXPLOSIVE INCIDENT DURING DEMOLITION GROUND OPERATIONS..... 1097
Mr. Melvin R. Bailey

SESSION - DESIGN OF STRUCTURES FOR EXPLOSIVES FACILITIES
Moderator - Dr. W. E. Baker

SIMPLIFIED APPROACH FOR DESIGN OF BUILDINGS CONTAINING ACCIDENTAL EXPLOSIONS..... 1105
Mr. Washington T. Char

OPTIMIZATION OF REINFORCED CONCRETE SLABS..... 1149
Mr. J. M. Ferritto

FEASIBILITY OF USING FIBERGLASS REINFORCED PLASTIC (FRP) BUILDINGS FOR AMMUNITION PLANTS..... 1169
Mr. Charles C. Huang

SESSION - RISK ANALYSIS AND PREDICTION II
Moderator - Mr. John Atkins

THE DIVISION'S APPROACH TO RISK ANALYSIS IN PRODUCTION AND STORAGE OF EXPLOSIVES..... 1195
Mr. Magne Solheim

HOW MUCH SHOULD WE BE WILLING TO PAY FOR EXPLOSIVES SAFETY?..... 1223
Mr. Thomas Schneider

SESSION - FIRING RANGE AND EXPLOSIVES DETECTION SAFETY
Moderator - Mr. Edmund Demberg

HANGFIRE PROTECTION AND CONTAINMENT..... 1249
Messrs. John Gaye and Bob Laurent

DANGEROUS LEAD-IN-AIR CONTENT PRODUCED IN INDOOR SHOOTING RANGES.. 1267
CPT P. R. Sulik, USAF

SAFETY ASPECTS OF TAGGING EXPLOSIVES FOR POST-DETONATION IDENTIFICATION..... 1273
Dr. Carl Boyars

DDESB R&D HIGHLIGHTS

FRAGMENT HAZARD INVESTIGATION PROGRAM..... 1291
Messrs. R.T. Ramsey, J.G. Powell, Jr., and W.D. Smith, III

ESKIMO TEST RESULTS AND PLANS..... 1317
Dr. T. A. Zaker

SESSION - CHEMICAL MUNITIONS DEMILITARIZATION AND HAZARD PREDICTION
Moderator - Mr. Lawrence Smith

ADVANCES IN THE DETECTION AND ANALYSIS OF CHEMICAL AGENTS..... 1325
Mr. Leslie Eng

A SIMPLIFIED METHODOLOGY FOR COMPUTING CHEMICAL HAZARD DISTANCES.. 1337
Mr. C. Glenvil Whitacre

THE CUTTING OF M-55 CHEMICAL ROCKETS WITH A 2kW CO_2 LASER..... 1365
Mr. Ona R. Lyman

THE ROLE OF THE SAFETY MANAGER IN SUPPORT OF CHEMICAL DEMILITARIZATION PROGRAMS..... 1379
Mr. Lawrence Smith

SESSION - HAZARDS CONTROL IN EXPLOSIVES OPERATIONS I
Moderator - Mr. Pete Rutledge

AN EVALUATION OF DRYING SYSTEMS FOR EXPLOSIVES..... 1389
Messrs. E.P. Bergmann, Alan Hartman, and A. B. Wenzel

SYSTEM SAFETY PROGRAM FOR MODERNIZATION AND EXPANSION PROEJCTS.... 1409
Mr. Joseph R. Drugmand

REMOTE-CONTROLLED NITRATOR FACILITY WITH MULTI-PRODUCT CAPABILITY. 1449
M.C. Hudson, P.R. Mosher, and W.A. Carr

SESSION - SHIPBOARD EXPLOSIVES SAFETY
Moderator - Mr. Catesby P. Jones

THE NAVY'S EXPLOSIVE SAFETY IMPROVEMENT PROGRAM FOR PIER SIDE MUNITIONS OPERATIONS..... 1461
Mr. Joseph Petes

A MODEL AND METHODS FOR CONTROL OF SYMPATHETIC DETONATION..... 1479
Mr. F. B. Porzel

SIMULATED TOMAHAWK MISSILE HANDLING ARC TEST RESULTS..... 1527
Mr. J. M. Ward

NAVY REQUIREMENTS FOR COMBAT SURVIVABLE PROPELLANTS AND EXPLOSIVES 1551
Dr. June T. Amlie

SESSION - EXPLOSION PROPAGATION TESTS AND RELATED SAFETY
Moderator - Mr. E. C. Teichmann

DETERMINATION OF SAFE SEPARATION DISTANCES FOR EXPLOSIVES AND PROPELLANTS IN SELECTED MANUFACTURING OPERATIONS..... 1561
Messrs. J.W. Gehring, A.B. Wenzel, J. Friesenhahn, & W.O. Seals

HAZARD CLASSIFICATION TEST OF COMPLETE ROUND 155mm PALLETS..... 1605
Mr. Harry J. Reeves

EXPLOSIVE SAFETY TESTS OF PERSONAL PROTECTIVE EQUIPMENT..... 1617
Mr. Glenn C. Pritchard

SESSION - HAZARDS CONTROL IN EXPLOSIVES OPERATIONS II
Moderator - Mr. Pete Rutledge

MANUFACTURE OF EXPLOSIVES EXTRUDED PRODUCTS..... 1637
Mr. Robert A. Lee

FLUID ENERGY MILLING OF HMX..... 1677
Mr. Walter J. Moodie

ENVIRONMENTAL EFFECTS ON ELECTROSTATIC SENSITIVITY OF ENERGETIC MATERIALS..... 1691
Messrs. L.D. Haws, L.W. Collins, and A. Gibson

SESSION - SUPPRESSION OF FRAGMENTS AND BLAST
Moderator - Mr. R. Vitali

SHIELDING OF FACILITIES FOR WORK WITH PYROTECHNIC AND EXPLOSIVE MATERIALS..... 1703
Dr. David J. Katsanis

SUPPRESSION OF FRAGMENT DAMAGE BY MEANS OF FRAGIBLE SURROUNDS..... 1751
Messrs. J.E. Backofen, Jr., L.J. Wolfson, and J.D. Shock

SHIELDS FOR DECELERATING MUNITIONS FRAGMENTS..... 1769
Mr. Joseph G. Connor, Jr.

CATASTROPHIC REACTION OF COMPARTMENTALIZED AMMUNITION - CAUSES AND PREVENTIVE MEASURES..... 1795
Dr. P. M. Howe and Dr. R. B. Frey

DESIGNING NUCLEAR PLANTS TO WITHSTAND PULSE AND IMPACT LOADS..... 1809
Mr. Alexander L. Florence

LIST OF ATTENDEES..... 1865

DATA FOR RISK ASSESSMENT OF ACCIDENTAL EXPLOSIONS IN PROPELLANT GROUND HANDLING AND TRANSPORT SYSTEMS

BY

VAN B. PARR AND PATRICIA K. MOSELEY

SOUTHWEST RESEARCH INSTITUTE
SAN ANTONIO, TEXAS

WORK PERFORMED FOR NASA LEWIS RESEARCH CENTER
CONTRACT NO. NAS3-20497
CR-3023

Data for Risk Assessment of Accidental Explosions in Propellant Ground Handling and Transport Systems

Van B. Parr and Patricia K. Moseley
Southwest Research Institute
San Antonio, Texas

ABSTRACT

This paper presents the results of statistical analyses of data on twenty-five events of explosions in propellant ground handling and transport systems. These results are taken from a soon-to-be published NASA report entitled "Workbook for Estimating Effects of Accidental Explosions in Propellant Ground Handling and Transport Systems," which was prepared for NASA Lewis Research Center by Southwest Research Institute, under contract number NAS3-20497.

Estimates of distributions of parameters and relationships between parameters which are useful in risk assessment are presented. Results include fragment weight distribution, mean fragment weight as a function of normalized yield, correlation between fragment range and fragment weight, correlation of fragment range to the ratio or mean fragment weight to vessel weight for cylindrical tanks, and correlation of fragment velocity to the ratio of energy to vessel weight. Tables of the data and graphs of the resultant distributions are included in the paper to support final conclusions.

1.0 INTRODUCTION

The material presented herein represents a portion of the results of a study which Southwest Research Institute performed for NASA Lewis Research Center under contract number NAS3-20497. The complete results are being published by NASA Lewis in workbook format. A companion paper in this seminar describes the content of the workbook more completely.

From the material presented in this paper and the companion paper, one should be able to make predictions of blast and fragment characteristics and effects for a range of possible explosion accidents in ground systems.

For convenience, all figures and tables follow the text.

2.0 ACCIDENT DATA

A literature search was conducted in which accident reports and other available, related data sources were reviewed for information on characteristics of fragments and pressure waves of bursting thick-wall, compressed fluid storage and transportation vessels. Fluids and gases considered in the survey were propane, anhydrous ammonia, oxygen, argon, air and propylene. Organizations and contractors contributing sources included the National Transportation Safety Board, Naval Surface Weapons Center, NASA Langley Research Center, Department of Transportation, National Technical Information Service and Ballistic Research Laboratory. Also, an incident which occurred in San Antonio, Texas during the accumulation of data, in which a propane storage tank exploded, was investigated for information on energy release. Data obtained from this literature were organized in a logical manner for the subsequent analysis. Records of the data include the reference and date of the explosion; the quantity

of the explosion source; the estimated energy release; the shape, volume, weight, material and dimensions of the container vessel; the number of fragments; the weights, ranges, trajectory elevations (if given) drag coefficients and shapes of the fragments; and any additional pertinent information. Each vessel was assigned an identifying number. Twenty-five vessel explosions form the data base. An example of these data are given in Tables 1 and 2.

Due to the limited amount of data on most of the events, it was desirable to group the data from like events in order to yield an adequate base for meaningful statistical analysis. From the data on the twenty-five events, the six groups of like events shown in Table 3 were obtained. Statistical analyses were performed on data from each of the groups to yield (as the data permitted) estimates of fragment range distribution, fragment weight distribution and fragment mean velocity as a function of the ratio of explosion energy to vessel weight. Other relationships were also investigated and the results are given in the following paragraphs.

3.0 FRAGMENT RANGE DISTRIBUTIONS

The fragment range data for each of the six event groups (see Table 3) were sorted in ascending order. For event groups 1, 2, 3, 4 and 6, the values for the range for the 10th to the 90th percentile in 10% steps were identified. For event group 5, the values from the 14.3 percentile to the 85.7 percentile in 14.3% steps were identified. Table 4 is a listing of these values.

Figures 1 and 2 are plots of the percentile points on log normal probability paper for events groups 1 and 2.

A "W" statistic [see Hahn and Shapiro (1967)]* for goodness of fit was calculated for each of the distributions. The approximate probability of obtaining the calculated test statistic, given that the chosen distribution is correct, was then determined. The results are shown in Table 5. As it is customary to consider probability values of "W" statistic exceeding 2 to 10% as adequate grounds for not rejecting the hypothesis that the data belong to the chosen distribution, the fits for the six event groups are more than adequate.

Figures 1 and 2 can be used to estimate the percentage of fragments which will have a range, R, equal to or less than a particular range.

For example, if we wished to estimate the percentage of fragments which would have a range equal to or less than 600 m for an explosion involving a rail tank car filled with propane (group 1), we would refer to Figure 1, and on the range axis (abscissa) at 600 m go upward to the intersection of the line. Then, at the intersection point read the percentage value from the ordinate, which is 96%. Conversely, if we wanted to know what range 90% of the fragments would not exceed, we would enter the chart on the 90% line, go over to the intersection of the line and read downward to the range axis the value of 380 m.

4.0 FRAGMENT WEIGHT DISTRIBUTIONS

Sufficient pertinent weight data were available only from event groups 2, 3 and 6. Table 6 is a listing of the percentiles of these event groups.

Figure 3 is a plot of the percentile points on log normal probability paper for event group 2.

---

*Hahn and Shapiro, Statistical Models in Engineering, John Wiley and Sons, Inc., New York, 1967.

Table 7 is a listing of the estimated means and standard deviations for the log normal (to the base e) distributions.

The calculated "W" statistic along with the approximate probability of obtaining the calculated test statistic, given that the chosen distribution is correct, is presented for each of the three event groups in Table 8. Since the probability values of the "W" statistic are 10% or greater, the fits for the three event groups are considered adequate.

Charts of this type can be used in the same manner as Figures 1 and 2 are used for fragment range.

5.0 MEAN FRAGMENT WEIGHT AS A FUNCTION OF NORMALIZED YIELD

In events 21, 22 and 23, spherical containers were pressurized until rupture. The spheres were constructed of steel with an approximate ultimate stress (σ_u) of 834 Mega Pascals (MPa). The spheres were the same volume for all three events. The wall thickness of the spheres was the same within events, but was different across events.

Pertinent data and calculated parameters for each of the spheres are given in Table 9, where $\bar{W}$ is the geometric mean fragment weight for each event, W(T) is the sphere weight for each event, V is the sphere volume, $\bar{P}$ is the average burst pressure for each event, and E_o is the energy of detonation of 1 gram of TNT or 4190 Joules (J).

Figure 4 is a plot of the normalized yield ($\bar{P}V/E_o$) versus mean fragment weight ($\bar{W}$) for the three events. One could estimate the mean (geometric) fragment weight for any decided ratio of $\bar{P}V/E_o$ from 693 to 2347.

The correlation coefficient, r, for the regression equation shown on Figure 4 was 0.9999, which indicates a high degree of correlation between $\bar{P}V/E_o$ and $\bar{W}$.

6.0 CORRELATION BETWEEN FRAGMENT RANGE AND FRAGMENT WEIGHT WITHIN EVENT GROUPS

Only three event groups (2, 3 and 6) contained sufficient fragment range and weight data for correlation analysis. Various curve fitting techniques were employed to determine if a predictable relationship existed between fragment range and weight as indicated by the data on the three events.

Figure 5 depicts the relationship of the fragment range to fragment weight for Group 2. The correlation coefficient is 0.79.

Figure 6 shows the relationship of the fragment range to fragment weight for Group 6. The correlation coefficient is 0.68.

7.0 CORRELATION ANALYSIS OF FRAGMENT RANGE TO THE RATIO OF MEAN FRAGMENT WEIGHT TO VESSEL WEIGHT FOR CYLINDRICAL TANKS

Five events with cylindrical tanks contained sufficient fragment weight information to determine the degree of correlation of fragment range to the ratio of mean fragment weight to vessel weight. It was necessary to group events 6 and 7 to have a sufficient sample size.

Table 10 presents the data by event number, the ratio of the arithmetic mean fragment weight ($\bar{W}$) to the vessel weight (W(T)), and the arithmetic mean fragment range ($\bar{R}$). Figure 7 is a plot of the points in Table 10 along with the prediction equation. The sample correlation coefficient is 0.987.

From Figure 7, one could estimate the mean fragment range for any decided ratio of mean fragment weight to vessel weight for the types of tanks in the events.

8.0 CORRELATION OF FRAGMENT VELOCITY TO THE RATIO OF ENERGY TO VESSEL WEIGHT

Only in event group 5 were there reports of mean velocity for fragments. Figure 8 is a plot of the relationship between the mean fragment velocity and the ratio of the energy to vessel weight. The velocities were chosen as the maximum velocity reported within an event for events 21, 22 and 23 (see Table 9). The correlation coefficient for the regression equation is 0.93.

One could use Figure 8 to predict the average velocity for fragments from bursting steel spheres over a range of an energy to vessel weight ratio of 4.5×10^7 to 6.05×10^7. However, the analytic predictions for fragment velocity presented in the workbook are more useful because they cover a much wider range of bursting vessel conditions.

9.0 SUMMARY AND CONCLUSIONS

Estimates of functions relating to fragment mass, velocity and range have been derived from accidental explosions in propellant ground handling and transport systems. These data may be used to estimate the effects of a postulated event involving similar transport systems. In addition, the analytical methods presented in a companion paper may be used to complement the estimation of effects of a postulated event.

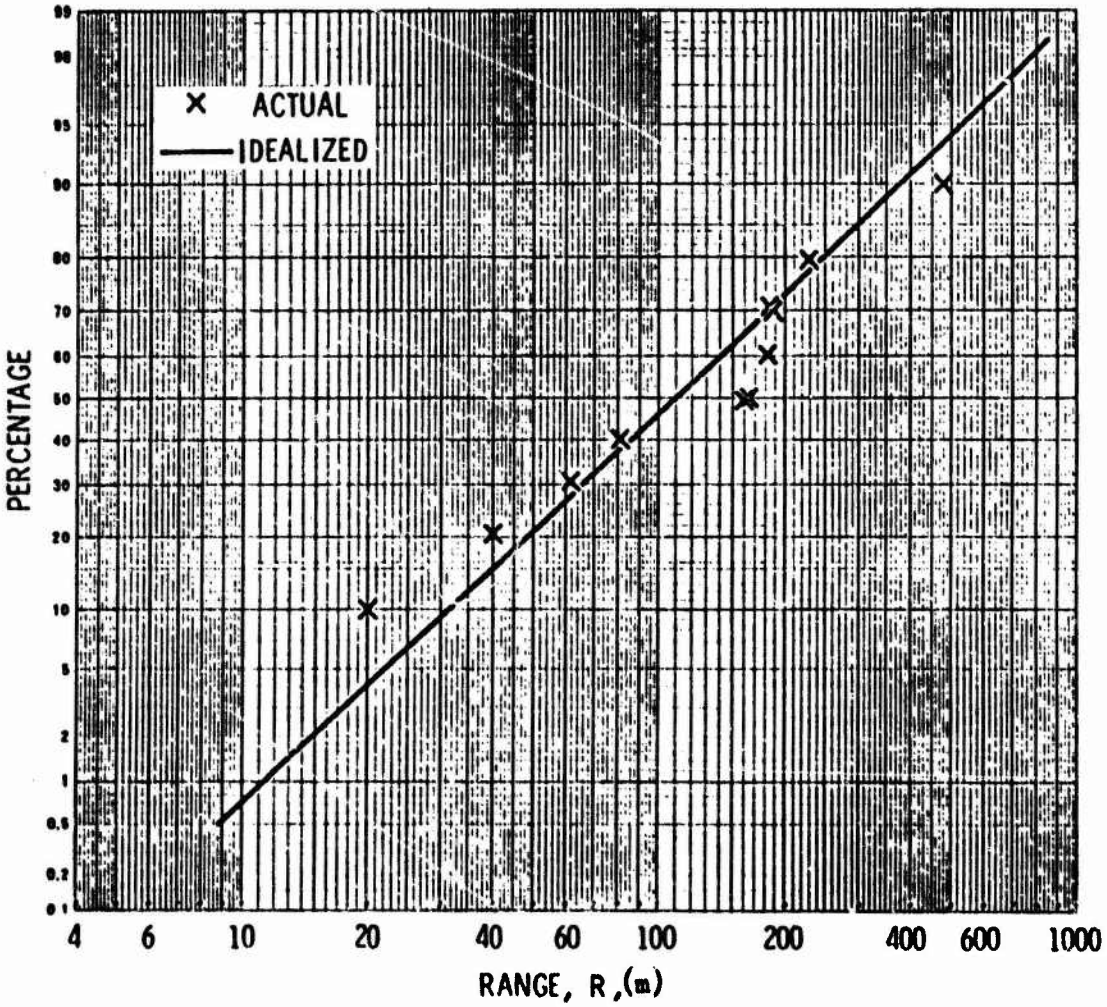

FIGURE 1. Probability Distribution—Fragment Range (Event Group 1 - Events 1, 2, 3, 18)

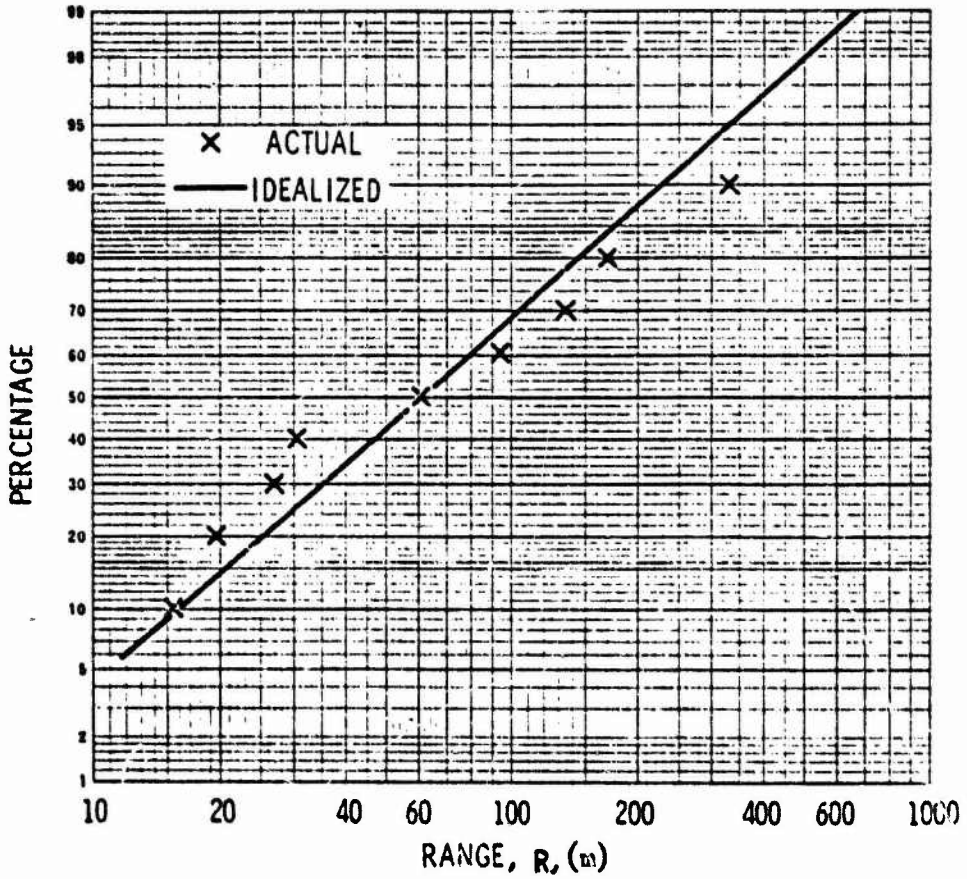

FIGURE 2. Probability Distribution—Fragment Range (Event Group 2 - Events 6, 7, 8, 9, 10, 13, 14, 15 and 19)

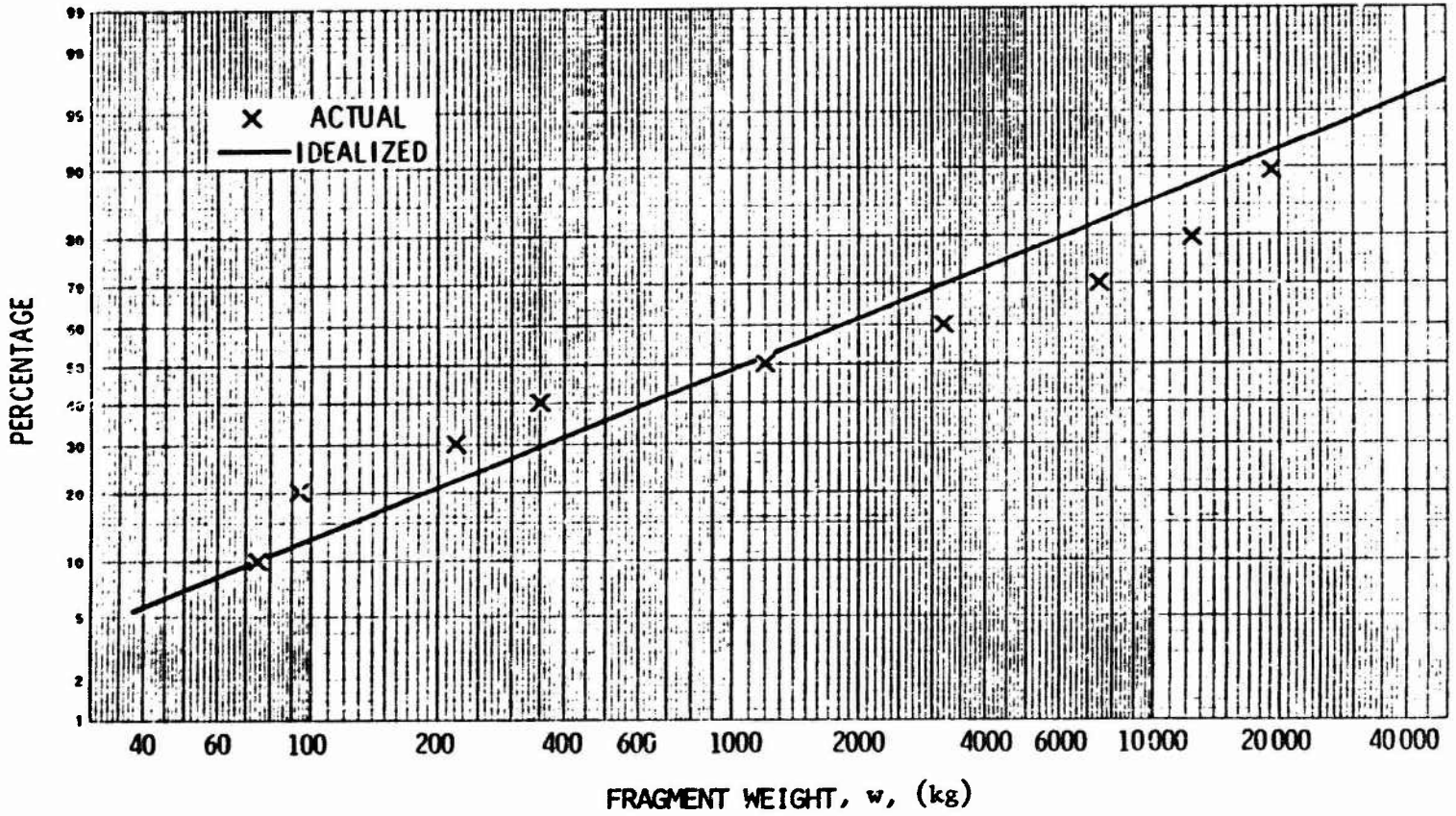

Figure 3. Probability Distribution-Fragment Weight (Event Group 2 - Events 6, 7, 8, 9, 10, 13, 14, 15, 19)

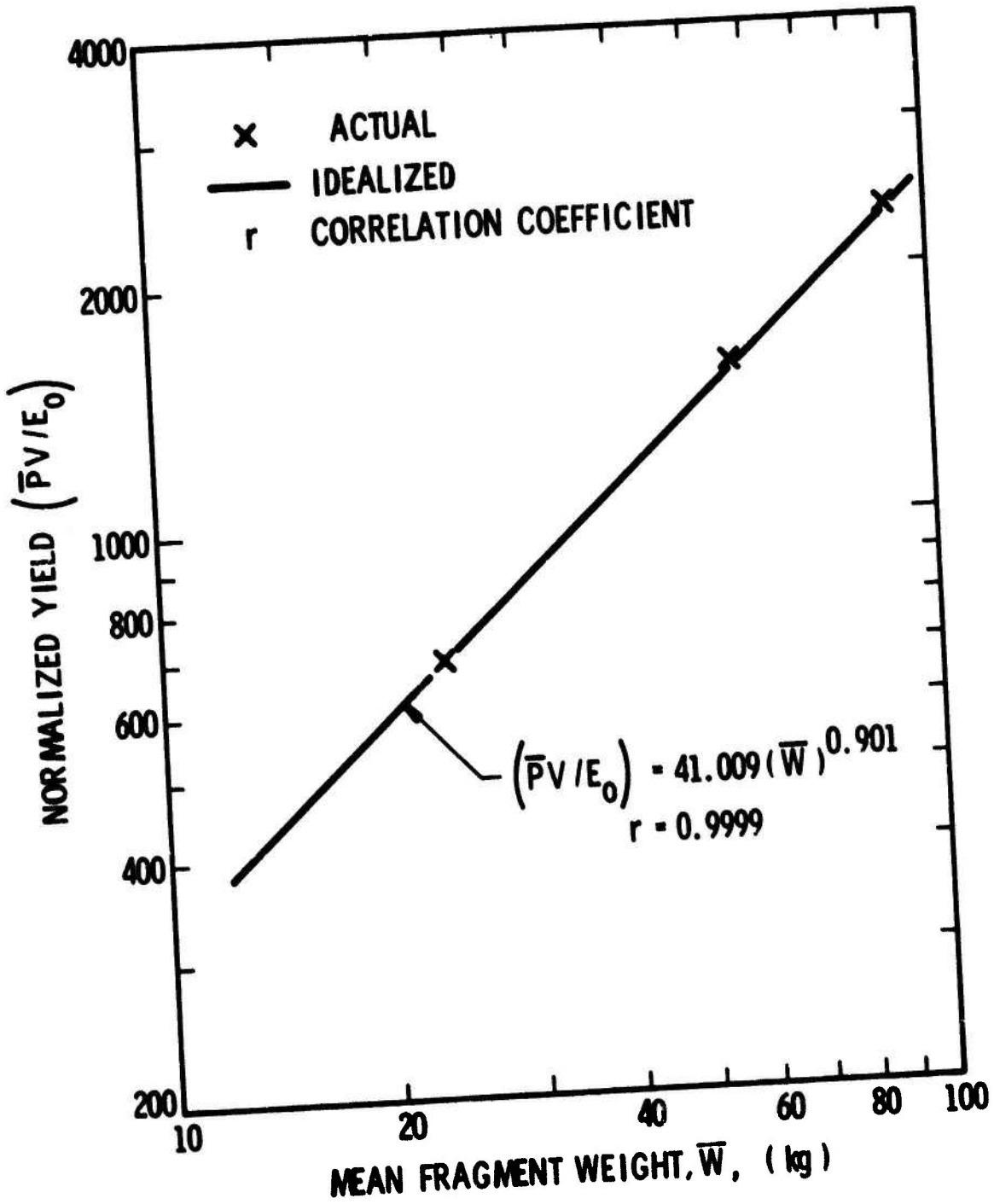

FIGURE 4. Normalized Yield Versus Mean Fragment Weight for Bursting Spheres

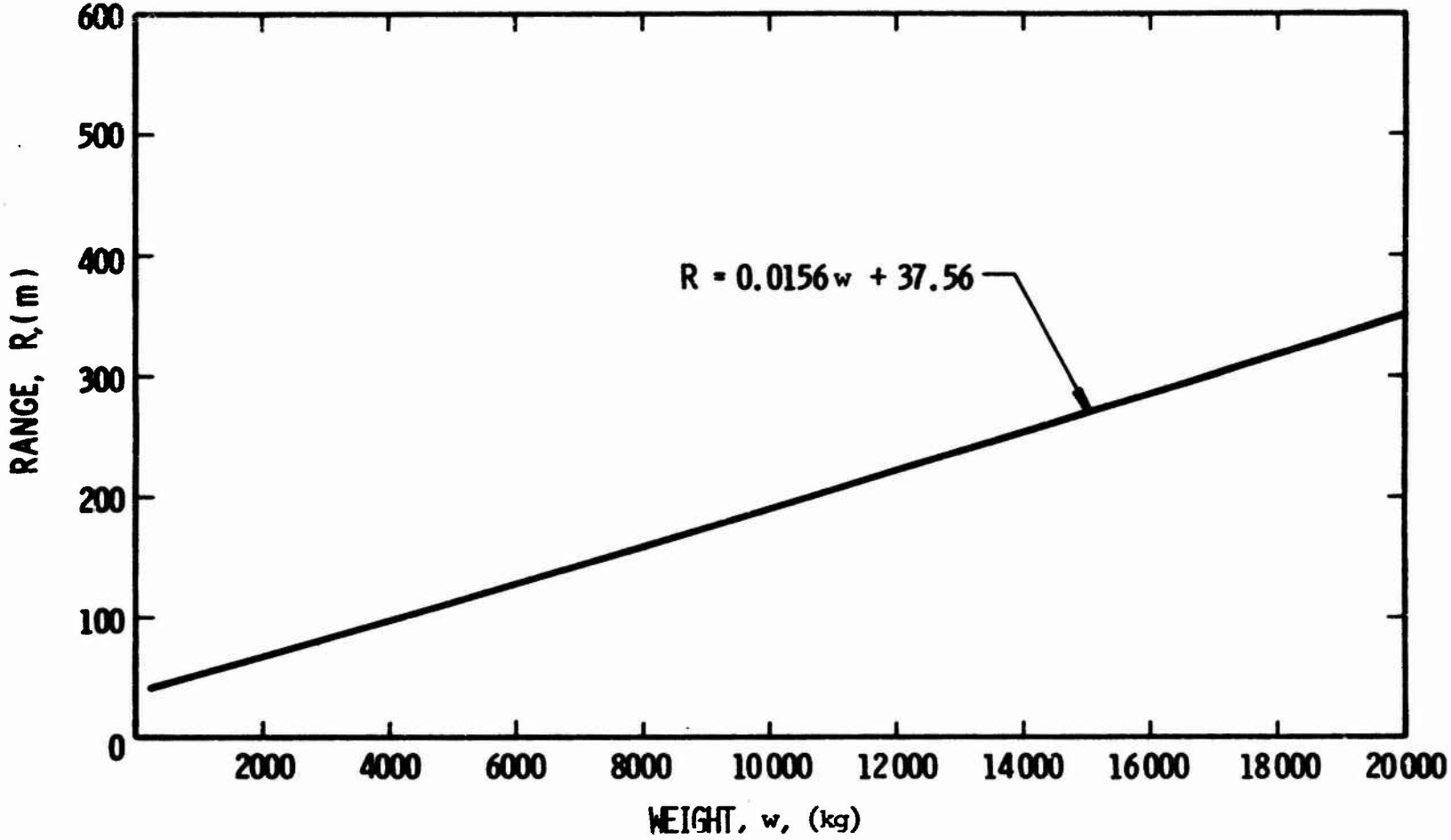

FIGURE 5. Fragment Range Versus Fragment Weight for Event Group 2 (Correlation Coefficient is .79)

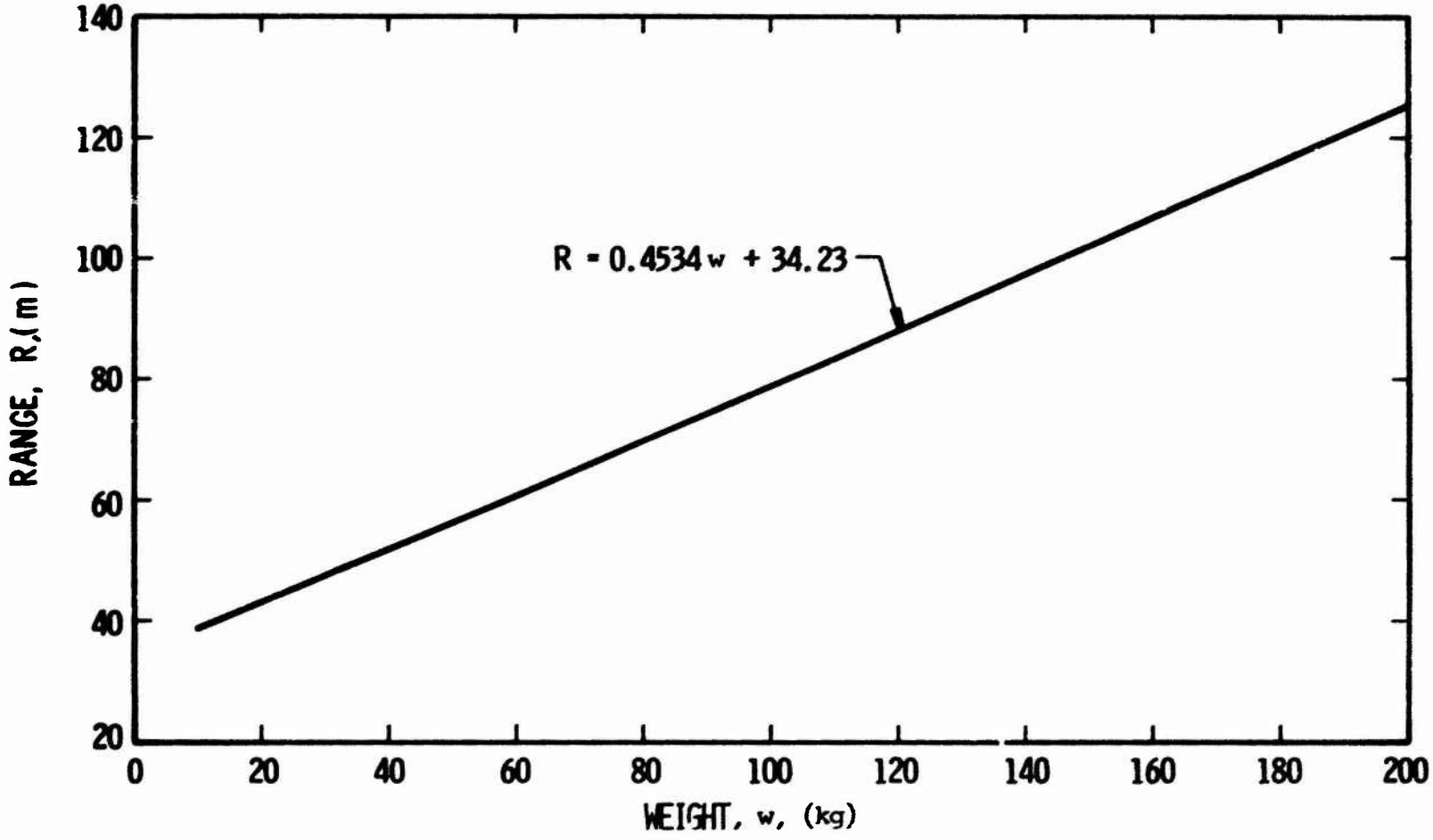

Figure 6. Fragment Range Versus Fragment Weight for Event Group 6 (Correlation Coefficient is .68)

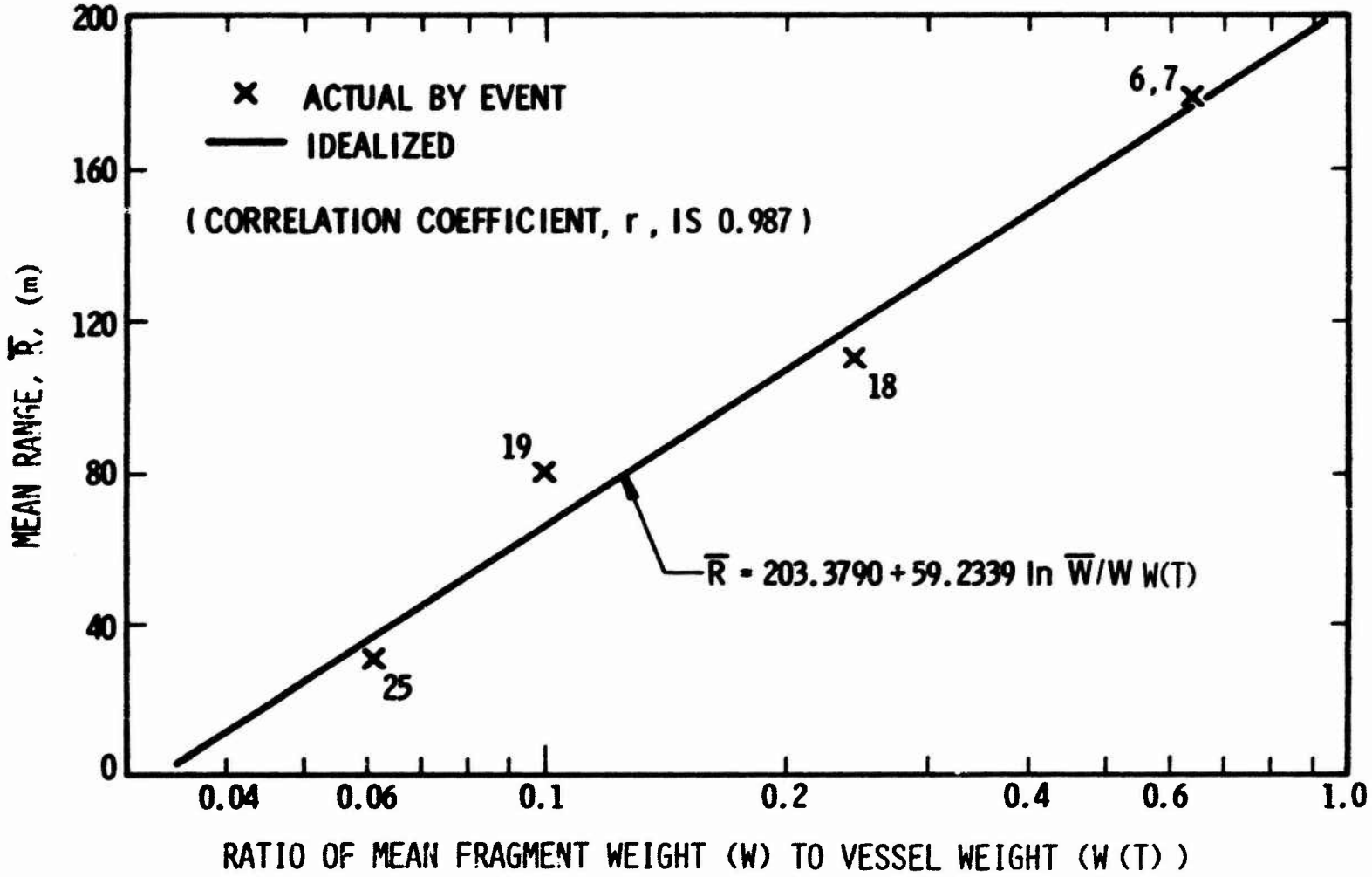

FIGURE 7. Range Versus the Ratio of Mean Fragment Weight to Tank Weight for Cylindrical Vessels (Events 6 and 7, 18, 19, 25)

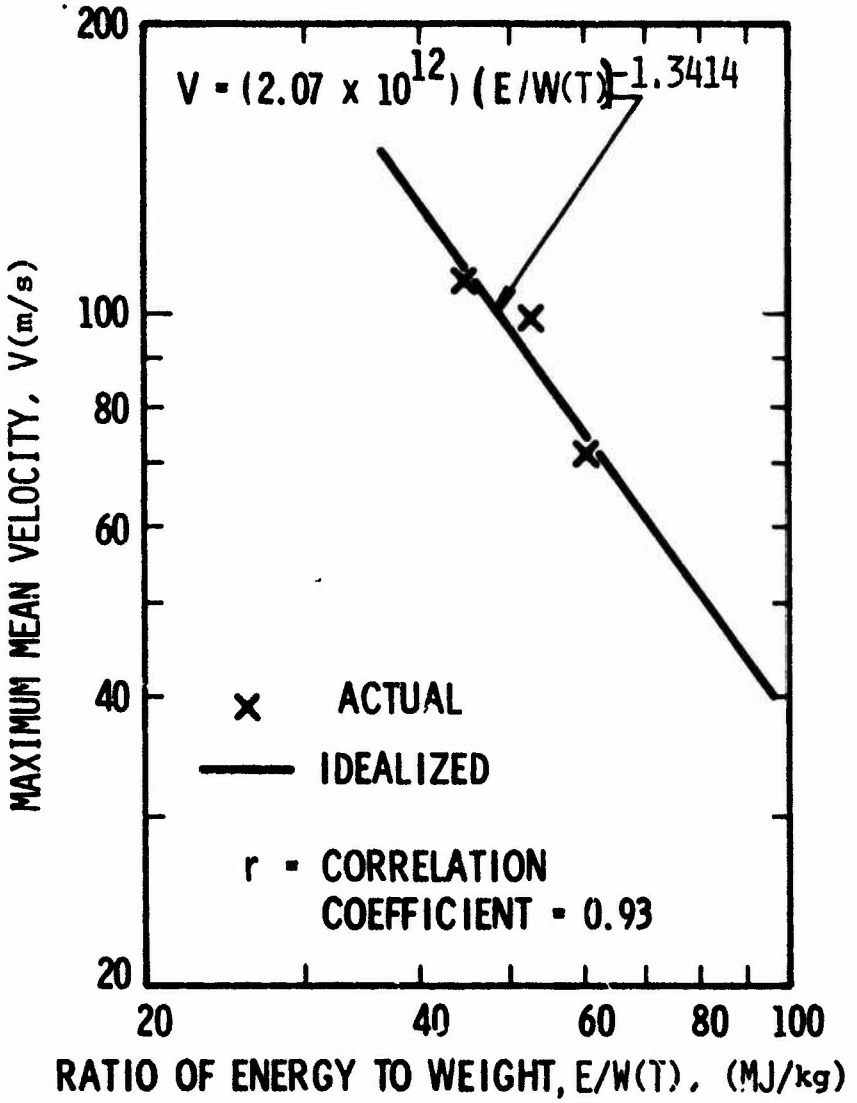

Figure 8. Maximum Mean Velocity Versus Ratio of Energy to Vessel Weight for Bursting Spheres

TABLE 1. Listing of Explosion Event Source and Vessel Data

		EXPLOSION SOURCE				VESSEL				
I.D. NUMBER	REFERENCE	MATERIAL	QUANTITY (M^3 OR KG)	OTHER DATA	ESTIMATED ENERGY (JOULES)	SHAPE	DIMENSIONS	VOLUME (M^3)	MASS (KG)	MATERIAL
1	NTSB-RAR-72-2 Train Derailment 6-21-70	Propane	62,700 kg = 31,300 m^3	Temp: 83°F Specific Gravity: 0.507	5.417×10^5 Joules	Railroad Tank Car #27 with Hemispherical heads	Inside diameter: 2.61m & 3.06m Surface Area: 183.14m^2 Thickness sheets 0.019m 0.02m Outage: 0.34m Length: 21m	30.07m^3	235,000 kg	A 212GrB Steel
2	NTSB RAR-72-2 Train Derailment 6-21-70	Propane	64,900 kg = 32.409m^3	Temp: 88°F Specific Gravity: 0.507	5.954×10^5 Joules	Tank car #28 with Hemispherical heads	Inside Diameter: 3.02m Surface Area: 181.53m^2 Thickness sheets: 0.016m, 0.011m Outage: 0.30m Length: 19.1m	20.71m^3	162,000 kg	TC128GrB Steel

TABLE 2. Listing of Explosion Event Fragment Data

I.D. NUMBER	TOTAL NUMBER FRAGMENTS	FRAGMENTS					
		MASSES (KG)	RANGE (M)	APPARENT TRAJECTORY ELEVATION	DRAG COEFFICIENT C_D	SHAPES OR OTHER DESCRIPTION	REMARKS
1	4		182m		1.20	East end hurled-	First in a series of ex
						eastward	plosions-dug a crater
							in track structure
			91.4m		1.20	West end hurled-	Struck & collapsed roof
						southwestward	of a gas station
			182m		0.82	Large Portion - (0.762m wide)	hurled southwesterly
			228m		0.82	large portion -	Hurled southwesterly.
							The force caused the
							next car (#28) to ro-
							tate with the north end
							elevated 10 ft higher
							than south end.
2	2		61.0m		0.82	South end -	hurled southward; en-
							tered a brick apartment
			487m		0.82	north end -	hurled northeast over
							several bridges & landed
							in a field & continued
							to roll

TABLE 3. Groups of Like Events Taken From the Twenty-five Explosion Events

Event Group Number	Event	Explosion Source		Vessel		
		Material	Energy Range, J	Shape	Mass, kg	Number of Fragments
1	1,2,3,18	Propane, anhydrous ammonia	1.487×10^5 to 1.288×10^6	RR Tank Car	25,542 to 235,409	14
2	6,7,8,9,10, 13,14,15,19	LPG	3814 to 3921.3	RR Tank Car	25,464	28
3	17	Air	5.198×10^{11}	Cylinder Pipe and Spheres	145,842	35
4	20,24	LPG, Propylene	549.6	Semi Trailer (cylindrical)	6,343 to 7,840	31
5	21,22,23	Argon	2.438×10^9 to 1.133×10^{10}	Sphere	46.26 to 187.33	14
6	25	Propane	24.78	Cylinder	511.7	11

TABLE 4. Percentiles For Plotting Fragment Ranges of the Six Event Groups

Percent	Event Group Numbers*					
	1	2	3	4	5	6
10.0	20.00	15.24	22.35	32.00		15.24
14.3					168.27	
20.0	40.00	19.81	40.64	51.51		17.68
28.6					202.69	
30.0	60.96	27.43	54.19	60.65		25.20
40.0	91.44	30.48	66.38	76.02		28.35
42.9					220.07	
50.0	161.00	60.96	68.41	85.04		31.39
57.2					346.25	
60.0	182.88	94.50	88.05	136.86		41.76
70.0	182.88	133.40	109.73	164.59		58.83
71.5					423.37	
80.0	228.60	167.64	115.82	238.96		119.79
85.8					512.06	
90.0	487.68	335.28	206.59	373.73		122.83

*Range in Meters

TABLE 5. Summary of "W" Test on Normality for Fragment Range Distributions for Event Groups 1 Through 6

Event Group No.	"W"	Probability
1	.964	.82
2	.951	.68
3	.986	.98
4	.980	.95
5	.936	.57
6	.917	.28

As it is customary to consider probability values of the "W" statistic exceeding 2 to 10% as adequate grounds for not rejecting the hypothesis that the data belong to the chosen distribution, the fits for the six event groups are more than adequate.

TABLE 6. Percentiles for Plotting Fragment Weights of Event Groups 2, 3 and 6

Percent	Event Group Numbers *		
	2	3	6
10	74.8	93.61	.0341
20	94.8	241.98	.967
30	220.0	399.28	.998
40	350.0	1,039.52	1.00
50	1,180.0	1,080.29	1.22
60	3,183.0	1,281.78	9.30
70	7,470.0	1,439.81	52.23
80	12,200.0	1,935.88	104.46
90	19,098.0	2,020.84	171.38

*Weight in kg.

TABLE 7. Listing of Estimated Means and Standard Deviations for Log-Normal Fragment Weight Distributions (to the Base e) for Event Groups 2, 3 and 6

Event Group No.	Estimated Mean	Estimated Standard Deviation
2	7.049131	2.117124
3	6.617446	1.051264
6	1.418576	2.784658

TABLE 8. Summary of "W" Test On Normality for Fragment Weight Distributions for Event Group 2, 3 and 6

Event Group No.	"W"	Probability
2	.920	.37
3	.860	.10
6	.914	.32

TABLE 9. Parameters of Bursting Spheres

Event	Shot No.	Fragment Weight Kg	Fragment Average Velocity, (m/s)	Burst Pressure, P, Pa	Volume, V (m^3)	Vessel Weight W(T), (kg)	Energy, J	Average(1) Fragment Weight, $\bar{W}$, kg	(2) $\frac{\bar{P}V}{E_o}$
21	1	22.49 23.77	96.9	1.044×10^8	.0283	46.26	2.438×10^9	23.14	693.43
	2	22.36 23.90	98.6	1.030×10^8	.0283	46.46			
	6	23.18 23.18		1.006×10^8	.0283	46.26			
22	3	69.18 66.90	107.59	2.372×10^8	.0283	136.08	6.078×10^9	55.69	1541.6
	7	48.99 42.41	83.52	2.193×10^8	.0283	136.08			
23	4	117.03 70.03	65.84	3.475×10^8	.0283	187.33	1.133×10^{10}	89.75	2347.1
	5	122.92 64.41	71.63	3.475×10^8	.0283	187.33			

(1) Geometric mean fragment weight

(2) $\bar{P}$ = Average burst pressure

E_o = Energy of detonation of 1 g TNT

TABLE 10. Mean Range and Ratio of Mean Fragment Weight to Vessel Weight for Cylindrical Tanks

Event	$\bar{W}/W(T)$	$\bar{R}$
6, 7	0.664	179.83
18	0.242	110.30
19	0.100	80.08
25	0.0612	39.20

WORKBOOK FOR ESTIMATING EFFECTS OF ACCIDENTAL EXPLOSIONS IN PROPELLANT GROUND HANDLING AND TRANSPORT SYSTEMS

BY

W. E. Baker
J. J. Kulesz
R. E. Ricker
P. S. Westine
V. B. Parr
L. M. Vargas
P. K. Moseley

Southwest Research Institute
San Antonio, Texas

REPRODUCED PAGE BLANK

ACKNOWLEDGEMENTS

Many staff members at Southwest Research Institute in addition to the authors contributed substantially to the work reported here. The authors gratefully acknowledge the special contributions of the following:

- Mr. T. R. Jackson, for assistance in debugging and running the complex TUTTI computer program for calculating two-dimensional blast wave properties.
- Ms. Deborah J. Stowitts, for organizing and editing the report.

We also gratefully acknowledge the help of Dr. Del Lehto, Naval Surface Weapons Center, White Oak Laboratory, for providing the TUTTI code documentation, and consulting on its use.

The technical support and guidance of our project manager at the NASA Lewis Research Center, Mr. Paul M. Ordin, contributed materially to the success of this work. In particular, he provided excellent technical guidance as input data for fragment characteristics.

I. INTRODUCTION

This paper describes a companion workbook to an earlier NASA workbook [Baker, et al[1]], NASA CR-134906, which was prepared to aid designers and safety engineers in predicting damage and hazards from accidental explosions involving liquid propellants and compressed gases in flight hardware. The new book, in contrast, is devoted to blast and fragment hazards for the same classes of accidental explosion sources in propellant ground handling and transport systems. Prediction methods which were thoroughly covered in the earlier workbook and which apply without change are not repeated. Instead, explosion hazards peculiar to ground storage and transport systems, or ranges of input parameters specific to these systems, are emphasized.

II. NATURE OF THE HAZARDS

The general nature of the hazards from accidental explosions in propellant handling systems is similar in many respects to the hazards which occur in such explosions in flight vehicles. These accidents cause damage by air blast loading, fragment or appurtenance impact, radiation from fireballs, or fire from ignition of combustible materials following an explosion. Damage can occur to buildings and other facilities, vehicles, and flora and fauna--including humans. Depending on the severity, type and location of explosion accident, the damage can range from minor to extensive.

The sequences of events or causes of accidental explosions in ground handling systems for liquid propellants and compressed gases can be quite similar to those which can occur in flight vehicles, or can differ markedly. Failure by material fatigue on overstress can occur in either case. But, many of the possible causes of flight vehicle explosions such as loss of thrust during launch, guidance system failure, or rupture of a bulkhead separating a fuel from an oxidizer, are inapplicable for ground handling systems. Conversely, transportation accidents followed by explosions are causes which are absent in flight vehicle accidents.

Ground handling systems usually have much less serious weight constraints than do flight vehicles. This difference dictates some of the differences in the nature of the hazards. Ground systems can employ relatively massive, ductile materials in pressure vessel and piping

construction. On failure, such vessels generate relatively few fragments compared to similar failures in flight-weight vessels. A failure of a long cylindrical vessel near one end can often result in most of the vessel remaining intact, and "rocketing" as the internal compressed fluid is ejected from the rupture. This mode of failure has never been observed in flight-weight pressure vessels or tankage, which have less ductility and instead break into a relatively large number of fragments. Pressure vessels used in ground systems are often of much larger capacity than flight systems. The total stored energy in compressed gases or total chemical energy in stored fuels and/or oxidants can then be much greater than for many flight systems.

There have unfortunately been many more accidental explosions involving fuels and compressed fluids in ground handling than in flight vehicles. There is a considerable body of accident report literature [see, for example, Strehlow & Baker[2,3]which highlight the probable types of accident. These are (not necessarily in order of probability):

1) Simple pressure vessel failure because of fatigue or flaw growth.
2) Vessel failure induced by impact during a transportation accident.
3) Vessel failure by overpressure because of overheating. This often follows a derailment accident with railroad tank cars.
4) Fuel leakage followed by a vapor cloud explosion.

Blast and some type of fragment or massive body impact usually result from the first three types of accident; the last type causes primarily a pressure wave and fireball; while the first three may or may not cause fireball or fire depending on the fluid and circumstances in the accident.

Assessment of the magnitudes and the effects of the blast and fragments for ground system explosions is the topic of the new workbook. [Baker, Kulesz, et al[4]].

III. CONTENTS OF THE WORKBOOK

From the material presented in the workbook, one should be able to make predictions of blast and fragment characteristics and effects for a

wide range of possible explosion accidents in ground systems. The body of the workbook gives the prediction methods in the form of graphs, equations, or tables. All detailed development and some computer programs are given in appendices. Given a number of accident scenarios, the material should allow prediction of:

1) Explosive energy yield or energy release
2) Characteristics of blast pressure waves generated by spherical and non-spherical explosions.
3) Effects of pressure waves on certain classes of targets or for blast loading conditions not covered in Baker, et al[1].
4) Characteristics of fragments generated by ground equipment explosions. This includes massive vessel parts which "rocket".
5) Effects of fragment impact not covered in Baker, et al[1]. including effects of fragment revetments on blast waves.

The scope of the material is deliberately limited to avoid duplication with the previous workbook. Typical examples of prediction curves and formulas available in the book, and some discussion of the procedures used to derive the curves, are now given.

Explosive Energy Release (Yield)

For compressed gas vessel bursts, an upper limit for total energy release can be obtained by using the equation proposed by Brode[5]. This formula is:

$$E = \left(\frac{p_1 - p_a}{\gamma_1 - 1}\right) V_1 \qquad (1)$$

where E is blast yield (energy), p_1 is initial absolute pressure in the vessel, p_a is outside atmosphere absolute pressure, γ_1 is the ratio of specific heats for the gas in the vessel, and V_1 is the internal volume. A slightly lower, but still conservative (high) estimate is based on isentropic expansion from initial burst pressure to atmospheric pressure [Baker[6], Brinkley [7]].

$$E = \frac{p_1 V_1}{\gamma_1 - 1}\left[1 - \left(\frac{p_a}{p_1}\right)^{\frac{\gamma_1 - 1}{\gamma_1}}\right] \qquad (2)$$

The equations given here for blast yield are based on the assumptions that all of the energy which can drive a blast wave does so, depending only on the energy release rate. For real situations, some energy must be absorbed by the vessel as it fractures, both in the fracturing process itself and in accelerating the vessel pieces for fragments to their maximum velocity. For failure of a compressed gas vessel, the energy absorbed in the fracture process is negligible because the vessel is already stressed to failure. But, the energy absorbed in accelerating vessel fragments can be significant. In experiments such as those of Esparza and Baker [8] and Boyer, et al[9] with pressurized glass spheres and Pittman[10,11] with metal pressure vessels, the fragments were observed with high speed cameras or other velocity measuring systems. In accidental vessel bursts, the velocities of fragments can be estimated by methods presented in the workbook. Knowing mean fragment velocity U and total mass M of the vessel, one can then compute the kinetic energy of the vessel fragments.

$$E_k = M U^2/2 \qquad (3)$$

To obtain an estimate of effective blast yield E_e for gas vessel bursts, one can then use either eq. (1) or (2) and subtract fragment kinetic energy, i.e.,

$$E_e = E - E_k \qquad (4)$$

Many fluids are stored in vessels under sufficient pressure that they remain essentially liquid at the vapor pressure corresponding to the storage temperature for the particular liquid. Examples are the fuels propane or butane which are normally stored at "room" temperature, methane (LNG) which must be stored at cryogenic temperatures, and refrigerants such as ammonia or the Freons which are also stored at room temperature. If a vessel containing such fluids fails, the resulting sudden pressure release can cause expansion of vapor in ullage space and partial flash evaporation of the liquid, and drive a blast wave into the surrounding air.

Because the properties of flash-evaporating fluids differ markedly from perfect gases, the methods for estimating blast yield for gas vessel bursts are inapplicable. Instead, one must know the complete thermodynamic properties of the fluid in the vessel as functions of state variables such as pressure, specific volume, temperature, and entropy.

For any expansion process from state 1 to state 2, the specific work done is defined as:

$$e = u_1 - u_2 = \int_1^2 p \, dv \qquad (5)$$

where u is internal energy, p is pressure, and v is specific volume. We assume that an isentropic expansion process occurs after vessel burst. This process is shown schematically in a p-v (pressure-volume) diagram in Figure 1, and in a T-s (temperature-entropy) diagram in Figure 2. The cross-hatched area in Figure 1 is the integral of equation (5), and therefore represents the specific energy e. Also shown in the two figures are the saturated liquid and saturated vapor lines, which bound the wet vapor region. Parameters P_c and T_c are the critical pressure and critical temperature, respectively. Whenever the expansion process occurs near or in the wet vapor region, as is always true for flash-evaporating fluids, the functional relationship between pressure and specific volume is quite complex and the integral in equation (5) cannot be obtained analytically. But, fortunately, there are tables of thermodynamic properties available for many fluids, and the internal energy u or enthalpy h defined as:

$$h = u + pv \qquad (6)$$

are tabulated for the entire wet vapor region and the superheat region, as functions of pressure and specific volume, or temperature and entropy.

Using thermodynamic tables, assuming isentropic expansion, and obtaining initial specific volume from:

$$v_1 = V_1/m \qquad (7)$$

where V_1 is vessel internal volume and m is total mass of fluid, one can than compute E from

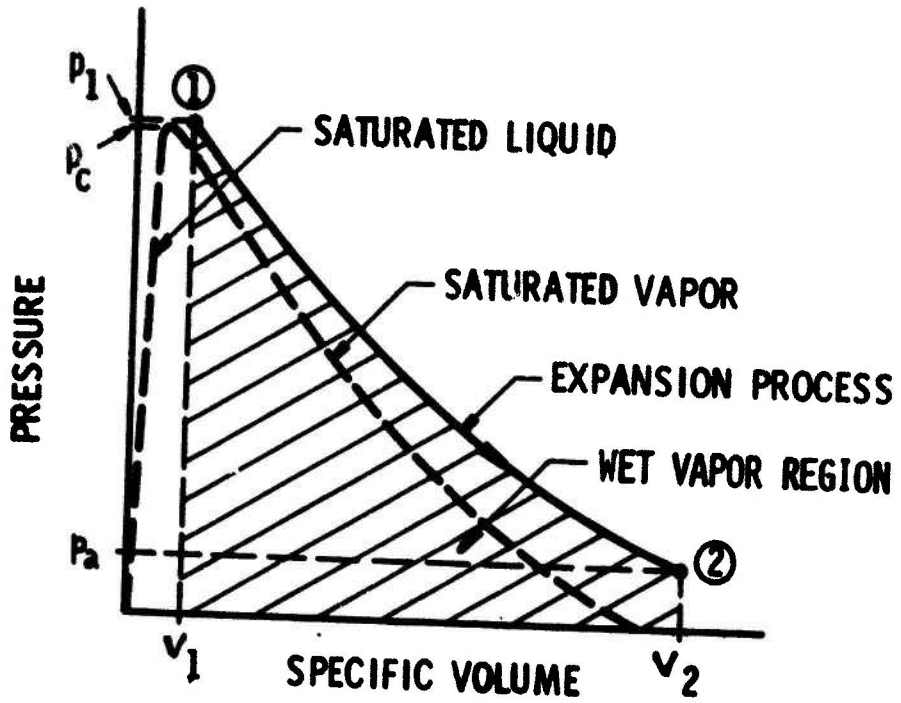

Figure 1. p-v Diagram of Expansion

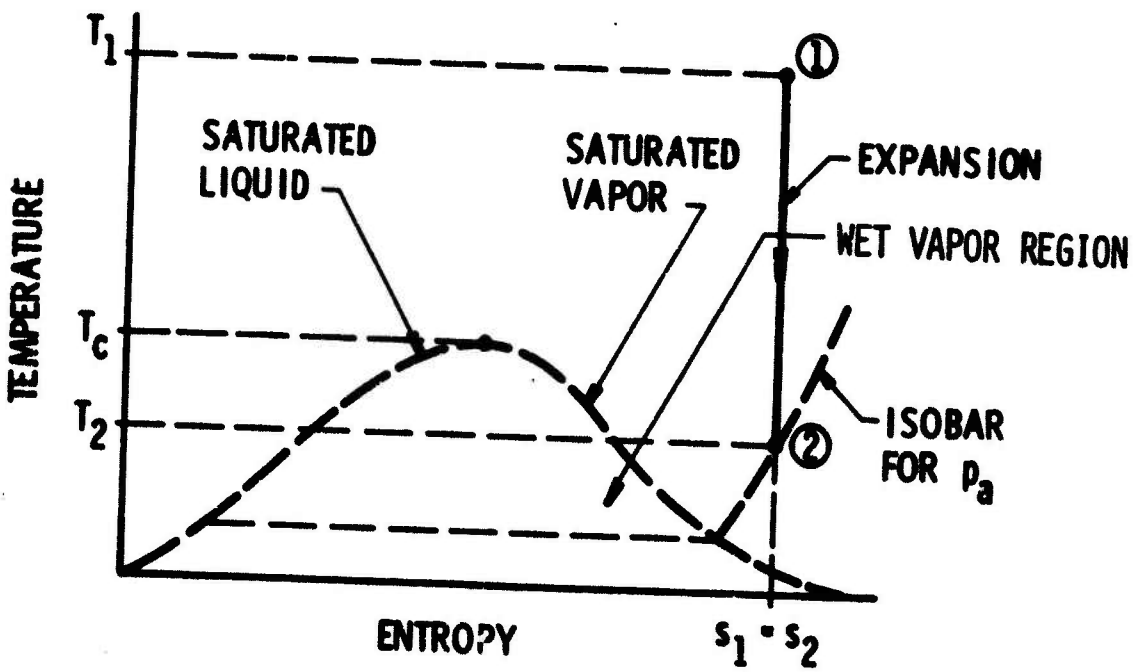

Figure 2. T-s Diagram of Expansion

$$E = m (u_2 - u_1). \qquad (8)$$

Some tables of thermodynamic properties for fluids which can be used to estimate blast yields by the process just described are the ASHRAE Handbook of Fundamentals[18] for refrigerants, Keenan, et al[12] for steam, and Din [13] for a number of fluids including fuels such as propane and ethylene.

The workbook contains some discussion of energy releases from vapor cloud explosions, and notes that estimates of these fields can only be very approximate with our current state of knowledge. An approximate procedure for estimating vapor cloud explosion yields is suggested, and a list of potentially dangerous fuels is given.

BLAST WAVE CHARACTERISTICS

New blast wave properties given in this workbook include results of recent measurements around bursting frangible pressure spheres [Esparza and Baker[8,14]] and results of some two-dimensional computer code predictions for the case of spherical pressure vessels separating into halves and releasing compressed gas. A typical measured pressure wave for a bursting, gas-filled sphere is shown in Figure 3, together with definitions of some properties which are not usually reported. The distinctive characteristics of this pressure-time trace are the pronounced negative phase compared to the positive phase, and the strong second shock wave. By contrast, waves from condensed explosives have much smaller negative phases and seldom have a discernible second shock. The parameters indicated in Figure 3 are defined as follows:

P_{s1} first shock side-on overpressure

$I_s^{(+)}$ positive phase impulse for first shock

$T_s^{(+)}$ duration of positive impulse for first shock

$I_s^{(-)}$ negative phase impulse for first shock

$T_s^{(-)}$ duration of negative phase for first shock

P_{s2} second shock side-on overpressure.

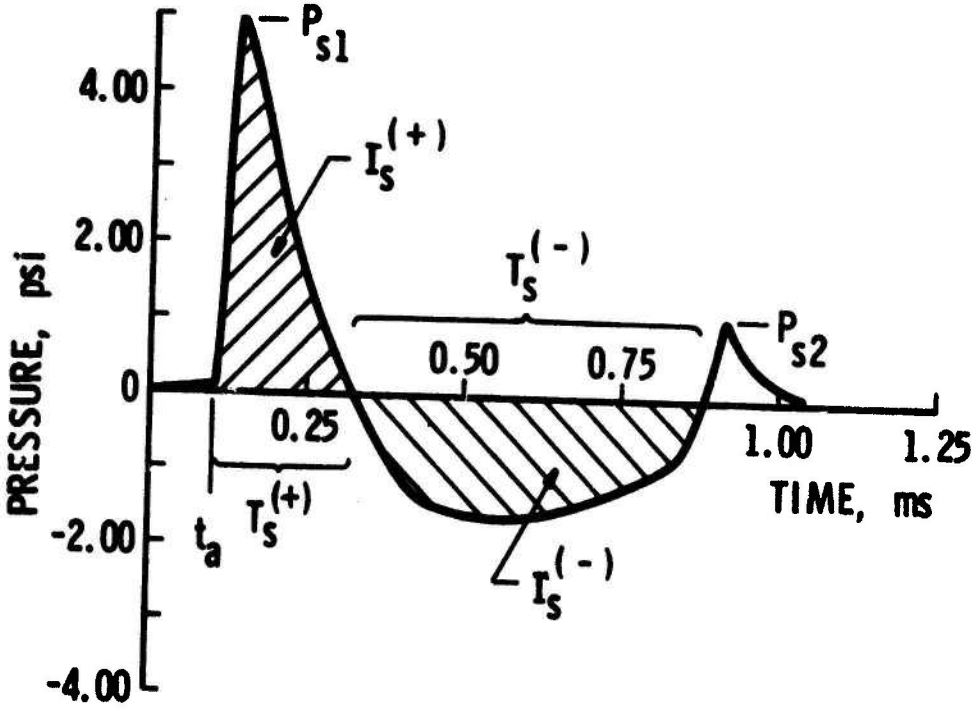

Figure 3. Typical Blast Pressure History for Frangible Gas Sphere Burst

Figures 4 and 5 show how two of the more usual scaled parameters, peak overpressure and positive phase impulse, compare with scaled Pentolite data and with one-dimensional (spherical) code calculations. The negative impulses are quite large for these bursts, as can be seen by comparing Figure 6 to Figure 5.

The two-dimensional computer code predictions were distilled down to graphs for scaled overpressure (Figure 7) and impulse (Figure 8) along the dividing plane between the two vessel halves as they separate, where the blast waves are the strongest.

BLAST WAVE EFFECTS

Because of the correlation of the blast effects prediction methods in Baker, et al[1] with blast wave properties, all of the graphs and equations in Chapter III of that reference are equally applicable for the ground burst accidents which are the topic of the new workbook. Topics covered in Baker, et al[1] are:

1) Thresholds for glass breakage.
2) Empirical blast damage estimates for residential buildings.
3) Toppling or overturning of vehicles and other objects.
4) Damage thresholds for beam structural elements.
5) Damage predictions for brittle and ductile rectangular plate elements.
6) Damage thresholds for rectangular membranes.
7) Blast injury estimates for humans.

Supplementary prediction curves based on further damage prediction analyses are given in the new book. These include:

1) Predictions for response of elastic beams (Figure 9)
2) Predictions for response of elastic-plastic beams (Figure 10)
3) Predictions for response of elastic-plastic "strings", i.e., narrow members with negligible bending stiffness (Figure 11)
4) Buckling thresholds for columns with dynamic axial loads (Figure 12).

The plots shown in Figures 9-12 are all cast into the form of dimensionless pressure-impulse (p-i) curves, and allow rapid prediction of response of these structural elements, if the blast loads, structural dimensions, and material properties are known. In these graphical solutions, the loading

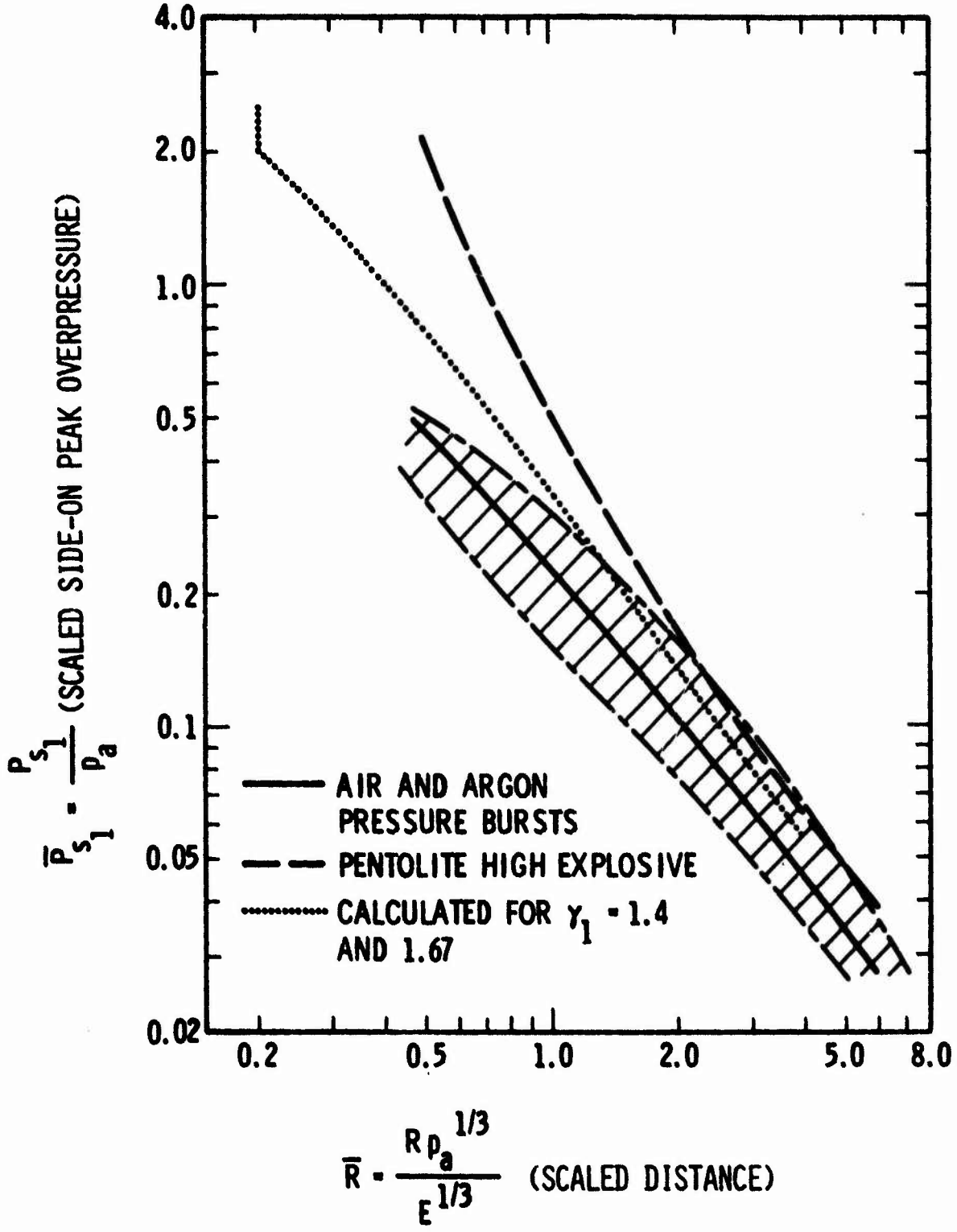

Figure 4. Scaled Side-On Peak Overpressure for First Shock From Bursting Gas Spheres

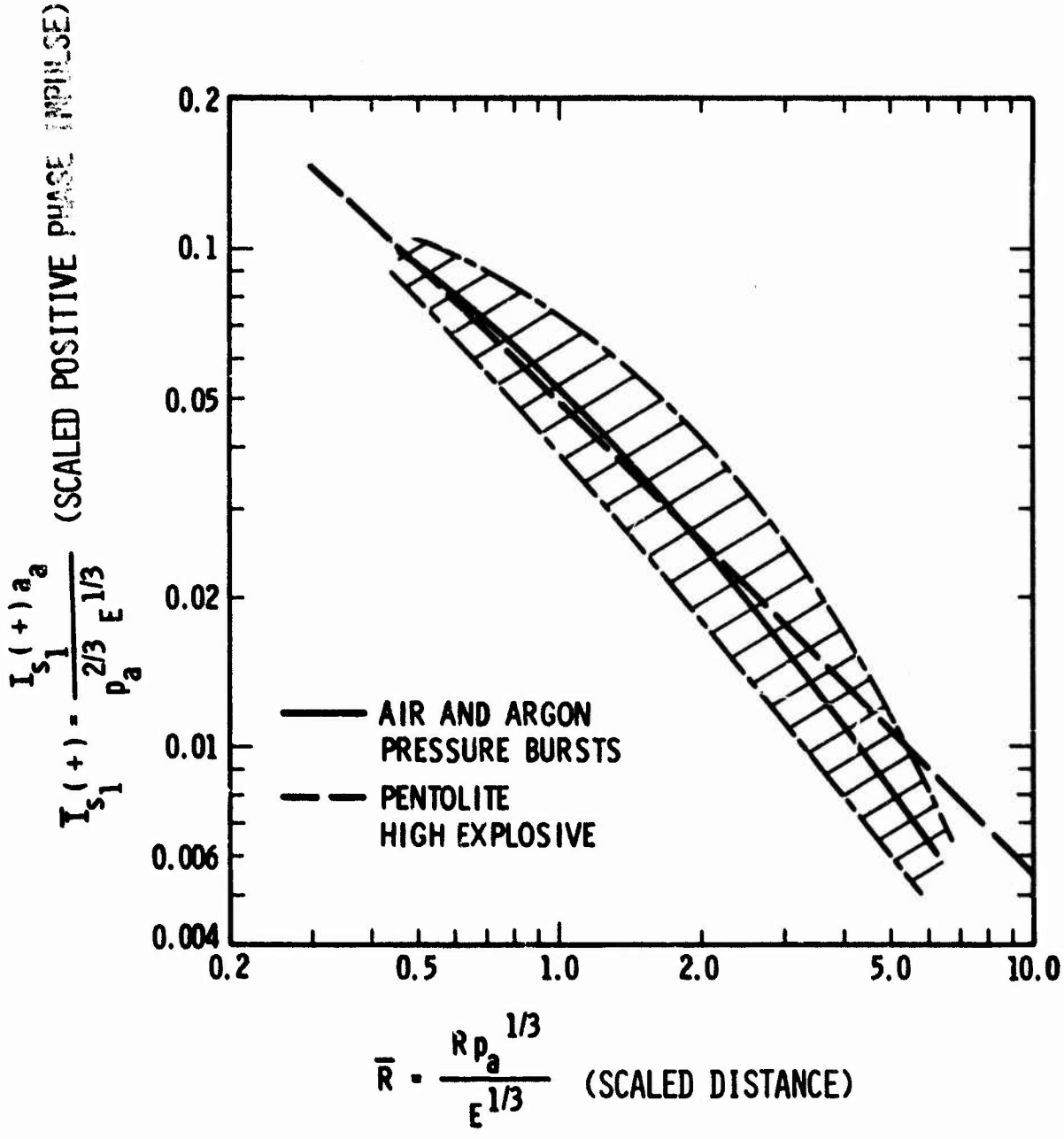

Figure 5. Scaled Side-On Positive Impulse From Bursting Gas Spheres

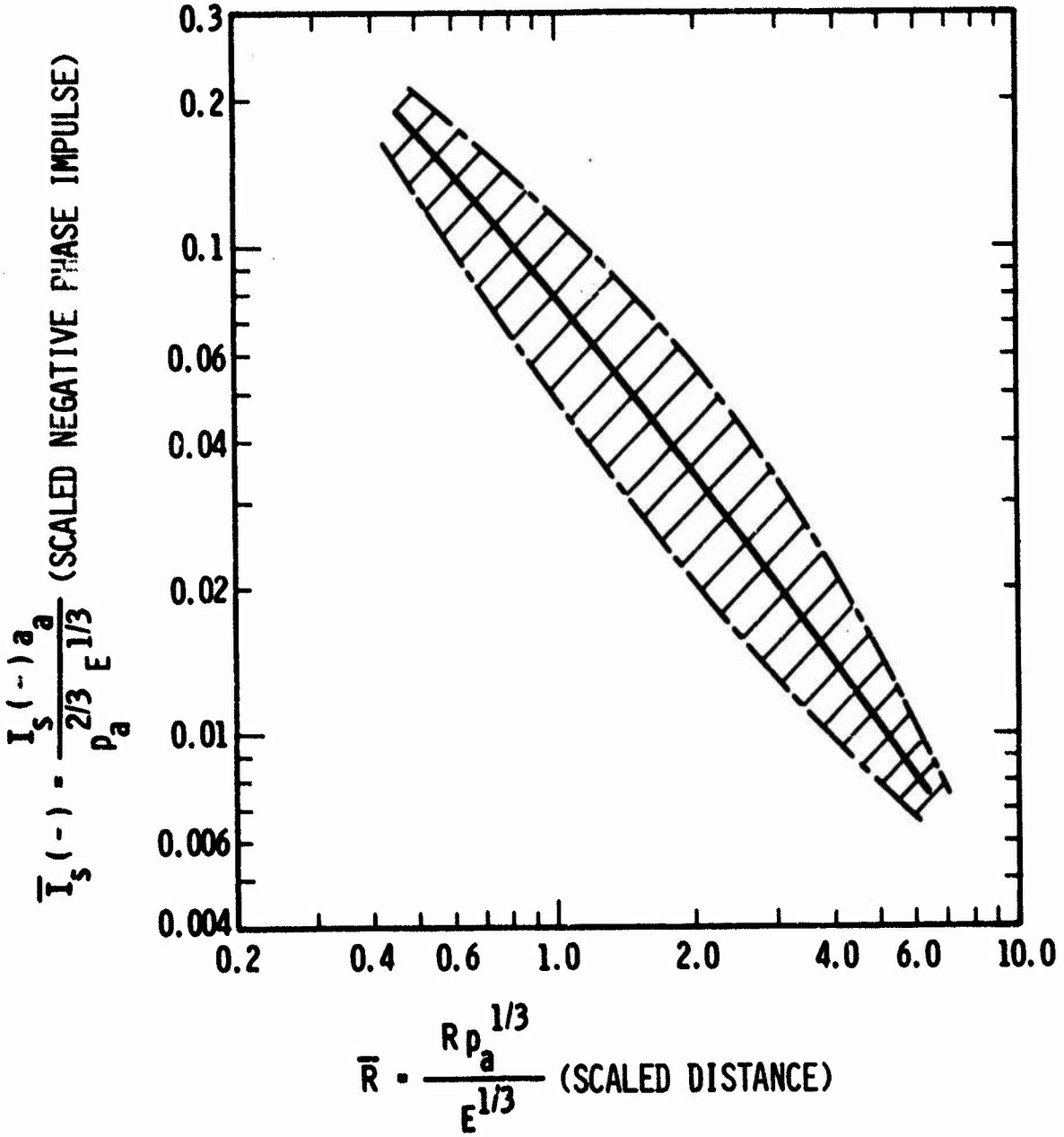

Figure 6. Scaled Side-On Negative Impulse From Bursting Gas Spheres

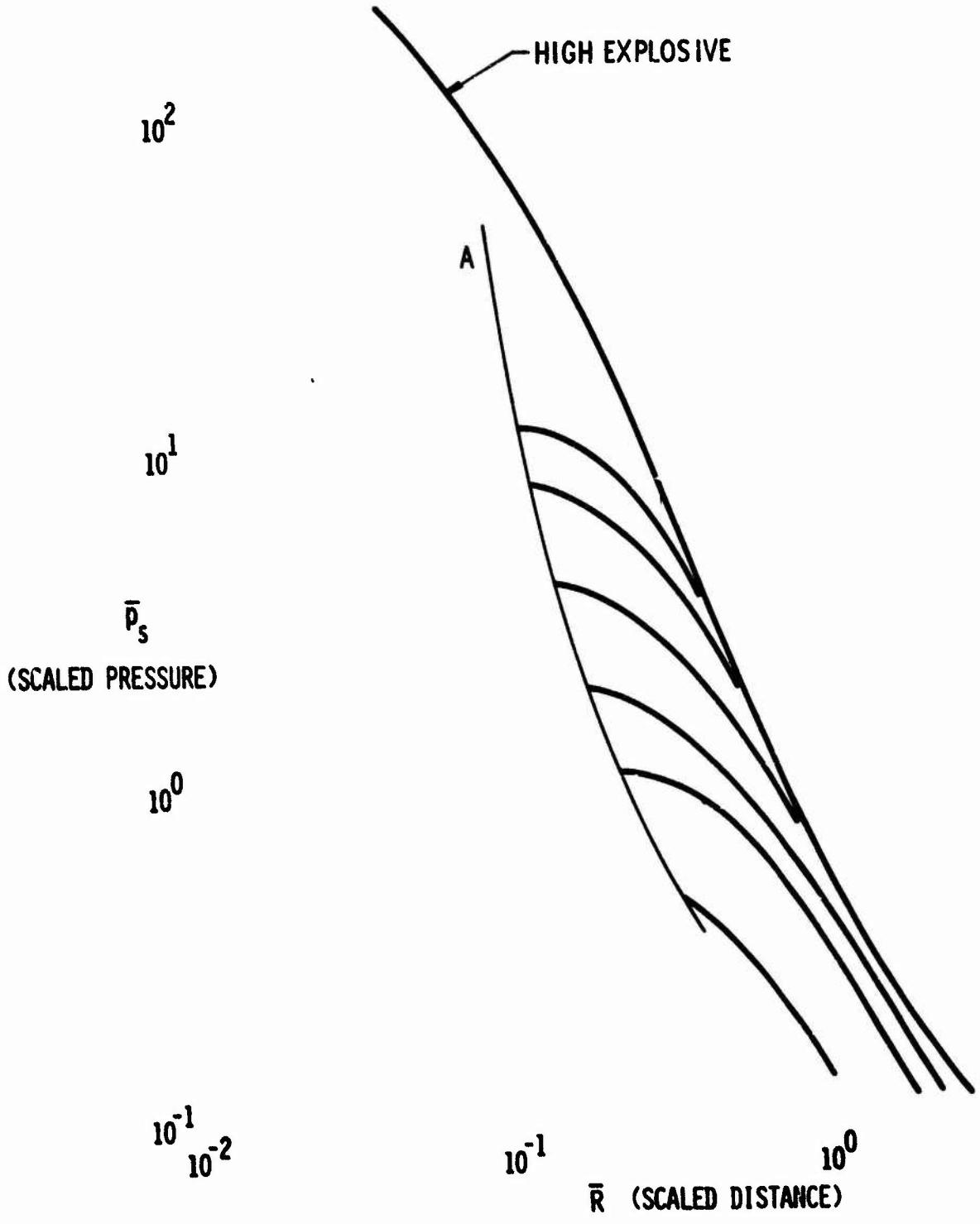

Figure 7. $\bar{P}_s$ vs. $\bar{R}$ for Overpressure Calculations.
Distance along Plane of Symmetry

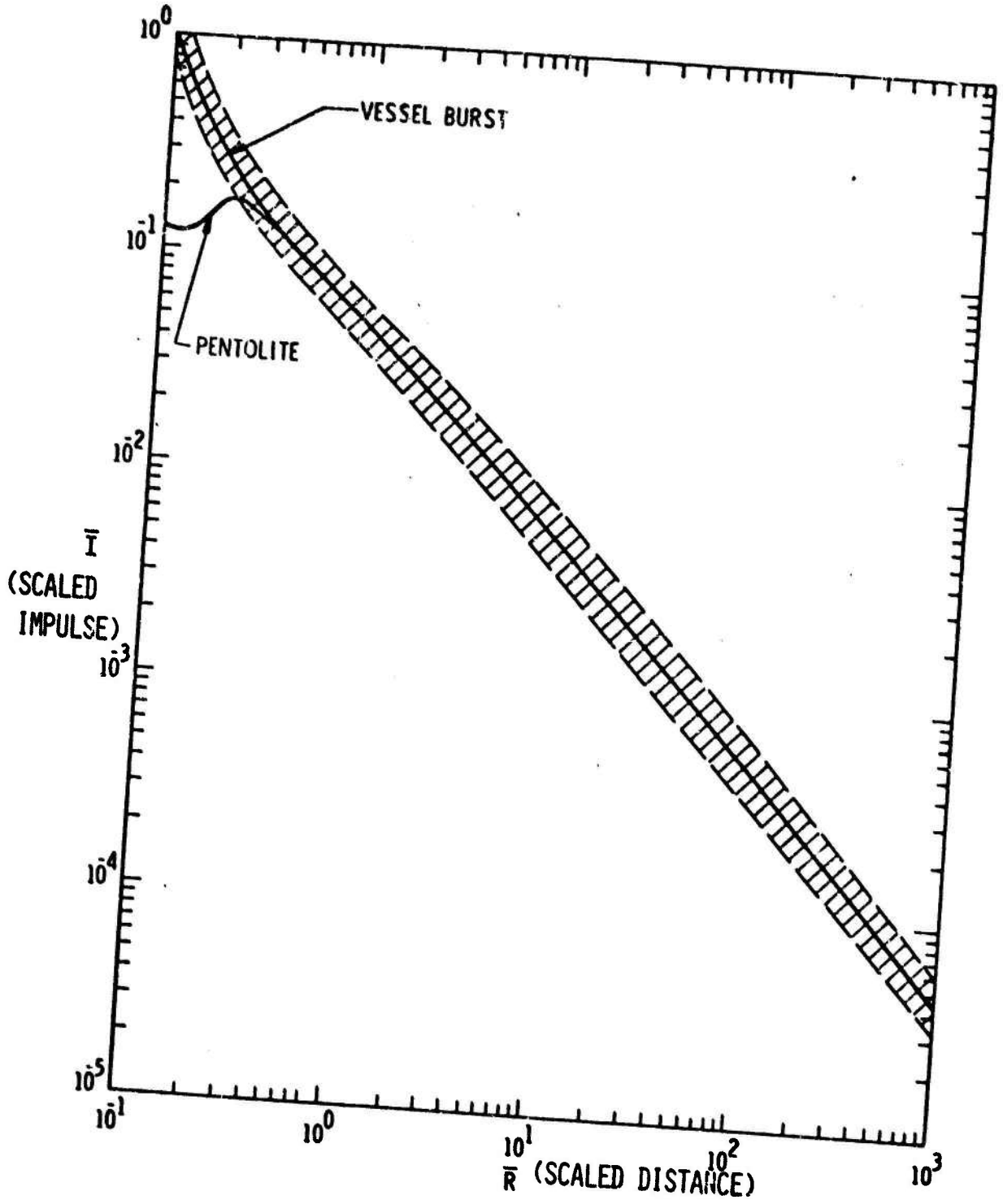

Figure 8. $\bar{I}$ vs. $\bar{R}$ for Pentolite and Gas Vessel Bursts

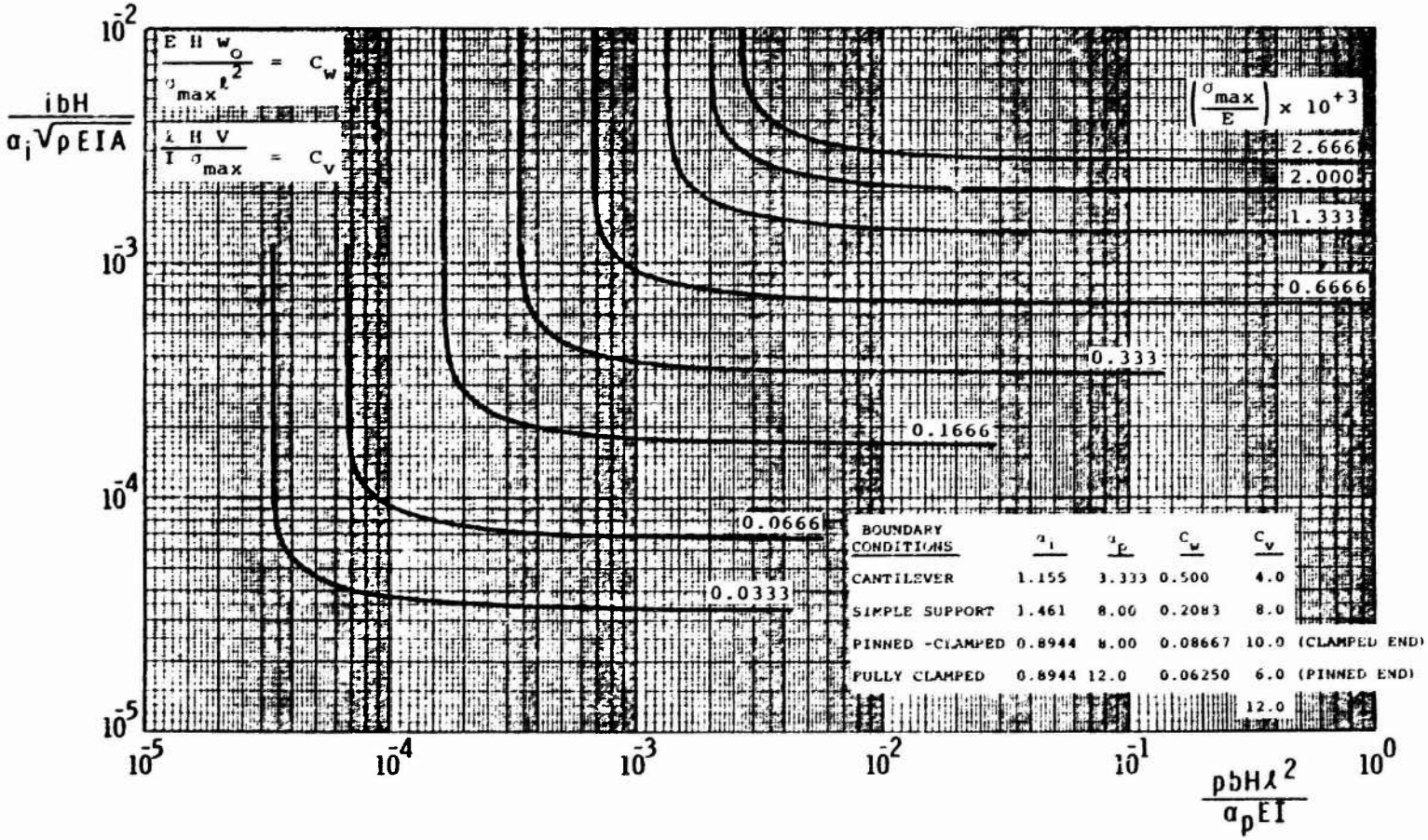

Figure 9. Stresses, Shears, and Deflections in Blast Loaded Elastic Beams

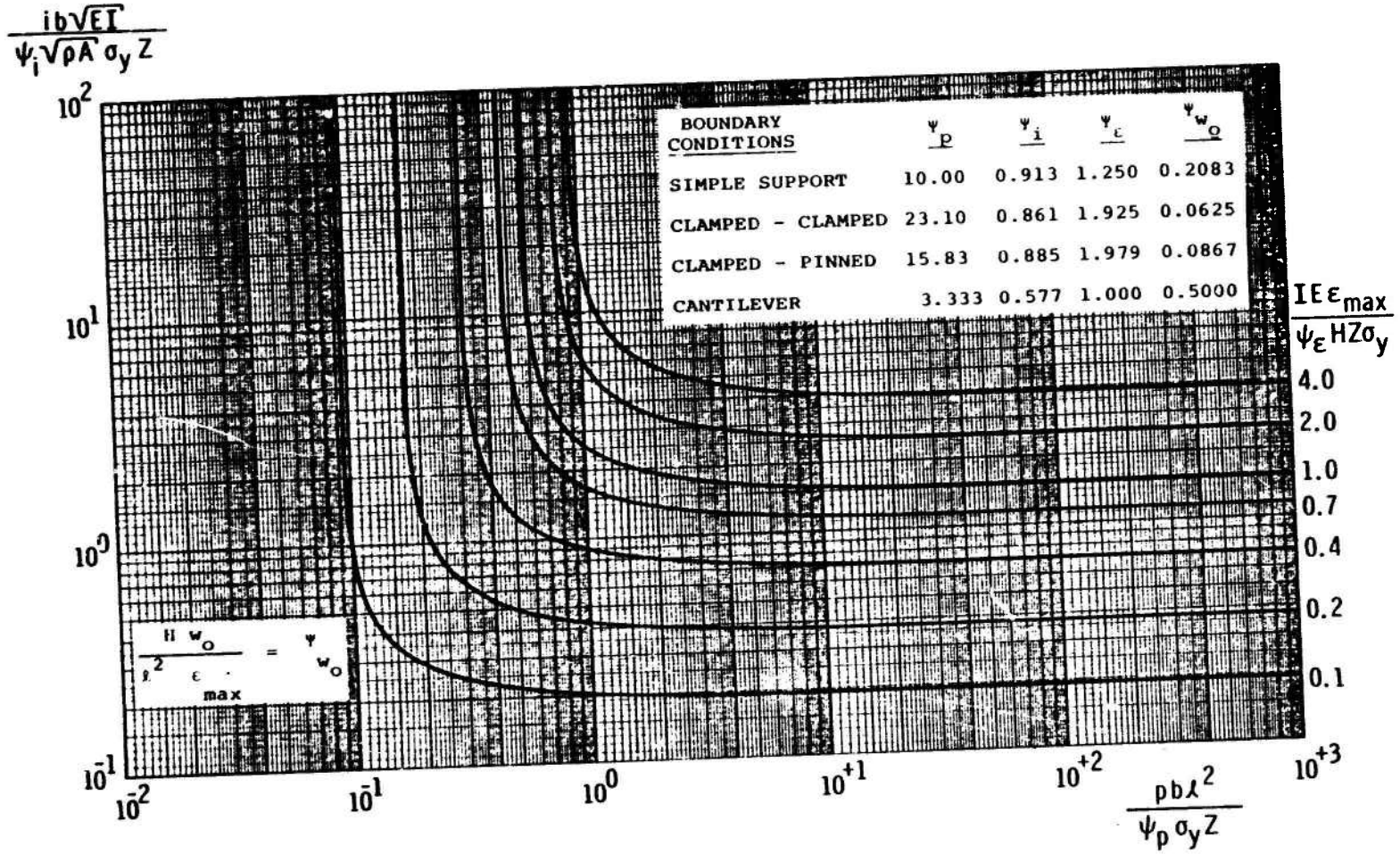

Figure 10. Elastic-Plastic Solution for Blast Loaded Beams

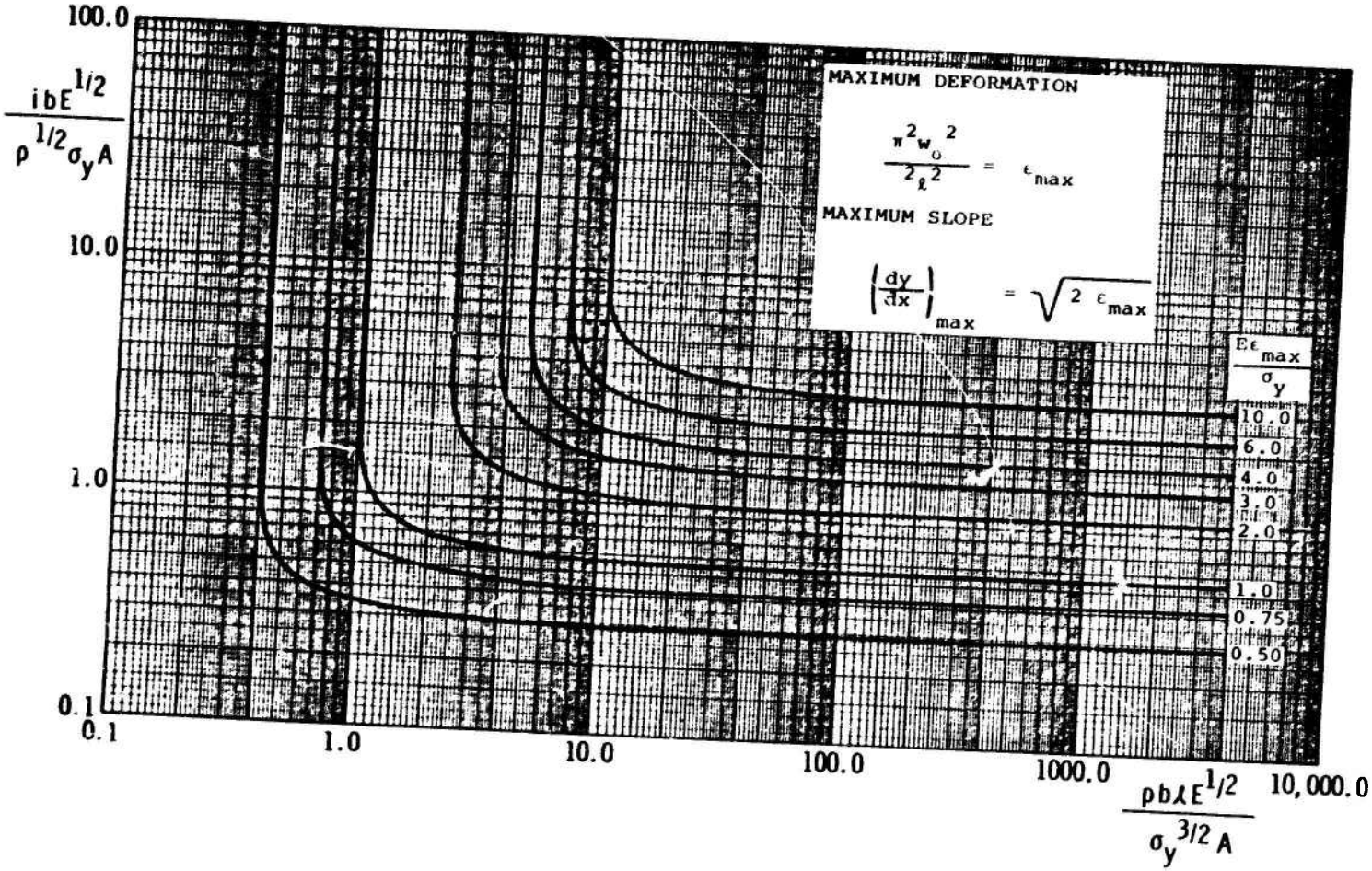

Figure 11. Elastic-Plastic String Solution

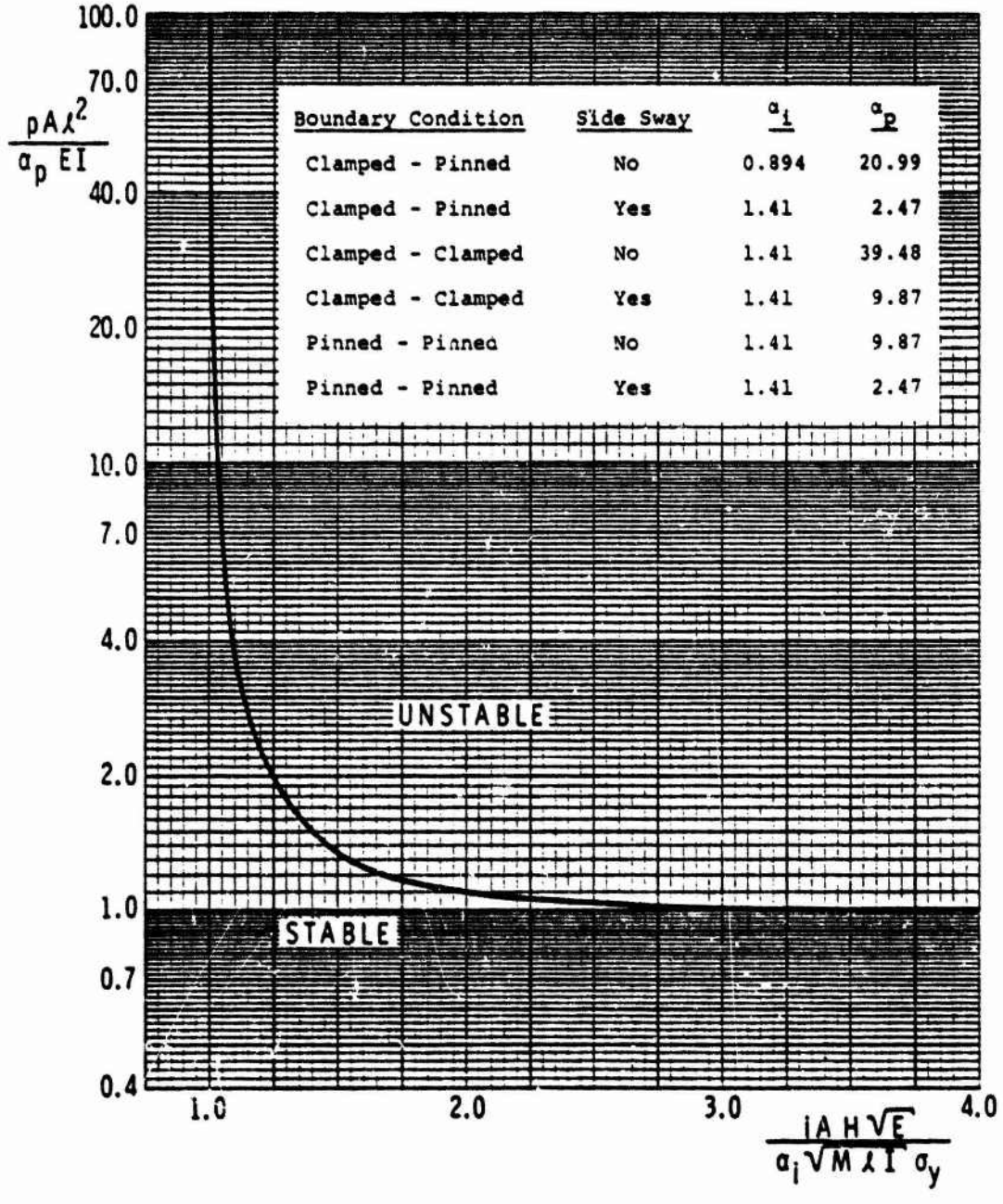

Boundary Condition	Side Sway	α_i	α_p
Clamped - Pinned	No	0.894	20.99
Clamped - Pinned	Yes	1.41	2.47
Clamped - Clamped	No	1.41	39.48
Clamped - Clamped	Yes	1.41	9.87
Pinned - Pinned	No	1.41	9.87
Pinned - Pinned	Yes	1.41	2.47

Figure 12. Buckling for Dynamic Axial Loads

is assumed to be uniform over the entire span of length ℓ. The beam has a loaded width b, a mass density ρ, a cross-sectional area A, a total depth H, an elastic modulus E, a maximum deformation w_o, a yield stress σ_y, and a second moment of area I. In Figure 10, the beam also has a plastic section modulus Z to be used in predicting response. Throughout these solutions, the stress-strain curve is assumed to be an elastic - perfectly plastic one without significant strain hardening or strain rate effects.

Different boundary conditions can be evaluated using Figures 9, 10 and 12 by inserting the appropriate nondimensional numbers, i.e., the appropriate Ψ or α coefficients from the tables in the figures. Figure 9 is actually a more specific form of Figure 10. Figure 9 is a bending beam solution for elastic response only, and, thus, allows one to estimate the shear forces at the supports. Provided the response is elastic, Figure 9 essentially yields the same solution as an elastically responding beam from the more generalized Figure 10 solution.

When a member undergoes large deformations relative to its thickness, or is axially constrained, the principal mode of energy dissipation can be extensional rather than bending. Figure 11 presents an elastic-plastic, one-dimensional, extensional solution. In this solution, one assumes that the ends are constrained from moving together so that in-plane forces can be developed. Once strain has been determined, the maximum deformation, the slope at the boundaries, and the magnitude of the anchoring force can all be determined using Figure 11.

Figure 12 shows a scaled pressure-impulse diagram for buckling of an axially loaded elastic column. The solid line in the figure is the threshold separating unstable column response from stable. If the nondimensional loads imparted to a column establish a point which is to the left and/or below the threshold line, then the column should remain stable. On the other hand, should these nondimensionalized loads establish a point above and to the right of the threshold, large permanent, unstable deformation should be expected. The new parameter in the figure, M, is the mass of the overlying floor, and A is the loaded area of the roof or floor over the column.

FRAGMENT CHARACTERISTICS

In Baker, et al [1], there was extensive coverage of such characteristics of fragments from flight-weight vehicles as initial velocities, size and mass distributions, fragment trajectories, and the distances of ranges the fragments

travelled. The data and prediction methods given in that reference were based on accident reports and tests with liquid propellant explosions and lightweight gas vessel bursts, development and exercise of a variety of special-purpose computer programs, and statistical analysis of test and accident data.

Accidental explosions in ground systems tend to produce very different types of fragments or missiles than do similar explosions in flight-weight systems. The most striking difference lies in the number of fragments generated, with the number usually being much less for the ground systems than for flight systems. This difference is primarily a function of the differences in storage or pressure vessel materials and construction. Relatively thick-walled vessels, made of ductile steels, dominate in ground storage and transport systems. These vessels often split, or fragment into only two pieces, after failure. Accidental explosions which generate more than a dozen vessel fragments are quite uncommon. For storage or transport vessels containing flash-evaporating liquids such as propane (LPG), a common failure mode is an asymmetric burst of a long cylindrical vessel, with the major part remaining intact and "rocketing" as the fluid exhausts and flashes. Accident reports of such failures show that the vessel can travel great distances, and of course cause major damage where they impact.

In the workbook, the results of studies on the characteristics of fragments from ground vessel explosions are presented, and the differences from fragmentation of flight-weight vehicles are highlighted. As before, a survey and statistical analysis of accident data is included; several new computer programs were developed and exercised; and prediction curves for various characteristics of the relatively large and massive fragments generated in accidental explosions in ground systems are presented. The results of the survey of accidents are reported in another paper in this seminar [Parr & Moseley[15]], while some of the prediction curves based on computer analysis are shown here.

Initial fragment velocities for cylindrical and spherical vessels bursting into n equal fragments can be estimated from Figure 13 for two fragments, ten fragments and one hundred fragments from spherical or cylindrical vessels. Three separate regions have been bounded to account for scatter: (1) cylindrical vessels bursting into multiple fragments; (2) spherical vessels bursting into halves or multiple fragments and (3) cylindrical vessels bursting into two fragments. Estimates

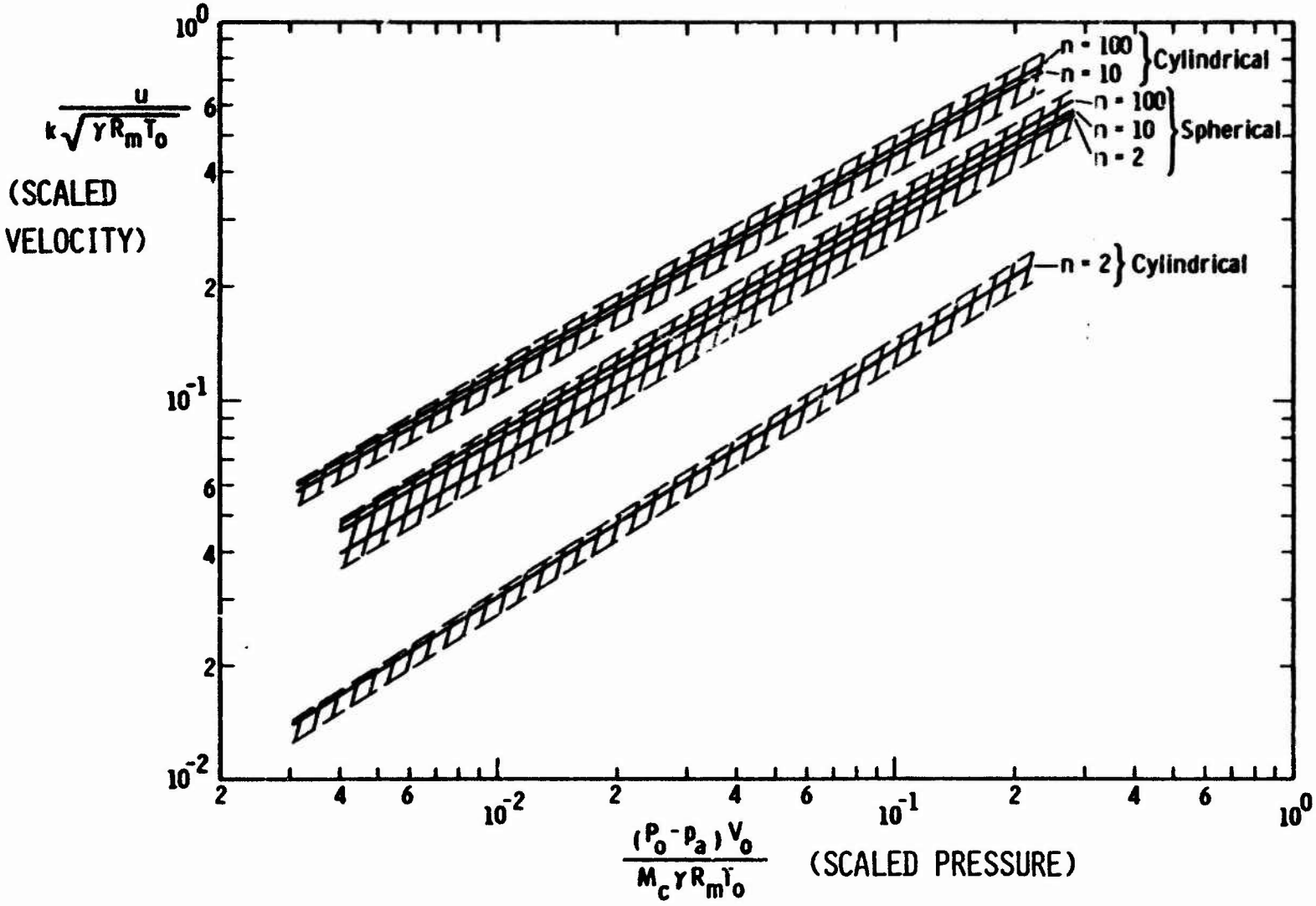

Figure 13. Initial Fragment Velocity vs. Scaled Pressure

of the initial velocities of cylinders and spheres can be extracted from the nondimensional terms read directly from the appropriate bounded regions on the graph. The two nondimensional terms in Figure 13 are:

(1) Nondimensional pressure term

$$= \frac{(P-p_a)V_o}{M_c \gamma R_m T_o} = \frac{(P-p_a)V_o}{M_c a^2_{gas}} = \frac{\text{(pressure - atm. pressure)(Volume)}}{\text{(Mass of container)(sound speed of the gas)}^2}$$

(2) Nondimensional velocity term

$$= \frac{u}{K\sqrt{\gamma R_m T_o}} = \frac{u}{K a_{gas}} = \frac{\text{(velocity)}}{\text{(constant)(sound speed of the gas)}}$$

where K equals 1.0 for equal fragments.

Our analysis and Figure 13 also apply to long cylinders breaking into two unequal parts, if difference in masses of the two parts is accounted for. Figure 14 includes the results of calculations for such failures, and is used as a simple adjustment factor to multiply predictions from Figure 13.

Efficient prediction curves for maximum ranges of free-flying fragments were developed for this workbook, using the computer code FRISB, which accounts for lift, drag and gravity forces during fragment flight. These scaled curves are given in Figure 15. Procedure for their use are:

Step 1. Calculate the lift/drag ratio = $\frac{C_L A_L}{C_D A_D}$ for the fragment.

Step 2. Calculate the velocity term = $\frac{\rho_o C_D A_D V^2}{Mg}$ for the fragment.

Step 3. Select the curve on the graph for the appropriate lift/drag ratio; locate the velocity term on the horizontal axis; find the corresponding range term, $\frac{\rho_o C_D A_D R}{M}$ and determine the range, R.

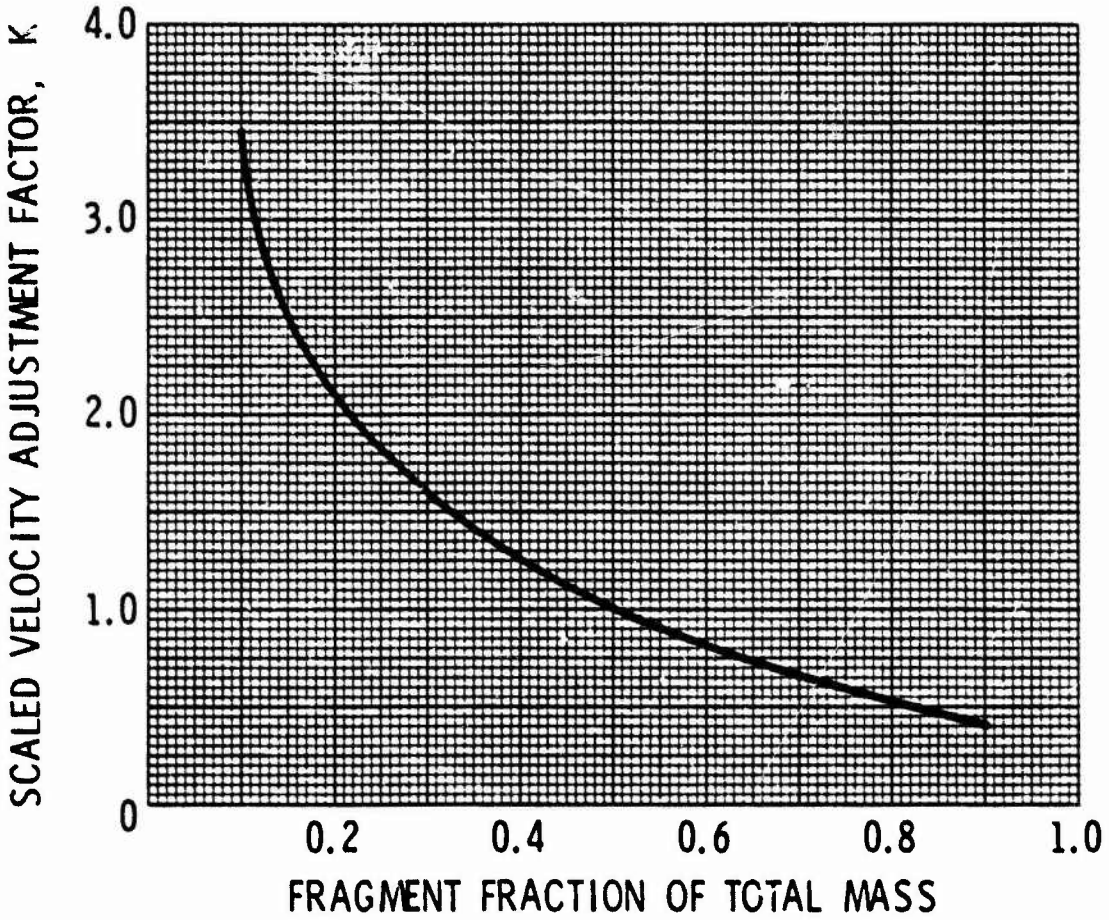

Figure 14. Adjustment Factor for Velocities for Unequal Mass Fragments

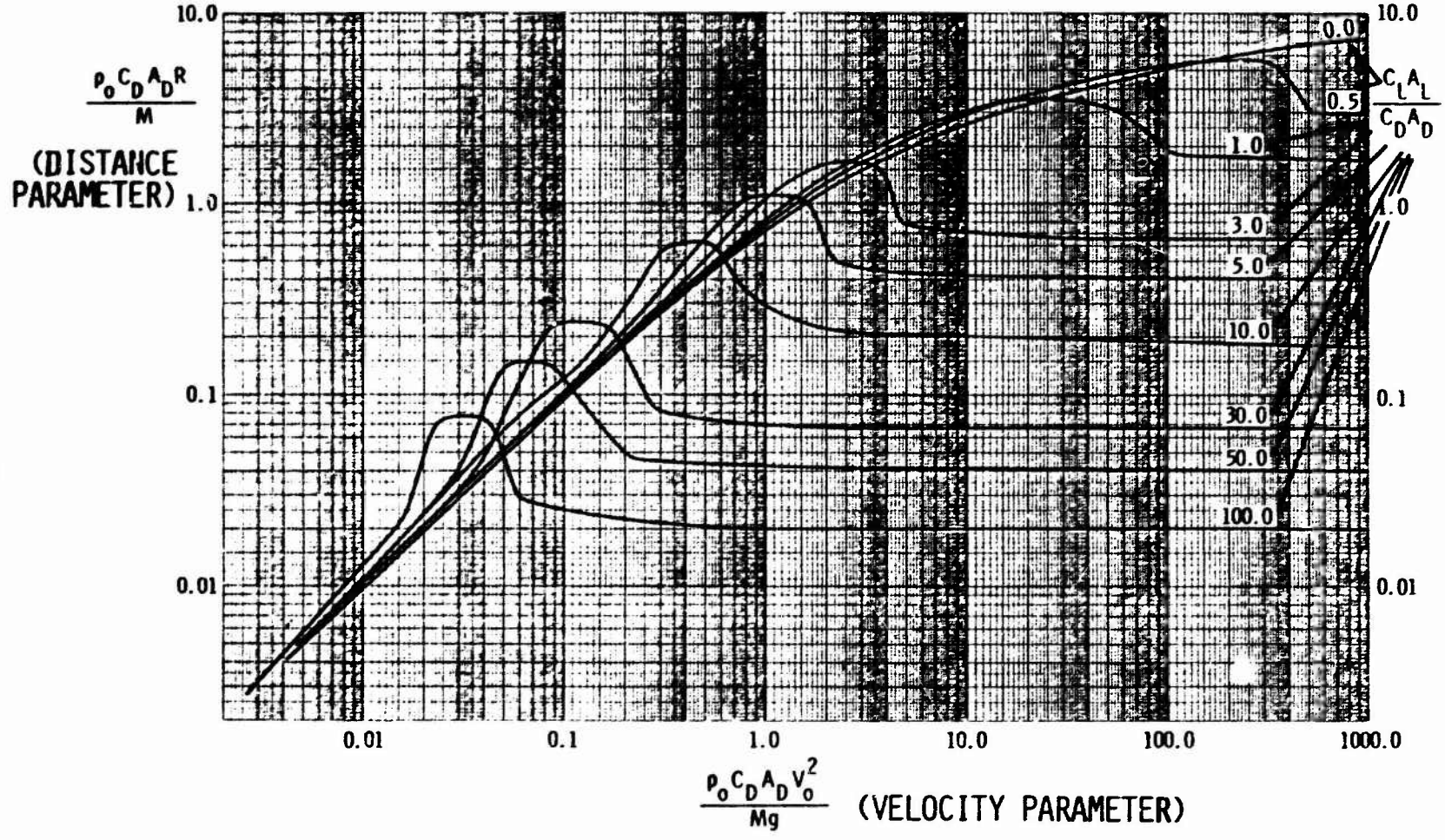

Figure 15. Scaled Curves for Fragment Range Prediction

For lift to drag ratios $\frac{C_L A_L}{C_D A_D}$ that are not on the curve, a linear interpolation procedure can be used to determine the range from the curve. Interpolation in the steep areas of the curve can cause considerable error and it is recommended that, for these cases, the computer code FRISB be exercised.

In an accident involving propellant (propane, butane, etc.) storage systems, large fragments (greater than one-fourth of the vessel) are sometimes generated which travel long distances. These large fragments are typically sections of the tank which break free intact and initially contain some entrapped propellant. These large fragments exhibit a rocketing behavior which results from the changing of all or part of the liquid propellant into a gas when the internal pressure is released during the fracturing of the vessel (flash evaporation). The gas escapes from the opening in the vessel in a manner similar to gas exiting a rocket motor and propels the somewhat stabilized fragment to great distances.

The physics of this process is complex, so consolidated prediction curves for trajectories of these rocketing fragments were not generated. But, we did develop a computer program entitled THRUST which can be used to calculate trajectories for rocketing fragments containing flash-evaporating fluids. This program is described in detail and listed in Baker, Kulesz, et al[4].

FRAGMENT IMPACT EFFECTS

In Chapter V of Baker, et al[1], some methods were given for prediction of effects of impact of typical fragments from accidental explosions involving flight-weight hardware. For the even more massive fragments typical of explosions in ground systems, the voluminous literature on terminal effects of military fragments and projectiles is of very little use. But, since the earlier workbook was prepared, some data and prediction methods have been developed related to impact effects of tornado-borne missiles. Generally, this class of missile lies within the range of masses and velocities for fragments from explosions in ground systems. Wooden poles and planks, pipes, pieces of steel reinforcing bar, and more massive bodies such as compact cars and entire storage tanks have been picked up and

hurled at damaging velocities by tornadoes. Much of this work is summarized in Peterson [16], and has its impetus in tornado-proof design requirements for nuclear plants.

Similarly, new nuclear plants must now be designed to be proof against other accidents including crash of aircraft on the containment structures, and external vapor-cloud explosions. Some preliminary design methods have evolved for massive, non-penetrating missile impacts to meet the aircraft crash design requirements. But, in spite of these recent additions to the literature, impact effects of quite massive, but crashable, missiles are not well enough known to be reduced to design graphs in this workbook.

In certain fixed ground installations having a high potential for accidental explosion, or limited real estate, barricades may be built in an attempt to attenuate blast waves and to reduce fragment hazards. The barricades may be earth beams, retaining walls backed by earth fill, or built-up walls of reinforced concrete, timber, or steel construction. Unless structures to be protected are located very close to the barricades, they are almost totally ineffective in attentuating blast waves. The waves simply diffract over the barricades and reform. Barricades are, however, quite effective in arresting fragments and may be worth constructing for that purpose alone. Some prediction graphs for blast attentuation for barricades of several forms located close to protected structures are given in the new workbook. No data or proven prediction methods exist for effects of barricades on non-ideal blast waves, so the predictions are limited to attentuations for condensed high explosives.

Some impact effects predictions on reinforced concrete and steel panels, based on scaled data from tornado-borne missile barrier testing, are given in the workbook. Sources for the basic data are discussed, and the curves generated, by Baker, Hokanson, et al[17], are given.

Figure 16 gives scabbing thresholds for steel pipes impacting normally on lightly reinforced concrete panels, with rebar percentages < 1%. In this figure, KE is impact kinetic energy, h is concrete panel thickness, d is pipe outside diameter, and t_w is pipe wall thickness. Length-to-diameter ratios (L/D) variable, but all are greater than 5:1. Each curve gives the scabbing threshold for a particular wall thickness ratio.

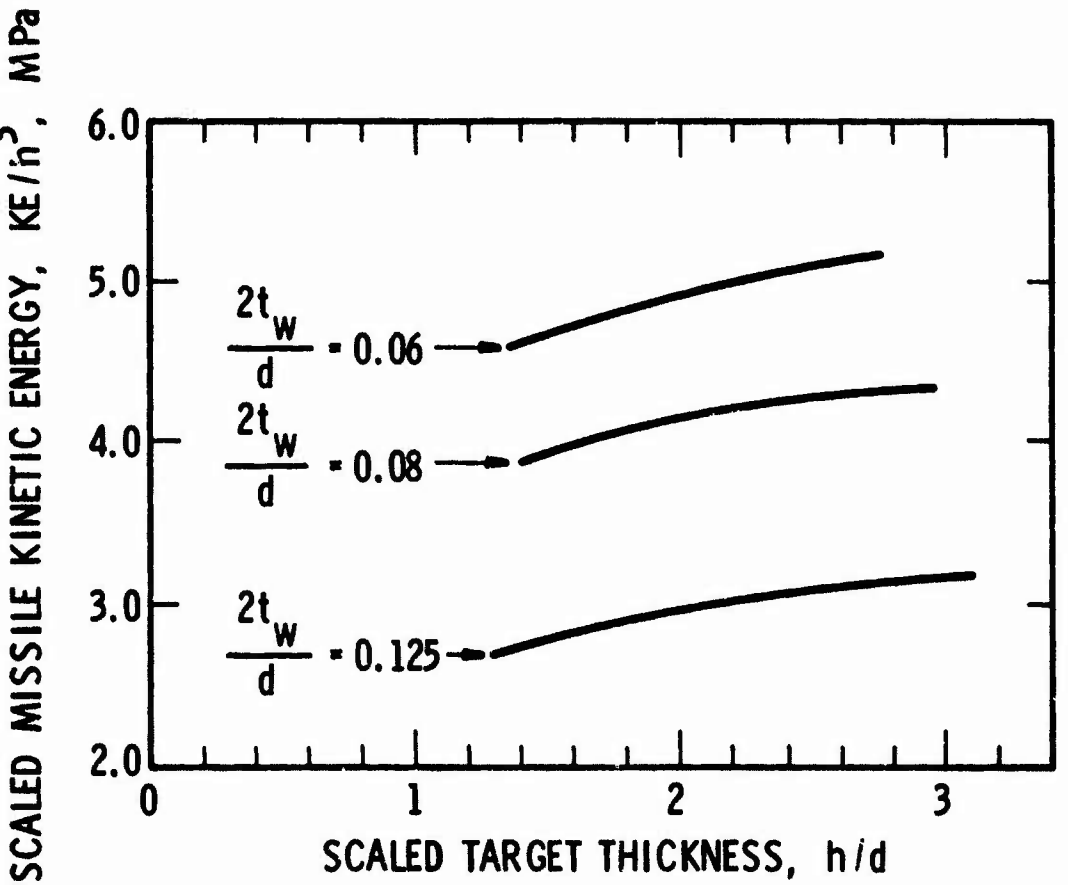

Figure 16. Scabbing Threshold for Mild Steel Pipes Impacting Reinforced Concrete Panels

Curves for scabbing caused by normal impact of solid rods, of material strong compared to the concrete, are given in Figure 17. The thresholds are quite different for slabs which are reinforced heavily enough for the rebar spacing to be significantly closer than the rod diameter (heavy reinforcing) and for spacing open enough that a rod can pass through without striking a rebar (light reinforcing). Rods were of ℓ/d ratios ranging from 1.75-40. A number of long wooden missiles were also fired against reinforced concrete panels, but these missiles were invariably defeated by the panels, with negligible damage to the panels themselves.

Baker, Hokanson et al[17] fit a penetration threshold curve for wooden missiles impacting large steel panels normally. This curve is reproduced here as Figure 18, and the empirically-fitted equation is given by

$$\frac{\rho_p V_s^2}{\sigma_t} = 1.751 \left(\frac{h}{d}\right)\left(\frac{\ell}{d}\right)^{-1} + 144.2 \left(\frac{h}{d}\right)^2 \left(\frac{\ell}{d}\right)^{-1}, \qquad (10)$$

Here, ρ_p is density of projectile material, V_s is striking velocity, and σ_t is yield strength of the steel plate material. Figure 18 applies for the test length-to-diameter ratio, $\ell/d = 31.1$. Equation (10) should also be limited to the ranges

$$5 \leq \ell/d \leq 40$$

$$0.042 \leq h/d \leq 0.1 \qquad (11)$$

IV. DISCUSSION

This workbook should be a definite aid to designers and safety engineers in predicting damage and hazards from accidental explosions in ground handling systems. It should prove to be a useful adjunct to our earlier workbook for predicting explosion hazards in flight systems, NASA CR-134906.

Parts of this work should have wider application than indicated by the title. The additional methods for rapid structural damage prediction

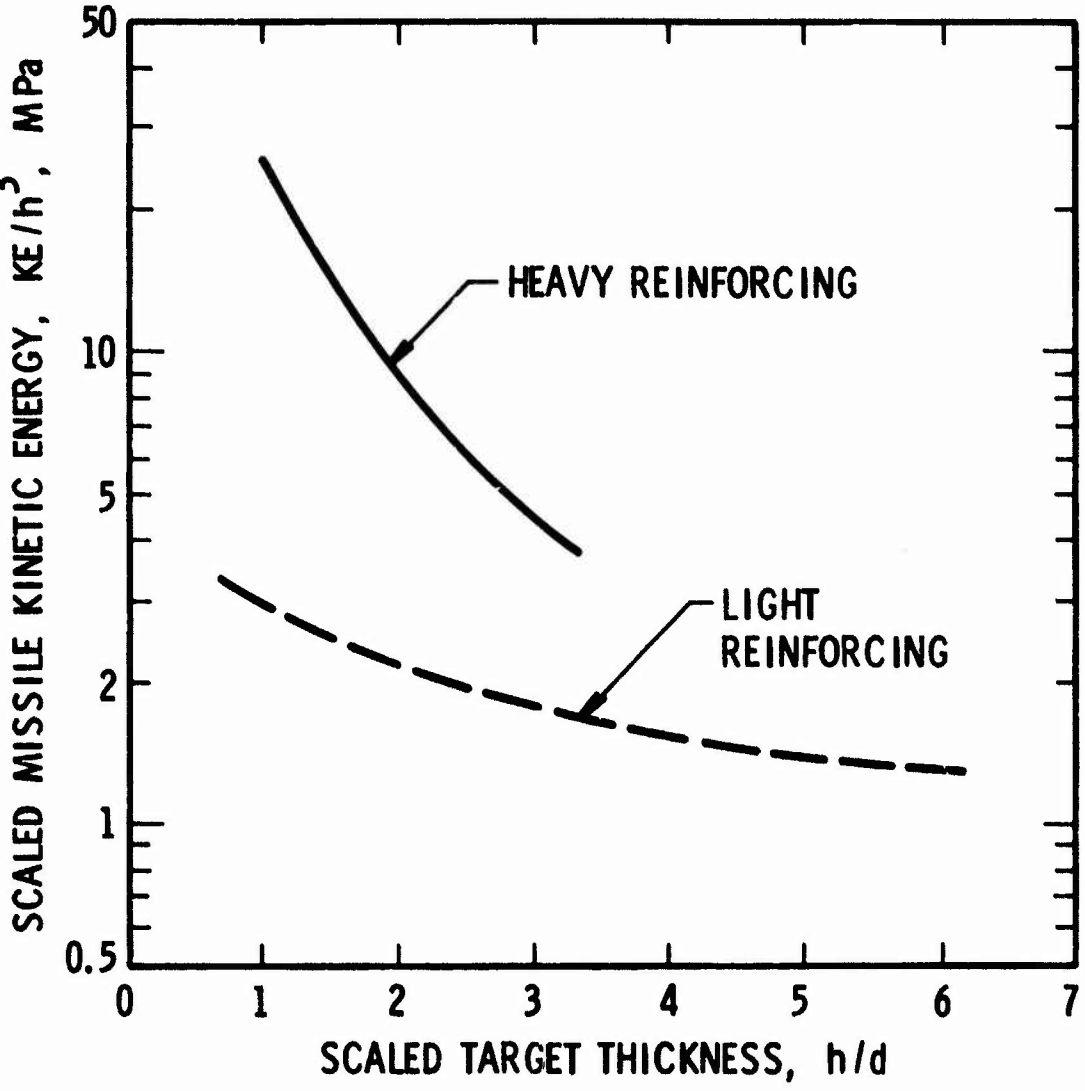

Figure 17. Scabbing Thresholds for Solid Rod Missiles Impacting Reinforced Concrete Panels

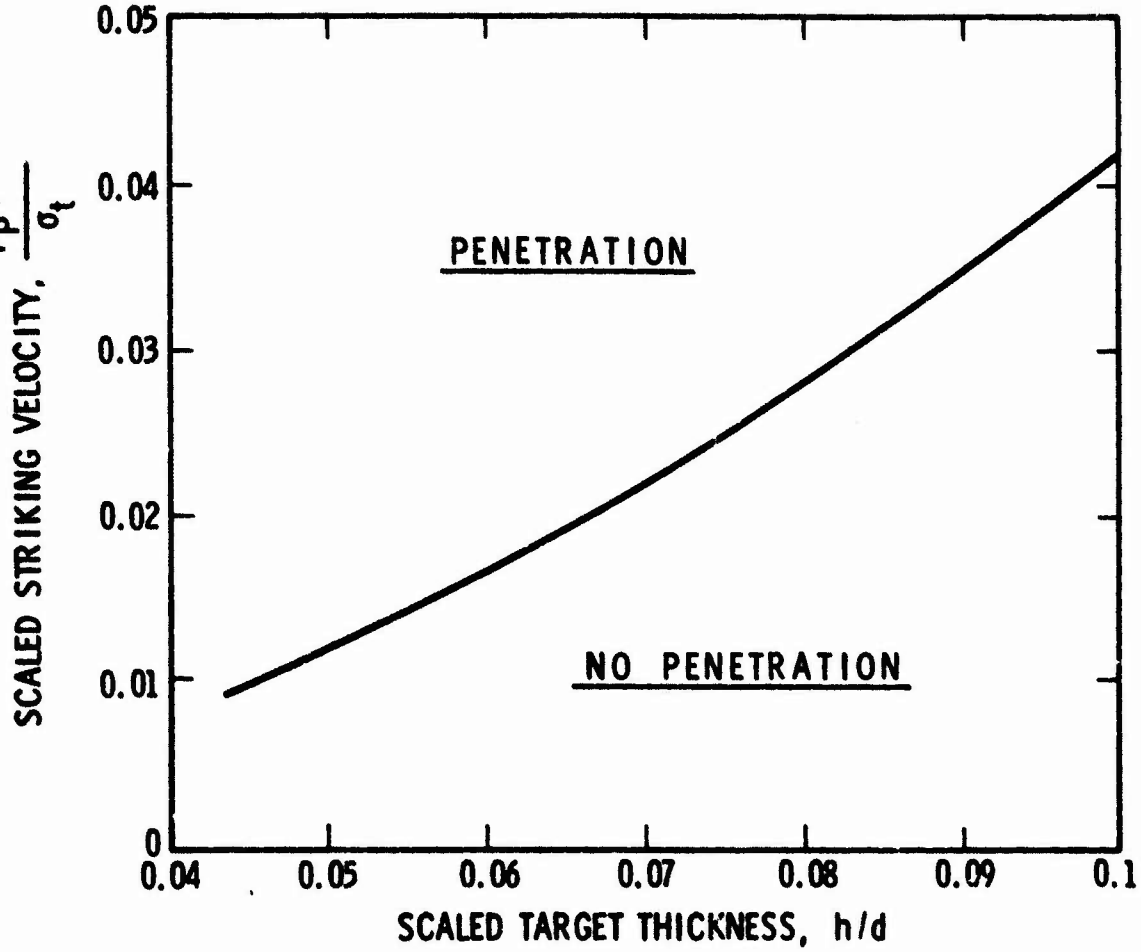

Figure 18. Prediction of Penetration Threshold for Steel Panels Impacted by Wooden Projectiles with $\ell/d = 31.1$

can be used for any blast source, provided the peak overpressures and positive impulses can be predicted. The computer programs and methods for prediction of velocities and trajectories of lifting fragments and thrusting burst vessels can be effectively applied to transportation accidents with tank cars and tank trucks containing many types of pressurized fluids, in addition to rocket propellants. The methods for estimating explosive energy release for flash-evaporating fluids can be used to predict severity of boiler explosions, or severity of blast for any type of liquid and gas mixture stored under high pressure. The data and prediction methods for effects of impact of massive fragments or missiles are not limited to fragments generated by accidental explosions in ground handling systems, and indeed were taken from other related studies.

A number of prediction curves are given in this work for the characteristics of blast waves from bursting gas pressure vessels, and some for bursting vapor spheres. These waves exhibit some characteristics which are distinctly different from blasts from condensed explosives such as TNT, including pronounced negative phases and pronounced second shocks. Most structural response or damage analyses account only for pressures and impulses in the first positive phase, and we therefore recommend further study of responses to waves with characteristics such as in Figure 3. It would also be very desirable to conduct more scaled experiments with bursting, pressurized vessels, to generate additional blast prediction curves.

Concurrent with the continuation of study of the character of blast waves from accidental explosions, one should also review, and alter if necessary, the prediction methods for structural response and damage in this workbook, in NASA CR-134906, and related references which assume that the wave can be described as a simple, single pulse. The basic analytic tools to do this are readily available, but application to as complex a loading pulse as Figure 3 will require careful application of these techniques, and almost invariably, some increase in complexity of response prediction.

Several related problems with potentially explosive ground storage and transport systems could perhaps be addressed in following

studies. One question concerns planning of in-service testing of pressure storage vessels to avoid or prevent accidental explosions. Many new and effective nondestructive testing methods and equipment have been developed in recent years, and applied in industries such as the nuclear power industry. For storage vessels of large volume and/or high pressure, where the hazards are great in the event of vessel failure, the frequency or thoroughness of such testing might be increased.

This workbook includes a number of prediction methods for fragment and missile impact conditions and locations near explosions, and some relatively new data and prediction curves for effects of impacts of relatively massive missiles. There is still a serious lack of data on massive missile impact effects. Scale model techniques have proven to be efficient in gathering enough data rapidly and relatively inexpensively to generate impact effects curves (see Figures 16 through 18), but most of the classes of missiles expected in accidental explosions have not been tested against industrial or residential "targets". We would certainly recommend a carefully planned model test program to fill this gap.

Looking into the future, we can perhaps anticipate an increasing shift to a hydrogen fuel economy. If this occurs, large volumes of hydrogen must be stored either as a compressed gas or as a cryogenic liquid, which would necessitate large volume storage near airports. Can this be done safely? A thorough safety study would have to precede any serious plans for such a change, with workbooks like this report providing part of the input to assess the hazards.

REFERENCES

1. Baker, W. E., Kulesz, J. J., Ricker, R. E., Bessey, R. L., Westine, P. S., Parr, V. B., and Oldham, G. A., (1975), "Workbook for Predicting Pressure Wave and Fragment Effects of Exploding Propellant Tanks and Gas Storage Vessels," NASA CR-134906, Contract NAS 3-19231, November 1975 (reprinted Sept. 1977).

2. Strehlow, R. A. and Baker, W. E., (1975), "The Characterization and Evaluation of Accidental Explosions," NASA CR-134779, Grant NSG 3008, June 1975.

3. Strehlow, R. A. and Baker, W. E., (1976), "The Characterization and Evaluation of Accidental Explosions," Progress in Energy and Combustion Science, 2, 1, pp. 27-60.

4. Baker, W. E., Kulesz, J. J., Ricker, R. E., Westine, P. S., Parr, V. B., Vargas, L. M. and Moseley, P. K. (1978), "Workbook for Estimating Effects of Accidental Explosions in Propellant Ground Handling and Transport Systems," NASA CR-3023, Contract No. NAS 3-20497.

5. Brode, H. L., (1959), "Blast Wave from a Spherical Charge," Physics of Fluids, 2, 217.

6. Baker, W. E., (1973), Explosions in Air, University of Texas Press, Austin, Texas.

7. Brinkley, S. R., (1969), "Determination of Explosive Yields," AIChE Loss Prevention, 3, 79-82.

8. Esparza, E. D. and Baker, W. E. (1977a), "Measurement of Blast Waves from Bursting Pressurized Frangible Spheres," NASA CR-2843, Grant NSG 3008, May 1977.

9. Boyer, W. D., Brode, H. L., Glass, I. I., and Hall, J. G. (1958), "Blast from a Pressurized Sphere," UTIA Report No. 48, Institute of Aerophysics, University of Toronto.

10. Pittman, J. F. (1972), "Blast and Fragment Hazards from Bursting High Pressure Tanks," NOL TR-12-102, U. S. Naval Ordnance Laboratory, Silver Spring, Maryland, May 1972.

11. Pittman, J. F. (1976), "Blast and Fragments from Superpressure Vessel Rupture," Report No. NWSC/WOL/TR 75-87. Naval Surface Weapons Center, White Oak, Silver Spring, Maryland, February 1976.

12. Keenan, J. H., Keyes, F. G., Hill, P. G., and Moore, J. G. (1969), Steam Tables, John Wiley & Sons, Inc., N.Y.

13. Din, F., Editor (1962), Thermodynamic Functions of Gases, Vol. 1, Ammonia, Carbon Monizide, and Carbon Dioxide, Vol. 2, Air, Acetylene, Ethylene, Propane and Argon, Butterworths, London.

14. Esparza, E. D. and Baker, W. E., (1977b), "Measurements of Blast Waves from Bursting Frangible Spheres Pressurized with Flash-Evaporating Vapor or Liquid," NASA CR-2811, National Aeronautics and Space Administration, Washington, D.C., November 1977.

15. Parr, V. B. and Moseley, P. K. (1978), "Statistical Analysis of Data from Accidental Explosions of Propellant Handling Systems," Minutes of the 18th Explosives Safety Seminar.

16. Peterson, R. E., Editor (1976), Proceedings of the Symposium on Tornadoes. Assessment of Knowledge and Implications for Man, Texas Tech. University, Lubbock, June 22-24, 1976.

17. Baker, W. E., Hokanson, J. C., and Cervantes, R. A., (1976), "Model Tests of Industrial Missiles," Final Report, SwRI Project No. 02-9153-001, Southwest Research Institute, San Antonio, Texas, May 1976.

18. ASHRAE Handbook of Fundamentals, (1972), Am. Soc. of Heating, Refrigerating and Air Conditioning Engineers, Inc., N.Y.

SPECIAL CONSIDERATIONS FOR SPACE TRANSPORTATION SYSTEMS PROCESSING AT KENNEDY SPACE CENTER

Mr. John R. Atkins
John F. Kennedy Space Center, Florida

INTRODUCTION

The impact of the Shuttle Program and the resultant effects on the how of doing business at Kennedy Space Center could never have been anticipated in 1970 when it was decided to use the VAB for stacking the solid rocket motors, the external tank and Orbiter. Although ordnance operations had been performed in the VAB during the Apollo Program, it was done under a severe limitation of numbers of people present during the operations. This was accomplished by limiting the performance of these operations to the period from 1800 Friday to 0600 Monday, and allowing only those persons actually required for the activities to be physically present in the VAB. Essentially, 25 solid propellant motors used for ullage, stage separation and escape system with a total weight of 4320# were attached to the various stages and to the command module. All initiators and electrical connections were installed and made after roll out to the pad and on T-1 day during the launch countdown preparation activities.

Imagine, if you will, the feelings and concerns when

directed to plan and develop policies for handling, per flight, 2 solid rocket motors 145 ft. in length, over 11 ft. in diameter and containing over 1 million pounds propellant, and at a launch rate of 40/year. (At that time the highest rate for Apollo was 3/year.) Taking into account the proposed launch rate, problems associated with launch and delivery rates of the solids, it was deemed a distinct possibility that under certain conditions as many as 4 full flight sets of solid rocket motors could be in the VAB. Studies also showed that in the late stages of the operational development testing of Orbiter 102 solids would be in the VAB almost 100% of the time and would always be present in the operational phases.

Accepting the conclusion that in time solids would always be in the VAB in various phases led to the following:

1. The VAB could not be utilized as general office, warehouse, testing labs, and assembly as was the case during Apollo.

2. Only ordnance operations and those activities necessary to assemble and test the space transportation system would be allowed in the VAB.

3. Manhours of exposure would be kept to a minimum consistent with operational requirements.

4. Maximum use would be made of the Explosives Safety Board in obtaining comments and suggestions on the proposed processing plans.

PROBLEM DEFINITION

During the preliminary studies of where to process the solid rocket motor segments prior to stacking in the VAB, the degree of risk to personnel, to facilities, and to program was always paramount. To quantify this total risk in a manner suitable for management decision, an approach evolved that made use of industry experience, Apollo VAB Study, [1/] various computer programs for effects of solid motor ignition, special studies to establish inadvertent initiation energy levels and Apollo problem tracking and closeout techniques. The first step was a study performed by Thiokol [2/] to do the following:

1. Propellant Characterization

Determine the response of the propellant to stimuli in order to relate it to in-process conditions, which are measurable and/or calculable. Response to measured energy stimuli will be determined in the Thiokol laboratories. Stimuli of interest are impact energy, frictional energy, heat energy and electrostatic energy. Knowing the response (probability of ignition) as a function of input energy, hazardous, non-hazardous or potentially hazardous classifications can be applied to various operations and/or items.

1/ Study of Kennedy Space Center Safety Hazards
TRW NAS10-3082, dated 22 September 1966

2/ Hazard Analysis of Solid Rocket Motor Assembly Operations
for Kennedy Space Center Vehicle Assembly Building
Thiokol NAS8-30490, dated 3 June 1977

2. Consequences of Ignition

The SRM propellant will be subject to other laboratory characterization tests designed to provide better insight into the consequences of ignition and means for minimizing damages. Surface propagation rate will be measured. This will give an indication of the gas evolution rate immediately after ignition. The effectiveness of water or other spray or fog on burning propellant surfaces will be evaluated. Thermal radiant flux levels vs. time-to-ignition will be determined experimentally, in order to judge segment-to-segment propagation behavior. Exhaust product composition, burning time, plume shape and temperature profiles for the several in-process or stacked configurations will be calculated. Estimates of ignition transient time and net propulsive force will also be calculated. This phase will be a subjective analysis, deducing precautions, procedures, and overall planning recommendations that will minimize injury and damage.

3. Operations Review

It is intended that Thiokol will conduct a thorough survey of the VAB, regarding SRM operations. It will be necessary to consult at length and in detail with NASA process planning personnel. Details of facilities, process flow, time lines, procedures, equipment and tooling design, design criteria, maintenance requirements, special tooling, GSE and component and subassembly configuration and characteristics will be provided by NASA to the degree necessary to assess potential hazards. It is proposed that cognizant NASA process, safety and facility personnel be assigned to

work with Thiokol's analyst in order to expedite the exchange of information. Other than overall operations, the following type of information will be included:

a. 250-ton Crane. What is design ultimate capacity? What is design yield capacity? What was initial load test? What is subsequent test load and frequency program? How, and how frequently, are cables inspected? How, and how frequently, are rails, cable blocks, drum bearings, etc., inspected and overhauled? What pre-operational checkout is employed each day or use?

b. Separation Motors. What handling and attachment method and equipment are planned? What configuration when attached? What are propellant characteristics? What preassembly will be done? What operations are performed after attachment? What is ignition system? How is it operated?

4. Identification for Ignition

Detailed steps and all associated hazards from segment operations, handling, component failures and human errors will be identified, and the magnitude of the potential stimulus calculated, measured or estimated. Potential for extraneous or peripheral hazards, such as electrical shorts, dropped objects, vapor generation and ignition and others will also be identified.

5. Mechanisms Producing Stimuli

Once the stimuli for initiation of a hazardous event is identified, the next step for resolving the hazard problem shall be to identify the mechanisms for producing the stimuli. Both direct and indirect

mechanisms shall be identified. Using the data generated above, probability of ignition will be determined. Also, the probability of the identified hazardous event occurring where propellant exists and ignite will be determined. Joint-to-joint impact or friction is not in itself hazardous if no propellant is in proximity to ignite, but failure of a crane cable during a segment lift will always expose propellant to a hazardous fall.

The overall probability for each hazard will then be computed simply as:

$P = P_e P_c P_i$ where

- P = Overall probability of ignition
- P_e = Probability of the hazardous event occurring
- P_c = Probability that propellant is exposed to the hazardous stimulus
- P_i = Probability that the stimulus magnitude will ignite the propellant

Summing these results for all hazardous events will give the estimated probability of incident.

6. Recommendations for Hazard Prevention

The recommendations and the analysis are actually an iterative procedure. When a particular hazard analysis deduces an overall probability of ignition considered unacceptable, it is not left there. Consideration is then given to methods, design changes or sequence changes that will reduce one of the component probabilities, thus reducing the overall probability. These then become the recommendations tendered for improving the process safety to an acceptable level.

7. Protective Measures

This final phase faces up the fact that to conduct the program, probability of ignition cannot be reduced to zero and we must look at what might happen if a hazard developed. Much of the data obtained above is applicable to analyzing this phase. Conflagration times, gas generation rates, plume shape, growth rate, quenching criteria, all enter into this evaluation. The goal would be to provide a system which would be cost effective and provide some means of minimizing damage if an event occurred.

REVIEW AND STATUS

The second step after completion of the study was to establish a system that maintained status on each study recommendation. A work sheet was designed which designated the individual and his organizational element responsible for working the recommendation. In addition, a KSC number was assigned that cross referenced to the study, statement of recommendation and status/comment. The work sheet was titled, "Solid Rocket Motor Hazard Analysis Report Sheet" and representative copies are included in the appendix.

STUDY RESULTS AND ACTIONS TAKEN

Inadvertent initiation of the propellant can occur as a result of friction, impact, heating or electrostatic discharge. Test results established safe energy levels as follows:

Friction	2,300 psi
Impact	2.7 ft. lb/in^2
Heating	4.98 BTU/ft^2
	$27^{\circ}F$/min to 520° radiant conduction
Electrostatic	1.3 Joules

The effects of inadvertent initiation of a single segment or combination of segments in any region of interest during specified time periods can be predicted. The effects of interest are overpressure, temperature, sound level and exhaust products. From the study it can be shown that once a segment is ignited it will burn completely in approximately 12 minutes. If a burning center segment is in an upright position and exhausting from the top a temperature of 1,024^{o}F would be expected at 180 ft. above the segment and 25 ft. radially distant.

The high bay area and surroundings would very rapidly be filled with smoke which would contain toxic constituents in concentrations that would be harmful to humans. It must be said in all candor that at KSC there is no question that a solid can be inadvertently ignited, however, we feel that the probability of such an occurrence is sufficiently low as to warrant accepting the risk.

Accordingly, our approach has been two-fold:

First - Do those things that preclude or minimize ignition;

Second - Do those things that given ignition prevent harm to humans and minimize effects on equipment and facilities.

There were 168 distinct recommendations that were identified by the study covering design, operating practices, procedures, housekeeping and training. Excluding the 40 recommendations dealing with design, over 50% of the recommendations were practices or policies in effect at KSC and had been identified in

various documents. Much of the remaining recommendations while common practice were not in our procedure or policy documents. These types of recommendations once included in a procedure or policy directive were marked closed. As mentioned previously precluding or minimizing inadvertent ignition was, and is, paramount in obtaining an acceptable safety risk factor. Many of the recommendations deal with this and typical examples are:

1) Certification of all segment handling equipment such as the cranes and handling slings. These equipments have been the subject of detailed hazard analysis, intensive periodic inspections and annually selective non-destructive tests.
2) Ensuring the resistance between vehicle and workstands, workstands and cranes, and workstands to facility ground is no greater than 1 ohm. One of the requirements prior to starting operations involving segments is verification of grounds by taking measurements at selected locations and providing the results of these tests to the Safety Office. (Typically the ohmic values do not exceed 0.1.)
3) Precluding objects striking exposed grain by use of covers on the segments, implementation of a tethered tool policy and installation of caging and toe boards in areas above and around the segments.

Protection of personnel and minimizing exposure is accomplished by:

1) Each first time operation such as off loading segments from the rail car, placement in workstands or placement on the mobile launcher platform will be done on a weekend with only minimum operational personnel present.

2) Egress routes have been established that allow evacuation time from work station to the egress route in less than thirty seconds and longest time to evacuate the building once in the egress route is 6 minutes.

3) A housing plan was developed that restricted not only the numbers of people allowed in the VAB but in addition limited the areas that could be occupied. With the exception of the external tank workstands and the integrating cells where the total vehicle is stacked, occupancy has been limited to the first five floors.

CONCLUSION

In summary, we feel that the many in-house reviews, discussions with industry, and the consultations with the DOD Explosives Safety Board have resulted in a system of management review and ensures proper consideration of safety requirements for all facets of activity in the VAB, both for now in the planning stages, and also allows for redirection as we gain operational experience.

SOLID ROCKET MOTOR HAZARDS ANALYSIS REPORT SHEET

NAME	ORGANIZATION	DATE
Scofield/Hornyek	SF-PRA-1	7-5-77

SF NUMBER	CONTRACTOR NUMBER	RECOMMENDATION
34 (same as item 133)	15 2.5 Ignition prevention recommendations	Dye penetrent inspect criticel welds, pins, clevises, etc., after proof test. ACTION CLOSED

STATUS/COMMENTS

KSC-STD-SF-0001C requires testing of these items prior to use. Maximum segment weight to be lifted is 320,000 lbs. The crane is rated at 500,000 lbs., and will have a current load test of 558,000 lbs., per Mr. Ray Phillips, SO-ENG, per phone conversation June 23, 1977. Contected Carloe Springfield, SO-LAB, June 29, 1977, and he indicated that dye penetrant inspection would not be as effective, in this case, as electromagnetic particle testing, on hooks or attachments manufactured from SAE 4140 heat treated steel. Dye penetrent used on painted surfaces also does not furnish satisfactory results. Mr. Springfield further suggested that, whichever tests were used, it be done prior to the load test as well as immediately following it, as this would provide a realistic "map" to facilitate fracture growth measurements, as well as an indication of previously existing surface flaws.

To TS for evaluation and further recommendations.

In memo of 8/2/77 TS stated that they annually proof-load test the cranes and magneflux the hooks; they believe this is sufficient. TS is not responsible for pins, clevises, and other component parts of lifting equipment/assemblies.

Further SF comment: As stated above, TS annually tests and inspects cranes, and hooks. KSC-STD-S-0001C requires operating organizations to proof-load test, annually, all slings, pins, clevises, and associated hardware as a complete assembly. The lifting hardware is tethered so that parts cannot be removed and replaced. The Standard requires tha lifting assembly be inspected periodically for wear, damage, and corrosion, however, it does not require dye penetrent inspection. Additionally, OMIs will require inspection verification of valid proof-load tests prior to equipment use. Apollo Program experience indicates this is sufficient. Based on this rationale, this recommendation is closed.

KSC FORM 07-1000 10/77 (ONETIME FORM - REPRINT NOT AUTHORIZED)

SOLID ROCKET MOTOR HAZARDS ANALYSIS REPORT SHEET

NAME	ORGANIZATION	DATE
Scofield/Hornyak	SF-PRA	7-12-77

SF NUMBER	CONTRACTOR NUMBER	RECOMMENDATION
31	12 2.5.1 Ignition Prevention (High Bays 2 and 4)	Procedures should require that both Thiokol and KSC inspectors verify the absence of all external propellant contamination before and after shipment, respectively. ACTION CLOSED

STATUS/COMMENTS

Transferred from SF-SOO SRM Report Sheet.

Ref. SF No. 64. A data package with certification of cleanliness will accompany shipped segments. KSC inspection not available at Thiokol plant.

KSC will be responsible for verifying certification is received and additional inspections performed as required during receiving inspection.

TO VO for appropriate action.

SVO agrees and the results will be put in the OMI's by USBI; however, KSC will verify only after shipment.

SF-SOO-1 to track and identify the procedure.

KSC FORM 07-1060 (6/77) (ONETIME FORM - REPRINT NOT AUTHORIZED)

SOLID ROCKET MOTOR HAZARDS ANALYSIS REPORT SHEET

NAME	ORGANIZATION	DATE
J. R. Reynolds	SF-SEC-3	August 8, 1977

SF NUMBER	CONTRACTOR NUMBER	RECOMMENDATION
14.	2.4.2 3	Provide each segment and partial or finished stack with external water spray coverage at a density of 0.25 gpm/sq. ft. or more on top and sides.

STATUS/COMMENTS

Water spray of each segment:

If segments can be stored x feet apart (x - minimum distance that propagation will not occur from segment-to-segment),then segment water spray is not necessary. Thiokol should provide the distance x (not mentioned in report TWR-11389), then KSC SP office should assess if the distance is acceptable to storage requirements.

If the distance is not acceptable to SP, then individual segment water spray protection is required. Water spray system can be arranged to be turned on manually by request of 1P10 communicator, after actuation of the fire alarm system. (Page 7-25 of TWR-11389 indicates there is 1 to 2 minutes to get the system on to prevent propagation of segments 17.17 feet apart center-to-center).

Water Spray of partial or finished stock:

Each stacking high bay (1 and 3) platform half has a manually operated deluge system (operated on site only) that protects the platform area. The platform deluge systems do not spray the segment stack.

KSC FORM 07-1969 (9/77) (ONE TIME FORM - REPRINT NOT AUTHORIZED)

RADFORD ARMY AMMUNITION PLANT

NITROGLYCERIN EXPLOSION

6 JANUARY 1978

PRESENTED TO

EXPLOSIVES SAFETY SEMINAR

LTC THURMAN WATTS

1003

PRECEDING PAGE BLANK

HUGHES INCORPORATED
OPERATING CONTRACTOR

PART I

GOOD AFTERNOON LADIES AND GENTLEMEN:

I AM LTC WATTS, THE COMMANDING OFFICER OF RADFORD ARMY AMMUNITION PLANT. MY DISCUSSION TITLED "MAJOR EXPLOSION IN CONTINUOUS NITROGLYCERIN MANUFACTURING FACILITY" RELATES TO INCIDENT WHICH OCCURED AT RAAP. I WILL INITIATE THE DISCUSSION WITH A DESCRIPTION OF WHAT HAPPENED AND SOME OF THE PROBLEMS FACED AND SOLVED BY THE COMMANDING OFFICER AND THE PLANT MANAGER. I WILL BE FOLLOWED BY MR. SKOGMAN WHO WILL DISCUSS THE IMPLICATIONS OF THE EXPLOSION AND ITS EFFECTS ON SAFETY STANDARDS.

FIRST AN EXPLANATION OF A GOCO PLANT. THE GOVERNMENT OWNS ALL OF THE FACILITIES BUT CONTRACTS THE OPERATION OF THE MANUFACTURING TO A COMMERCIAL CONTRACTOR. IN RAAP'S CASE HERCULES INCORPORATED.

AT 0605 HRS ON THE MORNING OF 6 JAN 1978, ONE DAY AFTER ACHIEVING A LEVEL OF 4.1 MILLION MANHOURS WITHOUT A LOST TIME INJURY, RADFORD ARMY AMMUNITION PLANT WAS ROCKED BY THE EXPLOSION OF 5,000 LBS OF NITROGLYCERIN. REPERCUSSIONS AND ECHOS WERE HEARD FOR MILES THROUGHOUT THE AGRICULTURAL AND INDUSTRIAL COMMUNITIES SURROUNDING THE PLANT. REPERCUSSIONS WILL ALSO BE FELT FOR YEARS TO COME WITHIN THE AMMUNITION COMMUNITY. IT IS THE CHAIN OF EVENTS SET INTO MOTION BY THAT EXPLOSION THAT I'M GOING TO DISCUSS TODAY.

DISCUSSION WILL CONSIST OF THREE BASIC PARTS, ORIENTATION ON RAAP, SIGNIFICANT PROBLEMS FACED AND SOLVED AND CURRENT OPERATING SITUATION.

THIS CHART SHOWS AN AERIAL VIEW OF PART OF THE MANUFACTURING AREA.



PORTION OF RADFORD UNIT

AERIAL VIEW LOOKING WEST

THIS SLIDE SHOWS THE PLANT'S LOCATION IN SW VIRGINIA - 41 MILES FROM ROANOKE, 4.5 HOURS WEST OF FT LEE AND RICHMOND, 6.5 HOURS SOUTH/SW OF WASHINGTON, DC ON ROUTE 81. THE PLANT CONSISTS OF TWO UNITS APPROXIMATELY 9 MILES APART. THE NEW RIVER UNIT, USED PRIMARILY FOR STORAGE AND THE RADFORD UNIT WHERE THE PROPELLANT IS MANUFACTURED. THE PLANT LIES PRINCIPALLY IN A VALLEY ALONG THE NEW RIVER WITH 3 CITIES IN THE IMMEDIATE VICINITY, RADFORD, BLACKSBURG AND CHRISTIANSBURG.

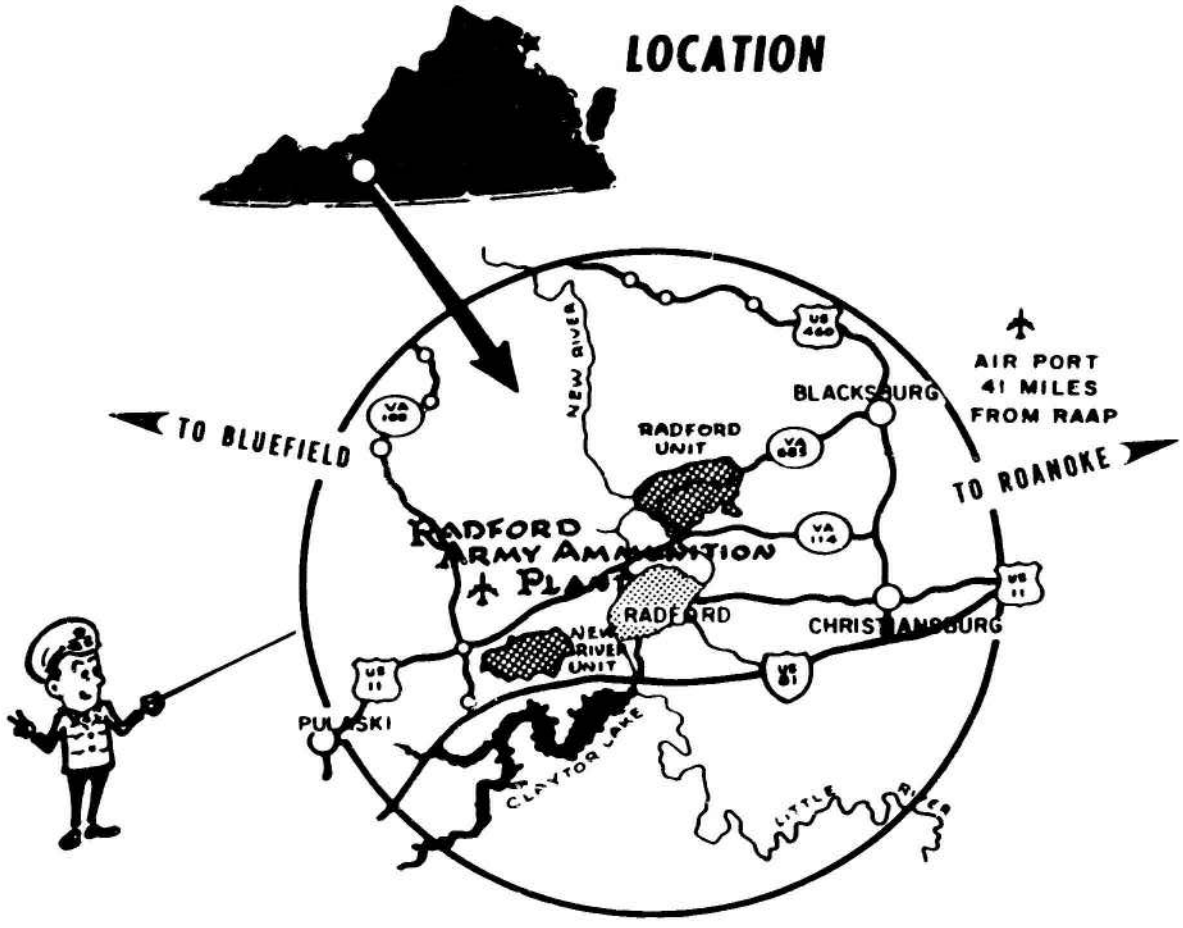
LOCATION
TO BLUEFIELD
TO ROANOKE
AIR PORT
41 MILES
FROM RAAP
NEW RIVER
BLACKSBURG
RADFORD
UNIT
RADFORD
ARMY AMMUNITION
PLANT
RADFORD
CHRISTIANSBURG
NEW
RIVER
UNIT
PULASKI
CLAYTOR LAKE
LITTLE
RIVER
US
460
VA
114
US
11
US
81

THE MANUFACTURE OF PROPELLANTS AND EXPLOSIVES IS AN ENERGY INTENSIVE PROCESS REQUIRING CONSIDERABLE UTILITIES CAPACITY. THE UTILITIES CAPABILITY IS LOCATED ON THE RADFORD UNIT OF APPROXIMATELY 4,100 ACRES.

RADFORD ARMY AMMUNITION PLANT

AREAS AND FACILITIES

		ROAD HARD SURFACE	RAILROAD STD. GAUGE	SECURITY FENCE
RADFORD UNIT	4,100 ACRES	126 MILES	26 MILES	21 MILES
NEW RIVER UNIT	2,895 ACRES	30 MILES	7 MILES	9 MILES
	6,995 ACRES			

BUILDINGS	1,240
SQUARE FEET UNDER ROOF	3,400,000 +

1011

UTILITIES CAPABILITITY

ELECTRICITY FOR A CITY OF 50,000 POPULATION	ELECTRICITY	580,000 K. W. H./DAY
WATER FOR ABOUT ½ THE CITY OF WASHINGTON, D.C.	FILTERED WATER	40 MILLION GALLONS/DAY
	RAW WATER	40 MILLION GALLONS/DAY
	DRINKING WATER	3 MILLION GALLONS/DAY
STEAM TO HEAT 10,000 HOMES	STEAM	23.5 MILLION POUNDS/DAY

THE RADFORD UNIT IS SPLIT BY THE NEW RIVER FLOWING EAST AND WEST AS IT FORMS WHAT IS CALLED THE HORSESHOE AREA CONNECTED TO THE MAIN PLANT BY A BRIDGE WHICH BELONGS TO THE ARMY.

THE MANUFACTURING PROCESS FLOWS TOWARD THE RIVER, PHYSICALLY DOWN HILL FROM THE ADMIN AREA THROUGH THE FINISHING AREA. NOTE THE LOCATIONS OF NITROGLYCERIN AREAS #1 AND 2.

RADFORD ARMY AMMUNITION PLANT

RADFORD UNIT

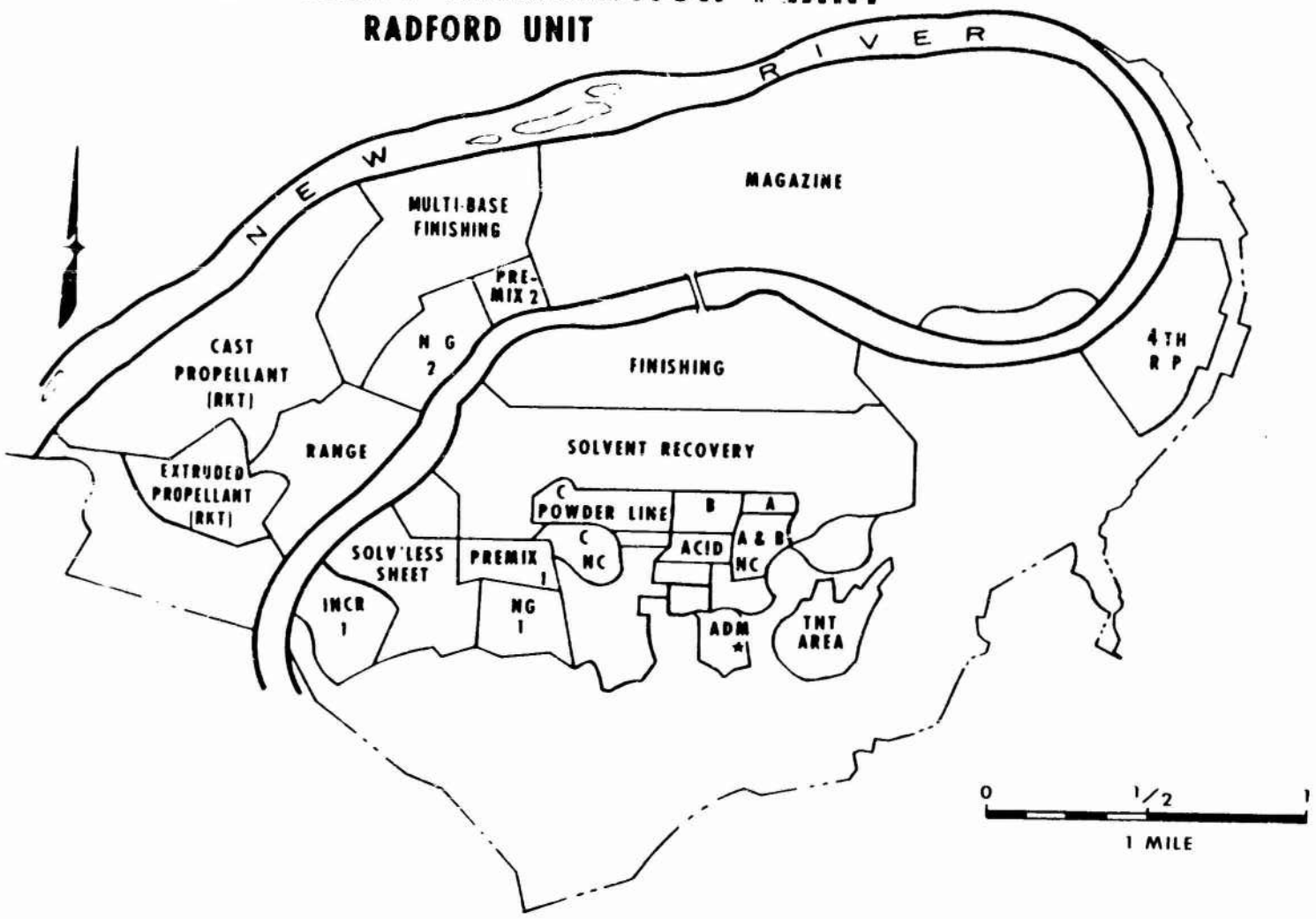

ON THIS SLIDE, THE TOP LINE IS THE BOTTOM LINE. WE MANUFACTURE PROPELLANT AND EXPLOSIVES WHICH IS PRIMARILY A CHEMICAL PROCESS. WE DO HAVE A 300 MILLION DOLLAR MODERNIZATION PROGRAM UNDERWAY AND A 90 MILLION DOLLAR POLLUTION ABATEMENT PROGRAM. THE POLLUTION ABATEMENT PROGRAM IS AT THE MOMENT RECEIVING MAXIMUM ATTENTION AS THE STATE OF VIRGINIA IS THREATENING SUIT AND ASSESSMENT OF PENALTIES WHICH COULD REACH 10,000 DOLLARS/DAY FOR EACH SOURCE FOR 27 MONTHS, TOTALLING MILLIONS OF DOLLARS.

RADFORD ARMY AMMUNITION PLANT

MISSION (ARMCOM REG 10-9)

- MANUFACTURE PROPELLANTS, EXPLOSIVES AND CHEMICAL MATERIALS AS ASSIGNED
- PROCURE AND MANAGE NECESSARY SUPPLIES, EQUIPMENT, AND ESSENTIAL MATERIALS
- OPERATE AND MAINTAIN ACTIVE FACILITIES
- PERFORM PRODUCT ASSURANCE FUNCTIONS IN SUPPORT OF PROCUREMENT AND PRODUCTION
- PERFORM PRODUCTION AND PROCESS ENGINEERING TASKS AS DIRECTED
- LAYAWAY AND MAINTAIN STANDBY FACILITIES
- RECEIVE AND MANAGE INDUSTRIAL AND FIELD SERVICE STOCKS AS DIRECTED
- PARTICIPATE IN INDUSTRIAL READINESS AND MOBILIZATION PLANNING
- PROVIDE SUPPORT SERVICE FOR TENANTS

THIS BUSY SLIDE IS THE CRUX OF THIS PORTION OF MY BRIEFING. IT IS DESIGNED TO REFLECT THE INTER-RELATIONSHIPS OF THE VARIOUS MATERIALS USED TO YIELD THE PROPELLANT PRODUCTS.

WE PROCURE THE MATERIALS ON THE LEFT. WE MANUFACTURE NITRIC AND SULFURIC ACID AND UPON COMBINATION OF THESE ACIDS WITH THE OTHER MATERIALS PURCHASED WE DERIVE NC, NG AND TNT. SINGLE BASE, DOUBLE AND TRIPLE BASE PROPELLANTS ARE REFLECTED HERE.

NOTEWORTHY AT THIS JUNCTURE IS THAT BETWEEN 50 AND 60% OF RAAPs PRODUCTION REQUIRES NG. AND DON'T FORGET THIS WHOLE PROCESS INVOLVES OVER 2,600 PEOPLE.

BASE MATERIALS FLOW DIAGRAM
FOR PROPELLANTS* MANUFACTURED AT RAAP

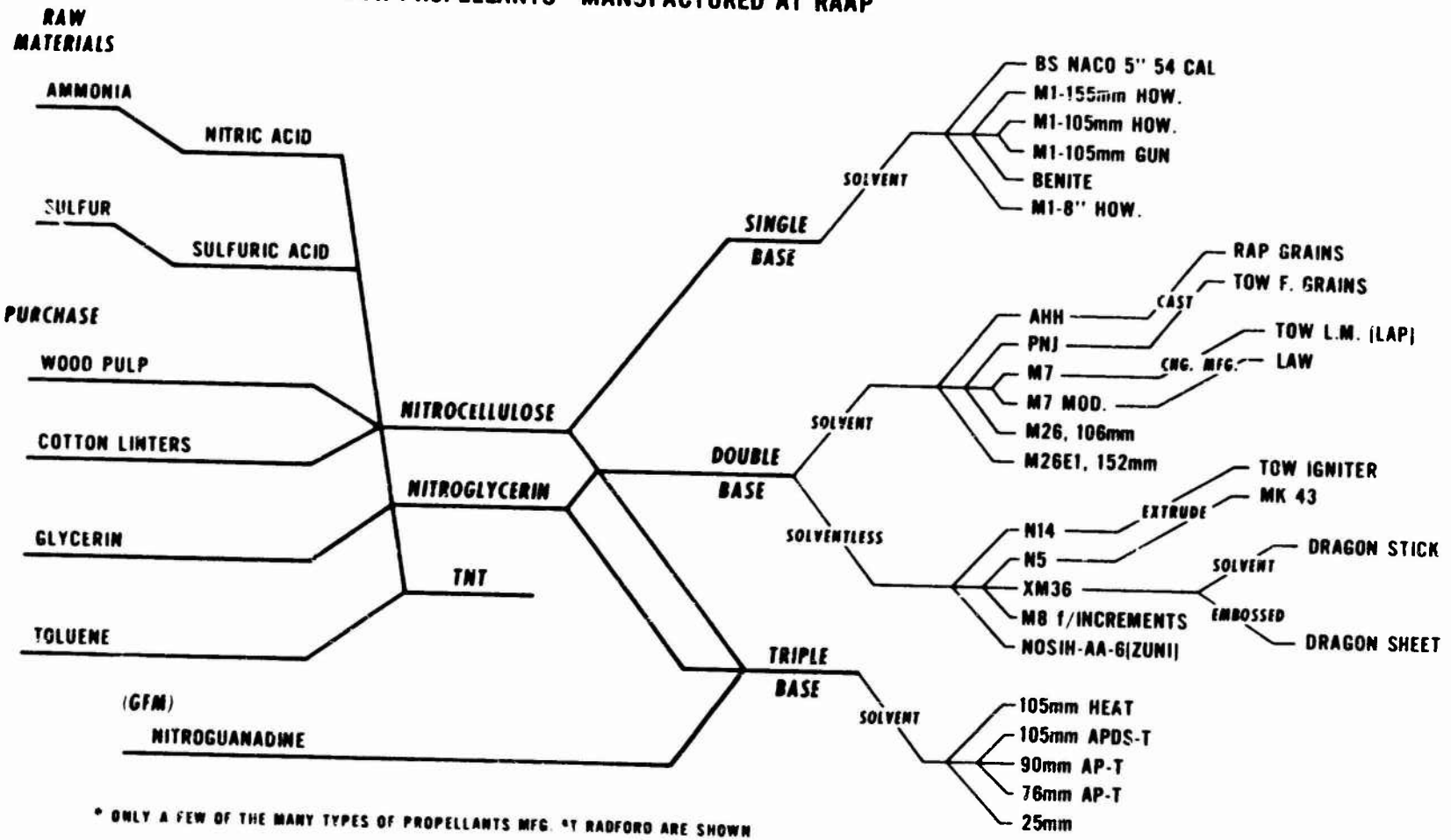

* ONLY A FEW OF THE MANY TYPES OF PROPELLANTS MFG. AT RADFORD ARE SHOWN

RAAPs MANUFACTURE OF NG IS SIGNIFICANT TO NOT ONLY THE ARMY BUT OTHER SERVICES AND COUNTRIES AS WELL. THE IMPORTANCE IS REFLECTED HERE BY PRODUCTS REQUIRING NG AND THE CUSTOMER REQUIRING THE PRODUCT. SO, THE MANUFACTURE OF NG AT RAAP TRANSCENDS THE LOCAL SITUATION OF RAAP, 2,600 WORKERS AND EVEN THE ARMY AS A SERVICE.

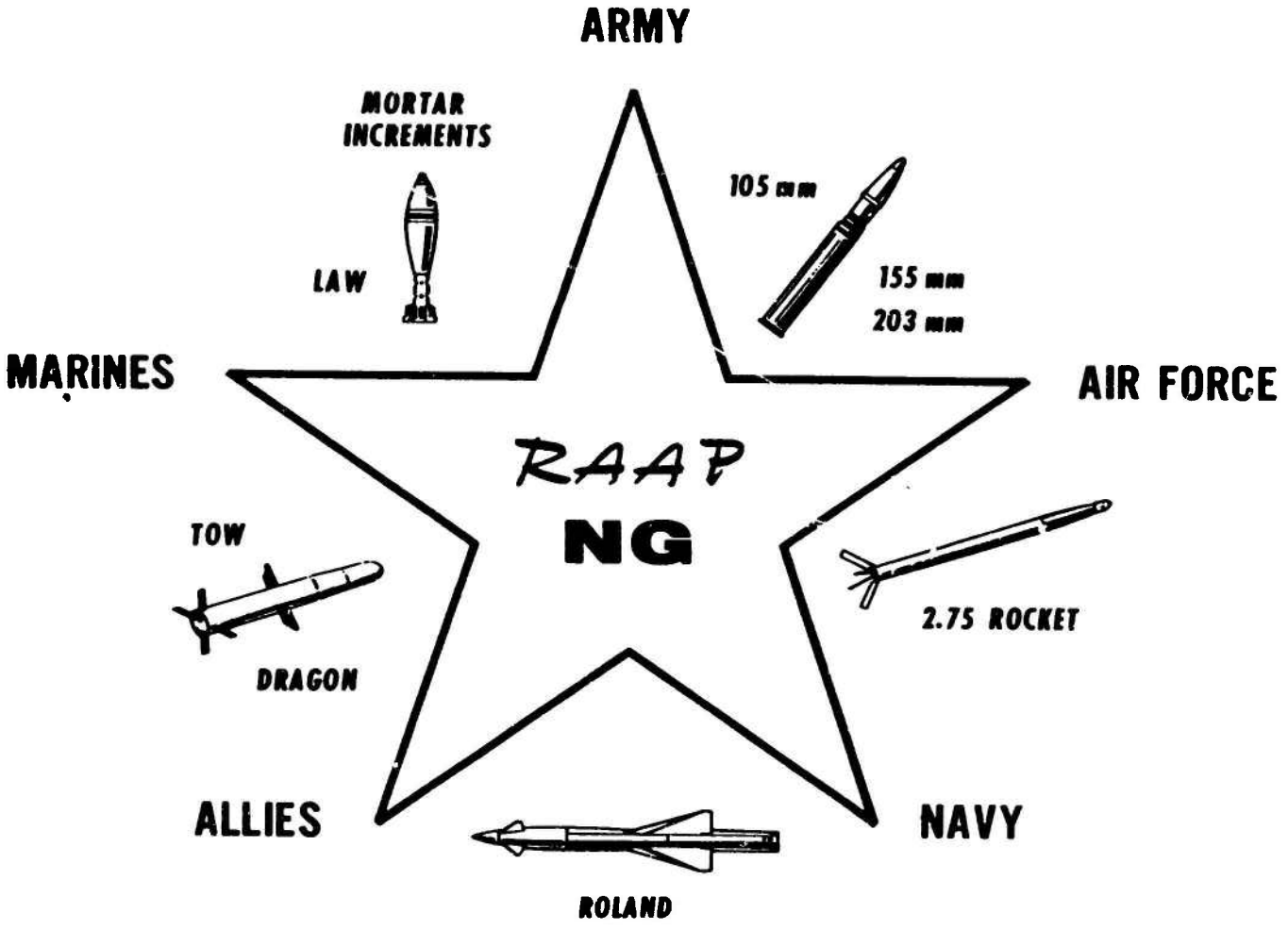
ARMY
MORTAR INCREMENTS
LAW
105 mm
155 mm
203 mm
MARINES
AIR FORCE
RAAP
NG
TOW
DRAGON
2.75 ROCKET
ALLIES
NAVY
ROLAND

THIS IS A LAYOUT OF THE NG AREA #2 SHOWING THE 3 STOREHOUSES AND THE NITRATION HOUSE. NITRATION WAS CONTINUOUS USING THE BIAZZI PROCESS AND THE NG FLOW TO THE STOREHOUSES WAS BY GRAVITY THROUGH A PLASTIC 1 1/2" FEED LINE WHICH RESTED IN A GUTTER. THE NITRATION BUILDING AND STOREHOUSE #1 (SHOWN IN RED) EXPLODED, STOREHOUSES #2 AND 3 (SHOWN IN YELLOW) DID NOT EXPLODE.


1021

PICTURE OF THE BIAZZI UNIT AS INSTALLED IN THE NITRATION BUILDING. NOTICE THAT IT IS ALL STAINLESS STEEL.

ON THE NEXT SLIDE I WILL ACTUALLY TRACE THE PROCESS.

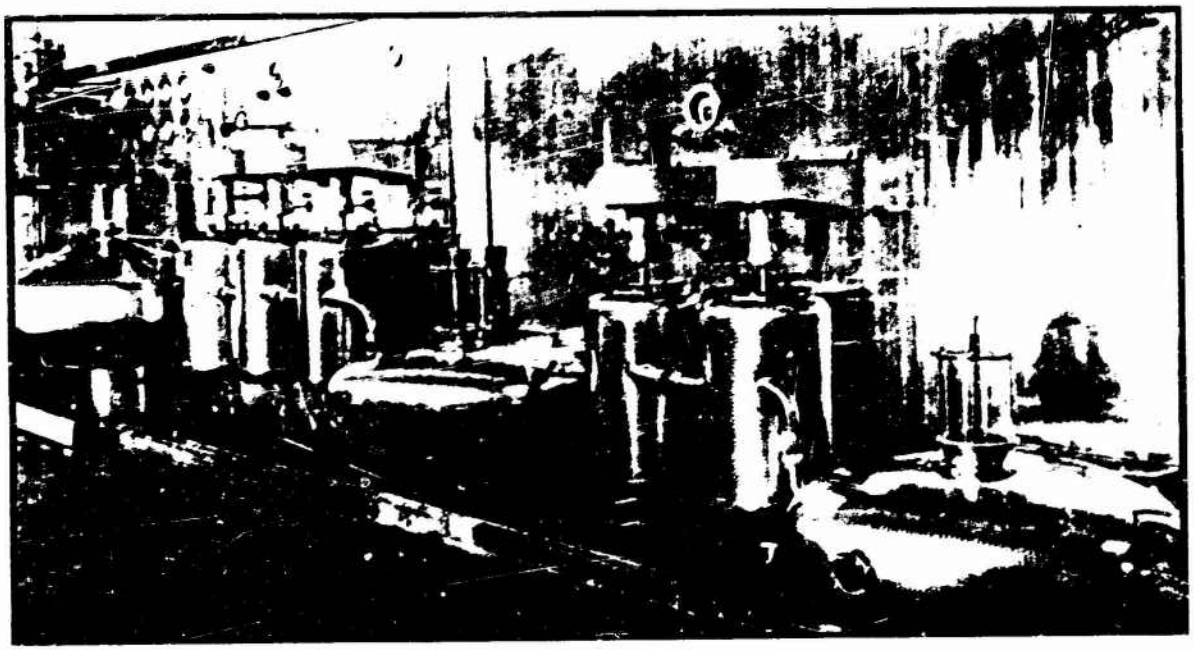

NG BIAZZI UNIT

I WILL RUN THROUGH THE NITRATION PROCESS VERY QUICKLY TO PROVIDE AN APPRECIATION OF ITS COMPLEXITY.

(DISCUSS SLIDE)

NITRATION PANEL

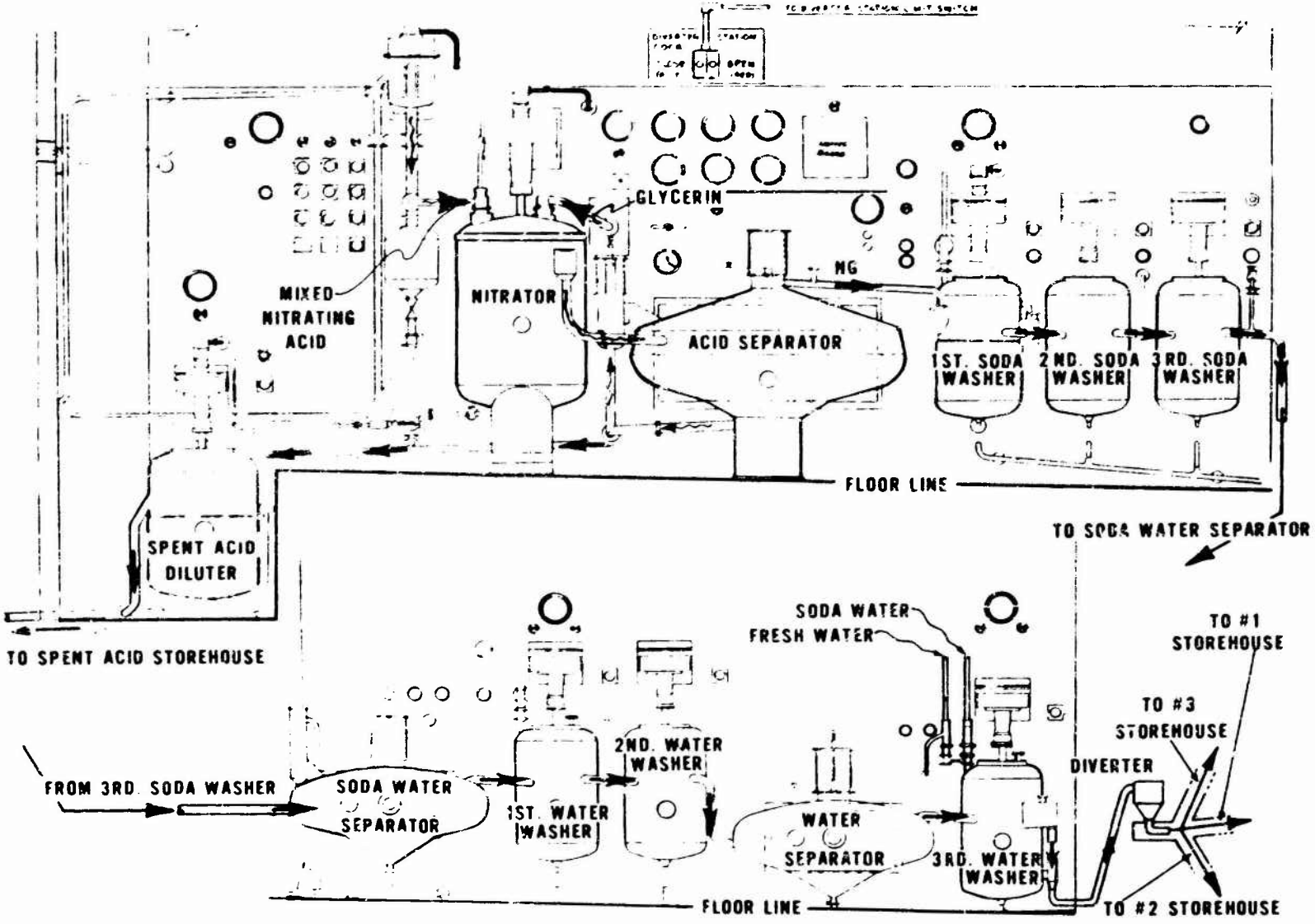

STATISTICS OF THE INCIDENT ARE SHOWN HERE.

(DISCUSS CHART)

IT SHOULD BE NOTED THAT OUR CAPABILITY TO MANUFACTURE NG IN AREA #2 WAS DESTROYED AND THAT TOTAL NG SUPPLY WAS NOW 8,000 LBS WHICH WAS LOCATED IN DAMAGED FACILITIES.

INCIDENT STATISTICS

0600 6 JAN 1978

- 5,000 OF 13,000 LBS OF NG EXPLODED
- ROCKED LOCAL COMMUNITIES
- MEASURED 1.3 ON RICHTER SCALE
- MAJOR PROPERTY DAMAGE TO NG AREA No. 2
- KILLED 2 PEOPLE, INJURED 8; 1 SERIOUSLY
- RENDERED NG AREA No. 2 UNUSABLE
- LEFT 8,000 LBS OF NG IN TWO DAMAGED STOREHOUSES

EFFECTS OF THE EXPLOSION ON STOREHOUSE #1 ARE SHOWN HERE WITH A BEFORE AND AFTER LOOK.

NG STOREHOUSE NO. 1

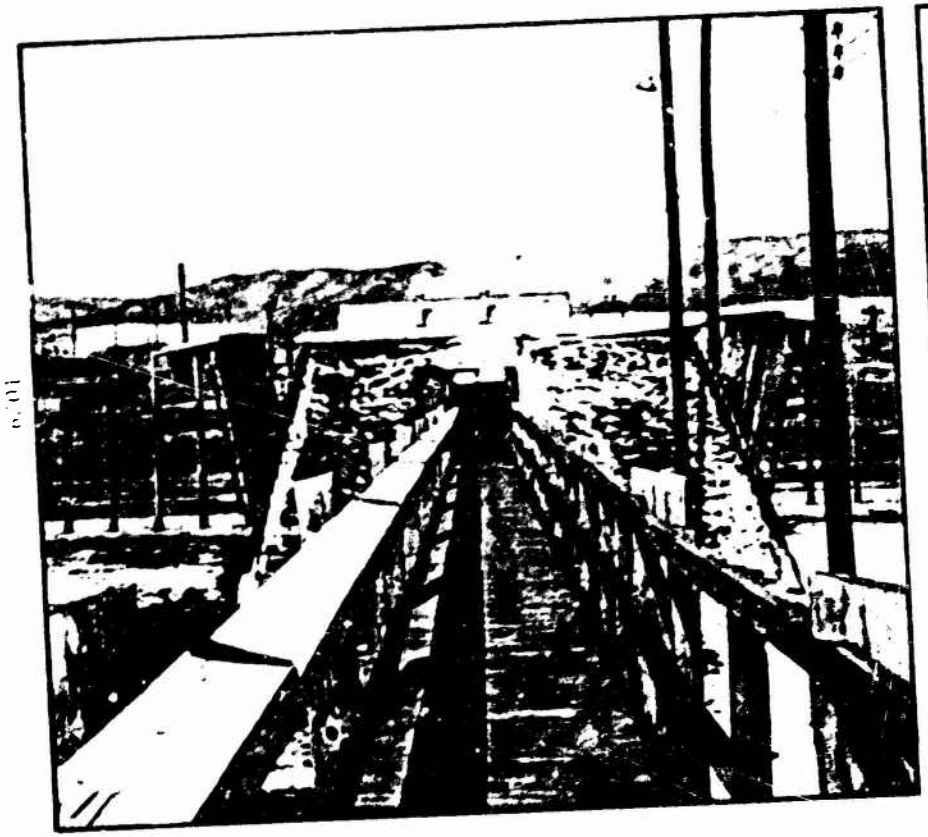

BEFORE

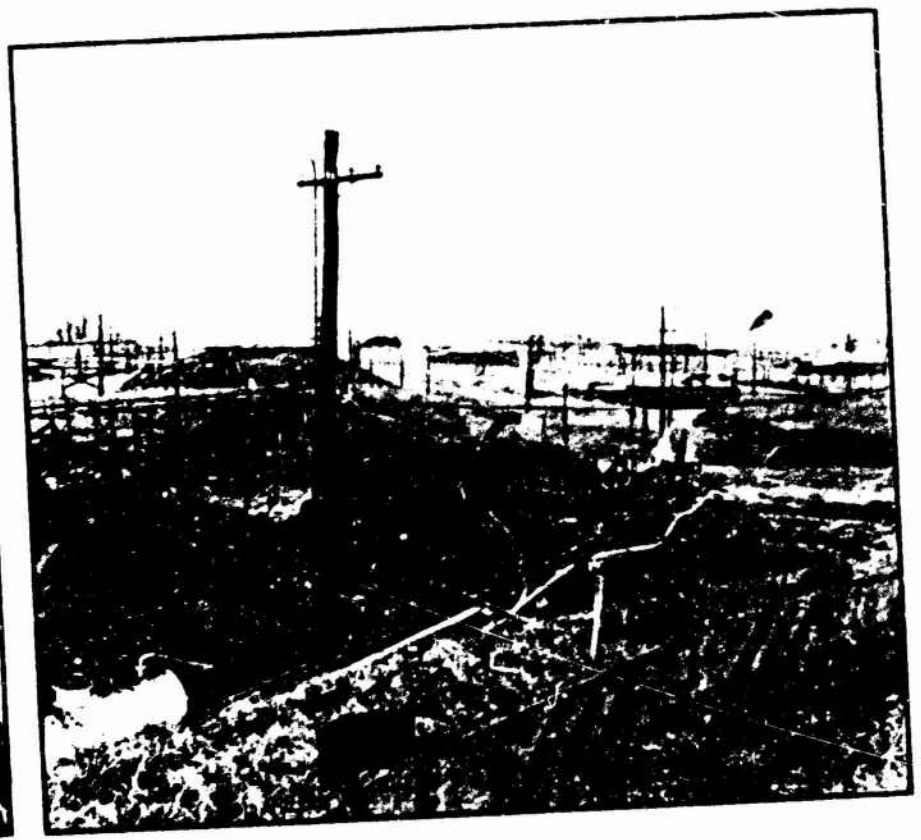

AFTER

THE EXPLOSION OCCURRED AT 0605 HRS. WE HAD ONLY THE NIGHT SHIFT WORKING AND THE MAIN WORKFORCE WAS TO START AT 0800 HRS. FOR THE MOST PART THE 6TH OF JANUARY WAS A "REACT" DAY. THE DEMANDS WERE GREAT. SOME OF THE PROBLEMS WHICH TEND TO LOOM THE LARGEST, AFTER THE FACT, ARE SHOWN HERE. I WILL DISCUSS EACH BRIEFLY.

A DAY THAT STARTED WITH A "BANG", ENDED WITH A GROAN AT APPROXIMATELY 0030 HRS 7 JAN, ANTICIPATING THE 0800 HRS MEETING THE NEXT DAY (SATURDAY) WITH ALL PRINCIPAL MEMBERS OF BOTH HERCULES AND MY STAFF. TO SET THE STAGE FOR RECOVERY ACTIONS.

SIGNIFICANT PROBLEMS

* *IMPACT ASSESSMENT*
* *MISSING PERSON*
* *OSHA*
* *PRESS*
* *RECOVERY*
* *RESPONSIBILITIES*

THE FIRST PROBLEM, OF COURSE, WAS IMPACT, PRODUCTION AND PEOPLE, HOW TO ASSESS AND LIMIT.

HERE ARE SOME OF THE CONSIDERATIONS. (DISCUSS)

AND HERE ARE OUR SOLUTIONS. (DISCUSS)

AS A RESULT OF THESE - NO OTHER AMMUNITION PLANT WAS IMPACTED AND THE TOTAL PERSONNEL IMPACT RANGED FROM 127 PEOPLE OUT FOR 1 DAY TO 8 PEOPLE OUT FOR 11 DAYS. A TOTAL OF 250 PEOPLE WERE AFFECTED BUT NO ONE WAS LAYED OFF. ONLY FURLOUGHED WITHIN PROVISIONS OF THE CONTRACT.

THIS WAS POSSIBLE PRIMARY BECAUSE HERCULES WORKED ITS MAINTENANCE CREW 24 HOURS/DAY, 7 DAYS/WEEK TO GET NG AREA #1 ON STREAM. NG AREA #1 IS A BATCH PLANT CONSTRUCTED IN 1945 AND NOT IN USE FOR NG PRODUCTION AT THE TIME.

IMPACT

PRODUCTS/PERSONNEL

PROBLEM

HOW TO MEET SCHEDULES AND LIMIT CONTRACTOR PERSONNEL LAYOFFS / FURLOUGHS

Considerations

60% OF PRODUCTION MULTI-BASE
8,000 LBS NG AVAILABLE
250 PEOPLE POTENTIALLY IMPACTED
MONTH AFTER CHRISTMAS
PROPELLANT SUPPLIES IN PIPELINE
HORRENDOUS WEATHER CONDITIONS

SOLUTIONS

- REALIGNED PRODUCTION SCHEDULE TO CRITICAL ITEMS AND THOSE THAT WERE LABOR INTENSIVE
- FILL WEATHER ABSENTEEISM WITH FURLOUGHED PERSONNEL
- ADVANCED FUTURE WORK (REBLEND)

THE MISSING PERSON PROBLEM WILL NEVER BE COMPLETELY SOLVED.

THE PROBLEM HAS NO SET SOLUTION AND WAS ONE OF THE WORST TO ADDRESS.

(DESCRIBE/DISCUSS CRATER AREA AND CONSIDERATIONS)

THESE ARE THE SOLUTIONS WE DEVELOPED. IT SHOULD BE NOTED THAT NO SPECIFICALLY IDENTIFIABLE REMAINS WERE EVER FOUND. SMALL REMNANTS OF MATERIAL WERE FOUND AND DETERMINED TO BE HUMAN TISSUE. THE FAMILY HELD THE FUNERAL 19 MAR 78, 9 WEEKS AFTER THE INCIDENT. THE STATE OF VIRGINIA LEGISLATURE PASSED A SPECIAL ACT DECLARING THOSE INVOLVED IN THE EXPLOSION LEGALLY DEAD IF THEY WERE STILL MISSING AFTER 6 MONTHS.

MISSING PERSON

PROBLEM

ONE MAN (CONTRACTOR EMPLOYE) ASSUMED TO HAVE BEEN IN STOREHOUSE - STILL MISSING

Considerations

AREA SNOW COVERED
BELOW FREEZING TEMPERATURES
DEBRIS/AREA UNDER CONTROL OF BOARD OF INQUIRY
CONTINUOUS PUBLIC CONCERN

SOLUTIONS

OBTAIN PERMISSION OF BOARD OF INQUIRY TO REMOVE DEBRIS
PHOTOGRAPH ENTIRE AREA INCLUDING AERIAL PHOTOS
BRING IN SEARCH DOGS FROM MDW-MP
MANUALLY REMOVE AND "SIFT" ALL DIRT IN CRATER AREA
CONDUCT SHOULDER TO SHOULDER SEARCH AS SNOW MELTS
CONTRACTOR MADE ALL PERSONAL CONTACT WITH FAMILIES
FUNERAL HELD 19 MARCH 1978

THE OSHA PROBLEM IS ALSO A KNOTTY ONE AND ONE YOU CANNOT SOLVE AT THE PLANT LEVEL.

THE CONSIDERATIONS WE HAD.

AND HERE ARE OUR SOLUTIONS.

ACTION IS CONTINUING ON A JOINT MEMO OF UNDERSTANDING BETWEEN DA AND DOL WHICH WILL RESULT IN OSHA BEING PERMITTED ENTRANCE INTO THE PLANT, UNDER, I HOPE, CERTAIN RESTRICTIONS.

OSHA

PROBLEM

OSHA DEMANDS ADMITTANCE TO "WHERE THE ACTION IS"
(EXPLOSIVE AREA)

Considerations

DARCOM/ARRCOM POLICY
PRECEDENTS
SEVERITY OF EXPLOSION (CASUALTIES)
OSHA REPS PERSONALLY PRESENT
DISTRICT DIRECTOR & ASST SEC OF LABOR INTEREST

SOLUTIONS

ADHERE TO CURRENT POLICY - ADMIT TO ADMIN AREA ONLY
SCHEDULE SECOND VISIT TO ADMIN AREA
HOSPITABLE AND ACCOMMODATING AS POSSIBLE

THIS ONE WILL SCARE HELL OUT OF YOU, AT LEAST IT DID ME. THE NEWS PEOPLE CAN RAISE YOU TO HEIGHTS YOU NEVER DREAMED OF OR CAN HAVE YOU TALKING IN YOUR SLEEP DURING DREAMS YOU WOULD LIKE TO FORGET.

CONSIDERATIONS WE HAD.

OUR SOLUTIONS WERE THESE. (DISCUSS)

THE RESULT OF THIS ONE WAS OBVIOUS. WE HAD AND, STILL DO, A GOOD PRESS.

MEDIA

PROBLEM

CONTINUOUS DEMANDS FOR NEW INFORMATION

Considerations

LOCAL COMMUNITIES FELT THE BLAST
NOTIFICATION OF NOK
FREEDOM OF PRESS - RIGHT TO KNOW
COMMUNITY ATMOSPHERE
COR MAKES RELEASES

SOLUTIONS

BE AS OPEN AS POSSIBLE
EARLY PRESS RELEASE (0700)
PRESS CONF AND PHOTO SESSION
TV INTERVIEW
ESTABLISHED SINGLE POC FOR MEDIA
FOLLOW-UP ON ALL DEFERRED INQUIRIES
LATER PRESS RELEASE WITH NAMES OF INJURED

THE PROBLEM OF RECOVERY IS TWO PRONGED - HOW TO GET BACK INTO PRODUCTION WITH MINIMUM IMPACT THEN HOW TO RESTORE THE PRODUCTION CAPABILITY IN THE DESTROYED AREA.

CONSIDERATIONS AVAILABLE. (DISCUSS)

OUR SOLUTIONS - ARE SHOWN HERE.

I AM DISAPPOINTED IN OUR LONG RANGE SOLUTION SINCE THE EFFORT IS EXPECTED TO TAKE 26 MONTHS - MAY 1980 WE HOPE TO BEGIN OPERATIONS IN AREA #2.

NO MATTER WHAT YOU DO, IT WILL TAKE ABOUT 2 YEARS TO GET YOUR PLANT BACK.

RECOVERY

PROBLEM

SHORT TERM FOR PRODUCTION
LONG TERM FOR RESTORATION

Considerations

PRODUCTION AHEAD OF SCHEDULE
NG AREA NO. 1 (BATCH) NOT OPERABLE WITHOUT MAINTENANCE
IMPACT ON ARMY & PERSONNEL (LOCAL & REMOTE)
ONLY ACTIVE AAP WITH NG CAPABILITY
COST OF OPERATION
EXPOSURE OF PERSONNEL

SOLUTIONS

SHORT RANGE

ACTIVATE NG NO. 1 ASAP - USE AVAILABLE FUNDS
REALIGN PRODUCTION SCHEDULE TO CRITICAL ITEMS AND MAXIMUM MANPOWER RQMTS

LONG RANGE

DEVELOP PROGRAM DOCUMENTS FOR RESTORATION
GET ALCON ON BOARD
UTILIZE CURRENT STATE OF ART TECHNOLOGY

1501

THIS "PROBLEM" WAS NOT A PROBLEM FOR RAAP, BUT COULD BE A SIGNIFICANT PROBLEM. WHO HAS WHAT RESPONSIBILITIES DURING A CRISES SUCH AS A BLOW ON A GOCO PLANT, MUST BE CLEARLY DEFINED IN ADVANCE OR YOU MUST OPERATE AS A TEAM WITH EACH SIDE DOING WHAT HE BELIEVES IS RIGHT AND COORDINATING IT WITH THE OTHER. OBVIOUSLY SOME THINGS CANNOT BE DONE WITHOUT SPECIFIC APPROVAL OF COR AND/OR ARRCOM.

CONSIDERATIONS.

THE SOLUTION TO THE RESPONSIBILITY PROBLEM IS MAKE DECISIONS AND DO THE JOB WHILE FULLY COORDINATING THE ACTIONS.

THE CO ACCEPTS FULL RESPONSIBILITY FOR DECISIONS THAT MUST BE COORDINATED WITH ARRCOM. COORDINATE LATER.

THE RELATIONSHIP OF CO AND PLANT MANAGER MUST BE SUCH TO PERMIT EACH TO FULFILL HIS RESPONSIBILITIES AND COORDINATE LATER.

RESPONSIBILITIES

PROBLEM

INTERFACE OF COR & CONTRACTOR IN THE MYRIAD OF ONGOING URGENT ACTIONS

Considerations

CO ULTIMATELY RESPONSIBLE
COR INTERFACES WITH THE PUBLIC
PLANT MUST BE SECURED
OTHER FUNCTIONS MUST CONTINUE
CONCERNS OF ARMY & CONTRACTOR HQ SIMILAR
REESTABLISH ATMOSPHERE OF NORMALCY

SOLUTIONS

CO ACCEPTS FULL RESPONSIBILITY FOR DECISION MAKING
WORK AS A TEAM IN ALL AREAS

THIS SLIDE REFLECTS, FROM A SAFETY VIEWPOINT, THE CURRENT RISKS THE ARMY IS TAKING RUNNING NG AREA #1. REMEMBERING THE IMPORTANCE OF NG TO THE OVERALL PROPELLANT PRODUCTION YOU DRAW THE CONCLUSION THAT PROPELLANT PRODUCTION MUST CONTINUE. WE HAVE ASSESSED ALL RISKS AND CONDUCTED A FORMAL HAZARD ANALYSIS IAW ARMCOM REG 385-4 AND CONCLUDED THAT THE RISKS ARE WITHIN ACCEPTABLE LIMITS.

THE RISKS ARE REFLECTED HERE TO DIFFERENTIATE BETWEEN THE CONTINUOUS NG AREA #2 AND BATCH AREA #1.

NEEDLESS TO SAY, WE ARE TAKING EXTRAORDINARY MEASURES TO ASSURE MAXIMUM SAFETY OF OPERATION.

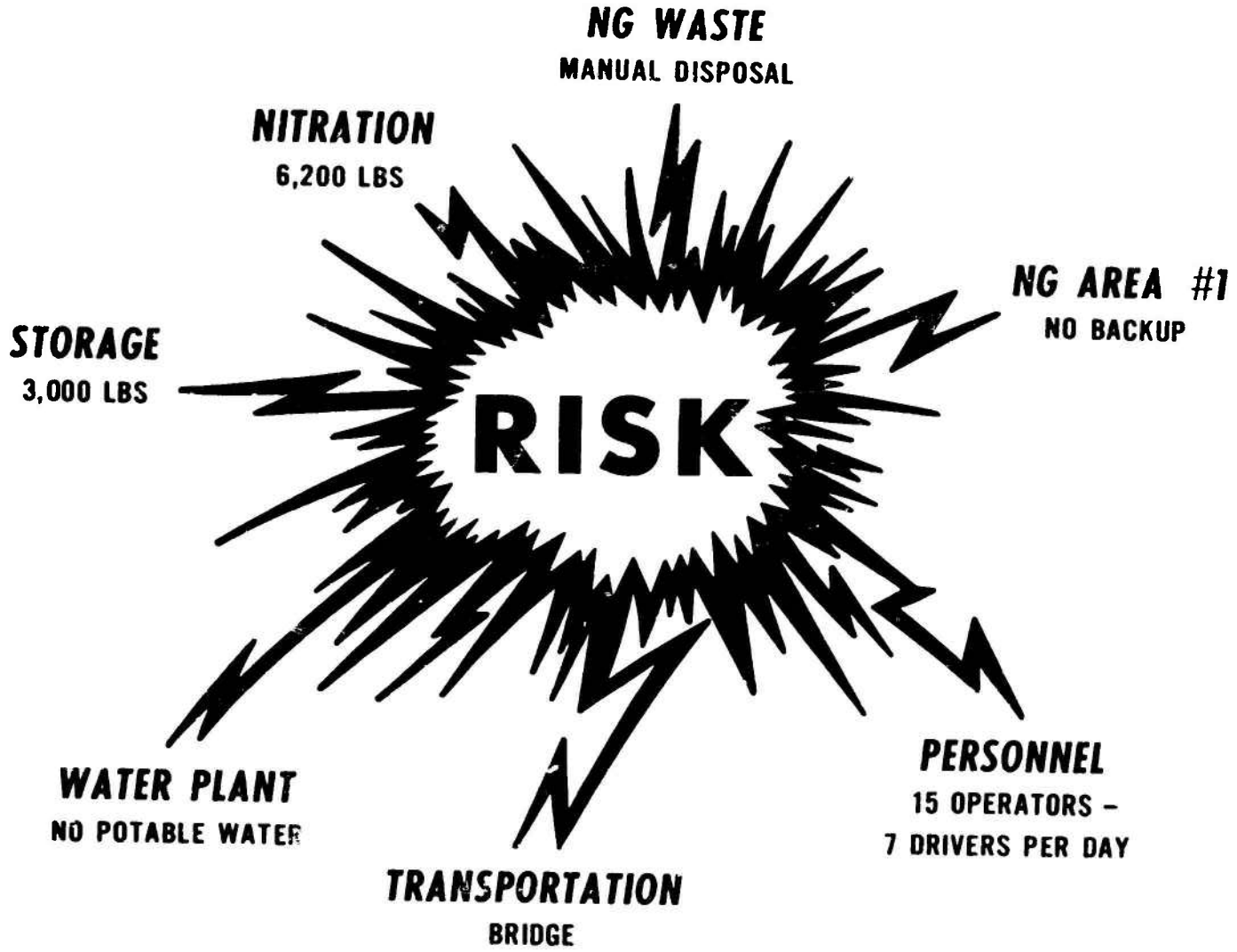
NG WASTE
MANUAL DISPOSAL
NITRATION
6,200 LBS
NG AREA #1
NO BACKUP
STORAGE
3,000 LBS
RISK
WATER PLANT
NO POTABLE WATER
PERSONNEL
15 OPERATORS -
7 DRIVERS PER DAY
TRANSPORTATION
BRIDGE

IN CONCLUSION, A BOARD OF INVESTIGATION WAS APPOINTED BY ARRCOM AND THE PRESIDENT OF THE BOARD WAS ON THE SCENE THE SAME DAY OF THE EXPLOSION. THE REPORT HAS BEEN COMPLETED AND MR. SKOGMAN WILL DISCUSS IT IN DETAIL AS WELL AS OTHER SAFETY IMPLICATIONS.

I WILL TAKE ANY GENERAL QUESTIONS YOU HAVE ON THE PLANT AT THIS TIME. HOWEVER, I WOULD LIKE YOU TO HOLD QUESTIONS ON THE EXPLOSION UNTIL MR. SKOGMAN IS FINISHED.

MR. SKOGMAN...

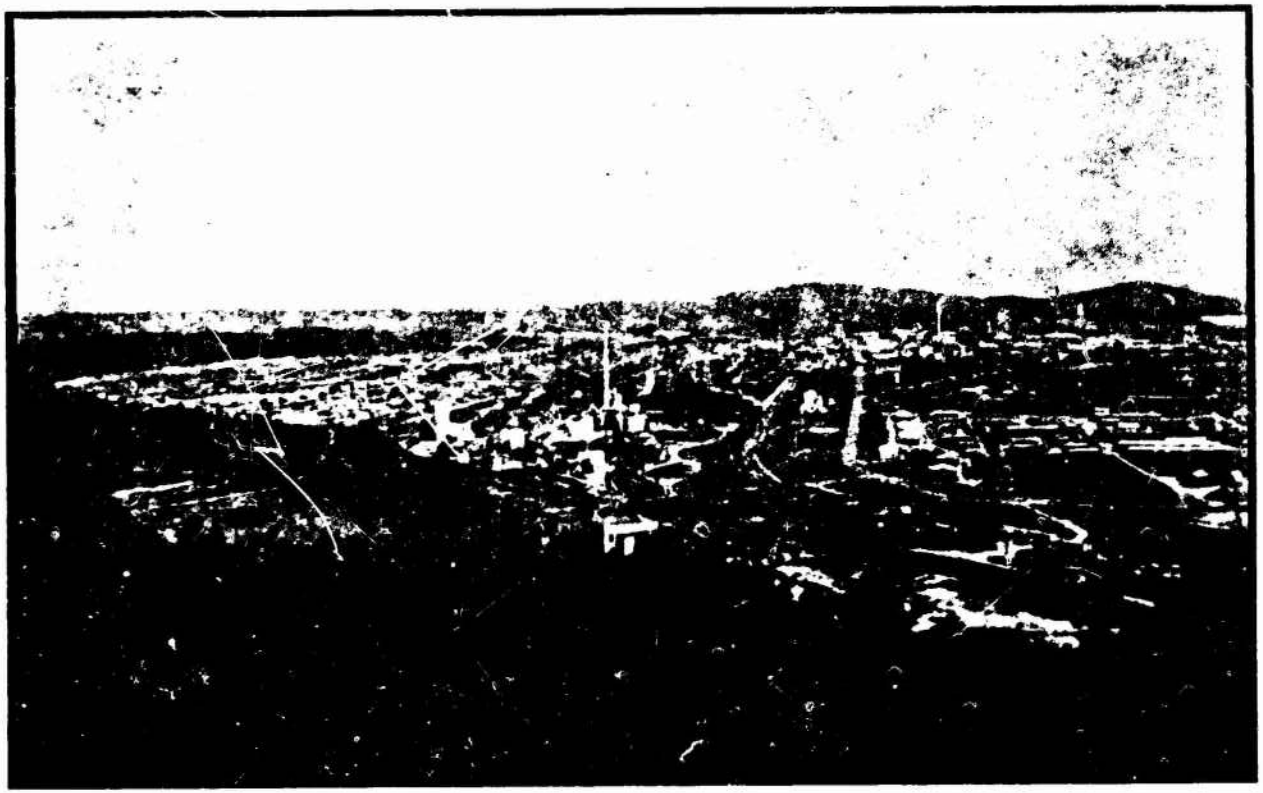

PORTION OF RADFORD UNIT

VIEW LOOKING EAST

PART 2

Gentlemen:

My name is Dave Skogman. I am a Safety Engineer with the Headquarters, US Army Armament Materiel Readiness Command at Rock Island, Illinois. I was a member of the Army Board of Investigation that was convened to determine the cause of the NG explosion at Radford and develop recommendations to prevent its recurrence. The composition of the Board of Investigation was as shown on Figure 1. The membership was chosen to provide the necessary expertise to investigate an accident of this type.

The President of the Board was COL Eure who was the Commanding Officer of Holston Army Ammunition Plant at the time of the accident. COL Eure established administrative control over the area of the explosion and arrived at Radford at 1430 on 6 January 1978. The first meeting of the Board with all member present was on 11 January 1978.

The box score that resulted from this incident was indeed impressive (Figure 2). But as seems to be the case in explosions of this magnitude, it could easily have been much worse. Only minutes before the incident, two Nitroglycerin Weigh Operators passed through the Nitrating House enroute to the NG Area Office and would undoubtedly have been severely injured or killed had they been in the Nitrating House at the time of the incident.

Figure 3 shows the relative locations of the injured personnel from the two primary explosive concentrations at the time of the incident. It was estimated that there were 675 pounds of NG in the Nitrating House and 4,200 pounds of NG in Storehouse #1. The fact that an operator was located in the Nitrating House at the time of the incident and survived can only be described as incredible. Furthermore, the required intraline distance for 700 pounds of NG is 80 and 160 feet, barricaded and unbarricaded intraline distance, respectively. Three of the casualties were within these minimum distances and were not seriously injured. The Nitrating House had reinforced concrete walls with earth barricades against the walls which most probably helped protect these individuals from more serious injury.

However, based on the quantity of NG involved, the degree of physical damage sustained and the close proximity of personnel to the explosion, it can certainly be seen that this casualty listing could easily have been much worse.

The Board estimated that at the time of the incident there were 4,200 pounds of NG in Storehouse #1, 677 pounds in the Nitrating House, and 123 pounds distributed in the Diverter Station and NG Conduit between the Storehouse and Nitrating House. The current minimum acceptable explosive quantity distance requirements for 4,200 and 700 pounds of high explosive are as shown on Figure 4. By definition, inhabited building

distance provides a high degree of protection to frame or masonry buildings from structural damage, to their occupants from death or serious injury, and reasonable protection to superficial parts such as window frames, doors, porches, and chimneys. Inhabited building distance does not provide protection against glass breakage or injury to personnel from glass breakage or hazardous fragments. Again by definition, intraline distance is expected to protect buildings from propagation of explosion due to blast effects but not against the possibility of propagation due to fragments. Buildings separated by intraline distance will probably suffer substantial structural damage.

Major explosions provide an opportunity to verify that the current explosive separation criteria are still acceptable and accurate. This chart (Figure 5) shows the estimate of damage to several buildings located at approximately inhabited building distance from the 4,200 pounds of NG at NG Storehouse #1. Effects ranged from door and window breakage to moderate structural damage and occupants of these buildings were protected from death or serious injury. In general, it can be said that the degree of protection predicted by inhabited building distance separation was verified.

Buildings located at intraline distance from NG Storehouse #1 did suffer substantial structural damage as predicted by current separation criteria, but propagation did not occur (Figure 6). The NG storage tanks in Storehouse #3 were displaced about 0.5 inches from the force

of the explosion and all the remaining NG storage tanks contained debris from the explosion. One very significant conclusion of the Board of Investigation needs to be emphasized at this point. There was 310 feet separation distance between NG Storehouse #1 and NG Storehouse #2. This distance meets the minimum unbarricaded intraline separation distance requirements; and therefore, the barricades that were in place exceeded the minimum acceptable requirements. Based on the extent of damage sustained and the sensitivity of NG, the Board concluded that these barricades probably prevented sympathetic detonation from occurring. In other words, exceeding the minimum requirements probably prevented a much more serious incident.

The sole purpose of the Board of Investigation was to determine the most probable casue of the incident and develop recommendations to preclude its recurrence. From a process and physical standpoint, the incident involved three distinct funtions and areas; the Nitrating House where the NG was produced; the NG Diverter Station and Conduit which transferred the NG from the Nitrating House to the Storehouse; and the Storehouse where the NG was stored until used (Figure 7). The first priority was to determine in which of these process areas the incident most likely was initiated in order to narrow the search for the most probable cause. Each of the three areas is shown here in order of increasing probability as determined by the Board; i.e., it was determined that initiation in the Diverter Station/NG Conduit was least likely,

and initiation in the storehouse was most likely. I will briefly discuss the rationale used in making this initial crucial determination.

The Board examined possible stimuli that could have initiated the incident in the Diverter Station/NG Conduit as shown on Figure 8. It is known that strongly acidic impure NG decomposes autocatalytically and exothermally which can lead to autoignition and detonation. This possibility was highly unlikely since the NG in the Conduit had already been subjected to soda water and water washes before leaving the Nitrating House. The possibility of human error was also discarded because the location of all personnel in the area was determined, and no one was working in the vicinity of the NG Conduit at the time of the incident. The third possibility considered was that an object struck the Conduit causing initiation. There was no evidence found of such an occurrence; and since there was no wind or storm in the area at the time, this possibility was discarded. It is known that a mixture of liquid and crystalline NG is more sensitive to shock than liquid NG. The NG Conduit was bathed in hot water, and the temperature of this water was monitored at the Nitrating House. If this water heating system had failed, which is unlikely, the only predictable result would have been the gradual freezing of NG and eventual blockage of the NG Conduit. An initiation stimulus would still have been required to have caused the incident.

Initiation in the Nitrating House was considered and concluded to be improbable for several reasons (Figure 9). Nitration had been going on for 9 hours prior to the incident which included a shift change, and all operations had been normal. The in-process inspection tests on the NG produced during this period showed that the NG was acceptable. The Nitrating House was manned with two experienced and knowledgeable operators. The surviving operator stated that all operations were normal prior to the incident. The surviving operator further stated that if strongly acidic NG capable of autoignition had been present in the nitration system, it would have been immediately perceived by the operator, and corrective actions initiated. Finally, two NG weigh operators had passed through the Nitrating House only minutes before the incident, and they stated that nothing abnormal was observed.

Nitration was stopped at 0530, and the incident occurred at 0605. According to this timetable, the operator in the storehouse would normally have been involved with sampling or skimming the NG storage tank or otherwise manipulating an NG specimen (Figure 10). This was the only area where such a situation prevailed. The second and most convincing factor that influenced the conclusion that the storehouse was the most probable initiation site was the testimony of an eye witness. This witness was standing approximately 50 feet from the Nitrating House with an unobstructed view of the wooden trough containing the NG Conduit between the Storehouse and the Nitrating House. This witness testified to seeing a streak of lightning 5 to 10 feet high along the top of the NG Conduit come up

from the Storehouse to the Nitrating House. The expected detonation velocity of unconfined liquid NG is 1,000 - 2,000 meters per second, and the Board, therefore, estimated that the time of propagation between the Storehouse and the Nitrating House was in the range of about 0.1 second. Based on known human comprehension capabilities and given the time of propagation, the Board concluded that a witness' ability to determine direction of travel was credible and in fact predictable.

With the conclusion that the incident originated at the Storehouse, the search for cause was narrowed to operations and potential initiation stimuli within the Storehouse. The Board viewed these initiation stimuli as separable into three main categories; Acts of God, human factors, or equipment failure (Figure 11).

Figure 12 shows possible initiation stimuli considered by the Board to be in the realm of Acts of God. Weather conditions at the time of the incident were as follows: Temperature 42° Fahrenheit, sky was cloudy, and there was no precipitation. The exact wind speed at the time of the incident is unknown, but testimony of personnel in the area indicates the wind speed was not excessive. The second possibility considered was that the Storehouse Operator suffered a blackout, convulsion, or heart attack that resulted in an error that initiated the incident. An interview with the Radford Medical Director confirmed that the Storehouse Operator was in good physical condition, and these possibilities were very unlikely. Sabotage, while perhaps is more appropriately classified

as the opposite of an Act of God was also considered and dismissed. All of the personnel in the area were experienced, reliable employees, and no unauthorized personnel were seen in the area prior to the explosion.

The second category of initiation stimuli considered was human factors. The possibilities considered are shown on Figure 13. Normal operations called for the transfer of NG from the outside catch tank to the inside catch tank using a bucket. According to testimony, this operation had been completed by another operator shortly before the incident, and therefore, the bucket would not have been in use at the time of the incident. The remaining three possibilities all involve an error at some point in the NG sampling operation.

Figure 14 is a floor plan of the NG Storehouse. The NG sampling operation involved using a rubber dipper to take a sample from tank #1 which was being filled, walking with the dipper in hand over the skimmer and drain hoses and down the stairs to the inside catch tank, and pouring the sample from the dipper into a rubber sample bottle over the inside catch tank. The following photographs illustrate some of the potential for error that were a part of this operation.

Figure 15 shows the operator in position to reach down into the storage tank and take a sample of NG. Although not shown here, it should be noted that the operator is standing on a two-step bench which he must step down from to the floor after the NG sample is taken.

Figure 16 shows the hoses that would have been in the operator's path of travel. Consider that the operator had to step over these hoses while holding a dipper of NG and a sponge.

Figure 17 shows the operator descending the stairs to the floor level on which the inside catch tank was located.

Figure 18 shows the operator filling the rubber sample bottle from the dipper over the inside catch tank. These pictures illustrate that the potential for a slip, trip, or fall were very real during this sampling operation. This potential becomes even more significant based on the fact that tank #1 would have been filled to the point where the operator could have been expected to be sampling at the time of the incident. Under the assumption that for whatever reason the operator either dropped or threw the sample dipper, a series of tests and analyses were conducted.

The analysis performed considered the initiation possibilities shown on Figure 19. The sample dipper could have been accidently dropped, swung laterally against a solid object such as the storage tank, or thrown upward or forward as might occur if the operator tripped and was about to fall. In addition, the free-fall drop height necessary to initiate an NG sample in the rubber sample bottle was determined. The tests performed duplicated as nearly as possible the actual conditions in the Storehouse.

Of the scenarios tested and analyzed, only the one shown on Figure 20 was assessed to produce sufficient impact energy to be capable of initiating 100 percent NG. Several conditions must be satisfied for this event to occur. First, the operator had to have been at the sampling station next to the storage tank on the two-step bench. Second, the dipper would have had to have been tossed 2.6 feet upward to attain minimum required free-fall of 3.6 feet. Third, the dipper had to have struck the edge of the stainless steel catch tank because the other lead and wood surfaces available do not deliver enough energy to the sample to exceed the threshold initiation level for NG. It is further pointed out that initiation of the NG sample in the vicinity of the catch tank does not automatically infer that sufficient shock energy would occur to sympathetically detonate the NG storage tanks. The initiation could have propagated to NG in the catch tank or along a thin film of NG in the rubber transfer hoses. There should not have been a significant quantity of NG in the catch tank at the time of the incident since the catch tank had been emptied approximately 50 minutes before the incident. The further the point of initiation from any NG in the catch tank or the transfer hoses, the less likely manual operation with the dipper was involved in the incident. Nevertheless, the Board concluded that manual operation with the dipper was a possible cause of the incident.

The third category of initiation stimuli considered by the Board was equipment failure (Figure 21). It was considered possible that the drop plug cam or the wooden cam race pin could have cracked or

separated and resulted in the unseating of the rubber drop plug by the agitated contents of the storage tank. This unseating of the drop plug would result in a very rapid flow of NG into the catch tank that would be immediately evident to the storehouse operator. The operator's first action would probably be to attempt to reseat the drop plug. There is one incident on record where the impact of a rubber drop plug on a stainless steel seat resulted in initiation of NG after 645,000 trials with the same drop plug. The exact cause of this incident was not determined but possibilities listed included impact, deterioration of the drop plug with resultant chance of hot spots or entrapped air bubbles, and contamination. After this incident, drop plugs were changed whenever they showed signs of wear, and 1,012,000 subsequent trials were conducted without incident. According to testimony, the rubber drop plug and the cam race pins had been changed on the tank being filled the day before the incident. Based on this new drop plug and the previously recorded 1,000,000 trials without incident, the Board concluded that initiation while attempting to reseat the drop plug was extremely unlikely. The second possibility considered was failure of the grounding system with resultant electrostatic initiation of NG. NG has a high threshold for electrostatic initiation. The NG storage tanks were grounded, and a buildup of electrostatic charge in flowing NG has not been detectable. A thorough annual inspection had been performed on this storehouse about 3 months prior to the incident, and the inspection report indicated that all grounding systems were acceptable. The latest safety inspection reports did not reveal any deficiencies associated with the grounding system. Based on these factors, the Board concluded that electrostatic

initiation was very improbable. The third equipment failure possibility considered was the NG jet used to transfer NG from the inside catch tank back to the storage tank.

Early in the investigation, the Board did not focus attention on the NG jets primarily because at the time of the incident, the jet would normally not have been in operation (Figure 22). The jets were of interest, however, in that an internationally recognized expert on NG operations testified that the jets in use at Radford could cause initiation of NG. In fact, a study of major explosions during the transport or storage of NG from 1950 to 1975 done by this expert identified five cases where the jet transfer system was identified as the most probable cause. The mode of initiation is thought to be the adiabatic compression of air bubbles producing sufficient heat to initiate NG. As the investigation continued, evidence was gathered which indicated that the inside catch tank may have had an abnormally large quantity of NG in it at the time of incident. If this were the case, the operator could have been in the process of jetting this NG from the catch tank back to the storage tank.

Under normal circumstances, the inside catch tank should have contained not more than 400 grams of NG at the time of the incident. Figure 23 shows fragments of the inside catch tank which were found as far as several hundred feet from the crater. Also, one of the fragments shows possible signs of having been in contact with detonating NG. This

indication along with the degree of destruction of the catch tank led the Board to conclude that the catch tank probably contained an abnormally large amount of NG at the time of the incident.

Figure 24 shows fragments of operating equipment found in and around the crater. The hose at the top of the picture is particularly significant. This hose was confirmed to be the hose on the output side of the NG jet in the storehouse. This hose shows clear evidence of having contained a detonation of some quantity of NG. Normal operation of the NG jets called for flushing this line of NG after use; and unless the jet were in operation at the time of the NG incident, this hose should not have contained any NG.

Figure 25 shows an unused jet with the jet recovered after the incident. The jet assembly involved in the incident was found approximately 1,600 feet from the crater. The machined stainless steel jet shows clear evidence of having sustained an internal stress such as would result from the detonation of NG in the assembly. The body, NG pick-up arm, and the discharge arm were expanded by comparison with an unused jet. The presence of NG in the jet assembly should only be possible if the jet were in operation at the time of the incident. The Board considered it unlikely that the observed expansion of the jet could have resulted from an explosion external to the jet since in that case, the jet assembly would probably have been slightly crushed or flattened. From the evidence of NG in the jetting hose and the evidence

of NG in the jet assembly itself, the Board concluded that initiation in the NG jet system was a possible cause of the incident.

The bottom line of an explosion investigation is to identify the most probable cause (Figure 26). As everyone in the explosives business knows this task is never easy, and in some cases is even impossible. However, after what I can assure you was a long, arduous, and sometimes heated debate, this Board of Investigation concluded that the most probable cause of the NG explosion at Radford on 6 January 1978 was initiation of NG in the jet system used to transfer NG from the inside catch tank to the storage tank. Use of the NG jets at Radford was stopped on 9 January 1978. A study is currently underway to identify a safer jet system. Gentlemen, that completes my presentation. Are there any questions?

MEMBERSHIP

BOARD OF INVESTIGATION

PRESIDENT	COL SAMUEL L. EURE	CHEMICAL CORPS
DEPUTY	DR. PETER C. K. LUI	CHEMICAL ENGINEER
MEMBER	DR. HAROLD J. MATSUGUMA	SUPERVISORY CHEMIST
MEMBER	MR. DAVID P. SKOGMAN	SAFETY ENGINEER
MEMBER	MR. DANIEL E. WALSH	CHEMICAL ENGINEER
MEMBER	MR. ALFRED E. MOREAU	ATTORNEY - ADVISOR
RECORDER	LT MARION D. RASHALL	CHEMICAL CORPS

1062

FIG. 1

INCIDENT STATISTICS

0600 6 JAN 1978

- 5,000 OF 13,000 LBS. OF NG EXPLODED
- ROCKED LOCAL COMMUNITIES
- MEASURED 1.3 ON RICHTER SCALE
- ESTIMATED PROPERTY DAMAGE TOTAL $3,455,000.00
- KILLED 2 PEOPLE, INJURED 8; 1 SERIOUSLY
- RENDERED NG AREA NO. 2 UNUSABLE

FIG. 2

LOCATION OF CASUALTIES

DISTANCE FROM EXPLOSION SITES	DESCRIPTION OF INJURIES
AT STOREHOUSE #1	FATALITY
AT NITRATING HOUSE	FATALITY
AT NITRATING HOUSE	SERIOUSLY INJURED
50 FT. FROM NITRATING HOUSE	SUPERFICIAL SCALP ABRASION
110 FT. FROM NITRATING HOUSE	CONTUSIONS BOTH KNEES AND RIGHT HAND, TINNITUS BOTH EARS
110 FT. FROM NITRATING HOUSE	CONTUSIONS BOTH KNEES AND LEFT ELBOW, TINNITUS BOTH EARS
192 FR. FROM STOREHOUSE	NO PHYSICAL INJURY, SEVERE NERVOUSNESS
310 FT. FROM STOREHOUSE	MIDLINE SCALP LACERATION
5000 FT. FROM STOREHOUSE	ABRASION OF LEFT WRIST
4200 FT. FROM STORE HOUSE	TINNITUS, RIGHT EAR

1064

FIG. 3

CURRENT QUANTITY DISTANCE REQUIREMENTS

QUANTITY OF EXPLOSIVES	IHBD *(FT.)	ID**(FT.)	BID***(FT.)
4200	685	310	155
700	355	160	80

1065

*IHBD - INHABITED BUILDING DISTANCE

**ID - INTRALINE DISTANCE

***BID - BARRICADED INTRALINE DISTANCE

FIG. 4

DAMAGE SUSTAINED AT IHBD FROM NG STOREHOUSE

BUILDING DESCRIPTION/TYPE OF CONSTRUCTION	DISTANCE (FT.)	ESTIMATE OF DAMAGE
PRE-MIX HOUSE/WOOD FRAME EARTH BARRICADES	815	$2,200
PRE-MIX HOUSE/WOOD FRAME EARTH BARRICADES	720	$2,887
NG AREA OFFICE/WOOD FRAME	675	$6,000
FORCED AIR DRY/WOOD FRAME EARTH BARRICADES	662	$1,812
AREA STORAGE BUILDING/WOOD FRAME	720	$ 579

1066

FIG. 5

DAMAGE SUSTAINED AT ID FROM NG STOREHOUSE

BLDG DESCRIPTION/TYPE OF CONSTRUCTION	DISTANCE (FT)	ESTIMATE OF DAMAGE
NG STOREHOUSE #3/WOOD FRAME EARTH BARRICADE	297	$37,500
NG STOREHOUSE #2/WOOD FRAME EARTH BARRICADE	310	$37,500
NG MIX HOUSE/WOOD FRAME	300	$37,500

1067

FIG. 6

PROCESS BUILDINGS/AREAS INVOLVED IN INCIDENT

- DIVERTER STATION/NG CONDUIT
- NITRATION BUILDING
- NG STOREHOUSE

FIG. 7

REASONS FOR ELIMINATING DIVERTER STATION/NG CONDUIT

- STABLE NG AFTER NITRATION
- NO OPERATOR INVOLVEMENT
- NO EVIDENCE OF ACT OF GOD
- NO EVIDENCE OF HOT WATER SYSTEM FAILURE

1069

FIG. 8

REASONS FOR ELIMINATING NITRATION HOUSE

- NINE HOURS OF NORMAL OPERATIONS
- NG PRODUCED DURING PRECEDING NINE HOURS WAS ACCEPTABLE
- EXPERIENCED, KNOWLEDGEABLE OPERATORS
- SURVIVOR TESTIFIED THAT OPERATIONS WERE NORMAL
- TWO WITNESSES PASSED THROUGH NITRATING HOUSE MINUTES BEFORE INCIDENT

1070

FIG. 9

REASONS FOR CONCLUDING THAT NG STOREHOUSE MOST PROBABLE INITIATION LOCATION

- NORMAL OPERATIONS REQUIRED MANUAL HANDLING OF NG
- EYEWITNESS OBSERVED "STREAK OF LIGHTNING" COMING TOWARDS THE NITRATION HOUSE FROM THE STOREHOUSE ALONG THE NG CONDUIT

1071

FIG. 10

NG STOREHOUSE
INITIATION CATEGORIES

- ACT OF GOD
- HUMAN FACTORS
- EQUIPMENT FAILURE

FIG. 11

1072

ACTS OF GOD

- WEATHER - WIND, RAIN, LIGHTNING
- OPERATOR ILLNESS - BLACKOUT, CONVULSION, HEART ATTACK
- SABOTAGE

1073

FIG. 12

HUMAN FACTORS

- DROPPED BUCKET CONTAINING NG
- DROPPED DIPPER INTO NG STORAGE TANK
- STRUCK SIDE OF STORAGE OR CATCH TANKS
- DROPPED NG SAMPLE DIPPER OR BOTTLE

1074

FIG. 13

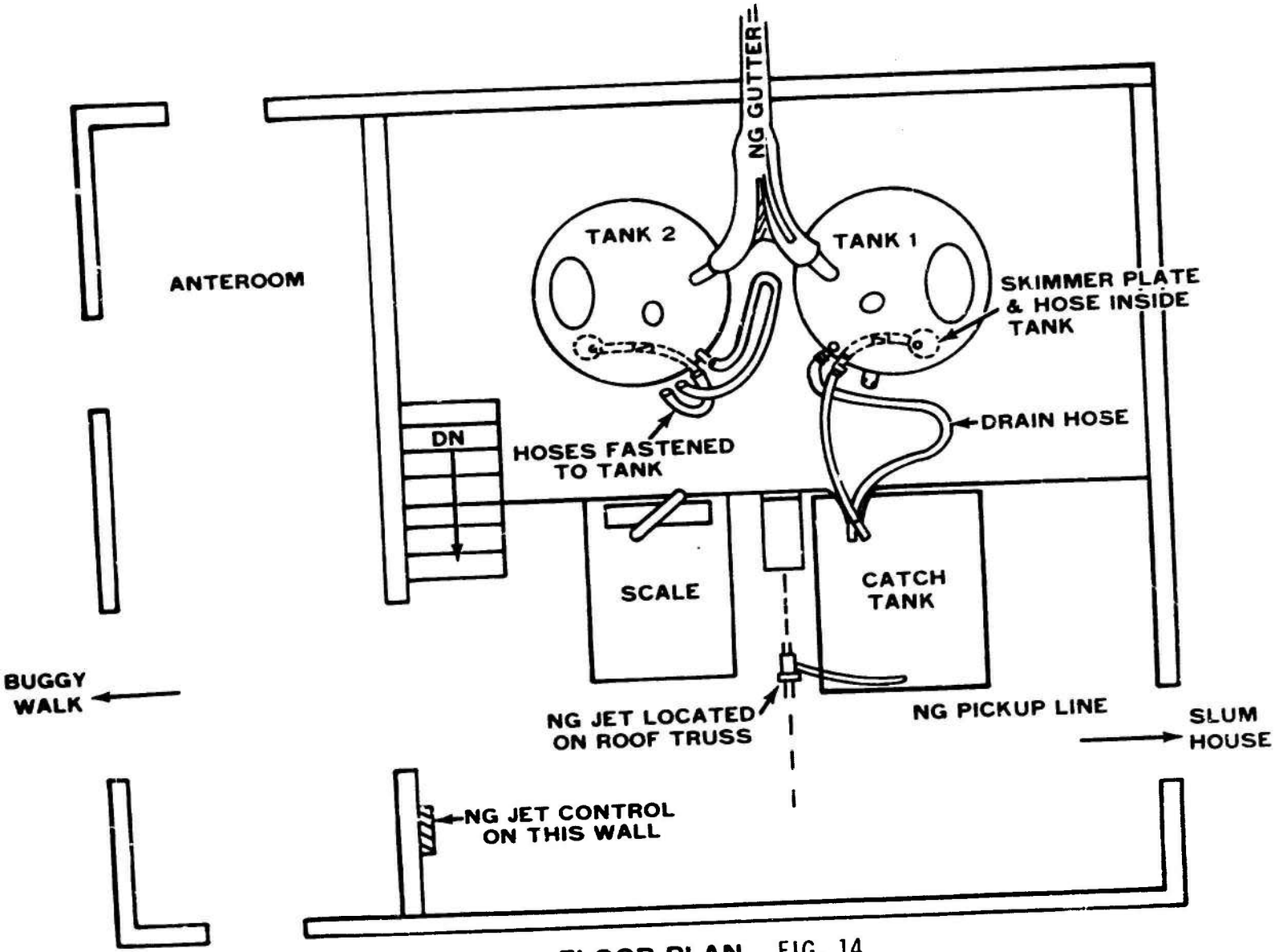

FLOOR PLAN FIG. 14



FIG. 15 : READY TO SAMPLE (AIR AGITATOR IS NOT ON).



FIG. 16 : HOSES ON FLOOR
(LOOKING TOWARD OPERATOR IN EXHIBIT



FIG: 17 : DESCENDING STAIRS.

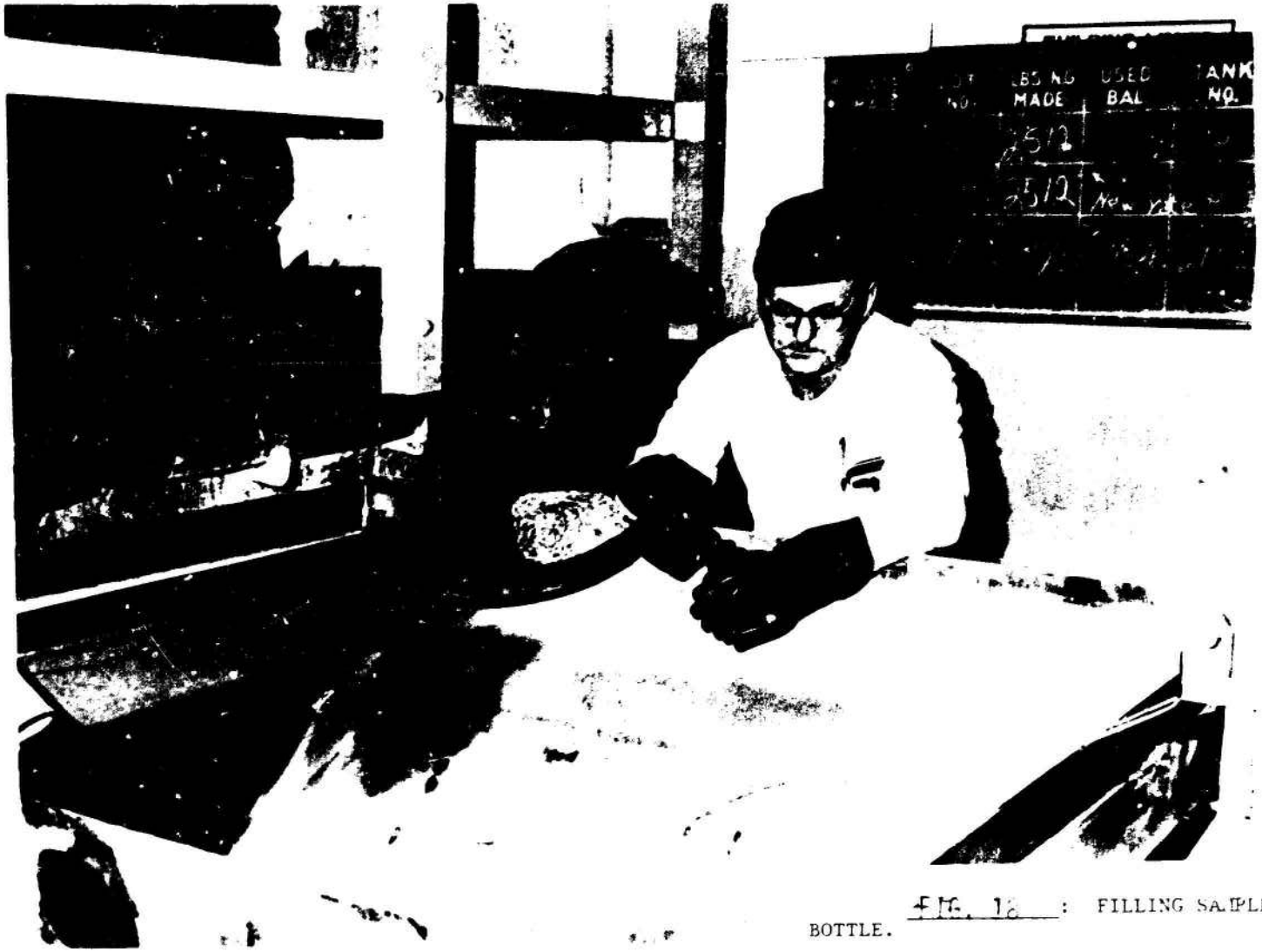

FIG. 12 : FILLING SAMPLE BOTTLE.

INITIATION POSSIBILITIES ANALYZED

- SAMPLE DIPPER
  - (1) ACCIDENTALLY DROPPED
  - (2) SWUNG LATERALLY AND IMPACTING A SOLID OBJECT
  - (3) THROWN FORWARD AS THE RESULT OF A TRIP OR FALL
- SAMPLE BOTTLE DROPPED

1080

FIG. 19

ANALYSIS RESULTS

- OPERATOR SLIPS/TRIPS AT SAMPLING STATION
- SAMPLING DIPPER IS THROWN FROM OPERATOR'S HANDS
- DIPPER IMPACTS EDGE OF STAINLESS STEEL CATCH TANK
- DIPPER FREE FALLS MINIMUM OF 8.6 FEET
- AVAILABLE IMPACT ENERGY CAPABLE OF INITIATING NG

1081

FIG. 20

EQUIPMENT FAILURE

- DROP PLUG ASSEMBLY
- EQUIPMENT GROUNDS
- NG RECOVERY JET

1082

FIG. 21

NG JET SYSTEM

- JETS HAVE BEEN IDENTIFIED AS CAUSE OF SIMILAR NG INCIDENTS
- FRAGMENTS OF CATCH TANK INDICATED POSSIBLE CONTACT WITH DETONATING NG
- EVIDENCE THAT NG JET WAS IN OPERATION AT THE TIME OF THE INCIDENT

1083

FIG. 22



FIG. 23 : FRAGMENTS OF INSIDE CATCH TANK, NG STOREHOUSE #1, SHOWING PROBABLE EFFECT OF DETONATION OF NG AGAINST METAL.



FIG. 24 : FRAGMENTS OF OPERATING EQUIPMENT FROM NG STOPEHOUSE #1 FOUND IN AND ABOUT THE CRATER.

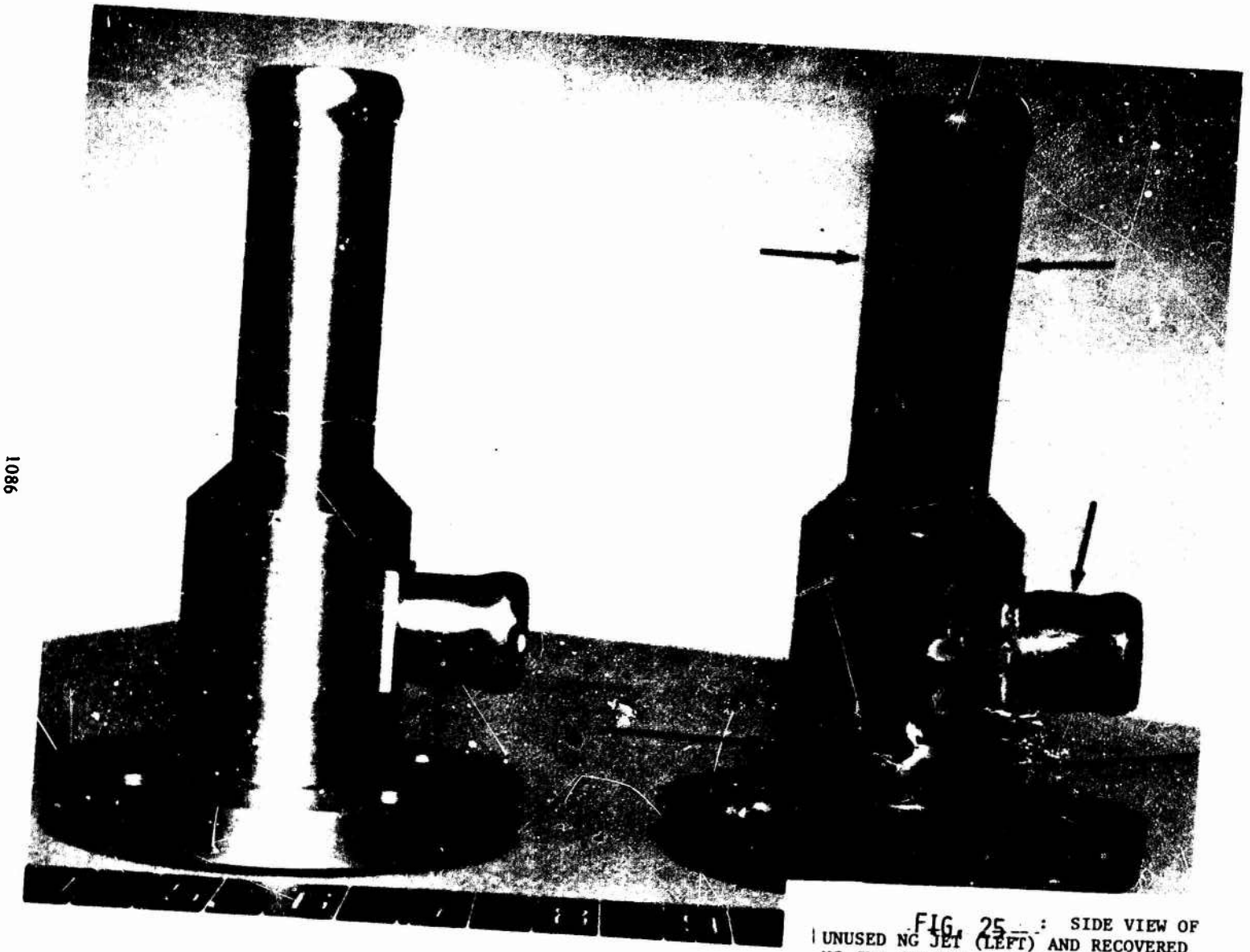

FIG. 25 : SIDE VIEW OF UNUSED NG JET (LEFT) AND RECOVERED NG JET (RIGHT). ARROWS SHOW DEFORMATION.

MOST PROBABLE CAUSE

EXPLOSION WAS CAUSED BY INITIATION OF NG IN THE JET SYSTEM USED TO TRANSFER NG FROM THE INSIDE CATCH TANK TO THE STORAGE TANK.

1087

FIG. 26

THE ACCIDENT WHICH OCCURRED AT

THE PONT-DE-BUIS GUN-POWDER FACTORY

ON 7TH AUGUST 1975

Mr. Jean Quinchon
Societe Nationale Des Poudres Et Explosifs
Paris, France

The Pont-de-Buis National Gun-Powder Factory in the department of Finistere was built in the reign of LOUIS XIV to supply the Brest naval dock-yards with gun-powder. From the end of the XIXth century onwards it was one of the establishments belonging to the French Government specialized in the manufacture of single-base powders and as a result of this connection it experienced intense activity at the time of the two World Wars. When it was incorporated into the Société Nationale des Poudres et Explosifs (National Propellants and Explosives Company) by the State in 1973, it was mainly producing single-base powders for ammunition for light and medium calibre arms and hunting rifle cartridges.

°
° °

On Thursday 7th August 1975, around 1.17 p.m., a series of explosions occurred in this powder-factory : unfortunately 3 workers were killed and 64 injured. The works were partially destroyed.

PRECEDING PAGE BLANK

Quite by chance, these explosions were recorded, thereby making it possible, afterwards, to reconstruct, to a certain extent, the likely sequence of events. A film was made six months after the explosion retracing the events leading up to the accident. It relied on this recording and on the various photos taken immediately after the accident.

(presentation of the film)

The exact causes of the accident have not yet been established. It is possible, however, to point out certain lessons we can learn from a complete study of the circumstances and consequences of this accident.

We will not dwell on the financial consequences of this accident for S N P E : setting right the damage, rebuilding the factory over a larger area and restoring output to its previous level, using modified processes, will have cost in all about 120 million francs (i.e. approximately 25 million dollars), only a small proportion of which was covered by insurance. This clearly confirms, solely from the economic standpoint, the extremely grave consequences of such an accident in an industry like ours and the need for ever-tighter safety measures.

The main lesson is that some single-base powders can explode by transition from combustion to detonation. It has long been known that powders can explode when subjected to sufficient priming, or to hot metal fragments at high speed. The Pont-de-Buis accident demonstrated that combustion, even in single-base powders, can degenerate into detonation once a certain critical confinement occurs. We have performed many tests ranging from the steel tube, several centimeters in diameter, up to hoppers or containers with several tons of single - or double-base powders. Processing these tests is a painstaking task which has not yet been completed. We can, however, now assert, that for each powder, there is, under defined operating conditions, a critical detonation height which must not be exceeded without accepting the risk. This critical height varies:

- firstly according to the nature of the powder i.e. its speed of combustion (but it also varies according to the degree of humidity and, to a lesser extent, the temperature)

- and secondly, with the type of confinement, i.e. the container's diameter, its shape and the mechanical resistance of the casing.

C H A R T 1

We thus strive, in every concrete case where our powders are manufactured or used, to determine the "critical confinement".

The second lesson is that from the damage noted at the time of these explosions, it has been possible to check out the validity of the information available on the material consequences of a detonation, providing it be considered that the detonation of 1 ton of single-base powder is equivalent in effect to that of approximately 0.6 ton of trinitrotoluene (T N T) : the damage caused at Pont-de-Buis by the initial explosion of 12 tons of single-base powder is, in actual fact, about the same as the damage which would have been caused by the explosion of 7 tons of T N T.

C H A R T 2

Until the Pont-de-Buis accident, the only risk taken into account in France in the manufacture of single-base powders was that of deflagration ; it had been measured that under these conditions the explosion of one ton of powder had effects equivalent to the detonation of 4 kg of T N T. It is confirmed here that the effects of a powder detonation are on a scale which is quite different from those of a deflagration.

The third lesson is that it does appear possible to shield oneself against the effects of a detonation, at least if one is at a sufficient distance from the heart of the explosion.

As the film shows, concrete of an adequate thickness, suitably reinforced by a specially designed metal frame, provides very good protection. On the other hand, old buildings (more than 50 years old), which were constructed of lower quality concrete over too large areas, had difficulty in resisting the shock-wave effects and collapsed.

C H A R T 3

Furthermore, the effects of the explosion of the dryers show that, before being destroyed, the walls of the dryers were able to deflect the effects of the detonation in preferential directions.

When it is not possible to guarantee the absence of detonation, appropriate safety-measures (distance, protection, barricades, etc...) are now taken.

° ° °

More and more often, however, we try to work in "intrinsic" safety, i.e. we try to make sure that we can avoid the risk of detonation through detailed knowledge of the pyrotechnical behaviour of the products manufactured, at every stage of their production and through an exhaustive study of the safety of the process.

A major research effort is required to reach this ambitious goal, including life-size explosion tests in a suitable setting. Every year we set aside a large amount of our budget for this purpose.

Dr Jean Q U I N C H O N
Directeur Sécurité Environnement

Pierre FONTAINE
Chef du Service Technique
Sécurité Environnement.

CRITICAL HEIGHT OF DETONATION (in meters)

Powders	Steel tubes	
	Ø 82.5/88.9 mm	Ø 200/202 mm
Single-base, non porous.	> 1	> 1.8
Double-base	0.15 - 0.25	0.3 - 0.4
Ball Powder	015 - 0.25	0.7 - 0.8
Single-base porous		0.5 - 0.9

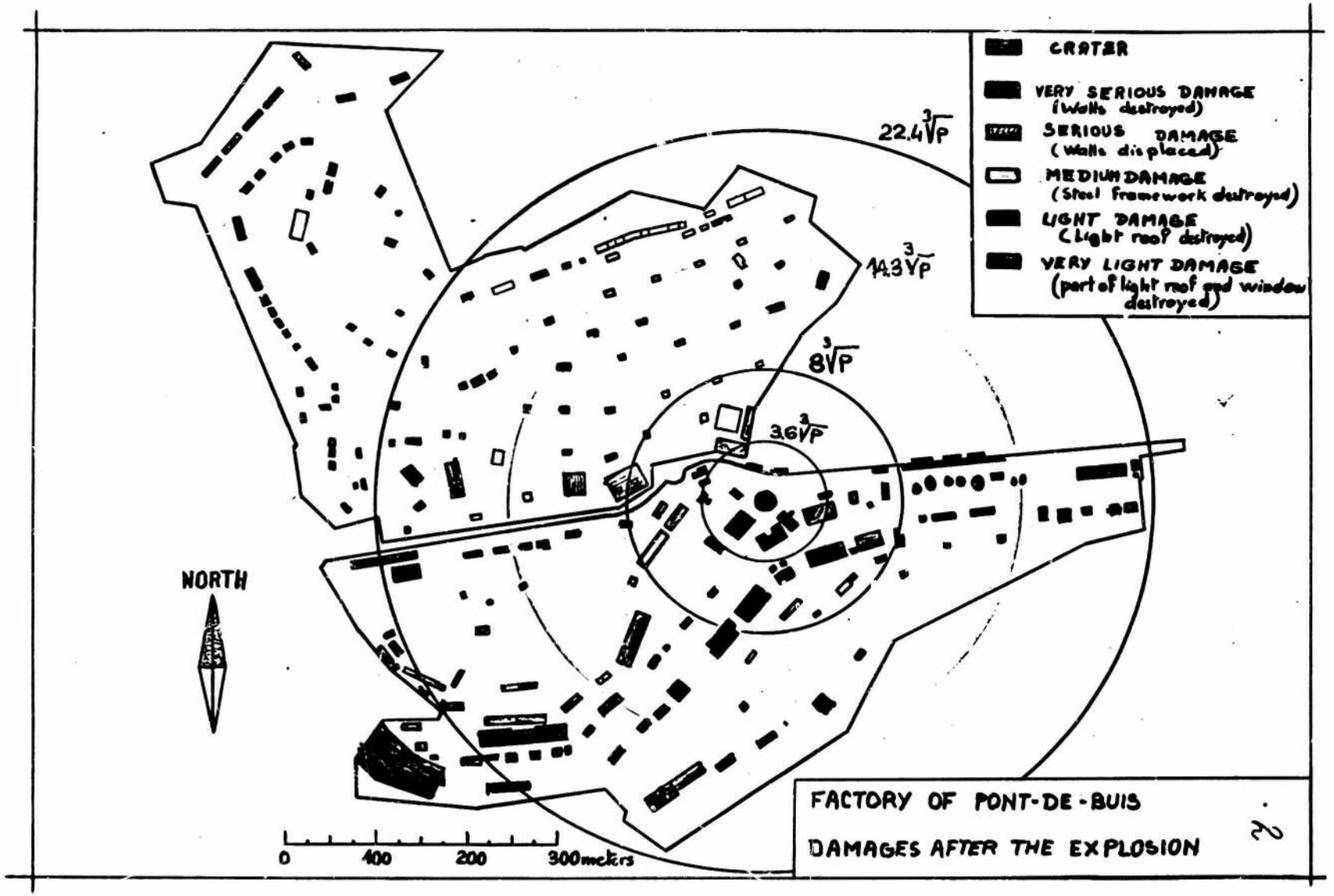
GRATER
VERY SERIOUS DAMAGE (walls destroyed)
SERIOUS DAMAGE (walls displaced)
MEDIUM DAMAGE (Steel framework destroyed)
LIGHT DAMAGE (Light roof destroyed)
VERY LIGHT DAMAGE (part of light roof and window destroyed)
22.4 ∛P
14.3 ∛P
8 ∛P
3.6 ∛P
NORTH
0
400
200
300 meters
FACTORY OF PONT-DE-BUIS
DAMAGES AFTER THE EXPLOSION
2

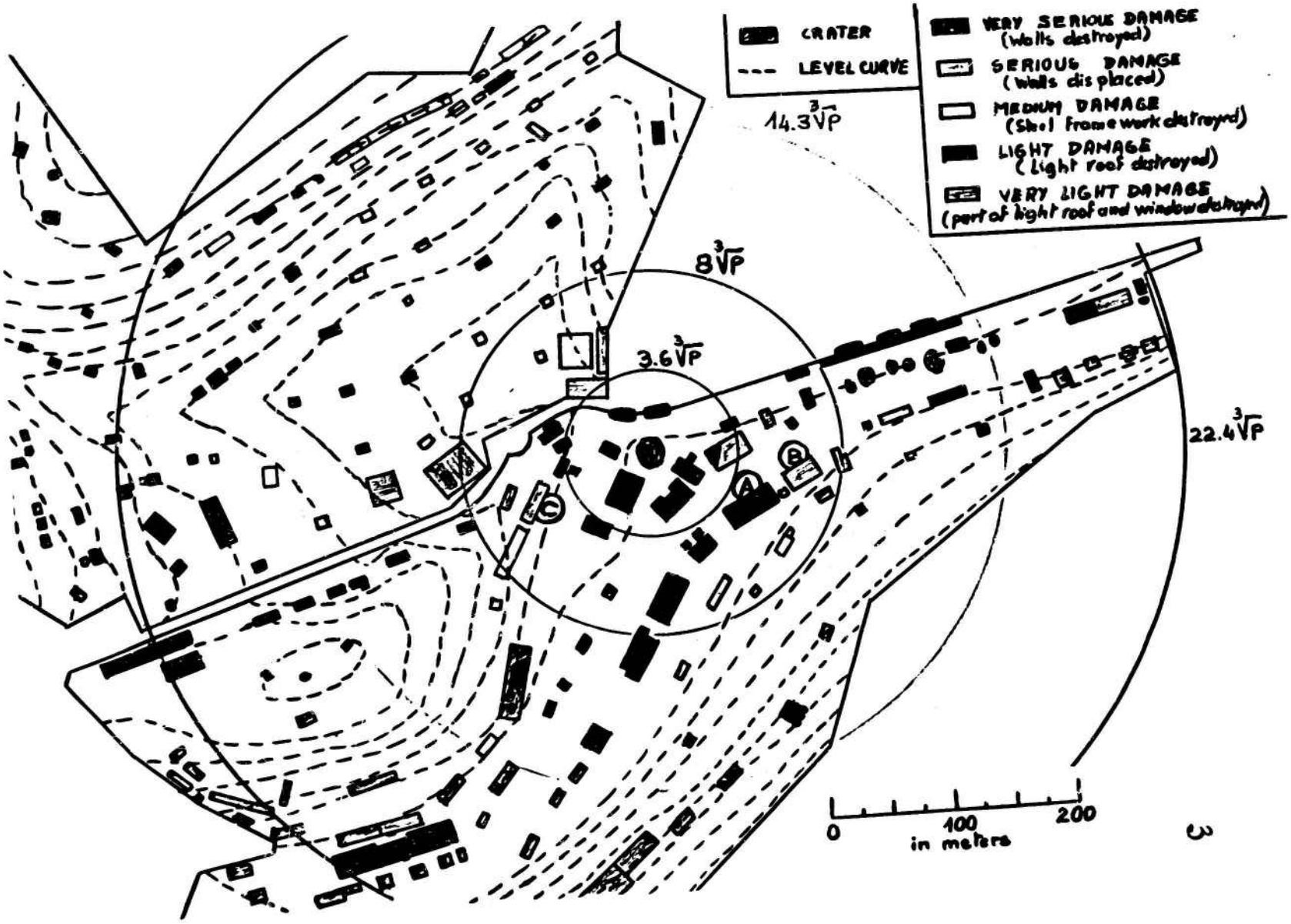
CRATER
LEVEL CURVE
VERY SERIOUS DAMAGE (walls destroyed)
SERIOUS DAMAGE (walls displaced)
MEDIUM DAMAGE (Steel frame work destroyed)
LIGHT DAMAGE (Light roof destroyed)
VERY LIGHT DAMAGE (part of light roof and window destroyed)
14.3∛P
8∛P
3.6∛P
22.4∛P
0
100
200
in meters

EXPLOSIVE INCIDENT DURING DEMOLITION GROUND OPERATIONS

Mr. Melvin R. Bailey
DARCOM Field Safety Activity
Charlestown, Indiana

Members and guests of the DoD Explosives Safety Board. It is a pleasure to address you today. The purpose of this discussion is to present a brief review of an accidental explosion involving M55 stab detonators at a demolition ground.

At approximately 1100 hours on 24 March 1977, an explosion occurred in the demolition area at one of the DARCOM depots. Approximately one week prior to the incident, the Army depot received a letter from a POPO plant indicating that 31,975 reject slider assemblies containing M55 detonators and loaded in aluminum tubes were being sent to the depot for demilitarization in accordance with Section J of Contract DAAA-0976-C-0089. The slider is a component of the M223 fuze which is used on M42 and M46 grenades that are the submunitions for the M483, 155MM projectile.

The detonators are received in nonpropagating packs from an Army ammunition plant and staked in the slider. After this operation the sliders are loaded into the aluminum tubes which are a rectangular cross section ($\frac{1}{2}$ inch wide by $1\frac{1}{2}$ inches high and 40 inches long). The loaded tubes are then transferred to another part of the process where they are used as slider assembly dispensers during fuze assembly manufacture (see Figure 1). The tubes containing slider assemblies received for demil were from various lots and had been rejected for a number of reasons, the most prevalent of which involved an unsatisfactory stake. The means by which the ends of the tubes were closed varied. A typical means employed masking tape on one end and an ordinary spring-type paper clip ($1\frac{1}{4}$ inches in width) on the other end. The clip was located in such a fashion as to allow the detonator end of the slider to protrude beyond the end of the tube.

The dispensers were transported by POV, a carryall-type van, to the depot. Apparently the tubes were lying about loosely in the cargo compartment (see Figure 2). Personnel at the gate noted that the vehicle had neither explosives placards nor fire extinguisher and refused entry until this could be corrected. The material was then transported to a building which is used for storage of material received from posts, camps, and stations. The tubes were then moved to the Demolition Ground along with a work order for their disposal provided by Maintenance Planning.

PRECEDING PAGE BLANK

Lacking a specific procedure other than the general demolition SOP which does not discuss destruction of this item, it was decided by the demolition foreman to remove the clip and dump the slider into an empty wooden ammunition box. Once the box became full, it was to be removed from the vicinity of a holding barricade and taken to a pit where it would be detonated.

Four men were assigned to the job, two of them were to hand the tubes to the other two who were to then remove the clip and dump the items into the box.

The operation had proceeded for some time (estimates of the number of sliders in the wooden box ranged from 2,000 to 20,000) when one of the men indicated that as he removed a clip from a tube, a detonation occurred. This individual and the man next to him received ruptured eardrums, burns over a large portion of their bodies, and eye damage. Both required eye surgery and were listed in serious condition. The injuries received by the other two men involved primarily eardrum rupture (see Figures 3 and 4).

Subsequent review at the site of the explosion revealed that clip removal was taking place approximately 50 feet from an explosive building which contained 108, 3.5-inch HE loaded warheads locked in a MILVAN and awaiting destruction. Slider assemblies were thrown an estimated 100 yards in all directions from the scene of the explosion. Bits of clothing and the remains of exploded slider assemblies were noted in the area. In addition, even though EOD personnel had reportedly cleared the area of all live items, several undetonated sliders and at least one loaded tube were noted.

CAUSES:

Direct Cause: Unknown

Possible Causes: The initial explosion could have occurred while removing a metal paper clip from the end of an aluminum tube when a detonator in a slide assembly was protruding from the end of the tube.

The explosion could have occurred when the slides and detonators were being placed into the box with the other detonators.

The explosion could have been caused by rough handling of the detonators.

REMARKS:

The aluminum tubes were not considered to be a non-propagating package for storage, transportation or handling purposes. The slide assembly with M55 detonator could be exposed past the end of the tube if the spring paper clip was not properly placed.

The slide assemblies, with the M55 detonator installed, were received from a privately owned, privately operated contractor activity that had requested the installation to destroy the detonators and salvage the aluminum tubes. The slide assemblies had failed to meet quality requirements and had been rejected for various reasons.

Investigation revealed that none of the personnel performing the destruction operation were familiar with the characteristics of the explosives involved.

RECOMMENDATIONS:

Items, or components of munitions containing explosives, should be carefully researched as to explosives characteristics prior to determining the disposal method. Disposal methods for the specific item or component should be incorporated into a Standing Operating Procedure that is sufficiently comprehensive to preclude unsafe handling or disposal procedures. (Reference paragraph 16-25, AMCR 385-100)

Personnel employed at the destruction area must be thoroughly trained regarding the nature of the materials handled, the hazard involved, and the precautions necessary. (Reference paragraph 27-13b, AMCR 385-100)

Incoming motor vehicles loaded with explosives, ammunition or other hazardous materials should be carefully inspected in accordance with AR 55-355, using DD Form 626, and positive action taken for unsatisfactory or unsafe shipments. (Reference paragraph 22-10, AMCR 385-100)

Review abstract report number ES-42, which refers to destruction of explosive items unfamiliar to the demolition crew.

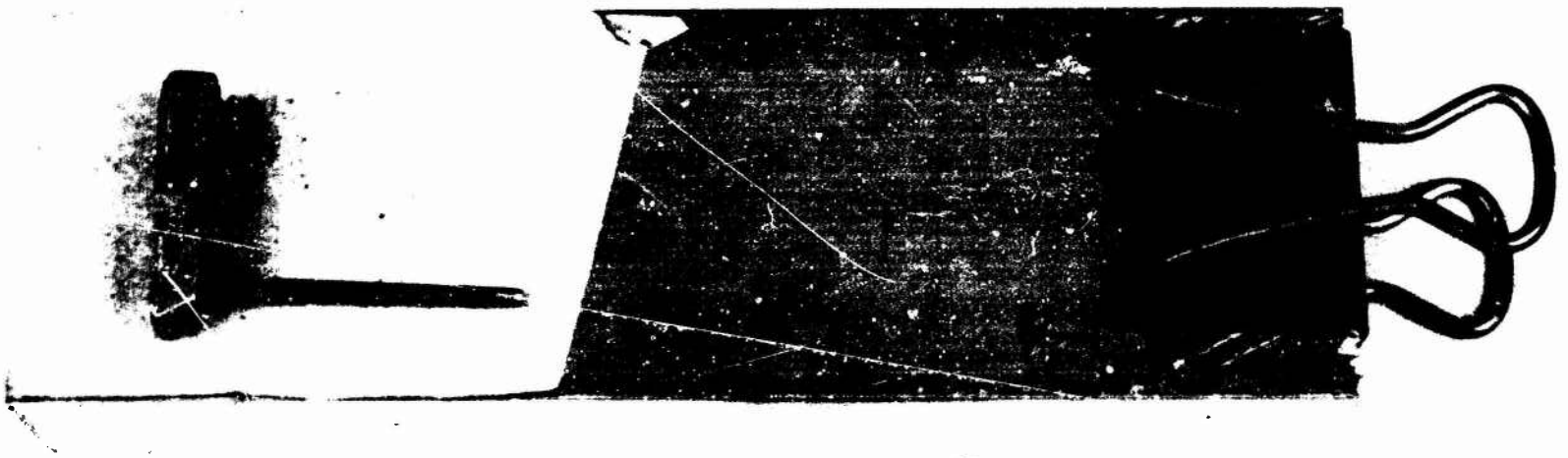



M55 STAB
DETONATOR



SLIDE
ASSEMBLY

METAL
PAPER CLIP

Figure 1



Figure 2



Fipure 3



Figure 4

Simplified Approach for Design of Buildings Containing Accidental Explosions

By Washington T. Char

US Army Corps of Engineers
Huntsville Division

In design of buildings, the designer is concerned with numerous building loads. Primary loads are live loads from people, vehicles, equipment and other movable objects. Earthquakes, wind and snow provide other sources of building loads let alone the building dead weight. In accidental chemical explosions, we encounter three effects: fireball, fragments, and airblast. Airblast phenomenology is the more complex and unique of these effects and is addressed in our designs.

Three common forms of protection are barricades, containment structures, and shelters. The primary purpose of barricades is to provide protection against fragments. Barricades offer some reduction of pressure, therefore separation, but this amount is not significant. Fig 2 (a) and (b) show differences in distance. Containment structures and shelters offer the greatest reduction in pressure and accordingly separation. Fig 2(c) shows no significant separation when explosions are fully or partially contained.

Present building separation criteria provide specific distance between source of explosion and building. However, when a barricade is included, this distance may be reduced by half. See Fig 3(a) and (b).

The advantage of hardened buildings is savings in real estate and facility costs. The disadvantage is the additional building cost for

PRECEDING PAGE BLANK

hardening. Although the advantages and disadvantages are worthy of mention, the main purpose of this paper is to demonstrate that buildings can be designed with reasonable simplicity to contain explosions. Before proceeding, we should examine the technical factors that must be considered in the design.

One factor is the jump associated with flexible expanding object resting on ground. As a box shaped object with relatively thin walls rapidly expands from an internal explosion, it will distend approaching a sphere. In the process, it reacts against the ground and lifts itself upwards or jumps off the ground. See Fig 4(a). To minimize the jump, the base is stiffened. Fig 4(b) shows the thickened base. To prevent vertical movement, in addition to stiffening the floor, the charge should be located nearer the floor than to the roof and footings should be buried deeper as illustrated in Fig 5(a). A more viable solution is to provide a small space or egg crate-like material between the floor and ground. Fig 5(b) shows a reasonable space below the floor. The space should be adequate not to allow the floor to react against the ground during the explosion.

When designing the building footings, we need to know the footing loads resulting from the explosion. In most situations, the explosives will be located close to the floor resulting in a net downward force, Fig 6(a). The pressure time history of this net force is shown in Fig 6(b). Although the spring constant as shown in the model, Fig 6(c), includes the foundation wall, K_F for the foundation wall should be

ignored since the subgrade reaction of the soil is invariably significantly larger. Knowing the pressure time history and the subgrade reaction of the soil, the footing loads can be calculated by a common formula which we will see later.

In the same manner as before, because the charge is closer to the right wall, the net force will be to the right. This will cause overturning which will additionally load the right wall footings. The rationale for the net pressure time history and spring constants are shown in Fig 7(a), (b), and (c).

The walls, roof, and floor of a structure may be modeled as a rectangular slab, Fig 8(a). However, if the structure is long relative to its width or height, it may be modeled as a one foot strip rectangular frame or a fixed end beam, Fig 8(b). Larger buildings should be framed and modeled as shown in Fig 9.

Knowing the factors that go into the design of a building subjected to internal explosions, the designer should examine the types of blast loads. Blast loads are of two types: pressure and impulse. Fig 10(a) shows close-in external line-of-sight blast to the walls designated by (1). These are impulsive loads. The load to the far wall designated by (2) is an incident pressure. Fig 10(b) shows an internal explosion. The load on the inside wall is a combination of a reflected impulse and incident pressure. This incident pressure is long time pressure, which is often referred to as a quasi static pressure as opposed to a static pressure which does not decay. Buildings containing internal explosions see this type of loading.

Associated with every loading function is a resistive function. The resistive function for most ductile materials can be depicted in the elastic, plastic and strain hardened ranges in a stress-strain relationship. A typical stress-strain diagram is shown in Fig 11(a). Since our designs are allowed to go plastic, we are only interested in the first two ranges: elastic and plastic. Fig 11(b) shows an idealization of the elastic-plastic bilinear resistive function.

There is a well defined relationship between the work done by external loads and the energy absorbed by structures. The relationship is expressed in an equation composed of the basic parameters from the loading and resisting functions as shown below and depicted in Fig 12.

$$\left(\frac{\frac{C_1 P_r}{r_y}}{\frac{r_m}{\pi t_1}\sqrt{2\mu-1}}\right)^2 + \frac{\frac{C_2 P_r}{r_y}}{\frac{r_m}{\pi t_2}\sqrt{2\mu-1} + \frac{1-\frac{1}{2\mu}}{1+0.7\left(\frac{r_m}{t_2}\right)}} = 1$$

This formula can be further simplified when the second pulse is static (no decay in pressure). See Figure 13.

$$\left(\frac{\frac{C_1 P_r}{r_y}}{\frac{r_m}{\pi t_1}\sqrt{2\mu-1}}\right)^2 + \frac{\frac{C_2 P_r}{r_y}}{1-\frac{1}{2\mu}} = 1$$

Obviously, because the pressure remains, the loading is more severe. Accordingly, a more conservative design results. This approach is more desirable and recommended, considering the inherent variance in design assumption and construction quality and workmanship.

Where openings in Walls occur, the appropriate design procedure is the yield line method. Fig 14 suggests that yield lines occur from corners of the wall to corners of the door. This is invariably the situation and the designer should include this in his first trial. Openings less than five percent of the gross area of the slab may be ignored; however, the rebars which would have gone through the openings should be located at the sides of the openings. As would be expected openings should not be located in the highly stressed areas.

In the appendix is an example problem that illustrates the approach discussed. The purpose of this example is to show the unique features of the design and does not include methods and procedures considered common to the designer. The design of the footings and design of the walls with openings are infrequent encounters and are illustrated.

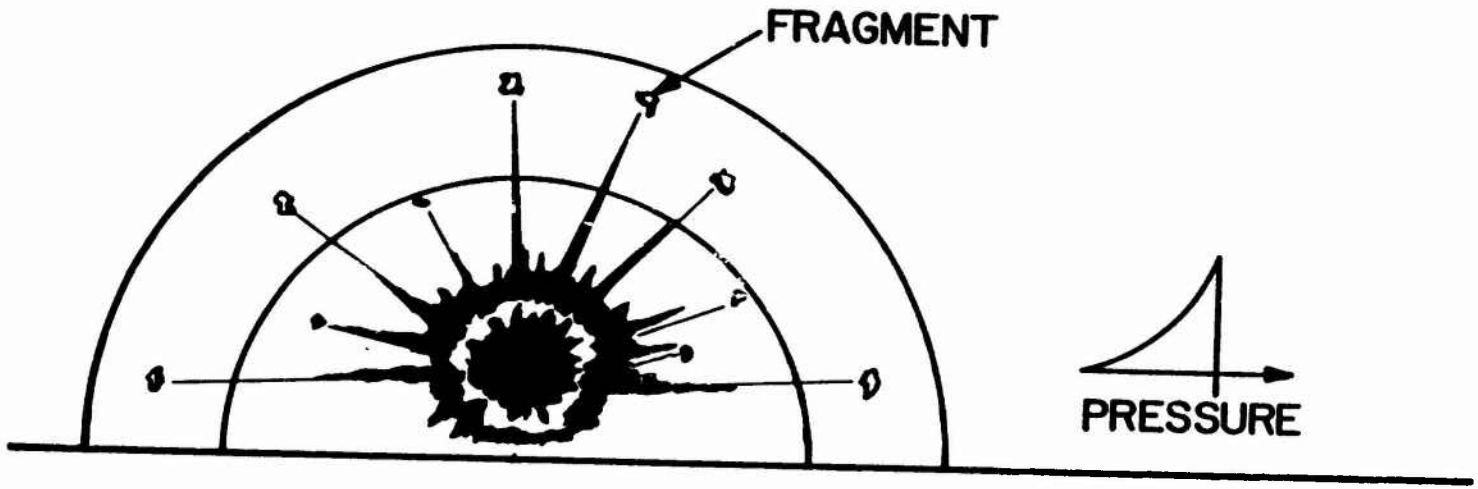

FREE FIELD BLAST ENVIRONMENT

FIG. 1

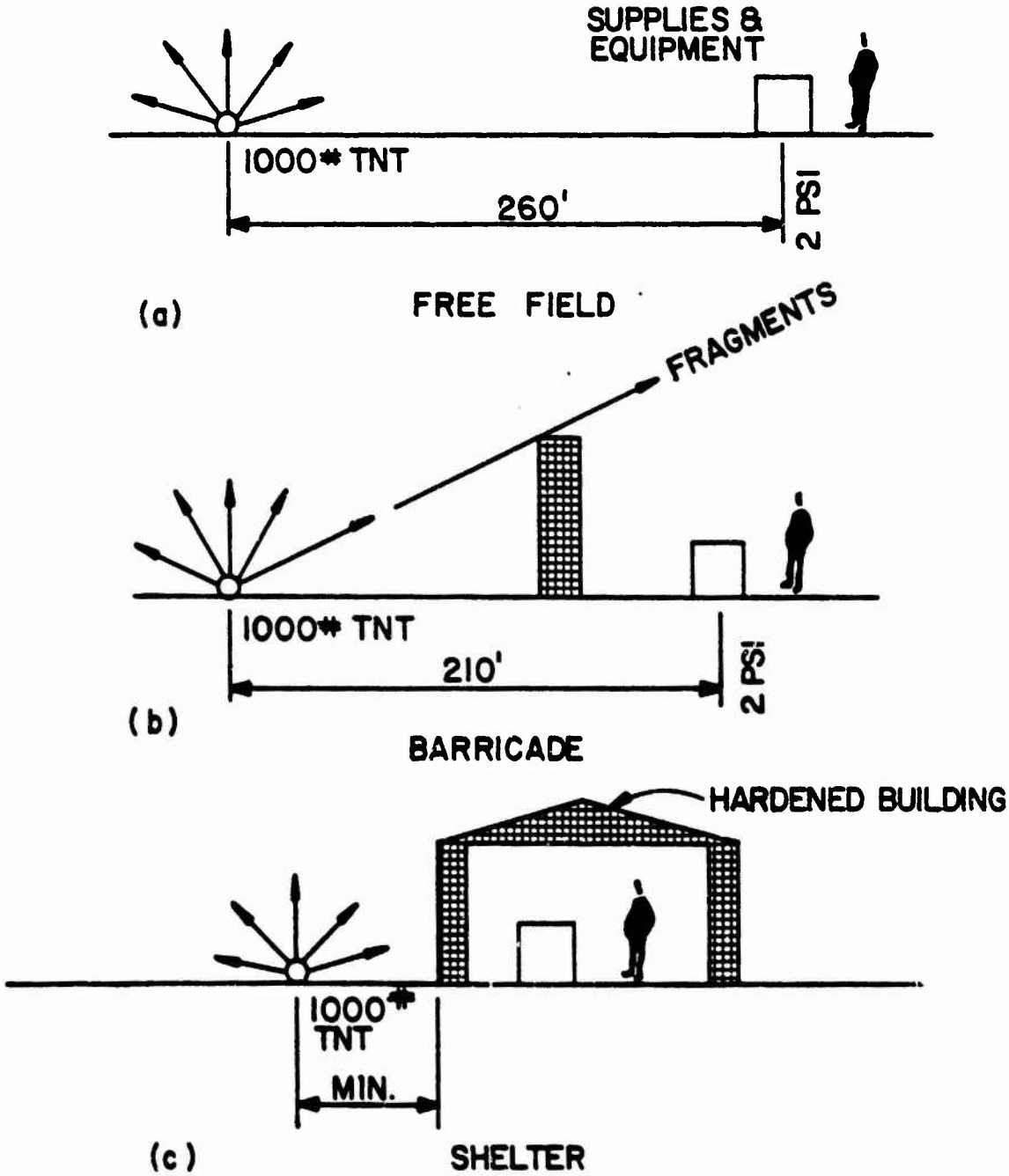

PROTECTION

FIG. 2

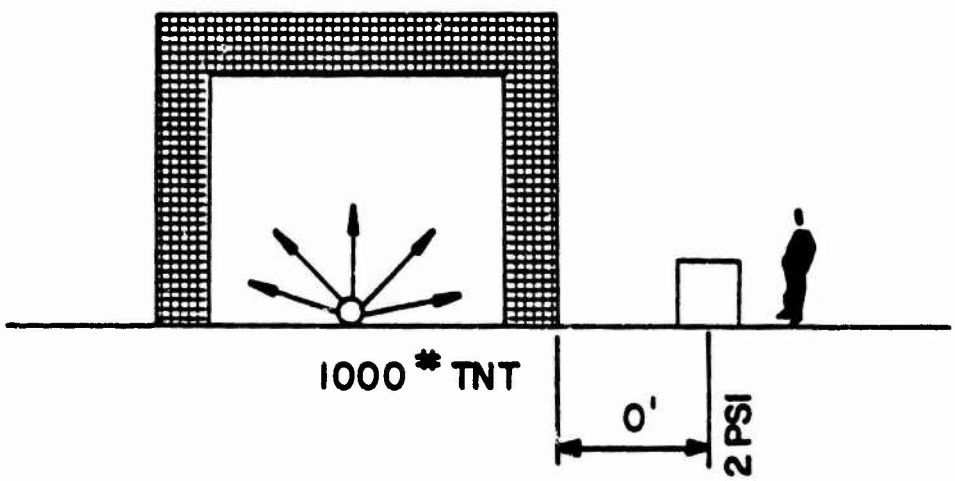

CONTAINMENT (SUPPRESSIVE SHIELDS)

FIG. 2 (b)

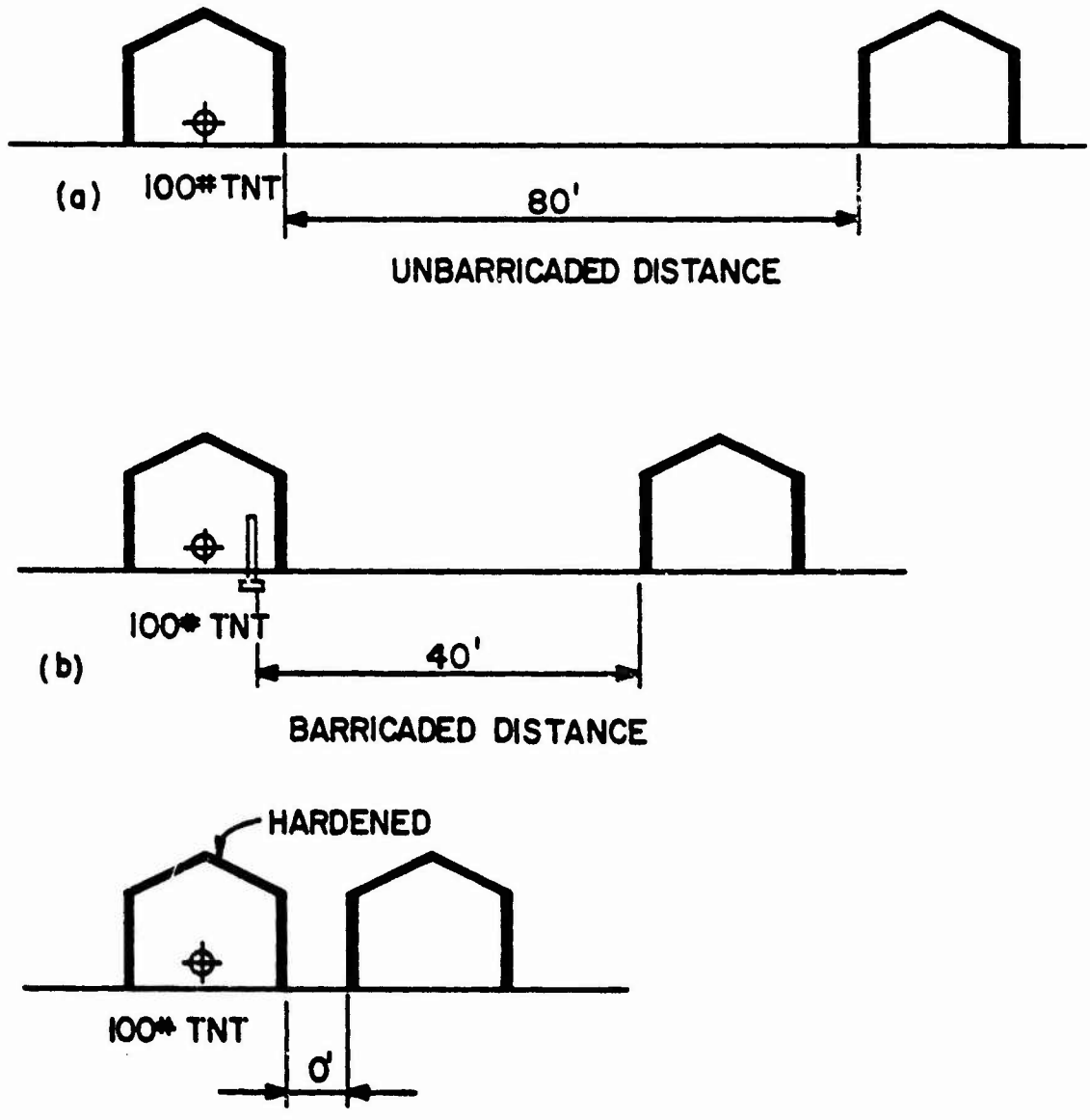

BARRICADE

FIG. 3

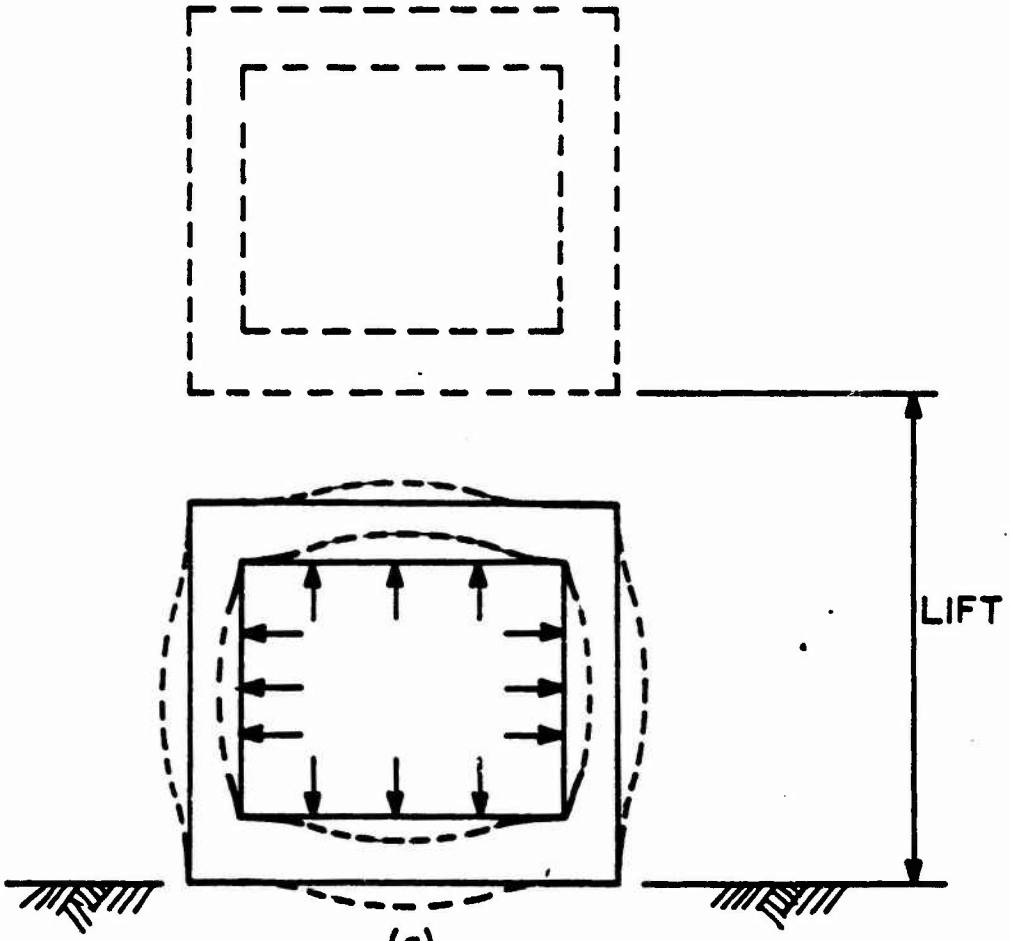

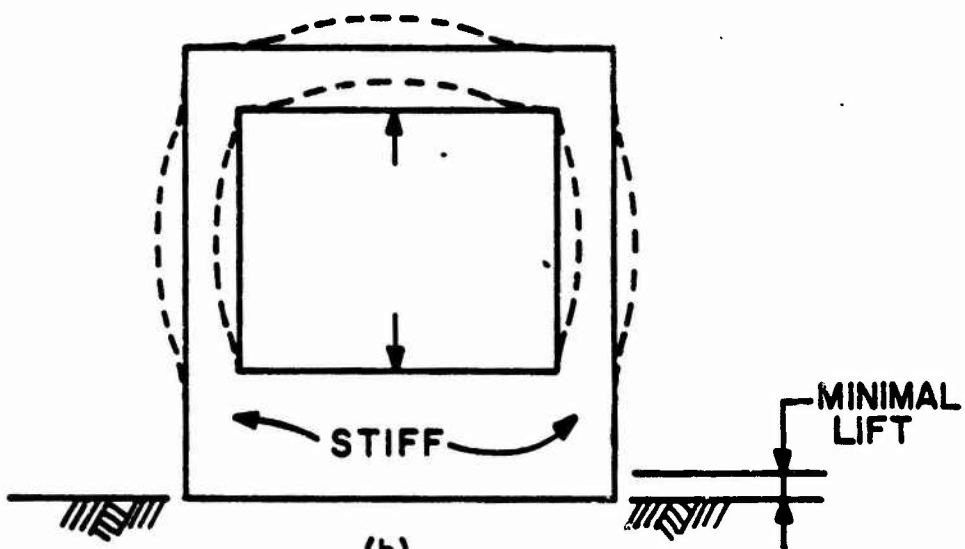

LIFT CAUSED BY MODIFIED CONFIGURATION

FIG. 4

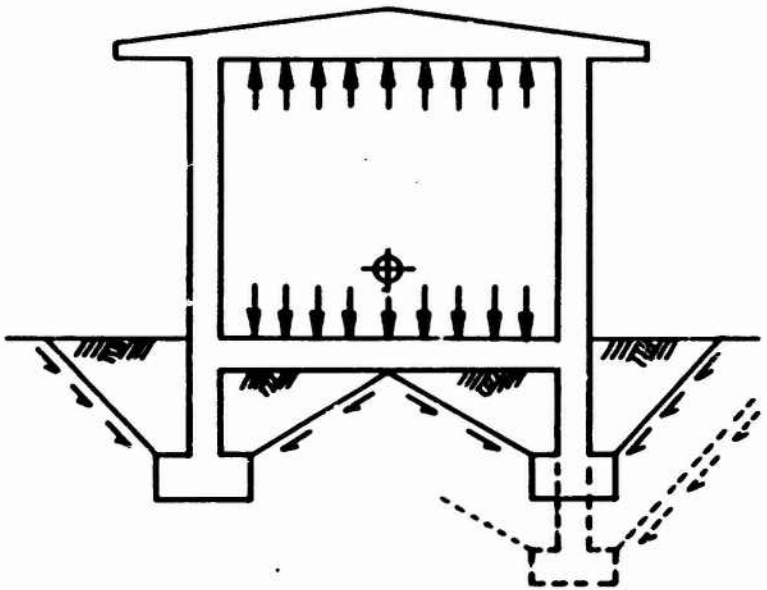

LIFT

(a)

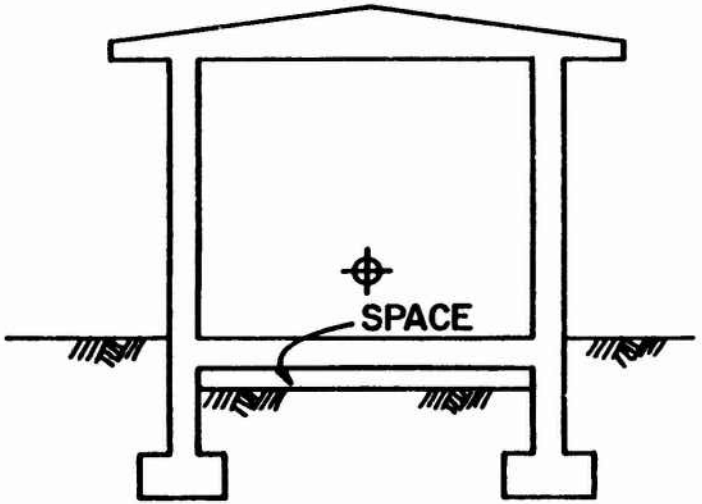

NO LIFT

(b)

PREVENT LIFT

- STIFFEN FLOOR
- LOCATE CHARGE NEAR FLOOR
- DESIGN FOOTINGS DEEP AND WIDE

FIG. 5

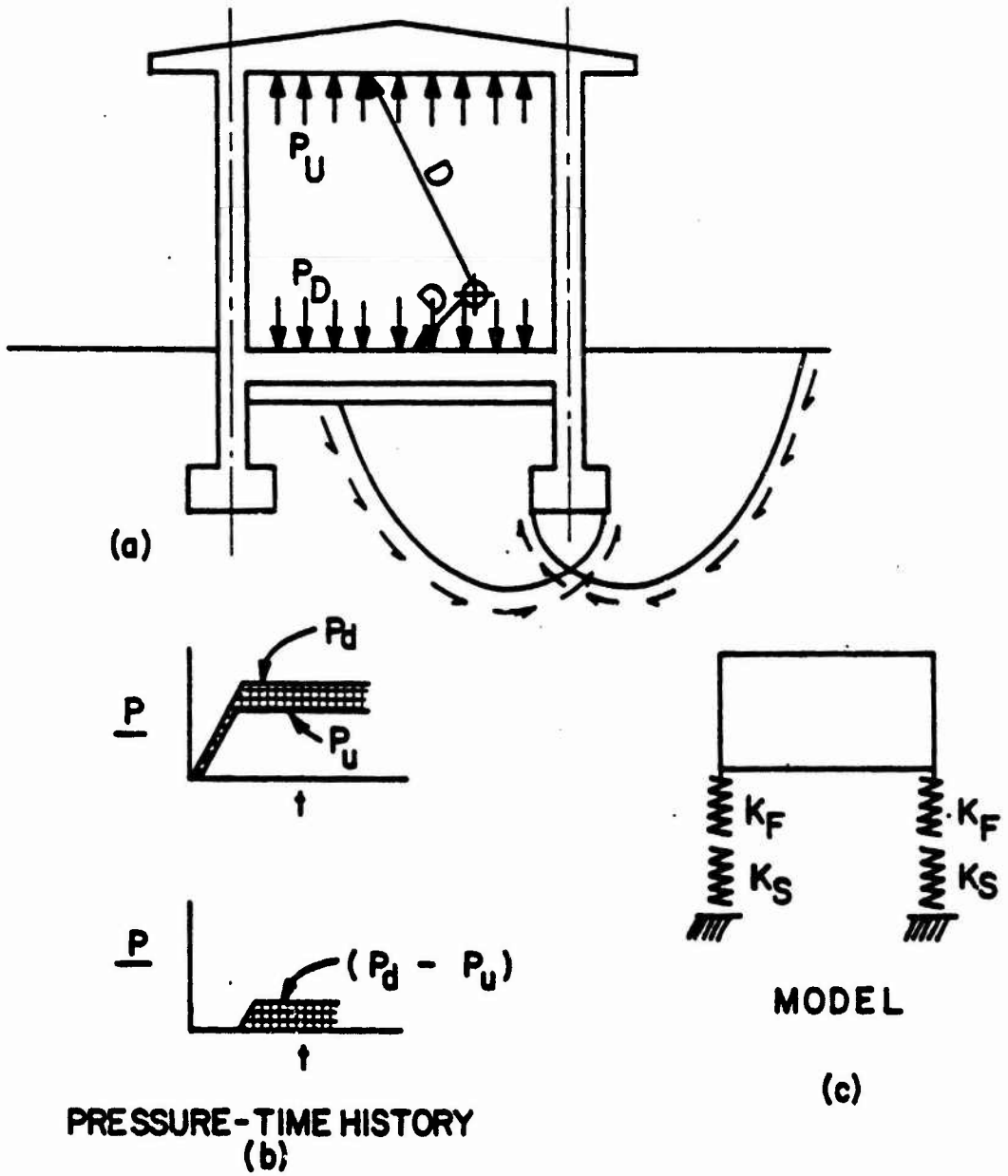

VERTICAL FORCE

FIG. 6

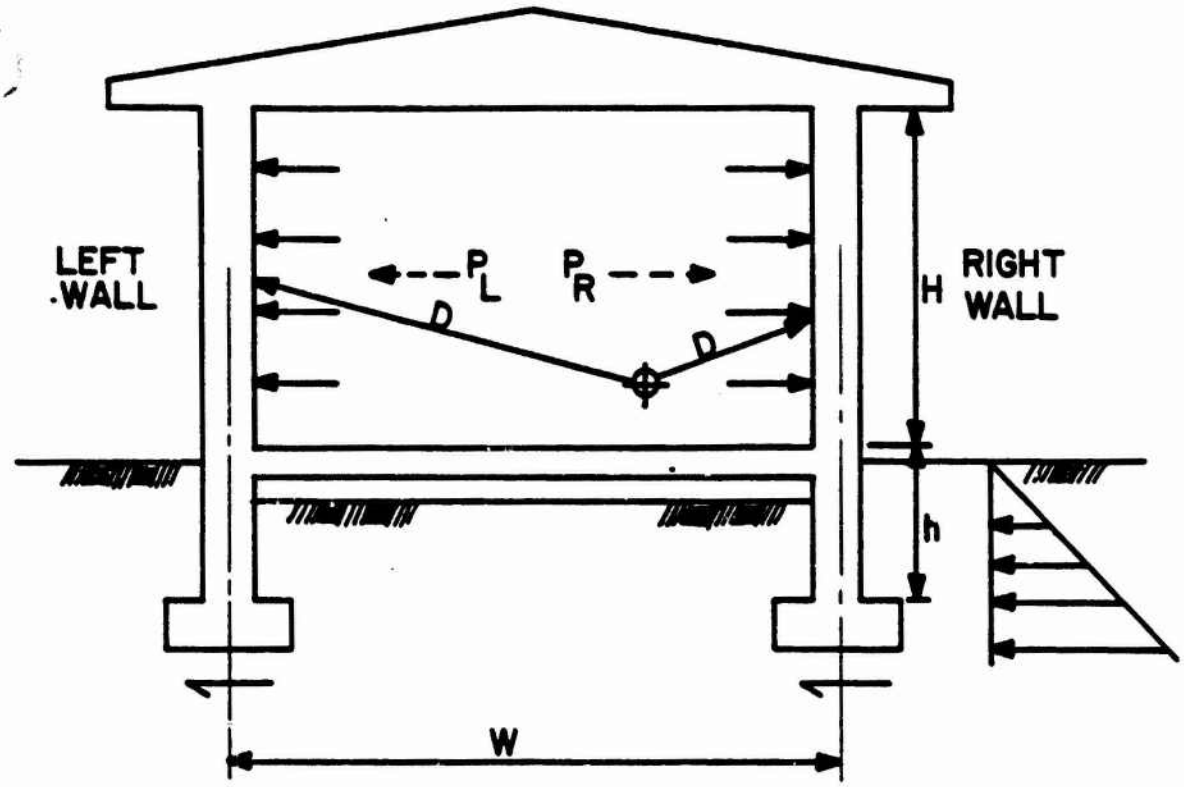

(a)

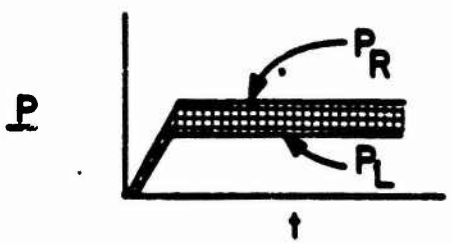

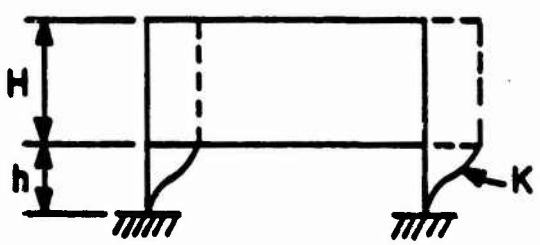

MODEL
(c)

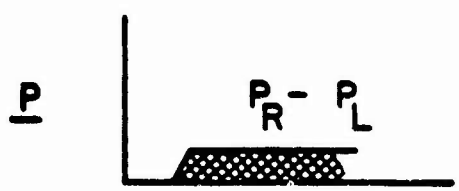

PRESSURE TIME HISTORY
(b)

LATERAL FORCE FIG. 7

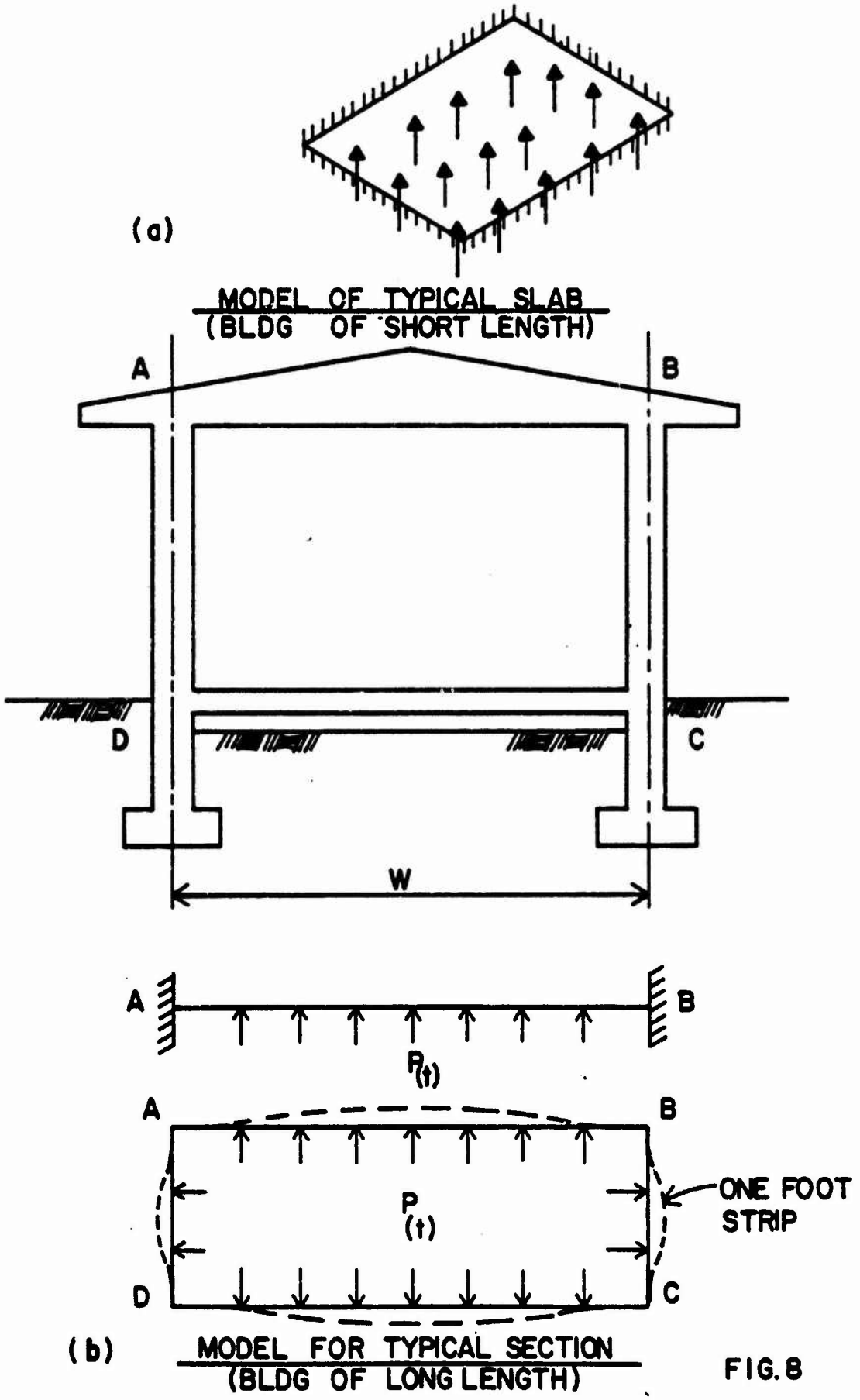
(a)
MODEL OF TYPICAL SLAB
(BLDG OF SHORT LENGTH)
A
B
D
C
W
A
B
R(t)
A
B
P
(t)
ONE FOOT
STRIP
D
C
(b)
MODEL FOR TYPICAL SECTION
(BLDG OF LONG LENGTH)

FIG. 8

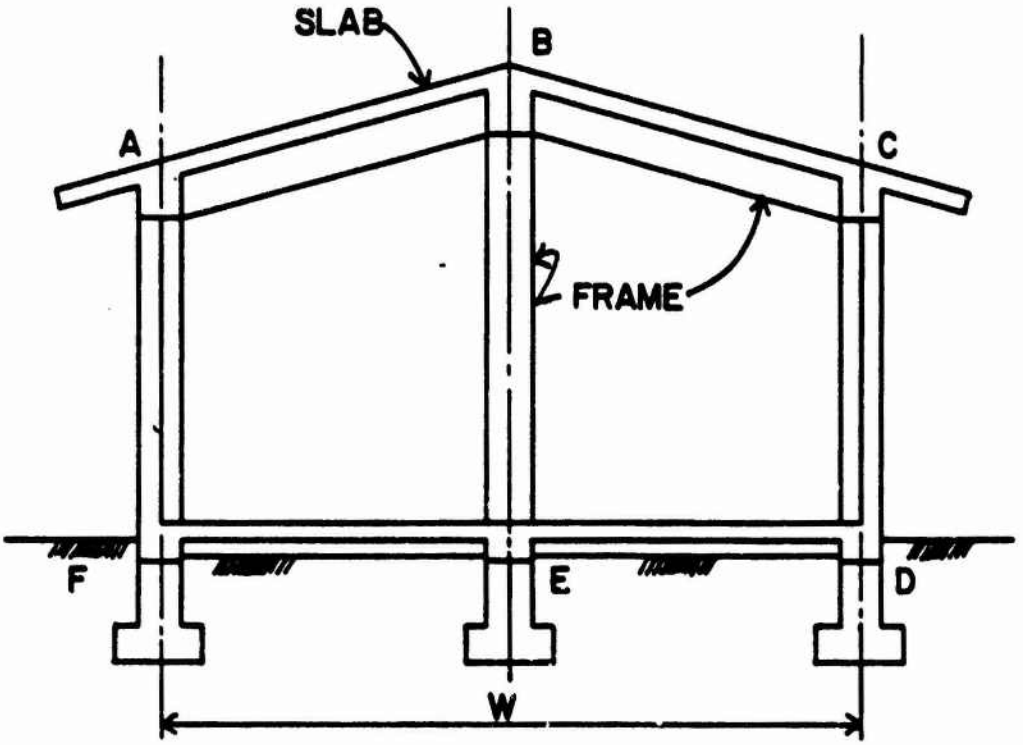

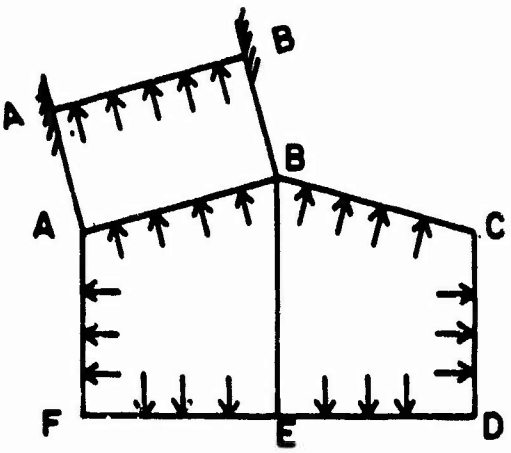

MODEL OF FRAME

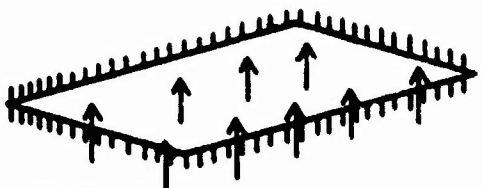

MODEL OF WALL, ROOF, FLOOR

FIG. 9

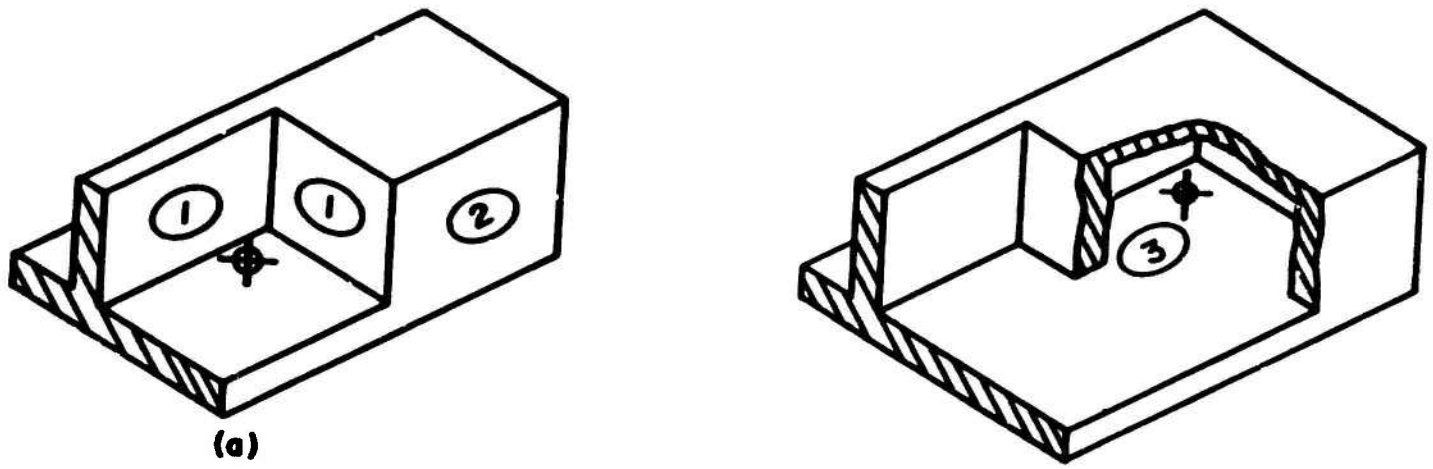

(a)

(b)

11.20

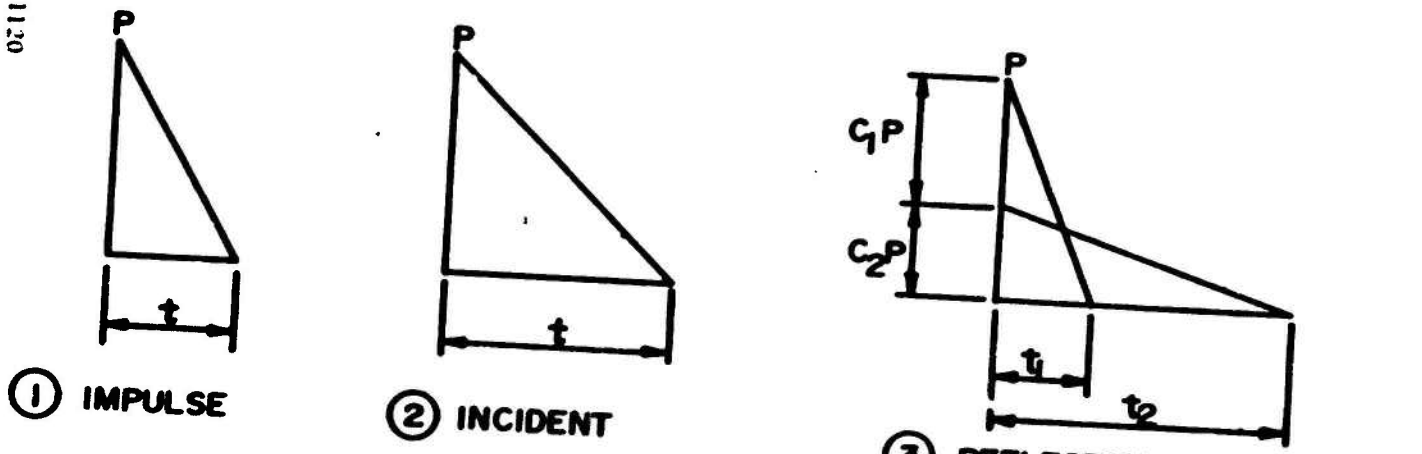

① IMPULSE

② INCIDENT

③ REFLECTION-QUASI STATIC

BLAST PRESSURES

FIG. 10

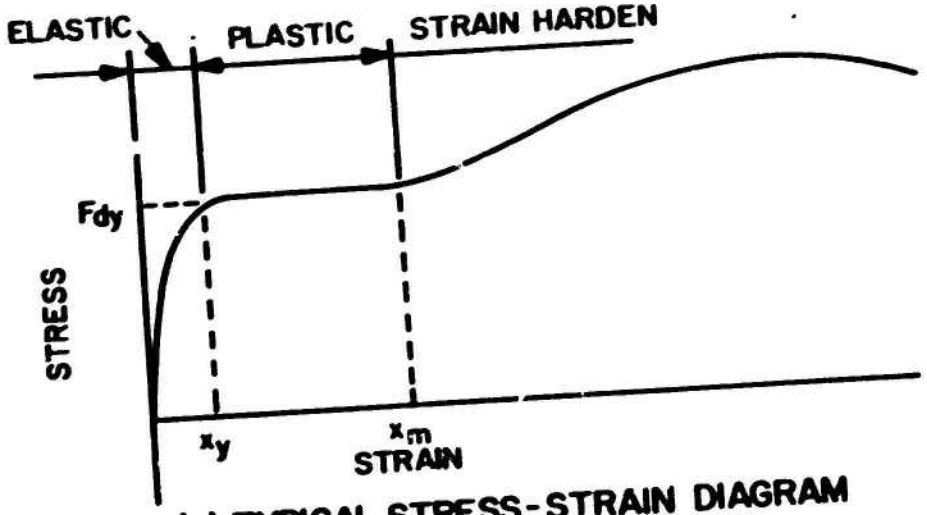

(a) TYPICAL STRESS-STRAIN DIAGRAM

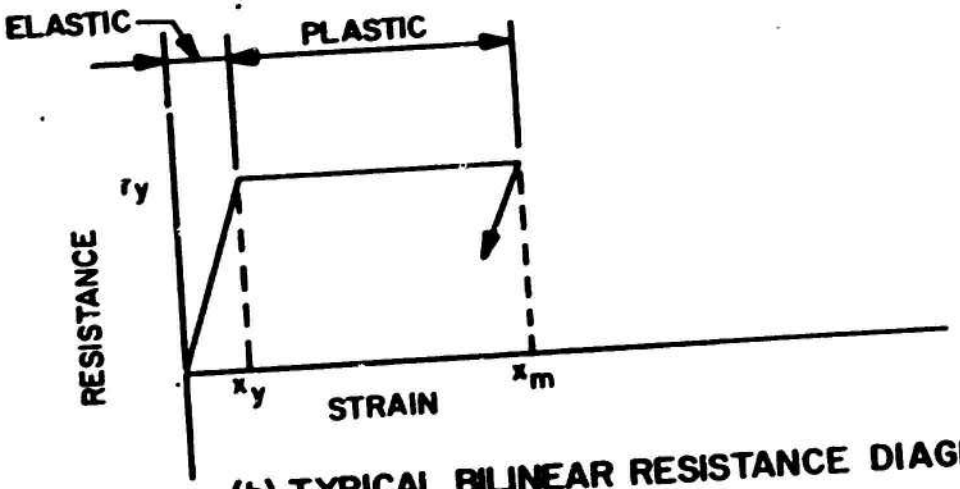

(b) TYPICAL BILINEAR RESISTANCE DIAGRAM

DYNAMIC MATERIAL STRAIN CHARACTERISTICS

FIG. II

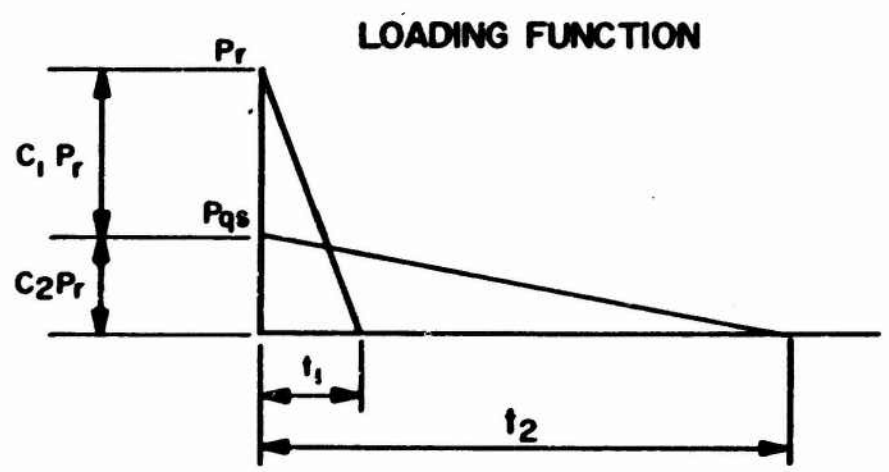

CONSERVATIVE P-t HISTORY
(DIRECT SOLUTION)

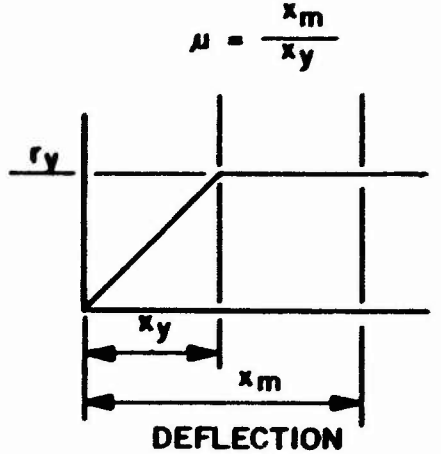

RESISTIVE FUNCTION

$$\left(\frac{\frac{C_1 P_r}{r_y}}{\frac{T_n}{\pi t_1}\sqrt{2\mu - 1}} \right)^2 + \frac{\frac{C_2 P_r}{r_y}}{\frac{T_n}{\pi t_2}\sqrt{2\mu - 1} + \frac{1 - \frac{1}{2\mu}}{1 + .7\left(\frac{T_n}{t_2}\right)}} = 1$$

P_r = REFLECTED PRESSURE

$P_{qs} = C_2 P_r$ = QUASI-STATIC PRESSURE

t_i = DURATION

T_n = PERIOD

x_y = YIELD DISPLACEMENT

x_m = MAXIMUM DISPLACEMENT

$\mu = \frac{x_m}{x_y}$ = DUCTILITY RATIO

r_y = RESISTANCE

GENERAL FORMULA

FIG. 12

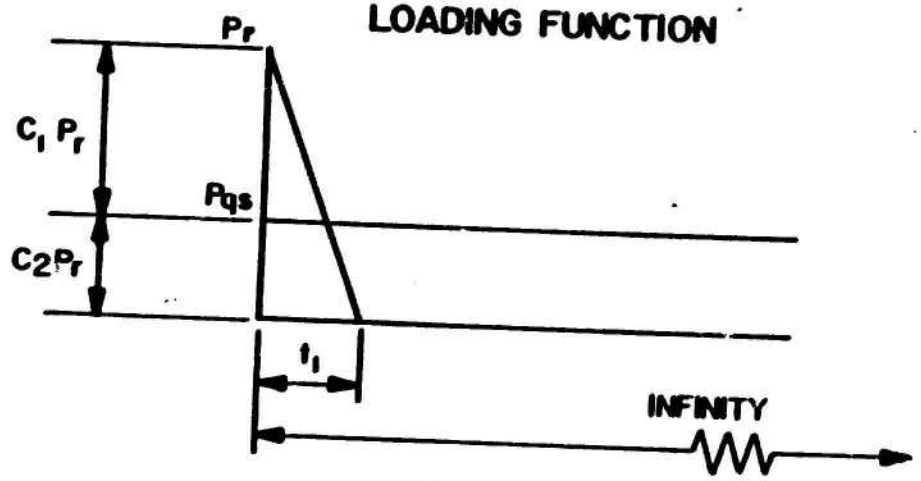

CONSERVATIVE P-I HISTORY
(DIRECT SOLUTION)

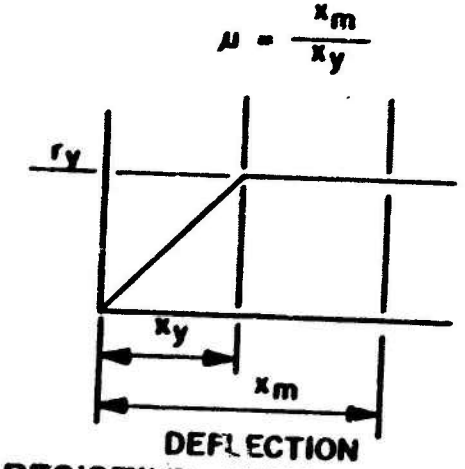

RESISTIVE FUNCTION

$$\left(\frac{\frac{C_1 P_r}{r_y}}{\frac{T_n}{\pi t_1}\sqrt{2\mu - 1}} \right)^2 + \frac{\frac{C_2 P_r}{r_y}}{1 - \frac{1}{2\mu}} = 1$$

P_r = REFLECTED PRESSURE

$P_{qs} = C_2 P_r$ = QUASI-STATIC PRESSURE

t_1 = DURATION

T_n = PERIOD

x_y = YIELD DISPLACEMENT

x_m = MAXIMUM DISPLACEMENT

$\mu = \frac{x_m}{x_y}$ = DUCTILITY RATIO

r_y = RESISTANCE

GENERAL FORMULA
FIG. 13

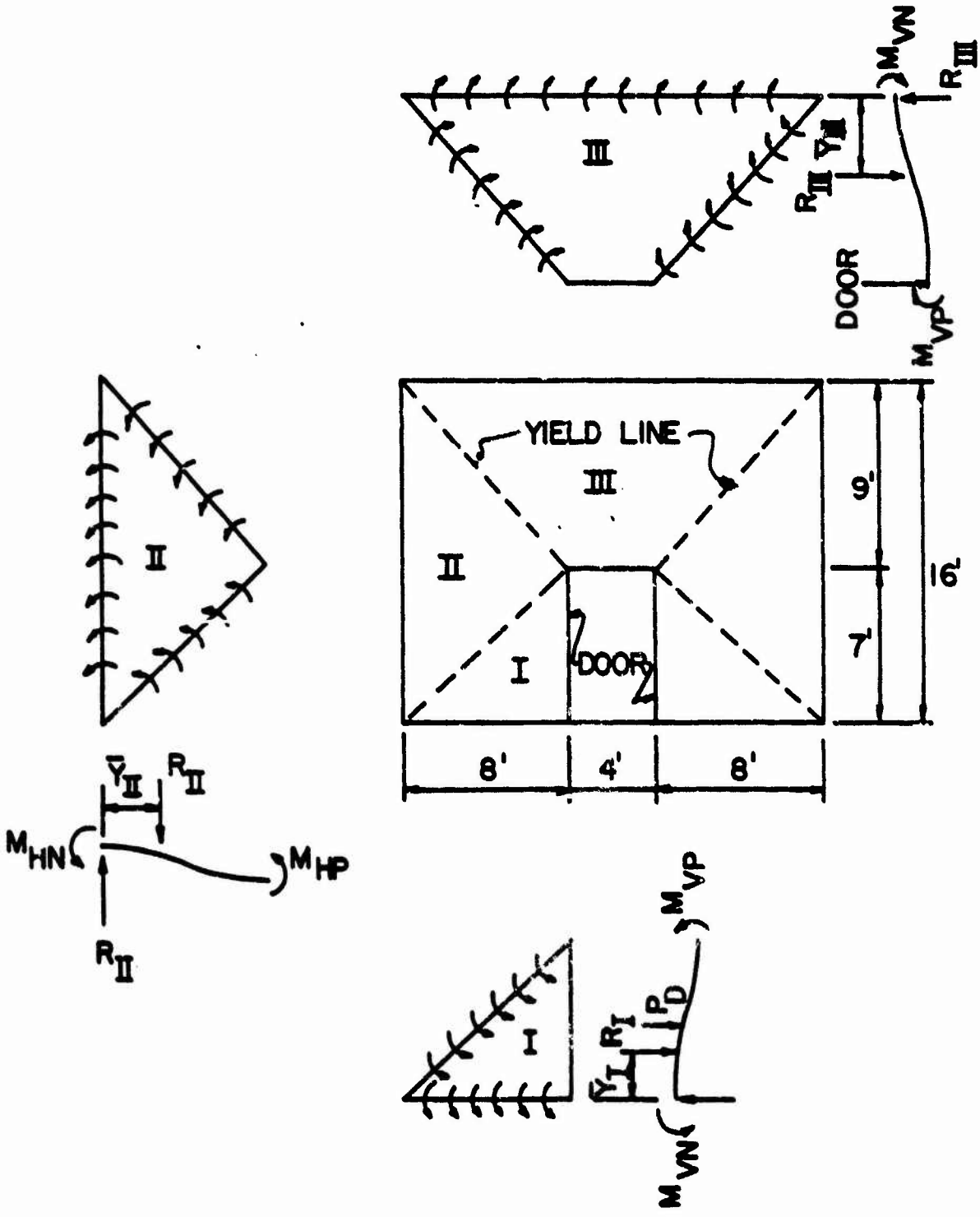
III
M_{VN}
R_{III}
R_{III}
$\bar{Y}_{III}$
DOOR
M_{VP}
YIELD LINE
III
II
I
DOOR
9'
7'
16'
8'
4'
8'
II
$\bar{Y}_{II}$
R_{II}
M_{HN}
M_{HP}
R_{II}
I
M_{VP}
P_D
R_I
$\bar{Y}_I$
M_{VN}

FIG. 14

APPENDIX

SUBJECT	COMPUTED BY:	DATE:
	CHECKED BY:	DATE:

GIVEN:

$E_c = 4.3 \times 10^6$ psi

$f'_{dc} = 5000$ psi

$f_{dy} = 44{,}000$ psi

$K_{soil} = 200$ lb/in.^{3}

Allow. soil Brg. = 6000 psf

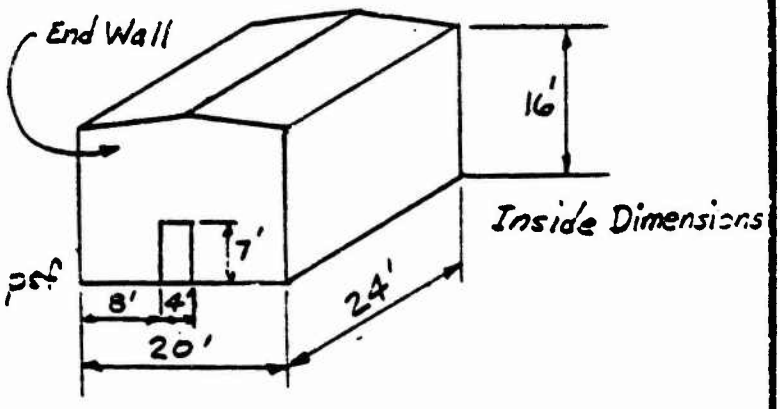

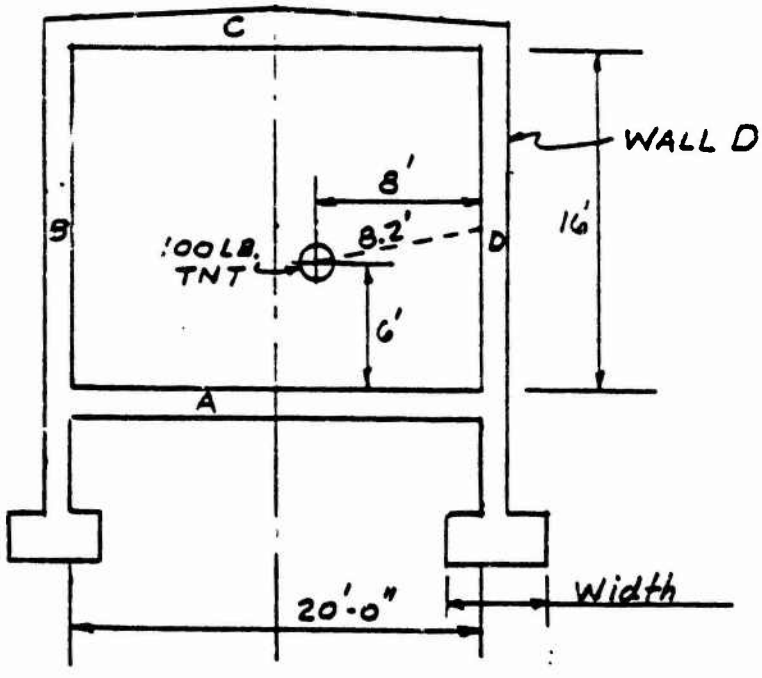

REINFORCED CONCRETE BUILDING

REQ'D: Design for single event

a. Thickness and reinforcing for Wall D
b. Thickness and reinforing in End Wall
c. Width of Footing

SUBJECT	COMPUTED BY:	DATE:
	CHECKED BY:	DATE:

DESIGN WALL D

$$Z = \frac{R}{W^{1/3}} = \frac{8.2}{(100)^{1/3}} = \frac{8.2}{4.64} = 1.77 \ ft/lb^{1/3}$$

FROM FIG. 3-6 IN S/S HANDBOOK

$P_r = 2200$ psi

$$\frac{i_r}{W^{1/3}} = 0.085 \ psi\text{-}sec/lb^{1/3}$$

$$i_r = 0.085\,(4.64) = 0.39$$

$$t_r = \frac{2i_r}{P_r} = 2(0.39)/2200 = 0.00036 \ sec.$$

$$= 0.36 \ ms$$

FROM FIG. 3-9 IN S/S HANDBOOK

$$\frac{W}{V} = \frac{100}{20 \times 16 \times 24} = 0.013 \ lb/ft^3$$

$P_{qs} = 85$ psi

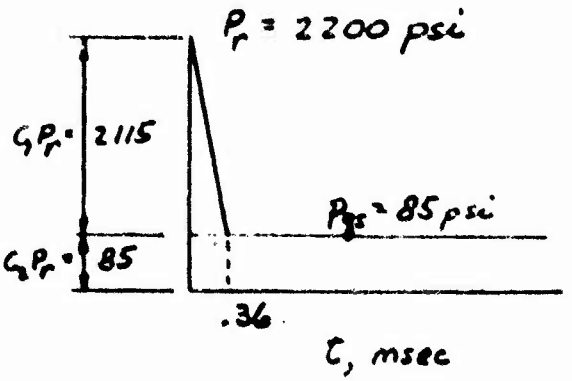

SUBJECT:	COMPUTED BY:	DATE:
	CHECKED BY:	DATE:

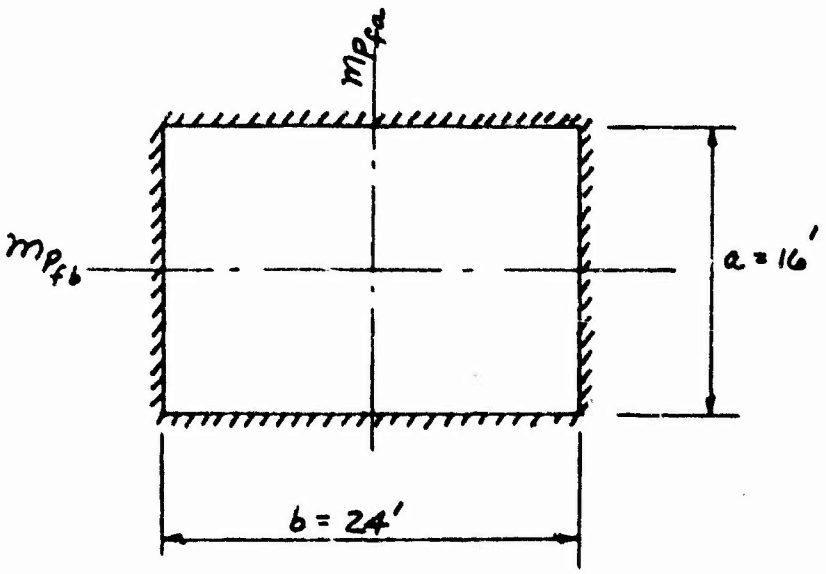

Assume $m_{Pfb} = m_{Psb} = m_{Pfa} = m_{Psa} = b\,m'_{Psb}$

SEE S/S HANDBOOK, TABLE 5-5.

$$\frac{a}{b} = \frac{16}{24} = 0.7$$

$$R_1 = 26.2\, m'_{Psb}$$

$$R_M = \frac{1}{a}\left[12(m_{Pfa} + m_{Psa}) + 9.8(m_{Pfb} + m_{Psb})\right]$$

$$R_M = \frac{24}{16}\left[12(2\,m'_{Psb}) + 9.8(2\,m'_{Psb})\right] = 65.4\, m'_{Psb}$$

$$K_1 = \frac{692\,E I_a}{a^2}$$

$$K_2 = \frac{201\,E I_a}{a^2}$$

SUBJECT:	COMPUTED BY:	DATE:
	CHECKED BY:	DATE:

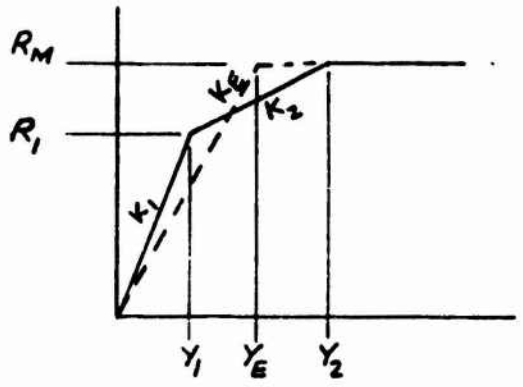

EFFECTIVE BILINEAR RESISTANCE FUNCTION

$$Y_E = Y_1 + Y_2\left(1 - \frac{R_1}{R_M}\right) \qquad \text{EQ. 5-50 TM5-1300}$$

$$Y_1 = \frac{R_1}{K_1}$$

$$Y_2 = \frac{R_M - R_1}{K_2} + \frac{R_1}{K_1}$$

$$\therefore \quad Y_E = \frac{R_1}{K_1} + \frac{R_1(R_M - R_1)}{K_1 R_M} + \frac{(R_M - R_1)^2}{K_2 R_M}$$

$$Y_E = \frac{m^{\circ}_{P_{sb}} a^2}{EI_a}\left[\overset{.038}{\frac{26.2}{692}} + \overset{.023}{\frac{26.2(65.4 - 26.2)}{692(65.4)}} + \overset{.117}{\frac{(65.4 - 26.2)^2}{201(65.4)}}\right]$$

$$Y_E = \frac{0.178\, m^{\circ}_{P_{sb}} a^2}{EI_a}$$

$$K_E = \frac{R_M}{Y_E} = \frac{65.4\, m^{\circ}_{P_{sb}}}{\frac{0.178\, m^{\circ}_{P_{sb}} a^2}{EI_a}} = 367\,\frac{EI_a}{a^2}$$

SUBJECT:	COMPUTED BY:	DATE:
	CHECKED BY:	DATE:

1ST TRIAL SECTION

TRY r_m (req'd) = 100 psi

$R_M = 100 \times 144 \times 16 \times 24 = 5{,}529{,}600$ lb.

$m^o_{P_{sb}} = \frac{5{,}529600}{65.4} = 84{,}550$ in-lb./in.

$m^o_{P_{sb}} = \rho_s b d^2 f_{dy} \left(1 - \frac{0.59 \rho_s . f_{dy}}{f'_{dc}}\right)$ EQ. 5-7 S/S HDBK.

$m^o_{P_{sb}} = .01\,(1) d^2 (44000) \left[1 - \frac{.59(0.01)(44000)}{5000 \times 1.25}\right]$

$m^o_{P_{sb}} = 422\, d^2$

$\therefore d = \sqrt{\frac{84550}{422}} = 14.1''$

$I_a = \frac{bd^3}{2}(5.5\rho_s + 0.083)$ EQ. 5-8 S/S HDBK

$I_a = \frac{1(14.1)^3}{2}(0.138) = 193.4$ in.^{4}/in.

$K_E = \frac{367 \times 4.3 \times 10^6 \times 193.4}{(12 \times 16)^2} = 8{,}279{,}200$ #/in.

$M_t = \frac{150 \times 17/12 \times 16 \times 24}{386} = 211$ lb-sec^2/in.

$T = 2\pi \sqrt{\frac{K_{LM} M_t}{K_E}} = 2\pi \sqrt{\frac{0.58 \times 211}{8{,}279{,}200}} = 0.024$ sec.

$= 24$ msec.

PROJECT:	COMPUTED BY:	DATE:
	CHECKED BY:	DATE:

Allowable $\mu = 15$

$C_1 P_r = 2115$

$C_2 P_r = 85$

$t_1 = 0.36$ msec.

$T/t_1 = \frac{24}{0.36} = 67$

$$\left(\frac{\frac{C_1 P_r}{r_m}}{\frac{T}{\pi t_1}\sqrt{2\mu - 1}} \right)^2 + \frac{\frac{C_2 P_r}{r_m}}{1 - \frac{1}{2\mu}} = 1 \qquad \text{Eq. 5-54, S/S HDBK}$$

$$\left(\frac{\frac{2115}{r_m}}{114.8} \right)^2 + \frac{\frac{85}{r_m}}{0.967} = 1$$

$$\frac{339.4}{r_m^2} + \frac{87.9}{r_m} = 1$$

$r_m^2 - 87.9\, r_m - 339.4 = 0$ (Solve by quadratic eq.)

$$r_m = \frac{87.9 \pm \sqrt{87.9^2 - 4(-339.4)}}{2}$$

$r_m = 91.6$ psi < 100

∴ Try 91.6 psi for selecting d.

SUBJECT:	COMPUTED BY:	DATE:
	CHECKED BY:	DATE:

2ND TRIAL SECTION

Try $r_m = 91.6$ psi

$R_M = 91.6 \times 144 \times 16 \times 24 = 5{,}065{,}100$ lb.

$m^{\circ}_{P_{sb}} = \frac{5{,}065{,}100}{65.4} = 77{,}448$ in-lb./in.

$d = \sqrt{\frac{77448}{422}} = 13.6''$

$I_a = \frac{1(13.6)^3}{2}(0.138) = 173.6$ in.^{4}/in.

$K_E = \frac{367 \times 4.3 \times 10^6 \times 173.6}{(12 \times 16)^2} = 7{,}431{,}600$ lb./in.

$M_t = \frac{150 \times 16/12 \times 16 \times 24}{386} = 199.0$ lb-sec^2/in.

$T = 2\pi\sqrt{\frac{0.58 \times 199}{7{,}431{,}600}} = 0.025$ sec.

$\frac{T}{t_1} = \frac{25}{.36} = 69.4$

$$\left(\frac{\frac{2115}{r_m}}{119}\right)^2 + \frac{\frac{85}{r_m}}{0.967} = 1$$

$$\frac{315.9}{r_m^2} + \frac{87.9}{r_m} = 1$$

$$r_m^2 - 87.9\, r_m - 315.9 = 0$$

$$r_m = \frac{87.9 + \sqrt{87.9^2 - 4(-315.9)}}{2} = 91.4 \text{ psi req'd.}$$

91.6 psi provided
∴ O.K.

SUBJECT:	COMPUTED BY:	DATE:
	CHECKED BY:	DATE:

TIME OF MAXIMUM RESPONSE, t_m

$$t_m = \frac{C_1 P_r t_1}{2(r_m - C_2 P_r)} \qquad \text{EQ.(5-57), S/S HDBK}$$

$$t_m = \frac{2115(.00036)}{2(91.6-85)} = 0.058 \text{ sec.}$$

SHEAR, V

$$F = 85 \times 144 \times 16 \times 24 = 4,700,200 \text{ lb.}$$

$$R_M = 91.6 \times 144 \times 16 \times 24 = 5,065,100 \text{ lb.}$$

$$\left.\begin{aligned} V_A &= 0.06F + 0.12R_M \\ V_B &= 0.10F + 0.22R_M \end{aligned}\right\} \text{ Table 5-5, S/S HDBK}$$

$$V_A = 0.06(4,700,200) + 0.12(5,065,100) = 889,800 \text{ lb.}$$

$$V_B = 0.10(4,700,200) + 0.22(5,065,100) = 1,584,300 \text{ lb.}$$

SUBJECT:	COMPUTED BY:	DATE:
	CHECKED BY:	DATE:

Vert. rebar

$A_s = 0.01 \times 13.6 \times 12 = 1.63^{\square"}$

Space #9 $= \frac{1}{1.63} \times 12 = 7.36"$ say $7"$

Hor. rebar

$A_s = 1.63 \times \frac{24}{16} = 2.45^{\square"}$

space #9 $= \frac{1}{2.45} \times 12 = 4.9"$

Say 5"

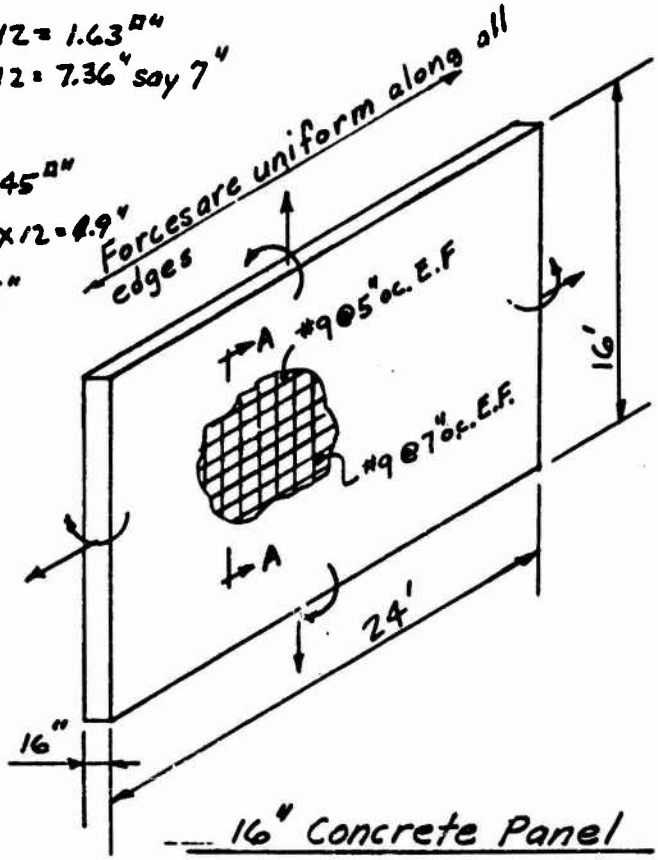

16" Concrete Panel

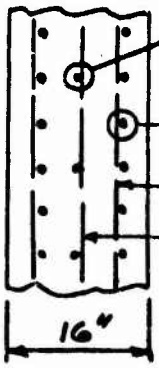

#9 @10" o.c.

#9@5" o.c. E.F.

#9@7" o.c. E.F.

#9@7" o.c. E.W.

Middle layer for axial load only

SECTION A-A

SUBJECT:	COMPUTED BY:	DATE:
	CHECKED BY:	DATE:

DETERMINE REBAR IN END WALL WITH DOOR

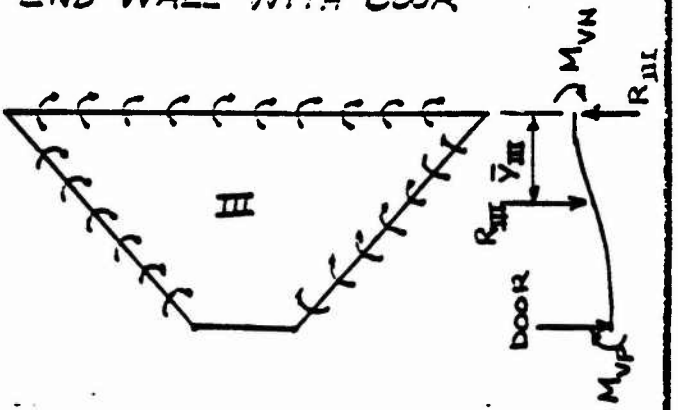

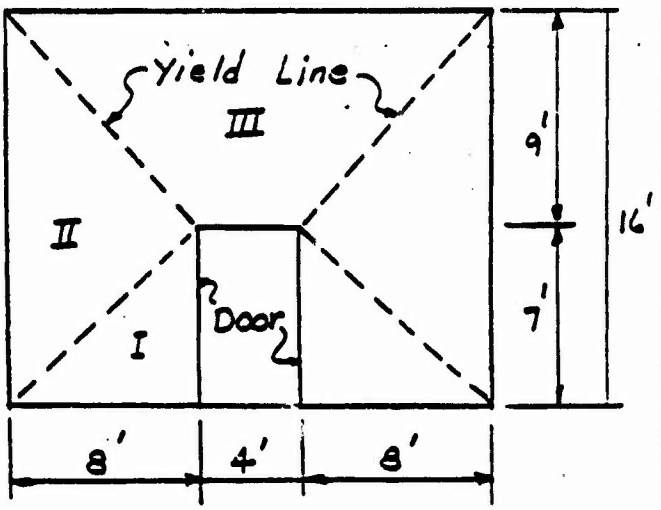

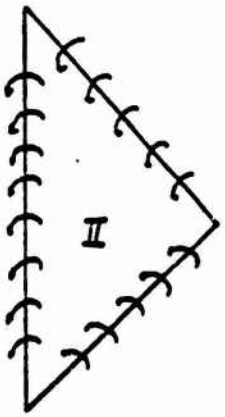

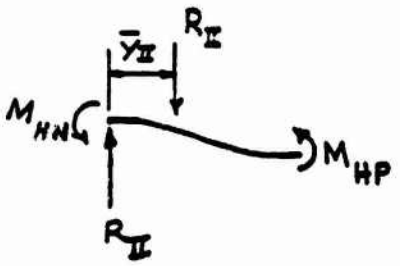

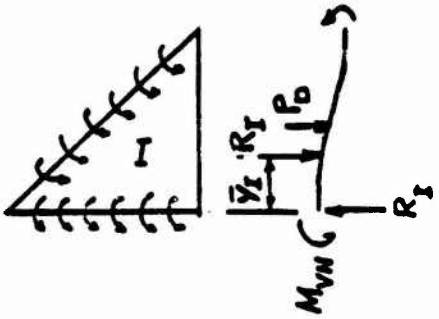

SUBJECT:	COMPUTED BY:	DATE:
	CHECKED BY:	DATE:

DOOR

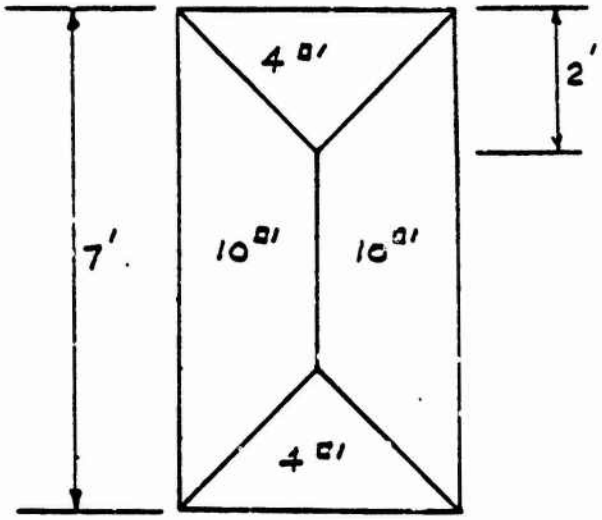

Area Contributing to loads on wall

Assume V_u of wall and door are the same

Let $M_{VN} = M_{VP}$

SECTION I (See Sheet 10)

Summation of moments about M_{VN}

$$8M_{VN} + 8M_{VP} - r_m A_I \bar{Y}_I - P_D\left(\frac{7}{2}\right) = 0$$

$$8M_{VN} + 8M_{VP} - 144\, r_m\left(\frac{8\times 7}{2}\right)\left(\frac{7}{3}\right) - 144\, r_m(10)\left(\frac{7}{2}\right) = 0$$

$$(9408 + 5{,}040)\, r_m = 16 M_{VI}$$

$$r_m = 0.0011\, M_{VI}$$

SUBJECT:	COMPUTED BY:	DATE:
	CHECKED BY:	DATE:

SECTION II

Summation of moments about M_{HN}

$$16 M_{HN} + 16 M_{HP} - R_{II} \bar{y}_{II} = 0$$

$$16 M_{HN} + 16 M_{HP} - r_m (144)\left(\frac{8 \times 16}{2}\right)\left(\frac{8}{3}\right) = 0$$

$$24576\, r_m = 32\, M_H$$

$$r_m = 0.0013\, M_{HII}$$

SECTION III

Summation of moments about M_{VN}

$$20 M_{VN} + 16 M_{VP} - R_{III} \bar{y}_{III} - 9 P_D = 0$$

$$20 M_{VN} + 16 M_{VP} - r_m (144)\left(\frac{4+20}{2} \times 9\right)\left[\frac{9}{3}\left(\frac{2 \times 4 + 20}{4 + 20}\right)\right]$$

$$-9(144)(4)\, r_m = 0$$

$$r_m = \frac{36\, M_{VIII}}{(54432 + 5184)}$$

$$r_m = 0.0006\, M_{VIII}$$

SUBJECT:	COMPUTED BY:	DATE:
	CHECKED BY:	DATE:

When rebars are the same in all directions, the moments are the same in all directions. Section III ($0.0006\, M_{VIII}$), Section I (0.0011) and Section II ($0.0013\, M_{HII}$) are respectively weakest to strongest. Accordingly to make r_m the same for all sections, consistent with the yield line theory, the following adjustments must be made.

Determine vertical moment required in Section III from $r_m = 0.0006\, M_{VIII} = 0.0011\, M_{VI} = 0.0013\, M_{HII}$

Obtain $0.0011\, M_{VI} = 0.0006\, M_{VIII}$

$$M_{VIII} = 1.833\, M_{VI}$$

Determine horizontal moment in Section II

$$0.0011\, M_{VI} = 0.0013\, M_{HII}$$

$$M_{HII} = 0.8462\, M_{VI}$$

SUBJECT:	COMPUTED BY:	DATE:
	CHECKED BY:	DATE:

Find value of M_{VI} in Section I

Use $r_m = 90.2$ psi (obtained from separate calc. for other end wall)

$d = 13.2$ in.

$r_m = 0.0011 M_{VI}$

$M_{VI} = \frac{r_m}{0.0011} = \frac{90.2}{0.0011} = 82{,}000$ lb-ft/ft

or 82,000 lb-in./in.

Find steel required in section I

$$M'_{ps} = \rho_s b d^2 f_{dy} \left(1 - \frac{0.59 \rho_s f_{dy}}{f'_{dc}}\right)$$

Obtain $7{,}666{,}560\rho_s^2 - 31{,}816{,}224\rho_s = -82{,}000$

$$\rho_s^2 - 0.24\rho_s + 0.00258 = 0$$

$$\rho_s = \frac{0.24 \pm \sqrt{.24^2 - 4(1)(0.00258)}}{2}$$

$$\rho_s = \frac{0.24 \pm 0.22}{2} = .23 \text{ or } \underline{\underline{.01}}$$

$A_s = .01 \times 13.2 \times 12 = 1.58$ sq. in.

Spacing #9 $= \frac{1.00}{1.58} \times 12 = 7.6$ in.

Say 7" o.c.

SUBJECT:	COMPUTED BY	DATE:
	CHECKED BY:	DATE:

Find vertical steel required in Section III

$M_{VIII} = 1.833\, M_{VI}$

$M_{VIII} = 1.833(82{,}000) = 150{,}300$ in-lb./in.

$$\rho_s(1)(13.2)^2(44{,}000)\left(1 - \frac{.59\rho_s(44)}{6.25}\right) = 150{,}300$$

$$7{,}666560\rho_s - 31843{,}800\rho_s = 159{,}300$$

$$\rho_s^2 - 0.24\rho_s + 0.0047 = 0$$

$$\rho_s = \frac{0.24 \pm \sqrt{0.24^2 - 4(1)(0.0047)}}{2}$$

$$\rho_s = \frac{0.24 \pm 0.20}{2} = 0.22 \text{ or } \underline{0.02}$$

$A_s = 0.02 \times 13.2 \times 12 = 3.17$ sq. in.

Spacing #9 $= \frac{1.00}{3.17} \times 12 = 3.79$ in. Say 3.5 in. o.c.

Find horizontal steel required in Section II

$M_{HII} = 0.8462\, M_{VI}$

$M_{HII} = 0.8462(82000) = 69{,}333$

Since 69,388 < 82,000 in-lb./in.

Use same steel as 82,000 in-lb./in.

or #9 @ 7" o.c. (See Section I)

SUBJECT:	COMPUTED BY:	DATE:
	CHECKED BY:	DATE:

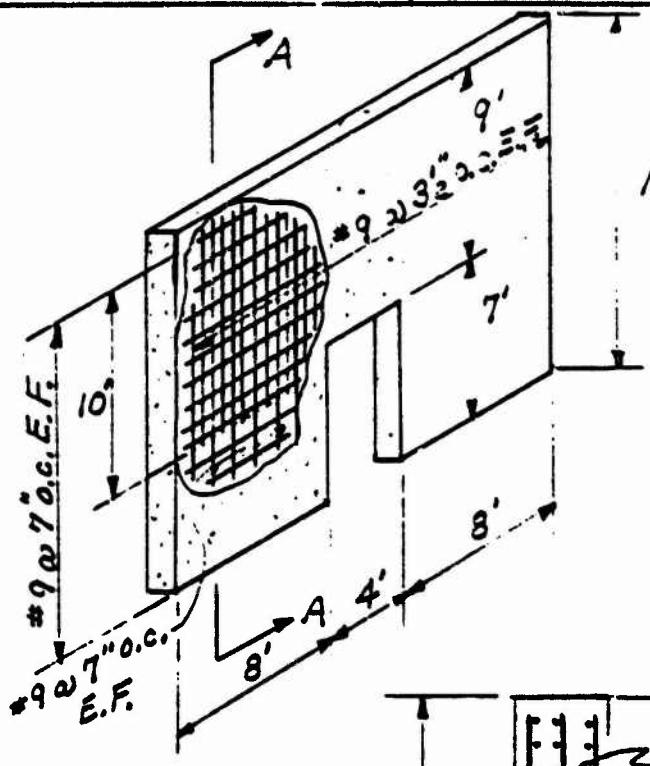

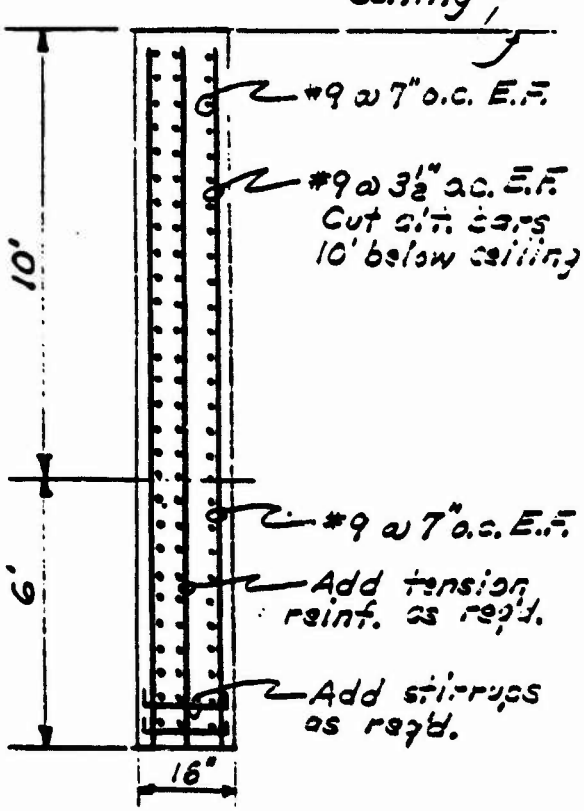

SECTION AA

SUBJECT:	COMPUTED BY:	DATE:
	CHECKED BY:	DATE:

FOOTING

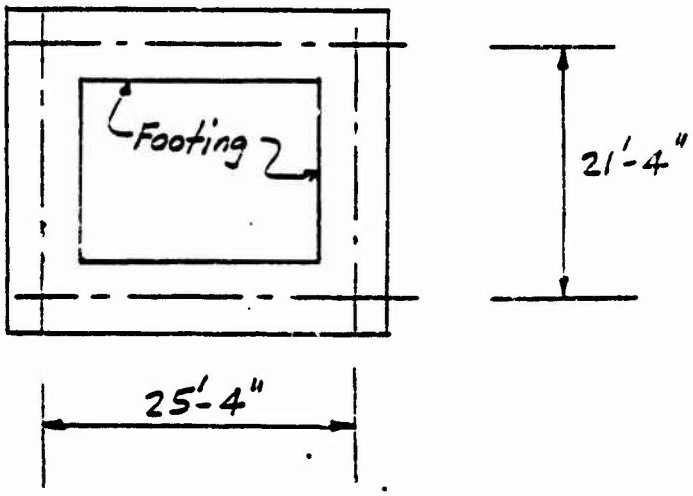

COMPUTE WEIGHT OF BLDG.

Outside Width = 20 + 2.67 = 22.67
Outside Length = 24 + 2.67 = 26.67
Outside Height = 16 + 3.00 = 19.00

Vol. = $(22.67 \times 26.67 \times 19.00 - 20 \times 24 \times 16) = 3808$ cu. ft.

Wt. = $150 \times 3808 = 571{,}000$ lb.

$M_t = 571{,}000/386 = 1480$ lb-sec^2/in.

Area of Ftg. Try W = 3'

Area = $3(2 \times 25.33 + 2 \times 21.33) = 280$ sq. ft.

K = $200 \times 280 = 56{,}000$ lb/in.

$$T = 2\pi\sqrt{\frac{M}{K}} = 2\pi\sqrt{\frac{1480}{56000}} = 1.02 \text{ sec.}$$

SUBJECT:	COMPUTED BY:	DATE:
	CHECKED BY:	DATE:

VERTICAL LOAD

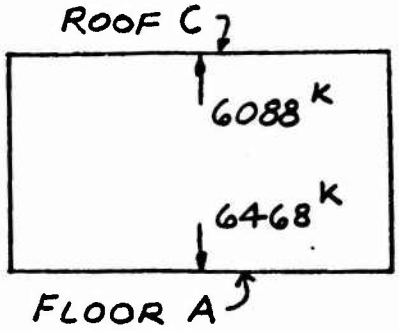

ROOF C

$T = 0.028$ sec

$\omega = 2\pi/.028 = 224$ rad/sec.

$\cos \omega t_{e1} = 1 - \frac{R_M}{F_1} = 1 - \frac{6197}{5875} = -0.0598$

$\omega t_{e1} = 1.626$

$t_{e1} = \frac{1.626}{\omega} = \frac{1.626}{224} = 0.007$ sec.

$t_m = \frac{i_r}{r_y - P_s} = \frac{0.325}{89.7 - 85} = 0.69$

ROOF

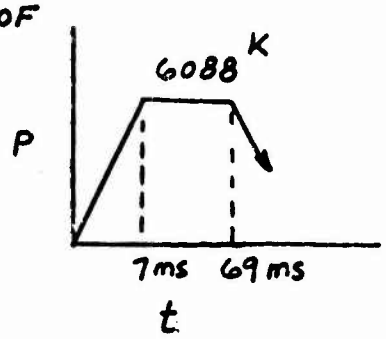

FLOOR

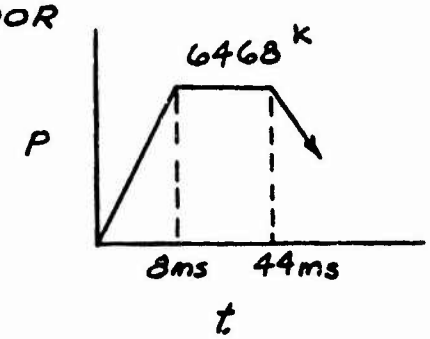

SUBJECT:	COMPUTED BY:	DATE:
	CHECKED BY:	DATE:

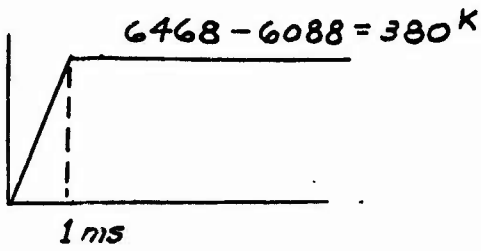

$\frac{t_r}{T} = \frac{1}{1020} = .001$ DLF = 2 (Fig. 2.9, Biggs p. 48)

$\therefore R_M = 380^K$

Req'd Area of Ftg. = $\frac{2 \times 380 + 571}{6} = 222$ sq.ft

FIND FOOTING WIDTH

$222 = w(2 \times 25.33 + 2 \times 21.33) = 93.32\,w$

$w = \frac{222}{93.32} = 2.38'$

TRY AREA = 222 sq.ft.

$K = 200 \times 222 = 44400$ lb/in.

$T = 2\pi\sqrt{\frac{M_t}{K}} = 2\pi\sqrt{\frac{1480}{44400}} = 0.57$ sec.

$\frac{t_1}{T} = \frac{.001}{0.57} = .0018$

SUBJECT:	COMPUTED BY:	DATE:
	CHECKED BY:	DATE:

HORIZONTAL LOAD

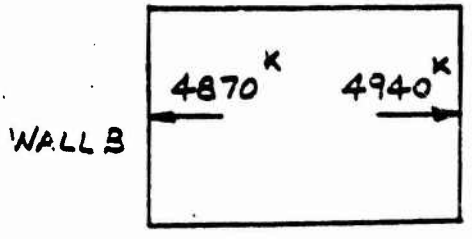

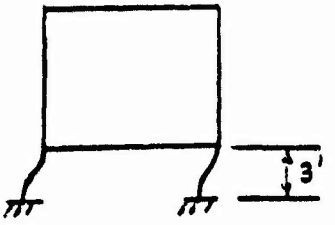

WALL B

$$\omega = \frac{2\pi}{T} = \frac{2\pi}{.025} = 251.$$

$$\cos \omega t_{e1} = 1 - \frac{R_M}{F_1} = 1 - \frac{89.5}{85}$$

$$\omega t_{e1} = 1.62$$

$$t_{e1} = \frac{1.62}{251} = 0.006 \text{ sec.}$$

$$t_m = \frac{i_r}{r_m - P_{qs}} = \frac{0.269}{89.5-85} = 0.060 \text{ sec.}$$

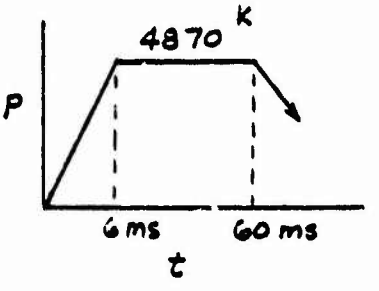

WALL D

$$\omega = \frac{2\pi}{T} = \frac{2\pi}{.025} = 251$$

$$\cos \omega t_{e1} = 1 - \frac{R_M}{F_1} = \frac{1-91.6}{85} = -.076$$

$$t_{e1} = \frac{1.647}{251} = 0.007 \text{ sec.}$$

$$t_m = \frac{0.39}{91.6-85} = 0.059 \text{ sec.}$$

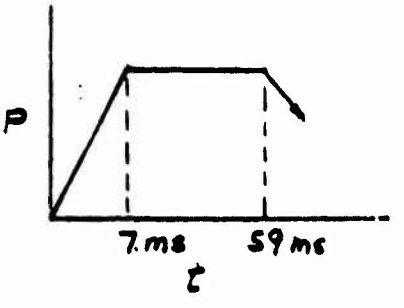

SUBJECT:	COMPUTED BY:	DATE:
	CHECKED BY:	DATE:

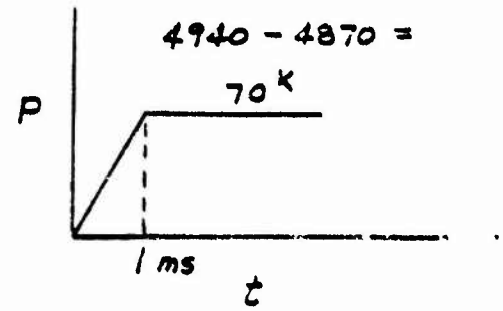

FOUNDATION WALL

$$I_a = \frac{bd^3}{2}(5.5\rho_s + 0.033)$$

$$I_a = \frac{(12\times24)(14)^3}{2}(5.5\times.005 + 0.033)$$

$$I_a = 43{,}663 \text{ in.}^4$$

$$K = \frac{24EI_a}{h^3} = \frac{24\times4.3\times10^6\times43663}{(3\times12)^3}$$

$$K = 96{,}580{,}000 \text{ lb./in.}$$

$$T = 2\pi\sqrt{\frac{M}{K}} = 2\pi\sqrt{\frac{1480}{96{,}580{,}000}} = 0.024 \text{ sec.}$$

$$\frac{t_r}{T} = \frac{1}{24} = 0.04$$

DLF $\simeq$ 2 Biggs p.43, Fig 2.9

SUBJECT:	COMPUTED BY:	DATE:
	CHECKED BY:	DATE:

EQUIVALENT STATIC LOAD

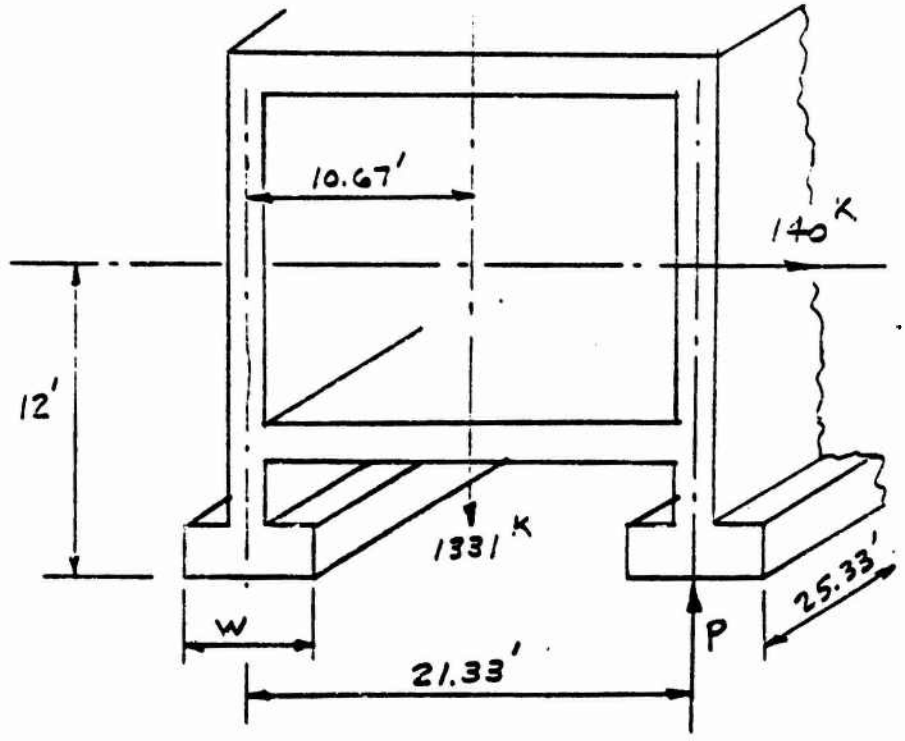

$$P = \frac{140 \times 12}{21.33} = 78.8^{K}$$

Additional width due to moment

$$w = \frac{2 \times 78.8}{6 \times 25.33} = 1.04'$$

Width due to vertical load = 2.38'

Additional width = 1.04'

Total width, w = 3.42'

Say 3'-6"

Optimization of Reinforced Concrete Slabs

by J. M. Ferritto [1]

INTRODUCTION

The Department of Defense has numerous facilities engaged in the production of various types of explosives and munitions used by military services. In most cases the production of ammunition utilizes assembly line procedures. Projectiles pass through various stages of preparation: filling with explosive, fuzing, marking, and packing. Hazardous operations, such as the filling of the projectile case with an explosive in a powder form and the compaction of the powder by hydraulic press, are accomplished in protective cells that are intended to confine the effects of an accidental explosion.

Most of the existing production facilities were built in the 1940s. With few exceptions, the manufacturing technology and existing equipment represent the state of the art as of 1940. The production equipment was operated extensively during World War II, again during the Korean conflict, and recently during the Southeast Asia war. Much of this equipment and the housing structures have been operating beyond their designed capacities [1]. The Department of Defense is conducting an ammunition plant modernization program [2] that is intended to greatly enhance safety in the production plants by protective construction, automated processing, and reduction of personnel involved in hazard operations. An automated procedure was required to give structural designers the capability to

---

[1]Senior Research Engineer Structures Division Civil Engineering Laboratory, Naval Construction Battalion Center, Port Hueneme, Calif.

PRECEDING PAGE BLANK

perform rapid analysis of the structural safety of blast-resistant construction. The design parameters interact in a complex way since the procedure is both nonlinear and dynamic. From a design point of view an optimization procedure was required to minimize cost and maximize safety since blast-resistant construction has been reported to cost 3 to 5 times as much as conventional construction. Therefore, the first objective was to automate the analysis procedures for determining structural response of reinforced concrete slabs having a bilinear stiffness representation and subjected to blast shock and gas pressures. Concrete slabs are the basic element forming sidewalls, roofs and floors of cells designed to confine the effects of accidental explosions. The second objective was to provide an optimum design procedure for laced (shear reinforced) and unlaced reinforced concrete slabs that will automatically produce a least-cost design for a given slab geometry, material properties, and explosive weight for both feasible and nonfeasible starting points.

ANALYSIS PROCEDURE

The procedure treats reinforced rectangular slabs with arbitrary boundary conditions, cross section properties, material properties and loading. The determination of the equivalent pressure load based on the quantity of explosive and cell geometry is based on Reference [3]. The computational procedure for the slab analysis utilizes reinforced concrete section properties to determine resisting moment, from which using yield line analysis techniques, the static resistance of the slab is determined. The stiffness of the slab is calculated using elastic plate theory.

Using the loading, resistance, stiffness and mass of the slab, the dynamic response of the slab is computed by time step iteration. The slab is modeled as an equivalent single degree-of freedom elasto-plastic system [4]. The design of the slab, based on its ultimate strength allows large nonlinear deformations to confine the effects of an accidental explosion. The deflections are limited in terms of support rotations.

Structural Optimization

The optimization problem consists of finding the least-cost structure that satisfies all the design constraints; or, stated in optimization terms: Find $\vec{X}$ such that $M(\vec{X})$ is a minimum and

$$g_i(\vec{X}) \leq 0 \qquad i = 1, 2, \ldots N$$

where $\vec{X}$ = vector of design variables

N = number of design constraints

g = vector of design constraints

M = objective function

Specifically for this problem the design variables selected are areas of steel reinforcement and thickness of concrete. The design constraints are minimum section properties and the flexural and shear limits. The objective function consists of the costs of formwork, concrete, and flexural and shear (lacing) reinforcement.

Fixed Variables

W = explosive weight

H = wall height

EL = wall length

h = height of explosive above floor

ℓ = distance of explosive from left side of wall

R_a = distance of explosive from wall

I = reflection code

f_{dc} = ultimate dynamic concrete strength

f_{dy} = dynamic yield strength of reinforcing steel

θ = rotation criterion

Design Parameters, X

$$X = \begin{cases} t_c & \text{concrete thickness} \\ AVT & \text{area of vertical reinforcing steel tension} \\ AVC & \text{area of vertical reinforcing steel compression} \\ AHT & \text{area of horizontal reinforcing steel tension} \\ AHC & \text{area of horizontal reinforcing steel compression} \\ AS & \text{area lacing steel} \end{cases}$$

Constraints, g (X)

$\delta(X) = \delta(\theta)$, maximum deflection

$V(X) \leq VC$ for $\theta \leq 2$ deg, maximum shear

$t_c \geq 12$, minimum thickness

$AV \geq 0.0025\ bd$

$AH \geq 0.0025\ bd$

} minimum steel reinforcement tension or compression

The methodology [5,6] selected used the unconstrained minimization approach. The problem is converted to an unconstrained minimization by constructing a function, ϕ, of the general form

$$\phi(\vec{X}, r) = M(\vec{X}) + P[g_1(\vec{X}), \ldots, g_n(\vec{X}), r]$$

For this problem the interior penalty function technique was selected. This methodology is suitable when gradients are not available, and, because the method uses the feasible region, a useable solution always results. The objective function is augmented with a penalty term that is small at points away from the constraints in the feasible region, but increases rapidly as the constraints are approached. The form is as follows:

$$\phi(\vec{X}, r) = M(\vec{X}) - r \sum_{j=1}^{N} \frac{1}{g_j(\vec{X})}$$

where M is to be minimized over all $\vec{X}$ satisfying $g_j(\vec{X}) \leq 0$, $j = 2 \ldots N$. Note that is r is positive, then, since at any interior point all of the terms in the sum are negative, the effect is to add a positive penalty to $M(\vec{X})$. As the boundary is approached, some $g_j(\vec{X})$ will approach zero, and the penalty will increase rapidly. The parameter, r, will be made successively smaller in order to obtain the constrained minimum of M.

Objective Function

$$\text{Cost} = M = H \cdot EL \cdot t_c \cdot C_c + (AV + AH)(EL \cdot H)C_s + (A_s)(EL \cdot H)C_L$$

where C_c = cost of concrete ($/cu ft)

C_s = cost of horizontal and vertical reinforcement ($/cu in.)

C_L = cost of lacing reinforcement ($/cu in.)

A_s = area lacing reinforcement ($/cu in.)

AV = vertical steel (tension and compression)

AH = horizontal steel (tension and compression)

$$\phi = M + r \sum_{j=1}^{N} \frac{1}{g_j(X)}$$

where r = penalty parameter.

The program requires a starting point in the feasible region before optimization can proceed. This is accomplished automatically by the program by incrementing the design variables until a feasible point is reached.

An algorithm which comprises the steps most commonly used is as follows:

1. Given a starting point, X_o, satisfying all $g_j(X) > 0$ and an initial value for r, minimize ϕ to obtain X_{min}.
2. Check for convergence of X_{min} to the optimum.
3. If the convergence criterion is not satisfied, reduce r by $r \leftarrow rc$, where $c > 1$.
4. Compute a new starting point for the minimization, initialize the minimization algorithm, and repeat from step 1.

The logic diagram for the interior penalty functions technique is shown in Figure 1.

The minimization for $\phi(X, r)$ shown in Figure 1 is accomplished by a method developed by Powell using conjugate directions [5,6].

Powell's method can be understood as follows: Given that the function has been minimized once in each of the coordinate directions

and then in the associated pattern direction. Discard one of the coordinate directions in favor of the pattern direction for inclusion in the next minimizations, since this is likely to be a better direction than the discarded coordinate direction. After the next cycle of minimizations, generate a new pattern direction, and again replace one of the coordinate directions.

Figure 2 is a logic diagram for the unconstrained minimization algorithm. The pattern move is constructed in block A, then used for a minimization step (blocks B and C), and then stored in S_n (block D) as all of the directions are up-numbered and S_1 is discarded. The directions S_n will then be used for a minimizing step just before the construction of the next pattern direction. Consequently, in the second cycle, both X and Y in block A are points that are minima along S_n, the last pattern direction. This sequence will impart special properties to $S_{n+1} = X - Y$ that are the source of the rapid convergence of the method.

Figure 2 shows a block requiring a one-dimensional minimization of α^* of the function $\phi(\overset{+}{X} + \alpha S_q)$. The one-dimensional minimization uses a four-point cubic interpolation. It finds the minimum along the direction S_q, where $\overset{+}{X}$ is the coordinate of the previous minimum. By trial and error it finds three points with the middle one less than the other two. It makes a qudratic interpolation, and then a cubic inter polation. If the actual function evaluated at the new interpolated point is not sufficiently close to that of the preceding point or if it is not sufficiently close to the interpolated function, then another cubic interpolation is made.

Discussion of Results

The objective function is segmentally linearly dependent on the design variables; however, the constraints are both linearly and nonlinearly related to the design variables. The minimum area of steel and minimum concrete thickness are linear constraints. Figure 3 shows the constraints and objective function considering for this example that reinforcement in tension and compression is the same and that vertical reinforcement is related to horizontal reinforcement (thus reduced variables for a 2-dimensional presentation). The shear stress and deflection are nonlinearly related to the thickness of concrete. The shear stress is further noted not to be convex. This will be discussed later. Figure 3 shows the useable region bounded by flexure, shear, and minimum steel constraints. The optimum least-cost solution is shown. This specific example solution considers an unlaced section; thus, the maximum shear constraint is active. Laced sections eliminate the shear constraint. If the number of sides supported were increased from 2 to 3, the design space would change as shown in Figure 4. There are two regions that are useable areas. Obviously, the lower one offers the least cost and, therefore, is more desirable.

There is clearly a complex interaction of constraints showing the effect of shear. Unfortunately, the optimum solution found by the program depends on the starting point selected. The program converges on the closest relative optimum. Several alternative starting points should be used to verify a questionable optimum. Revising the design parameters could possibly shift the constraints such that only one

useable solution would appear. However, a slight increase in shear stress (10%) can significantly reduce cost by allowing the near-optimum nonfeasible solution to be accepted, Figure 5.

The dual-space problem of finding a useable solution is peculiar to unlaced concrete slabs only because lacing (shear reinforcement) modifies the shear constraint. Nonautomated optimum design for unlaced conditions is almost impossible when one considers the complexity of the design space and the large number of iterations required when an initial solution is not feasible.

Cost data used in the program can be selected by the user. However, the data used herein is based on work by Picatinny Arsenal on contract with Ammann and Whitney [7]. Table 1 shows a comparison of unlaced and laced concrete walls for various boundary conditions. The example considers a 15-foot-high by 12-foot-wide (4.6 m x 3.7 m) wall subjected to a 200-psi (1,400 kPa) 10-ms triangular loading function. In all cases the laced concrete (12-degree rotation) is less expensive than unlaced (2-degree rotation) designs. For the unlaced sections ultimate deflections expressed as support rotation capacity must be limited to 2 degrees whereas laced sections are allowed to reach 12 degrees by virtue of the added concrete confinement provided by the lacing.

COMPARISON OF RESULTS TO FINITE ELEMENT TECHNIQUES

To evaluate the accuracy of the approximations made in the analytical technique described above, a comparison was made to a finite element

program, INSLAB [8]. Program INSLAB, is a finite element program having plate element with 12 degrees freedom. An elasto-plastic material model was used throughout this work. The model was defined by the elastic modulus, yield modulus, equivalent yield stress assuming rectangular section (yield moment divided by thickness squared) and Poisson's ratio. Yielding is determined by principal moments. Uniform pressure loading is input and mass is lumped at the modes based on material density and integrating the mass over the element interpolation function. The solution procedure uses time step integration assuming a constant acceleration between successive time increments.

A reinforced concrete slab supported on three sides was analyzed for a 400 psi (2,800 kPa) pressure load with 1.17 msec duration. The slab measured 4 ft by 4 ft with 6-inch thickness (1.2 m x 1.2 m x 0.5 m). Horizontal and vertical reinforcement was 0.18 sq in./ft (3.8 cm^2/m) both sides. A comparison of peak displacement from both the finite element and approximate solutions is shown in Figure 6.

The finite element analysis was performed using the computer program INSLAB, [3]. The mesh consisted of 80 elements each having 12 degrees of freedom. A time increment of 0.01 ms was used. The displacement difference at maximum value is about 13 percent.

Both techniques used an elasto-plastic analysis. The approximate solution uses a cracked moment of inertia averaged with a gross moment of inertia to determine stiffness. The finite element method uses a gross moment of inertia based on section thickness. However, the modulus of the concrete was reduced to account for reduction in stiffness resulting from cracking. The rise time of the load for the finite element solution

was increased to allow a number of steps before peak load. This effect is minimal since the loading is impulsive in nature and is thought to result in about a 5 percent reduction in peak displacement.

Figure 7 shows the deflection contours obtained by the finite element analysis and the yield line obtained from the approximate solution. The agreement is very good. The yield line marks regions of the plate assumed to displace as units. The contour lines tend to run parallel to the support and vertical yield line. This is the same mechanism predicted by the yield pattern since the slab deflects most along the vertical yield line varying linearly to the nondeflecting support.

CONCLUSION

An optimum design procedure is given for reinforced concrete slabs using the internal penalty function approach. The solution has been found to converge rapidly and at minimum computer cost. Results agree well with more refined finite element anlaysis. This program is in use by the Navy in the design of facilities to resist dynamic pressures, such as from accidental explosions.

REFERENCES

1. J. O. Gill et al. "Preliminary report on the modernization of the Naval ordnance production base and application of hazard risk analysis

technique," paper presented at the Fifteenth Explosive Safety Seminar, Department of Defense Explosive Safety Board, San Francisco, Calif, Sep 1973.

2. Arthur Mendolia. "A new approach to explosives safety," paper presented at the Fifteenth Explosive Safety Seminar, Department of Defense Explosive Safety Board, San Francisco, Calif, Sep 1973.

3. Departments of the Army, Navy, and Air Force. TM51300, NAVFAC P-397, and AFM 88-22: Structures to resist the effects of accidental explosions. Washington, DC, Jun 1969.

4. Civil Engineering Laboratory. Technical Note TN-1434: Development of a computer program for the dynamic nonlinear response of reinforced concrete slabs under blast loading, by J. M. Ferritto. Port Hueneme, Calif, Apr 1976.

5. R. L. Fox. Optimization methods for engineering design. Addison Wesley, Reading, Mass, 1971.

6. Advisory Group for Aerospace Research and Development. AGAARD No. 149: Structural design applications of mathematical programming techniques. NATO.

7. Picatinny Arsenal. TR-4441: Preliminary estimate of concrete thickness and construction costs of laced reinforced concrete structures, by R. Dede, R. Dobbs, N. Porcaro, and J. Rindner. Dover, N.J., Oct 1972.

8. Users Guide for INSLAB Code Agbabian Associates, El Segundo, Calif, Sep 1975.

List of Illustrations

Figure 1. Logic diagram for interior penalty function technique.

Figure 2. Logic diagram for minimization of $\phi(X)$.

Figure 3. Design space, 2 sides fixed.

Figure 4. Design space, 3 sides fixed.

Figure 5. Revised design space, 3 sides fixed.

Figure 6. Displacement history 4 ft x 4 ft (1.2 m x 1.2 m) concrete slab.

Figure 7. Deflection contour of 4 ft x 4 ft (1.2 m x 1.2 m) slab.

Table 1. Comparison of Optimum Solutions

(200 psi; 10 ms; wall, 12 ft L x 15 ft H)
(1,400 kPa; 10 ms; wall 3.7 m L x 4.6 m H)

N Sides	Shear Reinforcement/ Deflection	Cost ($)
	unlaced 2 degrees	3,290
	laced 12 degrees	2,289
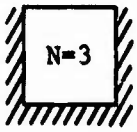	unlaced 2 degrees	2,753[a]
	laced 12 degrees	2,019
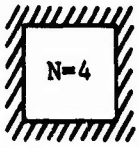	unlaced 2 degrees	2,001[a]
	laced 12 degrees	1,958

[a]Shear capacity slightly exceeded.

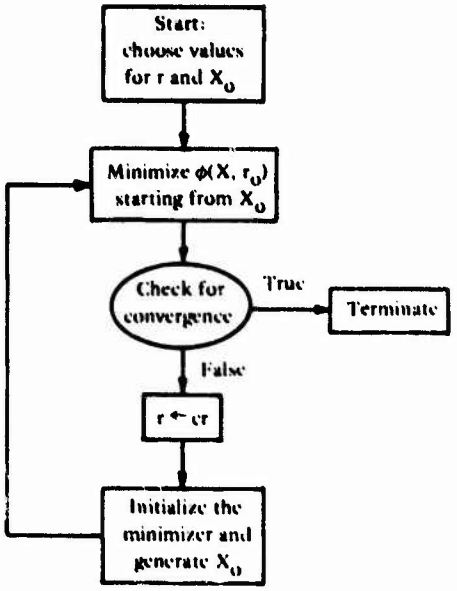

Figure 1. Logic diagram for interior penalty function technique.

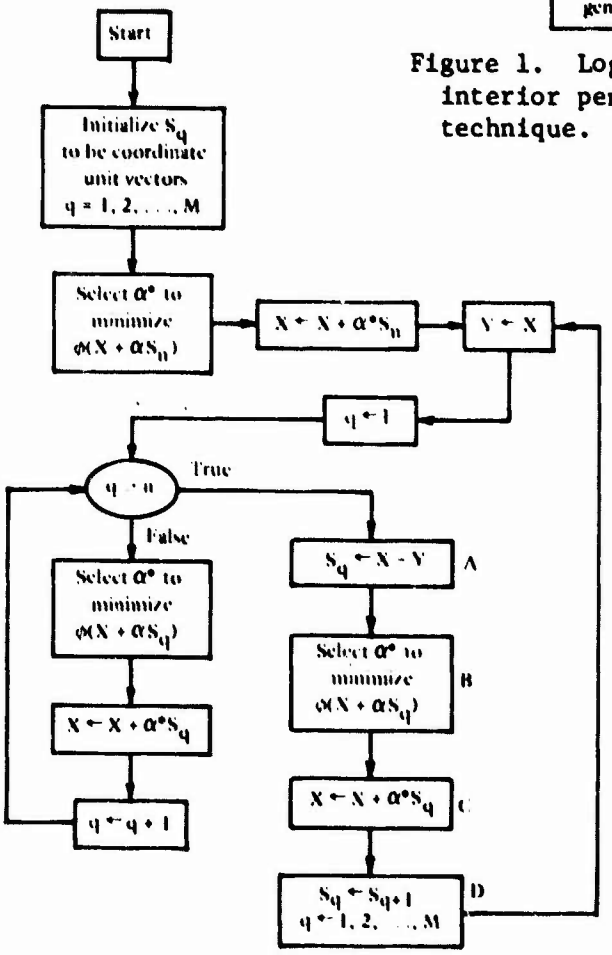

Figure 2. Logic diagram for minimization of $\phi(X)$.

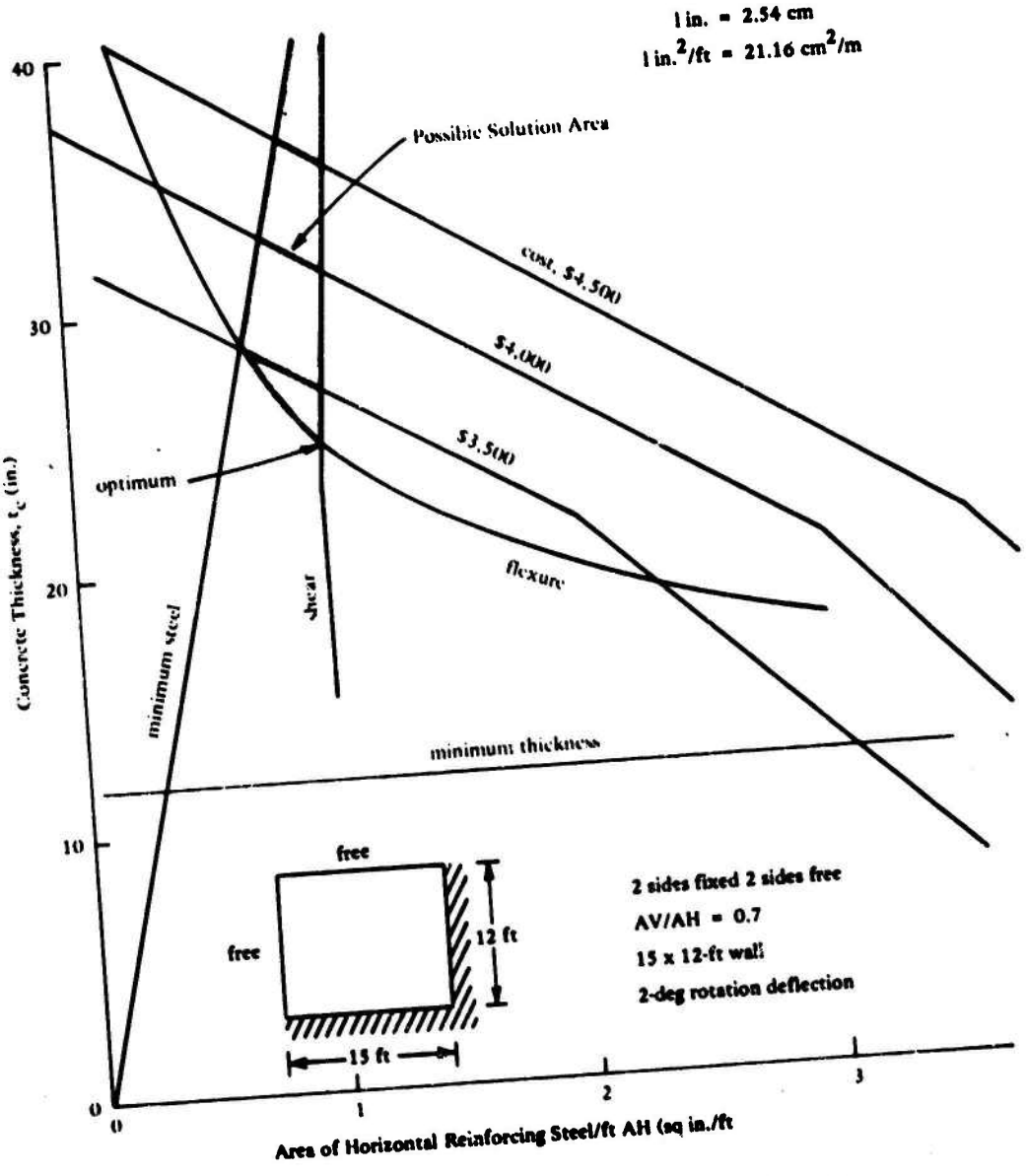

Figure 3. Design space, 2 sides fixed.

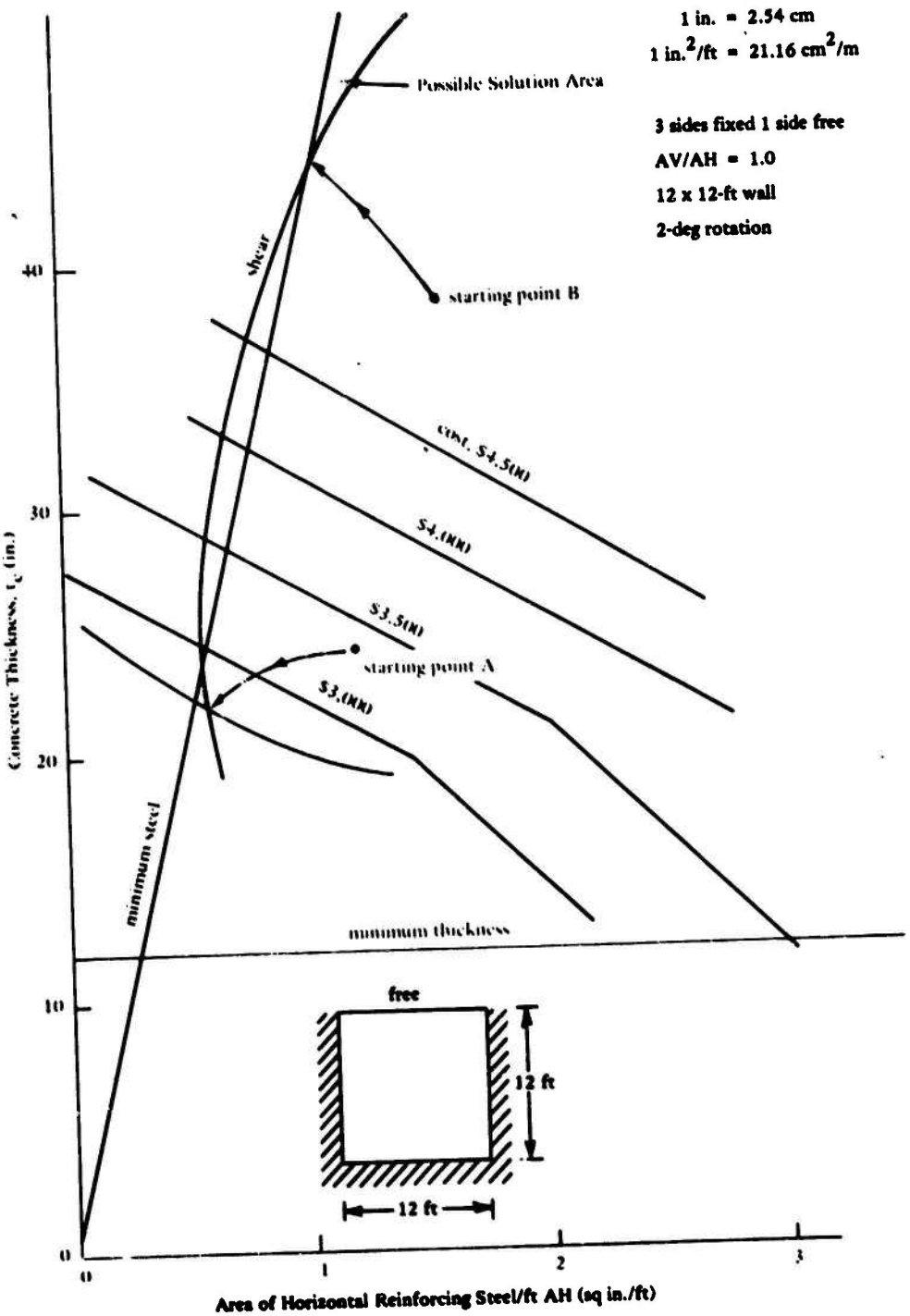

Figure 4. Design space, 3 sides fixed.

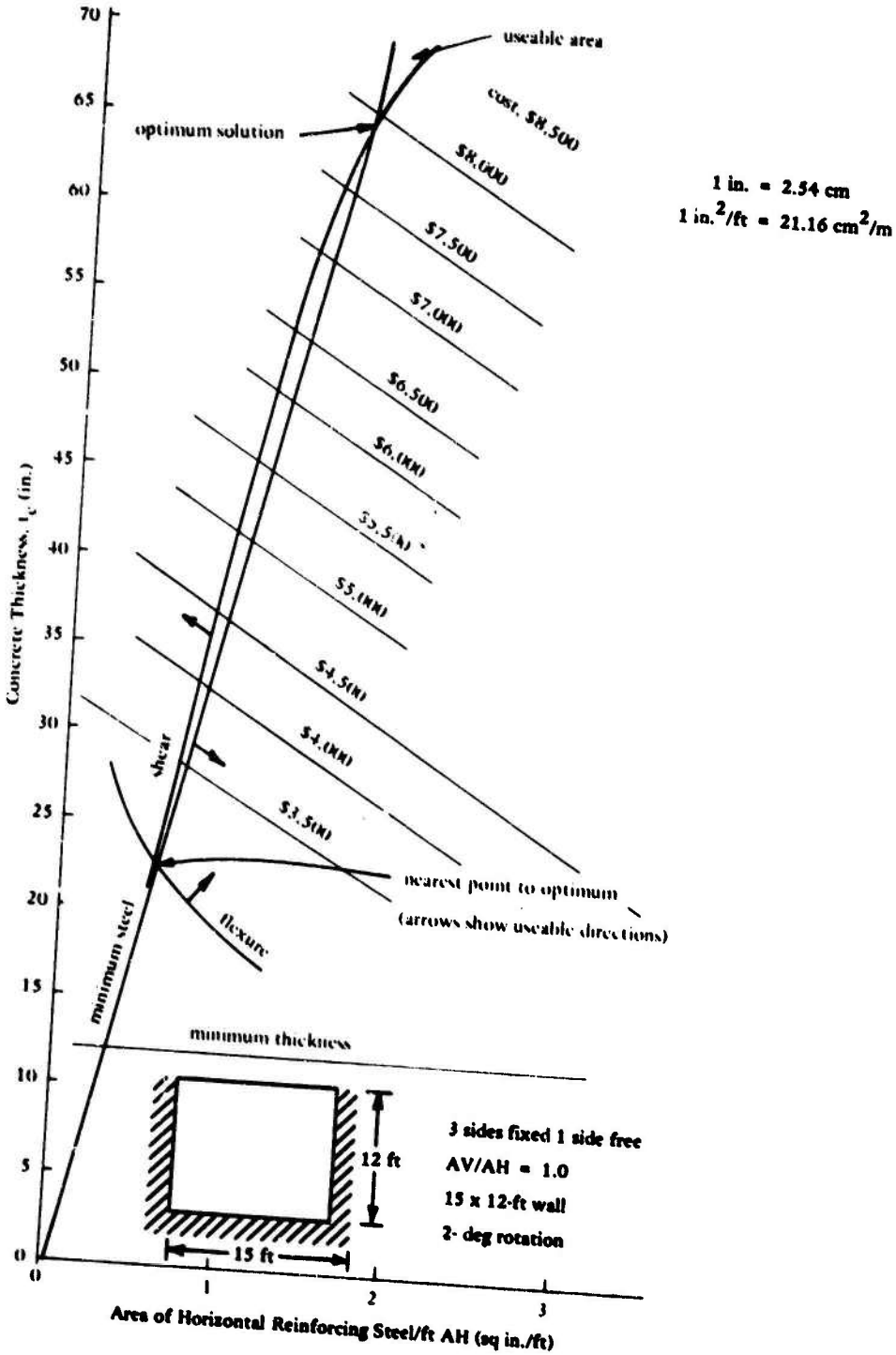

Figure 5. Revised design space, 3 sides fixed.

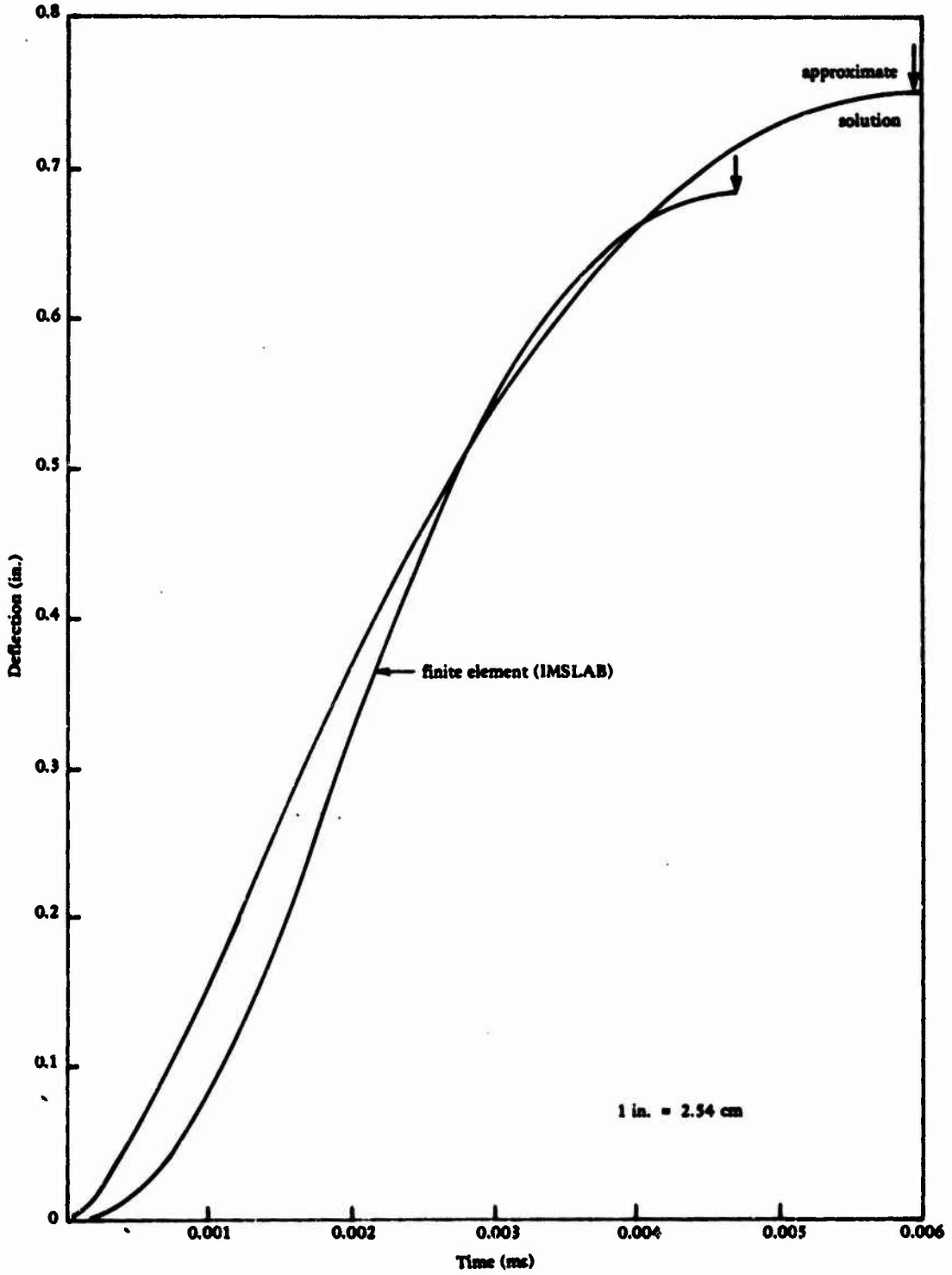

Figure 6. Displacement history 4 ft x 4 ft (1.2 m x 1.2 m) concrete slab.

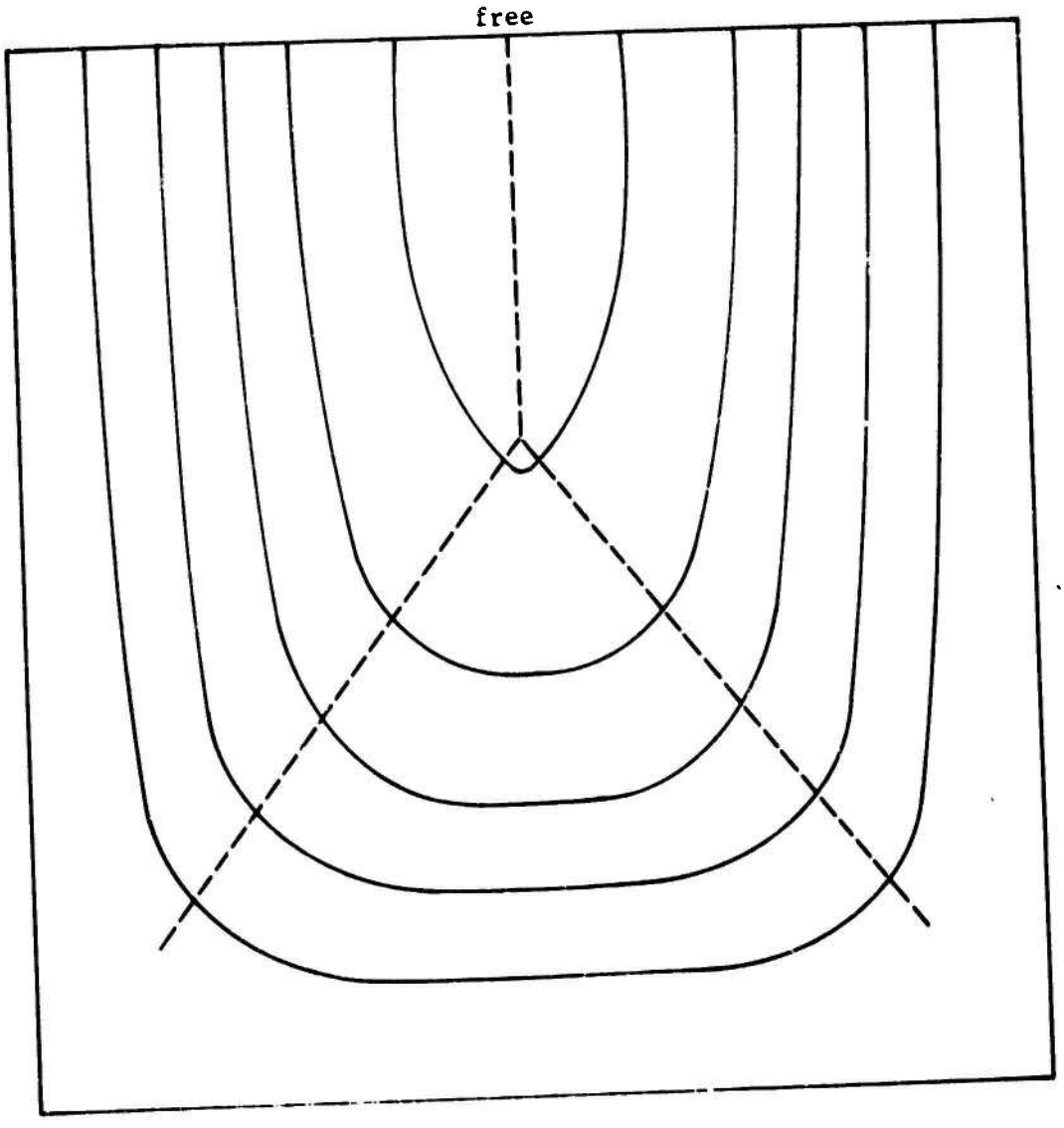

Figure 7. Deflection contour of 4 ft x 4 ft (1.2 m x 1.2 m) slab.

FEASIBILITY OF USING FIBERGLASS REINFORCED PLASTIC (FRP) BUILDINGS FOR AMMUNITION PLANTS

by

Charles C. Huang

US Army Engineer Division, Huntsville

1. INTRODUCTION

Fiberglass Reinforced Plastics (FRP) have made significant advances in technology and applications during the past years. Less than two decades ago, the first futuristic FRP house was unveiled at Disneyland, CA. Today the FRP industry is ready to market a variety of energy-saving, FRP residential houses. In chemical plants there are storage tanks, vats, hoods, and a host of structural and architectural items made from FRP, which are impervious to corrosive environments. Laminated panels with layers of FRP, plywood, and in certain applications with a core of foam are being used for semi-trailer bodies and cargo containers. FRP, having such desirable properties as being nonsparking, lightweight, corrosion resistant, smooth surface finish and impervious to water, appears to be an ideal building material for certain applications in ammunition plants. This paper presents the findings of a recent study* which investigates the technical and economic

---

* The study was prepared for the Office of DARCOM Project Manager for Munitions Production Base Modernization and Expansion. The author acknowledges that this paper was prepared based on the study conducted by his colleagues, Morgan Jones and Frank Shearer, both of USAEDH. The contributions from various FRP manufacturers to the study have been duly acknowledged in the report, listed as Reference 7.a of this paper.

feasibility of using FRP buildings for certain areas in propellent manufacturing plants where the presence of nitroglycerin (NG) vapor or nitrocellulose (NC) dust requires frequent washdown to prevent accumulation and to enhance safety.

2. MATERIALS

a. Resins

Most of the FRP components for structural applications are made of polyester resins with glass fiber for reinforcement. Phenolic resins for structural wall panels are emerging in Europe but are not as prevalent as polyester in the United States. Epoxy and acrylic resins are also available but are more expensive and difficult to mold than polyester resins. With various additives and pigments, and with different amounts of filler and fiberglass, polyester resins can be formulated to meet special requirements of mechanical properties, color, fire retardancy*, smoke development characteristics, ultraviolet ray absorption, chemical compactibility and cost.

b. Reinforcing

Fiberglass reinforcement consists basically of a bundle of glass filaments called rovings. The rovings can be woven into fabric or chopped into short lengths and bonded to form mats. Resin soaked woven fabrics, bonded mats, or chopped rovings are laid over molds to form desired FRP products (molding process). Resin impregnated rovings can be continuously

---

* Safety criteria for certain buildings require noncombustible construction materials. Use of fire retardent FRP in lieu of noncombustible material in such cases will require a waiver.

wound over a mold to form cylindrical, conical, and other complicated curved surfaces (filament winding process). Structural shapes, e.g., wide flange or I beams, channels, angles, rods, tubes, and flat sheets are made by soaking reinforcing elements in resin and then pulling them through a die (pultrusion process). Regardless of the manufacturing process, the amount and orientation of fiberglass reinforcing elements in an end product determines its mechanical properties. The strength of an FRP component is strongest in the direction of the reinforcing element; therefore, the characteristics of having varying mechanical properties in different directions must be taken into consideration during FRP building design.

c. Insulation

The insulation material commonly used with FRP is cellular foamed polyurethane.* The foam can be sprayed on or rigid foam sheets can be bonded to an FRP surface. Composite panels are made from layers of FRP with a foam core. Layers of plywood are often added for strength and rigidity.

3. FRP COMPONENTS

a. Pultruded Parts

Off-the-shelf FRP structural and architectural items available for building construction are made by the pultrusion process. Pultruded shapes, sheets, double-wall panels, etc., are formed by passing fiberglass strand rovings, mats or woven fabrics through a bath of polyester resin. The resin-impregnated reinforcing elements are then fed continuously into a temperature

---

* Polyurethane foam insulation of 2 lb/ft^3 density with the lowest smoke developed rating of 150 still exceeds the current DOD criteria. A waiver will have to be applied for applications for which the use of the foam is justifiable.

controlled die. As the cured product is pulled from the die it is cut into predetermined lengths. Pultrusion is a highly efficient manufacturing process. The equipment presently available for making pultruded structural wide flange or I beams, etc., is up to 13 inches square and for making double wall panels up to 60 inches wide and two inches deep. Standard stock items available for prompt delivery are not as large as the limiting sizes indicated above. Special runs, subject to minimum quantity restrictions, can be ordered for non-stock items.

b. Molded Parts

Large building subassemblies such as various wall units, arched roof, etc., cannot be manufactured by the pultrusion process. They are usually made by the molding process. This process involves manual operations in varying degrees dependent on the production quantity involved and the extent of tooling used. For a small production quantity, layers of fiberglass reinforcing materials are placed over or into a mold by hand. The amount of resin and reinforcing materials, which control the strength and dimensional accuracy of an end product, are greatly influenced by the skills of the worker. The curing process takes place in the atmosphere or in an autoclave depending on the production quality and quantity required. For larger quantity productions, more investment in tooling and production equipment will enhance quality control and effect production cost reduction. For example, FRP parts for automobile bodies are produced by an automated molding process.

c. Filament Winding

FRP liquid storage tanks, rocket motor skirts and nozzles, submarine antennas and the like are subject to heavy loads and severe operating environments. Stringent mechanical properties requirements which call for multi-directional fiberglass reinforcement and exacting quality control can be attained by winding fiberglass rovings over a mold. This is a relatively expensive process and its applications for FRP building construction have not been identified by the study.

4. FRP BUILDINGS

Three FRP buildings, all having dimensions of 60 feet X 30 feet, representing three design approaches were evaluated from technical and economic viewpoints. The first building investigated has a standard frame structure of beams and columns similar to the conventional metal building. All the structural members used are of pultruded FRP shapes. The second building utilizes a shell construction which would provide more rigidity than the frame structure. The third one was adapted from an FRP prototype residential house being developed by an FRP manufacturer for large quantity production. The features of these buildings are given in the following paragraphs:

a. Standard Frame FRP Building

Figures 3-1, 3-2 and 3-3 depict the concept of this building. This is a conventional beam and column framing system made from pultruded FRP structural members with bolted connections. The exterior wall and roof panels are insulated double wall FRP panels. Three types of panels were investigated and each will be described later. The structural frame

was designed in accordance with the design guides* provided by FRP manufacturers. The low modulus of elasticity of FRP (2.3×10^6 psi for FRP as compared with 29×10^6 psi for steel and with 10×10^6 psi for aluminum) creates problems of deflection and elastic instability under loads. For instance, the standard FRP structural shapes are inadequate for a clear span of 30 feet due to excessive deflection and a center column for each bay must be provided.

The beam and purlin size selection is based on beam deflection and the column is based on elastic stability. As a result the stress level in the members is rather low. This indicates that the frame building system does not provide efficient use of FRP material and its cost may not be competitive with other type building systems such as shell construction.

The three wall panels investigated for use with the structural frame are off-the-shelf items that have been used successfully for various applications. Their features are described below:

(1) Composite Panel. This panel (Figure 3-4a) with two layers of plywood provides adequate strength to span from the floor to the roof without horizontal girts or tie rods, thus eliminating the ledges along the wall for dust collection. The foam core provides required insulation. This panel can be fabricated in sizes 10 feet wide and up to 200 feet long

---

* The ASCE Structural Plastic Research Council is preparing two manuals: "Properties Classification Manual," and "Design of Plastics Structural Components." The manuals, when available, will provide more design guidance.

without joints or seams. If the practical limit in length for handling is assumed to be 30 feet, for a 60 foot x 30 foot building, it would require only one joint for each of the 60 foot walls. The work involved in the preparation of vapor/liquid impervious joints would be reduced to a minimum. Further, the panel's inner surface has a bonded gel-coat finish similar to FRP bathtubs and pleasure boats. This finish can be made fire retardant and imprevious to water and many chemicals.

(2) Pultruded Panel. This panel (Figure 3-4b) is a pultruded box section of 48 inches wide and 2 inches deep with intermediate longitudinal diaphragms at 6-inch intervals. The voids are filled with polyurethane foam for insulation. The panel has a recess along each edge to provide lap joints to hold the panels together, and it can be made to meet specified strengths. It is lighter than the composite panel described previously and can be framed vertically from the floor to the roof, without horizontal supports. Since the panel is only 4 feet wide, joint preparation for sealing against explosive vapor/dust will be required at 4-foot intervals. This means more field work during building erection and subsequent maintenance (recaulking or resealing). Further, the surface finish of the pultruded panel is not as smooth as the gel-coated surface on the composite panel.

(3) Molded Panel. This is a proprietary item (Figure 3-4c) consisting of an inner and outer molded FRP skin with a polyurethane foam core. The 4-foot wide panel has its edges bent outward to form flanges to facilitate bolting the panels together to form a wall or a roof. Some of the buildings for housing switchgear in electric substations are made from this type panel.

The inner surface has a gel-coat finish and the outer surface has a durable finish for exterior exposure. One drawback of this panel is its width which requires caulking and sealing of the seams between panels at 4-foot intervals. For a relatively small building, the walls and roof can be made from the panels to form a shell which is structurally adequate without additional structural frames.

b. FRP Semi-Arch Building

The semi-arch concept (Figures 3-5, 3-6, and 3-7) was investigated because a shell structure is usually more efficient (i.e., to attain a higher ratio of carrying capability to the weight of FRP used) than a frame building system of beams and columns. A semi-arch building is formed by bolting together a number of prefabricated semi-arch segments. When all the joints between segments are properly sealed the entire interior surface will be smooth and free from any protrusion due to structural members.

The size and shape of semi-arch segment was developed in consultations with manufacturers for constructability based on the largest autoclave presently available. The segments, according to one manufacturer's view, can be fabricated by hand lay-up/vacuum mold/autoclave curing process. For a small quantity production, the mold would consist of male and female parts and produce one segment at a time.

With the existing facilities at the manufacturer's plant, the estimated production rate for such a segment is rather slow. Heavy investment for more molds and larger size autoclaves is not justifiable unless a large quantity of the building is in demand. Obviously, this labor intensive fabrication method cannot be expected to result in a relatively inexpensive building of this type.

c. FRP PREFAB Building

Since quantity production is the key to cost reduction, an attempt was made to adapt certain FRP houses being developed for large-quantity production to the 60 foot x 30 foot building under study. Two proprietary prototype buildings have been built and a third improved version is under development by Molded Fiber Glass Co. (MFG), Astabuhla, Ohio. The concept shown in Figure 3-8 was developed with the aid of the manufacturer's architect. This building system will utilize the standard components and subassemblies in the FRP residential houses to be marketed for quantity production. As the market expands and production costs lower, it is expected that FRP buildings constructed by this approach would result in cost effective buildings for use in ammunition plants.

5. FRP BUILDING COSTS

The estimated costs for the FRP buildings described earlier are summarized in Tables 3 and 4. The estimates were developed from the material cost data furnished by manufacturers. The costs for shipping, handling, and erection were estimated based on the total weight for each building system and the degree of complexity in erection and labor skills needed. It should be noted that the costs for site preparation, foundation, and equipment and utilities installations are not included in the estimates.

As expected, the specially designed semi-arch building system costs more than the other two. The building adapted from the residential houses would have the most cost reduction as the quantity increases. It must be recognized that such a significant cost reduction is attainable predicated upon the expectation that the FRP residential houses would be able to capture

the housing market as planned. Therefore, the actual amount of cost reduction due to quantity as indicated here can be verified only when marketing of the FRP residential houses is underway. Nevertheless, the trends indicate clearly that the adaptation of commercially available standard components to a particular application is the approach that results in cost saving.

It is also interesting to note that there is a very small difference in costs among the frame-structured buildings using three different FRP panels for walls and roof. This indicates that the cost differentials of the three panels are small and the selection of the panel will be based more on their technical features than on cost.

Figure 3-11 provides a comparison not only among the three FRP buildings studied, but also between FRP and preengineered steel buildings. The cost indicated here for preengineered building includes the work involved in the special treatment of the joints and seams and wall surfaces in order to meet the same washdown requirements for FRP buildings. However, one must recognize that the cost comparison between FRP and preengineering steel buildings as indicated does not provide the whole picture, because the inherent advantages and disadvantages of FRP and metal buildings are not amenable to quantitative comparison. In fact, the steel building is not an acceptable structure by the safety community for housing NG operations.

Thus far the comparisons have been made on the initial costs of the buildings. Through the subsequent years of operations, seams and joints will require rework to maintain vapor/dust-proof feature. Bolts in certain

areas may have to be tightened or replaced. The surface of the walls may need refinishing to maintain required smoothness. Taking into consideration all necessary maintenance during the years, a life cycle cost analysis for a 25 year service life was made for the three types of FRP buildings and the insulated preengineered steel building. The results are tabulated in Table 4. It is interesting to note that the difference in cost between the steel building and the FRP building adapted from prefabricated residential houses is about 13 percent.

6. CONCLUSIONS

a. The best approach to providing an all FRP building of 60 feet x 30 feet for use in ammunition plants would be to adapt it from standard FRP residential houses that are being developed by the FRP industry for the housing market (Molded Fiberglass Company, Astabuhla, Ohio is one of such developers). Utilizing quantity-produced standard wall and roof units would reduce the initial building cost. Specially designed FRP buildings using pultruded FRP structural shapes or molded components would not be cost effective because the quantity for each particular application is small.

b. Small buildings of shear wall-type construction can be produced by modular flanged FRP panels (similar to Figure 3-4c except no extensive interior structural framing). The largest building of this type construction built by PACS Industry, Inc., Great Neck, New York is 20 feet x 68 feet with a peaked roof which has been used for housing switchgear. This type of ready made FRP-panel building could be utilized if an immediate need for relatively small FRP buildings should arise.

c. At the Radford Ammunition Plant, some of the future buildings in which propellent dust presents hazards is planned to have "inside-out" wood structures. The wood frame is inclosed by an inside wall only; thus, leaving the structural frame exposed on the outside. The hidden cavities for dust accumulation, which normally exist between the walls of conventional double-wall buildings, are eliminated in the "inside-out" construction. The interior plywood walls are to be caulked and sealed and painted for dust and water proofing. It can be envisioned that this type construction will have low initial building cost. However, it will require more maintenance and it also lacks insulation.

The FRP-plywood panel (similar to Figure 3-4a such as those made by Lunn Laminates, Inc., Wyandanch, New York) could be used for the interior wall of the "inside-out" wood building. This type panel would require fewer joints and seams (because large size panels are available) and a very smooth gel-coat surface finish. These features are desirable from both operating and maintenance viewpoints and make the FRP-plywood panel a better wall system for the "inside-out" construction than does the plywood panel.

d. In planning or designing FRP buildings for ammunition plants, one must recognize the fact that some of the FRP characteristics are still not fully known and require attention for each particular application. Such characteristics include the following:

(1) Deformation of FPP structural members under load tends to increase with time. The creeping characteristic is not fully known and more data should be collected from existing prototype buildings.

(2) FRP structural members, when subject to sustained elevated temperatures, lose a large percentage of their load-carying capacity. For example, the strength of FRP may reduce up to 50 percent in a 200°F environment. This factor must not be overlooked in designing FRP structures.

(3) The effects of static buildup on FRP surfaces should be investigated to establish safe grounding methods.

7. REFERENCES

a. HNDTR-78-33-ED-SR, 15 July 1978, "Feasibility of Using Fiberglass Reinforced Plastic (FRP) Structure for NG Operations."

b. HNDTR-78-34-ED-SR, 1 May 1978, "Standard Details Study for NG, NC, SB and MB Facilities."

c. DOD 4270.1-M, 1 October 1972, Department of Defense Construction Criteria Manual.

d. AMCR 385-100, Safety Manual.

COPPS OF ENGINEERS U.S. ARMY

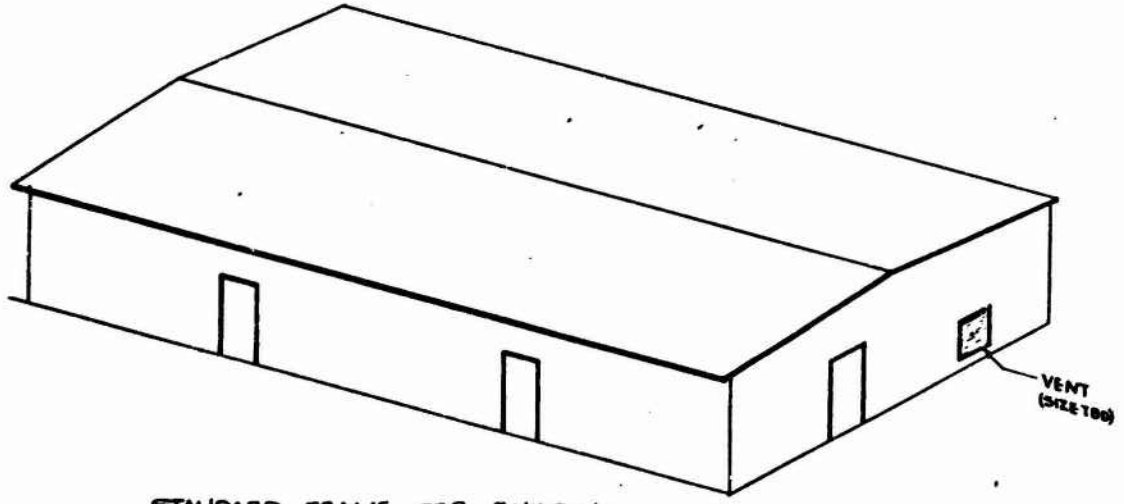

STANDARD FRAME FRP BUILDING

NOTE 1. FOR WALL & ROOF PANEL LAYOUT SEE FIGURES 3-4a THRU 3-4c

FIGURE 3-1

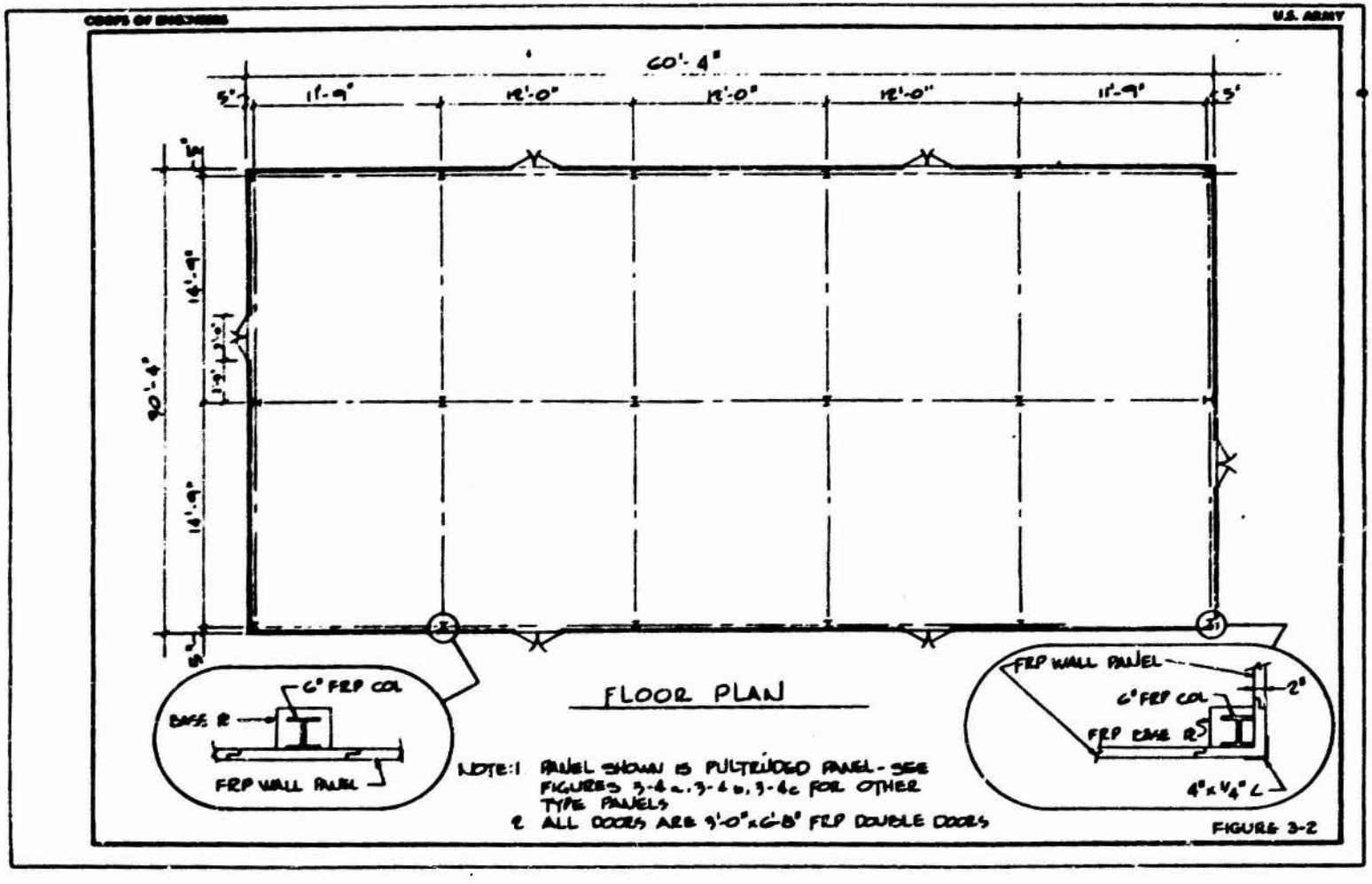
CORPS OF ENGINEERS
U.S. ARMY
60'-4"
5"
11'-9"
12'-0"
12'-0"
12'-0"
11'-9"
5"
5"
14'-9"
30'-4"
15'-3"
14'-9"
5"
6" FRP COL
BASE R
FRP WALL PANEL
FLOOR PLAN
FRP WALL PANEL
6" FRP COL
2"
FRP EDGE R
4"x 1/4" L
NOTE: 1 PANEL SHOWN IS PULTRUDED PANEL - SEE FIGURES 3-4a, 3-4b, 3-4c FOR OTHER TYPE PANELS
2 ALL DOORS ARE 3'-0"x6'-8" FRP DOUBLE DOORS

FIGURE 3-2

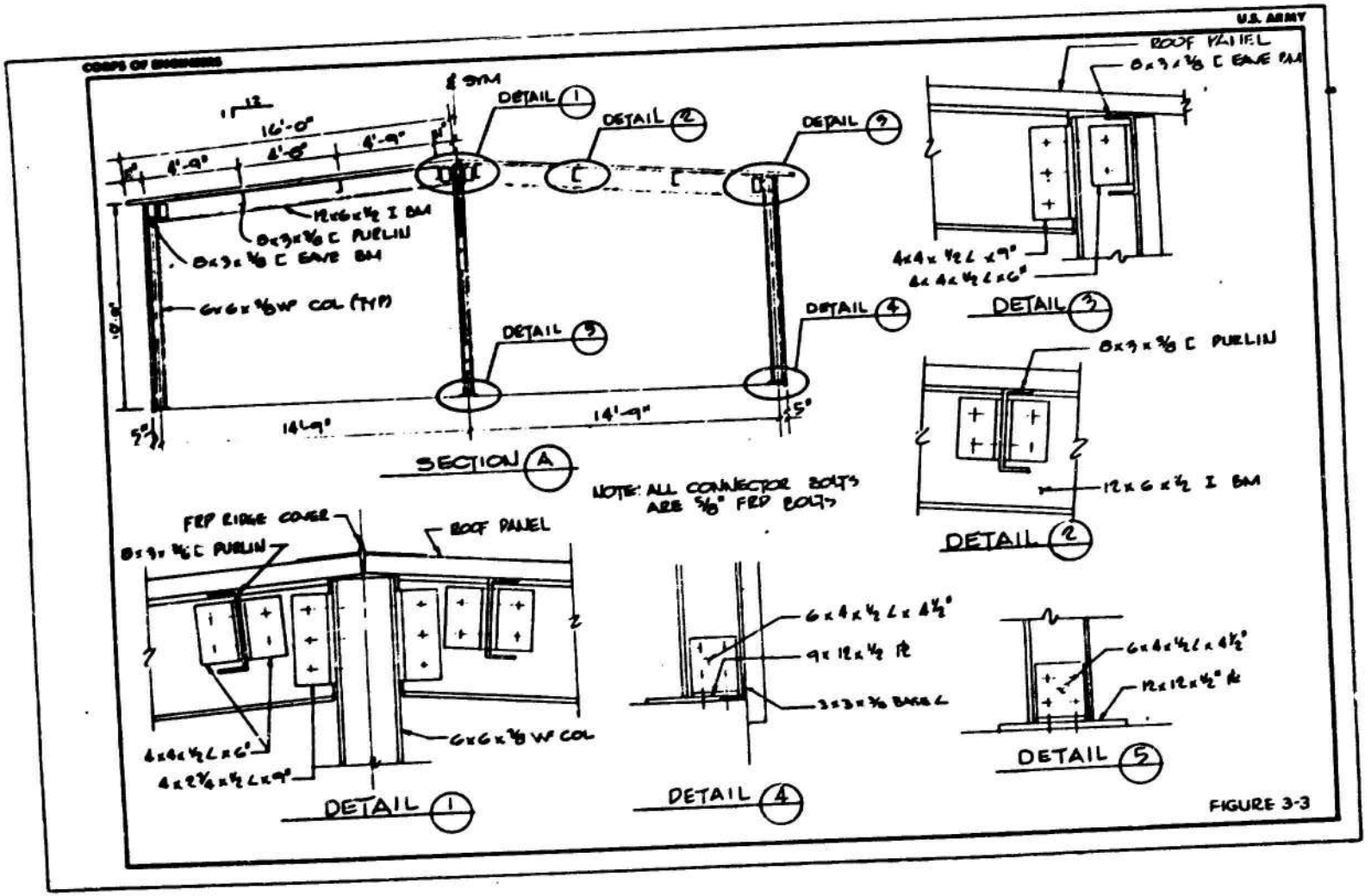
CORPS OF ENGINEERS
U.S. ARMY
DETAIL 1
DETAIL 2
DETAIL 3
DETAIL 4
DETAIL 5
16'-0"
4'-9"
4'-8"
4'-9"
12x6x½ I BM
8x3x⅜ C PURLIN
8x3x⅜ C EAVE BM
6x6x⅜ WF COL (TYP)
14'-9"
14'-9"
5"
5"
SECTION A
NOTE: ALL CONNECTOR BOLTS ARE ⅝" FRP BOLTS
ROOF PANEL
8x3x⅜ C EAVE BM
4x4x½ L x 9"
4x4x½ L x 6"
8x3x⅜ C PURLIN
12x6x½ I BM
FRP RIDGE COVER
8x3x⅜ C PURLIN
ROOF PANEL
4x4x½ L x 6"
4x2¾x½ L x 9"
6x6x⅜ WF COL
6x4x½ L x 4½"
9x12x½ PL
3x3x⅜ BASE L
6x4x½ L x 4½"
12x12x½" PL

FIGURE 3-3

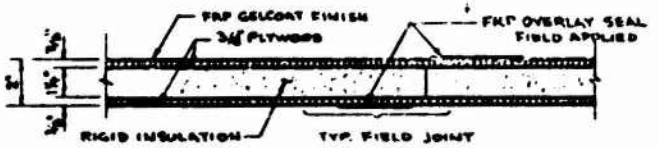

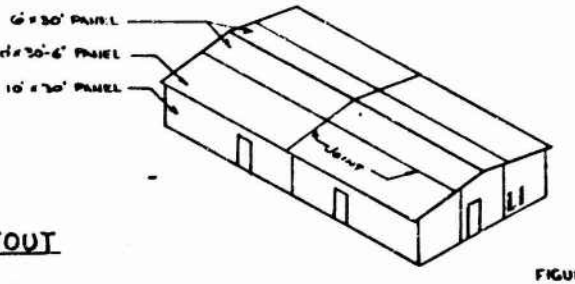

COMPOSITE PANEL EXTERIOR LAYOUT

FIGURE 3-4a

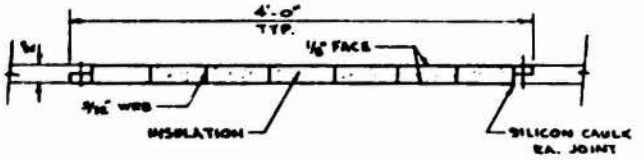

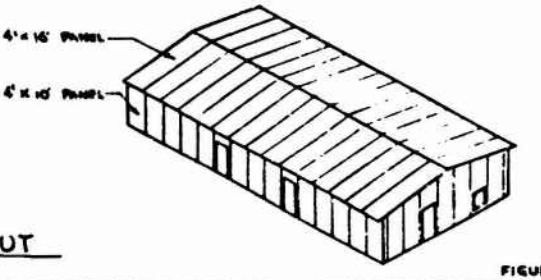

PULTRUDED PANEL EXTERIOR LAYOUT

FIGURE 3-4b

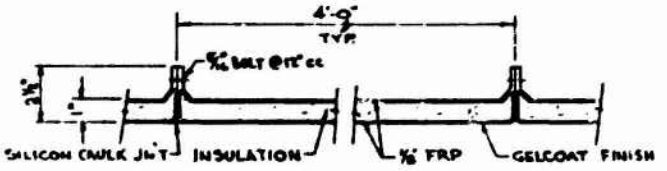

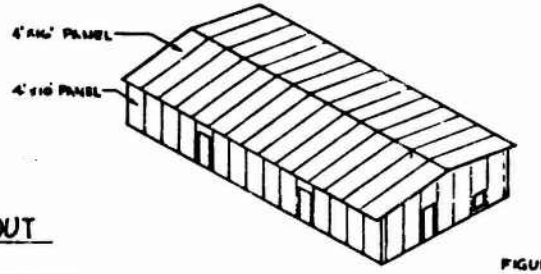

MOLDED PANEL EXTERIOR LAYOUT

FIGURE 3-4c

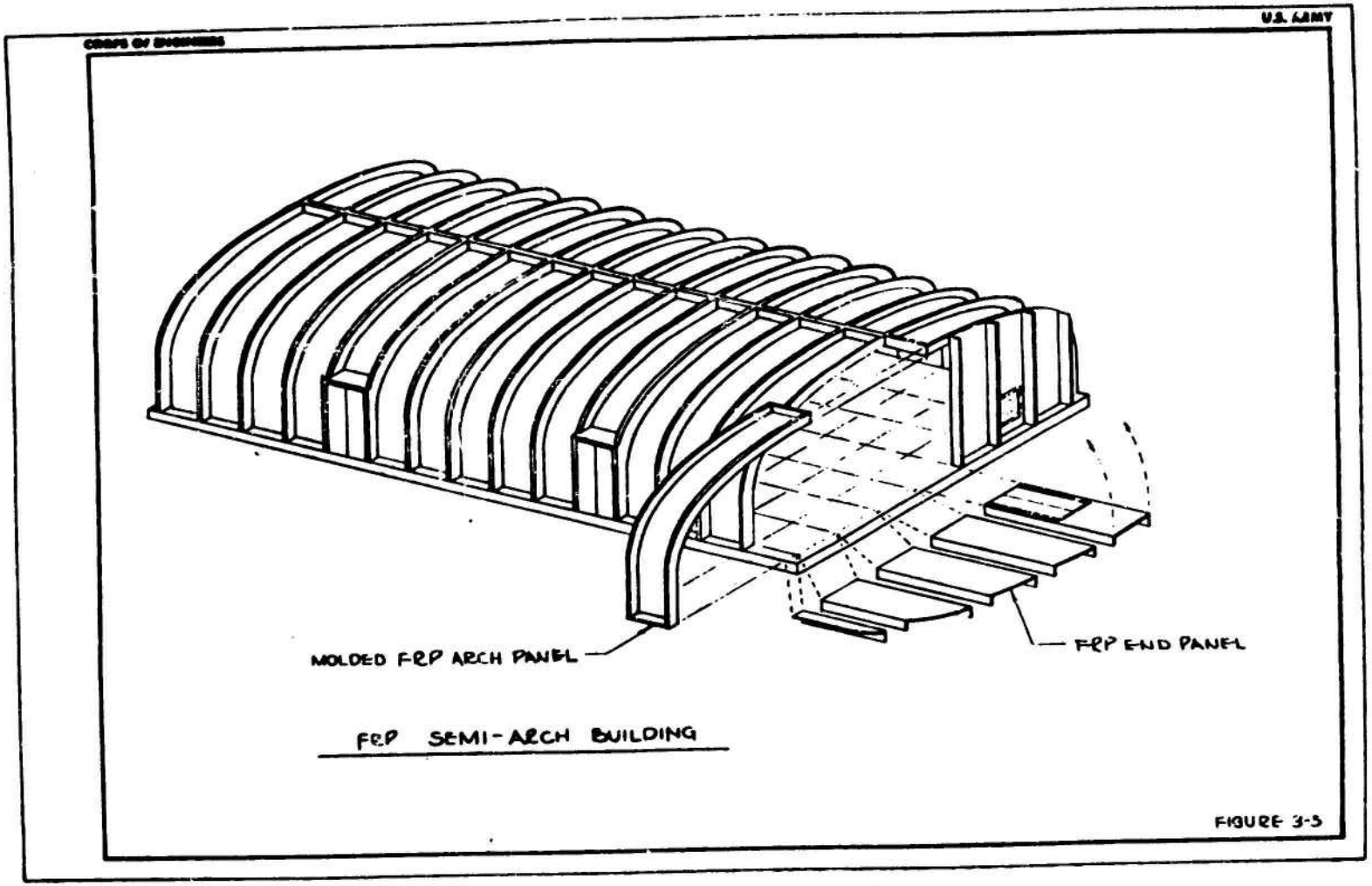
U.S. ARMY
CORPS OF ENGINEERS
MOLDED FRP ARCH PANEL
FRP END PANEL
FRP SEMI-ARCH BUILDING

FIGURE 3-3

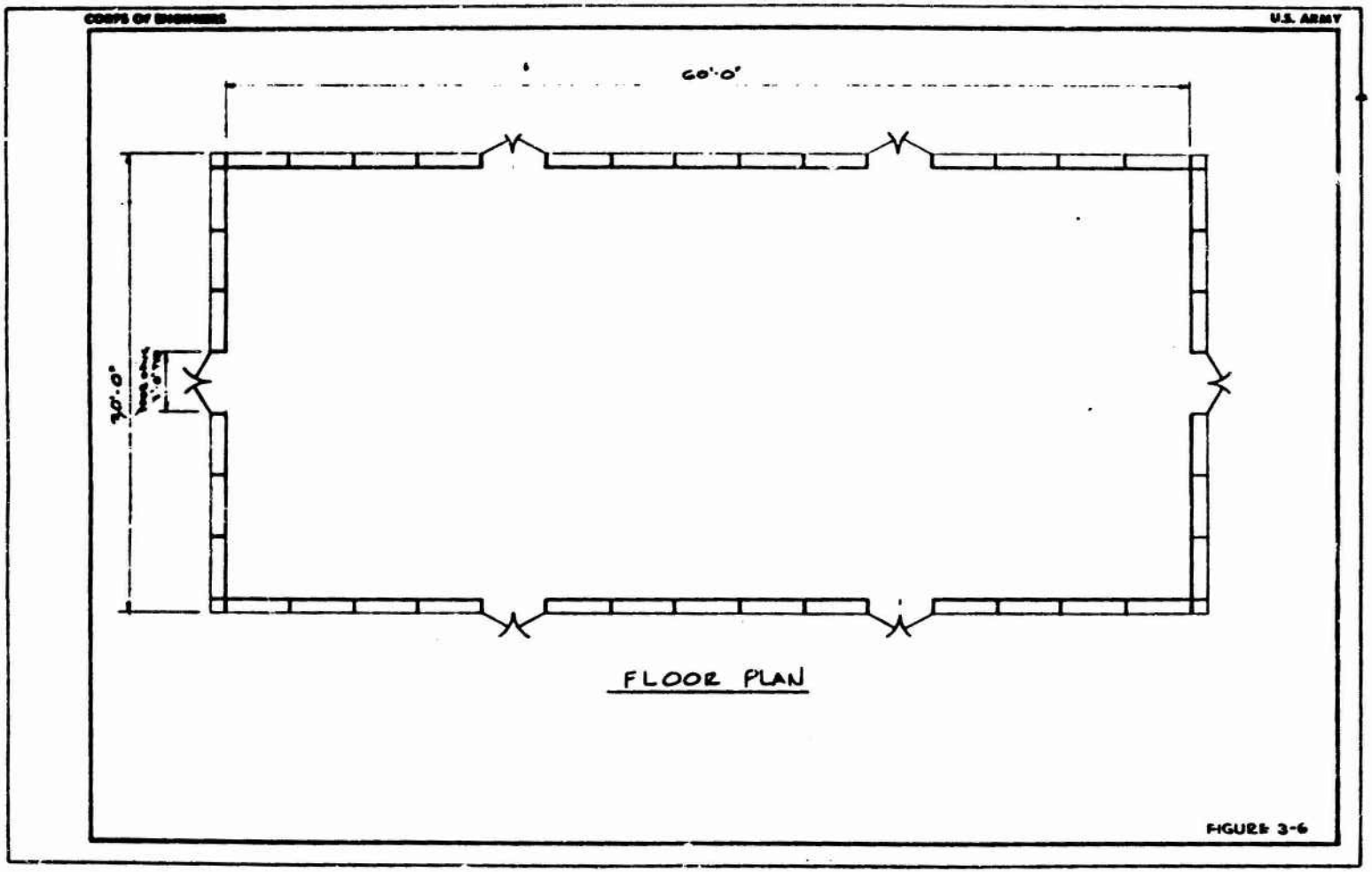
CORPS OF ENGINEERS
U.S. ARMY
60'-0"
30'-0"
FLOOR PLAN
FIGURE 3-6

CORPS OF ENGINEERS U.S. ARMY

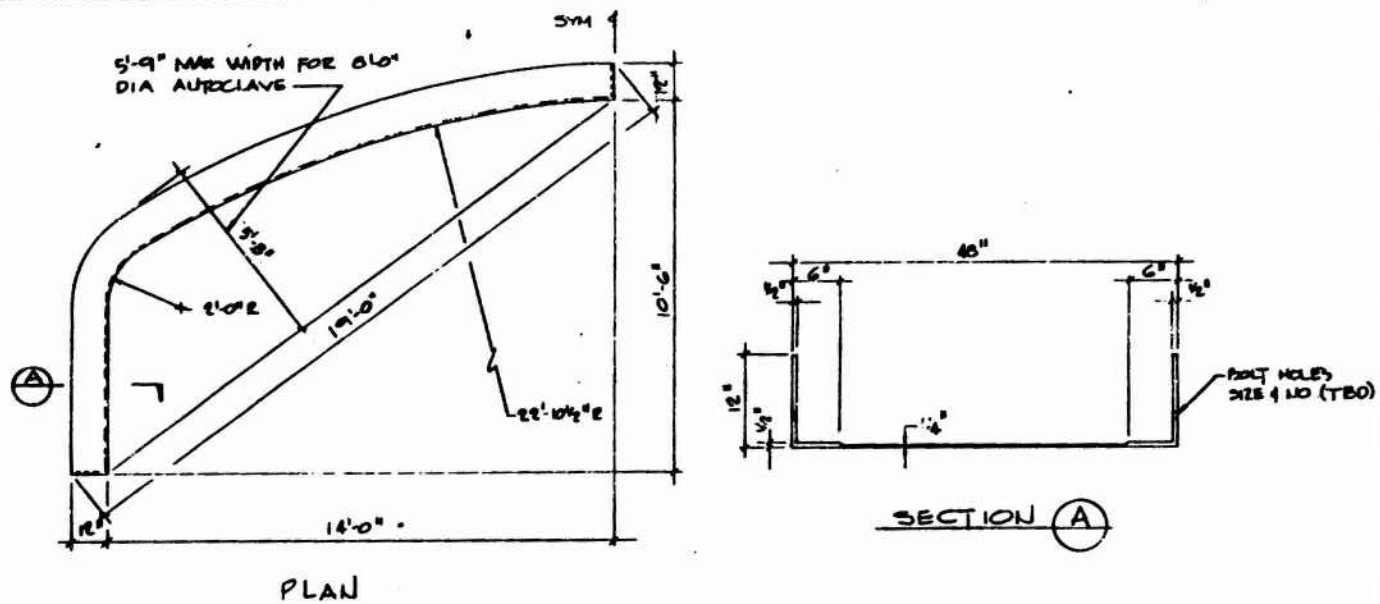

FIGURE 3-7

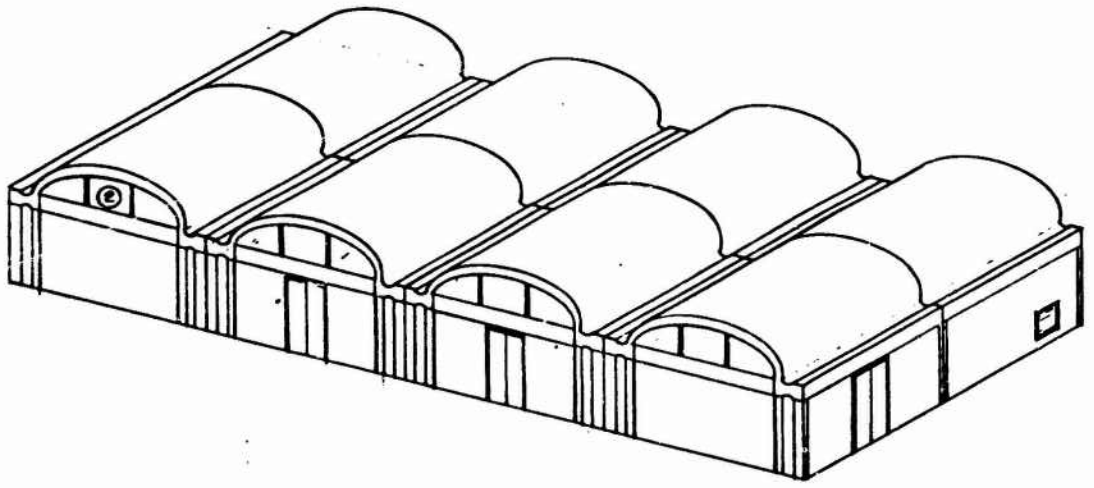

FRP MFG PREFAB BUILDING

FIGURE 3-8

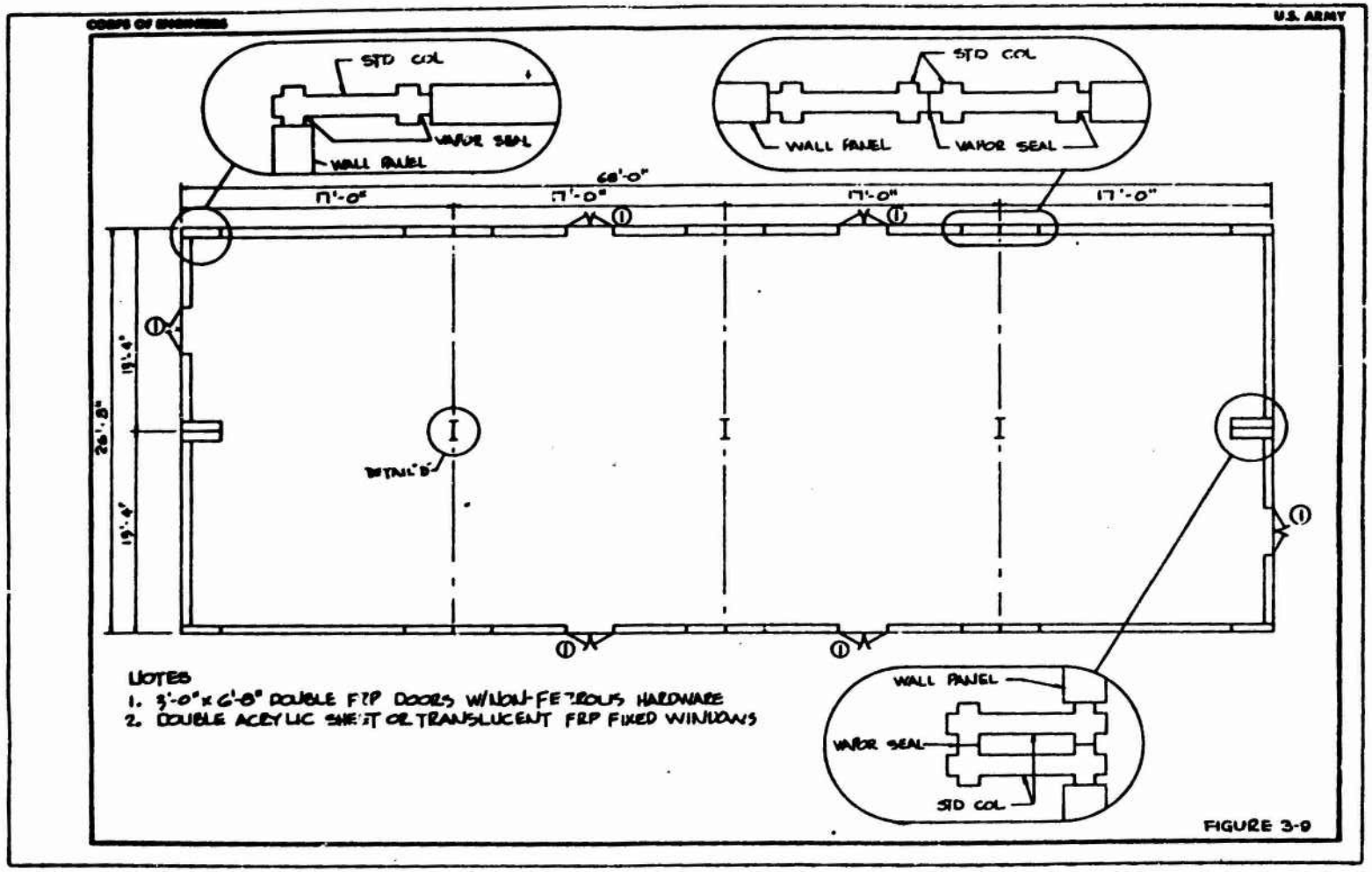
CORPS OF ENGINEERS
U.S. ARMY
STD COL
VAPOR SEAL
WALL PANEL
STD COL
WALL PANEL
VAPOR SEAL
60'-0"
17'-0"
17'-0"
17'-0"
17'-0"
20'-8"
19'-4"
19'-4"
DETAIL "B"
NOTES
1. 3'-0" x 6'-8" DOUBLE FRP DOORS W/NON-FERROUS HARDWARE
2. DOUBLE ACRYLIC SHEET OR TRANSLUCENT FRP FIXED WINDOWS
WALL PANEL
VAPOR SEAL
STD COL

FIGURE 3-9

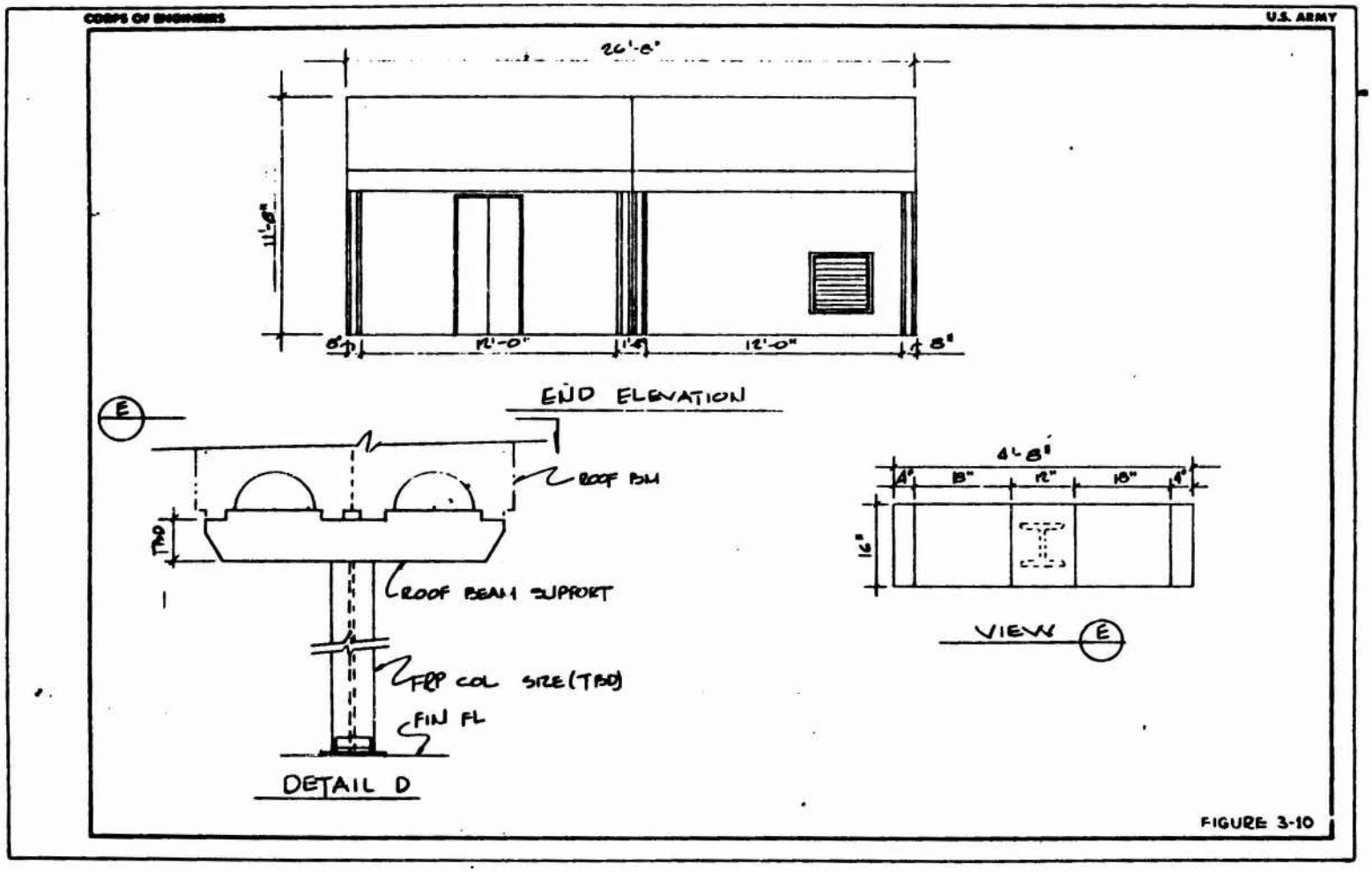
CORPS OF ENGINEERS
U.S. ARMY
26'-0"
11'-6"
6"
12'-0"
1'-6"
12'-0"
8"
END ELEVATION
E
ROOF BEAM
TBD
ROOF BEAM SUPPORT
FRP COL SIZE (TBD)
FIN FL
DETAIL D
4'-8"
A"
B"
12"
10"
4"
16"
VIEW E

FIGURE 3-10

FRP BUILDING COSTS
QUANTITY COMPARISON CURVES

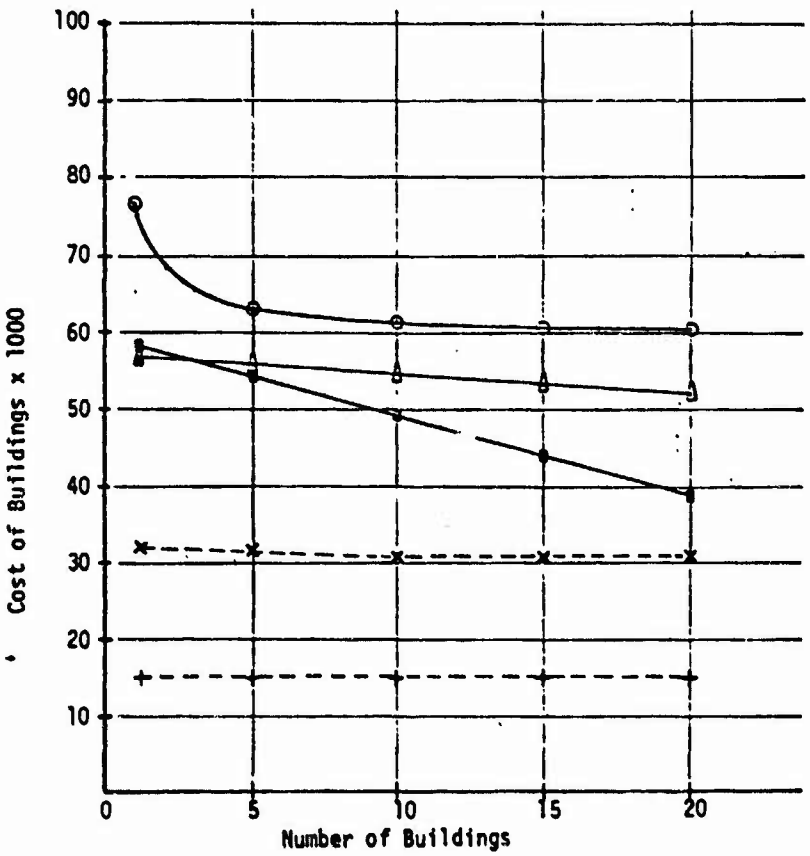

Δ-FRP Pultruded Frame Buildings
o-FRP Semi-Arch Buildings
□-MFG FRP Prefab Buildings
×-Standard Pre-engineered Steel Buildings/Insulated Panels
+-Standard Pre-engineered Steel Buildings (No Insulation)

Figure 3-11 Quantity Comparison Curves

TABLE 3

ESTIMATED COST FOR QUANTITY PROCUREMENT (1978 DOLLARS)

TYPE OF BUILDING	NUMBER OF BUILDINGS				
	1	5	10	15	20
FRP Pultruded Shape Bldg.(a)	$56,000	$54,000	$53,600	$52,500	$51,400
(b)	56,500	55,300	54,100	53,000	51,900
(c)	57,000	55,800	54,600	53,500	52,400
FRP Semi-Arch Building	76,900	63,000	61,300	60,700	60,400
FRP Prefab Building	58,400	53,500	48,600	43,700	38,800
Mod. Preengineered Steel Building, Insulated	32,000	31,800	31,600	31,600	31,600

TABLE 4

ESTIMATED COST PER SQUARE FOOT FLOOR AREA (1978 Dollars)

TYPE OF BUILDING	NUMBER OF BUILDINGS				
	1	5	10	15	20
FRP Pultruded Shape Bldg.(a)	$31.11	$30.00	$29.78	$29.17	$28.56
(b)	31.39	30.67	30.06	29.44	28.83
(c)	31.67	31.00	30.33	29.72	29.11
FRP Semi-Arch Building	42.72	35.00	34.06	33.72	33.56
FRP Prefab Building	29.95	27.44	24.92	22.41	19.90
Mod. Preengineered Steel Building, Insulated	17.78	17.68	17.56	17.56	17.56

(a) Plywood Reinforced FRP Panel, (b) Pultruded FRP Panel, (c) Lay-up FRP Panel.

ALL ESTIMATED COSTS SHOWN ARE FOR BUILDINGS ERECTED ON A PREVIOUSLY CONSTRUCTED SLAB. COSTS FOR THE CONCRETE SLAB, MECHANICAL, ELECTRICAL AND SITE WORK ARE NOT INCLUDED.

TABLE 5

LIFE-CYCLE COST

TOTAL COST IN CONSTANT DOLLARS AND PRESENT WORTH

	PULTRUDED FRAME			FRP	FRP	STEEL
	Pultruded Panel	Plywood Laminate	Molded Panel	Semi-Arch Building	Prefab Residential Type	PE Steel Building
Unit Price/S.F.	$28.83	$28.56	$29.11	$33.56	$19.90	$17.56
(1) Investment Cost	51,900	51,400	52,400	60,400	38,800	31,600
(2) Maintenance Cost						
(a) Surface Treatment with Gel-Coat		1,560	1,560	1,560	1,560	1,560
without Gel-Coat	3,120					
(b) Tighten or Replace Fasteners	1,863	772	1,096	1,096	0	1,544
(c) Recaulk Joints	2,120	680	2,120	1,600	280	3,200
(d) Damage Repair	116	116	116	116	116	600
(3) Total Cost (Constant-1978 Dollar)	59,119	54,528	57,292	64,772	40,756	38,504
(4) Present Worth (Inflated and Discounted)	54,787	52,513	54,222	62,013	39,444	34,246

DYNO INDUSTRIER A.S

Explosives Division

NORWAY

A PRESENTATION OF
THE DIVISION'S APPROACH TO RISK ANALYSIS
IN PRODUCTION AND STORAGE
OF EXPLOSIVES

MR. MAGNE SOLHEIM

1. Background

From the number of fatalities in the production of commercial NG-explosives in Western Europe over the last 15 years, and from an estimate of the number of employees, the number of fatalities per 100 million working hours can be calculated.

For comparison, the official Norwegian statistics for 1970 are shown:

Explosives production in Western Europe	50 fatalities/100 million working hours
Mining industry, Norway	35 fatalities/100 million working hours
Total industry, Norway	5,5 fatalities/100 million working hours

The comparison shown above and the reactions that occured after several accidents in the first part of the 1970's was the reason for Dyno's decision to start a more systematic approach to the problem of reducing the number of accidents.

Dyno's explosives plants are all placed in populated areas less than 30 miles from Oslo. One of the first and most important tasks was therefore to find criteria vis-a-vis our surroundings. Up till now all our work has been based on the assumption that an accident will occur (probability = 1).

2. Criteria

Dyno's criteria for external and internal conditions are shown in fig. 1. This kind of criteria made it possible to plan and arrange our production and storage areas in a better way than the traditional quantity distance tables.

3. Applications of the criteria

3.1 General approach

All of Dyno's explosives plants have been studied with respect to these criteria, using a "Questionnaire" shown in fig. 2.

The various buildings and transport routes have been analysed and classified. In this work we also have used a datasheet shown in fig. 3. This analysis has been the base for several decisions and changes, some of which are substantial, which have been carried out.

3.2 Work in the Gullaug plant

As the map in fig. 4 shows, the Gullaug plant is situated on a peninsula.

Boundaries set up by the criteria versus the nearest dwellings, shops, schools, roads and factories are shown.

All explosives activities were situated on the part of the plant area outside these boundaries.

The quay with up to 400 tons and some magazines containing 50 tons each (sum 600 tons) were found not to be acceptable.

The conclusion of the first stage was therefore that the Gullaug plant fulfilled the demands versus the surroundings, if the quay and the magazines were removed.

The next questions were whether the internal criteria were fulfilled, and if the remaining area satisfied our demands for the present and future concerning space.

Fig. 5 shows how the plant was arranged when the work started.

The numbered areas were found not to fulfill the criteria due to the distances to the workshops and roads. The amount of explosives in process in these buildings was too high and since there was no practical way of reduction the following major decisions were made

- Production of TNT hade to be stopped
- Production of TNT-slurry, ANFO and detonating cord had to be moved. This was taken into account in the new plant layout.
- The quay and the magazines had to be moved out of the plant area.

These projects are mostly finished by now.

In the plant we have 3 categories of traffic

- Personell
- Undangerous goods
- Dangerous goods

These categories will all affect the risk situation.

Personell transport represents a risk problem only if it goes through or stops in dangerous areas.

Transport of dangerous goods will be a problem by endangering the route.

This led to that serveral roads and routes had to be changed. New routines for personell transport (buses and private cars, parking places) were introduced. In order to acheive a rational transport of dangerous goods it was decided to build a sorting/intermediate storage terminal for finished products from where the goods are transported to the magazine area. This terminal has been in operation since early 1976 and consists of 5 igloos for 8 tons each.

Final conclusions

The analysis which has been roughly described above led to a disposition plan for the area which is shown in fig. 6.

As the plan shows the transport of personell and undangerous goods are led in in one end of the plant and the dangerous goods are taken out in the other.

Further on the area has been divided into areas which give place both for the present production and for future activities. Along the borderlines between the different areas we have planted trees which act as screens mostly for fragments.

4. Types of buildings, model tests

4.1 Buildings

Fig. 7 shows in principle the various types of buildings used in the production areas and also indicates their place in time.

From a safety point of view the totally buried, concrete building and the steel houses are very much alike. Both have a well defined effect in reducing the shock pressure in the area close to an explosion compared with the conventional mounded building. In the matter of debris the steel house is to be preferred.

When the question comes to arranging a layout for an explosives production plant where space is limited these constructional properties combined with our kind of criteria are very valuable.

The development of these constructions started earlier than our risk analysis and from other motives. Without this work, however, we would have met much bigger problems in satisfying our internal criteria.

4.2 Model tests

Our model tests can be separated in 3 separate parts:

- Tests referring to the cylindrical, concrete construction.
- Steel house tests.
- Spot tests to investigate special constructions and layouts.

As shown in fig. 7 the cylindrical concrete building type was taken into use in the late 1960's. After having built 1 mixing plant and 1 cartridging plant of this type, it was decided to make a model test on the latter in order to investigate more closely the condition for the operators in their control room.

A model was built in scale 1 : 10. The test was carried out by the Norwegian Defence Construction Service. The conclusion from the test led among other things to a reinforcement of the doors in the control room. Data from this test also provided valuable background for the building of 2 remote controlled mixing plants at one of our plants.

The model tests for the double-walled steel house started in 1971. A series of tests in scale 1 : 10, 1 : 4 and 1 : 2 were made. The most important questions were

- pressure distribution
- impulse
- debris, vertical and horizontal
- data for constructional calculations

The tests gave us the following answers:

- Pressure distribution as shown in fig. 8 (Scale 1 : 2). Roughly the pressure at a distance of 10 metres is reduced by 8% and from 50 - 350 metres by 30%.

- Impulse reduction at 10 metres distance about 70% and at 50 - 350 metres 40%.

- Very concentrated debris downfall as shown in fig. 9.

- No horizontal fragments.

Other advantages in using this type of building is

- Compact layouts which leeds to cheaper transportation systems.

- Simple foundations, see fig. 9.

- Flexibility in building and mooving plants.

Fig. 10 and 11 show part of the layout of two production lines at one of our plants and results of model tests made of these.

The problem was as follows:

In order to achieve a satisfactory regularity in production it was necessary to introduce a buffer storage of explosives between the mixing and cartridging operation. The buffer sizes were 1 400 and 1 600 kg. The space available was restricted and it was therefore decided to run a series of model tests in scale 1 : 10 of various constructions in order to determine the pressure propagation. The results led to a construction which gives marked pressure reduction in certain directions which again made it possible to arrange the production line as shown.

When planning our Pilot plant, we also ran a series of model tests in scale 1 : 14 which led to the construction and layout we have today. Generally speaking model tests are looked at as a very useful tool of determining possible layouts and constructional details.

5. Storage of explosives

5.1 General background

Our main storage area is placed in a valley about 3 km from the plant. Fig. 12 shows a map of the magazine area. The magazines numbered 1 - 5 are of the box type and were built in the 1960's. The magazines 7 - 10 are of the igloo type and were built in 1974/75 and represented the first step of moving the magazines out of the plant area. The dotted magazines 11 - 17 are future magazines.

In order to allow a further expansion of the magazine area (11 - 17) the Norwegian Explosive Inspector demanded that a risk analysis should be made. The Swiss consultant firm Basler & Hofmann were hired for this job, and the work started late in 1976. The analysis was divided in 2 stages:

- Is it recommendable to build further magazines area and what amount of explosives could be stored?

- What could be the most probable causes for an explosion?

5.2 Result of the analysis, stage 1

Fig. 13 shows the principles for the approach to the analysis, and fig. 14 defines the terms "individual risk" and "group risk".

Every magazine and in some cases a sum of 2 magazines represents an "event", i.e. a potential explosion, and were analysed for effect on the surrounding population. The result of these calculations are shown in fig. 15.

The most important conclusions are:

- An explosion in magazine 1, 2 or 3 will probably propagate to all three.

- An explosion in magazine 4 og 5 will propagate to the other magazine.

- Building magazines 11, 12, 13 and 14 make very little change in the risk situation.

- Increasing the amount of explosives in magazines 7 - 14 up to 250 - 350 tons has little effect on the risk.

- Magazine 15 should be limited to 70 - 80 tons.

- Magazines 16 and 17 should not be built.

The value of Re = 1 corresponds to what is normally accepted in Switzerland with a probability of 10 - 3 (i.e. 1 explosion every 1000 year).

The discussion of the report, where also the Explosives Inspector participated, led to the following conclusions:

- Magazine 2 and 4 will not be used for explosives storage in the future.

- The maximum allowable amount of explosives in an igloo magazine should be set to 150 tons (with reference to the ESKIMO-program).

- The allowable amount of explosives in magazine 7 - 10 was increased from 70 to 100 tons.

- The new magazines 11 - 14 will be built for 150 tons.

- Magazine 6 (not built) may be built for 150 tons.

5.3 Result of the analysis, stage 2

As mentioned the conclusions of stage 1 were based on a probability of 10^{-3} of an explosion. A rough check was made in this stage.

Stage 2 consisted of a very detailed and thorough analysis of possible causes and probabilities in order to get as good confirmation of our earlier assumptions as possible.

Fig. 16 shows the model for the analysis. All the different links in the various chains of events were studied. The result of the analysis is shown in fig. 17.

The conclusion was that the probability at the time of the analysis was to high, but that it can with simple means be lowered to an acceptable level. This work will very soon be finished.

FIG. 1

DYNO, CRITERIA VERSUS SURROUNDINGS

Fatality rate $P_f = 0.1 \cdot 10^{-8}$

This is lower than the risk of being killed by fire in Norway.

	MAX. ALLOWED AIR PRESSURE	MIN. DISTANCE DUE TO FRAGMENTS
1. Dwellings	50 mb	400 m
2. Public roads	80 mb	2/3 x 1 i.e. 270 m
3. Shops	30 mb	3/2 x 1 i.e. 600 m
4. Schools, churches etc.	22 mb	2 x 1 i.e. 800 m

The minimum distance due to fragments is based on maximum 1 lethal fragment per 56 m^2.

DYNO'S INTERNAL CRITERIA

Fatality rate $P_f = 5 \cdot 10^{-8}$

This is identical with the average value for Norwegian industry.

1. Departments who have no connection with the production and storage of explosives — 50 mb

2. Departments directly involved in production and storage of explosives — 100 mb

3. Production or storage departments dependant on each other, explosives under transportation, packed and protected explosives — 200 mb

4. Inside a production or storage department. People working inside buildings should not be exposed to air pressure higher than — 350 mb

   or to ground shock exceeding 8 g, velocity 3 m/sec.

   The people should not be exposed to fragments.

FIG. 2

CHECK PROCEDURE, RISK ANALYSIS

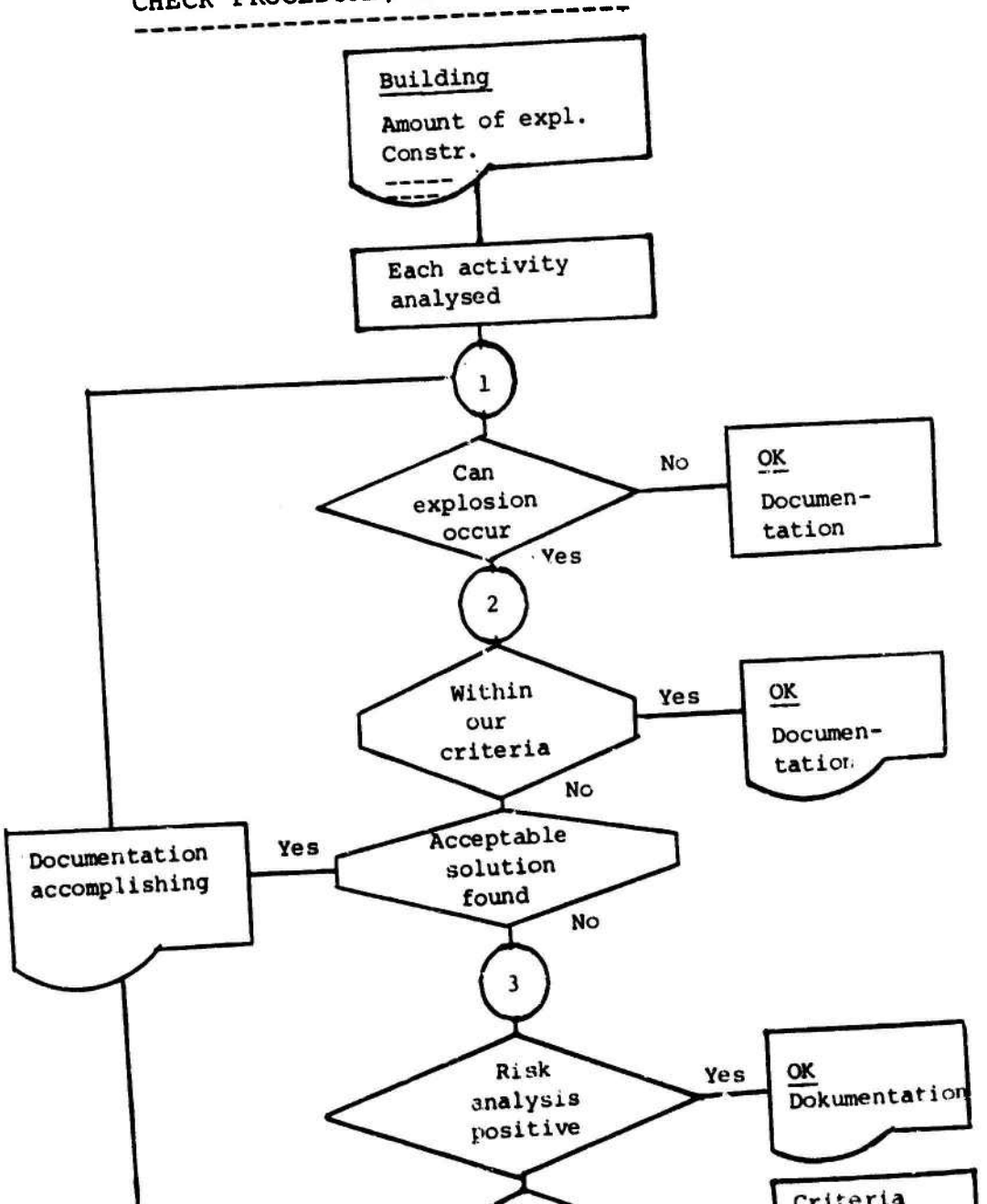

FIG. 3

DYNO INDUSTRIER A.S

ANALYSIS OF INTERNAL CONDITIONS

Building No.: A 46

Function : Cartridging
Remote controlled
Rollex

Terrain profile. Scale:

DONOR PROPERTIES:

Max. allowed amount : 100 kg

Equivalent amount TNT, Q_1: 90 kg

Max. amount by accident : 200 kg

Equivalent amount TNT, Q_2: 180 kg

Type of building, construction:

Light wooden building surrounded by mound

Fragments:

Distant: Much
Nearby : Little

Reduction factor for P_{max} due to type of building (50 m distance):

0.7

EXPOSED PERSONS:

Max. number: 3

Number of persons	1	2	3	4	5
Average time of exposure per shift	0.5	0.3	0.2		
Number of persons x time per shift	0.5	0.6	0.6		

Sum: Number persons x exp. time per shift 1.7

Average: Exposed number x exposed time per hour: 0.2

Average manhours per day for cleaning: 2

Remarks:

ACCEPTOR PROPERTIES:

Neighbour-build. No.	Same depa-t-ment?	Distance s meter	Q_1 (Q2) kg	$f=\frac{d}{\sqrt[3]{Q}}$	Pmax free charge mbar	Red. factor donor	Red. factor acceptor	Red. Pmax.
A-55	Yes	34	300	5.1	460	0.4	0.7	130
A-49	Yes	90	1 300	8.2	210	0.75	0.7	110
A-54	No	175	5 400	10.0	155	1	0.9	140
A-56	Yes	35	720	3.9	680	1	0.9	610
A-73	No	325	35 000	9.1	190	1	1	180
A-47	Yes	40	320	5.8	340	0.8	1	270

Remarks - conclusion

Criteria can not be fulfilled ☐ Criteria can be fulfilled ☐ Satis-factory ☐

FIG. 4

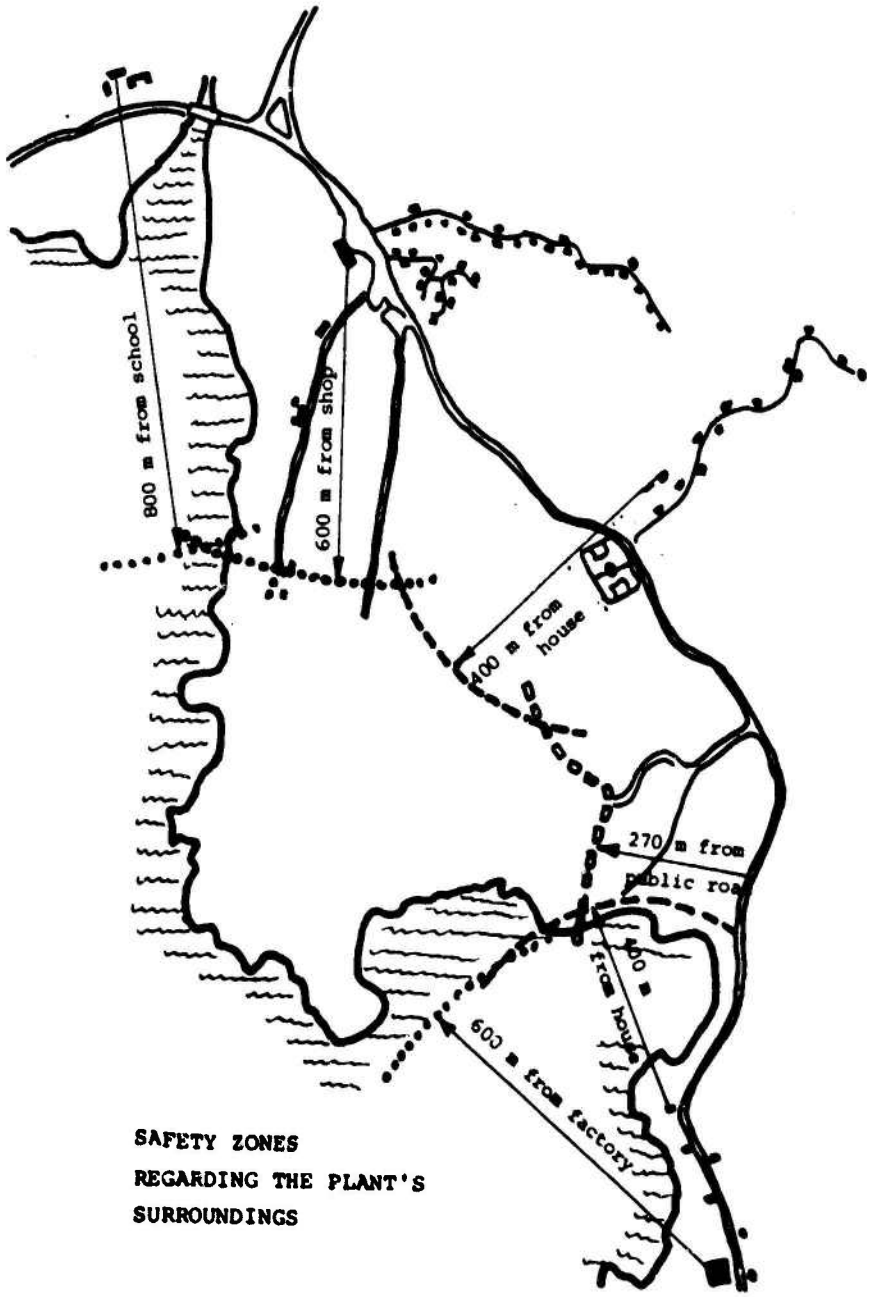

SAFETY ZONES
REGARDING THE PLANT'S
SURROUNDINGS

FIG. 5

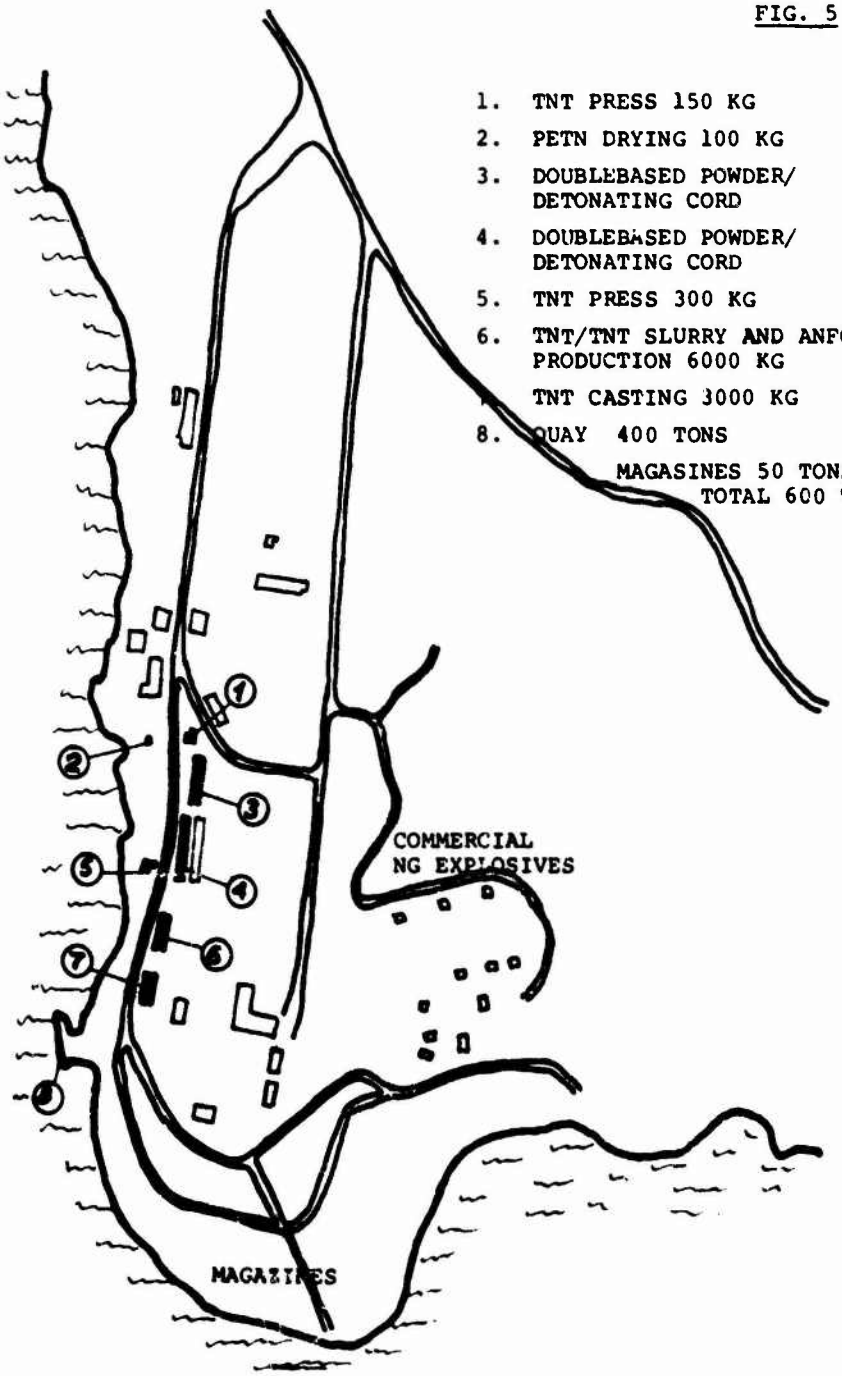
1. TNT PRESS 150 KG
2. PETN DRYING 100 KG
3. DOUBLEBASED POWDER/ DETONATING CORD
4. DOUBLEBASED POWDER/ DETONATING CORD
5. TNT PRESS 300 KG
6. TNT/TNT SLURRY AND ANFO PRODUCTION 6000 KG
7. TNT CASTING 3000 KG
8. QUAY 400 TONS
MAGASINES 50 TONS EACH, TOTAL 600 TONS
COMMERCIAL NG EXPLOSIVES
MAGAZINES

FIG. 6

DISPOSTION OF PLANT AREA,
GULLAUG FABRIKKER

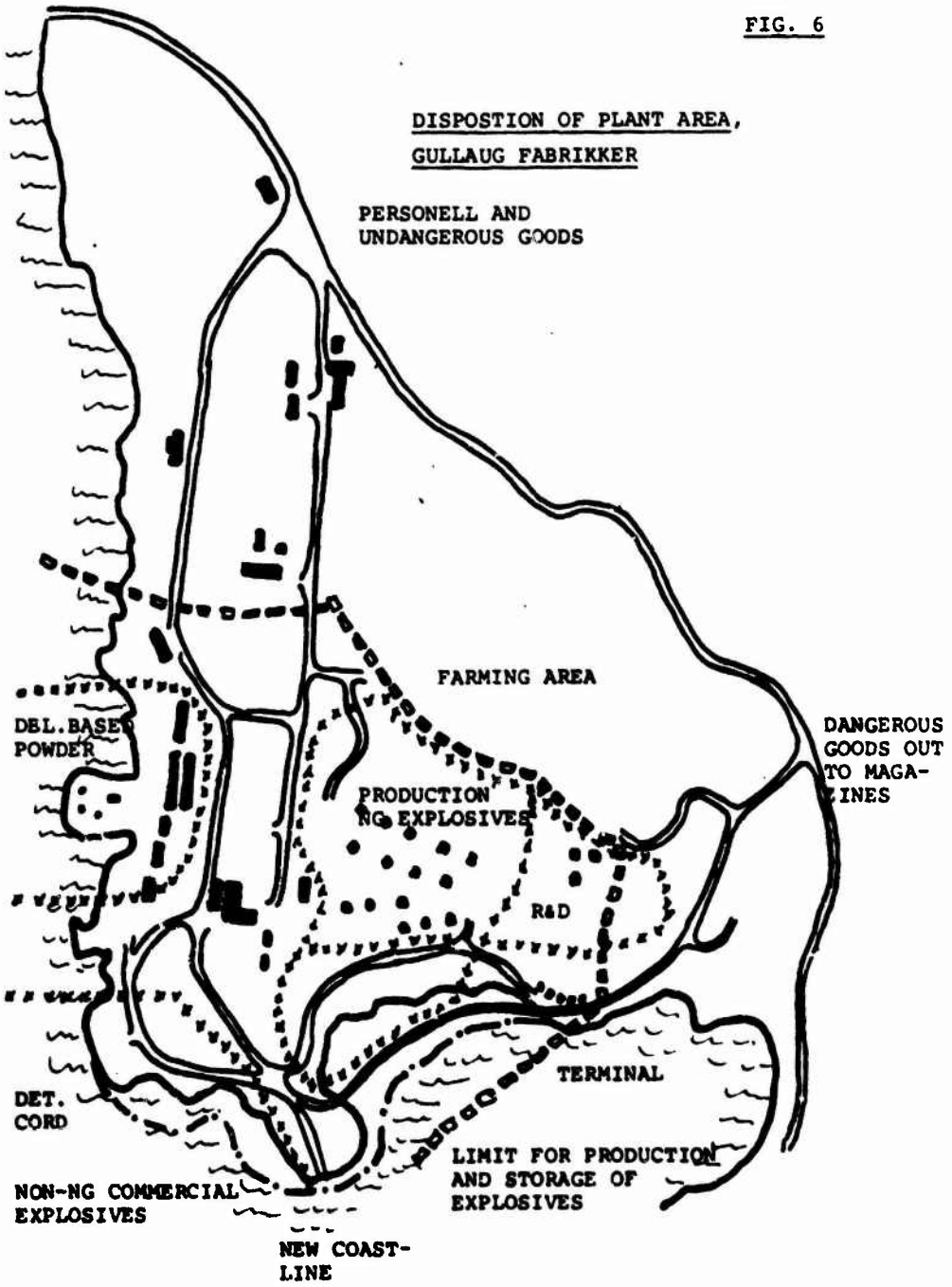

FIG. 7

VARIOUS TYPES OF PRODUCTION BUILDINGS

Convential light wooden building with mound. Built until end of 1960's.

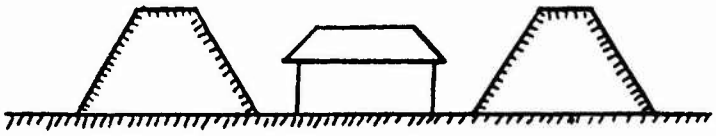

Cylindrical concrete building. Roof of laminated wooden beams with thin wooden cover. Totally buried. Built in end of 1960's and early 1970's.

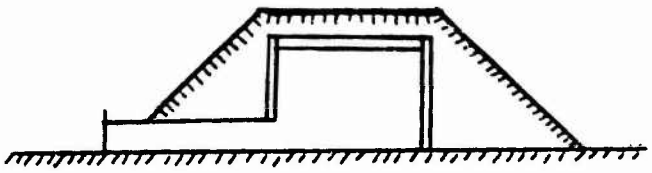

Cylindrical double-walled steel houses. Sand filled between walls and the roof.

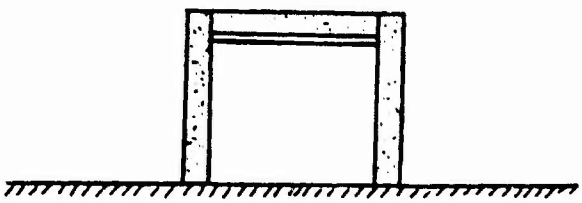

FIG. 8

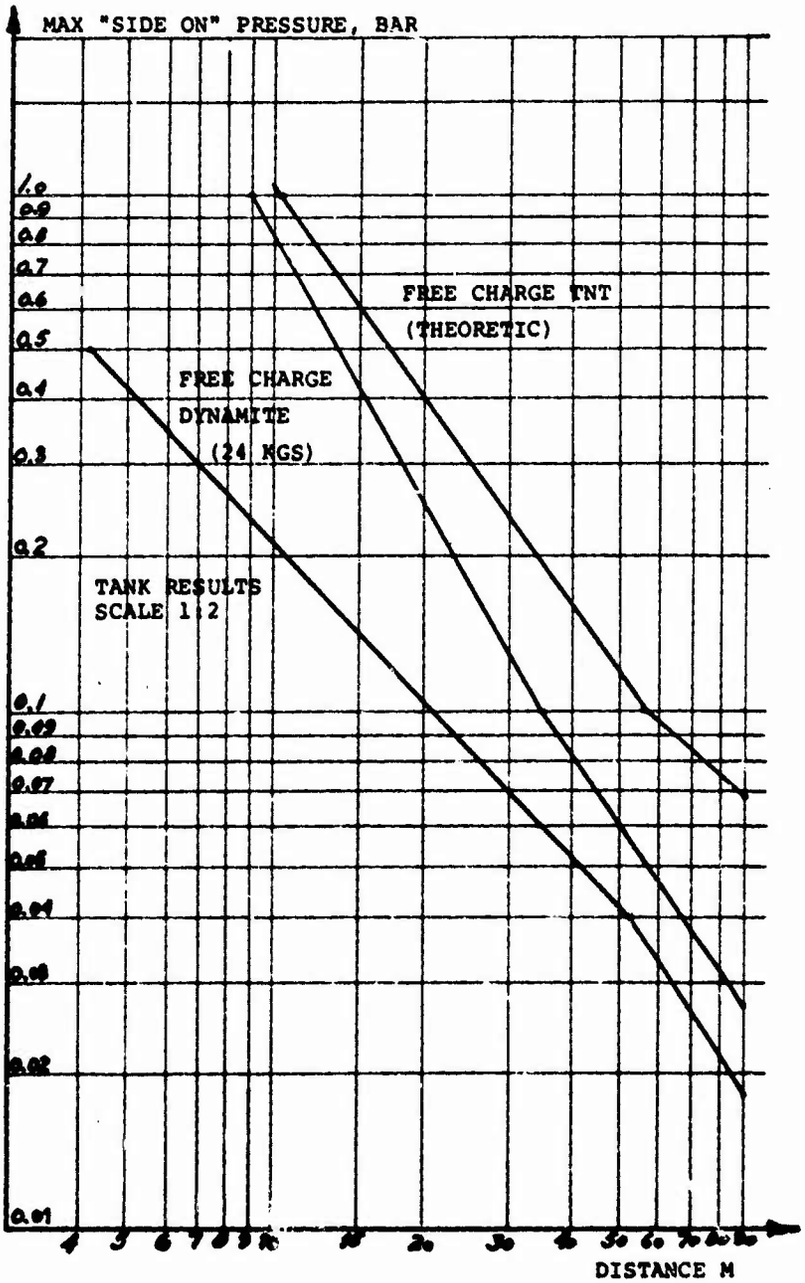
MAX "SIDE ON" PRESSURE, BAR
1.0
0.9
0.8
0.7
0.6
0.5
0.4
0.3
0.2
0.1
0.09
0.08
0.07
0.06
0.05
0.04
0.03
0.02
0.01
FREE CHARGE TNT
(THEORETIC)
FREE CHARGE
DYNAMITE
(24 KGS)
TANK RESULTS
SCALE 1:2
4
5
6
7
8
9
10
20
30
40
50
60
70
80
90
DISTANCE M

FIG. 9

THROWOUT OF DEBRIS

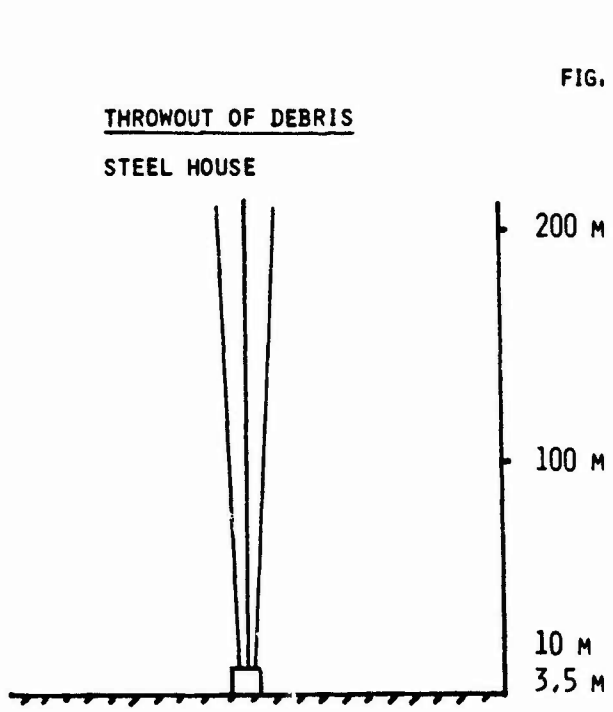

3 - 5 DEGREES ANGLE OF THROWOUT.

10 - 15 SECONDS FOR SAND TO FALL DOWN.

FOUNDATION FOR STEEL HOUSE

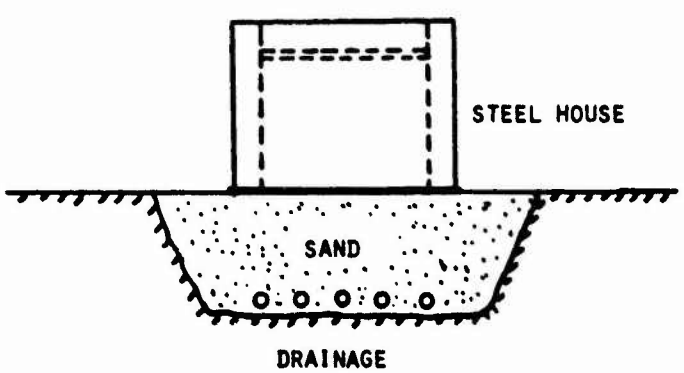

FIG. 10

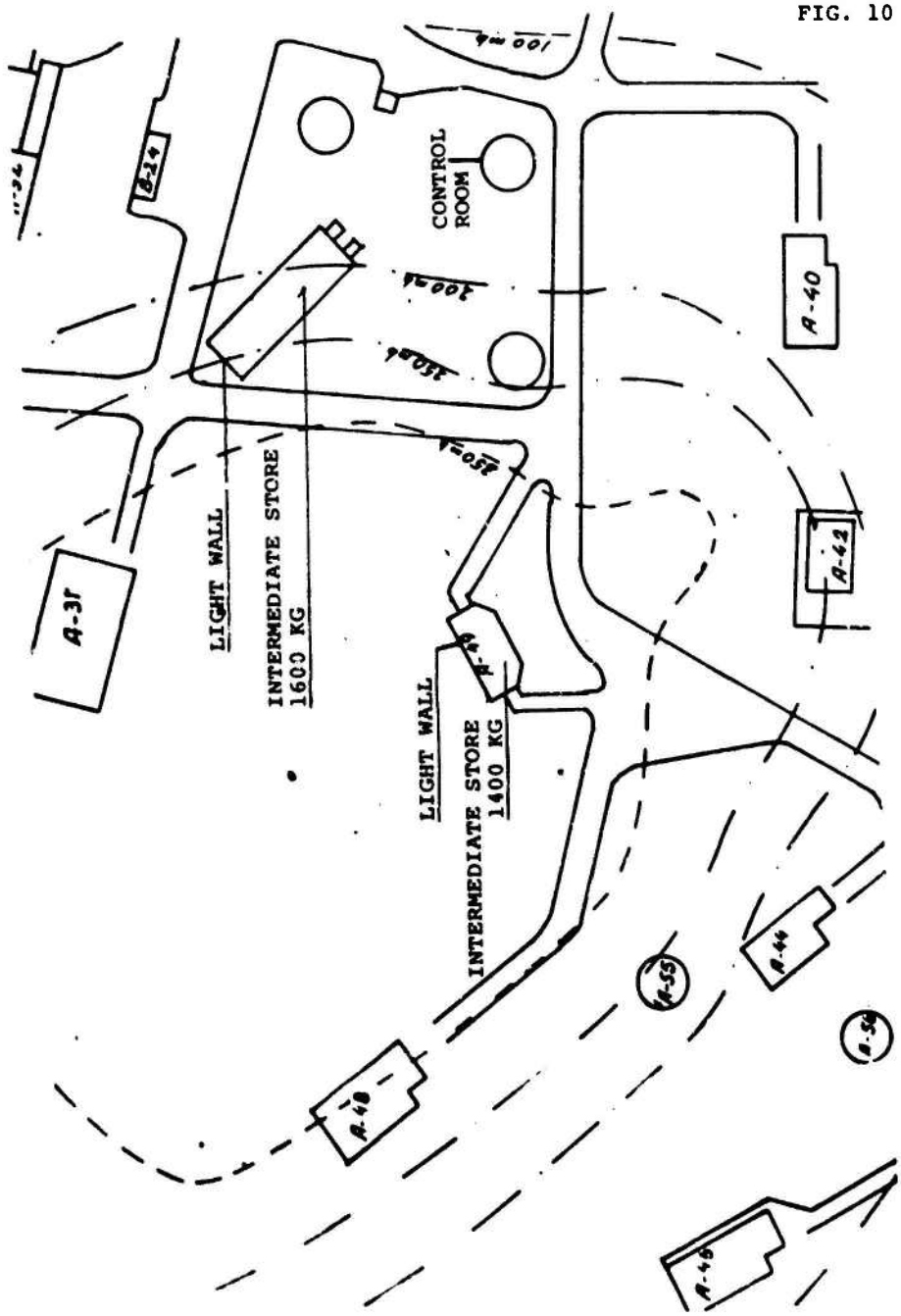
CONTROL ROOM
A-40
A-42
A-31
LIGHT WALL
INTERMEDIATE STORE 1600 KG
LIGHT WALL
INTERMEDIATE STORE 1400 KG
A-44
A-48
A-45

FIG. 11

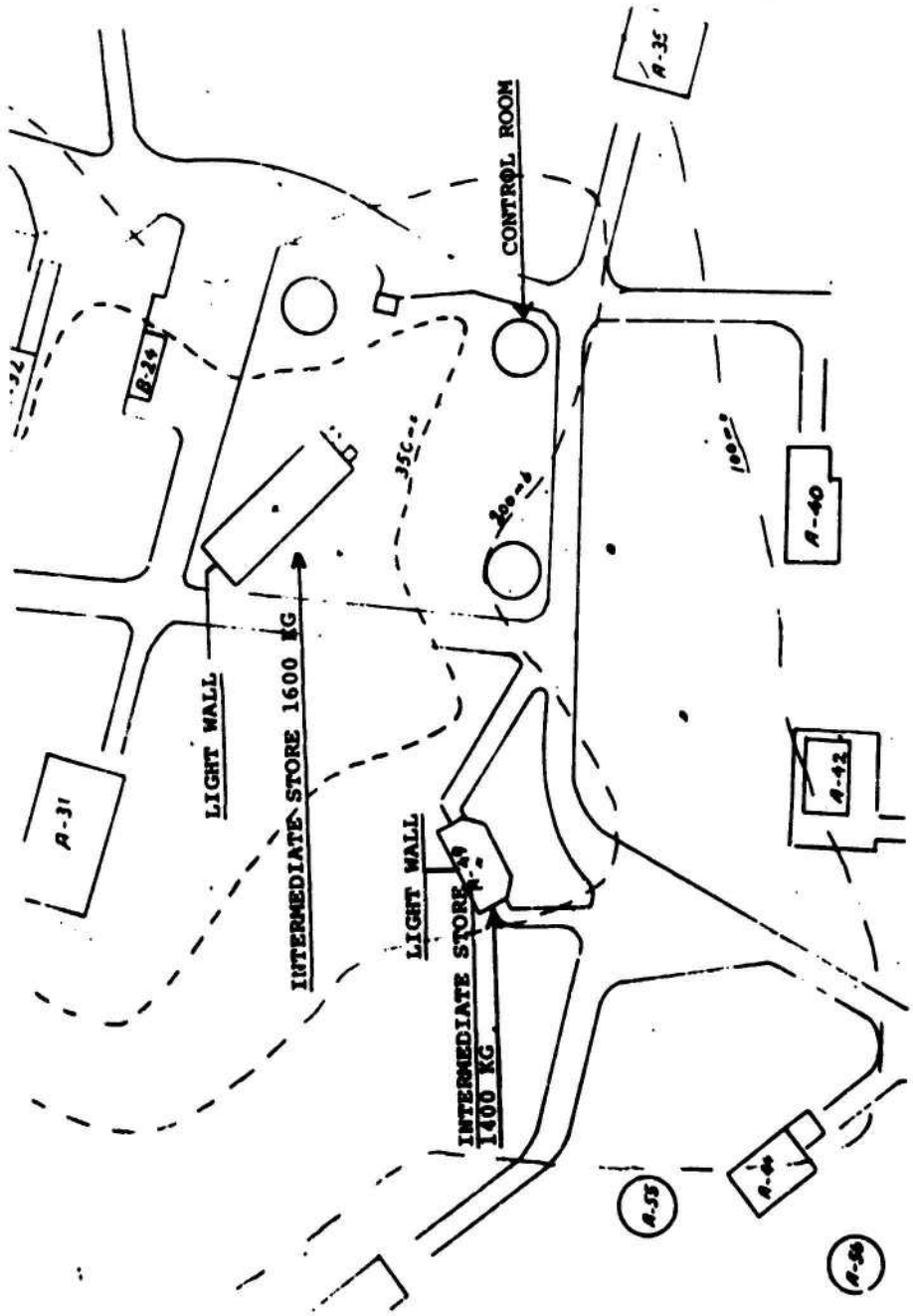
CONTROL ROOM
LIGHT WALL
INTERMEDIATE STORE 1600 KG
LIGHT WALL
INTERMEDIATE STORE
1400 KG
A-31
A-35
A-40
A-42
B-24

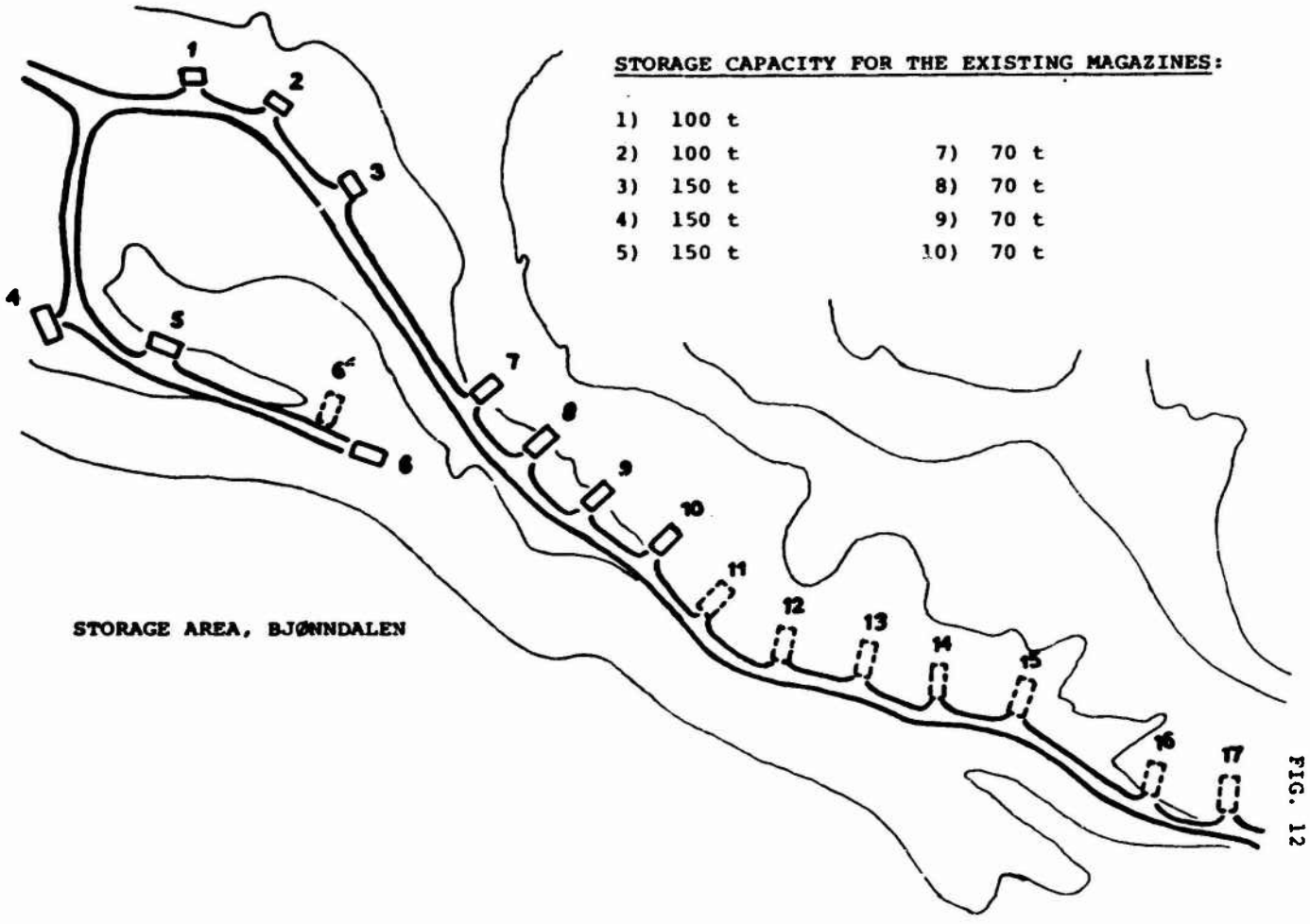

STORAGE CAPACITY FOR THE EXISTING MAGAZINES:

1)	100 t		
2)	100 t	7)	70 t
3)	150 t	8)	70 t
4)	150 t	9)	70 t
5)	150 t	10)	70 t

STORAGE AREA, BJØNNDALEN

FIG. 12

FIG. 13

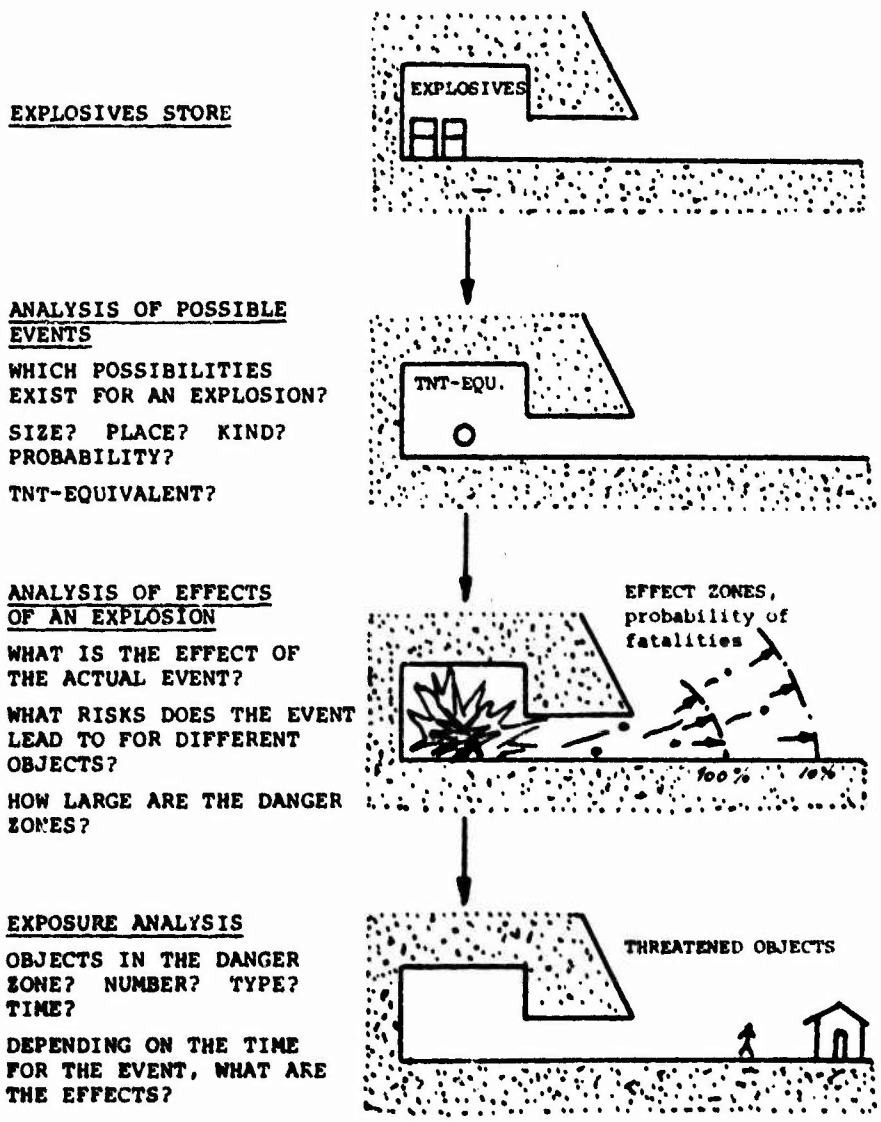
EXPLOSIVES STORE
EXPLOSIVES
ANALYSIS OF POSSIBLE EVENTS
WHICH POSSIBILITIES EXIST FOR AN EXPLOSION?
SIZE? PLACE? KIND? PROBABILITY?
TNT-EQUIVALENT?
TNT-EQU.
ANALYSIS OF EFFECTS OF AN EXPLOSION
WHAT IS THE EFFECT OF THE ACTUAL EVENT?
WHAT RISKS DOES THE EVENT LEAD TO FOR DIFFERENT OBJECTS?
HOW LARGE ARE THE DANGER ZONES?
EFFECT ZONES, probability of fatalities
100 %
10 %
EXPOSURE ANALYSIS
OBJECTS IN THE DANGER ZONE? NUMBER? TYPE? TIME?
DEPENDING ON THE TIME FOR THE EVENT, WHAT ARE THE EFFECTS?
THREATENED OBJECTS

FIG. 14

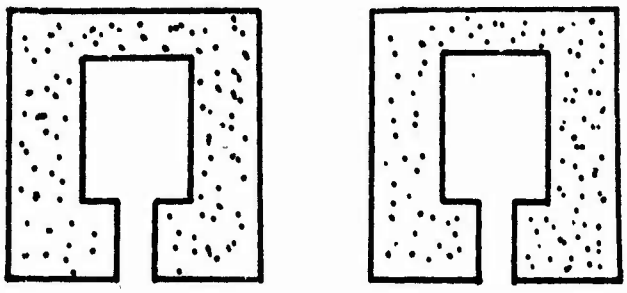

NUMBER OF PERSONS PRESENT	2 (ALWAYS THE SAME PERSONS)	40 (ALWAYS THE SAME PERSONS)
PRESENCE	90%	25%
PROBABILITY OF AN EXPLOSION	W_E	W_E
MAX. INDIVIDUAL RISK *	0,9 W_E	0,25 W_E
GROUP RISK **	1,8 W_E	10 W_E

* INDIVIDUAL RISK - PROBABILITY OF LETHALITY x AVERAGE PRECENSE PER INDIVIDUAL

** GROUP RISK - PROBABILITY OF LETHALITY x AVERAGE NUMBER OF PEOPLE PRESENT

FIG. 15

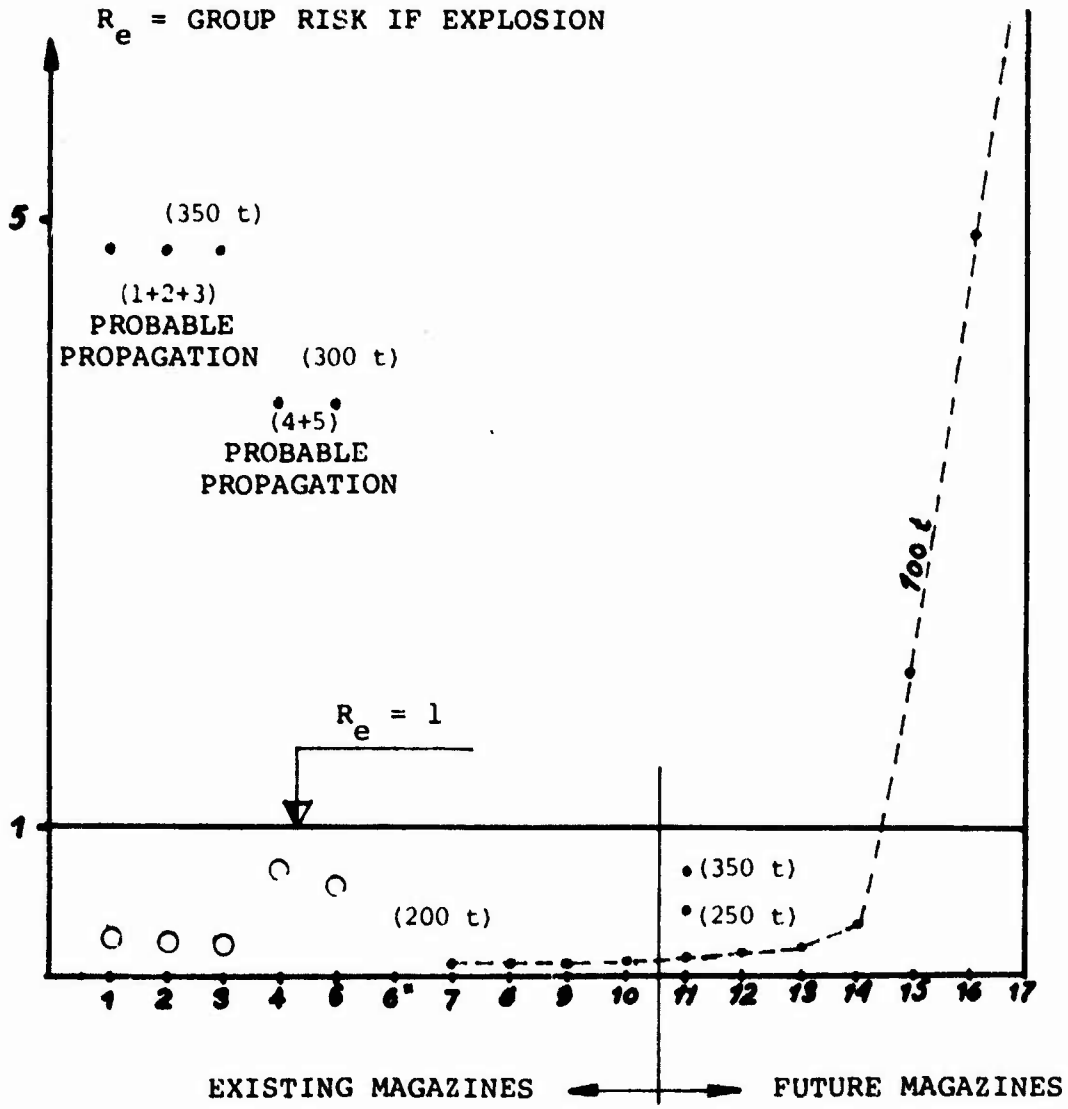

SUMMARY OF THE VALUES FOR R_e (GROUP RISK IF EXPLOSION):

- ● = R_e VALUE FOR THE PRESENT ARRANGEMENT. PROPAGATION TAKEN INTO ACCOUNT.
- O = R_e VALUE FOR EACH MAGAZINE AT THE PRESENT ARRANGEMENT WITHOUT PROPAGATION.
- - - - = R_e VALUE CURVE FOR 100 TONS.

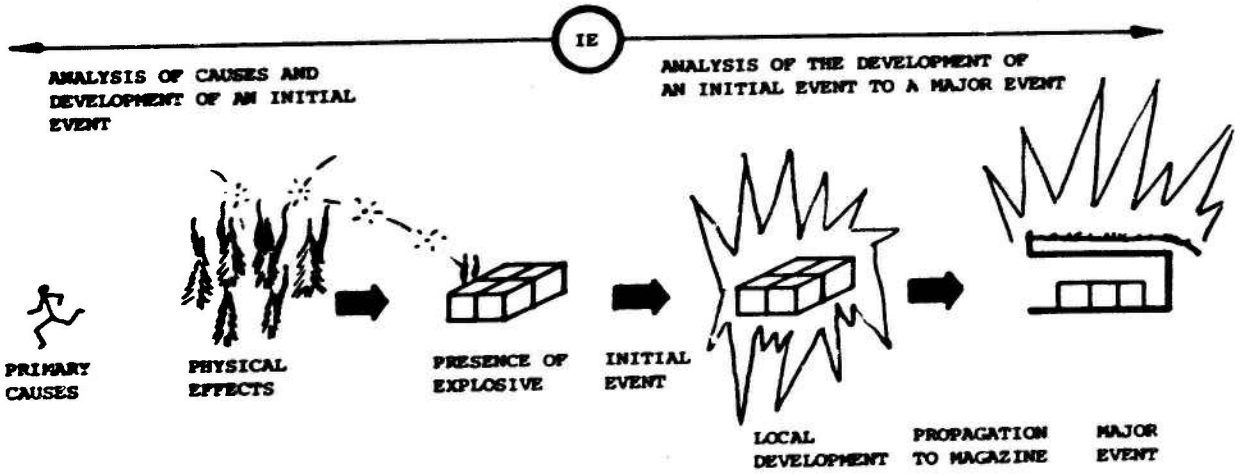

CORRESPONDING MODEL ELEMENTS

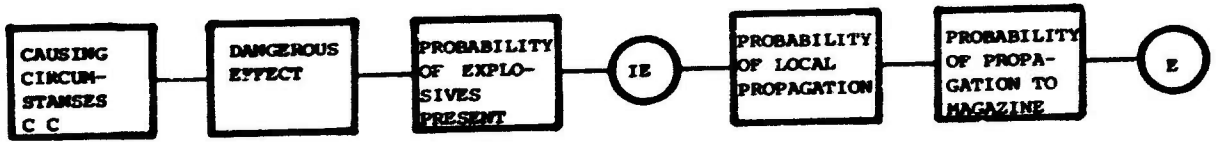

FIG. 16

FIG. 17

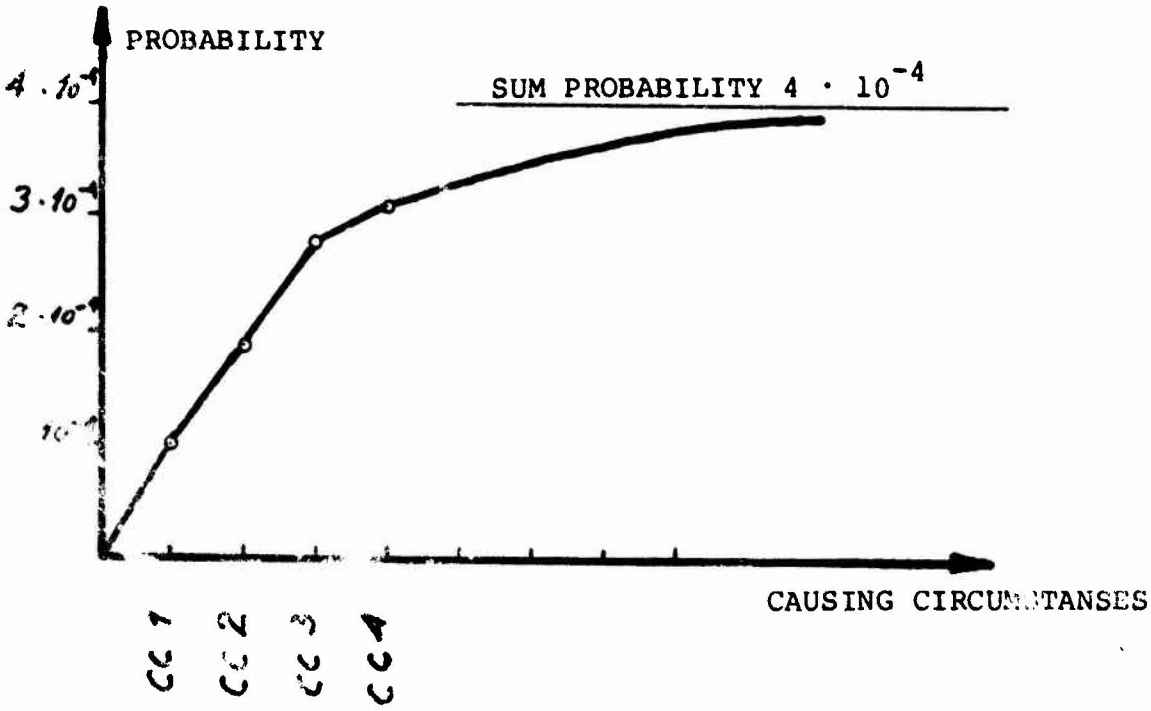

		PROBABILITY
C C 1:	FORKLIFT [illegible] EXPLOSIVES	$10 \cdot 10^{-5}$
C C 2:	FAULTY ELECTRICAL SYSTEM	$9 \cdot 10^{-5}$
C C 3:	SABOTAGE	$9 \cdot 10^{-5}$
C C 4:	MAINTENANCE ACTS (WELDING ETC.)	$3 \cdot 10^{-5}$
SUM MOST IMPORTANT CAUSES		$3{,}1 \cdot 10^{-4}$
SUM OTHER CAUSES		$0{,}9 \cdot 10^{-4}$
TOTAL PROBABILITY PR. MAGAZINE		$4 \cdot 10^{-4}$

WITH 10 - 12 MAGAZINES IN THE APEA:

PROBABILITY $\sim 5 \cdot 10^{-3}$

HOW MUCH SHOULD WE BE WILLING TO PAY FOR EXPLOSIVES SAFETY ?

Th. Schneider
Basler & Hofmann
Consulting Engineers
Zurich, Switzerland

Abstract

It becomes more and more accepted that safety considerations should be based on quantitative risk predictions. The data and tools for such predictions have been improved considerably in the last years.

In contrast to this, we still have considerable difficulties concerning the problem of decision criteria in this field.

In this paper, a model is discussed which allows to make consistent decisions for safety measures. The model is based on the fact that the safety of any system is basically determined by the money we invest for safety measures. As we are always confronted with limited funds in reality, we will always attend only limited safety. This problem is discussed in more detail for the example of fatal accidents. Furthermore, the fact is discussed that striving for a constant risk level does not bring us the maximum possible benefit for our investments; we should rather introduce the marginal costs for safety as a decision criterion, thus e.g. the price we are paying to save a human life.

Paper presented to

Eighteenth Explosives Safety Seminar, 12-14 September 1978
El Tropicano Hotel, San Antonio, Texas, U.S.A.

PRECEDING PAGE BLANK

Introduction

In recent years, it has become more and more accepted that safety problems should be solved on the basis of a prediction of the risks which are involved in an activity. According to this, we can observe increasing efforts to improve the technical data and tools for such risk or hazard predictions also in the field of explosives.

An inevitable consequence of such risk predictions is that we realize very clearly the following fact (figure 1): Safety problems are a matter of two questions. By predicting risks only, or, in other words, answering the question "What can happen?", we have not yet solved our problem. The second question "What do we accept?" is equally important and by no means easier to answer. But when we look at the effort made until today to answer these two questions, we find that it is hardly balanced. As a result of this, we still come up with solutions for many safety problems which - seen from a broader point of view - are neither consistent nor economically optimal.

In this paper, I would like to present some ideas concerning the problem of risk appraisal or safety decisions. We have started to apply these ideas in various safety problems in Switzerland, among others in explosives safety.

How do we express risk or safety?

Of course I have to restrict myself in this short paper to certain parts of this wide problem. So I shall only speak about fatal accidents here. However, other categories of damage - even accidents involving only property damage - raise a lot of equally important questions.

If we look at an activity which includes a fatal risk for the persons involved, this risk can be presented as follows (figure 2):

The risk and therefore the safety of any single individual involved in this activity is just a matter of its probability to be killed in an accident. The risk of all the other persons involved does not affect this individual risk.

If we plot the individual risk for each person of the group, e.g. in decreasing order as you see it in this figure, we recognize another quantity: the risk of the group as a whole which corresponds to the sum of all individual risks and which is represented by the area under this curve. This group risk is the value we usually find in our accident statistics.

Thus, we find that the risk of an activity is characterized by two things: the area under the curve and the shape of the curve. It is easy to see that these are two quite different aspects of a risk situation. So I can e.g. keep the area or group risk constant and vary the distribution of the individual risks (figure 2a). This will not change anything in our accident statistics, but for certain persons it can change the individual risk level significantly.

In summary, we can say that we will have to look at both the individual and the group risk. However, in this paper I will restrict myself to the group risk problem only and it is important to keep this in mind.

What is actually competing with safety?

So, if we are concerned with the group risk, our task is obviously to reduce the area under this curve or - in other words - the number of fatalities in the safety records of this activity to an acceptable level.

Well, why don't we reduce it to zero? Everybody who has ever been confronted with real projects will know the answer to this question. But let me mention an example, although I may not give you the actual figures (figure 3):

In Switzerland, a program has been initiated to improve the safety of the large ammunition storages. The first step in this program consisted in a risk analysis of the entire storage system as it existed at that time. This gave us a value R_e which is actually a prediction of the fatalities we expect the system to produce if we leave it as it is.

In the second step, we did not yet worry about the problem of acceptable risks. We just started to think about the measures which could reduce the

existing risks. So we made a list of all the different possible measures like structural improvements, reduction of explosives quantities, moving ammunition from one storage to another and so on. For all these measures it has been investigated what effect they would have in the risk analysis and what risk reductions they would provide. On the other hand, it was clear that all these measures would cause costs. These costs were comparatively easy to estimate. Now, we were able to rank all the measures according to their benefit/cost-ratio, and we plotted them as indicated in figure 3 with decreasing effectiveness.

What did we realize? The degree of safety we can achieve is basically a matter of the money we are investing for safety measures. Thereby, it is typical that for increasing costs we obtain decreasing risk reductions but that at no price we shall reach absolute safety. This is surely not surprising, but the question is now: which point on this curve represents the correct or optimal solution? This is the problem we are going to discuss here.

A first approach to our problem

In the following example I would like to demonstrate a basic principle which is decisive for the solution of our problem (figure 4). In this figure, three systems are shown, each one represented by a curve analogous to the curve we have just seen before. The three systems, e.g. three explosives storages, differ in the initial risk and in the shape of the curve representing the possibilities for risk reductions. Let's assume we have to improve these three systems.

What can we do in such a situation? Normally, we would tend to specify safety requirements more or less explicitly by an acceptable risk level; let's call it R^*. If we now apply this risk level to each of our three systems, we get total costs of C^*. This is shown in figure 4a. Our solution is now represented by a residual total risk of $3 \times R^*$ and total costs of C^*.

The question is now: is this the best solution we can obtain for our investment C^*?

Basic mathematics tell us that this is indeed not the best solution! We can see that easily without mathematics. In system 3 we spend a big part of our money without decreasing the risk very much. On the other hand, we could reduce the risk in system 1 significantly with much less money. So, if we would transfer money from one system to another, we could improve the safety of the three systems.

Not only the mathematicians but also the economists know this problem very well, and many of you have probably already realized what the solution is.

Figure 5 shows this solution. It is easy to understand and also to prove that we obtain the minimal risk for our three systems if we distribute our investment C* in a way that the slope of the three curves is the same in each of the chosen points. Then, the total risk $R_1' + R_2' = R_3'$ is minimal. Now, we cannot transfer money from one system to another anymore and decrease the total risk at the same time.

Let's assume that we have understood that the slope of the risk-cost curve should be our criterion rather than a fixed risk level. But there is one thing we may dislike now: everybody will understand what a risk level means, but not necessarily what the meaning of this slope is. Let's look at this slope a bit closer. We can say that this slope indicates the ratio of the risk and the costs at this point. The economists call it the marginal costs. We can say that it is the costs we pay per risk unit at this particular point. But what is our risk unit? In the case of fatal group risk which we discuss here, it is nothing else but one human life saved. Thus, our slope has a very clear meaning: it is the money we pay to save a life!

A second approach to our problem

Let us now look at our problem in another way. The problem of trade-off between risk reduction and safety costs is often presented in the way of figure 6. This figure shows that if we add more and more safety measures to a system, the expected damage will decrease and the costs will increase. I think most

problem.

In this kind of figure, our attention is usually drawn to the fact that the sum of these two curves, thus the total costs, has somewhere a minimum. This minimum looks somehow very much like the solution of our problem, and in many cases it is with no doubt the solution.

If we have e.g. a transport company which wants to find the best maintenance policy for its trucks, this will surely be a good way to look at the problem. The more this company is investing in maintenance, the less repair costs can be expected, and it is quite plausible that there will be an optimal policy which causes minimal total costs. This is a very common way of thinking in many economic problems.

But probably you have realized that in this example a decisive condition is fulfilled which allows us to make use of this optimization criterion. We can of course make the sum of these two curves only as long as both curves are expressed in the same units. For the transport company both the repair and the maintenance costs will be expressed in monetary terms, and there is no problem in adding them.

But unfortunately <u>our</u> problem does not fulfill this requirement (figure 7). One of our curves gives the number of fatalities we have to expect during the lifetime of our system. The other curve, the safety costs, will be expressed in monetary terms. Thus, we have the problem of adding apples and pears.

Now, do we really have to abandon our nice solution of minimal total costs in this situation? Somehow, we have the feeling that even if we cannot add the two units, the basic problem is still the same. This basic problem is that we have to make up our mind in the trade-off between two competing values. We know that we are not able to pay an infinite price for the safety of our system, but we also know that for a limited price we can hardly get absolute safety.

non-transparent and unconscious negotiation. But let us assume that in this example people have thought and discussed very intensively about this trade-off and have agreed on a particular solution (figure 7a). Everybody has therefore agreed that investing more money would not pay off, investing less money would result in an unacceptable risk situation.

But does this not mean that at this point we have found the balance between our two competing values? Thus, if we think in terms of an ideal sum of these two values, this sum is obviously increasing in either direction from this point. But if we accept this - and I think we have to - we can state the following: there is exactly one transformation of our fatality curve into a dollar curve which would produce this solution as the optimal one if we add it with the cost curve (figure 7b). The trick how to find this curve consists in transforming the risk curve until it has the inverse slope of the cost curve at the point of the chosen solution.

If we now look at our new transformed curve, we have to realize that with the choice of our solution we have done the same as if we had assigned a certain monetary value to a human life. Or if we look at it the other way round by defining the ultimate price we would pay to save a human life, we can transform our fatality curve into a dollar curve and easily find our optimal solution.

Well, we realize that we end up with exactly the same conclusions as in our first approach. The criterion which is the only one that will allow us to make consistent decisions and get the highest benefit from our invested money is the price - or rather the marginal costs - we are willing to pay to save a human life.

How much should we pay to save a human life?

Now, as we know what our criterion should be, we would like to know what we should pay to save a human life in quantitative terms.

Quite a lot has been written about the problem of putting a monetary value to a human life. The following figure shows that there have been basically three approaches (figure 8):

The first approach is based on purely economic considerations on an industrial management basis. Thus, only the costs resulting for a company from fatal accidents are compared with the costs for preventive measures.

Since this first approach is surely not quite satisfactory from a higher point of view, a second group of approaches tries to assign a value for a human life by making overall economic considerations. One of this kind of approaches e.g. is based on the lifetime earnings of a person.

Many objections have been brought up against these approaches and I personally think that it is really quite irritating to reason what a human life is worth.

But I think now that the third approach I would like to mention is quite different in this respect. Here, we do not ask any longer how much a human life is worth, but we ask the much more realistic question: how much are we willing to pay for a human life? The example in the last section has shown that we can virtually not avoid to answer this question when we decide about projects and of course also regulations. In the following, we always refer to this third philosophy.

If we now come to the question how high this price should be, the next problem is whether we are dealing with just one single price in all different risk situations. From a theoretical point of view one might argue that there should be no reason to pay different prices for a human life in different situations. But a look at the real world reveals that our safety efforts are actually quite different in different areas.

Well, I think it is not our task to change the world, but primarily to understand it. So, what we tried in the following model is to explain our today's behaviour in its tendency by finding out the hidden rules. This way we try to accept the feelings of the people, but at the same time eliminate the inconsistencies caused by lack of transparence.

Let me explain you in the next figure four categories of risks we have defined (figure 9). These categories seem to be appraised differently by the society. The governing parameter is the relation between the following three groups of persons:

- the persons affected by the risk of an activity
- the persons involved in an activity, thus having a direct benefit from it
- the persons responsible for the risk control

In the first category, these three groups are identical. Here we are virtually talking of fully voluntary risks. In a second category, the three groups are generally regarded as more or less identical. Typical examples are most of the traffic accidents and a large part of the occupational accidents. In the third category now, the persons affected are still more or less identical with the persons involved, but the persons responsible for the risk control are different. Examples for this category are special occupational accidents as we have them e.g. in the explosives industry or in other industries where complicated production facilities include the possibility of ususally rare but extensive dangerous events. And finally in the last category all three groups are not identical anymore. These risks are the typical involuntary risks, where e.g. people are affected by risks of activities they have nothing to do with.

In figure 10 finally, now you find a proposition for the actual values of our criterion. This figure is the result of an evaluation of many different research studies as well as case studies. Of course I cannot discuss here the whole background of this curve. You might be astonished that these values are varying within such wide limits. But we must be aware that in this figure we are dealing with the whole range of activities of our civilization. If we look at one specific activity which we should be able to locate quite easily in this figure, there will of course be only one value or at least a quite narrow range for our criterion.

In figure 10a I have plotted two points: one for explosives industry employees and one for third party risk from ammunition storage. One is approximately 2 Mio SFrs., the other 10 Mio SFrs. per life saved. So, all our safety efforts e.g. in explosives factories would be governed by one value. This value is our criterion for consistency and guarantees that we achieve the maximum benefit for the money we spend.

Of course, these values must still be regarded as propositions and there should be a lot of discussions about them. But I think it is worth while to start working with such hypotheses, because this is the only way to get the experience and the feeling necessary for sensible discussions about the important questions of safety criteria.

* *
*

We have to add two points at the end of this paper which have not been touched in the verbal presentation for reasons of simplification.

The first concerns the assumption that we are dealing with more or less predictable risks. As soon as risks are not predictable with an acceptable degree of reliability, additional aspects have to be taken into account. If we mention the problem of predictability we have to state clearly what we regard as predictable and unpredictable risks. When talking about unpredictable risks, we think of risks such as the overall impact of the nuclear energy production of the long term effects (e.g. genetic effects) of chemicals in our environment. On the other hand, all risks of comparatively simple technologies (e.g. explosives technology) are regarded as basically predictable.

The second point concerns the problem, that if we have accidents with more than one fatality at the same time, the question of non-linear utility functions has to be considered. We refer here to the basic theory of decision under uncertainty. But even if we come to the conclusion that we have to introduce what is called an aversion function, the ideas shown in this paper would still be valid. The difference would be that we have to introduce our new utility unit instead of directly referring to saved lifes as our unit.

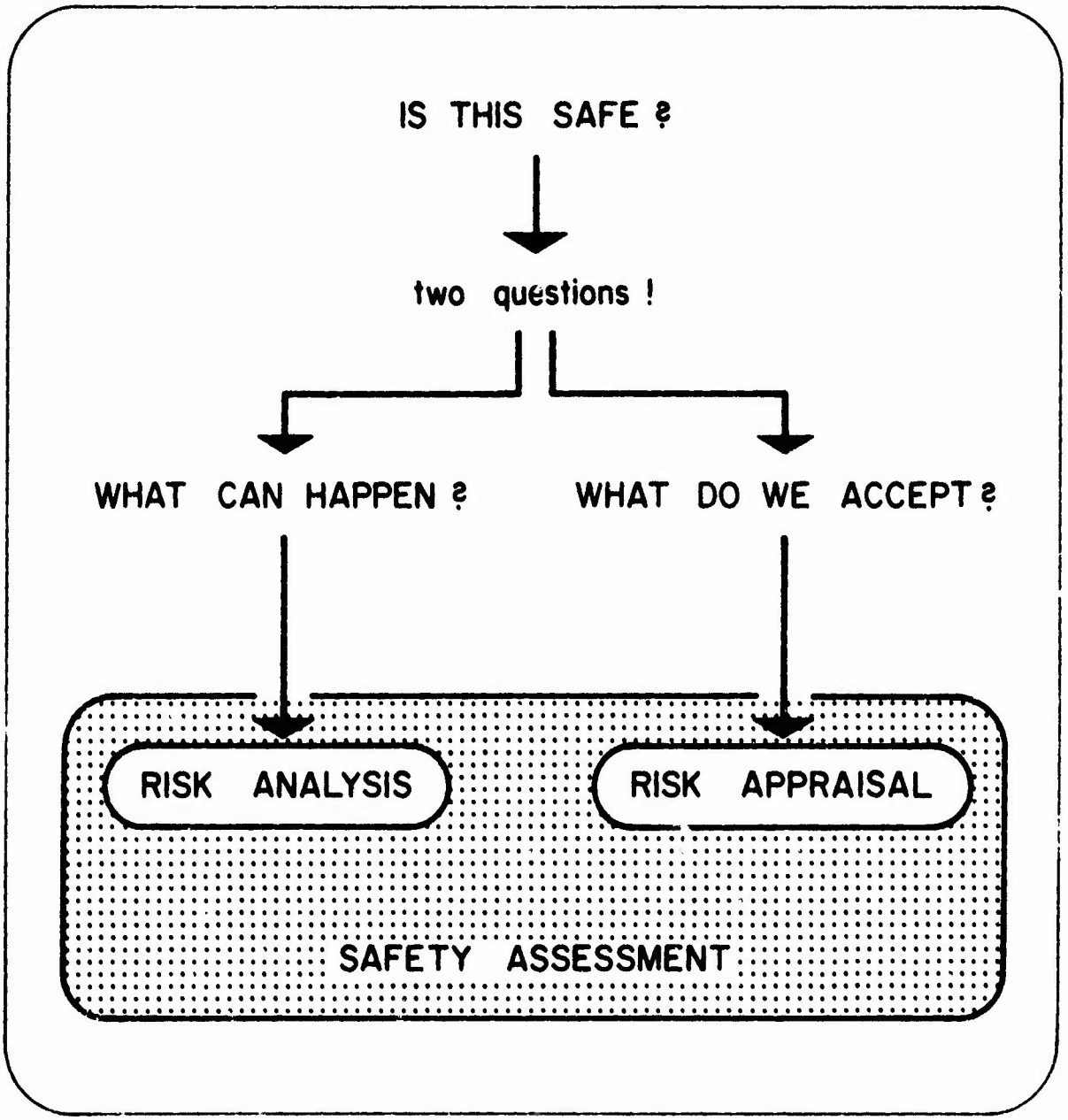
IS THIS SAFE ?
two questions !
WHAT CAN HAPPEN ?
WHAT DO WE ACCEPT ?
RISK ANALYSIS
RISK APPRAISAL
SAFETY ASSESSMENT

(1)

Risk of an activity for a group of n persons

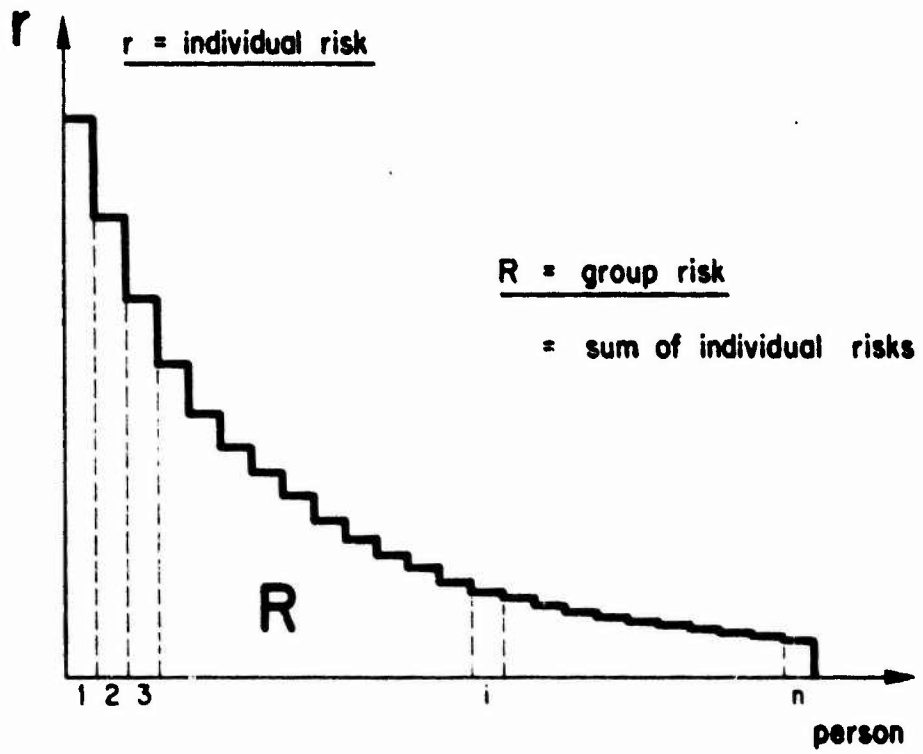

r = probability of death per year

R = expected number of fatalities per year

(2)

Risk of an activity for a group of n persons

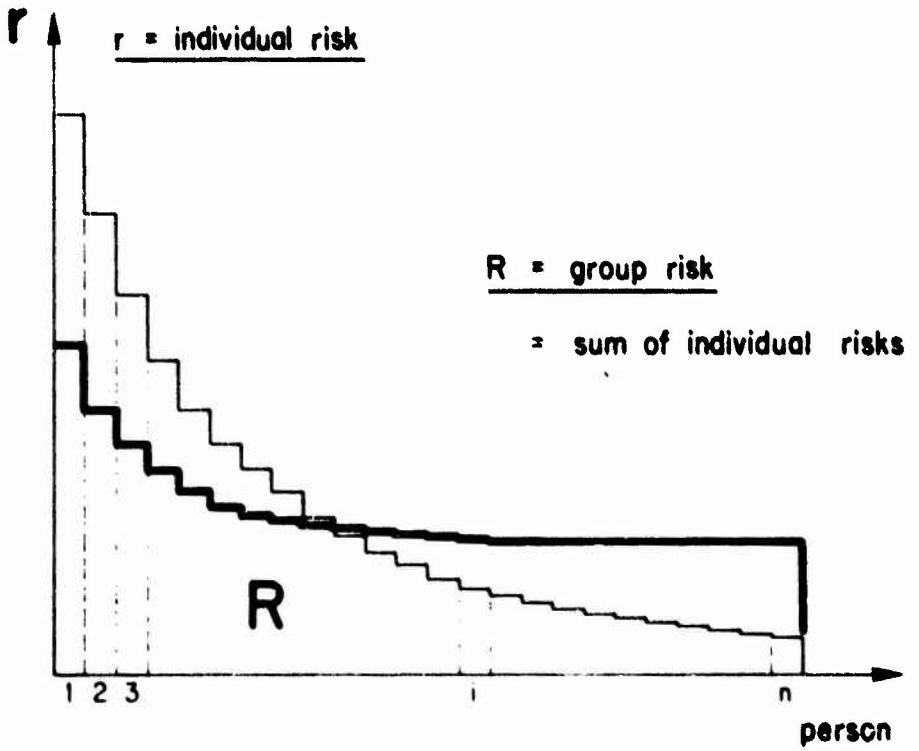

r = probability of death per year

R = expected number of fatalities per year

2a

Relation between risk and costs for safety

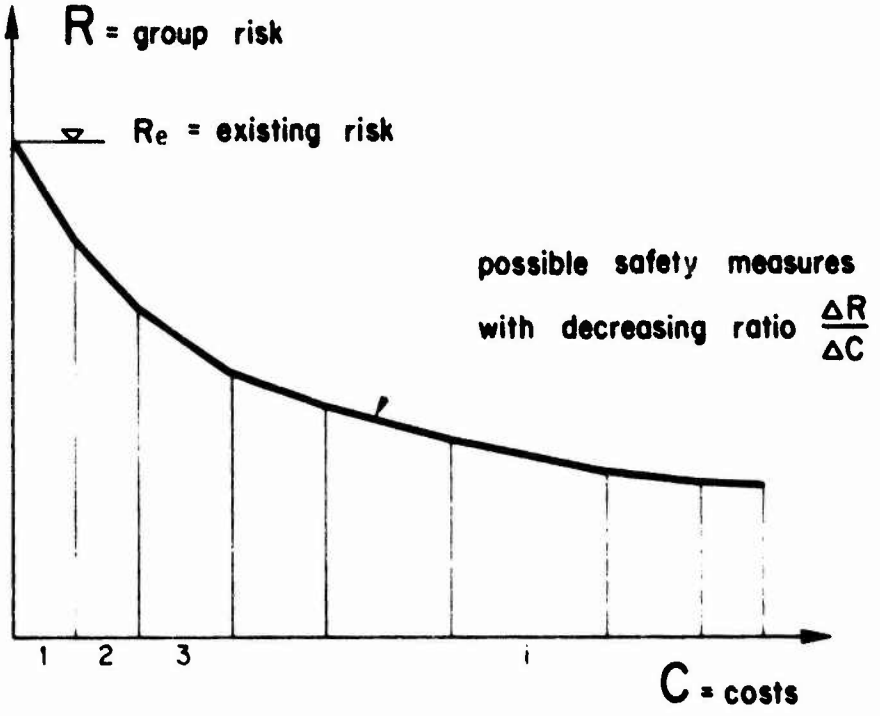

Problem: which point on the curve represents the solution?

(3)

Best safety solution for three systems

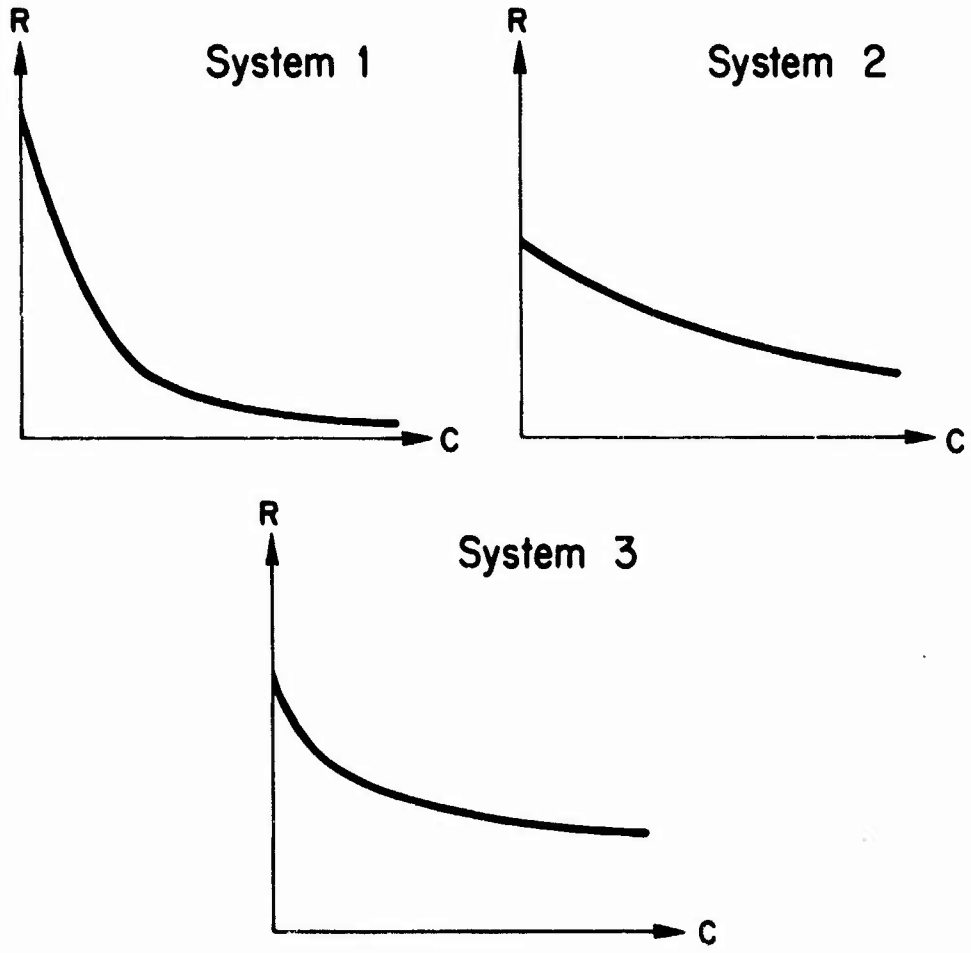

Best safety solution for three systems

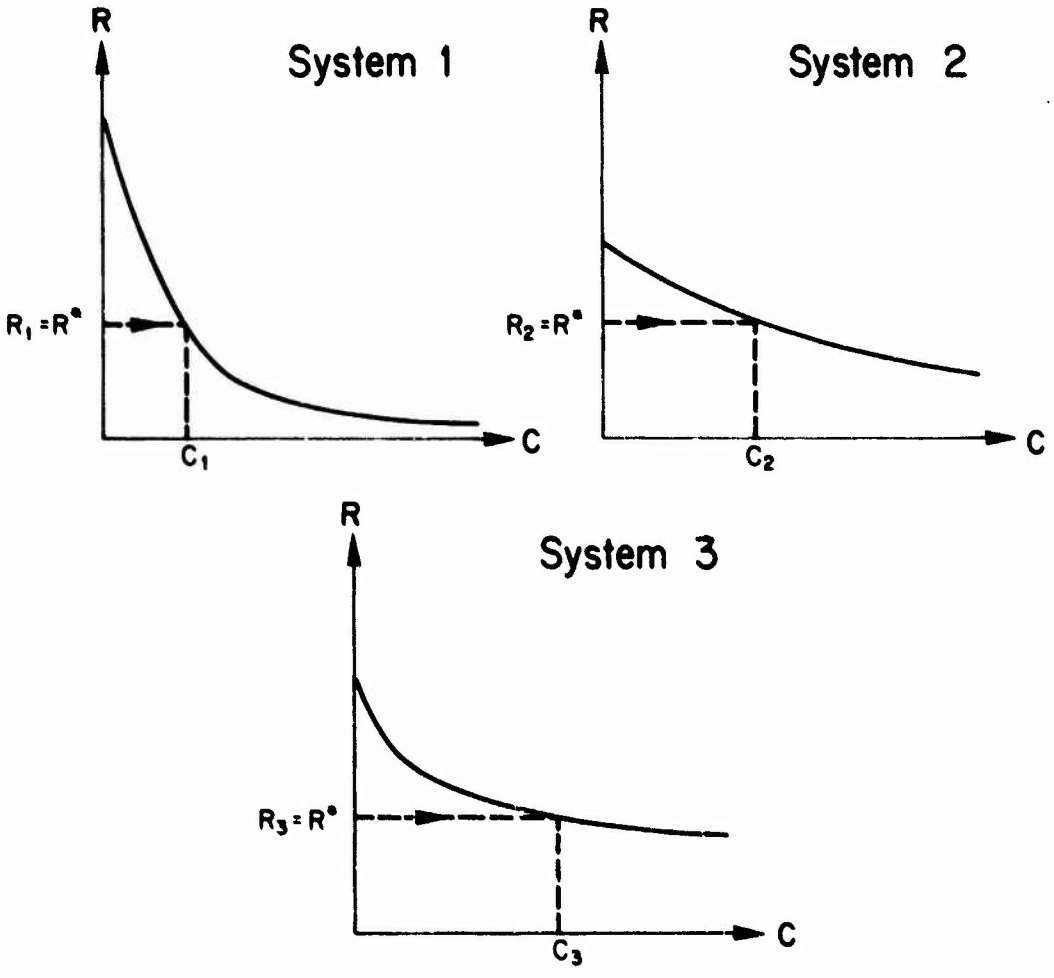

With constant risk level : $R_1 + R_2 + R_3 = 3R^*$

→ total costs : $C_1 + C_2 + C_3 = C^*$

Question: is this the best solution ?

Best safety solution for three systems

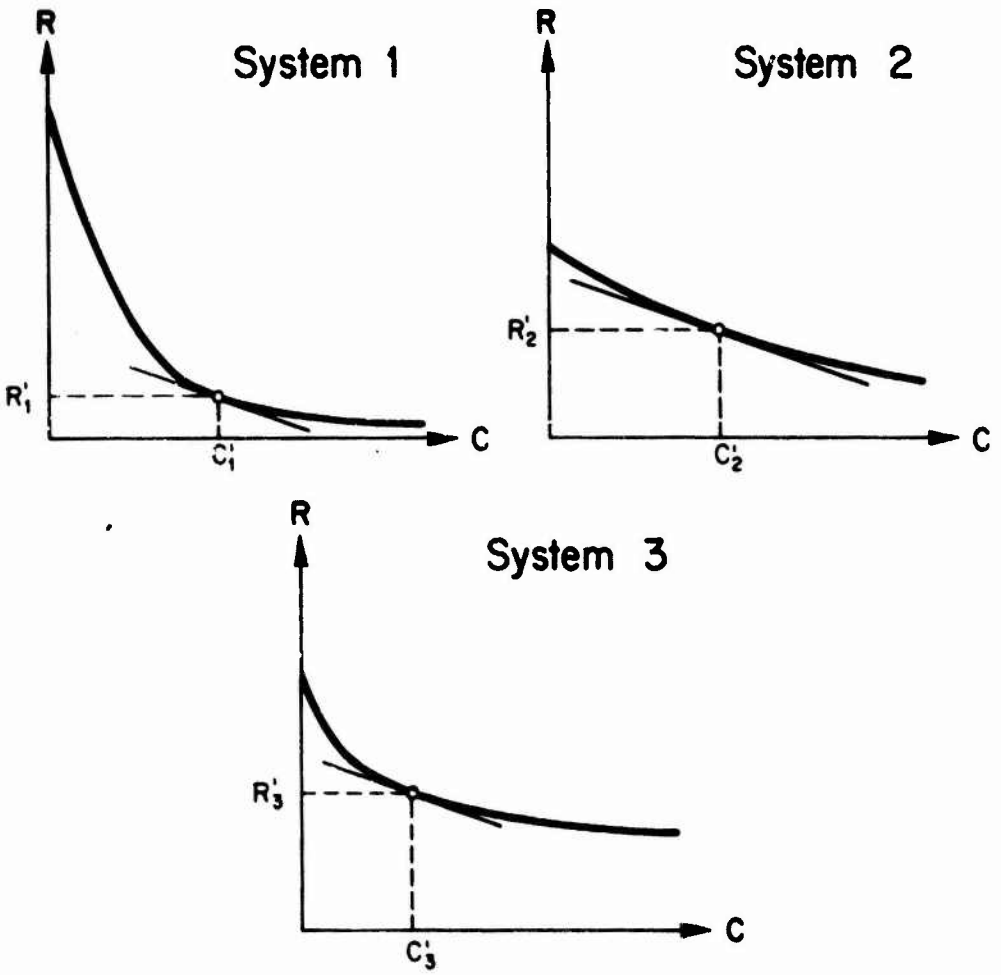

For the same total costs $C'_1 + C'_2 + C'_3 = C^*$

→ we get now $R'_1 + R'_2 + R'_3 = 2.5R^* < 3R^*$

Solution : same slope !

i.e. same marginal costs !

Trade-off between two competing aspects

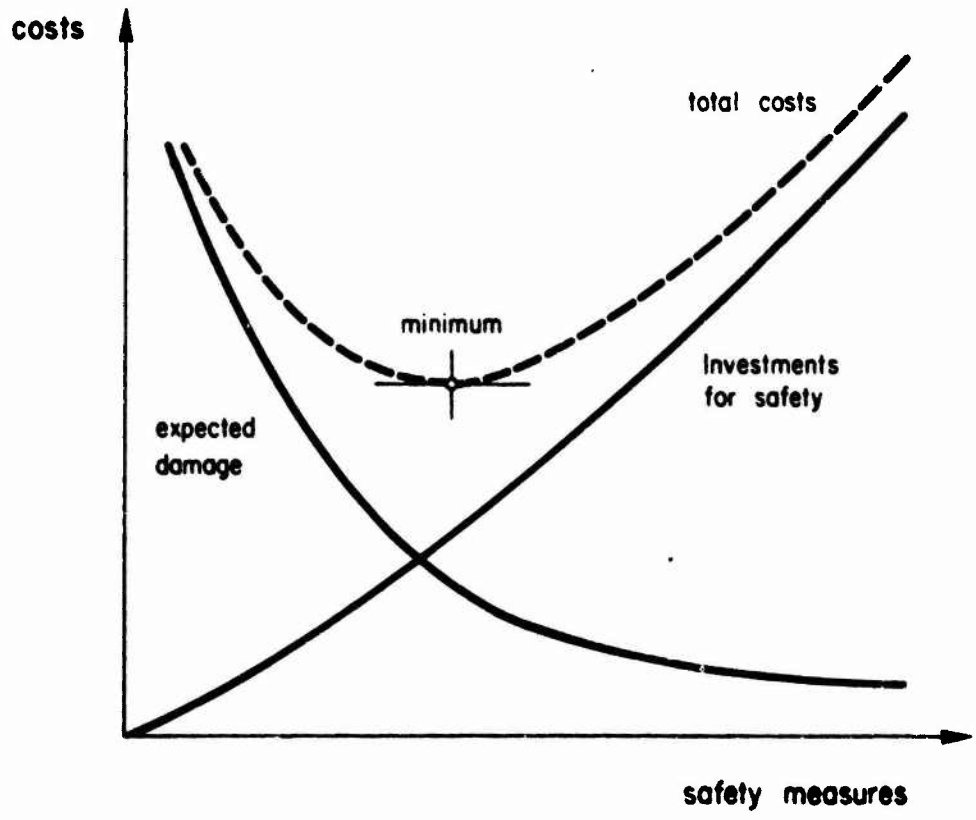

Question: Is this minimum our solution?

Trade - off between different units

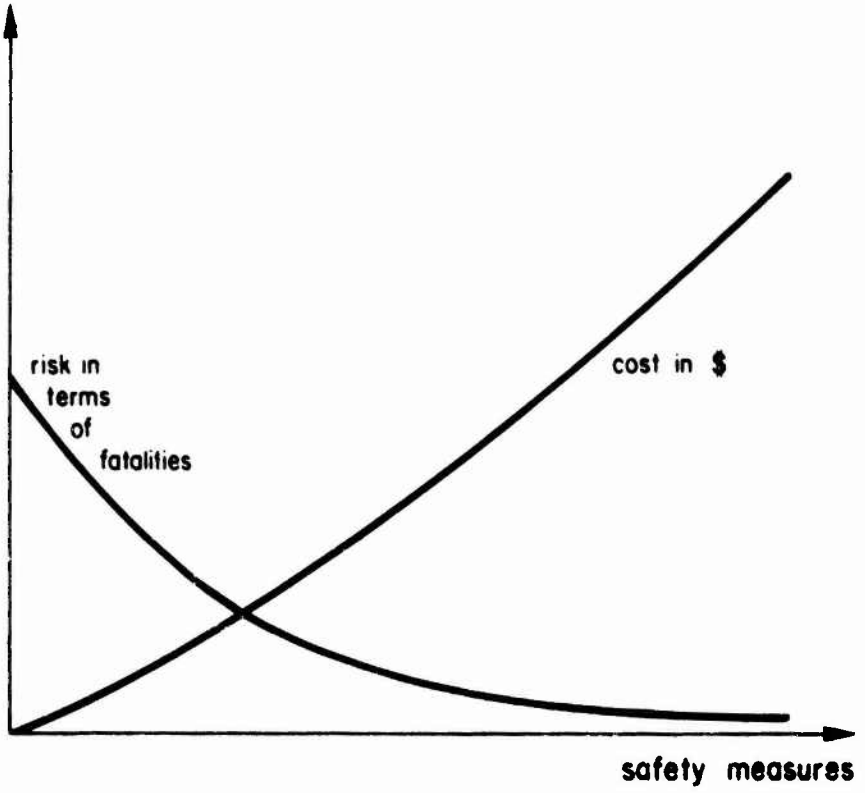

7

Trade - off between different units

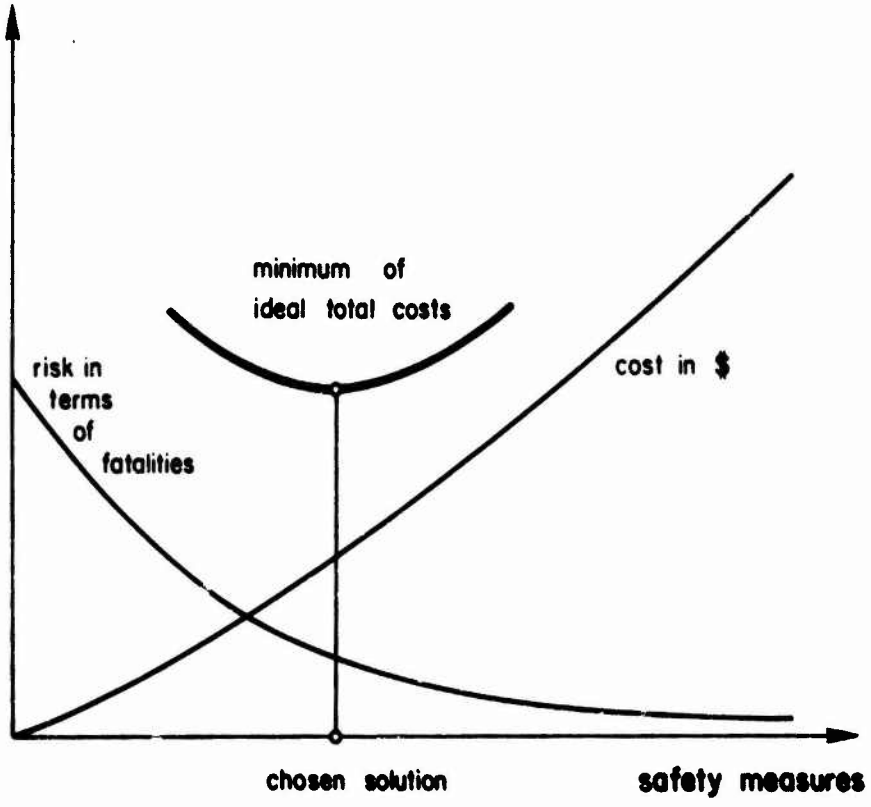

7a

Trade - off between different units

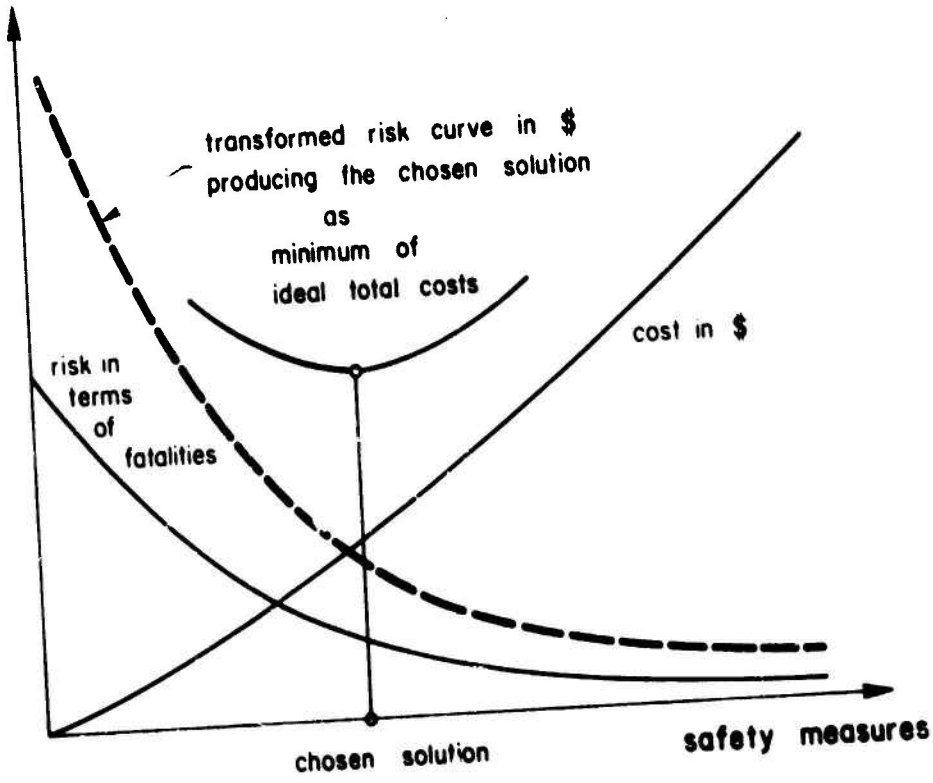

Solution: transform risk unit into $ - unit !

(7b)

How much do we pay for a human life ?

Three approaches :

- What costs does a fatal accidents cause for the company ? (e.g. insurance premium)
- What is the overall economic value of a human life ? (e.g. lifetime earnings)
- What are we willing to pay to save a human life ?

Four categories of risks

Parameter is relation between

- persons affected by the risks of the activity
- persons involved in the activity
- persons responsible for the risk control

Category 1 :

persons affected $=$ persons involved $=$ persons responsible

Category 2:

persons affected $\simeq$ persons involved $\simeq$ persons responsible

Category 3:

persons affected $=$ persons involved $\neq$ persons responsible

Category 4:

persons affected $\neq$ persons involved $\neq$ persons responsible

Proposed limits for willingness-to-pay for different risk categories

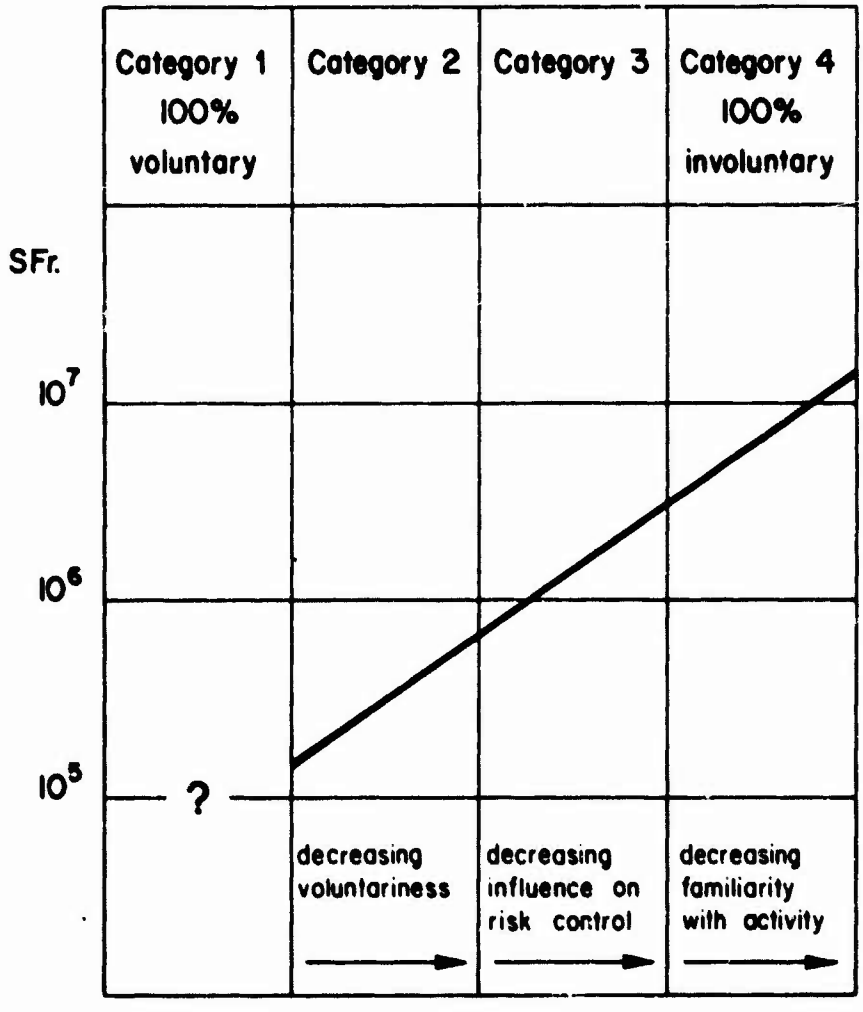

Proposed limits for willingness-to-pay for different risk categories

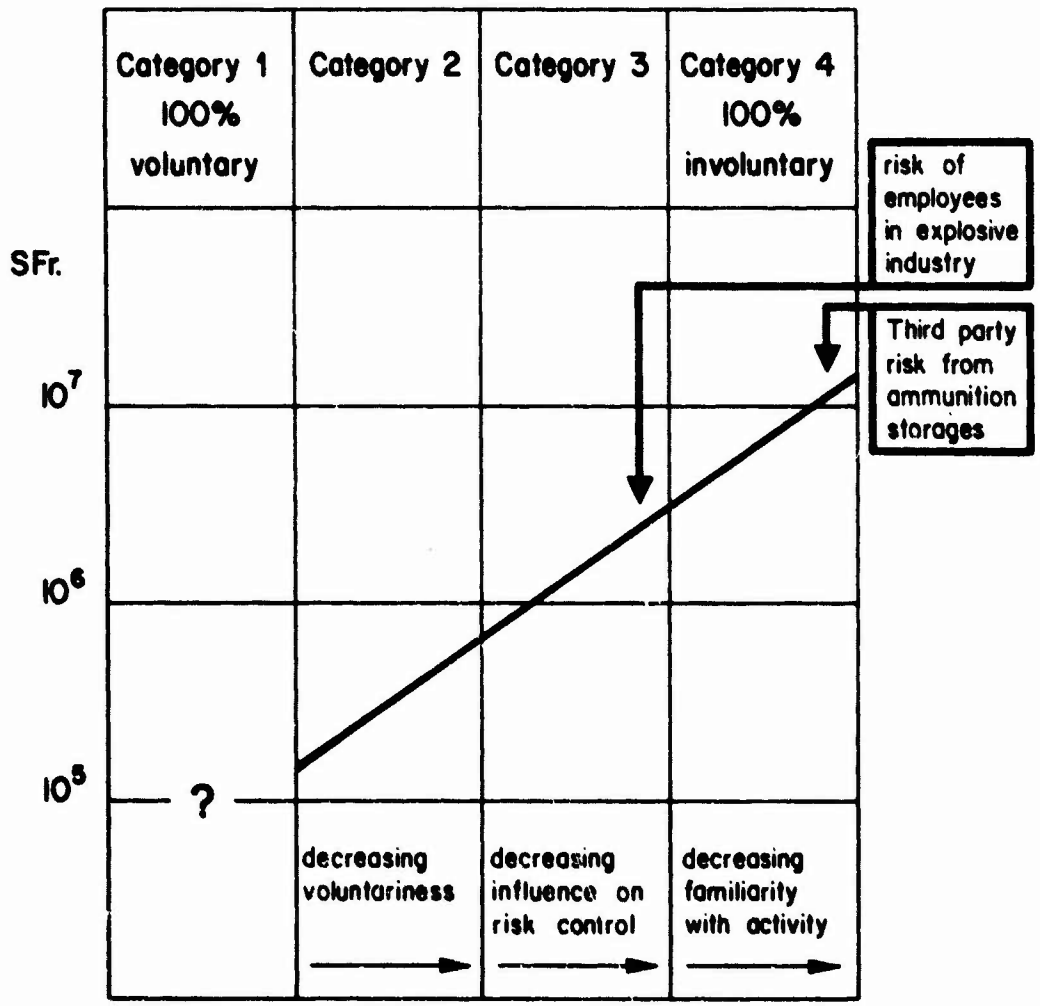

10a

SEPTEMBER 1978

Hangfire Protection and Containment



By:

John Gaye
Design Engineer

Bob Laurent
Design Engineer

ARMAMENT SYSTEMS DEPARTMENT
BURLINGTON, VERMONT

GENERAL ELECTRIC

PRECEDING PAGE BLANK

HANGFIRE PROTECTION AND CONTAINMENT

A major safety concern inherent in a high rate of fire gun system is the danger of a hangfire round and subsequent resulting damage. As a brief explanation, a hangfire is an ammunition defect in which the action time (time from strike to projectile muzzle exit) exceeds the maximum specified time. In externally-powered guns, this can result in detonation of the round in the gun with an unlocked gun bolt or, if a longer delay occurs, in detonation exterior to the gun. In either case, damage will occur to the gun and feed system and possibly inflict damage to the inside of a gun compartment. This is the hazardous concern and does require some type of containment.

In a typical 20-mm gun and feed system installation, the probability of hangfire occurrence is said to be quite low, with an approximate frequency rate of one hangfire in 200,000 rounds. Even with this low probability, adequate protection is required to prevent possible damage. The gun and round handling units attached to the gun do provide adequate protection. They are usually made of steel or aluminum housings with internal steel guides and gates. The conveyor through which the ammunition flows, made of steel round carriers guided through an aluminum-framed chuting, does not offer much protection. This is where some additional containment feature is needed to protect against the exploding debris of a hangfire.

In making a determination for protecting against hangfire, an evaluation of both brass and steel-cased ammunition was conducted. The U.S. Military Services are in the process of changing from brass to steel-cased ammunition and it was suspected that steel-cased rounds would have a more pronounced hazardous effect. The relatively higher strength of the steel case may allow higher over-pressures, damage, and fragment velocities. A test was conducted which confirmed these suspicions. Both a brass-cased and a steel-cased round were detonated within a piece of flexible conveyor chuting. A large cardboard box was placed over the test setup to indicate the amount and size of fragment penetration after detonation of the round. Many pieces of chute and case penetrated the box from the brass-cased round. A similar amount of fragment penetration was noted with the steel-cased round plus a large hole from the blast effect appeared on the side of the box. Through these tests it was concluded that any subsequent testing should use steel-cased ammunition, as it appeared to result in a more hazardous condition.

The F-18 Gun System was the specific application in which the development of a new protective cover was needed. All previous applications which required protective covers over some portion of the feed system were developed and tested using brass-cased ammunition. As the F-18 Gun System cover development concluded, it was recommended that previous programs re-evaluate their particular designs using steel-cased ammunition. In the F-18 Gun System, fired ammunition leaves the port side of the gun and enters into the flexible conveyor assembly. It

was at this area that a protective cover was needed to contain any possible hangfire rounds. With the F-18 Gun System mounted in the nose of the aircraft, aft of the radar package and in front of the pilot, many items within the gun compartment are vulnerable to damage from a hangfire, and necessitate a protective cover.

In beginning the evaluation for the F-18 protective cover, similar construction and material were used for the first configuration cover as were used on previous applications. Four plies of ballistic nylon per MIL-C-12369 were used for the first sample. Two grommets on one side of the cover were included as pressure relief vents. The cover was placed over a section of conveyor similar to the test setup used for evaluation of ammunition. A steel-cased round was detonated within this cover. The cover totally failed by permitting the projectile, case, and part of the chuting to exit through the cover, and was deemed unacceptable.

To confirm the impact of the steel-cased ammunition, a brass-cased round was detonated within a protective cover of the same construction. All debris was contained within the cover which showed the lesser hazard of this type of ammunition, and that the typical four-ply nylon design was adequate.

The second configuration cover was similar to the first with the addition of four 1" x 6" nylon reinforcing straps sewn into the case end of the cover. A steel-cased round was detonated within this chute. There was some seam and stitching failure and the projectile penetrated about two-thirds of the way through the cover. However, all debris was contained within the cover. This design appeared to be an improvement over the original design; however, still considered somewhat marginal due to the stitching failures and amount of projectile penetrations.

The third series of tests included two configurations of covers. The first was made of four plies of nylon with four extra plies over the projectile and of the cover, four grommets for venting instead of two, and four reinforcing straps, 2" x 6", over the case end of the cover. The second configuration was made of four plies of Kevlar cloth and the same grommets and reinforcing straps as the nylon configuration. A steel-cased round was detonated in each of these two configurations. With the nylon cover, some stitching failure was noted and the projectile penetrated about one-half inch through the cover. All debris was contained within the cover. In the Kevlar cover, there was no stitching failure, the projectile penetrated about one-half inch through the cover, and all debris was contained.

The significant features learned from this particular test were that the nylon with the reinforcing straps can contain the exploding round, the Kevlar thread does not fail and is superior to nylon thread, and that four grommets can be used to provide more venting.

In the final series of tests to confirm the design configuration, two sample covers were fabricated. Four plies of nylon with four additional plies in the projectile area, four grommets, Kevlar thread used throughout, and four reinforcing straps made up the final configuration. One of the samples did not have the reinforcing straps. It was felt that perhaps the Kevlar stitching alone could hold the cover together without the additional straps. When the round was detonated within this cover, the stitching did hold; however, the nylon failed at the seam and permitted the case to exit the cover.

The cover with the reinforcing straps did prove to be the superior design. It contained all debris without any seam or stitching failure. The projectile did penetrate through the cover by about one-half inch, which was considered acceptable. A second round was detonated within the same cover. Some evidence of unweaving and stitching failure was noted, the grommets were loosened, and the projectile did penetrate the cover by the same one-half inch. The cover did contain all of the debris. Although the cover would have to contain only one detonation, the second detonation did strongly indicate the design to be completely satisfactory to contain a hangfire. The selection of nylon over Kevlar material was based on cost and ease of fabrication. The cover represented the lowest cost, lightest weight design which would provide the necessary safety precaution to be used for this application.

Many things were learned in conducting these series of tests, particularly the greater hazard posed by the steel-cased ammunition. In an environment such as an aircraft gun compartment, an uncontained exploding round could do a great deal of damage to vital components of the aircraft. However, with a fairly simple low-cost ballistic nylon cover, this threat can be fairly well minimized. With the most emphasis placed on firing ammunition at a high rate of fire, the safety aspect of those late fired rounds is not being overlooked.

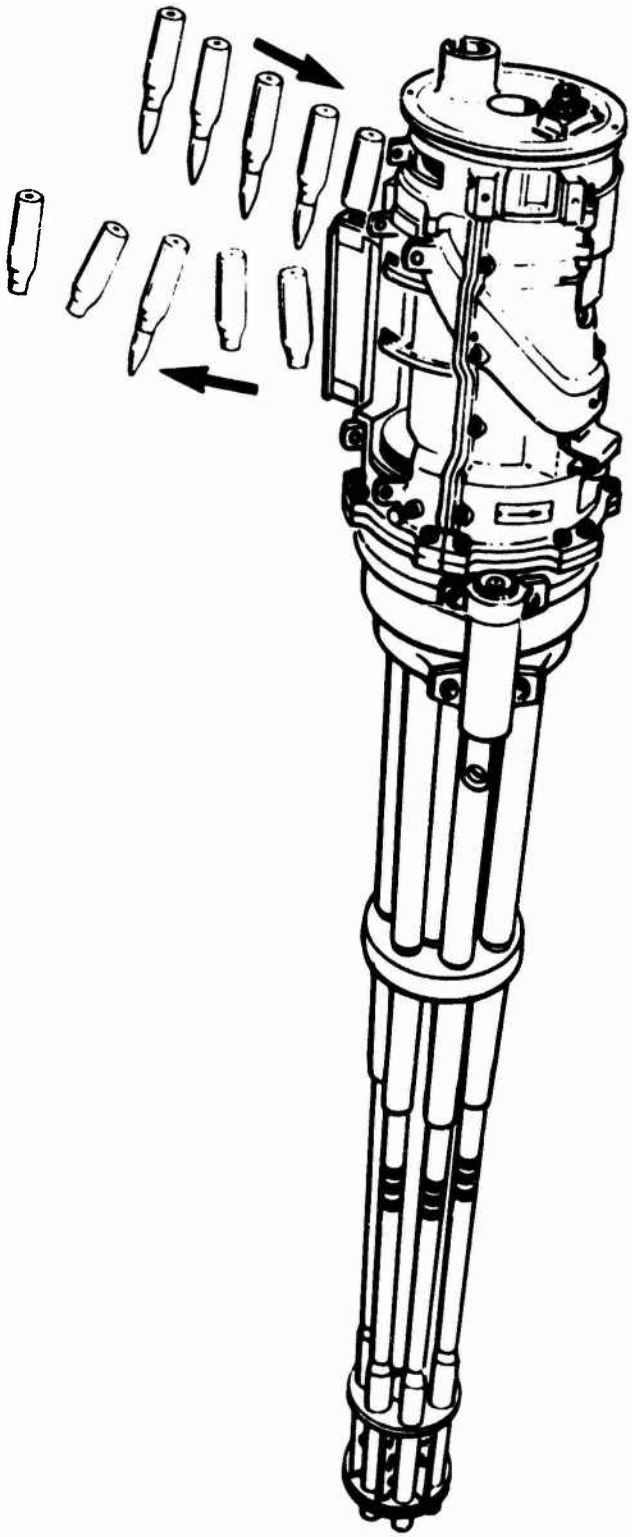

Figure 1. Location of Hexfire

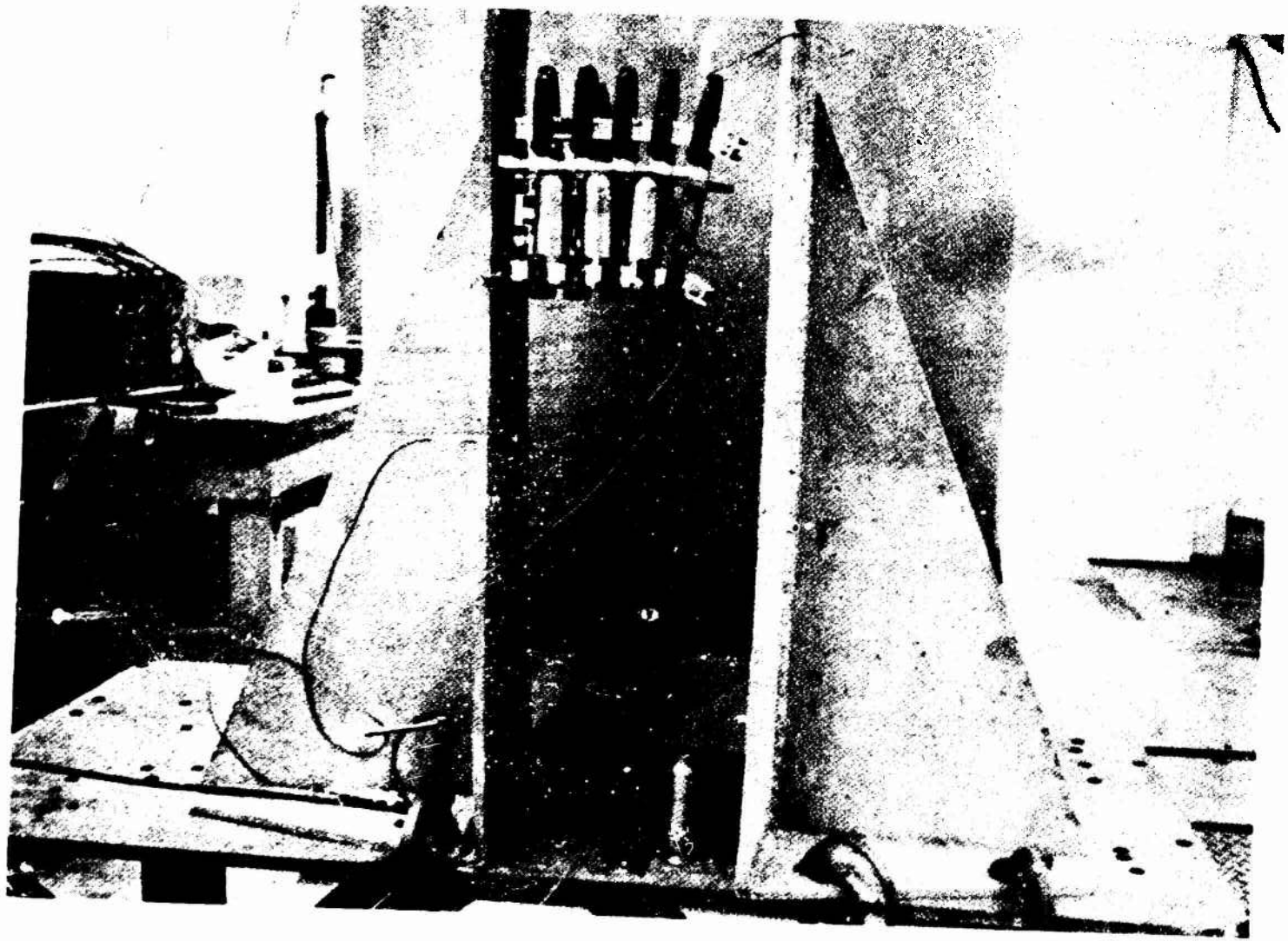

Figure 2. Ammunition Test Setup

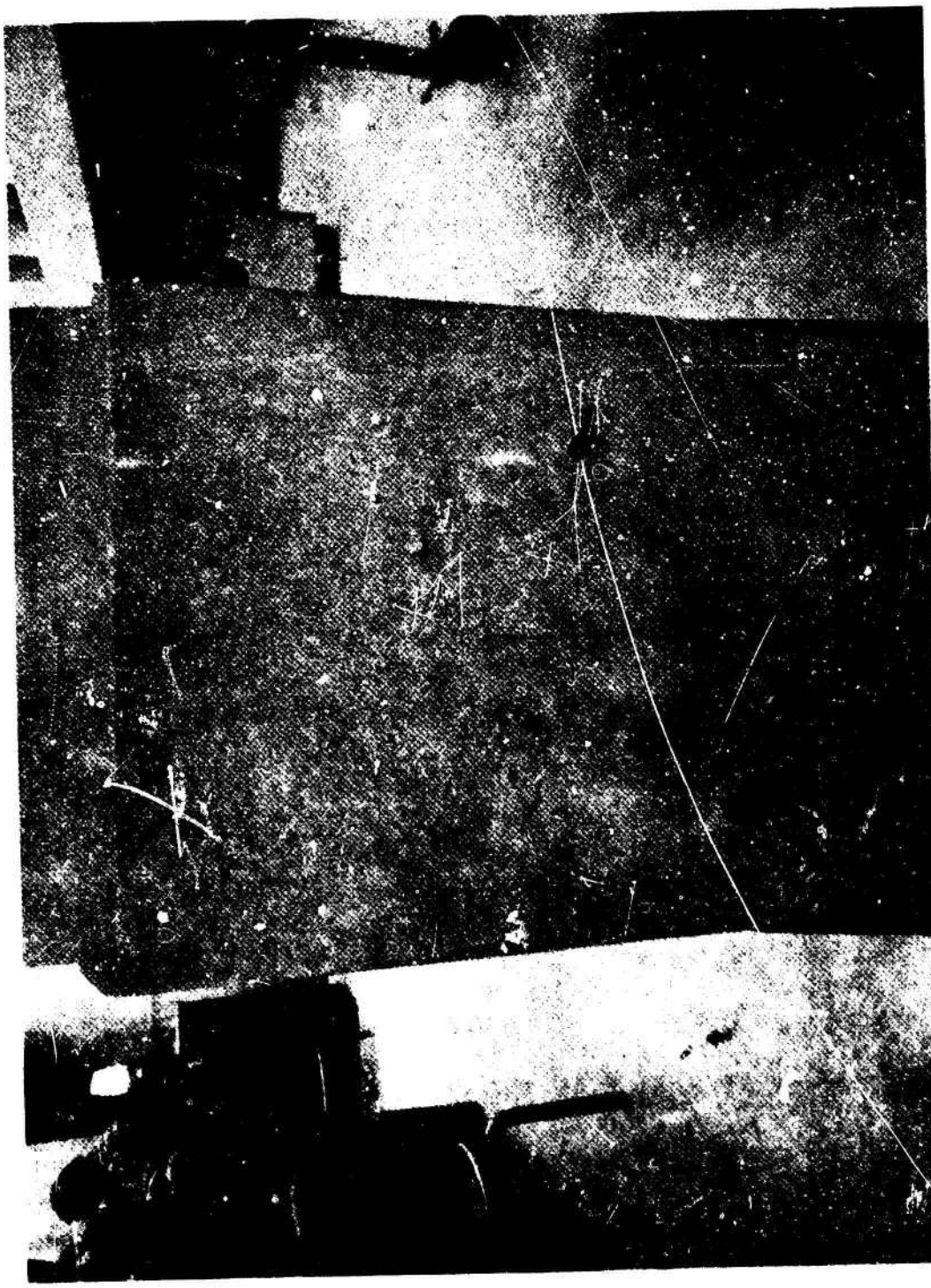

Figure 3. Result of Brass-Cased Round

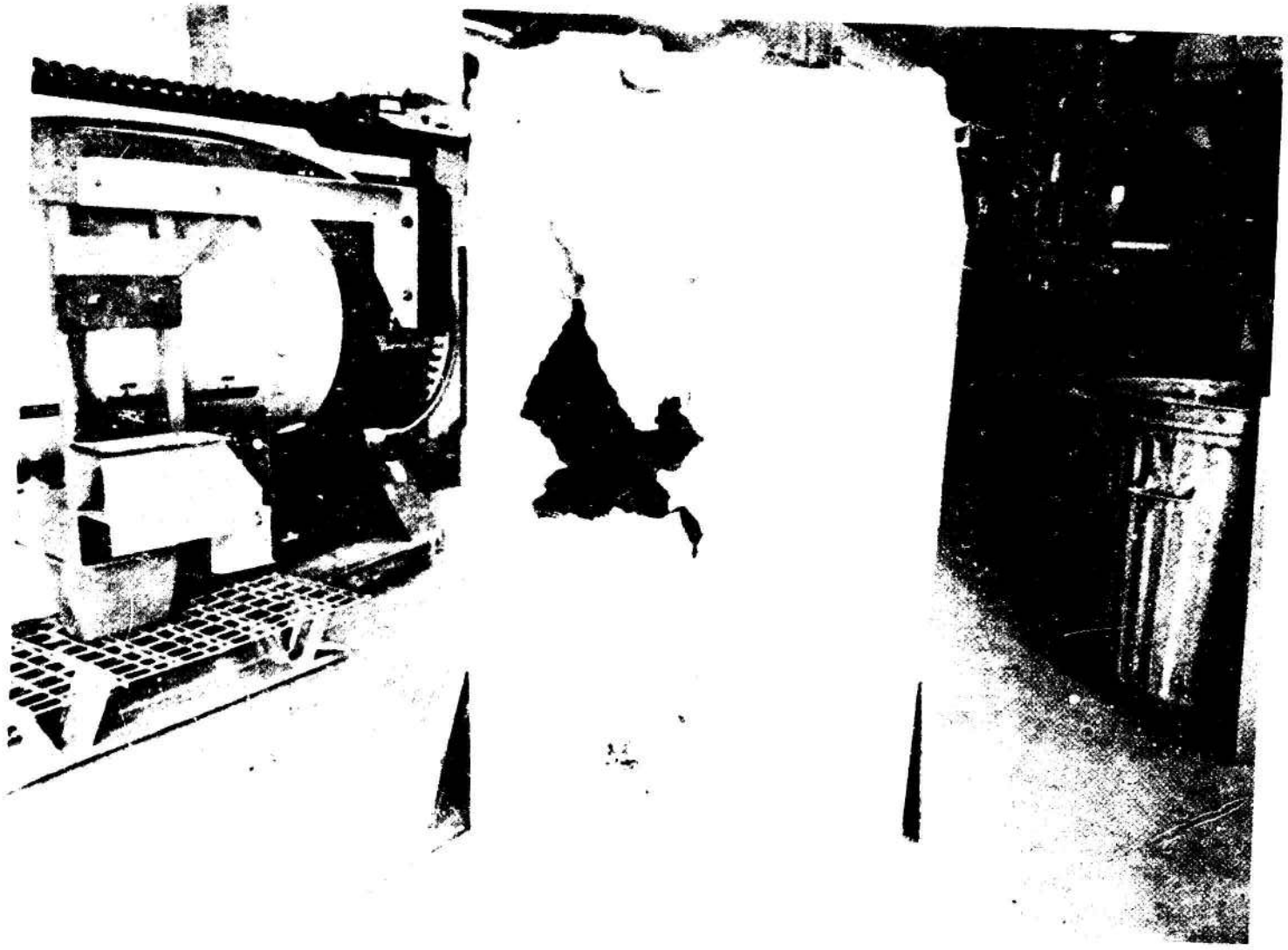

Figure 4. Result of Steel-Cased Round



Figure 5. F-18 Gun System

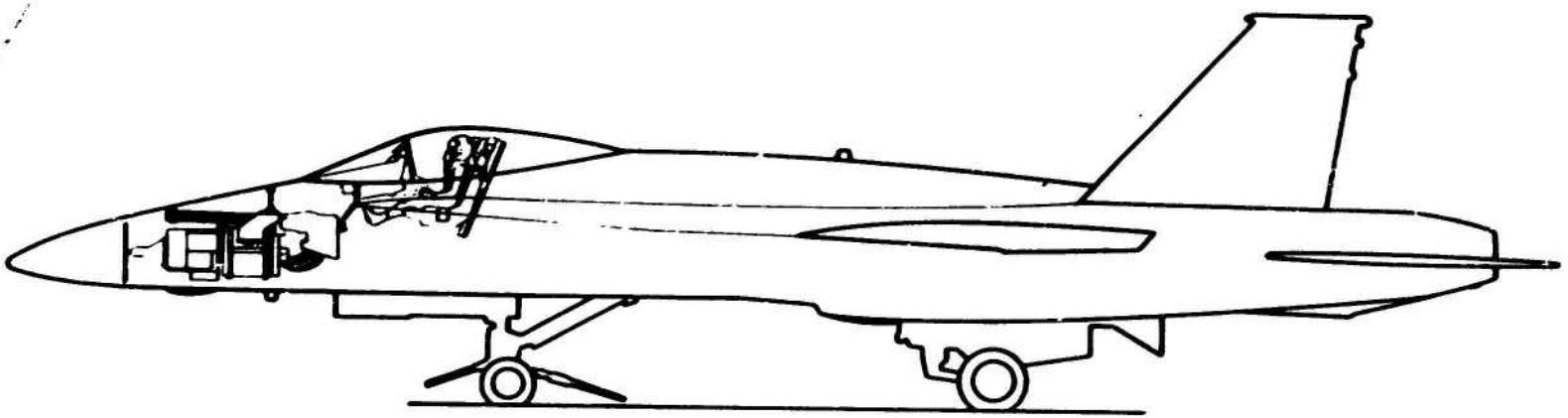

Figure 6. Gun System Location in F-18 Aircraft - Sketch

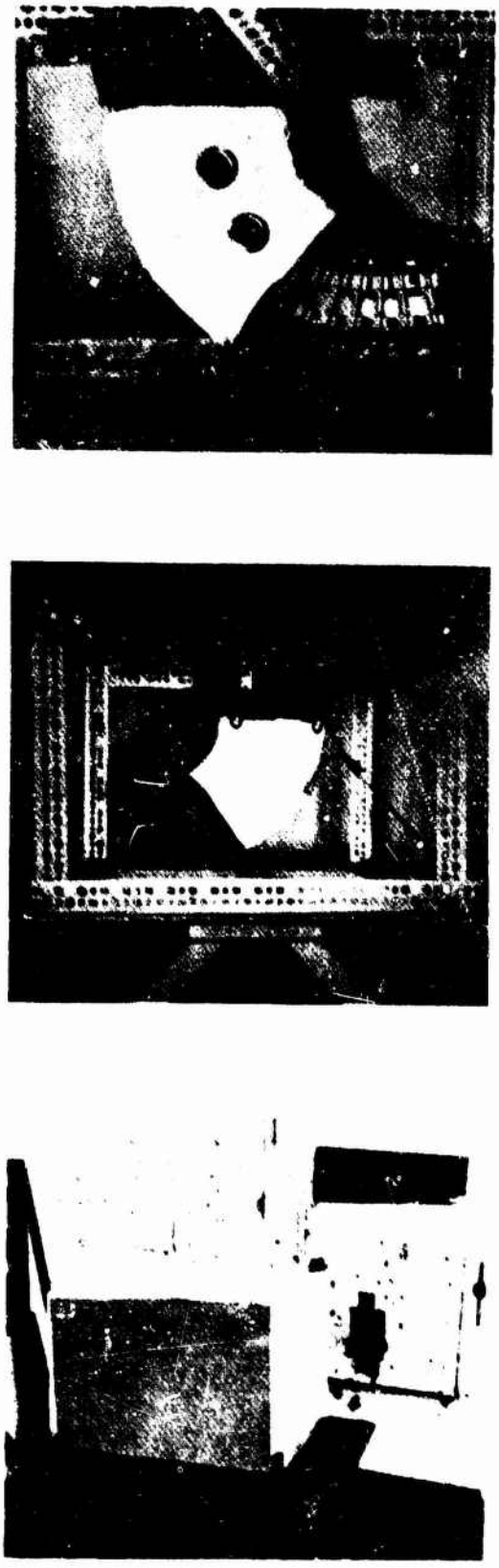

Figure 7. Test Setup for Cover Evaluation

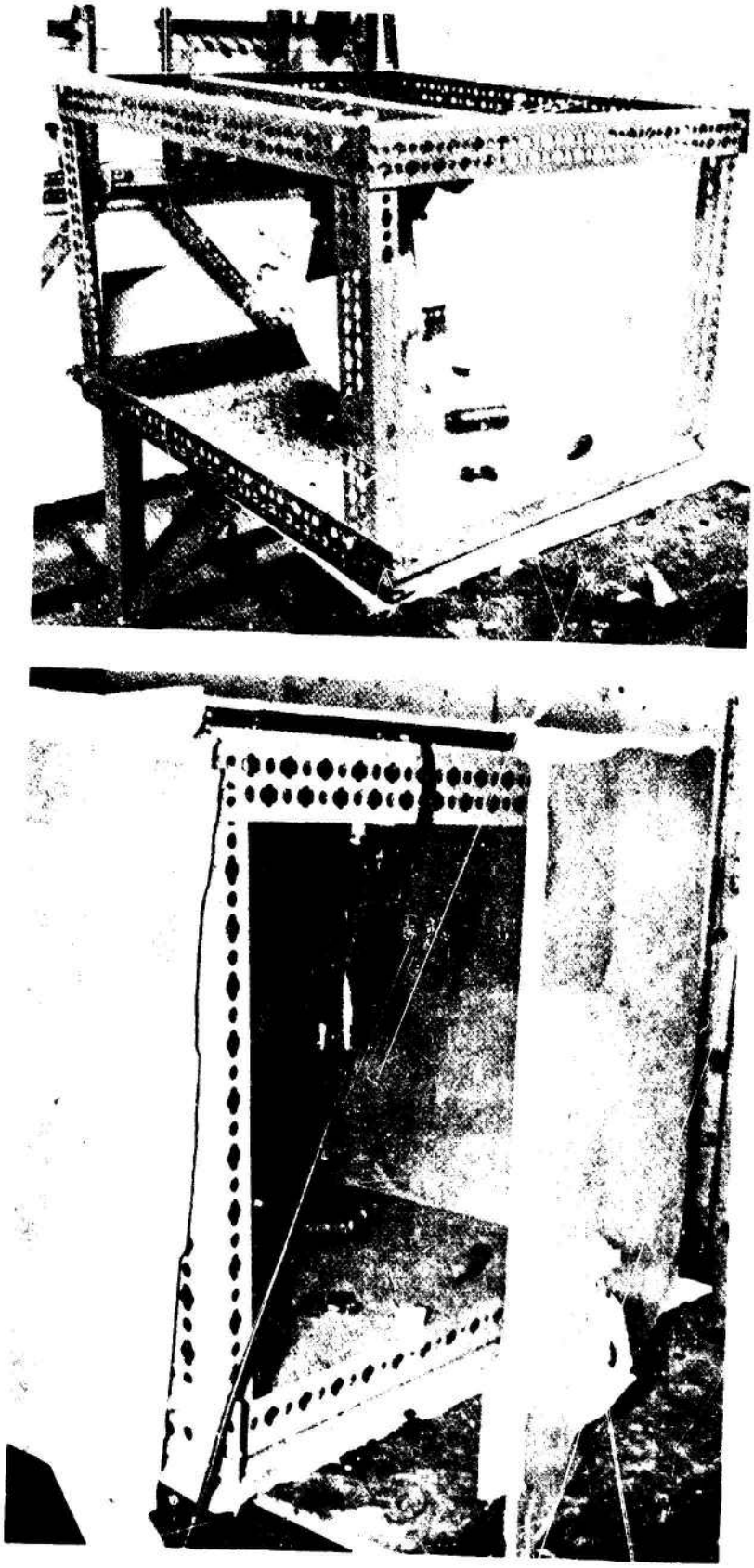

Figure 8. Results of Initial Test

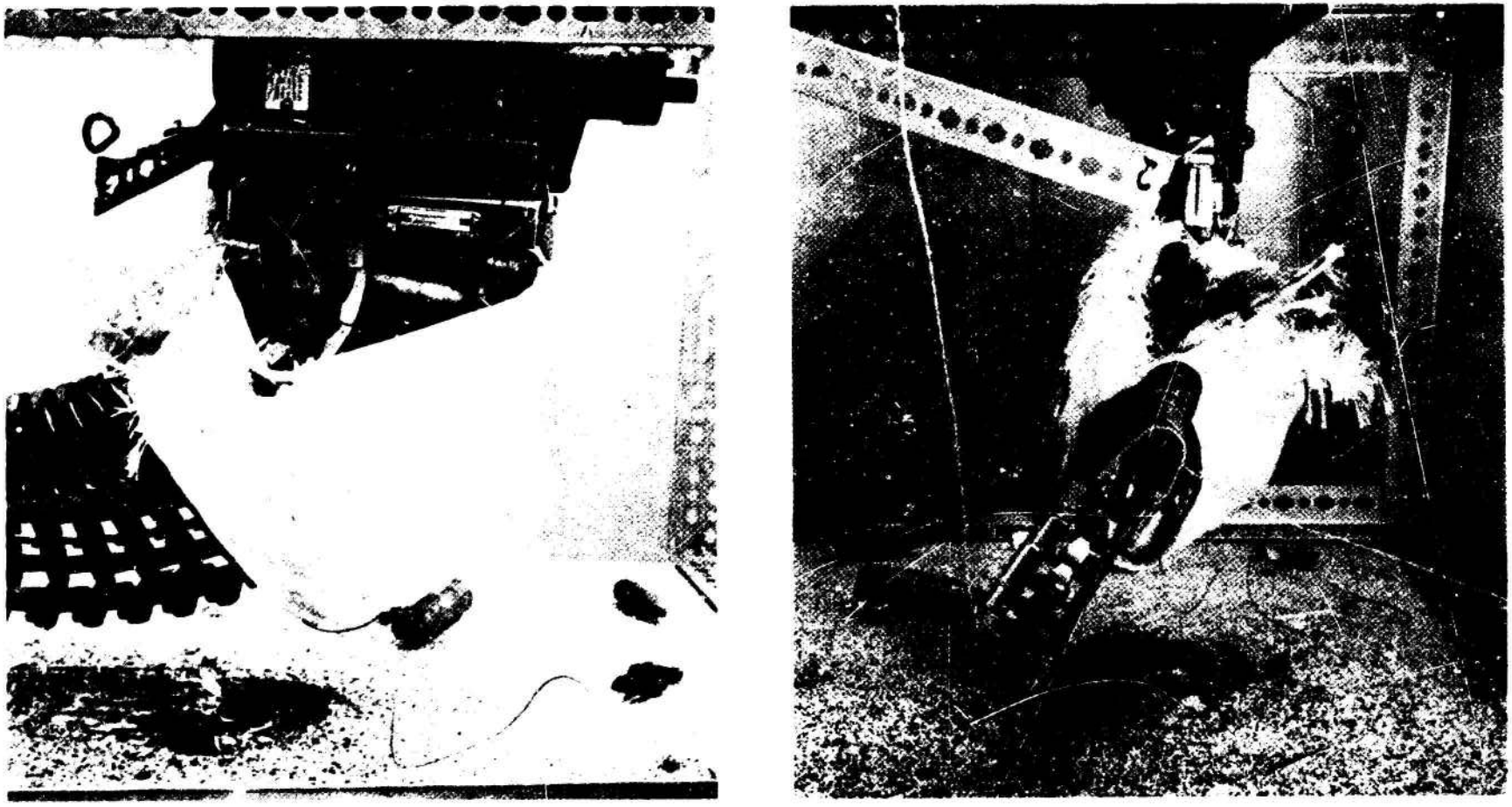

Figure 8. Results of Initial Test – Continued



Figure 9. Results of Second Test – With Straps

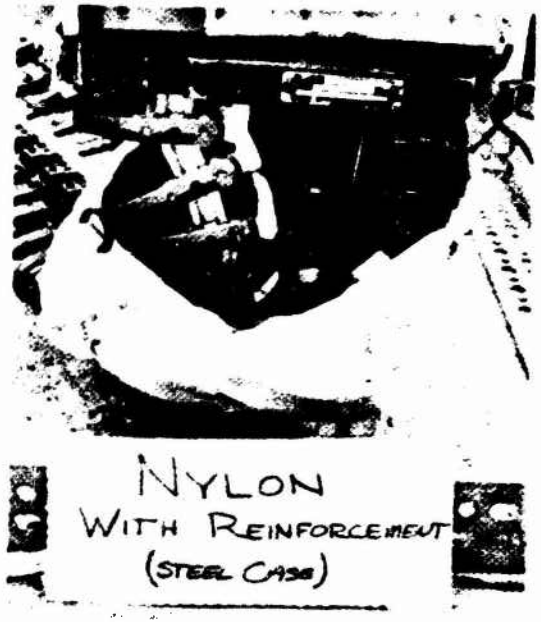

NYLON



KEVLAR



KEVLAR – NO STRAPS

Figure 10. Results of Third Test



WITHOUT STRAPS

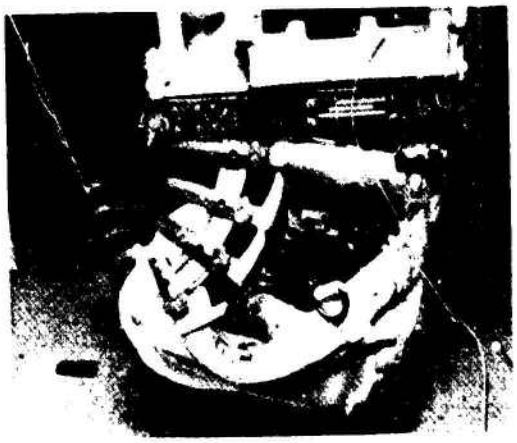

WITHOUT STRAPS

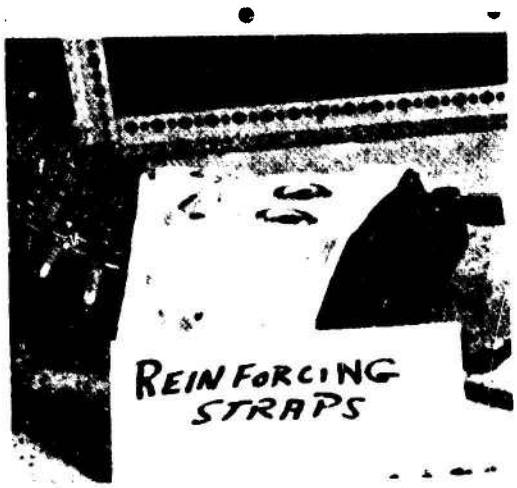

WITH STRAPS

Figure 11. Results of Fourth Test

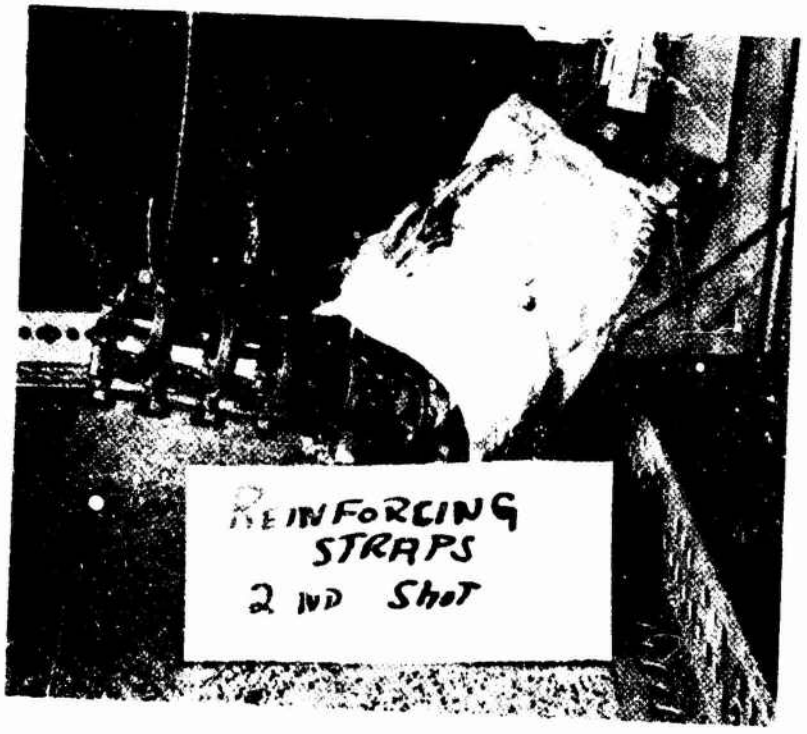



SECOND SHOT

Figure 11. Results of Fourth Test Continued



Figure 12. F-18 Gun System with Protective Cover

"DANGEROUS LEAD-IN-AIR CONTENT PRODUCED IN INDOOR SHOOTING RANGES"

CPT P. R. Sulik, USAF
Alaskan Air Command
Elmendorf AFB, AK

INTRODUCTION

As a person who has always been very interested in firearms and shooting, I have had the opportunity to fire weapons under many types of conditions. One facility that I have been using more and more each year is the indoor shooting range, especially when I wish to fire a handgun. While using these ranges, I have always been concerned over the quantity, and possible harmful effects, of smoke, lead particles, and especially lead fumes. I knew that lead can be very harmful when inhaled or ingested into the body but I did not know what quantities would be required in order to reach the danger level. Even more important, I did not know if the level produced during indoor firing was, in fact, high enough to be harmful.

I realized that every range is different due to the size, type of ventilation system, and amount of firing. However, I did feel that a significant problem might well exist, and therefore, I began to delve into the subject. Specifically, I wanted to find out what types of tests had been conducted in this area and what findings had been produced.

I talked with various indoor range personnel and was told that Environmental Health Services had been studying this very problem. Subsequent conversations with Environmental Health personnel revealed that a lead-in-air problem does exist on a broad scale and encompasses both military and civilian facilities. I also learned that only recently has the required amount of attention even begun to be focused on this problem; and, while many range problems have been identified and corrective action formulated, in many cases this corrective action has been postponed repeatedly due to lack of funds. Even more distressing, however, is the fact that responsible personnel at many ranges may not even know that a lead-in-air problem exists at their ranges, and that is the reason for my report.

As a source of data, I chose to use the results of tests and studies conducted by trained personnel who had the time, manpower, and facilities to perform such work. I conducted no basic research myself. I simply studied the work of others and used their findings to substantiate my theory that a problem exists. Furthermore, while the researchers produced very detailed findings for each range they studied and provided their results to a relatively small group, I wished to report on all ranges in general and to address a very large and diversified audience.

"DANGEROUS LEAD-IN-AIR CONTENT PRODUCED IN INDOOR SHOOTING RANGES"

The purpose of this paper is to help eliminate the health hazard of lead-in-air produced in indoor shooting ranges. To accomplish this goal, I would like to use a two-step approach. First, and most important, I want to make appropriate personnel aware of the hazard that may exist in their ranges, and second, I would like to offer some suggestions on how to about correcting this problem.

Perhaps it would be best to start by presenting a brief description of how lead-in-air is produced. When a cartridge is fired, the powder charge produces very hot, expanding gases which propel or drive the bullet forward. These hot, burning gases produce an effect much like a cutting torch and actually burn away a small amount of the base of the bullet. Furthermore, as the bullet is driven down the barrel, a tremendous amount of heat and friction is generated causing a certain amount of lead erosion to take place. The final result is that the lead which has been rubbed off the sides of the bullet, plus the lead which has been burned off the base of the bullet, are all blown out of the barrel by the expanding gases. It is this combination of lead fumes and small particles which consititute the lead-in-air that is so harmful to the body.

Designers of indoor shooting ranges have always been aware that this problem existed to some degree. Therefore, practically all indoor ranges have some type of ventilation system. The problem, however, is that many of the ventilation systems in use simply are not capable of accomplishing their purpose. This deficiency is usually due to inadequate capacity and/or inefficient design.

To be effective, the ventilation system must be capable of circulating enough air so that the lead-in-air content never exceeds 0.15 milligrams of lead per cubic meter of air, even during periods of heaviest firing activity. Testing at the three ranges used as the basis for this report, however, produced the following results:

Lead-in-Air Content

Milligrams of lead per cubic meter of air
($0.15\ mg/m^3$ = maximum safe level for a normal work day)

Range	Highest Reading	Lowest Reading	Average Reading	Factor (Average Reading Divided) By 0.15
#1	2.63	0.27	1.27	8.5
#2	7.76	0.45	2.69	18.0
#3	6.50	2.70	4.95	33.0

NOTE: #1. At Range #2, the ventilation system was corrected in accordance with the recommendations of the study group. A follow-on test then revealed that the

lead-in-air content, which had averaged 2.69 mg/m^3 or a factor of 18, was reduced to an average of 0.07 mg/m^3 or a factor of .47.

NOTE: #2. It should be noted that a lead-in-air content of 0.45 mg/m^3 is permissable for short periods of time (2-3 hours) and would not prove harmful to personnel who only fire on an infrequent basis. However, this level of concentration could prove harmful to full-time range personnel who are exposed on a daily basis.

In addition to being able to circulate a sufficient quantity of air, it is equally important that the ventilation system be properly balanced. That is, the intake air and the exhaust air must match, in both volume and rate of flow. In the two ranges where the air flow was measured, a significant imbalance was detected, as illustrated in the following chart:

Intake Air versus Exhaust Air
(Cubic Feet of Air Per Minute)

Range	Intake Air	Exhaust Air	Difference
#1	1,012	3,277	2,265
#2	6,900	4,200	2,700

A third and equally important consideration in regard to the ventilation system applies to the pattern of air flow. To be a truly effective ventilation system, intake air must enter the room uprange, flow past the shooters, continue past the bullet trap area and then be exhausted at the downrange end of the building. Studies indicate that the most effective method is to exhaust 30% of the contaminated air halfway between the shooters and the bullet trap, and then exhaust the remaining 70% just behind the bullet trap. The main point, of course, is to ensure a smooth sweeping air flow which provides fresh air to the shooters and forces out contaminated air downrange.

However, since correction of ventilation system is often a lengthy process, several interim solutions may be applied. The most obvious, of course, is simply to reduce the number of shooters that are permitted to fire at any one time. By thus reducing the rate at which lead-in-air is produced, even an inadequate ventilation system should be able to maintain a safe environment. This action, however, will require that firing be conducted over longer periods of the day and may even require that some firing be done at night time and/or weekends.

A second interim solution would require that (copper) jacketed bullets be used instead of lead bullets. Comparison tests at one range revealed that bullets made entirely of lead produced two and a half times as much lead-in-air content as jacketed bullets. The primary reason for this difference is the presence of the metal jacket which prevents lead erosion from the sides of the bullet. Jacketed bullets, however, are seldom used since lead bullets are less expensive, less likely to ricochet and more readily available.

While on the subject of bullet designs, one type deserves special mention due to its widespread use. This bullet, called the wadcutter, offers several advantages which have made it the all-time favorite for use in indoor shooting ranges. Since wadcutter ammunition is designed primarily for target work, it is superbly accurate and very pleasant to shoot due to its moderate recoil and reduced muzzle blast. However, because of the unique wadcutter design, which assures more bearing surface in the bore of the weapon, these bullets generate more friction while moving down the barrel and consequently produce more lead-in-air than any other type of bullet. Therefore, use of this ammunition should be restricted whenever it becomes necessary to reduce the rate at which lead-in-air content is produced.

SUMMARY

It is probably safe to say that a significant health hazard may well exist at many indoor shooting ranges. To properly assess the extent of this hazard, each range must be evaluated on an individual basis. If the ranges for which you are responsible have been tested and found to be safe, they require no further attention other than occasional testing to reaffirm their safe status.

However, if you are not sure of the status of your ranges, then by all means notify the appropriate personnel and request that a lead-in-air content test be conducted. The Environmental Health Services Office on your base, or within your area, is probably the best place to contact first. If they cannot help you, they will at least be able to refer you to an agency that can help.

At the three ranges mentioned in this report, a definite health hazard had existed for an undetermined length of time. Yet, it was not until someone questioned the safety of the air and requested that it be tested, that the problem was fully realized and corrective action initiated. In fact, testing revealed lead-in-air content readings that were 8.5, 18, and 33 times the maximum safe level.

Once you have determined that you have a lead-in-air problem at your range, the only real solution is to install a proper ventilation system. In some cases, a modification of the existing system may be adequate and in other cases installation of an entirely new system may be required. In either case, the same agency that helped you identify the problem should be able to assist you in formulating a solution.

When considering the ventilation system - remember, fresh air should enter the room from the uprange end, flow past the shooters and then be exhausted from the downrange end. Intake air must equal exhaust air and the total volume circulated must be enough to ensure that the lead-in-air content never exceeds 0.15 mg/m^3. The effectiveness of this solution was clearly demonstrated at Range #2, where impressive results were achieved. The lead-in-air content, which had averaged 18 times the maximum safe level, was reduced by 97%, simply by correcting the ventilation system.

Until a proper ventilation system can be installed, several interim solutions may be applied. These solutions include reducing the number of shooters who are permitted to fire at any one time, using jacketed bullets instead of lead bullets, and restricting the use of wadcutter ammunition. It must be remembered, however, that these are merely short term solutions and as such do not address the basic problem.

Hopefully, this report will help to focus attention on a problem that is both dangerous and widespread. Lead-in-air is a serious problem, but it is one that can be identified and corrected when responsible people take the necessary action.

REFERENCES

Annual Industrial Hygiene Survey Report, (7 June 1977), Elmendorf Air Force Base, Alaska

Industrial Hygiene Survey Report, (6 March 1975 - 31 January 1977), United States Air Force Academy, Colorado

Anania, Thomas L., Lucas, James B., M.D., and Seta, Joseph A., (1974) Lead Exposure at an Indoor Firing Range, HEW Publication No. (NIOSH) 74-100, U.S. Department of Health, Education and Welfare, Cincinnati, Ohio

Safety Aspects of Tagging Explosives for Post-Detonation Identification

Carl Boyars
The Aerospace Corporation
955 L'Enfant Plaza, S. W., Suite 4000
Washington, D. C.

A number of bills have been introduced in the House of Representatives and Senate of the United States which require the tagging of commercial explosives for detection and for post-detonation identification as an aid in the apprehension of criminal bombers. It is possible that, at some future date, this requirement may be extended to military explosives as well.

In developing and evaluating taggants, various aspects of compatibility with the manufacturing processes and the performance of the products must be considered. Safety is, of course, a critical item. In this paper, the test data that have been obtained to demonstrate the safety of tagging various explosives will be described in detail.

Explosives identification tagging refers to the addition of tiny coded particles to explosives during their manufacture that can survive detonation, be recovered and decoded, and, through distribution records, allow the explosives to be traced back to the last legal possessor. These tags are incorporated in quantities of 0.05% to 0.1% by the explosives manufacturers into their formulations.

The taggant for post-detonation identification which is now being evaluated on a fairly large scale was developed by the 3M Company. The identification code is given by a multi-layered particle, viewed through a microscope, in which the layers differ in color (Figure 1). Each color is assigned a number corresponding to the electrical resistor color code. The number of possible colored layer permutations is obviously quite large.

The regular 3M taggant consists of a laminated melaminealkyd core encapsulated in polyethylene wax. The core is color-coded by the inclusion of various pigments. One of the layers normally includes iron particles to make the taggant magnet-sensitive, and one or both exterior layers include one of three fluorescers which respond to UV irradiation. The normal taggant core (unencapsulated) is called a Type A taggant. A Type B taggant (unencapsulated), made with melamine-acrylic resin, was tested in the early stages of taggant development, but this "hard" taggant sensitized explosives while the Type A "soft" taggant did not. The Type A core encapsulated with polyethylene wax is called Type C. When Type C is

evaluated for use in specific explosives, both Type A and Type C are often subjected to compatibility tests because of the possibilities of inadvertent omission of polyethylene coating from the Type C or of removal of the polyethylene coating at some stage in the processing of explosives. The most complete test of chemical compatibility of taggants with explosives involves using "first article blends" of taggants. These consist of a mixture of three different color-coded taggants which include, among them, all the different pigments and phosphors as well as the magnet-sensitive additive. Other experimental cores and encapsulating materials have also been evaluated for 3M. The test data on Type A and Type C have always shown that these taggants do not increase the hazards of explosives processing or handling.

The test methods used for compatibility evaluations (sensitivity, thermal stability, aging, and performance) are those used in the explosives industry, although there is a general lack of standardization between manufacturers as to test procedures, apparatus, and interpretation. In general, each manufacturer will want to satisfy himself, by test procedures he selects, that a proposed additive (i.e., taggant) is compatible with his process.

The tests generally compare the response of explosives (with and without taggant) to the impact of a falling weight, to a sliding frictional type impact, to electrostatic discharge, and to various thermal inputs. A positive response to electrical or mechanical energy input may be defined as any evidence of reaction or as a defined extent of reaction, e.g., explosion. Test results may be reported as the energy level necessary to give positive responses 50% of the time or as the energy level which will give a single positive response in 10, 20, or more trials (Threshold Initiation Level = TIL).

Thermal tests may consist of determining:

(1) At what temperature exotherms occur, i.e., DTA (differential thermal analysis) or DSC (differential scanning calorimetry);

(2) The rate of gas evolution at a given temperature, e.g., Taliani or Vacuum Stability tests;

(3) The time required for a color reaction (e.g., Abel test) which indicates the presence of nitrogen oxide gases, which are decomposition products in those explosives containing nitrate esters, e.g., dynamites but not most aqueous gelled slurries; and

(4) The time required for explosion.

Tests of performance assure that the explosive containing taggant functions as well as the same explosive without taggant.

Compatibility of taggant was measured with a number of different types of commercial explosives: dynamites; gelled aqueous slurries (usually called slurries or water gels, depending on the manufacturer's preference); cast boosters; and black powder. The data obtained are tabulated as follows:

Table I --- Compatibility of Type A Taggant

(a) With dynamites (and their ingredients)
(b) With aqueous gelled slurry explosives (and their ingredients)
(c) With cast boosters (and their ingredients)
(d) With black powder

Table II --- Compatibility of Type B Taggant

(a) With cast boosters (and their ingredients)
(b) With dynamites (and their ingredients)
(c) With black powder

Table III Compatibility of Type C Taggant

(a) With dynamites (and their ingredients)
(b) With aqueous gelled slurry explosives (and their ingredients)
(c) With cast boosters

The Tables compare directly various explosives with and without taggant added, subjected to a variety of tests of sensitivity and stability and performed by a number of different organizations. Despite attempts at elegance in reporting test results by some of the organizations, e.g., the computation of energy values in drop weight tests and the computation of force values in friction tests, the absolute values have no significance here; only the relative values of tagged versus untagged explosive are relevant. It is obvious that there are instances of sensitization by the obsolete Type B taggant but not one case of sensitization or unstabilization in the numerous tests of Type A and Type C taggants.

The relaxation time for dissipation of an electrostatic charge relates to electrostatic discharge hazards. This parameter was measured by Hercules for Type C taggant and found to be 900 sec. For comparison,

the aluminum powder which Hercules incorporates in one of its gelled aqueous slurry explosives was found to have a relaxation time of 820 seconds. Thus, the taggant properties in this regard are quite similar to those of a standard ingredient of explosives.

Besides all this evidence of safety, it can be mentioned in passing that all tests of performance, of changes on aging, and of manufacturability of the explosives have shown that these taggants have no adverse effect.

The work reported has been carried out under the sponsorship of the Bureau of Mines (Department of the Interior) and the Bureau of Alcohol, Tobacco and Firearms (Department of the Treasury).

W-02460

Reading A Color-Coded Taggant

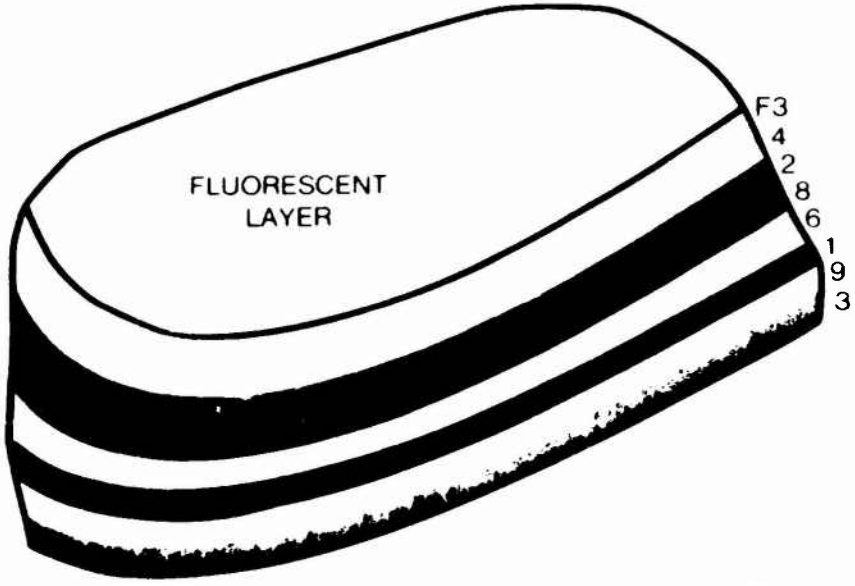

F34286193

COLOR CODE	
0	BLACK
1	BROWN
2	RED
3	ORANGE
4	YELLOW
5	GREEN
6	BLUE
7	VIOLET
8	GRAY
9	WHITE

1277

Table I

Compatibility of Type A Taggant

With dynamites (and their ingredients)

Material	Test By	Test Type	Result	Conclusion
Vibrogel	Hercules ABL	Drop Weight (TIL)	4.2×10^4 J/sec	
Vibrogel with taggant			4.2×10^4 J/sec	
Red HA	Hercules ABL	Drop Weight (TIL)	2.6×10^4 J/sec	
Red HA with taggant			2.6×10^4 J/sec	No significant difference on addition of taggant.
Tamptite Gelatin Extra 60%	Hercules ABL	Drop Weight (TIL)	6.5×10^4 J/sec	
Same with Taggant			6.5×10^4 J/sec	
Unigel	Hercules ABL	Drop Weight (TIL)	2.6×10^4 J/sec	
Unigel with Taggant			3.3×10^4 J/sec	
Vibrogel	Hercules ABL	Friction (TIL)	1.85×10^8 N/m^2	
Vibrogel with Taggant		3m/sec	7.3×10^8 N/m^2	
Red HA	Hercules ABL	Friction (TIL)	8.7×10^8 N/m^2	
Red HA with Taggant		3m/sec	5.9×10^8 N/m^2	No significant difference on addition of taggant.
Tamptite Gelatin Extra 60%	Hercules ABL	Friction (TIL) 3m/sec	7.2×10^8 N/m^2	
Same with Taggant			4.8×10^8 N/m^2	
Unigel	Hercules ABL	Friction (TIL)	4.2×10^8 N/m^2	
Unigel with Taggant		3m/sec	6.0×10^8 N/m^2	
Gelobel AA	Bureau of Mines	Drop Weight	37.2 cm	Difference not significant.
Gelobel AA with 0.56 taggant			34.8 cm	
EGDN	Atlas	Sliding Rod	55"-no reaction	
EGDN with Taggant			55"-no reaction	No difference

Table I (Cont.)

Compatibility of Type A Taggant

With aqueous gelled slurry explosives (and their ingredients)

Material	Test By	Test Type	Result	Conclusion
GEL-POWER A-2 GEL-POWER A-2 with taggant	Hercules ABL	Drop Weight (TIL)	$>2.4 \times 10^5$ J/sec 2.0×10^5 J/sec	No significant difference
GEL-POWER A-2 GEL-POWER A-2 with taggant	Hercules ABL	Friction (TIL)	6.2×10^8 N/m^2 7.4×10^8 N/m^2	No signficiant difference.
*10% H_2O, 25% MMAN, duPont 15% SN, 50% AN same with 1% taggant		Chemical Stability (7hrs. on steam bath)	No significant difference in type or concentration of metal ions in the water.	No leaching of ions from tags; no effect on stability of gels.

1279

*MMAN = monomethylamine nitrate; SN=sodium nitrate; AN=ammonium nitrate

Table I (Cont.)

Compatibility of Type A Taggant

With cast boosters (and their ingredients)

Material	Test By	Test Type	Result	Conclusion
PETN PETN with 0.05% taggant	Bureau of Mines	Drop Weight	19.1 cm 21.5 cm	Difference not significant
Pentolite Pentolite with 0.05% taggant	Bureau of Mines	Drop Weight	84.0 cm 85.0 cm	Difference not significant
Pentolite (1 gram) Taggant (1 gram) Pentolite + taggant (1 gram each)	Naval Ordnance Station	90°Vacuum Stability	0.24ml gas in 40hrs 0.16ml gas in 40hrs 0.70ml gas in 40hrs	Difference negligible
PETN PETN with 0.05% taggant	Bureau of Mines	BAM Friction (TIL)	2 kg 2 kg	No difference
Pentolite Pentolite with 0.05% taggant	Bureau of Mines	BAM Friction (TIL)	8 kg 8 kg	No difference

Table I (Cont.)

Compatibility of Type A Taggant

With black powder Material	Test By	Test Type	Result	Conclusion
FFFg black powder same + 1 taggant particle	Bureau of Mines	Drop Weight	66.6cm 67.5cm	No significant difference
same + 5 taggant particles			65.0cm	
Tailings (finest dust) of black powder same + 1 taggant particle	Bureau of Mines	Drop Weight	84.6cm 85.0cm	No significant differences
same + 5 taggant particles			95.0cm	Possible desensitization (slight)
FFFg black powder same + 5 taggant particles	Bureau of Mines	BAM Firction (TIL)	0/10 at 36 kg 0/10 at 36 kg	No difference
Tailings (finest dust) of black powder same + 5 taggant particles	Bureau of Mines	BAM Friction (TIL)	0/10 at 36 kg 0/10 at 36 kg	No difference

Table II

Compatibility of Type B Taggant

With cast boosters (and their ingredients)

Material	Test By	Test Type	Result	Conclusion
PETN	Bureau of Mines	Drop Weight	22.2cm	Difference not significant
PETN with 0.05% taggant			22.4cm	
Pentolite	Bureau of Mines	Drop Weight	81.3cm	Taggant sensitizes
Pentolite with 0.05% taggant			38.0cm	
PETN	Bureau of Mines	BAM Friction (TIL)	2.0kg	Friction due to the rough rubbing surfaces of the apparatus is greater than any friction that might be introduced by taggant.
PETN with 0.05% taggant			2.0kg	
Pentolite	Bureau of Mines	BAM Friction (TIL)	8.0kg	
Pentolite with 0.05% taggant			8.0kg	

With dynamites (and their ingredients)

EGDN	Atlas	Sliding Rod	55"-no reaction	Taggant sensitizes.
EGDN with taggant			55"-explosion	
Gelobel AA	Bureau of Mines	Drop Weight	37.2cm	Taggant sensitizes.
Gelobel AA with 0.05% taggant			23.0cm	

Table II (Cont.)

Compatibility of Type B Taggant

With black powder

Material	Test By	Test Type	Result	Conclusion
FFFg black powder	Bureau of Mines	Drop Weight	66.6cm	No significant differences
same + 2 taggant particles			70.5cm	
same + 6 taggant particles			71.0cm	
Tailings (finest dust) of black powder	Bureau of Mines	Drop Weight	84.6cm	No significant differences
same + 2 taggant particles			87.0cm	
same + 6 taggant particles			93.0cm	Possible desensitization (slight)
FFFg black powder	Bureau of Mines	BAM Friction (TIL)	0/10 at 36kg	No difference
same + 6 taggant particles			0/10 at 36kg	
Tailings (finest dust) of black powder	Bureau of Mines	BAM Friction (TIL)	0/10 at 36kg	No difference
same + 6 taggant particles			0/10 at 36kg	

Table III

Compatibility of Type C Taggant

With dynamites (and their ingredients)

Material	Test By	Test Type	Result	Conclusion
Vibrogel Vibrogel with taggant	Hercules ABL	Drop Weight (TIL)	4.2×10^4 J/sec 4.2×10^4 J/sec	
Red HA Red HA with taggant	Hercules ABL	Drop Weight (TIL)	2.6×10^4 J/sec 2.2×10^4 J/sec	No significant difference on addition of taggant.
Tamptite Gelatine Extra 60% same with taggant	Hercules ABL	Drop Weight (TIL)	6.5×10^4 J/sec 4.2×10^4 J/sec	
Unigel Unigel with taggant	Hercules ABL	Drop Weight (TIL)	2.6×10^4 J/sec 4.2×10^4 J/sec	
Nitroglycerin Nitroglycerin with taggant	Hercules ABL	Drop Weight (TIL)	3.45×10^4 J/sec 2.6×10^4 J/sec	
Vibrogel Vibrogel with taggant	Hercules ABL	Friction (TIL) 3m/sec	1.85×10^8 N/m^2 1.3×10^8 N/m^2	
Red HA Red HA with taggant	Hercules ABL	Friction (TIL) 3m/sec	8.7×10^8 N/m^2 8.7×10^8 N/m^2	No significant difference on addition of taggant, except possible desensitization of nitroglycerin
Tamptite Gelatine Extra 60% same with taggant	Hercules ABL	Friction (TIL) 3m/sec	7.2×10^8 N/m^2 7.2×10^8 N/m^2	
Unigel Unigel with taggant	Hercules ABL	Friction (TIL) 3m/sec	4.2×10^8 N/m^2 7.5×10^8 N/m^2	
Nitroglycerin Nitroglycerin with taggant	Hercules ABL	Friction (TIL) 3.3×10^8 N/m^2	0.3m/sec 0.6m/sec	

Table III (Cont.)

Compatibility of Type C Taggant

With dynamites (and their ingredients) (cont'd)

Material	Test By	Test Type	Result	Conclusion
Vibrogel Vibrogel with taggant	Hercules ABL	Electrostatic Discharge (TIL)	0.075T 0.075J	
Red HA Red HA with taggant	Hercules ABL	Electrostatic Discharge (TIL)	0.075J 0.075J	No difference on addition of taggant
Tamptite Gelatine Extra 60% same with taggant	Hercules ABL	Electrostatic Discharge (TIL)	0.075J 0.075J	
Unigel Unigel with taggant	Hercules ABL	Electrostatic Discharge (TIL)	0.024J 0.024J	
EGDN EGDN with taggant	Atlas	Sliding Rod	55"-no reaction 55"-no reaction	No difference
EGDN EGDN with taggant	Atlas	Drop Weight	18cm 30cm	Desensitization by taggant
EGDN EGDN with taggant	Atlas	Heat (Abel)	49 min. 60+ min.	NO_2 pick-up by taggant
90/10 EGDN/NG same with taggant	Atlas	Sliding Rod	55"-no reaction 55"-no reaction	No difference
90/10 EGDN/NG same with taggant	Atlas	Heat (Abel)	35 min. 40 min.	No significant difference

Table III (Cont.)

Compatibility of Type C Taggant

With aqueous gelled slurry explosives (and their ingredients)

Material	Test by	Test Type	Result	Conclusion
Tovex® 800 Tovex® 800 with 0.1% taggant	duPont	Drop Weight	above max. ht. of apparatus	No difference
Tovex® 800 Tovex® 800 with 0.1% taggant	duPont	Sliding Rod	above max. of apparatus	No difference
Tovex® 700, 800, &320 same with 0.1% taggant	duPont	Projectile Impact	No significant differences	
*5.5% H_2O, 29.5% MMAN, 15% SN, 50% AN same with 10% taggant *5.2% H_2O, 28.0% MMAN, 14.25% SN, 47.5% AN same with 10% taggant	duPont	Thermal Stability (350°F Bath)	No exotherms or decomposition	No differences
Tovex® 700, 800, &320 same with 0.1% taggant	duPont	Hot Tip Test (White Heat)	No burning or detonation; smoke only.	No differences
Tovex® 700, 800, &320 same with 0.1% taggant	duPont	Hot Bar Test (250°C)	No burning or detonation; smoke only.	No differences

*MMAN = monomethylamine nitrate; SN = sodium nitrate; AN = ammonium nitrate.

Table III (Cont.)

Compatibility of Type C Taggant

With aqueous gelled slurry explosives (and their ingredients) (cont'd)

Material	Test By	Test Type	Result	Conclusion
GEL-Coal GEL-Coal with 0.1% taggant*	Hercules	Drop Weight (TIL)	100cm 100cm	No difference
GEL-Power GEL-Power with 0.1% taggant*	Hercules	Drop Weight (TIL)	100cm 100cm	No difference
GEL-Coal GEL-Coal with 0.1% taggant*	Hercules	Friction (8 ft/sec)	112 lbs. 90 lbs.	No significant difference
GEL-Power GEL-Power with 0.1% taggant*	Hercules	Friction (8 ft/sec)	83 lbs. 82 lbs.	No significant difference
GEL-Coal GEL-Coal with 0.1% taggant*	Hercules	Electrostatic Discharge (TIL)	6.25 joules 6.25 joules	No difference
GEL-Power GEL-Power with 0.1% taggant*	Hercules	Electrostatic Discharge (TIL)	6.25 joules 6.25 joules	No difference
GEL-Coal GEL-Coal with 0.1% taggant*	Hercules	75°C Taliani	8 mm 9 mm	No significant difference

* Also contained 0.1% Westinghouse taggant.

Table III (Cont.)

Compatibility of Type C Taggant

With aqueous gelled slurry explosives (and their ingredients) (cont'd)

Material	Test By	Test Type	Result	Conclusion
GEL-Power GEL-Power with 0.1% taggant*	Hercules	75°C Taliani	10 mm 11 mm	No significant difference
GEL-Coal GEL-Coal with 0.1% taggant*	Hercules	75° Weight Loss (DOT)	4.85% 4.88%	No significant difference
GEL-Power GEL-Power with 0.1% taggant*	Hercules	75°C Weight Loss (DOT)	3.75% 3.80%	No significant difference
GEL-Power A-2 GEL-Power A-2 with taggant	Hercules ABL	Drop Weight (TIL)	$>2.4 \times 10^5$ J/sec $>2.4 \times 10^5$ J/sec	No difference
GEL-Power A-2 GEL-Power A-2 with taggant	Hercules ABL	Friction (TIL) 3m/sec	6.2×10^8 N/m^2 8.7×10^8 N/m^2	Desensitization by taggant
GEL-Power A-2 GEL-Power A-2 with taggant	Hercules ABL	Electrostatic Discharge (TIL)	1.26 J 1.26 J	No difference

*Also contained 0.1% Westingho

Table III (Cont.)

Compatibility of Type C Taggant

With cast boosters (and their ingredients)

Material	Test By	Test Type	Result	Conclusion
PETN PETN with 5% taggant	duPont	Drop Weight	29cm 31cm	Difference not significant
PETN PETN with taggant	Trojan	Drop Weight	10% lower than PETN alone	Difference not significant
PETN PETN with 5% taggant	duPont	Sliding Rod	25% positive 5% positive	Possible desensitization by taggant
Pentolite (1 gram) Taggant (1 gram) Pentolite + taggant (1 gram each)	Naval Ordnance Station	90°C Vacuum Stability	0.24ml gas in 40 hrs. 0.18ml gas in 40 hrs. 0.60ml gas in 40 hrs.	Difference negligible

FRAGMENT HAZARD

INVESTIGATION PROGRAM

by

RICHARD T. RAMSEY
JOSEPH G. POWELL, Jr.
WILLIAM D. SMITH III

NAVAL SURFACE WEAPONS CENTER
Dahlgren, Virginia 22448

PRECEDING PAGE BLANK

1. INTRODUCTION

The Department of Defense Explosives Safety Board (DDESB) is conducting a continuing program to evaluate the fragment hazards produced by the accidental detonation of stored munitions. In support of this effort, the Naval Surface Weapons Center was funded in July 1975 to conduct the Fragment Hazard Investigation Program. The purpose of the program is to provide the DDESB with the necessary fragmentation data to improve or to substantiate the quantity-distance (QD) standards for the safe and efficient storage of stacked munitions according to specific hazard classifications. Previous programs attempted to use far-field fragment recovery in limited predetermined areas to quantify the hazards. The current program will use near-field fragment characterization data to develop an empirical relation to predict far-field fragment density. The ultimate goal is to provide a methodology for the determination of QD standards for all hazard classifications. The hazard classification under investigation in this report is the Mass-Detonating Hazard Materials (Class 1, Division 1).

The major effort of this program to date has been focussed on the mass-detonating Army M107 155mm (TNT loaded) projectile. Arena fragmentation tests of various projectile stacking configurations have been conducted concurrent with supporting analytical studies. Fragmentation data were generated on projectile clusters which simultaneously detonate and on those which detonate by means of natural communication. The largest projectile cluster detonated during the test program was the 155mm projectile shipping pallet (eight projectiles).

This paper presents the experimental findings from the static detonations of M107 155mm projectiles (TNT loaded) in various storage pallet configurations. A fragmentation model characterizing the simultaneous detonation of a pallet of eight projectiles, and a preliminary description of the detonation scheme for a pallet which detonates by means of natural communication is presented. From these experimental findings equations for far-field fragment densities and ranges have been developed and are presented.

2. TEST PROGRAM

2.1 OBJECTIVE

The objective of the test program is to collect the necessary fragmentation data to evaluate the far-field fragment hazards produced by the detonation of projectiles stacked in typical storage configurations. In this program the evaluation of the far-field fragment hazards is based on close-in fragmentation data. The fragmentation data includes polar and azimuthal spatial reference for fragment weights, numbers, velocities and presented areas.

2.2 APPROACH

The initial test program was divided into two major efforts. The initial effort was a series of arena tests designed to characterize projectile clusters that were simultaneously detonated. This test series began with three repeated single round detonations in a fragmentation arena. The data from these tests were compared with available literature to ensure the adequacy of the testing and data collection procedures. These data were used as baseline data for the comparison of data from the detonation of projectiles in a cluster. The test series continued with the simultaneous detonation of projectiles in increasingly larger clusters in fragmentation arenas. The second effort was a follow-on test sequence based on identical projectile cluster configurations, except, the projectile clusters were detonated by means of natural communications. This was accomplished by priming only one projectile in the cluster configuration. The location of the donor projectile was varied throughout the test series to investigate the effect on the fragmentation data.

2.2.1 TEST METHOD

For both test series the fragmentation data were collected in specially constructed fragmentation arenas. The arenas were designed to determine the fragment weights, numbers, and velocities as a function of polar and azimuthal angle. Fragment weight and number data were obtained by collecting the ejected fragments in a fiber-board building material marketed under the trade name Celotex. The Celotex was configured in bundles, 4' x 4' x 8', and positioned in the test arena according to fragment collection zone requirements. The fragments were extracted from the Celotex after the test; cleaned, weighed, and documented according to spatial zones. The presented areas of the fragments were measured with a planimeter or an Electro-Optic Icosahedron gage depending upon fragment size. The fragment velocity data were recorded with high speed motion picture cameras equipped with millisecond timing generators. The cameras recorded the detonation of the projectiles and the fragment scintillations on 22-gauge mild steel witness panels marked according to the required spatial zones. Figure 1 is a sketch of a typical arena with the steel witness panels and Celotex. During the conduct of the test program, it became necessary to deviate from this arena design to obtain specific data. For example, arenas were conducted with 360° of Celotex, as well as, 360° of witness panels. The spatial requirements for each arena design were based on previous arena test data and the projectile cluster configuration under investigation.

2.2.2 PROJECTILE CLUSTER CONFIGURATIONS

All of the projectile cluster configurations detonated throughout the test program were subsets of the standard shipping pallet design. The pallet consits of eight vertical projectiles spaced seven inches

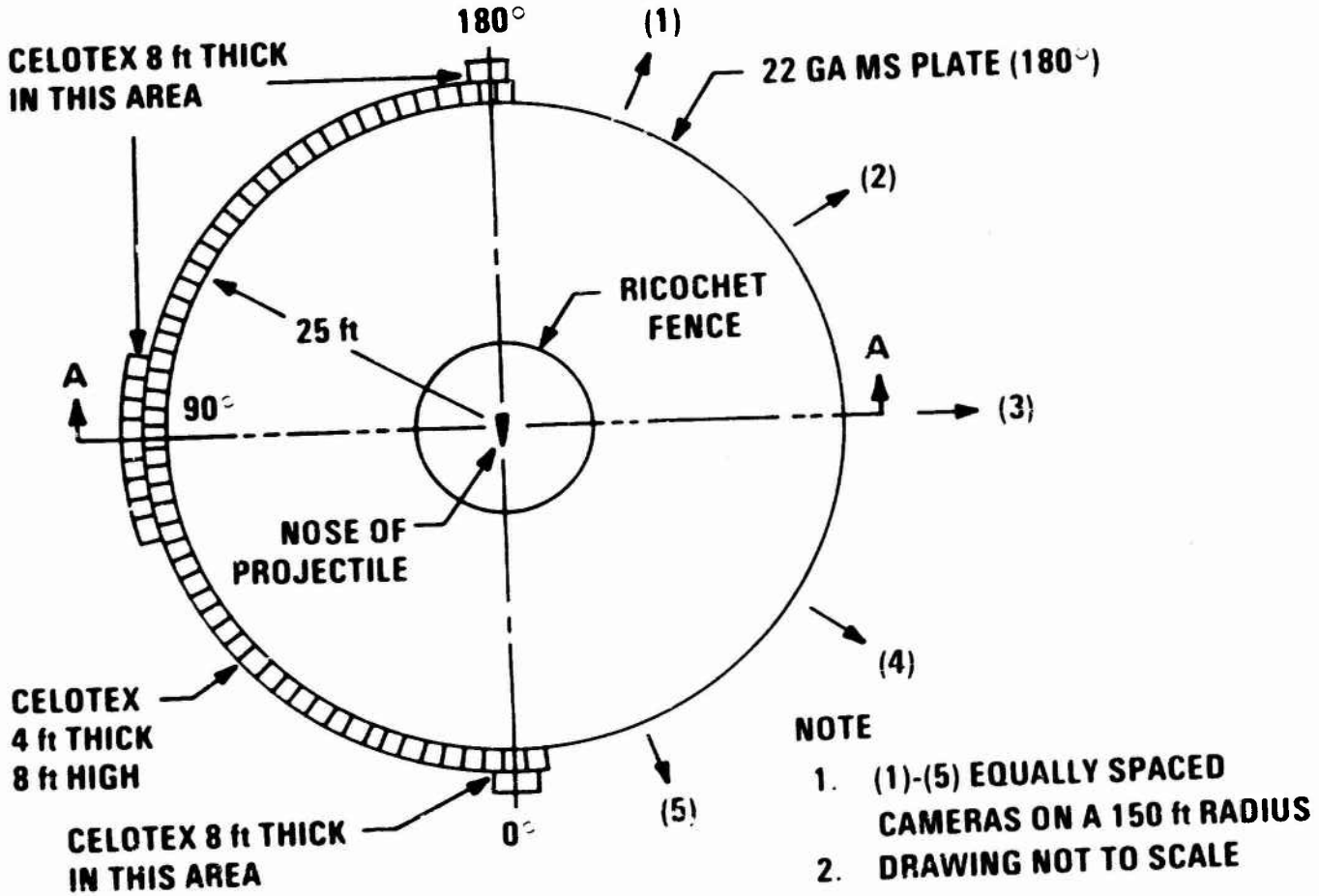

FIGURE 1

TYPICAL FRAGMENTATION ARENA LAYOUT

center-to center and banded in a two by four matrix. The projectile configurations were based on multiples of two projectiles for symmetry. This provided a one-to-one relationship between fragment collection sectors and fragment velocity sectors.

The projectile clusters were detonated in a horizontal or vertical position depending upon azimuthal and polar zone requirements. For discussions in this report a polar angle arena is defined as an arena designed to determine the fragment weights, numbers, and velocities as a function of polar angle with respect to the axis of symmetry of a horizontal projectile cluster. Likewise, an azimuthal arena was designed to collect the same information as the polar arena except as a function of azimuthal angle with respect to the axis of symmetry of a vertical projectile cluster.

2.3 SIMULTANEOUS DETONATION

The single round and the nine multiple round projectile configurations shown in Figures 2 and 3 were used to collect the fragmentation data. Each cluster configuration was assigned a specific identification number and simultaneously detonated in either a polar or azimuthal angle arena. The clusters were tested in the order presented in Figures 2 and 3, from left to right, then top to bottom. The space between any two adjacent projectiles was defined as the interaction area. An example of the geometric boundaries designated as the interaction areas (IA) for configuration QD-155-04 is shown in Figure 2.

2.3.1 DETONATION SCHEME

For the cluster configurations that were simultaneously detonated all of the projectiles were primed. Simultaneity was achieved by using equal lengths of DuPont 49 grain per foot detonating cord. The detonating cord was fashioned into the harness initiation device shown in Figure 4. Each leg of the harness was crimped with a DuPont P-3 detonator and positioned in a modified U. S. Army M564 PD nose fuze. The entire arrangement was assembled on the projectile cluster and remotely initiated by detonating a Hercules Vibrodet HC-15 blasting cap at the harness junction.

2.3.2 OBSERVATIONS

As stated before, the interaction area is defined as the space between any two adjacent projectiles in a projectile cluster configuration. This spacing was maintained throughout the test series at the shipping pallet design of seven inches center-to-center.

After the conduct of several fragmentation arenas, it became obvious that the interaction areas would be a contributing factor in far-field fragment distribution. These areas were generating fragment



BASE LINE ARENA
TEST NO.
QD-155-01
(POLAR ARENA)

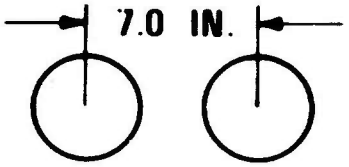

TEST NO.
QD-155-02
(POLAR ARENA)

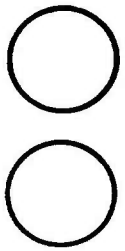

TEST NO.
QD-155-03
(POLAR ARENA)

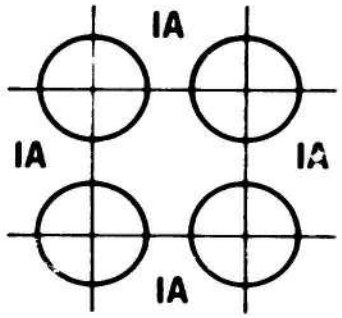

TEST NO.
QD 155-04
(POLAR ARENA)

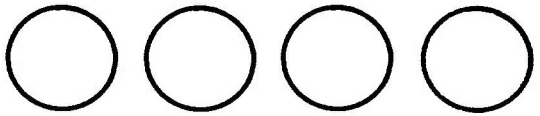

TEST NO.
QD-155-05
(POLAR ARENA)

NOTES:
1. CIRCLES DENOTE PROJECTILES ORIENTED HORIZONTALLY
2. IA DENOTES INTERACTION AREA

FIGURE 2

PROJECTILE CLUSTER CONFIGURATIONS

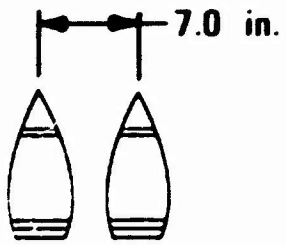

TEST NO.
QD-155-09
(AZIMUTHAL ARENA)

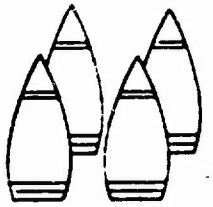

TEST NO.
QD-155-10
(AZIMUTHAL ARENA)

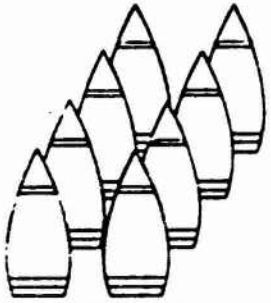

TEST NO.
QD-155-12
(AZIMUTHAL ARENA)

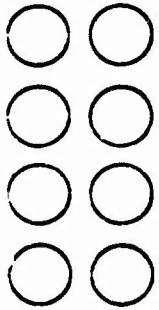

TEST NO.
QD-155-08
(POLAR ARENA)

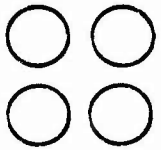

TEST NO.
QD-155-4R
(POLAR ARENA)

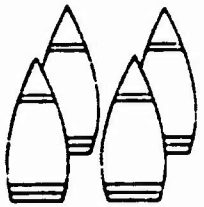

TEST NO.
QD-155-10R
(AZIMUTHAL ARENA)

NOTE: CIRCLES DENDTE PROJECTILES
DRIENTED HORIZDNTALLY

FIGURE 3

PROJECTILE CLUSTER CONFIGURATIONS

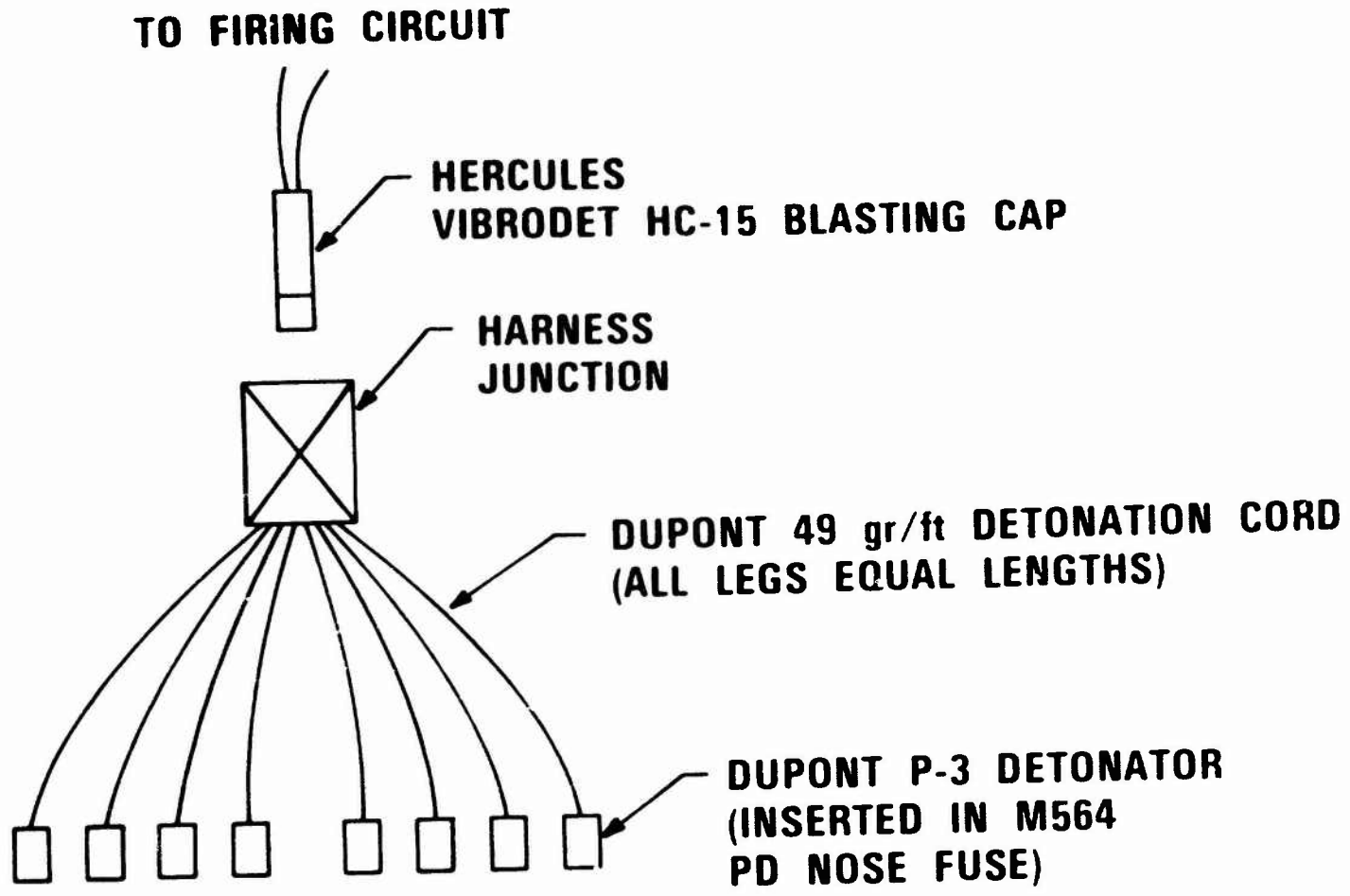

FIGURE 4

HARNESS INITIATION DEVICE FOR FULL PALLET CONFIGURATION

concentrations at extremely high velocities (6000 ft/sec to 8700 ft/sec) as compared to single round fragmentation data. An example of these high velocity jets is shown in Figure 5. These data were recorded at a 25 ft. stand-off from the simultaneous detonation of a full pallet of eight projectiles. The azimuthal location at 180° is the interaction area located at one end of the pallet. The 270° location is a combination of the three interaction areas on one side of the pallet. In both locations the impact points of the concentrations show no signs of angular shifts and fragment velocities in excess of 8000 ft/sec were recorded. For all other locations outside the interaction area, the magnitude of fragment velocities was similar to a single round detonation.

2.4 NATURAL COMMUNICATION

This testing effort is currently in progress. The projectile cluster configurations shown in Figure 6 were used to collect the fragmentation data. To date, two repeated firings of the four configurations have been conducted in azimuthal arenas consisting of 360° of mild steel witness panels. Also, the four-porjectile configuration was detonated in an azimuthal arena consisting of 360° of Celotex, and the full pallet configuration number 3 was detonated in an azimuthal arena consisting of 180° of Celotex and witness panel.

2.4.1 DETONATION SCHEME

The detonation by means of natural communication was achieved by priming only one projectile in the cluster configuration. A Hercules Vibrodet HC-15 blasting cap assembled in a modified U. S. Army M564 PD nose fuze was used for the detonation. For all tests to date, all projectiles detonated.

2.4.2 OBSERVATIONS

In this test series the high velocity fragment concentrations being generated at the interaction areas were found to have an appreciable angular shift in the azimuthal impact points. This was expected since the detonation scheme was not simultaneous. At the completion of the 360° witness panel tests, the fragment hole count data showed that the azimuthal shifts were completely predictable and depended upon the primed projectile location. The angular shifts fall into three categories as follows:

(a) A shift of approximately eleven degrees which occurs when two adjacent projectiles are non-simultaneously detonated by a third projectile. The width of the concentration is approximately 35 degrees.

(b) A twenty-eight degree shift which results when a projectile detonates a single adjacent projectile. The width of the concentration is approximately 45 degrees.

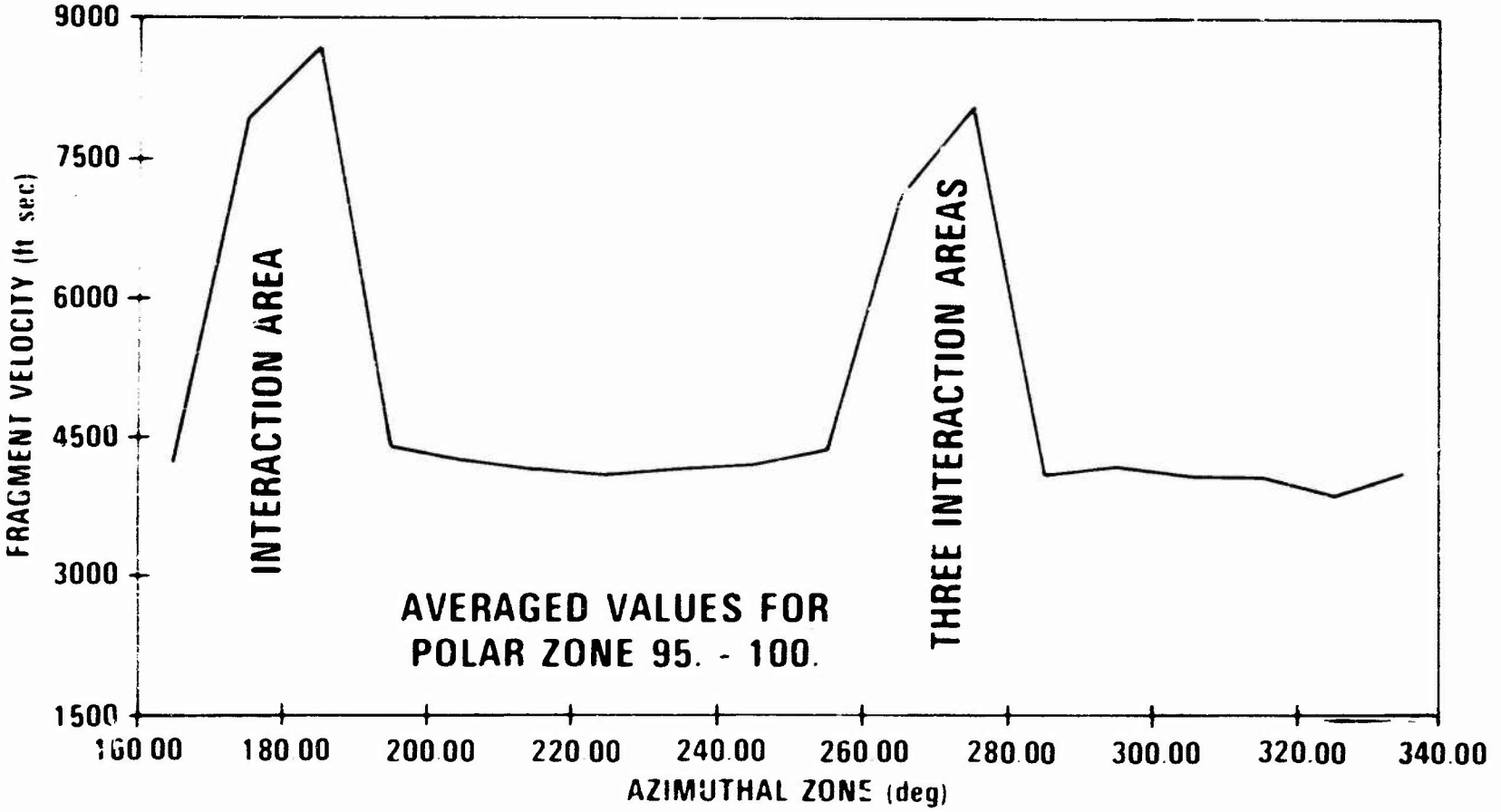

FIGURE 5

AVERAGE FRAGMENT VELOCITIES
FOR THE
SIMULTANEOUS DETONATION OF A FULL PALLET

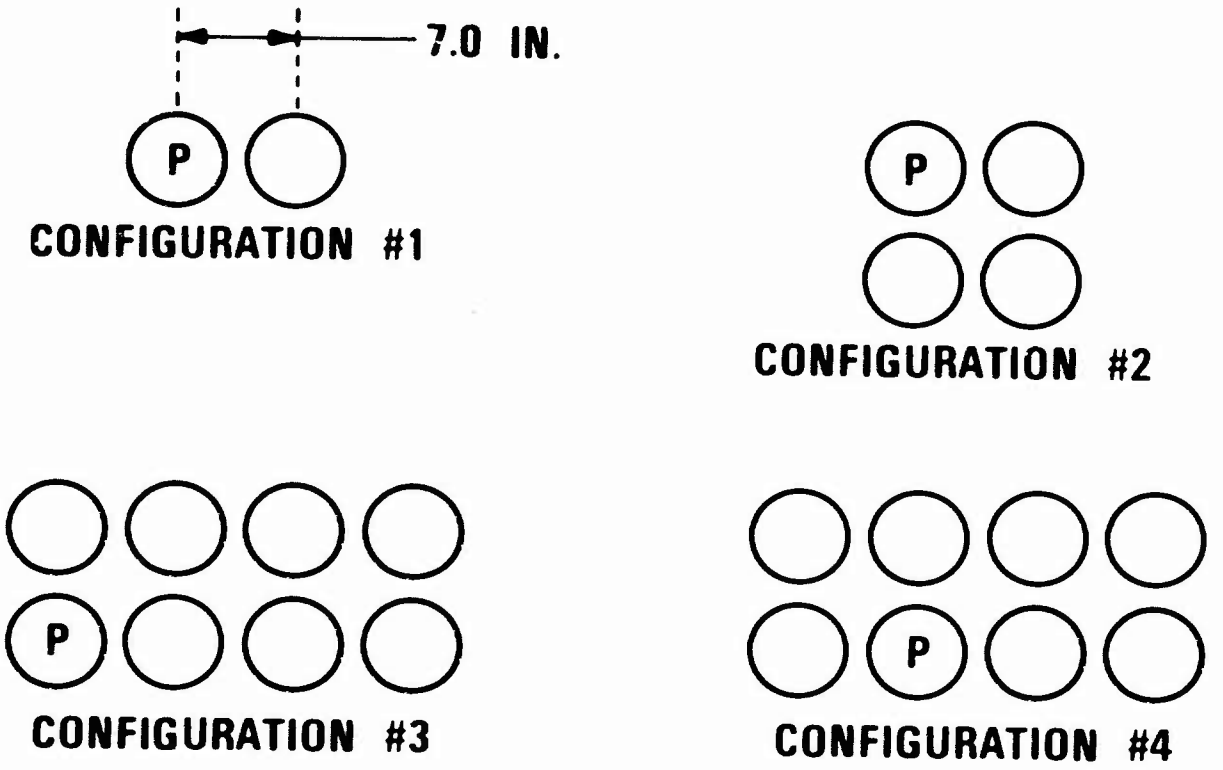

FIGURE 6

PROJECTILE CLUSTER CONFIGURATIONS

(c) No shift in the concentration occurs when two adjacent projectiles are simultaneously detonated by another source. The width of the concentration is approximately 35 degrees.

Figure 7 illustrates the concentration locations for a full pallet detonation. The largest number of fragments appear to come from the end of the pallet farthest from the detonation source (projectiles number 4 and 5). Additionally, fragments from the interior of the pallet appear to be escaping. This is evidenced by the concentration formed at 315° which is apparently from the simultaneous detonation of projectile numbers 2 and 8.

3. ANALYSIS OF RESULTS

3.1 FRAGMENTATION MODEL

The experimental findings from the simultaneous detonation of multiple projectiles were used to develop a fragmentation model. Detailed comparisons of the data from this test series, as well as other available literature, led to several observations. The first of these is that the abundance of data from these tests is not sufficient to validate a model of the simultaneous detonation of a group of projectiles for the entire polar region of interest (polar zones 0° - 180°). However, there is sufficient data for polar zones 80° to 110° to develop a relatively simple model. The model characterizes the simultaneous detonation of groups of two, four and eight projectiles.

A detailed step-by-step verification of the model has been documented in the NSWC Technical Report No. TR-3664 and will not be presented in this paper. However, the basic model assumptions are presented, as well as, MOTT Plots and Fragment Ballistic Density data for reference. A sketch of the geometric boundaries pertinent to the model description is shown in Figure 8. The basic model assumptions for simultaneous detonation are as follows:

(a) The metal in the shaded area (interior casing in Figure 8) does not enter into the fragment distribution but is instead trapped in the interior area.

(b) The available metal weight outside of the interaction area (Area B in Figure 8) will be equal to the metal weight from an equivalent area of a single projectile and will display fragment velocities similar to that of a single projectile.

(c) The available metal weight of the interaction area (Area A in Figure 8) will be concentrated in a narrow beam (approximately 30° wide) with fragment velocities larger than those of a single projectile and will be equal to the metal weight from an equivalent area of a single projectile.

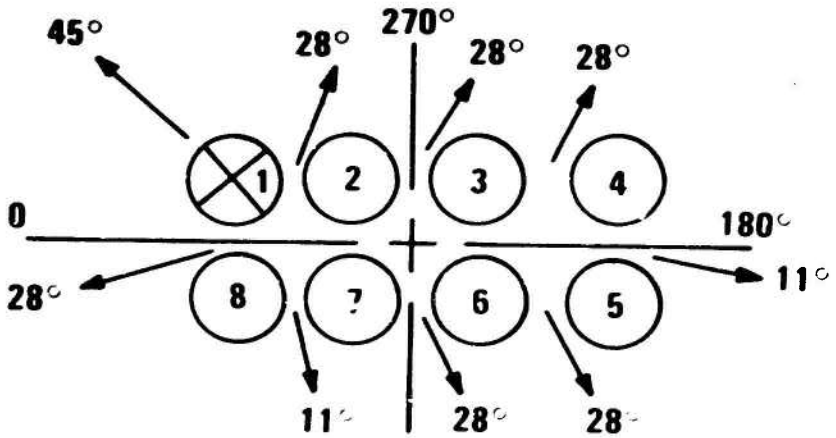

PROJECTILE NOS.	AZIMUTH FRAGMENT CONCENTRATION LOCATION	
	PREDICTED	ACTUAL*
1 & 2	242°	240°
2 & 3	242°	240°
3 & 4	242°	240°
4 & 5	170°	173°
5 & 6	118°	127°
7 & 8	118°	127°
8 & 1	101°	107°
8 & 2	28°	23°
	315°	322°

*DATA FROM TEST NO. QO-155-S8

FIGURE 7

FRAGMENT CONCENTRATION LOCATIONS
FOR
DETONATION OF PROJECTILE NO. 1

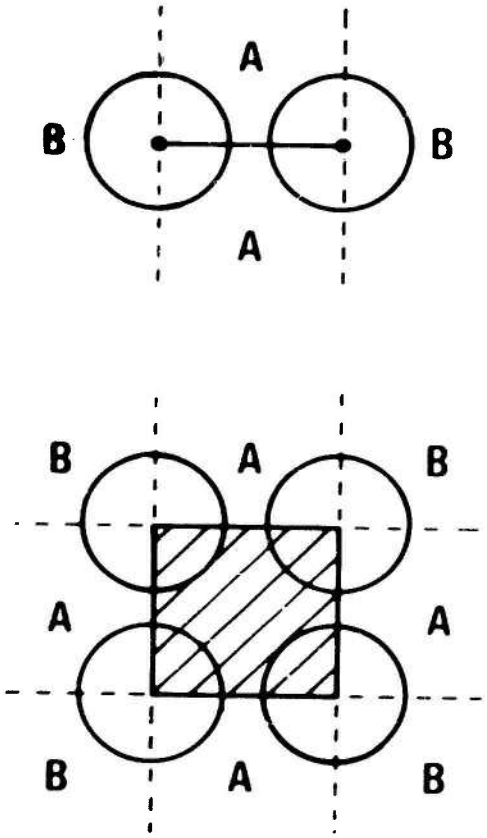

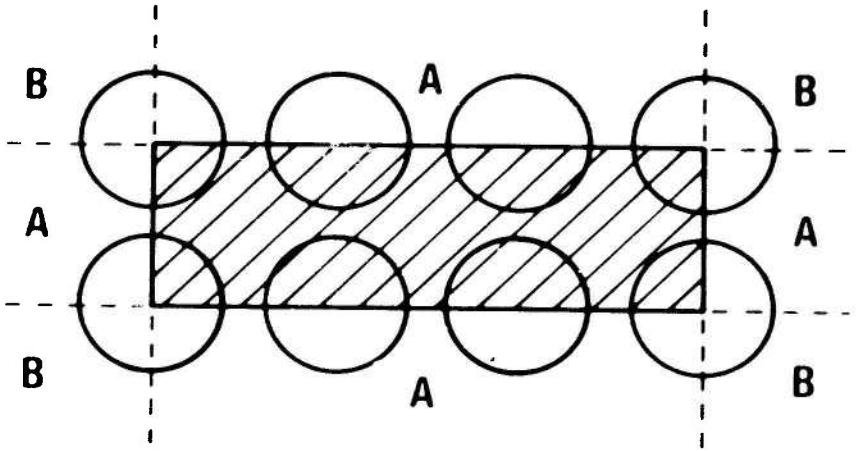

NOTE:

1. ZONE A DENOTES PROJECTILE INTERACTION AREAS
2. ZONE B DENOTES AREA OUTSIDE THE PROJECTILE INTERACTION AREAS

FIGURE 8

FRAGMENTATION MODEL BOUNDARIES
FOR
SIMULTANEOUSLY DETONATED PROJECTILE CLUSTERS

(d) The slope of the fragment weight number curves (MOTT Plot) for areas A and B of Figure 8 will approximate the slope of the single projectile weight number curve. A MOTT Plot comparison is shown in Figure 9.

(e) The average ballistic density of the fragments from Areas A and B will be similar to the average ballistic density of fragments produced by a single projectile. A comparison of the ballistic density curves is shown in Figure 10.

A simple fragmentation model has not been developed for the natural communication detonation tests. However, preliminary review of the test data indicates that some of the large fragments (2 pounds and greater) trapped within the shaded area of Figure 8 in the simultaneous tests are being propelled out of the pallet. The average ballistic density of the fragments also appears to be similar to that of a single round.

3.2 ANALYSIS OF TEST DATA

The test data were analyzed in order to develop an emperical relation to predict far-field density. The development was based upon relations which characterized the fragment shape (Number-Gamma distribution) and the fragment range (two-dimensional particle trajectory model).

3.2.1 NUMBER-GAMMA DISTRIBUTION

Figure 11 presents a plot of the fragment number-gamma distribution for both simultaneous and natural communication tests. The similarity of the curves lead to the development of the following relation:

$$N(\gamma > \gamma_1) = N_o e^{-\left(\frac{M}{\gamma}\right)^{1/3}} \qquad (1)$$

where N_o = constant of proportionality (dimensionsless)

M = slope of the line (lb/in^2)

Values of N_o are presented below:

Configuration	Detonation Scheme	N_o
Full Pallet	Simultaneous	5.83×10^6
Full Pallet	Natural Communication	8.18×10^5

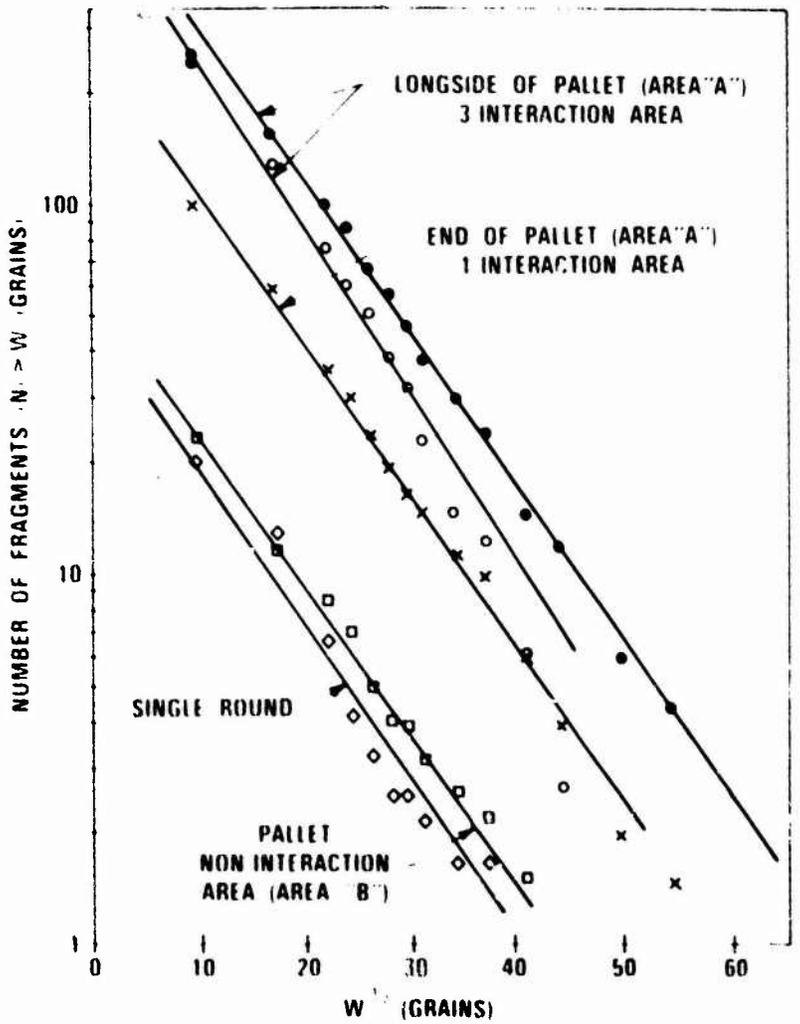

FIGURE 9

MOTT PLOT

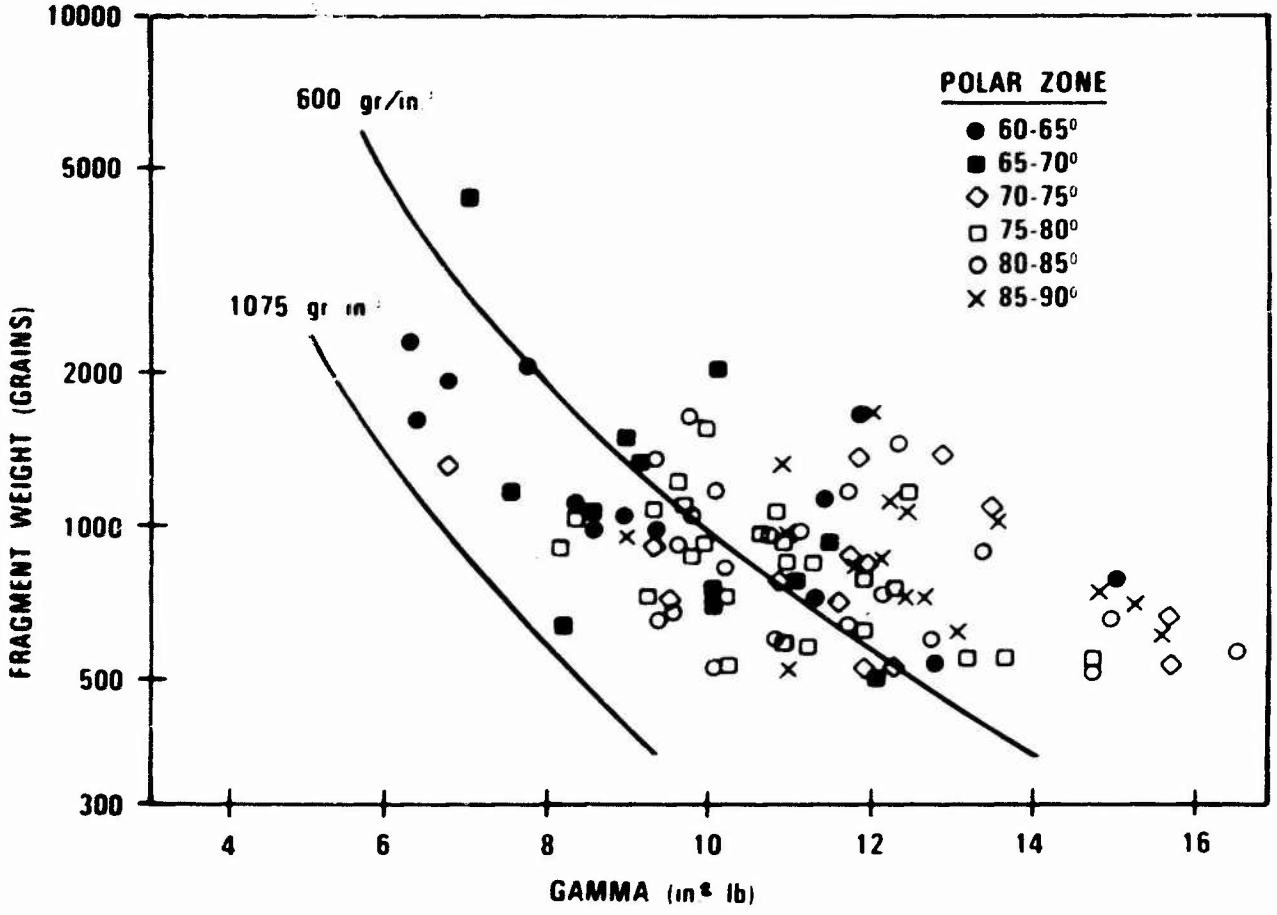

FIGURE 10

DISTRIBUTION OF FRAGMENT WEIGHT VERSUS GAMMA
FOR A
SIMULTANEOUSLY DETONATED PALLET

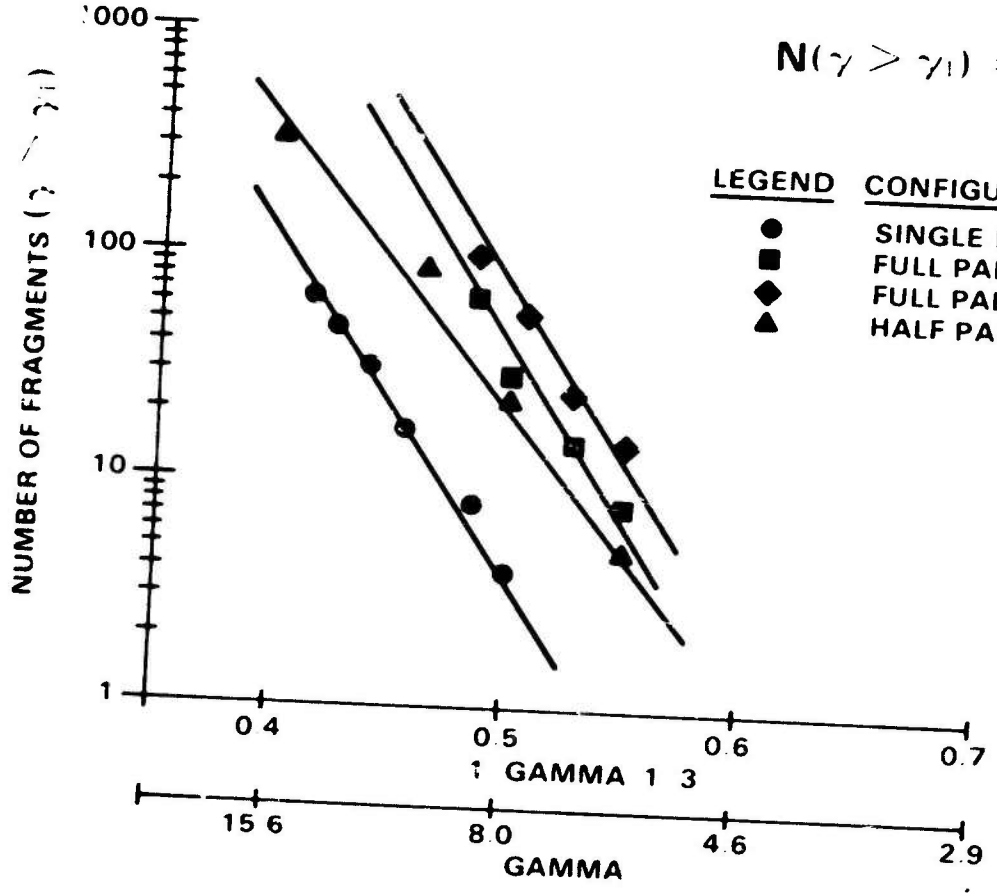

$$N(\gamma > \gamma_1) = N_0 e^{-(\frac{M}{\gamma})^{1/3}}$$

LEGEND	CONFIGURATION	POLAR ZONE	DETONATION SCHEME
●	SINGLE ROUND	80 -110	----
■	FULL PALLET	90 -100	SIMULTANEOUS
◆	FULL PALLET	85 -120	SIMULTANEOUS
▲	HALF PALLET	75 -90	NATURAL COMMUNICATION

FIGURE 11

NUMBER-GAMMA DISTRIBUTION

3.2.2 FRAGMENT RANGE

A good approximation for the range of individual fragments is provided by a two-dimensional particle trajectory model. Figure 12 presents typical results of the model for several Gammas as a function of ejection angle. The maximum fragment range is obtained for ejection angles between 5° and 45°. A good fit to the data for this range of ejection angle, Gamma between 2.0 to 20.0 in^2/lb and initial velocities of 3000 to 10000 ft/sec is provided by

$$R = 7920 \left(\frac{V}{1000}\right)^{0.275} \gamma \left[0.18\left(\frac{1000}{V}\right)^{0.275} - 1\right] \qquad (2)$$

where R = range (ft)

V = velocity (ft/sec)

Substituting the velocity of interaction area fragments (8700 ft/sec) into equation (2) yields

$$R = 14358\ \gamma^{-0.901} \qquad (2a)$$

or solving for γ

$$\gamma = 41100/R^{1.11} \qquad (2b)$$

3.2.3 FRAGMENT DENSITY

Substituting equation (2b) into equation (1) yields

$$N(R>R_1) = N_o\ e^{-K_1 R_1^{0.37}} \qquad (3)$$

where $N(R>R_1)$ = number of fragments with range R greater than R_1 in an area of one degree width

K_1 = constant developed from the test data

Equation (3) provides a relation for the number of fragments as a function of the experimentally developed constant N_o. If it is assumed that

$$N_o = N_{IA}\ N_{OA} \qquad (4)$$

where N_{IA} = number of interaction areas

N_{OA} = N_o per interaction area

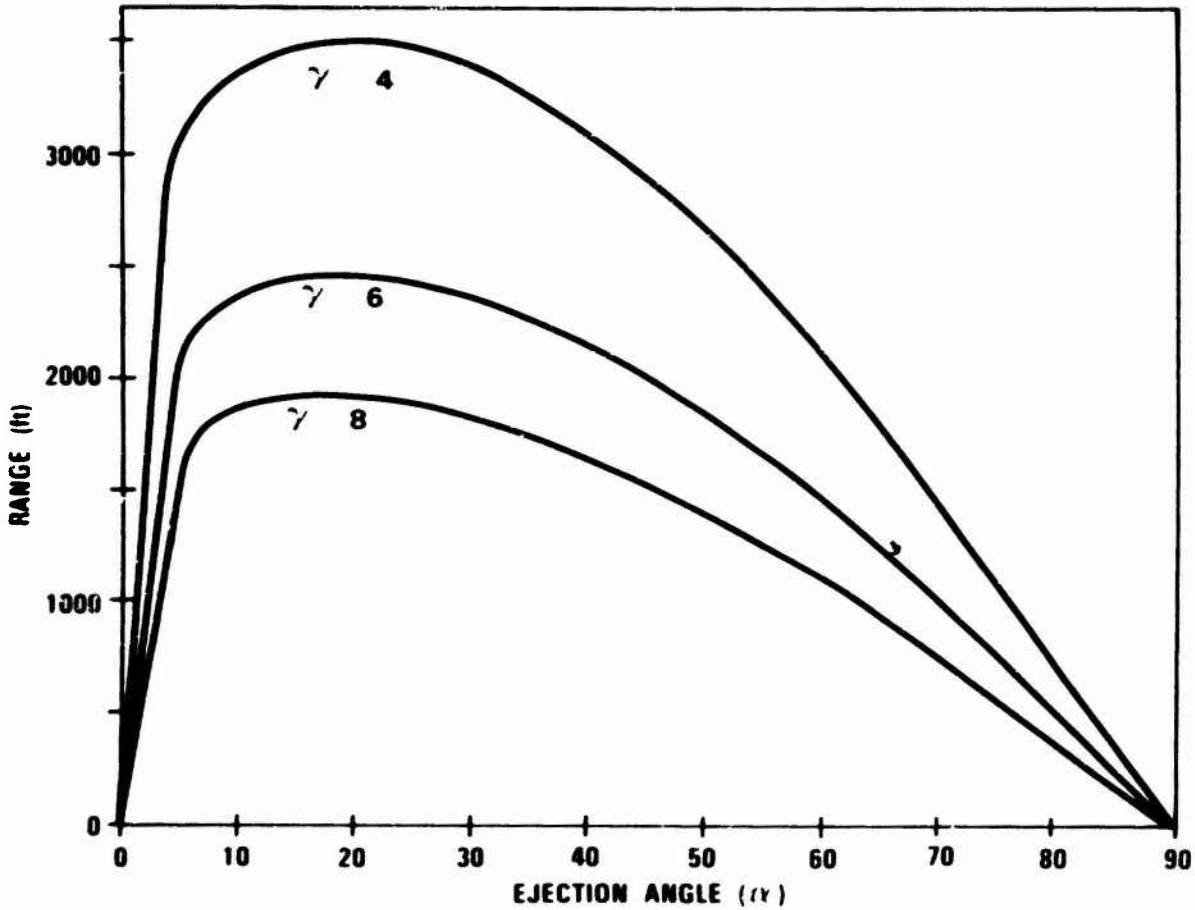

$R = f(V, \gamma)$

FOR $5° < \alpha < 45°$

$\gamma = \bar{A}/W \ \frac{\text{sq in.}}{\text{lb}}$

FIGURE 12

TYPICAL FRAGMENT RANGE DATA
PROVIDED BY PARTICLE TRAJECTORY MODEL

Equation (3) becomes

$$N(R>R_1) = N_{IA}\, N_{OA}\, e^{-K_1\, R_1^{0.37}} \tag{5}$$

The desired relation for fragment density is of the form

$$\frac{dN}{dA} = \frac{dN}{dR}\,\frac{dR}{dA} \tag{6}$$

where $\frac{dN}{dA}$ = number of fragments per unit area

Dropping the subscript from R and differentiating equation (5) yields

$$\frac{dN}{dR} = 0.37R^{-0.63}\, N_{IA}\, N_{OA}\, e^{-K_1\, R^{0.37}} \tag{7}$$

The area of one degree of azimuth angle is

$$dA = \frac{2\pi R dR}{360} \tag{8}$$

or

$$\frac{dR}{dA} = \frac{57.3}{R} \tag{8a}$$

Substituting equation (7) and *8a) into equation (6) yields the final relation

$$\frac{dN}{dA} = \frac{-19.4\, N_{IA} N_{OA}}{R^{1.63}}\; e^{-K_1\, R^{0.37}} \tag{9}$$

The accuracy of equation (9) can be evaluated by comparing the predicted fragment density to the actual fragment density for the 155mm projectile test ESKIMO I. Figure 13 compares the results of equation (9) using N_{OA} for a full pallet of 155mm projectiles detonated simultaneously to the actual ESKIMO I collection data for a row of 275 projectiles (N_{IA} = 274).

It should also be realized that equation (9) predicts the density of all fragments whether hazardous (terminal kinetic energy ≥ 58 ft-lb) or not. A useful relation can be developed from the equations for terminal velocity in free fall and kinetic energy to define a hazardous fragment. It is

$$W_{HAZ} = 198.63\gamma \tag{10}$$

where W_{HAZ} = weight of a hazardous fragment (grains). Figure 14 presents the results of applying equation (10) to the test data and plotting the percent of hazardous fragments as a function of gamma and range. It is obvious from the plot that the majority of far-field fragments (R>2300 ft) will be hazardous.

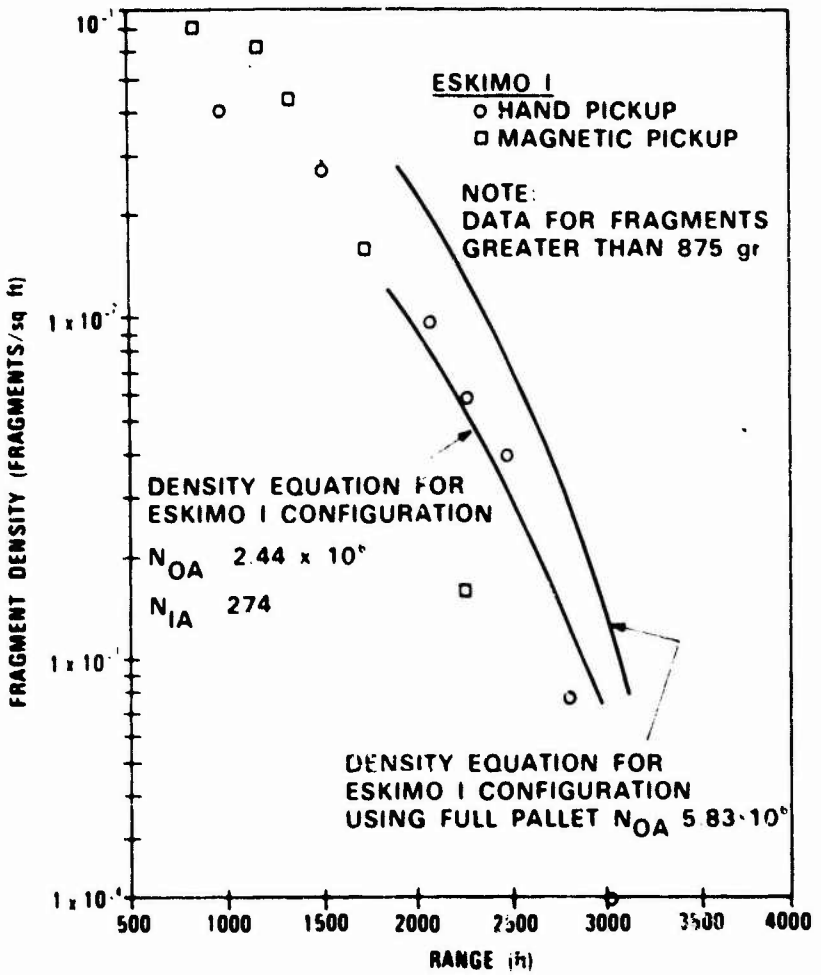

FIGURE 13

COMPARISON OF PREDICTED FRAGMENT
DENSITY TO THE ESKIMO 1 TEST RESULTS

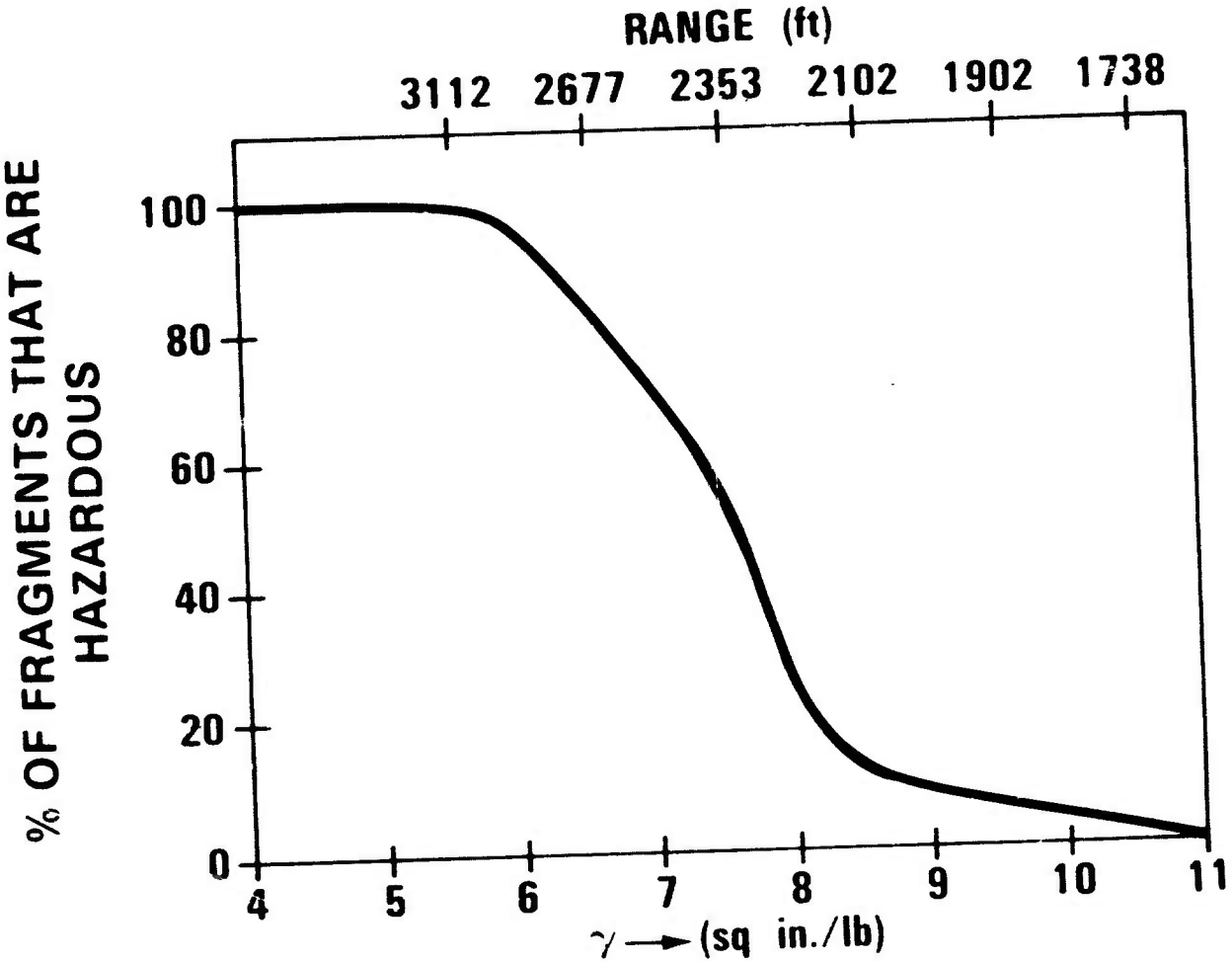

FIGURE 14

DISTRIBUTION OF HAZARDOUS FRAGMENTS
AS A FUNCTION OF GAMMA AND RANGE

3.2.4 IMPLICATIONS OF THEORY UPON EXISTING QD CRITERIA

The equation developed above implies that an important determinant of fragment density is the configuration of the stack (i.e., the number of potential interaction areas). In order to determine the impact of the theory upon the existing $KW_{EX}^{1}/_{3}$ criteria it was decided to compare the predicted fragment density for a stack of projectiles in different stack configurations to the existing QD criteria for the same size stack.

The stack configurations used for 5000 155mm projectiles (75000 lbs TNT) are presented below:

STACK CONFIGURATION			MAXIMUM NUMBER OF POTENTIAL
LENGTH	WIDTH	HEIGHT	INTERACTION AREAS (N_{IA})
250	20	1	249
500	10	1	499
1000	5	1	999

Figure 15 presents the results of equations (9) and (10) for these stack configurations and using N_{OA} from the full pallet natural communication test ($N_{OA} = 8.18 \times 10^{5}$). Using Figure 15 to compare the densities to the existing QD criteria of 1685 feet (75000 lbs of explosive) shows that the existing blast criteria ($KW_{EX}^{1}/_{3}$) for inhabited buildings may underestimate the fragment hazards.

3.2.5 OBSERVATIONS

The test program and concurrent analytical effort provides a methodology which can be used to determine the far-field fragment hazards produced by the detonation of a pallet of 155mm projectiles. Specifically, it is apparent that the interaction areas possess a greater potential for excellent agreement of the predicted fragment density with the ESKIMO I test data indicates that small-scale testing may be used to obtain quantity-distance data.

4. CONTINUING EFFORT

It is planned to continue the test and analysis effort to determine if the theoretical framework developed for the single pallet can be applied to multiple pallet stacks. A series of tests will be conducted to collect far-field fragment data from large stacks of 155mm projectiles.

Tests of Non-Mass Detonating ammunition (Class 1, Division 2) have recently been started to gather far-field fragment data. Pallets of 40mm AA and 105mm cartridges are being subjected to bon-fire tests. Fragments from the tests are being collected and analyzed to determine the potential fragment hazards.

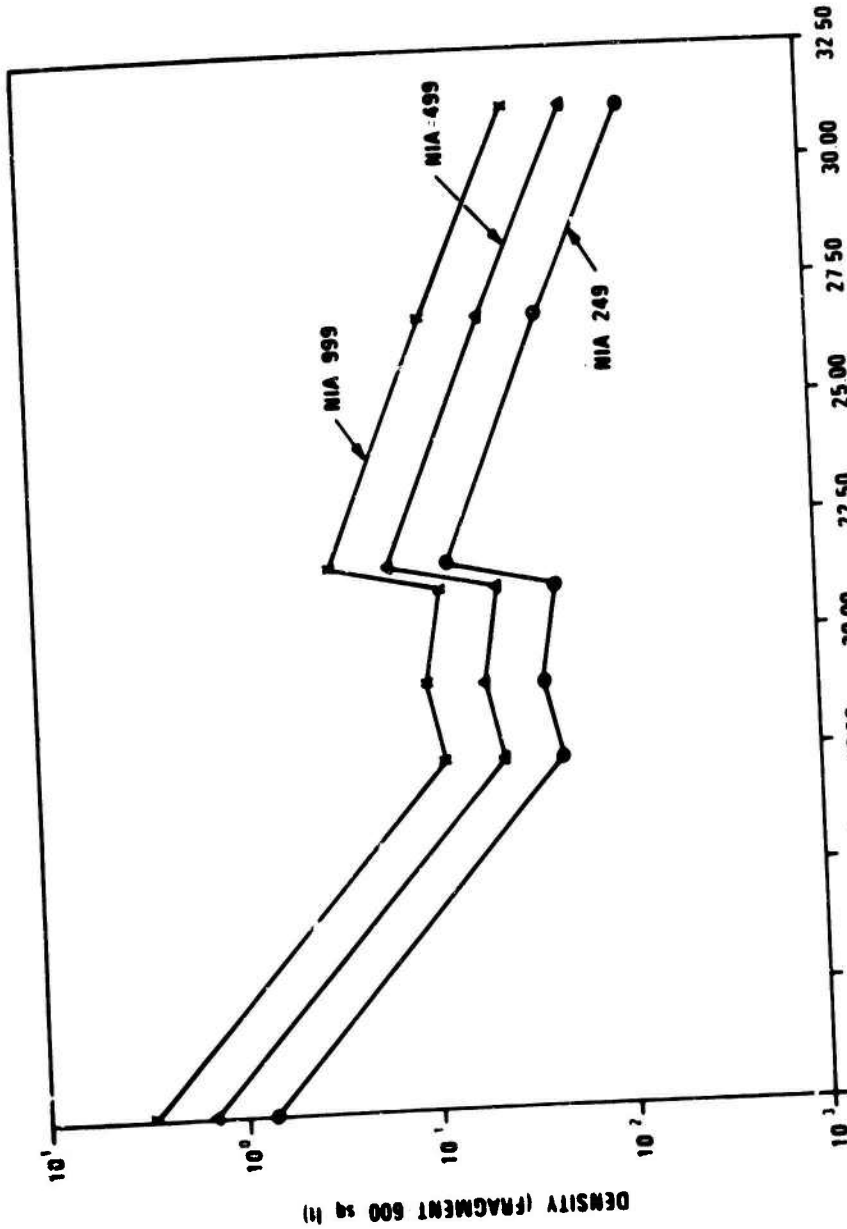

FIGURE 15

PREDICTED HAZARDOUS FRAGMENT DENSITY

ESKIMO TEST RESULTS AND PLANS

T. A. Zaker
Department of Defense Explosives Safety Board

ESKIMO V

ESKIMO V was the fifth in a series of explosion tests of full-scale earth-covered magazine structures conducted at the Randsburg Wash Test Range, Naval Weapons Center, China Lake, California. The test took place on 17 August 1977.

Objectives

The objectives of ESKIMO V were to justify eliminating concrete thrust beams, a costly structural feature, from the design of the oval steel-arch igloo, Office, Chief of Engineers Drawing 33-15-73; to confirm the safety of applying current side-to-side igloo separation distances to concrete-arch igloos, which had never been tested at such small separations; and to demonstrate once again at full scale the blast suppressing characteristics, and consequently the greater safety, of earth-covered storage compared with aboveground storage.

Test Structures

Two test structures were subjected to explosive blast loading approximating that from explosion of the contents of an earth-covered magazine at the minimum side-to-side distance permitted by standards. Formerly existing concrete thrust beams were removed from the oval steel-arch magazine remaining from previous ESKIMO tests, and the earth fill was replaced. This magazine had been tested with thrust beams in ESKIMO III, with a 24-m long donor igloo containing 159,000 kg of tritonal in M117 (340-kg) bombs. Permanent deformation sustained by the oval arch in ESKIMO III was so slight as to permit retesting without rebuilding the arch.

The light-gage steel arch acceptor igloo northwest of the site of the ESKIMO III donor, significantly damaged in that test, was demolished. Near the same site a noncircular concrete arch (Freloc) magazine was constructed in accordance with U.S. Army Engineer Command, Europe Drawing 33-15-13. This magazine has a cross section similar to the oval steel arch and may be economically competitive with it in some localities. The cross section consists of a shallow elliptical arch supported on vertical side walls. Concrete arches, however, had never been tested at the smallest igloo separations permitted by standards. The current distances had essentially all been established in tests of steel-arch igloos.

PRECEDING PAGE BLANK

Explosion Source

A hemispherical stack built up of 3.6-kg TNT demolition blocks, near the site of the ESKIMO III donor igloo, was utilized without any earth cover as the explosion source. The stack was sized and positioned to produce peak overpressure and impulse equal to the values measured in ESKIMO III on the surface of the earth cover of the acceptor magazines to either side of the donor. The average values of pressure and impulse measured at the surface of the earth cover over the centerlines of the ESKIMO III acceptor igloos were 6 bars and 45 bars-ms, respectively.

Approach

Model tests and analysis conducted by the Ballistic Research Laboratory were directed toward determining the size and position of the aboveground hemispherical charge required to produce the same loadings on the acceptor igloos as did the ESKIMO III donor.

These model simulations, using cast pentolite hemispheres at 1/30 linear scale, showed that a 34,000-kg TNT hemisphere located midway between the two acceptor igloos with their centerlines 94.5 m apart would produce air blast loadings that match quite closely the pressures and impulses measured in ESKIMO III on the surface of the earth cover and side fill of the acceptor structures in that test. The comparison between the scale-model experiments and ESKIMO III is reported in another paper at this Seminar.* The ESKIMO V test area layout is shown in the accompanying diagram.

In addition to extensive blast loading and arch response measurements on the test structures, free-field blast measurements were made for purposes of comparing the blast output of the ESKIMO V explosion source with the standard pressure and impulse curves for aboveground hemispherical charges. A related purpose was to reveal the existence of any anomalies of the blast field in directions of interest.

Results

The explosion source performed as anticipated from the model-scale experiments conducted beforehand. A crater about 25 m in diameter was formed. Blast measurements on the surface of the earth fill over the centers of the acceptor arches yielded good agreement with the predictions of the model tests.** The aboveground hemisphere, consisting of 34,000 kg of explosive, produced the same levels of air blast overpressure and impulse on acceptors 47 m from its center as did nearly five times that quantity

---

* C. N. Kingery, "Blast Parameters from Munition Storage Magazine Model Studies," Minutes, 18th Explosives Safety Seminar, September 1978.

** Kingery, ibid.

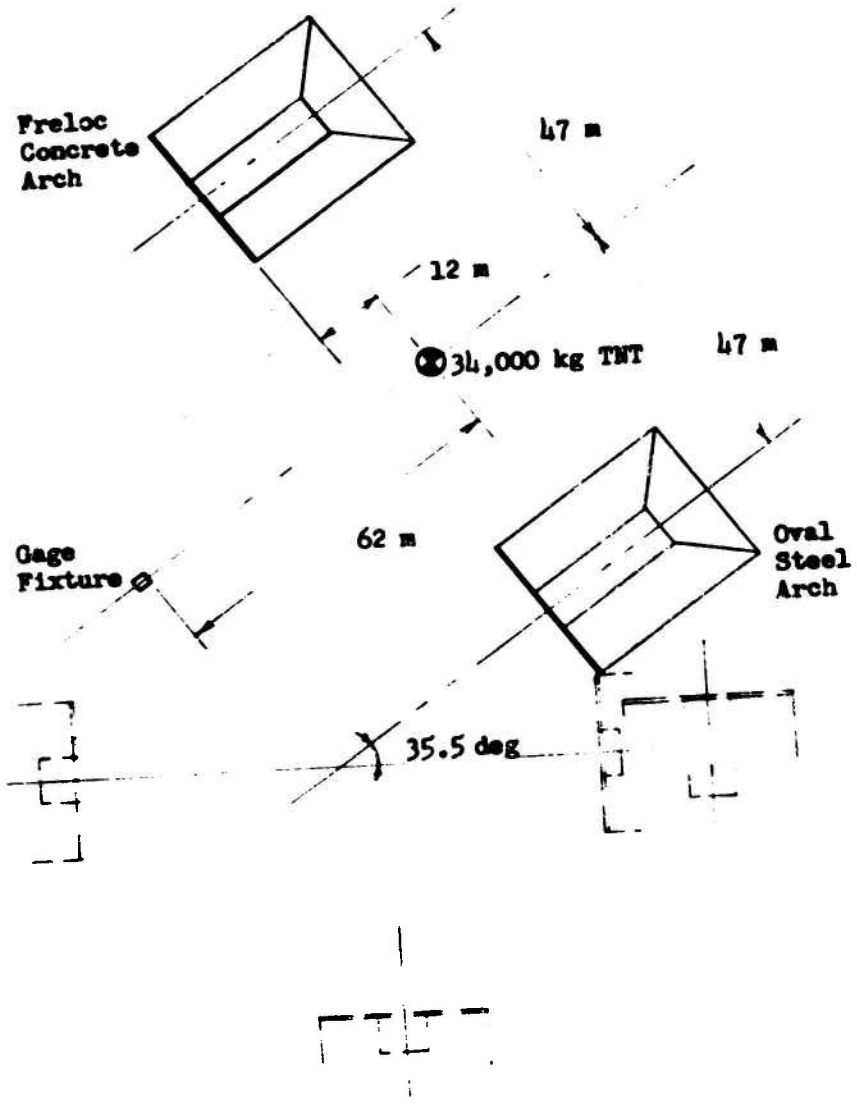

ESKIMO V Test Area Layout

(160,000 kg) under earth cover in ESKIMO III, with only 35 m between donor and acceptor magazine centerlines.

Permanent deformations of the steel and concrete arches were not visible to the unaided eye, but were readily measurable. Relative to the centerline of the floor of each igloo, the maximum inward radial movement in the midsectional plane occurred at the arch crown. In the steel arch the incremental downward permanent deflection was about 5 cm, while in the concrete arch it was about half that value. There was no significant spalling or material loss from the inside surface of the concrete arch or side walls, except for minor chipping from joints, such as that between the floor slab and the side wall. Local spalling occurred from the inside face of the headwall of the concrete igloo near the door opening, evidently due to bending of the slab caused by blast forces acting on the pilaster projecting forward of the outside face of the headwall at the side of the door opening toward the donor.

ESKIMO V demonstrated an ample margin of safety against catastrophic collapse of both the thin-shell concrete arch and the oval steel arch with thrust beams omitted, under air blast loading on the surface of the earth fill above equivalent to that from explosion of the contents of a full-size magazine at the minimum side-to-side separation distance permitted by standards.

ESKIMO VI

A sixth test in the ESKIMO series is being planned. Its objective will be to evaluate the explosion resistance of flat-roofed earth-covered reinforced concrete construction characteristics of magazines used by the U.S. Navy for storage of smokeless powder, projectiles, and missiles. Such magazines consist of three or more bays, the concrete slab roof being supported on interior columns and covered with a uniform thickness of earth. There is no adequate basis at the present time for allowing these magazines to be located at the minimum separation distances permitted between standard tested magazines. Large-scale testing thus far has been confined to steel and concrete magazines of the arch type, an inherently strong structural form. Concern has been expressed by some authorities for the safety of large, flat roof spans on isolated interior supports.

Large multibay magazines are needed for the storage of missile motors filled with detonable, high-energy solid propellant. Current design studies aimed at modifying these magazines to accommodate large motors have raised the question of the applicability of minimum separation distances, associated with high levels of potential blast loading, to this type of magazine. On the other hand, it is possible that the design techniques do not adequately allow for the suppression of blast by earth cover, and testing may justify significant economies in the strengthened versions of these magazines. Earth-covered multibay structures may also prove economical as explosion-resistant buildings for other potential applications such as ammunition manufacturing facilities.

Participants

ESKIMO VI will be sponsored jointly by the U.S. Navy and the Department of Defense Explosives Safety Board (DDESB). It is expected that the test will be conducted in 1979 at the site of previous ESKIMO tests at the Naval Weapons Center (NWC). The detailed design of the test will be developed in a design study to be performed by the Naval Civil Engineering Laboratory (CEL) under DDESB sponsorship.

The test design study will be supported by small-scale model experiments sponsored by DDESB at the U.S. Army Ballistic Research Laboratory (BRL). These model tests will be conducted to determine the blast loadings to which large flat-roofed magazines would be subjected from an explosion in one of them, at the minimum separation distances now permitted for earth-covered arch-type igloos. Model tests will also be conducted to simulate specific alternative test area layouts recommended in the design study, in order to verify that blast loadings in the test will approximate actual field conditions.

TEST DESIGN CONSIDERATIONS

The test design study will result in a recommended scale of the ESKIMO VI test (whether to conduct it at full scale or at some reduction from full scale in the interest of economy). It will lead to a design for the explosion source or donor, and will specify an optimum layout of test structures. Recommendations will be made for instrumentation to be installed in the test structures for various measurements of structure response. To this end, predictions will be made of the response levels to be expected in the test, by approximate methods as required for the specification of instrument types and output level.

Scale of Test

The geometric scale of ESKIMO VI, which will determine the size of test structures and, at least in part, the quantity of donor explosives, will be selected so as to provide an optimum balance among the factors of cost, instrument coverage, expected data return, and confidence in the modeling of structure response. It is expected that a linear scale factor between 1:10 and unity (full size) will be chosen, the value probably being closer to the latter. It should be possible to model structural response adequately provided the scale reduction is not excessive. On the other hand, even a modest reduction of scale leads to significant savings in material and explosives. For example, a reduction of 20 percent in the linear dimensions reduces the material quantities by about half.

The choices available in the design of the explosion source include a complete flat-roofed magazine constructed to standard specifications, an accurate reduced-scale replica of such a magazine, a crude full-scale (or reduced-scale) mockup, or an unenclosed stack of explosives. Successful modeling of the effect of earth cover on the blast fields from explosions

in arch-type magazines at very small scale, accomplished by BRL under DDESB sponsorship, has shown that construction details and the strength of structural elements of the donor magazine do not play an important role in determining the blast fields. This suggests that a crude mockup of the magazine housing the donor explosives may be adequate for the test, whether conducted at full scale or at somewhat reduced scale. The donor explosive charge will be arranged within so as to approximate a realistic storage configuration.

Test Structure Selection

In order to resolve uncertainties as to the adequacy of existing flat-roofed magazines proposed for general explosive ammunition storage, and to attempt to justify economies in the adaptation of similar magazines to large missile storage, a variety of structures, or partial structures and structural components, will be tested. It will be one of the tasks of the test design study to determine the mixture and positioning of exposed structures so as to maximize the return of data on the investment of resources in the test.

Of particular interest is the existing design of the Navy Smokeless Powder and Projectile Magazine Type IIB, which has been proposed for more versatile use in ammunition storage than originally contemplated when the magazine was designed. The resistance of the earth-covered roof slab, which is supported by columns at isolated interior points, is of major concern. Preliminary indications from model testing are that the greatest loads are exerted on the roof when the magazine is forward of the donor at the minimum front-to-rear distance permitted by standards. Also of concern is the vulnerability of the front wall and door construction facing the side or rear of the donor.

A second flat-roofed, earth-covered structure, Navy Missile Magazine Type I, is being redesigned to house large solid propellant missiles. Again, the exposures of concern are the roof forward of the donor and the front wall facing the side or rear. Currently applicable design methods and loading estimates appear to lead to high construction cost for the redesigned structure. If testing of this structure in ESKIMO VI shows these procedures to be excessively conservative, significant cost savings may be realized without compromise of safety.

A test design study will determine the feasibility of exposing components or segments of these structures in ESKIMO VI rather than complete buildings, at either full or reduced scale. It may prove practicable to design test structures incorporating only those components considered most vulnerable, such as intermediate column-supported roof spans.

Consideration will be given to other untested magazine designs of wide interest, such as portal style reinforced concrete magazines of UK or German design. The noncircular concrete arch (Freloc) magazine exposed in ESKIMO V to explosive loading simulating conditions at the minimum side-to-side

separation between magazines remains at the NWC site. The previous test left the headwall and door virtually undamaged and available for exposure in ESKIMO VI. It represents a target of opportunity from which additional response information can be gained, provided the test area layout can be designed so that the main aims of the test are not compromised. In general, it will be a part of the strategy of test design to make maximum use of assets remaining at the ESKIMO site from previous testing.

PRETEST SUPPORTING STUDIES

The design of ESKIMO VI will be developed with the aid of model experimental and analytical studies to better anticipate levels of loading and response, and to verify that the configuration of the donor and exposed structures will constitute a valid test approximating conditions of actual magazine storage.

Blast Model Study

Model experiments will be conducted by BRL at 1/50 scale to determine blast loadings on three-bay Type IIB magazines at minimum distances permitted in the directions forward, to the side, and to the rear of the donor. The results will be compared with similar results already in hand from tests on models of arch-type magazines, to assess the effect on the blast loadings due to the flat roof and the relatively smaller mass of earth fill associated with it, as well as the large internal magazine volume. Type I magazines are sufficiently similar that the results will also be applicable to these, inasmuch as the structural strength of the donor building is much less important than the mass of its components in determining the external blast field.

Experiments will also be conducted modeling accurately the configuration (or configurations) of the donor and the test structure exteriors recommended as a result of the design study. These experiments will validate the overall test design in regard to the blast levels to be anticipated, and will provide data for the calibration of ESKIMO VI blast instrumentation.

Response Predictions

As part of the test design study, approximate predictions will be made of the response of the test structures and structure components. These estimates will be made in sufficient detail to guide the positioning of response instrumentation and the calibration of dynamic strain and motion transducers.

Should the performance of the structures in ESKIMO VI be such as to require a more detailed understanding and interpretation of the observed behavior, additional response analyses, perhaps using finite-element numerical techniques, may be undertaken after the test for this purpose.

Instrumentation Recommendations

The positioning of air blast gages by type, and the levels to which they will be calibrated, will be based on the recommendations of BRL as a result of the final pretest model-scale simulation of the ESKIMO VI test structure array.

Soil stress gages will be located in the earth fill at positions such as to facilitate estimating the loadings on earth-covered surfaces and the attenuation of blast by earth. The positioning of these gages will be based on recommendations resulting from the test design study by CEL, and possible consultation with the U.S. Army Engineer Waterways Experiment Station.

Measurements will be made of reinforcing bar strain at critical locations determined by CEL from approximate predictions of structure response. The predictions will also be used as the basis for setting strain gage sensitivity levels.

Motion instrumentation will include accelerometers, velocity gages, and linear variable differential transformers for dynamic displacement measurements. These will be positioned and calibrated on the basis of the results of the response predictions of the test design study. Recommendations will also be made by CEL for high-speed motion-picture photography, specifying camera positions and framing rates for quantitative assessment of structure motion.

ADVANCES IN THE DETECTION AND ANALYSIS OF CHEMICAL AGENTS

BY

LESLIE ENG

OFFICE OF THE PROJECT MANAGER FOR
CHEMICAL DEMILITARIZATION
AND INSTALLATION RESTORATION
ABERDEEN PROVING GROUND, MD

This work is sponsored and funded by the Office of the Project Manager for Chemical Demilitarization and Installation Restoration, Aberdeen Proving Ground, Maryland.

ABSTRACT

Early detection of toxic chemical agents in the atmosphere is necessary to provide adequate protection for personnel against hazardous exposure. In the plant environment, chronic exposure to sublethal concentrations of contaminants is a primary concern. Efforts to develop monitors capable of rapid response to extremely low concentrations of chemical agents are described.

ADVANCES IN THE DETECTION AND ANALYSIS OF CHEMICAL AGENTS

Ever since World War I when the German armies employed toxic chemical agents as a tactical weapon on a large scale, the United States has been concerned with defensive programs to neutralize the effectiveness of these toxic chemicals against personnel. The first step in any defensive measure is the early detection of toxic chemicals in the atmosphere. Initially, the human physical senses were relied upon to provide this early detection. The chemical agents employed during World War I could be seen or smelled at high concentrations. However, with the advent of the anticholinesterase or nerve agents during the World War II period, the human senses were no longer reliable indicators of the presence or absence of chemical agents since the nerve agents were colorless, tasteless, and odorless at toxic concentrations. Chemical and/or instrumental methods of detection were then developed to provide an early detection and warning capability to protect the battlefield soldier.

Under battlefield conditions, agent concentrations in the atmosphere were expected to be relatively high immediately after a chemical attack and to decrease as the agent dissipated in the atmosphere. Personnel exposure to chemical agents was expected to consist of high periodic concentrations rather than low continuous concentrations. Detection methods were, consequently, directed towards high concentrations of short duration rather than low concentrations over extended periods.

To train military personnel in the detection of toxic chemical agents, Chemical Agent Identification Sets (ID Sets) were developed and manufactured by the Department of the Army (DA) from the 1930's to 1960's. These ID Sets were distributed to Department of Defense installations for use by all services. Through the use of these sets, personnel could become familiar with the appearance, color, and odor of some of the toxic chemical agents and demonstrate to themselves the ability of chemical agent detector kits to detect the various agents. In April 1971, the Army declared the ID Sets obsolete. The task of disposing of the ID Sets became the responsibility of the Office of the DA Project Manager for Chemical Demilitarization and Installation Restoration (OPM CDIR).

The disposal of the ID Sets will be accomplished under production plant conditions. Under these conditions with the continuous presence of agent containers, personnel exposure to low concentrations of a number of chemical agents over extended periods may be possible. With the development of highly sophisticated ventilation and containment process equipment, chronic exposure to sublethal concentrations becomes the main concern in ensuring worker safety rather than exposure to acute concentrations. Concentration levels to which workers may be exposed for up to eight hours per day indefinitely and suffer no effects are referred to as time weighted averages (TWA). Each of the agents contained in the ID Sets has its individual TWA, and it is to this concentration

level that current detection techniques are directed in order to monitor the safety of the work environment.

The detection methods developed for the field were found to be inadequate for determination of the low TWA concentrations required in the plant. In order to measure these low levels, analytical techniques employing bubblers were developed. These bubbler techniques required sampling for longer periods of time or at high flow rates in order to observe the TWA concentration. The collection media were then transported to a chemical laboratory for analyses. The total procedure required more time than the field methods but did result in the ability to observe very low concentrations of chemical agents. With bubblers, sampling times alone range from thirty minutes to two hours. Transportation and analyses require additional time.

In an effort to obtain more rapid responses to protect workers on chemical demilitarization programs, the OPM CDIR has developed and is developing monitors that will respond to TWA concentrations of chemical agents in a matter of minutes rather than hours. These monitors represent application of state-of-the-art technology to minimize potential hazards during demil operations. A monitor for the nerve agent, GB, has been developed under the aegis of the OPM CDIR and is currently being tested with simulants at the Chemical Agent Munitions Disposal System site at Tooele Army Depot, UT. This monitor is based on the familiar enzyme technique for detecting anticholinesterase compounds. The atmosphere is sampled automatically and placed in contact with an enzyme. The presence of an anticholinesterase compound destroys the enzyme and prevents the enzyme from engaging in a subsequent color producing chemical reaction. The absence of color is then taken as an indication of the presence of an anticholinesterase compound in the atmosphere. These monitors require solution replenishment only once a week which minimizes the need for operator attention. Alarms from TWA concentrations of GB are realized in approximately ten minutes.

Another monitor, the Automatic Continuous Air Monitoring System (ACAMS), is curently being developed for the OPM CDIR under contract with Southern Research Institute for use in the program for the disposal of ID Sets. The ID Sets disposal program presents a unique situation over other current demil programs in that several toxic chemical agents must be monitored simultaneously in the presence of possible analytical interferents arising from the incineration process. In the past, monitoring for a single agent at TWA concentrations and at the same time requiring specificity and rapid response has frequently been a difficult task. The ACAMS concept requires specificity and rapid response at TWA concentrations for multiple agent contamination. In addition, the current effort requires delivery of an operational system in less than fourteen months.

In order to provide the necessary specificity, the current ACAMS utilizes a gas chromatograph (GC) as the basic analytical instrument. GC's are used extensively in modern analytical laboratories for the

separation of components in gas or liquid samples. The separation is affected by a GC column to varying degrees depending upon the physical and/or chemical properties of the components. Under a given set of carefully controlled conditions, the time required for a particular compound to traverse or elute from the column is highly reproducible. This retention time is indicative of the particular compound.

Once a compound elutes from the column, its presence is determined by the GC detector. These detectors provide a degree of specificity in that they tend to be more sensitive to compounds of particular compositions. Recent advances in detector technology have made modern detectors more stable and more specific than their predecessors. The ACAMS utilizes the Hall electrolytic conductivity detector recently developed by Tracor Instruments. Reported sensitivity for this unit is ten picograms or ten trillionths of a gram for chlorine. Since the majority of toxic chemical agents contain chlorine, this detector appears to be ideal for the ACAMS application.

To reduce the required operator attention, the ACAMS will be microprocessor controlled. Recent advances in microprocessor/microcomputor technology have been applied extensively to analytical instrumentation by instrument manufacturers. Microprocessor based instruments are currently capable of automatically controlling tasks from injection of the sample to reducing the output data. In the ACAMS, the various functions will be initiated electronically after predetermined parameters are entered on a keyboard by the operator. The ACAMS will then function automatically and alarm when the TWA of an agent is reached.

Table 1 lists the chemical agents along with their TWA concentrations contained in the ID Sets. While chloroform is not classified as a chemical agent, recent evidence has shown that it is a hazardous material, and, consequently, it is included in the list of compounds to be monitored. Of the agents listed, some are not included in the current ACAMS effort. Chloroacetophenone (CN) was not included since the quantities contained in the ID Sets were quite small and represented less than a half of one percent of the analytical workload. The arsenic containing agents, lewisite (L) and adamsite (DM), were also not included although they represent almost fourteen percent of the analytical workload. Lewisite was deleted based on previous experiences of difficulty in analysis by gas chromatography. DM was deleted when examination of its physical properties indicated that it would not be amenable to analysis by gas chromatography. Other methodology will be utilized for these compounds. The remaining agents in Table 1 were included in the ACAMS program.

To date, investigations have indicated that suitable conditions exist for the GC analysis of all of the agents considered for ACAMS except for the nitrogen mustard, HN1. HN1 was found to decompose in the gas chromatograph at temperatures less than 150°C. Use of lower temperatures resulted in retention times of 15-20 minutes which were considered excessive

for the ACAMS program. Pursuit of a resolution to the HN1 problem was considered to be sufficiently time consuming in that it could jeopardize the timely availability of a monitor for the other agents. Consequently, HN1 was deleted from the current ACAMS requirements.

Although suitable parameters for the individual GC analysis of each of the agents have been identified, the problem of combining these parameters in a mutually compatible system still remains. To complicate the compatibility problem, the mustards and GB must be preconcentrated on a solid sorbent in order to detect their TWA concentrations. Air sampling is performed by passing the air through a tube containing the solid sorbent for a specified time at a fixed flow rate. The agents are adsorbed on the solid and held until the sampling period is complete. The tube is then heated, and the agents are desorbed and injected into the GC for analysis.

Those agents not requiring preconcentration are injected into the GC by an air sampling loop as shown in Figure 1. A vacuum pump draws air through an empty column or loop of specific volume. All connections are made through a multiport valve. To inject an air sample, the valve is actuated, and the air trapped in the loop at the time of actuation is swept by the carrier gas into the GC for analysis. The valve is returned to its original position, and, when the analysis cycle is completed, the valve is again actuated to inject another air sample.

To circumvent possible problem areas and to simplify the ACAMS requirements for simultaneous monitoring for multiple agents, the actual composition of the various ID Sets was examined as shown in Table II. As can be seen from the table, many of the particular sets contain only one agent. The X548 and X550 Sets contain L and HN1 for which no ACAMS capability is currently planned. The ACAMS will monitor only for the HN3 in the X302 Set. In the K955 Set, only the HD and PS will be observable by the ACAMS.

In the K945 Set, HD and GB must be monitored simultaneously. This is the only ID Set that contains the nerve agent GB. The difficulty in this simultaneous monitoring is that the GB is more amenable to detection by a flame photometric detector (FPD) than the Hall detector. While the FPD has been used for the detection of HD, it cannot detect HD and GB simultaneously. The FPD is sensitive to the phosphorus atom in GB and to the sulfur atom in HD. However, the detector cannot be sensitive to sulfur and phosphorus at the same time since the individual sensitivities are provided by appropriate narrow band light filters. The use of one filter precludes the use of the other filter. This problem could be resolved in several ways. Two FPD's could be used, but this seems unreasonable since the Hall detector is available for HD detection. The problem now reduces to how to direct the single column effluent to two separate detectors. If the column effluent were split by passing it through a Y connection as shown in Figure 2, half of the sample could enter the FPD while the other half could enter the Hall detector.

The disadvantage of this method is that by splitting the sample, the sensitivity is reduced by half since only half of the sample reaches any one detector.

A more viable solution is through the use of a valve as shown in Figure 3. The valve could direct the flow from the column to the FPD until the retention time for GB has elapsed. At this time, the valve switches automatically to divert the flow from the column to the Hall detector. The valve can be controlled by the microprocessor that has been incorporated into the ACAMS. This option allows for realizing the full detection limit of the collected sample.

Referring back to Table II, the K951 through K954 Sets represent the largest ACAMS challenge in two senses. Not only must four agents be monitored simultaneously, but these sets represent 60 percent of the total number of ID Sets. As mentioned previously, while most of the agents can be injected into the GC directly, the HD must be preconcentrated. Studies performed thus far have demonstrated the separation and detection of HD, PS, and chloroform in a mixture. One of the problems encountered is the separation of CK and CG which are found together in the K953 and K954 Sets. However, their TWA's are sufficiently close that setting the alarm level at the lower of the two (CK) will allow a safety factor regardless of which of the agents is present and makes the separation unnecessary.

It can be gathered from this presentation that the technology developed thus far in the ACAMS program will allow the assembly of monitors capable of rapidly detecting single chemical agents at their TWA concentrations. However, the objective of ACAMS is to monitor for multiple agents simultaneously. Through refinement and expansion of its capabilities, the ACAMS has the potential of being a single monitor for many of the toxic chemical agents. By constantly pressing state-of-the-art technology, the ACAMS concept is not only possible, but probable. A successful ACAMS and similar instruments will contribute markedly towards the protection of personnel against exposure to low concentrations of chemical agents and thus provide a greater degree of safety in the work environment.

TABLE I. AGENTS CONTAINED IN THE ID SETS

AGENT	TWA mg/m^3	TWA ppb
HD	0.003	0.464
HN1	0.003	0.434
HN3	0.003	0.361
CG	0.2	50
CK	0.05	20
PS	0.7	100
GB	0.0001	0.018
CHLOROFORM	240	50×10^3
L	0.003	0.35
DM	0.05*	
CN	0.3	50

* AS ARSENIC

TABLE II. AGENT COMPOSITION BY ID SET

ID SET	AGENTS
K941	HD
K942	HD
X547	HD
X551	HN3
X302	HN1, HN3
X552	PS
K955	HD, PS, L, CN, DM
K951, K952	HD, CG, PS, Chloroform, L
K953, K954	HD, HN1, CG, CK, Chloroform, L
K945	HD, GB, L
X545	CG Simulant
X548	L
X550	HN1

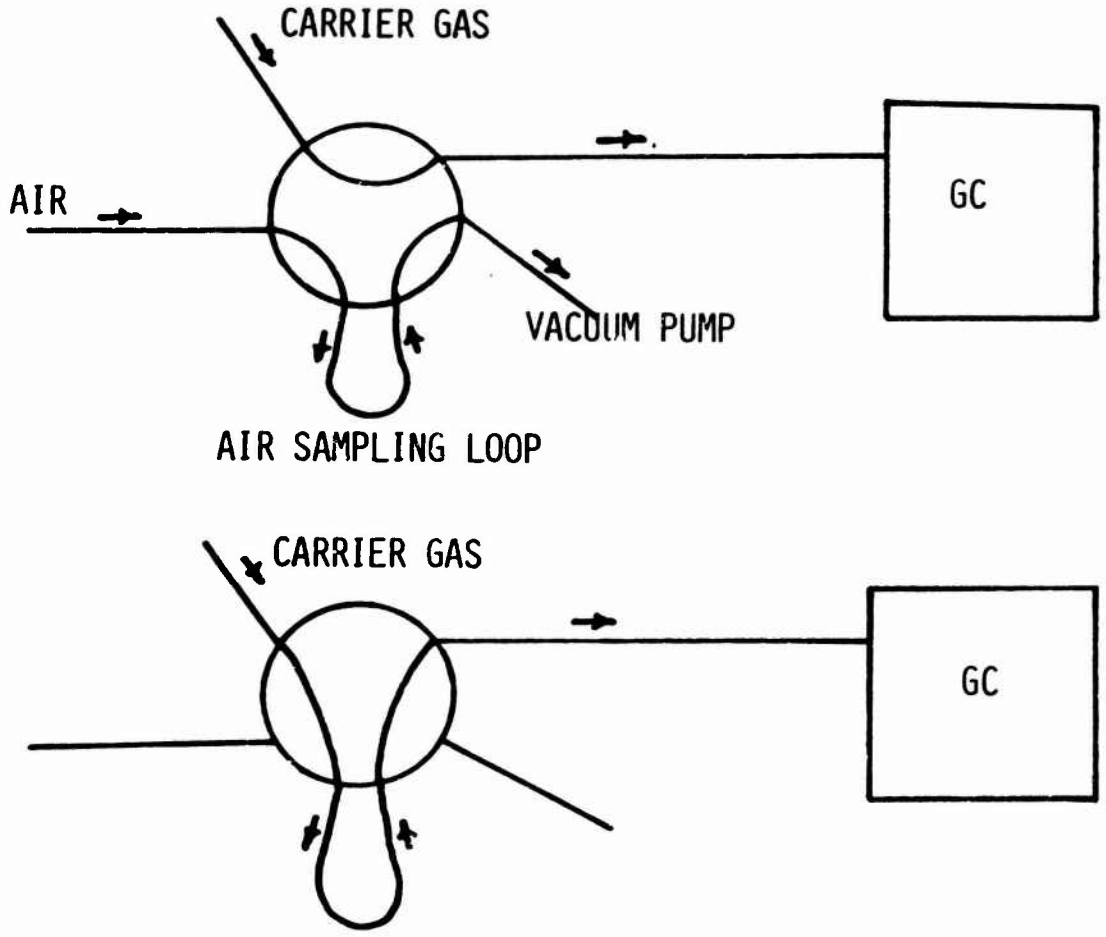

FIGURE 1. OPERATION OF AN AIR SAMPLING LOOP

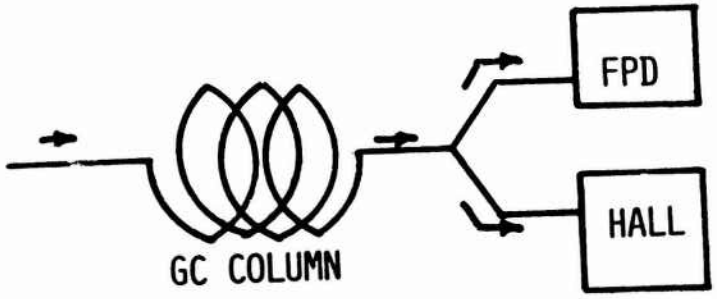

FIGURE 2. "Y" SPLITTER OPTION

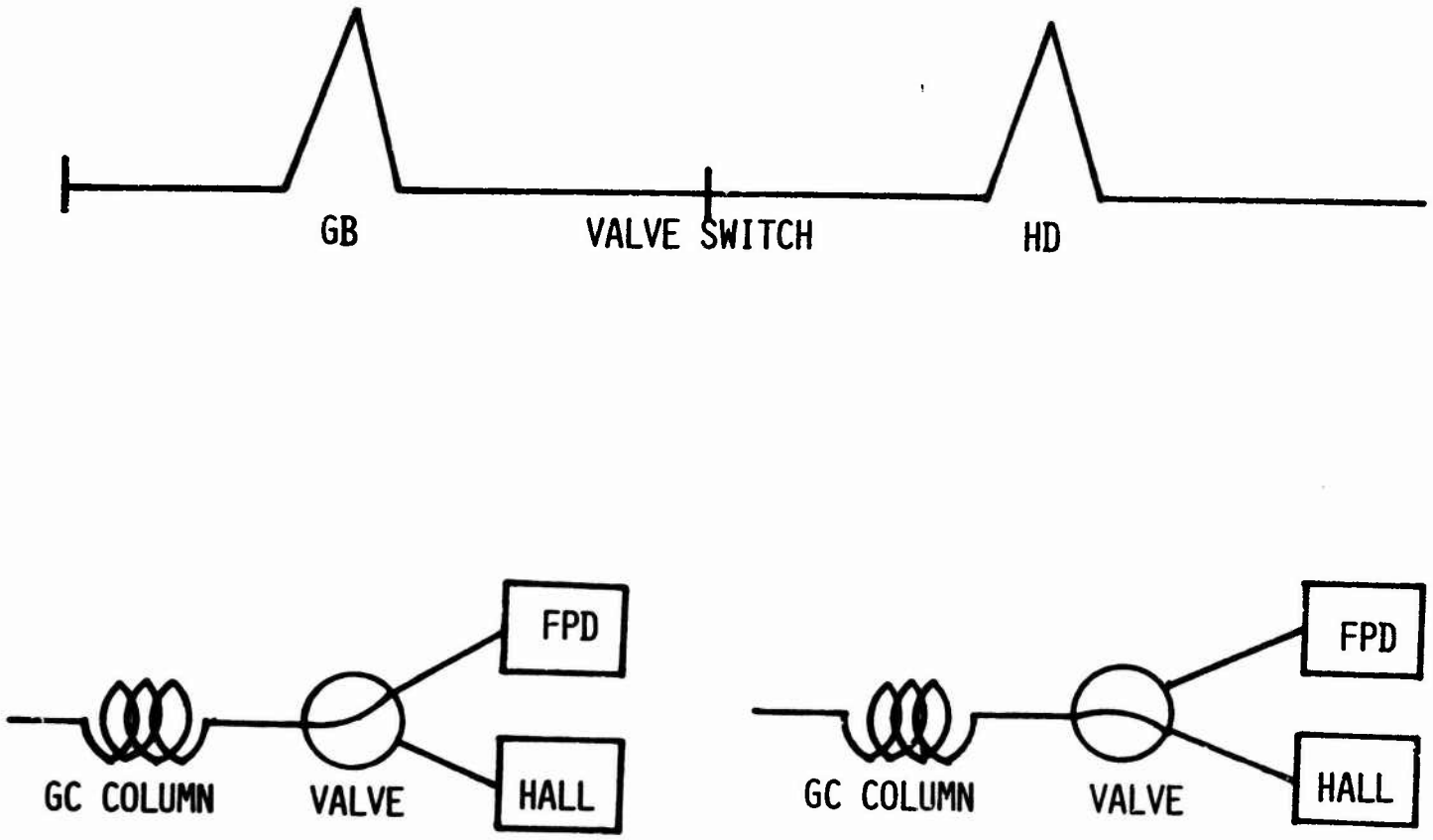

FIGURE 3. VALVE SWITCHING OPTION

A SIMPLIFIED METHODOLOGY FOR COMPUTING CHEMICAL HAZARD DISTANCES

C. Glenvil Whitacre

Systems Assessment Office
Chemical Systems Laboratory
Aberdeen Proving Ground, MD 21010

PRECEDING PAGE BLANK

A SIMPLIFIED METHODOLOGY FOR COMPUTING CHEMICAL HAZARD DISTANCES

1. SCOPE

1.1 Objective. It is the objective of this task to develop a methodology for the solution of the Gaussian diffusion model which is simple enough to be performed on a pocket calculator. It is intended that this would include the effect of the bounded mixing layer[1] and the 2-minute dosage correction[2] as employed with some agents.

1.2 Background. The Methodology for Chemical Hazard Predictions, which was agreed upon by the Technical Advisor to the Chemical Standards Working Group of the Department of Defense Explosives Safety Board in 1974, was published as DODESB Technical Paper No. 10[2] in March 1975. The mathematical representation of this methodology was stated in very general form and its inherent complexity prevented its immediate adoption for field work.

In 1976, a system of graphic aids was prepared by the Systems Assessment Office, Chemical Systems Laboratory, and was published by DARCOM in March 1977 as a Handbook for Chemical Hazard Prediction.[2] In June 1977, ARCSL-TR-77049[3] was published by Systems Assessment Office to document a complete computer program of this methodology.

Since the Handbook[1] was developed as the basic implementing document of this methodology, it was presented in generalized form which attempted to portray all the variables of the model over the ranges of interest. This document was large, containing some 170 graphs, but still treated many variables as factor corrections to a first estimate.

The computer program, documented as ARCSL-TR-77049, was also developed as a basic tool and attempted to cover all of the methodology in the most concise manner. As a result, the program is made up of eight subroutines containing some 1000 Fortran statements. The program is fast, relatively easy to use, and will be maintained on the ARRADCOM Univac 1108 computer at Aberdeen Proving Ground, Maryland, for remote use through the telephone.

There remained, however, an area of quick field applications which neither of these approaches satisfied completely. An approach was sought which would approximate some of the more complex procedures in the methodology and lead to simple statements which could be programmed on the pocket calculator.

1.3 Approach. Two computational procedures were of particular concern in simplifying this methodology. Both the infinite sum used to compute the transition from the Gaussian to the Box Model* and the iterative procedure used to compute the 2-minute correction** were complex and time consuming.

From the many curves which had been produced for the Handbook,[1] it was evident that the transition from the Gaussian to the Box Model occurred over a relatively short distance, and an approach was sought to define this zone as a function of stability and height of the mixing layer. Once the transition zone was defined, simple equations were used to compute the dosage versus distance curve as three log-log segments representing the Gaussian Model, mixing layer transition, and Box Model.

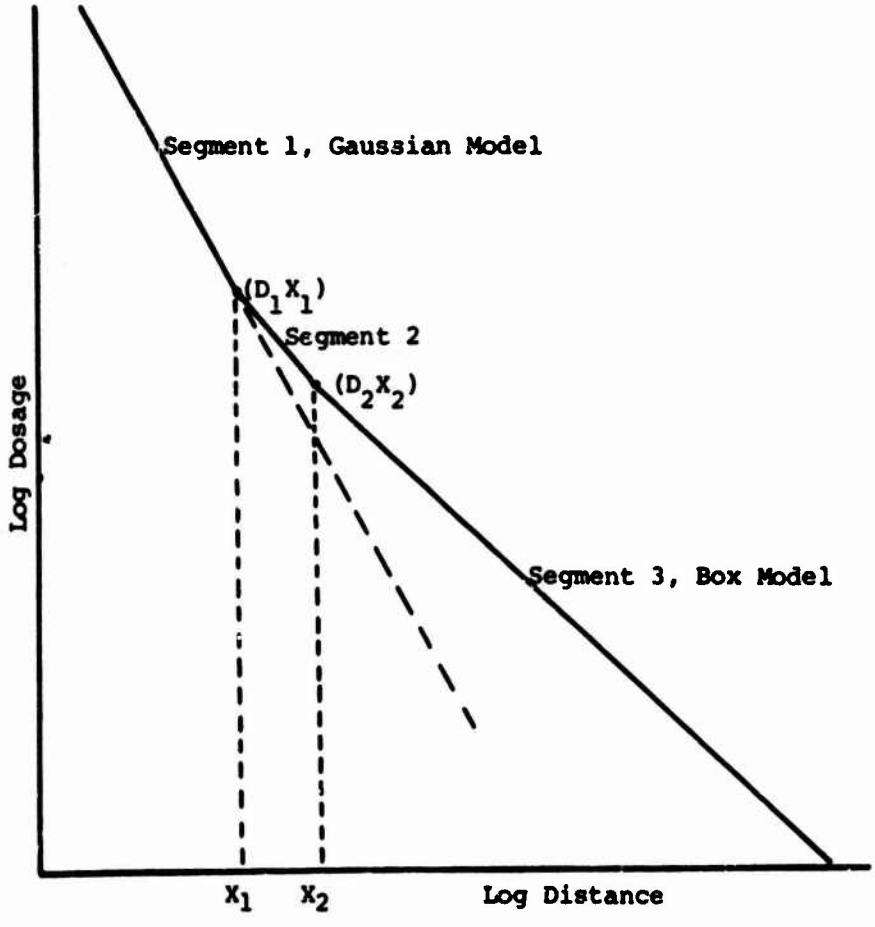

*Diffusion under an inversion cap with vertical distribution uniform.

**A correction for some agents where effects are dependent on time of accumulation.

In order to simplify the 2-minute corrected methodology as reproduced in Technical Paper No. 10,[2] the full iterative program was executed and the final dosage correction factor at each distance was converted to an effective time of exposure. This effective time was then fitted as a function of stability, wind speed, and distance, and a simple algebraic statement of the 2-minute correction was substituted into the diffusion equation and solved directly for distance.

Finally, the mixing layer and 2-minute corrections were combined to complete the model. Simple algebraic expressions were used to approximate these unknown functions with the condition that deviations would be biased to produce a safe-sided estimate of the hazard distance.

2. METHODOLOGY

2.1 Effect of the Mixing Layer. When a Gaussian cloud encounters a physical boundary such as the ground surface or an elevated inversion cap,[1] the fraction of the cloud reaching the boundary is reflected back to reinforce the concentration and increase the dosage within this mixing layer. A model based on multiple reflections from these bounding surfaces was outlined in ORG 17[4] in 1958. This approach was reproduced in Technical Paper No. 10[2] indicating that the factor which augments the dosage at any downwind distance can be expressed as follows:

$$F_R = \frac{1}{2} \sum_{i=1}^{\infty} \left[\exp\left[-\frac{1}{2}\left(\frac{2iH_m - H - Z}{\sigma_z} \right)^2 \right] + \exp\left[-\frac{1}{2}\left(\frac{2iH_m - H + Z}{\sigma_z} \right)^2 \right] + \exp\left[-\frac{1}{2}\left(\frac{2iH_m + H - Z}{\sigma_z} \right)^2 \right] + \exp\left[-\frac{1}{2}\left(\frac{2iH_m + H + Z}{\sigma_z} \right)^2 \right] \right] \quad (1)$$

where

F_R is the reflective contribution to the dosage at distance, x

H_m is the height of the mixing layer (m)

H is the height of the source (m)

Z is the height of the sampler (m)

$\sigma_z = \sigma_{zr} \left(\frac{x}{x_{zr}} \right)^{\beta}$, the vertical distribution of the cloud as defined in the Handbook[1] (m)

When one is interested in dosages near the ground, Z can be taken as zero and the expression simplifies to the following:

$$F_R = \sum_{i=1}^{\infty} \left[\exp \left[-\frac{1}{2} \left(\frac{2iH_m+H}{\sigma_z} \right)^2 \right] + \exp \left[-\frac{1}{2} \left(\frac{2iH_m-H}{\sigma_z} \right)^2 \right] \right] \quad (2)$$

A special version of the program reported in ARCSL-TR-77049 was written to capture the downwind distances at which the reflective model first departed from the Gaussian Model by a specified amount, ΔE, and then where the reflective model approached the Box Model by the same difference. These distances are referred to as X_1 and X_2 and define the transition zone.

Tables 1 and 2 list values of X_1 and X_2 for different stabilities and heights of the mixing layer. The results shown are for $\Delta E = .01$.

TABLE 1. VALUE OF X_1 AS A FUNCTION OF STABILITY AND H_m

H_m (m)	A	B	C	D	E	F
100	282	550	1023	2138	3548	7079
200	468	1096	2188	4786	8511	17783
300	617	1660	3467	7762	14125	30903
400	759	2188	4786	10965	19953	44668
600	1023	3311	7413	17783	33113	77624
800	1259	4467	10233	24547	47863	112201
1000	1479	5495	13188	32359	63095	151355
2000	2399	10965	28840	72443	151355	380188

TABLE 2. VALUE OF X_2 AS A FUNCTION OF STABILITY AND H_m

H_m (m)	A	B	C	D	E	F
100	427	955	1862	4074	6918	14454
200	692	1905	4074	9120	16596	36308
300	933	2884	6310	14791	27542	63095
400	1148	3802	8710	20893	39811	91201
600	1514	5754	13804	33113	66069	158489
800	1862	7586	19055	46773	93325	234422
1000	2188	9550	23988	60256	123026	316226
2000	3631	19055	52481	138038	295119	794324

It was found that the data shown in Tables 1 and 2 could be fitted by expressions of the following form:

$$X_1 = C_1 H_m^{1/\beta} \quad (3)$$

$$X_2 = C_2 H_m^{1/\beta} \quad (4)$$

where

X_1 and X_2 defines the transition zone (m)

C_1 and C_2 are constants for each stability

β is the slope of the sigma Z curve

The derived values of C_1 and C_2 are listed in Table 3 as a function of stability. The diffusion parameters, as taken or derived from Technical Paper No. 10,[2] are also tabulated for use in the equations 5 and 6. The reference σ values have been transformed to one meter as will be discussed under equation 6. Values of σ_y are given for both instantaneous (ins) and continuous (con) sources as discussed in the Handbook.[1]

TABLE 3. METEOROLOGICAL PARAMETERS

Parameter	A	B	C	D	E	F
σ_{y1} (ins)*	0.09	0.0633	0.048	0.0634	0.0754	0.0796
σ_{y1} (con)**	0.27	0.1899	0.125	0.1268	0.1508	0.1592
σ_{z1}	0.0222	0.11	0.119	0.0898	0.0879	0.0791
α	1.	1.	1.	0.9	0.8	0.7
β	1.4	1.	0.9	0.85	0.8	0.75
C_1	10.5	5.5	6.13	9.49	11.2	15.3
C_2	15.9	9.55	11.2	18.1	21.9	31.1

*ins = instantaneous

**con = continuous

2.2 Total Dosage: Segment 1, $X < X_1$

If one considers total dosage near the ground from a point source release near the ground, the dosage-distance relationship is defined as follows:

$$D(X) = \frac{Q}{60\pi\, \sigma_y(x)\sigma_z(x)u} \qquad (5)$$

where

D(X) is the total dosage at X (mg-min/m^3)

Q is the source strength (mg)

u is the wind speed (m/sec)

$$\sigma_y(x) = \sigma_{yr}\left(\frac{x}{x_{yr}}\right)^{\alpha} \text{ (m)}$$

$$\sigma_z(x) = \sigma_{zr}\left(\frac{x}{x_{zr}}\right)^{\beta} \text{ (m)}$$

By transferring the reference distances, x_{yr} and x_{zr}, to one meter, this is further simplified to:

$$D(X) = \frac{Q}{60\pi\ \sigma_{y1}\sigma_{z1} u\ x^{\alpha+\beta}} \tag{6}$$

where

$$\sigma_{y1} = \sigma_{yr}(x_{yr})^{-\alpha}$$

$$\sigma_{z1} = \sigma_{zr}(x_{zr})^{-\beta}$$

or the inverse solution:

$$x = \left[\frac{Q}{60\pi\ \sigma_{y1}\sigma_{z1}\ D\ u}\right]^{1/\alpha+\beta} \qquad x < x_1 \tag{7}$$

where D is the dosage of interest (mg-min/m^3).

2.3 Total Dosage: Segment 3, $X > X_2$

The total dosage in segment 3 can be calculated from the following:

$$D(X) = \frac{Q}{60\ \sqrt{2\pi}\ \sigma_{y1}\ H_m\ x^{\alpha}} \tag{8}$$

or

$$x = \left[\frac{Q}{60\ \sqrt{2\pi}\ \sigma_{y1}\ D\ H_m}\right]^{1/\alpha} \qquad x > x_2 \tag{9}$$

2.4 Total Dosage: Segment 2, $X_1 < X < X_2$

Considering that the distance between X_1 and X_2 is relatively small, it was decided to approximate this segment as a log-log straight line between points (D_1, X_1) and (D_2, X_2). The value, D_1, is taken at X_1 on segment 1 and D_2 is taken at X_2 on segment 3. A straight line segment will slightly overestimate the dosage in this region and thus provide a conservative (safe-sided) estimate of the distance.

Employing equations 6 and 8,

$$D_1 = \frac{Q}{188.5\ \sigma_{y1}\sigma_{z1}\ u\ X_1^{\alpha+\beta}} \tag{10}$$

$$D_2 = \frac{Q}{150.4\ \sigma_{y1}\ H_m\ u\ X_2^{\alpha}} \tag{11}$$

then

$$S = \frac{\ln(X_2/X_1)}{\ln(D_2/D_1)} \tag{12}$$

and

$$X = X_1 \left(\frac{D}{D_1} \right)^S \tag{13}$$

3. TWO-MINUTE CORRECTION

3.1 Instantaneous Sources with 2-Minute Correction. A copy of the program for computing dosage with the 2-minute correction, as defined in ARCSL-TR-77049,[3] was modified to output the effective time, t_e, of dosage accumulation as a function of downwind distance. Data were generated for a variety of conditions and fitted to a general equation.

$$t_e = \frac{0.005\ x^{0.9294}}{u} \tag{14}$$

where

t_e is the effective time of dosage accumulation (min)

0.9294 is the slope of the sigma-x curve

Given this effective time of exposure, one can then consider the time correction factor for the dosage[2] to compute the effective dosage at any distance.

$$M = 0.827\ t^{0.274} \qquad t > 2 \text{ min} \tag{15}$$

where

M is the factor by which the required dosage is increased

t is the time of dosage accumulation (min)

3.1.1 Two-Minute Corrected Dosage: Segment 1, $X < X_1$

By setting $t = t_e$ and multiplying D by the factor of M (combining equations 7, 14, and 15), the following equation can be used to calculate distance in segment 1. This equation is also subject to the condition that

$$x > [400\ u]^{1.076}$$

which represents the distance at which the time of dosage accumulation will exceed 2 minutes as calculated from equation 14.

$$x = \left[\frac{Q}{36.51\ \sigma_{y1}\sigma_{z1}\ D\ u^{0.726}}\right]^{1/\alpha+\beta+0.255} \qquad \text{for } X_1 > X > X_T \tag{16}$$

where

$$X_T = (400\ u)^{1.076}$$

For $X < X_1$ and X_T, use equation 7.

3.1.2 Two-Minute Corrected Dosage: Segment 3, $X > X_2$

By combining equations 9, 14, and 15, the 2-minute correction in segment 3 can be computed subject to the same restriction in t_e.

$$x = \left[\frac{Q}{29.13\ \sigma_{y1}\ H_m\ D\ u^{0.726}}\right]^{1/\alpha+0.255} \qquad X > X_2 \text{ and } X_T \tag{17}$$

3.1.3 Two-Minute Correction of Dosage: Segment 2, $X_1 < X < X_2$

Following the same approach outlined above, when $X > X_T$,

$$D_1 = \frac{Q}{36.51\ \sigma_{y1}\sigma_{z1}\ u^{0.726} X_1^{\alpha+\beta+0.255}} \tag{18}$$

$$D_2 = \frac{Q}{29.13\ \sigma_{y1}\ H_m\ u^{0.726} X_2^{\alpha+0.255}} \tag{19}$$

The distance is then computed using equations 12 and 13. If $X < X_T$, then equations 10 and 11 are used instead of equations 18 and 19.

3.2 Semicontinuous Source with Two-Minute Correction. The special computer program referred to in section 3.1 was executed for a range of release times to provide estimates of t_e for the semicontinuous release. These data were fitted to a generalized model as follows:

$$t_e = \left[0.281\ t_s^2 + \frac{0.000025}{u^2}\ x^{1.8588} \right]^{1/2} \tag{20}$$

where

t_s is the source release time (min)

For small values of X, equation 20 takes on a constant value based on the value of t_s. At large values of X, the values are the same as those obtained from equation 14. In the transition between these two extremes, the value of t_e is underestimated slightly which in turn provides a safe-sided estimate of hazard distance.

3.2.1 Semicontinuous Source with Two-Minute Correction. Segment 1

Following the approach outlined in section 3.1.1, the equation for the hazard distance to doage, D, from source, Q, is as follows:

$$\left[0.281\ t_s^2 + \frac{0.000025}{u^2}\ x^{1.8588} \right]^{0.137} x^{\alpha+\beta} = \frac{Q}{155.9\ \sigma_{y1}\sigma_{z1}\ u\ D} \tag{21}$$

$$X_1 > X > X_{TS}$$

where

$$X_{TS} = \left[\frac{(4 - 0.281\ t_s^2)\ u^2}{0.000025} \right]^{0.538} \qquad (22)$$

For values of $X < X_1$ and X_T, equation 7 is used.

It is noted that equation 21 is not solved for the downwind distance, X. Due to the form of the equation, it was decided to arrive at a value of X by successive approximation. This approach is practical on a programmable electronic calculator of the pocket-size variety. (Experience has shown that some solutions can take a minute or more, but it's automatic and it does get there.)

3.2.2 Semicontinuous Source with Two-Minute Correction. Segment 3

Distances that fall in segment 3 are computed in a similar manner using the following:

$$\left[0.281\ t_s^2 + \frac{0.000025}{u^2}\ x^{1.8588} \right]^{0.137} x^{\alpha} = \frac{Q}{124.4\ \sigma_{y1}\ H_m\ D\ u} \qquad (23)$$

$$X > X_2 \text{ and } X_{TS}$$

3.2.3 Semicontinuous Source with Two-Minute Correction. Segment 2, $X > X_{TS}$

The values of D_1 and D_2 are computed in segment 2 from the following equations:

$$D_1 = \frac{Q}{155.9\ \sigma_{y1}\sigma_{z1}\ u\ X^{\alpha+\beta}} \left[0.281\ t_s^2 + \frac{0.000025}{u^2}\ X_1^{1.8588} \right]^{-0.137} \qquad (24)$$

$$D_2 = \frac{Q}{124.4\ \sigma_{y1}\ H_m\ u\ X^{\alpha}} \left[0.281\ t_s^2 + \frac{0.000025}{u^2}\ X_2^{1.8588} \right]^{-0.137} \qquad (25)$$

4. COMPUTATIONS WITH THE SIMPLIFIED METHODOLOGY

With the exception of equations 21 and 23, all of these equations can readily be solved on a pocket calculator which has a fractional power function (y^x). The only complication is the determination of the proper segment and, thus, the selection of the proper equation for X. The complete logic for making this selection is shown in Figure 1.

In order to test the simplified methodology and the logic in Figure 1, two Fortran computer programs were written. These programs contain 42 and 56 statements as compared to 334 for subroutine DOSDIS. One provides solutions for instantaneous releases and the other for semicontinuous releases. Each program has the option of solving either the total dosage or 2-minute corrected dosage methodology. These programs are very similar and one program could provide all four solutions if provisions were made to select the proper reference sigma-y values for instantaneous and continuous solutions. The two Fortran programs are listed in Appendix A, where the inputs are defined.

Once the logic was tested with the Fortran program, this approach was coded for the TI-59 pocket calculator. The 60 memory words were used to store the stability-dependent parameters (σ_{y1}, σ_{z1}, α, β, C_1, C_2) so that the set required for any specific run could be selected by indirect addressing.

These programs were published as SINST and SSCS in ARCSL-TR-78010, A Simplified Methodology for Computing Chemical Hazard Distances, dated January 1978.

5. THE FIELD HANDBOOK

Programs SINST and SSCS had proven that a pocket calculator with the simplified methodology could provide estimates of the downwind chemical hazard, but they still were not a very neat (efficient) package for field use. It was decided to combine the instantaneous and semicontinuous into one program and, if possible, add source geometry and the inhalation-deposition model from Technical Paper No. 10.

The approach of solving for X as a function of D was abandoned in favor of D as a function of X. In this approach, the dosage is calculated at successively larger distances until the dosage falls below the value of interest. The last two values are then used to interpolate for X at the required dosage.

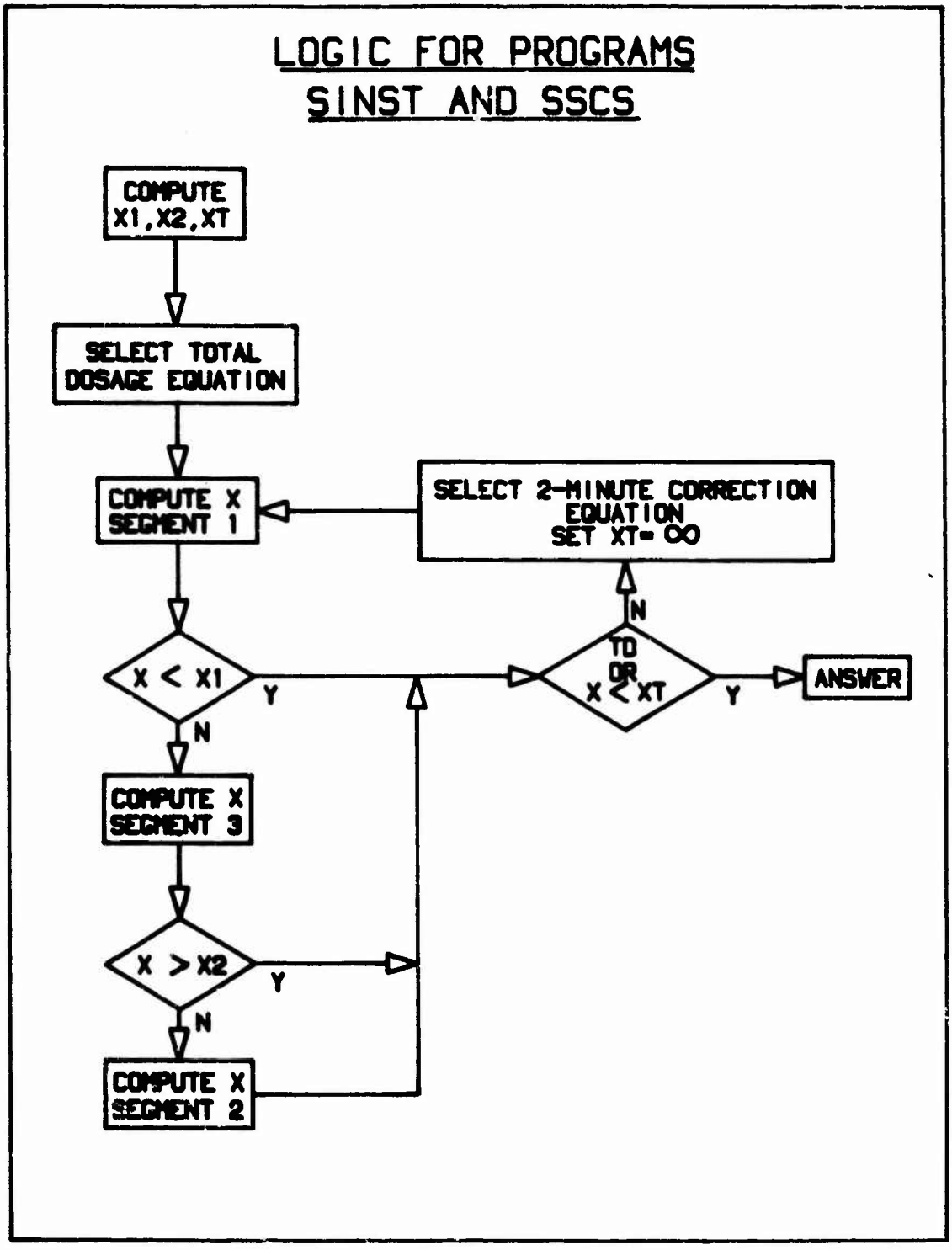
LOGIC FOR PROGRAMS
SINST AND SSCS
COMPUTE X1, X2, XT
SELECT TOTAL DOSAGE EQUATION
COMPUTE X SEGMENT 1
SELECT 2-MINUTE CORRECTION EQUATION SET XT= ∞
N
X < X1
Y
TD OR X ≤ XT
Y
ANSWER
N
COMPUTE X SEGMENT 3
X > X2
Y
N
COMPUTE X SEGMENT 2

FIGURE 1

Program SGDX was designed as a short general purpose dosage as a function of X calculator. The loop which estimates dosage or intravenous dose contains four statements which are executed selectively to solve either the Gaussian or the Box Models with or without 2-minute correction and with or without inhalation-deposition. These are lines 39 through 42 of the Fortran listing given in Appendix A. The logic for Program SGDX is shown in Figure 2.

By using the available options, Program SGDX will solve all the variations of the diffusion model presented in the Handbook. The TI-59 program code is listed in Appendix B.

To round out the methodology from Technical Paper No. 10 and the Handbook, Program SEVP was written to compute the evaporation rate from a spill. This is a shortened version of subroutine EVAP reported in ARCSL-TR-77049.

Subroutine STAB was expanded to compute the sun elevation angle given location, date, and time. The new program is called PSST (Pasquill Stability Selector after Turner). With the other inputs (cloud cover, cloud height, and wind speed), this program will select the Pasquill stability category for a given place and time. Figure 3 is a flow chart of Program PSST. The Fortran program is listed in Appendix A and the TI-59 code, in Appendix B.

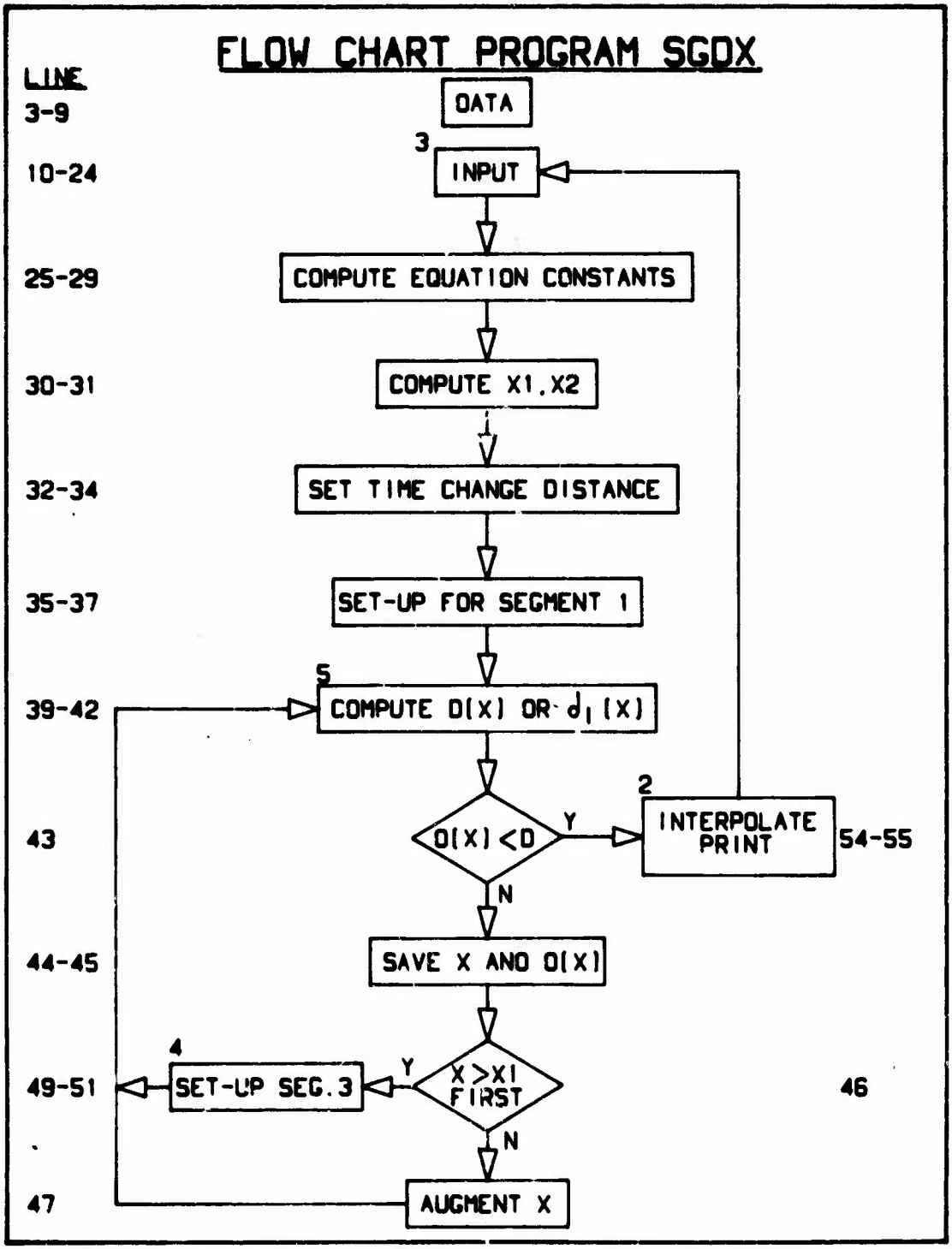
FLOW CHART PROGRAM SGDX
LINE
3-9
DATA
3
10-24
INPUT
25-29
COMPUTE EQUATION CONSTANTS
30-31
COMPUTE X1, X2
32-34
SET TIME CHANGE DISTANCE
35-37
SET-UP FOR SEGMENT 1
5
39-42
COMPUTE D(X) OR $d_1(X)$
2
43
D(X) <0
Y
INTERPOLATE PRINT
54-55
N
44-45
SAVE X AND D(X)
4
49-51
SET-UP SEG. 3
Y
X >X1 FIRST
46
N
47
AUGMENT X

FIGURE 2

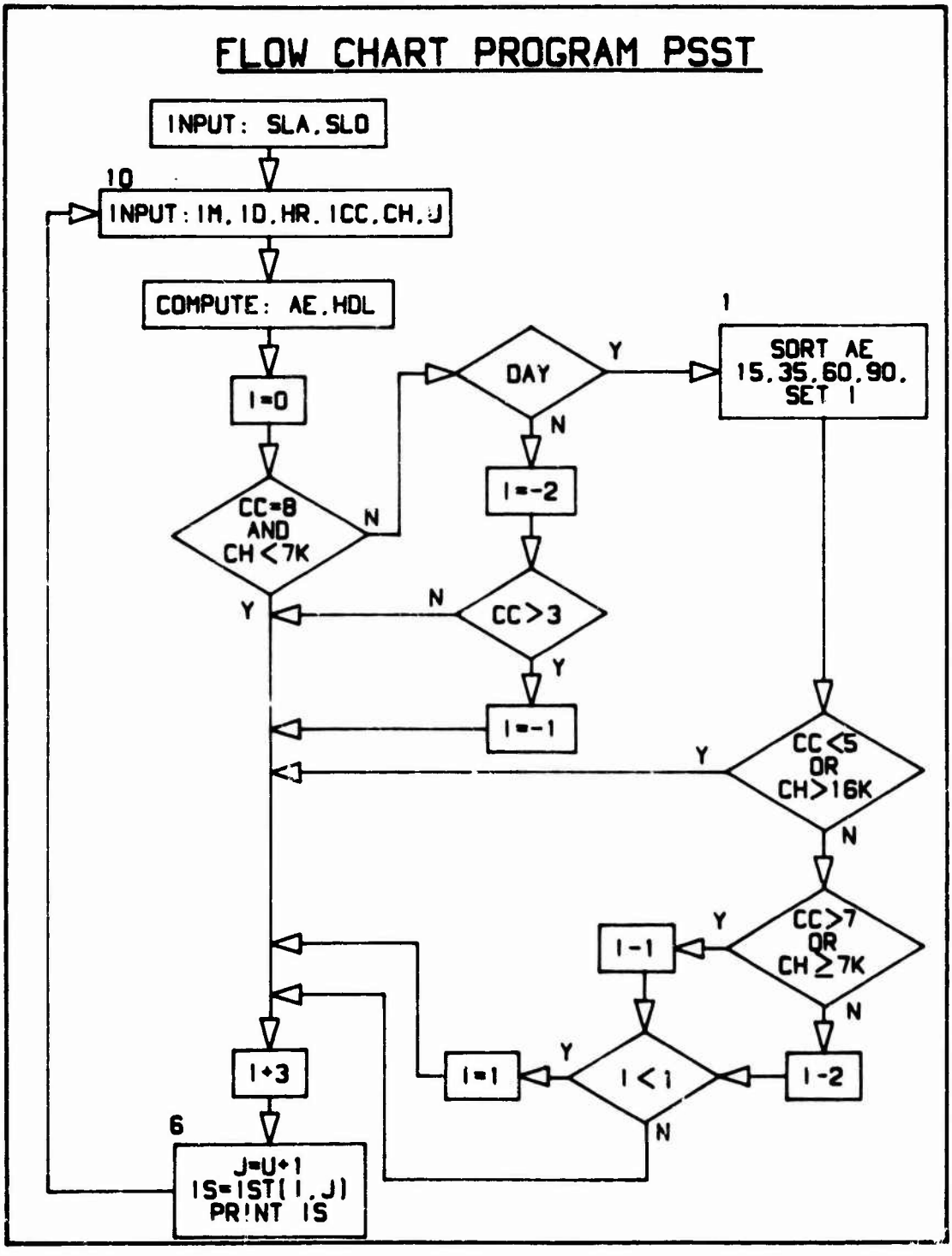
FLOW CHART PROGRAM PSST
INPUT: SLA, SLO
10
INPUT: IM, ID, HR, ICC, CH, J
COMPUTE: AE, HDL
I=0
DAY
Y
N
1
SORT AE
15, 35, 60, 90,
SET 1
I=-2
CC=8
AND
CH<7K
N
Y
N
CC>3
Y
I=-1
CC<5
OR
CH>16K
Y
N
CC>7
OR
CH≥7K
Y
I-1
N
I+3
I=1
Y
I<1
I-2
N
6
J=J+1
IS=IST(I,J)
PRINT IS

FIGURE 3

REFERENCES

1. Handbook for Chemical Hazard Prediction. Safety Document. US Army Materiel Development and Readiness Command. March 1977.

2. Methodology for Chemical Hazard Prediction. Department of Defense Explosives Safety Board Technical Paper No. 10. March 1975.

3. Whitacre, C. Glenvil, Robinson, Philip E., Kneas, William L., and Freeman, Alan L. ARCSL-TR-77049. Computer Program for Chemical Hazard Prediction. June 1977. UNCLASSIFIED Report.

4. Milly, George H. ORG Study No. 17. Atmospheric Diffusion and Generalized Munitions Expenditures. Operations Research Group. Army Chemical Center, Maryland. May 1958.

APPENDIX A

FORTRAN PROGRAMS

Program SINST estimates the distance to a specified dosage of interest for either total dosage or 2-minute corrected dosage.

When Program SINST is executed, it will request the following information:

INPUT: Q, u, D, HML, IS, IT

where

Q is source strength (mg)

u is wind speed (m/sec)

D is dosage ($mg\text{-}min/m^3$)

HML is height of the mixing layer (m)

IS is one of digits 1 through 6 corresponding to stability categories A through F

IT is an indicator, IT = 0 for total dosage

IT = 1 for 2-minute correction

Variable format is followed. All real numbers are written with a decimal point and fields are separated by commas.

The program outputs X_1, X_2, and X,

where

X_1 is the distance at which reflection from the inversion cap begins

X_2 is the distance at which vertical mixing is uniform

X is the distance at which the dosage of interest occurs

Program SSCS estimates the distance to a specified dosage of interest from a semicontinuous (uniform release for a finite time) source. The estimate is made for either total dosage or 2-minute correction. When Program SSCS is executed, the following input is requested:

INPUT: Q, TS, u, D, HML, IS, IT

where

TS is the release time (min)

Program SGDX

The program will type:

INPUT: Q, SYS, SZS, TS, u, D, HML, IS, IT

where

Q is the source (mg)

SYS is the source sigma-y (m)

SZS is the source sigma-z (m)

TS is the source release time (min)

(TS = 0 is instantaneous)

u is the wind speed (m/sec)

D is the dosage of interest ($mg\text{-}min/m^3$)

Intravenous dose, d_I, (mg) when IT = 3 or 4

HML is the height of the mixing layer (m)

IS is one of digits 1 through 6 indicating stability

(IS = 7 will request meteorological parameters)

IT is an indicator, IT = 1 for total dosage

IT = 2 for 2-minute correction

IT = 3 for inhalation-deposition

IT = 4 for inhalation-deposition without 2-minute correction

The line continues to type headings for the output columns, X_1, X_2, and X. As soon as the value of IT is input and the return key is pressed, the computer will complete the calculation and list X_1, X_2, and X on the next line. The program is then ready for the next set of input values, starting with Q.

Optional Inputs

If IS in the above statement is input as 7, the program will request the following:

INPUT: ALF, SY1, BTA, SZ1, C_1

where

ALF is the slope of the sigma-y curve

SY1 is the reference sigma-y at X = 1

BTA is the slope of the sigma-z curve

SZ1 is the reference sigma-z at X = 1

C_1 is the reference value for computing X_1 (see text)

Program PSST

The program will request:

INPUT: SLA, SLO

where

SLA is the station latitude

SLO is the station longitude

The program will then request:

INPUT: IM, ID, HR, ICC, CH, u

where

IM is the number of the month

ID is the day of the month

HR is the time in hours (24-hour day)

ICC is the cloud cover, in eights (1/8)

CH is the cloud height (ft)

u is the wind speed (m/sec)

The program will output sunrise, sunset, sun elevation angle, and the selected stability. The times for sunrise and sunset are output in hours and minutes; the sun elevation angle is in degrees. The program loops back to the input of IM, ID, HR, etc., if additional runs are needed.

THIS PAGE IS BEST QUALITY PRACTICABLE
FROM COPY FURNISHED TO DDC

PRØGRAM SINST

```
      C  SHØRT TØTAL DØSAGE (IT=0)/SHØRT 2-MIN CRT (IT=1)/SA0/CCW
         DIMENSIØN SY1(6),ALF(6),SZ1(6),BTA(6),C1(6),C2(6)
         DATA SY1/.09,.0633,.048,.0634,.0754,.0796/
         DATA SZ1/.0222,.11,.119,.0898,.0879,.0791/
         DATA ALF/1.,1.,1.,.9,.8,.7/
         DATA BTA/1.4,1.,.9,.85,.8,.75/
         DATA C1/10.5,5.5,6.13,9.49,11.2,15.3/
         DATA C2/15.9,9.55,11.2,18.1,21.9,31.1/
       3 PRINT 101
     101 FØRMAT ('INPUT: Q,U,D,HML,IS,IT')
         READ 100,Q,U,D,HML,IS,IT
         APB=ALF(IS)+BTA(IS)
         HRB=HML**(1./BTA(IS))
         ALFI=ALF(IS)
         XT=1.E36
         IF (IT .EQ. 1) XT=(400.*U)**1.076
         X1=C1(IS)*HRB
         X2=C2(IS)*HRB
         QYZDU=Q/(188.4*SY1(IS)*SZ1(IS)*D*U)
         QYHDU=QYZDU*1.253*SZ1(IS)/HML
       5 X=QYZDU**(1./APB)
         IF (X .LT. X1) GØ TØ 4
         X=QYHDU**(1./ALFI)
         IF (X .LT. X2) GØ TØ 2
       4 IF (X .LT. XT) GØ TØ 1
         UE=U**.274/.1937
         QYZDU=QYZDU*UE
         QYHDU=QYHDU*UE
         APB=APB+.255
         ALFI=ALFI+.255
         XT=1.E36
         GØ TØ 5
       2 D1=QYZDU/X1**APB
         D2=QYHDU/X2**ALFI
         S=LØG(X2/X1)/LØG(D2/D1)
         X=X1/D1**S
         GØ TØ 4
       1 PRINT 200,X1,X2,X
         GØ TØ 3
     100 FØRMAT ( )
     200 FØRMAT(23X,'  X1=',1PE10.3,'  X2=',E10.3,'  X=',E10.3,' M')
         END
```

THIS PAGE IS BEST QUALITY PRACTICABLE
FROM COPY FURNISHED TO DDC

PRØGRAM SSCS

```
      C  SHØRT SEMI-CØNT (IT=0) W/2-MIN CØRR (IT=1)/SA0/CGW
         DIMENSIØN SY1(6),ALF(6),SZ1(6),BTA(6),C1(6),C2(6)
         DATA SY1/.27,.1899,.125,.1268,.1508,.1592/
         DATA SZ1/.0222,.11,.119,.0898,.0879,.0791/
         DATA ALF/1.,1.,1.,.9,.8,.7/
         DATA BTA/1.4,1.,.9,.85,.8,.75/
         DATA C1/10.5,5.5,6.13,9.49,11.2,15.3/
         DATA C2/15.9,9.55,11.2,18.1,21.9,31.1/
         PRINT 101
     101 FØRMAT(' INPUT: Q,TS,U,D,HML,IS,IT',6X,'X1',8X,'X2',8X,'X (M)')

       3 READ 100,Q,TS,U,D,HML,IS,IT
         APB=ALF(IS)+BTA(IS)
         HRB=HML**(1./BTA(IS))
         ALFI=ALF(IS)
         ET=.281*TS*TS
         RU=.000025/(U*U)
         X1=C1(IS)*HRB
         X2=C2(IS)*HRB
         QYZDU=Q/(188.4*SY1(IS)*SZ1(IS)*D*U)
         QYHDU=QYZDU*1.253*SZ1(IS)/HML
         IF (IT .EQ. 0) GØ TØ 5
         XT=0.
         IF (TS .GT. 3.77) GØ TØ 6
         XT=((4.-ET)/RU)**.538
       5 X=QYZDU**(1./APB)
         IF (X .LT. X1) GØ TØ 4
         X=QYHDU**(1./ALFI)
         IF (X .LT. X2) GØ TØ 2
       4 IF (X .LT. XT .ØR. IT .EQ. 0) GØ TØ 1
       6 CALL XE(QYZDU,APB)
         IF (X .LT. X1) GØ TØ 1
         CALL XE(QYHDU,ALFI)
         IF (X .GT. X2) GØ TØ 1
         QYZDU=QYZDU/(.827*(ET+RU*X1**1.8588)**.137)
         QYHDU=QYHDU/(.827*(ET+RU*X2**1.8588)**.137)
         XT=1.E36
       2 D1=QYZDU/X1**APB
         D2=QYHDU/X2**ALFI
         S=LØG(X2/X1)/LØG(D2/D1)
         X=X1/D1**S
         GØ TØ 4
       1 PRINT 200,X1,X2,X
         GØ TØ 3
     100 FØRMAT ( )
     200 FØRMAT (25X,3F10.0)
         SUBRØUTINE XE(FQ,P)
         E=FQ/.827
         X=0.
         DX=1.E5
       7 X=X+DX
         IF (((ET+RU*X**1.8588)**.137*X**P) .LT. E) GØ TØ 7
         X=X-DX
         DX=DX/10.
         IF (DX .GE. 1.) GØ TØ 7
         RETURN
         END
```

THIS PAGE IS BEST QUALITY PRACTICABLE
FROM COPY FURNISHED TO DDC

PRØGRAM SGDX

```
      C  SHØRT INST(TS=0)/SEMI-CØNT  W/MIXING LAYER  W/TD(IT=1)
      C  W/2-MIN-CRT(IT=2)  W/VX INH-DEP(IT=3)  W/SRC SIG /SA0/CGW
         DIMENSIØN SYII(6),SYIC(6),ALF(7),SZI(7),BTA(7),CI(7)
         DATA SYII/.09,.0633,.048,.0634,.0754,.0796/
         DATA SYIC/.27,.1899,.125,.1268,.1508,.1592/
         DATA SZI/.0222,.11,.119,.0898,.0879,.0791,0./
         DATA ALF/1.,1.,1.,.9,.8,.7,0./
         DATA BTA/1.4,1.,.9,.85,.8,.75,0./
         DATA CI/10.5,5.5,6.13,9.49,11.2,15.3,0./
         PRINT 101
     101 FØRMAT(' INPUT: Q,SYS,SZS,TS,U,D,HML,IS,IT',
        $6X,'X1',8X,'X2',8X,'X (M)')
       3 READ 100,Q,SYS,SZS,TS,U,D,HML,IS,IT
         IF (IT .NE. 0) GØ TØ 7
         PRINT 102
     102 FØRMAT (' INPUT: TMP,NM,IT')
         READ 100,TC,FNM,IT
         Q=Q*(.5+.00782*TC)*FNM
       7 SYI=SYIC(IS)
         IF (TS .EQ. 0.) SYI=SYII(IS)
         IF (IS .NE. 7) GØ TØ 8
         PRINT 103
     103 FØRMAT (' INPUT: ALF,SYI,BTA,SZI,CI')
         READ 100,ALF(7),SYI,BTA(7),SZI(7),CI(7)
       8 B=(SYS/SYI)**(1/ALF(IS))
         C=(SZS/SZI(IS))**(1./BTA(IS))
         QFI=Q*.01*U**2.38
         ET=.281*TS*TS
         RU=.000025/(U*U)
         X1=CI*HML**(1./BTA(IS))
         X2=X1*1.76/BTA(IS)**.468
         XT=0.
         IF (ET .LT. 4.) XT=((4.-ET)/RU)**.538
         IF (IT .EQ. 1 .ØR. IT .EQ. 4) XT=1.E36
         XC=X1
         QF=Q/(188.5*SYI*SZI(IS)*U)
         X=10.
       5 IF (X .GT. XC) X=X1
         D2=QF/(X+B)**ALF(IS)
         IF (X .LE. X1) D2=D2/(X+C)**BTA(IS)
         IF (X .GT. XT) D2=D2/(.827*(ET+RU*X**1.8588)**.137)
         IF (IT .GT. 2) D2=.00325*D2+QFI/X**2.38
         IF (D2 .LT. D) GØ TØ 2
         XS=X
         DI=D2
         IF (X .EQ. X1) GØ TØ 4
         X=X*1.584893192
         GØ TØ 5
       4 XC=1.E36
         QF=Q/(150.4*SYI*HML*U)
         X=X2
         GØ TØ 5
       2 IF (X .EQ. 10.) GØ TØ 6
         X=XS*(D/DI)**(ALØG(X/XS)/ALØG(D2/DI))
       6 PRINT 200,X1,X2,X
         GØ TØ 3
     100 FØRMAT ( )
     200 FØRMAT (33X,3F10.0)
         END
```

THIS PAGE IS BEST QUALITY PRACTICABLE
FROM COPY FURNISHED TO DDC

PRØGRAM PSST

```
      C  PASQUILL STABILITY CATEGØRY SELECTØR/ TURNER/ SA0 CGW
         DIMENSIØN AC(4),IST(7,8),ISTA(6),IDC(12),SE(4)
         DATA AC,ISTA/15,35,60,90,'A','B','C','D','E','F'/
         DATA IST/6,6,4,3,2,1,1, 6,6,4,3,2,2,1, 6,5,4,4,3,2,1,
        $          6,5,4,4,3,2,2, 5,4,4,4,3,3,2, 5,4,4,4,4,3,3,
        $          4,4,4,4,4,3,3, 4,4,4,4,4,4,4,3/
         DATA IDC/0,0,3,3,4,4,5,5,5,6,6,7/
         DATA VE,SE,HY/79.9775,92.78,93.64,89.83,89.,182.62/
         DATA PH,PI,P2,RD/1.570796,3.141593,6.283185,57.2958/.
         PRINT 101
     101 FØRMAT (' INPUT: SLA, SL0')
         READ 100,SLA,SL0
     100 FØRMAT ( )
         A=SLA/RD
         PRINT 102
     102 FØRMAT (' INPUT:IM,ID,HR,ICC,CH,U'10X,'SR',4X,'SS',
        $ 4X,'AE',4X,'STB')
      10 READ 100,IM,ID,HR,ICC,CH,U
         DJ=(IM-1)*31-IDC(IM)+ID
         DV=DJ-VE
         IF (DV .LT. 0.) DV=DV+365.
         DT=DV
         D0 7 I=1,4
         IF (DT .LT. SE(I)) G0 T0 8
       7 DT=DT-SE(I)
       8 DL=SIN(PH*((I-1)+DT/SE(I)))*.4091
         EQ=(10.*SIN((DV+89.)/HY*P2)+7.75*SIN((DV+78)/HY*PI))/60.
         HDL=AC0S(-.014538/C0S(A)/C0S(DL)-(TAN(A)*TAN(DL)))/.2618
         TC=12.+EQ+(SL0/15.-AINT(SL0/15.))
         SR=((TC-HDL)-AINT(TC-HDL))*.6+AINT(TC-HDL)
         SS=((TC+HDL)-AINT(TC+HDL))*.6+AINT(TC+HDL)
         AE=ASIN(SIN(A)*SIN(DL)+C0S(A)*C0S(DL)*C0S((HR-TC)*.2618
         I=0
         IF (ICC .EQ. 8 .AND. CH .LT. 7000.) G0 T0 6
         IF (HR .GT. (13.-HDL) .AND. HR .LT. (11.+HDL)) G0 T0 1
         I=-2
         IF (ICC .GT. 3) I=-1
         G0 T0 6
       1 D0 2 I=1,4
         IF (AE .LT. AC(I)) G0 T0 3
       2 C0NTINUE
         I=4
       3 IF (ICC .LT. 5 .0R. CH .GT. 16000.) G0 T0 6
         IF (ICC .GT. 7 .0R. CH .GE. 7000.) G0 T0 4
         I=I-2
         G0 T0 5
       4 I=I-1
       5 IF (I .LT.1) I=1
       6 I=I+3
         J=U+1.
         IF (U .GT. 6.) J=8
         IS=IST(I,J)
         PRINT 200,SR,SS,AE,ISTA(IS)
     200 FØRMAT (32X,3F6.2,4X,A1)
         G0 T0 10
         END
```

APPENDIX B

LISTING OF TI-59 CODE FOR PROGRAMS SINST, SSCS, SGDX, SEVP, PSST

Copies of Appendix B will be available from the author upon request.

THE CUTTING OF M-55 CHEMICAL ROCKETS WITH A 2kW CO_2 LASER

Ona R. Lyman

USAARRADCOM
U.S. Army Ballistic Research Laboratory
Aberdeen Proving Ground, MD

This work was sponsored and funded by the Project Managers Office for Chemical Demilitarization and Installation Restoration, Aberdeen Proving Ground, Edgewood Area, Maryland.

ABSTRACT

Background studies leading up to this task are described and the rationale for determining the feasibility of laser cutting of the M-55 rocket is given. The facilities for the experiment are described and experimental test plans presented. Early submission requirements preclude the presentation of experimental results in the written paper, but preliminary results should be available for oral presentation.

I. INTRODUCTION

The study of the feasibility of sectioning M-55 Chemical Rockets is the third task the Ballistic Research Laboratory (BRL) has undertaken for the Program Manager for Chemical Demilitarization and Installation Restoration (CDIR). Because information on the two previous tasks has received limited distribution, the results will be summarized here as background to the current program.

II. LASER CUTTING OF CHEMICAL PROJECTILES

The first task was to determine the feasibility of cutting chemical projectiles with high power continuous lasers. The results of this task are reported by Mr. K. Frank in BRL MR 2756[1]. The 155mm chemical projectile was selected for the test object. Because industrial facilities with no explosive handling capabilities were to be used, several inert projectiles were equipped with thermocouples as shown in Figure 1. The experimental cuts were made at United Technologies Research Center, at Harford, CT and at AVCO, Everett Research Laboratory. Laser power levels of 3kW, 6kW and 10.5kW were used. The 155mm projectile has a wall thickness of 1.5 cm at the place where the cuts were made. Cutting speeds of 1.48, 2.21 and 4.2 cms per sec were achieved using an oxygen gas jet to assist the cutting, see Figure 2. No

PRECEDING PAGE BLANK

measurable temperature increase was recorded at either thermocouple location during the cutting, although temperatures up to 150°C were recorded at the junction of the burster tube and projectile wall about 2 minutes after the cut. Temperatures in the wax explosive simulant reached a high of 82°C about 3 minutes after the cut. The experiments demonstrated that laser cutting of projectiles can be an efficient operation with CO_2 lasers available commercially.

A few experiments were also performed on completely inert M-55 rockets. Cutting speeds of 3.4 cm/sec were demonstrated for the fiberglass shipper/launcher tube, and 2.5 cm/sec for the shipper/launcher tube backed by the steel motor case with laser powers of 3.0 kilowatts.

III. LASER ASSISTED BURNING OF BURSTER TUBE EXPLOSIVES[2]

For this test series two types of burster tubes were filled with Composition B and Tetryl and tested. The burster tube diameters used were 2.54 cms and 4.1 cms of varied lengths. The burster tubes were placed inside a cylindrical steel shield with one end open which was surrounded by a sand bag barrier. The laser beam was brought into the shield via mirrors and focussed on the open end of the burster tube with a spherical mirror. The entire setup was outside the building housing the BRL 2kW CO_2 laser.

As might be expected the mass burning rate for the larger diameter tube was greater than that for the smaller tube, although not as much greater as the exposed area ratio. This may be explained by effects of the burster tube walls. When laser intensities, ranging from 18 kW/cm^2 to 0.2 kW/cm^2, were used to assist the burning, burning times were shortened considerably. Rather unexpectedly the length of the burster tube being tested was an important parameter. Laser assisted mass burning rates measured ranged from 4 grams/sec to 1.4 grams/sec compared to 0.4 grams/sec average for the Composition B filled tube burning unassisted. There are several anomolies that need to be investigated before a final model of laser assisted burster tube burning can be developed. These will be addressed when the current efforts on cutting M-55 rockets allow these tests to be scheduled. Regardless of the model development, it has been shown that laser assisted burning of burster tube explosives can reduce burning times by a factor of 3 or more.

IV. LASER CUTTING OF M-55 ROCKETS

In this section the reasoning that makes laser cutting of M-55 rockets a desirable goal and background data that indicate that there is a possibility for successful sectioning of the live munition will be discussed.

A. Background

The current procedure for cutting the M-55 chemical rocket into seven sections for demilitarization, uses circular saws under a sodium carbonate solution with the entire operation inside an agent confinement area. Maintainance, even of a routine nature, becomes a difficult, time-consuming operation under these conditions. Protective clothing is required for individuals performing maintainance work and decontamination is required after the work is completed. Initial testing has shown that commercial CO_2 lasers are capable of performing the cutting of the various rocket materials (i.e., aluminum, steel, and fiber-glass). Table I shows cutting speeds and power requirements obtained by Mr. Frank[1] for these materials. The advantage obtained by the laser is that the laser, and its auxillary equipment, can be located externally to the agent containment structure thus making maintainance a rather easy routine task. Inside the containment structure only some relatively cheap beam steering and focussing mirrors are required in addition to material handling equipment. A method of getting the laser energy into the containment structure is required, but can be handled within the state-of-the-art and requires no special development program.

The one area of uncertainty in the laser sectioning of M-55 rockets is: can a laser be used to cut the rocket motor without igniting it? In searching the available literature there is evidence that suggests laser cutting of propellant may be possible. For non-reactive solid targets there exist a large number of papers which treat the heat transfer problem of laser irradiated targets (see Refs. 3, 4, 5 for example). Harrach[6] has developed a model for thermal ignition of high explosive by lasers. In this paper he shows that at intensity levels above some critical value the explosive can be vaporized away without igniting the solid material. Table II, by Harrach, shows the predicted value for four explosives. Notice that the required intensities to exceed this critical intensity is well below levels obtainable with a rather modest CO_2 laser.

A variety of papers exist on the ignition of solid propellants by radiant energy. The most pertinent to our problem are Hightower[7], Bush and Williams[8], Liñán and Williams[9,10], Kindelan and Williams[11], Liñán and Crespo[12] and Kindelan and Liñán[13]. Hightower[7] used an arc image furnance as his ignition source for experiments on ammonium perchlorate propellants. He shows that ignitions times were shortest with Oxygen as the environmental gas and longest with Helium. A result attributable to the high values of specific heat and thermal conductivity of Helium compared to Oxygen.

The theory of ignition of solid materials exposed to uniform radiant flux of energy is developed in References 8 thru 13. In very general terms, three methods of ignition are developed which depend on the nature and composition of the propellant. One may have initiation of an exothermic reaction in the condensed phase of the propellant, or an

Table I. Cutting of Composite Cylinders by Gas-Assisted CO_2 Laser

t_1 mm	t_2 mm	t_3 mm	P kW	Gas -	Speed cm/s	T sec	W kWs
5.1	0	0	3.0	CO_2	3.50	7.9	24
5.1	2.5	7.6	3.0	O_2	2.54	10.9	33
5.1	2.5	8.9	6.0	CO_2	0.64	43.2	259
5.1	2.5	10.7	6.0	CO_2	0.42	65.8	295
5.1	2.5	0	6.0	CO_2	1.27	21.8	131
5.1	2.5	0	3.0	O_2	2.54	10.9	33
5.1	0	0	10.5	Air	17.0	1.6	16.8
5.1	2.5	9.7	10.5	He	2.54	10.9	114

t_1: wall thickness of outer cylinder (Fiberglass tube)

t_2: motor case (steel)

t_3: warhead (aluminum, innermost cylinder)

d_1 = 124.5mm

d_2 = 115mm, airspace between outer cylinder and rocket assembly

$(t_1 + t_2 + t_3)/d_1$ = 0.04 - 0.20

t: time required to complete circular cut

W = P.T: energy required for complete cut

NOTE: Data obtained on M55 rocket assembly

Table II.

Explosive	I* kW/cm^2
PETN	1.86
RDX	1.9
HMX	1.1
TNT	0.05

For values of I<I* the explosive is expected to burn, but for I>I* the explosive is expected to vaporize and be removed without igniting the solid material.

exothermic reaction at the surface of the propellant, or lastly an endothermic gasification process followed by an exothermic reaction in the gas phase adjacent to the solid surface. The effects of reactions rates, and thermal processes are explored in detail by Williams, Liñán, and Kindelan in the referenced papers. It is not at all clear how the proposed tests on the M-55 rocket motor will compare to these theoretical analyses, because the proposed tests are to be made on propellant encased in a motor case; the energy is delivered to a very small area; radiant energy intensities can be very large; and the spectral distribution of energy is very narrow, which may effect energy absorption. In spite of the uncertainty of success for these tests (success is defined as sectioning an M-55 rocket without igniting the propellant) the possible advantages justify a feasibility study.

B. Approach

The M-55 rocket must be cut in the 6 locations indicated in Figure 3 prior to treatment in the demilitarization process. You will note that three of the cuts must be made through the rocket motor. Furthermore, the cuts must be made with the rocket in its shipper/launcher tube. Thus, one must first cut through the fiberglass tube, then the steel motor case and then the propellant. Previous work (Ref. 1) shows that cutting of the shipper/launcher tube and the motor case present no problems. Therefore our efforts will be directed primarily toward the safe cutting of propellant.

The initial experiments will be performed with thin, ≈ 5mm thick, slices of M28 propellant from the rocket motor. A very finely focussed laser beam (diameter of the focal spot less than 1mm) will be used, and a jet of Helium gas will be used to dilute and cool the vaporized material from the solid propellant. This combination was selected as the most likely to result in successful cutting of the propellant. Once successful cutting is demonstrated the range of cutting parameters will be examined, i.e., laser power, focal spot diameter, sample feed rate, gas flow rate and angle of attack of the gas jet. After sufficient knowledge has been obtained thicker samples will be tested until thicknesses equal to the rocket motor radius have been tested. Following this test series will be experiments with a thin steel plate on the exposed surface of the propellant to simulate the motor case. Finally with all parameters optimized cutting tests will be performed on sections of M-55 rocket motors.

C. Progress

Prior to starting experimental work, a suitable location had to be found where it would be safe to work with the complete munition. It should be noted here that no tests with munitions containing chemical agents will be made in this test series or at this location. The actual rocket used will be the M-61 which is a training round identical to the M-55 rocket except that the M-61 contains no agent. Safe working

conditions for handling explosives and propellant are required however. The site selected was range 15 in the BRL test area on Spesutie Island at the Aberdeen Proving Ground. The existing reinforced concrete building at this location had to be expanded and the electrical service upgraded in order to accomodate the CO_2 laser. Figure 4 shows a drawing of the facility. This facility was completed in early June of 1978 and provides an excellent opportunity for laser experiments on explosives and propellants.

Although the BRL laser is rated for 2 kW of output power, power levels as high as 4 kW have been achieved. These outputs are multimode and consequently are not readily focussed to a small spot and tend to have radiation levels around the focal spot which have significant power. While the experimental site was being prepared the BRL CO_2 laser was returned to the manufacturer for modification. The major modifications included the installation of a rigid truss frame for mounting the laser mirrors and the installation of an unstable resonator mirror system. These modifications result in a laser output beam which is single mode and hence easily focusable. The total power out of the laser will be reduced, but intensities in the focal spot will be larger. Figure 5 shows a sketch of the unstable resonator configuration. One characteristic of this unstable resonator configuration is an output beam with an annular cross section. Figure 6 shows a focussing system which uses this characteristic to allow on axis spherical mirror focussing of the laser beam. This technique is appropriate for the pilot plant operations also as spherical mirrors are significantly cheaper than those with aspherical surfaces. Also it is important when using spherical mirrors to be able to perform experiments on the optic axis of the mirror to avoid aberrations.

D. Status

The schedule for this task has slipped principally because of construction delays in the modification of the building at the test range. Modifications were completed in June of 1978, and the laser system and optical system are being installed during July. Although there are no experimental results to report at this time it is hoped that some preliminary test data will be available for oral presentation at the September meeting.

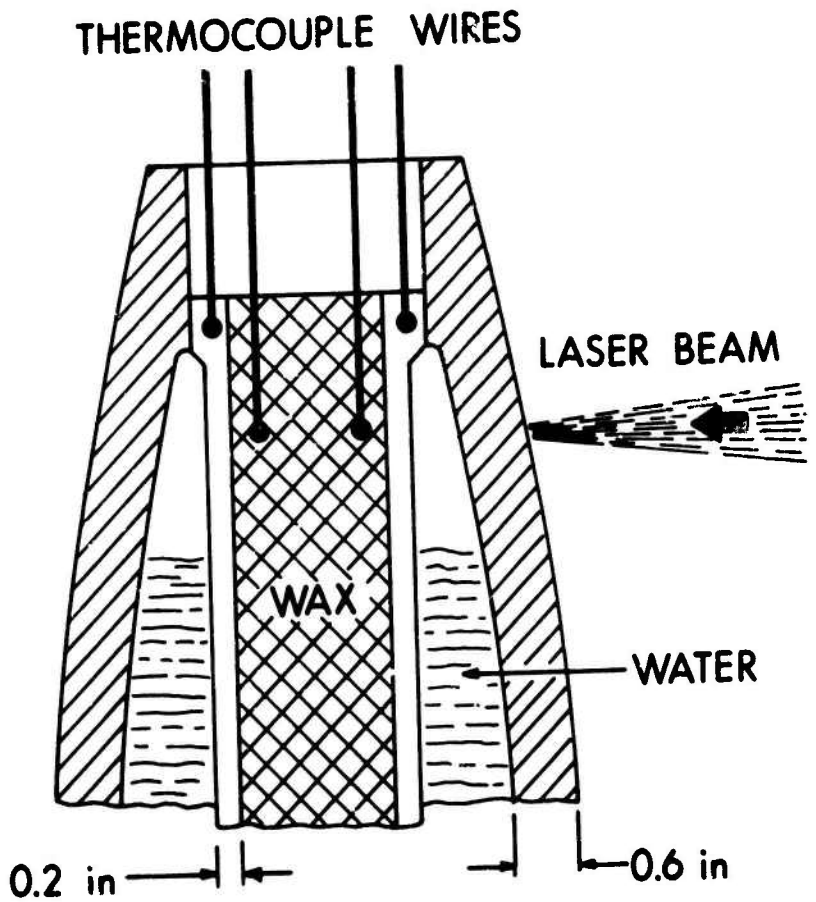

Figure 1. 155mm Inert Gas Projectile Showing Location of Thermal Sensors During Laser Cutting of the Projectile

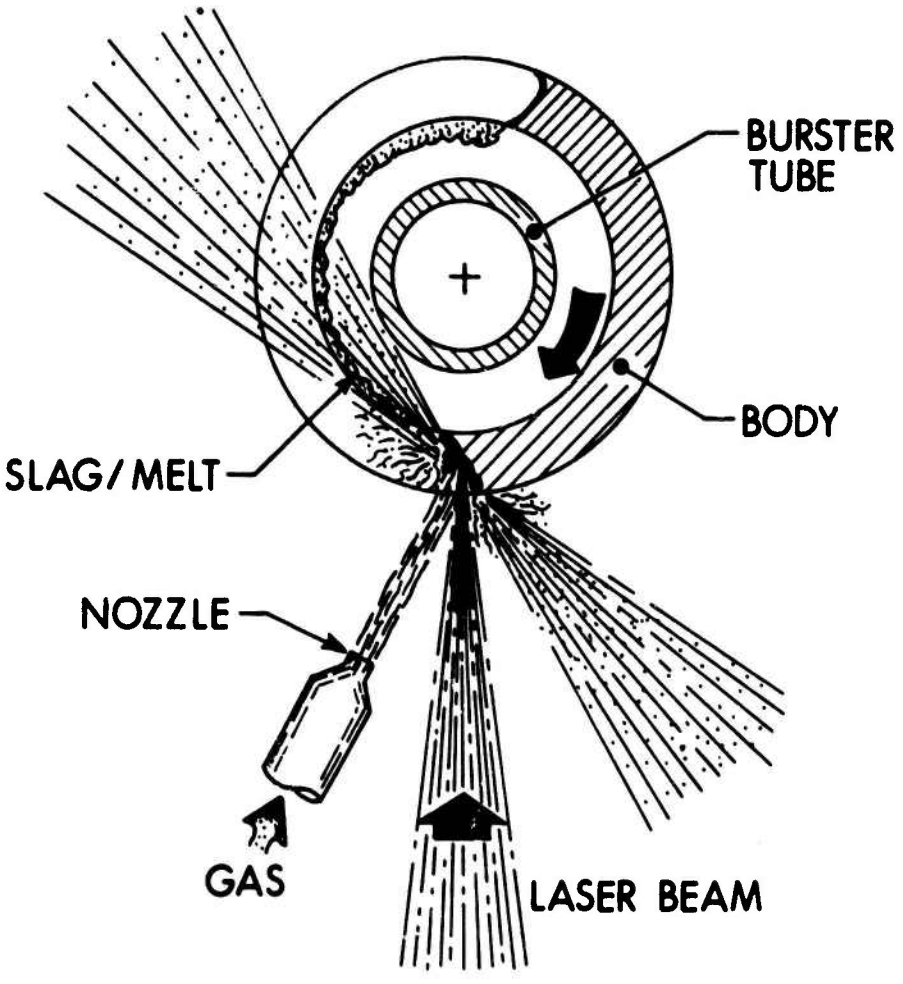

Figure 2. Orientation of Projectile, Laser Beam, and Gas Jet

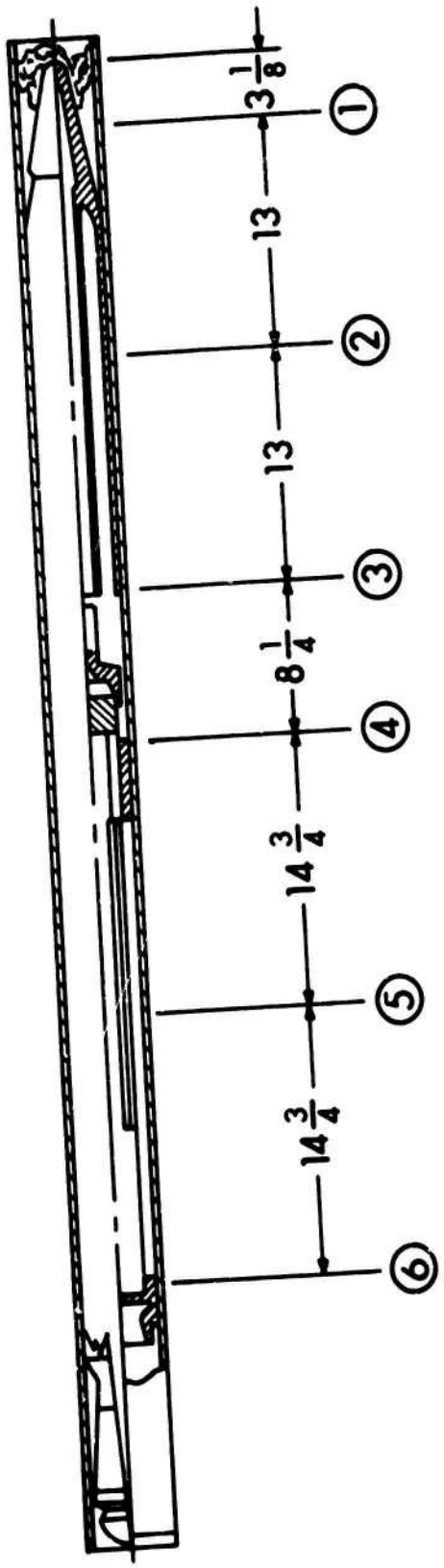

Figure 3. M-55 Rocket Showing Location of Desired Laser Cuts

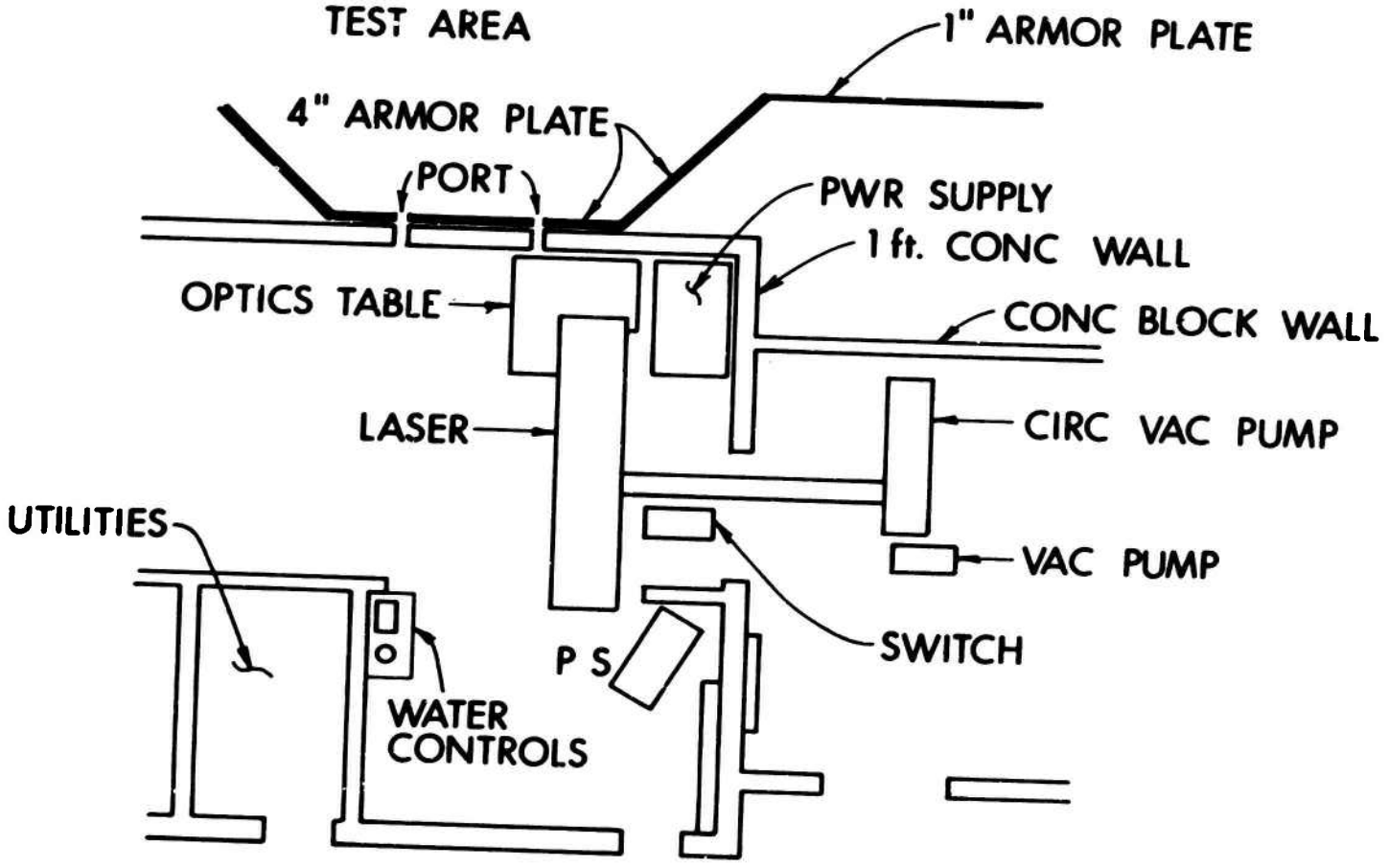

Figure 4. Plan of the Laser/Explosive Test Area

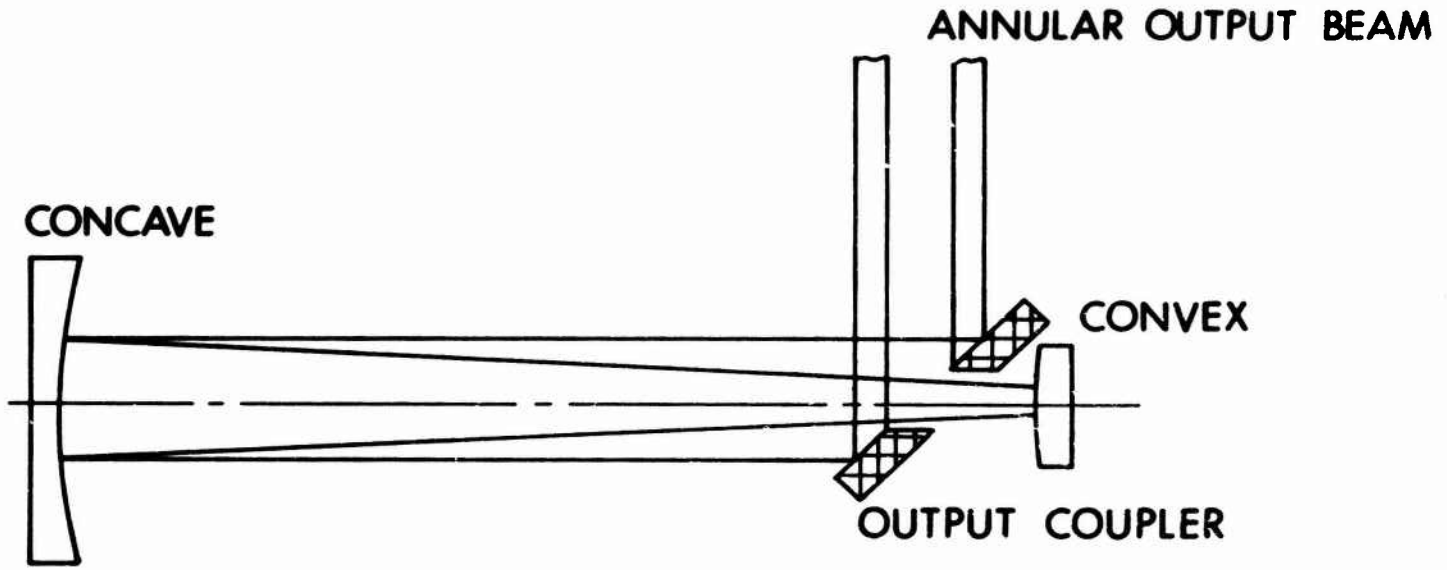

Figure 5. Unstable Resonator Mirror Configuration for the CO_2 Laser

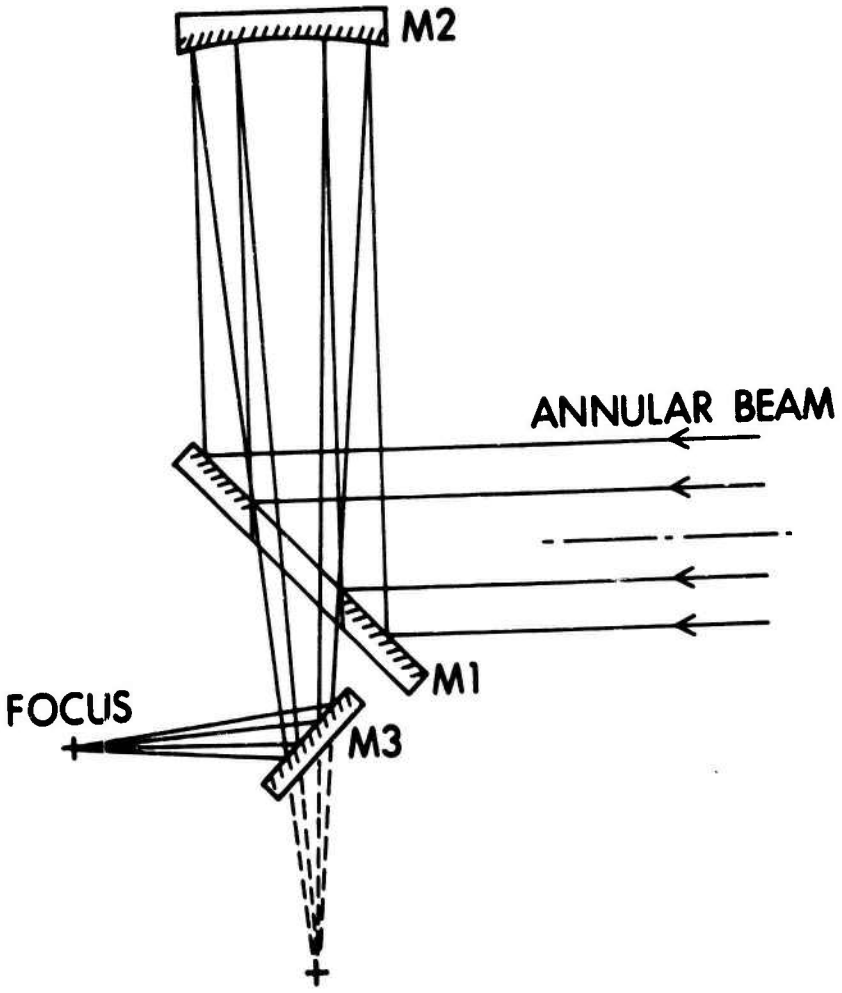

Figure 6. Diagram of the Focussing System for the Annular Crossection Laser Beam

REFERENCES

1. K. Frank and R. Roszak, BRL MR 2756, "Feasibility Experiments on the Demilitarization of Chemical Munitions by High Power Lasers. Part I: Cutting Experiments," June 1977.

2. J. Paszek, K. Frank, and R. Roszak, "Feasibility Experiments on the Demilitarization of Chemical Munitions by High Power Lasers. Part II: Burster Tube Burning Experiments," to be published.

3. Carslaw and Jaeger, Conduction of Heat in Solids, 2nd Edition, Oxford at the Clorendon Press, 1959.

4. W. W. Duley, "CO_2 Lasers, Effects and Applications," Academic Press, 1976.

5. H. J. Breaux, BRL R 1834, "Simple Formulas for CW Laser Burnthrough Times when Radial Heat Conduction is Significant," September 1975.

6. R. J. Harrach, "Estimates on the Ignition of High Explosives by Laser Pulses," Journal of Applied Physics, Vol. 47, No. 6, June 1976, pp 2473 - 2482.

7. Hightower, J. D., "Investigation of the Effect of Environmental Gases and Pressure on the Ignition of Solid Rocket Propellants," Naval Weapons Center, TP 4431, October 1967.

8. Bush, W. B. and Williams, F. A., "Radiant Ignition of a Surface-Cooled Reactive Solid," Acta Astronautica, Vol. 2, pp 445 - 462, Permagon Press, 1975.

9. Liñán, A. and Williams, F. A., "Theory of Ignition of a Reactive Solid by a Constant Energy Flux," Combustion Science and Technology, Vol. 3, pp 91 - 98, 1971.

10. Liñán, A. and Williams, F. A., "Radiant Ignition of a Reactive Solid with In-Depth Absorption," Combustion and Flame, Vol. 18, pp 85 - 97, 1972.

11. Kindelan, M. and Williams, F. A., "Radiant Ignition of a Combustible Solid with Gas - Phase Exothermicity," Acta Astronautica, Vol. 2, pp 955 - 979, Permogen Press, 1975.

12. Liñán, A. and Crespo A., "An Asymtotic Analysis of Radiant and Hypergolic Heterogeneous Ignition of Solid Propellants," Combustion Science and Technology, Vol. 6, pp 223 - 232, 1972.

13. Kindelan, M. and Liñán, A., "Ignition of a Reactive Material by Hot Gases," Air Force Office of Scientific Research, AROSR-TR-77-0004, Vol. 15, November 1976.

THE ROLE OF THE SAFETY MANAGER IN SUPPORT OF CHEMICAL DEMILITARIZATION PROGRAMS

I. INTRODUCTION

A. Good morning, my name is Lawrence Smith; I am the Safety Manager for the Office of the Project Manager for Chemical Demilitarization and Installation Restoration (OPMCDIR), Aberdeen Proving Ground, Maryland.

B. This portion of the Chemical Munitions Demilitarization and Hazard Prediction Session is devoted to a discussion of safety management methods and philosophy leading to the successful safety record compiled during the disposal of lethal chemical warfare agents and munitions during the past six years. This safety record is the result of a total commitment to safety and a team effort from the participating personnel of the Defense Department through the OPMCDIR and the installations where the programs were accomplished.

II. BACKGROUND

A. The OPMCDIR is responsible for providing intensive and centralized management for the timely and effective accomplishment of the demilitarization of hazardous chemical substances and munitions including lethal, incapacitating and other chemicals as specified by the Department of the Army.

B. Demilitarizatrion is the act of destroying the military advantages inherent in certain types of equipment or materiel. Demilitarization in effect, prevents the further use of equipment or materiel for its originally intended military or lethal purpose. More specifically, the chemical demilitarization process involves the following major technical steps:

PRECEDING PAGE BLANK

(1) Separation of the agent and the explosive components.

(2) Detoxification of the Agent.

(3) Thermal deactivation of the explosives.

(4) Decontamination of residual material.

C. The chemical demil projects represent a significant technical achievement. In a period of a few years, the Army has successfully planned, designed, fabricated, tested and operated complex facilities for the demil and disposal of toxic chemical agents and munitions. Since 1972 when the chemical demil office was formed, no fatalities or serious injuries have occurred in any demil operation sponsored by the Project Manager's Office. The following successful chemical demil operations have been completed with absolute safety to workers or nearby heavy populated areas:

COMPLETED CHEMICAL DEMIL PROGRAMS

Location	Completion Date	Agent	Item/Amount
Johnston Island	Nov 73	GB (nerve)	19 M55 Rockets
Rocky Mountain Arsenal	Mar 74	H (mustard)	3,407 Ton Containers
Rocky Mountain Arsenal	Nov 74	GB (nerve)	40,000 Gallons Stored in Underground Tanks
Edgewood Arsenal	Aug 75	Lethal and Nonlethal	65 Drums
Rocky Mountain Arsenal	Nov 75	GB (nerve)	2,422 Ton Containers
Rocky Mountain Arsenal	Aug 76	GB (nerve)	106 Honest John Warheads
			1,222 M139 Bomblets
			39,532 Bomblet Halves
Rocky Mountain Arsenal	Sep 76	GB (nerve)	21,114 M34 Cluster Bombs
Dugway Proving Ground	Sep 76	GB (nerve)	395 M55 Rockets
Dugway Proving Ground	Sep 77	GB (nerve)	1,515½ M139, E139 Bomblets
Rocky Mountain Arsenal	Mar 77	GB (nerve)	1 Weteye Bomb

D. This safe and successful record of the disposal of over 1,500,000 gallons of lethal chemical warfare agent is an exemplary accomplishment attributed to the planners, managers and workers of the OPMCDIR and the installations involved. These additional chemical demil programs are currently being planned or are nearing completion: Chemical Agent Munitions Disposal System, Drill and Transfer System, Agent AC Bomb Disposal, BZ Cluster Bomb Downloading, Agent CG Ton Container Disposal, and Chemical Agent Identification and Training Sets Demilitarization.

III. BASIC PRINCIPLES

Based upon my personal experience and training, I have defined three basic principles which I use in my role as a safety manager. These principles are emphasized throughout the life-cycle of a demil program and are integrated wherever possible. I think of these three principles as the keystones to hold together the eight elements of the Army safety program. These three principles are: assure management commitment; keep safety involved throughout; and interface completely with local safety personnel.

A. Management Commitment

As in all good safety programs, the necessary emphasis on safety must begin at the top and be carried through all echelons of management and supervision to the workers who actually perform the task. The OPMCDIR successful safety record is a reflection of a firm commitment by top Army management to a clearly defined safety policy for the enlistment of all echelons of management and supervision in support of the safety effort. This commitment to safety in chemical demil programs has been firmly defined by the Army as follows:

(1) Absolute safety.

(2) Maximum protection for operating personnel.

(3) Absolute assurance of total containment of agent.

(4) Incontrovertible data to justify personnel safety, security and community safeguards.

The effectiveness of the chemical demil safety program is dependent upon top management's active support of these commitments and the skill of the safety manager in focusing this support into a meaningful effort.

B. Local Safety Interface

OPMCDIR is considered a staff office and not an operational element. OPMCDIR managers and engineers cause actions to be taken by operating elements by providing plans, funds, direction and control of the program for the demilitarization of substances designed for disposal. The installation where the actual demil is done, supplies the manpower, utilities and support for accomplishing the program. Integration of past demil safety experience and site specific safety criteria developed during the early stages of a project must be carried through and implemented by the local installation. Local safety personnel must be consulted and plans coordinated with them to assure uniform direction of the safety program during day-to-day safety of construction and actual demil operations.

C. Safety Manager Involvement

It is my belief that the safety manager functions best as a coordinator of expertise. It is not his job to operate the system. Based upon the Army's total commitment to safety the safety manager's proper role is simply to make things happen. He is actually an influencer of action; he must influence other people to make the correct decisions or to make the necessary changes to guarantee equipment, facilities, procedures, and personnel conform to stringent safety criteria and can perform their intended operational functions. The job of the safety professional is no longer that of the engineer or technician alone. Short term corrections such as those usually resulting from routine safety inspections on the operating line are of relatively small impact to the total safety program in the long run. Those corrections which have a more permanent impact on the safety of operations are instituted during the initial planning and design of the program. Those who can bring more permanent solutions into effect are the project engineers, the managers. That is why the safety manager must work through management in order to be effective. By themselves, safety managers cannot prevent accidents. With the skill to influence the demil program managers, a safety manager can have significant influence even with a small staff. This influence must begin with the project concept and continue through the entire life of the project. Development of a chemical demil program follows a typical life cycle from start to finish. The safety manager's role in influencing this life cycle development is considerably strengthened if he is made aware of all program management plans as they develop and progress. It is much simpler and more acceptable to management if safety criteria is incorporated during the initial planning and design phases. A typical life cycle follows these stages:

(1) Design Concept

(2) System Development

(3) Authorization Documentation

(4) Equipment Fabrication/Facility Construction

(5) Project Systemization

(6) Preoperational Survey

(7) Operations

(8) Cleanup, Layaway

IV. INTEGRATION OF PRINCIPLES INTO PROJECT LIFE CYCLE

The degree of safety achieved in a demil project is directly dependent upon the skill of the Safety Manager in integrating these three general principles into the safety program at each stage of the project life cycle.

A. Design Concept

1. A concept proposing a technical approach to the conduct of the demil operation is developed. It may only be a paper study of alternatives or it may require a demonstration of the technical feasibility.

2. The safety manager's role is to highlight to management the special areas of safety consideration. He must provide safety references and requirements and identify standards which are not currently available and require development. Attendance at planning meetings is crucial to influencing and understanding management actions during this stage. Decisions will have major impact on the total project and must not compromise safety. Local safety personnel where the project will be consumated must be kept aware of plans and decisions as should safety personnel of any supporting organizations.

B. System Development

1. System development is the development and engineering of the project process and associated equipment and facilities. It could involve pilot or full scale equipment and process studies. Data will be generated to validate the process for scale-up. Equipment drawings, specifications, personnel requirements and site information will be prepared. Draft environmental documents will be prepared.

2. The safety manager must furnish or evaluate safety design criteria and participate in technical design program reviews. He must also describe safety tests or data needed and begin development or unavailable safety standards. Engineering drawings, maintenance manuals, demil plans, environmental plans and safety site plans must receive safety input. With a management commitment to safety obtained in earlier stages, the ability to influence design and plans is increased. Cooperating safety offices must be kept informed and assist in making decisions so that a uniform safety approach is achieved.

C. Authorization Documentation

1. A compilation of documents are needed to inform, justify, prove technical details and receive project approval. A safety assessment of the proposed location of the operation, a site plan, must be approved by DDESB. Hazard Zone Calculations defining a danger zone for a maximum credible accident must be submitted. A Final Safety Submission providing detailed procedures, facility descriptions, and technical documentation also must be submitted and approved by DDESB.

2. These documents are prepared by the installation where the work is to be accomplished with the aid of the OPMCDIR. The safety manager will assist in the preparation, review and staffing. He will answer any questions during the chain-of-command review and will remain a record of approvals.

D. Equipment Fabrication/Facility Construction

1. Full-scale process equipment will be fabricated or procured, necessary facilities and utilities erected, and process and support equipment and utilities unstalled. Ancillary equipment necessary to assure safety and environmental pollution control will also be erected. Standing operating procedures and employee training programs will be drafted.

2. The Safety Manager will attend management status reviews, visit the construction site and review its development against drawings to assure accurate incorporation of all safety designs. He will assure local safety personnel are included as the facility is constructed and will review or assist the local installation in the preparation of SOPs and training programs.

E. Project Systemization

1. The process and equipment will be evaluated during this phase to determine the capability of the facility to meet design goals as regards production rates, maintainability, personnel training, safety, and environmental controls.

2. The Safety Manager now aids the Program Managers in establishing test requirements and ensuring that safety verification of design criteria is included in the test program. He provides input to local operator training and reviews test data.

F. Preoperational Survey

1. Prior to conducting actual toxic chemical agent operations, an operation using simulated agent or inert items will be conducted. This is intended to permit identification and correction of any unsafe condition before conducting operations with hazardous materials.

2. To assure that facilities developed under OPMCDIR jurisdiction conform to approved safety criteria and can perform intended operational functions, a preoperational survey is conducted. Only upon a positive recommendation by the survey team and approval by the PM may actual toxic agents be introduced to the facility.

3. The Safety Manager acts as the chairman of the PMO preop team. Team members are assembled from organizations knowledgeable in agent operations. The local installation safety office and the next higher command safety office are requested to provide members. The survey team coordinates all recommendations with top management to assure the appropriate emphasis is given.

G. Operations

1. The production scale demil operation is carried out during this phase. The operation may take only a day or two or may continue for several years. The plant is operated on 1, 2, or 3 shifts depending on the requirements, money, and schedule developed. Engineering changes are made as experience is gained to increase productivity or safety.

2. The Safety Manager will monitor, inspect and audit the plant to assure safety achieved in design is maintained and adequate during operations. He will analyze accidents, incidents, and failures to identify unsafe conditions. He will review engineering change proposals (ECP), production improvement proposals (PIP), and operator deficiency reports to assure that safety is not degraded. He also conducts studies or pre-operational surveys of modifications and reviews operating and maintenance publication changes for safety requirements, cautions, etc.

3. These actions are conducted in cooperation with the local installation safety office and all recommendations or comments are discussed with the local commander and the OPMCDIR program managers.

H. Cleanup and Layaway

1. This phase covers the decontamination, dismantling, layaway or destruction of the equipment and facilities used during demilitarization operations. It also covers the disposal of any agent containers and by-products resulting from the demilitarization operations. In some instances the clean equipment may be transported to another site for reuse. In cases where sale or further handling by commercial firms is proposed, certification of the product as to safeness to handle and freedom from contamination must be furnished.

2. The Safety Manager will review cleanup and decontamination plans and SOPs. He will assist in coordinating approvals of decon levels and methods. Decon standards and limits for agent concentrations allowable following cleanup must be developed. He will also monitor the actual decontamination and disposal operations and assure materials for disposal are adequately marked and documented.

I. Top management commitment provides the necessary backing and authority for the Safety Manager. Safety Manager involvement throughout the program makes engineers and managers aware of safety interest, responsiveness, and availability for assistance in decision making. Local safety interface assures uniformity in directing the safety program from planning sessions to daily operations.

V. PITFALLS IN THE SAFETY MANAGER'S ROLE.

A. Two pitfalls, however, can reduce the effectiveness of the Safety Manager and must be avoided. One is the undue dependence on standards, regulations, and codes for the answers to all safety problems. The other is the inability to be reasonable and practical with engineers and managers when developing and implementing the safety program.

1. It would make the job of the safety manager rather simple and easy if mere conformance to written standards was an adequate assurance of safety. However, undue reliance on safety standards as a safety remedy may subvert professional management activities needed to assure adequate emphasis on the more significant, long-term safety program. Confronted by a mass of regulations, some managers have allowed themselves to define the safety mission as compliance with regulations rather than development of comprehensive planning. We must move away from the concept of code or regulation compliance only and spend more of our time in the area of an inclusive, all embracing safety program.

2. As an influencer of actions, the Safety Manager must routinely work with the project managers and engineers who are professionals at their jobs. He must maintain their respect for himself and their respect for uncompromising safety. Chemical demil is new and unique; safety guidance must be provided for unprecendented operations not covered by existing regulations or experience. In the absence of generally accepted and uniformly understood guidance, the Safety Manager must approach the implementation of the safety program with practicality and reasonableness. He should not claim exclusive jurisdiction over a body of knowledge but must listen to and accept the experience and concepts of the professional managers and engineers with whom he works. However, he must understand that the safety professional, as an expert in accident prevention, is held to a higher standard of care than those who are not. He must be flexible at times in the method of achieving safety, but he must also know where to draw the line and refuse to compromise.

VI. CONCLUSION.

A. Management commitment, safety involvement, and local interface have served to provide the safety program for chemical demil projects with the control and direction necessary to achieve our goals without harm to personnel or the environment. To accomplish this, the Safety Manager must be privy to all matters and must have direct access to the boss for a decision in the event he is unable to coordinate the necessary action. He must not put undue reliance on written standards and he must be flexible in his approach.

B. Safety is not a one-man show. Safety cannot be allowed to stagnate. Everyone must be involved and we must be alert to change and be ready to give thoughtful consideration to innovation. Safety is a choice and not an accident; that choice can be influenced by the role of the Safety Manager. Safety is a profession where the success is measured by counting the failures. The OPMCDIR, local installations, major and subordinate commands, and the Department of Defense, in cooperation, have been successful and have measured up to the job of lethal chemical demilitarization--while establishing an admirable safety record.

AN EVALUATION OF DRYING SYSTEMS FOR EXPLOSIVES

Prepared for:
The Eighteenth DOD Explosives Safety Board Seminar
12-14 September 1978
San Antonio, Texas

By:
E. P. Bergmann[1]
Alan Hartman[2]
A. B. Wenzel[3]

This paper summarizes work sponsored by Munitions Production Base Modernization, USARRADCOM

[1]Senior Engineer, Southwest Research Institute
[2]Munitions Production Base Modernization, ARRADCOM
[3]Director, Department of Ballistics and Explosives Sciences, Southwest Research Institute

PRECEDING PAGE BLANK

I. INTRODUCTION

This project was directed toward evaluating the options for drying "A" Composition products at Holston AAP, Kingsport, Tennessee. The products of interest are A-3, A-4, A-5 and A-7 explosives. Current drying methods used for Compositions A-3, A-4 and A-5 are not adequate for incorporation into continuous production lines. A faster and more efficient method of drying these compositions is required. The current A-7 production process incorporates three Wolverine Jetzone dryers to reduce the water content of the A-7 from approximately eight percent to two percent. Three dryers are used in series to effect the drying. These dryers have problems in controlling the start-up and steady state phases of production and in the tendency to generate relatively high levels of dust.

The primary objective of this program was to review drying alternatives and select the "best" dryer for each product-given no present investment and state-of-the-art drying capability. The second objective was to select the optimum dryer based on development to improve the current state-of-the-art. A third objective, developed during the course of the program, was to select the best alternative for line 1; the A-7 line in which the Wolverine dryers are installed. The primary and secondary objectives were met. There were insufficient data or funds to fully explore the background needed to provide a valid basis for selecting the best option for the third objective.

Three fundamental problems were encountered during this project which must be discussed briefly to put the proper prospective on the analysis. The first problem relates to the state-of-the-art of dryers. Text books on drying processes are generally vague on the relationship between the material, the initial moisture, the particular method of drying and the drying duration. This is primarily due to the lack of predictability of the drying process. Even such a simple problem

as predicting the time to evaporate water from a pan placed somewhere in a room is beyond the theoretical capability of drying technology. It is apparent, then, that the prediction of the drying capability is an empirical process whereby some experimentation is required before drying rates can be indicated.

The second problem relates to the difficulty in accurately predicting dryer costs. Part of the problem relates to the variability of manufacturers in their cost structure, part relates to the lack of publication of general cost trends of dryers and part relates to the vagueness of drying capability which reflects itself in the cost vagueness.

The third problem is the general lack of interest of dryer manufacturers. The market is small, the production run is short, the problem is difficult and there is a reluctance to "get involved with the government red tape." These problems, then, limit the depth of the engineering analysis that is fruitful and the rigor of the conclusions which can be drawn - but not necessarily the validity of the conclusions. The analysis that is presented in this report is not a strict cost/effectiveness study of dryer options. It is, however, an engineering assessment of eight dryer options based on function, safety and cost.

II. DISCUSSION

Eight dryer types were evaluated in terms of their functional characteristics, their tendency to produce hazards, and their costs. An overall assessment was then made. There are many dryer types that could have been postulated as having a potential value for drying explosives. However, only those dryer types that have previously been used for products that tend to produce dust (not necessarily the explosives) were considered because they provide a general basis of having the drying potential with a demonstrated level of safety. The eight dryer types considered are:

- Tray Dryer. The material is placed on a tray(s) and dried by conduction and convection.
- Drum Dryer. The material is placed on the outside of a heated drum.
- Rotary Dryer. Similar in principle to the common clothes dryer.
- Fluidized Bed Dryer. A stream of air is directed on or through the material.
- Pneumatic Dryer. The airstream drys and transports the material.
- Spray Dryer. Material is sprayed from a nozzle into an airstream.
- Vacuum Dryer. A tray dryer in which a partial pressure is drawn to facilitate drying.
- Microwave Dryer. A high frequency voltage heats the water molecules.

The eight dryer types were evaluated in terms of eight functional characteristics: control sensitivity, off-spec product sensitivity, state-of-the-art required, maintenance level expected, product drying compatability, dust potential, development risk and suitability potential.

Since the analysis of a drying process is still largely an empirical procedure and since specific dryer characteristics are not

available, a subjective evaluation was made. This was accomplished by a comparative analysis using the fluidized bed as a baseline. In such an analysis each characteristic, which can be weighted, is assigned a value of 5 for the baseline dryer. All other dryers are then evaluated as being better or worse than the baseline dryer for each characteristic. The better dryers are assigned values between 5 and 10 and the worse dryers are assigned values between 5 and 1. The overall assessment is then made by adding the points for each dryer for a total score. The dryers are then ranked based on their score. No attempt was made to put a weighting factor on each dryer characteristic. Such factors are normally established by management or by the process engineer.

On a Functional Basis the Dryers are Ranked as Follows:

- Vacuum Dryer ranks number one primarily because it has the least control sensitivity, appears to be compatible with all of the A-X products and should be suitable now for pilot model evaluation. The primary drawback is that it is a batch dryer.
- Microwave Dryer is ranked second because it should provide low control sensitivity and the best potential for drying A-3 explosive. Unfortunately little is known about its adaptability to drying explosives. Pilot model testing is not recommended because such testing may be premature, but development type testing is certainly in order.
- Tray Dryer is ranked third. It is expected that the tray dryer can dry all of the explosive products except A-3. That product may also be dried but there exists some doubt that it can be dried effectively in a reasonable number of passes.
- Rotary Dryer is ranked fourth because it has less control sensitivity than the fluidized bed dryer but more than the tray dryer. The rotary dryer will probably experience

difficulty drying the A-3 product but it should be capable of drying the other products.

- Fluidized Bed Dryer is ranked fifth because it is control sensitive and has limited capability in drying the A-3 explosive.
- Drum, Pneumatic and Spray Dryers are ranked sixth, seventh and eighth respectively but they do not appear to be particularly applicable to the A-X products.

A failure modes and effects analysis (FMEA) was conducted on each of the eight dryer types. In order to facilitate this analysis, a work/breakdown structure was generated in a generic form and for each dryer type. Figure 1 shows the general dryer work/breakdown structure. It consists of four primary elements: (1) Into Dryer Transport System, which moves the product into the dryer; (2) Dryer, which drys the product; (3) Exhaust system, which collects and removes the dust generated by drying; and (4) Out of Dryer Transport System, which moves the product from the dryer to the next step in the process.

Of primary concern to this program is work/breakdown structure (WBS) element 2, The Dryer. That element, then, has been expanded in Figure 1 to eleven sub-elements which make up the major subsystems of a dryer. Not all dryers have all of the subsystems. The subsystems are then peculiarized to each dryer type and the FMEA is conducted. Hazard categories are estimated and placed according to the categories defined in MIL-STD-882, dated 15 July 1969, whereby:

- Category I-Negligible....will not result in personnel injury or system damage.
- Category II-Marginal....can be counteracted or controlled without injury to personnel or major system damage.
- Category III-Critical....will cause personnel injury or major system damage, or will require immediate corrective action for personnel or system survival.
- Category IV-Catastrophic....will cause death or severe injury to personnel, or system loss.

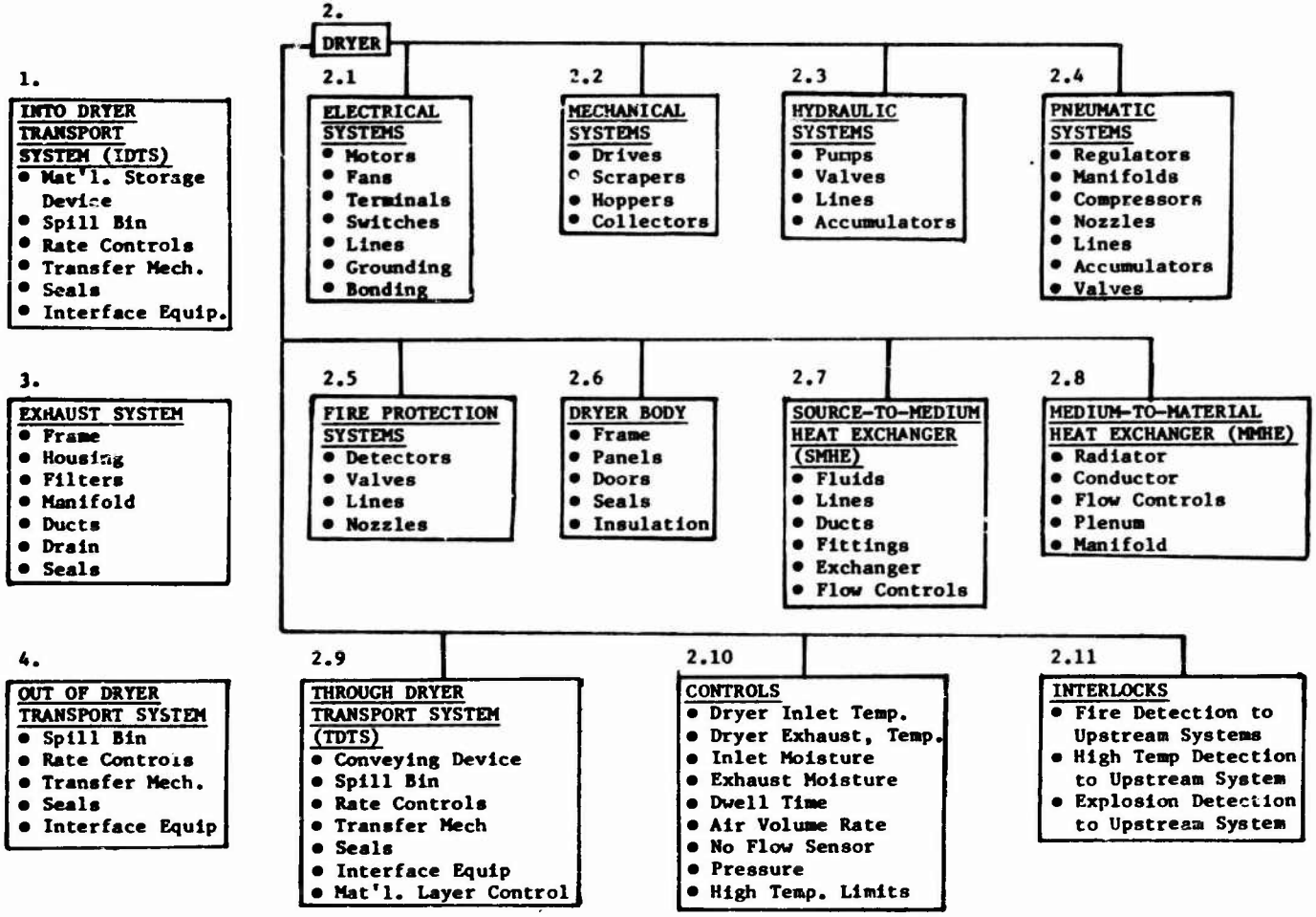

FIGURE 1. GENERAL DRYER WORKBREAKDOWN STRUCTURE

In addition, the probability of occurrence for each hazard has been estimated in gross terms. Three probability levels have been assigned: low, moderate and high. If gross numerical values ranging from 1 to 4 for the hazard categories and from 1 to 3 for the probabilities are assigned, gross estimates of risk can be made. For instance, a Category I combined with a low probability would have a risk level of 1 (1 x 1), whereas a Category IV hazard combined with a high probability would be assigned a risk level of 12 (4 x 3).

Table 1 is a compilation of the risk levels for each dryer type and major subsystem. On an overall basis, the following are noted:

- None of the dryer types offer a really safe option. Perhaps this could have been expected.
- Vacuum and microwave dryers appear to be somewhat less hazardous than the other dryers, although it is difficult to reconcile the use of strong electrical energy in close proximity to an explosive (microwave dryer).
- If the overall risk (Σ) is divided by the number of major subassemblies, the average risk per subassembly ($\bar{\Sigma}$) is estimated. It is seen that $\bar{\Sigma}$ is almost uniform across the dryer types.

In terms of each major subassembly the following are noted:

- Mechanical System. In general the mechanical system is not a prime risk source. The drum and rotary dryers, however, do indicate a risk sensitivity in this system. The drum dryer is sensitive because the drum temperature must be high to effect drying over a short residence time. If the drum should stop, the hazard is present. A rotary dryer has about six mechanical subsystems that contribute to the risk level. As with reliability and maintainability, there is a payoff for simple systems.

TABLE 1. RISK LEVEL DISTRIBUTION

Major Subsystem \ Dryer Type	Tray Dryer	Drum Dryer	Rotary Dryer	Fluidized Bed Dryer	Pneumatic Dryer	Spray Dryer	Vacuum Dryer	Microwave Dryer
Electrical System	23	24	22	23	23	23	22	32
Mechanical System	7	15	11	1	0	6	4	3
Hydraulic System	0	0	0	0	0	0	0	15
Pneumatic System	0	0	0	21	21	21	0	0
Fire Protection System	33	33	33	33	33	33	33	33
Dryer Body	10	3	11	9	9	9	13	9
Source-to-Medium Heat Exchanger	16	18	18	18	18	18	17	0
Medium to Material Heat Exchanger	16	17	17	0	0	0	9	0
Through Dryer Transport System	13	0	0	12	0	0	0	6
Controls	29	25	25	26	25	25	26	23
Interlocks	12	12	12	12	12	12	11	14
Σ	159	147	149	155	141	147	135	135
Σ'	18	18	19	17	20	18	17	17

- Hydraulic System. The only dryer with a hydraulic system is the microwave dryer which requires that the power supply be cooled. A need for an interlock between the hydraulic system and the primary dryer power is indicated.
- Pneumatic System. The fluidized bed, pneumatic and spray dryers use pneumatic systems. The risk levels of these systems are high primarily because of their inherent tendency to produce dust. If the probability of providing an effective control for dust explosion potential were factored into the risk assessment, these three dryer types (as well as the rotary dryer) would have a significantly increased risk level.
- Dryer Body. The primary factor in the dryer body is to provide blow-out capability to prevent the amplification of an explosion. The drum dryer has a clear advantage in this regard, since the explosive is located on the outside of the drum.
- Through Dryer Transport System. This system is a factor if a conveyor is used to transport the product through the dryer.
- Medium-to-Material Heat Exchanger. This subsystem represents a significant contribution to the overall risk (about 10%). The primary areas of concern are the ability to produce a uniform heat distribution over the product and the consequences of failing to transfer the correct level.
- Electrical System. The electrical system controls and distributes the electrical energy in the dryer. For thermo-mechanical dryers, this system consists of motors, fans, bonding, grounding, wiring, switches, and fuses. As with any electrical system in close proximity to explosives, the dryer electrical system is a major source of potential hazard. Category IV type hazards can be obtained from bonding, grounding, and switch failures.

- Fire Protection System. The fire protection system is not in the functional flow of the dryer system and therefore does not cause a hazardous event. It is an essential subsystem, however, in that it can contain or mitigate the effect of a fire. This brief study indicated that each of the elements of the fire detection system is critical, i.e., failure of one element could negate the effectiveness of the system. The detectors have the highest probability or failure since their primary failure mode is failure to detect because of dust obscuration of the sensor.
- Source-to-Medium Heat Exchanger. This subsystem converts steam heat from the primary source to hot air, which is circulated through the dryer. Under normal operations, the intake air flow damper is a possible source of a problem. If the damper fails to close, the air could be overdriven, resulting in a dusty product which, in turn, could contribute to a hazardous event. Incorporation of a damper designed to be normally closed would mitigate this problem.
- Controls. Controls govern the process flow and monitor particular process parameters. Typically controls include: source-to-medium heat exchanger supply air controller; steam control valves; dry and wet bulb temperature sensors; intake air damper; manifold damper; intake air temperature limit switch; exhaust air damper; no air flow sensor; and intake air pressure sensor. Failure of controls can lead to an over-heated producted or to the generation of excessive dust.
- Interlocks. Interlocks are structured to prevent a failure from cascading into a hazardous event, or to stop the flow of material into a failure in which a fire or an explosion has occurred. Generally both material flow and energy must be shut down. Since failure of an interlock

could lead to a catastrophic situation, some redundancy of interlocks is desirable.

Typical hazards associated with each dryer type include:

Tray Dryer

The tray dryer has several areas which must be successfully treated if a safe system is to be effected. This dryer type, as well as most other dryers, is susceptible to dust generation and distribution. Some dust can be expected to be generated as the product is cascaded from tray to tray. This dust can settle into the turbo fan cavity, into the drive and out of the dryer if seals are not properly designed, installed, and maintained. Since several of the seals will need to be of the dynamic type, frequent inspection will be required to assure proper function. Uniformity of air distribution is also critical to minimum dust production. Mechanical system failures should be controllable to prevent hazardous events. Blowout proof panels will be needed to mitigate the pressure buildup if an explosion occurs. Based on the analysis conducted, a safe tray dryer for the A-X products is within the state-of-the-art.

Drum Dryer

The drum dryer is not considered to be an inherently safe dryer for explosives because the drum temperature must be high to effect the proper level of drying within the relatively short residence time. Any failure that stops the drum has the potential of initiating a fire, and any failure of the high temperature control system could result in a fire or explosion. Proper controls and interlocks should be able to prevent a runaway temperature. However, the drum drive failure consequence remains as an inherent problem that would require a demonstrated solution before the drum dryer could be found to be acceptable.

Rotary Dryer

The rotary dryer has two inherent problem areas: product

buildup on the flights and the generation of dust. Product buildup can be minimized by the use of low airflow through the dryer. Since the dust potential for the rotary dryer is the primary effect which leads to a hazardous event, dust control must be demonstrated to assure a safe dryer.

Fluidized Bed Dryer

Fluidized bed dryers are made with several types of through dryer transport systems. This analysis considered only the shaker conveyor. The primary hazard of a fluidized bed dryer relates to the dust. Pneumatic system balance is essential to minimize dust. This balance, in turn, requires state-of-the-art design practices to be incorporated into the intake manifold, baffles, nozzles, and exhaust plenum. Available data do not indicate that sufficient consideration was given to these areas to show that the fluidized bed dryer will be safe.

Pneumatic Dryers

The pneumatic dryer has a relatively low total risk level because it is simple and has few mechanical and electrical parts. However, it is not an inherently safe dryer. Indeed, Palmer[1] recommends that pneumatic dryers be isolated from work areas. Enough controls and interlocks can be incorporated into the design to make the dryer safe from mechanical and electrical system failures. The state-of-the-art is considered to be insufficient to provide the requisite safety for the pneumatic system.

Spray Dryers

The spray dryer has the pneumatic system hazards of a pneumatic dryer plus the problems associated with the spray mechanism. The nozzles, which tend to clog frequently, do not present a major hazard, although a blocked line filled with explosive must be treated with

[1]K. N. Palmer, Dust Explosions and Fires, Chapman and Hall, Ltd., London, England, 1973.

respect. Spray dryers also have a tendency for the product to collect on the walls of the dryer. Frequent cleaning is necessary to prevent the accumulation from becoming a hazard. Given the particle range for the A-X products, the pneumatic system state-of-the-art of the spray dryer is not considered to be sufficient to offer a safe drying option.

Vacuum Dryer

The vacuum dryer has perhaps the most benign environment for the drying of explosives. Batch constraints require that the explosive be hand placed into and out of the dryer, thereby easing the hazards associated with two adjacent systems. The temperature can be set at a relatively low level since a partial pressure is inherent in the drying process and the air flow is so low that there should be little dust. The primary area of concern is the vacuum valve which could pinch particles of explosives drawn into the exhaust system. The vacuum dryer is clearly the safest dryer type, and its design is well within the state-of-the-art.

Microwave Dryer

There are two generic problem areas for the microwave dryer, the electrical system and the mechanical system. The primary problem in the mechanical system is the consequence of a jammed conveyor. In such an instance, the explosive could overheat unless an interlock is provided to shut off the power. In the electrical system the primary source of trouble would be a failure of the line voltage regulator. In some regulators, failure permits the passage of high voltage which, in turn, could result in an overheated product. A fail-safe regulator would be needed. All of the remaining electronic subsystems appear to have a fail-safe mode--either reducing the voltage amplitude or the frequency at failure. A hydraulic system is needed to cool the power supply, and failure of the system requires an interlock with the electrical power for effective limitation of the

hazard. There is no question as to the state-of-the-art of the desgin of a microwave dryer. There is some question as to whether the hazards postulated are indeed the hazards or if additional hazards are to be found. Since the microwave dryer has not been evaluated experimentally for explosive products, it must be assessed as a risk until a proper evaluation has been conducted.

The hazards assessments ranking based on the scores from Table 1 is given in Table 2.

TABLE 2. DRYER RANK BASED ON HAZARDS ASSESSMENT

Gross Rank	Dryer Type
1	Vacuum Dryer
2	Microwave Dryer
3	Pneumatic Dryer
4	Drum Dryer
5	Spray Dryer
6	Rotary Dryer
7	Fluidized Bed Dryer
8	Tray Dryer

No accurate basis for a general cost assessment of dryer types was found. A search of The Open Literature Data Files of Engineering Index and Chemical Abstracts indicated that there were no dryer cost assessment articles in either data base. Some information (about 15 years old) was uncovered, indicating that costs can be estimated on a Log Linear Basis of one dryer parameter - usually surface area. Those trends were compiled and used to a limited extent. Two cost data points were available on microwave dryers. These data were used to estimate cost trends for those particular dryer types. Cost trends for the remaining dryer types were estimated by using those trend equations that appeared to best fit the dryers.

Table 3 summarizes the cost by dryer type. The data are presented in terms of increasing cost which provides a cost rank to the dryer. It is always tempting to explain a trend after it has been shown, however, no consistent trend is indicated. The high airflow dryers, by virtue of their relative simplicity and small size are the least cost options. This is as expected. The trend of trading air flow for surface area (size) would be expected to continue so that the expected cost rank would be: 1) pneumatic dryer, 2) fluidized bed dryer, 3) spray dryer, 4) rotary dryer, 5) tray dryer, 6) vacuum dryer and 7) drum dryer. The first three dryers are in the expected order. The drum dryer is somewhat less expensive than expected and the rotary dryer is somewhat more expensive. The vacuum and tray dryers appear to be within 10% of a common cost which would be expected. The microwave dryer has historically been an expensive dryer option and appears as such in this assessment.

...BLE 3. DRYER COSTS

Gross Rank	Gross Cost Thousands of Dollars	Dryer Type
1	300	Pneumatic Dryer
2	325	Fluidized Bed Dryer
3	750	Spray Dryer
4	825	Vacuum Dryer
5	900	Drum Dryer
6	900	Tray Dryer
7	1,200	Rotary Dryer
8	3,500	Microwave Dryer

The eight dryer type options must be assessed on some basis. If each operational characteristic of each dryer type could be quantified, the dryer options could be assessed on a cost/effectiveness basis. Clearly such an assessment is not possible because the data are limited. The method used, then, makes an initial assumption that dryer capabilities are distributed according to their rank.

Since the dryers were assessed in three categories (function, hazard and cost) the combined ranking is possible based on the summation of the rank points. Successive filters were then added in each of the categories to eliminate the undesirable candidates. Finally, the remaining options were graded in terms of assets and liabilities.

Table 4 represents the rank summary of the dryer option based on their rank in each of the categories. Except for the vacuum dryer, which has a clear rank advantage, the dryers follow a relatively smooth trend in terms of rank points.

Some of the dryer types were eliminated based on undesirable characteristics. The pneumatic and spray dryers are eliminated because they are very control sensitive and as such they have a high development risk. Drum dryers were also eliminated from a functional viewpoint because it is doubtful that they can be made to work without an increase in the initial moisture level. Such an increase would be counterproductive. Microwave dryers were eliminated based on their high initial cost. Four dryer types, then, remained as candidates.

Table 5 is a compilation of the assets and liabilities of the four candidate dryer types. Based on this assessment, the vacuum and tray dryers were recommended. The fluidized bed dryer has an advantage in cost and in low residence volume of explosive, however, it has an inherent control problem which requires extensive rework before a functional dryer can be made to work. On these bases the fluidized bed dryer is not recommended. The rotary dryer is also not recommended because it has no inherent advantage over any of the remaining dryer options.

The vacuum and tray dryers were recommended as candidate dryers. The final selection must be made on the basis of verification of drying ability by pilot models, explosive residence volume, and final cost

TABLE 4. RANK SUMMARY WITHOUT FILTER

Dryer Type	Gross Overall Rank	Gross Functional Rank	Gross Hazards Rank	Gross Cost Rank	Rank Points
Vacuum Dryer	1	1	1	4	6
Pneumatic Dryer	2	7	3	1	11
Microwave Dryer	3	2	2	8	12
Fluidized Bed Dryer	4	5	7	2	14
Drum Dryer	5	6	4	5	15
Spray Dryer	6	8	5	3	16
Tray Dryer	7	3	8	6	17
Rotary Dryer	8	4	6	7	17

TABLE 5. ASSETS AND LIABILITIES

Dryer Type	Assets	Liabilities	Recommended ?
Vacuum Dryer	• "Best Dryer for A-3" • Safest Dryer • Low Development Risk • Simple Dryer • Good Control Sensitivity	• Batch Dryer • High Cost • High Residence Volume of Explosive	Yes
Fluidized Bed Dryer	• Lowest Cost Dryer • Low Residence Volume of Explosive	• Poor Control Sensitivity • Won't Dry A-3 • Tends to Produce Dust • High Development Risk	No--Dryer Inherently a Problem
Tray Dryer	• 2nd Best Dryer for A-3 • Good Control Sensitivity • Low Development Risk	• High Cost • High Residence Volume of Explosive	Yes
Rotary Dryer	• Low Residence Volume of Explosive	• High Cost • Poor Control Sensitivity	No--Dryer has no Inherent Advantage

constraints. The vacuum dryer appears to have the highest probability of drying the A-3 product. The batch characteristics may make the vacuum dryer unattractive although it should be possible to incorporate some semi-continuous ability into a vacuum dryer design.

III. CONCLUSIONS

The following conclusions are drawn:

1) There exists a very limited ability to predict accurately the dryer performance or the cost without some experimentation.

2) Dryer manufacturers, as a group, have little incentive to develop dryers capable of drying explosives.

3) High air flow dryers tend to cause control problems for the A-X products unless the air flow within the dryer is uniformly distributed and controlled.

4) The "best" drying mechanism appears to be the microwave dryer since its energy is directly coupled to the water. This dryer type is not recommended on a near term basis, however, because it has a high cost and needs a detailed assessment.

5) The "best" near term dryer is a vacuum dryer. It should provide the requisite capability if the in-process storage is not excessive for the particular line.

6) The "next best" near term dryer is the tray dryer.

Office of the
Project Manager

MUNITIONS PRODUCTION BASE

MODERNIZATION AND EXPANSION

Dover, New Jersey

1409

SYSTEM SAFETY PROGRAM

FOR

MODERNIZATION AND EXPANSION PROJECTS

PRESENTED AT

DEPARTMENT OF DEFENSE

18TH EXPLOSIVES SAFETY SEMINAR

PRESENTED BY

JOSEPH R. DRUGMAND

SAFETY ENGINEER

12-14 SEPTEMBER 1978




DEPARTMENT OF THE ARMY
UNITED STATES OF AMERICA
1775

ABSTRACT

THIS PRESENTATION DESCRIBES THE APPLICATION OF A SYSTEM SAFETY PROGRAM TO PRODUCTION FACILITIES WHICH ARE BEING MODERNIZED OR EXPANDED TO MANUFACTURE VARIOUS MUNITIONS USED BY THE UNITED STATES ARMED FORCES.

OUTLINE

- BACKGROUND
- CONTENTS OF MEMORANDUM
- DOCUMENTATION
- HAZARD ANALYSES

OUTLINE

THE PURPOSE OF THIS PRESENTATION IS TO EXPLAIN THE SYSTEM SAFETY PROGRAM USED IN THE MODERNIZATION AND EXPANSION PROGRAM. I SHALL ACCOMPLISH THIS BY COVERING THESE TOPICS.

DOD CONVENTIONAL AMMUNITION PRODUCTION BASE
GOVERNMENT OWNED FACILITY LOCATIONS



DOD CONVENTIONAL AMMUNITION PRODUCTION BASE

GOVERNMENT OWNED FACILITY LOCATIONS

FIRST I'LL BRIEFLY EXPLAIN WHAT THE MODERNIZATION AND EXPANSION PROGRAM IS AND WHAT WE DO IN IT. THE PROJECT MANAGER'S OFFICE MANAGES SEVERAL HUNDRED PROJECTS FOR CAPITAL INVESTMENTS AT 23 GOVERNMENT-OWNED, CONTRACTOR-OPERATED PLANTS AND FOUR GOVERNMENT-OWNED, GOVERNMENT-OPERATED PLANTS SHOWN ON THIS CHART.

LOCATION OF GOVERNMENT PLANT EQUIPMENT PACKAGE LINES

IN PRIVATE SECTOR

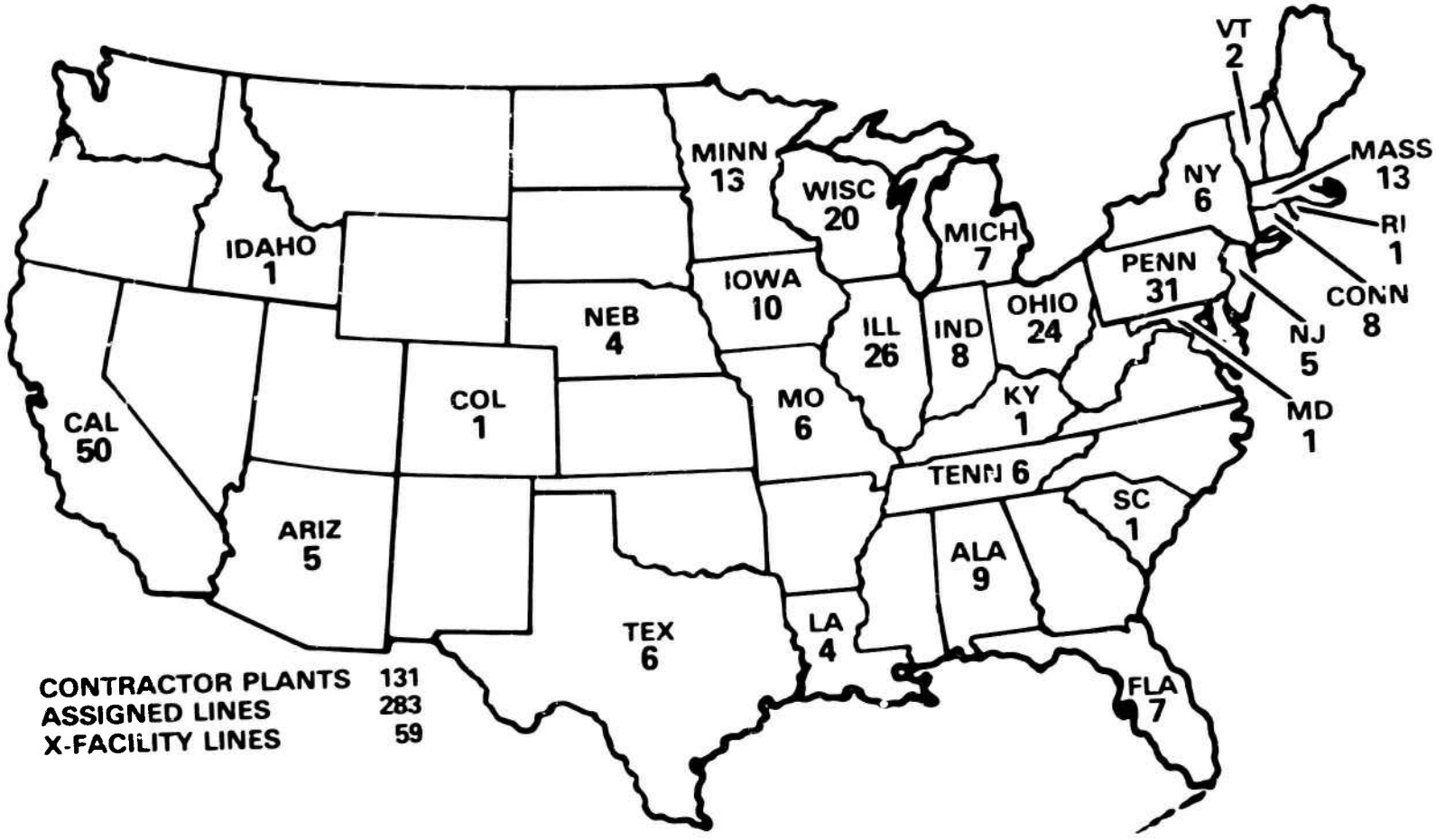

1416

LOCATION OF GOVERNMENT

PLANT EQUIPMENT PACKAGE LINES

IN PRIVATE SECTOR

ALSO, WE MANAGE SIMILAR PROJECTS AT 131 CONTRACTOR PLANTS WHICH UTILIZE GOVERNMENT EQUIPMENT, OR A MIX OF GOVERNMENT AND PRIVATELY-OWNED EQUIPMENT. THIS PLANT DISTRIBUTION IS GEOGRAPHICALLY SHOWN ON THIS CHART. THESE PROJECTS ARE DESIGNED TO MODERNIZE THE MUNITIONS FACILITIES AND INCREASE THEIR PRODUCTION CAPABILITIES. THE PROGRAM VALUE HAS RANGED FROM 150 TO 250 MILLION DOLLARS PER YEAR. THE PROGRAM BEGAN IN THE LATE 1960'S AND IS PLANNED TO CONTINUE INTO THE 1990'S.

REASONS FOR SYSTEM SAFETY PROGRAM

- ACCIDENT PREVENTION
  - COST EFFECTIVE
  - INTERRELATES COMPONENTS
  - QUANTIFY

REASONS FOR SYSTEM SAFETY PROGRAM

THE SYSTEM SAFETY PROGRAM, WHICH IS THE SUBJECT OF THIS PRESENTATION, IS ONE OF MANY PROGRAMS PROSECUTED AS A PART OF THE TOTAL MODERNIZATION AND EXPANSION PROGRAM; HOWEVER, IT IS AN EXTREMELY IMPORTANT PART BECAUSE THROUGH IT WE ARE, TO A LARGE EXTENT, DETERMINING THE FUTURE SAFETY RECORD, THAT IS THE ACCIDENT EXPERIENCE OR LACK OF ACCIDENTS, IN THE NEW PRODUCTION FACILITIES. THERE ARE ADDITIONAL REASONS FOR HAVING THE PROGRAM. FIRST, THE SYSTEM SAFETY PROGRAM IS COST EFFECTIVE; THAT IS, IT SAVES MORE MONEY THAN IT COSTS TO DEVELOP AND IMPLEMENT. THIS OCCURS THROUGH AVOIDING EXPENSIVE ENGINEERING CHANGES LATE IN THE PROJECTS, AS WELL AS THE OBVIOUS SAVINGS FROM AVOIDING ACCIDENTS. THE ARMY STRONGLY ADVOCATES THIS APPROACH THROUGH A SYSTEM OF REGULATIONS. SECOND, WE MUST ALSO ANALYZE POSSIBLE INTERRELATED OCCURRENCES TO SEE WHAT EFFECT THEY WILL HAVE ON THE TOTAL SYSTEM. THIS IS NEEDED BECAUSE SAFETY-CODE REGULATIONS DEAL WITH ISOLATED RATHER THAN INTERRELATED COMPONENTS AND DESIGNING COMPLEX FACILITIES SIMPLY TO COMPLY WITH SAFETY-CODE REGULATIONS IS GROSSLY INADEQUATE. AND THIRD, WE DESIRE TO QUANTIFY THE PROBABILITIES OF ACCIDENTS OCCURRING IN ORDER TO PROVIDE OBJECTIVE INFORMATION FOR MAKING MANAGEMENT DECISIONS.

SYSTEM SAFETY PROGRAM MEMORANDUM OUTLINE

- POLICY
- PROCEDURES
- RESPONSIBILITIES
- REQUIREMENTS
- APPENDICES
  - I : SAFETY CRITERIA
  - II : HAZARD ANALYSIS
  - III : SAFETY SITE PLANS & FINAL SAFETY REVIEW SUBMISSIONS
  - IV : TNT EQUIVALENTS
  - V : SUPPLEMENTARY INFO FROM ARRCOM SAFETY BULLETINS
  - VI : SUPPLEMENTARY INFO FROM OFFICIAL CORRESPONDENCE

SYSTEM SAFETY PROGRAM

MEMORANDUM OUTLINE

OUR SYSTEM SAFETY PROGRAM IS MANAGED THROUGH A MEMORANDUM ENTITLED "SYSTEM SAFETY PROGRAM FOR MODERNIZATION AND EXPANSION PROJECTS." THE MEMORANDUM, WHICH SERVES AS A HANDBOOK FOR OUR PROJECT ENGINEERS, IS USED DURING ALL PHASES OF OUR PROJECTS. THIS VIEWGRAPH SHOWS A BRIEF OUTLINE OF THE MEMORANDUM. COPIES OF THE COMPLETE MEMORANDUM CAN BE OBTAINED BY GIVING ME YOUR ADDRESS AFTER THIS PRESENTATION.* THE MEMORANDUM HAS HAD WIDESPREAD DISTRIBUTION WITHIN OUR OWN ORGANIZATION AND IN ALL ORGANIZATIONS PARTICIPATING IN THE MODERNIZATION AND EXPANSION PROGRAM. THE MEMORANDUM IS IN GREAT DETAIL AND UNIQUE SINCE IT IS TAILORED TO OUR PROGRAM. APPROXIMATELY EVERY SIX MONTHS IT IS UPDATED BY ADDING LESSONS LEARNED, THE LATEST REQUIREMENTS OF HIGHER AUTHORITIES, AND THE LATEST TECHNOLOGY.

---

* COPIES OF DRCPM-PBM MEMORANDUM 385-3, SYSTEM SAFETY PROGRAM FOR MODERNIZATION AND EXPANSION PROJECTS, CAN BE OBTAINED BY REQUESTING THEM FROM:

PROJECT MANAGER
MUNITIONS PRODUCTION BASE MODERNIZATION & EXPANSION
US ARMY MATERIEL DEVELOPMENT AND READINESS COMMAND
ATTN: DRCPM-PBM-T-SF (MR. JOSEPH R. DRUGMAND)
DOVER, NEW JERSEY 07801

AUTOVON 880-6706
COMMERCIAL (201)328-6706

SYSTEM SAFETY PROGRAM
SIGNIFICANT DOCUMENTS

- PRELIMINARY HAZARD ANALYSIS
- TOTAL SYSTEM HAZARD ANALYSIS
  - SUBSYSTEM HAZARD ANALYSES
  - SYSTEM HAZARD ANALYSIS
  - OPERATING AND SUPPORT HAZARD ANALYSIS
- HAZARD ANALYSIS MONTHLY PROGRESS REPORTS
- HAZARD ANALYSIS TEST DATA

- SAFETY SITE PLAN
- FINAL SAFETY REVIEW SUBMISSION

SYSTEM SAFETY PROGRAM

SIGNIFICANT DOCUMENTS

THE SIGNIFICANT DOCUMENTS GENERATED BY OUR SYSTEM SAFETY PROGRAM ARE SHOWN ON THIS VIEWGRAPH. THIS PRESENTATION WILL CONCENTRATE ON THE MORE UNUSUAL HAZARD ANALYSIS DOCUMENTS SHOWN IN THE UPPER PORTION OF THIS VIEWGRAPH. I SHALL CONCENTRATE ON HAZARD ANALYSIS BECAUSE IT IS THE METHOD USED FOR DISCOVERING AND DETERMINING THE EFFECTS OF INTERRRELATED OCCURRENCES, ESPECIALLY THOSE WHICH CAN CAUSE CATASTROPHIC ACCIDENTS, WHEREAS SAFETY SITE PLANS AND FINAL SAFETY REVIEW SUBMISSIONS DEAL WITH THE WELL KNOWN TOPICS OF SITING FACILITIES AND SAFETY-CODE REGULATIONS.

WITH MOST PROJECTS THE ANALYSES INCLUDE BOTH A PRELIMINARY HAZARD ANALYSIS AND A TOTAL SYSTEM HAZARD ANALYSIS. THE TOTAL SYSTEM HAZARD ANALYSIS IS COMPRISED OF SUBSYSTEM HAZARD ANALYSES, A SYSTEM HAZARD ANALYSIS AND AN OPERATING AND SUPPORT HAZARD ANALYSIS. FOR OUR PURPOSES, THE DEFINITIONS OF THESE ANALYSES ARE THE SAME AS THOSE GIVEN IN MIL-STD-882A. THE NEW TERM WE INTRODUCE IS "TOTAL SYSTEM HAZARD ANALYSIS" WHICH IS A COMBINATION OF THE THREE ANALYSES SHOWN BELOW IT ON THE VIEWGRAPH. TOTAL SYSTEM HAZARD ANALYSIS INCLUDES THE ENTIRE PRODUCTION FACILITY ASSOCIATED WITH THE PRODUCTION OF THE SUBJECT MATERIEL. I WANT TO POINT OUT THAT BECAUSE OF THE UNIQUE REQUIREMENTS OF OUR FACILITIES, WE REQUIRE OUR HAZARD ANALYSIS CONTRACTORS TO ANALYZE ADDITIONAL SYSTEMS THAT ARE PART OF MUNITIONS FACILITIES, SUCH AS, PROCESS CONTROL SYSTEMS, LIGHTNING PROTECTION SYSTEMS, UTILITIES, AND FIRE DETECTION AND SUPPRESSION SYSTEMS.

USUALLY THE PRELIMINARY HAZARD ANALYSIS IS PERFORMED DURING THE DEVELOPMENT OF THE EQUIPMENT FUNCTIONAL CRITERIA AND COMPLETED BY THE TIME THE EQUIPMENT FUNCTIONAL CRITERIA IS BASELINED. THE TOTAL SYSTEM HAZARD ANALYSIS IS STARTED WHEN THE CONTRACT IS AWARDED TO AN ARCHITECTURAL/ENGINEERING FIRM OR EQUIPMENT DESIGNER FOR CONCEPT DESIGN AND THE ANALYSIS IS UPDATED THROUGH THE FINAL DESIGN. OCCASIONALLY, THE CIRCUMSTANCES OF A PROJECT CAUSE SOME EXCEPTIONS TO OCCUR REGARDING HOW THESE ANALYSES ARE SCHEDULED.

HAZARD ANALYSIS SPECIFICATIONS

- DEFINITIONS
- QUANTITATIVE GOALS
- REPORTS
- MILESTONES

HAZARD ANALYSIS SPECIFICATIONS

I SHALL EXPLAIN OUR HAZARD ANALYSIS SPECIFICATIONS DEVELOPMENT IN SOME DETAIL BECAUSE WE BELIEVE WE HAVE A NEW APPLICATION WHICH CAN BE ADAPTED FOR USE IN OTHER AREAS.

PREVIOUSLY, NO ONE HAD DEVELOPED SPECIFICATIONS FOR HAZARD ANALYSES OF MUNITIONS FACILITIES FOR USE IN CONTRACTS.

THESE SPECIFICATIONS ARE DESIGNED TO ASSURE THAT THE GOVERNMENT RECEIVES FULL VALUE FOR WHAT IT PAYS FOR, THAT IS, ALL REQUIRED ANALYSES ARE ADDRESSED, REALISTIC QUANTITATIVE GOALS ARE ESTABLISHED, AND THE CONTRACTOR'S REPORTS AND RECOMMENDATIONS ARE IN A USABLE FORM WITH PROBLEM AREAS HIGHLIGHTED.

ON THIS CHART ARE THE MAJOR SUBJECT AREAS ADDRESSED BY THE SPECIFICATIONS. UNDER DEFINITIONS, WE DEFINED MANY TERMS AS THEY APPLY TO OUR PROJECTS. UNDER QUANTITATIVE GOALS, WE ESTABLISHED GOALS FOR THE PROBABILITIES OF ACCIDENTS OCCURRING AND STATISTICAL REQUIREMENTS FOR HOW THE ANALYSES SHALL BE PERFORMED. UNDER REPORTS, WE SPECIFIED THE REQUIRED REPORTS AND FORMATS. UNDER MILESTONES, WE TIME PHASED AND INTERRELATED THE PROGRESS OF THE HAZARD ANALYSES WITH OTHER ACTIVITIES.

ADDITIONALLY, MY OFFICE MAINTAINS AN UPDATED BIDDERS LIST OF FIRMS QUALIFIED TO PERFORM HAZARD ANALYSES. THIS LIST IS USED TO SOLICIT PROPOSALS FOR PERFORMING THE HAZARD ANALYSES.

USING THE SPECIFICATION DOES NOT SIGNIFICANTLY INCREASE THE COST OF THE SAFETY PROGRAM. WE ARE SIMPLY CRYSTALLIZING OUR NEEDS BY MORE CAREFULLY SPECIFYING WHAT THE CONTRACTOR SHALL DO, WHAT DEFINITIONS SHALL BE USED, WHAT THE STATISTICAL REQUIREMENTS ARE AND HOW THE RESULTS SHALL BE REPORTED. ACTUALLY, THE SPECIFICATIONS ARE COST EFFECTIVE, THAT IS, THEY SAVE MORE MONEY THROUGH COST AVOIDANCE THAN THEY COST TO DEVELOP.

THE APPROACH IS ALSO BENEFICIAL IN MOLDING A TEAM OPINION, BETWEEN PROJECT ENGINEER AND SAFETY ENGINEER, AS TO THE HAZARD ANALYSIS OBJECTIVES SOUGHT FOR THE PROJECT.

THESE SPECIFICATIONS ARE DEVELOPED FOR ALL MODERNIZATION AND EXPANSION PROJECTS, EVEN THOSE WHICH DO NOT INVOLVE EXPLOSIVES, PROPELLANTS OR PYROTECHNICS BECAUSE CATASTROPHIC LOSSES CAN ALSO OCCUR IN INDUSTRIAL OPERATIONS FOR NON-ENERGETIC MATERIALS.

THE REMAINING VIEWGRAPHS PROVIDE EXAMPLES OF HOW WE TREAT THE DEFINITIONS, QUANTITATIVE GOALS, REPORTS AND MILESTONE ELEMENTS IN OUR SPECIFICATIONS.

DEFINITION DEVELOPMENT

HAZARD/ACCIDENT CATEGORIES

- MIL-STD-882A
- EQUIPMENT DAMAGE
- PERSONNEL INJURIES
- ACCIDENT DEFINITIONS

DEFINITION DEVELOPMENT

HAZARD/ACCIDENT CATEGORIES

THIS VIEWGRAPH SHOWS THE AREAS WE CONSIDERED IN DEVELOPING OUR DEFINITIONS FOR ACCIDENTS. IN THE NEXT FOUR VIEWGRAPHS, I SHALL DISCUSS THESE AREAS IN SOME DETAIL.

HAZARD CATEGORIES

(MIL-STD-882A DTD 28 JUNE 1977)

I.	CATASTROPHIC	MAY CAUSE DEATH OR SYSTEM LOSS
II.	CRITICAL	MAY CAUSE SEVERE INJURY, SEVERE OCCUPATIONAL ILLNESS, OR MAJOR SYSTEM DAMAGE
III.	MARGINAL	MAY CAUSE MINOR INJURY, MINOR OCCUPATIONAL ILLNESS, OR MINOR SYSTEM DAMAGE
IV.	NEGLIGIBLE	WILL NOT RESULT IN INJURY, OCCUPATIONAL ILLNESS, OR SYSTEM DAMAGE

HAZARD CATEGORIES

(MIL-STD-882A DTD 28 JUNE 1977)

THIS VIEWGRAPH SHOWS THE CURRENT DEPARTMENT OF DEFENSE DEFINITIONS FOR HAZARD CATEGORIES INCLUDED IN MIL-STD-882A. HOWEVER, THESE DEFINITIONS COMBINE EQUIPMENT AND PERSONNEL CONCERNS IN EACH HAZARD CATEGORY.

FOR QUANTIFICATION PURPOSES, WE CHOSE TO TREAT EQUIPMENT AND PERSONNEL SEPARATELY. ALTHOUGH WE ABIDE BY THESE MIL-STD-882A CONCEPTS, WE DIFFERENTIATE BETWEEN EQUIPMENT AND PERSONNEL WITHIN EACH MIL-STD CATEGORY.

DEFINITIONS OF EQUIPMENT DAMAGE

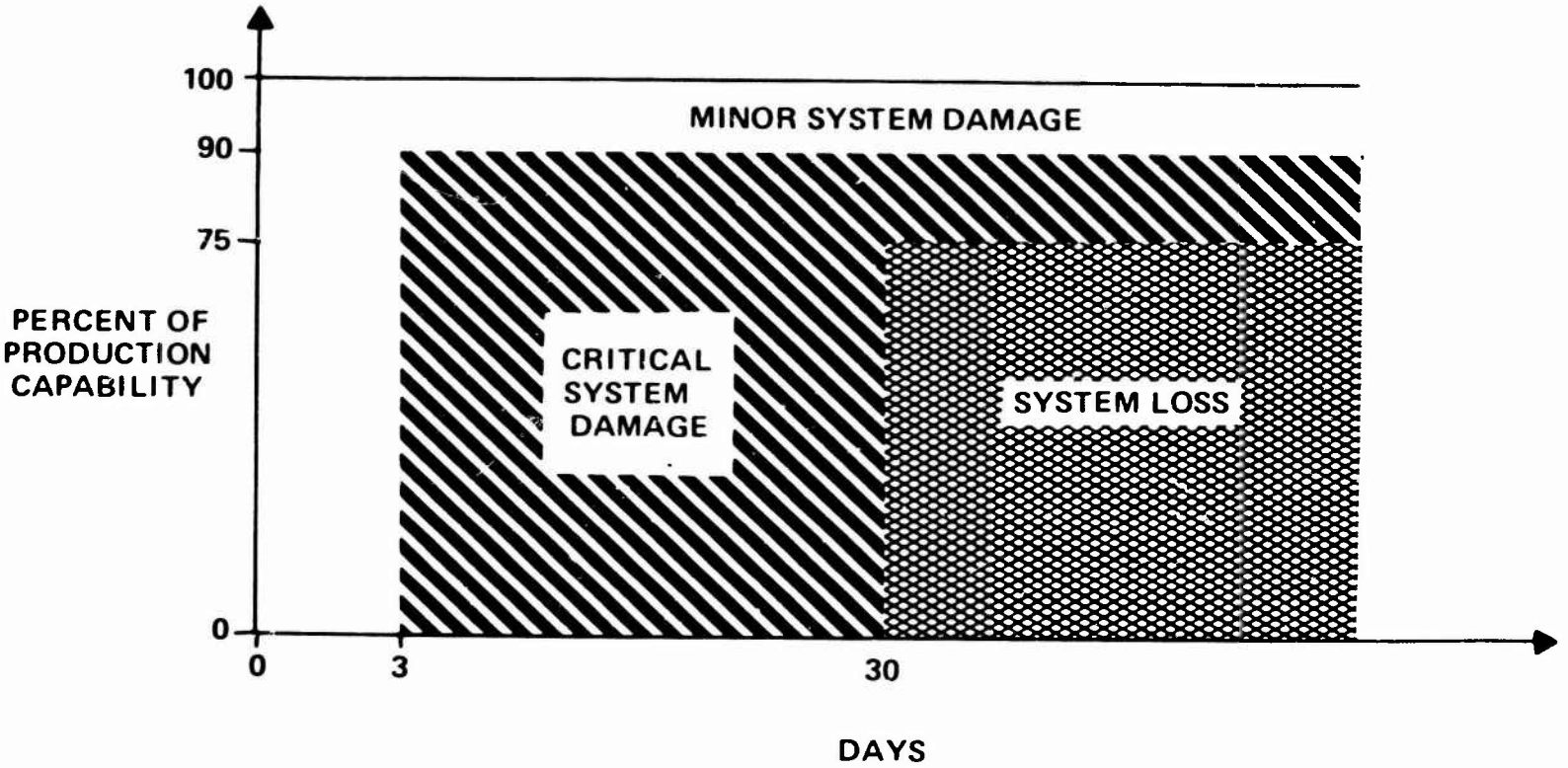

DEFINITIONS OF EQUIPMENT DAMAGE

THIS VIEWGRAPH GRAPHICALLY SHOWS THE DEFINITIONS WE USE FOR CATEGORIZING EQUIPMENT DAMAGE. THESE DEFINITIONS ARE CONSISTENT WITH MIL-STD-882A, BUT THEY ADD A QUANTITATIVE DIMENSION. THE 30-DAY, ZERO PRODUCTION POINT ASSOCIATED WITH SYSTEM LOSS WAS SPECIFIED BY THE COMMANDING GENERAL RESPONSIBLE FOR THE PLANTS. WITH THIS AS A BASE POINT, MY OFFICE DEVELOPED THE OTHER DEFINITION PARAMETERS. NOW CONTRACTORS HAVE MORE DEFINITIVE PARAMETERS FOR IDENTIFYING ACCIDENT CATEGORIES FOR EQUIPMENT.

DEFINITIONS OF PERSONNEL INJURIES

1434

AMERICAN NATIONAL STANDARDS INSTITUTE
STANDARD Z16.1-1967

METHOD OF RECORDING AND MEASURING WORK INJURY EXPERIENCE

DEFINITIONS OF PERSONNEL INJURIES

FOR THE DEFINITIONS FOR PERSONNEL INJURIES, WE RELIED ON THIS COMMONLY ACCEPTED ANSI STANDARD FOR REPORTING INJURIES. THIS STANDARD CAREFULLY DEFINES PERMANENT TOTAL DISABILITY, PERMANENT PARTIAL DISABILITY, AND TEMPORARY TOTAL DISABILITY. THIS SET OF DEFINITIONS, ALSO, FITS INTO THE SCHEMA USED IN MIL-STD-882A AND IS SUSCEPTIBLE TO QUANTIFICATION.

ACCIDENT DEFINITIONS

ACCIDENT CATEGORY	EQUIPMENT	PERSONNEL
IA	SYSTEM LOSS LARGE SCALE ENVIRONMENTAL DAMAGE	– – – –
IB	– – – –	DEATH PERMANENT TOTAL DISABILITY
IIA	CRITICAL SYSTEM DAMAGE SOME ENVIRONMENTAL DAMAGE	– – – –
IIB	– – – –	PERMANENT PARTIAL DISABILITY
IIIA	MINOR SYSTEM DAMAGE SOME ENVIRONMENTAL DAMAGE	– – – –
IIIB	– – – –	TEMPORARY TOTAL DISABILITY OR LOST TIME INJURY NOT COVERED BY CATEGORIES IB OR IIB
IV	NO DAMAGE	NO INJURY

ACCIDENT DEFINITIONS

HAVING DEVELOPED DEFINITIONS FOR EQUIPMENT AND PERSONNEL, WE FORMULATED AN OVERALL SYSTEM OF DEFINITIONS SUSCEPTIBLE TO QUANTIFICATION FOR THE FOUR CATEGORIES OF ACCIDENTS YOU SEE HERE. NOTICE THAT THIS SYSTEM SEPARATES EQUIPMENT AND PERSONNEL.

ADDITIONALLY, UNDER EQUIPMENT WE DEFINED LARGE SCALE ENVIRONMENTAL DAMAGE AS REQUIRING ONE MILLION DOLLARS OR MORE TO CORRECT, AND SOME ENVIRONMENTAL DAMAGE AS REQUIRING LESS THAN ONE MILLION DOLLARS TO CORRECT.

QUANTITATIVE GOALS

EACH PROJECT SHALL HAVE THE FOLLOWING, OR LOWER, MEAN PROBABILITY VALUES AS DESIGN GOALS FOR THE ENTIRE PRODUCTION FACILITY ASSOCIATED WITH THE PRODUCTION OF THE SUBJECT MATERIEL:

ACCIDENT CATEGORY	ACCIDENTS PER FACILITY · HRS	ACCIDENTS PER MAN · HRS
IA	10^{-6}	– – – –
IB	– – – –	10^{-7}
IIA	10^{-5}	– – – –
IIB	– – – –	10^{-6} *
IIIA	10^{-3}	– – – –
IIIB	– – – –	10^{-6} *
IV	1	1

*NOTE: THE SUM OF THE PROBABILITIES OF A CATEGORY IIB OR IIIB ACCIDENT OCCURRING SHALL BE 10^{-6} PER MAN-HOUR OR LOWER.

QUANTITATIVE GOALS

THIS VIEWGRAPH SHOWS THE QUANTITATIVE GOALS THAT RESULTED FROM OUR DEFINITIONS. WITH THESE GOALS WE ARE REQUIRING THAT EACH NEW FACILITY BE AT LEAST AS SAFE AS THE OLD FACILITY. I SHALL BRIEFLY PRESENT THE RATIONALE FOR EACH OF THESE VALUES BEGINNING WITH THE CATEGORIES FOR WHICH WE HAVE THE MOST STATISTICAL INFORMATION. THE CATEGORY IB VALUE IS BASED ON A STUDY OF ARMY AMMUNITION PLANT ACCIDENT EXPERIENCE FROM 1949 TO 1973. THE CATEGORY IIB AND IIIB VALUES ARE BASED ON PLANT EXPERIENCE FOR THE LAST DECADE. CATEGORY IV IS A SAFE SITUATION WHEREIN NO INJURIES OR DAMAGE OCCURS, SO THAT GUIDELINES ALLOW UP TO ONE INCIDENT PER HOUR. HOWEVER, WE REALIZE THAT THIS FREQUENCY WILL CAUSE SOME PRODUCTION PROBLEMS, AND WE ANTICIPATE THAT OTHER CONSTRAINTS MAY DICTATE HAVING A LOWER PROBABILITY IN SELECTED PROJECTS FOR CATEGORY IV. THE CATEGORY IIIA VALUE IS BASED ON APPROXIMATING THE FREQUENCY OF INTERRUPTIONS THAT NORMAL OPERATIONS CAN TOLERATE WITHOUT JEOPARDIZING PRODUCTION GOALS. THIS, TOO, MAY NEED TO BE LOWER FOR SELECTED PROJECTS DUE TO OTHER CONSTRAINTS. THE CATEGORY IIA AND IA VALUES ARE BASED ON GENERAL PLANT EXPERIENCE. AS NEW DATA ARE ACCUMULATED, WE WILL MODIFY THESE PROBABILITY GOALS TO REFLECT THE NEW INFORMATION. THE VALUES FOR CATEGORY IA AND IIA ARE THE ONES THAT ARE MOST LIKELY TO CHANGE, WHEREAS, THE OTHER VALUES ARE UNLIKELY TO CHANGE SIGNIFICANTLY. IN THE FUTURE, WE ANTICIPATE THE ADDITION OF COEFFICIENTS TO EACH PROBABILITY VALUE, AND THEREBY ADVANCING FROM THE ORDER OF MAGNITUDE CONCEPT WE HAVE AT THIS TIME.

ALONG WITH THESE QUANTITATIVE GOALS, WE SPECIFY DETAILED STATISTICAL REQUIREMENTS THE CONTRACTOR MUST COMPLY WITH AS AN INTEGRAL PART OF THE HAZARD ANALYSES.

TOTAL SYSTEM HAZARD ANALYSIS REPORTS

- SAFETY CRITERIA AND REGULATIONS
- INDEPENDENT, DEPENDENT AND SIMULTANEOUS FAILURES
- NORMAL OR ABNORMAL OPERATION
- DATA
- TOTAL SYSTEM PROBABILITIES

TOTAL SYSTEM HAZARD ANALYSIS REPORTS

THIS VIEWGRAPH SHOWS THE TOPICS WE SPECIFY TO BE REPORTED UPON. SINCE YOU ARE FAMILIAR WITH THE FIRST THREE, I SHALL NOT ELABORATE ON THEM. IN REGARD TO THE FOURTH TOPIC, WE REQUIRE THAT THE CONTRACTOR SUBMIT ALL OF THE TEST DATA HE PRODUCES IN CONJUNCTION WITH THE REPORTS WHICH WE SPECIFY.

ON THE NEXT VIEWGRAPH WE WILL SEE THE FORMAT WHICH WE DEVELOPED FOR REPORTING THE TOTAL SYSTEM PROBABILITIES OF OCCURRENCE FOR THE VARIOUS CATEGORIES OF ACCIDENTS.

EXAMPLE OF FORMAT TO REPORT TOTAL SYSTEM PROBABILITIES

		PROBABILITY OF CAT. IIB OR IIIB ACCID. PER MAN-HR	EXPECTED TIME BETWEEN CAT. IIB OR IIIB ACCIDENTS
WORSE CASE:	95% CLim	1.0×10^{-5}	100,000 MAN-HRS
MEAN:	50% CLev	1.0×10^{-6}	1,000,000 MAN-HRS
BETTER CASE:	95% CLim	5.3×10^{-7}	1,900,000 MAN-HRS

EXAMPLE OF FORMAT TO REPORT

TOTAL SYSTEM PROBABILITIES

WE WANT THE HAZARD ANALYSIS CONTRACTOR TO DETERMINE AND REPORT THE INFORMATION SHOWN ON THIS VIEWGRAPH WHENEVER FEASIBLE. IF HE CANNOT DETERMINE THESE VALUES, THEN HE MUST REPORT WHY HE CANNOT DETERMINE THEM.

WE DEVELOPED THIS FORMAT FOR PROBABILITY REPORTING TO GIVE THE PROJECT ENGINEER THE MEAN VALUE, THE CONFIDENCE LIMITS, AND THE EXPECTED TIME BETWEEN ACCIDENTS FOR EACH CATEGORY OF ACCIDENT FOR THE TOTAL SYSTEM. FURTHERMORE, THIS FORMAT PROVIDES INTERPRETATION OF THE MEANING OF THE PROBABILITY VALUES. THIS REDUCES THE POSSIBILITY THAT AN UNACCEPTABLY HIGH PROBABILITY OF AN ACCIDENT WILL GO UNNOTICED. ALSO, IT PROVIDES A SUCCINCT SUMMARY OF THE RESULTS OF THE ANALYSIS AND THE DISPERSION OF THE PROBABILITY DISTRIBUTION.

EXAMPLES OF DATA ITEMS REQUIRED BY SYSTEM SAFETY PROGRAM

ATCH NR _____ TO EXHIBIT _____ CONTRACT DATA REQUIREMENTS LIST SYSTEM/ITEM _____

TO CONTRACT/PR _____ CATEGORY _____ CONTRACTOR _____

1. SEQUENCE NUMBER	2. TITLE OF DESCRIPTION OF DATA / 3. SUBTITLE	6. TECHNICAL OFFICE	10. FREQUENCY	12. DATE OF 1ST SUBMISSION	14. DISTRIBUTION AND ADDRESSEES (Addressee – Regular Copies/Repro Copies)
4. AUTHORITY (Data Item Number)	5. CONTRACT REFERENCE	7. DD250 REQ / 8. CODE / 9. APP CODE	11. AS OF DATE	13. DATE OF SUBSEQUENT SUBM/EVENT ID	
001	2. Safety Analyses & Hazard Evaluation Rpts 3. Preliminary Hazard Analysis	6. DRCPM-PBM-T-SF	10. ASREQ	12. See Blk 16	DRCPM-PBM-T-SF 1/0 DRCPM-PBM- 1/0 Plant COR 1/0 DRSAR-SF 1/0 DRDAR-SFS 1/0 Technical Dir 1/0 DRXOS-ES 1/0 13. TOTAL 7/0
DI-H-1326A(M) MOD #710	5. SOW Para 4.1	7. DD / 8. / 9.	11. ASREQ	13. See Blk 16	
16. REMARKS Prepare in accordance with modified DD Form 1664 and DRCPM-PBM Memorandum 385-3. Due _____.					
002	2. Safety Analyses & Hazard Evaluation Rpts 3. Total System Hazard Analysis (TSHA)	6. DRCPM-PBM-T-SF	10. ASREQ	12. See Blk 16	DRCPM-PBM-T-SF 1/0 DRCPM-PBM- 1/0 Plant COR 1/0 DRSAR-SF 1/0 DRDAR-SFS 1/0 Technical Dir 1/0 DRXOS-ES 1/0 13. TOTAL 7/0
DI-H-1326A(M) MOD #711	5. SOW Para 4.2	7. DD / 8. / 9.	11. ASREQ	13. See Blk 16	
16. REMARKS Prepare in accordance with modified DD Form 1664 and DRCPM-PBM Memorandum 385-3. Draft due _____. Final due _____.					
003	2. Industrial Reports, GOCO Plants 3. Mfg Rech Rpt (MANTECH) Prog Proj Status Rpt	6. DRCPM-PBM-T-SF	10. MTHLY	12. See Blk 16	DRCPM-PBM-T-SF 1/0 DRCPM-PBM- 1/0 Plant COR 1/0 DRSAR-SF 1/0 DRDAR-SFS 1/0 Technical Dir 1/0 DRXOS-ES 1/0 13. TOTAL 7/0
DI-L-1415 #712	5. SOW Para 4.3	7. NO / 8. / 9.	11. 0	13. 21 calendar days after cutoff	
16. REMARKS Complete Paras 1,2,3,4,5,6 & 11 of AR 700-90 MANTECH Rpt for 1st two mo of qtr. Complete all paras of AR 700-90 MANTECH Rpt for last mo of qtr. Data gener for TSHA shall be submitted for rev as it is gener. First rpt due 21 cal days after 1st full mo following contract award.					
004	2. Test Reports 3. Data	6. DRCPM-PBM-T-SF	10. MTHLY	12. See Blk 16	DRCPM-PBM-T-SF 1/0 DRCPM-PBM- 1/0 Plant COR 1/0 DRSAR-SF 1/0 DRDAR-SFS 1/0 Technical Dir 1/0 DRXOS-ES 1/0 13. TOTAL 7/0
DI-T-4024(M) MOD #713	5. SOW Para 4.8	7. NO / 8. / 9.	11. 0	13. 21 calendar days after cutoff	
16. REMARKS Prepare in accordance with modified DD Form 1664 and DRCPM-PBM Memorandum 385-3. First report due 21 calendar days after first full month following contract award.					

PREPARED BY: JOSEPH R. DRUGMAND, DRCPM-PBM-T-SF — DATE — APPROVED BY — DATE

DD FORM 1423 REPLACES EDITION OF 1 APR 68, WHICH IS OBSOLETE

EXAMPLE OF DATA ITEMS REQUIRED BY SYSTEM SAFETY PROGRAM

FOR THE CONVENIENCE OF THE PEOPLE USING OUR SPECIFICATIONS, THE MEMORANDUM DESCRIBING OUR SYSTEM SAFETY PROGRAM HAS COPIES OF THE NECESSARY CONTRACT DATA REQUIREMENTS LISTS AND DATA ITEM DESCRIPTIONS. THIS VIEWGRAPH IS A CONTRACT DATA REQUIREMENTS LIST SHOWING HOW TO SPECIFY ON THIS FORM THE HAZARD ANALYSIS REPORTS, MONTHLY PROGRESS REPORTS AND DATA REPORTS.

EXAMPLE OF MILESTONE

MILE-STONE NUMBER	RESPON ORG	TITLE, DEFINITION AND SCHEDULING
1131	PLANT	START TOTAL SYSTEM HAZARD ANALYSIS (TSHA)—DATE THE CONTRACT IS AWARDED TO START TSHA. SCHEDULE THIS MILESTONE CONCURRENTLY OR AFTER MILESTONE 1130.

EXAMPLE OF MILESTONE

WE MONITOR OUR PROGRESS ON A PROJECT THROUGH A MILESTONE SYSTEM. THIS IS AN EXAMPLE OF THE PERTINENT MILESTONE INFORMATION PROVIDED TO PROJECT ENGINEERS. EACH MILESTONE IS DESCRIBED BY A MILESTONE NUMBER, ORGANIZATION RESPONSIBLE FOR MEETING THE MILESTONE, TITLE, DEFINITION, AND SCHEDULING INFORMATION. THE MEMORANDUM DESCRIBING OUR SYSTEM SAFETY PROGRAM HAS A COMPREHENSIVE LIST OF THESE MILESTONES.

IN CLOSING, I WANT TO SUMMARIZE A FEW POINTS. FIRST, WE TAILORED OUR SYSTEM SAFETY PROGRAM TO OUR OWN NEEDS. SECOND, WE DESIGNED OUR MEMORANDUM WHICH DESCRIBES THE PROGRAM AS A HANDBOOK FOR OUR PROJECT ENGINEERS. THIRD, WE DEVELOP DETAILED SPECIFICATIONS FOR HAZARD ANALYSES AND ALL OTHER ASPECTS OF OUR PROGRAM THAT WE EXECUTE, WHETHER IN-HOUSE OR THROUGH CONTRACT. AND FOURTH, WE BELIEVE WE HAVE SOME FACETS IN OUR HAZARD ANALYSIS SPECIFICATIONS WHICH CAN BE ADAPTED FOR USE IN OTHER AREAS.

REMOTE-CONTROLLED NITRATOR FACILITY WITH MULTI-PRODUCT CAPABILITY

by

M. C. Hudson, P. R. Mosher, and W. A. Carr
Naval Ordnance Station, Indian Head, Maryland

INTRODUCTION

A continuous, automatic, remote-controlled nitration plant has been built at the Naval Ordnance Station, Indian Head, Maryland. The nitration plant is capable of producing a variety of nitrate-esters by appropriate changes in process vessels and controls. The plant has many unique features for process development and for safety.

The fundamental design concept of the plant was that it be a nitration process development facility capable of producing a variety of nitrate-esters with minimum exposure of personnel and a high degree of safety in operation. Personnel of the Naval Ordnance Station, Indian Head worked with HansPeter Moser Processing of Corseaux, Switzerland and defined the design criteria. The criteria were:

(1) for operations with known processing parameters such as for NG;

(2) for new and unique processing such as continuous nitration of MTN and TEGDN; and

(3) for instrumentation that would provide safe, remote-controlled processing. The plant design criteria also required that equipment and control modifications necessary to change products be minimized and made as nearly error-proof as possible. These criteria were quite satisfactorily met in the completed facility. It is the first plant to produce MTN and TEGDN by continuous process. The plant can manufacture NG (nitroglycerin), MTN (metriol trinitrate), PGDN (propylene glycol dinitrate), DEGDN (diethylene glycol dinitrate), and TEGDN (triethylene glycol dinitrate). Other products possible include solid nitrate esters such as PETN.

Note:
Design parameters of this plant are proprietary to Moser processing.

PRECEDING PAGE BLANK

Basic criteria for process vessels were:

- vessels containing hazardous product would be of minimum size consistent with reaction retention time and heat transfer requirements.

- the stirrer must emulsify the product.

- cooling capacity should be maximum attainable.

- workmanship to be suitable for NG service.

To date, equipment for NG, MTN, and TEGDN processing has been utilized and successfully produced products meeting quality control requirements.

The NG process is depicted in Figure 1. The nitrator is common to all current products. It has slightly larger capacity than necessary for NG to allow nitration of esters with high heat of reaction. Its cooling system is new. A "hair-pin" cooler, with U-shape tubes vertically oriented below a top manifold plate was developed. This improves heat transfer over that of a continuous coil cooler and reduces coolant loop inlet-to-outlet temperature increase. It also removes all welds from exposure to the acid contents. The nitrator also is jacketed for additional cooling and for nitrating solids which could "salt-out" on cooling coils.

The NG/spent acid separator is similar to those of other continuous processes. It is a static separator with the nitration effluent emulsion entering tangentially to give a slow stirring action. This allows product to separate and rise to the top above the spent acid layer. The top section of the separator is glass as shown in Figure 2. This allows remote TV observation of the separating product. Depth of the product layer can be controlled remotely and once the float system is adjusted, control of product layer and overflow is automatic. The spent acid is decanted thru a controlled overflow. It is automatically diluted with water to dissolve remaining product and improve downstream safety. Dilution with water is used only on spent acid that is stable enough to be treated.

The other vessels in the NG process are washers and separators similar to those of many continuous nitration facilities. The only unique feature of these vessels is the use of electronic control on the washer stirrer motors to allow changing stirrer speed. This change can be made remotely from the control room. Soda water and fresh water can be remotely added to the washers. The water separators have interface floats so that product level in these vessels can be observed by TV. This arrangement of vessels is utilized for most products with some changes for different product requirements. Principles of operation are common and available in other literature hence, will not be further discussed.

Process schematic for TEGDN is shown in Figure 3. Note the continuous drowner which is a new and unique feature. Because of low stability of the spent acid from TEGDN and certain other nitrate esters processing, previous production has been by batches which are quickly drowned in ice water to cool and separate the product and quenched acid. In this plant, the nitrator effluent, product and spent acid emulsion, is not allowed to separate in a static separator but is continuously drowned by chilled water. The continuous drowner is located in the nitrator emergency drown tank which is filled with chilled water to maximize cooling capacity. The continuous drowner stirs and dilutes the emulsion and allows the product to settle out. The nitrate-ester is then picked up by an eductor using chilled water as the motive force and lifted to the acidic water separator. This separator is installed on the panel in place of the static separator utilized for NG, etc. From here the TEGDN is continuously displaced to the washer system. The acidic water overflows from the continuous drowner to the main drowner tank and is then educted to a neutralization tank in the spent acid house.

Control of feed material flow is essential to safe continuous nitration. In this plant, one motor drives the mixed acid pump which then drives the polyol pump. Any failure in this system results in stopping the polyol pump thus preventing addition of polyol to the nitrator without adding acid which is a hazardous condition. The pumps are variable speed thru their gear drives and provide variable feed ratio in addition to rate. Acid flow is checked by volume in a gauged container. Polyol flow is checked by weight in a scale tank. Polyol lines to the pump from the various supply tanks comes thru non-interchangeable fittings only one of which can be "made". A retractible tube with control interlocks feeds polyol to the nitrator. Certain alarm conditions result in polyol arm retraction from the nitrator and interruption of nitration.

The plant is controlled by a combination of pneumatic systems with intrinsically safe electronic sensor feedback. The control console, Figure 4, is located in a barricaded structure remote from the nitrator house. In automatic operation, a pneumatic punch card programmer operates necessary components in the plant. This programmer establishes the order of various operating events to put the plant on-stream and operates valves, pumps, and stirrer motors automatically as necessary to maintain continuous nitration. The shutdown/washdown operations are also programmed. The programmer will not advance if interlocked conditions are not satisfied. Also, the programmer turns off or "bridges" some interlocks during startup when operating conditions have not stabilized thus preventing shutdown by automatic control response to alarm situations.

To change products, sections of the control console are changed. The electrical and pneumatic connectors are keyed and non-interchangeable so that improper plug-in is impossible. These control changes coordinate with changes in process vessels.

The control console also has recorders to document process parameters. The data is used to optimize production rates, and investigate equipment modifications.

To provide for control system safety and integrity, there are over 100 intrinsically safe relays to transmit signals from sensors mounted on valves and stirrer shafts, etc. An example of a valve body mounted, two-position sensor is shown in Figure 5. Also, all critical product feed, coolant flow, and instrumentation lines are traced with a pneumatic system. In particular, thermocouple wells into the process vessels are traced. If any line is not properly connected, the tracer system cannot be closed and pneumatic pressure will not buildup to deactivate the interlock and allow the plant to begin nitration.

Instrumentation for nitrator operation and safety are:

- bimetal thermometer (for start-up preparation)
- pneumatic temperature transmitter for brine control and safety alarm
- pneumatic temperature transmitter for recording and safety
- electric thermostat for drowning
- stirrer rpm transmitter for safety, indication, and recording
- Redox meter on effluent emulsion

The instrumentation in the static separator are:

- temperature transmitters same as in the nitrator
- interface controller for spent acid overflow and product layer depth
- automatic skimmer for displacement of ester on shutdown
- poor separation transmitter

The continuous drowner/separator has temperature and product level sensors. Washer instrumentation is stirrer rpm and temperature sensors. There are pH meter to measure washer effluent and product conditions.

Product transfer from the nitrator was orginally by gravity. In this system, separated product was displaced through a water filled detonation trap to a water filled line. The product, in the form of individual droplets, rolls down this line to the hold house. This system is successfully utilized in Europe and worked with NG in this plant although the as-installed elevation available between nitrator and hold house at Indian Head was marginal as far as providing the driving force.

When initial continuous nitrations of MTN were made, it was found that the product, which is considerably more viscous than NG, would not flow at a satisfactory rate. As time and need for product did not allow for modifying as-installed positions to provide a greater slope, an eductor system was installed in the final separator to transfer product to hold house.

In summary, the Naval Ordnance Station, Indian Head has a unique multi-product nitration facility capable of producing 100 kilograms per hour of high quality nitrate esters. By virtue of modular design allowing process vessels to be relocated and control systems to be switched at connectors in the control cabinets, the plant can be easily changed from one product to another. This versatility allows pilot scale study of nitration parameters that would be important in designing a large production plant.

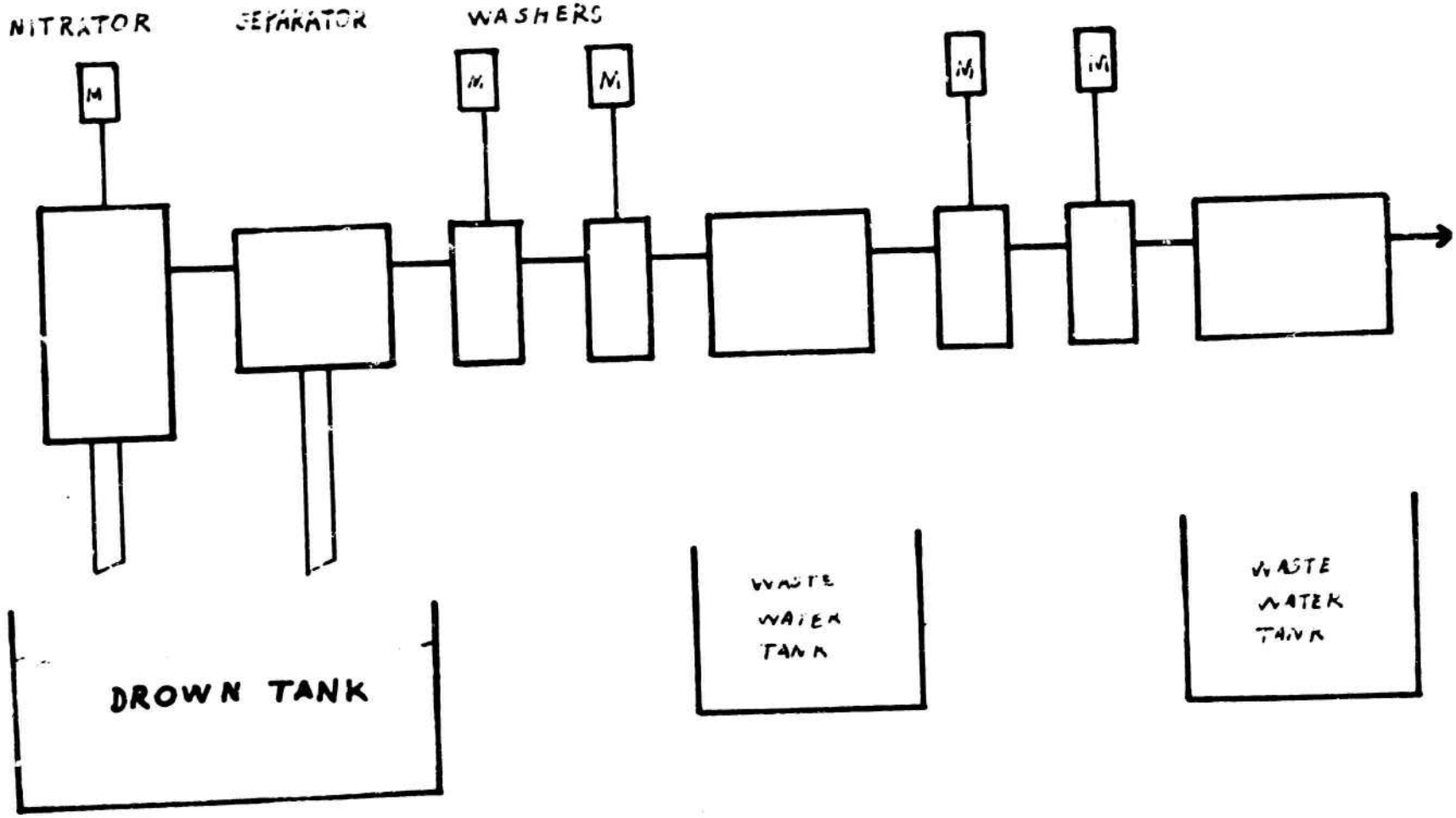

FIGURE 1 NITROGLYCERIN ARRANGEMENT

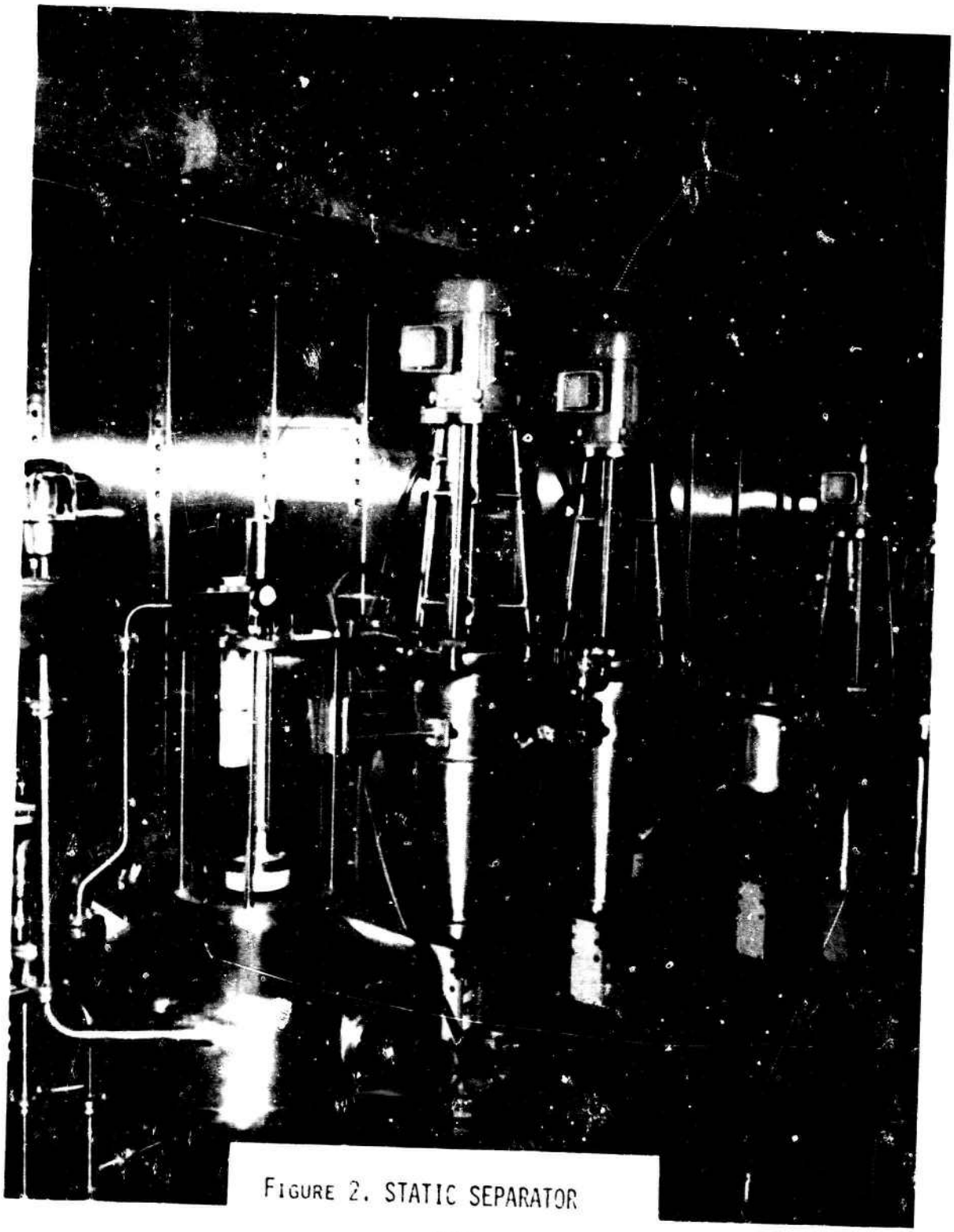

FIGURE 2. STATIC SEPARATOR

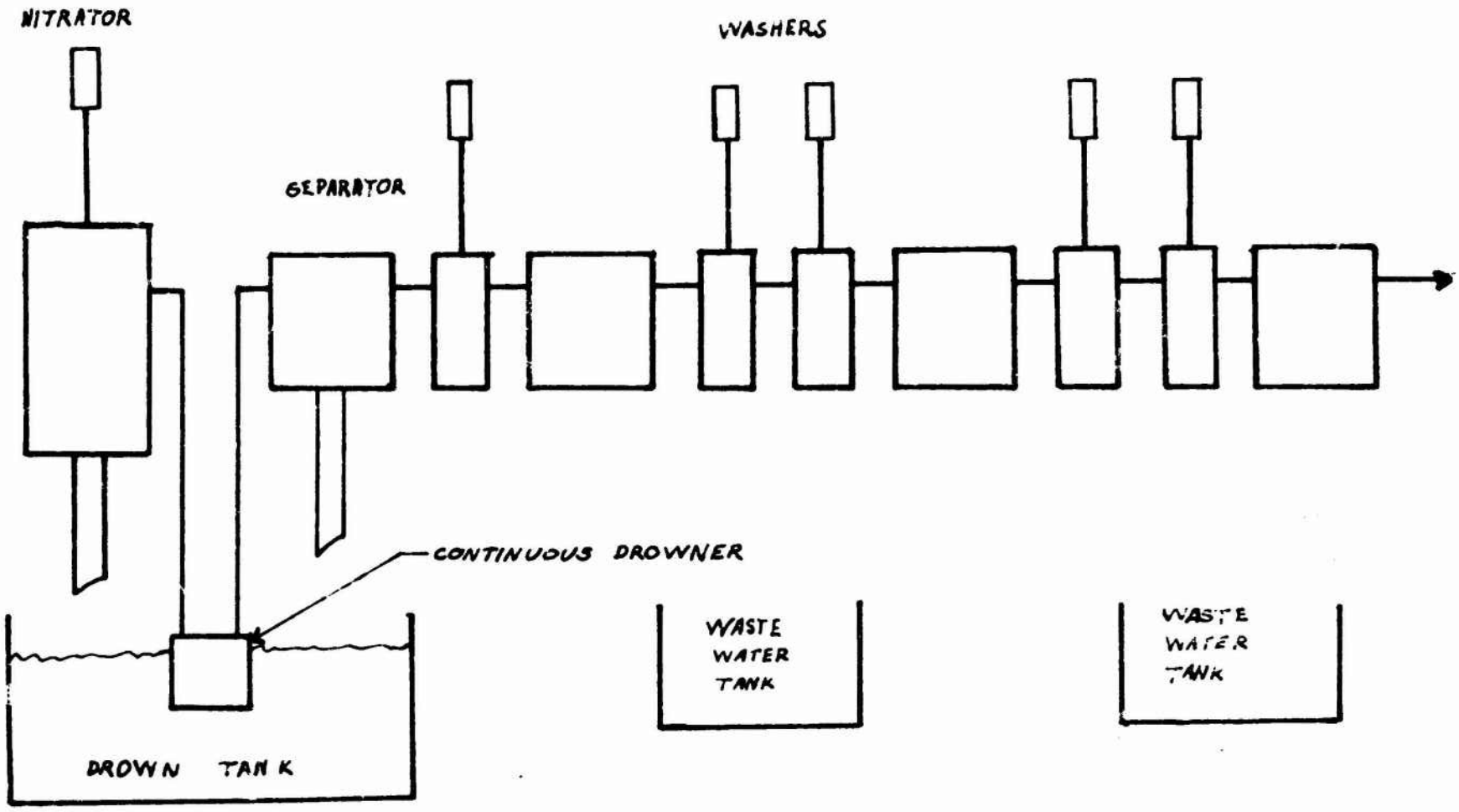

FIGURE 2 TEGDN ARRANGEMENT

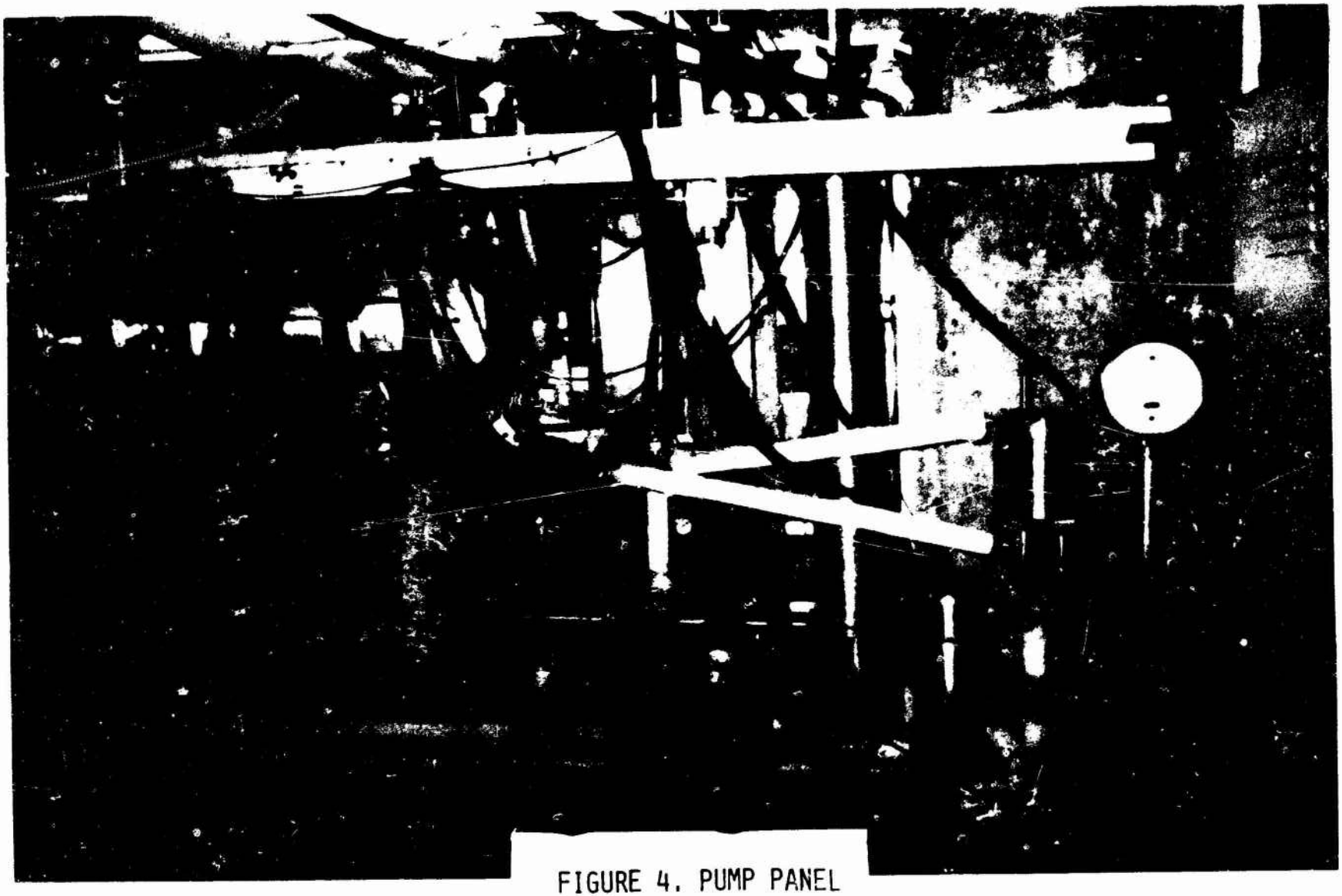

FIGURE 4. PUMP PANEL

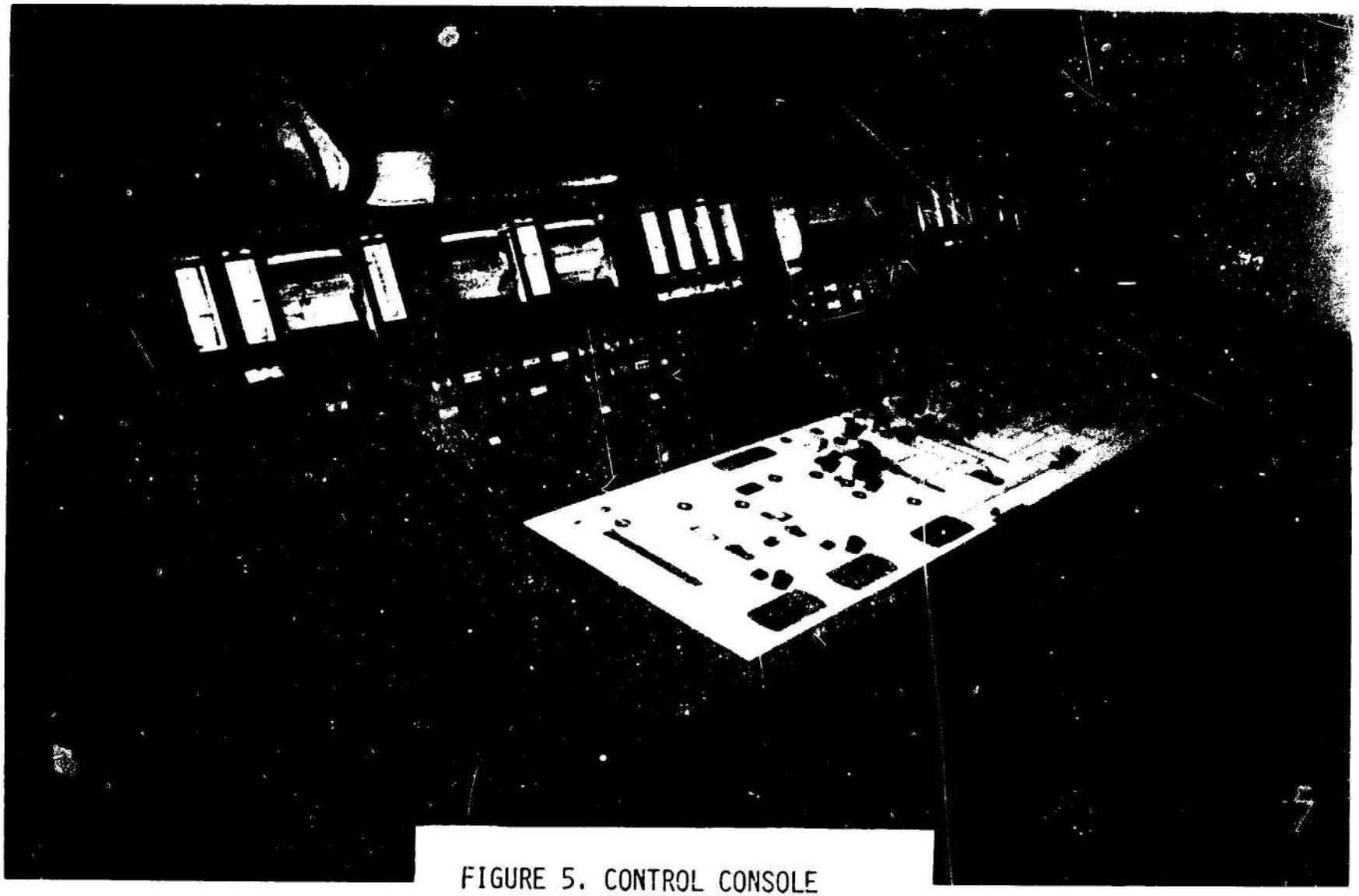

FIGURE 5. CONTROL CONSOLE

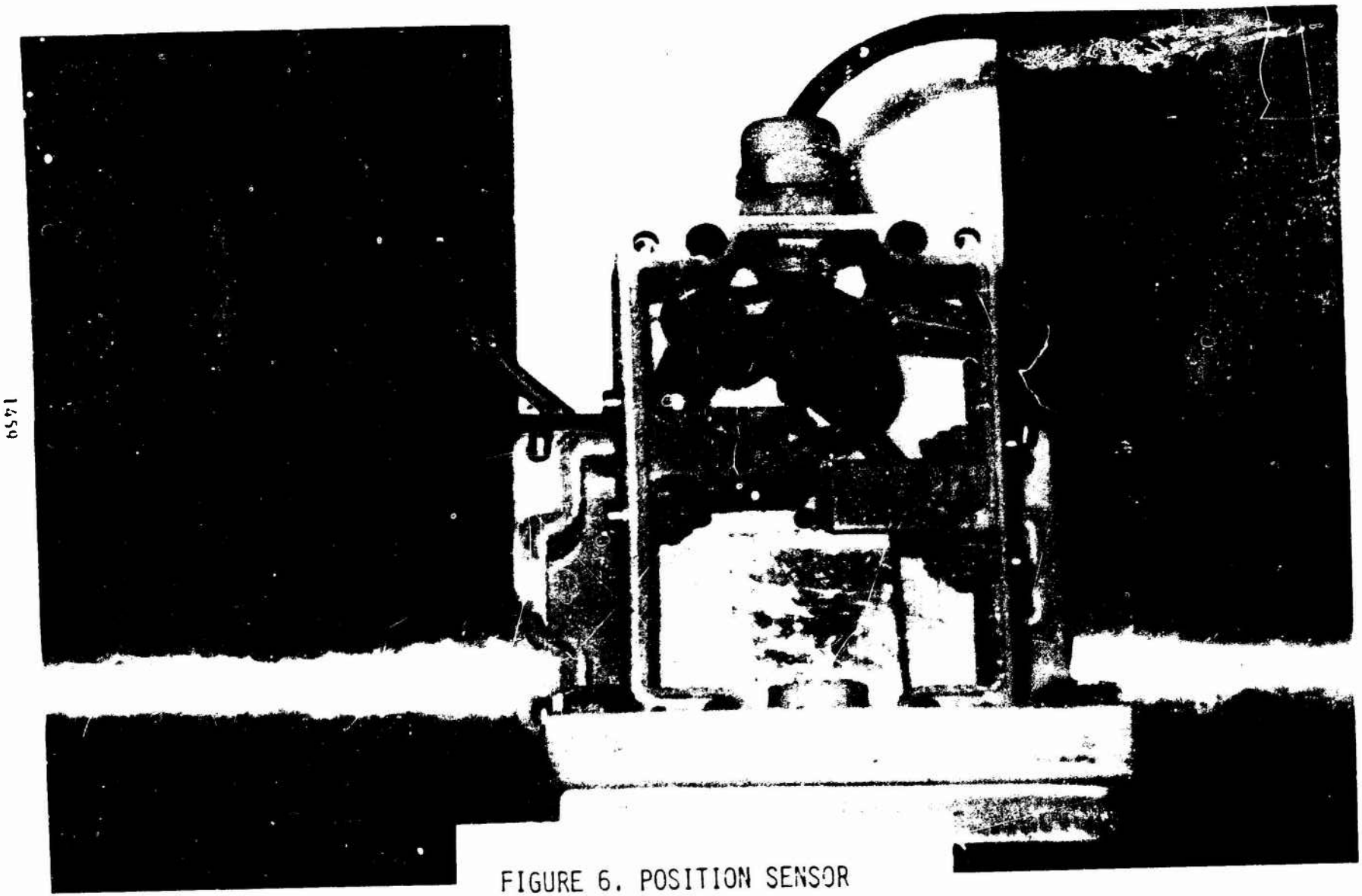

FIGURE 6. POSITION SENSOR

THE NAVY'S EXPLOSIVE SAFETY IMPROVEMENT PROGRAM FOR PIER SIDE MUNITIONS OPERATIONS

by

J. Petes
Naval Surface Weapons Center

About three years ago, CNO initiated the Navy Explosives Safety Improvement Program (NESIP). It wasn't that there were a rash of accidents involving explosives - the Navy's explosive safety record is excellent. Rather, the program was started in order to assess the Navy's compliance with DDESB standards in its many operational environments, and to improve controls over waivers and explosive safety problems in general. A collateral objective is to develop military construction programs to eliminate such problem areas where possible. One major element in the NESIP is that which I will describe, that designated Milestone E-2 (Fig. 1).

This Milestone has as its objective the development of analyses and testing programs to obtain realistic data in regard to explosives hazards which may be experienced in Navy ship berthing ports during the handling of small quantities of ammunition between ships and shore activities. This we call the Navy "topping off" scenario because the objective is to handle only enough ammunition to top off any minor shortage in the ship's magazine. I will discuss the scope of the work, the methods and approaches used, and some of the results we have attained.

Blanket application of the Q-D standards severely hampers Navy operations in port. It is through waivers that the Navy must operate in many of these daily, necessary functions - and the elimination of waivers is a continuing Navy objective.

The Navy believes that many of the waivers can be eliminated without compromising accepted hazard criteria by applying DDESB ground rules to specific Navy operations or scenarios. The accepted hazard criteria, Fig. 2, in physical terms, permits no more than one psi of airblast pressure, and no more than one hazardous fragment in a unit area of 600-ft^2, where a hazardous fragment is defined as one with an impact energy greater than 58-ft lb.

The basic Navy problem is illustrated in Figure 3. The Q-D tables call for a hazard arc of 1,250-ft when up to 30,000-lb of fragmenting munitions are being handled. Only operations essential to the task are permitted within this arc. But at many of our ports, this arc encompasses all sorts of normal naval base activities such as pursued in office buildings, residences, commissaries, and such. At some ports, public roads are within the arc.

PRECEDING PAGE BLANK

We would like to reduce the arc to something more compatible with the amount of explosives handled in topping off operations. By direction, the Navy has limited ammunition handling at these ports to no more than 1,500-lb net explosive weight (NEW) in any given operation. Intuitively one would guess that if a 1,250-ft arc is appropriate for 30,000-lb NEW, then something less than 1,250-ft would constitute an acceptable hazard arc when, for instance, unloading munitions with 1,500-lb NEW from a truck at the pier. If the lesser arc could be realized, a large area for the other base activities would be freed from restrictions. If the arc could be reduced to 500-ft, it would hardly extend beyond the pier.

But how much less than 1,250-ft can this arc be reduced, if indeed it can be reduced? That's our job in Milestone E-2 (Fig. 4) - to determine through analysis and tests, the hazard arc for the maximum credible explosion during topping off operations, and if practicable, to reduce this arc.

In the task, we are concerned with all the different munitions (except nuclear) that the Navy handles in topping off and on-off inspection type operations, and all ships and submarines on which the munitions go. We follow the munitions from the time they arrive at the pier to the time they are safely secured in the ships magazines or launchers. And we keep asking the question: What if a round explodes here, what if it goes off there, and what are the consequences as far as Q-D is concerned? Note, we don't ask how an accident happens - the how is not the issue.

In most ports, it is convenient to consider four general scenarios (Fig. 5). In the pier handling situation, we are limited to 1,500-lb NEW. A 1,500-lb explosion produces a pressure of about one psi at 500-ft; since this pressure coincides with the acceptable blast criterion, our real concern is the fragment hazard generated by this explosion. What is the fragment distribution and areal density surrounding the explosion for any of the munition - torpedoes, missiles, shells, bombs - and their transport vehicle that may be involved? How large is the acceptable fragment arc? We try to answer these questions.

The pier explosion may have larger implications that its own Q-D arc; it may set off munitions in and on the ship that is being topped. (This is the second scenario.) Some of our ships are relatively thin skinned with magazaines extending out to the hull and above the water line. Their magazines may be vulnerable to the fragments from the pier accident. And the munitions topside - torpedoes and ASROCs - may be

vulnerable because the launchers are essentially weather shields only.

Will the on-board munition detonate as a result of the pier accident? If so, 10,000-lb and more NEW may be involved. Now, we have to determine, first, the mass detonation probabilities of the munitions, or the maximum credible explosion, that may occur and, then, the consequences of this explosion in Q-D terms - blast, fragment, and debris hazards versus distance.

The third scenario concerns intraship propagation of explosions. We have to assess the probability of a detonation at one location of a ship propagating to another location. For instance, will a torpedo detonation in the workshop of a submarine tender (AS) or a destroyer tender (AP) detonate the torpedoes in the magazine directly below the workshop? As in the pier to ship scenario, the maximum credible explosion has to be determined first and then the blast, fragment, and debris hazards.

The last scenario involves ship to ship propagation. Will they occur, and if so, what are the consequences?

It would take forever if we were to investigate each of the items in these scenarios individually. Fortunately, there is a common thread among all of them (Fig. 6). The maximum credible explosion really is the Quantity of the Q-D tables, and the hazard is the Distance. The quantity is a function of the sympathetic detonation probability of the munitions involved and the hazard is a function of the blast and fragmentation. These two items - sympathetic detonation and effects, i. e., blast and fragments, - provide the technological base for solving most of our problems.

We are looking at sympathetic detonation (Fig. 7) for pairs of munitions and clustered weapons in terms of sources of initiation such as blast, single, and multiple fragment impacts, massive debris impacts, thermal inputs, synergistic effects, and explosive sensitivity and energy. And we are studying fragmentation (Fig. 8) characteristics of exploding munitions and their surrounds such as the truck in which the munitions arrive at the pier and the ship's structure around the explosion. We determine such things as the number, size, shape, velocity, trajectory, areal density, and impact energy of these fragments.

With sympathetic detonation and effects information in hand, we apply them to the specific scenarios of concern through analysis and tests. And thus, we can provide answers in terms of distances at which acceptable hazards are attained.

In Figure 4, I indicated that one of our objectives is to reduce the distances and maximum credible explosion if practicable. The basic technology is applicable to designing

means to do this (Fig. 9). On one hand, we can use inhibitors between rounds to prevent sympathetic detonation and so reduce the maximum credible explosion. On the other hand, we can design shields to surround an explosion source so that fragment trajectories can be restricted and thus reduce hazard distances.

The preceding is in general and in brief a description of the objectives, scope, and approaches of the NESIP Milestone E-2 program. Now, even more briefly, some of the results will be described.

We have developed (Fig. 10) general analytical means for fragment generation and characterization and for determining sympathetic detonation probabilities. For cased munitions and their close-in surrounds, the fragment characteristics are summarized in what we call FEN charts relating fragment energy, number, size, and distance. We have these for specific weapons such as torpedoes, missiles, and projectiles and will prepare them for other munitions as we progress in the program. The analytical model for sympathetic detonation will be described in some detail by Fran Porzel in a following paper at this Seminar.

Figure 11 shows some of the scenarios we have tested and analyzed and the munitions involved. Most of the work thus far has been with the pier handling situations. We have demonstrated that two Mk 16 torpedoe warheads totalling 1,500-lb NEW and detonated simultaneously produce an acceptable blast and fragment areal density beyond 500-ft provided that a sand shield or barrier is used on the truck transporting the torpedoes. It turned out that the truck cab was a major source of fragments; a 10-in thick sand barrier between the warheads and the cab reduced the breakup of the cab to acceptable limits.

We have determined that 5"/54 projectiles loaded with Explosive D will not detonate in pallet or magazine stacking configurations; there is no sympathetic detonation between rounds even when the rounds are in contact one with the other. However, 5" rounds filled with Composition A-3 explosive will detonate in these configurations. But, we found that the use of 3/4-in thick steel plates between rounds inhibits sympathetic detonation. So, for a pallet load of 48 rounds, each round containing about 8-lb of explosive, the maximum credible explosion is only 8-lb, i.e., the donor, when the inhibitors are used. The fragment distribution and blast from this single round is well below the acceptable hazard criteria at 500-ft.

We found that Composition A-3 loaded 76mm projectiles in operational configurations such as on pallets on the pier, and in magazine storage in ready service racks and on the gun loading ring aboard an FFG-7 class ship, are not prone to sympathetic detonation. The space between rounds in these configurations is larger than P_{D50}, where P_{D50} is the distance between rounds at which there is a 50% probability of detonation propagation between donar and acceptor. The 76mm round is fixed - the projectile is fixed to the propellant cartridge. Although the receptor projectile does not detonate at operational spacings, the cartridge case is penetrated by donor projectile fragments resulting in the burning of some of the propellant. This burning may provide a cookoff environment for the receptor projectiles; we are looking into this.

Tests with a mockup of the Tomahawk weapon have been conducted; the results show that beyond 500-ft the acceptable hazard criteria have been met.

Intraship scenarios have been investigated. For instance, we determined that in the geometries we have aboard an AD and an AS, the deck plating is sufficient to prevent detonation of a receptor torpedo warhead in the magazine from the fragments and blast of a donor torpedo in the workshop directly above the torpedo magazine. Now we are investigating the effects of acceptor torpedo translations one against the other and against the bulkheads and deck, and the thermal inputs of the donor torpedo in the confined volume of the magazine. In similar tests, we have determined that on an FFG-7, the detonation of a 76mm projectile in its magazine will not detonate a receptor Mk 46 torpedo warhead in the magazine directly below the 76mm magazine. The warhead burns vigorously. This now is our concern: Will the burning explosive provide a cookoff environment to the other warheads in the magazine? We are investigating this.

We have done a lot and we have much more to do. Our basic technology is fairly well developed and operable. It is used for analysis and test guidance. Together - analysis and tests - they are giving the answers to the questions asked: What are the Q-D values for specific Navy scenarios? So far we have met the hoped for 500-ft arc, sometimes with the use of inhibitors and shields, sometimes without them. We realize that when the maximum credible explosion yield gets to be larger than 1,500-lb, we may not be able to attain 500-ft; so be it. Whatever it turns out to be, it will at least be real and defensible, not just a limitation imposed by general regulations.

ACKNOWLEDGEMENTS

Milestone E-2 of this CNO initiated program has been ably guided by J. Connelly of OPNAV 411 and supported by the Naval Sea Systems Command with E. W. Daugherty (NAVSEA 04H3) at present, and Dr. A. Amster (NAVSEA 0332) formerly, providing much appreciated technical liason. The development of the details of the objectives and their prosecution is the work of many persons too numerous to mention. Two, however, merit singling out: F. B. Porzel of NSWC(WO) for his enthusiastic and comprehensive technical guidance and analyses of all facets of the task, and P. McLain of the TERA Group of the New Mexico Institute of Mining and Technology for his skillful direction of the tests.

NAVY EXPLOSIVES SAFETY IMPROVEMENT PROGRAM

MILESTONE – E

DEVELOP/IMPROVE NAVY-DDESB INTERFACE TO OBTAIN FULLER RECOGNITION OF NAVY SCENARIOS AND READINESS REQUIREMENTS.

E-2 – DEVELOP TESTING

PROGRAM TO OBTAIN DATA IN SUPPORT OF NAVY INTERPRETATION OF DDESB STANDARDS RE NAVY SCENARIOS.

FIGURE 1



GUIDE LINE 1

DDESB CRITERIA FOR ACCEPTABLE HAZARD

1468

- 1 PSI OR LESS BLAST PRESSURE
- 1 HAZARDOUS FRAGMENT OR LESS PER 600 SQ. FT. (1.67 FRAGS/1000Ft^2)
- HAZARDOUS FRAGMENT HAS IMPACT ENERGY OF 58 FT-LBS OR MORE

FIGURE 2

THE PROBLEM

- 448 WAIVERS AT 12 TIDEWATER PORTS
- COST TO CORRECT VIA NEW CONSTRUCTION, AT SEA REPLENISHMENT - > 600 M

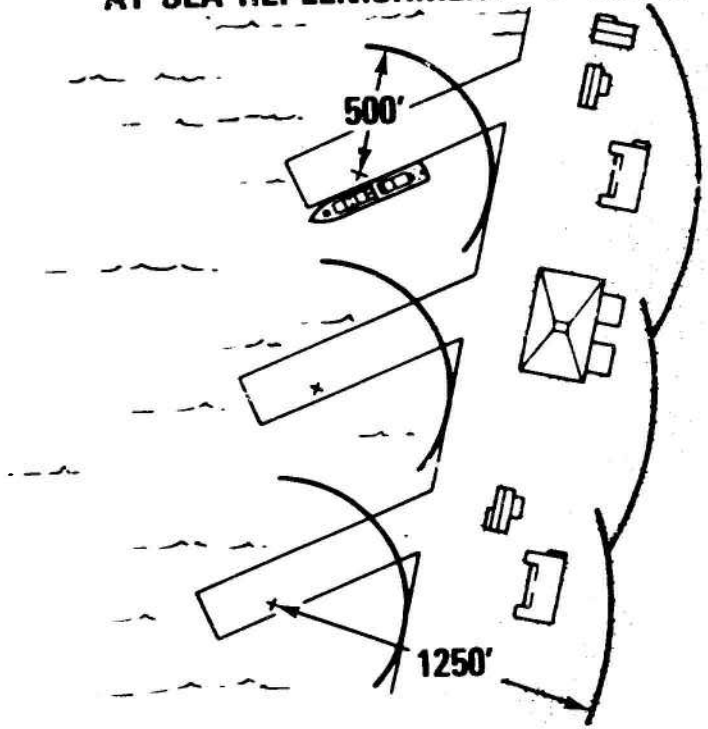

1469

THE SOLUTION –

ESTABLISH NEW QUANTITY-DISTANCE TAILORED TO OPERATIONS AT EACH PORT

FIGURE 3



OBJECTIVES

1470

- DETERMINE HAZARD DISTANCES FOR PRESENT OPERATIONS
- REDUCE DISTANCES AND MAXIMUM CREDIBLE EXPLOSION WITHOUT COMPROMISING SAFETY

FIGURE 4

NESIP SCENARIOS

A. PIER HANDLING

- TORPEDOES
- PROJECTILES
- BOMBS
- MISSILES

} FRAGMENT DISTR. BEYOND 500-FT FOR < 1500-LBS NEW

B. PIER TO SHIP

- ALL SHIPS
- ALL MUNITIONS
- TOPSIDE
- MAGAZINES

} MAX. CREDIBLE EXPLOSION, FRAG. DISTR., & BLAST

C. INTRA-SHIP EVENT

- AO/AS WORKSHOP TO MAGAZINE
- TOPSIDE TO TOPSIDE
- TOPSIDE TO MAGAZINE
- MAGAZINE TO MAGAZINE

} MAX. CREDIBLE EXPLOSION, FRAG. DISTR. , & BLAST

D. SHIP TO SHIP EVENT

- SHIPS AT PIER
- NESTED SHIPS & SUBS

} MAX. CREDIBLE EXPLOSION, FRAG. DISTR., & BLAST

FIGURE 5



1472

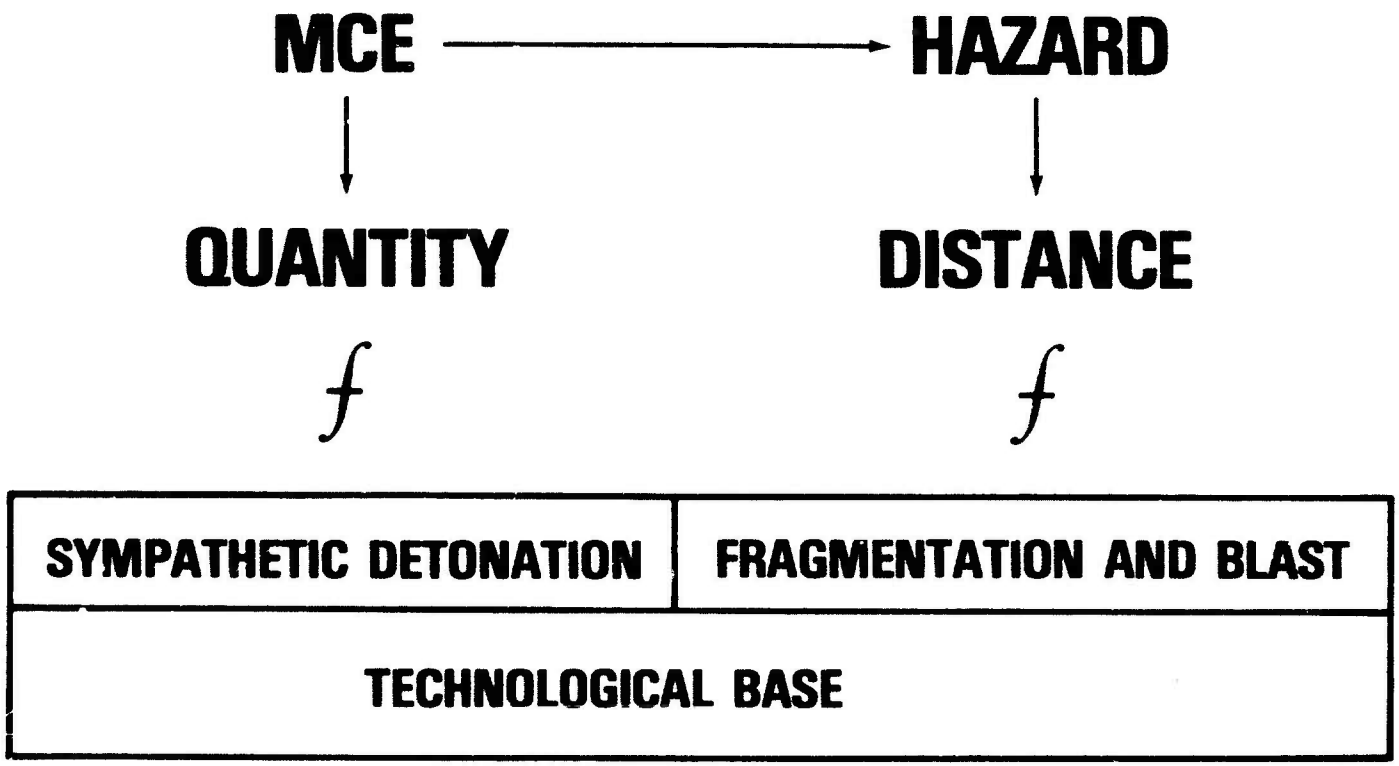

FIGURE 6



SYMPATHETIC DETONATION OF SINGLE PAIRS & CLUSTERED MUNITIONS

- BLAST
- SINGLE FRAGMENT IMPACT
- MULTIPLE FRAGMENT IMPACTS
- MASSIVE DEBRIS IMPACT
- THERMAL INPUT
- SYNERGISTIC EFFECTS
- EXPLOSIVE SENSITIVITY & ENERGY

1473

FIGURE 7



FRAGMENT CHARACTERISTICS OF EXPLODING MUNITIONS & SURROUNDS

- NUMBER
- SIZE
- SHAPE
- VELOCITY
- TRAJECTORY
- AREAL DISTRIBUTION
- IMPACT ENERGY

1474

FIGURE 8

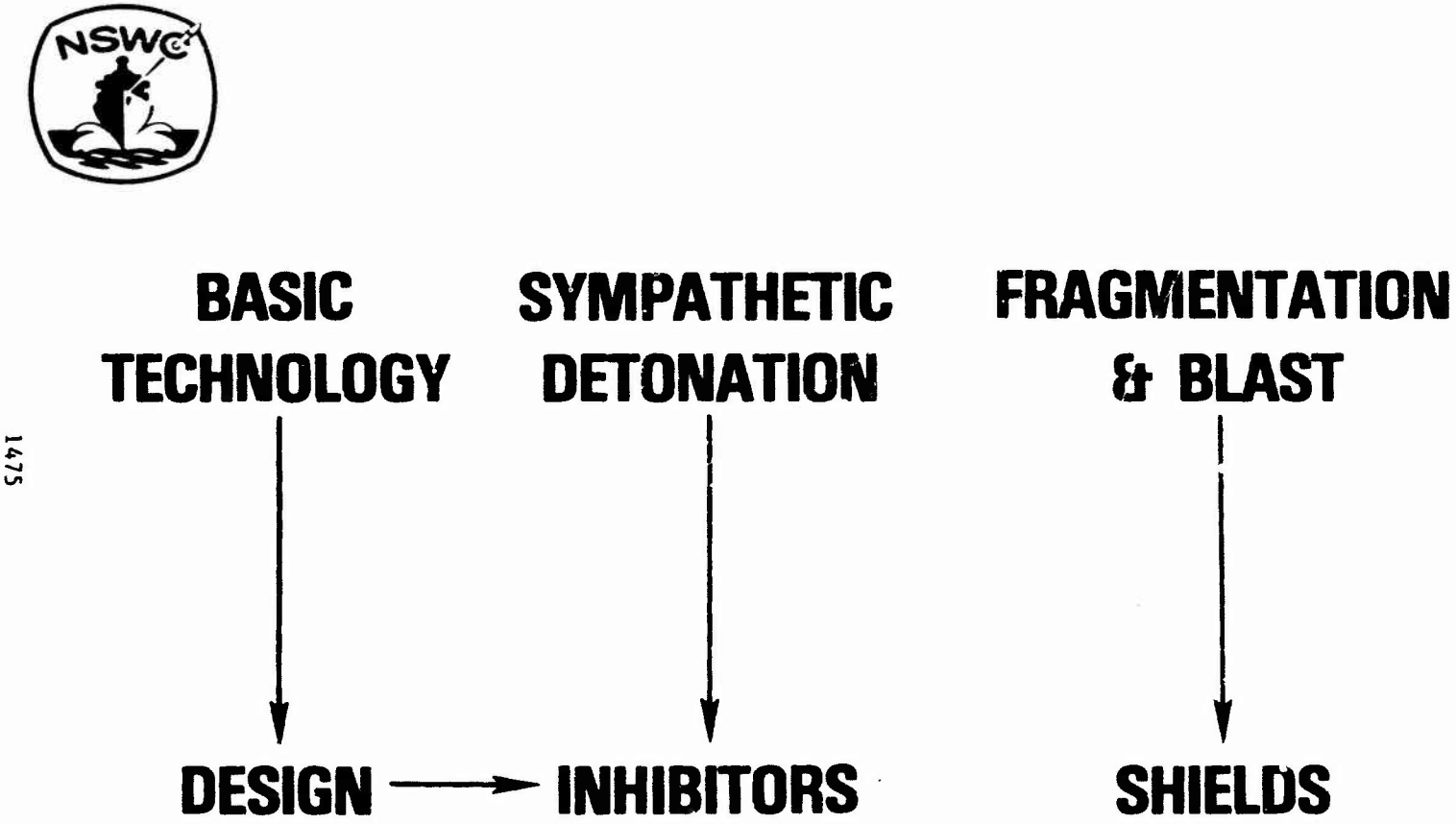

1475

FIGURE 9



DEVELOPED GENERAL ANALYTICAL MEANS FOR

- **FRAGMENT CHARACTERIZATION**
  - E.G. SIZE, AREAL DISTRIBUTION, IMPACT ENERGY
  - PRIMARY & SECONDARY
- **SYMPATHETIC DETONATION DETERMINATION**
  - SINGLE & MULTIPLE FRAGS. & MASSIVE DEBRIS
- **INHIBITOR & SHIELD DESIGN**

1476

FIGURE 10

TESTS

MUNITION	TEST FOR		SCENARIO	COMMENTS
	S.D.*	FRAG.		
MK16 TORPEDO W.H.	✓	✓	ON PIER	O.K. AT 500' WITH SHIELD FOR 1,500 LBS NEW - ALL TORPEODES
5"/54 PROJ. EXPLD	✓	✓	ON PIER (PALLET)	NO S.D.*
				IN MAGAZINE PROBABLY NO S.D.*
5"/54 PROJ. COMP. A-3	✓	✓	ON PIER (PALLET)	MASS DETONATION;
				WITH ¾" INHIBITOR, NO S.D.*
76mm PROJ COMP. A-3	✓		ON PIER (IN TANKS)	NO MASS DETONATION
			ON SHIP (IN TANKS & BARE)	NO MASS DETONATION - BUT COOK-OFF HAZARD?
TOMAHAWK		✓	ON PIER	O.K. AT 500'
MK16 TORPEDO W.H.	✓		AD/AS	NO S.D.* WITH 5/16 PLATE & 40" SPACING
76mm PROJ. V.S. MK46 TORPEDO W.H.	✓		FFG-7 MAGAZINE	NO S.D.* BUT DEFLAGRATION

* S.D.= SYMPATHETIC DETONATION

FIGURE 11

A MODEL AND METHODS FOR CONTROL OF SYMPATHETIC DETONATION

by

F. B. PORZEL
Naval Surface Weapons Center
White Oak Laboratory, Silver Spring, Md

INTRODUCTION

This paper is part of the Navy Explosive Safety Improvement Program (NESIP) just described by Mr. Petes of the Naval Surface Weapons Center. The work is sponsored by OP 411 through NAVSEA 04H3 (Safety Office). To guide and plan the tests, and evaluate the results we have developed and nearly completed a technology base encompassing safety hazards for a broad spectrum of Navy weapons. The NESIP technology base is largely based on the unified theory of explosions, (UTE, NOLTR 72-209, 1972), which was also described briefly in the last two DDESB Safety Symposia (DDESB XVI and XVII, Porzel). UTE provides a simple comprehensive way to predict and evaluate the blast from virtually any explosion; the technology base includes sympathetic detonation determinations and the prediction of fragment sizes, distribution, trajectories, areal density and residual energy on impact.

Sympathetic detonation is a key part and end product of this technology base for safety problems, mainly because the Navy has no single conventional weapon which by itself, if accidentally detonated, produces a blast or fragment hazard at 500 feet that exceeds criteria deemed acceptable by the DOD Explosive Safety Board. Hazardous scenarios arise only from sympathetic detonation of two or more warheads. If sympathetic detonation can be prevented, the whole specter of cataclysmic explosions from mass detonation is virtually exorcised.

Various modes of sympathetic detonation have been heretofore suggested:

- Direct Shock
- Fragment Impact
- Cook off
- Translational Impact
- Radiation (Laser, X-Rays)

Sympathetic detonation, like most real world problems, is far too complex to aspire for precise, rigorous solutions in every case, and is far too broad in scope to risk descriptions which apply well but only to specialized situations. Instead, we will follow the UTE approach: to seek out the controlling

PRECEDING PAGE BLANK

variables that are necessary to describe the phenomena in every case, and to use approximate, average values for less consequential details. For example, it makes sense to aim a cannon just as accurately as is necessary to accomplish the mission -- not as accurately as possible -- because it becomes a waste of time and is misleading to dwell on details that fall well within the inherent probable error of the whole system. UTE is both a tool and a discipline; a tool for pioneering research when information is sparse, and a discipline that demands and insures that what we profess in one field be consistent in what we profess in every other field that involves the same or analogous phenomena.

For these reasons, the emphasis in this paper is twofold, to show that:

- The basic mechanisms of sympathetic detonation are themselves straightforward hydrodynamic phenomena, but
- Cumulative effects such as multiple impacts of fragments and synergistic effects between modes of energy will often produce detonation where the single events, isolated modes by themselves, are too weak to do so.

MODEL FOR SYMPATHETIC DETONATION

Let us first review some facts. Regardless of the complexities of sympathetic detonation, here are a set of well-established facts about them. They are also a set of facts which any theory must explain or accommodate in order to be credible.

1. Energy density is the controlling variable. Sympathetic detonation is not unique to pressure, as the large-scale gap test might suggest, or to temperature as cook-off might suggest, or to velocity of fragment impact, to deformation of the explosive or to translational impact. It may result from any or all of these causes, the common denominator is energy density.

2. Threshold for initiation exists. We know that some critical energy density must exist below which the explosive will never detonate however long it is exposed to the thermal or mechanical stresses. For a given geometry, the large scale gap test, for example, provides just such definite and reproducible initiation pressures. To make that statement more definite, Figure 1 shows the initiation pressure for cast explosives as a function of percent RDX in various mixtures with other more inert materials. Figure 2 is the same graph for pressed explosives. These are compilations recently done for the NESIP program.

3. Critical size. If the source for detonation is too brief or the impacting fragment is too small, the detonation wave will die out, however intense the stimulus may be. We know that because innumerable times a second, cosmic rays and particles bombard explosives with vastly greater energy density than is necessary to initiate an explosion locally, yet they do nothing to the explosive as a whole, except perhaps to "age" it.

4. Synergistic effects. We know that under certain conditions, effects appear to be cumulative. For example, if explosives are exposed to fire they appear to become sensitive to small impacts which will set them off. There is an old saying that a second bullet down the same hole will always set off an explosive.

5. Reaction energy proportional to stimulus. Less widely known, but well established from SUSAN tests is the observation that the energy release from an explosion is a function of the input energy. Up to the point of detonation, low impact velocity produces small explosions, high impact velocities produce large explosion energies. The reaction may die out for purely chemical reasons, and/or many mechanical reasons, such as physical break-up of the explosive charge in the complex geometry of the impact. Once a full detonation is achieved, it is evidently more than enough to initiate another detonation. So, at high enough impact energies, the explosion wave becomes self-sustaining and the energy release is no longer a function of the impacting energy.

Conceptual Model. Before we set up criteria for detonation, we need to ask "Why is an explosion, in the first place?" Figure 3 is a classical model of potential energy which answers that question, along with the facts just mentioned. The abcissa is volume; it could also be space because volume depends only on the spacing r between the atoms, $V \sim r^3$. It could be the volume of a unit mass or of a mole, but let us think of it as the volume of a single molecule, that is, the total volume of a definite number of atoms such as carbon, nitrogen, hydrogen and oxygen, but not necessarily always having the same molecular structure. The ordinate is the energy density, the potential energy of these atoms at a given volume. A prerequisite that any material be a solid or liquid is such a potential well as shown. It simply requires at least one close range repulsive force, which tends to drive the atoms apart, and one close-range attractive force which tends to pull the atoms together. At some distance marked by the bottom of the potential well, the two opposing forces just equal each other,

and the molecule remains in a stable configuration at the bottom of the well.

Of course there are really a great many positive and repulsive forces in a complex structure of such a molecule. There may well be a whole series of potential wells - much more complex than shown here.

To explain explosives requires also a long range repulsive force shown by the long sloping curve to the right. At a large enough separation between molecules, the constituents become a gas and the far right hand portion of the graph can be approximated by the ideal gas law or the corresponding expression for the mixture of explosive debris.

What else does it take to be a practical explosive? It requires only that the depth of the potential well be small compared with the peak at E_c. So, if the molecule can be energized to E_c by whatever process, and the atoms separated, the debris will "slide" down toward the deeper well at infinite separation, releasing far more energy than was required to raise it to E_c in the first place. As in any chain reaction, the important point is that we first have to invest energy for each molecule, and the ratio of energy released to energy invested must be fairly large in order to raise several adjoining molecules up to or exceeding the critical energy required for each of them to reach E_c. Otherwise, the energy released from one molecule simply appears as excitation energy of several adjoining molecules, none of which have received enough energy to raise them up to the critical energy E_c.

We need also to recognize that the same numbers of atoms could be arranged in many different structures or combinations of simpler molecules for each given volume. The complete set of energy-volume curves requires at least one more axis directly out of the paper, representing variable compositions. The whole energy may be represented by a surface, something like a mountain side, full of hills, valleys and lakes, in all directions. The surface itself is an "equilibirum" state. Imagine a raindrop which may actually start (energized) above the surface, fall on to the surface and eventually find its way from the top of the mountain to the valley below, not necessarily on a bee-line going over the tops of ridges to river valley, but moving in three dimensions circuitously from one lake or a stream to the next. Better yet, if the mountains were represented by an irregular, but smooth surface, and a steel ball were rolled down, it might indeed be carried over some ridges by its own momentum. It still move in a three dimensional path. The path might be different for different rolls, depending on how highly it was energized in the first

place. So even if the beginning and end product were the same, releasing the same amount of energy in the long run, the rate of release might be entirely different. Like the difference between a waterfall and following a stream bed from top to bottom. The analogy here is the difference between detonation and burning, even though the chemistry looks the same. One of the central ideas in the unified theory of explosions is just this point: the difference between prompt and delayed energy.

Criterion. It is convenient to summarize the main features of this model and of the facts cited earlier by means of the following criterion

$$\int (E - E_c)\, dt > H_{minimum}$$

without arguing that this is an exact or final expression. The criterion says:

1. The energy can be in any form, hence the term E rather than pressure, temperature, velocity or deformation.

2. E must exceed some critical energy, E_c, necessary to lift it out of the potential well, or the molecule will never decompose however long a time t it is energized.

3. The energy may be cumulative, hence the integral.

4. Time is of essence, as they say, because it is not sufficient merely to raise the molecule to some high energy -- as in a collision with a cosmic ray - It must remain in the high energy state long enough for the molecule to expand and disorganize without falling back into the original potential well.

5. This excess action summarized by the integral must exceed some minimum action, H, sufficient to activate more than one nearest neighbor if the explosive chain is to propagate and grow as a chain reaction.

How such a criterion expression translates into other criteria involving pressure, temperature, velocity or size, will depend upon the shock strength and the size of the stimulus itself. At some shock strengths, the energy will be proportional to P^2, suggesting the criterion

$$P^2 t = \text{constant}$$

At higher shock strengths, involving non-linear compression, or due to the existence of voids, the energy will be proportional to P, suggesting a criterion

$$Pt = \text{constant}$$

Finally, the region and time of activation may be so long as to guarantee that each molecule will disorganize, as in cook-off or fully developed detonation waves, which will simply require that

$$P = \text{constant}$$

For each such case, time t may be replaced by a distance d using the local sound speed c, $d = t/c$. In the acoustic approximation and if $E \sim P^2$, pressure, P, and material velocity, V, are proportional, then P^2t leads to V^2d which is $Vd^{1/2}$ = constant which is sometimes called the Jacobs criterion. Under conditions where $E \sim P$,

$$Pt \text{ leads to } Vt \text{ or } Vd = \text{constant}$$

a form recently found by Howe (ARBRL 02048). For fully developed detonation waves

$$P = \text{constant leads to } V = \text{constant}$$

These regimes are displayed graphically and compared with test data in Figure 3a. It shows the velocity, V, required to detonate Comp B high order (ordinate) as a function of the fragment size d (abscissa). At the highest velocity and pressure levels, the circles are data for 105 mm shells impacted by relatively small fragments as correlated by Howe in ARBRL TR 02048; in this regime the criterion Vd = constant evidently applies. At moderate velocities and pressure, involving somewhat larger "fragments", the SUSAN test results and the large scale gap tests (NOL TR 74-40) suggest that a criterion $Vd^{1/2}$ = constant applies. For SUSAN data and LSGT, the "fragment" was taken as the diameter of the explosive itself. At the lowest velocities involving massive debris, the experiments suggest we have reached the regime where V = constant. These last experiments are described later in this report, using 70 pound projectiles fired from the IITRI 12" gun facility (DDESB XVII, Rindner). P = constant, V = constant, are really the tacit assumption we make whenever we use almost any of the classic criteria used for sensitivity: large scale or small scale gap tests, SUSAN impact velocity, fragment impact velocity, or drop tests.

In summary, each criteria is correct under certain conditions and incorrect under others. Much analysis remains to be done, but they all appear to be special cases of a minimum action criterion $\int(E - E_c)dt$. This criterion also promises a way to correlate the many existing different sensitivity tests.

METHODS OF INHIBITING PROPAGATION

We turn now to some methods for preventing sympathetic propagation as suggested by this criterion.

First let us see which of the damaging variables are capable of causing detonation between neighboring 5"/54 shells. Figure 4 shows pressure-distance curves as was calculated with the unified theory of explosions (NOLTR 72-209) for a 5"/54 shell loaded with 7.8 pounds of Composition A-3 explosive. Near the top is a horizontal dashed line at 16 kilobars which is the initiation pressure of explosive A-3 as indicated by large scale gap tests. To use a current cliche, it is the bottom line for sympathetic detonation. Far below it, with a maximum at 32 bars, is the side-on blast pressure. It is too small by orders of magnitude to cause detonation in an adjacent round. The total pressure head is produced mostly by the dynamic pressure (dashed line) of the debris from the explosive products, and includes the average value of the fragments energy. When the total head strikes another explosive, it produces the reflected pressure shown; we see that it is barely sufficient to cause direct shock initiation at the warhead surface of an abutting round or one perhaps few centimeters distant.

The upper three full lines show the pressures induced locally by typical fragments from a 5"/54 projectile. The average fragment with an impact pressure of 13 kbars is too slow to cause detonation. The fastest fragments which are possible can cause detonation of bare A-3 out to a considerable distance, about 30 meters, before drag forces set in to lower the impact velocity. But when such an isolated fragment strikes the shell case of the donor, it must share its momentum with the receptor case, reducing the average velocity by a typical factor of two, bringing it below the initiation pressure. The top most line is a fragment moving at 4200 f/s which is required for 30 gram fragment according to fragment impact tests (Ref. Roslund).

The overall conclusions from Figure 4 are:

1. Direct shock is not likely to cause sympathetic detonation of 5"/54 Composition A-3 loaded shells.

2. Single small fragments are incapable of producing detonation in 5"/54 shells loaded with A-3.

3. The cumulative effect of multiple impacts from closely spaced small fragments are required to induce detonation in these shells.

The calculations also suggest that sympathetic detonation of 5"/54 shells with A-3 are marginal at best and it could be readily dea ated with modest amounts of shielding.

Similar calculations can readily be made for other warheads using UTE.

Guided by the model, we are concerned only with fragment initiation, not blast initiation. The following processes show promise for inhibiting sympathetic propagation from fragments.

1. Absorption

2. Stand-off

3. Scattering

After a brief discussion of them, we will incorporate these processes in the design of a system capable of preventing sympathetic detonation within the spatial dimension of existing pallets of 5"/54 shells, or to other similar munitions.

Absorption. The large scale gap test (NOLTR 74-40) is an obvious method and is monumental evidence that sympathetic detonation can be inhibited simply by imposing a thickness of absorber like plastic cards, between the donor and the acceptor. Moreover, the LSGT provides an encyclopedia of data as a rough guide to the amount of absorber required. (See figure 5)

The LSGT shows that about 2.5 inches of plastic are required to inhibit detonation of A-3 in the confinement and geometry provided by the large scale gap tests. The equivalent mass of a dense material (but poorer absorber) like steel is provided by a steel plate about .3 inches thick. This is a first guess as to the thickness of steel required and that is about what the P_d50 thickness turns out to be.

These inhibitor or absorber thicknesses would hold, provided the attenuation were a matter of momentum transfer by a smooth planar shock or by single fragments. For the 5"/54, the donor case does not provide the absorber thickness required because it transmits the high reflected pressure it produced in the explosive and is later driven by the impulse of the explosive debris. But, the acceptor case is an attenuator. To a first approximation the attenuation offered by the shell cases is somewhat offset by the reflection and multiple impact processes.

A fact which is very clear from the pressure-distance curve in Figure 4: fragments are a way of concentrating energy well above what the smooth shock wave can produce.

Standoff is a way to capitalize on the inherent divergence from any spherical or cylindrical explosion merely because the fragments move outward on radial lines. Divergence is the reason for the first and most obvious thing to know about explosions: the farther away the better.

As shown in Figure 6, a given size plate will apparently increase in effectiveness as it is placed farther from the donor simply because it subtends less momentum and energy than it would suffer at the closer distance.

Standoff or divergence is the crux of the question why P_d50 occurs at short distances for some munitions. For other munitions, sympathetic detonation may be a matter of fragment energy and single fragment size. We saw from the UTE calculations, sympathetic detonation could be produced at very large distances, or many meters.

Summing up: UTE calculations, arena tests and single impact tests agree that typical fragments from any 5"/54 shell are too weak to detonate another projectile; multiple impacts are required and their cumulative effect can fall off sharply at short distances because of divergence or standoff.

Scattering. By scattering (Figure 7), I refer to deflection of fragments out of the beam of fragments traveling along radial lines. It is similar to the way photons are scattered without being absorbed by a thin translucent screen, or by fog. The outgoing fragments from a shell case move radially outward as in the upper part of the figure. But upon striking the scattering medium shown below, they diverge outward from the original solid angle of the beam within which they were contained. This is a powerful method, provided the scatterer is not too wide, otherwise it begins to scatter as many fragments back into the beam as were scattered out. We want to use an inhibitor no wider than necessary.

Inhibitor module. These processes for absorption have been incorporated in the design shown in Figure 8. The intent is to put individual rounds in modules (like a milk carton) with minimum size inhibitors and placed only where needed. An alternate idea: the inhibitor bars could be placed between the rounds in a standard pallet.

The inhibitors shown serve two purposes:

1. They absorb momentum and energy from the donor.

2. They stiffen the module walls.

We wish to keep the absorber as thin as necessary to save weight. The inhibitors are as narrow as possible in order to maximize scattering. We can do nothing to exploit stand-off of course if the shells are to be placed within a standard pallet. The module itself or the pallet spacing does provide an important air gap between the donor and the acceptor; this gap allows a rarefaction to develop between each interface so that the momentum is the only means for transmitting the action from one shell to the next.

Finally, the module serves two other purposes: One is for protection against cook-off; the thin case or wall, together with the air gap between the carton and the shell is an excellent thermal insulator. And second, the modules being square, they can can readily be banded together in any size pallets of their own. They can be stacked without breaking loose in heavy seas and rolling back and forth. The USS BADGER STATE was lost that way in World War II (DDESB XV, Osborn).

INHIBITOR TESTS

We turn now to a series of experiments with 76 mm shells, 5"/54 shells, Mk 16 torpedoes and mock-ups for a variety of warheads including the Mk 46 torpedoes. They test the ideas and methods of protection discussed so far. The main thrust of the results is to show, as the theory indicated, that sympathetic detonation is no preemptive problem for any of the Navy munitions and scenarios considered. Taken together most Navy munitions either do not detonate at all or the detonation appears to be preventable with modest inhibitors.

76 mm Projectile. Figure 9 illustrates a test set-up and results for 76 mm projectiles. The objective was to determine the distance at which there is a 50% chance of high order detonation. The 76 mm is a high velocity round containing about 1.35 pounds of high explosive A-3 and has a 0.4 inch thick steel case. It is like a small version of the 5"/54 shell. The so-called P_d50 distance is obtained by varying the spacing between donor and acceptor according to an "up and down" technique -- use a larger separation on the test next if a detonation occurs and use a smaller separation when detonation does not occur (ASJ, June 1953). The graph at the bottom shows the results in the form of probability of detonation (the ordinate) as a function of the separation between the shells (the abscissa). The P_d50 distance calculated with the up-and-down convention is shown by the large cross, slightly over 3 cm or about 1.2 inches. The fractions indicate the number of detonations out of shells fired at

each distance, for example 2/2 means 2 out of 2 shells detonated (when the spacing was about 1.3 cm) and 7/9 means 7 out of 9 detonated (when the spacing was 2.5 cm., or 1 inch).

The 76 mm shells are shipped and stored in an aluminum case, which protects the propellant and cartridge cases. The shipping case insures that the separation between rounds is larger than the P_d50 separation, hence, there is little probability of sympathetic detonation between rounds. Even without the shipping case, and because of the rotating bands shown on the sketch, it is not easy in operational situations to stand two shells upright and space them as close as the P_d50 separation. In any case, wherever bare rounds are stored, as in the ready racks below the gun turrets, the separation is always substantially larger than the P_d50 separation found here. In various tests so far, we have exposed probably a hundred 76 mm shells to 76 mm donor projectiles, some without their shipping containers in simulated ready racks. We have never had even a low order detonation among them.

In short, there is no problem of sympathetic detonation between Navy 76 mm projectiles; no inhibitor is required.

5"/54 Projectiles. We turn to results with the 5"/54 shells.

There is no need to show a graph similar to Figure 9 for P_d50 results for the 5"/54 projectiles loaded with Explosive D. No sympathetic detonation occurred even when the donor and potential acceptor were butted against each other side-by-side.

A whole truckload is more dramatic. Shown here in Figure 10 are two full pallets, 96 rounds, complete with fuzes. A central round of the forward pallet was detonated. Figure 11 shows the result: The truck was hardly damaged, lots of shells were thrown around, but not a single detonation; not even low order or burning occurred among the 95 potential acceptors. Unfortunately, the 5"/54 Explosive D shell is now obsolete. Perhaps second thoughts about Explosive D are in order in view of the wide current effort to develop insensitive high explosives.

5"/54 shells loaded with composition A-3 are more sensitive. The initiation pressure from large scale gap tests is about 16 kilobars for A-3, compared with 32 kbars for Explosive D. The P_d50 separation distance for our first lot of 5"/54 projectiles is shown by the dashed line on the right of Figure 13. The P_d50 separation using the up-and-down technique was about 28cm, (11 inches); a similar distance is obtained by simply joining the experimental points by broken lines as shown. Hence, we would expect complete detonation in the

normal pallet where the shells are separated by 1 inch and 2 inches. In the truck test (Figure 12) similar to the one just described for explosive D, (Figs. 10, 11) we used one full pallet of shells plus a token row 40" away to represent the front row of another pallet. The result in Figure 12 leaves no question that all rounds detonated. More significantly, the propagation jumped the 40 inch gap between the two pallets, setting off the token row. The P_d50 separation between pallets is larger than for single shells. Clearly, there is a problem with the A-3 loaded 5"/54 shells.

By this time we ran out of the early lot of 5"/54 shells and had ordered more. The newly arrived ammunition was of older manufacture dating to the early 1960's and contained many different lots. We will refer to it as the polyglot. Folklore states that older ammunition is more sensitive. We redid the P_d50 with the polyglot and the results are shown by the full line in Figure 13. The P_d50 for this older ammunition is now about 16 cm; about half what we see for the newer ammunition on the right side. . There is a smooth decrease in the probability of detonation from 100% detonation at 5 cm to virtually 0% at 24 cm except for a single round which happened to detonate at 30 cm. The truckload of pallets would doubtlessly still have detonated.

It is sobering to realize that two different lots of ammunition can vary by a factor of 2 in sensitivity output. The question is: "Is the difference real?"

In preparation for a test of the design for the inhibitor module , a new type of P_d50 test was undertaken. This time we placed a steel plate, 3 inches and 1.5 inches wide and about 15 inches long between the projectiles and, varied the thickness. The results are shown on Figure 14. For the 3" wide plate the first lot of newer ammunition showed a P_d50 thickness of about 0.4 inches, varying from complete detonation with 1/4 inch thickness to no detonations with 3/4 inch thickness. The P_d50 thickness for the older vintage polyglot was only .21 inches, again about half as much as the new ammunition; again, the probability decreased smoothly from complete detonation at 0 separation to no detonations at 3/8 inches. Some conclusions:

1. The difference in sensitivity between lots, a factor of 2, is confirmed.

2. Only modest thicknesses of steel, like 3/4", are needed to inhibit sympathetic detonation, and the inhibitors are easily fit within a standard pallet.

The next set of experiments concerned the width of the plate. At first thought it might seem that the wider the plate the better. But Figure 15 shows that this is not so. The wider shield subtends proportionately more energy and momentum of the projectile, as indicated by the rays B and B', whereas the narrower inhibitor absorbs less momentum and energy, that lying between the rays A and A', so less overall energy is transferred to the acceptor. With the narrower plate, fragments lying outside A and A' would strike at more glancing incidence, would have to penetrate much steel and never reach the explosive. But, with the wider plate, to the extent that the plate remains intact, about twice as much energy or momentum is collected and eventually brought to bear on point C. These are not intended to be precise arguments, but to show the general trends and reasons why the larger plate should be a poorer inhibitor than the narrower plate. It is strongly reminiscent of what we found for shielding and reported in the last symposium (DDESB XVII, Porzel): the minimum size shield was best, one that was just sufficient to do the job required and no more.

The P_d50 thickness tests for A-3 5"/54 shell were repeated this time with a plate only 1 1/2 inches wide. The results are shown in Figure 16. Sure enough, for the newer lot ammunition, the P_d50 thickness was reduced from about .4 inches, as seen in Figure 14 to about .25 inches, as shown here by the dashed line. And for the older polyglot ammunition, the thickness was reduced from about .21 inches for the 3" plate, down to .06 inches with the 1 1/2" plate. Again we confirm the substantial difference in sensitivity, the older ammunition being less sensitive.

From the graph we again note the remarkable result that a strip of steel 1 1/2 inches wide and 1/8 to 3/8 inch thick, depending on the lot of explosive, would be sufficient to completely inhibit sympathetic detonation between 5"/54 shells even with so sensitive an explosive as A-3. All the damage seen on the previous photograph of the truck for the pallet of 5"/54 would be reduced to the insignificant effect produced by Explosive D.

This is a good point to note both in summary and in anticipation of further results; the 5"/54 shell is the worst hazard we have so far tested among Navy munitions. Yet, it is possible to prevent sympathetic detonation by plates of steel 1/8 to 3/8 inch thick.

To test the module concept, experiments were first done with arrays of 24 and 29 shells, approximately a quarter of a standard pallet, see Figure 17. They were placed on a large steel plate, 1" thick which served as a witness plate for sympathetic detonation: Experience shows that such a plate is a go-no-go device that either perforates when a high order detonation is achieved or otherwise shows little sign of damage. A central round in the array was detonated. The result: No sign of detonation except under the donor round, where it verified that the donor did go high order. All the shells were recovered, many with the fuzes still intact. Three of the closest neighbors were broken severely by mechanical action of the explosion from the donor round.

These tests have been repeated twice since then with the same result. The 3/4" thick inhibitors completely supress sympathetic detonation.

A confirmatory test was done with an array of 48 shells in a standard pallet, Figure 18. Again, only the donor detonated; the witness plate showed only a single (new) hole below the donor, and all the rounds were accounted for. Had the pallets been placed on a truck the results would have been just the same as the Explosive D on the truck; barely any damage to the truck.

Mk 16 Torpedo

We turn now to thin-skinned weapons and some experiments with Mark 16 torpedoes. This warhead contains about 747 pounds of HBX-3 and has a bronze case about 1/8" thick. Calculations with UTE show the case is thin enough and the fragment velocities are high enough that a single fragment can be sufficient for initiation at long distances.

Figure 19 is a fortunate photograph which verifies single fragment initiation. The test is similar to a P_d50 test with shells; the warheads were placed upright on thick witness plates, and in this photograph the donor and acceptor were 32 feet apart. We see here a single fragment, still outrunning the fireball; it strikes the lower side of the warhead, which then bursts with the characteristic white heat of a detonation, not the yellowish flame of burning. The witness plates and craters left no doubt that detonation occurred for 32 feet separation and would do so for smaller separations. It would probably be a waste of ammunition to test at longer distances; the Mk 16 would detonate on the small chance of a single energetic fragment striking it.

Sympathetic detonation of the torpedoes is relatively easy to defeat. First, according to UTE calculations, we do need about 2 feet separation to prevent sympathetic detonation by the direct shock. Given that separation, all that is then required is a relatively thin plate, although substantially thicker than the warhead case, just enough to bring the donor case fragment below the initiation velocity. The first test was done with a 5/8 inch plate, shown in Figure 20. The upper torpedo was the donor, the lower torpedo was the acceptor. The result: No detonation. We know that because:

1. About 100 pounds of unburned explosive was recovered from the craters and surrounds.

2. Massive fragments of the acceptor warhead were found, about a foot across, which could never have been so large had the acceptor detonated.

3. All the plate fragments recovered showed numerous craters from impacts but always only on one side, clearly the side facing the donor.

4. Plate fragments were found beneath the acceptor in the crater, where they never could have been driven had it detonated.

These tests were repeated 3 times with a 5/16 inch plates, with the same separation between warheads (Figure 21). This time the warheads were placed upright on a witness plate. Another witness plate was set vertically to the side. The acceptor shadowed the donor fragments so that any fragments from a detonated acceptor could be identified. The results in all three cases were the same as with the 5/8 inch plate: No detonation occurred: as shown byno marks found on the horizontal witness plates, by the absence of acceptor fragment craters on the vertical witness plate and most definitely by finding much unburned explosive in the vicinity. Some acceptor explosive did ignite when it struck the witness plate, and on one test, recovery was delayed for about one-half hour while the scattered explosive burned itself out.

These experiments are themselves an almost definitive case against the mechanism of sympathetic detonation by translational impact. Theory argues against it, too. The shock wave from the donor which sets the acceptor into motion is equivalent to the reflected shock which passes through it when the acceptor is stopped by the vertical witness plate. We then ask: If the shock from the donor were too weak to detonate the acceptor initially, is it likely to hurl the acceptor with sufficient velocity to cause detonation by the stagnation pressure? These tests and arguments suggest translational impact does not apply, at least to thin cased weapons.

Figure 22 shows how not to design an inhibitor: Make it thick enough to transmit the donor shock directly and to prevent scattering. This shield is a 1/4 inch of steel faced with a foot of wood, and contains far more mass than the 5/16" steel plate. The two warheads are almost close enough to detonate by direct shock according to the UTE calculations. The results left no doubt that the acceptor detonated. The witness plate showed a large dent below the acceptor; detonation occurred and was immediate.

There is no paradox here between the two experiments. In the first experiment, using a 5/16" plate and a large separation, only a small fraction of the donor energy impinged on the acceptor, the distance was large enough to be beyond direct shock initiation, and the plate was just thick enough to inhibit fragment initiation. In the second "sandwich" experiment, the spacing was close enough for direct shock initiation, a wide sector of the donor energy was captured by and contained within the shield which when impinged on, and perhaps wrapped around the acceptor case converging inward on the acceptor. The facts remain: The thin plate and standoff inhibited the detonation; the sandwich shells did not prevent it.

Massive Debris

We have described experiments with high speed fragments from thin cased weapons and lower speed fragments from thick cased weapons. We turn to a series of experiments with massive masonry debris at very low speeds. Mock ups of various Navy warheads with HBX-1, HBX-3 and H-6 were tested but of particular interest is PBXN-103 because it is one of the most difficult of explosives to detonate, but one of the easiest to ignite by burning.

The gun shown in Figure 23 is the Illinois Institute of Technology's 12 inch air gun at La Porte, Indiana (DDESB XVII, Rindner). IITRI did the experiments for us. The projectiles were essentially an 8 x 8 x 12 inch block of brick masonry, mortared and banded together and weighing about 70 pounds.

Some test predictions and results for PBXN-103 are shown in Figure 24. The abscissa is the debris velocity in feet/second. The ordinate is a blast pressure that was measured from the target. Labelled here in psi, it corresponds, as in the SUSAN tests to slight reactions, moderate reaction, vigorous reaction and finally detonation as shown. The circles joined by straight lines are SUSAN test data for PBXN-103 but modified to account for the fact that here the debris was brick rubble, whereas, in the SUSAN tests the projectile impacted on a massive steel plate. The box on the upper right shows predictions one makes on the basis of large scale gap tests; there the characteristic size of the explosive or activation zone is $d \cong 3$ inches instead of $d \cong 8$ inches for the brick masonry. The lower horizontal dashed line is the pressure one predicts for a free air explosion of the test geometry and charge weight; the upper horizontal dashed line is the corresponding reflected pressure expected from full detonation over a perfectly rigid plane -- or as if the target plate were "infinite" in extent for the SUSAN tests. The box is bounded on the left by the velocity required if the driving debris were in direct contact with the explosive, as in the SUSAN tests, and on the right, for free debris striking the explosive. On the basis of analysis of SUSAN tests, we would predict a threshold for ignition by brick debris -- zero output pressure -- to be around 300 f/s. From the experiment we found that the threshold is about 350 f/s for PBXN-103 in a .145 thick aluminum case, and around 520 f/s for PBXN-103 in a .25 inch thick steel case. This is good agreement in view of all uncertainties; a blind use of the SUSAN test data disregarding the difference between steel and brick would have suggested that PBXN-103 could ignite at a velocity below 100 f/s.

Table 1 shows the results for impact of masonry debris on the four explosives and cases tested. In no case did detonation or even moderate reaction occur, even for debris velocities in excess of 800 f/s. Burning of PBXN-103 occurred in three cases, at 386 f/s with a .145" aluminum case and above 500 f/s in a .25" steel case. Two of the latter shots produced slight pressure pulses, which may be taken as evidence of some reaction equivalent to a small fraction of a pound of TNT, but it is not much more than the energy of impact of the debris.

It is noteworthy that these experiments with massive debris were done as part of a typical safety problem under the NESIP program. The question: Would the detonation of 65,000 pounds of explosive in a small brick building with 9" thick wall induce sympathetic detonation to thin-cased explosives stored in another such building 90 feet away? The answer to the question was: No problem. The common NAVY explosives are too insensitive even to burn under those conditions, let alone detonate.

TABLE 1

PRELIMINARY TEST RESULTS

Brick Impacting on Thin Cased Warheads

Explosive	Case thick., in.	Measured velocity f/s	Detonation	Burn	Press. psi	Remarks
PBXN-103	Alum	207	No	No	0	Case intact
	.145	311	No	No	0	
		386	No	Yes	0	Vigorous burn, 1 min.
PBXN-103	Steel .25	357	No	No	0	Case intact, reused @ 509 fps
		500	No	Yes	.27	Scattered explosive.
		509	No	No	0	No reaction, same case as at 357 fps
		722	No	Yes	Trace	
H-6	Steel	201	No	No	0	Case dented
	.125	356	No	No	0	
		797	No	No	0	
HBX-1	Steel .125	196	No	No	0	Case still intact
		916	No	No	0	
HBX-3	Alum.	203	No	No	0	No reaction
	.125	398	No	No	0	Scattered
		812	No	No	0	explosive, but no reaction

SUMMARY

Under the Navy Explosive Safety Improvement Program we have found:

1. Sympathetic detonation is a straightforward hydrodynamic phenomena which can be explained and quantitatively described by simple, approximate but comprehensive methods such as the unified theory of explosions (NOLTR 72-209).

2. The controlling variables for sympathetic reactions can be summarized by the criterion

$$\int (E - E_c)\, dt > H_{minimum}$$

which requires some stimulus, E, greater than a critical value, E_c, which lasts for time, t, long enough for the induced reaction to be self-sustaining.

3. Experimental data sufficient to supply critical parameters in the above criterion already exist from standard, well-known measurements such as the large scale gap test and SUSAN tests.

4. An effective means of inhibiting sympathetic detonation, when needed: Use thin narrow plates to scatter and absorb fragment energy, provided there is sufficient (but small) stand-off necessary to "vent" the energy and prevent initiation by direct shock.

5. We have designed and successfully tested the following devices to inhibit sympathetic detonation:

Case	Warheads and Explosive	Inhibitor
Thick cases	76 mm projectile, A-3	None required
	5"/54 Explosive D	None required
	5"/54, Comp. A-3	.75 x 1.5 x 15" steel plate, w/o standoff
Thin case (high speed dense frags)	Mk 16 Torpedo	.31 inch thick plate w/40 inch standoff
Thin case	PBXN-103 .125" Al case	No burning below 300 f/s
(massive soft debris)	PBXN-103 .25" steel case	No burning below 500 f/s
	H-6, HBX-1, HBX-3 typical cases for mines destructors	No burning at 800 f/s

As an overall summary for Navy explosives and warheads so far tested, we find either that no hazard exists, or that sympathetic detonation can be prevented by relatively modest inhibitors.

ACKNOWLEDGEMENT

NESIP is in fact a broad project, the joint effort of many people. The author is indebted, on one hand to John Connelly of OP 411, Ed Daugherty of the NAVSEA Safety Office and to Joseph Petes of White Oak all of whom steer the project. On the other hand, were Phil McLain of the TERA group, New Mexico Institute of Mining and Technology, Ed Swider of the IIT Research Institute and Gruver Martin of White Oak Lab, NSWC, all of whom did the experiments.

REFERENCES

ARBRL TR 02048 — "The Phenomenonology of Internal Communication and Techniques for Prevention," Phillip Howe, U.S. Ballistics Research Laboratory, Aberdeen, Md., March 1978.

ASJ June 1953 — "The Up-and-Down Method with Small Samples", K.S. Brownlee, J.L. Hodges, J.R. and M. Rosenblat, University of Chicago, 1953 June, American Statistical Journal.

DDESB XV (OSBORN) — "The Navy's Development of Explosive Safety Procedures for Loading and Damaging of Ammunition Cargo Aboard Ships," p. 329, Vol 1, D. Osborn, Minutes of the 15th DOD Explosives Safety Seminar, Sep 1973.

DDESB XVI (PORZEL) — "Damage Potential from Real Explosions: Total Head and Prompt Energy", F.B. Porzel, in Minutes of 16th Explosives Safety Seminar Vol I, p. 633, DDESB, Washington, D.C., Sep 1974.

DDESB XVI (RINDNER) — "Safe Separation and Secondary Fragment Impact Studies," Minutes of the 16th Explosive Safety Seminar, DOD Explosives Safety Board, 1974, R.M. Rindner, R.S. Kukuvka.

DDESB XVII (PORZEL) — "Design of Lightweight Shields Against Blast and Fragments," F.B. Porzel, in Minutes of 17th Explosives Safety Seminar, Vol. II, p. 1247, Washington, D.C., Sep 1976.

DDESB XVII (HOWE) — "En Masse Detonation of Explosive Stores," Phillip M. Howe, Minutes of the 17th Explosives Safety Seminar, Sep 1976.

DDESB XVII (RINDNER) — "Experimental Determination of Explosive Sensitivity to Fragment Impact," R.M. Rindner, C. Petino, and H. Napadensky, p. 1587, Minutes of the 17th Explosives Safety Seminar, Department of Defense Explosive Safety Board, Sep 1978.

NOLTR 72-209 — "Introduction to a Unified Theory of Explosions", F.B. Porzel, Naval Ordnance Laboratory, White Oak, Md., Sep 1972.

NOLTR 74-40 "The NOL Large Scale Gap Test III. Compilation of Unclassified Data and Supplementary Information for Interpretation of Results", Donna Price, U.S. Naval Ordnance Laboratory, 8 Mar 1974.

ROSLUND Private Communication.

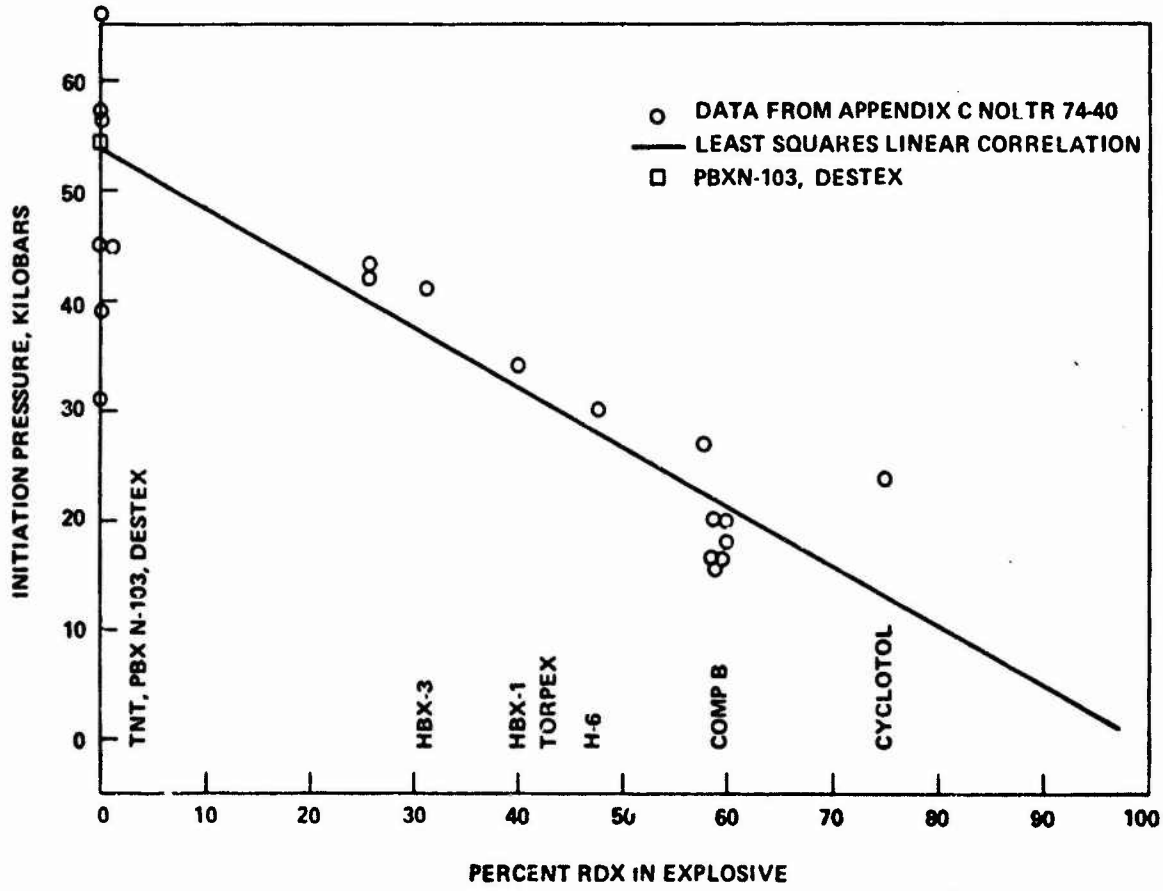

FIGURE 1. INITIATION PRESSURES FROM LARGE SCALE GAP TESTS CAST CHARGES: RDX/TNT/INERT MATERIALS.

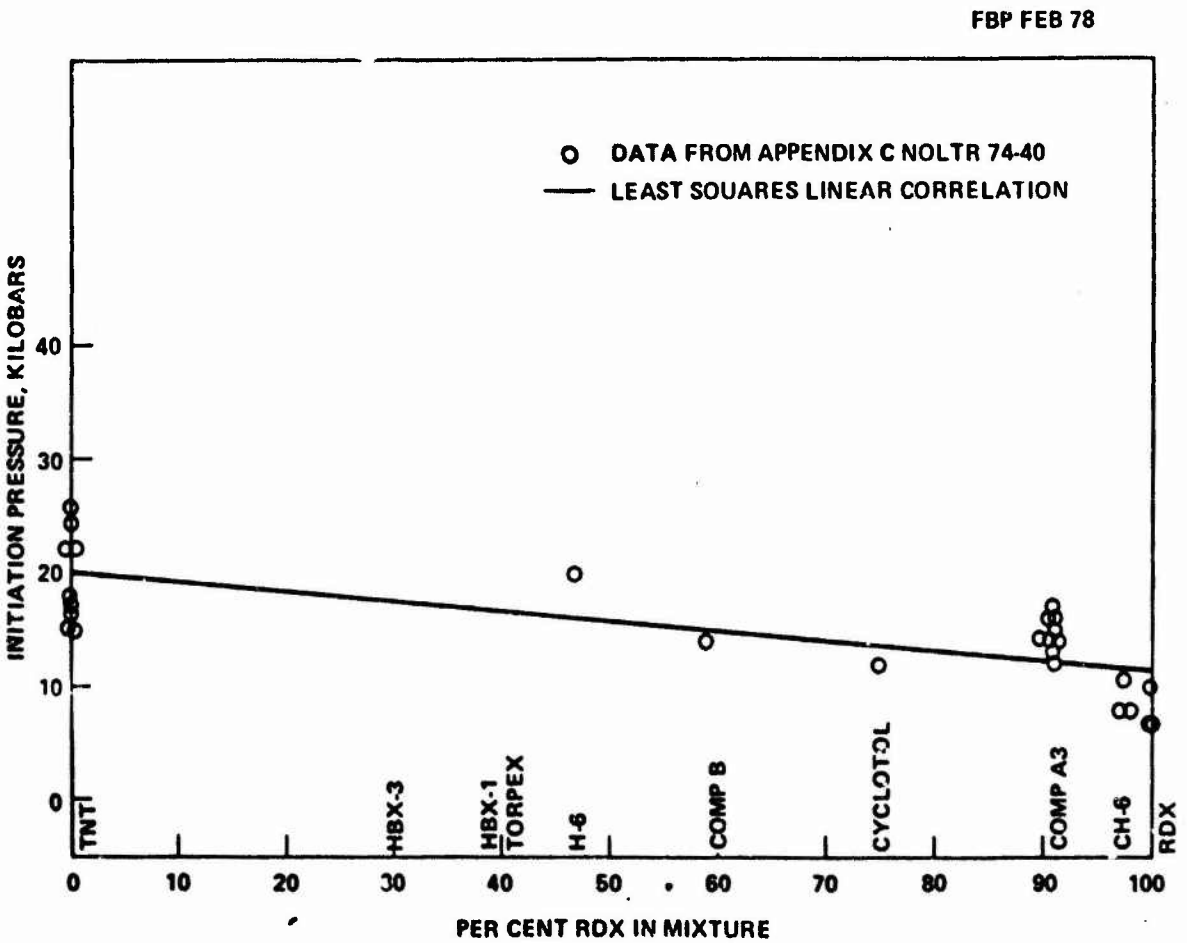

FIGURE 2. INITIATION PRESSURE FROM LARGE SCALE GAP TESTS PRESSED CHARGES: RDX/TNT/INERT MATERIALS.

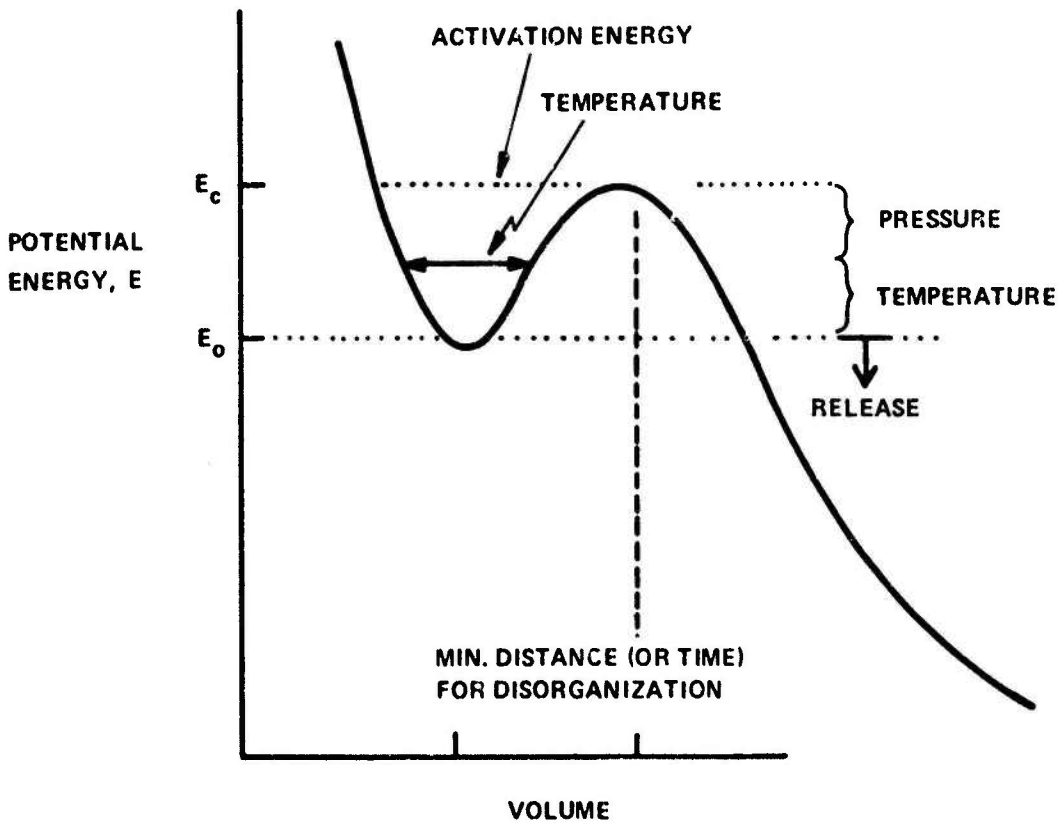

MINIMUM ACTION REQUIRES

1) ACTIVATION ENERGY AND
2) LONG ENOUGH TIME TO DISORGANIZE THE STRUCTURE

FIGURE 3. SIMPLIFIED POTENTIAL WELL OF AN EXPLOSIVE.

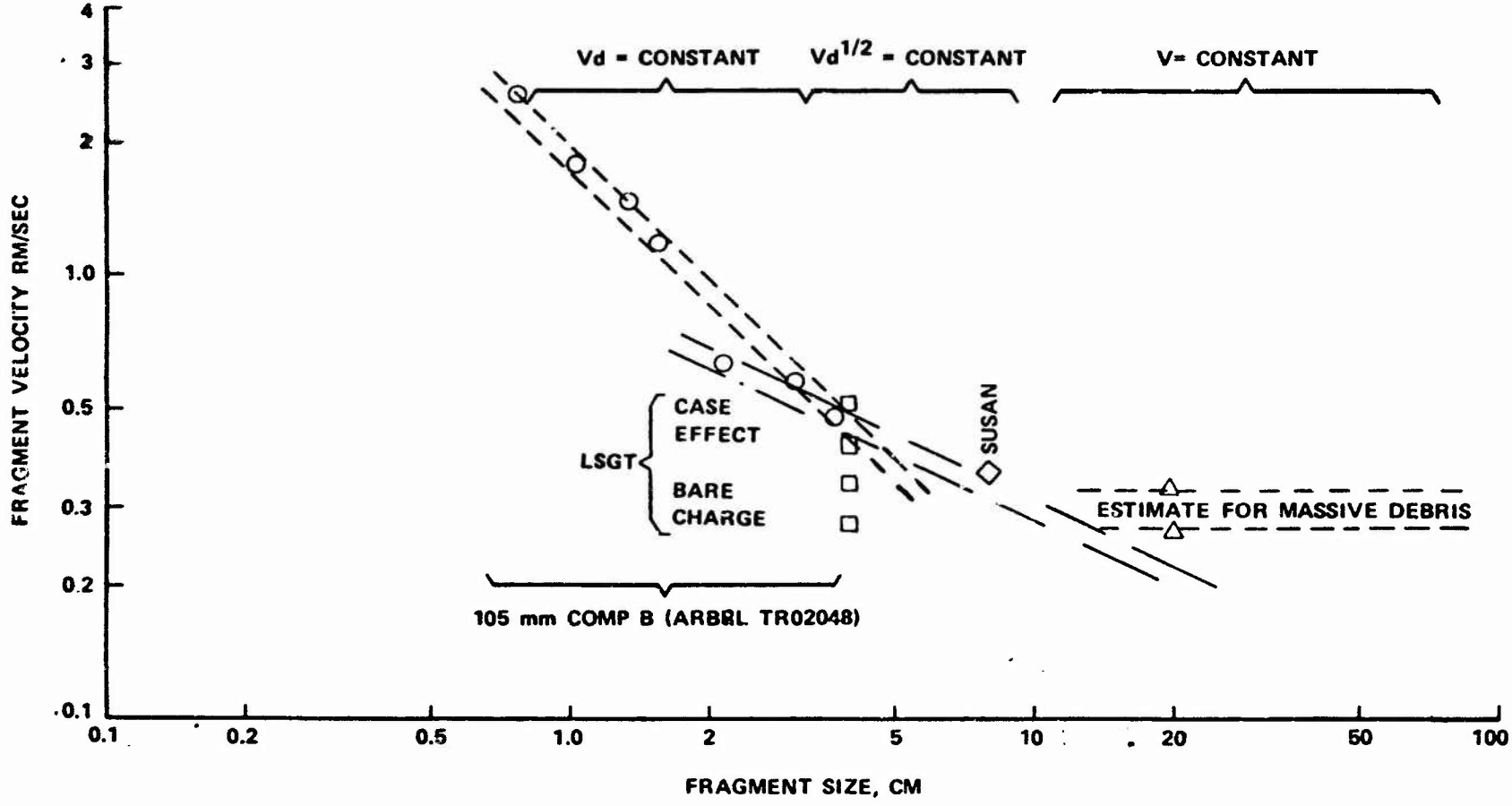

FIGURE 3 A CORRELATION OF CRITERION VD^{η} = CONSTANT
In various regimes for full detonation of composition B.

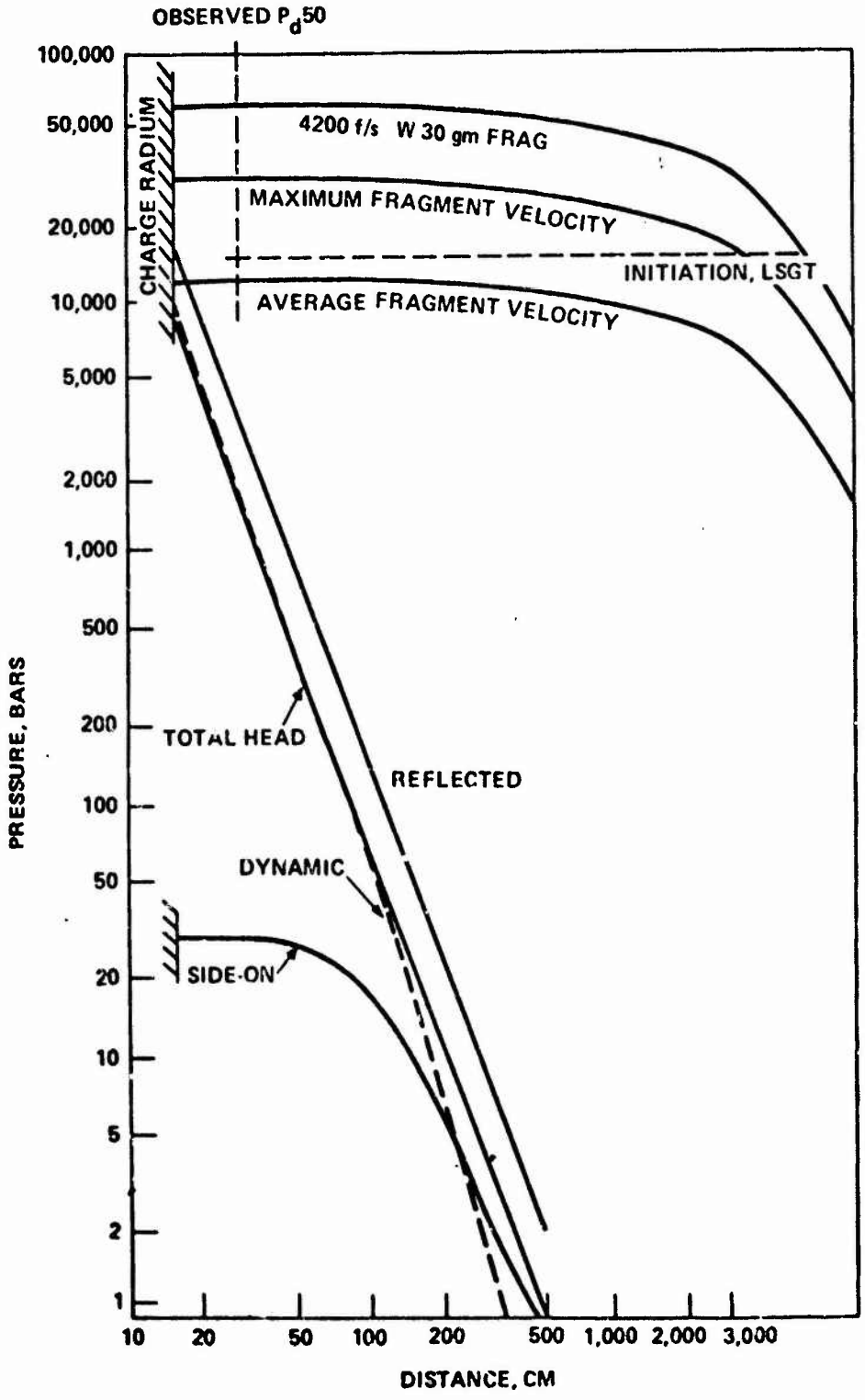

FIGURE 4. PRESSURE-DISTANCE FOR 5"/54 PROJECTILE.

7.8 lbs. A-3 in 70 lbs steel case UTE predictions, spherical equivalent.

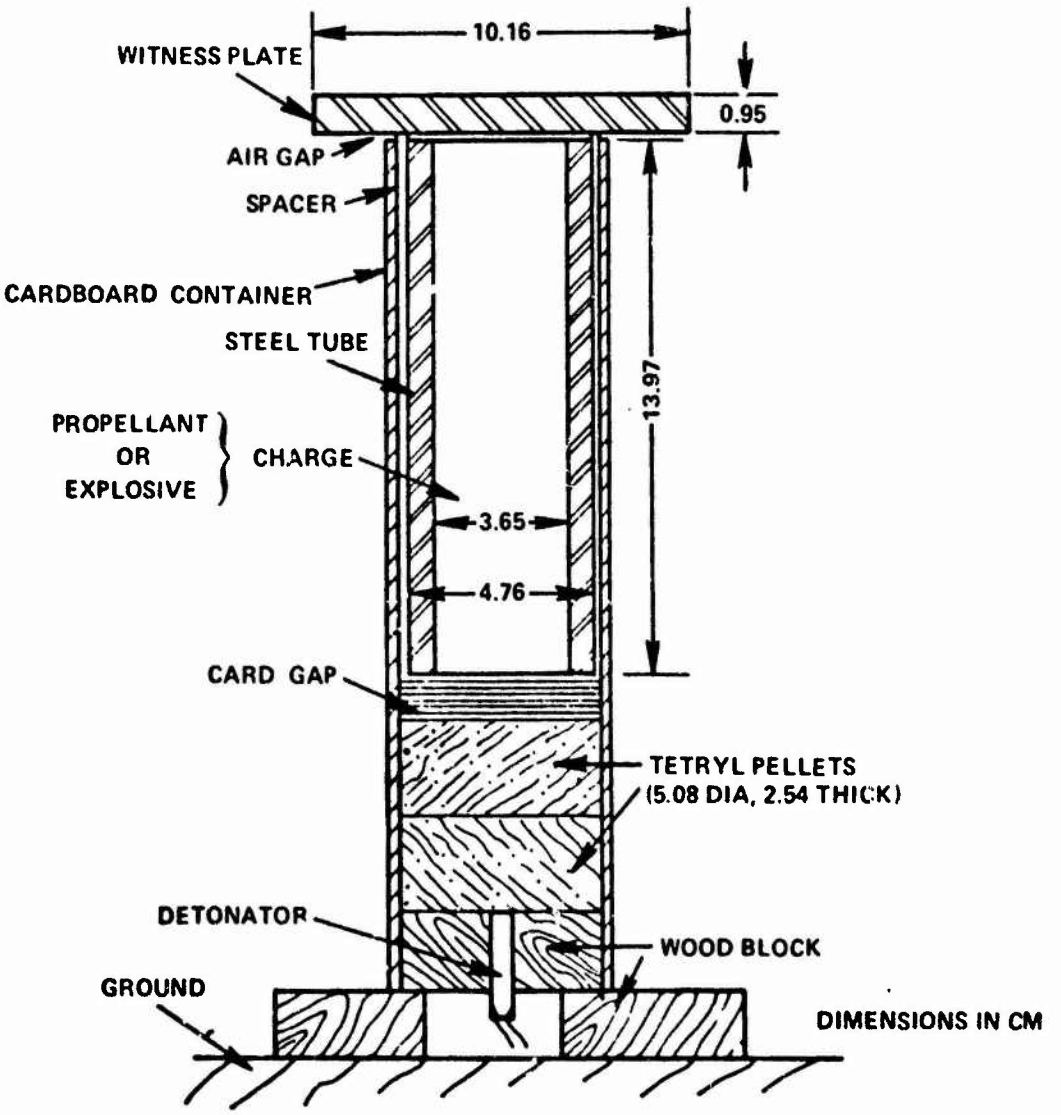

FIGURE 5. LARGE SCALE GAP TEST ASSEMBLY.

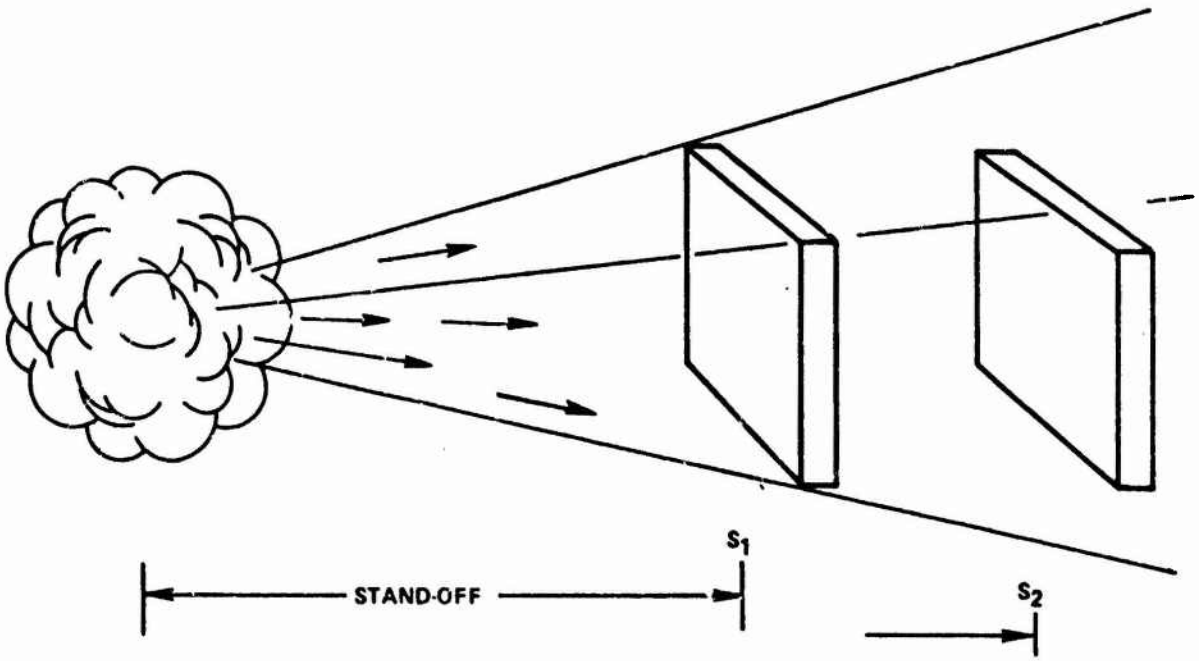

FIGURE 6. SHIELD STAND-OFF AND EFFECTIVENESS

For the same area, thickness and weight of shield, the geometry shows that the more distant shield at S_2 will be more effective than the closer shield at S_1, by the factor $(S_2/S_1)^2$.

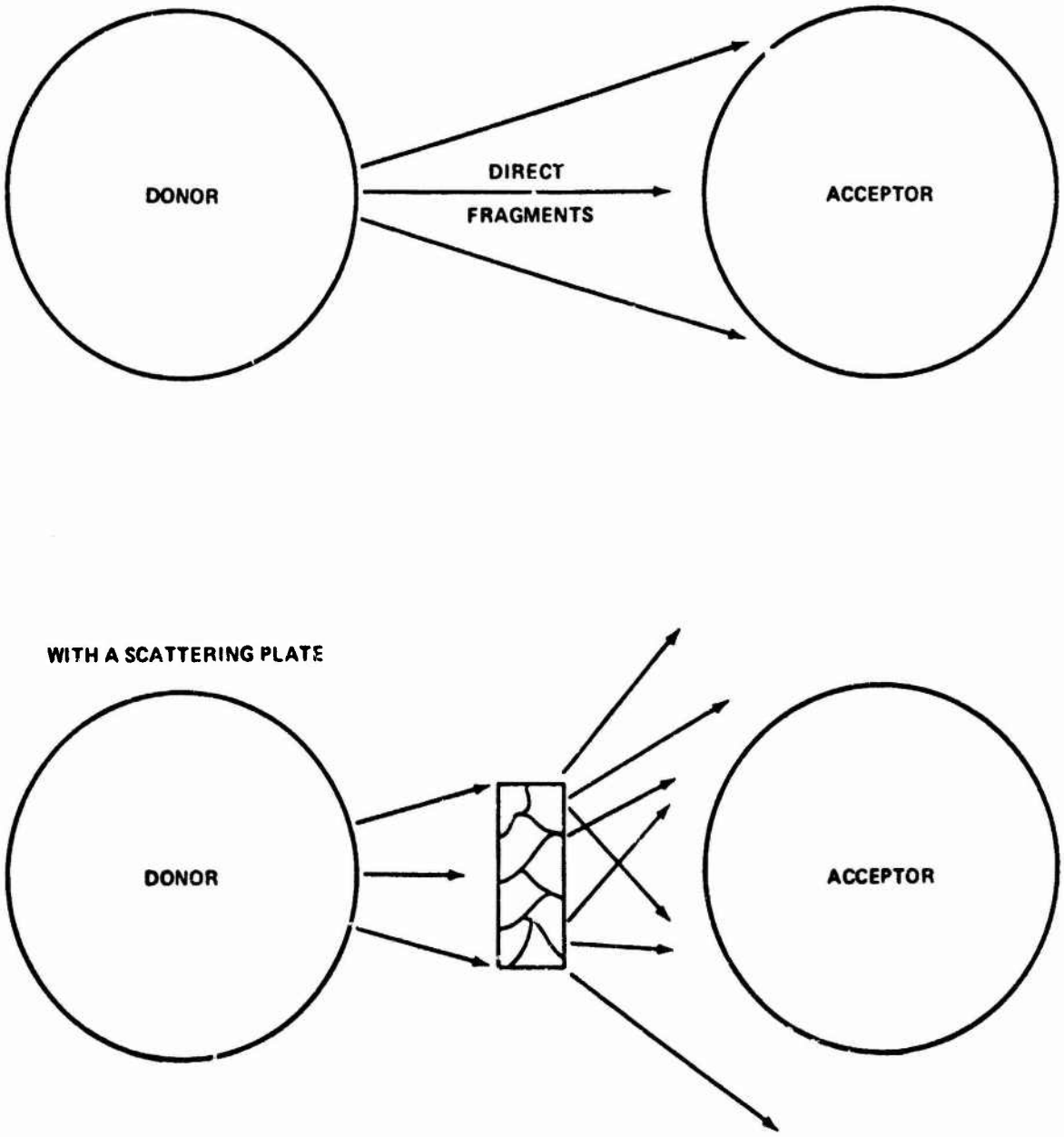

FIGURE 7. SCATTERING MECHANISM.

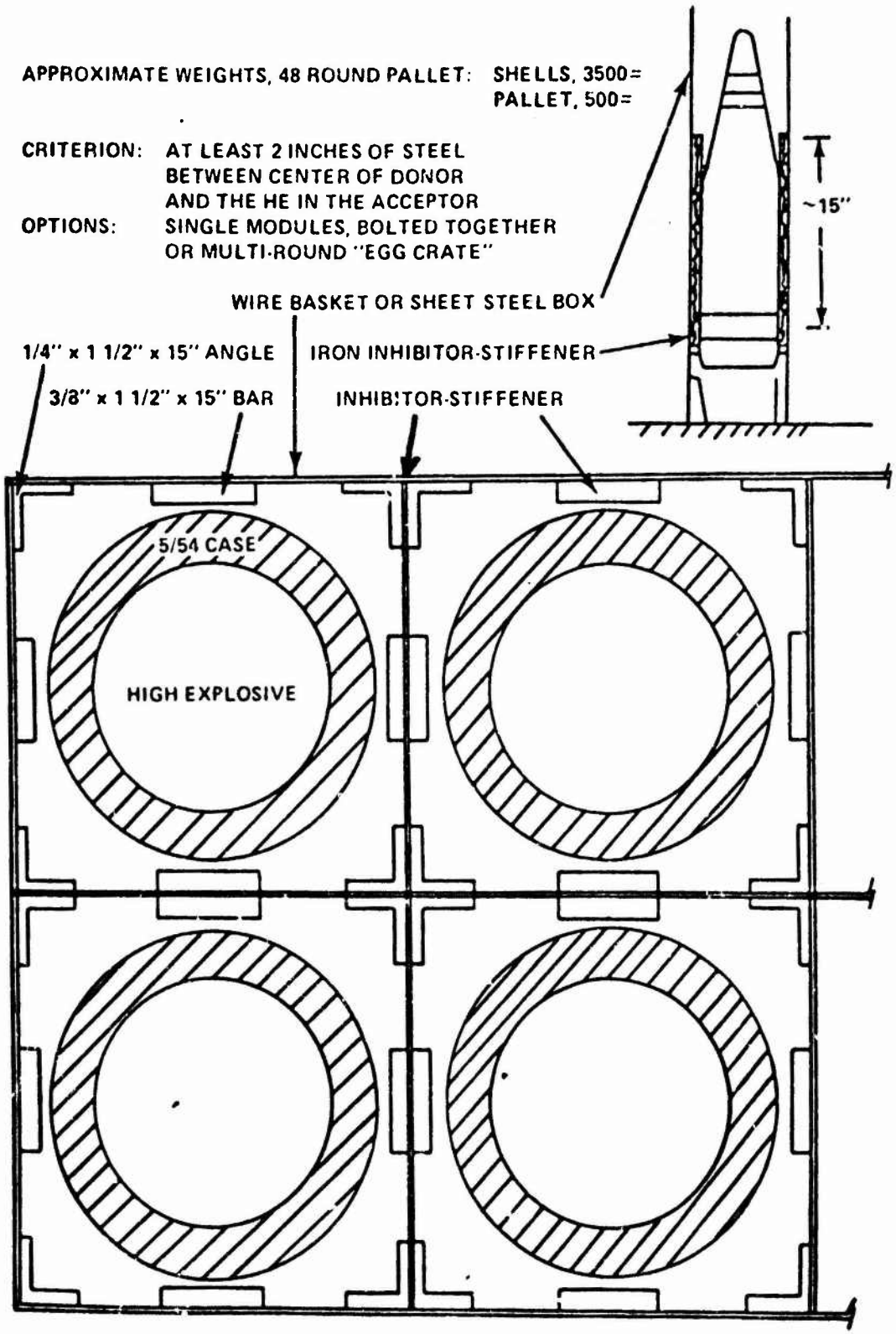

FIGURE 8. OPTIMISTIC DESIGN FOR A MODULAR CONCEPT FOR AN INHIBITING PALLET FOR 5"/54 SHELLS TO PREVENT SYMPATHETIC DETONATION.

TEST ARRANGEMENT:

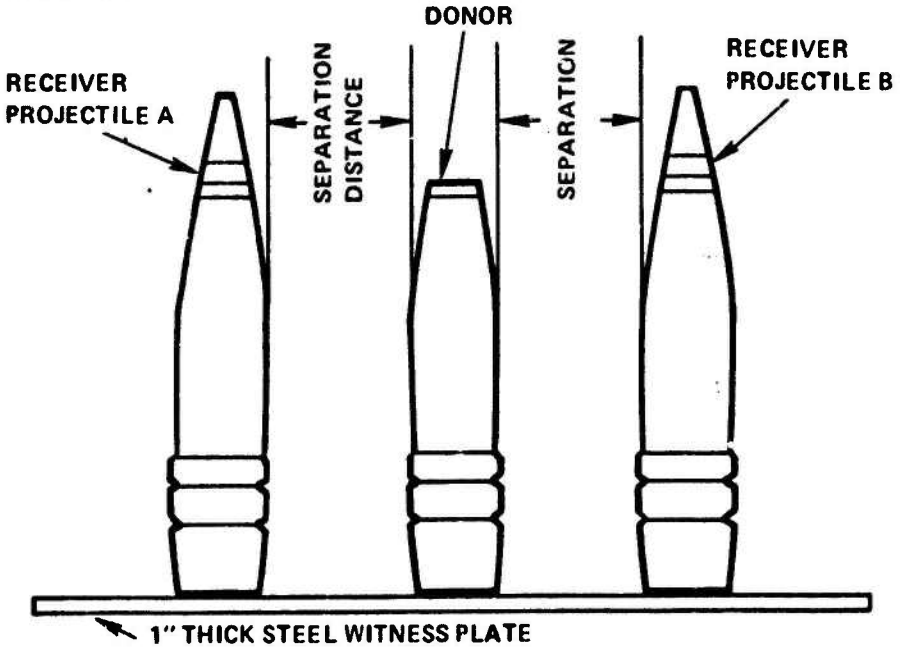

RESULTS:

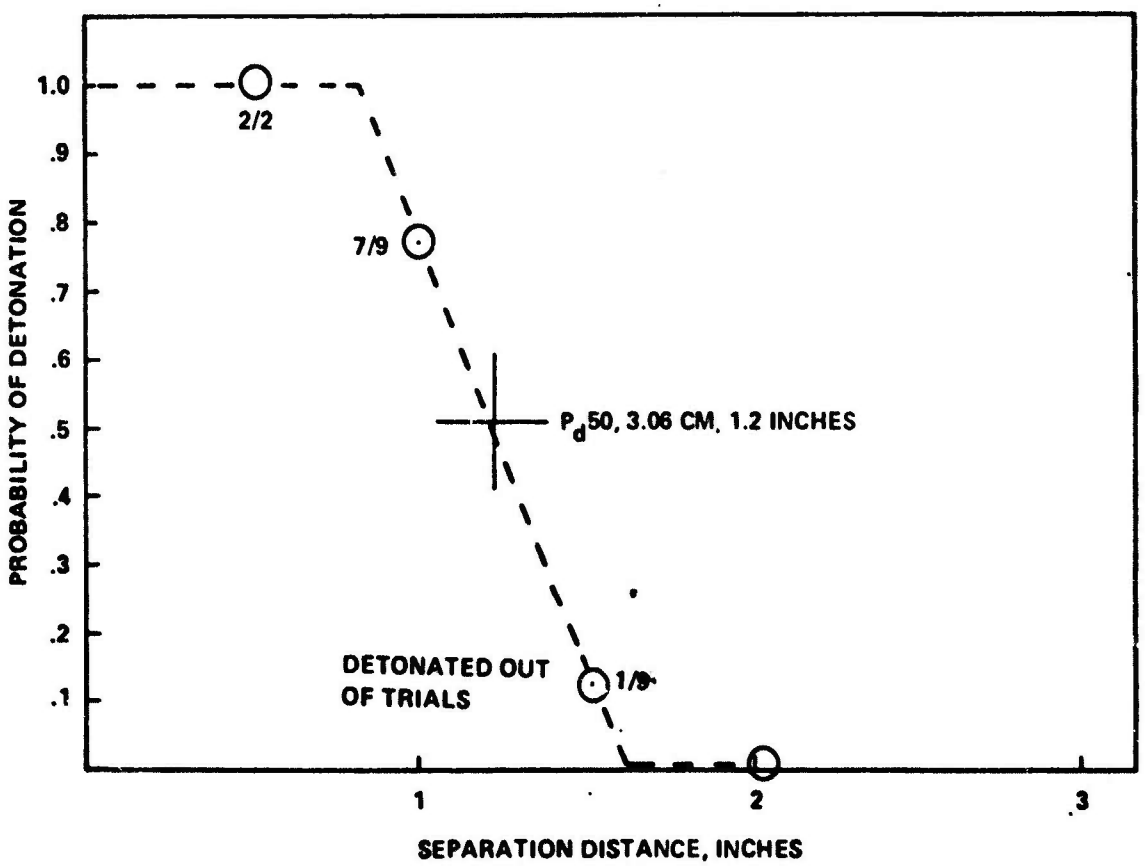

FIGURE 9. P_d50 SEPARATION TEST: 76 mm SHELL WITH EXPL. A/3.

TEST OBJECTIVE: Part of a series of tests to determine a distance value for fifty percent probability of sympathetic high order detonation between 76 mm HE-PD SF projectile MK 166 MOD 0, with fuze, Lot #1315-00-488-0978 ALN 6-C-76 with no shielding.

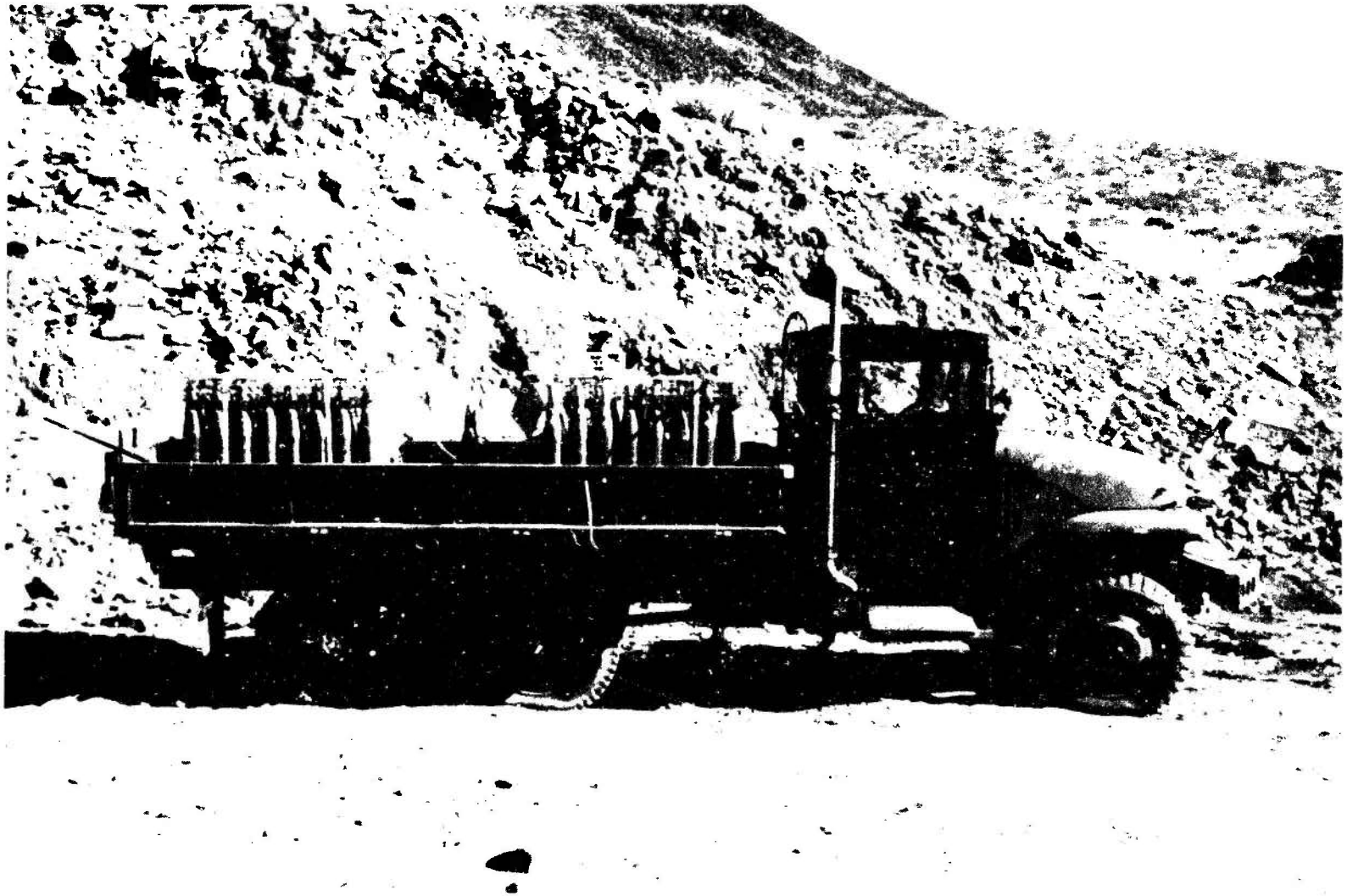

FIGURE 10. BEFORE THE TEST, 5"/54 WITH EXPLOSIVE D.

Two full pallets, 96 rounds were present. A single donor shell was used in the forward pallet.

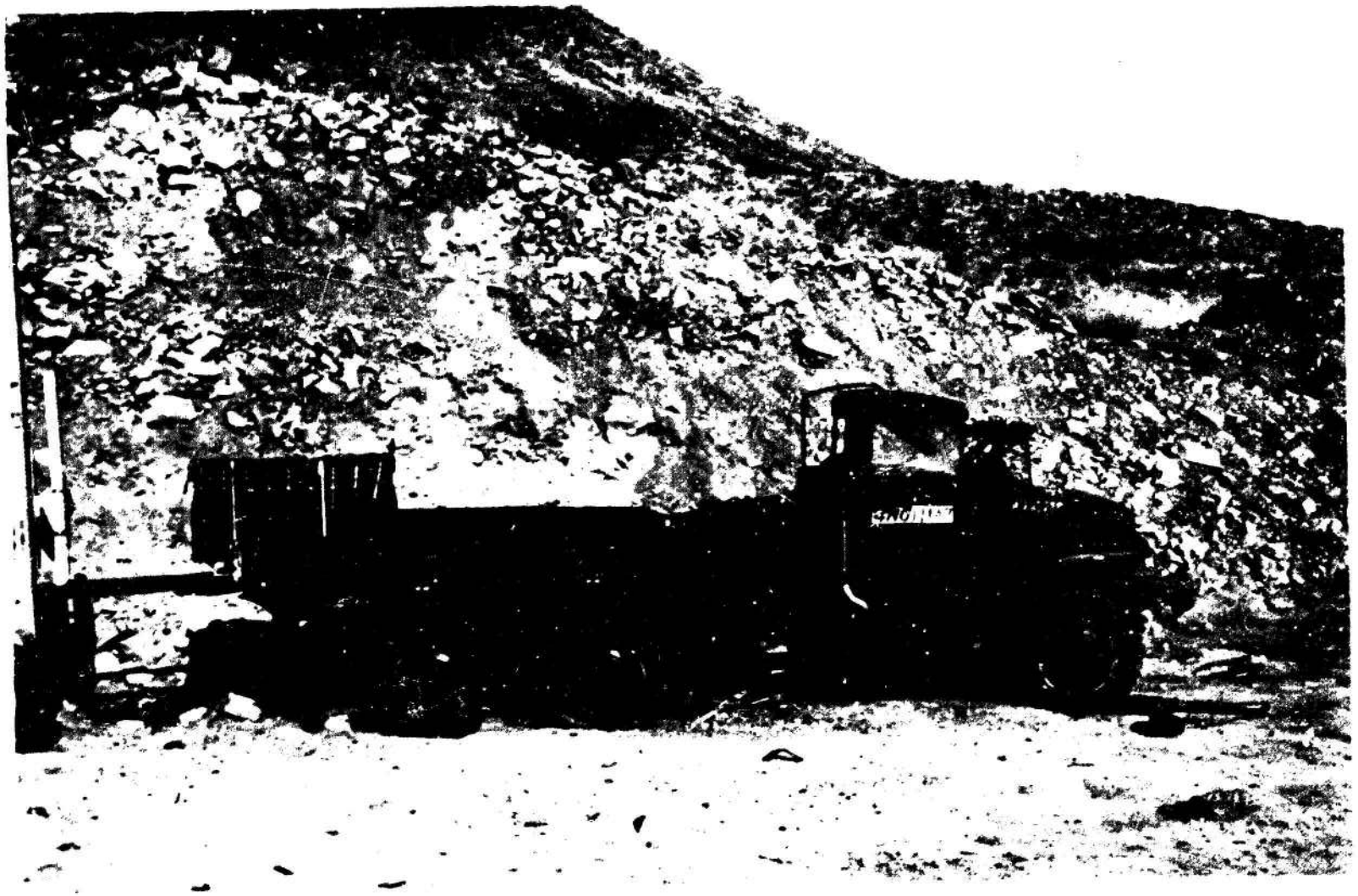

FIGURE 11. AFTER THE TEST, 5"/54 PROJECTILES WITH EXPLOSIVE D.

Only the donor detonated, all shells were recovered. The rear pallet was simply shoved back about two feet.



FIGURE 12. AFTER THE TEST, 5"/54 WITH COMP. A-3.

One full pallet, 48 rounds plus a token row at 40" distance. All rounds detonated.

TEST ARRANGEMENT:

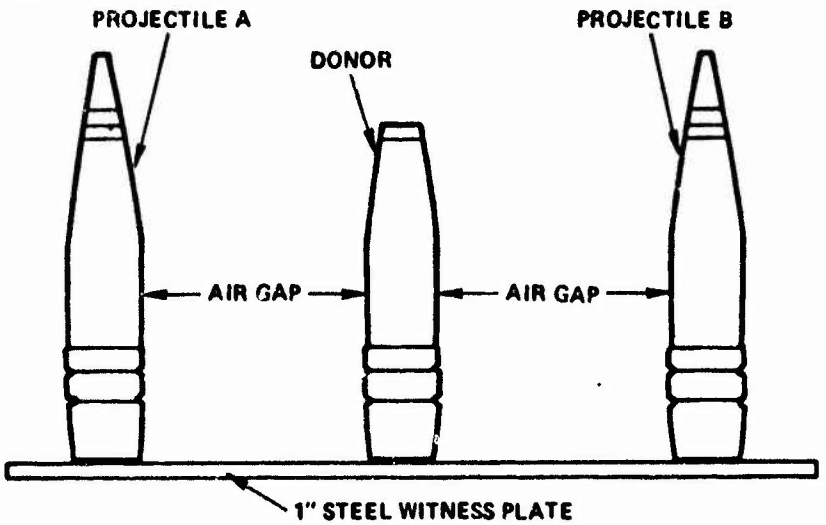

RESULTS:

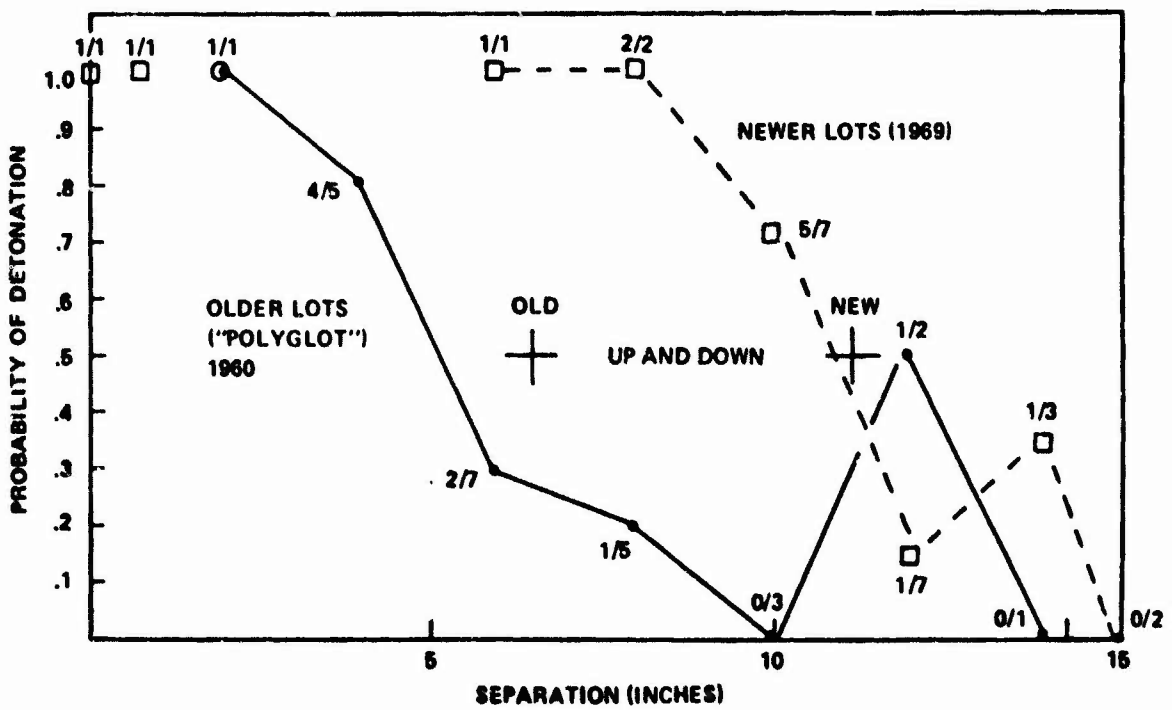

FIGURE 13. P_d50 SEPARATION TEST. 5"/54 W/A-3.

TEST OBJECTIVE: Part of a series of tests to determine a distance value, for fifty percent probability of sympathetic high order detonation between 5-inch/54 caliber, MK 41-0, Comp A3 (Den. 1.60) loaded, HC projectiles. Nose Fuze 30-3. Base Fuze 31-3. Aux. Det. 52-3. All parts and components for Guns MK 16 and MK 18-0.

TEST ARRANGEMENT:

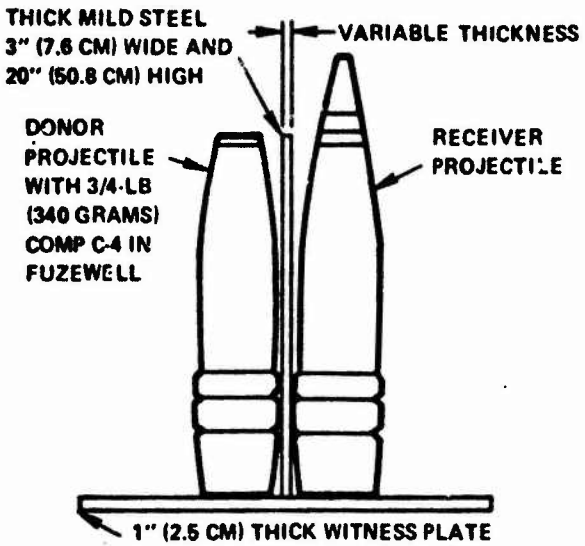

RESULTS:

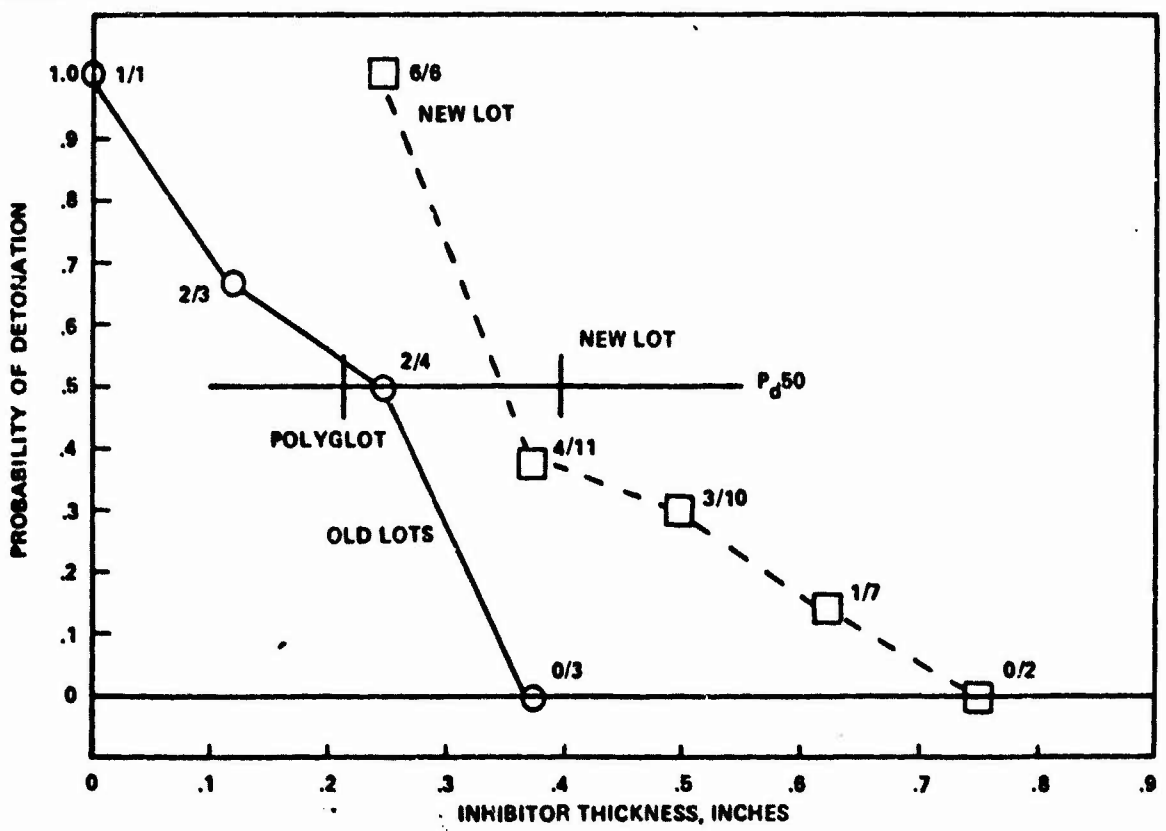

FIGURE 14. P_d50 THICKNESS. 3" WIDE PLATE TEST, 5"/54 W/A-3.

TEST OBJECTIVE: Part of a series of tests to determine a distance value for fifty percent probability of sympathetic high order detonation between 5"/54, HE-VT, Comp A-3 loaded projectiles with 3" (7.6 cm) wide mild steel shielding between the projectiles.

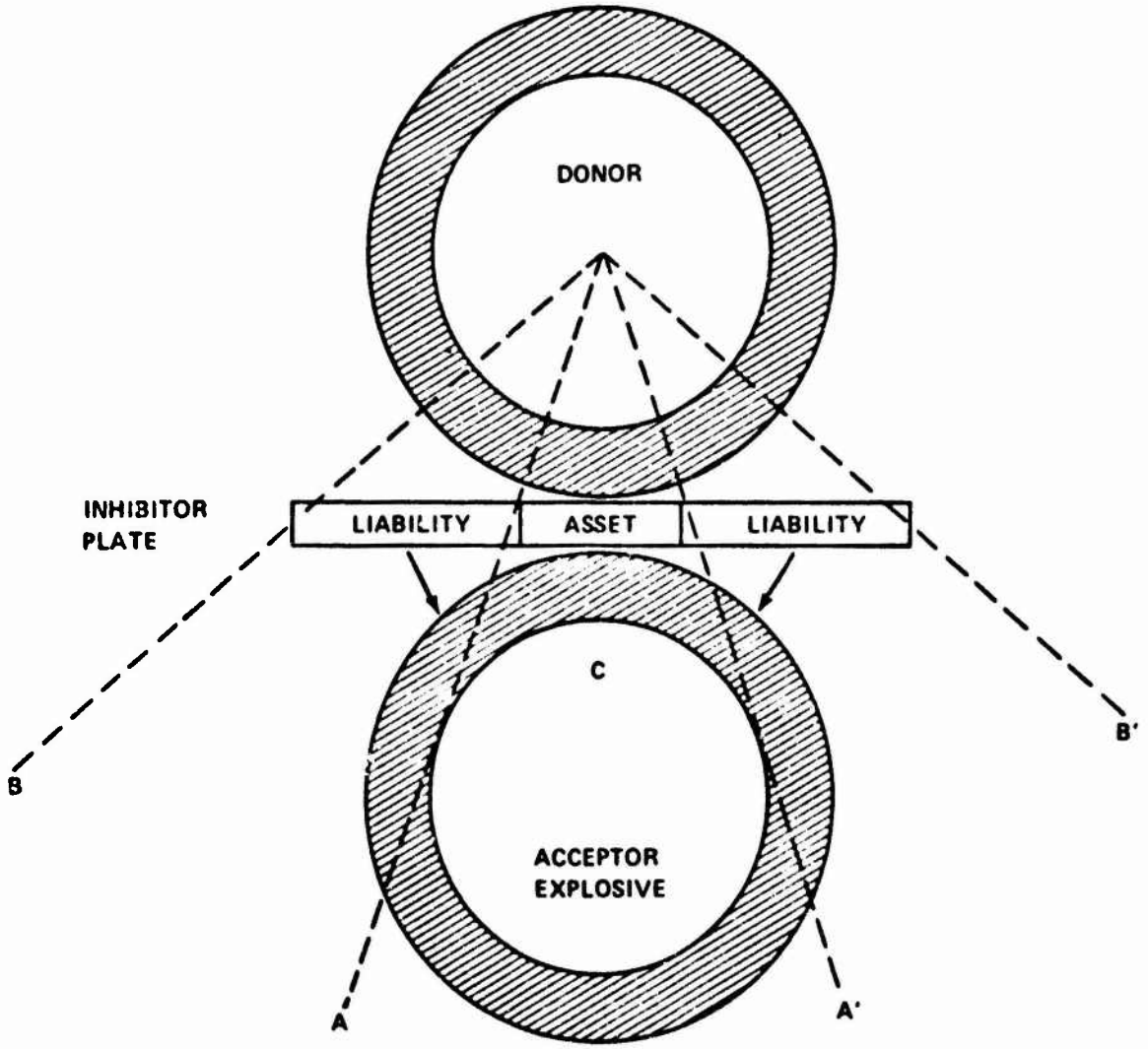

FIGURE 15. KEEP THE INHIBITOR PLATE NARROW.

Too wide an inhibitor increases loading of the donor and prevents scattering of the inhibitor near the point of contact C.

TEST ARRANGEMENT:

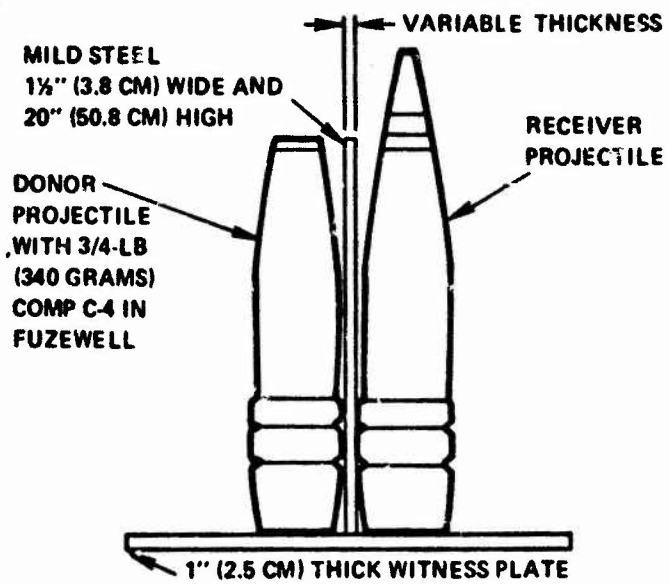

RESULTS:

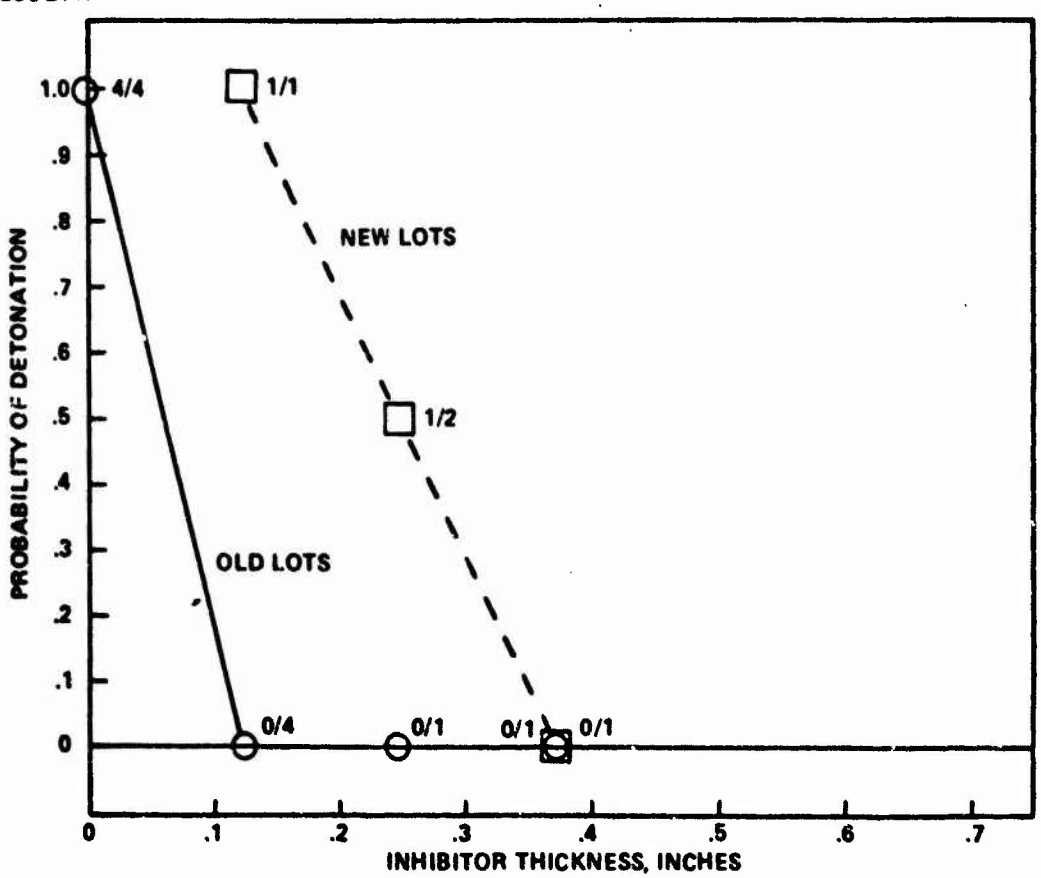

FIGURE 16. P_d50 THICKNESS 1½" WIDE PLATE TEST, 5"/54 W A/3.

TEST OBJECTIVE: Part of a series of tests to determine a distance value for fifty percent probability of sympathetic high order detonation between 5"/54, HE-VT, Comp A-3 loaded projectiles with 1½" (3.8 cm) wide mild steel shielding between the projectiles.

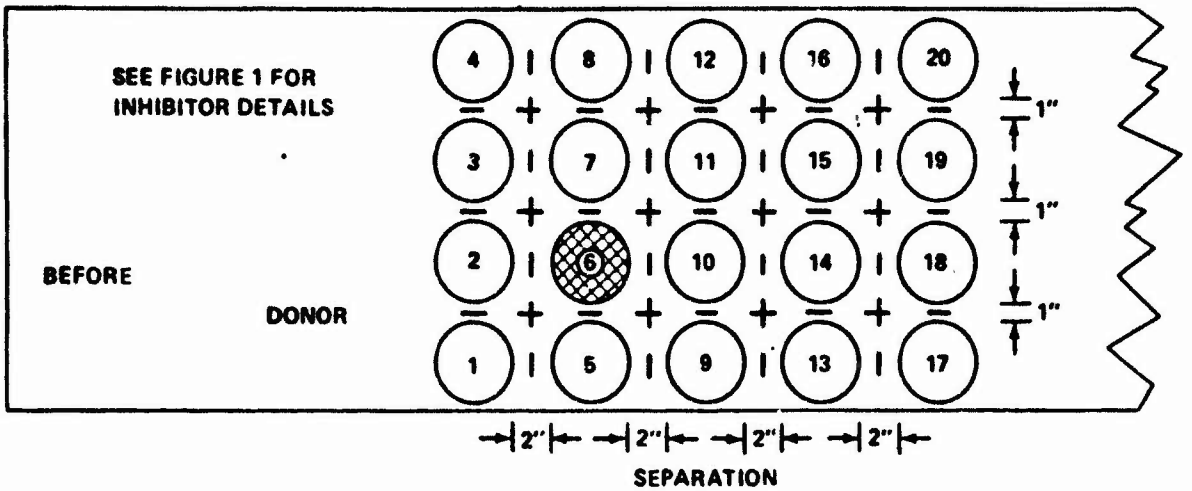

RESULTS: NO SYMPATHETIC DETONATIONS; HOLE FROM DONOR ONLY 16 OF 19 ACCEPTORS FOUND IMMEDIATELY, 13 INTACT AND MOSTLY WITH FUZES, 3 SPLIT OPEN, 3 BURIED OR BROKEN UP.

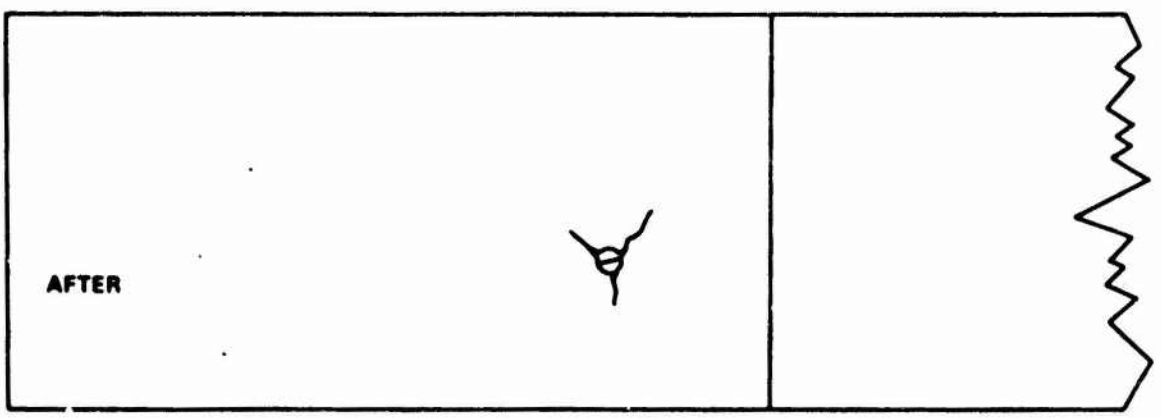

FIGURE 17. INHIBITOR TEST, AWC420A8, 20 APRIL 1978.
5"/54 MK 41-0 Projectile with VT fuzes, A-3 Loaded, 20 rounds
P_d50 = 6.4 inches separation, single rounds without inhibitors
Full pallet will detonate across 48" gap



BEFORE



AFTER

FIGURE 18. FULL PALLET TEST OF INHIBITOR FOR 5"/54 WITH COMP. A3

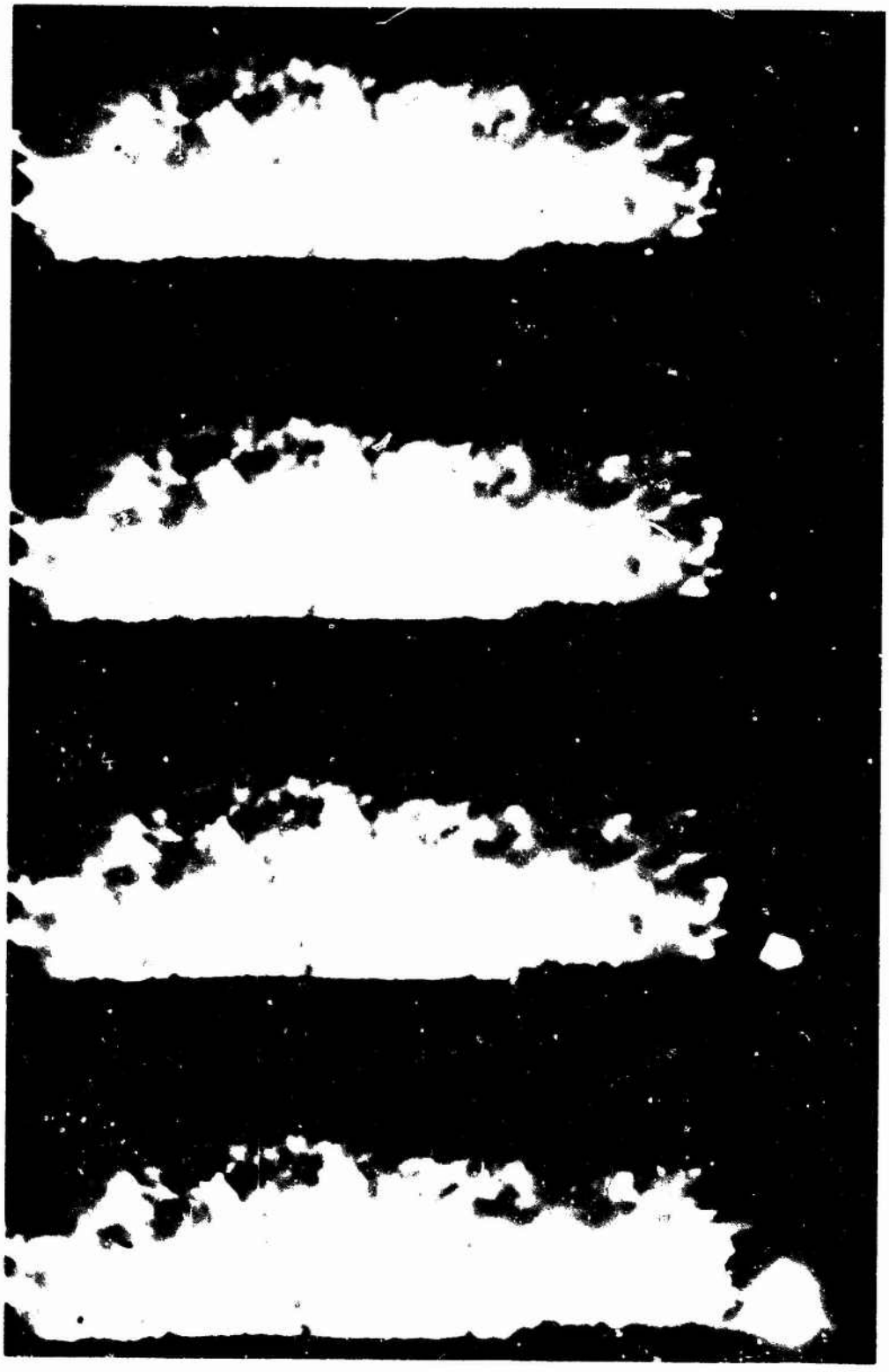

FIGURE 19. SINGLE FRAGMENT DETONATES MK 16 TORPEDO AT 32 FEET

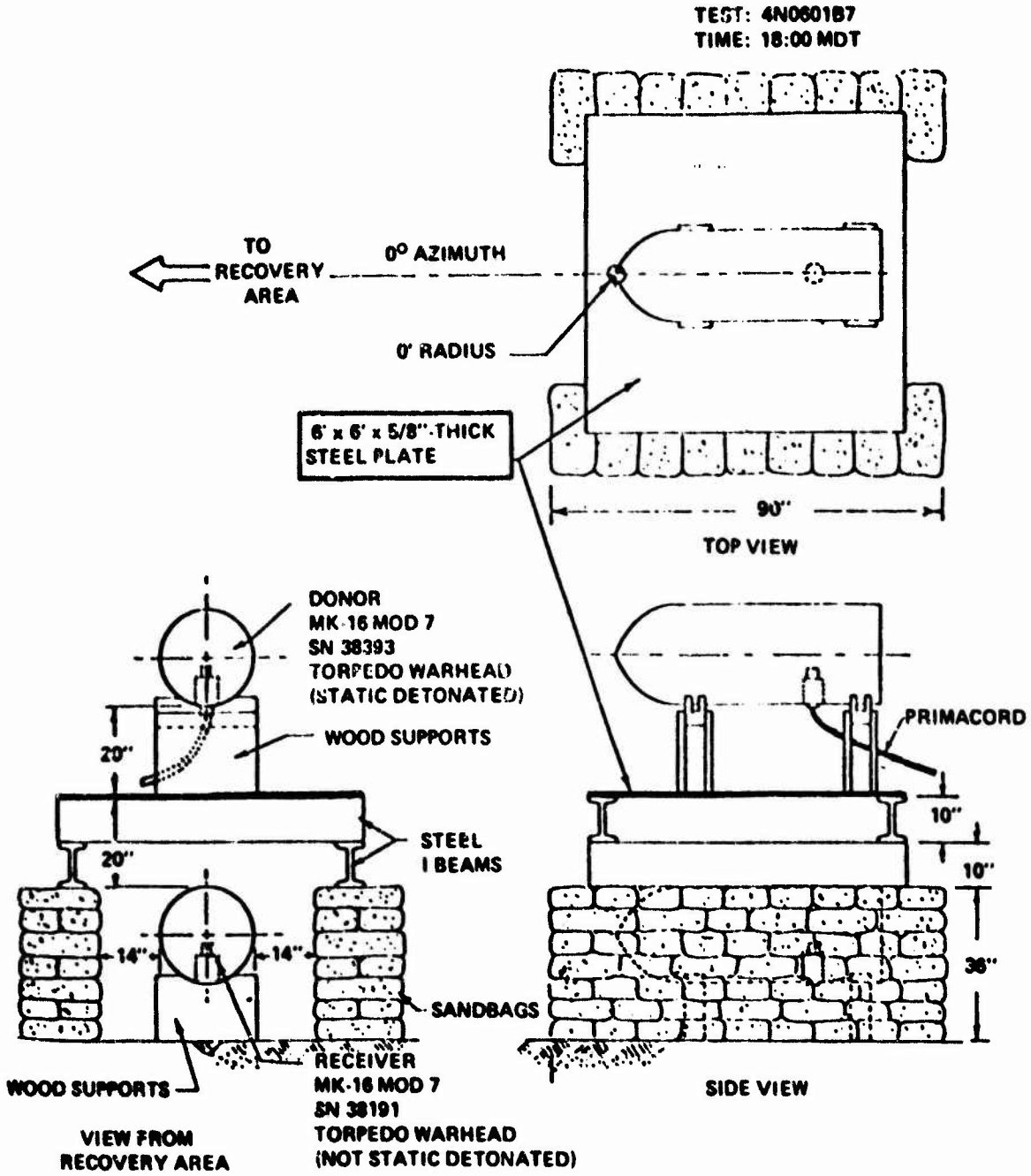

FIGURE 20. TEST OF 5/8" INHIBITOR FOR MK 16 TORPEDO.

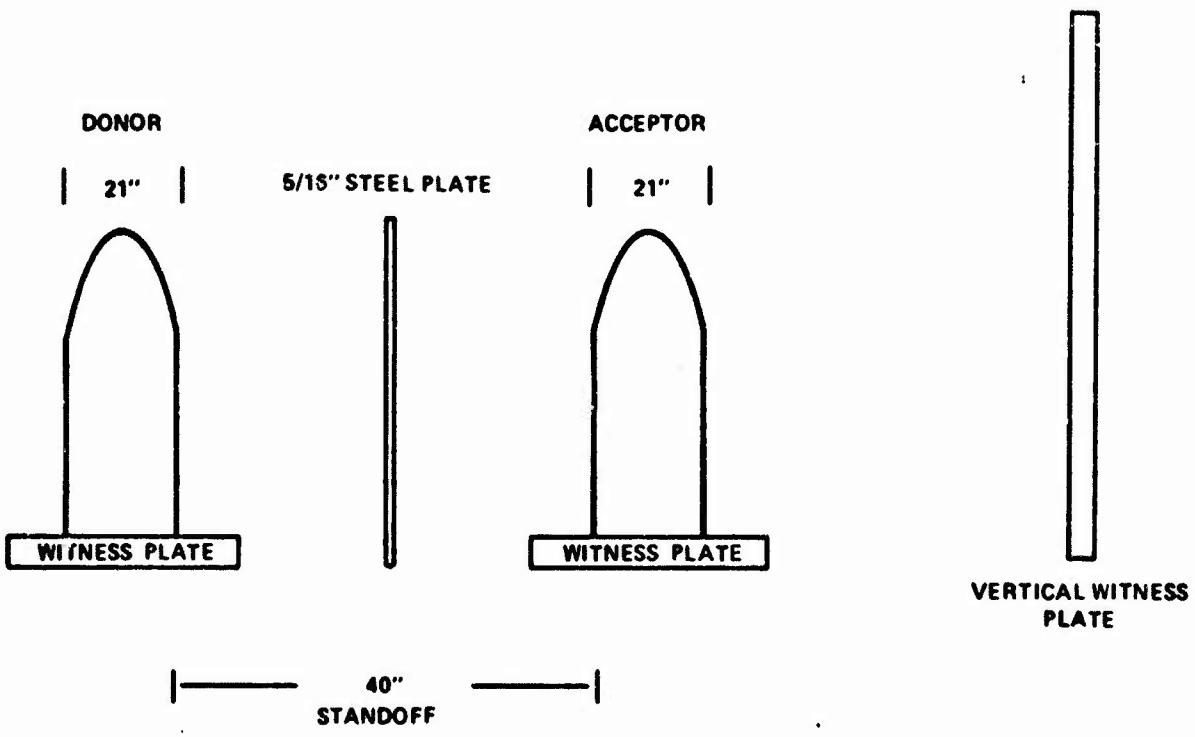

FIGURE 21. MK 16 TORPEDO WARHEADS% 747 POUNDS HBX-3 IN 1/8" BRONZE CASE.

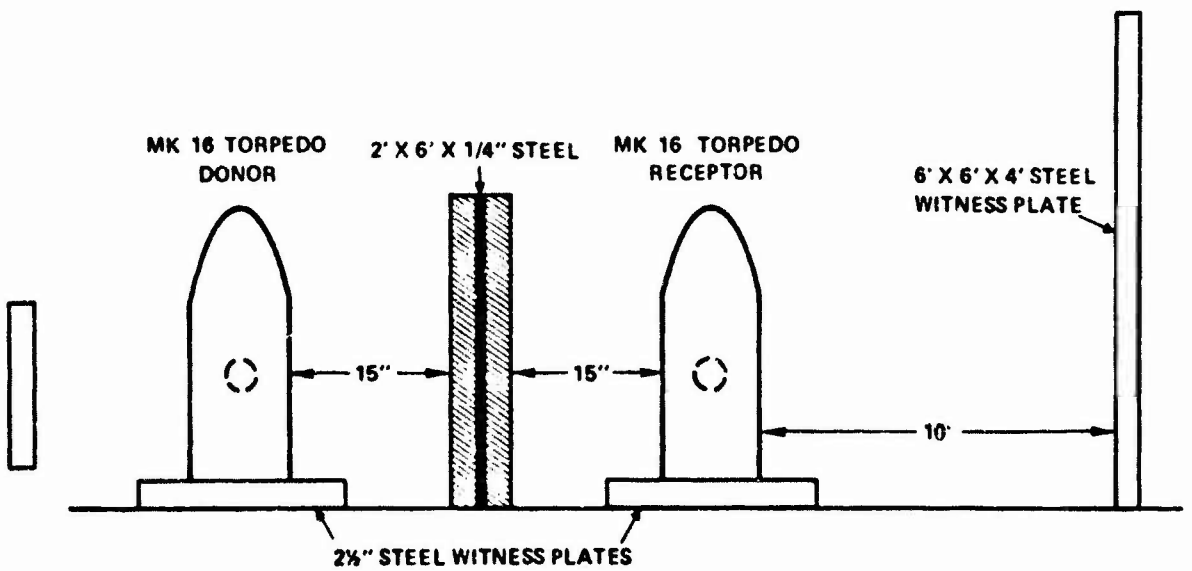

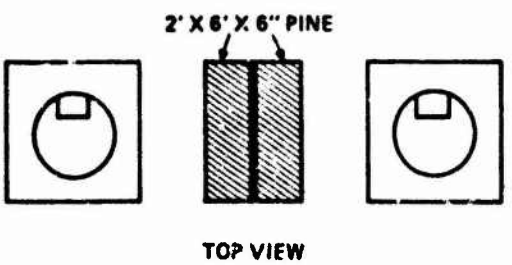

FIGURE 22. SET UPS FOR WOOD-STEEL SANDWICH INHIBITOR TESTS.

The acceptor detonated high order.

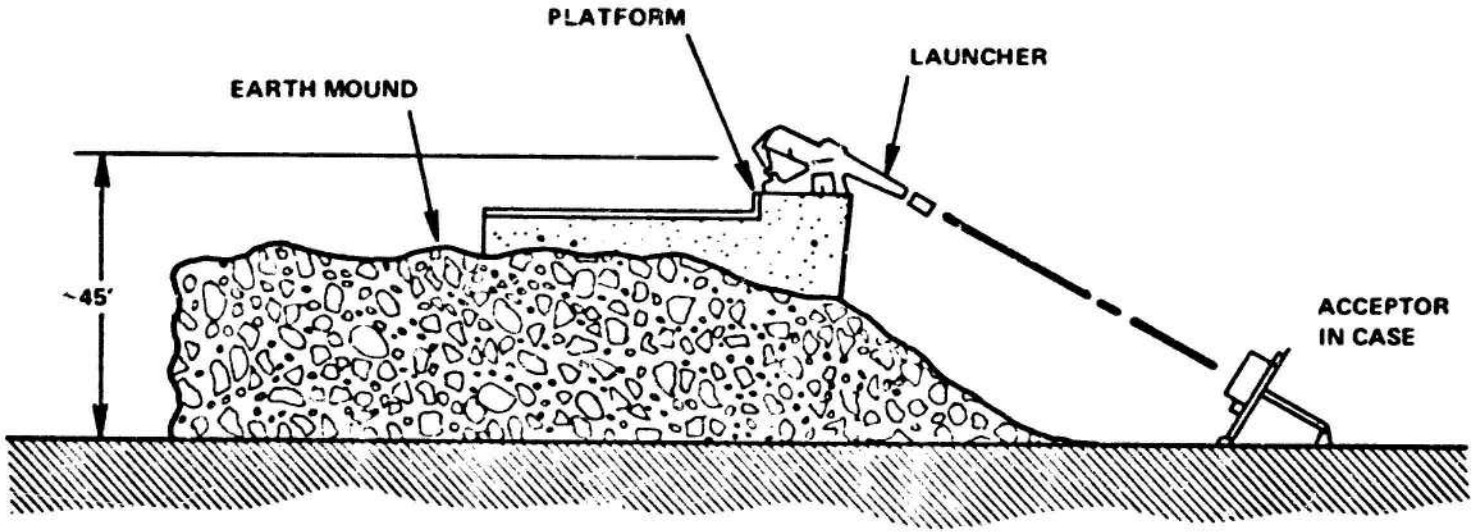

FIGURE 23. TWELVE INCH AIR-GUN FACILITY OF IITRI.

The current tests used ≅70 pound projectiles varying from 200 to 800 fps. The facility will accommodate up to 400 pound projectiles and velocities up to 1,000 f/s

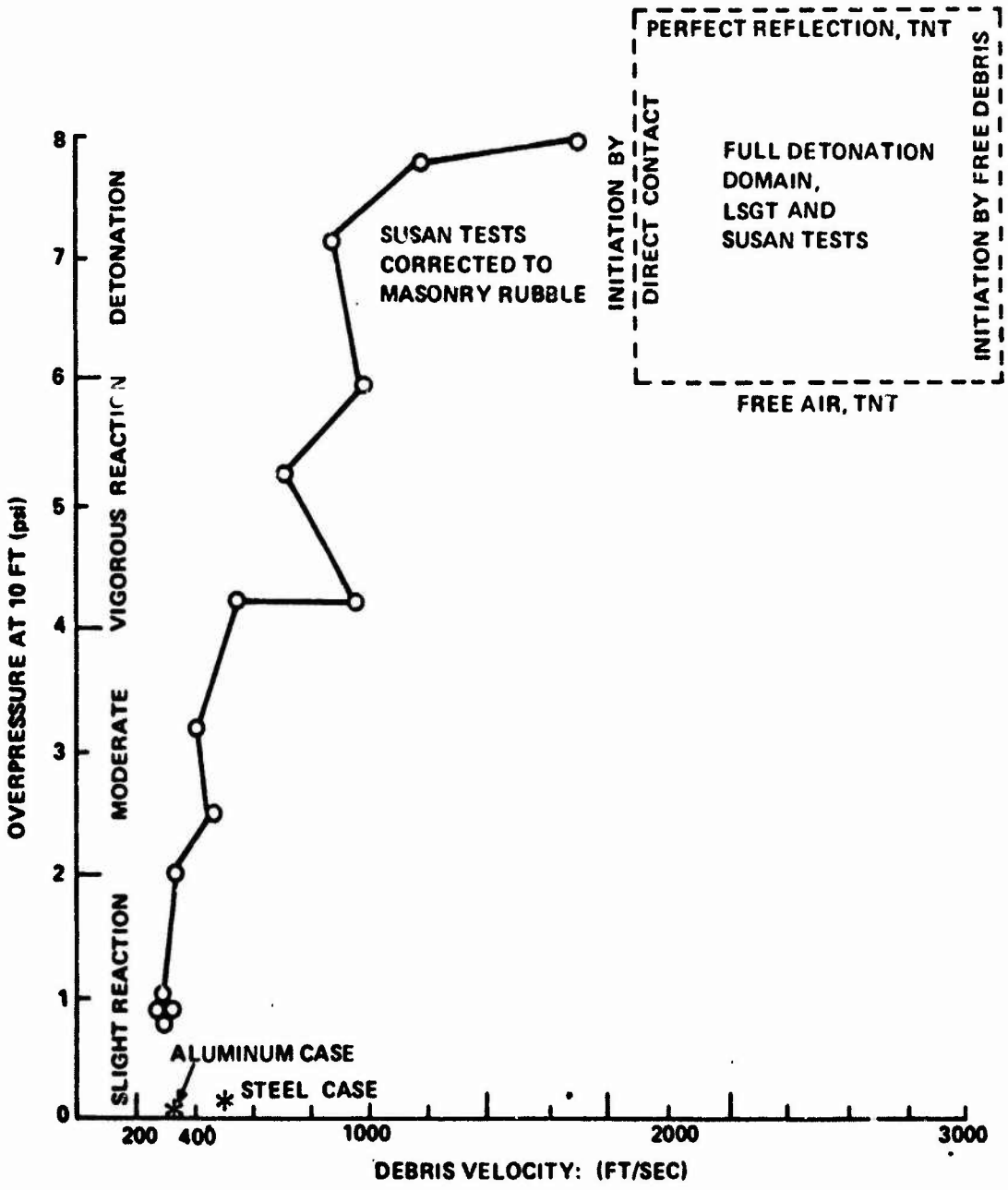

FIGURE 24. CORRELATION OF LARGE SCALE GAP TEST, SUSAN TESTS AND CONCRETE RUBBLE TESTS FOR PBX N103.

The box labelled LSGT shows the domain for full detonation of PBX N103, depending on direct contact for free flying debris and efficiency of:

O SUSAN TEST DATA (IMPACT ON STEEL) WERE CORRECTED TO CORRELATE WITH FREE FLYING MASONRY DEBRIS.

* MASONRY RUBBLE TESTS, ITTRI AIR GUN FACILITY.

SIMULATED TOMAHAWK MISSILE HANDLING ARC TEST RESULTS

by

J. M. Ward
Naval Surface Weapons Center
White Oak, Silver Spring, Maryland

1. INTRODUCTION

1.1 BACKGROUND

The work reported here was performed as part of the Navy Explosive Safety Improvement Program (NESIP). In the past, the Navy has been issued Explosive Safety Quantity Distance (ESQD) waivers at the tidewater port complexes during explosive handling operations which were necessary to maintain fleet operational readiness requirements. The ESQD arc of 1250 ft was established for 30,000 lb net HE; however, the requirement is applied to any quantity of fragmenting ordnance below this amount unless a specific safe* handling arc has been established. Herein lies the problem - ESQD waivers had to be issued for operations such as ordnance transfers, where the quantity of munitions involved was much less than 30,000 lb net HE, but where no appropriate safe handling arc had been established. The NESIP, as one of its objectives, has been concerned with establishing these safe handling arcs for various items of ordnance and their associated operations for handling.

One ordnance item of interest to the Navy is the TOMAHAWK cruise missile (HE warhead) which will be involved in future Naval operations. The study reported here was undertaken to establish the safe handling arc for the TOMAHAWK missile (HE warhead) when it is handled at a pier as part of off- and on-loading of a ship.

1.2 ACCEPTABLE HAZARD HANDLING ARC

A safe (acceptable hazard) handling arc is represented in Figure 1. Inside the arc, the density of impacting hazardous fragments is $\rho_H > (1/600)$ ft^2; that is, there are more than one hazardous fragment impacts per 600 ft^2 of area. Outside of the arc, the density of hazardous fragments is $\rho_H < (1/600)$ ft^2; that is, there is less than one hazardous fragment impact per 600 ft^2 of area. The area referred to in the definition is horizontal ground surface area. A fragment is considered hazardous when it possesses an impact energy of 58 ft-lb or greater. A second criterion is used to define acceptable hazard: the blast pressure outside the arc shall be no more than 1 psi.

*The word "safe" as used in the term "safe handling arc" signifies "acceptable hazard".

One of the major objectives in the NESIP is to establish a safe handling arc for munitions handling at the pier, and specifically, for the work reported here, for the handling of a TOMAHAWK missile.

1.3 OBJECTIVE

The objective of the work was to determine the safe handling arc for the TOMAHAWK cruise missile (HE warhead) in a transport configuration representative of future Naval ordnance transfer operations between a ship and the pier.

Experimental tests were to be performed to compare with results predicted with a simple analytical model developed as part of the NESIP technology base.

A fragment shield was to be designed and tested, if necessary, in order to provide a safe handling arc on the order of 500 ft.

1.4 SUMMARY

The safe handling arc for the simulated TOMAHAWK missile in a representative transport configuration was determined to be $\sim$ 500 ft. A fragment shield design was not required.

This paper briefly describes the simple analytical model developed for predicting safe handling arcs, the experimental tests, and the method of analyzing the recovery area data. All important assumptions for both the analytical model and the data analysis are presented so that, if necessary, most simplifying assumptions can be easily identified and then modified to improve the approximation for future analyses. The various elements of the experimental model are discussed briefly to describe the degree of simulation involved in building the models. Model dimensions and weights cited are only approximate.

Only the recovery area fragment data and results are published here. A complete test report will be published

as a Naval Surface Weapons Center Technical Report at a later date.

2. ANALYTICAL MODEL

The analytical model used to predict the safe handling arc for the TOMAHAWK missile was developed by F. B. Porzel and was presented at the 17th Explosives Safety Seminar (Reference 1).

2.1 IMPORTANT PARAMETERS

The simple model is based on the following main assumptions.

(a) Spherical symmetry - The fragment density is averaged over all polar angles. Side-spray enhancement is not included.

(b) Uniform initial velocity - There is no fragment velocity distribution, all fragments have the same initial velocity.

(c) Constant drag coefficient - The drag coefficient for fragments in supersonic flight is used. The fragment velocity decays exponentially as does the fragment energy.

(d) Flat trajectory - Only the low-angle trajectory path is considered and this path is computed as straight-line. The high-angle trajectory path solution is ignored. Since the low-angle trajectory path produces the more hazardous fragment impact, the effect of this assumption is to overestimate the number of hazardous fragment impacts (energy > 58 ft-lb).

(e) Trajectory-normal fragment areal density - The fragment areal densities normal to the trajectory path are calculated. Corrections for terminal angle of fall at the horizontal ground surface are not made. Because of this assumption, the areal density of fragment impacts is overestimated.

(f) Fragment characteristic size - The fragment characteristic size (L1) is usually assumed to be one-half the thickness of the case material unless fragment size distribution data are available. In this case L1 is determined by a fit to the available data (see (g) below).

Reference 1. Porzel, F. B., "Design of Lightweight Shields Against Blast and Fragments," Minutes of the Seventeenth Explosives Safety Seminar, Department of Defense Explosives Safety Board, 14-16 September 1976, Vol. II, p. 1247.

(g) Fragment size distribution - The fragment sizes are assumed to follow the distribution

$$N(>L) = N_0 \exp(-L/L1)$$

where $N(>L)$ = The number of fragments with characteristic dimensions larger than L

N_0 = The total number of fragments = $W/(6\rho(L1)^3)$

$L1$ = The characteristic fragment size

L = Mean fragment size = $(\text{mass}/\text{density}/\text{shape factor})^{1/3}$

W = Case weight

ρ = Case material density.

(h) Uniform shape factor - The shape factor S is used to relate the fragment mass to its mean dimension by $M = S\rho(L)^3$.

(i) Fragment initial velocity - The explosive energy is assumed to be equipartitioned between the internal and kinetic energies of the explosion gas products and case debris. The initial fragment velocity is determined when the total mass and the explosive energy output are specified.

(j) Energy equivalent - The TNT energy equivalent used is 720 cal/gram.

The analytical model is very simple to apply and is quite useful for providing an estimate for the safe handling arc. The analytical model was instrumental for planning purposes in the design of the experimental tests.

2.2 PREDICTIONS

The preliminary predictions for the TOMAHAWK safe handling arc are given in the Fragment Energy and Number (FEN) chart, Figure 2. These calculations considered only the case material for the HE warhead - at the time of these calculations, six months before the experimental test, detailed information about the missile, capsule, and shipping container had not yet been collected. The results are based on the assumption that the characteristic fragment dimension for the warhead case was $L1 = 1.0$ cm with a shape factor of $S = 0.4$ and that the initial fragment velocity was $V_i = 6{,}000$ ft/sec with a constant drag coefficient of $C_D = 1.3$.

Hazardous fragment densities occur in the region labelled "Unacceptable Hazard Zone" in Figure 2. In this part of the

graph, hazardous fragments (> 58 ft-lb energy) have an areal density greater than (1/600) ft^2 (1.67 fragments/1000 ft^2). Figure 2 indicates that the safe handling arc is somewhat less than 500 ft for the assumed fragment model. The R = 500 ft curve just misses passing through the "Unacceptable Hazard Zone". These calculations were very useful for determining what specific tests to perform and which test parameters had to be simulated more exactly.

Just prior to the test, when all the information on the missile, capsule, and shipping container were well in hand, updated predictions for the safe handling arc were made. The results, not shown here, indicated that the safe handling arc was somewhat greater than 500 ft.

3. TOMAHAWK MODEL

The TOMAHAWK cruise missile is shown in boosted flight configuration in Figure 3. Two full-scale pseudo-models of the missile including capsule and shipping container were constructed. These models used the same baseline HE warhead intended for the TOMAHAWK, but for the rest of the missile only major dimensions and weight distributions were simulated. The missile models were fabricated with an aluminum alloy that has material properties very similar to the TOMAHAWK missile skin. Both the capsule and the shipping container models were constructed with the same metal alloys surrounding the warhead section as is proposed for the TOMAHAWK design. All skin thicknesses for the missile, capsule, and the shipping container models were chosen to match the proposed design dimensions for the TOMAHAWK.

Each of the three container models was painted a separate color to aid in identifying sources of recovered fragments.

The various elements of the model are discussed briefly in the next five sections to provide details on the scope of the model design. Dimensions and weights cited are only approximate.

3.1 WARHEAD

The warhead section used for the TOMAHAWK model was the 1,000-lb conventional fragmentation warhead section of a surplus air-to-ground missile. Some modifications were made to the missile frame around the warhead section to represent longitudinal and ring stiffeners present in the TOMAHAWK design.

3.2 MISSILE

The missile model was fabricated from surplus air-to-ground missile sections which had material properties quite similar to those of the proposed aluminum alloy for the TOMAHAWK design. Each of the missile model sections was built to approximate length and total weight specifications of the TOMAHAWK design, Figure 4(a). Exact center-of-gravity (C.G.) locations for specific items of internal equipment were not controlled, only the total weight for each missile section was modelled. Ballast material in each of the model sections was selected so as to be representative of the type and distribution of actual material (electronics, hardware, fuel, etc.) present in the real missile. Some examples are given below.

(a) The model guidance section contained surplus aircraft guidance equipment.

(b) The model fuel tank section contained the proper quantity of water as ballast to match the weight of the jet fuel. The water ballast was included to determine how far liquid would be dispersed by the explosion. Jet fuel was not on board the model because only a fuel fire would have been produced (not a sympathetic detonation) which would not have contributed to the fragment hazard associated with the warhead detonation.

(c) The model engine section contained a jet accessory pack which simulated the cruise engine.

(d) The model booster section contained the proper quantity of sand to represent the booster propellant. An evaluation was made of the possibility of sympathetic detonation of the booster propellant produced by warhead detonation. When the sensitivity data of the propellant along with booster/warhead geometry were analyzed, the conclusion was that sympathetic detonation was highly unlikely. The warhead and the booster are separated by 10 feet of internal missile equipment. Sand was used to simulate the booster propellant weight so as to determine how far the booster section would be thrown relative to the dimensions of the area of water (which simulates jet fuel) dispersal. The booster section could be a potential late-time hazard because of cook-off in the fuel fire.

3.3 CAPSULE

TOMAHAWK missiles bound for submarine duty are to be encapsulated in order to mate with the inside dimension of the torpedo tube. The capsule is constructed of stainless steel

and it presents an added fragment source for a Navy TOMAHAWK configuration. For this reason, the capsule was included in the model design. A schematic of the simulated capsule is given in Figure 4(b). Capsule sections in the vicinity of the warhead section were fabricated with the same stainless steel alloy (including heat treatment) as specified in the proposed TOMAHAWK design.

3.4 SHIPPING CONTAINER

There are several proposed designs for the TOMAHAWK shipping container. The design which would represent the worst fragment hazard should an accidental warhead detonation occur was simulated for these tests. An end-view diagram of the model is given in Figure 5. Basically the model consisted of two half-cylinders 31 inches in diameter and approximately 23 feet in length with an overhead plate and five support cradles. The styrofoam shown in the figure was added to the model to aid in mounting the overhead plate.

3.5 TRANSPORTATION VEHICLE

A surplus 2-1/2-ton military cargo truck was used to represent a transport vehicle for the TOMAHAWK missile. The total weight of the encapsulated missile plus the shipping container was approximately 6,000 lb which is less than the highway payload limit (10,000 lb) for this type of truck. However, the truck had a bed length of 12 ft whereas the shipping container model was 23 ft in length which produced an 11 ft overhang that was supported by steel I-beams (see Figure 6). The warhead section of the model was positioned on the truck bed above one of the wheel axles with the truck cab located forward of the warhead section.

The specific type of truck used in the test would, of course, not be used for actual transport of a TOMAHAWK cruise missile because the truck bed is far too short. However, the truck was adequate for the explosive test performed since the warhead section was completely contained on the truck bed for the test configuration. Any truck fragment hazardous beyond 500 ft (from ground zero) would come from a source in the vicinity of the warhead section.

4. TEST DESCRIPTION

The explosive tests were performed at TERA, New Mexico Institute of Mining and Technology, Socorro, New Mexico. The West Valley Test Area, the site of the test, is shown in Figure 7. The truck/missile location is shown at the 0-ft radius position. There were two tests, one test with the truck facing

side-on to the recovery area and the other configuration where the truck was oriented face-on towards the recovery area.

The warhead was detonated with a C-4 booster and a primacord lead; the warhead fuze was removed.

The camera coverage was somewhat different for the two tests, but generally there were seven high-speed data cameras and three documentary cameras to record the event.

Two blast gages were located at the 300-ft radius from ground zero (about the 1 psi overpressure range) and four rows of Celotex-pack fragment catchers, used for measuring fragment impact velocities, were positioned as indicated in Figure 7.

The recovery area represented by the grid network (which defines the 25 recovery area sectors) given in Figure 7, is bounded by terrain contours indicated in the figure by dashed lines.

A witness sheet, used for measuring fragment initial velocities, was placed about 57 ft from ground zero.

5. FRAGMENT RECOVERY AND TRAJECTORY CALCULATIONS

5.1 FRAGMENT RECOVERY

Following the explosive event, a recovery team was brought in to collect fragments located inside the recovery area. The fragment data were classified into three mass ranges:

(a) mass < 6 grams - The number and the total mass of all fragments collected per recovery area sector were recorded.

(b) 6 < mass < 28 grams - The mass of the individual fragment collected and the recovery area sector were recorded.

(c) mass > 28 grams - The mass of the individual fragment collected and the location coordinates within the recovery area were recorded.

A mass and a range (relative to ground zero) were identified with each fragment collected in the recovery area. For fragments in mass range (a), mass less than 6 grams, an average mass value was used. The range associated with each fragment corresponded to the radius from ground zero to the nearest boundary of the recovery area sector; for example, all fragments collected in sector 25 (Figure 7) were ascribed a range of 500 ft.

The fragment impact radius was equated to the fragment range (where the fragment finally landed) which overestimates the fragment impact radius. Fragments impact and then bounce to different locations. The assumption here is that the flux of the fragments bouncing into a recovery area sector is greater than the flux of fragments bouncing out of the recovery area sector. So, when only considering fragments collected within a recovery area sector, the number of impacts per recovery area sector is overestimated.

The trajectories of fragments stopped by the vertical Celotex targets (Figure 7) were estimated and their impact locations were included in the fragment recovery area data.

5.2 FRAGMENT TRAJECTORY CALCULATIONS

The impact energies of the recovered fragments were determined by ballistic trajectory calculations. A particle model (three-degrees-of-freedom* with variable drag coefficient) computer code was used. Instead of computing the particular trajectory required to place a fragment at its recovered location, which would have taken some iterations (also there were many fragments collected), a series of ballistic trajectories were computed which were used to represent the fragment trajectories. The series of trajectories (272 separate trajectories) are outlined below.

(a) Two fragment materials were considered - steel and aluminum

(b) Eight fragment masses were selected for each material

1 - 6 - 10 - 20 - 28 - 40 - 60 - 100 grams

(c) Seventeen angles of elevation were chosen for each mass

1 - 2.5 - 5 - 10 - 15 - 20 - 25 - 30 - 35 - 40 - 45 - 50 - 55 - 60 - 70 - 80 - 89 degrees

Additional input conditions which were needed in order to make the trajectory calculations are fragment initial velocity, presented area, and drag coefficient. These input parameters are discussed below.

The intial velocity chosen for all fragments was 8300 ft/sec. The first fragment to strike the witness sheet at 57 ft from

*No wind velocity components (for instance, cross winds) were included, so actually the trajectory calculations only involved two-degrees-of-freedom.

ground zero had an average velocity of 6200 ft/sec. To determine the initial fragment velocity, the fragment mass must be known. If the characteristic fragment dimension (L1 = 1.0 cm (see Figure 2) discussed in Section 2) for the warhead case material was chosen (from warhead arena test data) then approximately 8300 ft/sec is obtained for the initial fragment velocity. This value is somewhat below the side-spray fragment velocity obtained from arena tests for the warhead alone without the added mass of the missile, capsule, and shipping container.

The presented areas for the fragments were computed from the fragment masses using the fragment shape factor for the warhead case material. For aluminum fragments, originating from the missile and the shipping container, the shape factor was derived from the steel fragment shape factor by making a correction for density.

The drag coefficient curve used was taken from Figure 17 in Reference 2. It is the variable drag coefficient for a rotating cube based roughly on the average projected frontal area of the cube when rotating. The drag curve is sketched below.

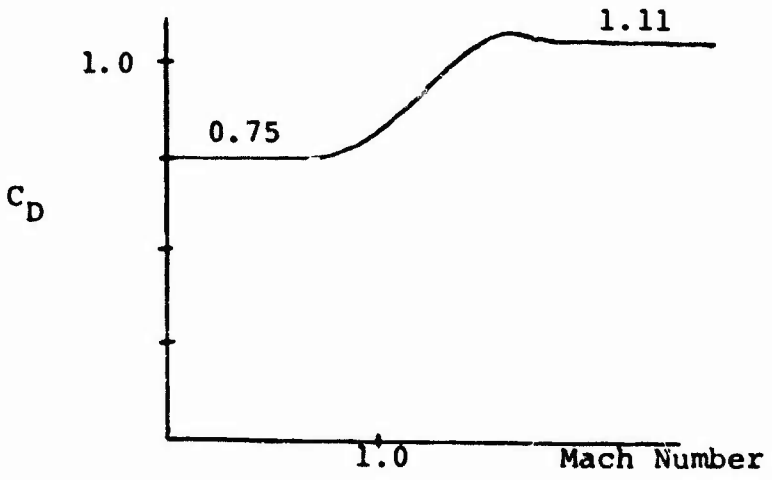

5.3 FRAGMENT HAZARD FACTOR

For each fragment impact location out to the maximum range, there are two trajectory solutions - the low-angle trajectory

Reference 2. Hoerner, S. F., "Fluid-Dynamic Drag," published by the author, 1965.

and the high-angle trajectory. The fragment impact energies for each of these trajectories can be quite different. For example, a 10-gram steel fragment with an 8300 ft/sec initial velocity impacting at 700 ft from a low-angle trajectory has an energy of 58 ft-lb whereas had the fragment arrived via a high-angle trajectory, the impact energy would have been 3 ft-lb. Thus, it is very important to determine the proportion of low-angle trajectory to high-angle trajectory impacts in a given recovery area sector. This was done using computed trajectory results displayed in the manner shown in Figure 8. In the figure, the impact range is given as a function of launch elevation angle for a specified mass, material, and initial velocity. From this figure, the result is obtained that 5% of the 10-gram steel fragments with an initial velocity of 8300 ft/sec impacting between 700-800 ft arrive via low-angle trajectories. The basic assumption here is that the fragment mass source is uniformly distributed with respect to angle. In the model tested, this was not the case. Because of the presence of the overhead plate on the shipping container model, more of the total mass was available for high-angle fragment trajectories than was predicted when it was assumed that the mass was uniformly distributed with angle. So for the calculations presented here, the proportion of fragments computed to have low-angle trajectories was overestimated; that is, the proportion of hazardous fragments was overestimated.

To help with the bookkeeping for analyzing the proportion of hazardous fragments to total number of fragments in a particular recovery area sector, a coefficient termed the fragment hazard factor (F_H) was defined. The definition, which applies to a specific fragment material and mass (one of the mass values listed in Section 5.2) and varies with recovery area sector*, is given below.

(a) If both the low-angle and high-angle trajectories produce hazardous fragment impact energies (> 58 ft-lb), then $F_H = 1$.

(b) If neither the low-angle nor the high-angle trajectories produce hazardous fragment impact energies, then $F_H = 0$.

(c) If the low-angle trajectory produces a hazardous fragment impact energy but the high-angle trajectory does not, then F_H is set equal to the proportion of low-angle to high-angle trajectories computed for the particular recovery area sector.

*F_H variation with azimuth is not included. Therefore, recovery area sectors 23-25 (Figure 7) all have the same value for F_H.

Tables were set up for each fragment material (steel and aluminum) which provided the fragment hazard factor (F_H) for each fragment mass listed in Section 5.2 and for each recovery area sector. Fragment mass interpolation within the table was not made. For example, fragments with masses in the range 6 < fragment mass < 10 grams were treated as 10-gram fragments for determining F_H.

The fragment hazard factor was used in the following manner. If an 8-gram steel fragment was collected from recovery area sector 23 then that fragment would be counted as 0.05 hazardous fragments. This follows from definition (c) above and the result given above that 5% of the 10-gram steel fragments with an initial velocity of 8300 ft/sec impacting between 700-800 ft (which bounds the range of recovery area sector 23) arrive via low-angle trajectories.

6. RECOVERY AREA FRAGMENT DISTRIBUTIONS

Figures 9 and 10 present the total fragment and hazardous fragment distributions for both simulated TOMAHAWK explosive tests. Also included in the figures is the distribution of allowed hazardous fragments per recovery area sector.

The total fragment distributions were obtained from the recovery operation. All fragments collected for each test are represented in the figures.

The hazardous fragment distribution was determined by applying the appropriate fragment hazard factor (F_H), described in Section 5.3, to each collected fragment taking into account the fragment material and mass, and the specific recovery area sector.

The allowed hazardous fragment distribution gives the number of hazardous fragments acceptable in each recovery area sector such that the hazardous density does not exceed (1/600) ft^2. This distribution was obtained by dividing the area of each recovery area sector by 600 ft^2.

For the side-on TOMAHAWK test (see Figure 9) the results indicate that the number of hazardous fragments per recovery area sector does not exceed the acceptable number of hazardous fragments for any of the recovery area sectors between 500 - 1,000 ft range. Note that the total number of fragments per recovery area sector is relatively large, but the greater majority of these fragments have impact energies less than 58 ft-lb.

For the face-on TOMAHAWK test (see Figure 10) the number of hazardous fragments per recovery area sector does not exceed the acceptable number of hazardous fragments for any of the recovery area sectors between 500 - 1,000 ft range. In fact, the number of hazardous fragments are quite small in comparison with the acceptable number of hazardous fragments for all these recovery area sectors. In addition, the total number of fragments per recovery area sector does not exceed the acceptable number of hazardous fragments for any recovery area sector beyond the 800 ft range.

A comparison of the fragment distributions between Figures 9 and 10 indicates that the side-on fragment spray from the TOMAHAWK is far more hazardous than the face-on spray, as expected. This is in agreement with arena test data for the warhead (without the missile, capsule, and shipping container surround) which does not include the shielding effects of the guidance section of the missile nor the presence of the truck cab for the face-on test configuration.

7. CONCLUSIONS

Tests were performed to determine the safe handling arc for the TOMAHAWK cruise missile (HE warhead). The experimental results agree quite well with predictions. Both the tests and the simple analytical model indicated that the safe handling arc is approximately 500 ft for the model configuration tested. The full-scale model included a 1,000-lb conventional fragmentation warhead encased in simulated missile, capsule, and shipping container models which was then loaded onto a surplus military cargo truck. Inclusion of the booster propellant and the jet fuel in the model was determined to be unnecessary.

The analytical model, the test procedures, and the method of data analysis described are applicable for evaluating the safe handling arc for a wide spectrum of other ordnance items such as HARPOON and torpedoes.

ACKNOWLEDGEMENTS

This work is a portion of the Navy Explosive Safety Improvement Program (NESIP) under the cognizance of OP 411 and supported by NAVSEA 04H3. Overall guidance was provided by J. Petes of NSWC(WO). Technical support and analysis was supplied by F. B. Porzel, also of NSWC(WO). Conduct of the tests was under the able direction of J. P. McLain of the TERA Group of the New Mexico Institute of Mining and Technology.

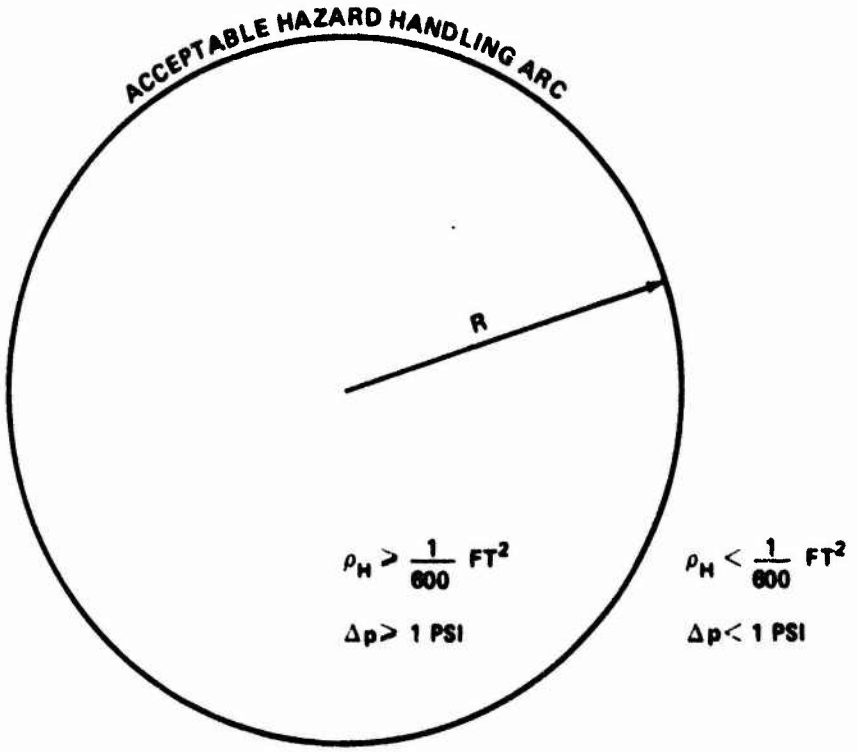

THE AREAL DENSITY OF HAZARDOUS FRAGMENTS* ρ_H IS LESS THAN ONE PER 600 FT^2 AND THE BLAST PRESSURE IS LESS 1 PSI BEYOND THE ACCEPTABLE HAZARD HANDLING ARC.

*HAZARDOUS FRAGMENT: FRAGMENT KINETIC ENERGY GREATER THAN OR EQUAL TO 58 FT-LB.

FIGURE 1 ACCEPTABLE HAZARD HANDLING ARC

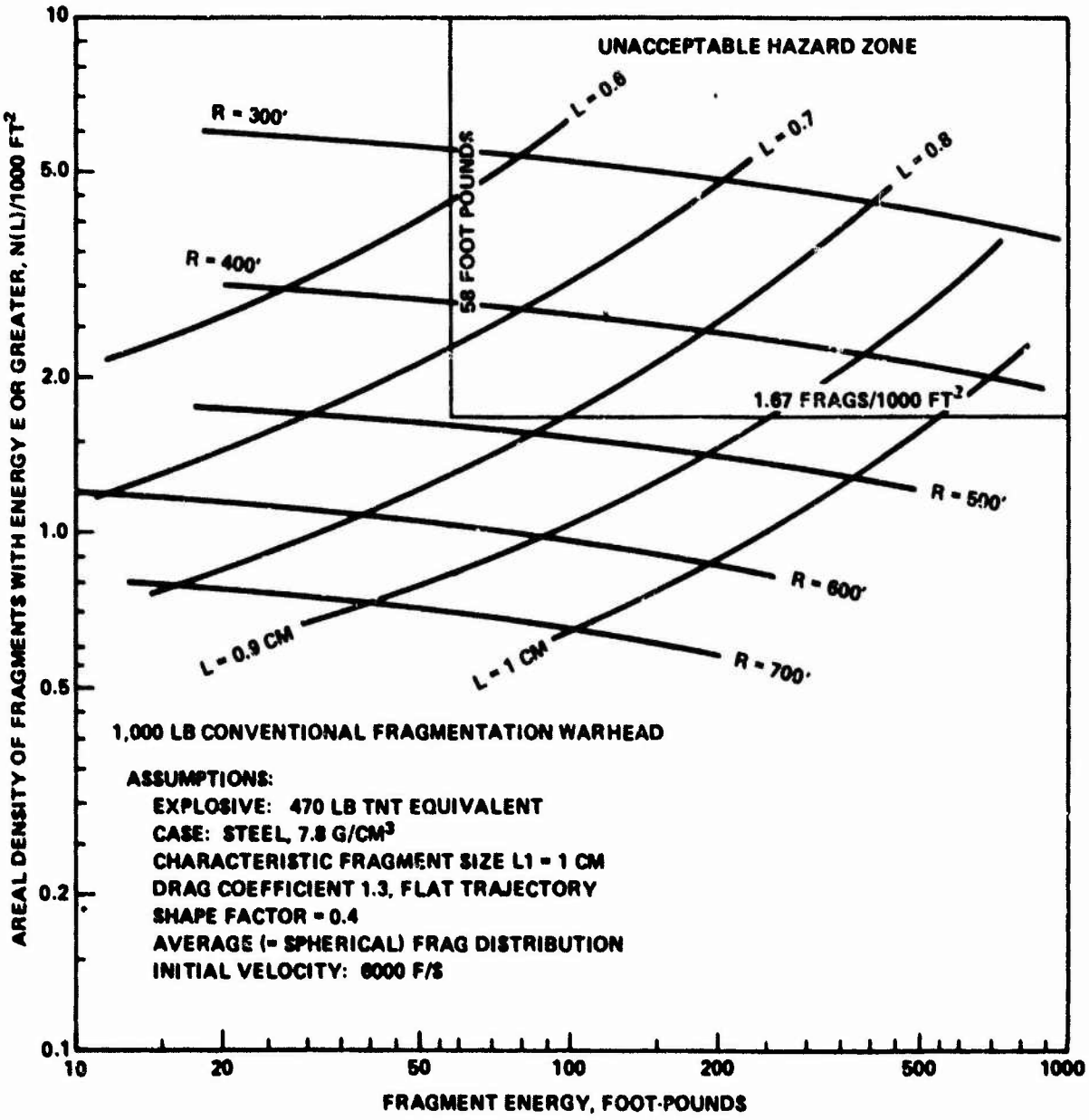

FIGURE 2 FRAGMENT ENERGY AND NUMBERS (FEN CHART)

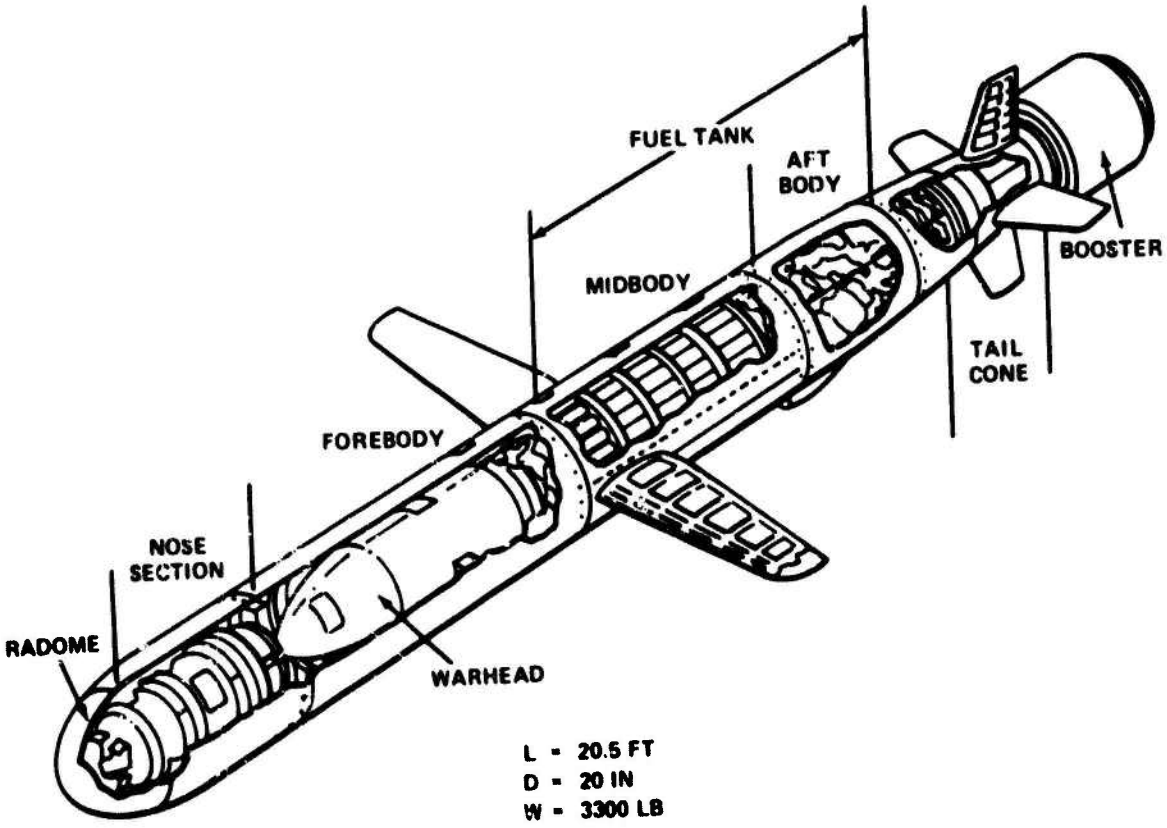

FIGURE 3 TOMAHAWK

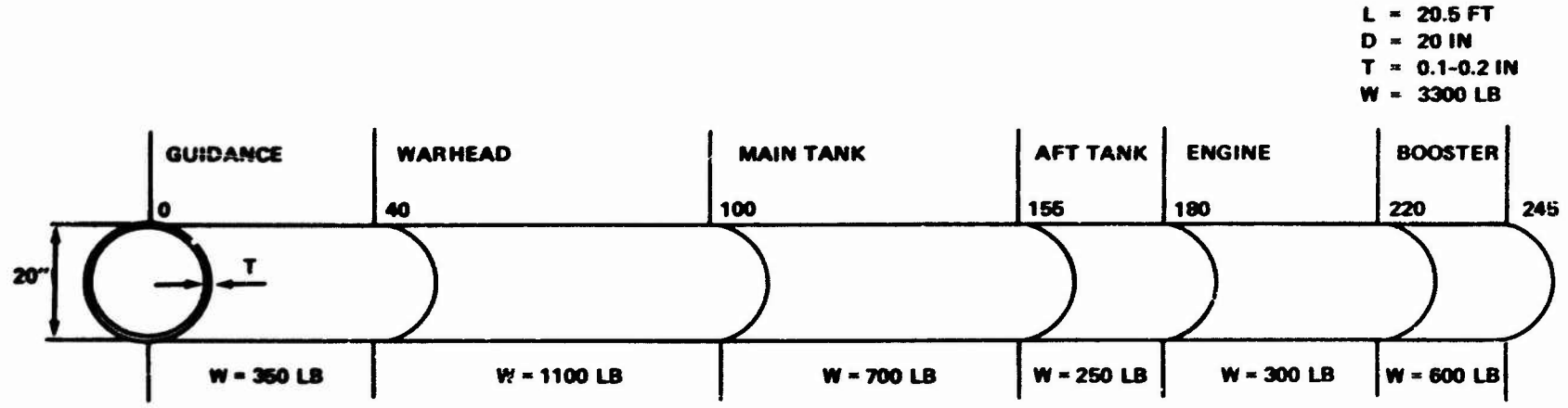

FIGURE 4(a) TOMAHAWK MISSILE MODEL

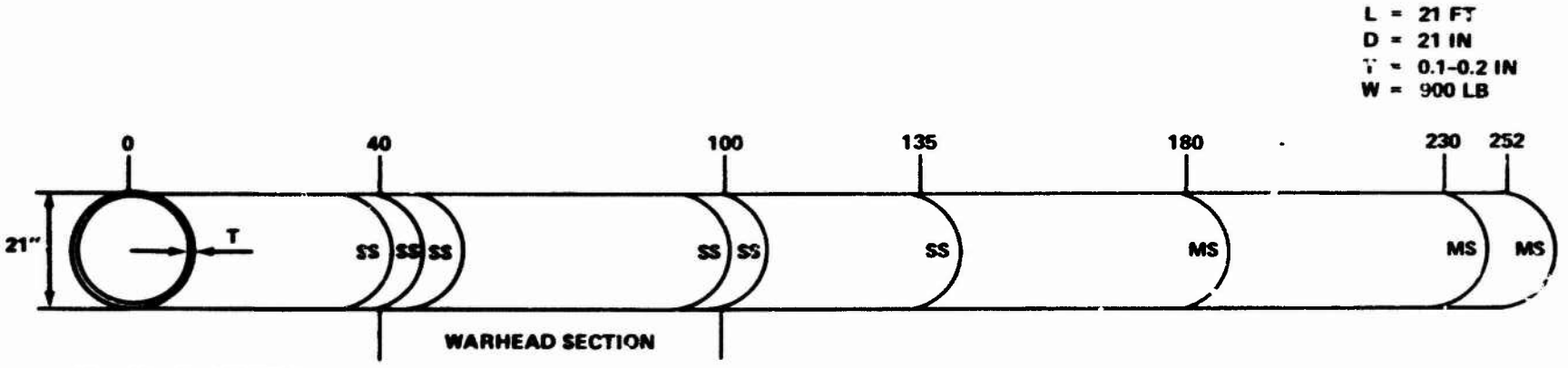

SS : STAINLESS STEEL
MS: MILD STEEL

FIGURE 4(b) TOMAHAWK CAPSULE MODEL

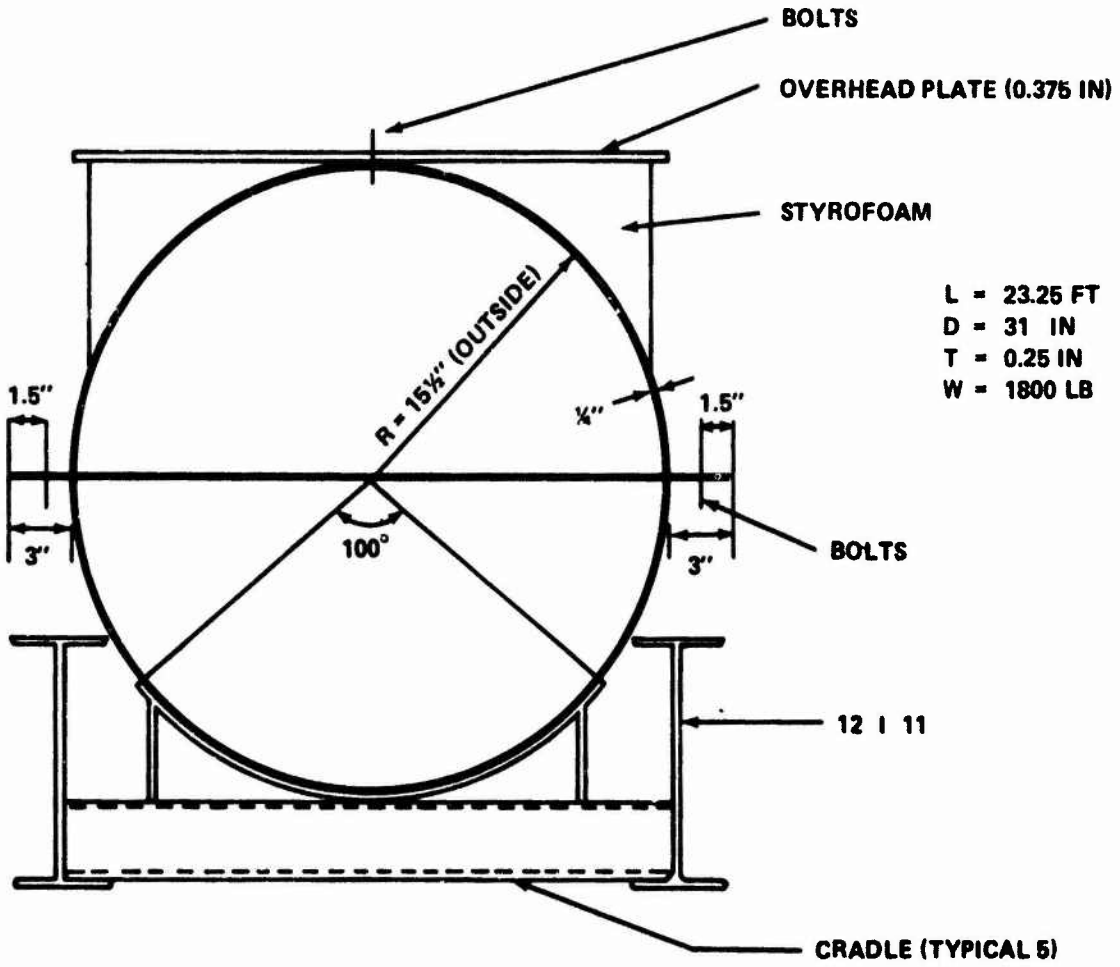

FIGURE 5 TOMAHAWK SHIPPING CONTAINER MODEL (END VIEW)

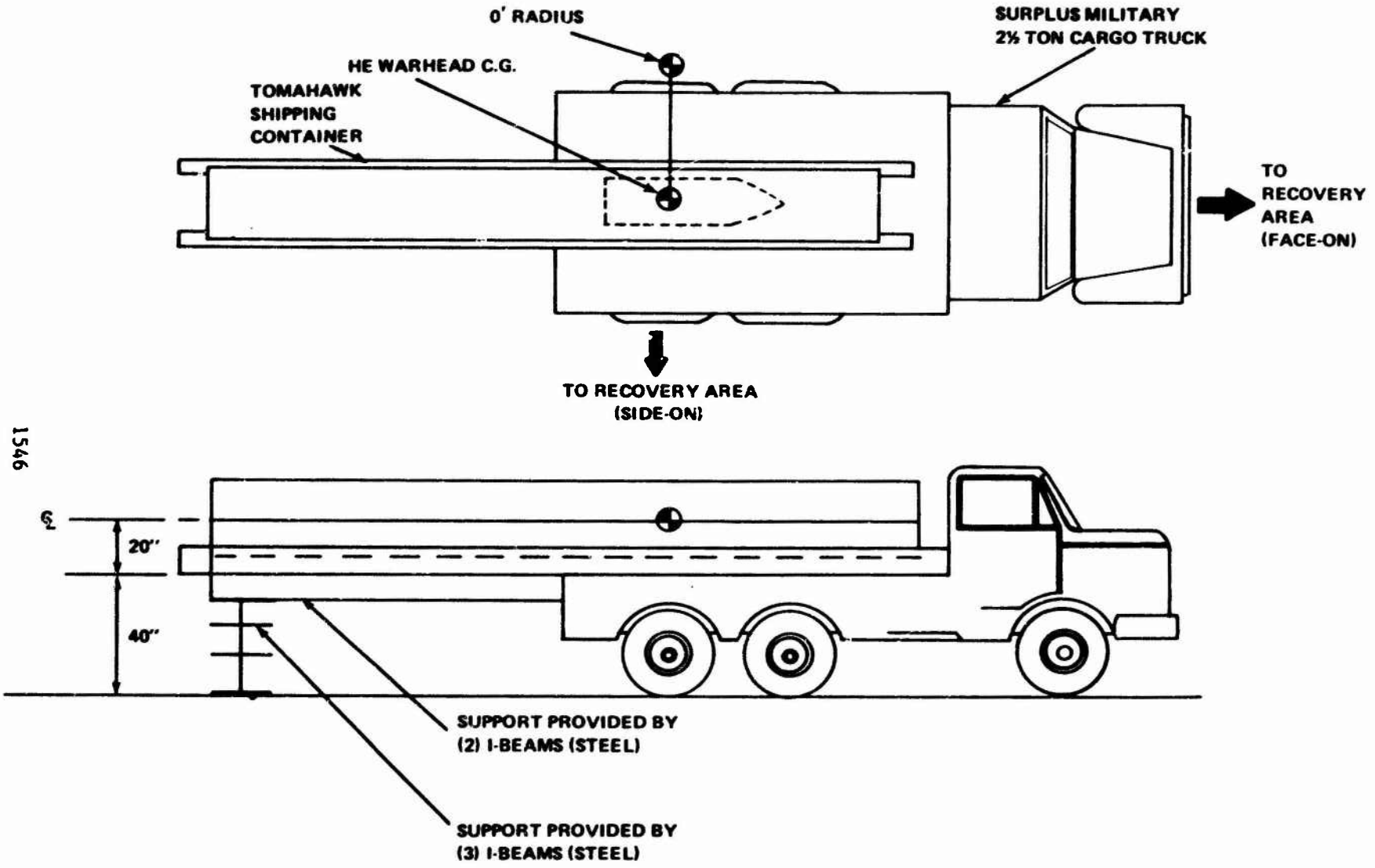

1546

FIGURE 6 MISSILE/TRUCK GEOMETRY

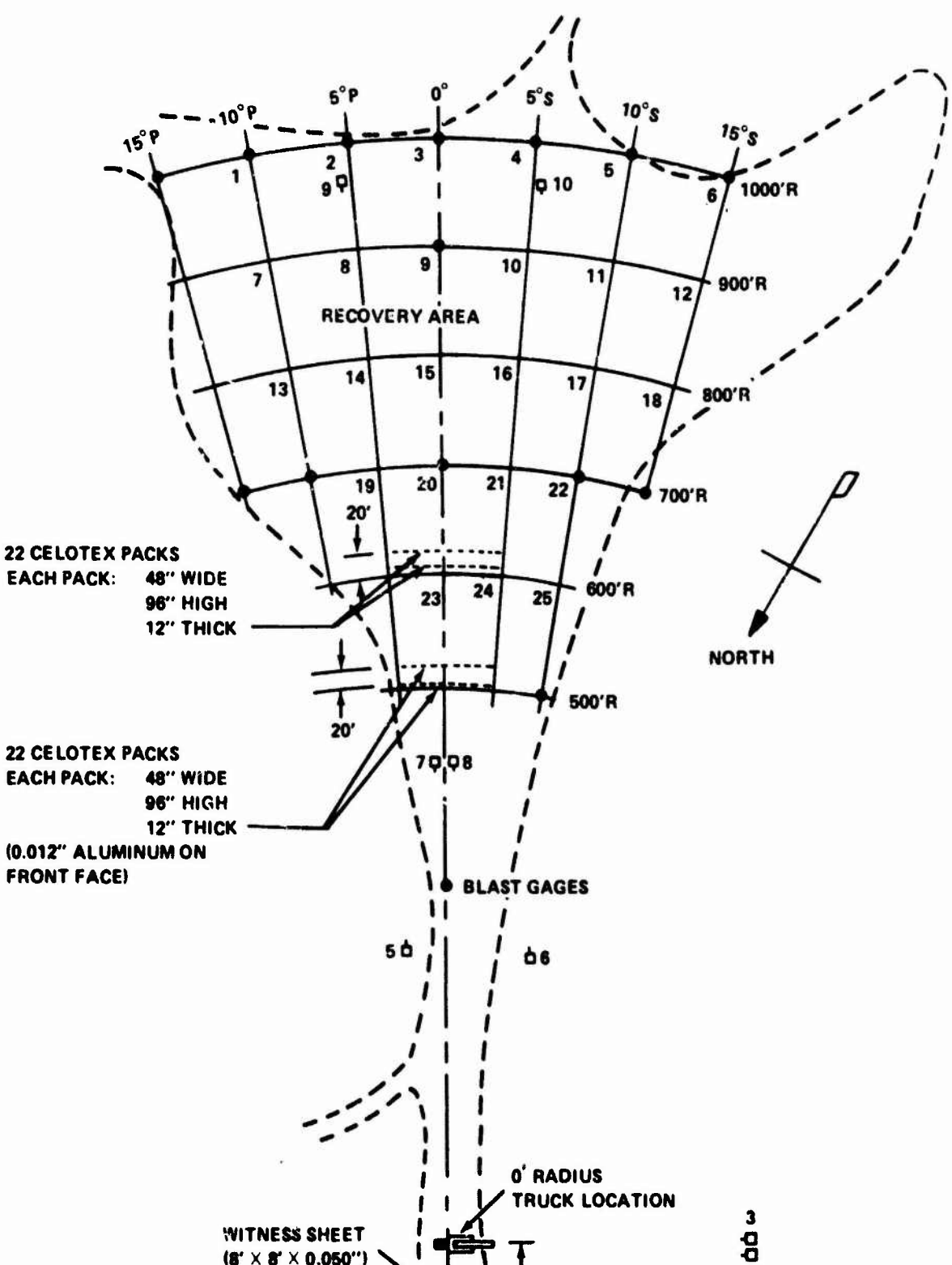

FIGURE 7 WEST VALLEY TEST AREA

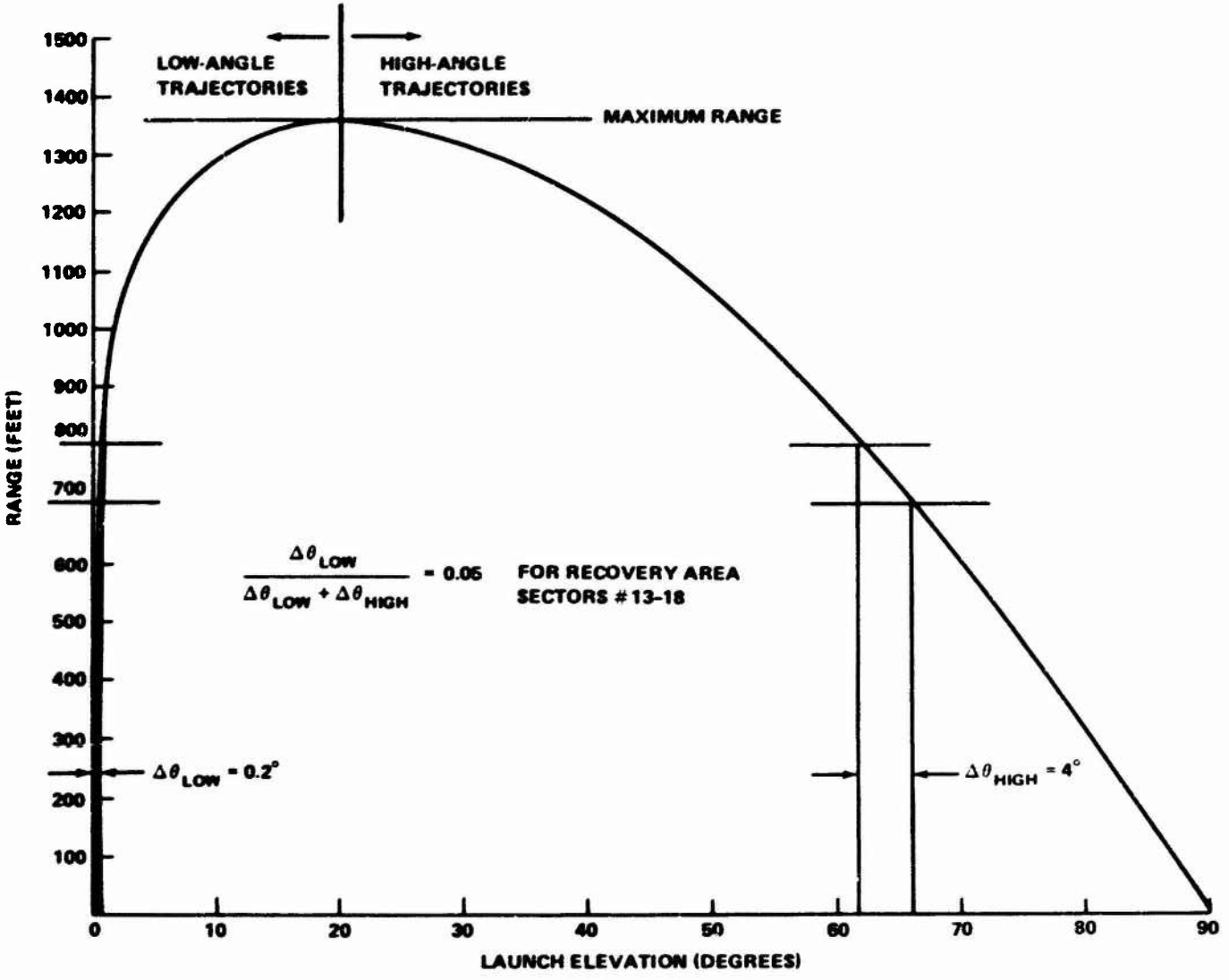

FIGURE 8 IMPACT RANGE VERSUS LAUNCH ANGLE FOR 10 GRAM STEEL FRAGMENT WITH INITIAL VELOCITY OF 8300 FT/SEC

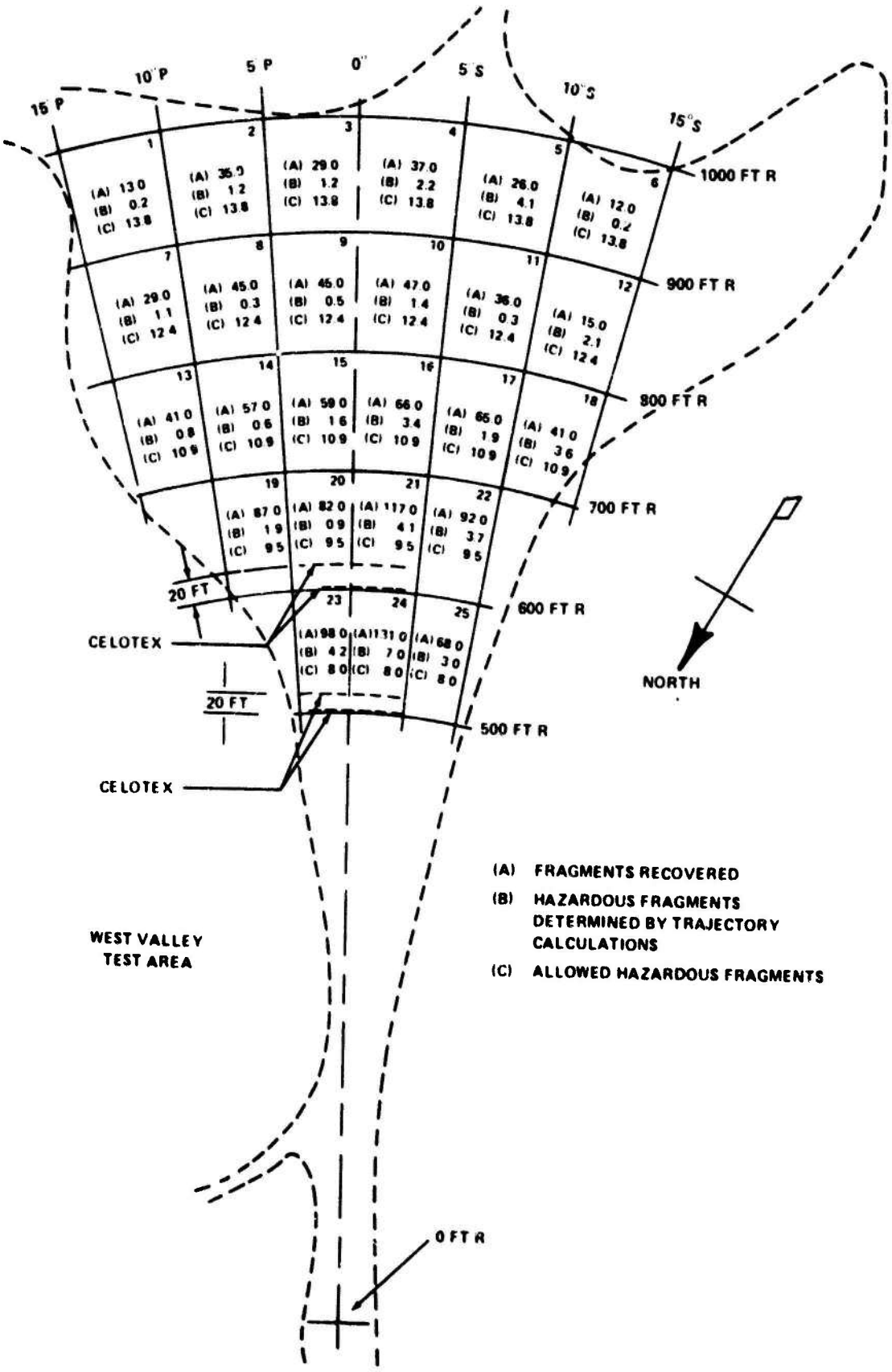

FIGURE 9 FRAGMENT DISTRIBUTIONS FOR SIDE-ON TEST CONFIGURATION

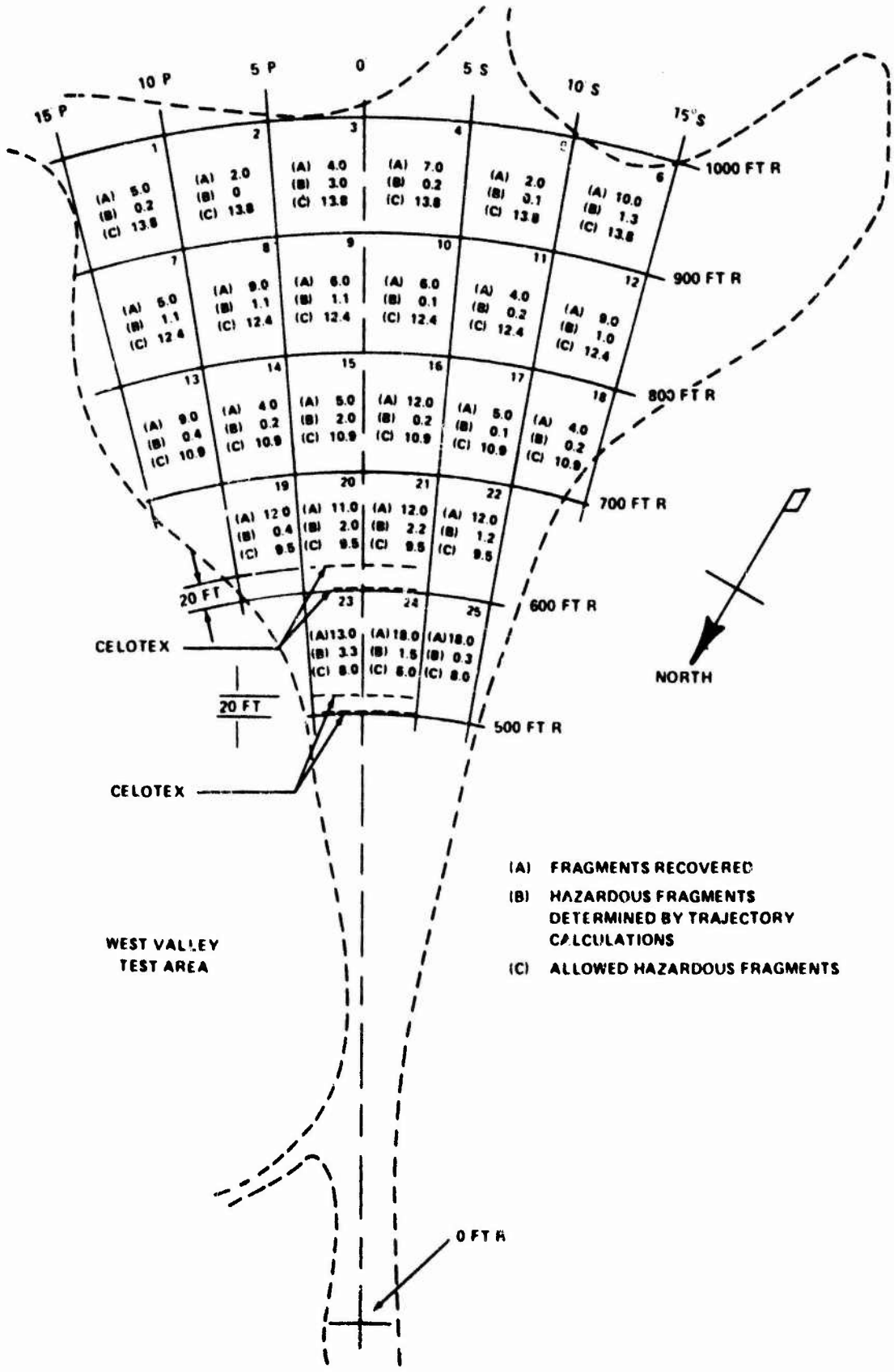

FIGURE 10 FRAGMENT DISTRIBUTIONS FOR FACE-ON TEST CONFIGURATION

NAVY REQUIREMENTS FOR COMBAT SURVIVABLE PROPELLANTS AND EXPLOSIVES

Dr. J. T. Amlie
Naval Material Command
Washington, D.C.

Insensitive high explosives and propellants or IHEP are currently being addressed in a major study of the subject by Department of Energy Laboratories and the Department of Defense. There are two primary tasks in the study: the first looks at what the technology can provide, and the second looks at the effectiveness of these materials. From the viewpoint of Naval Weapon Combat Survivability, there are two specific interests: survivability of the weapon incorporating these materials once launched, and survivability of the launch platforms in combat should the weapons be struck. I should point out here that the word weapon as used throughout the paper refers to expendable ordnance.

A potential benefit in use of IHEP will be, for Navy combatant ship design - on the flexibility that might be obtained in magazine and weapon placement, the reduction in high strength protective material requirements, and mitigation of damage which might result from taking a magazine hit. For naval aircraft, use of IHEP in weapons would contribute greatly to survivability of aircraft if we go to conformal carriage.

There are many considerations regarding IHEP of producibility, availability of raw materials, production availability, processability, effectiveness, cost, and reliability that will not be addressed in this paper.

The paper will address the benefits that might be afforded by IHEP in terms of three aspects that relate to weapons combat survivability: performance, survivability of the weapon under attack in flight to the target, and survivability of the weapon on the platform (and thus of the platform and its weapon function) when the platform is attacked by conventional weapons.

Performance of weapons must not be degraded by use of IHEP because performance is the primary requirement for weapons. Weapons are designed for kill power against particular targets, and defensive weapons are part of the insurance of combat survivability of launch platforms. With the guidance accuracy of our weapons today and our increasing knowledge of target vulnerability, we can better specify the warhead performance needed to kill a given target. An example of this approach is the combination of a Navy developed explosive and warhead design concepts, which in the HARPOON Missile Warhead obtain the desired combination of performance and insensitivity.

Insensitivity of the weapon in flight into the target is an increasingly important feature of weapon performance. Fragment attack from enemy defensive weapons should not be able to cause the rocket motors and warheads of our weapons to detonate in flight to the target.

The same explosive and propellant properties that provide invulnerability for weapons attacking targets apply to the larger problem of weapon survivability on the launch platorm, and the survival of the platform and its capability to perform assigned missions. The goals of weapon combat survivability given attack by enemy weapons, are to (1) limit the damage to the launching platform to the minimum possible, and (2) preserve the function of as many weapons as possible.

Of continuing concern aboard ship is the ability to deal with the threat of fire, which in peacetime might be characterized as a primary threat and in combat as a secondary effect on conventional weapon attack. We have made great strides with the Navy cook-off improvement program, and a very difficult job has been successfully accomplished so that our bombs and rockets now reach the goal of surviving in the fast cook-off fire for more than five minutes (Figs. 1 & 2). This work has been done as a backfit program with "fixes". More significantly for the future, we have developed designs for rocket motor and warhead cases so that the case opens and the energetic material burns rather than having the possibility of transition to a detonation under confinement. The Navy has developed a series of explosives, the PBX explosives, that have been shown to burn rather than detonate in the fast cook-off fuel fire, when tested as a fill in bomb cases. Results of comparative tests are dramatic. Figure 3 shows the test setup, Figure 4 shows the test site after a test of bombs loaded with standard fill and Figure 5 shows the test site after a test of bombs loaded with PBX-116.

The second desirable objective for shipboard weapons in combat is for resistance to fragment attack. To assess this resistance, in combination with other development tests, WR-50 requirements are applied and many munitions have in the past been accepted on the basis of resistance to detonation of a rocket motor (without the igniter), or a warhead (without the booster) when impacted by one 20-MM AP round at service velocity. One can argue without conclusion about the threat size, but I think it would be prudent to consider the reality of attack by weapons that represent a greater threat than a 20-MM round, as well as the reality of multiple fragment attacks.

There are several thresholds for detonation of weapons, given fragment attack. There is the low-velocity impact by massive rubble, as demonstrated in tests by Napadensky at IITRI, detonation by fragment impact at velocities near the ballistic limit of the case, and shock initiation. This film of tests by Sewell at the Naval Weapons Center, China Lake, will demonstrate the effects of impact by 20-MM AP rounds at a velocity near the ballistic limit of the case, the deflagration-to-detonation transition (DDT), and shock initiation of detonation, (NOTE: the difference in DDT and shock initiation is evidenced by time to detonation: a few milliseconds for shock initiation, and from hundredsof milliseconds to minutes for the DDT process.)

Another consideration for insensitivity of shipboard weapons in combat is for survivability on impact. Weapons that operationally are required to penetrate hard surfaces usually incorporate front-end design for shock attenuation. However, side-on impact becomes important in ship magazines where high translational velocities can be induced in stowed munitions by blast and shock loadings from detonation of large threat warheads. Protection against side-on impulsive loading is not a design requirement, and the level of response if any would be a function of explosive properties.

Tests of the Navy PBX explosives indicate that they will better contend with the side-on impulsive loading issue. The resistance to detontion as shown in the fast cook-off test correlates with improved resistance to bullet impact and target impact properties as demonstrated in Figure 6.

Another element of concern for ships under attack by enemy weapons is the question of sympathetic detonation of our weapons. Depending on the enemy weapon attack in combat, the reactions that may occur in a ship magazine may range from ignition of one or more rounds to further ignitions, the deflagration to detonation transition, cook-off, detonation, or sympathetic detonation. These events pose an undesirable hazard to the ship. It is not reasonable to expect to reach the point of complete insensitivity of munitions, and improvements here in combat survivability may well be a matter of degree. If the properties of energetic materials are such that we can reduce the likelihood and severity at each step in the chain of events, we will have made a significant contribution.

The Navy is determining the safe separation distance for various weapons as one of the tasks in its NESIP or Naval Explosive Safety Improvement Program given the design mode initiation of one round, and will perform tests of the sympathetic detonability of the new PBX series of explosives.

There has been a natural tendency to emphasize the hazard associated with explosive-filled warheads. There is as much concern with the response of rocket motors to combat threats. While future trends for explosives are promising, trends with solid propellant developments are not comparable in all cases.

First, the so-called "New Generation" solid propellants for application in air-to-air guided missile rocket motors. These formulations produce minimum smoke and provide some increase in performance, but have been classified under the old system of classification as Class 7. The response of a representative Class 2 propellant and of the new generation propellants to bullet impact is shown in a film of tests at the Naval Weapons Center. Should these new propellants be introduced aboard ship as surface-launched derivatives of air-to-air missiles or if we

incorporate them into surface launched missiles, we may within the context of what I have been discussing increase the vulnerability of our ships as well as aircraft. There would, of course, be implications for Navy in terms of quantity-distance relationships.

On the positive side, the Navy has developed a composite propellant as a candidate for a large surface-launched missile that produces minimum smoke and has substantial improvement in performance over the current missile propellant, and reacts by burning quietly when impacted by a shaped charge.

This paper is not complete without some mention of Navy Gun Propellants. The propellant in the 76-MM cartridge, for example, does react when impacted by fragments, but the level of reaction in tests conducted to date has been limited to combustion, deflagration, and pressure rupture of the cartridge case.

The goal of the Navy Combat Survivability Program in propellants and explosives is to work toward use of formulations in weapons that will not detonate when attacked by enemy weapons in combat, but instead respond with a less violent reaction that we can cope with by ship design.

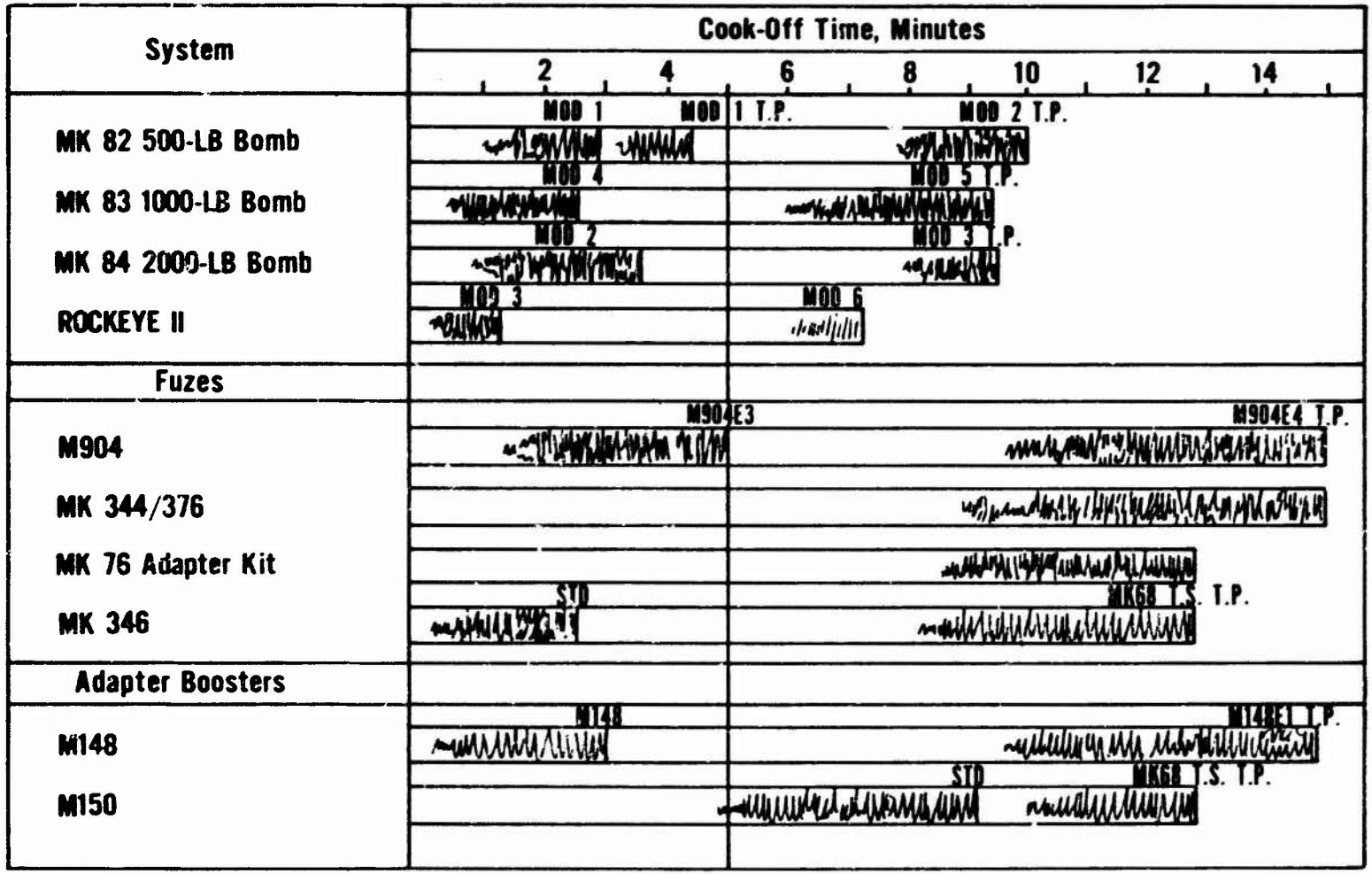

Figure 1. Bomb Cook-Off Improvement Program Status

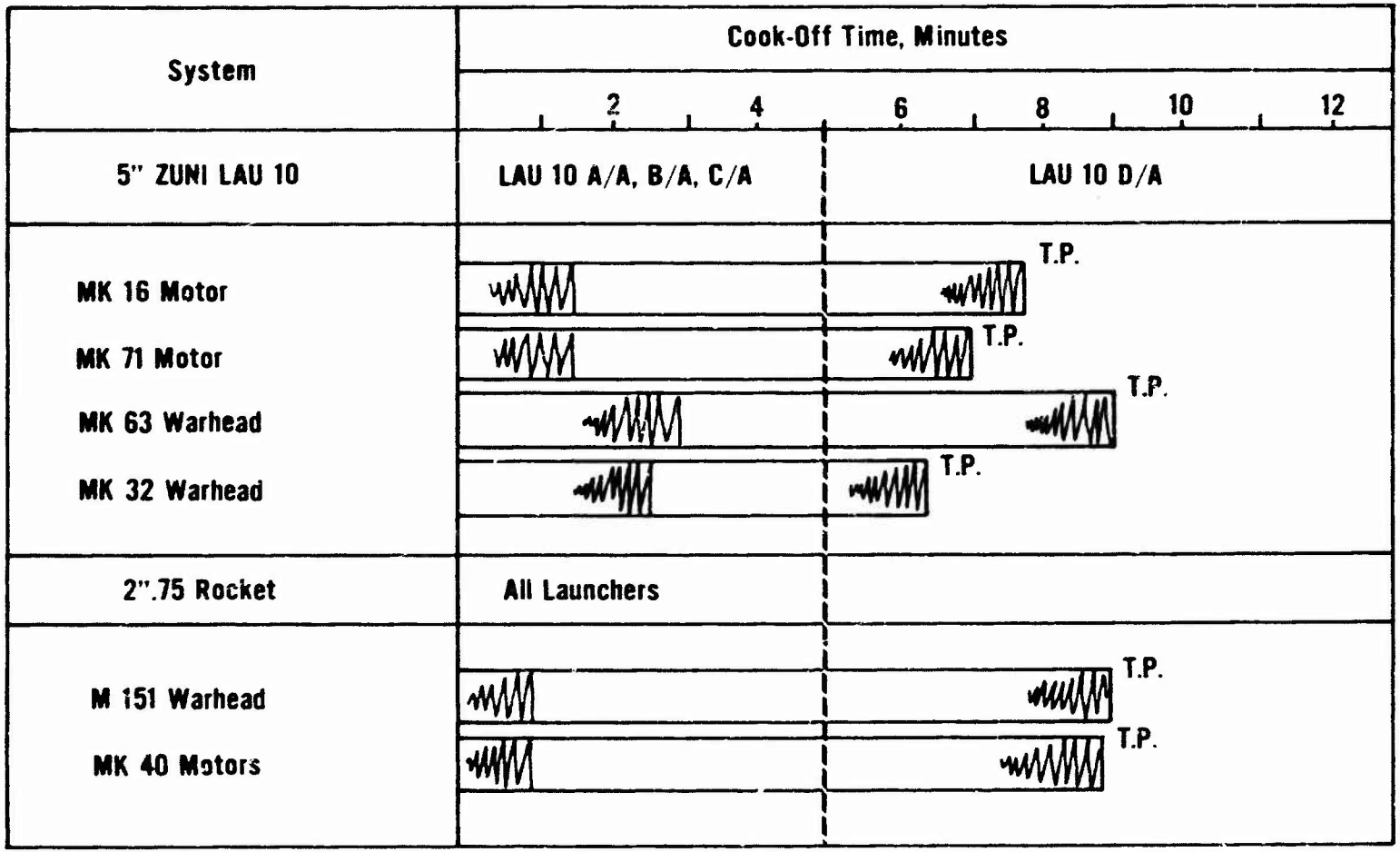

Figure 2. Cook-Off Times for Rockets With and Without Thermal Protection (T.P.)

1556
UNCLASSIFIED
UNCLASSIFIED

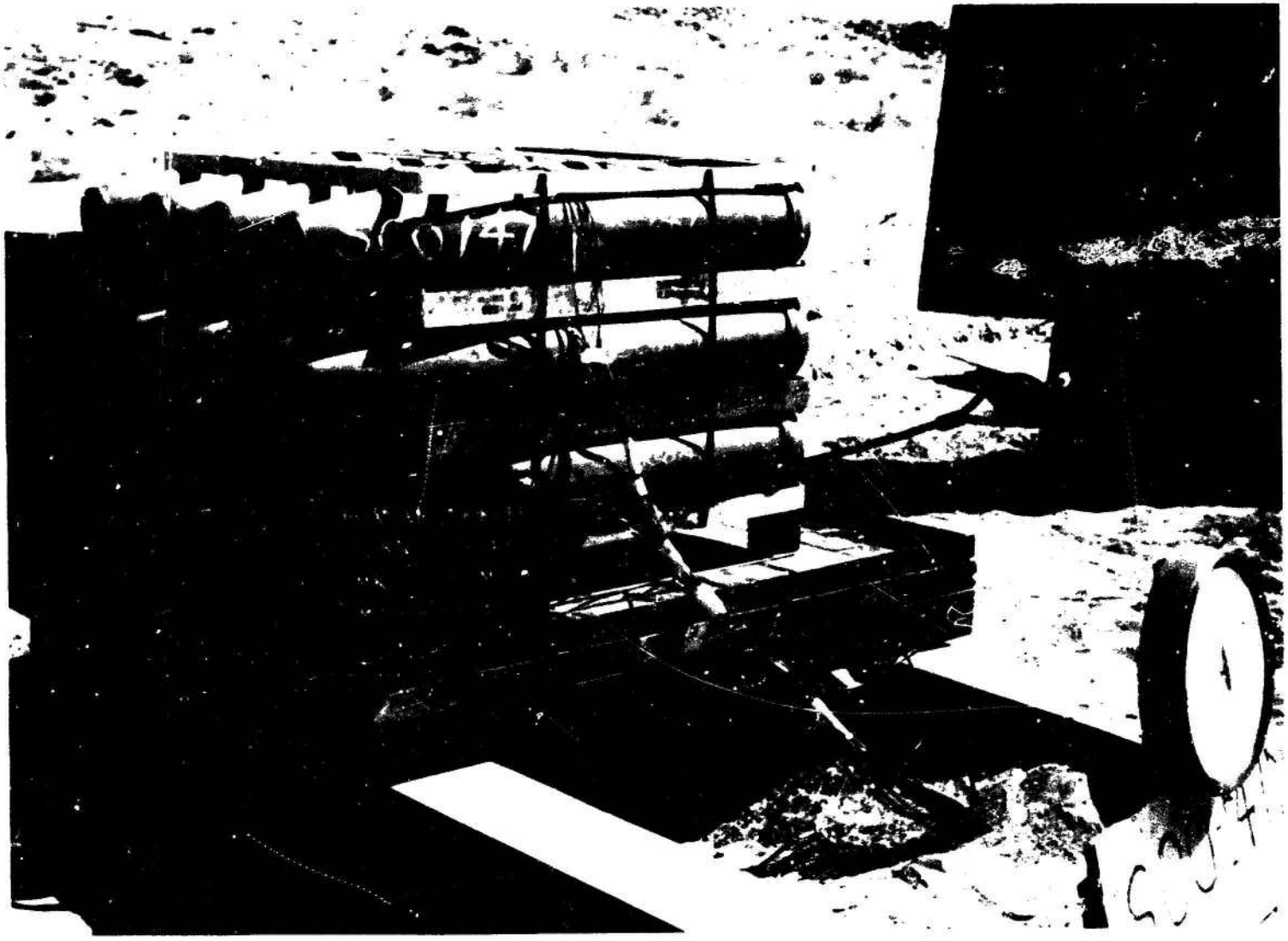

FIGURE 3. COOK-OFF TEST SETUP WITH FOUR Mk 81 BOMBS FROM ROSEVILLE INCIDENT AND EIGHT SAND-FILLED CASES

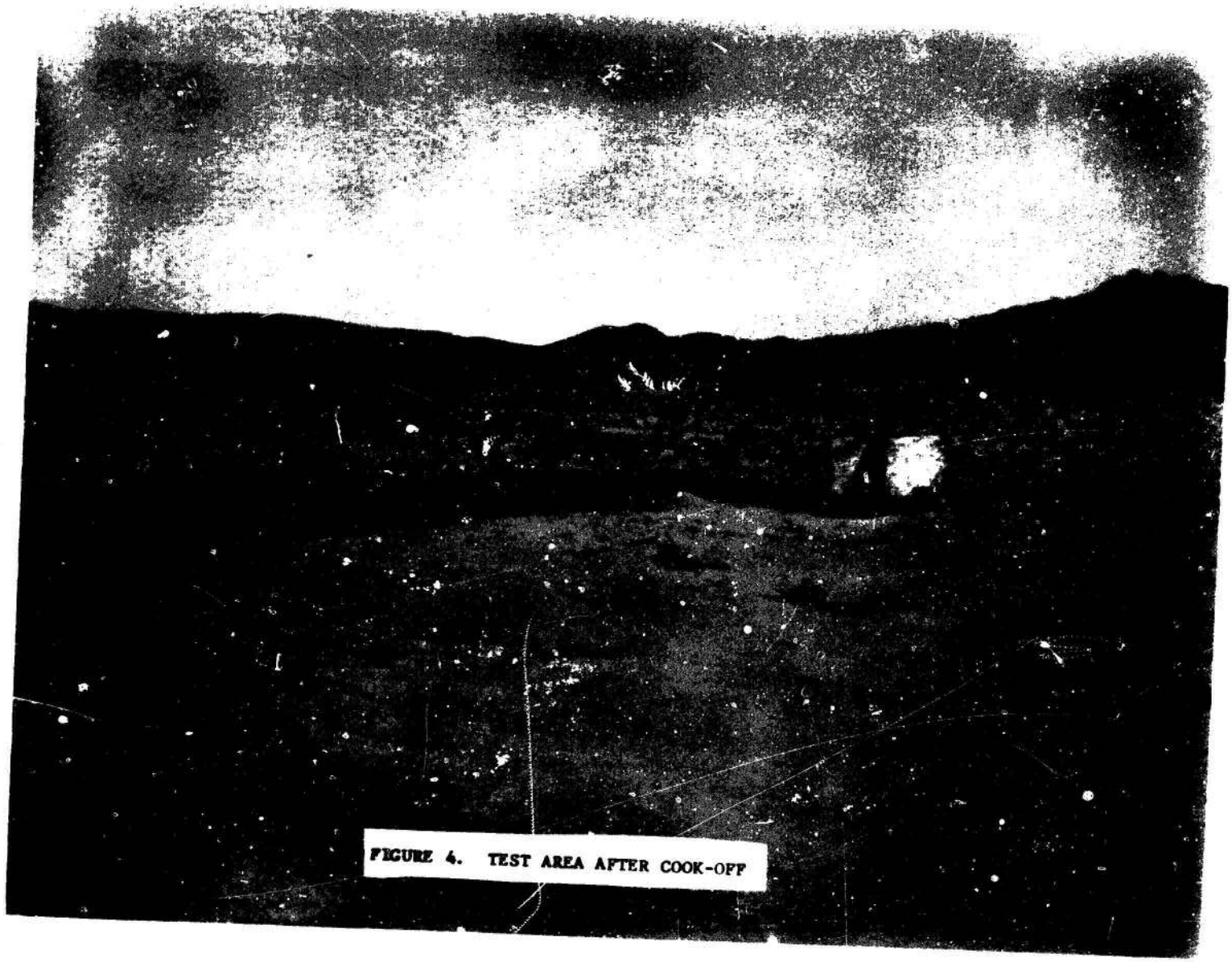

FIGURE 4. TEST AREA AFTER COOK-OFF



FIGURE 5. TEST AREA AFTER COOK-OFF OF BOMBS FILLED WITH PBXC116

PBX SENSITIVITY TEST RESULTS

EXPLOSIVE	TEST	WARHEAD	RESULTS
PBXC-116	50 CAL. BULLET IMPACT	CONFINED IN STEEL PIPE	30/30 NO REACTION
PBXN-106	50 CAL. BULLET IMPACT	CONFINED IN STEEL PIPE	9/12 SOME EXPLOSIVE BURNED
PBXN-106	TARGET IMPACT SENSITIVITY	MK82 BOMB	IMPACT AT 660 TO 1,180 FT/SEC REINFORCED CONCRETE 8/8 NO REACT-IONS
PBXW-107	TARGET IMPACT SENSITIVITY	MK82 BOMB	SAME AS ABOVE 4/4 NO REACTION

DETERMINATION OF SAFE SEPARATION DISTANCES FOR EXPLOSIVES AND PROPELLANTS IN SELECTED MANUFACTURING OPERATIONS

by

J. W. Gehring
A. B. Wenzel
J. Friesenhahn
Southwest Research Institute

Wm. O. Seals
ARRADCOM

for

Department of Defense Explosives Safety Seminar
September 12-14, 1978

ARRADCOM - Contract No. DAAA21-76-C-0255

ABSTRACT

In support of the U. S. Army Plant Modernization Program and with the guidance of the ARRADCOM, Manufacturing Technology Division, SwRI has conducted a number of full-scale tests to determine the safe separation distances to prevent explosive propagation. These tests simulated the operating conditions and confining environments in selected in-plant procedures where, because of production requirements or equipment constraints, intralined distances had to be held to an absolute minimum consistent with safety regulations. In parallel with the full-scale tests, analytical techniques were used to substantiate the experimental evidence and to indicate how these results could be applied to other critical situations in new production plant designs.

The paper will discuss the results of the experimental test firings and the methods to analytically predict safe separation distances for the operations which have been examined. Values of minimum safe separation distances will be given for ten in-plant processes as noted in Figure 1.

LIST OF FIGURES

FIGURE NO.	
1	LISTING OF SAFE SEPARATION TESTS
2	TYPICAL BLAST PRESSURE VS DISTANCE PLOTS
3	FLOW DIAGRAM FOR DETERMINING SAFE SEPARATION DISTANCE OF CASED CHARGES
4	SIDE VIEW OF 15 m TUNNEL
5	VIEW OF 120 m REINFORCED TUNNEL
6	76 kg OF COMPOSITION A-7 IN TOTE BIN ON ROLLER CONVEYOR
7	ACCEPTOR TOTE BIN SURROUNDED BY CELOTEX WITNESS SHEETS IN TUNNEL CONFINEMENT
8	VIEW OF TUNNEL DAMAGE AFTER SHOCK Note Acceptor Tote Bin Survived Blast
9	SAFE SEPARATION TESTS OF CARDBOARD BOXED CYCLOTOL IN TUNNEL CONFINEMENT
10	VIEW OF ACCEPTOR BOX OF CYCLOTOL AFTER HAVING SURVIVED DETONATION OF DONOR BOX
11	7075-T6 ALUMINUM BOXED CYCLOTOL ON SIMULATED PENDANT CONVEYOR
12	OVERALL VIEW OF DONOR AND TWO ACCEPTOR BOXES OF CYCLOTOL WITH NO CONFINEMENT
13	M-1 PROPELLANT IN 68 kg FIBER DRUMS ON SIMULATED CONVEYOR
14	REMAINS OF M-1 DRUMS AFTER TEST Note That Both Acceptor Drums Burned and That Tunnel Was Not Damaged
15	SAFE SEPARATION TESTS OF THE COMPLETE BLU BOMBLET Note C-4 Charge to Detonate Donor Bomblet
16	SAFE SEPARATION TESTS OF BLU HEMISPHERES ON LOOSE CANVAS CONVEYOR

LIST OF FIGURES (Cont.)

FIGURE NO.

17 SAFE SEPARATION TESTS OF BLU HEMISPHERES IN HOLDING FIXTURE

18 DAMAGED, BUT NOT DETONATED, BLU BOMBLET AFTER TEST

19 VIEW OF BLU BOMBLET POURING TRAY AFTER SAFE SEPARATION TEST

20 SAFE SEPARATION TESTS OF SHIPPING DRUMS CONTAINING 2.3 kg OF M-10 PROPELLANT
Note That Donor Drum Has Burned Without Damage to Acceptor Drums

21 M-10 FEED HOPPER IN TEST STAND

22 VIEW OF TWO HOPPERS AFTER CRITICAL HEIGHT TESTS
Note Different Degrees of Damage to the Hopper Base

23 81 mm MORTAR INCREMENTS IN HOLDING FIXTURES
Note That Donor Increment Has Burned Without Damage to Acceptors

24 25 CENTER CORE IGNITERS IN PLASTIC TOTE BIN

25 TOTE BINS OF BOXED IGNITERS ON DUAL CONVEYOR SYSTEM
Note Single Line Water Deluge System to Protect Acceptor Tote Bins From Extraneous Fires

26 SUMMARY OF SAFE SEPARATION AND CRITICAL HEIGHT TEST RESULTS

FIGURE 1

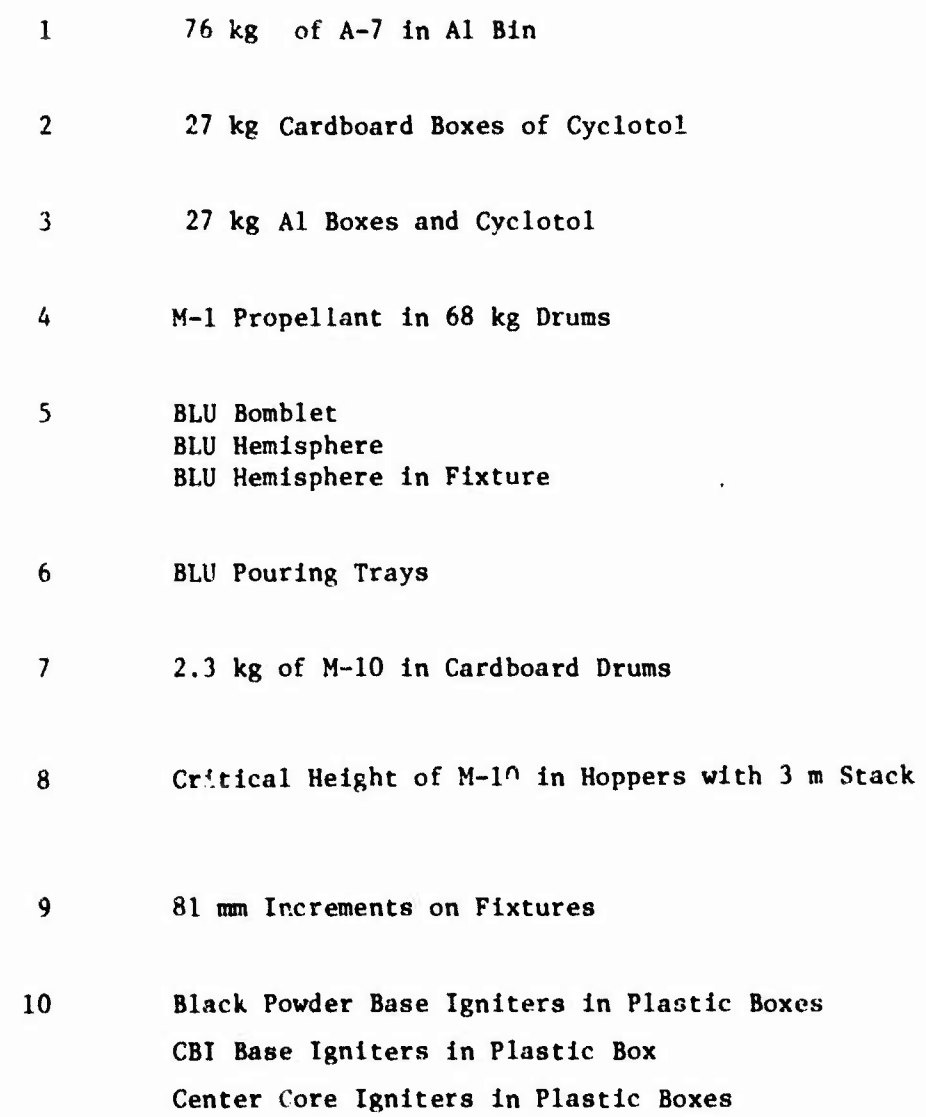
1
76 kg of A-7 in Al Bin
2
27 kg Cardboard Boxes of Cyclotol
3
27 kg Al Boxes and Cyclotol
4
M-1 Propellant in 68 kg Drums
5
BLU Bomblet
BLU Hemisphere
BLU Hemisphere in Fixture
6
BLU Pouring Trays
7
2.3 kg of M-10 in Cardboard Drums
8
Critical Height of M-10 in Hoppers with 3 m Stack
9
81 mm Increments on Fixtures
10
Black Powder Base Igniters in Plastic Boxes
CBI Base Igniters in Plastic Box
Center Core Igniters in Plastic Boxes

I. INTRODUCTION

This paper describes a series of full-scale test evaluations which was conducted in support of the U.S. Army Plant Modernization Program and the activities of the Lone Star, Kansas, Iowa, Milan and Indiana Army Ammunition Plants. The tests were performed under the guidance of the Manufacturing Technology Division of ARRADCOM, Dover, New Jersey, and were aimed at determining critical design criteria for plants currently undergoing either extensive modification or the construction of totally new manufacturing plants.

The questions to be answered by the test series centered on the determination of whether these manufacturing activities can be controlled or limited such that a major detonation will not propagate to adjacent activities; and, should a fire be ignited at any point in the process activities, can this fire be controlled through either limitation of the safe separation distance and/or application of a water deluge system to extinguish extraneous fires. It was most important that a determination be made of the hazard classification of these activities and that some prediction be made of the extent of damage should a detonation occur, since extensive modification would have to be made to the existing facilities and/or construction plans if these operations remained a Class 1.1 explosive operation as opposed to the much less hazardous Class 1.3 operation.

The series of tests was conducted to evaluate specific processing operations in which a detonation or fire could conceivably result in major property damage and even loss of human life. The test series spanned a broad spectrum of in-plant activities ranging from the determination of the safe separation of tote bins carrying A7 explosive from the receiving building to the shell-loading facility. In this activity each tote bin contained 76 kg of A7 explosive which is extremely vulnerable to ignition by either detonation or shock. In succeeding tests, safe separation distances were evaluated for cardboard

boxes containing 27 kg of Cyclotol explosive and for a similar quantity of Cyclotol after it has been transferred to metal boxes and is being transported on a pendant conveyor. Each of the above tests represented a severe explosive environment should a detonation occur in any of these transport boxes. Other tests of a less severe nature, were conducted to determine the safe separation of M-1 propellant shipping barrels, the pouring and transporting of the BLU Bomblets through the in-plant assembly operations, the loading of M-10 propellant into 81 mm mortar increments, and the transport of boxed igniter charges for loading into the 200 mm (8-in.) and 155 mm propelling charges.

As a safety measure, each of these in-plant activities is normally conducted in buildings which are separated by some physical separation distance. This distance is designed such that a detonation or fire event in one building should not be propagated to any adjacent building. This same philosophy is applied to operations within any single building. Each activity is normally separated by a blast wall or is conducted at a sufficiently distant point such that propagation should not occur as a result of a single event. These distances, however, must be established for each activity and in an environment which simulates the potential confinement of that specific operation. Each processing activity is, however, connected by either a tunnel ramp conveyor system between buildings or an intrabuilding conveyor which transports the inprocess materials from activity to the next. It is along these conveyor systems and tunnel ramps that propagation is most likely to occur. Also, in establishing these safe separation distances, minimum distances are always of vital importance since greater separations would require more real estate, additional building costs, and a slowing of the production process. Therefore, in making the safe separation determinations the test director is always seeking means to either dissipate the blast effects or lessen the fragment hazard.

The tests to be described in this paper resulted in several suggestions enabling the reduction of some safe separation distances. Typical of these suggestions was the recommendation to use 7075-T6 aluminum as the tote bin material because this alloy is brittle, and will fragment into smaller pieces, each of which will have less mass than their steel counterparts. The velocity of small lightweight fragments is reduced appreciably through air and is , therefore, of less hazard to adjacent tote bins for manufacturing operations. Also, it was determined that a tunnel ramp did indeed offer blast confinement which did contribute to the focusing of fragments down the tunnel thus increasing minimum safe separation distances. In the case of propellant transporting systems,it was determined that by controlling the size of the shipping containers a transition from deflagration to detonation could be prevented; and, should a fire occur, that fire could be extinguished by the use of a water deluge system.

II. SAFE SEPARATION-ANALYTICAL APPROACH

Two approaches are possible for determining minimum safe separation distances for in-plant operations of an explosive material. The first of these is to determine the safe separation distance through a purely analytical approach using the relationships that have been established by many investigators over recent years. The second and often the only totally acceptable method is through the conduct of full-scale tests in the simulated in-plant environment. The analytical approach is most valid under simplistic conditions where the evaluation is made of the blast and fragment hazard generated by a single detonating charge in an open environment. Manufacturing operations are, however, always encumbered by process machinery, each of which is engulfed in a nearby explosion and contributes secondary fragments to the hazard problem. Many times, therefore, it is difficult to depend on a strictly analytical approach when the process activity is confined by such things as steel roller conveyors, operating machinery, tunnel ramp walls or building walls, and even more important operating personnel. To evaluate the

in-plant processes addressed in this paper, an analytical approach was used to approximate the minimum safe separation distance and then full-scale tests were conducted to clearly demonstrate that safe separation distances had been established.

To determine the safe separation distance on an analytical basis, one first looks at the fireball and pure blast pressures generated by the detonation of a quantity of high explosive in question. For purposes of brevity in this paper, the reader is simply referred to Reference No. 1, a reference which deals in detail with the behavior of a detonation front as it expands through free air. The air shock generated by a quantity of high explosive falls off in pressure exponentially as the standoff distance is increased. For reference, a blast pressure versus distance plot is given in Figure 2, for four different weights of TNT at distances ranging from 1.22 to 122 meters from the point of detonation. From these plots and others given in Reference 1, one can estimate that the fireball emanating from an explosive blast will propagate not much more than about 3 meters and that the pressure pulse is significantly reduced by separation distances ranging from 3 to 30 meters. For the most part, therefore, it is possible to rule out the propagation of a detonation from a donor charge to an acceptor charge as being due to fewer impulsive loading or to adiabatic heating. Attention is therefore directed more to establishing a methodology for determining the safe separation distance in a fragment environment, fragments which are generated either from the shell casing or secondary fragments picked up from the adjacent environment. This methodology has been established and is presented in Figures 3a through 3c and is based upon the relationships which were established in References 2 through 5. The methodology consists of determining the size and velocity of a typical fragment through the use of the Gurney equations and then estimating the vulnerability of an adjacent acceptor charge to a fragment of this predicted mass and velocity. The methodology then proceeds through a process whereby the thickness of a shield

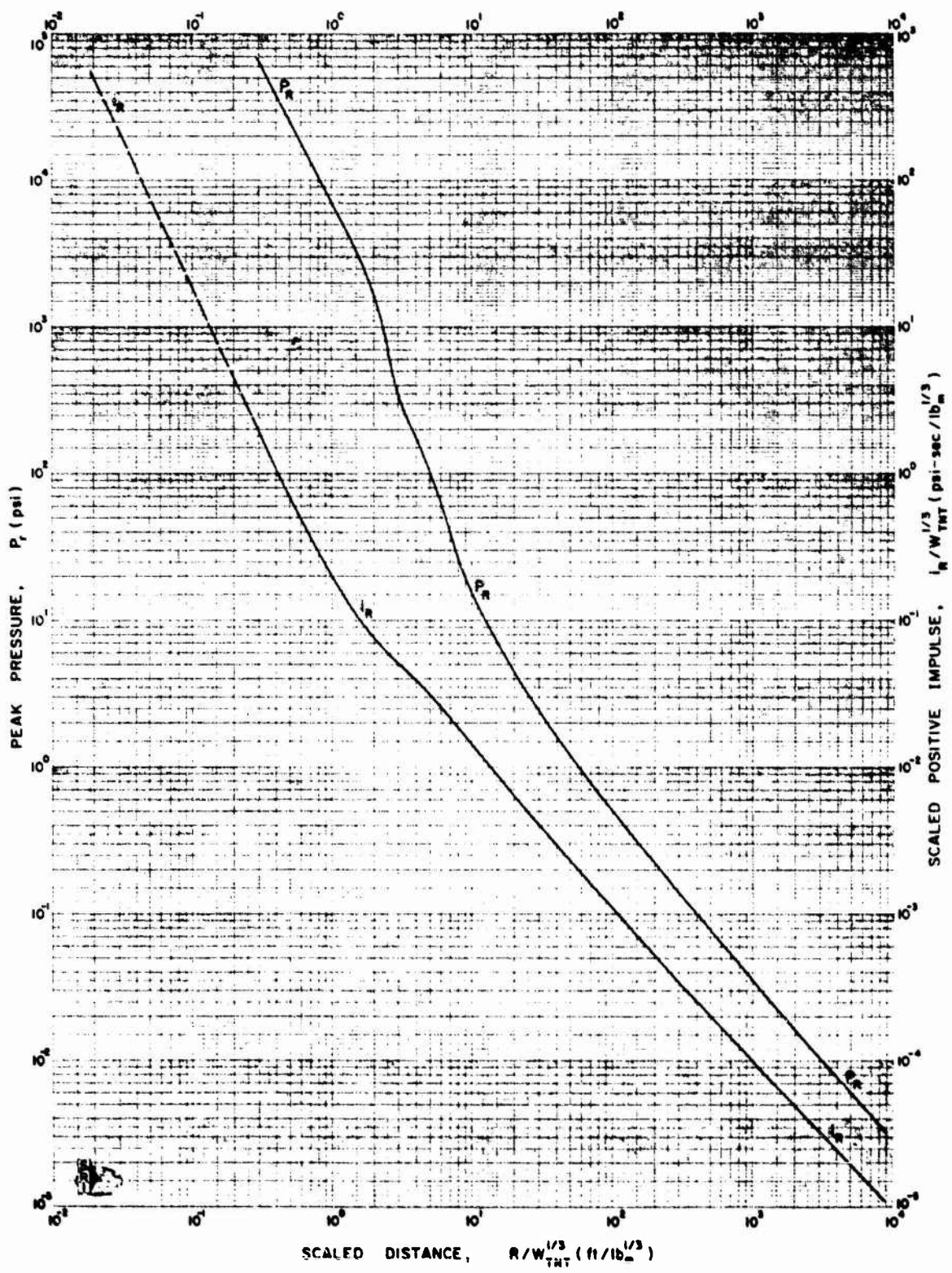

FIGURE 2. BLAST PRESSURE VS. SCALED DISTANCE

FLOW DIAGRAM FOR DETERMINING SAFE SEPARATION DISTANCE OF CASED CHARGES

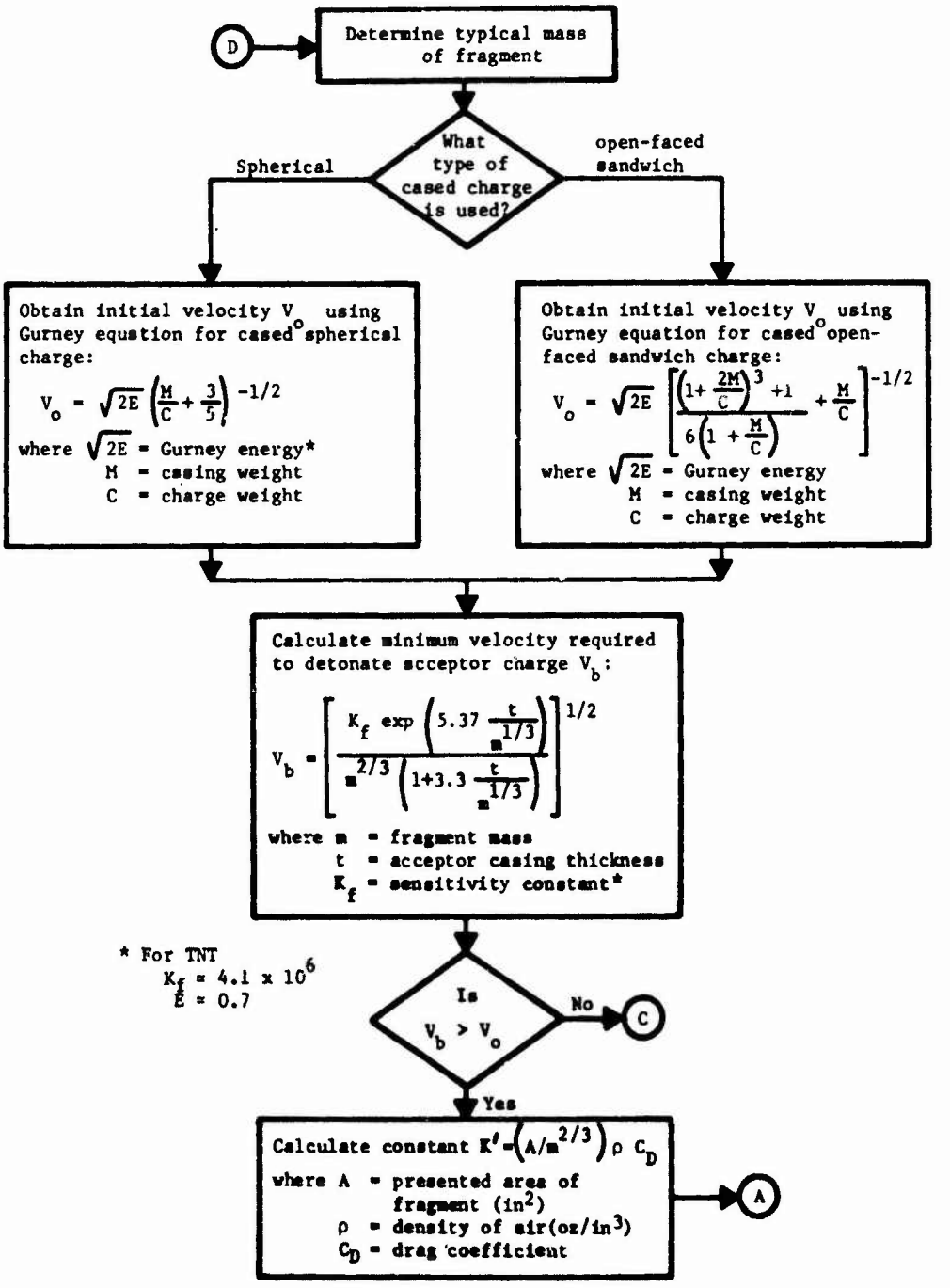

FIGURE 3a

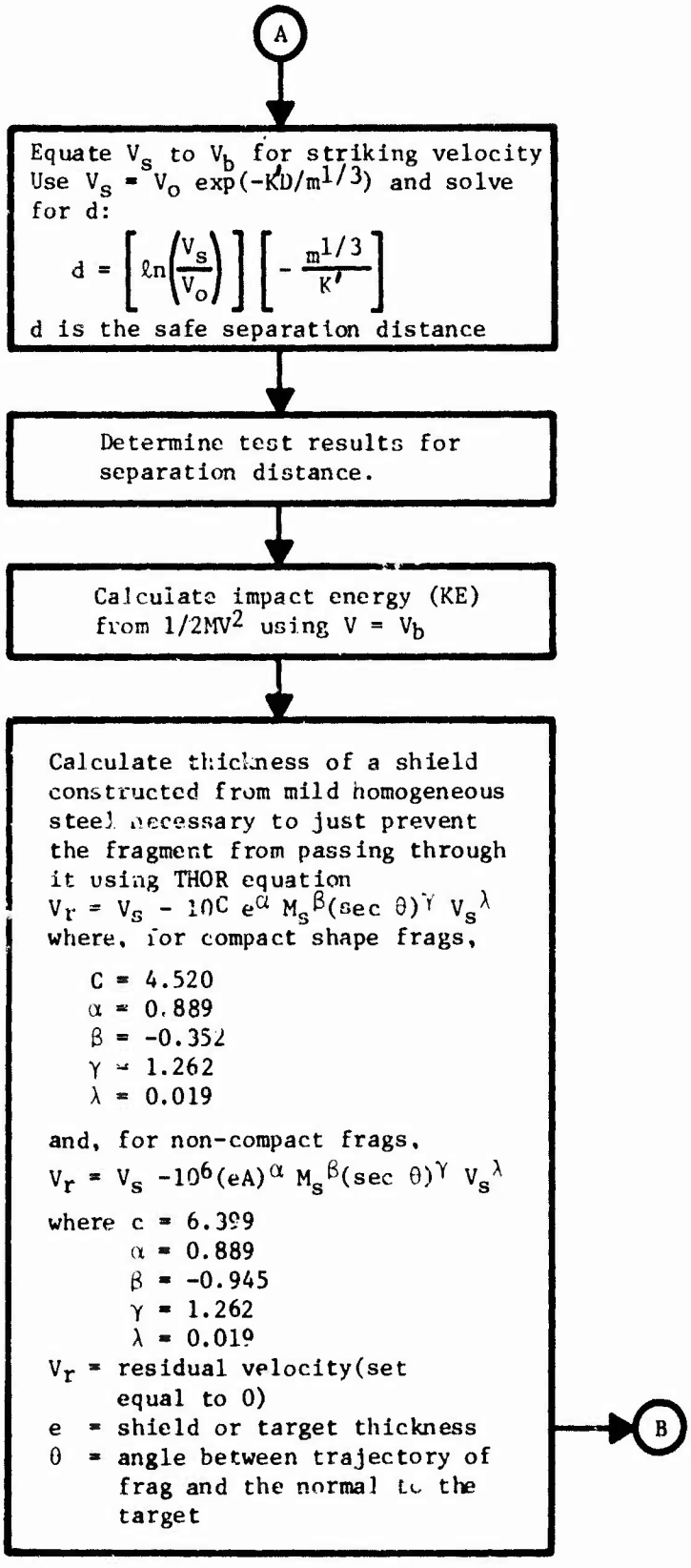
A
Equate V_s to V_b for striking velocity
Use $V_s = V_o \exp(-KD/m^{1/3})$ and solve for d:
$d = \left[\ln\left(\frac{V_s}{V_o}\right)\right]\left[-\frac{m^{1/3}}{K'}\right]$
d is the safe separation distance
Determine test results for separation distance.
Calculate impact energy (KE) from $1/2MV^2$ using $V = V_b$
Calculate thickness of a shield constructed from mild homogeneous steel necessary to just prevent the fragment from passing through it using THOR equation
$V_r = V_s - 10C\, e^{\alpha} M_s^{\beta} (\sec\theta)^{\gamma} V_s^{\lambda}$
where, for compact shape frags,
C = 4.520
α = 0.889
β = -0.352
γ = 1.262
λ = 0.019
and, for non-compact frags,
$V_r = V_s - 10^6 (eA)^{\alpha} M_s^{\beta} (\sec\theta)^{\gamma} V_s^{\lambda}$
where c = 6.399
α = 0.889
β = -0.945
γ = 1.262
λ = 0.019
V_r = residual velocity(set equal to 0)
e = shield or target thickness
θ = angle between trajectory of frag and the normal to the target
B

FIGURE 3b

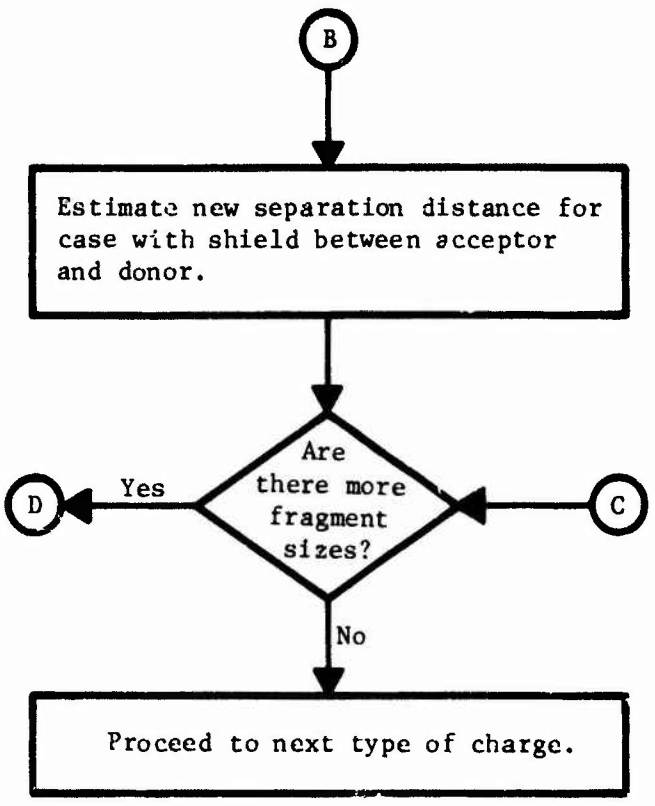
B
Estimate new separation distance for case with shield between acceptor and donor.
Are there more fragment sizes?
Yes
D
C
No
Proceed to next type of charge.

FIGURE 3c

can be determined to prevent propagation to an adjacent acceptor charge. This "shield" could, of course, be the adjacent shell casing or the transport container for the high explosive.

To determine the effects of confinement on the propagation of blast and fragments from a detonating explosive charge, a different procedure was followed which is described in detail in References 6 and 7. That procedure will not be presented in this paper, however, it was demonstrated that the shock front moving away from a detonating charge could be reflected from the walls of any nearby confinement (i.e., tunnel ramp) and that this shock front could act to focus fragments in a preferred direction along a process line.

In closing, these procedures permit the estimation of safe separation distances and establish guidelines for the conduct of full-scale safe separation tests. The analytical determination of the approximate safe separation distance is also of importance in minimizing the required number of expensive full-scale test firings required to demonstrate the safe separation distance to the satisfaction of the plant designer.

III. SAFE SEPARATION - TESTS AND TEST RESULTS

For purposes of brevity in this presentation, let us consider two basic problems and view typical test set-ups. The first of these generic problems is the establishment of safe separation distances between explosive materials as they are being transported through a tunnel ramp between buildings which separate the process activities. In Figure 4, a side view is given of a typical 15 m long segment of a conveyor system passing through a tunnel ramp. These tunnels are normally constructed only for weather protection and are deliberately made of lightweight (frangible) construction. The ramp shown in Figure 4 is constructed atop a concrete slab and is fabricated of 3.8 cm angle iron frames overlaid with aluminum siding. Another ramp configuration seen in Figure 5 is a reinforced structure fabricated of



FIGURE 4. SIDE VIEW OF 15 m TUNNEL

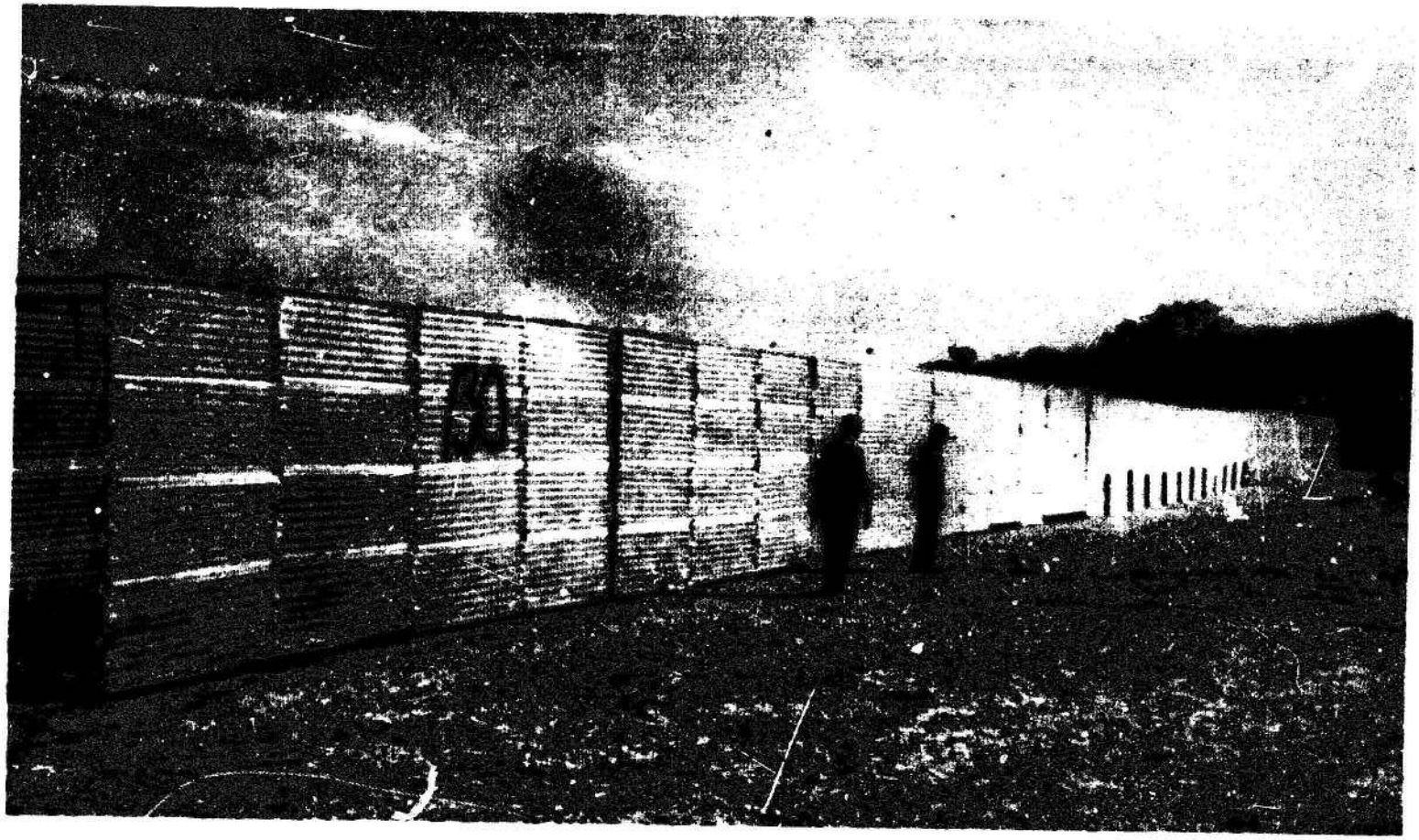

FIGURE 5. VIEW OF 120 m REINFORCED TUNNEL

7.6 cm angle iron, Transite siding and riveted fiberglass panels, and staked into the ground to simulate confining support. This structure is more typical of that used in the more severe weather climates and, for our tests, was used for the evaluation of safe separation distances between tote bins conveying 76 kg of A-7 explosive. This tote bin resting on a steel roller conveyor can be seen in Figure 6 and the acceptor tote bin placed 39 m down the tunnel from the acceptor is seen in Figure 7. The acceptor tote bin shown here is surrounded with wallboard witness material which was used to measure fragment size distribution and velocity should any fragments arrive at the far end of the tunnel. In Figure 8, the aftermath of the test shot is seen wherein the donor tote bin has been detonated and caused complete destruction of the mid section of the 120 m long tunnel, yet the far end of the tunnel and the acceptor tote bin is seen not to have been detonated by the blast and fragments generated from the detonation of the acceptor.

In a series of tests, it was determined that a stainless steel box tote bin would generate sufficiently large fragments having a velocity which would cause propagation to the acceptor tote bins. When the tote bin material was changed to 7075-T6 aluminum, it was possible to reduce the minimum safe separation distance to 39.6 m, a value which was consistent with the plant design established at both the Holston and Lone Star Plants. In a series of 50 confirmatory tests (25 shots), this safe separation distance was verified.

Continuing the discussion of the establishment of safe separation distances within a tunnel ramp conveyor system, the next series of tests examined the conveyance of boxed Cyclotol, each box containing 27 kg of 70/30 Cyclotol. These tests were conducted for the cases wherein the boxed Cyclotol was contained in the cardboard receiving boxes, and for the case wherein the Cyclotol has been unpacked and transferred to metal boxes which are then conveyed on a pendant (overhead) conveyor. The cardboard boxed Cyclotol is shown in Figure 9 spaced at a distance of 3.7 m between containers and operating along a steel roller conveyor



FIGURE 6. 76 kg OF COMPOSITION A-7 IN TOTE BIN ON ROLLER CONVEYOR



FIGURE 7. ACCEPTOR TOTE BIN SURROUNDED BY CELOTEX WITNESS SHEETS IN TUNNEL CONFINEMENT



FIGURE 8. VIEW OF TUNNEL DAMAGE AFTER SHOCK NOTE ACCEPTOR TOTE BIN SURVIVED BLAST

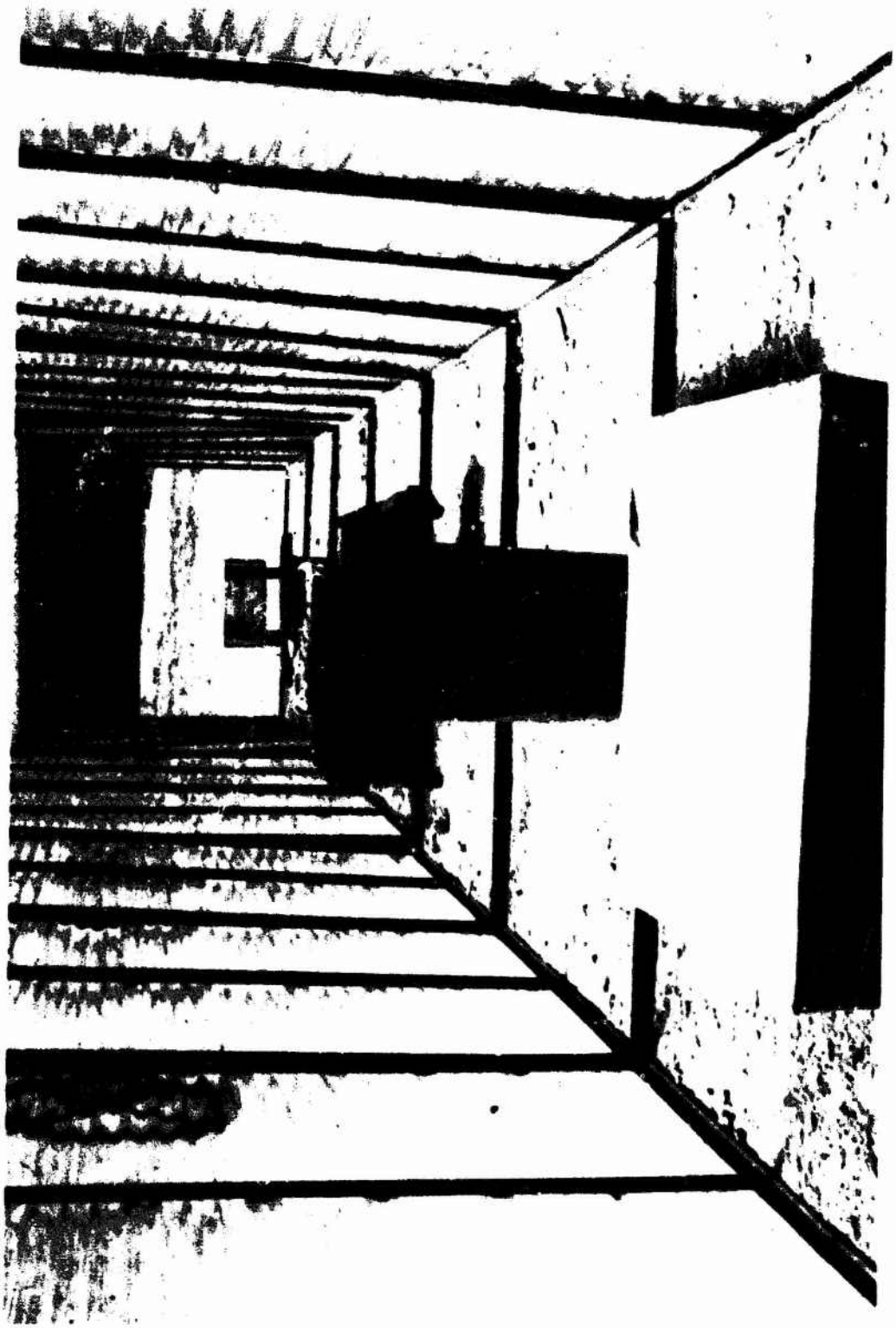

FIGURE 9. SAFE SEPARATION TESTS OF CARDBOARD BOXED CYCLOTOL IN TUNNEL CONFINEMENT

inside a lightweight tunnel. Upon detonation of the donor charge, propagation did not occur to either of the acceptors, although in some instances severe damage was felt by the acceptor box. A typical acceptor box after detonation is shown in Figure 10.

It was of particular importance at the Milan AAP and Kansas AAP that this same 3.7 m separation distance could be maintained after the Cyclotol was transferred to a metal box and conveyed on a pendant conveyor. In a series of tests using steel boxes, 6061-T6 aluminum and 7075-T6 aluminum, it was clearly demonstrated that both steel and 6061-T6 boxes would produce massive high velocity fragments and a safe separation distance in excess of 10 m would be necessary. When the tote bin material was changed to the more brittle 7075-T6 aluminum, the fragment problem was significantly reduced and the safe separation distance could be reduced to 3.7 m without propagation as shown in Figures 11 and 12. This safe separation distance was also verified through a series of confirmatory tests.

In support of the igniter bag loading operation at the Indiana Army Ammunition Plant, a series of tests was conducted to determine the minimum safe separation of large fiber drums each containing 68 kg of M-1 propellant. These drums moving along a steel roller conveyor inside a tunnel ramp configuration as seen simulated in Figure 13. Prior tests had demonstrated that this quantity of M-1 propellant contained in the fiber barrels would not transcend into a high order detonation should a fire be ignited within the barrel; hence, the problem was one of fire propagation and not of high order explosive propagation. Nonetheless, it was of extreme importance to determine a minimum safe separation to prevent this fire propagation, which is seen in Figure 14, to have propagated to each of the acceptor drums. Through the conduct of a number of full-scale test firings, the minimum safe separation to prevent fire propagation was established at 4.6 m and it was further demonstrated that the fire would cause only minimum damage to the conveyor system and tunnel walls. For these tests, however, the inside of the tunnel was lined with 15.8 mm gypsum board to shield the metal walls from the excessive heat.



FIGURE 10. VIEW OF ACCEPTOR BOX OF CYCLOTOL AFTER HAVING SURVIVED DETONATION OF DONOR BOX



FIGURE 11. 7075-T6 ALUMINUM BOXED CYCLOTOL ON SIMULATED PENDANT CONVEYOR



FIGURE 12. OVERALL VIEW OF DONOR AND TWO ACCEPTOR BOXES OF CYCLOTOL WITH NO CONFINEMENT

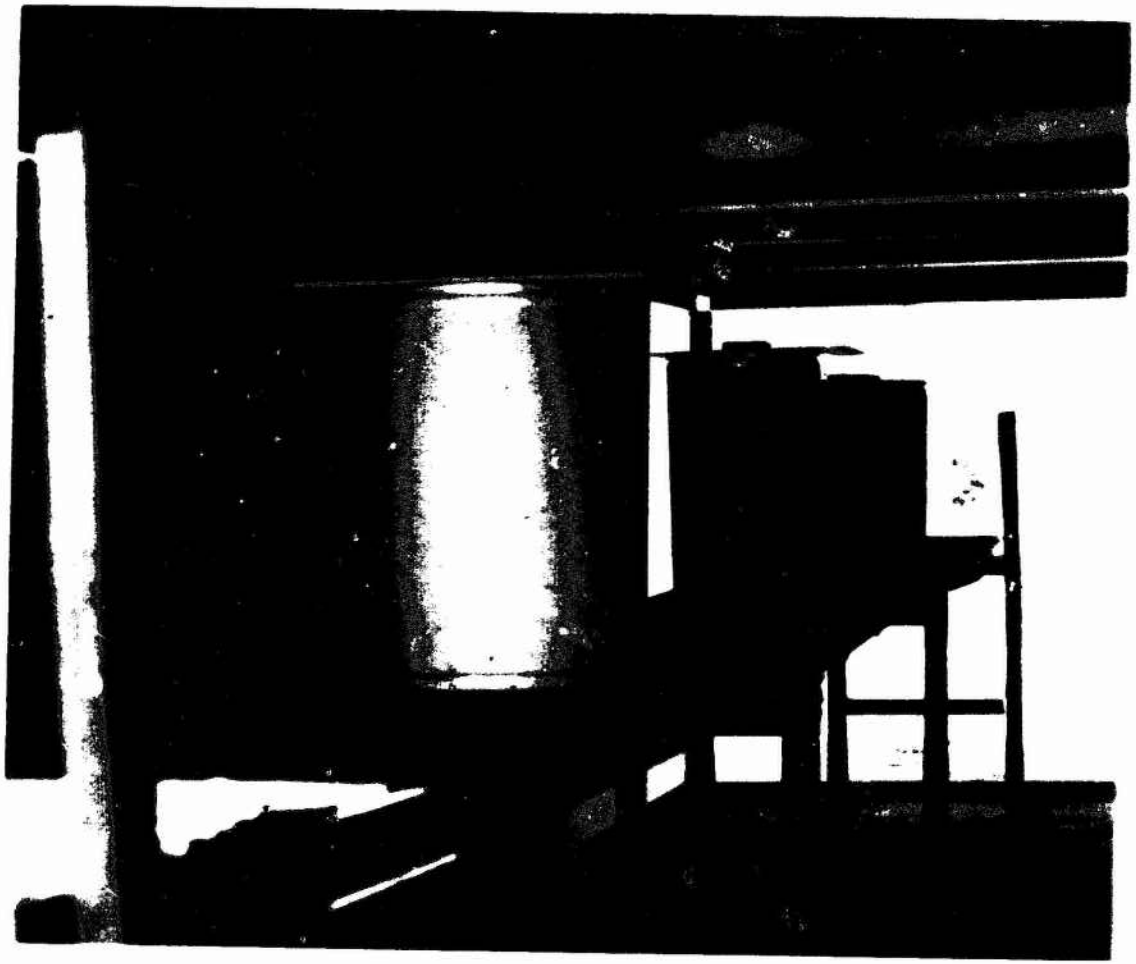

FIGURE 13. M-1 PROPELLANT IN 68 kg FIBER DRUMS ON SIMULATED CONVEYOR



FIGURE 14. REMAINS OF M-1 DRUMS AFTER TEST
Note that both Acceptor Drums burned and that tunnel was not damaged.

In support of the Milan AAP and Kansas AAP, the next series of tests concentrated on the establishment of safe separation distances during the process operation for the manufacture on the BLU Bomblets. In Figure 15 three complete BLU Bomblets are shown resting on a canvas conveyor system, the center bomblet is primed with C-4 explosive and an electric blasting cap prior to test firing. A safe separation for these bomblets was established at 25 mm, a distance which could easily be accommodated with the use of a Serpentex compartmented conveyor as opposed to the smooth canvas conveyor currently being used. This view of the complete BLU Bomblets represents the termination of the fabrication process, however, several other steps in their manufacture were also investigated. In Figure 16 the BLU hemispheres are seen on a simulated canvas conveyor and in Figure 17 those same hemispheres are seen after they have been placed in the holding fixture prior to final machining. In the final slide of this series, Figure 18, we see one of the acceptor BLU Bomblets after the test. Note that this bomblet has been completely perforated by a fragment yet detonation did not occur. The safe separation distances which were established for this test series were as follows: for the complete BLU Bomblet, 25 mm; for the BLU hemispheres loose on the canvas conveyor, 12 mm; and for the BLU hemispheres held in a test fixture, the fixtures can be touching one another without risk of propagation.

During the investigation of the safe separation distances involved in the BLU Bomblet manufacturing processes, the safe separation distances of the melt-pour trays were also studied. These melt-pour trays are an egg crate type configuration, each tray containing 16 bomblets with a high explosive riser in the amount of either 2 kg or 3.4 kg of Cyclotol. Each of these riser heights was investigated and it was found for the 3.4 kg riser case, a safe separation distance of 1.5 m was necessary whereas with only a 2 kg riser, the pouring trays could be touching one another without propagation. An acceptor pouring tray after the test is seen in Figure 19.



1589

FIGURE 15. SAFE SEPARATION TESTS OF THE COMPLETE BLU BOMBLET
Note C-4 Charge to Detonate Donor Bomblet

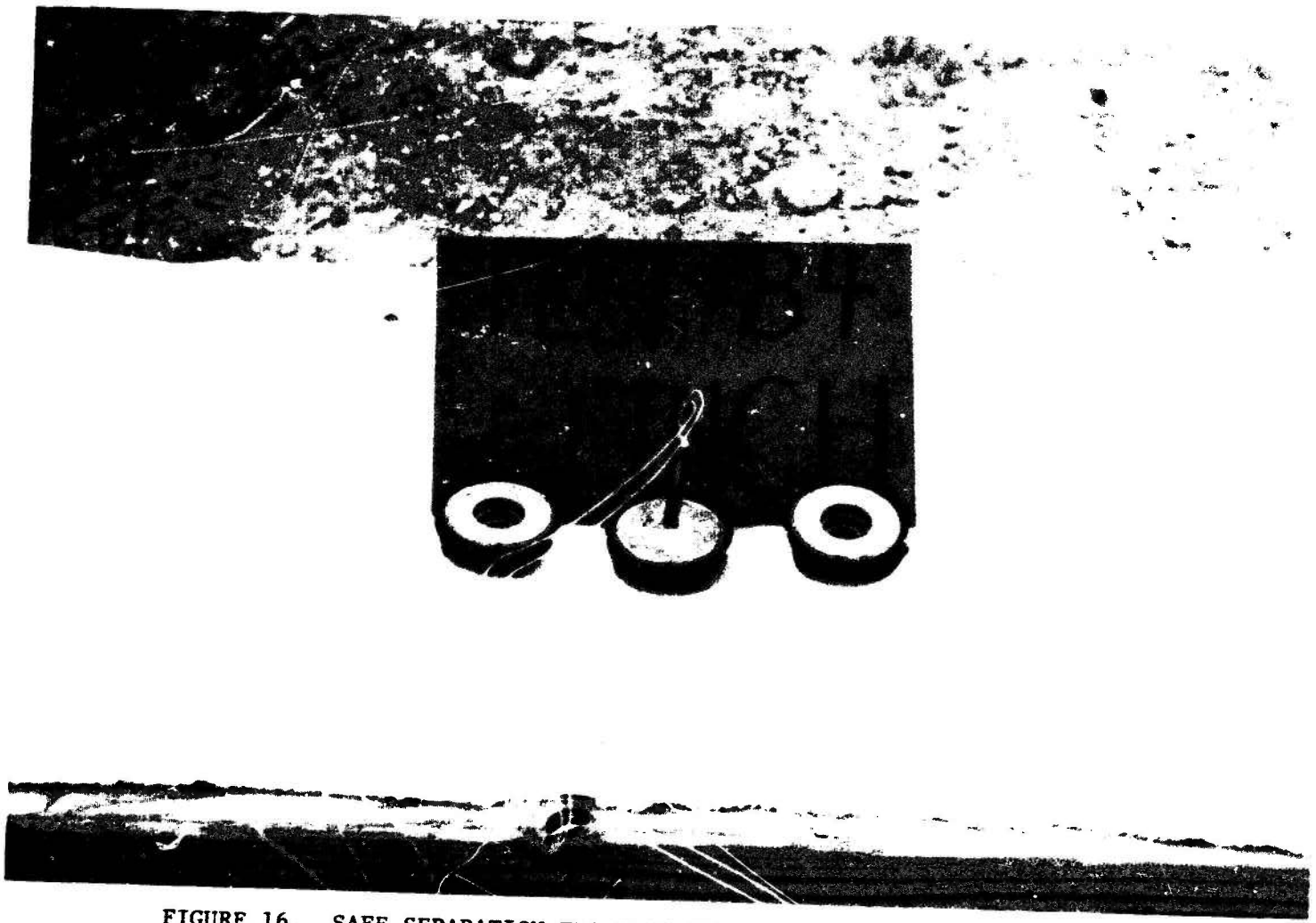

FIGURE 16. SAFE SEPARATION TESTS OF BLU HEMISPHERES ON LOOSE CANVAS CONVEYOR

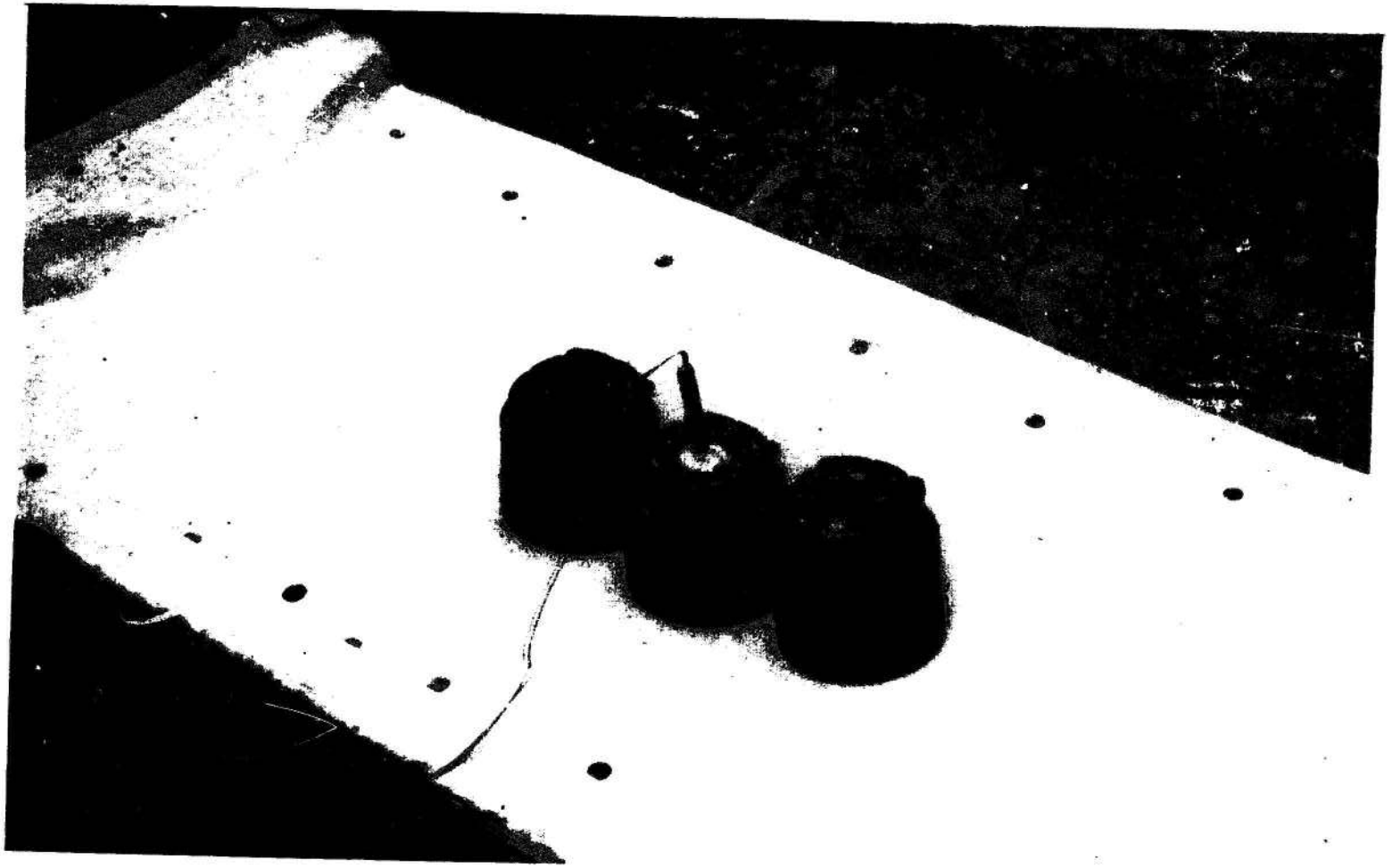

FIGURE 17. SAFE SEPARATION TESTS OF BLU HEMISPHERES IN HOLDING FIXTURE



FIGURE 18. DAMAGED, BUT NOT DETONATED, BLU BOMBLET AFTER TEST



FIGURE 19. VIEW OF BLU BOMBLET POURING TRAY AFTER SAFE SEPARATION TEST

In the next series of safe separation tests, the various processes involving M-10 propellant loading into the 81 mm mortar increments were studied. These processes ranged from the arrival of the shipping drums of M-10 propellant at the assembly site through their unloading into hoppers and finally, to the loading and processing of the 81 mm increments themselves. The first of these processes is seen in Figure 20, wherein a safe separation distance for the M-1 cardboard shipping drums, each containing 2.3 kg of propellant, were evaluated. Since the M-10 propellant burns very rapidly, a fire in the donor drum quickly consumes the propellant and with such speed that even the cardboard drum is not burned in the process. Consequently, the acceptor drums are safe even when they are touching the donor drum. In Figure 21 a processing hopper is seen in the test fixture used for a series of tests to determine the critical height of M-10 as it is offloaded into these processing hoppers. In a series of tests using hoppers as shown in this figure and also with hoppers that were fitted with a 3 m extension stack, a critical height of M-10 propellant was established at 31.8 cm. Beyond this height a fire in the M-10 propellant would transcend into a high order detonation and totally destroy the hopper. Two levels of damage are seen in Figure 22. The hopper on the left in this view contained 15 cm of propellant and the damage to the base of the hopper can be clearly seen. After the M-10 is loaded into the 81 mm mortar increments, these increments are transported along the conveyor line while held in a metal fixture. These fixtures can be seen in Figure 23. In this view, the donor increment has been burned without propagation to either acceptor increments placed on either side. It was determined in this series of tests that a minimum safe separation distance of 25.4 cm was necessary when a simple barrier was not placed between each of the holding fixtures. When a simple plywood barrier, only 10 cm in height, was placed between the fixtures, this safe separation distance can be reduced to 7.6 cm. This minimum safe separation distance was critical at the manufacturing facility in order to maintain the required production rates for this item.



FIGURE 20. SAFE SEPARATION TESTS OF SHIPPING DRUMS CONTAINING 2.3 kg of M-10 PROPELLANT. Note that Donor Drum has burned without Damage to Acceptor Drums.

1596

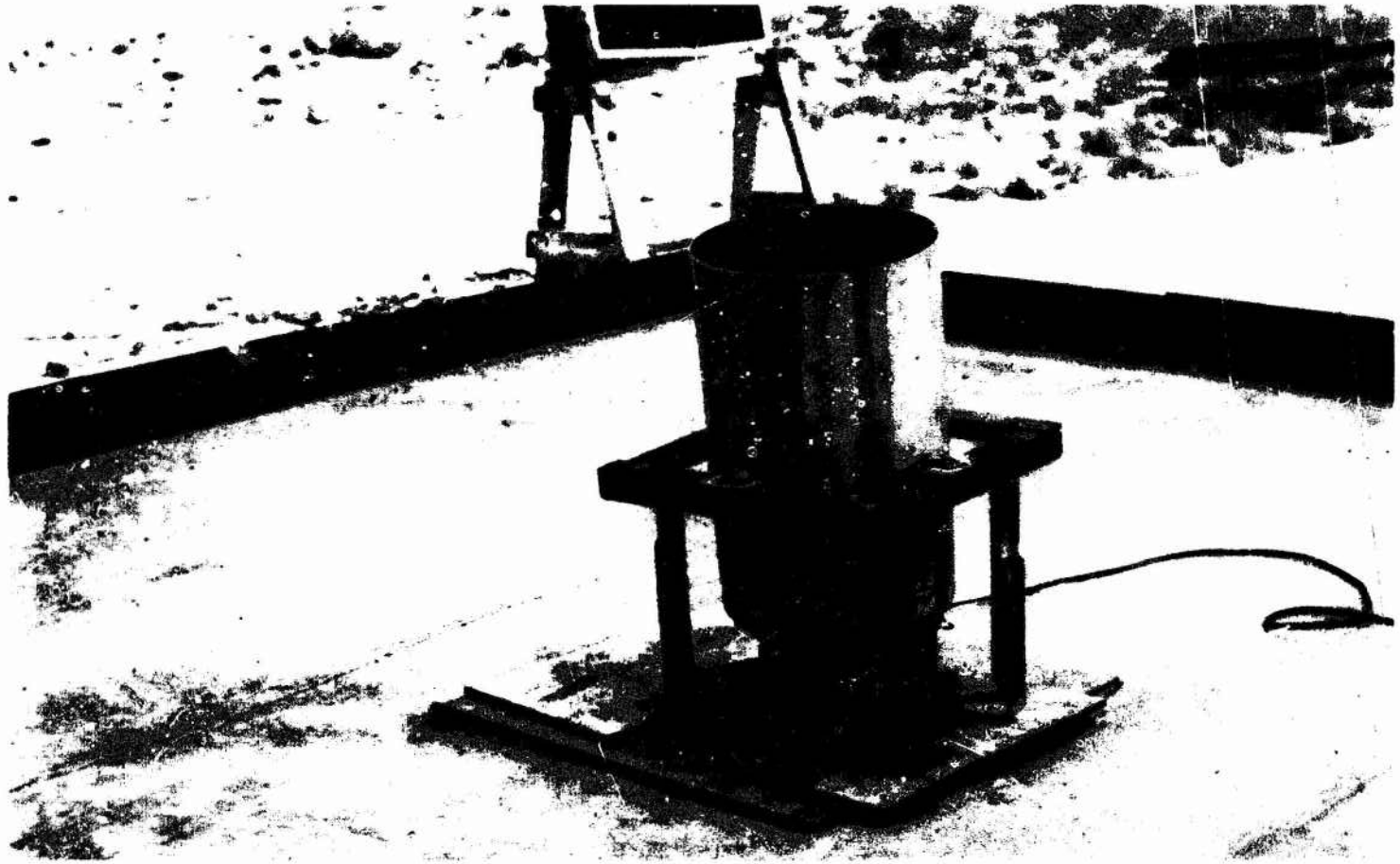

FIGURE 21. M-10 FEED HOPPER IN TEST STAND

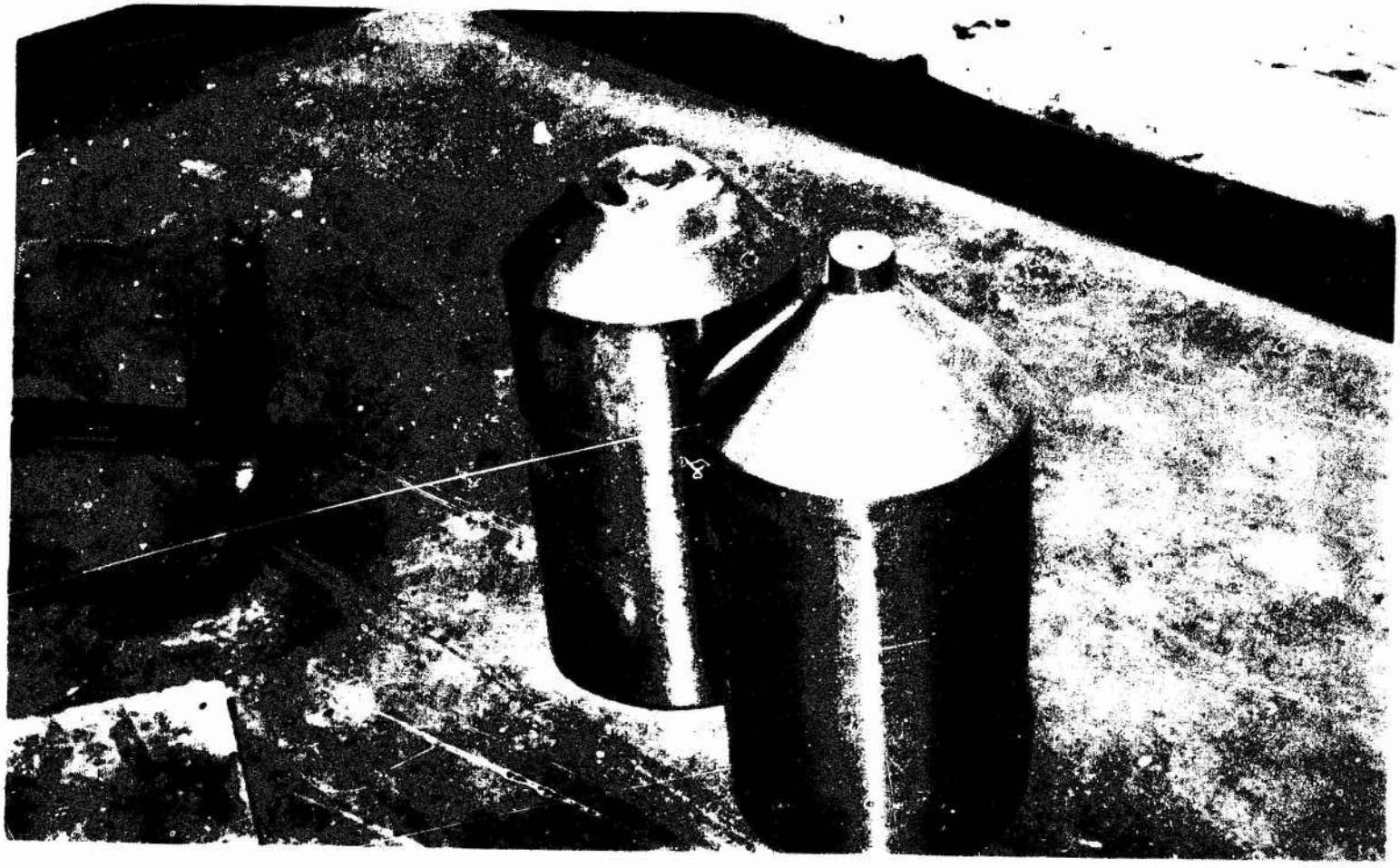

FIGURE 22. VIEW OF TWO HOPPERS AFTER CRITICAL HEIGHT TESTS
Note different degrees of damage to the hopper base.

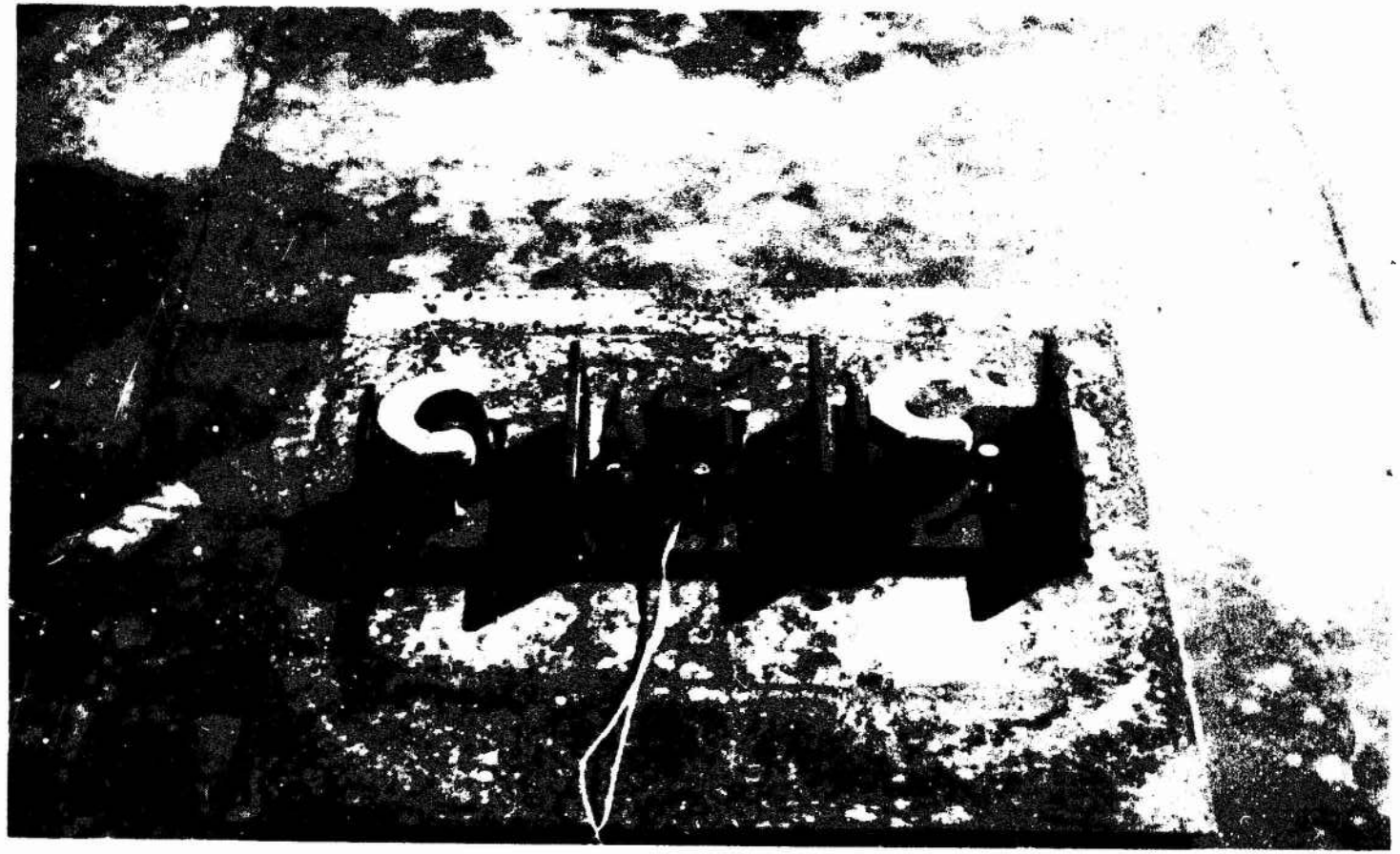

FIGURE 23. 81 mm MORTAR INCREMENTS IN HOLDING FIXTURES. Note that Donor increment has burned without damage to Acceptors.

In the last of the test series to be briefly described in this paper, was the processing of base igniter pads for eventual loading into the 155 mm or 200 mm(8-in.) Howitzer propelling charges. These igniter charges come in several varieties, the details of which will be passed over in the interests of brevity; however, each is loaded with nominally 140 grams of black powder placed in the base of a cotton sack. This cotton sack is then ultimately filled with M-1 propellant. Typical center core igniters are seen in Figure 24 and the task was to establish safe separation distances for plastic boxes containing these igniter pads. These plastic boxes containing the igniter pads pass along steel roller conveyors as seen in Figure 25. It was determined through a series of tests that boxes containing either the black powder base igniters or the center core igniters could be touching one another without fear of propagation. For the case of the igniters containing the clean burning igniter (so-called CBI) a safe separation distance of 0.3 m was necessary. In all three cases, it was also determined that due to gas generation upon ignition in any individual box, the burning bags would be ejected out of the box and strewn around the surrounding area. Should one of these burning bags fall on the lid of an adjacent box, it could eventually burn through the lid thus causing propagation. To eliminate this problem it was suggested that a water deluge system be used to extinguish these extraneous fires, and as seen in Figure 25, a single line overhead deluge system was designed to effectively combat these fires as they occurred.

IV. CONCLUSIONS

For purposes of brevity in this paper, a summary of the safe separation and critical height test results of each of the ten test series is summarized in Figure 26. As has been noted in the foregoing discussions, each of these test results and the safe separation distances which were established has been incorporated into the rapidly developing U.S. Army Modernization Program. In many instances, particularly in the establishment of a 39 m standoff for the A7 tote bins, the established

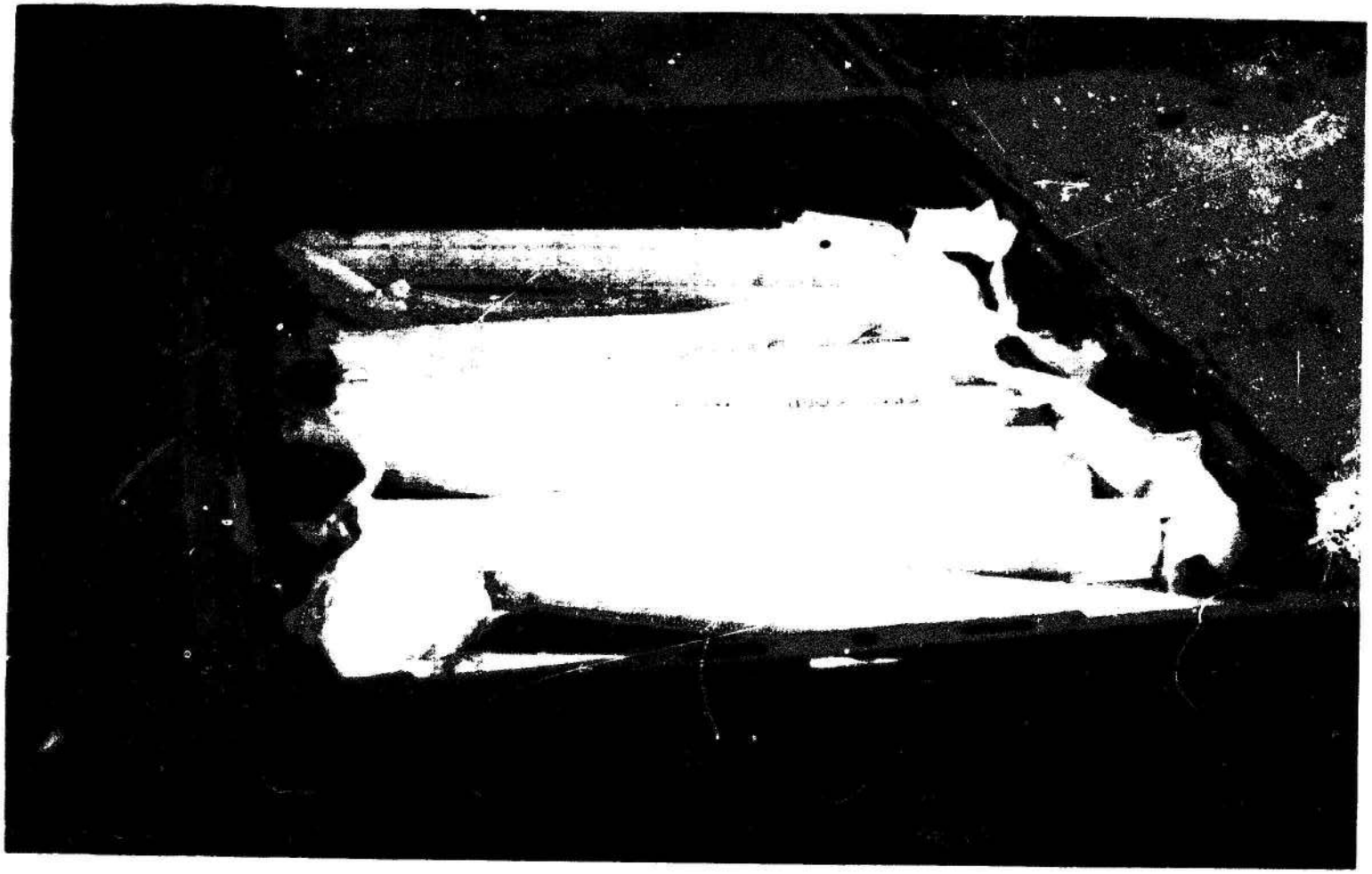

FIGURE 24. 25 CENTER CORE IGNITERS IN PLASTIC TOTE BIN



FIGURE 25. TOTE BINS OF BOXED IGNITERS ON DUAL CONVEYOR SYSTEM
Note single line water deluge system to protect
Acceptor Tote bins from extraneous fires.

FIGURE 26

Summary of Safe Separation and Critical Height Test Results

	Item	Safe Separation	Critical Hgt.
1	76 kg of A-7 in Al Bin	39.0 m	NA
2	27 kg Cardboard Boxes of Cyclotol	3.7 m	
3	27 kg Al Boxes of Cyclotol	3.7 m	
4	M-1 Propellant in 68 kg Drums	4.6*	NA
5	BLU Bomblet BLU Hemisphere BLU Hemisphere in Fixture	2.5 cm 1.2 cm Touching	
6	BLU Pouring Trays	Touching	
7	2.3 kg of M-10 in Cardboard Drums	Touching*	NA
8	Critical Hgt. of M-10 in Hoppers with 3 m Stack	NA	31.8 cm
9	81 mm Increments on Fixtures	7.6 cm w/barrier 25.4 cm w/o barrier	NA
10	Black Powder Base Igniters in Plastic Boxes	Touching*	NA
	CBI Base Igniters in Plastic Box	0.3 m*	NA
	Center Core Igniters in Plastic Boxes	Touching*	NA

*Water deluge recommended to extinguish extraneous fires

distances negated the need for additional real estate or for extensive plant modifications. Similarly, the established 3.7 m standoff for cardboard boxes of Cyclotol and a similar standoff for the aluminum boxed Cyclotol allowed the Milan AAP to use existing facilities without further modification. The recommended safe separation distances for the various BLU Bomblet assembly operations also resulted in significant savings at the Milan and Kansas AAP's. These safe separation distances, particularly in the case of the pouring trays using a 2.0 kg riser, enabled the loading plant to operate with the currently existing conveying facilities and with the currently in-use pouring trays.

Finally, the determination that the plastic boxes transporting the base igniters for the 155 mm and 200 mm (8-in.) Howitzers could be touching one another without propagation was a significant result for the Indiana AAP. The determination that a simply installed water deluge system could control and extinguish extraneous fires was a recommendation that could easily be incorporated into the plant at minimal cost and would permit the plant to maintain the production capacity required.

References

1. W. E. Baker, Explosions in Air, University of Texas Press, Austin, Texas, May 1973, pp. 150-113.

2. "Behavior and Utilization of Explosives in Engineering Design" 12th Annual Symposium - Held 2-3 March 1972, pages 116 and 117 by New Mexico Section ASME and University of New Mexico College of Engineering; Copies available from 1972 Symposium General Chairman, 2917 Dakota Street N.E., Albuquerque, New Mexico 87110.

3. Prevention and Protection Against Accidental Explosion of Munitions, Fuels, and Other Hazardous Mixtures, Annals of the New York Academy of Sciences, Vol. 152, Art. 1, pp 1-913 New York, Published by the Academy, Oct. 28, 1968.

4. Richard M. Rindner, Response of Explosives to Fragment Impact from Annals of the New York Academy of Sciences, Oct., 28, 1968, pp 250-268.

5. The Resistance of Various Metallic Materials to Perforation by Steel Fragments; Empirical Relationships for Fragment Residual Velocity and Residual Weight (U), Project Thor Technical Report No. 47, Ballistic Research Laboratories, Aberdeen Proving Ground, Maryland, April 1961.

6. A. B. Wenzel, R. M. Rindner, Determination of the Effects of Shielded Tote Bins on the Safe Separation of 168 Lb of Comp A-7 Explosive, ARLCD-CR-77012, September 1977.

7. J. W. Gehring, R. M. Rindner, W. O. Seals, Determination of Safe Separation of Aluminum Tote Bins Containing 76.2 kg of A-7 Explosive, ALRCD-CR-78021, January 1978.

HAZARD CLASSIFICATION TEST OF COMPLETE ROUND 155mm PALLETS

Harry J. Reeves

Vulnerability Survivability Division
US Army Ballistics Research Laboratory
US Armament Research and Development Command
Aberdeen Proving Ground, Maryland 21005

HAZARD CLASSIFICATION TEST OF COMPLETE ROUND 155mm PALLETS

Harry J. Reeves

Vulnerability Survivability Division
US Army Ballistics Research Laboratory
US Armament Research and Development Command
Aberdeen Proving Ground, Maryland 21005

ABSTRACT

To determine the Quantity-Distance restrictions associated with the storage of complete round pallets of 155mm ammunition requires that the potential contribution of the propellant to blast overpressures be known or estimated if the projectiles detonate en masse.

This paper presents the results of tests that were conducted to compare pressure profiles generated when the HE projectiles on a complete round pallet detonate en masse. The pallets were designed to transport and store sixteen 155mm HE projectiles, propelling charges, and fuzes. One, four, and eight pallet arrays were tested using live and inert propelling charges.

INTRODUCTION

The Ballistic Research Laboratory (BRL) in support of DEA-A-74-TN-1182 with the Dutch Government conducted a series of tests to evaluate the storage hazards associated with the use of a complete round pallet designed to transport and store sixteen rounds (HE projectiles), propelling charges, primers and fuzes) of 155mm ammunition. This effort was funded by the Joint Technical Coordinating Group For Munitions Effectiveness (JTCG/ME). Tests were conducted by the TERA Group at the New Mexico Institute of Mining and Technology.

A. Objectives

The objectives of this effort were to (1) determine the contribution of the propelling charges to blast overpressures when the HE projectiles on the complete round pallet detonate en masse, and (2) expand the data base that can be used to resolve similar problems analytically. To determine the contribution of the propelling charges to blast overpressures experimentally, field tests were conducted wherein selected HE projectiles on one, four, and eight pallet arrays (with and without propelling charges) were statically detonated. Air blast parameters measured at selected distances from the pallet (s) were then used to estimate the TNT weight equivalency of each test.

B. Background

The time required to issue ammunition to artillery units at forward area supply points can be critical in the event of a combat emergency. One means of reducing the issue time is to incorporate into the logistic system complete round palletization of separate-loading artillery ammunition (projectiles, propelling charges, primers and fuzes).

Unfortunately, storing the HE projectiles (Hazard Division 1.1) and the propelling charges (Hazard Division 1.2) in the same magazine could result in an increase in the number of magazines required to store a given number of rounds. This is a consequence of mixed Hazard Division storage regulations[1] which require that the explosive filler weight and the propellant weight be combined and the total weight be considered as Hazard Division 1.1 in determining Quantity-Distance restrictions at a storage site.

The Quantity-Distance restrictions define the minimum permissable distance between a potential explosion site containing a given quantity of explosives and inhabited buildings, public traffic routes, etc.

When the total explosive weight at a storage site is known and all the explosives detonate en masse, then the air blast parameters (peak overpressure, impulse and duration of the shock wave) at known distances from the site can be calculated using standard techniques[2,3] that have been in use for many years. Conversely, measured air blast parameters at selected distances from a detonation can be used to estimate the total explosive weight.

[1]Manual on NATO Safety Principles for the Storage of Ammunition and Explosives, 1977.

[2]C.N. Kingery, "Air Blast Parameters Versus Distance for Hemispherical TNT Surface Bursts", Ballistics Research Laboratory Report No. 1344, September 1966 (AD811673)

[3]H.J. Goodman, "Compiled Free-Air Blast Data on Bare Spherical Pentolite", Ballistic Research Laboratories Report No. 1092, February 1960 (AD235278)

SCOPE OF STUDY AND TEST PROCEDURES

A total of eight pallet tests and five calibration tests were conducted in support of this effort. The overpressure versus time history of the shock wave was recorded at twelve distances for each test.

A. Description of Pallets

In practice the sixteen complete rounds will be secured to a special pallet, see Figure 1. For test purposes the pallets were omitted in the one and four pallet simulation tests. However, pallets were used in the eight pallet tests where the pallets were stacked two high, see Figure 2. In the one and four pallet tests, see Figure 3 and 4, the projectiles and propelling charge cans were placed on a large steel plate and arranged so that geometric relationship between them was the same as if they were palletized.

All tests were conducted using M107 HE (15.4 lbs. Comp B) projectiles and propelling charge cans containing either four M4A1 (13.4 lbs. M1) propelling charges or an equal volume of inert propellant. Fuzes and primers were not required to satisfy the test objectives and were omitted.

Selected projectiles on each pallet were primed by filling their fuze wells with composition C-4 and inserting the knotted end of a length of Primacord. All Primacord leads were of equal length and were tied together at a junction point as shown in Figures 2 and 3. The junction point was connected, by a long length of Primacord, to a remotely located mechanical - electrical safety block.

In the first single pallet test only one projectile was statically detonated. In the remaining tests a multiple point initiation scheme was employed by detonating one projectile in each vertical and horizontal row. The multiple point scheme was used to minimize directional effects.

B. Test Set-Up

Two test sites were used. At each site the air blast parameters were recorded at twelve stations as shown in Figure 5. At test location "A" the distance from ground zero to the stations were kept constant while the pallet parameters were varied. At location "B" the distance from ground zero to the stations was varied from test to test in an attempt to monitor similar pressures as a function of distance and total explosive and propellant weight for each array.

C. Instrumentation

The KSP Industries Model PT-309-2 pressure transducer was used in all tests. It contains a piezoelectric sensing element which has a nominal charge sensitivity of 610 pico-coulombs per psi, and a natural frequency greater than 120 KHz.

The signals were amplified and recorded on a Consolidated Electrodynamics Corporation Model 3300 magnetic tape recorder. The system provided a data bandpass of from near zero to 20 KHz.

The tapes containing the analog data recordings were digitized at a sampling rate of 100 KHz (real time) in preparation for computer processing which yielded values of peak overpressure, arrival times, duration and impulse.

To minimize ground shock effects, the pressure transducers were flush mounted, via a Teflon collar, to aluminum blocks. The aluminum blocks were then positioned in the ground, at selected distances, and insulated from the hard rock-filled terrain by several inches of sand.

RESULTS AND OBSERVATIONS

The air blast parameters recorded at each station were used to estimate a TNT equivalent weight factor (EWF) for each test configuration. The final data form is a ratio of the EWF of pallets with live propelling charges to the EWF of pallets with inert propelling charges.

A. Air Blast Parameters

The peak overpressure (P_m), arrival time (t_a), positive duration (t_t) and positive pressure impulse (I) histories of an explosive event can all be used to estimate an EWF. However, in this series of tests only the peak overpressure and arrival time data were used. Only mean values of EWF are presented in this paper. Detailed results of all tests will be presented in a formal BRL report to be published at a later date.

The EWF in this effort is defined as the weight of a hemispherical TNT charge, detonated on the surface of the earth, required to produce the same air blast parameters that were observed for each pallet (s) configuration.

1. Peak Overpressure. The pressure versus time histories for each test were plotted and examined for quality. Approximately 15% of the records were of poor quality and rejected due to ground shock effects and fragment/debris impacts on the aluminum blocks housing the transducers. The remaining pressure time histories were used to determine the peak overpressure at each station and generate EWF's using the cube root scaling laws and the "Blast Parameters Versus Scaled Distance" table Reference 2. The average EWF based on the peak overpressures (W_p) are listed in Table I together with ratios showing the contribution of the propelling charges to blast overpressures in terms of changes in the EWF. Tests 1 and 4 were unique and not used in forming the EWF ratios.

2. Arrival Time. The pressure versus time histries were also used to measure arrival times. An EWF based on the arrival time (W_{ta}) was then calculated using the method described in Reference 4 for each station. This method involves (a) forming a ratio of the measured distance to the measured arrival time, (b) forming a ratio of the scaled distance to the scaled arrival time using the "Blast Parameters Versus Scaled Distance" table in reference 2, (c) determine the scaled distance when the two ratios are equal and (d) use cube root scaling laws to determine an EWF. The average EWF for each test are listed in Table I together with ratios showing the contribution of the propelling charges to blast overpressures.

3. Positive Duration and Impulse. The quality of the pressure versus time histories deteriorated with time in many cases due to noise, ground shock,fragment/debris impact, and what appeared to be thermal drifting. Therefore, no effort was made to estimate EWF's based on positive duration or impulse test results. These data will be provided in a formal report to be published at a later date.

B. Observations

In general, the EWF's based on arrival times (W_{ta}) were greater than the EWF's based on peak overpressures (W_p). The relatively poor agreement between the average values in Test 4 can be attributed to differences in the data base. In Test 4 a total of six data points were used in calculating W_p in contrast to eight data points for W_{ta}. The two additional points used in the W_{ta} solution were relatively high, 3500 lbs. versus an average value of 2320 lbs., and are probably the result of focusing.

[4] C.N. Kingery and W.F. Jackson, "Blast Screening Tests for the Alternate Explosive Fill Program", Ballistic Research Laboratory Memo Report No. 2236, October 1972 (AD 907354).

The results of Test 1 show that the detonation of only one projectile can lead to the en masse detonation of all the projectiles.

If it is assumed that propellant and TNT are equally effective on a weight basis in producing blast overpressures, then the equivalent weight of a pallet, in lbs. of TNT, with and without propellant can be calculated using the following formula from Reference 5:

$$W_{pallet} = W_{HE}\ KF + W_{prop}$$

Where

W_{HE} = total explosive filler weight of all sixteen projectiles.

K = conversion factor, Comp B to TNT.

F = factor given by the modified Farro formula to account for the energy expended in projectile breakup (0.635 for the 155mm projectile).

W_{prop} = total weight of all sixteen propelling charges.

Using these values the EWF's for pallets with and without propelling charges are 386.5 and 214.4 respectively. These values yield a ratio of 2.45 compared to an overall average value of 2.50 from the test data.

CONCLUSIONS

The contribution of the propelling charges to blast overpressure can be equated to TNT, on an equal weight basis, when assessing the storage hazards associated with the use of the pallet evaulated in this study.

The detonation of only one projectile in a group of pallets can result in the en masse detonation of the remaining projectiles.

No additional testing is required.

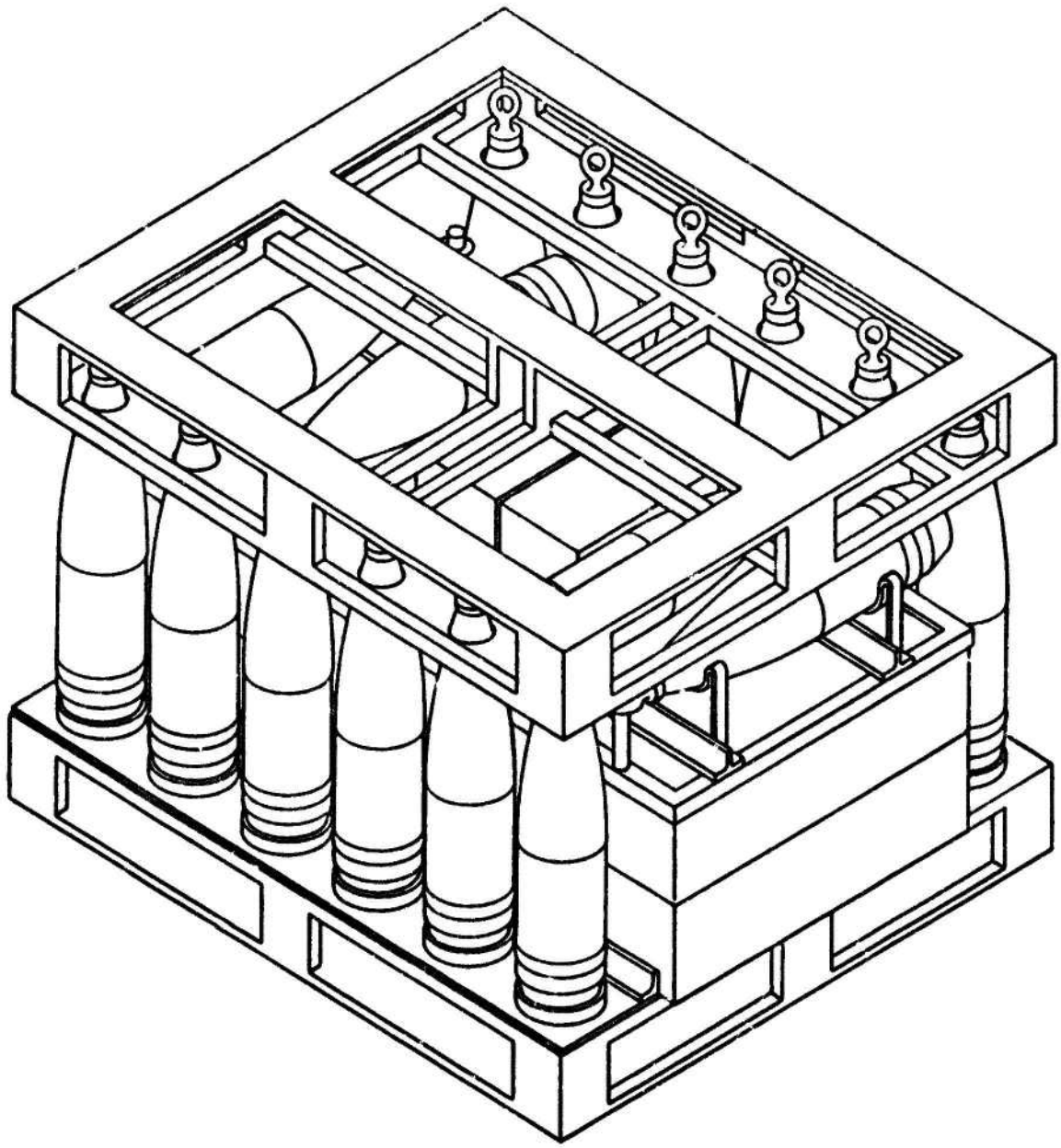

Figure 1. Complete Round Pallet For 155mm Ammunition

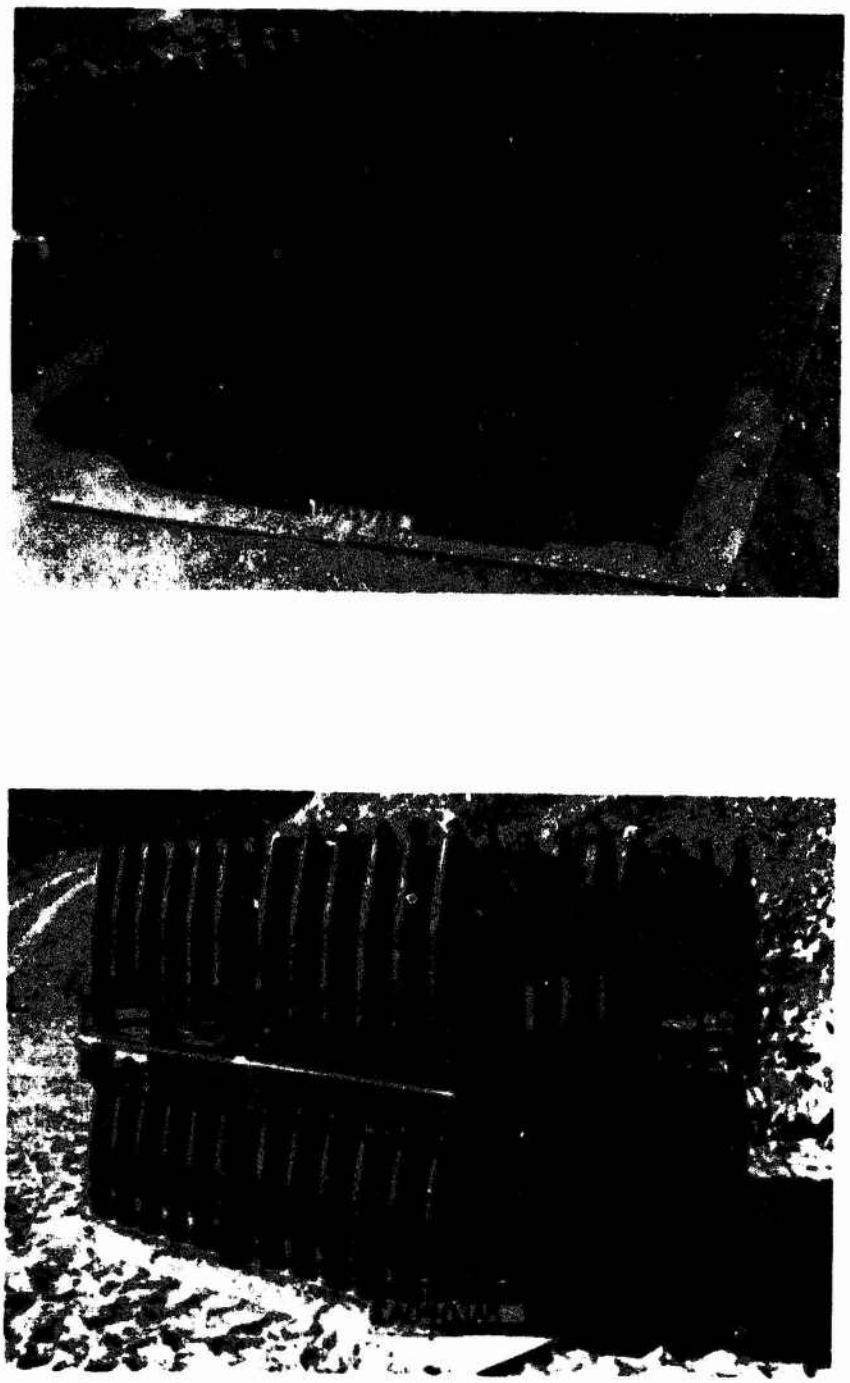

Figure 2. Eight Pallet Array

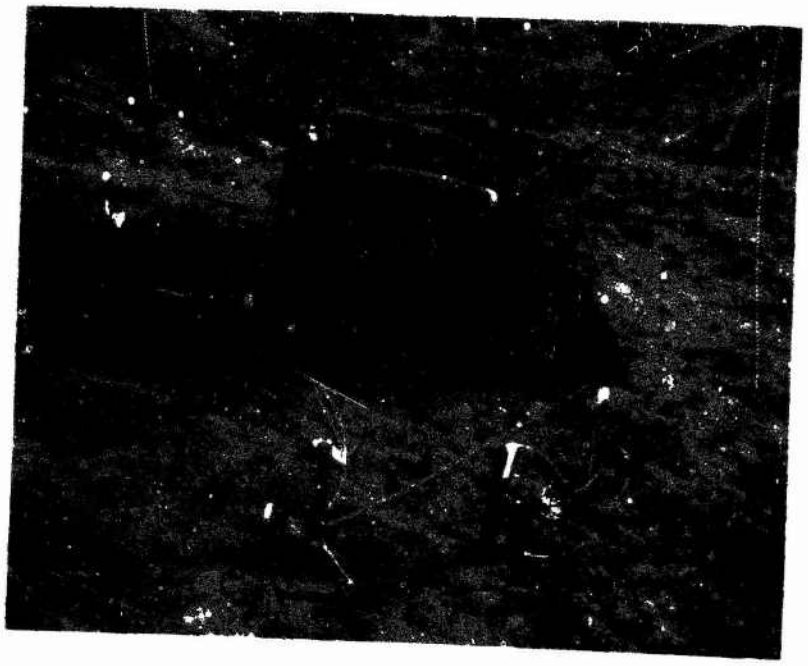

Figure 3. Single Pallet Array



Figure 4. Four Pallet Array

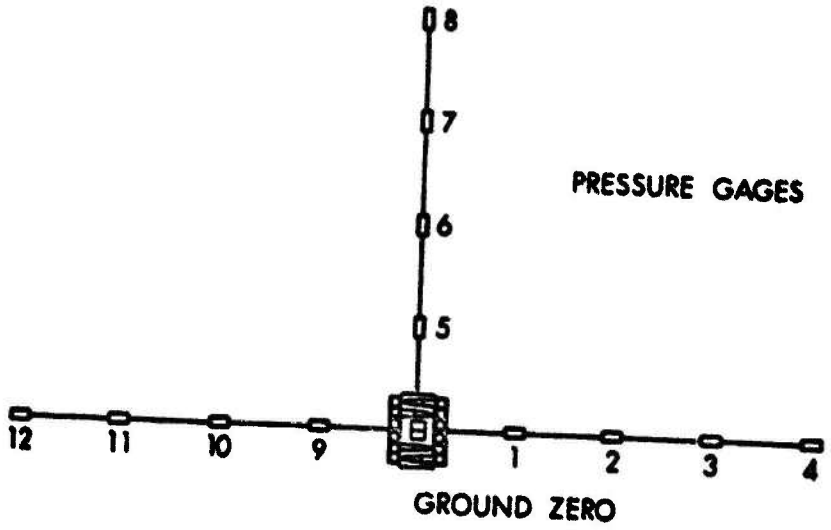

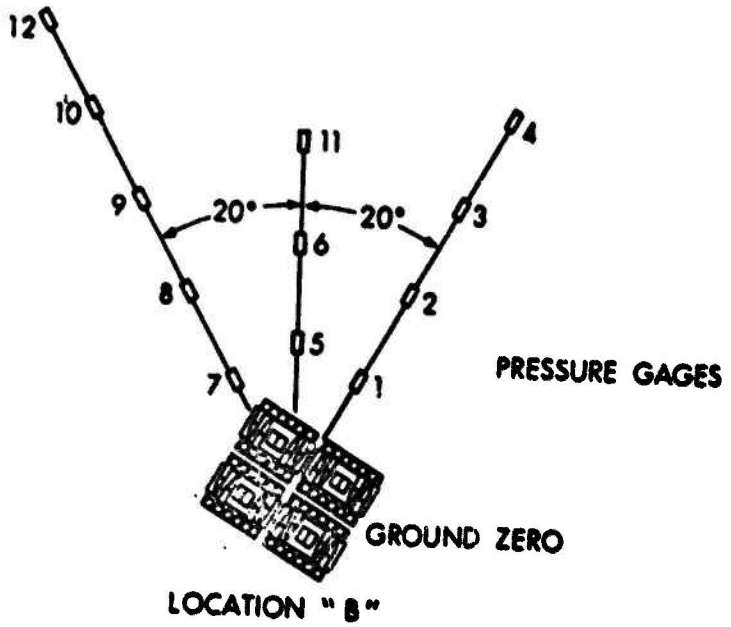

Figure 5. Field Test Set-Up

TABLE I. TEST RESULTS - AVERAGE EQUIVALENT WEIGHT FACTORS

TEST	TEST SITE	NO OF PALLETS	PROPELLANTS NO	PROPELLANTS YES	W_p (lbs)	W_p Ratio	W_{ta} (lbs)	W_{ta} Ratio	REMARKS
1	A	1		X	352				Single point initiation test.
2	A	1	X		140		202		
3	A	1		X	372	2.66	503	2.49	Ratios formed from Tests 2 and 3.
4	A	4		X	1213		2320		
5	B	4	X		519		622		
6	B	4		X	1450	2.79	1417	2.28	Ratios formed from Tests 5 and 6.
7	B	8	X		1311		1864		
8	B	8			3676	2.80	4289	2.30	Ratios formed from Tests 7 and 8.

W_p: TNT Equivalent Weight Factor based on peak overpressure averages.

W_{ta}: TNT Equivalent Weight Factors based on arrival time averages.

EXPLOSIVE SAFETY TESTS OF PERSONAL PROTECTIVE EQUIPMENT

GLENN C. PRITCHARD *

BUREAU OF MINES

WASHINGTON, D.C.

ABSTRACT

Explosive safety regulations require the use of personal protective equipment where work involves the processing, testing, or handling of propellants, explosives, pyrotechnics, and initiating devices. The need or rationale behind such regulations is not always accepted by operating personnel.

As a result, research at the Naval Weapons Center, China Lake, California, was initiated to evaluate: (a) types of protective eyewear to determine their effectiveness in flame- and fragmentation-environments; (b) types of protective clothing to determine their effectiveness in a flame-environment; and (c) types of commonly worn socks to determine the effectiveness of each in meeting present (electrical) conductivity standards.

This paper concerns itself with the criteria used to evaluate each type of equipment and limitations of such equipment. Variables needing control during the evaluation phase or during future tests are also discussed.

* Mr. Pritchard was previously affiliated with the Naval Weapons Center, China Lake, California before assuming his present position with the Bureau of Mines.

INTRODUCTION

Current explosives safety regulations require the use of personal protective equipment where work involves the processing, testing or handling of hazardous materials, such as propellants, explosives, pyrotechnics, and initiating devices. The regulations are intended either to preclude the accidental initiation of high-energy materials, or should initiation occur, to minimize the resultant injury to operating personnel by providing the necessary protection[1].

The need or rationale behind the use of personal protective equipment is not always accepted or is sometimes questioned by personnel. The purpose of the following tests is to provide data that can be used to validate the rationale. In addition, it is felt that perhaps too much credence has been placed in the use of other forms of personal protective equipment not designed nor intended for specific ordnance operations, yet nonetheless, used for such.

This report summarizes the results of three separate studies involving personal protective equipment at the Naval Weapons Center (NWC)[2].

The first series of tests involved the evaluation of five types of protective eyewear to determine the effectiveness of each in a flame-environment and in a fragmentation-environment.

The second series of tests involved three types of safety attire (clothing) to determine the effectiveness of each in a flame-environment.

The third series of tests involved the evaluation of five types of commonly worn socks to determine the effectiveness of each in meeting present (electrical) conductivity standards for ordnance operations.

For ease of presentation, this report is delineated into three separate sections.

[1]Naval Sea Systems Command. Ammunition and Explosives Ashore: Safety Regulations for Handling, Storing, Production, Renovation and Shipping. (NAVSEA OP-5, Vol. 1, Fourth Revision, 1 December 1977).

[2]Naval Weapons Center. Safety Evaluation Tests of Personal Protective Equipment for Ordnance Operations, by Glenn C. Pritchard, China Lake, Calif., NWC, 1978 (Technical Publication TP 6008, publication UNCLASSIFIED).

EYEWEAR TESTS

Five types of eyewear were tested at the Naval Weapons Center. The five types were: (a) safety glasses (polycarbonate-composition), (b) visitor glasses (polypropionate-composition), (c) splash goggles (polycarbonate-composition), (d) nitrometer mask (acetate-composition) and (e) faceshield (acetate-composition).

METHOD

Fragmentation

A standard U.S. Army Engineers blasting cap was placed so that it was centrally located to all five types of eyewear. The vertical orientation of the blasting cap enabled fragments resulting from an electrically-initiated detonation to project out radially in all directions. This insured high velocity fragment impact to all protective eyewear. Distance separation between the blasting cap and each type of eyewear was 18 inches; picked because it simulated personnel working at bent-arms length with the cap, which is a common practice. The vertical centerpoint of each eyewear type was located at the same height above ground level as the blasting cap.

All subsequent fragmentation damage to eyewear was assessed using total impacts, deflections, embedments, and complete penetrations. To assess effectiveness, a relative protection factor was used. It was determined by adding the total number of deflections and embedments and then dividing this value by the total number of impacts. All subsequent values for each eyewear were multiplied by 100 to yield a relative protection factor in percent.

Visual observations were recorded by 35 mm black and white, and color, stills.

RESULTS AND DISCUSSION

Fragmentation

In assessing the damage, not only the occurrence: such as deflection, embedment and penetration, must be considered, but the extent of each. Lenses of eyewear with a large percentage of deflections and shallow embedments are considered most desirable. Those with deep embedments to the very point of complete lens penetration are less desirable; and, of course, complete penetration of the lens is least desirable and totally unacceptable.

Safety Glasses (Spectacles). Not surprising is the fact that the polycarbonate-composition safety glasses withstood high-velocity impact from the fragmenting blasting cap. Fifty percent of the fragments were deflected from the lens, while the other 50% were embedded in the lens (See Table 1). No fragments came close to penetrating the entire thickness of the lens. The inside of the lens was smooth to the touch and as such indicates the appropriateness of requiring safety glasses to be worn during ordnance operations. It must be realized that the test performed simulated

Table 1. Fragmentation Test of Different Eyewear Types

Eyewear Type	Fragmentation				Relative[a] Protection Factor
	Total Impacts	Deflection	Embedments	Complete Penetration	
Safety Glasses (Spectacles)	4	2	2	0	100%
Visitor Glasses (Spectacles)	16	1	13	2	88%
Splash Goggles	9	0	7	2	78%
Nitrometer Mask	41	13	14	14	66%
Faceshield	46	7	22	17	63%

[a]The relative protection factor is determined by adding the total number of embedments and deflections, and then dividing this value by the total number of impacts. Multiplying by 100 will yield a relative protection factor in percent.

a small-scale ordnance mishap. It is not known whether large-scale blasts with subsequent fragmentation would be attended sufficiently by the eyewear; however, personnel would probably not survive due to massive whole-body trauma from severe fragmentation and over-pressure.

Visitor Glasses (Spectacles). Only two of 16 fragments actually penetrated the thickness of the polypropionate-composition lenses (See Table 1). This would be expected for low-velocity metal chips and filings, however, it was not expected (intuitively) for high-velocity schrapnel. The fact that all but three of the fragments were embedded indicates the relative strength of the lenses. However, the fragments that were embedded could be felt from the inside of the lens, thus indicating almost complete penetration.

It must be kept in mind that visitor glasses are intended to be worn by visitors and not by operating personnel directly involved in the hazardous work. Typically, most visitors do not get close enough to the operation and as such probably need no more protection than that provided by the visitor glasses.

Although tests were not conducted using the visitor glasses in combination with personal prescription glasses (not government-issued and approved), the current test results would seem to indicate that there would be sufficient attenuation to prevent eye damage when using this combination.

Splash Goggles. Two fragments completely penetrated the polycarbonate-composition lenses, while seven were sufficiently embedded in the lenses so that they could be felt from the inside of the glasses (Table 1). Goggles typically are used in chemical processing operations where liquid splash protection is needed. The goggles were not designed nor intended primarily for high-velocity impact protection and should not be used for such.

Faceshield Visor (Nitrometer Mask) and Faceshield. Neither the nitrometer mask nor the faceshield provided the protection desired in a fragmenting environment (Table 1). Approximately one out of every three fragments was able to penetrate the shield lens. Because of the .040" thickness of the shield lens, in both the nitrometer mask and the face-shield, all embeded fragments could be felt from the inside. These acetate-composition shields are intended for chip and dust impact, mainly generated by inert machining operations, and liquid splash operations.

METHOD

Burn

A 12-ounce pile of smokeless, single-based, nonperforated powder was situated in front of each type of eyewear. To simulate the typical angle at which personnel would be handling propellant or pyrotechnic powder on a work bench, each set of eyewear was placed 20° off vertical

from the powder, in addition to 18 inches away. Eighteen inches was picked because it was felt that bench level to eye level separation for average-sized personnel approximated this value.

A small powder bag, ignited by an M60 fuse lighter and safety (time) fuse, initiated the train which was set up parallel to and in front of the eyewear. Wooden stands were constructed to insure each eyewear maintained its proper orientation during the test.

The wind velocity at the time of the burn test was 5-9 knot gusts from the southwest. Ignition took place upwind from the eyewear. All eyewear were exposed to high temperature radiation and hot combustion gases. The duration of each 12-ounce pile fire was about 8 seconds. The burn time of the propellant train between piles was about 5 seconds. The total duration of the test was about 60 seconds. Visual observations were recorded by 35 mm black and white, and color, stills.

All subsequent burn damage to eyewear was assessed as none, light, moderate, heavy, or extensive.

RESULTS AND DISCUSSION

Burn

During the propellant burn test, no instrumentation was present to indicate the actual temperatures that the eyewear sustained. Also, no method was available to determine thermal conductivity of the individual eyewear. One can assess the resultant damage due only to thermal radiation and combustion gases. It is possible that some eyewear experience a more severe test than others, but it is not considered significant since the test duration was, in a sense, 'overkill.' Each eyewear experienced about an 8 second burn, which is much more than personnel would be subjected to if any bodily movement away from the flame was possible. The severity of the burn to the face, eyes, and body would be dependent upon the extent and time duration of flame contact, and type of compositional material of the eyewear.

Safety Glasses (Spectacles). It is not surprising that the safety glasses withstood both the thermal radiation and the hot combustion gases as a result of the propellant burn (See Table 2). As before, however, it should be realized that the test simulated a small-scale ordnance mishap and that a large-scale mishap would cause with virtual certainty, massive whole-body trauma, even though the glasses may have attenuated the fire.

The duration of the test was approximately one-minute, which included about 8 seconds of severe flame exposure to the safety glasses. Personnel would not normally be subjected to such a situation and thus the extent of damage may be looked upon as a 'worst case' test situation.

Visitor Glasses (Spectacles). The visitor glasses held up remarkably well to the burn (See Table 2). The lack of damage indicates the relative heat-resistant capabilities of the glasses. Not known is the temperature sustained by the glasses, but results indicate that the visitor glasses experienced no more damage than the government-issued safety glasses. As such, visitors using this type of eyewear are more than likely receiving the same amount of frontal flame protection as that provided by the safety

Table 2. Burn Test of Different Eyewear Types

Eyewear Type	Burn Damage[a]			
	Lens	Side Shields	Frontal Frame	Temple Frame
Safety Glasses (Spectacles)	Light	Moderate	Moderate	Light
Visitor Glasses (Spectacles)	Light	Moderate	Light	Light
Splash Goggles	Light	Light	Light	Light
Nitrometer Mask	Extensive	--	Extensive	--
Faceshield	Extensive	--	Extensive	--

[a]All damage to eyewear is assessed as none, light, moderate, heavy or extensive.

glasses. However, temple and brow protection may not be as great. In addition, no melting occurred and thus supports the idea that skin infection would not occur from a melted spectacle and flesh interaction.

Splash Goggles. Even more surprising than the assessed results of the visitor glasses, was the results of the splash goggles (Table 2). Burn damage to all portions of the eyewear was assessed as light. Consequently, the goggles received the most favorable rating among the five types of eyewear tested. The results should be viewed with some amount of caution. The goggles were located at the end of the propellant train, and as such, may not have received the same amount of thermal input as the other eyewear. Indeed, the wooden stand supporting this eyewear seemed less charred (near the eyewear) than the other stands.

Faceshield Visor (Nitrometer Mask) and Faceshield. Visual observations after the test led to 'extensive' damage assessments for both eyewear types (Table 2). Personnel wearing such eyewear would have experienced severe burns, probable inhalation of toxic combustion by-products from these shields, and probable skin infection from the interaction of the melted shields and flesh. Unless immediate evacuation were possible, the mask and shield would appear to be of no value in a flame-environment.

SUMMARY

This section describes fragmentation and burn tests made to determine the effectiveness of eyewear used in ordnance operations and to indicate the hazards to personnel should they be exposed to burning materials or explosive detonations. Observation of eyewear damage as a result of the tests indicates the following:

1. The purpose of the eyewear selected and thus the operation in which the eyewear is to be used, must always be kept in mind.

2. The apparent differences among all eyewear types tested can probably be attributed to lens thickness, lens composition, cross-linked chemicals used to facilitate lens strength, manufacturing differences of each company producing the eyewear, and other possibly unknown variables. Purchase of any such eyewear should include an attempt to take into account the aforementioned variable.

3. Realistically, the only eyewear providing adequate burn and light fragmentation protection is the polycarbonate safety glasses (spectacles). All other eyewear do not appear to be designed sufficiently to be used singularly in explosive operations for operator protection.

4. Polypropionate visitor glasses (spectacles) and polycarbonate splash goggles appear to have limited appropriateness during fragmentation-potential operations only when worn over personal prescription glasses or government-issued safety glasses.

5. Polypropionate visitor glasses (spectacles) and polycarbonate splash goggles appear to be appropriate to wear during burn-potential operations regardless of whether personal prescription or government-issued safety glasses are worn underneath.

6. The acetate nitrometer and acetate faceshield masks appear to have only limited appropriateness for ordnance operations, and only when worn in conjunction with government-issued safety glasses. The shields would appear to provide only immediate protection in a fire. Unless personnel wearing such equipment could remove themselves, or be removed, almost immediately from the fire, extensive melting in addition to possible smoke and toxic combustion by-product inhalation would cause incapacitation. The shields do provide some fragmentation attenuation, but the degree of such would prohibit them from being worn unless accompanied by government-issued safety glasses.

7. Discussions with several manufacturing and distributing firms indicate that the nitrometer mask and faceshield could be produced using either a polycarbonate or polypropionate composition; in place of the acetate material used. This would substantially increase the protection factor due to the increased strength. Fragmentation and burn tests could then be accomplished using the stronger compositions.

8. All eyewear evaluated should perform better (than that reported) in other than ordnance operations, where low-velocity chips, metal filings, and dust exists (e.g., machining operations of inert components).

9. Tests should be made to determine the maximum amounts of explosives and propellants, maximum fragment weights, and minimum distances for which each eyewear type will offer protection.

10. Tests should be made to attempt to validate some of the aforementioned comments involving personal prescription eyewear used in conjunction with visitor glasses (spectacles), splash goggles, and faceshields.

11. Tests should be conducted using thermocouples to determine actual temperatures sustained by the eyewear, and to assist in determining thermal conductivity of such eyewear.

12. The American National Standards Institute (ANSI Z87.1)[3] does not concern itself with high-velocity impact situations. Only those protection requirements involving low-velocity impact are discussed. An apparent deficiency in this area would appear to exist.

[3]American National Standards Institute. American National Standard for Occupational and Educational Eye and Face Protection, New York, N.Y. 1968(ANSI Z87.1).

CLOTHING TESTS

Three types of safety attire were tested at the Naval Weapons Center. The three types were: (a) flame-retardant treated coveralls (powder uniform) with all-cotton underclothing only, (b) flame-retardant treated coveralls with street clothing worn underneath, and (c) flame-retardant treated coveralls with a flame-suit worn over the coveralls.

METHOD

Three manakins were placed on one side of a table, on which was approximately 30 pounds of composite propellant shavings salvaged from processing operations and laid to a depth of 5- to 6- inches. One manakin wore government-issued cotton coveralls, cotton underwear and a cotton T-shirt. The T-shirt and cotton underwear were made of 100% combed-cotton. The coveralls, or powder uniform as is called in many processing facilities, was made of tightly woven, smooth, cotton fabric and treated with a diammonium phosphate or ammonium sulfomate flame-retardancy solution. The coveralls were of the type that require flame proofing after each laundering. The coveralls in this test had recently been laundered and flame-proofed.

A second manakin wore the government-issued cotton T-shirt and underwear. Over the underclothing were worn a cotton flannel shirt and blue denim jeans, both of which did not receive the flame retardant treatment. Over the shirt and jeans were worn the government-issued cotton coveralls. A third manakin wore a Firetex flame suit over the government-issued coveralls, T-shirt, and underwear.

Thermocouples were placed on each manakins' breast. To insure most likely contact between the manakin and the clothing, the breast area was chosen over other bodily areas. A fourth thermocouple was placed on the manakin outfitted with cotton underclothing and coveralls only. The location was on the neck of the manakin and as such, was unprotected.

Honeywell 19 recorders powered by a portable generator were used to record all thermocouple data. There were no zero time indicators on the two Honeywell recorders used. The zero time was arbitrarily chosen and is felt to be accurate only to within a couple of seconds.

The relative protection given by the various clothing types was evaluated by thermocouple data and visual observation. Visual observations were recorded by 35 mm color stills.

RESULTS

At the time of propellant ignition, the wind was blowing away from the safety-clothes-only manakin and toward the street-clothes-and-safety-clothes manakin. The safety-clothes-only manakin was exposed primarily to high temperature radiation, whereas the manakin with street clothing was exposed to both the radiation and the hot combustion gases. The

street clothes manakin with safety clothes experienced a more severe test than the safety-clothed manakin as a result of this additional exposure.

The duration of the burn was about 7-10 seconds, which is more than personnel would be subjected to, if any bodily movement away from the fire was possible. In this sense, the test represents an 'overkill' situation.

Safety Clothes Only. The manakin wearing only the government-issued cotton underclothing and coveralls was protected the least, according to the data provided by the thermocouple recorders and visual observation. As pointed out in the previous paragraphs, this manakin was the least exposed to fire. The cotton coveralls were charred, as was the T-shirt. The cotton underwear were scorched. The maximum temperature recorded was 385°F, reached five seconds after the initial temperature (See Figure 1).

All damage inflicted was at or above the table level.

Safety Clothes and Street Clothes. The manakin with government-issued safety clothes and street clothes underneath was protected much more than the manakin with safety clothes alone, according to the thermocouple data (See Figure 1). After two seconds of the initial temperature rise, a maximum of 195° was reached. This was the first of three noticable rises in temperature; the next occurring about 13 seconds later and reaching 220°F. Finally, 40 seconds after ignition propellant, the ignition of the street clothes occurred. The maximum rise then reached 435°F. The street clothes burned in the midriff section of the manakin, except where the flannel shirt had been tucked into the blue jeans. The jeans themselves received some burning in the belt and pocket area. So badly burned were the T-shirt and coveralls, that they disintegrated upon being touched. The underwear were virtually undamaged.

All damage inflicted was at or above the table level.

Safety Clothes and Flame Suit. The manakin wearing the flame suit over the coveralls was the most protected (See Figure 1). An initial, conspicuous temperature rise occurred about 5 seconds into the burn and reached a maximum of 125°F after about 8 seconds. The flame suit, however, was embrittled by the fire. For the chest area where the flame suit did not protect the coveralls, light scorching occurred. The fire was able to propagate up the sleeves of the flame suit, causing extensive damage to the coverall sleeves underneath. No glove gauntlets were being worn by the manakin during the test.

All damage inflicted was at or above the table level.

DISCUSSION

The resultant data is not too surprising. More protection is certainly gained by more clothing. NAVSEA OP-5, Volume 1, Ammunition and Explosives Ashore, indicates that street clothes may be worn under a powder uniform in operations where they are used for fire protection and to keep the worker's clothes from being contaminated. The NAVSEA

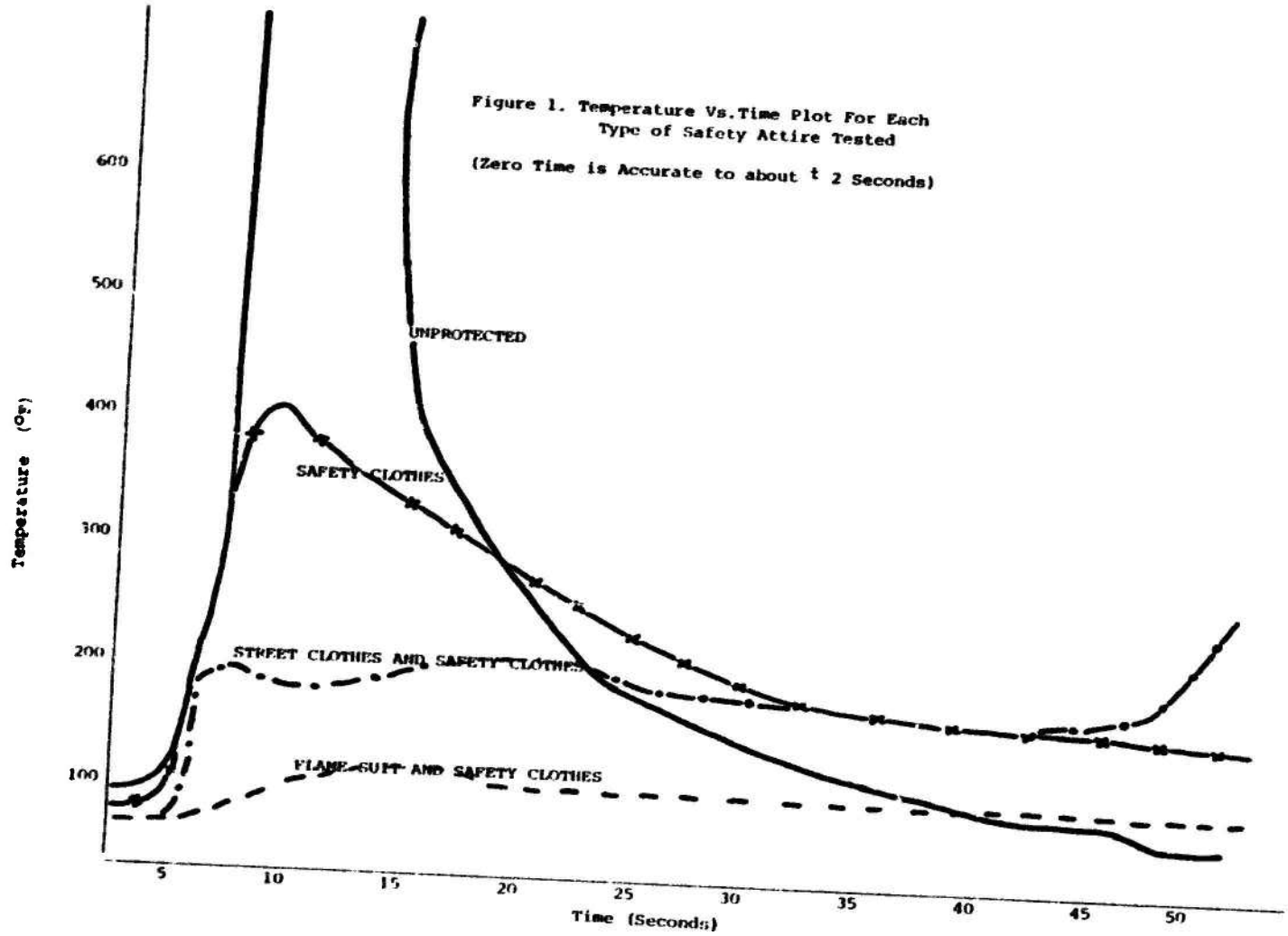

Figure 1. Temperature Vs.Time Plot For Each Type of Safety Attire Tested

(Zero Time is Accurate to about ± 2 Seconds)

document, however, goes on to indicate that in operations where static electricity creates a hazard, all clothing worn under powder uniforms shall be made of cotton.

The use of the flame suit provides the best protection of the safety gear evaluated. However, again the question of static electricity must be raised. Worker mobility and comfort must also be a consideration.

Decisions must be analyzed and the risks weighed in determining the trade off between comfort and thermal protection, static versus non-static producing clothing, and combinations thereof.

Although street clothes do burn, this test showed an extended time delay before they ignited. Any movement on the part of personnel away from the fire would have certainly precluded this ignition occurrence. A similar statement about the government-issued coveralls and underclothing can be made. Seven to ten seconds is a long time to be exposed to a propellant fire. The purpose of this protective clothing is not to 'fight' a fire, but to enable speedy and safe egress from one. Intuitively, all three protective outfits tested provide this capability. Of course, unprotected areas of the body, e.g., hands, face and neck would experience severe burns without immediate evacuation. In this circumstance, additional protection would be needed.

SUMMARY

This section describes flame tests made to determine the relative protection of safety attire (clothing) used in ordnance operations and to indicate to personnel the hazards should they be exposed to burning materials. Current Naval explosives safety regulations , in addition to observation of damage to the clothing as a result of the test, indicates the following:

1. All cotton clothing: coveralls, T-shirt, underwear, and socks must be worn in operations where the generation of static electricity would create a hazard.

2. When static electricity is of no concern and in operations where additional fire protection is needed, street clothes may and should be worn under a powder uniform.

3. Considering average personnel reaction time to a fire where less than massive amounts of propellant are involved, and assuming ease of emergency egress, coveralls and all-cotton undergarments are safe and appropriate clothing to wear in flame-potential environments.

4. Where flame suits are considered desirable (e.g., large-scale propellant and pyrotechnic operations), they need to be of such blend and construction that static electricity can be as easily dissipated as with cotton gear. In addition, personnel comfort and mobility must be a salient factor when determining the use of such suits. Indeed, the degree of protection provided by a flame suit may be outweighed by its static-producing capabilities and its lack of comfort.

SOCK TESTS

Five types of socks were evaluated at the Naval Weapons Center. The five types were: (a) 100% cotton (thin), (b) 75-85% cotton/25-15% nylon, (c) 100% cotton (thick), (d) 100% nylon, and (e) 75% orlon/25% nylon.

METHOD

Socks of the various types were issued to a number of personnel. The tests were conducted by having each person put on one kind of sock with his conductive shoes. A conductivity reading was taken immediately. A Safe-T-Ohm, Model TM, shoe tester was used for all readings. After the immediate reading, additional readings were taken at specified time intervals. This report focuses on the first 120 minutes.

During the testing period, personnel continued to perform their regularly assigned functions. This was done to simulate as near as possible the conditions personnel would normally experience in their work environment. Due to remote work locations, some extensive travel, and incongruous work schedules, all personnel were not tested with all sock types. In addition, not all personnel were tested at each of the specified time intervals.

RESULTS AND DISCUSSION

Table 3 shows the percent of sock types falling within specified conductivity ranges as a function of time. To facilitate ease of discussion, 'K' ohms will be used to indicate 1,000 ohms, while 'M' ohms will be used to indicate 1,000,000 ohms.

100% Cotton (Thin) Socks. Thin socks, of 100% cotton composition, registered the most satisfactory readings. This occurred not only immediately after personnel put on the socks, but for the entire two-hour evaluation period. The requirement for socks of high cotton content in ordnance operations involving electrostatic hazard potential appears to be validated by the results of this test. Cotton is hygroscopic, and as such will readily absorb moisture from the atmosphere or from the feet of personnel. Moisture collected on the feet of personnel is absorbed and transmitted through the sock to the inner sole of the conductive shoe. The shoe then provides a path to ground to bleed off electrostatic charge buildup.

Internal body resistance and built-in shoe resistance keep readings from reaching unacceptably low values. Current NAVSEA explosive safety requirements allow a minimum shoe reading of 25K ohms. Several 40K, 50K, and 60K ohm readings were registered during the cotton sock test, however, none approached minimum acceptability.

One somewhat disturbing aspect associated with the 100% cotton (thin) socks was the fact that 10% of the readings registered above the 1M ohm maximum immediately after putting on the socks. For operations where the generation of static would create a hazard, regulations require socks of high cotton content. No time element is involved, yet the test data

Table 3.Percent of Sock Types Failing Within Specified Conductivity Ranges as a Function of Time

Type of Socks	Range of Conductivity[a]	Approximate Time[b]					
		Immediately	15	30	45	60	120
100% Cotton (Thin) Socks	0-500K	80%	100%	100%	100%	100%	100%
	>500K-<1M	10%	-	-	-	-	-
	≥1M	10%	-	-	-	-	-
75-85% Cotton/ 25-15% Nylon Socks	0-500K	77%	100%	100%	100%	100%	100%
	>500K-<1M	-	-	-	-	-	-
	≥1M	23%	-	-	-	-	-
100% Cotton (Thick) Socks	0-500K	29%	71%	100%	100%	100%	100%
	>500K-<1M	-	29%	-	-	-	-
	≥1M	71%	-	-	-	-	-
100% Nylon Socks	0-500K	27%	25%	44.5%	20%	64%	62.5%
	>500K-<1M	9%	12.5%	11.0%	-	-	12.5%
	≥1M	64%	62.5%	44.5%	80%	36%	25%
75% Orlon/ 25% Nylon Socks	0-500K	10%	-	28.6%	17%	37.5%	37.5%
	>500K-<1M	10%	14.3%	-	-	-	12.5%
	≥1M	80%	85.7%	71.4%	83%	62.5%	50%

[a] K = 1,000 ohms
M = 1,000,000 ohms

[b] Time is in minutes

indicates that perhaps as long as 15 minutes may be needed before maximum safety, through acceptable conductivity readings, can be achieved.

75-85% Cotton/25-15% Nylon Socks. Socks with all cotton content have become increasingly difficult to procure. Cotton socks typically have a reinforced heel and toe made of nylon. The small percentage of nylon has generally not affected the hygroscopicity of the cotton, and the test results in this report would appear to validate this. After 15 minutes, all readings registered 0-500K ohms. The only difference between the all cotton (thin) socks and the cotton/nylon socks appeared to be in the readings achieved immediately after putting on the socks. Twenty-three percent of the personnel wearing the cotton/nylon socks had readings greater than 1M, as opposed to 10% for cotton (thin) socks. Based upon the test results, 15 minutes would appear to be needed to achieve maximum acceptable conductivity.

100% Cotton (Thick) Socks. Thick socks, of 100% cotton composition, revealed some surprisingly unsatisfactory readings. In fact 71% of the personnel wearing this sock type registered over 1M ohms resistance immediately upon donning them. Only 29% fell into the acceptable range. It should be understood that the requirement for socks with high cotton content is applicable to those of thin construction only. As stated before, cotton is hygroscopic. However, permeation of moisture through thick socks takes longer than through thin socks. As a consequence, acceptable conductivity readings take longer to achieve. The test data seems to substantiate this. After 15 minutes, 71% of the readings were in the 0-500K ohm range and 29% were in the >500K-<1M range. Fifteen minutes appears to be the minimum time to achieve acceptable conductivity. Thirty minutes seems most appropriate.

100% Nylon and 75% Orlon/25% Nylon Socks. Both types of synthetic socks worn by personnel registered entirely unsatisfactory readings. After two hours, 25% of the personnel wearing 100% nylon socks registered above 1M ohm. Fifty-seven percent of the personnel wearing 75% orlon/25% nylon socks registered above 1M ohm even after the two hour test period. Synthetics do not absorb moisture readily. In addition they provide good insulative effects. Both these aspects contribute to their ability to maintain an electrical charge for extended time periods before bleed-off occurs. This could be catastrophic in those operations where electrostatic discharge may initiate loose explosives or pyrotechnic powder, or vapor-air mixtures within ignitable limits.

VARIABLES

Several of the sock types proved to be effective for the hazardous conditions found in ordnance operations. However, many variables were found that affect the adequacy of conductivity afforded by the various type of socks. Variables that merit consideration are listed below under the general headings of shoe tester, weather conditions, shoe conditions, work conditions and individual differences. These variables should not be considered all-inclusive.

Shoe Tester. The shoe tester used in this particular test, the Safe-T-Ohm, has a scale range of 0 ohms to 1,000,000 ohms. This range is highlighted green to indicate acceptability. Above 1,000,000 ohms is highlighted red to indicate unacceptability. However, in the red region there is no scale and as a consequence, there is no satisfactory method to determine whether the sock readings are just slightly above acceptable conductivity or infinitely above. One only knows that the reading is unacceptable, not the extent of this unacceptability. There is probably enough machine-error variability to make the shoe tester readings near the red/green borderline region a concern.

Weather Conditions. Relative humidity must be controlled in order to obtain reliable conductivity measurements over time. A high humidity may cause enough moisture on the socks and feet of personnel to cause most, if not all, readings, regardless of sock content, to be within acceptable limits. Similarly, a low humidity may keep even cotton socks at high levels. Hygroscopicity is the ability to absorb moisture. If there is little moisture in the air, such as may be found in the desert winter months, hygroscopic socks will experience difficulty in moisture absorption. Consequently, readings may stay elevated for extended time periods.

In summary, cold versus warm weather conditions, coupled with wet versus dry climatic conditions are variables that must be considered and controlled when evaluations of this nature are performed. This is why daily checks are important in high hazard areas (e.g., primary explosive and pyrotechnic operations), per NAVSEA explosive regulations.

Shoe Conditions. Ideally, the conductivity of shoes should be determined before socks are tested so that a baseline of data can be established. Shoes in good condition may initially show a conductivity reading as low as 25K ohms. Likewise, shoes in bad condition may lead to greater than 1M ohm readings, even with 100% (thin) cotton socks.

Dirt, grime, grease, and wax are just a few of the materials that may provide sufficient insulative effects to prevent reliable and accurate conductivity readings, unless removed from the soles of the conductive shoes.

Work Conditions. Pedestrian traffic may be a crucial variable in evaluating sock conductivity. Field work that involves a great deal of activity on the part of personnel should lead to copious amounts of

perspiration, and as such, adequate conductivity measurements. Likewise, office work involving a good deal of sendentary activity, and only sporadic field work, may preclude perspiration buildup and thus raise most readings above acceptability, regardless of sock content.

Individual Differences. Some personnel may naturally perspire regardless of their activity, while others who do active work may not perspire at all. Blood circulation plays a major part, and of course, is different with different people. Test results would seem to verify this; the same personnel generally showed higher readings on all types of socks - especially initial readings. In summary, individuals must know their peculiarities to truly derive maximum safety through the use of socks and shoes.

SUMMARY

This section describes conductivity tests made to determine the relative conductivity of various sock types that may be worn in ordnance operations and to indicate to personnel the acceptability or unacceptability of such socks. Current NAVSEA explosives safety regulations, in addition to observations of sock conductivity as a result of the tests, indicate the following:

1. Where conductive shoes are required to be worn, only lightweight socks of high cotton content should be worn.

2. Even after donning lightweight (thin) socks of 100% cotton content, perhaps as long as 15 minutes may be needed before adequate conductivity readings can be achieved.

3. Seventy-five to 85% cotton socks, with some nylon reinforcement meet the requirement of high cotton content and appear to provide acceptable conductivity readings after a 15 minute waiting period.

4. Thick 100% cotton socks do not appear to meet current NAVSEA requirements, and test results seem to support this. Thirty minutes may be an appropriate waiting period, after donning heavy cotton socks, before hazardous operations should commence. This is a somewhat long waiting period and may be economically impractical.

5. Synthetic socks do not meet current requirements and this is reinforced by the data. Their use in ordnance operations should be precluded, especially where electrostatic discharge is a concern.

6. Many variables affect sock conductivity. To gain a reliable hold on actual sock conductivity, control of these variables is needed.

SUMMARY

This report summarizes the results of tests conducted at the Naval Weapons Center (NWC) to evaluate the effectiveness of personal protective equipment used in areas involving the processing, testing, and storing of high energy materials.

A more detailed discussion of the criteria used to evaluate the equipment, the limitations of each type of equipment, and variables to be controlled or included during the evaluation phase or during future tests can be found in "Safety Evaluation Tests of Personal Protective Equipment for Ordnance Operations." (Footnote 2).

Protective equipment described herein was purchased for limited applications and use by NWC. The results and implications derived from the test applications should be evaluated cautiously. Although different types of protective equipment were found acceptable for ordnance evironments, some variables probably did intervene to prevent a totally accurate analysis.

It is apparent that research programs are needed to obtain data in which some of the aforementioned variables are controlled. It is hoped that this report will stimulate an interest in that direction.

MANUFACTURE OF EXPLOSIVES EXTRUDED PRODUCTS

Robert A. Lee
THIOKOL CORPORATION/Louisiana Division
Louisiana Army Ammunition Plant
Shreveport, Louisiana

In 1973, a project was established to design and develop a prototype extruder for Composition C4 Explosives. It was intended to completely design a new facility at Louisiana Army Ammunition Plant for production of extruded items.

This presentation will include slides and a discussion of the production facilities and operational flow in producing the M112 Demolition Block. It will cover the entire operation from receipt of the bulk Composition C4 Explosives, extrusion, assembly and pack operations. Following the slide presentation, a short film will be shown covering these same operations.

Slide 1

Receive COMP C4 Explosives from the magazine.

Slide 2

Visual inspection of the COMP C4 Explosives to detect foreign objects. At this point, the C4 is introduced into the conveyor system in buckets as shown in the lower right hand corner.

PRECEDING PAGE BLANK

Slide 3

Overall view of the explosives being introduced into the conveyor. You will note the overhead speaker as these employees have constant two-way communication with the Control Room.

Slide 4

The overhead conveyor transports the explosives through a covered ramp to the extruder. Bucket in right hand corner is in position to dump COMP C4 into the extruder hopper.

It is interesting to note that the inbound and out feed ramps plus the extruder building are protected by automatic sprinklers. The systems in the extruder building are hi-speed, activated by ultra-violet detectors. These detectors also activate the sprinklers in both ramps in addition to the ones in the building.

Slide 5

The extruder showing the outfeed and reject conveyor.

Slide 6

This slide depicts the lower barrel and die head on the extruder. There are two extruders in the building separated by a TM 5-1300 wall.

Slide 7

As the extruded material exits the die head, it is measured by photoelectric cell. When the proper length is detected, the cutter is automatically triggered and severs the block from the ribbon. As the block proceeds to the short section of conveyor in front of the cutter, it is automatically weighed. If it is within tolerances, it proceeds to the outfeed conveyor. If out of tolerance, the block is fed back into the hopper for re-extrusion.

Slide 8

The products are extruded remotely. This slide shows the interior of the remote control room's closed circuit TV screens. This is the view the operator sees in order to operate the equipment.

Slide 9

The Quality Control Inspector measures the block.

Slide 10

The Quality Control Inspector checkweighs the block.

Slide 11

Blocks are removed from the conveyor and placed in trays.

Slide 12

The trays are placed in index buggies and transported to the assembly line.

Slide 13

This is an overall view of the demolition block assembly line.

Slide 14

The operator inserts the demolition block in plastic bag.

Slide 15

Machine which seals the end of the bag after the air has been evacuated.

Slide 16

Infrared equipment shrinks the plastic bag tightly to the block. The temperature of the infrared tunnel and speed of the conveyor are sensitive and rigidly controlled to prevent the block from over-heating. The entrance and exit tc this heat shrink operation are protected by ultra-violet fire detectors and rate-of-rise electronic detectors. The temperature within the tunnel is checked by thermo-couples periodically to determine the exact temperatures the blocks are receiving in transient.

Slide 17

This is a view as the blocks exit the heat shrink tunnel.

Slide 28

This is the automatic stenciling machine.

Slide 19

Operators cutting double face pressure sensitive tape.

Slide 20

Operator applying the double face tape to the demolition block.

Slide 21

The finished product ready to be packed out.

Slide 22

Wire bound boxes are assembled on the line for packout.

Slide 23

Operator preparing barrier bags for insertion into the wire bound boxes.

Slide 24

Here the bag is being inserted into the box.

Slide 25

Demolition blocks are packed into the barrier bag.

Slide 26

The air is evacuated from the barrier bag and the bag is then heat sealed.

Slide 27

The boxes are closed and sealed.

Slide 28

The lot number is then stenciled onto the box.

Slide 29

The boxes of demolition blocks are transported by conveyor to an adjacent building where they are palletized.

Slide 30

Boxes are loaded onto trucks for disposition.

Slide 31

An interesting item is the construction of the TM 5-1300 wall. The amount of steel this wall contains is almost unbelievable. It is very difficult to pour and compact the wet concrete around the steel lacing. This TM wall is designed for 250 pounds of explosives and actually separates the two extruders.

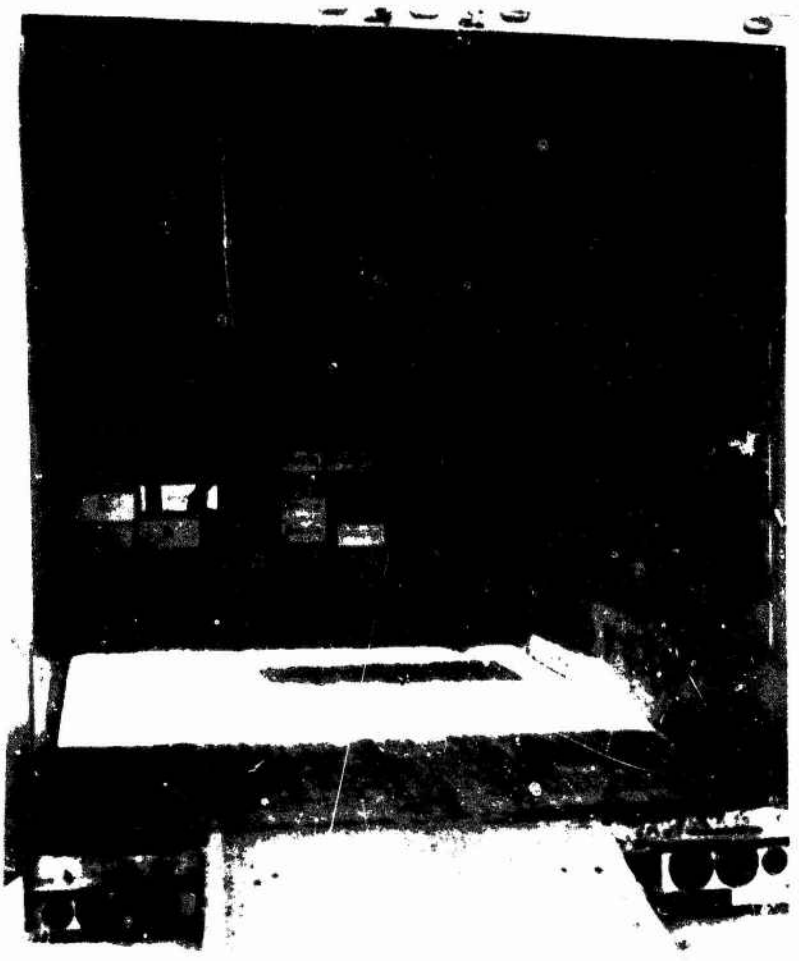

Slide 1



Slide 2

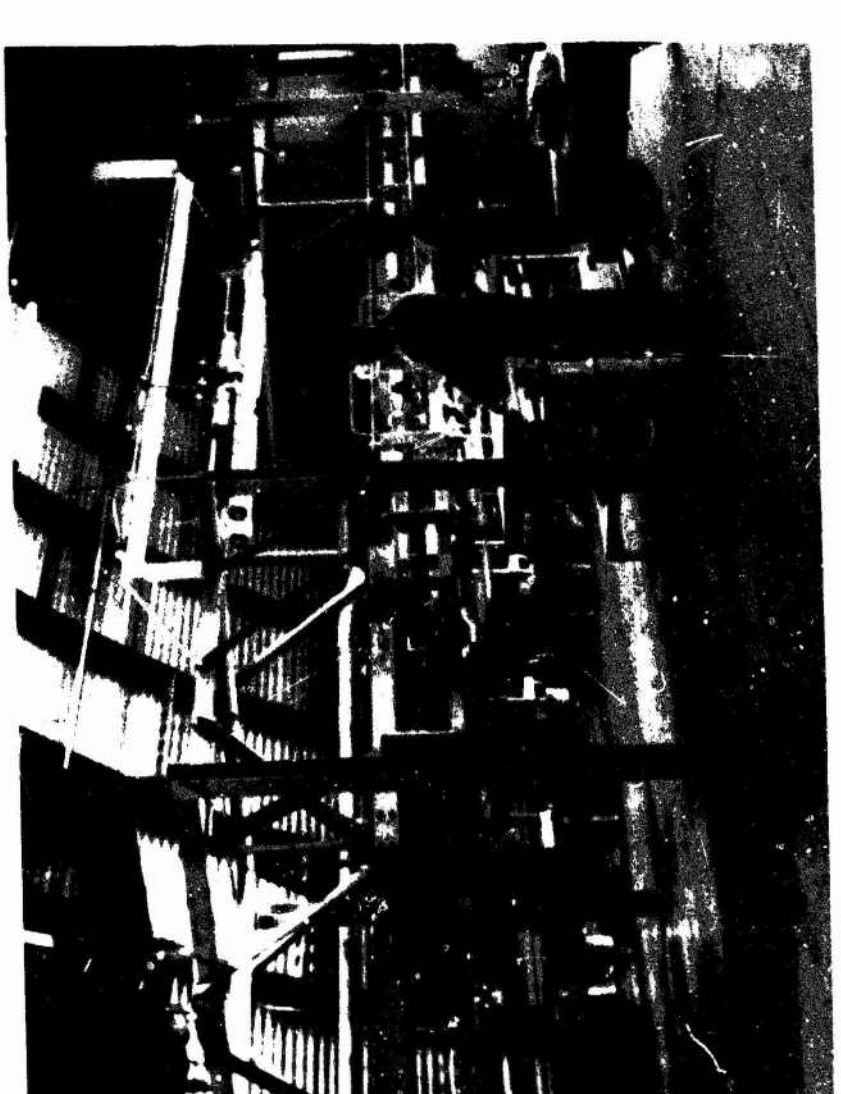

Slide 3

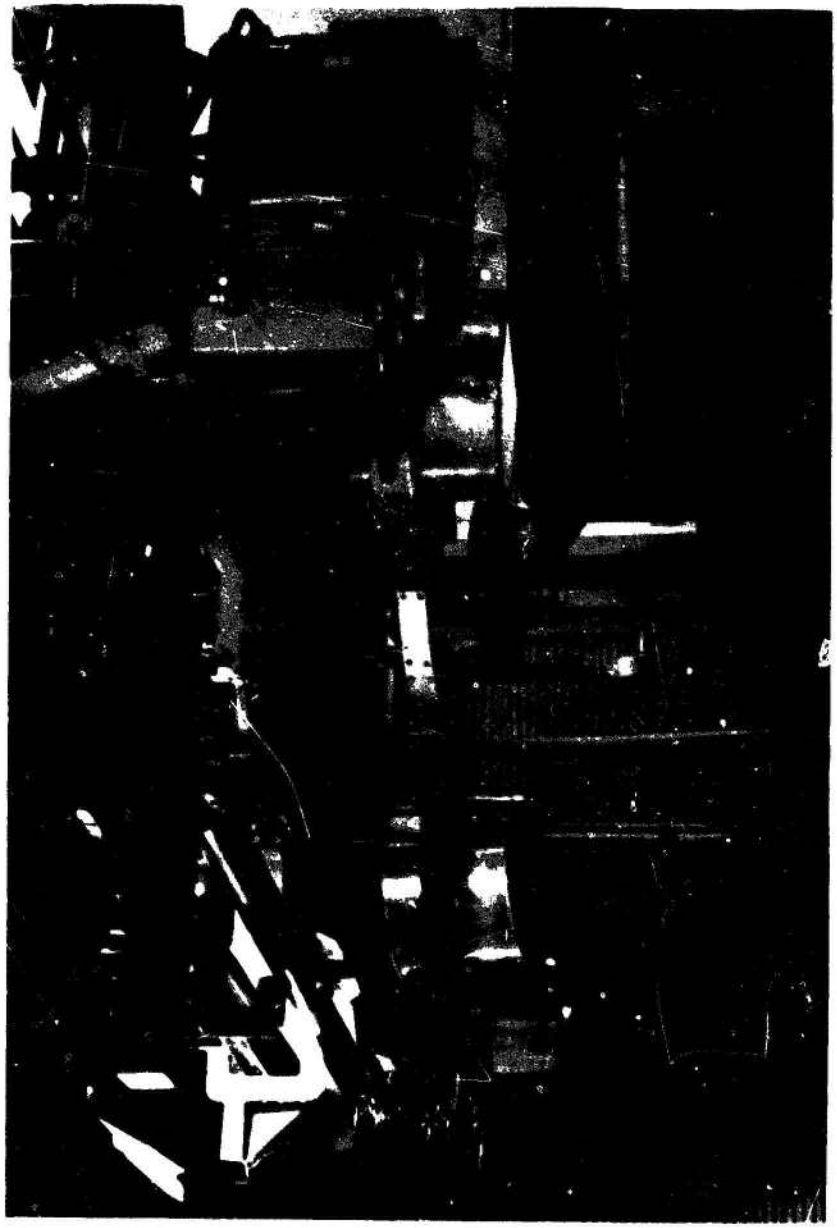

Slide 4



Slide 5



Slide 6

Slide 7

Slide 8

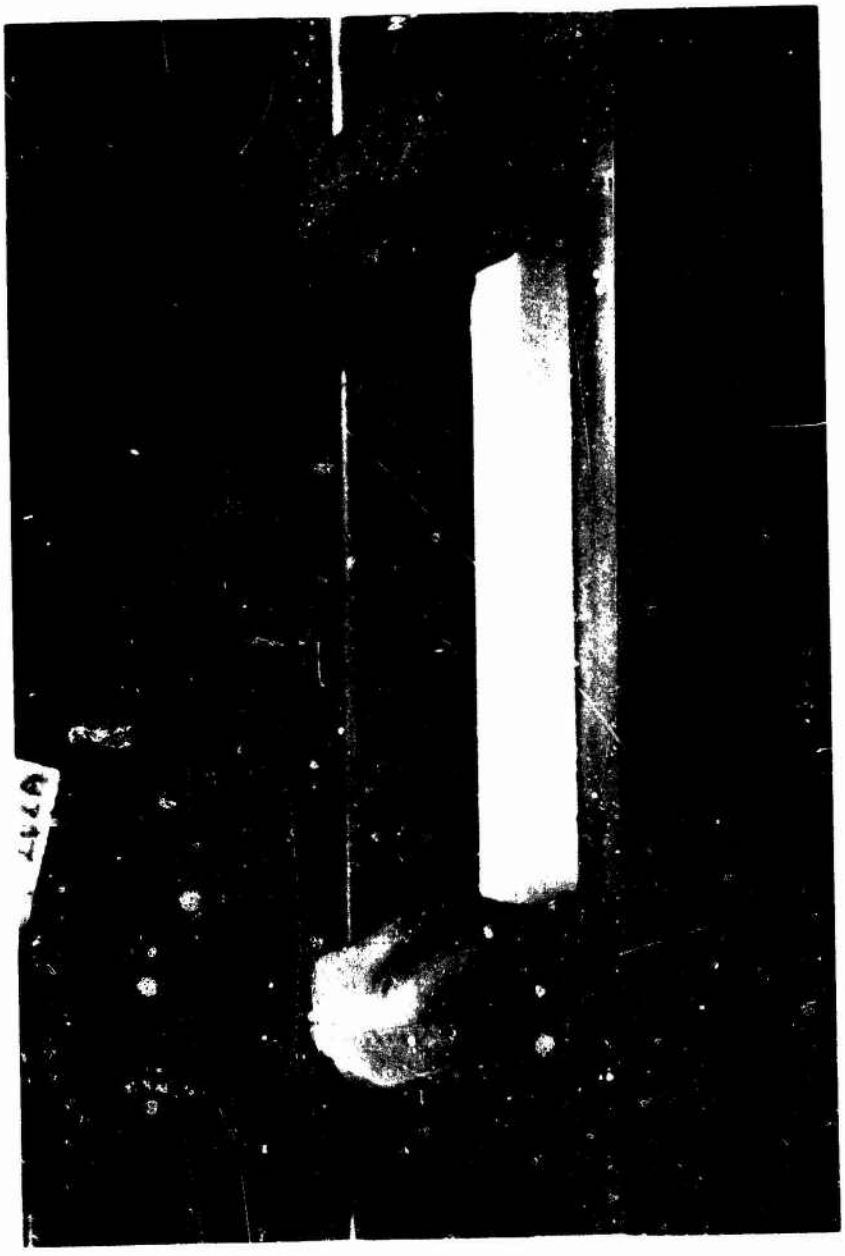

Slide 9

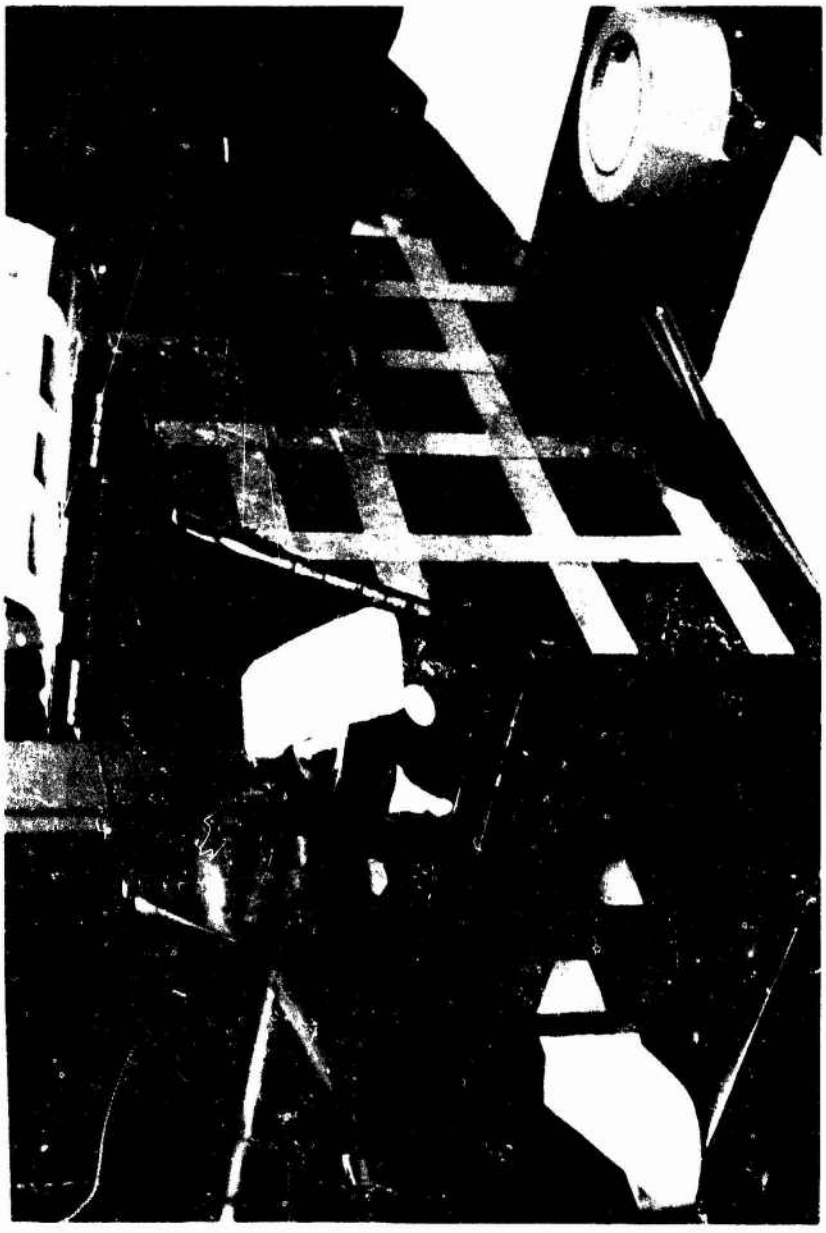

Slide 10

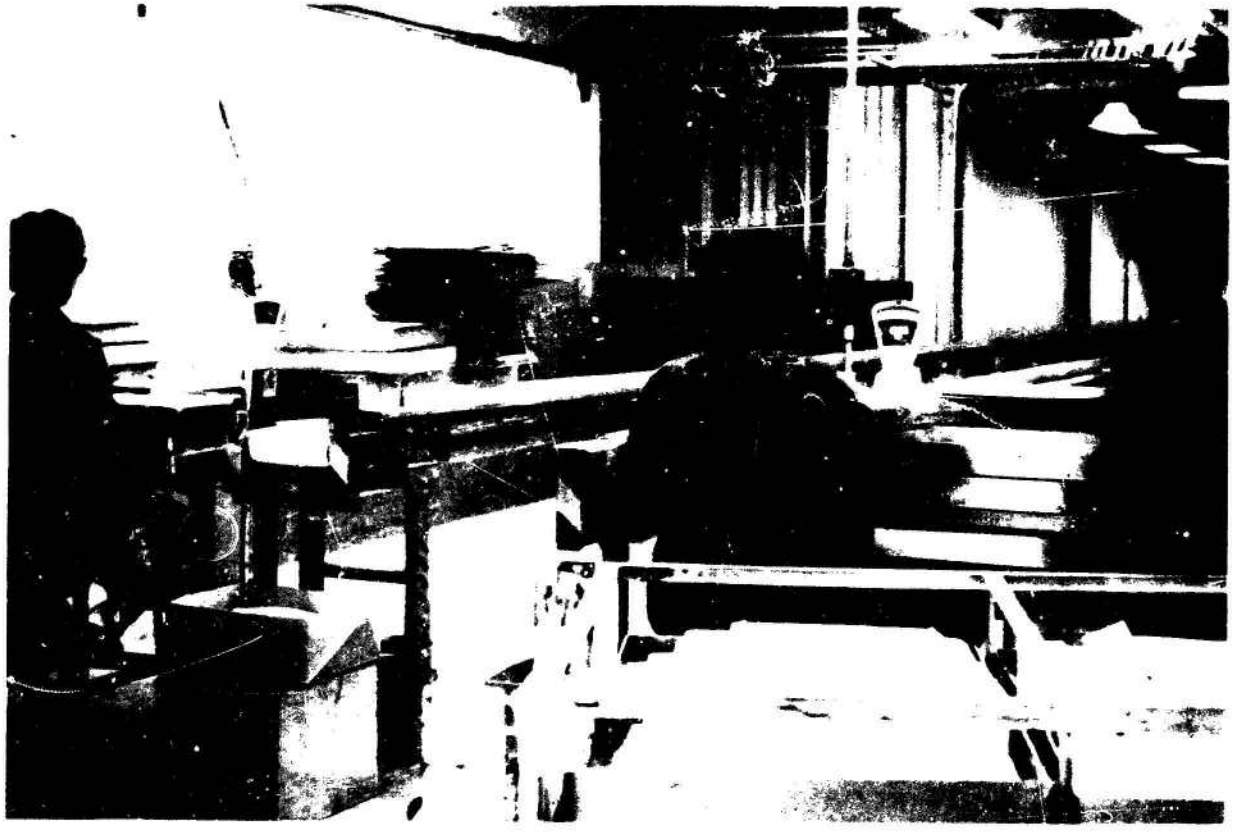

Slide 11

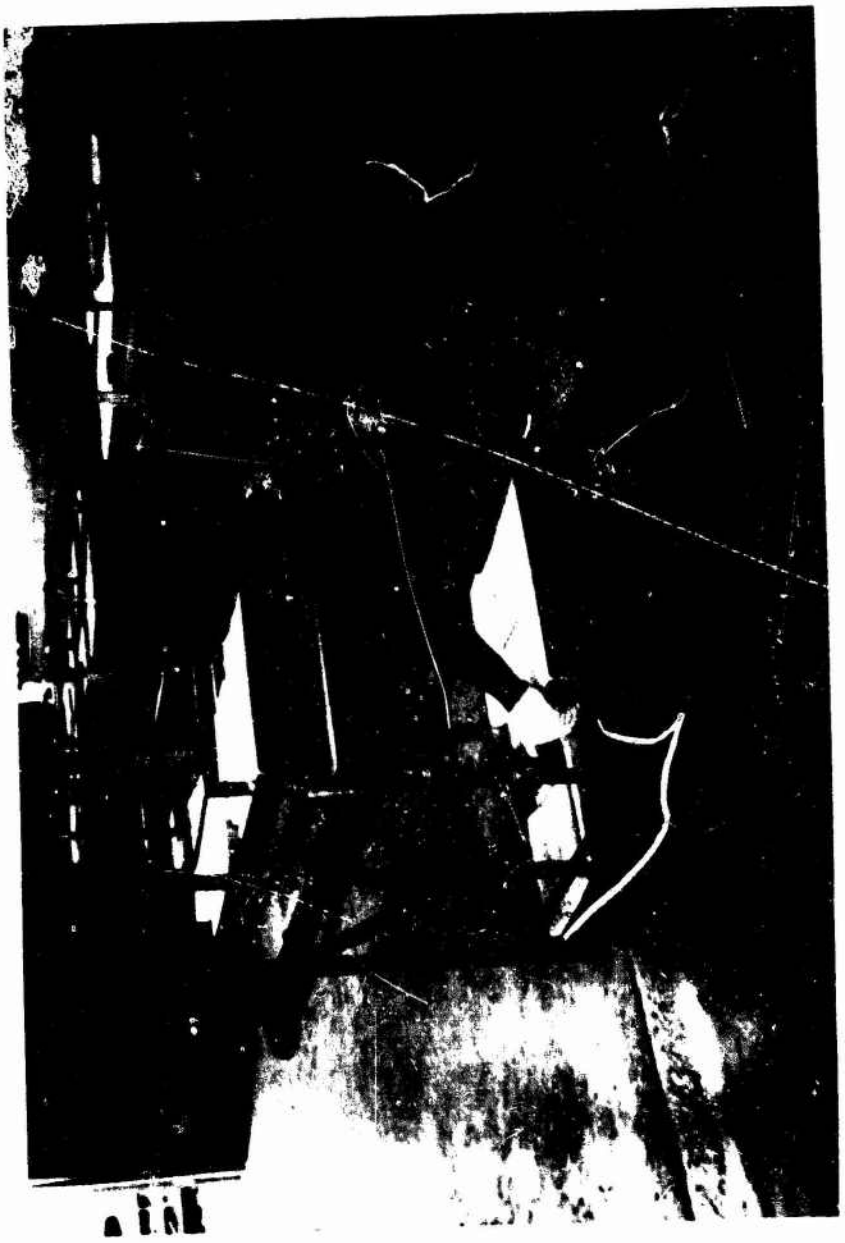

Slide 12

Slide 13

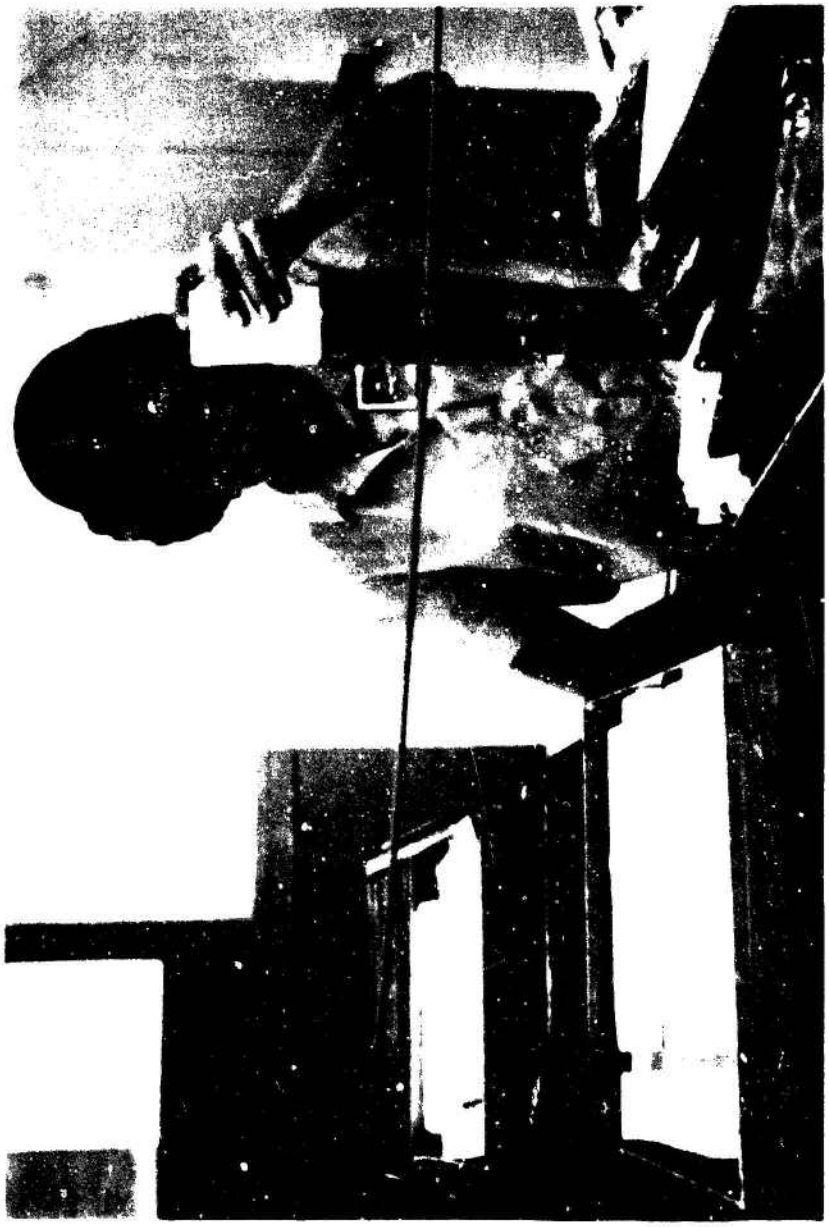

Slide 14

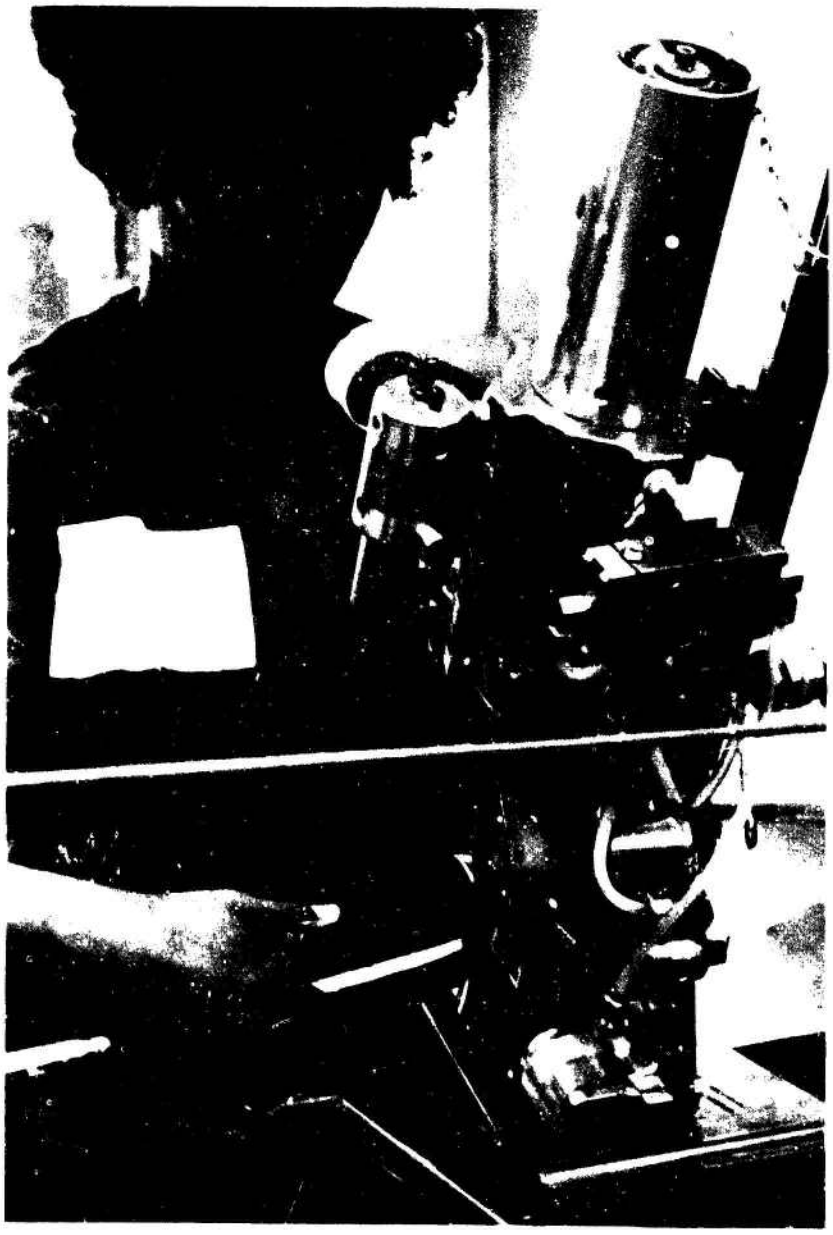

Slide 15

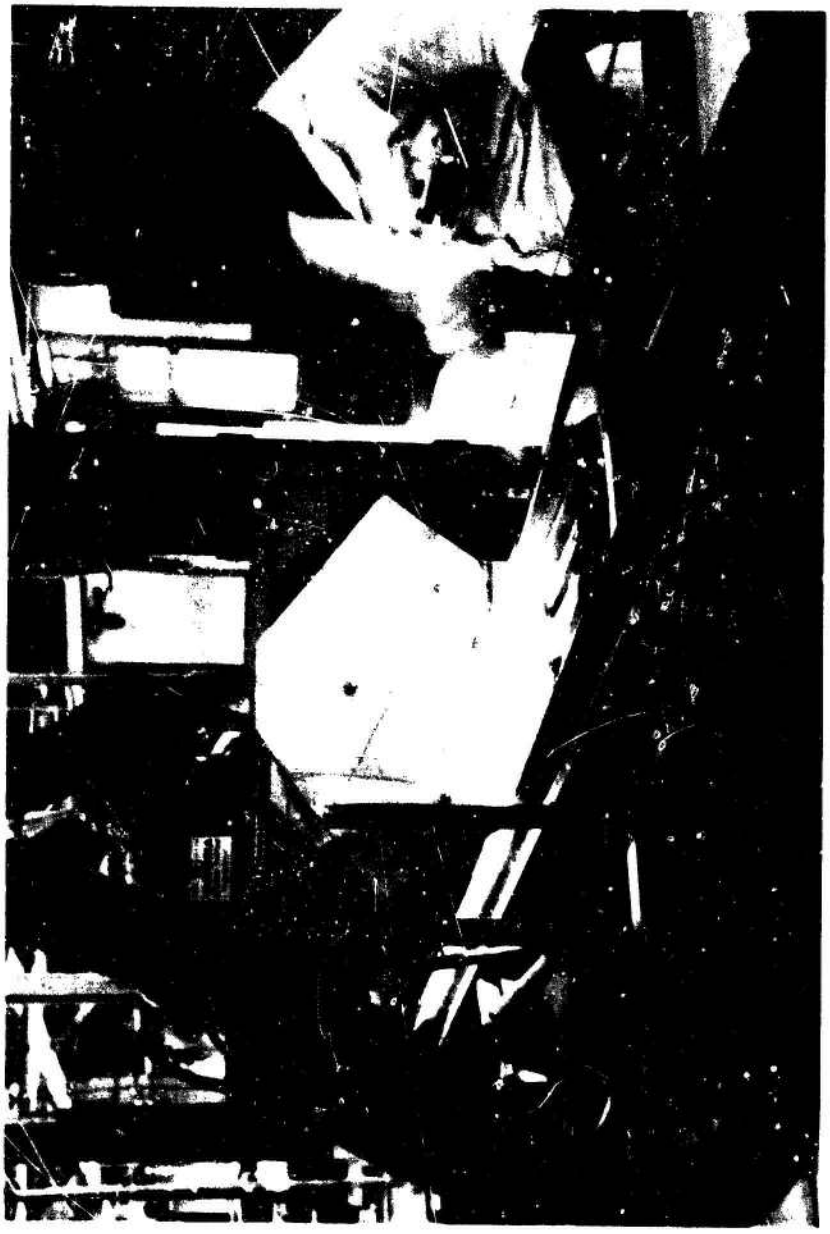

Slide 13

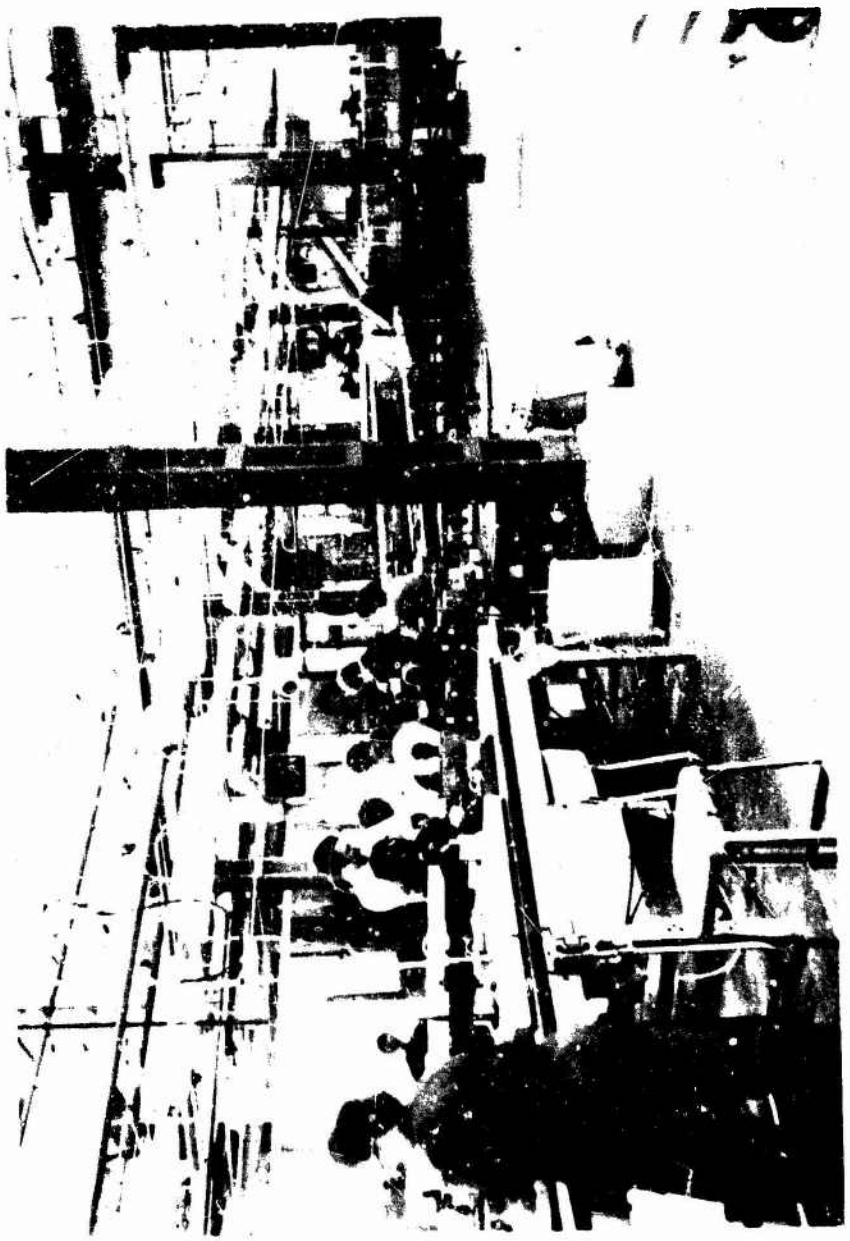

Slide 17

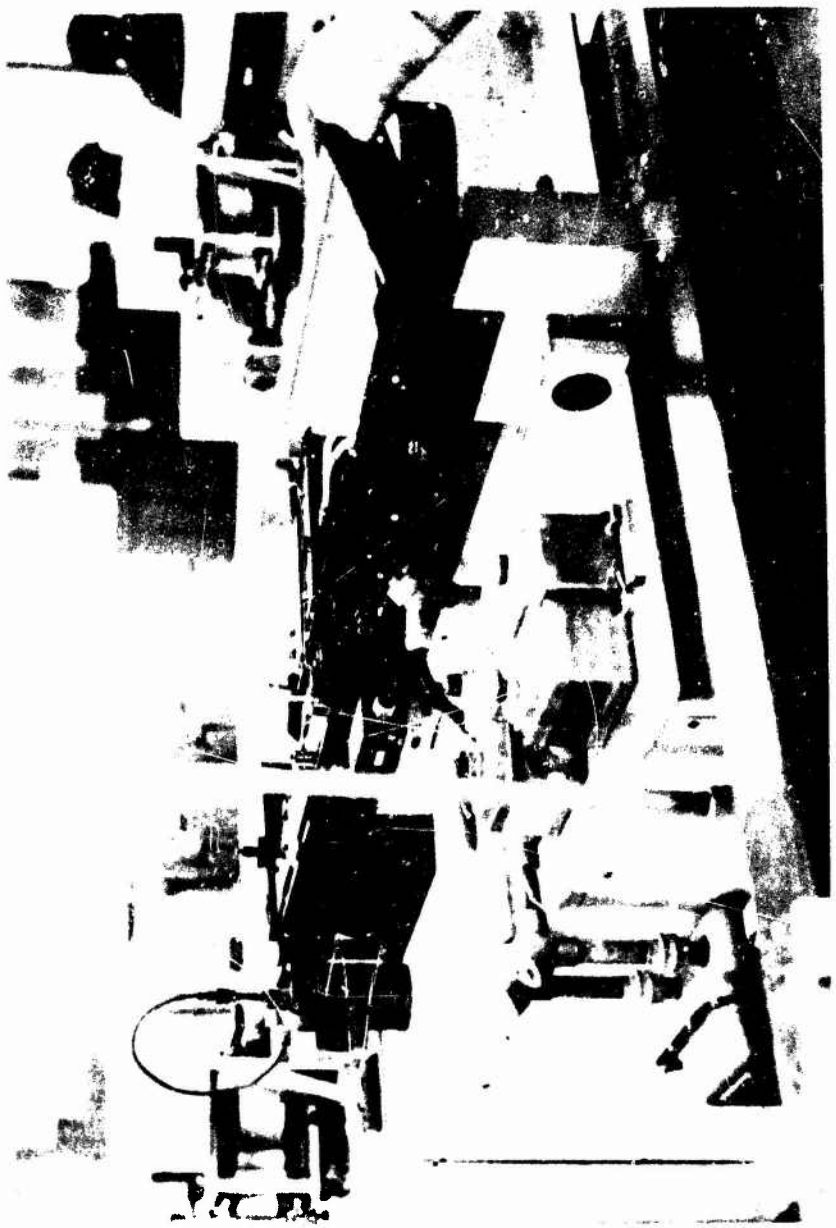

Slide 18



Slide 19



Slide 20

Slide 21



Slide 22



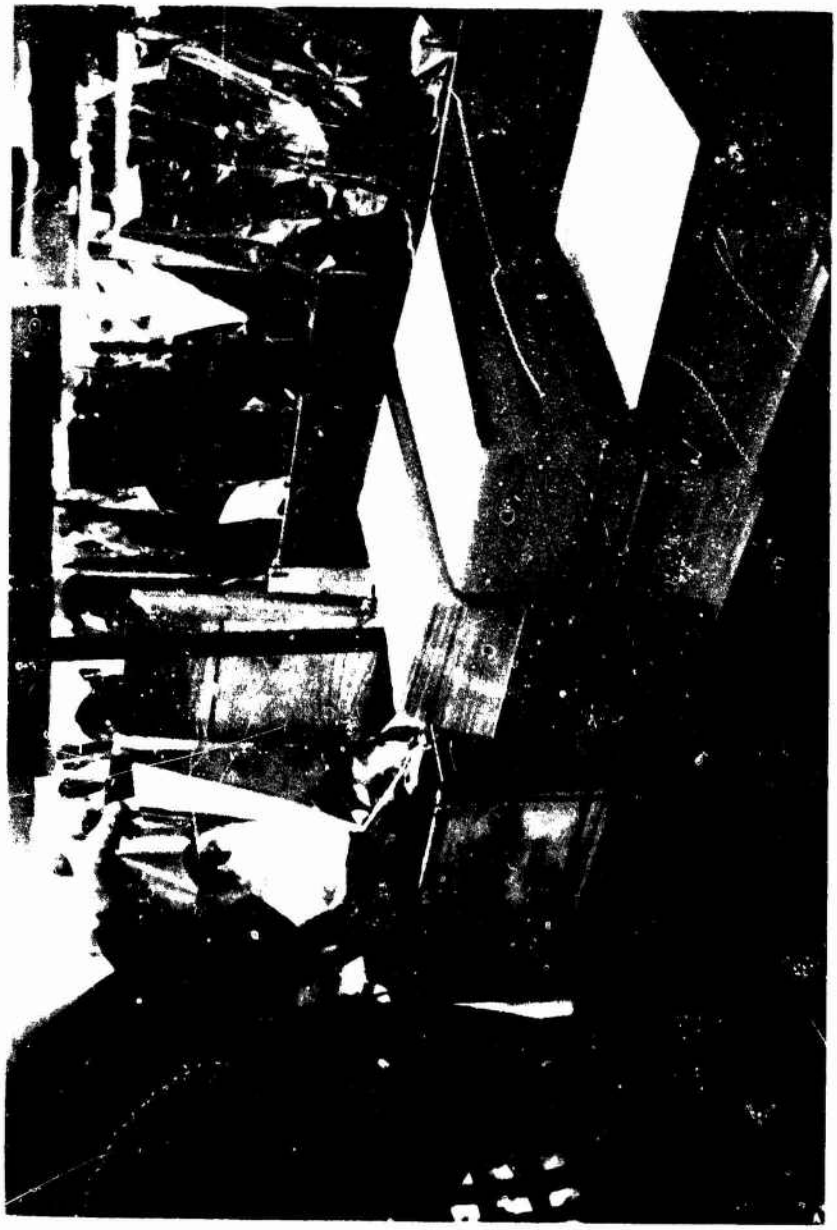

Slide 24



Slide 25

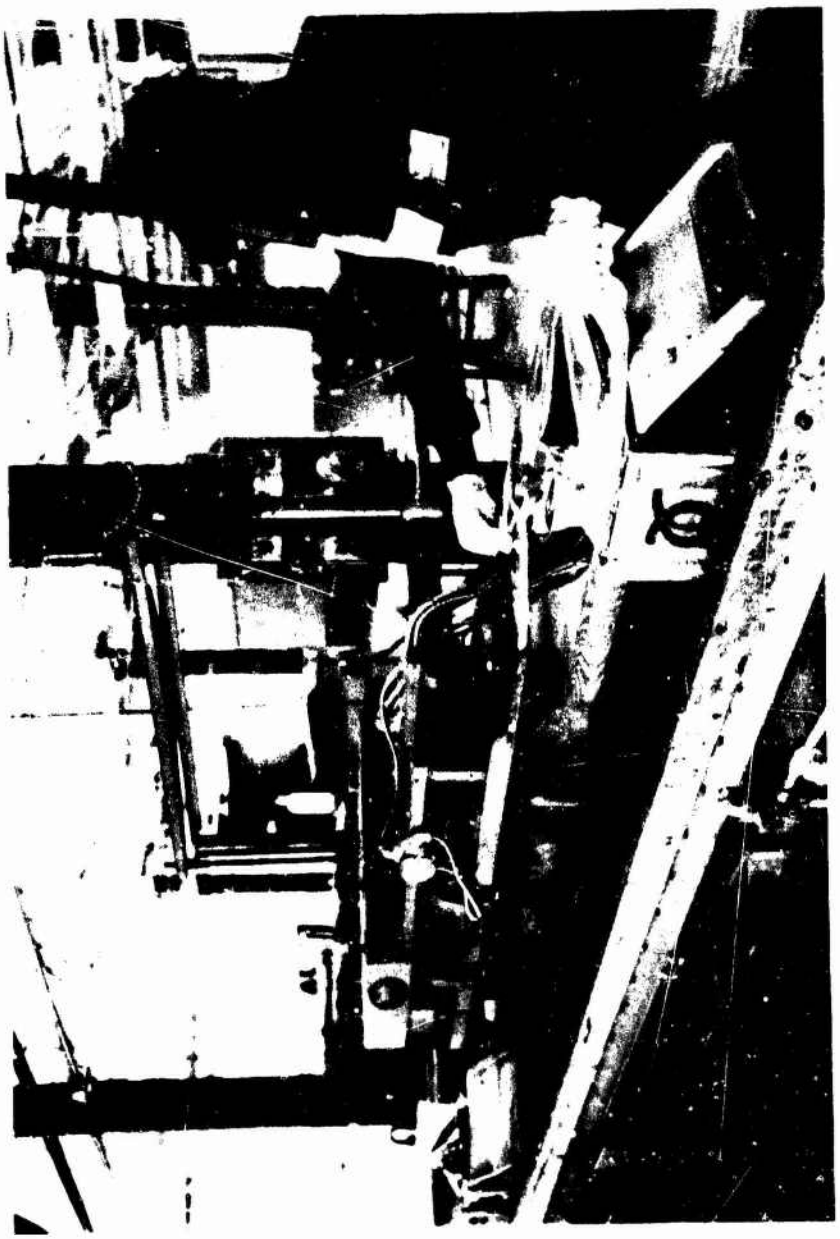



Slide 27

Slide 28

Slide 29



Slide 30

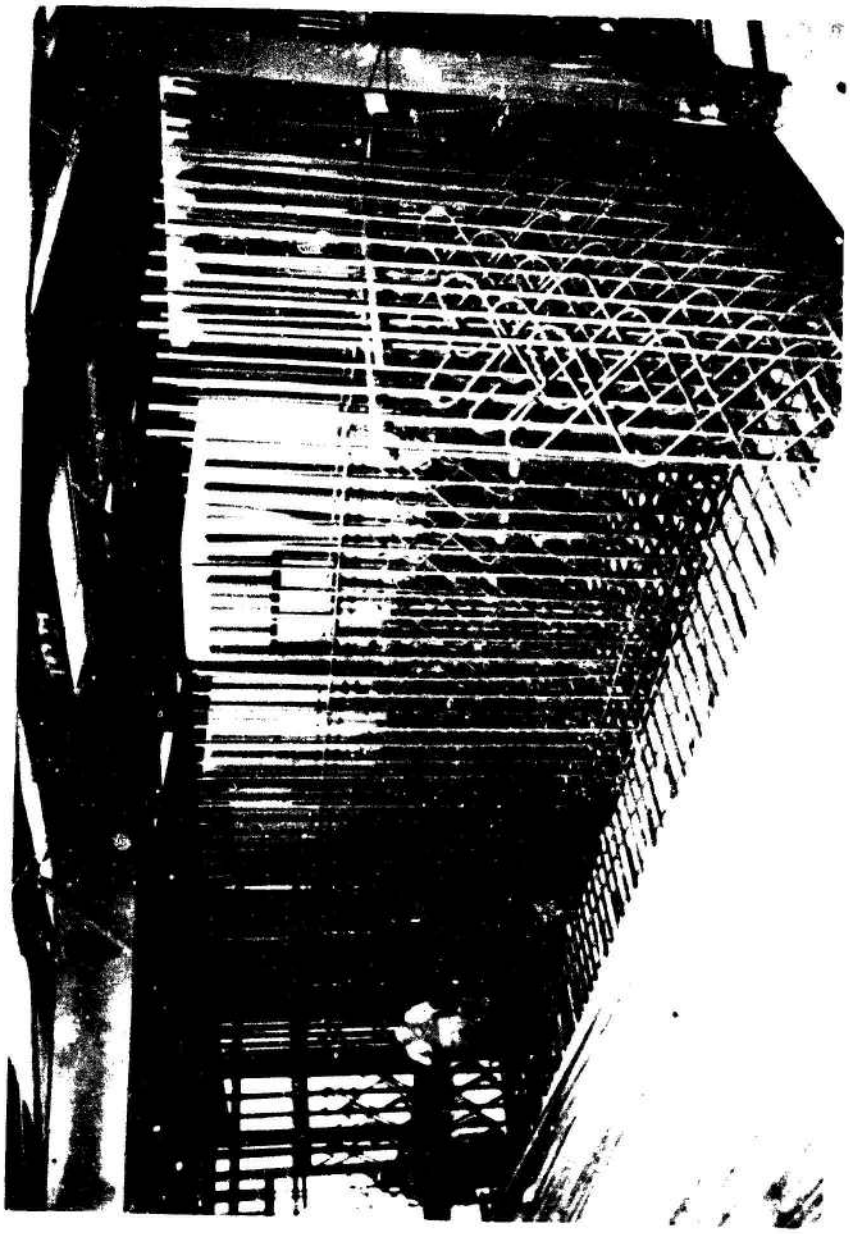

Slide 31A

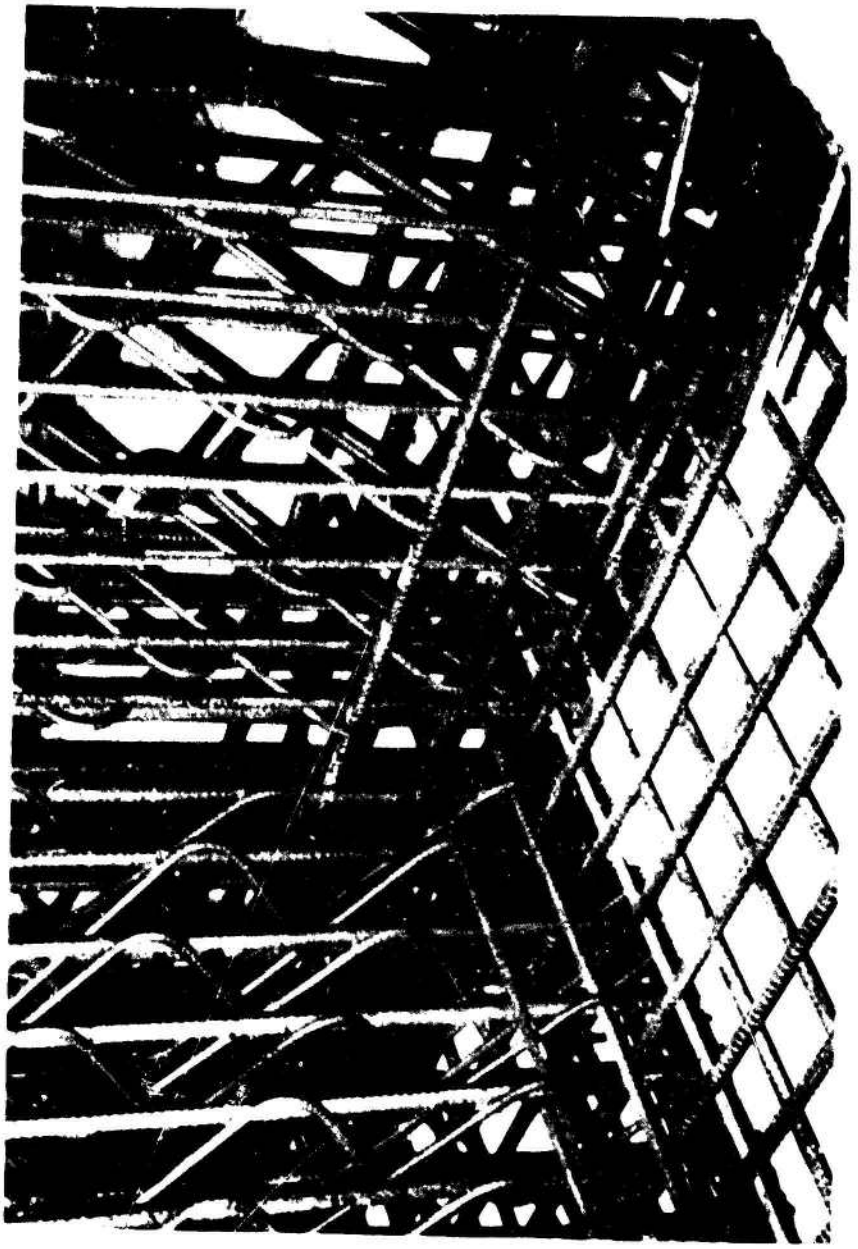

Slide 31B

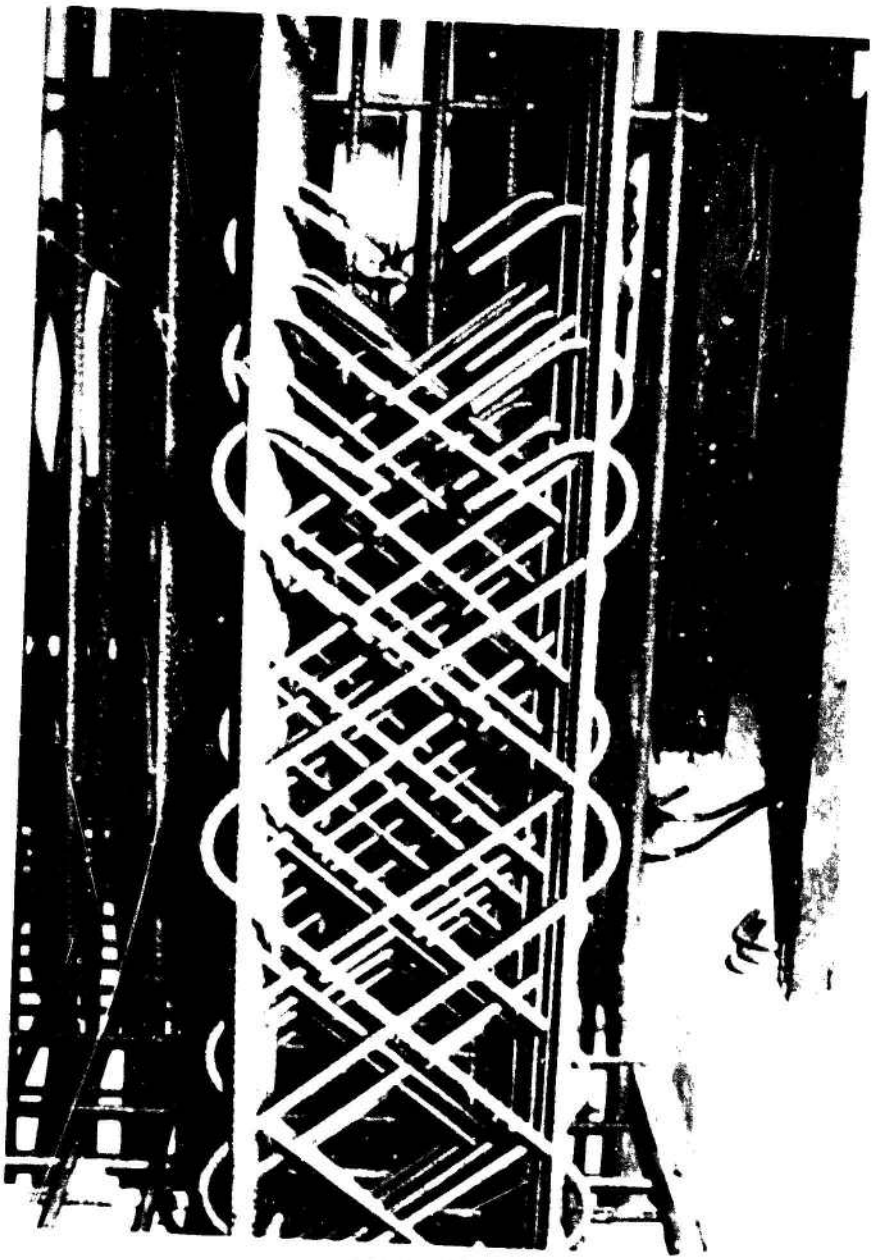

Slide 310

FLUID ENERGY MILLING OF HMX

Walter J. Moodie
Mound Facility*
Miamisburg, Ohio 45342

ABSTRACT

Fine-particle HMX powders are of interest for a variety of applications in Department of Energy weapons programs. A process is described for producing these materials in two stages: first, precipitation to yield a relatively coarse, free-flowing product of the desired polymorph, followed by dry grinding in a fluid energy mill using air as the working fluid. Surface area of the final product can be specified over a wide range by varying the parameters of the grinding operation. Inherent safety features of this type of mill are discussed, in addition to several operating procedures which further increase the safety of the grinding process.

INTRODUCTION

The firing characteristics of detonators and other explosive devices which use powdered explosives are determined to a significant extent by the particle size, size distribution, and particle shape of the explosive powder. This has led to a demand for fine particle size HMX powders for a variety of applications in Department of Energy weapons programs.

With other explosive compounds, such as PETN or RDX, particle size can be controlled over a wide range by suitable selection and control of the parameters of the recrystallization process, such as type of solvent and precipitating agent, solution concentration, temperatures, order of addition, addition rate, type of agitation, etc. With HMX the situation is complicated by the fact that HMX occurs in four polymorphic forms: alpha, beta, gamma and delta. Some of the pertinent properties of these polymorphs are compared in Table 1.

*Mound Facility is operated by Monsanto Research Corporation for the U.S. Department of Energy under Contract No. EY-76-C-04-0053.

PRECEDING PAGE BLANK

The beta form is the most stable at ordinary temperatures, and also has the lowest impact sensitivity, therefore beta HMX is the preferred polymorph for current detonator applications. Unfortunately, high surface area pure beta HMX cannot be recrystallized directly (to the best of our knowledge), as conditions which produce a very fine crystal size also favor the formation of the other polymorphs, usually alpha or gamma. In other words, conditions which favor the formation of beta HMX also promote crystal growth, resulting in relatively large crystals and correspondingly low surface area.

FLUID ENERGY MILLING - INHERENT SAFETY FEATURES

Thus, some form of particle reduction is necessary to produce high surface area beta HMX. Ball milling (wet) has been used, but one drawback to this method is the inherent potential of contamination from the wear products of the grinding media. A second disadvantage is the tendency of the finely divided product to form a dense cake in the filtering and drying process to remove the carrier liquid. This leads to a lumpy product and the lumps are usually quite difficult to break up. We have employed a dry grinding process utilizing a fluid energy mill, with a view to minimizing these problems. The use of a fluid energy mill for grinding explosives was reported by Albus in 1964 [1].

The following features of this type of mill are important from the safety standpoint, although they obviously do not guarantee the safety of any specific application:

- absence of heat build-up (Joule-Thompson effect provides cooling)
- no moving parts
- no metal-to-metal friction or moving contact
- no compaction of powder
- no electrical or mechanical spark source.

To provide additional perspective from the safety standpoint, HMX is compared with other explosives with respect to selected physical properties in Table 2.

RECRYSTALLIZATION OF BETA HMX

As mentioned previously, the recrystallization of HMX to produce predominantly beta HMX yields a relatively low surface area product. The process we use is a scaled-up and modified version of a Picatinny Arsenal small scale (5 g) procedure. HMX is dissolved in dimethylsulfoxide (DMSO), filtered, and added slowly to an ethanol/acetone mixture with stirring. The filtration apparatus and the precipitation vessel are shown in Figures 1 and 2, respectively. Initial crystallization consists of a mixture of the polymorphs, mostly beta and gamma, but essentially complete transition to the beta form

occurs during the latter stages of the addition and during a subsequent digestion period. The slurry is also cooled during the digestion, to increase yield. The batch is then filtered, washed with ethanol, and oven dried at 60°C. Batch size is 1400 g, yield approximately 92-94%. The final product is 95+% beta HMX, usually with a trace of alpha and/or gamma HMX, is free flowing, and has a surface area of approximately 1400 cm^2/g (equivalent spherical diameter = 22.6 μm).

OPERATING PRINCIPLE OF THE FLUID ENERGY MILL

The low surface area product of the precipitation process is used as feed material for the fluid energy mill, Model MJ-4, manufactured by Fluid Energy Processing and Equipment Company, Hatfield, Pa. This is the lab scale model of the mill; it is also available in several larger sizes. The mill is shown assembled in Figure 3 and disassembled in Figure 4. Air enters the grinding chamber as high velocity jets through nozzles around the inner surface of the manifold. Feed material is drawn into the chamber by a venturi jet, and introduced into the highly turbulent vortex of the grinding chamber. Particle reduction occurs primarily by collision between particles, with relatively little occurring as a result of impact with the chamber surfaces. Ceramic liners are used to reduce wear and to minimize metal contamination. Centrifugal force tends to keep the larger particles in the grinding zone, i.e., toward the outer edge of the grinding chamber, while the finer particles move toward the center where they are removed in the exhaust air stream to the collector system. The latter consists of a stainless steel vessel with a deflector on the inlet to provide centrifugal separation in addition to gravity settling. The air exhausts through a microweave nylon filter cloth backed up by a heavy filter paper and supported by expanded metal. The complete apparatus, including screw feeder, fluid energy mill, and collector system, is shown in Figure 5.

SAFETY PROCEDURES

With the inherent safety features of the fluid energy mill listed previously, the chief potential hazards associated with the milling operation are considered to be the impact energy due to particle collisions and the possibility of a spark due to static discharge. The following safety precautions are included as part of the operating procedure:

1. Grinding of explosives limited to those materials with relatively low impact and spark sensitivity.

2. Multiple grounding of equipment to prevent accumulation of static charge.

3. Drive motor and vibrating motor of feeder totally enclosed and air purged to keep dust out of potential spark source areas.

4. Speed control unit (non E P) located out of the operating area.

5. Grinding performed in increments with minimum quantity in the system at any given time.

6. Remote operation -- operators outside processing cell during grinding, protected by blast wall. Cell has one blow-out wall.

7. Standard precautions -- conductive floors and shoes, cleanliness, awareness, avoid complacency, etc.

OPERATING EXPERIENCE AND CONTROL

To date, approximately 90 grind increments have been made without incident, the quantity (i.e., wt of feed) ranging from 10 to 192 g, with an average of 96 g. Products have been obtained with surface areas from approximately 3600 to 31,000 cm^2/g (equiv. spherical diameter 8.77-1.02 μm). The products are well dispersed and free from lumps. Handling properties are generally good, although very fine powders are susceptible to accumulating a static charge and thus can become difficult to handle if worked excessively.

The surface area dependence upon the principal control parameters, manifold pressure (more exactly, manifold supply pressure) and feed rate, is shown in Figures 6 and 7. Increasing the manifold pressure increases the particle velocity and collision energy, resulting in greater reduction of particle size. Reducing the feed rate, thereby increasing residence time, also works in the direction of reducing particle size. The surface areas shown were measured after baking the powders and thus are slightly lower than the corresponding values after grinding but before baking. The graphs indicate that control of the process is fairly satisfactory, assuming a uniform feed rate can be maintained. This in turn requires that the feed material have good flow properties as any tendency to pack in the screw will result in an erratic feed rate. The scanning electron micrographs (SEM) in Figure 8 show the reduction in particle size for a typical grind. Note the different magnification for these two SEM's.

SUMMARY

Dry grinding of beta HMX has been accomplished on a small scale in a fluid energy mill with air as the working fluid. A screw feeder is used to provide a uniform feed rate, and a specially designed collector system separates the product from the exhaust air. The surface area of the product can be controlled, within fairly narrow limits, over a wide range by varying air pressure and feed rate. Inherent safety features of this type of mill and special working precautions, including adequate grounding of equipment and remote operation, combine to increase the safety of the process.

REFERENCE

1. Albus, F. E., "The Modern Fluid Energy Mill," Chemical Engineering Progress, 60, No. 6, June 1964, pp. 102-106.

Table 1 - SELECTED PROPERTIES OF THE HMX POLYMORPHS[a]

Property	HMX Polymorph			
	Beta	Alpha	Gamma	Delta
Crystal System	Monoclinic	Orthorhombic	Monoclinic	Hexagonal
Habit	Massive	Needles	Massive, Platy	Rods, Needles
Stability Range, °C	To 146	146 - 156	>156	Metastable, All Temps
Density, g/cm^3	1.90	1.82	1.76	1.80
Impact Sensitivity, cm	31-32	5 - 50	6 - 25	6 - 12

[a]Reference: Physical and Chemical Properties of RDX and HMX, Holston Defense Corporation, Control No. 20-P-26, Series A, March 1962.

Table 2 - SELECTED PROPERTIES OF HMX AND OTHER EXPLOSIVES[a]

Property		HMX	RDX	PETN	TNT
Molecular wt.		296.2	222.1	316.2	227.1
Density, g/cm^3		1.900	1.806	1.77	1.654
M.P., °C		285-287	205	139-142	80.9
ΔH_{det} (exper), kcal/g		1.48	1.51	1.49	1.09
ΔH_f, kcal/mol		+17.93	+14.71	-128.7	-15
Thermal Stability, cm^3 gas at 120°C					
0.25 g for 22 hr		<0.01	0.02-0.025	0.10-0.14	0.00-0.012
1 g for 48 hr		0.07	0.12-0.9	-	∿0.005
Detonation Velocity, km/sec		9.11 (ρ = 1.89)	8.70 (ρ = 1.77)	8.26 (ρ = 1.76)	6.93 (ρ = 1.64)
Impact Sensitivity, H_{50}, cm:	Type 12 tooling	33	28	11	80
	Type 12B tooling	40	-	-	>177
Gap Test, mm	Small scale	-	4.8-5.6 (ρ = 1.735)	4.8-5.6 (ρ = 1.757)	0.20-0.41 (ρ = 1.624)
	Large scale	70.7 (ρ = 1.07)	61.8 (ρ = 1.750)	69.4 (ρ = 0.81)	49.4 (ρ = 1.626)

[a]Reference: Dobratz, B. M. (ed.), Properties of Chemical Explosives and Explosive Simulants, Lawrence Livermore Laboratory Report UCRL-51319, Rev 1, July 31, 1973.

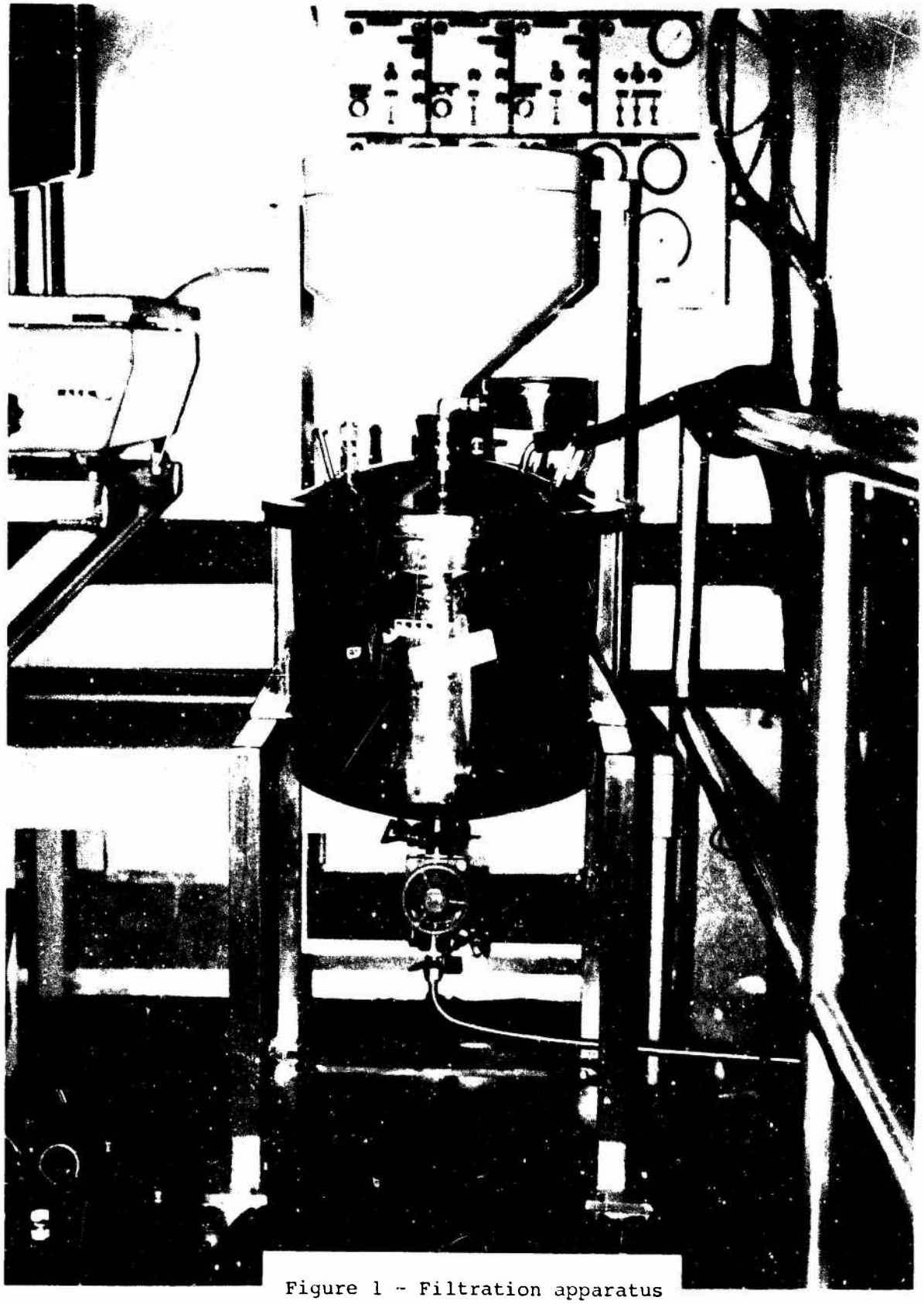

Figure 1 - Filtration apparatus

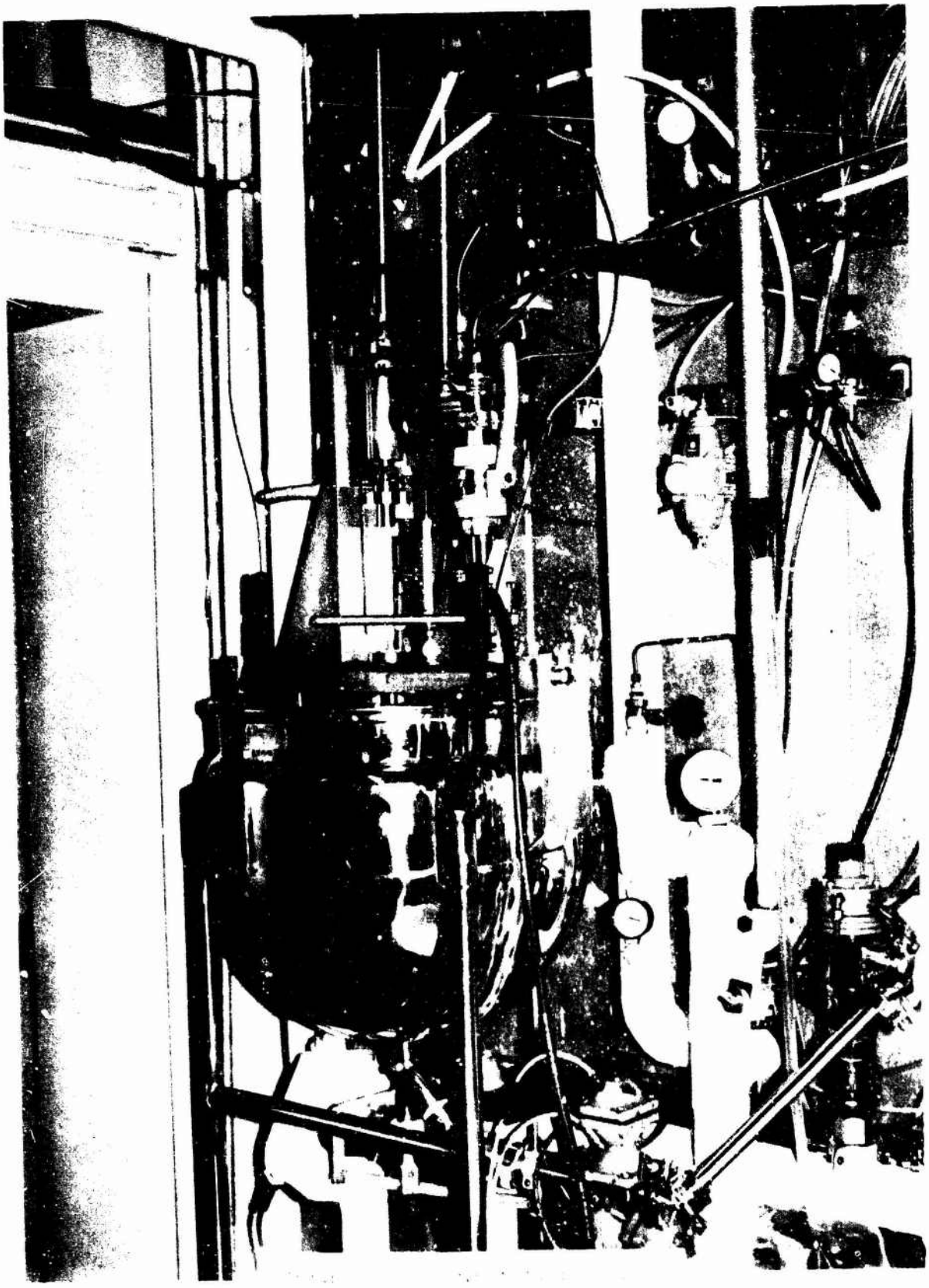

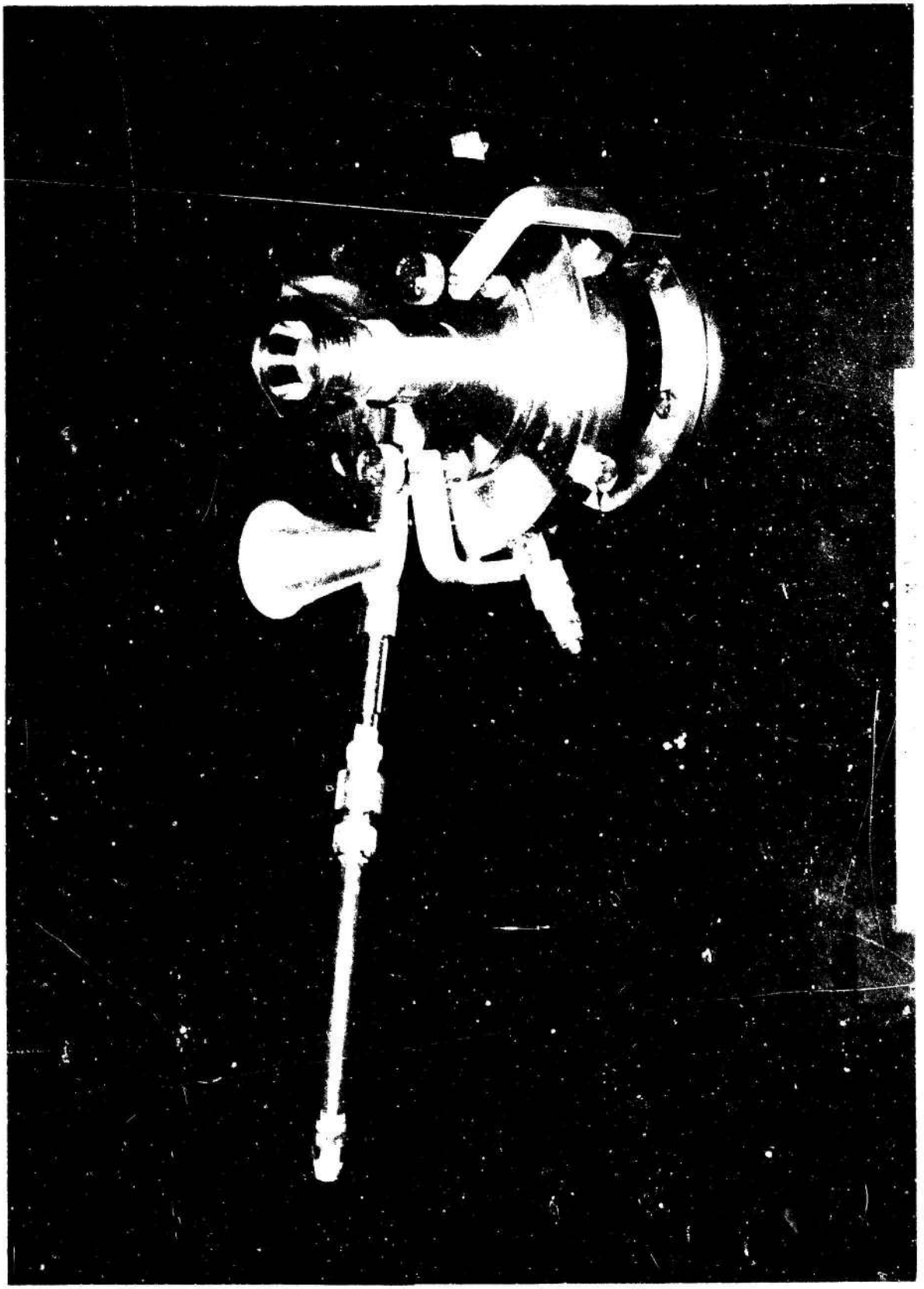

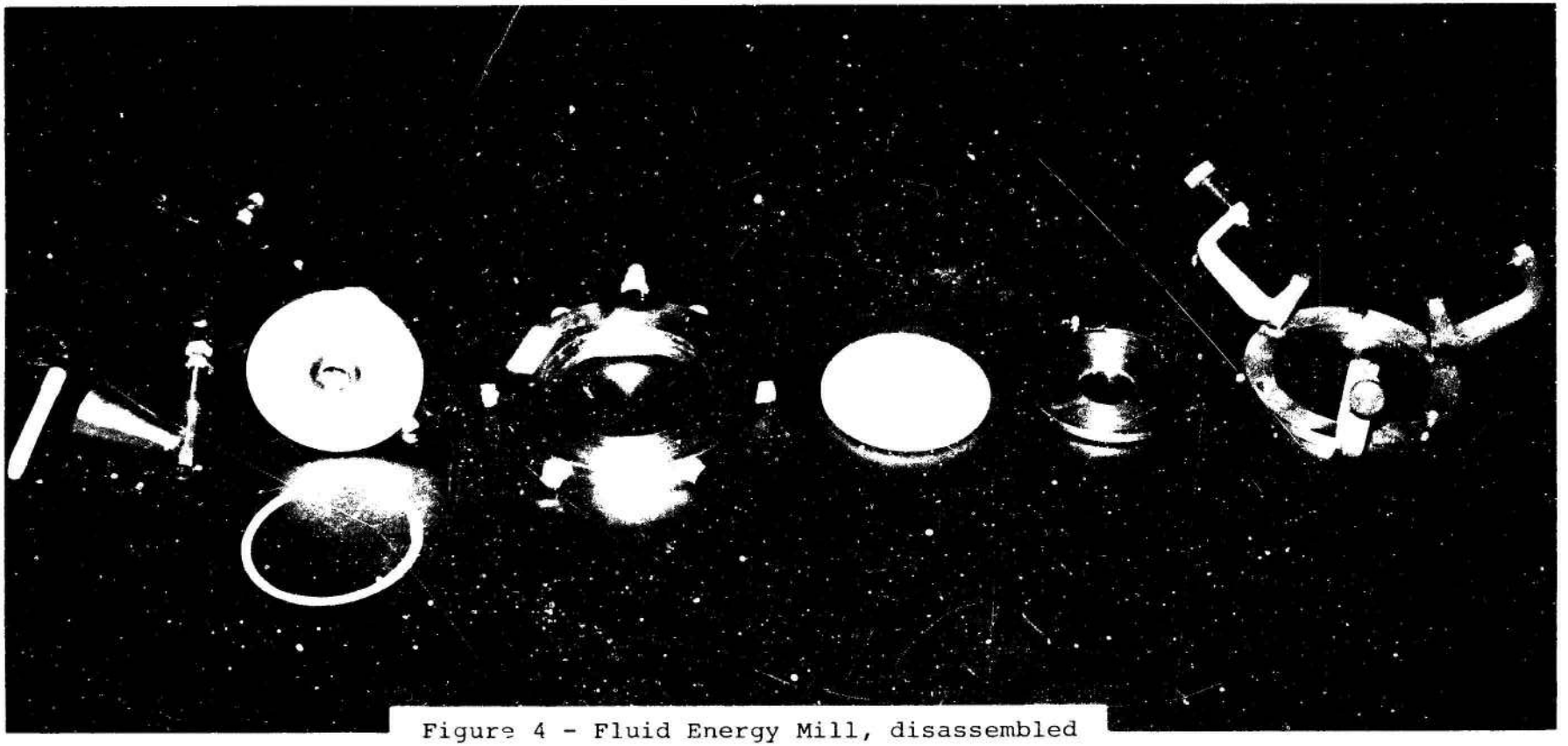

1686

Figure 4 - Fluid Energy Mill, disassembled

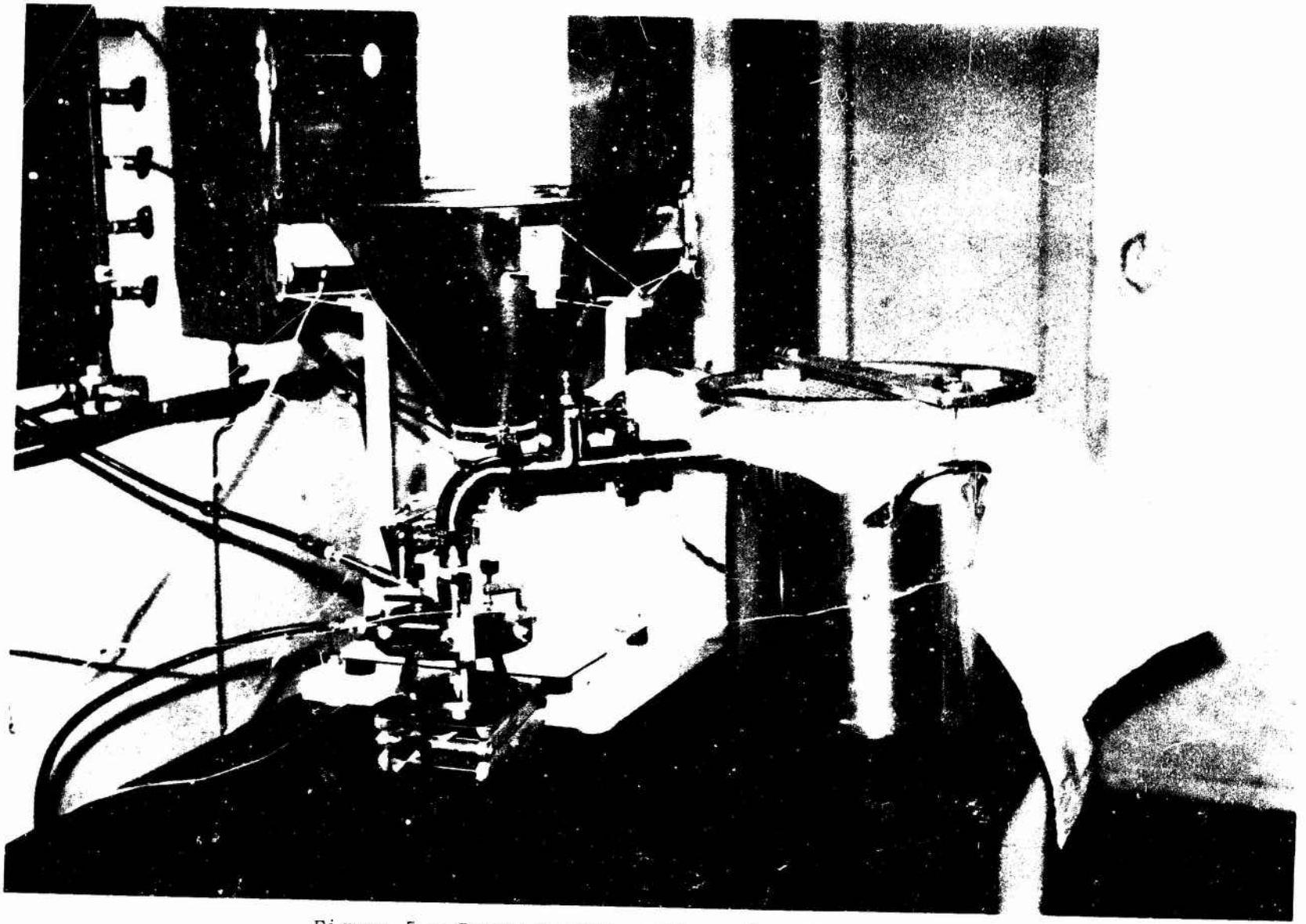

Figure 5 - Screw feeder, mill, and collector system

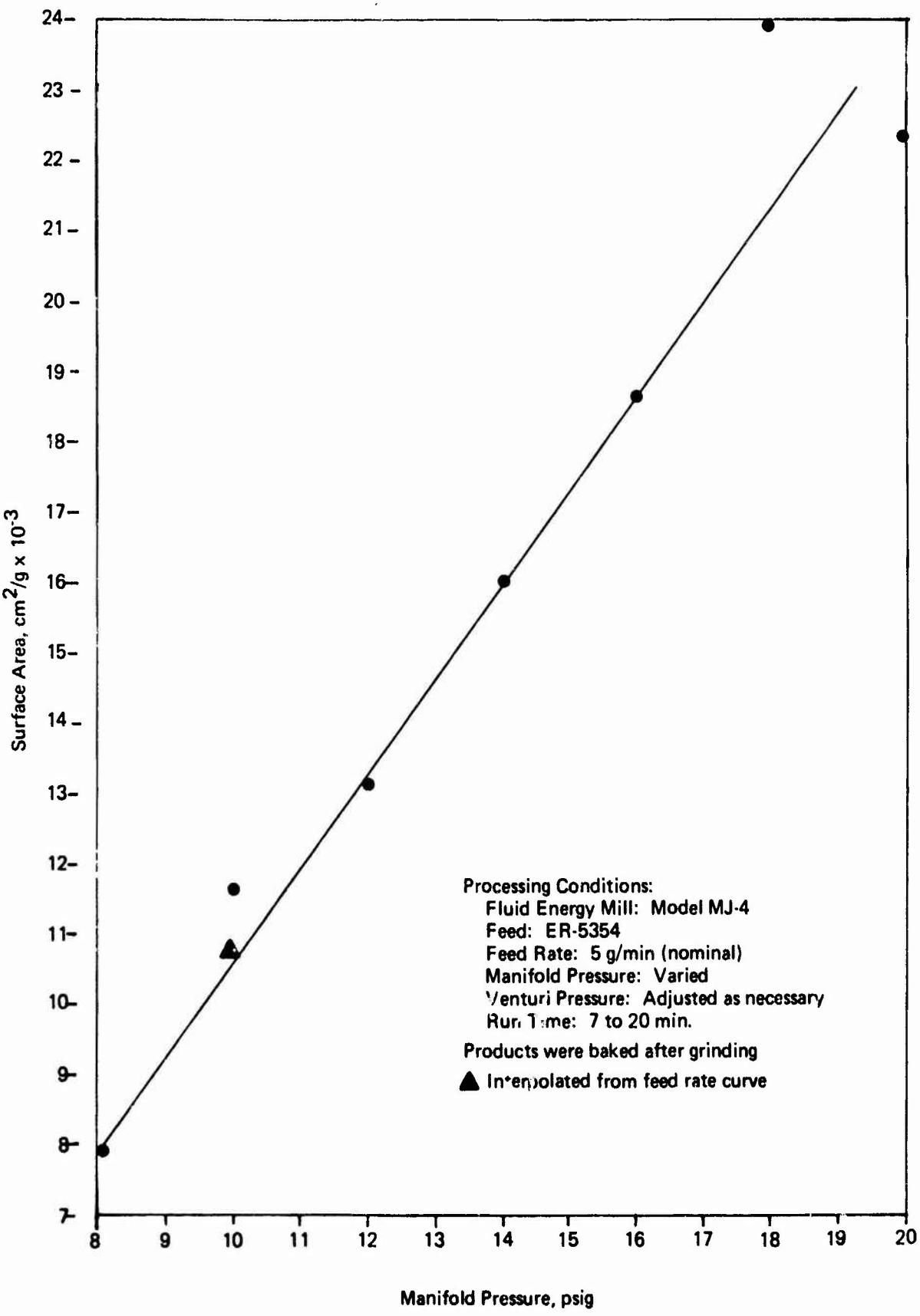

Figure 6 - Grinding of HMX: Effect of manifold pressure on surface area.

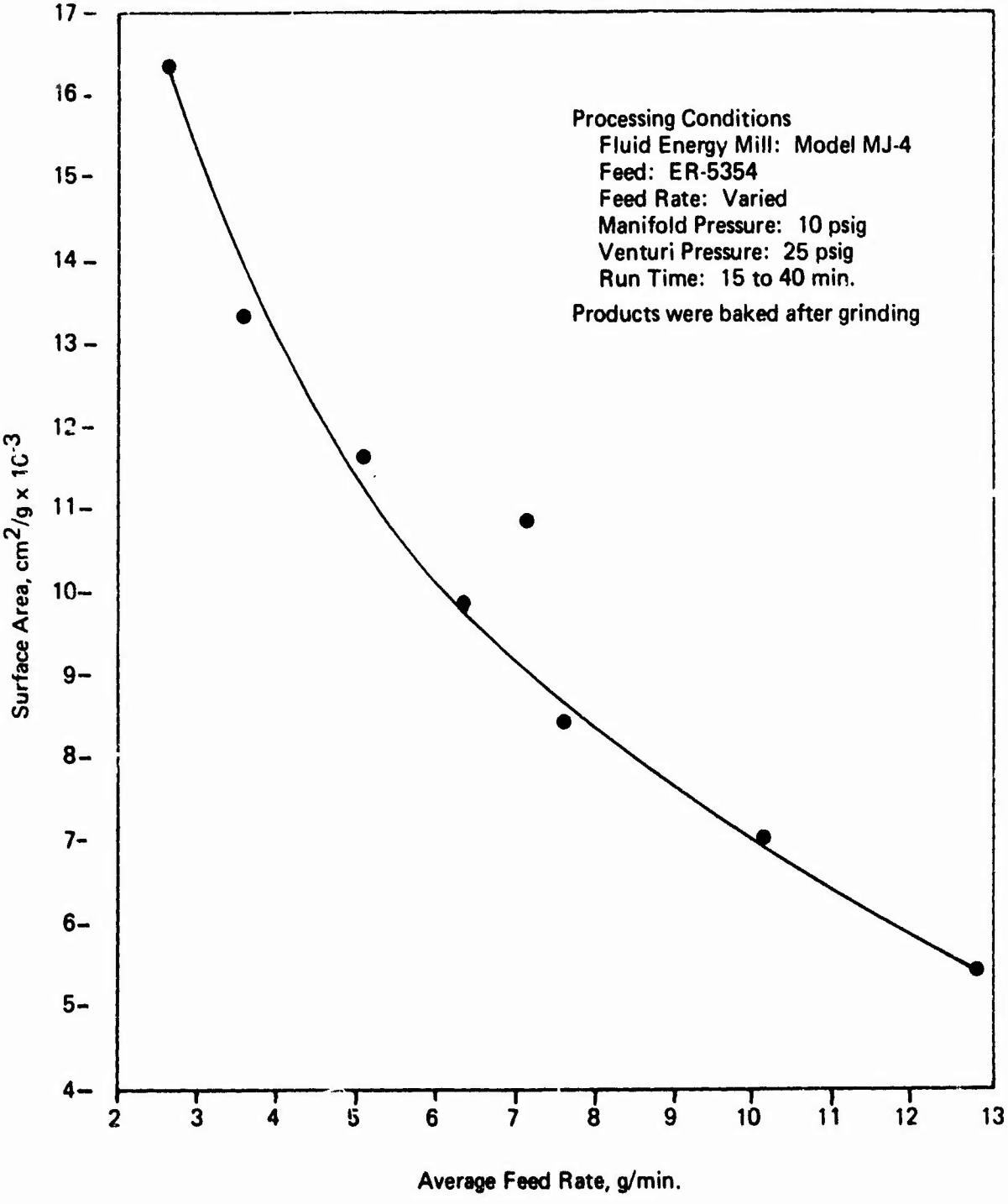

Figure 7 - Grinding of HMX: Effect of feed rate on surface area.



ER 5343

150 X

PRECIPITATED PRODUCT
1380 m^2/g

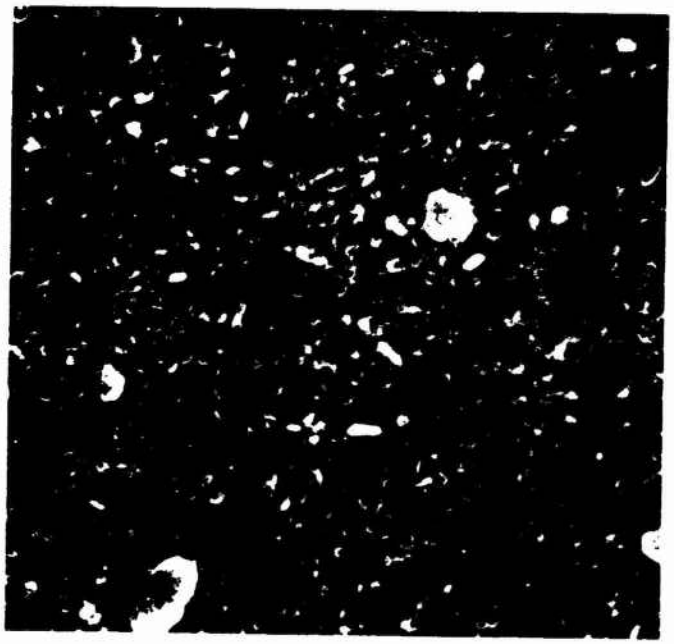

ER 5375

700 X

FLUID ENERGY MILLED PRODUCT
21,980 cm^2/g

SEMs OF UNMILLED AND MILLED BETA HMX

Figure 8 - SEM's of unmilled and milled beta HMX

EIGHTEENTH DOD EXPLOSIVES SAFETY SEMINAR

El Tropicano Hotel
San Antonio, Texas
September 12-14, 1978

ENVIRONMENTAL EFFECTS ON ELECTROSTATIC SENSITIVITY OF ENERGETIC MATERIALS

L.D. Haws, L.W. Collins, and A. Gibson

Monsanto Research Corporation

Mound Facility*

Miamisburg, Ohio 45432

ABSTRACT

The surroundings, in addition to the chemical and physical nature of the energetic material itself, markedly affect the sensitivity of energetic material to electrostatic stimuli. In particular, the effects of temperature, humidity and gas composition on the electrostatic sensitivity of selected pyrotechnic ingredients and compositions are being investigated; preliminary results are presented here. In similar gaseous environments, ignition phenomena were also characterized by thermal analysis techniques. Data from this type of study should be a valuable aid in establishing sound operational safety criteria for processes involving these materials.

*Mound Facility is operated by Monsanto Research Corp. for the U.S. Department of Energy under Contract No. EY-76-C-04-0053.

Introduction

Within the past few years, a number of agencies involved in the design of explosive devices have made a commitment to utilize energetic compositions which meet performance requirements but are less susceptible to accidental initiation than currently used primary explosives. One type of energetic material which shows promise in a number of applications is metal powder/oxidizer pyrotechnic compositions. Although these materials have a long history of use in certain areas, recent applications extend into functions traditionally dominated by primary explosives. This prospect of increased usage of pyrotechnics necessitates thorough scientific studies into the physical and chemical properties of these materials in order to guarantee component reliability and personnel safety.

One of the primary concerns in the handling of pyrotechnic mixes is the accidental electrostatic initiation through discharge from a human body. While we can measure the sensitivity of a material to electrostatic discharge, relatively little is known as to the mechanism of the spark interaction or the factors which affect the spark sensitivity. In order to properly evaluate the safety of pyrotechnic compositions, we felt that controlled testing must be performed to delineate those factors which influence the susceptibility of a material to spark initiation. The results of these experiments will be discussed and related to the safe handling of pyrotechnic materials.

Experimental Conditions

In order to evaluate the factors which influence the spark sensitivity of pyrotechnic materials, a versatile electrostatic sensitivity tester was fabricated to control environmental and instrumental parameters designated by the experimental design. The construction and operational details of this instrument have been reported previously[1]. Although the electrical resistance and capacitance in the electrostatic discharge circuit can be varied with this instrument, all testing reported here used constant values of 500 ohms and 600 pF since these values have been shown to be a reasonable electrical simulation of a human body.[2] Sample size and geometry were maintained as constant as possible, as were spark gap width and electrode surface condition.

For each data point, a sample weighing approximately 10 mg was placed in the electrode cavity and the spark gap adjusted to the proper dimensions. The chamber was then sealed, and, where appropriate, evacuated, and back-filled with a selected gas composition. The voltage was then selected, the capacitors discharged across the gap, and the results, "ignition" or "no-ignition," were recorded. In order to qualify as a "no-ignition," a spark must have been visually observed to cross the gap. Otherwise, the capacitors were again charged and discharged without changing the sample. If the spark was observed but no ignition occurred, the same sample was simply rotated to expose fresh material to the spark and again tested at the higher voltage. Voltage was varied and the data reduced according to the Bruceton technique.

Factors Influencing Spark Sensitivity of Pyrotechnics

Because the physicochemical nature of the spark initiation of pyrotechnics is not well understood, experiments were conducted to identify material and environmental factors which are relevant to this process. Five different factors were investigated:

1. Fuel surface area
2. Fuel composition
3. Humidity
4. Atmospheric composition
5. Temperature

The first two factors are characteristics of the pyrotechnic fuel and can practically be varied only within limits established by required performances and mechanical criteria. However, the last three factors generally do not affect powder performance and are controllable in production environments. These factors then illustrate the two approaches to pyrotechnic safety - 1) selection and alteration of constituents, and 2) control of work and handling environment.

Influence of Fuel Properties

In order to establish the relationship between fuel characteristics (surface area and composition) and electrostatic sensitivity, samples of TiH_x where x = 0.69, 1.53 or 1.93 were fractionated into narrow particle size ranges using a Bahco Microparticle

Classifier. The fractions were then blended with potassium perchlorate in the ratio of 33 wt % TiH_x to 67 wt % $KClO_4$ and spark tested as previously described. Threshold spark sensitivity was found to depend upon both the surface area and composition of the fuel as shown by the graph in Figure 1. These curves show that the spark sensitivity increases as the hydride content decreases or as the surface area increases. Thus, pyrotechnic compositions of TiH_x/$KClO_4$ can be made safer by decreasing the fuel surface area or increasing the hydrogen content within the constraints of performance, mechanical, and stability requirements.

Of significance also was the fact that pyrotechnic compositions of $TiH_x/KClO_4$ were less sensitive than the corresponding TiH_x fuel alone. This phenomenon is shown in Table 1.

Influence of Environmental Factors

Experience tells us that it is easier to generate a spark from the body in the dry Western states than in the more humid regions of the country. It therefore seems reasonable that humidity might influence the tendency of a material to be ignited by spark although the exact relationship may not be obvious. Since our instrument permits control of the atmosphere surrounding the test sample, some quantification of the relationship was possible. As the humidity increased, the spark sensitivity of the sample decreased as shown in Table 2. Since the spark sensitivity at the low humidity is about twice that at the higher humidity, the hazard of accidental ignition in production processes can be substantially reduced by working at an elevated humidity. Due to the possible damaging effect of moisture on the stability of some pyrotechnic powders, a compromise sometimes must be reached to balance risk of powder degradation with handling safety. For most operations, a working humidity of 40-60% seems to be a reasonable compromise.

Atmospheric composition was found to be a key element in the spark initiation of the TiH_x powders and pyrotechnics. Some minimum quantity of oxygen is necessary for spark initiation to occur. This effect is shown in Figure 2. Above this minimum requirement, the threshold is independent of oxygen concentration. However,

below this minimum level, threshold sensitivity decreases rapidly to values greater than 50 kV. This is a strong indication that spark initiation occurs through a fuel-oxygen reaction rather than through a pyrotechnic reaction. Thus the possibility of spark initiation can be completely eliminated by working in an inert atmosphere such as argon. It should also be noted that while nitrogen gas is sometimes used for an inert atmosphere, comparison of Figure 2 with Figure 3 (See also Table 3) shows that the electrostatic sensitivity is greater in oxygen/nitrogen mixtures than in oxygen/argon mixtures, indicating a fuel-nitrogen reaction. Although no ignition occurred in pure nitrogen, oxygen contamination would be more serious in a nitrogen atmosphere than in an argon atmosphere since the minimum oxygen concentration required for ignition is lower in nitrogen than in argon.

Several of the pyrotechnic samples were tested at 100°C to determine if they became more sensitive as the temperature increased. No statistically significant difference was found between the sensitivities obtained for the high temperature and ambient temperature tests. Thus, within reasonable limits, temperature alone will not sensitize a pyrotechnic to spark initiation and does not influence handling procedures. However, "hot" pyrotechnics are generally drier and may be more sensitive than material equilibrated with room humidity since comparisons were based on a constant, very-low humidity test condition.

Summary

The experiments which have been described show that TiH_x pyrotechnic compositions can be made less sensitive to accidental electrostatic discharge initiation by using material with a low surface area or by increasing the hydrogen content of the fuel. However, both of these factors must be balanced against performance criteria established for the blend. Alternatively, the likelihood of accidental electrostatic discharge initiation can be eliminated by handling the powders in an oxygen-free environment or greatly reduced by working in high humidity conditions. It was also demonstrated that increasing the temperature of the blend to 100°C did not substantially affect the spark sensitivity of the material.

References

1. L.D. Haws, R.C. D'Amico, and A. Gibson, "Design, Development and Application of a Versatile Electrostatic Sensitivity Tester," Minutes of the Seventeenth Explosives Safety Seminar, Vol. 2, 1423 (1976).

2. T.J. Tucker, "Spark Initiation Requirements of a Secondary Explosive," Annals of the New York Academy of Sciences, 152, 643 (1968).

TABLE 1

THE SPARK SENSITIVITY OF TITANIUM HYDRIDE POWDERS
IS REDUCED ON COMBINATION WITH POTASSIUM PERCHLORATE

NOMINAL THRESHOLD SENSITIVITY, kV		PYRO BATCH NUMBER
TiH_x ONLY	$TiH_x/KClO_4$ (33/67)	
< 1	< 1	P03022
< 1	3	P03013
< 1	8	P03068
< 1	29	P03069
< 1	≥50	P03057
2	26	P03054
2	37	P03053
2	≥50	P03052
4	≥50	P03039
6	15	P03058
7	45	P03032
9	13	P03060
9	≥50	P03048
16	≥50	P03028
22	≥50	P03050
≥50	≥50	P03026
≥50	≥50	P03047

TABLE 2

INCREASING THE HUMIDITY CAUSES A SIGNIFICANT REDUCTION IN ELECTROSTATIC SENSITIVITY

CHAMBER HUMIDITY %	THRESHOLD	
	POTENTIAL, kV	ENERGY, mJ
10	11.5	39.6
45	13.6	55.5
65	17.0	86.7
85	27.7	230.1

TABLE 3

ELECTROSTATIC SENSITIVITY IS SIGNIFICANTLY AFFECTED BY THE OXYGEN CONTENT OF THE ENVIRONMENT

COMPOSITION OF ENVIRONMENT, VOL %			THRESHOLD SENSITIVITY, kV	
OXYGEN	NITROGEN	ARGON	Ti	$Ti/KClO_4$
5	95	0	>50	>50
10	90	0	11.6	15.8
15	85	0	4.7	6.7
21.0 (AIR)	78.0	0.9	2.6	5.7
30	70	0	2.1	5.9
50	50	0	1.5	6.1
5	0	95	>50	>50
10	0	90	>50	>50
15	0	85	7.9	16.9
30	0	70	1.7	4.6
50	0	50	1.8	5.7
0	30	70	>50	>50
0	80	20	>50	>50

1699

ELECTROSTATIC SENSITIVITY OF $TiH_x/KClO_4$ IS A FUNCTION OF FUEL SURFACE AREA AND HYDROGEN CONTENT

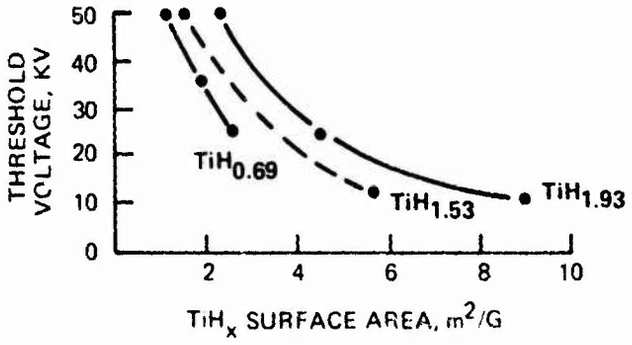

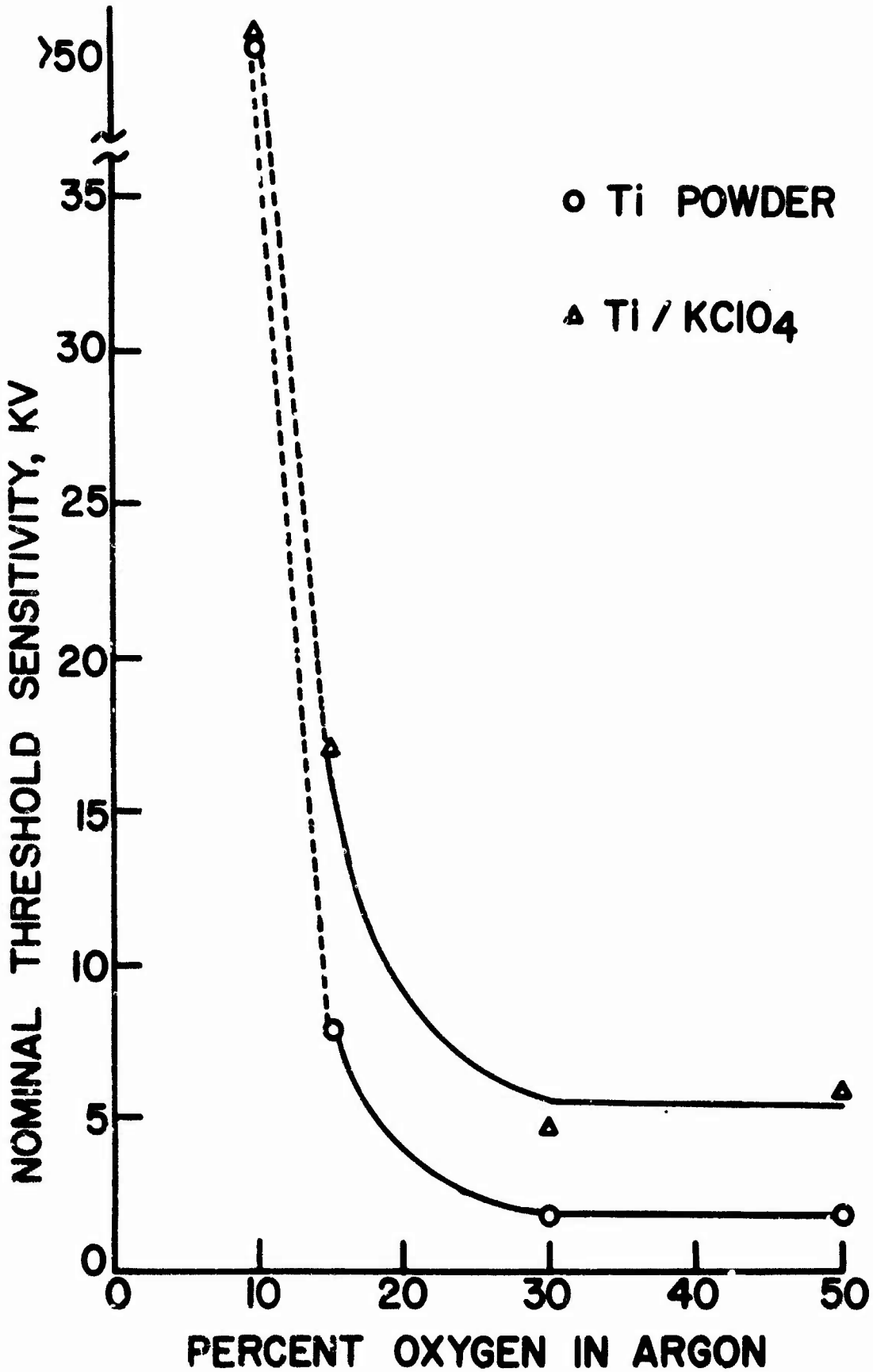
>50
35
30
25
20
15
10
5
0
NOMINAL THRESHOLD SENSITIVITY, KV
o Ti POWDER
▲ Ti / KClO4
0
10
20
30
40
50
PERCENT OXYGEN IN ARGON

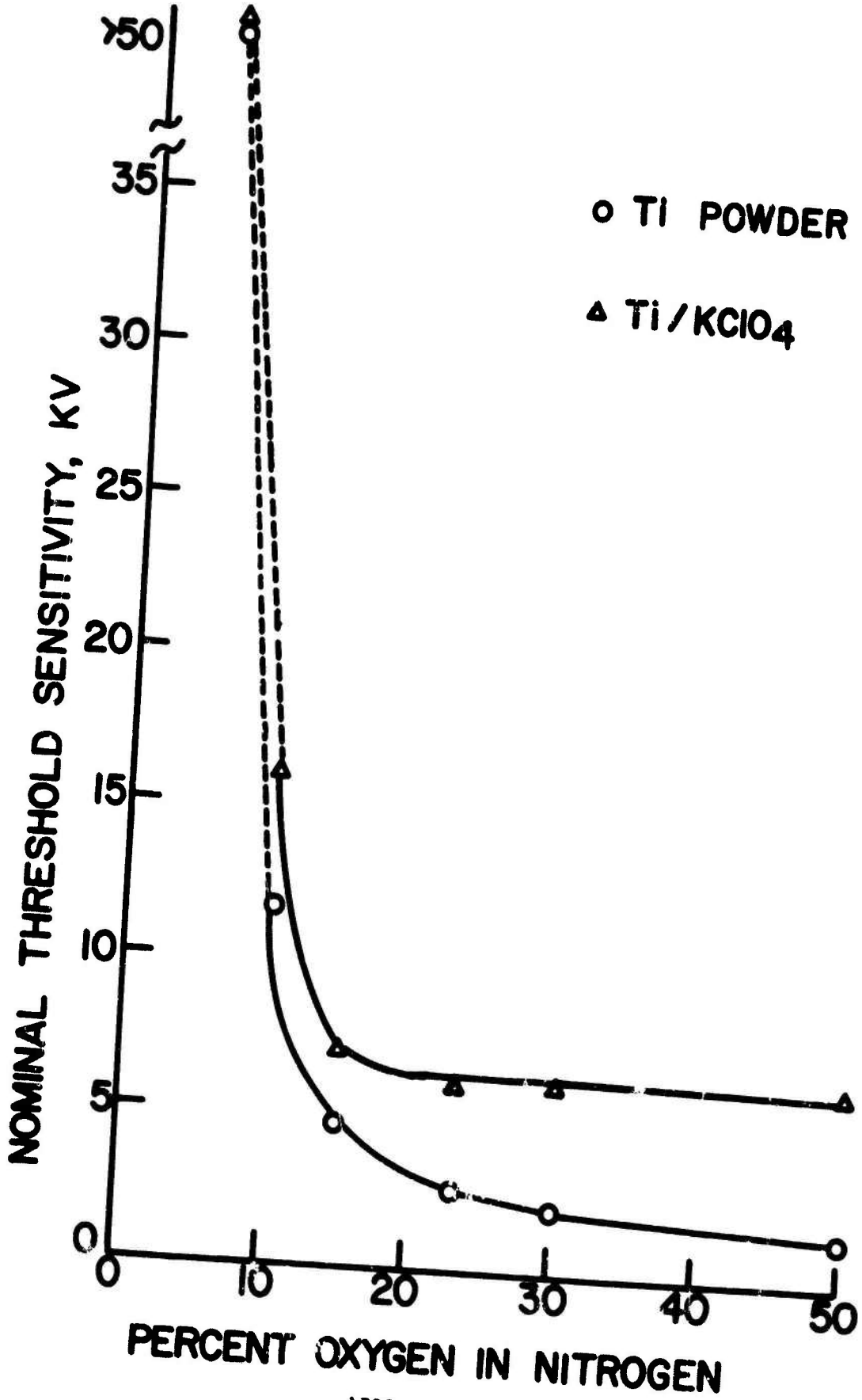
>50
35
30
25
20
15
10
5
0
NOMINAL THRESHOLD SENSITIVITY, KV
o Ti POWDER
▲ Ti/KClO4
0
10
20
30
40
50
PERCENT OXYGEN IN NITROGEN

SHIELDING OF FACILITIES FOR WORK WITH PYROTECHNIC AND EXPLOSIVE MATERIALS

BY

DR. DAVID J. KATSANIS

DEPARTMENT OF THE ARMY
US ARMY ARMAMENT RESEARCH & DEVELOPMENT COMMAND
CHEMICAL SYSTEMS LABORATORY
MUNITIONS DIVISION
ABERDEEN PROVING GROUND, MD 21010

SHIELDING OF FACILITIES FOR WORK WITH PYROTECHNIC AND EXPLOSIVE MATERIALS

David J. Katsanis
Chemical Systems Laboratory
Aberdeen Proving Ground, MD 21010

ABSTRACT

A relatively new concept is presented for protection to the area surrounding hazardous work with explosives. Suppressive shields are vented composite steel structures which are designed to confine all fragments from an accidental detonation and to suppress hazardous blast and flame effects to a safe level.

Department of Defense Explosives Safety Board has approved five groups of suppressive shields for protection of munitions production operations in US Army Ammunition Plants. Safety approved shields encompass seven different designs which range in size from a two foot diameter steel shell (Shield Group 6) to a ten foot diameter steel cylinder (Shield Group 3).

Studies have been conducted to develop a technological base for accurate determination of shield performance parameters. It was found early in the program that available data base was inadequate for accurately predicting the blast, fire and fragment effects that would occur as a result of an accidental detonation of an explosive in a shield environment. Indepth studies resulted in development of suppressive shield design procedures published in the Suppressive Shield Design Handbook which provides information needed for design of facilities where explosive materials are used in hazardous operations.

Details on safety approved shields will be presented with technology study results.

INTRODUCTION

Viewgraph 1 - Title

Suppressive shields are a relatively new concept for providing protection to the area surrounding hazardous work with pyrotechnic and explosive material. At present, these operations are either limited to small quantities, widely dispersed, or segregated by barricades. Suppressive shields provide an alternative in the form of a vented steel enclosure.

Viewgraph 2 - Suppressive Shield Schematic

This schematic illustrates the concept of a suppressive shield. The enclosure usually consists of a structural steel framework with built-up panels of steel angles, I-beams, perforated plate, or louvered panels. The space between panel components allow gaseous products of combustion to pass through while suppressing flame, and in case of a detonation, reducing blast overpressure to a safe level. There is no direct path through the panel for fragments to pass through. All fragmentation effects are confined within the enclosure.

The shields can be any size. They can be small transportable laboratory shields or large structures in a building similar to the concrete barricades sometimes used.

Viewgraph 3 - Typical Concrete Cubicles

Typical reinforced concrete barricades are shown here. The barricades are designed as cubicles with three walls to withstand direct blast pressure and to prevent propagation of a detonation from one area to the next.

They do not prevent hazardous run-up reactions where a fire can start in one cubicle and, through pyrotechnic dust in the air or accumulation on equipment, spread from one cubicle to another until the entire facility is in flames.

In the event a detonation occurs, the cubicles do not prevent wide dispersal of damaging primary and secondary fragments, nor do they prevent blast overpressure leakage beyond the open edges. The blast overpressure from the open edges of the cubicle can spread over the outside of the building wall and sometimes is large enough to make the walls collapse. A special reinforced building design can prevent this, but adds considerably to building cost.

Since suppressive shields are full enclosures, they perform in a different way from these cubicles.

Viewgraph 4 - Suppressive Shield Characteristics

Suppressive shields will:

- Confine all fragments from a detonation.
- Attenuate blast pressure to a safe level in all directions.
- Reduce fireball diameter sufficiently to prevent spreading of the fire beyond the local area.

Another particularly attractive feature of suppressive shields is that they are modular in design for quick erection and modification to provide maximum protection and flexibility.

Viewgraph 5 - General Configuration of Suppressive Shield Groups

Several general classes of shield designs have been conceived. As shown here, some have cylindrical or spherical configuration while others are rectangular frame and panel designs.

Generally the configuration is governed by the dominant hazard, i.e., blast, fragment or flame. If blast pressures are the factors which are most important in design of the structure, the shield will usually have a cylindrical or spherical shape. The rectangular frame and panel structures are typically used where the dominant hazard is flame.

In my presentation today, I will be discussing the Group 6 Shield and the Group 5 Shield to illustrate details of two typical applications. The Group 6 Shield illustrates a unique spherical design which is small and portable for use with laboratory quantities of primary explosives. The Group 5 Shield demonstrates the modular design concept that makes suppressive shields an attractive alternative to inflexible concrete barricades.

DISCUSSION OF GROUP 6 AND GROUP 5 SHIELD DESIGNS

Viewgraph 6, Group 6 Shield

The Group 6 Shield is spherical. The requirement for this shield is that an operator be capable of transporting on a push cart small quantities of extremely hazardous primary explosive material. It is not feasible to vent this shield because of the hazardous material involved and the close proximity of the operator.

The two foot diameter spherical steel shell is 1/4 inch thick and weighs about 200 pounds. A rectangular tray is used to carry 10 cups which would carry about 70 grams each of lead azide in a typical application. Total weight of explosive is limited to 700 grams lead azide or equivalent.

I will illustrate one interesting use of this shield. Although it is not a laboratory application, it is interesting because it shows how quantities of initiating or primary explosions can be handled in detonator production without exposing operating personnel to explosive hazards.

Viewgraph 7, Group 6 Shield on Cart with Operator

Use of this shield will result in about 3 million dollars savings in modernization of the detonator production line at Iowa Army Ammunition Plant. Costly automatic conveyors are replaced by a manual system which makes use of the Group 6 Suppressive Shield mounted on a cart as shown. The ring at the front mates with an opening in a storage barricade.

Viewgraph 8, Test Fixture Set-Up

This fixture for mechanical function testing illustrates the attachment of the shield to the barricade. The operator rolls the cart up to the barricade. The clamp at the barricade is closed and locks the shield to the barricade. Transport mechanisms remove the tray with explosive material from the shield. At no time is the operator exposed to explosive hazards.

A series of tests were conducted to verify the adequacy of the design.

Viewgraph 9, METV Before Test 6

This is a photograph of the set up for proof test of the system. The Group 6 test shield is supported by a wooden frame and is attached to the storage barricade in the middle of the photograph.

Viewgraph 10, Summary of Proof Test Data

Summary data from proof tests show that the Group 6 Shield and the Storage Barricade are adequately designed. The system contained all effects from blast of service charge with a sound level of 146 db outside the shield. One hundred forty-six is roughly the noise level from firing a service rifle such as the M-16 rifle. Ear protection is desirable but a single exposure will often produce no ear damage. This indicates a safe environment for the operator. A charge weight of 307 grams C-4 (37% above the design service charge) was required to rupture the shield. The proof charge which is 25% above service charge caused a bulge in the bottom of the shield but no rupture.

Now, I would like to discuss an entirely different suppressive shield design. The Group 5 suppressive shield is designed for use with pyrotechnic material.

Although the example I will be showing here is a large fixture, these shields can be scaled down in size for laboratory use or modified to meet special requirements.

Viewgraph 11 - Group 5 Panels on Ground

One of the features that adds to suppressive shield utility is their

modular design illustrated here. These panels for the Group 5 shield are laid out by the foundation ready for assembly.

Each panel is about 10 feet long and 5 feet wide. When erected they form a cube 10 feet long on each side.

Viewgraph 12 - Category 5 Panel Section

Each panel is a composite structure with a double row of interlocking structural steel angle beams arranged as shown in the viewgraph. There are three perforated plates, one on the outside and two on the inside. Wire screening was added between the panel layers for additional flame suppression, but it proved ineffective. Tests demonstrated that there was sufficient exposed metal surface to suppress flames effectively without the addition of metal screens.

Viewgraph 13

Here, the panels are being moved into place. The modular characteristic simplifies the alteration of facilities to meet changing requirements.

Viewgraph 14 - Group 5 Shield

This is the Group 5 shield ready for test. This shield has been approved for use with 1.84 pounds of C-4 or 30 pounds of illuminant mix.

The Group 5 shield is especially designed for flame suppression. The structure is not as heavy as those intended to withstand the comparatively large transient blast overpressures of a detonation. The design has a large surface area and volume of steel to absorb heat and suppress flames. The venting of gaseous products of combustion precludes significant pressure and burning rate increase inside the shield with propellant or pyrotechnic material.

To determine limits on flame suppression capability of this shield, thermal suppression studies have been conducted beyond those required for the safety approval proof tests mentioned previously.

Viewgraph 15 - Suppressive Shield Group 5 Testing

The tests are summarized on this viewgraph.

Single base, multiperforated, M10 gun propellant in bulk was used in the propellant tests. The illuminant material is a 50:50 mix of sodium nitrate, and powdered magnesium. The safety approval tests were conducted with a smaller charge weight than that shown, 30 pounds of the illuminant mix. To be complete, the proof test charge of 2.5 pounds is shown. That charge weight stressed the shield structure to its limit and was not increased.

Viewgraph 16 - Sensor Location for Group 5 Suppressive Shield Tests

Instrumentation layout for the tests is shown here (see table below: Instrumentation for Group 5 Suppressive Shield Tests). Burning time was measured using photocells in the shield wall. Thermocouples in the bulk pyrotechnic were used to obtain an indication when the material was completely burned. Static overpressure was measured on large charges to estimate confinement effects. Radiant heat flux outside the shield was measured with Keithley 860 flux meters. Blast pressure was recorded inside and outside the shield when explosive material was detonated in the shield. High speed motion picture coverage was included on all shots. Video display of each test in the instrument building was also recorded.

Viewgraph 17 - Free Field Illuminant Test Configuration

For comparison, free field temperatures and pressures were measured using instrument configuration shown here. Thermocouples were on a line in one direction spaced at 5 foot intervals and pressure was measured in a direction perpendicular to the thermocouple line. Black and white, and color film coverage was also included.

Viewgraph 18 - Test Set Up

This is a photograph of a typical test set up. The open shield door was closed during test.

INSTRUMENTATION FOR GROUP 5 S/S TESTS

Measurement Number	Parameter	Transducer	Amplifier	Installed Time Constant	Recorder
00	Timing	N/A	N/A	----	Sangamo 4700
01	Burning Time	Photocell Monsanto	Transdata	1 msec	Sangamo 4700
02	Burning Time	MT-2	NEFF109-6	1 msec	Sangamo 4700
03	Burn Rate	Fe-Constantan	NEFF109-6	100 msec	Sangamo 4700
04	Burn Rate	Thermocouple	NEFF109-6	100 msec	Sangamo 4700
05	Burn Rate	Breakwire	N/A	1 msec	Sangamo 4700
06	Static press	MB151-DBZ-177 in Tube	NEFF109-6	10 msec	Sangamo 4700
07					Sangamo 4700
08					Sangamo 4700
09	Static press	PCB101A02 in Baffle Mount	NEFF109-6	10 msec	Sangamo 4700
10	Blast press (face-on)	ST-2 in Wall Mount	PCB401A13	200 msec	Sangamo 4700
11	Heat flux	Keithley 860	N/A	1 sec	Sangamo 4700
12					
13					
14	Heat flux	Keithley 860	N/A	1 sec	Sangamo 4700
41	Blast press	ST-7H in Aerodynamic Probe	PCB401A11	200 msec	Biomation 610B
42	"				
43	"				
44	"				

Viewgraph 19 - Heat Flux as a Function of Time

Heat flux data transients five feet from outside of the shield (about 10 feet from the charge) are shown with dashed lines. The solid lines are from heat flux measurements about 10 feet from charges burned in the open. This is the same total distance from the charge as for the shield tests. Comparison between open air and shielded heat flux shows 85% reduction in peak radiant flux for a shielded 50 pound charge.

Preliminary propellant tests using a maximum charge weight of 590 pounds of M-10 single base multiperforated propellant in bulk with 0.0185 inch web resulted in no pressure rise in the shield. High radiant heat flux outside the shield wall indicated a need for improved thermal suppression. This work is not finished. The viewgraph lists some areas where more study is needed.

Viewgraph 20 - Research Needed

An exhaustive search of the literature to identify hazards and improved thermal suppression techniques has revealed a need for more research in this area.

Methods do exist for estimating free field radiant flux, fireball diameter, and burning time for unconfined pyrotechnic material, but there is, at present, no method to compute attenuated thermal effects when a suppressive shield is used. Predictive models are needed.

Investigation of nonuniform venting has been initiated, but that work is not complete. Much work is required to develop the basic technology necessary to design optimal shields for flame suppression.

As a result of extensive investigation of blast and fragment effects the technology for those hazards is well understood. Predictive techniques for suppressive shield performance in attenuating blast and fragment hazards have been developed. The next few viewgraphs just briefly indicate the scope and results of that investigation.

SAFETY APPROVED SHIELDS

Viewgraph 21 - Safety Approved Suppressive Shields

To insure that Department of Defense safety offices approve site plans which incorporate suppressive shields, we have designed, fabricated, and proof tested several designs as listed here.

The characteristics of the shields approved by the Department of Defense Explosives Safety Board are summarized in the viewgraph. They include sizes and charge weights typical to munitions manufacturing, but they can be scaled up or down in size or charge weight to meet special laboratory requirements.

As this table indicates, suppressive shields are approved for use in hazardous operations involving explosive charge weights up to the equivalent of 37 pounds 50/50 pentolite for Group 3 and 30 pounds of illuminant mix for Group 5.

Approved shield sizes range from the 2 foot diameter spherical steel shell of Group 6 to the 11½ foot diameter cylindrical Group 3 shield.

The operator safe distance shown is the distance from the exterior wall that an operator can be located and not be injured by blast overpressure or flame venting from the shield when detonation or deflagation occur within the shield.

TECHNOLOGY SUMMARY

Viewgraph 22 - Applied Technology Participants

The suppressive shield designs that we have been discussing are based on a major four-year effort by organizations listed here.

The roles they played are indicated on the viewgraph.

The lead organization for suppressive shield technology development was Edgewood Arsenal, now called Chemical Systems Laboratory. Recent

Army reorganization has reassigned responsibility for suppressive shielding to Large Caliber Weapon Systems Laboratory, ARRADCOM, at Dover, New Jersey.

Viewgraph 23 - Technology Flow Chart

Technology development has proceeded along the lines illustrated in this flow chart.

Hazards identified are classified as blast, fragment and fireball. Description of each of these hazards is essential to design of a shield. Each of these hazards poses a special problem to the designer and requires consideration not only in terms of its own features, but also in terms of combined effects of all hazards acting together.

The next step is to develop procedures to predict suppression of blast, fragment and flame hazards. The nature of the suppression governs the magnitude of the loads imposed on the structure. A safe, economical shield must be designed to withstand loads imposed. Suppression and design tradeoffs are made to obtain the best shield which satisfies hazard suppression requirements to provide a safe environment at minimal cost.

On blast environment, a predictive capability for characteristics of free air blast is available in the literature. In the technology program techniques were developed for defining internal transient and quasi-static blast overpressures, pressure loads on the shield and attenuated pressure external to the shield.

The second major element to be considered in the design of a suppressive shield is the fragment threat. As we initiated our technology studies we found much was known about primary fragment hazards but little was known about secondary fragment hazards. Primary fragments are those from material in direct contact with detonating composition. Secondary fragments are from surrounding equipment, not in direct contact with the composition that detonates.

It was necessary to establish a methodology to predict secondary fragment hazards and fragment suppression characteristics of the composite structural steel walls of a suppressive shield.

Viewgraph 24- Suppressive Shield Technology Summary

As a result of the Suppressive Shielding Program, engineering methodology is available for modifying or scaling approved designs to meet specific munitions plant requirements. Where approved designs do not exist to meet certain requirements there is an engineering methodology for design and proof test of new shields.

This methodology is presented in an engineering design handbook for suppressive shields, published by the US Army Corps of Engineers, Huntsville Division, Huntsville, Alabama.

Viewgraph 25 - Suppressive Shield Engineering Design Handbook

This viewgraph is a list of the chapter titles in the handbook. The information contained in each chapter is also shown.

Methods for modifying suppressive shields to meet specific production line requirements are given in Chapter II - Safety Approved Shields.

If a new shield must be designed, Information in Chapters III, IV and V are used.

Chapter VI - Structural details, has recommended designs for personnel doors, conveyor doors, as well as other penetrations for utilities and the like.

Economic analysis methods and quality assurance factors are included.

With this handbook, scientists or engineers requiring hazardous operation protection can select, modify or design a suppressive shield for their required use. This handbook is available through DDC or National Technical Information Service and provides an alternative protective method previously not available to provide increased protection to personnel involved in hazardous operations.

Gentlemen, it has been my pleasure to brief you today. Thank you for your attention.

BIBLIOGRAPHY

1. Ammunition and Explosives Ashore, Department of the Navy Publication, OP-5, including Volume I, NAVSEA OP-5/1 "Safety Regulations for Handling, Storing, Renovation and Shipping", Volume II, NAVORD OP-5/2, "Storage Data", Volume III, NAVSEA OP-5/3, "Advance Bases", and all revisions thereto. (U)

2. Ammunition and Explosives Safety Standards, DOD 5154.4S, Department of Defense, Office of the Assistant Secretary of Defense (Installations and Logistics), March 1978. (U)

3. Baker, W.E., The Elastic Plastic Response to Thin Sperical Shells to Internal Blast Loading, Paper No. 59-A-95, Applied Mechanics Division, American Society of Mechanical Engineers, February 1959. (U)

4. Baker, W.E. and Oldham, G.A., Estimates of Blowdown of Quasi-Static Pressures in Vented Chambers, EM-CR-76029, Report No. 2, Edgewood Arsenal, Aberdeen Proving Ground, Maryland, November 1975. (U)

5. Baker, W.E., et al, Analysis and Preliminary Design of a Suppressive Structure for a Melt Loading Operation, EM-CR-76056, Edgewood Arsenal, Aberdeen Proving Ground, Maryland, May 1976. (U)

6. Beedle, L.S., Plastic Design of Steel Frames, John Wiley and Sons, Inc., New York, N.Y., 1958. (U)

7. Biggs, J.M., Introduction to Structural Dynamics, McGraw-Hill Book Co., New York, N.Y., 1964. (U)

8. Building Code Requirements for Reinforced Concrete, ACI Standard 318-71, American Concrete Institute, Detroit, Mich., 1971. (U)

9. Building Construction Cost Data, Robert Snow Means Co., Inc., 100 Construction Plaza, Duxbury, Mass., Latest Edition. (U)

10. Crawford, R.E., Higgins, C.J. and Bultmann, E.H., The Air Force Manual for Design and Analysis of Hardened Structures, AFWL TR 74-102, Air Force Weapons Laboratory, Kirtland AFB, N.M., October, 1974. (U)

11. Dede, M., et al, Preliminary Estimate of Concrete Thicknesses and Construction Costs of Laced Reinforced Concrete Structures, Technical Report No. 4441, Picatinny Arsenal, Dover, N.J., October 1972. (U)

12. Design of Structures to Resist the Effects of Atomic Weapons, Structural Elements Subjected to Dynamic Loads, U.S. Army Corps of Engineers Manual TM5-856-4, December 1965. (U)

13. Design of Structures to Resist Nuclear Weapon Effects, American Chemical Society of Civil Engineers Manual of Engineering Practice No. 42, ASCE, New York, N.Y. (U)

14. Engineering Design Handbook: Explosions in Air, Part I, AMC Pamphlet 706-181, Headquarters U.S. Army Materiel Command, Latest Edition. (U)

15. Esparza, E.D., Baker, W.E., and Oldham, G.A., Blast Pressures Inside and Outside Suppressive Structures, EM-CR-76042, Report No. 8, Edgewood Arsenal, Aberdeen Proving Ground, Maryland, December 1975. (U)

16. Explosive Safety Manual, AFM 127-100, Department of the Air Force, Washington, D.C., 2 December 1971. (U)

17. Final Report Application of Suppressive Structure Concepts to Chemical Agent Munition Demilitarization System (CAMDS), Report EA-FR-2B02, Edgewood Arsenal, Aberdeen Proving Ground, Maryland, July 27, 1973. (U)

18. Gray, B.H., Williamson, G.R., and Batson, G.B., Fibrous Concrete Construction Material for the Seventies, Construction Engineering Research Laboratory, Champaign, Ill., May 1972. (U)

19. Gregory, F.H., Analysis of the Loading and Response of a Suppressive Shield When Subjected to an Internal Explosion, Minutes of the 17th Explosive Safety Seminar, Denver, Colorado, September 1976. (U)

20. Harris, C.M., and Crede, C.E., Shock and Vibration Handbook, McGraw-Hill Book Co., New York, N.Y., 1961. (U)

21. Healey, John, et al, Design of Steel Structures to Resist the Effects of HE Explosions, Technical Report 4837, Picatinny Arsenal, Dover, New Jersey, August 1975. (U)

22. Headey, John, et al, Primary Fragment Characteristics and Impact Effects on Protective Barriers, PA TR 4903, Picatinny Arsenal, Dover, N.J., December 1975. (U)

23. Henry, I.G., The Gurney Formula and Related Approximations for the High Explosive Deployment of Fragments, PUB-189, Hughes Aircraft Co., AD813398, April 1967. (U)

24. Hoggatt, C.R. and Recht, R.F., Fracture Behavior of Tubular Bombs, J. Appl. Physics, Vol. 39, No. 3, February 1968, pp. 1856-1862. (U)

25. Hubich, H.O. and Kachinski, R.L., Explosive Waste Removal Systems for Suppressive Shields, EM-CR-76002, Edgewood Arsenal, Aberdeen Proving Ground, Md., August 1975. (U)

26. Johnson, C. and Moseley, J.W., Preliminary Warhead Terminal Ballistic Handbook Part I, Terminal Ballistic Effects, NWL Report No. 1821, NAVWEPS Report No. 7673, U.S. Naval Weapons Laboratory, Dahlgren, Virginia, March 1964. (U)

27. Joint Munitions Effectiveness Manual, FM101-62-3, Manual of Fragmentation Data, 15 September 1973. (C-XGDS-3)

28. Katsanis, D.J., Safety Approval of Suppressive Shields, EM-TR-76088, Edgewood Arsenal, Aberdeen Proving Ground, Md., August 1976. (U)

29. Keenan, W.A. and Tancreto, J.E., Blast Environment from Fully and Partially Vented Explosions in Cubicles, Technical Report R828, Civil Engineering Laboratory, Naval Construction Battalion Center, Port Hueneme, California, November 1975. (U)

30. Kennedy, J.E., Explosive Output for Driving Metal, in Behavior and Utilization of Explosives in Engineering Design, ASME and Univ. of New Mexico, March 1972, Albuquerque, New Mexico. (U)

31. Kennedy, R.P., A Review of Procedures for the Analysis of Design of Concrete Structures to Resist Missile Impact Effects, Nuclear Engineering and Design, Vol. 37, 1976, pp. 183-203. (U)

32. Kingery, C.N., Air Blast Parameters Versus Distance for Hemispherical TNT Surface Bursts, BRL Report No. 1344, Aberdeen Proving Ground, Maryland, September 1966. (U)

33. Kingery, C.N., Schumacher, R.N., and Ewing, W.O., Jr., Internal Pressures from Explosions in Suppressive Structures, BRL Interim Memorandum Report No. 403, Aberdeen Proving Ground, Maryland, June 1975. (U)

34. Kinney, G.F. and Sewell, R.G.S., Venting of Explosions, Naval Weapons Center, NWC Technical Memorandum 2448, China Lake, California, July 1974. (U)

35. Koger, D.M. and McKown, G.L., Category 5 Suppressive Shield Test Report, EM-TR-76001, Edgewood Arsenal, Aberdeen Proving Ground, Maryland, October 1975. (U)

36. Lasseigne, A.H., Static and Blast Pressure Investigation for the Chemical Agent Munition Demilitarization System: Sub-Scale, Rpt. EA-FR-4C04, November 30, 1973. (U)

37. Levmore, S., Air Blast Parameters and Other Characteristics of Nitroguanidine and Guanidine Nitrate, PA TR 4865, Picatinny Arsenal, Dover, N.J., November 1975. (U)

38. Malvern, L.E., Propagation of Longitudinal Waves of Plastic Deformation in a Bar of Material Exhibiting a Strain-rate Effect, J. App. Mech., Vol. 18, pp. 203-8.

39. Manual of Steel Construction, Seventh Edition, American Institute of Steel Construction, Inc., New York, N.Y., 1970. (U)

40. Melin, J.W., Numerical Integration by Beta Method, ASCE Conference on Electronic Computation, Kansas City, Mo., 1968. (U)

41. Mott, N.F., A Theoretical Formula for the Distribution of Weights of Fragments, AC 3742 (British) March 1943. (U)

42. Mott, N.F., The Theory of Fragmentation, AC 3348 (British), January 1943. (U)

43. Nagy, J., et al, Explosibility of Miscellaneous Dusts, United States Department of the Interior, Bureau of Mines, Report of Investigations 7208, December 1968. (U)

44. Napadensky, H. and Swatosh, J., TNT Equivalency of Black Powder, IITRI TR J6289-4, IIT Research Institute, Chicago, Ill., September 1972. (U)

45. Napadensky, H. and Swatosh, J., TNT Equivalency of Large Charges of Black Powder, IITRI TR J6289-4, IIT Research Institute, Chicago, Ill., February 1974. (U)

46. Napadensky, H., Swatosh, J., Humphreys, A., and Rindner, R., TNT Equivalency Three Pyrotechnic Composition, PA TR 4628, Picatinny Arsenal, Dover, N.J., June 1974. (U)

47. Nelson, K.P., The Economics of Applying Suppressive Shielding to the M483A1 Improved Conventional Munition LAP Facility, EM-TR-76087, Edgewood Arsenal, Aberdeen Proving Ground, Md., January 1977. (U)

48. Nelson, K.P., Spherical Shields for the Containment of Explosions, EM-TR-76096, Edgewood Arsenal, Aberdeen Proving Ground, Md., March 1977. (U)

49. Newmark, N.M., "Computation of Dynamic Structural Response in the Range Approaching Failure," Proceedings of the Symposium on Earthquake and Blast Effects on Structures, Los Angeles, Calif., 1952. (U)

50. Oertel, F.H., Jr., Evaluation of Simple Models for the Attenuation of Shock Waves by Vented Plates, BRL Report No. 1906, Aberdeen Proving Ground, Maryland, August 1976. (U)

51. Petes, J., "Blast and Fragmentation Characteristics," Annals of the New York Academy of Sciences, Vol. 152, Article 1, October 1968, pp. 283-317. (U)

52. Proctor, J.F., Blast Suppression/Predictive Model, WBS 4333, Monthly Technical Report, November 1975, Naval Surface Weapons Center, White Oak, Silver Spring, Maryland. (U)

53. Proctor, J.F., Internal Blast Damage Mechanisms Computer Program, 61 JTCG/ME-73-3, Joint Technical Coordinating Group for Munitions Effectiveness, April 1973. (U)

54. Proctor, J.F. and Filler, W.S., A Computerized Technique for Blast Loads from Confined Explosions, 14th Annual Explosives Safety Seminar, New Orleans, Louisiana, 8-10 November 1972, pp. 99-124. (U)

55. Rakaczky, J.A., The Suppression of Thermal Hazards from Explosions of Munitions: A Literature Survey, BRL Interim Memorandum Report No. 377, Aberdeen Proving Ground, Maryland, May 1975. (U)

56. Ricchiazzi, A.J. and Barb, J.C., A Tentative Model for Predicting the Terminal Ballistic Effects of Blunt Fragments Against Single and Spaced Targets, A Comparison of Predicted and Experimental Results, BRL Memorandum Report 2578, Aberdeen Proving Ground, Maryland, January 1976. (U)

57. Roark, R.J. and Young, W.C., Formulas for Stress and Strain, McGraw-Hill Book Co., New York, N.Y., 5th Edition, 1975. (U)

58. Safety Criteria for Modernization and Expansion Projects, DRCPM-PBM Memorandum No. 385-3, Latest Edition. (U)

59. Safety Manual, AMCR 385-100, Hq, U.S. Army Materiel Command, Alexandria, Va., Latest Edition. (U)

60. Salmon, C.G. and Johnson, J.E., Steel Structures-Design and Behavior, Intext Educational Publishers, Scranton, Pa., 1971. (U)

61. Seely, F.B. and Ensign, N.E., Analytical Mechanics for Engineers, John Wiley & Sons, Inc., New York, N.Y., 3rd Edition, 1948. (U)

62. Seely, F.B., and Smith, J.O., Advanced Mechanics of Materials, Second Edition, John Wiley and Sons, Inc., New York, N.Y., August 1961. (U)

63. Schroeder, F.J., Kachinski, R.L., Schnapfe, R.W., Koger, D.M., McKivrigan, J.L. and Jezek, B.W., Engineering Design Guidelines, Drawings, and Specifications for Support Engineering of Suppressive Shields, EM-CR-76097, Edgewood Arsenal, Aberdeen Proving Ground, Md., December 1976. (U)

64. Schumacher, R.N. and Ewing, W.O., Jr., Blast Attenuation Outside Cubical Enclosures Made Up of Selected Suppressive Structures Panel Configurations, BRL Memorandum Report No. 2537, Aberdeen Proving Ground, Maryland, September 1975. (U)

65. Schumacher, R.N., Kingery, C.N., and Ewing, W.O., Jr., Airblast and Structural Response Testing of a 1/4 Scale Category I Suppressive Shield, BRL Memorandum Report No. 2623, Aberdeen Proving Ground, Maryland, May 1976. (U)

66. Shear and Diagonal Tension, Report of ACI-ASCE Committee 326, ACI Manual of Concrete Practice-Part 2, American Concrete Institute, Detroit, Mich., 1968. (U)

67. Shelter Design and Analysis, TR-20 (Vol. 4), Defense Civil Preparedness Agency, Washington, DC, July 1972.

68. Shields, Operational for Ammunition Operations, Criteria for Design of, and Tests for Acceptance, Mil Std 398, U.S. Government Printing Office, Washington, D.C., 5 November 1976. (U)

69. Structures to Resist the Effects of Accidental Explosions, TM5-1300, Department of the Army Technical Manual, NAVFAC P-397, Department of the Navy Publication, AFM 88-22, Department of the Air Force Manual, Washington, D.C., June 1969. (U)

70. Study of Suppressive Structures Application to an 81 mm Automated Assembly Facility, Report EA 1002, Edgewood Arsenal, Aberdeen Proving Ground, Maryland. 16 April 1973. (U)

71. Suppressive Shields, Structural Design and Analysis Handbook, HNDM-1110-1-2, U.S. Army Corps of Engineers, Huntsville Division, Huntsville, Alabama, 18 Nov 77. (U)

72. Swatosh, J., Cook, J., and Price, P., Blast Parameters of M26E1 Propellant, PA TR 4901, Picatinny Arsenal, Dover, N.J., December 1976. (U)

73. Swatosh, J., et al, and Levmore, S., Blast Parameters of Lead Azide, and Tetracene, PA TR 4900, Picatinny Arsenal, Dover, N.J., December 1974. (U)

74. Swatosh, J. and Napadensky, H., TNT Equivalency N-5 Slurry and Paste, IITRI TR J6278, IIT Research Institute, Chicago, Ill., September 1972. (U)

75. Swatosh, J. and Napadensky, H., TNT Equivalency of Nitroglycerine, IITRI TR J6312, IIT Research Institute, Chicago, Ill., September 1973. (U)

76. Swatosh, J., et al, and Price, P., TNT Equivalency of M1 Propellant (Bulk), PA TR 4885, Picatinny Arsenal, Dover, N.J., December 1975. (U)

77. Swisdak, M.M., Jr., Explosion Effects and Properties Part I - Explosion Effects in Air, NSWC/WOL/TR 75-116, Naval Surface Weapons Center, White Oak, Silver Spring, Maryland, October 1975. (U)

78. Symonds, P.S., ASME Colloguium on Behavior of Materials Under Dynamic Loading, Ed., N.J. Huffington, November 1965. (U)

79. System Safety Program for Systems and Associated Sub-systems and Equipment Requirements for, Mil Std 882, U.S. Government Printing Office, Washington, D.C., 15 July 1969. (U)

80. Tanner, W.S. and Warnicke, C.H., Support Test for the Fabrication of a Suppressive Shield for a Naval Ordnance Disposal Facility, DPG-DR-74-304, US Army Dugway Proving Ground, Dugway, Utah, December, 1973. (U)

81. Tomlinson, W.R., Jr., and Sheffield, O.E., Engineering Design Handbook, Properties of Explosives of Military Interest, AMC Pamphlet No. 706-177, Headquarters, U.S. Army Materiel Command, January 1971. (U)

82. Trott, B. Dale, et al, Design of Explosion Blast Containment Vessels for Explosive Ordnance Disposal Units, Picatinny Arsenal, Dover, N.J., June 1975. (U)

83. Trott, B. Dale, et al, The Blast and Fragment Containment Capability of Portable Chambers, N00174-74-C-0219, Naval Explosive Ordnance Disposal Facility, Indian Head, Md., September 1975. (U)

84. Warnicke, C.H., Added Support Tests of the Suppressive Shield for Naval Ordnance Disposal Facility, DPG-DRI-74-313, US Army Dugway Proving Ground, Dugway, Utah, September 1974. (U)

85. Weibull, H.R.W., Pressures Recorded in Partially Closed Chambers at Explosion of TNT Charges, Annals of the New York Academy of Sciences, 152, Art. 1, pp. 356-361, October 1968. (U)

86. Wenzel, A.B., et al, An Economic Analysis of the Use of Suppressive Structures in the Lone Star Army Ammunition Plant 105-mm High Explosive Melt-Pour Facility, EM-CR-76032, Edgewood Arsenal, Aberdeen Proving Ground, Md., November 1975. (U)

87. Wilcox, W.R., Shield Group 5 Suppressive Shield Plastic Liner and Propellant Testing, Contractor Report AR-TSD-CR-78001, NASA National Space Technology Laboratories, February 1978. (U)

88. Winter, G., et al, Design of Concrete Structures, McGraw-Hill Book Co., New York, N.Y., 1964. (U)

89. Zilliacus, S., Phyillaier, W.E., and Shorrow, P.K., The Response of Clamped Circular Plates to Confined Explosive Loadings, Naval Ship R&D Center Report 3987, NSRDC, Bethesda, Maryland, February 1974. (U)

90. 81 mm Suppressive Shielding Technical Data Package, Report EA-4E33 Edgewood Arsenal, Aberdeen Proving Ground, Maryland, January 1974. (U)

SHIELDING OF FACILITIES FOR WORK WITH PYROTECHNIC AND EXPLOSIVE MATERIAL

1725

David J. Katsanis

CHEMICAL SYSTEMS LABORATORY
US ARMY ARMAMENT RESEARCH AND DEVELOPMENT COMMAND
ABERDEEN PROVING GROUND, MARYLAND

VIEWGRAPH 1 -- TITLE

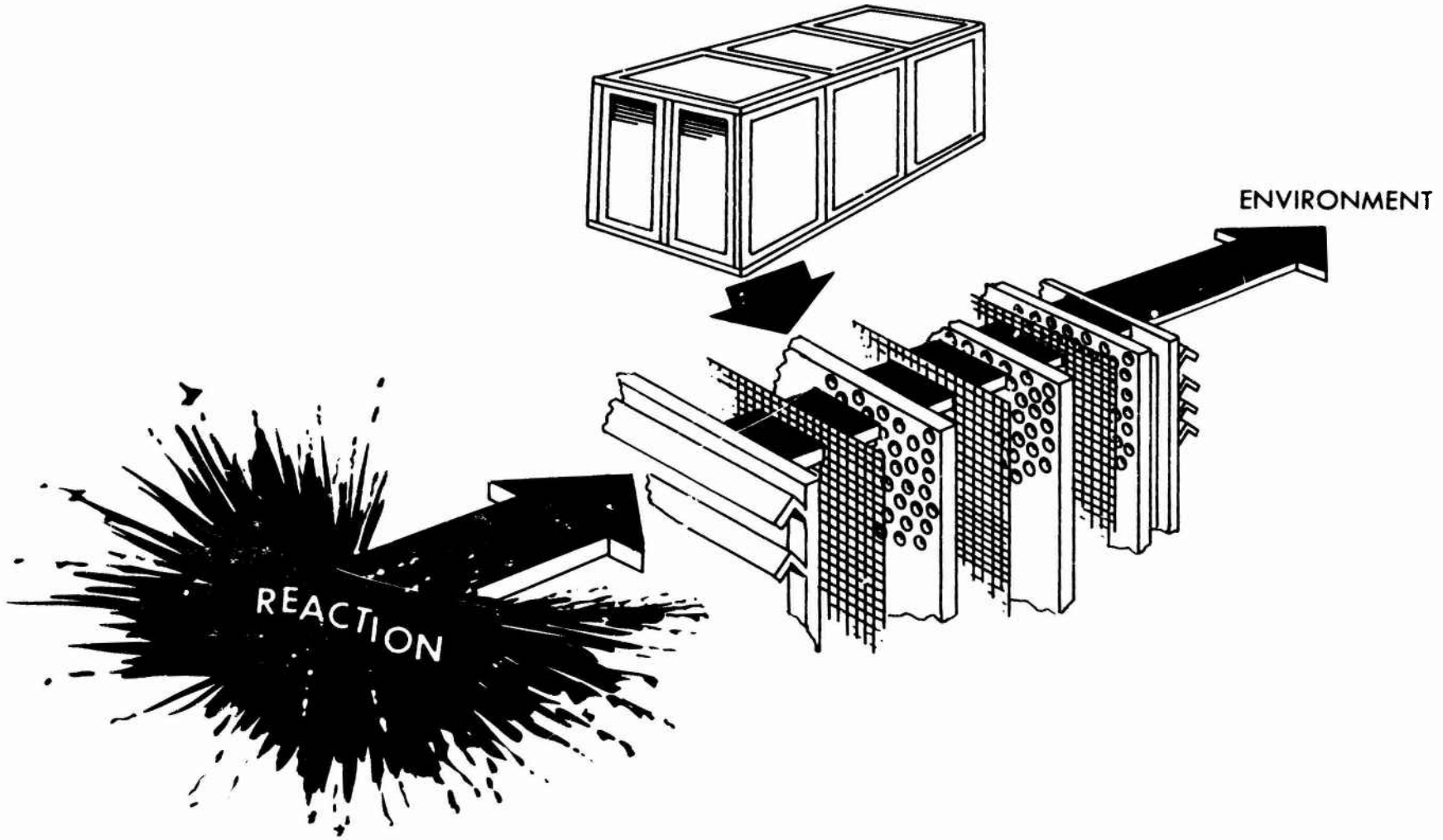

1726

VIEWGRAPH 2 -- SUPPRESSIVE SHIELD
SCHEMATIC

CONVENTIONAL STRUCTURE

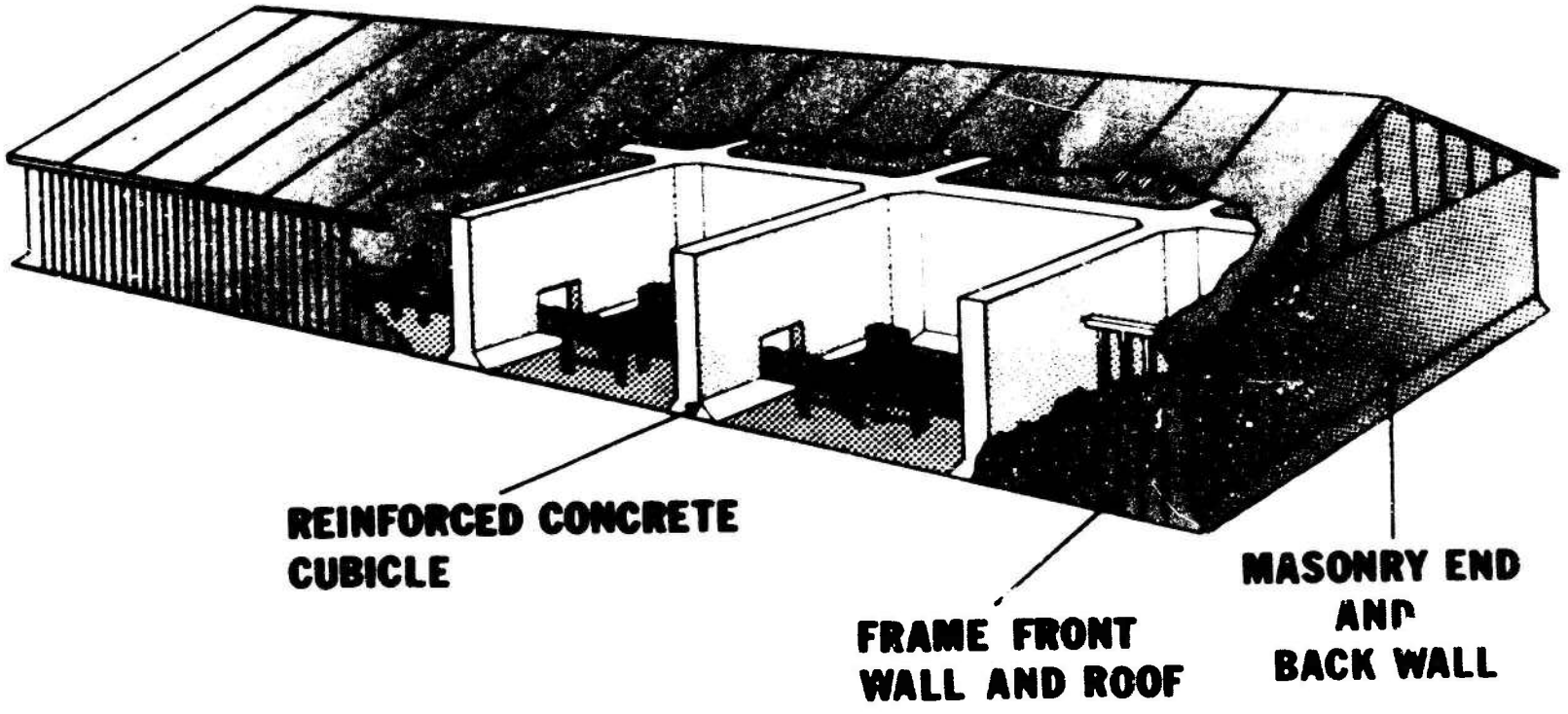

1727

VIEWGRAPH 3 -- TYPICAL CONCRETE CUBICLE

SUPPRESSIVE SHIELDING ENCLOSURE

1728

- FRAGMENT CONTAINMENT
- BLAST SUPPRESSION
- FLAME ATTENUATION

VIEWGRAPH 4 -- SUPPRESSIVE SHIELD CHARACTERISTICS

GENERAL CONFIGURATION OF SUPPRESSIVE SHIELD GROUPS

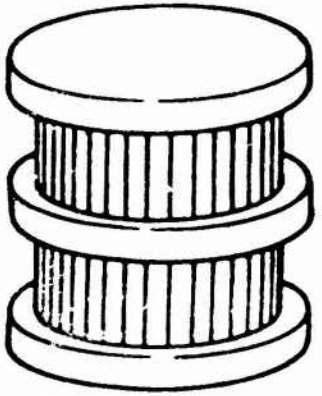

GROUPS 1, 2 AND 3

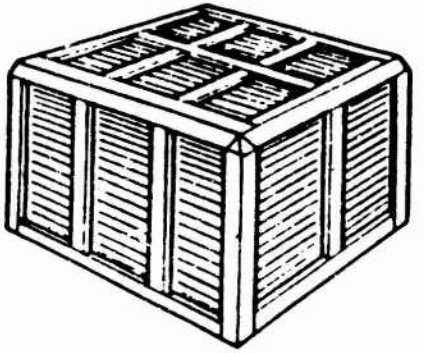

GROUP 4



GROUP 6

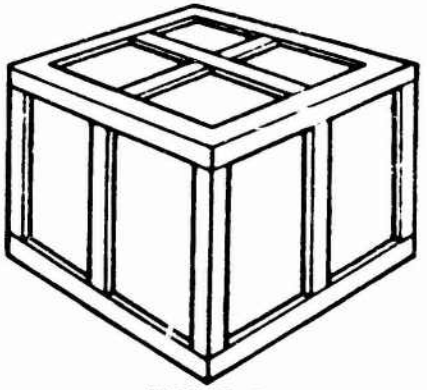

GROUP 5



GROUP 81MM

1729

VIEWGRAPH 5 -- GENERAL CONFIGURATION OF SUPPRESSIVE SHIELD GROUPS



GROUP 6 SUPPRESSIVE SHIELD

GROUP 6 SUPPRESSIVE SHIELD

DESIGN FEATURES

- VERY HIGH PRESSURE APPLICATIONS (1500 - 2000 PSI)
- MINIMAL FRAGMENT THREAT
- PERSONNEL CLOSE BY

TYPICAL APPLICATION

- CART TO TRANSPORT PRIMER MIX FROM PROCESS BUILDING TO DETONATOR ASSEMBLY BUILDING (DETONATOR BACKLINE - IOWA AAP)

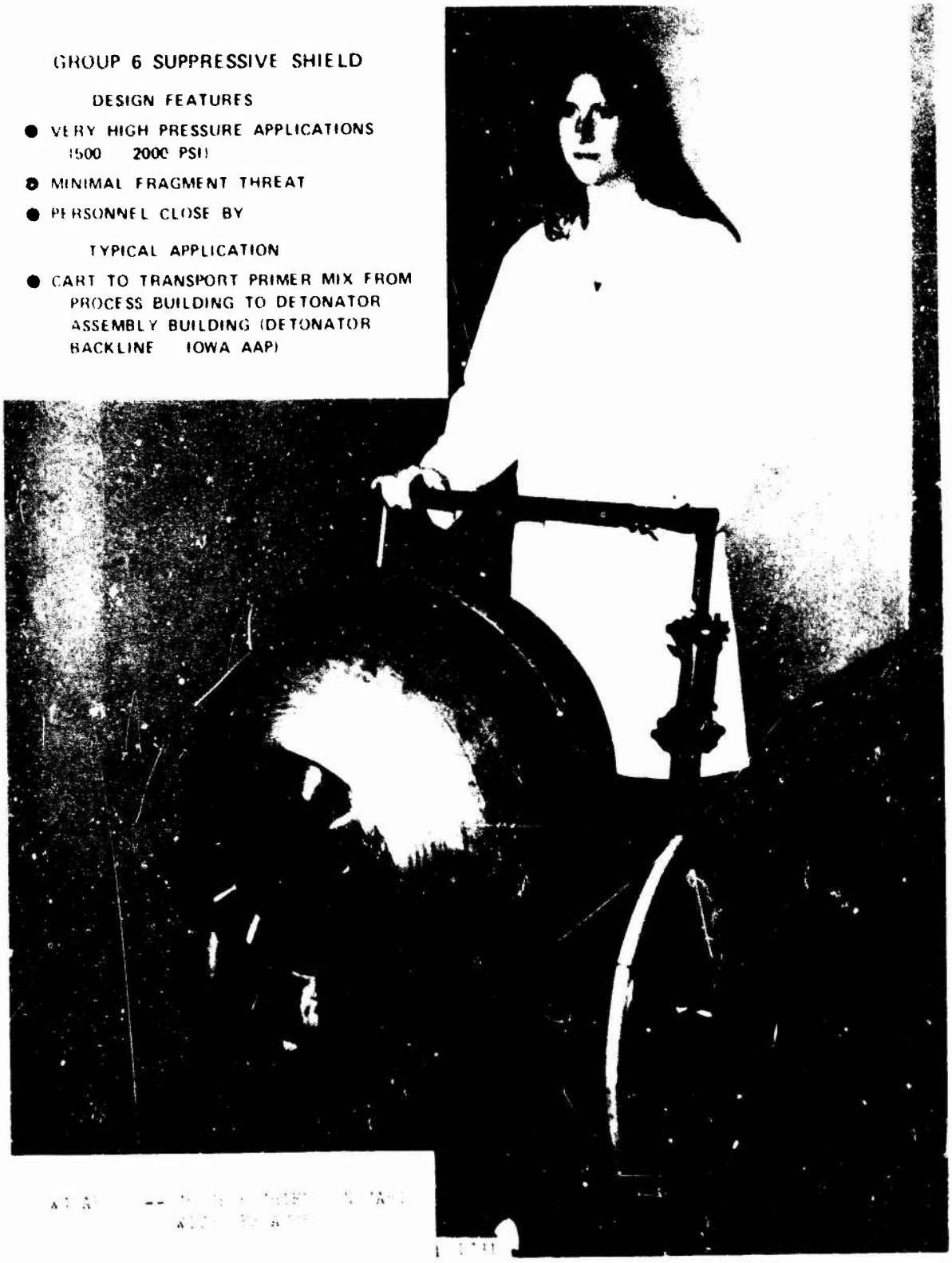

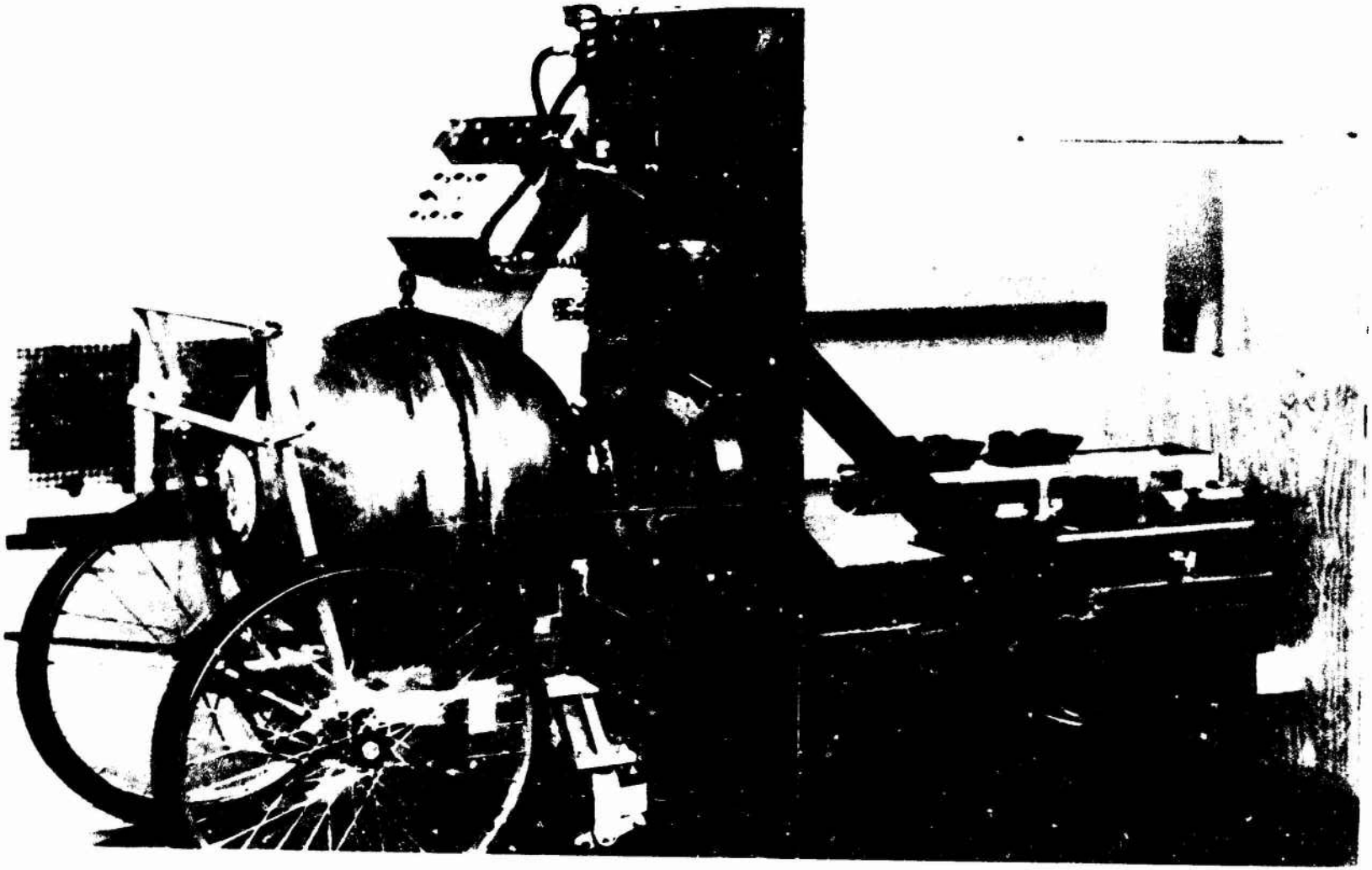

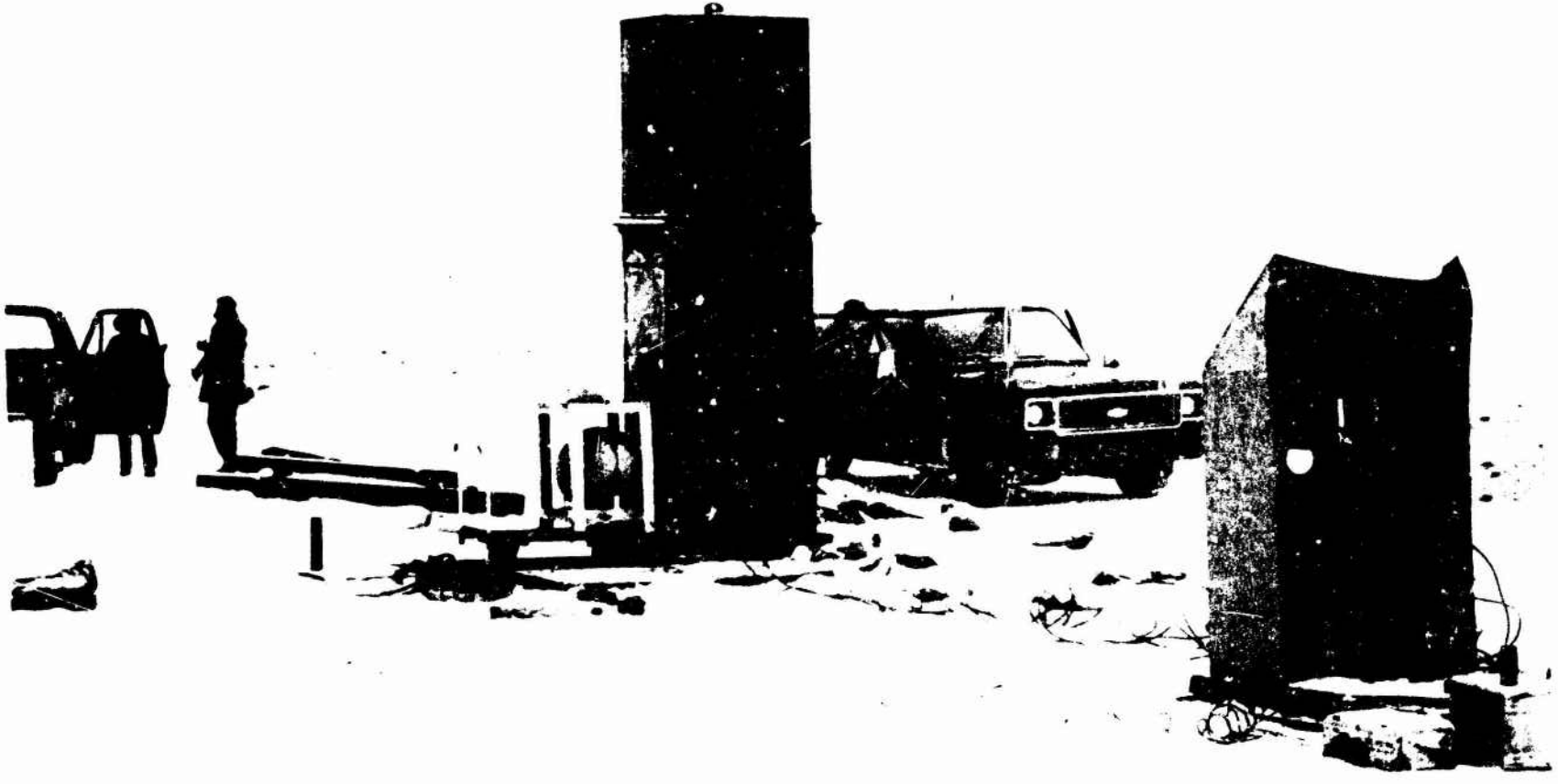

TABLE I. SUMMARY OF PROOF TESTS

MANUAL EXPLOSIVE TRANSPORT SYSTEM

ITEM	CHARGE			FUNCTION	
	WEIGHT* (gm)	COMPOSITION	LOCATION		
GROUP 6 SHIELD	708	NOL	CENTER	SATISFACTORY	
GROUP 6 SHIELD	567	LEAD AZIDE	10 CUPS	SATISFACTORY	
GROUP 6 SHIELD AND STORAGE BARRICADE	567	NOL	CENTER	SATISFACTORY, SOUNDLEVEL	- 146 db ON SCALE A
GROUP 6 SHIELD	250	C–4	CENTER	SATISFACTORY	89% PROOF CHARGE
GROUP 6 SHIELD	280	C–4	CENTER	SATISFACTORY	100% PROOF CHARGE
GROUP 6 SHIELD	307	C–4	CENTER	SATISFACTORY	111% OVER PROOF CHARGE SHIELD RUPTURED
GROUP 6 SHIELD AND STORAGE BARRICADE	222	C–4	CENTER	SATISFACTORY	

	NOL	C-4
* SERVICE CHARGE	567 gm	224 gm
PROOF CHARGE	708 gm	280 gm

VIEWGRAPH 10 -- SUMMARY OF PROOF TEST DATA

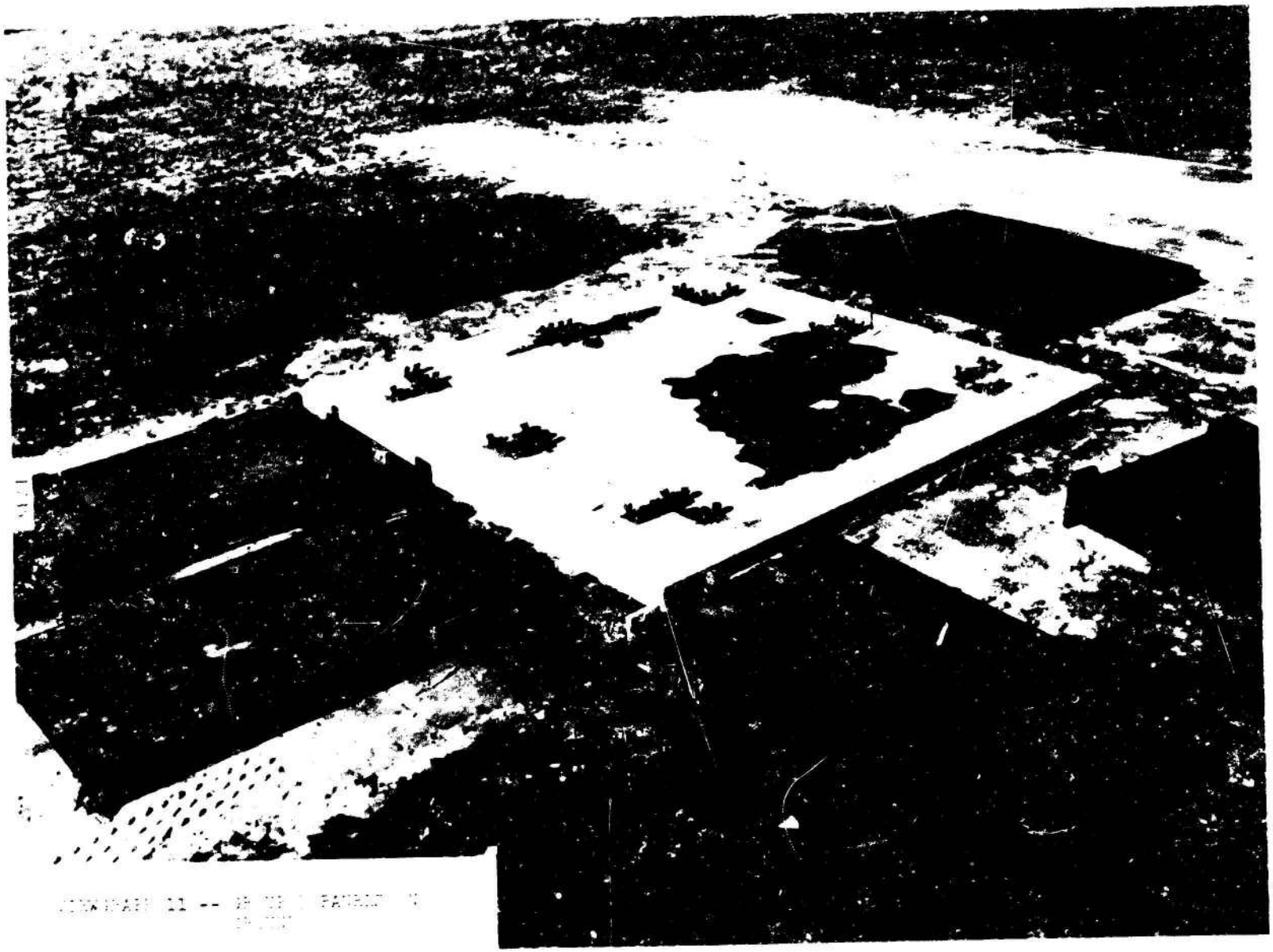

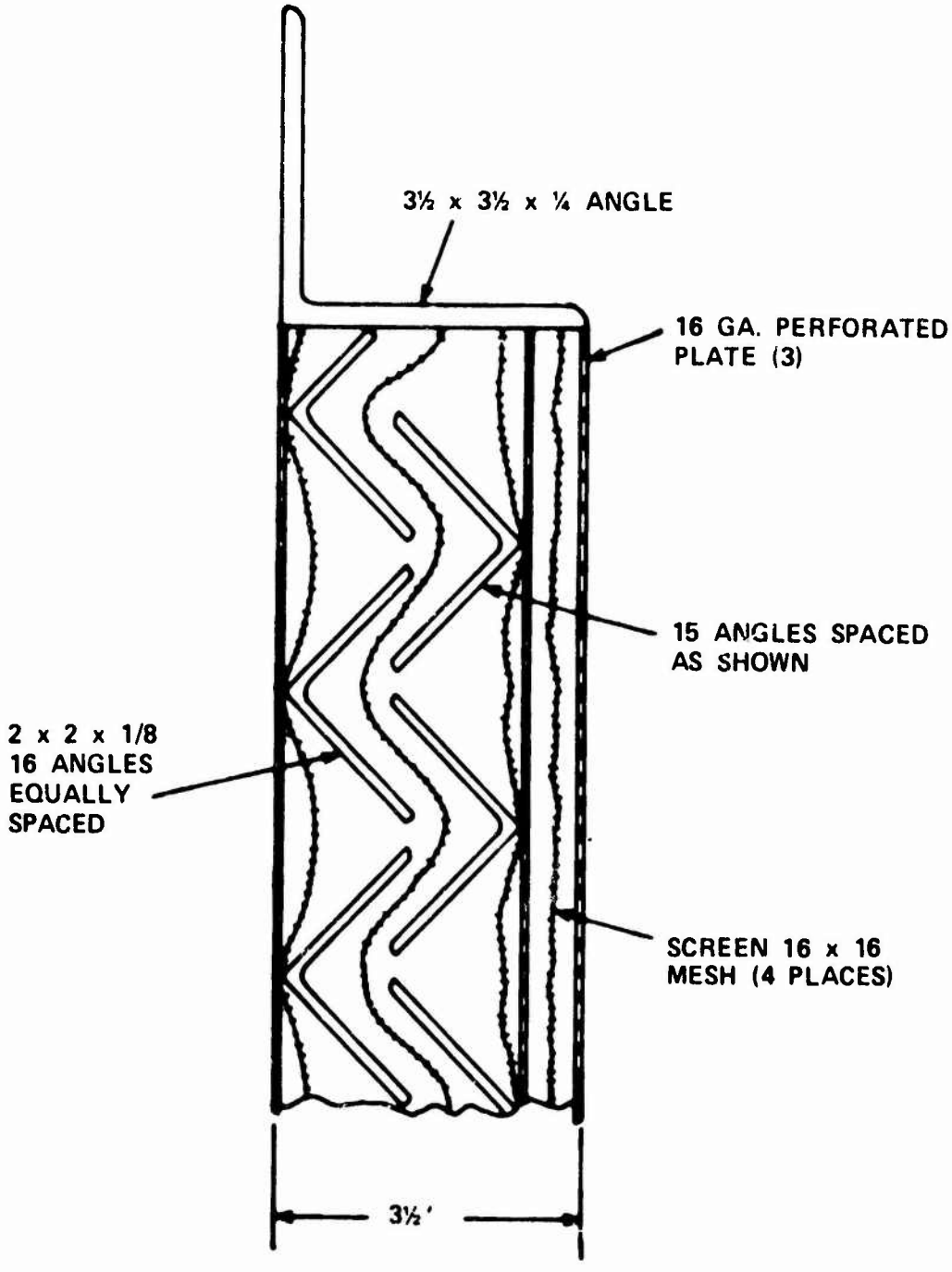

VIEWGRAPH 12 - CATEGORY 5 PANEL SECTION

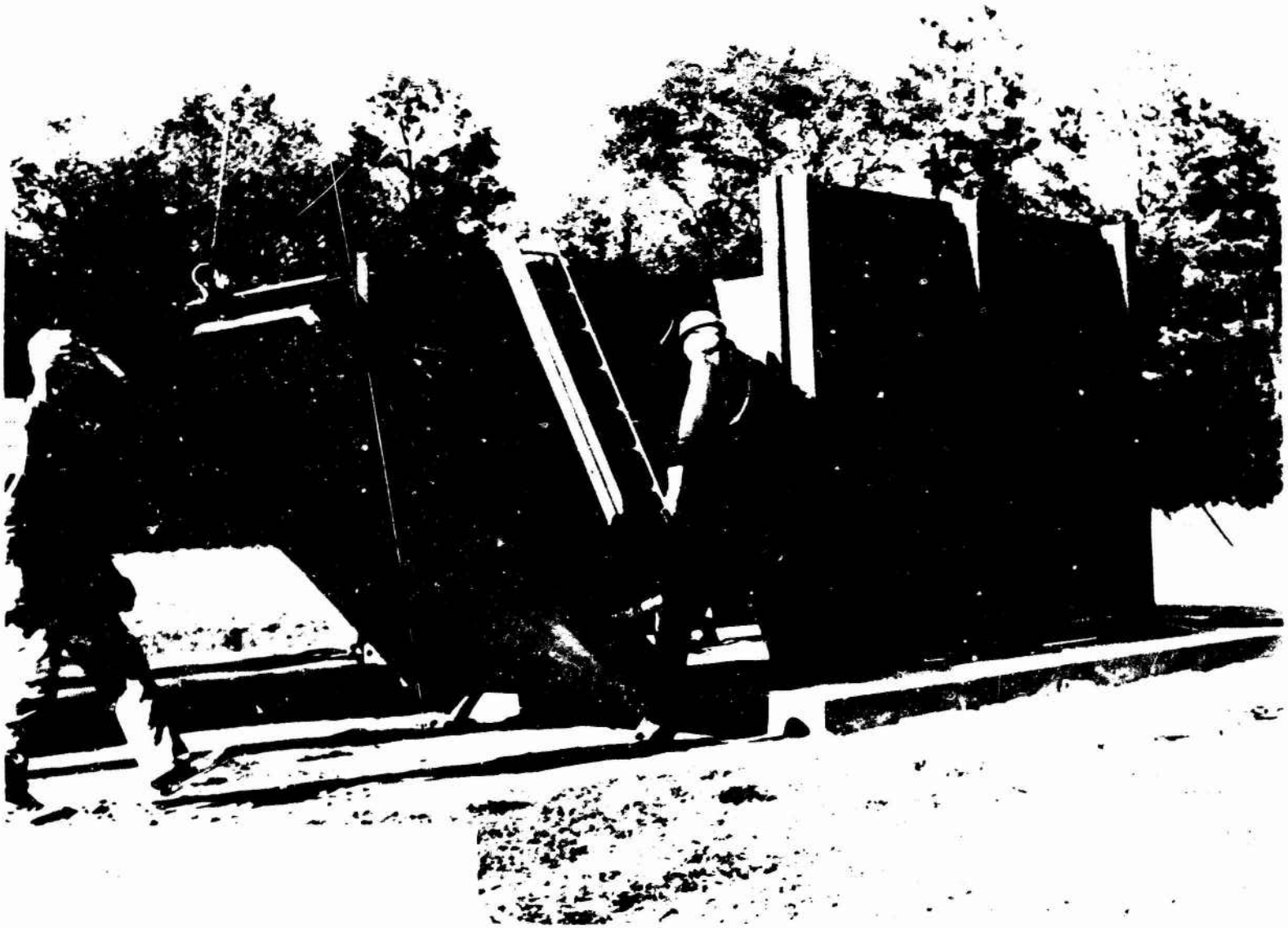



TABLE II. SUMMARY OF TESTS WITH SHIELD GROUP 5

MATERIAL	CHARGE WEIGHT	TYPE OF TEST
M10 GUN PROPELLANT	270 Kg (590 Lb.)	EXPLORATORY
ILLUMANT MATERIAL (50:50 SODIUM NITRATE–POWDERED MAGNESIUM)	22.7 Kg (50 Lb.)	EXPLORATORY
EXPLOSIVE MATERIAL (C-4)	1.1 Kg (2.5 Lb)	PROOF

1739

VIEWGRAPH 15 -- SUPPRESSIVE SHIELD GROUP 5 TESTING

SENSOR LOCATIONS FOR GROUP 5 S/S TESTS

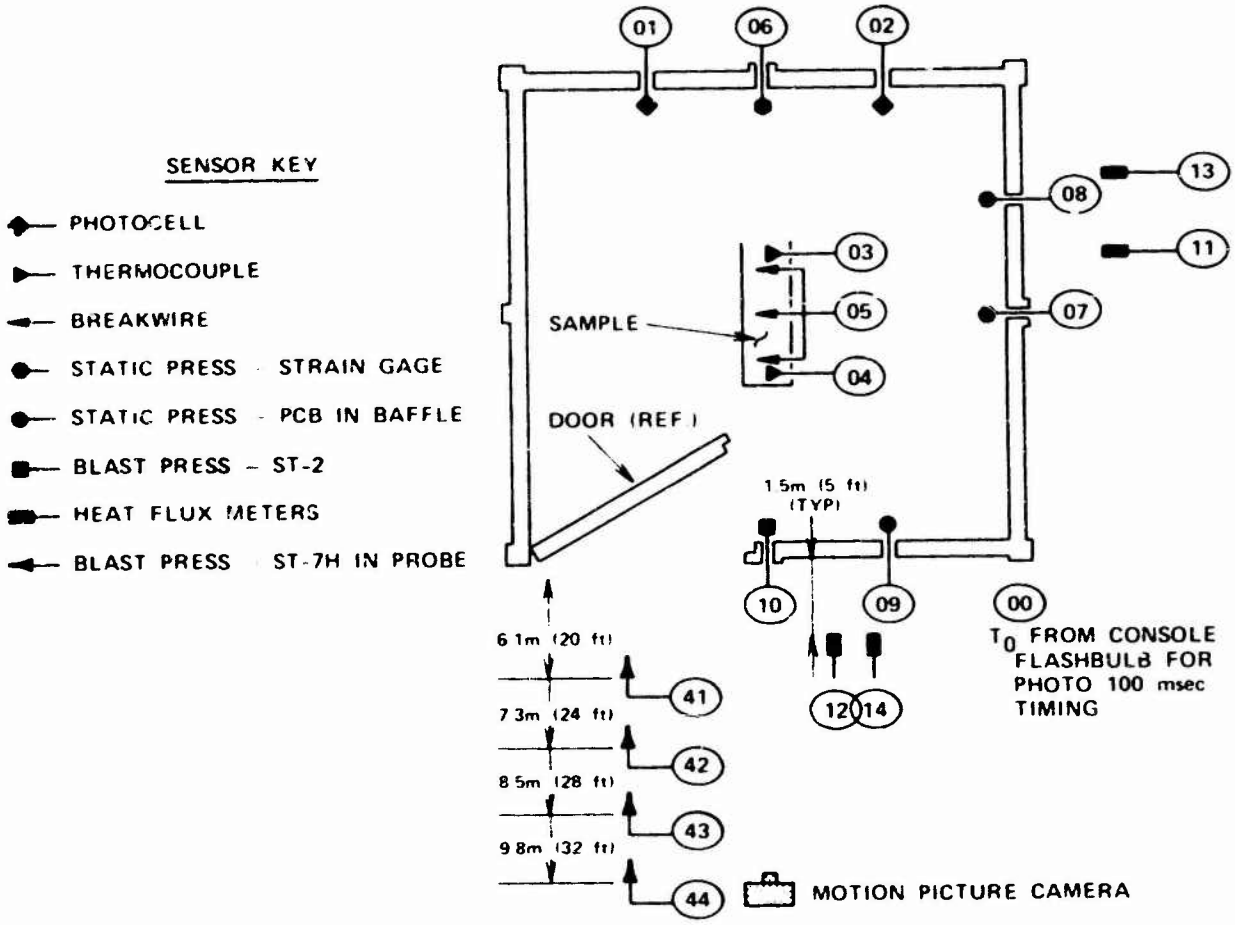

1740

VIEWGRAPH 16 -- SENSOR LOCATION FOR GROUP 5 SUPPRESSIVE SHIELD TESTS

FREE FIELD ILLUMINANT TEST CONFIGURATION

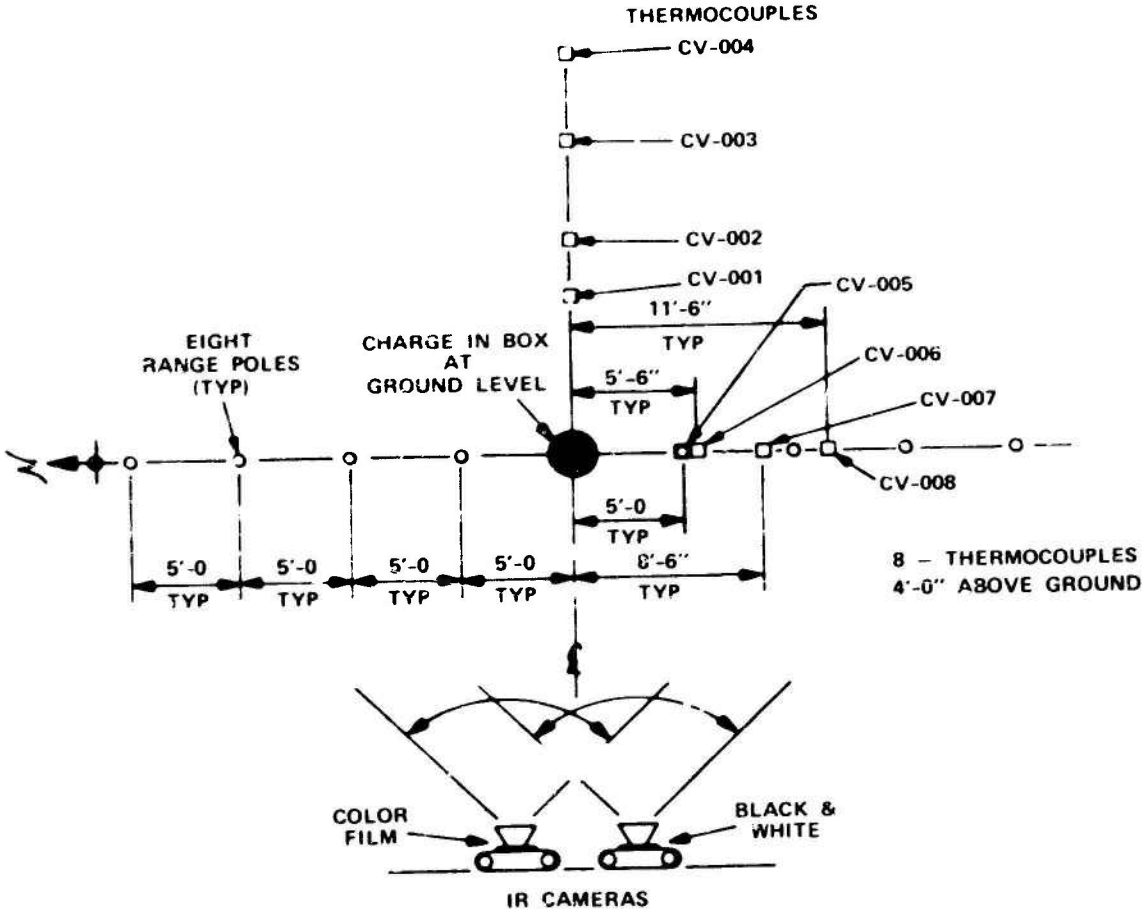

20 LB CHARGE – 30 FT. MINIMUM COVERAGE
30 LB CHARGE – 40 FT. MINIMUM COVERAGE
50 LB CHARGE – 60 FT. MINIMUM COVERAGE

VIEWGRAPH 17 -- FREE FIELD ILLUMINANT TEST CONFIGURATION



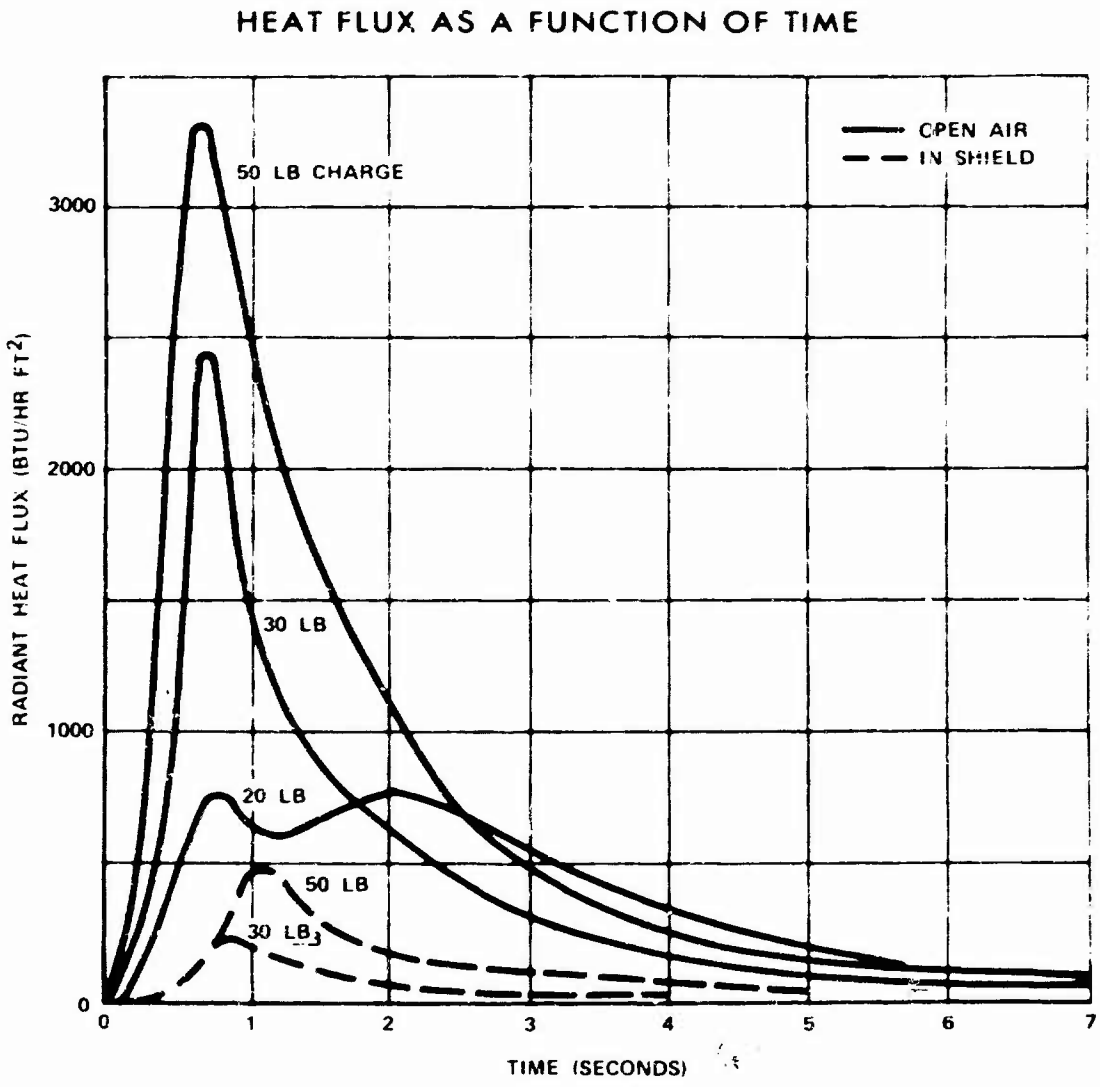

VIEWGRAPH 19 -- HEAT FLUX AS A FUNCTION OF TIME

RESEARCH NEEDED

HAZARD DEFINITION

IMPROVED THERMAL SUPPRESSION TECHNIQUES

SUPPRESSED FIREBALL CHARACTERISTICS

- DIAMETER
- BURNING TIME
- RADIANT FLUX

EFFECT OF NON-UNIFORM VENTING

VIEWGRAPH 20 -- RESEARCH NEEDED

TABLE V SAFETY-APPROVED SUPPRESSIVE SHIELDS

SHIELD TYPE	MATERIAL LIMIT	OPERATOR SAFE DISTANCE	SIZE
		FT	FT
GROUP 3	37 LB OF PENTOLITE	6.2	11.25 DIAMETER x 10 HEIGHT
GROUP 4	9 LB OF PENTOLITE	19	9.2 x 13.1 x 9.3 HEIGHT
GROUP 5	1.84 LB OF C-4	3.7	10.4 x 10.4 x 8.5 HEIGHT
	30 LB OF ILLUMINANT MIX	2	
GROUP 6	13.6 OZ OF PENTOLITE	1	2 DIAMETER
81 mm	TWO 81 mm ROUNDS 2.8 LB OF C-4	3	14 x 18.7 x 12.4 HEIGHT

1745

VIEWGRAPH 21 -- SAFETY APPROVED SUPPRESSIVE SHIELDS

TABLE VI

SUPPRESSIVE SHIELDING

APPLIED TECHNOLOGY PARTICIPANTS

ORGANIZATION	ROLE
CHEMICAL SYSTEMS LABORATORY	TECHNICAL DIRECTION
BALLISTICS RESEARCH LABORATORY	MODELING – BLAST, FRAGMENTATION
NASA - NATIONAL SPACE TECHNOLOGY LABORATORY	FABRICATION AND TESTING
SOUTHWEST RESEARCH INSTITUTE	ANALYSIS – SCALING LAWS
NAVAL SURFACE WEAPONS CENTER	COMPUTER CODES – BLAST SUPPRESSION
U.S. ARMY CORPS OF ENGINEERS	DYNAMIC STRESS ANALYSIS – STRUCTURES
DUGWAY PROVING GROUND	FABRICATION AND TESTING
U.S. ARMY MATERIAL SYSTEMS ANALYSIS ACTIVITY	COST EFFECTIVENESS ANALYSIS
AAI CORPORATION	ENGINEERING SUPPORT

1746

VIEWGRAPH 22 -- APPLIED TECHNOLOGY
PARTICIPANTS

TECHNOLOGY FLOW CHART

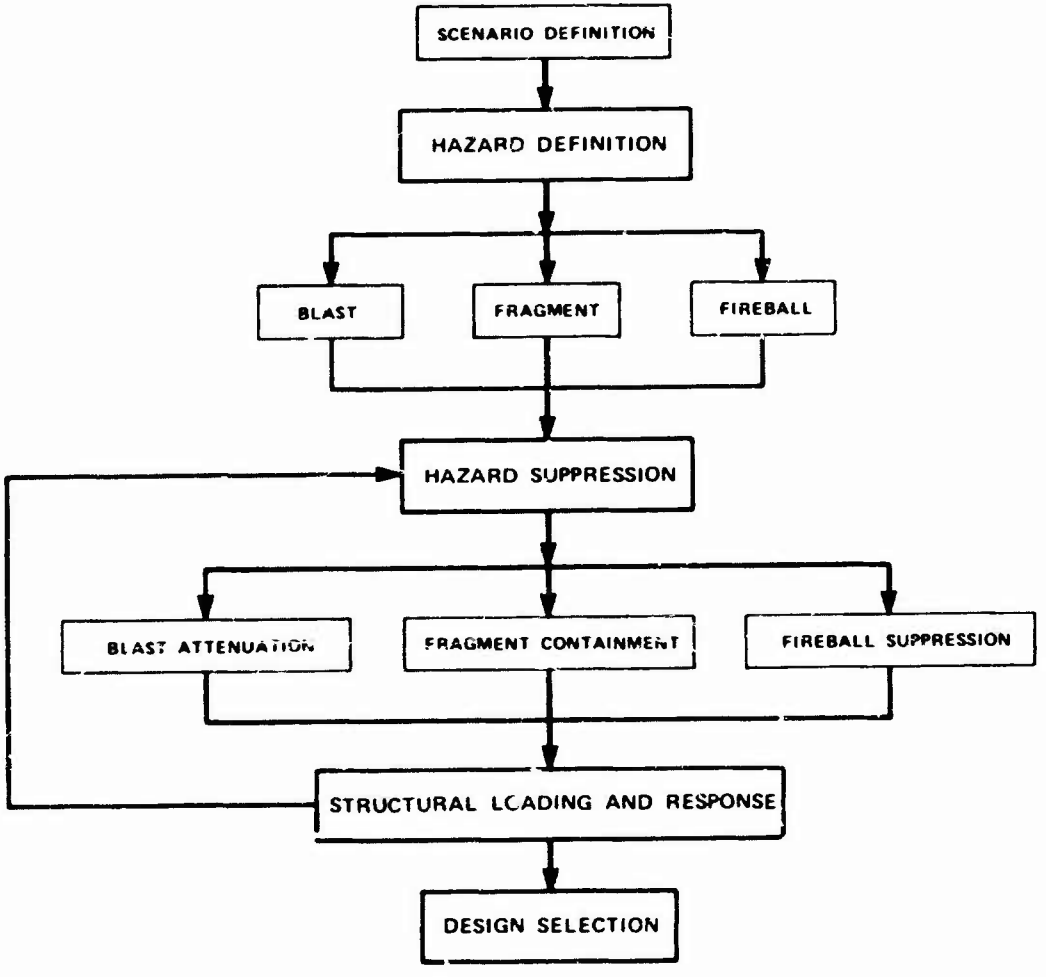

VIEWGRAPH 23 -- TECHNOLOGY FLOW CHART

SUPPRESSIVE SHIELD

TECHNOLOGY SUMMARY

- NO TECHNOLOGY BARRIERS
- PREDICTIVE CAPABILITY AVAILABLE
- SCALING LAWS APPEAR VALID FOR SMALL EXPLOSIVE CHARGES

VIEWGRAPH 24 -- SUPPRESSIVE SHIELD
TECHNOLOGY SUMMARY

TABLE VII

SUPPRESSIVE SHIELDING ENGINEERING DESIGN HANDBOOK

CHAPTER I.	INTRODUCTION	
		– HISTORY OF THE PROJECT
		– USE OF HANDBOOK
CHAPTER II.	SAFETY APPROVED SUPPRESSIVE SHIELDS	
		– DESCRIPTION AND USE OF APPROVED SHIELDS
CHAPTER III.	EXPLOSIVE ENVIRONMENTS	
		– METHODS FOR COMPUTATION OF HAZARDS AND SUPPRESSION
CHAPTER IV.	SUPPRESSIVE SHIELD STRUCTURAL BEHAVIOR	
		– MATERIAL PROPERTIES AND ACCEPTABLE RESPONSE
CHAPTER V.	STRUCTURAL DESIGN AND ANALYSIS	
		– METHODS FOR DYNAMIC STRESS ANALYSIS
		– DESIGN PROCEDURES
CHAPTER VI.	STRUCTURAL DETAILS	
		– DOORS, PENETRATIONS, LINERS
CHAPTER VII.	ECONOMIC ANALYSIS	
		– METHODS
CHAPTER VIII.	ASSURING STRUCTURAL QUALITY	
		– QUALITY ASSURANCE
APPENDIX		
		– ENGINEERING DRAWINGS OF SAFETY APPROVED SUPPRESSIVE SHIELDS
		– ENGINEERING DESIGN CHARTS
		– SAMPLE ECONOMIC ANALYSIS

1749

VIEWGRAPH 25 -- SUPPRESSIVE SHIELD ENGINEERING DESIGN HANDBOOK

SUPPRESSION OF FRAGMENT DAMAGE BY MEANS OF FRANGIBLE SURROUNDS*

by

J. E. Backofen, Jr.
Battelle, Columbus Laboratories
Columbus, Ohio

and

L. J. Wolfson and J. D. Shock
U. S. Naval Explosive Ordnance Disposal Facility
Indian Head, Maryland

* Sponsored by the U.S. Naval Explosive Ordnance Disposal Facility, Indian Head, Maryland, under Contract No.'s N00174-74-C-0219, N00174-75-C-0190, and N00174-77-C-0128.

PRECEDING PAGE BLANK

SUPPRESSION OF FRAGMENT DAMAGE BY MEANS OF FRANGIBLE SURROUNDS

by

J. E. Backofen, Jr.
Battelle, Columbus Laboratories
Columbus, Ohio

and

L. J. Wolfson and J. D. Shock
U. S. Naval Explosive Ordnance Disposal Facility
Indian Head, Maryland

ABSTRACT

Frangible surrounds consisting of sand have been used successfully within spherical portable complete containment vessels to suppress pipe bomb fragmentation damage. Initial design criteria for frangible surrounds constructed with sand or plaster-of-Paris have been established for the effective suppression of fragment damage. More effective materials have been identified. The mechanisms of preventing fragment damage have also been identified.

INTRODUCTION

Battelle's research on fragment damage suppression began during a research program for the development of portable chambers to contain the blast and fragments from "terrorist" pipe bombs.* During this program the technical monitor, Mr. Lennard Wolfson of the U.S. Naval Explosive Ordnance Disposal Facility, suggested that an additive mass annulus of sand could slow down the initial velocity of the fragments so that they would not perforate the chamber's walls.[1]**

---

* A paper on the development and testing of these chambers has been presented during the "Safety in Transport" session of this Seminar.

** References are listed at the end of the paper.

Mr. Joseph Backofen of Battelle's Columbus Laboratories had also previously used a similar technique of an annulus of water in the form of a disposable pool in which a large soft plastic bucket was immersed so that fragments from prototype controlled fragmentation shells exploded in the bucket could be slowed down and collected without damaging them or Battelle's 8-lb-capacity containment facility.[2] On the basis of the past experience, Mr. Wolfson's concept was expanded to include an air gap of variable size between the explosive-filled pipe and the sand annulus so that the restraint medium would not need to be matched to any particular threat. This configuration would also then allow the restraint medium to be sized to the maximum containment capacity of the chamber and still permit its use with any smaller threat.

Upon successful completion of the objectives of the first program, it was suggested that research continue separately on the subject of frangible surrounds. Two other research programs were funded in the next two years to find an expression that would enable engineering estimates of the amount of materials that would be needed to suppress a particular fragmenting munition and to determine the effectiveness of various frangible restraint materials.

OBJECTIVE

The summed objectives of the three programs can be expressed by the following:

- Develop a practical inexpensive lightweight method of suppressing fragment damage to portable containment structures.
- Determine ways to scale a controllable parameter that determines the threshold for fragment damage.
- Determine the sequence and significance of the interactions between the fragments, frangible surround, and the structure.

TECHNICAL DISCUSSION

The effort expended in the first program quickly demonstrated that a relatively thin annulus/layer of sand could be used to suppress fragment damage to the inside of the containment structure. This research was performed in a 2-foot-long section of 3-ft-diameter pipe lined with one foot square witness plates. Composition C-4 explosive filled 6-inch lengths of 2-inch-diameter schedule 40 pipe with a single end cap were suspended within the annulus of restraint material and above a layer of restraint material/air gap/witness plate. Figure 1 illustrates the arrangement and results of a typical experiment.

In the series of eleven experiments it was determined that a thickness of 2.5 inches would be required. This annulus of sand could be in contact with the pipe or up to an air gap of one pipe radius away and still be sufficient to preclude damage to the containment structure. This restraint was used successfully in contact with pipe bombs exploded within the 2-ft-diameter portable spherical complete containment chamber. The sand precluded fragment damage to the walls and door operating mechanism of the chamber.[1]

Although this frangible additive mass annulus of sand concept was sufficient for use in the portable containment chamber, the nature of the discovery warranted further investigation to identify the processes removing energy from the fragments. These processes were at first confusing for the following reasons:

(a) Placing the additive weight into the Gurney equation for fragment velocity from fragmenting cylindrical shells yielded velocities high enough that the fragments should have perforated the witness plates.

(b) Using (a) to generate the same velocity for both fragments and sand and then assuming that the fragments remain behind the sand[3] until witness plate impact would still allow the fragments to perforate the sand[4,5] and witness plates.

The initial experiments of the second program were done in an open chamber set up as shown in Figure 2. The plates were instrumented with aluminum foil arrival switches. The time of arrival and witness plate damage were noted for a series of twenty experiments having eighteen different configurations of explosive filled pipe, air gap, and restraint medium. Later

experiments utilized arrival switch instrumented witness plates and two channels of 300 Kev Field Emission radiograph equipment as shown in Figures 3 and 4 to get pictures of the interactions between the fragments and the frangible restraint media. A sample radiograph is shown as Figure 5. In these thirty experiments the size of the explosive filled pipe, the air gap, and the material used in the frangible surround were varied in twelve different configurations to form a matrix of fragment velocity and witness plate damage data. The materials used in the surround included sand, plaster-of-Paris, and hollow ceramic microballoons.*

The general progression of events after detonator firing was determined to be the following[6]:

- The explosive detonates and accelerates the pipe.
- The pipe fragments.
- The fragments impact the inner wall of the restraint medium cylinder (frangible surround).
- The restraint material and pipe fragments fly toward the witness plates.
- The blast wave reaches the witness plates.
- The restraint material reaches the witness plates.
- The fragments collide with the restraint material.
- The fragments may collide with the witness plates.

The theory previously expressed as (b) that the frangible surround was simply coming to rest and then being impacted by the fragments which could then penetrate the relatively thin layer and the witness plate was put to test by firing a pipe having a charge hollowed out so that the fragment velocities approximated those measured. Figure 6 illustrates the results. The fragments perforated the witness plates.

The second program's experiment data implied that a unit length strip explosive charge to pipe + frangible surround mass ratio of less than 0.058 was generally required to suppress significant (measurable by hand and eye) indentations in the witness plates. The following relationship was also determined for the velocity of the frangible surround material and fragments before impact at the witness plates.

---

* Eccospheres FAA manufactured and supplied by Emerson & Cuming, Inc., Northbrook, Illinois.

$$[m_f + m_r + \frac{c}{2}][1 + 0.0221\ (\frac{c}{m_f + m_r})^{-0.927}]V_f^{\,2} = 2Ec \qquad (1)$$

where

m_f, m_r, and c are the unit length weight of the pipe, restraint medium, and explosive charge respectively, lb/in.

V_f is the velocity of the fragments, ft/sec

2E is the square of the Gurney velocity for C-4, $\sqrt{2E}$ = 7880 ft/sec[7].

This equation is a form of an energy balance like the Gurney equation, but it also includes a term for energy expended during disruption of the frangible surround.[6]

Since the matrix of experiments from the second program was rather large and sparsely populated, a follow-on effort was funded a year later to substantiate the scaling relationships, investigate the interactions occurring at the witness plate surface, and examine the effectiveness of other materials. The research in this third program confirmed the velocity scaling relationship for a larger variety of explosive charge to total mass ratios per unit length, $c/(m_f + m_r)$, ranging from 0.038 to 0.11.[8] Figures 7 and 8 illustrate the reduction of flash radiograph position data by graphical methods into velocity data for the two programs. The lack of far-field damage to the reinforced concrete walls of Battelle's 40-ft-diameter complete containment facility was noted for each experiment in order to provide far-field damage data. The threshold of damage to near-field witness plates was further substantiated to be at a $c/(m_f + m_r)$ of 0.058 for sand and plaster-of-Paris frangible surrounds.[8] However, frangible surrounds made from materials such as microballoons, plaster/microballoon mixtures, and sand/epoxy suppressed damage at $c/(m_f + m_r)$ of 0.120, 0.106, and 0.087 respectively. The scaling relationship for fragment/media velocity had to be changed to the following in order to account for the greater absorption of energy by the microballoon restraint medium.[8]

$$[m_f + m_r + \frac{c}{2}][1 + 0.0375\ (\frac{c}{m_f + m_r})^{-0.967}]V_f^{\,2} = 2Ec \qquad (2)$$

Both this equation and the previous equation are fitted through their respective data points in Figure 9. Sufficient experiments were not performed with plaster/microballoon mixtures or sand/epoxy to enable a determination of their increased effectiveness.

The flash radiographs taken during the third program illustrated the following:

- The restraint medium (frangible surround) cloud reaches the witness plates.
- The restraint medium packs up at high pressure on the surface of the witness plates as the plates accelerate under the impulse.
- The fragments impact the compressed restraint medium.

This demonstrated that the restraint medium was impacting to form an impervious barrier on the surface of the plate. This has not been analyzed to date. The dynamic compaction cannot be estimated at the present time because the impacts occur as individual particles, each of which can generate a "water hammer" impact pressure. This pressure, however, can only be held by the particle for a brief period related to the speed of sound in the particle and its dimension along the impact velocity vector. Unfortunately, the speed of sound in the particles and impacting particle sizes are unknown. However, on the basis of observations in a few experiments using Primacord-filled glass tubing surrounds and a shock-mounted Susquehanna Instruments ST-4 piezoelectric pressure transducer, these time durations are anticipated to be of submicrosecond order.(9)

From these observations, it can only be concluded that the impacting restraint medium forms a very dense protective covering on the surface of the witness plates and that this layer absorbs the impact of the fragments. The effectiveness of this layer is dependent upon the material used for the frangible surround. The effectiveness is also somewhat dependent upon the velocity of impact of the material against the witness plates and the impact velocity of the fragments.

The delivery of significantly more mass over a longer period of time at the surface of a structure can lead to enhanced coupling.(10) This enhanced "blast" must be able to be withstood by the structure being protected from fragment damage. In the case of the spherical portable chamber using cylindrical pipe bombs and sand as the restraint material in the surround, this led to a significant egg shape after three experiments.

CONCLUSIONS

Initial design criteria for frangible surrounds constructed with sand or plaster-of-Paris have been established for the effective suppression of fragment damage. More effective materials have been identified. The mechanisms of preventing fragment damage have also been identified. But more research for fragment damage protection by this technique still remains to be performed.

REFERENCES

(1) Trott, B. D., Backofen, J. E. Jr., and White, J. J. III, "Blast and Fragment Containment Capability of Portable Chambers", Final Report on Contract No. N00174-74-C-0219 to U.S. Naval Explosive Ordnance Disposal Facility, Indian Head, Md., by Battelle, Columbus Laboratories, Columbus, Ohio, September 1975 (AD A-024 493).

(2) McCurdy, H. R., Peterson, J. H., and Meiners, K. E., "Investigation of Advanced Powder Metallurgy Techniques Applicable to Improved Five-Inch/54 Projectiles", Final Report on Contract No. N00178-73-C-0092 to Naval Weapons Laboratory, Dahlgren, Va., by Battelle, Columbus Laboratories, Columbus, Ohio, December 15, 1973.

(3) Fugelso, L. E., and Rathmann, C. E., "Effect of Earth Cover on Far-Field Fragment Distribution", Technical Report on Contract No. DAAB09-73-0010, to Department of Defense Explosives Safety Board, Washington, D.C. by General American Research Division, General American Transportation Corporation, Niles, Ill., December 1973 (AD 915 482L).

(4) Allen, W. P., Mayfield, E. B., and Morrison, H. L., "Dynamics of a Projectile Penetrating Sand", Journal of Applied Physics, 28, pp. 370-376, 1957.

(5) Allen, W. P., Mayfield, E. B., and Morrison, H. L., "Dynamics of a Projectile Penetration Sand, Part II", Journal of Applied Physics, 28, pp. 1331-1335, 1957.

(6) Backofen, J. E. Jr., "The Interaction of Steel Fragments From an Exploding Device and Mass Addition Fragment Restraint Systems", Final Report on Contract No. N00174-75-C-0190 to U.S. Naval Explosive Ordnance Disposal Facility, Indian Head, Md., by Battelle, Columbus Laboratories, Columbus, Ohio, January 21, 1976 (AD B015 931L).

(7) The JANNAF Hazards Working Group, "Chemical Rocket/Propellant Hazards", Volume 1, General Safety Engineering Design Criteria, Chemical Propulsion Information Agency, The Johns Hopkins University, Applied Physics Laboratory, CPIA Publication 194, May 1972 (AD 889 763).

(8) Backofen, J. E. Jr., and Schola, W. F., "Scaling the Interaction of Steel Fragments from an Exploding Device and Mass Addition Fragment Restraint Systems", Final Report on Contract No. N00174-77-C-0128 to U. S. Naval Explosive Ordnance Disposal Facility, Indian Head, Md., by Battelle, Columbus Laboratories, Columbus, Ohio, December 7, 1977.

(9) Backofen, J. E. Jr., and Schola, W. F., "Rapid Clearance of Area-Denial Munitions by Explosively Generated Shock Waves", Final Report No. NEODF 2-1 to U.S. Naval Explosive Ordnance Disposal Facility, Indian Head, Md., by Tactical Technology Center, Battelle, Columbus Laboratories, Columbus, Ohio, September 1977.

(10) de Klerk, A., "Measurement of Near-Field Blast Effects of Fluidically Encased Explosive Charges", NWC TP 5857, Naval Weapons Center, China Lake, Ca., by Denver Research Institute, Denver, Colorado, May 1976.

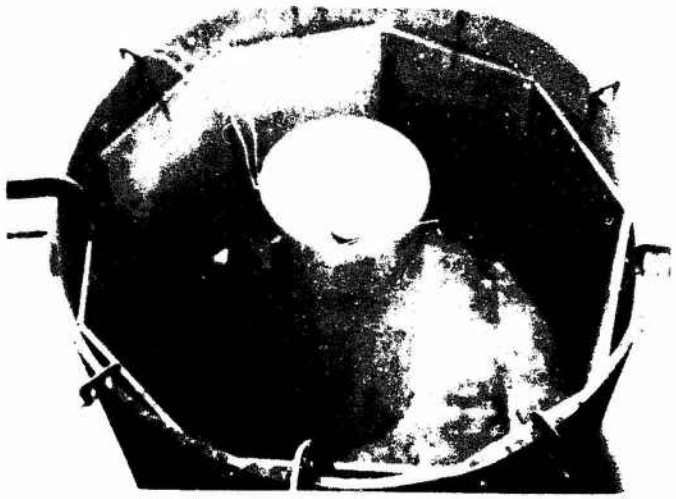

(a) Arrangement of Experiment



(b) Witness Plates After Experiment

FIGURE 1. SAMPLE EXPERIMENT WITH SAND FILLED FRANGIBLE SURROUND

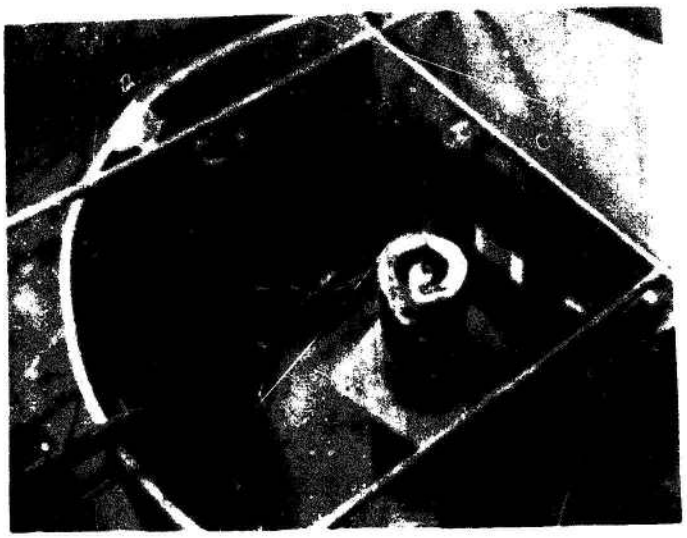

FICURE 2. OPEN CHAMBER EXPERIMENTS WITH WITNESS PLATES INSTRUMENTED FOR ARRIVAL TIME



FIGURE 3. TYPICAL EXPERIMENT FOR THE FLASH RADIOGRAPHY INVESTIGATION OF THE INTERACTIONS OF FRAGMENTS AND RESTRAINT MATERIALS

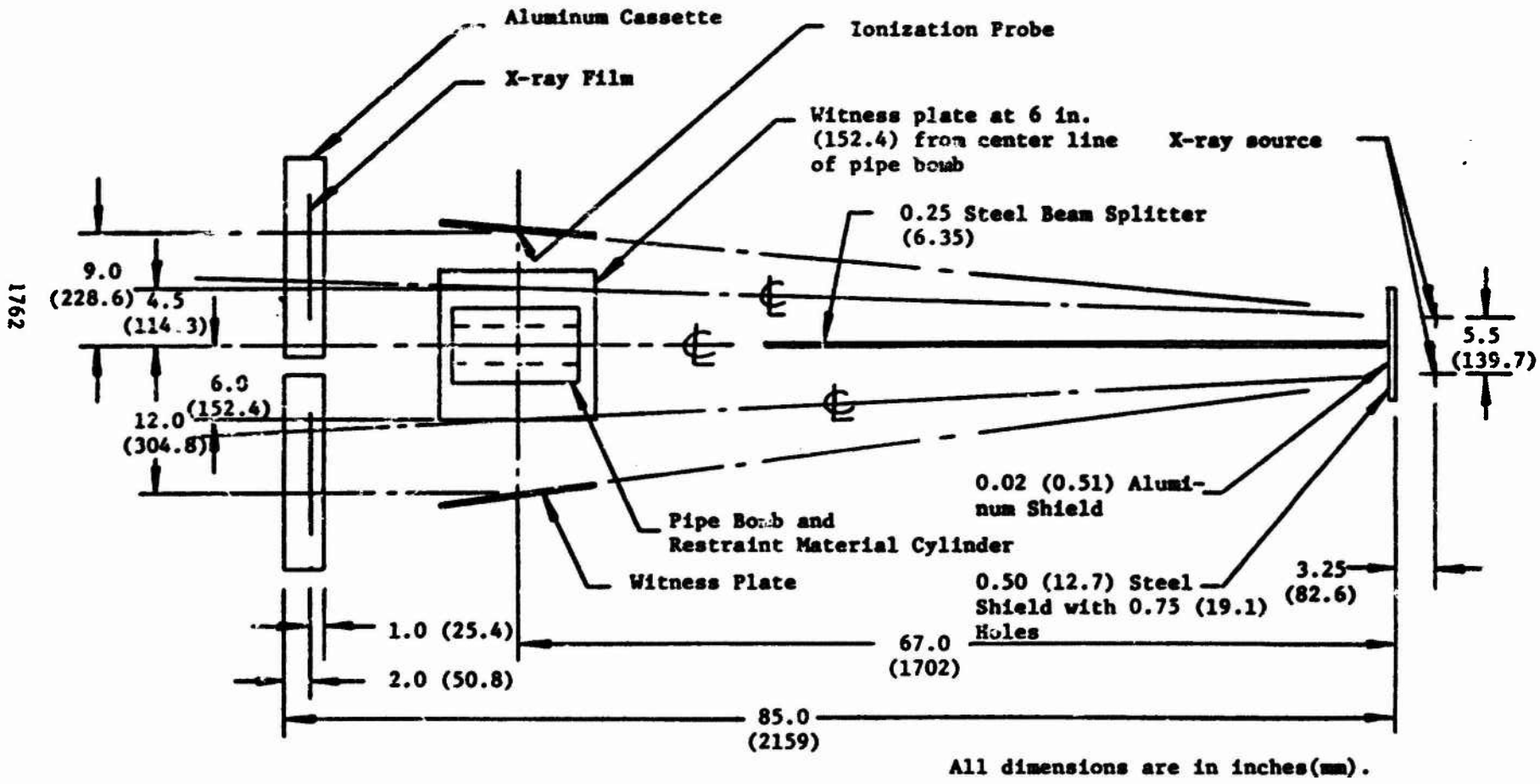

FIGURE 4. PLAN VIEW OF FLASH X-RAY EXPERIMENT GEOMETRY

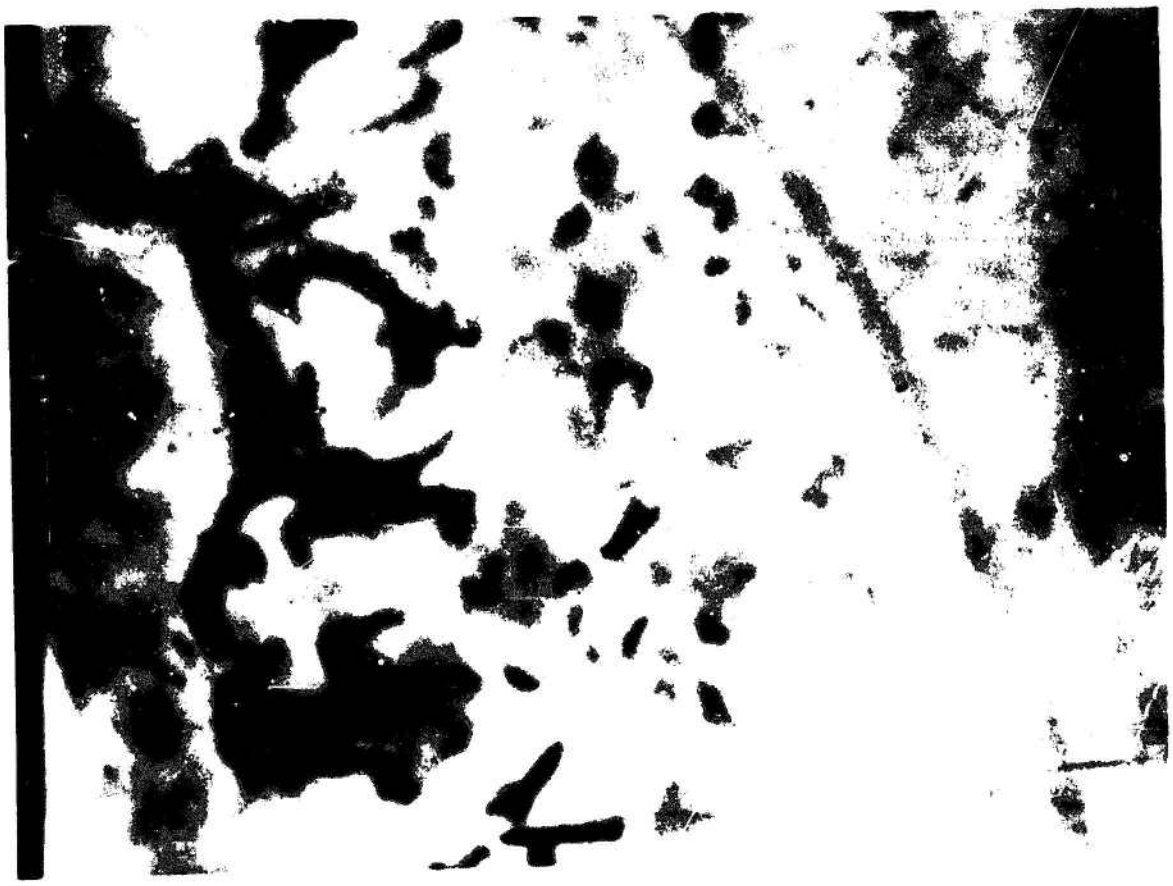

FIGURE 5. FLASH RADIOGRAPH OF A PLASTER RESTRAINT MEDIUM JUST IMPACTING A WITNESS PLATE AT 9 INCHES FROM THE CENTERLINE OF EXPERIMENT NUMBER 108 (TAKEN AT 200 μsec)

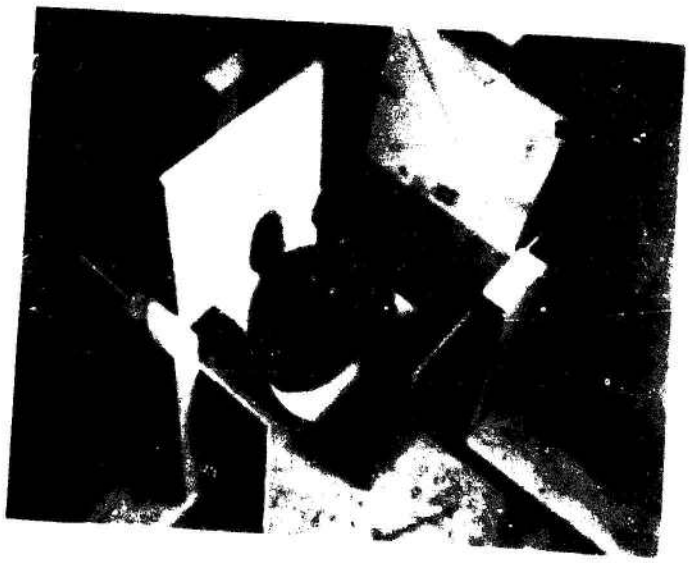

(a) Arrangement

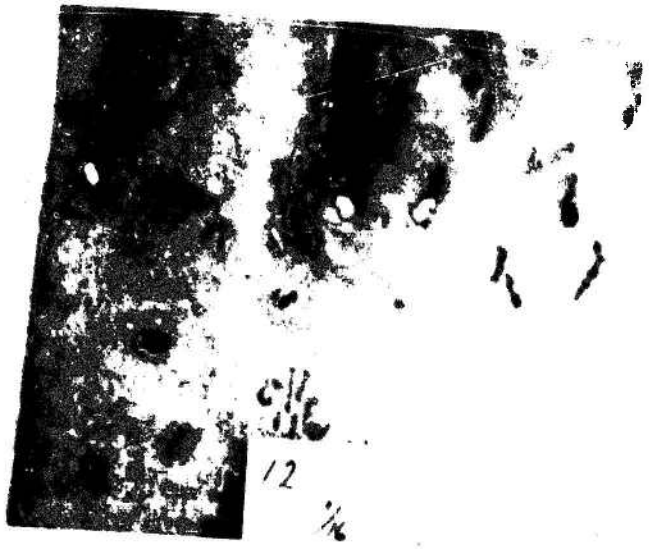

(b) Damage to Witness Plate Precoated with 0.19 Inch of Hardened Plaster-Of-Paris

FIGURE 6. EXPERIMENT ARRANGEMENT USED TO STUDY FRAGMENT DAMAGE TO WITNESS PLATES PRECOATED WITH HARDENED PLASTER-OF-PARIS AND TYPICAL DAMAGE TO ONE OF THE WITNESS PLATES

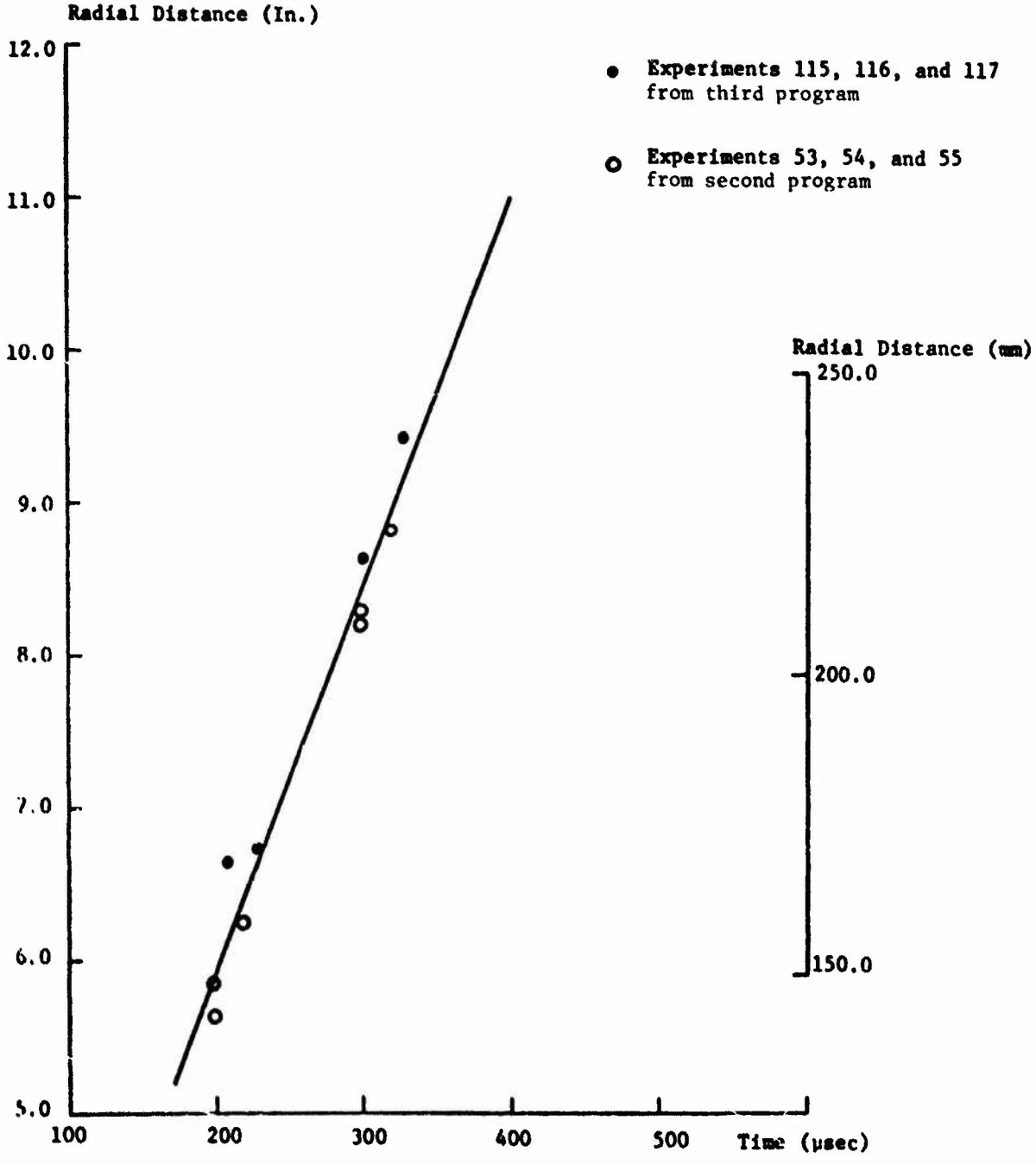

FIGURE 7. AVERAGED FRAGMENT LOCATIONS VERSUS TIME FOR SIX EXPERIMENTS

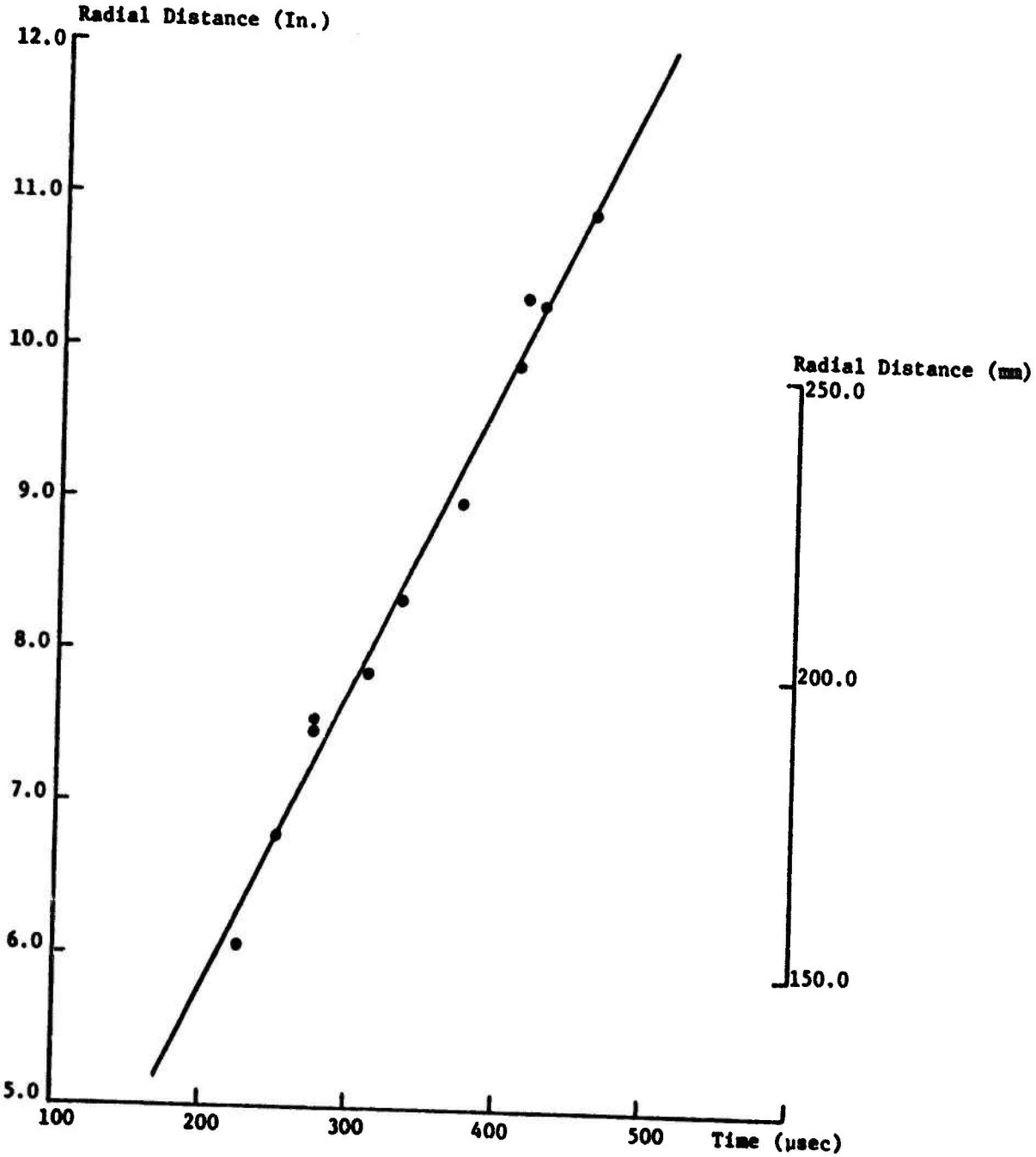

FIGURE 8. AVERAGED FRAGMENT LOCATIONS VERSUS TIME FOR SEVEN EXPERIMENTS

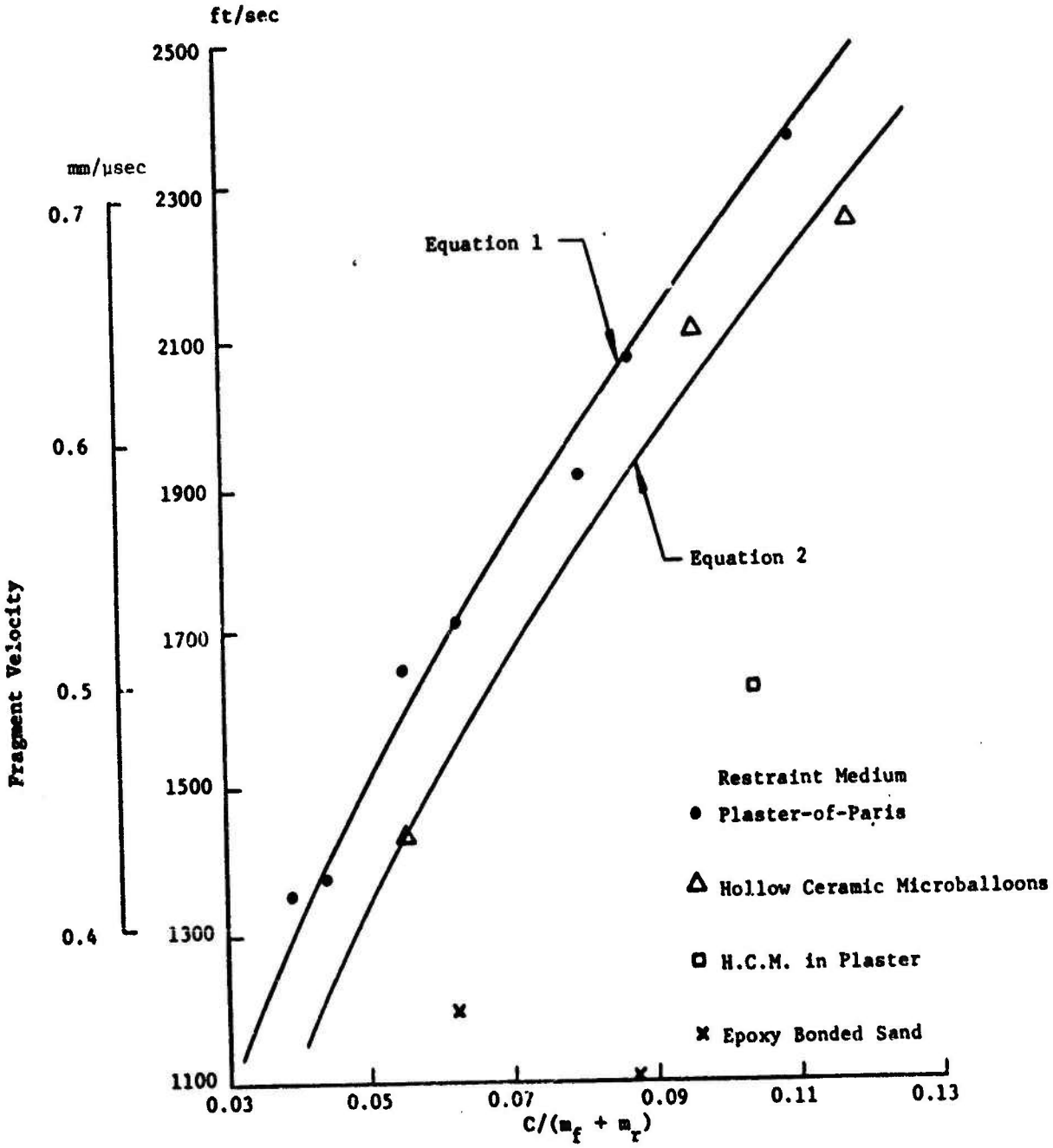

FIGURE 9. CORRELATION OF THE VELOCITY OF THE FRAGMENTS TO THE SCALING RELATIONSHIPS

SHIELDS FOR DECELERATING MUNITIONS FRAGMENTS

Joseph G. Connor, Jr.
Naval Surface Weapons Center
White Oak, Silver Spring, Maryland

INTRODUCTION

The tests described below were conducted to determine the relative effectiveness of several common materials as fragment decelerators. A flat sample of each material was placed in the spray of explosively driven steel case fragments between a Composition A-3 loaded 5"/54 projectile and a Celotex recovery pack. Three of four recovery packs around each projectile were shielded by one of the candidate materials; the fourth pack was an unshielded control.

Five tests, involving fifteen material samples were conducted at the New Mexico Institute of Mining and Technology. This report concerns the rationale of the tests and the relation of shield parameters to fragment interception efficiency. Further tests are indicated to confirm the choice of "best" shield material from this limited series of tests.

The ultimate reason for conducting these tests is to find a shield which will prevent too many hazardous fragments from traveling too far from an accidental detonation. A "hazardous" fragment, for purposes of the present work, is defined as one whose kinetic energy exceeds 58 ft-lb. A fragment with this energy has gone "too far" if, at or beyond a range of 500 ft, more than one is found in an area of 600 ft^2.

TEST SET UP

As many as four 4 ft by 8 ft collection packs were placed on the ground with the 8 ft side horizontal and tangent to a circle of 15 ft radius centered on the longitudinal axis of the projectile. The projectile was mounted base down at such a height that the 4 ft dimension of the collection packs approximately covered the polar angles between 90° and 105°. (See Figure 1). Test firings indicated that the most dense spray of fragments is found in this polar angle range.

The shield material samples were placed parallel to the collection packs at a distance of 2 ft from the projectile. The samples were all 2 ft high and 3 ft wide -- large enough

PRECEDING PAGE BLANK

to completely shadow the collection packs so that no fragments were able to travel directly from a projectile to a collection pack without passing through the shield. The materials were ranked according to the fragment velocities determined from mass and penetration depth in the Celotex packs.

General photographic coverage was provided on all tests. On the last three shots, aluminum sheets 0.12 in thick were fastened to the front of each recovery pack to produce a visible flash of light when a high speed fragment strikes the metal sheet. Fastax cameras running at a nominal rate of 5000 frames/second were positioned so that detonation light and fragment flashes from the aluminum sheets could be observed and timed. From these times of arrival at the front face of the Celotex packs an average velocity over the 15 ft flight path can be determined. This velocity is the instrumental velocity discussed later in this report.

SHIELD MATERIALS

Design of an effective shield requires choosing a type of material and determining the thickness necessary to do the job. The exact configuration for an efficient, practical shield can be determined easily once these two parameters are specified.

Shield materials for the first tests were chosen for their inertial properties. One can expect about 10 lb of steel case fragments to be ejected toward one of the Celotex packs which cover the polar angles between 90° and 105° and a bit less than 90° in azimuth. From momentum transfer considerations, if these fragments all strike an obstacle weighing about 100 lb their velocity will be reduced by about 90%. A 5/8 in steel plate 2 ft by 3 ft in area weighs about 150 lbs; one was available and was taken as a starting point. Other shields on the first round of tests had about the same arealdensity as the steel plate. This approach will indicate the effect of material choice alone -- eliminating density as a parameter. The materials used in the first six shields are listed in Table 1.

Because these shields were massive enough to preclude practical use, a second test series was conducted using different materials with areal densities smaller than those in the first series. Materials were chosen with properties other than inertia which were expected to be effective in breaking up or decelerating fragments. In particular, woven materials,

such as Kevlar or nylon cloth and wire rope blasting mats, have directional tensile properties which tend to make the materials catch and deflect incident fragments. The seven samples chosen for the second series of tests are described in Table 2.

DATA REDUCTION

Fragments were recovered from the Celotex recovery packs and cleaned. The mass of each fragment and its penetration depth in the recovery pack (to the nearest 1/2 inch) were recorded and used to determine fragment velocity at the front face of the Celotex. Initial velocity, at the shell case, was determined for each fragment assuming a flat trajectory and constant aerodynamic drag. Fragment velocity at 500 ft was calculated similarly. These values as well as fragment kinetic energy at various locations were all determined with a digital computer code.

The area/mass ratio is determined from the fragment shape factor and fragment mass as follows:

$$A/M = 0.0922\ M^{-1/3}$$

where: A = presented area (in^2)

M = fragment mass (grams)

Fragment velocity was determined from mass and Celotex penetration using an empirical relation determined for fragment velocities between 3000 and 6000 ft/sec. The fragments were 5/16" x 5/16" x 5/8" "cubelets". The relation reads as follows (Reference 1):

$$V = C\ P\ (A/M)$$

where: V = fragment velocity (ft/sec)

P = penetration depth (inches)

A = fragment presented area (in^2)

M = fragment mass (grains)

$C = 2 \times 10^5$

1. Private communication, R.G. Sewell, NWC, China Lake.

Fragment velocity at various distances from the projectile was determined from the measured velocity at the Celotex recovery pack by assuming constant aerodynamic drag and a flat trajectory. The expression developed from these assumptions is:

$$V_R = V_o\, e^{-0.121(A/M)R}$$

$$= V_C\, e^{0.121(A/M)R_C}\, e^{-0.121(A/M)R}$$

$$= V_C\, e^{0.121(A/M)(R_C - R)}$$

where: V_R = velocity at distance R (ft/sec)

V_o = velocity at projectile case (ft/sec)

V_C = velocity at Celotex (ft/sec)

A/M = fragment area/mass ratio (in^2/gram)

R_C = Celotex stand off from projectile (ft)

R = distance from projectile

$0.121 = 1/2\, C_D\, \rho_o \times (12\ in/ft) = 1/2(1.28)(.01574\ gm/in^3)$

For fragments that pass through a shield the velocity at the Celotex can be interpreted as the residual velocity characteristic of the material. This is a reasonable approximation because of the supersonic speed with which the fragments travel the short path length between the shield and the collection pack.

Kinetic energy at the recovery pack and at 500 ft from the projectile is calculated from the usual expression: $KE = 1/2\, M\, V^2$, using the appropriate velocity.

Total and average mass of fragments recovered from each pack are calculated, as are total and average fragment kinetic energy absorbed. Also, an arithmetic average of fragment velocities behind each shield material is calculated.

An arithmetic average of all penetration depths in each collection pack was calculated. A velocity was determined by using this average penetration with the average mass of fragments recovered from the pack in the empirical penetration relation. The velocity calculated in this way is similar to the instrumental velocity measured in the usual arena tests.

RESULTS

A summary of the characteristics of the fragments recovered from all the Celotex packs is shown in Table 3. The fifth line is simply an average of the first four. The remaining items are listed in order of decreasing areal density by group, and, within each group, in order of increasing total fragment weight recovered from the Celotex packs.

The average fragment mass for each pack is the total mass of fragments divided by the total number of fragments found in the pack. The average penetration is also simply the arithmetic average of all penetrations recorded. The velocity in the last column is determined by substituting these averages into the empirical relation discussed in the preceding section. However, because the fragments recovered from the Celotex are of irregular shapes and are smaller than those for which the relation was determined, the values reported here should not be considered typical of 5"/54 projectile fragments.

Initial qualitative observations based on the information in Table 3 include the following:

- Behind the denser shield materials the average fragment mass is higher and the average velocity is generally smaller than behind the other shield materials. Thus, smaller fragments are screened out and larger ones are decelerated.

- The 5/8" steel plate significantly reduces the number and velocity of the fragments it allows to pass. The reductions are greater than for any of the other materials tested.

- Behind the single blast mat, average fragment mass is the smallest of all the materials tested. Large fragments are broken into smaller pieces which are readily decelerated by drag forces to a velocity such that they are no longer hazardous. (No blast mat fragments were included in the count.)

NUMBER AND MASS OF FRAGMENTS. The shields of high areal density pass relatively few large fragments, while the shields of lower densities pass more smaller fragments. It appears that the kinds of materials used for the lower density shields effectively break up large fragments but are less effective at removing them from the fragment spray. The major difference between the heavier and the lighter shields (other than density) is that the lighter materials all possess some degree of

tensile strength in one or more directions. For example, the blast mats consist of steel cables woven in two perpendicular directions; the tensile strength of the cable adds to the energy required to break through the shield. The heavier materials generally exhibit little structural cohesiveness and can be visualized as simply inertia to be overcome by the incident fragments.

The heavier materials apparently are punctured by an initial cloud of small fragments; their residual velocity is too low for them to subsequently reach the recovery pack. The hole in the shield thus produced permits unobstructed passage of the later arriving larger fragments. Conversely, the lighter materials have sufficient tenacity to deflect the initial cloud of smaller fragments without suffering a complete perforation.

Both the total mass and the number of fragments recovered tend to increase with decreasing shield density. The average fragment mass does not vary markedly though it tends to decrease slightly with shield density. The single blast mat is an unusual case because both the number of fragments recovered and their average mass are distinctly different from the other shields in its weight class.

FRAGMENT VELOCITY. Most of the fragment velocities reported here were based on the empirical penetration/velocity relation described above. The equation is not necessarily valid for all velocities or all fragment sizes since it is based on a limited amount of data. Tests are currently under way which will illuminate this relation, and, perhaps, determine different relations for various ranges of fragment mass, velocity and energy.

Because of the uncertainty associated with using the empirical relation outside the range for which it was determined, the fragment parameter comparisons among shield materials are expressed in terms of the ratio of the parameter in question to the same parameter, determined in the same way, for the fragments recovered from the unshielded control packs. The relative effectiveness of each of the shield materials can be established in this way. The difference between the velocities determined from the empirical equation and the "true" values will be embodied in a multiplicative factor, if the correct relationship between penetration and velocity turns out to be of the same form as the empirical equation.

Initial Velocity. An average velocity is determined by measuring the time of arrival of many fragments at a fixed distance from the munition in an arena test. The fixed distance is divided by each time of arrival and the resulting velocities

are averaged. The fragment initial velocity characteristic of the particular munition is calculated from this average by assuming constant aerodynamic drag and determining the velocity at the munition case that would produce the observed average velocity at the fixed observation point.

For the present tests, two approaches were used to determine initial fragment velocity: analysis of high speed photographs, and extrapolation from Celotex penetration measurements.

Photographic information is somewhat limited because the aluminum flash panels were visible on film on only two of the four control packs. Several fragment velocities were determined from observed times of arrival at the flash panels; these were averaged and extrapolated back to the projectile case as just described to determine an initial velocity. The velocity so determined is 3300 ft/sec.

Three different average velocities can be calculated from penetration data:

- Each individual fragment velocity is determined and all such values averaged; the result is 6930 ft/sec.
- Each individual fragment penetration depth is averaged; this value is used with average fragment mass in the empirical relation; the result is 5645 ft/sec.
- The median penetration is used with the median fragment mass in the empirical relation; the result is 7150 ft/sec.

These values are summarized in the following table:

Photographic	3300 ft/sec
Velocity Average	6930 ft/sec
Penetration Average	5645 ft/sec
Penetration Median	7150 ft/sec

The values shown above are the reason that comparisons among shield materials in the following discussions are meaningful in terms of ratios rather than absolute values of velocity and kinetic energy. The photographic result is the most dependable; it is in substantial agreement with the 3000 ft/sec initial velocity found in arena tests in the 90° to 105° polar angle range. The Celotex penetration mechanism is too fraught with unknowns to be entirely trustworthy in an absolute sense.

Residual Velocity. The computer code produces a velocity for each fragment determined from its mass and penetration depth; this velocity at the Celotex is extrapolated back to the projectile case to find an initial velocity. Since the fragments have passed through a shield in all cases except the controls, the velocity so calculated is not a true initial velocity. However, it can be interpreted as the velocity of the fragment as it leaves the shield material since the initial fragment velocity is high and the travel distance to the shield is short. In other words, these velocities are characteristic of the residual velocity which characterizes each shield material.

Table 4 lists the fragment velocities calculated in the above manner. The ratio of each velocity to the average of the initial velocities determined from the control packs is listed in the last column. (The ordering of the rows in the table is that of increasing value of this ratio.) Wood appears to be the best shield from this point of view; it would be necessary to determine the residual velocity behind a thinner slab of wood before any firm statement or conclusion can be made. The other shields generally fall in the order of increasing shield density.

Velocity at 500 ft. Fragment masses and velocities at the 500 ft range from the munition are required in order to determine compliance with the safety criterion for energy. Masses of recovered fragments have just been discussed. Velocity at 500 ft can be determined from the velocities at the Celotex packs from the assumption of constant aerodynamic drag and flat trajectory. The weak link in this procedure is the empirical relation among Celotex penetration, fragment mass and velocity. As observed above, the velocities determined using this relation are high compared to the same velocities determined from photographs, which are perhaps more accurate. Therefore the error in fragment energies determined from these velocities tends to be conservative from the safety point of view.

Fragment velocities at the 500 ft range for each shield and the controls have been grouped according to fragment mass, and the arithmetic average calculated for each mass. Figure 2 contains points for 53 fragment masses recovered from the four control packs. Also shown on the figure is the power function of the form $V = A M^B$ which best fits the points in the least square sense. Least square fits of the same function to the velocity/mass data for all the shields were also made; these are compared to the control pack data on the succeeding Figures 3 to 5.

Figures 3 through 5 show comparisons between the least square fits to the shield data and the fit to the control data. The three graphs show the data from heavy, intermediate and lightweight shields. At 500 ft behind some of these shields fragment velocities greater than those behind the controls were found. This is due to experimental uncertainties and not to any real effect.

The shield materials tested, except for some of the densest ones, provide no real reduction in fragment velocity at 500 ft from the projectile. The utility of the shields therefore stems from their ability to reduce the number and size of the fragments that arrive at 500 ft.

FRAGMENT KINETIC ENERGY. Kinetic energy can be determined in several ways from the fragment masses and velocities detailed in the preceding sections. Two of the many possible calculations are singled out for consideration here; each provides a means of judging the relative efficiency of the shield material samples tested. Because it is impossible to isolate and examine the motion of an individual fragment in a Celotex pack, the energies of large groups of fragments must be examined. This approach is more meaningful in a statistical sense, anyway.

One method of studying shield effects on groups of fragments involves expressing the total fragment kinetic energy absorbed by each shield as a fraction of the energy carried by unshielded fragments. A large value of this fraction implies less energy carried by those fragments which survive passage through the shield in question.

Another assessment of the shields can be made by ranking them according to the total kinetic energy remaining at 500 ft from the projectile. This is a useful approach because the safety criterion requires that no more than one fragment per 600 ft^2 carry an energy exceeding 58 ft lb at 500 ft.

The number of fragments actually reaching the 500 ft range with energy exceeding any particular value will be less than the number determined by using velocities determined from the empirical relation for Celotex penetration depth. The results given below are overestimates and therefore conservative from the safety point of view.

Kinetic Energy Absorbed in Shields. The total kinetic energy delivered to each Celotex pack by all fragments greater than 1 gram mass was determined. This quantity is the sum of the values of $1/2\ m\ V^2$ for each fragment recovered from a particular pack. The energies so determined will be high because the velocities were calculated with the empirical penetration relation.

The kinetic energy fraction, f, is the ratio of the total kinetic energy carried by all the fragments recovered from a shielded recovery pack to the total energy carried by all the fragments recovered from an (average) unshielded control pack. The fraction, f, ranges from 0.0 for a completely shielded pack to 1.0 for a control pack.

The fraction F = 1 - f is defined as the kinetic energy fraction absorbed by a particular shield. F characterizes the shield materials more specifically than does f.

Figure 6 illustrates the variation of F as a function of shield areal density, A_D. Five of the fifteen points representing shield materials fall close to a single straight line: the points representing water and Kevlar 29, and the three points representing blast mats of various thicknesses. The least square straight line through these five points was found to be represented by the following expression:

$$F = 0.0143\ A_D + 0.360$$

That a straight line can be faired through these five points is significant for at least two reasons. First of all it indicates that absorbed kinetic energy is linearly dependent on shield mass. Secondly, note that three different materials produce points falling near the same line with good correlation. In some way Kevlar 29 in a basket weave cloth is similar in fragment impeding ability the blast mat "cloth" formed of 1/4" steel airplane cable. These two materials with their tensile and cohesive properties somehow resemble water - which possesses neither of these characteristics.

Another least square line is shown on the graph: it represents the agglomeration of points above the five just mentioned. The materials represented by these points fall near the following line:

$$F = 0.0173\ A_D + 0.494$$

The slopes of the two lines are not significantly different from one another; closer analysis may show them to be more nearly alike. Note that the point representing wood again appears "best" in that it is higher on the plot than any other except steel.

The two remaining points, Nylon and GRP, do not really fit with either of the groups near the least square lines. From a practical point of view they can be disregarded because they are below all the other points; that is, the materials function inefficiently as fragment kinetic energy shields.

Kinetic Energy at 500 ft. The number of fragments reaching a 500 ft range with a kinetic energy exceeding 58 ft-lb are listed in Table 5. Actual numbers for each shield are probably less than those listed because the energies are overestimated by the velocities obtained from the Celotex penetration formula.

Because of the uncertainty surrounding the empirical penetration relation, the ranking of shield materials is best made in terms of the ratio in the last column. The values in the last column are more representative of the effect of a given shield on fragment energy at 500 ft than are the actual values themselves, which are listed in the preceding column. Wood again appears to be a good shield choice.

The areal density of fragments exceeding 58 ft-lb is an even more useful bit of information. Such densities can be estimated by determining the surface area on a sphere of 500 ft radius which is shielded by the 32 ft^2 (4' x 8') Celotex recovery packs located 15 ft from the projectile. The area can be calculated as a ratio:

$$A_{500}/A_{15} = (4\pi R_{500}^2)/(4\pi R_{15}^2)$$

or

$$A_{500} = A_{15}\ (500/15)^2 = 35556\ ft^2$$

Only 26 fragments exceeding 58 ft-lb kinetic energy are estimated to reach a range of 500 ft from an unshielded projectile (Table 5). This is 26/35556 = 0.0073 fragments per square ft or (.0073)(600) = 0.44 fragments per 600 ft^2. It is obvious from this calculation that a single round 5"/54 Mk 41 projectile presents an acceptable fragment hazard at 500 ft. Since the velocities determined from Celotex penetrations are thought to be too high, the value of 0.44 fragments/600 ft^2 is also high. With a fragment decelerating shield in place, the fragment density will be even lower.

CONCLUSIONS

The purpose of the tests described in this paper has been to determine the relative merits of several materials as decelerators of explosively driven steel case fragments. Absolute values of fragment number, velocity and kinetic energy are incidental to this purpose. Fragment Energy and Number (FEN) chart analysis, as described in a previous discussion (Reference 2), has shown that six to eight unshielded projectiles of the type fired for these shield tests present an acceptable fragment hazard at 500 ft. The present test results are not inconsistent with this analytical conclusion.

---

[2] F.B. Porzel "Design of Lightweight Shields against Blast and Fragments", Minutes of the Seventeenth Explosives Safety Seminar, September 1977

The fragment shield samples tested in this series can be segregated into three general classes according to areal density: heavy, medium and light weight. The most efficient performers in each of the three classes are determined from the following measured or derived parameters:

- Number of fragments > 1 gram recovered from Celotex.
  Fewer fragments implies better shield performance.

- Average mass of recovered fragments.
  Large average mass implies that the smaller fragments were stopped, leaving only large, high drag, fragments in the spray.

- Average penetration depth in Celotex at 15 ft range.
  Shallow penetration implies:

  - low residual velocity

  - low velocity at 500 ft

  - few fragments exceeding 58 ft-lb at 500 ft

  - large kinetic energy absorbed by shield.

- Fragment velocity at various ranges.
  Since fragment velocity is determined by drag coefficient in addition to varying directly with penetration and inversely with the cube root of mass, separate consideration of mass and penetration may be misleading.

The above parameters are listed in Table 6 for the two most effective shields in each weight category. Similar values, determined by the same procedures, for the unshielded control packs are included for comparison. As indicated earlier, the velocities derived from Celotex penetrations (the basis for the last three values in each column of the table) are suspect because of the uncertainty inherent in the use of the empirical penetration relation. The results shown in the table are, however, indicative of the relative performance of the shield materials.

Using the (high) velocities derived from the empirical relation, the number of hazardous fragments reaching 500 ft is below the criterion of one in 600 ft^2. At the end of the preceding section it was shown that less than one fragment in 600 ft^2 is expected at 500 ft from an unshielded projectile; any of the shield materials tested will permit this density or less at 500 ft.

A single layer of wire rope blasting mat is efficient at breaking fragments into smaller pieces. If this material is used as a primary shield, the smaller fragments it allows to pass can be decelerated effectively into the "non-hazardous" class by one of the lighter granular or fibrous materials, such as sheet rock or wood. A weight saving is achieved by using the blast mat for only the first layer and the lighter materials in succeeding layers.

The effectiveness of the granular materials strengthens the original hypothesis that the important parameter in determining a good fragment shield is its inertia. However, the blast mat and Kevlar results indicate that there are other materials properties, like tensile strength, which also might be exploited for the present application.

ACKNOWLEDGEMENTS

This work is a portion of the Navy Explosive Safety Improvement Program(NESIP) under the cognizance of OP411 and supported by NAVSEA 04H3. Overall guidance was provided by J. Petes of NSWC(WO). Technical support and analysis was supplied by F. B. Porzel, also of NSWC(WO). Conduct of the tests was under the able direction of J. P. McLain of the TERA Group of the New Mexico Institute of Mining and Technology.

TABLE 1

Shield Materials Used in First Test Series

Material	No. Layers	Nominal Areal Density (lb/ft^2)
5/8" Mild steel plate	1	27
7" wide fiber transmission belt	8	25
Pine 2 x 12's	6	25
3" layer sand, 1/4" plywood box	1	26
1/8" fiberglass PC board + 1/2" rubber mat	4	25
6" layer water, 1/4" plywood box	1	31

TABLE 2

Shield Materials Used in Second Test Series.

Material	No. Layers	Nominal Areal Density (lb/ft^2)
Ballistic Nylon cloth	40	4
Kevlar 29 Basket weave cloth	30	4
1/2" Gypsum wallboard (sheet rock)	6	10
Door mats: tire treads on heavy wire	4	10
30" wide fiber transmission belt	4	10
Glass Reinforced Plastic armor	1	10
Blasting mats; woven 1/4" steel cable	1	9
" "	2	18
" "	3	27

TABLE 3. Fragments Greater Than 1 Gram Recovered From Celotex Packs.

SHIELDS		FRAGMENTS				
Material	Approx. Density (lb/ft^2)	Number Recovered (> 1 gm)	Total Mass Recovered (gm)	$\bar{M}$ (gm)	$\bar{P}$ (in)	V (ft/sec)
Control	0	63	889	14	9.5	4685
"	0	46	902	20	12.2	5392
"	0	58	900	16	11.9	5714
"	0	49	927	19	12.2	5466
Avg.Control	0	54	904	17	11.4	5288
5/8" Steel	27	7	133	19	4.6	2048
7" Belt	25	14	279	20	4.3	1905
11" Wood	25	16	328	20	2.8	1215
3" Sand	26	30	363	12	2.6	1345
Fibr/Rubber	25	28	453	16	3.3	1561
6" Water	31	49	532	11	4.1	2198
3 Blast Mats	27	50	689	14	5.5	2752
2 Blast Mats	18	63	754	12	6.2	3235
Sheet Rock	10	42	477	11	6.5	3463
4 Door Mats	10	65	715	11	5.6	3014
1 Blast Mat	9	88	726	8	6.6	3906
4 Belts	10	49	744	15	6.7	3236
GRP	10	62	948	15	7.4	3581
Kevlar 29	4	47	666	14	8.9	4414
Nylon	4	67	818	12	9.2	4769

$\bar{M}$ = Arithmetic average mass of recovered fragments
$\bar{P}$ = Arithmetic average Celotex penetration depth
V = Velocity at Celotex, determined from penetration equation using $\bar{M}$, $\bar{P}$ and presented area $A = 0.09222\ \bar{M}^{-1/3}$

Note: The fragment velocities recorded here should not be considered typical of 5"/54 projectile fragments because they are based on the empirical penetration/velocity relation which was determined for fragments in different size, shape and velocity ranges from those recovered here.

TABLE 4. Residual Velocities Behind Shield Samples

Shield Material	Approx. Density (lb/ft^2)	Residual Velocity (ft/sec)	Ratio ($V_R/5645$)
Average Control	0	5645	1.00
11" Wood	25	1291	.23
3" Sand	26	1447	.26
Fiberglass/Rubber	25	1668	.30
7" Belt	25	2027	.36
5/8" Steel	27	2180	.39
6" Water	31	2371	.42
3 Blast Mats	27	2951	.52
4 Door Mats	10	3250	.58
4 Belts	10	3463	.61
2 Blast Mats	18	3481	.62
Sheet Rock	10	3731	.66
GRP	10	3831	.68
1 Blast Mat	9	4243	.75
Kevlar 29	4	4731	.84
Ballistic Nylon	4	5129	.91

TABLE 5. Number of Fragments at 500 Ft With Energy Exceeding 58 ft-lb.

Shield Material	Approx. Density (lb/ft^2)	N>58 ft-lb at 500 ft	Ratio (N/26)
Control	0	26	1.00
5/8" steel	27	2	.077
7" Belt	25	2	.077
11" Wood	25	3	.12
Fiberglass/Rubber	25	3	.12
3" Sand	26	4	.15
Sheet Rock	10	10	.38
6" Water	31	12	.46
3 Blast Mats	27	13	.50
4 Door Mats	10	14	.54
Kevlar 29	4	16	.62
1 Blast Mat	9	16	.62
4 Belts	10	17	.65
2 Blast Mats	18	19	.73
Ballistic Nylon	4	25	.96
GRP	10	25	.96

TABLE 6. Parameters of Fragments Passed by the Most Effective Shields

	CONTROL	Heavy		Medium		Light	
		WOOD	SAND	Sheet Rock	1 Blast Mat	Kevlar	Nylon
Number of fragments > 1 gram	54	16	30	42	88	47	67
Average fragment mass (gm)	17	21	12	11	8	14	12
Average fragment Penetration (in)	11.3	2.8	2.6	6.5	6.6	8.9	9.2
Average fragment velocity (ft/sec)							
Initial	5645						
Residual		1291	1447	3731	4243	4731	5129
at Celotex	5466	1215	1345	3463	3906	4414	4769
Number of fragments exceeding 58 ft-lb at 500 ft range	26	3	4	10	16	16	25

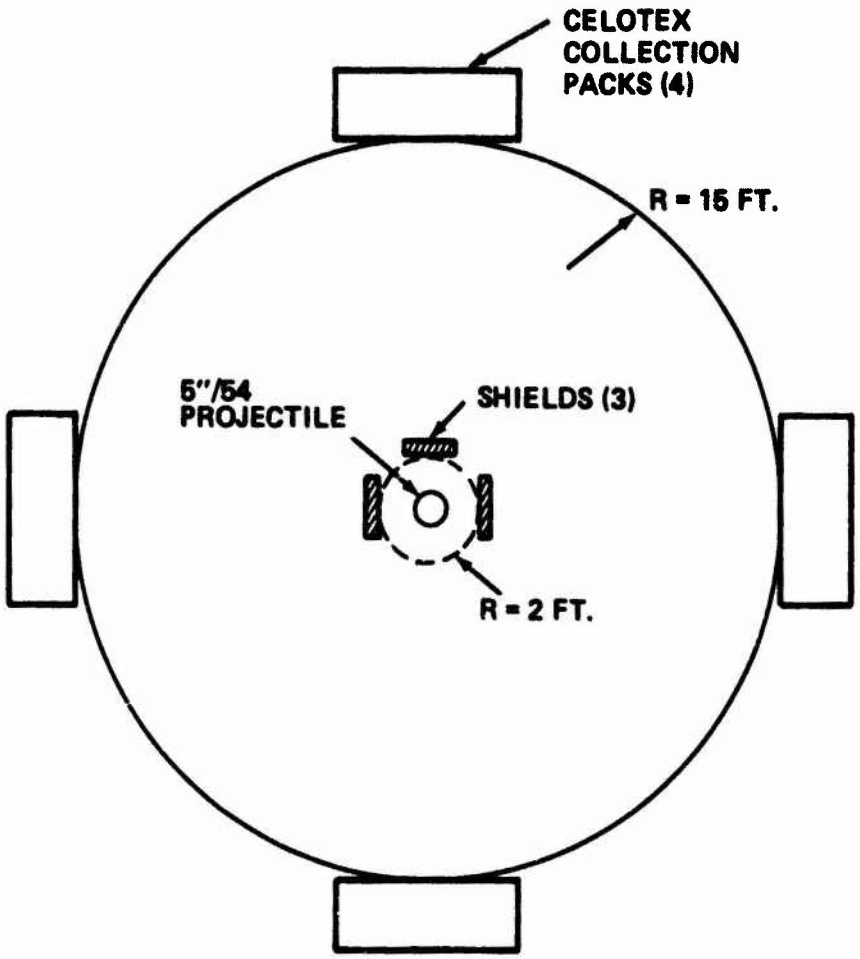

FIGURE 1a SHIELD TEST LAYOUT

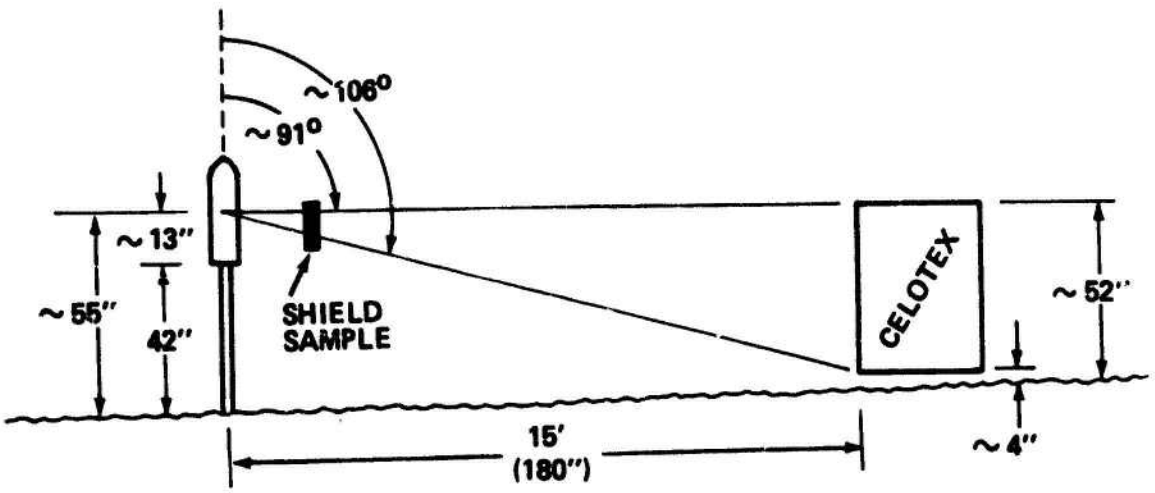

ELEVATION

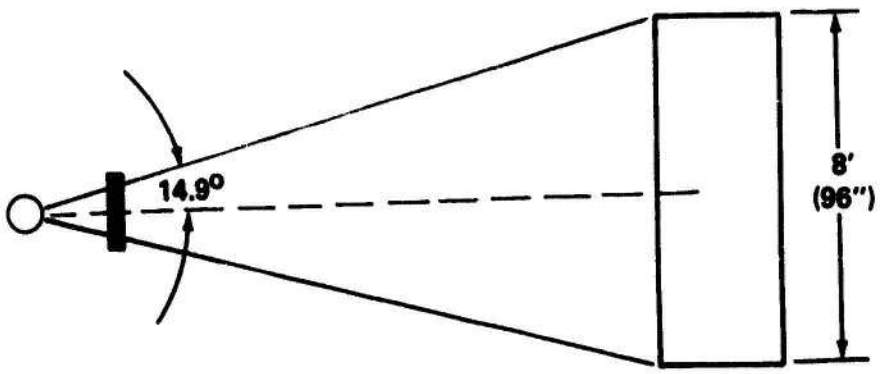

PLAN

FIGURE 1b SHIELD TEST GEOMETRY

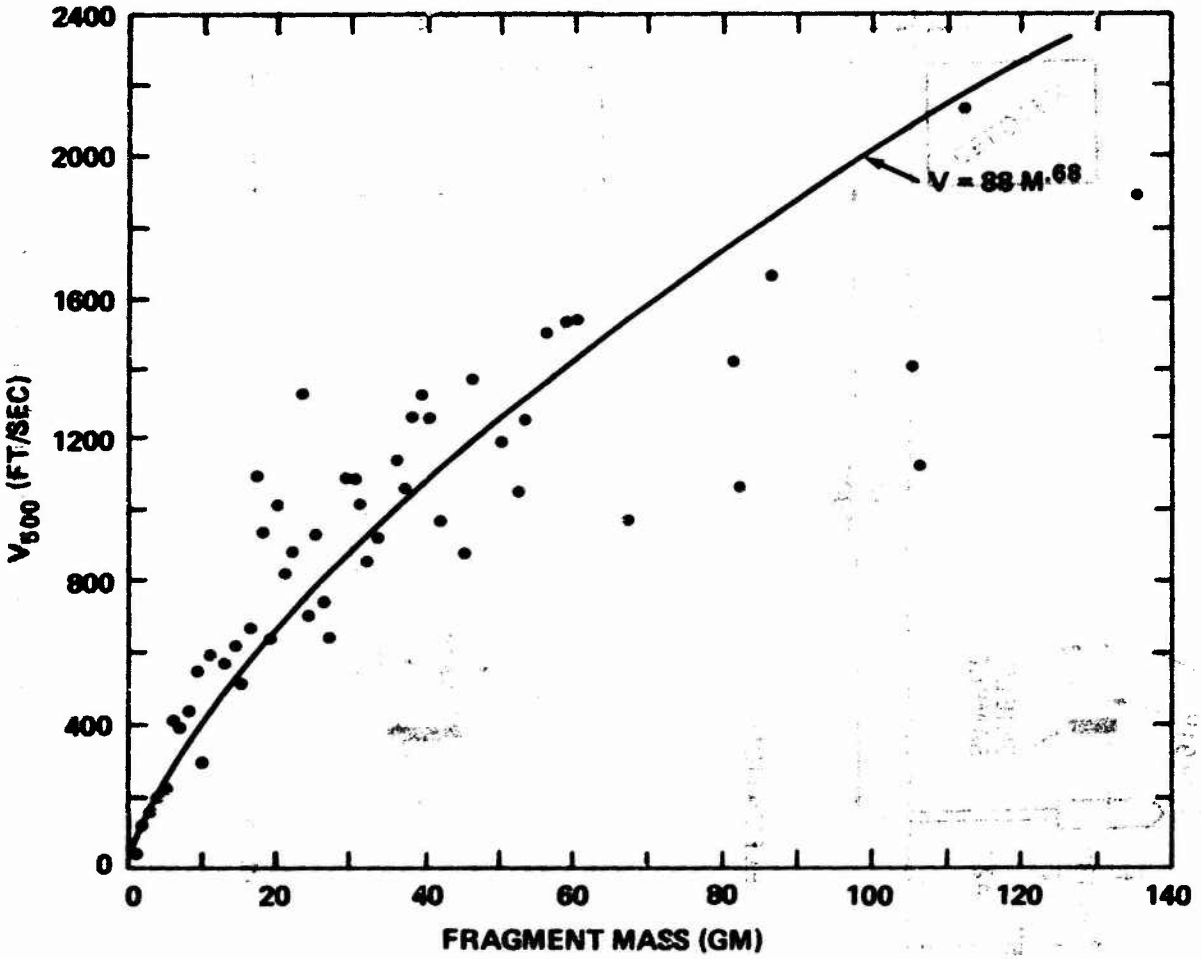

FIGURE 2 FRAGMENT VELOCITY AT 500 FT. RANGE

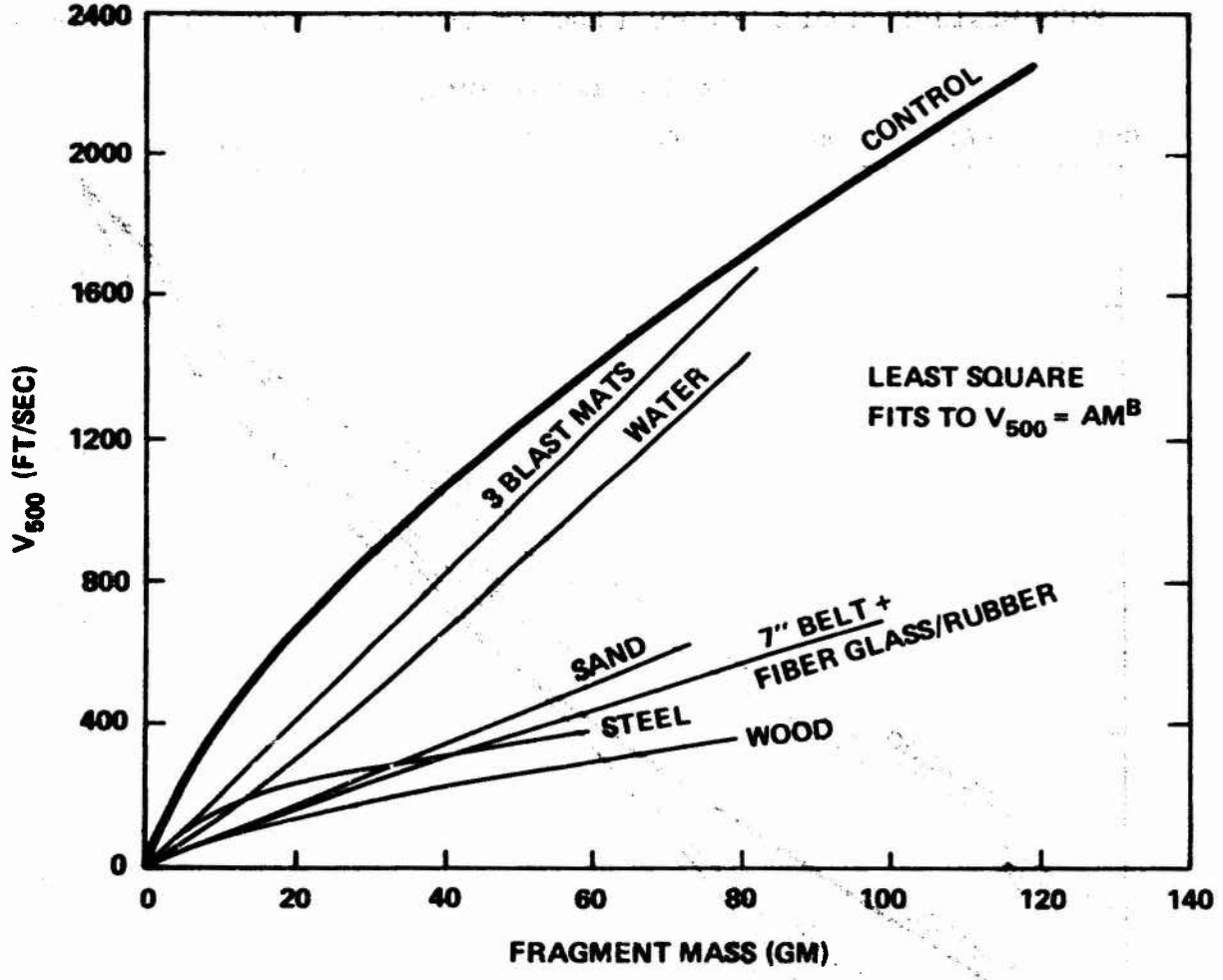

FIGURE 3 FRAGMENT VELOCITY AT 500 FT. RANGE; 25 TO 31 LB/FT^2 SHIELDING

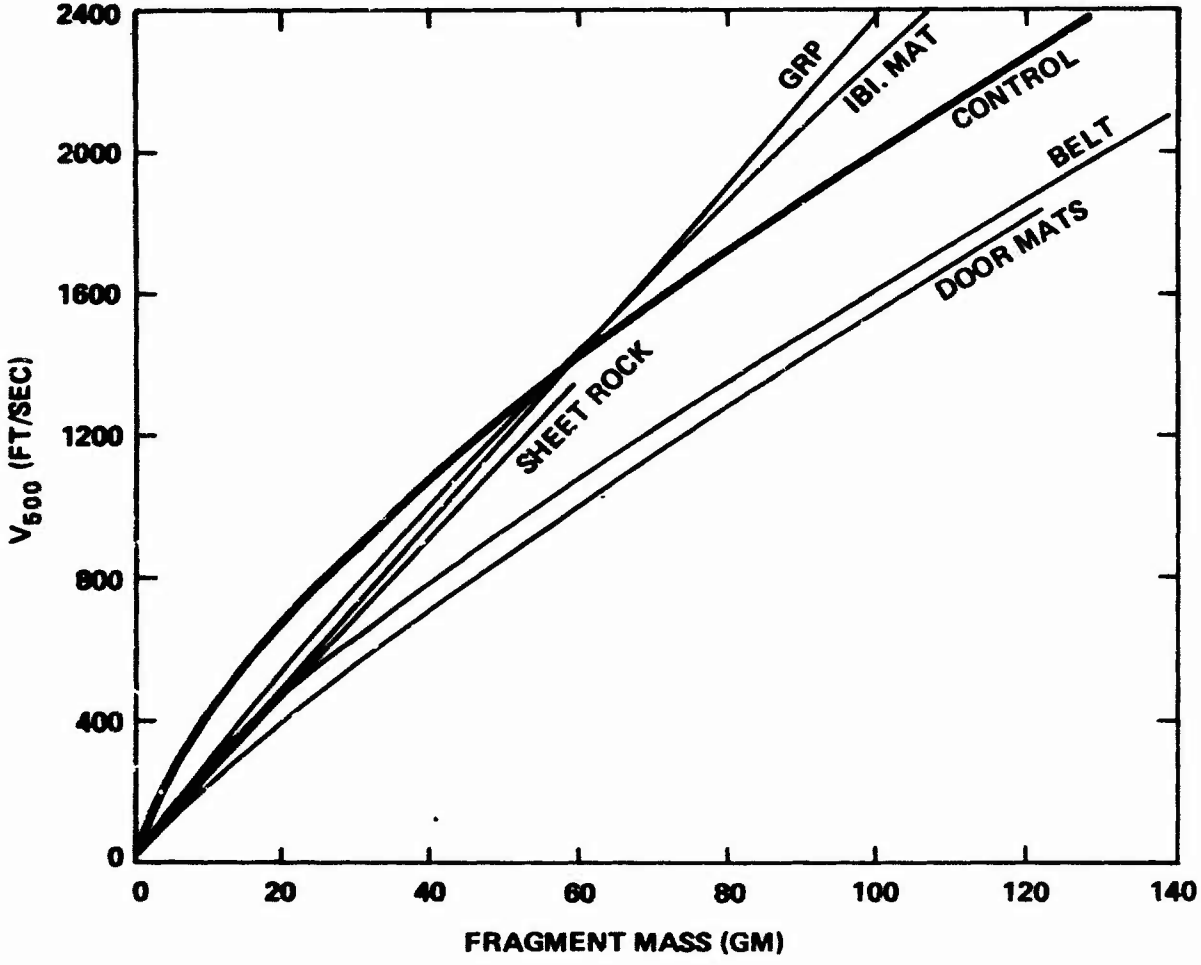

FIGURE 4 FRAGMENT VELOCITY AT 500 FT. RANGE; 9 TO 10 LB/FT^{2}SHIELDS

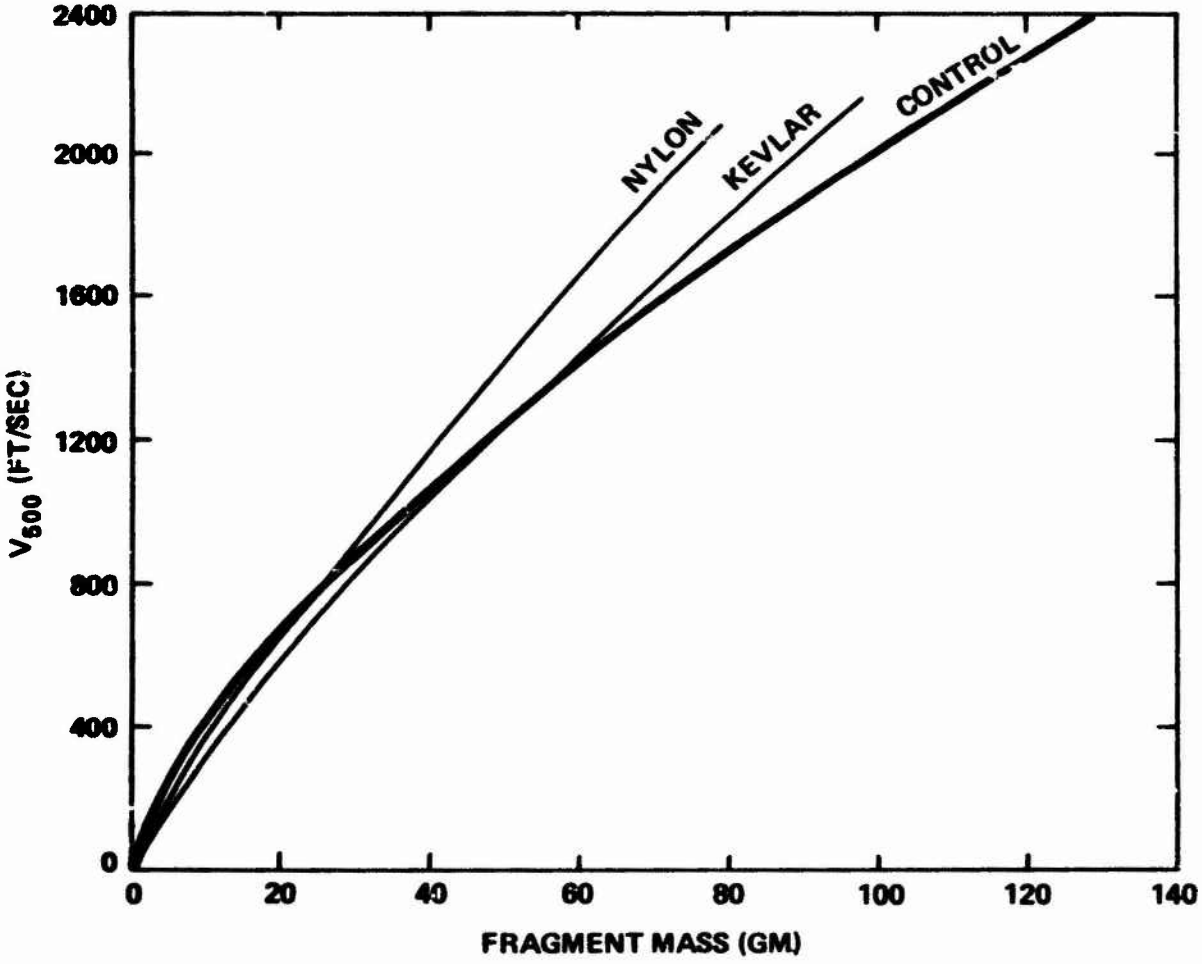

FIGURE 5 FRAGMENT VELOCITY AT 500 FT. RANGE; 4 LB/FT^2 SHIELDS

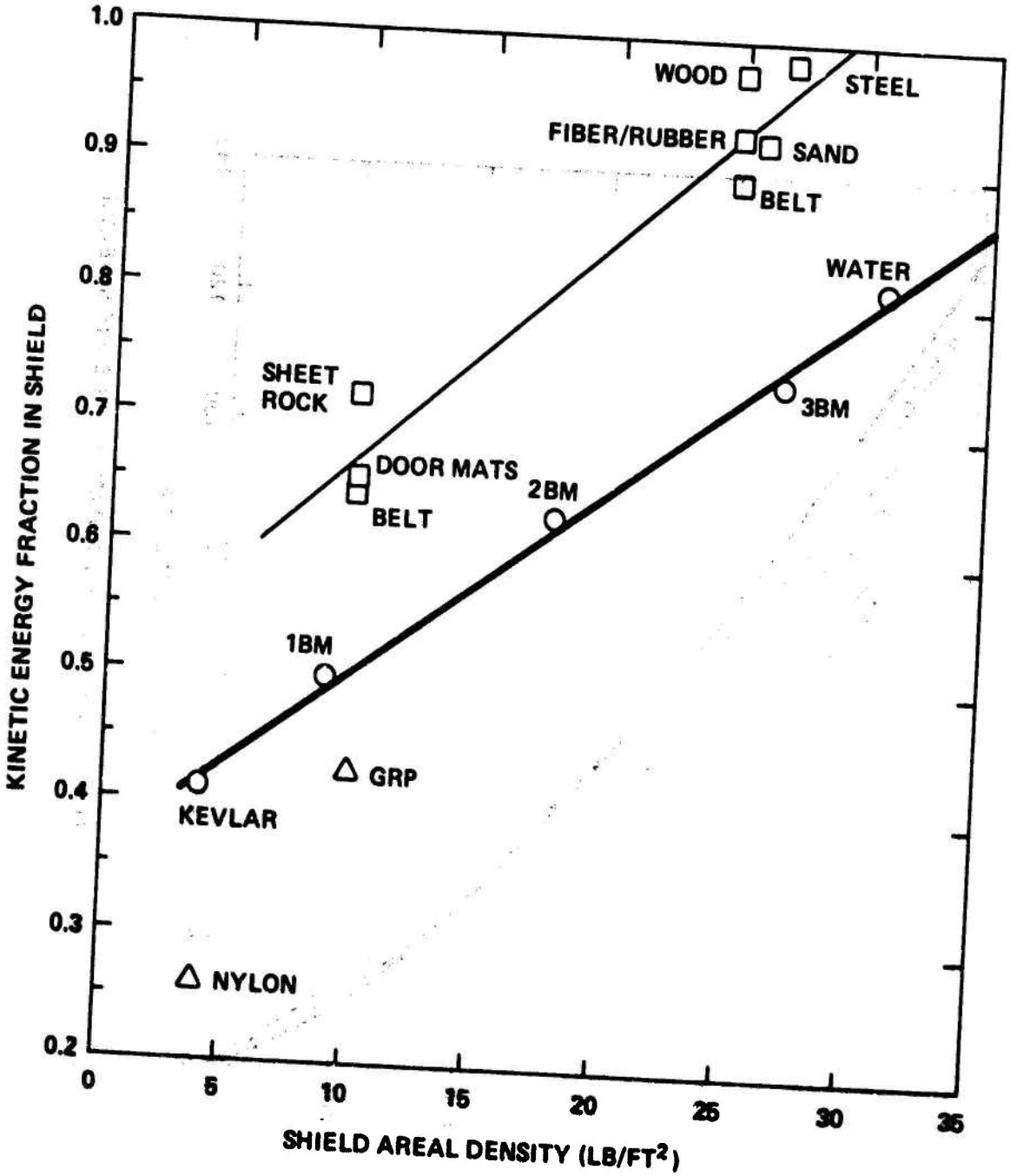

FIGURE 6 FRAGMENT KINETIC ENERGY ABSORBED BY SHIELDS

CATASTROPHIC REACTION OF COMPARTMENTALIZED AMMUNITION - CAUSES AND PREVENTIVE MEASURES

*PHILIP M. HOWE, Ph.D
ROBERT B. FREY, Ph.D
BALLISTIC RESEARCH LABORATORY
ABERDEEN PROVING GROUND, MD 21005

INTRODUCTION

While it is feasible to design a tank ammunition compartment which will survive the detonation of a single warhead, the design of a compartment which will survive the detonation of most or all of the warheads and which falls within the weight and space constraints imposed by the vehicle design is not currently possible; the detonation of 40 warheads (the planned complement) will destroy compartment and fighting vehicle. In previous research (1) we have shown that catastrophic reaction of munitions can occur under conditions much less strenuous than those required for classical shock initiation, which has been studied extensively for bare charges. These catastrophic reactions play an extremely important role in determining munition vulnerability, and in the rapid propagation of explosion through stacks of munitions. Typically, these catastrophic reactions take place in the 100-700μsec time frame, consume essentially all of the explosive, and may appear to be detonations to the observor interested in assessing damage potential. To understand the mechanisms of initiation of these reactions, and to devise preventive techniques suitable for safe transportation and storage, and vulnerability reduction of armored fighting vehicles, we have undertaken analyses and a variety of experiments. Pertinent results are summarized in this paper.

Interround Communication and the Role of the Casing

When a munition such as a 155mm artillery shell is detonated, nearby munitions are subjected to multiple fragment impacts, airblast, and severe loading from the explosive products. Initiation of the target munitions can occur, as a result of a single, massive, high velocity fragment, as a result of multiple fragment impacts occurring nearly simultaneously, or as a result of the severe blast loading delivered by fragments and explosive products. One might conjecture that some measure of protection would be provided the target munitions by heavy walled casings, but it must be remembered that a heavy walled protective casing of a target round implies massive lethal fragments when such a round serves as the donor.

Because there is a variety of parameters which may affect interround communication, a series of experiments was performed to establish a data base and to provide insight with respect to the pertinent mechanisms. Munitions from the inventory were used rather than specially designed test fixtures, because the former would provide a much needed practical data base and because analysis had shown that the variations in geometry from munition to munition could be accounted for and would not weaken the validity of the results. Each experiment involved three munitions placed collinearly upon a 2.5 cm steel witness plate (see Figure 1).

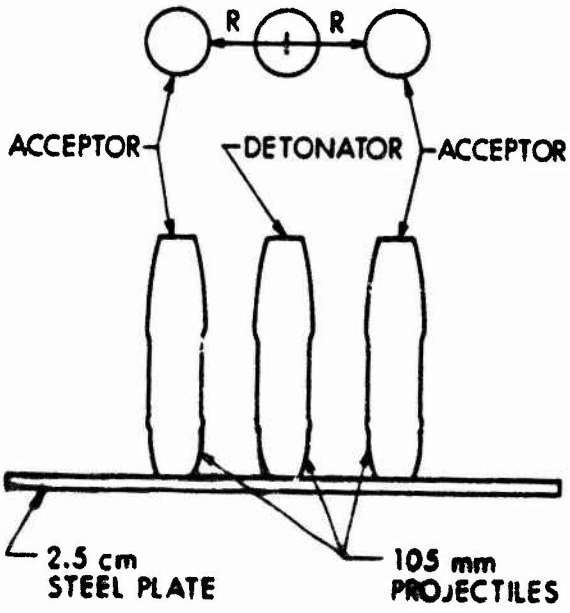

Figure 1. Schematic of typical test configuration for interround communication

The two outer munitions served as targets for the center warhead which was deliberately detonated via primacord embedded within some C-4 plastic explosive which filled the fuze cavity. (In some cases, target warheads contained fuzes. However, fuze presence did not change threshold response, and there was no evidence in any experiment to indicate that the fuze contributed to reaction of the target warheads). The donor wall thickness, diameter, and explosive content, and acceptor wall thickness, diameter, and explosive content were varied. Data were obtained for munitions containing composition B ($60\%_{w}$ RDX, $40\%_{w}$ TNT) and composition A-3 (91% RDX 9% wax).

The condition of the acceptor warheads and the witness plate was examined after each experiment to determine acceptor response. When a donor was detonated in the design mode, it always perforated the witness plate and this was taken as a crude but effective indicator of acceptor detonation. For each type of warhead pair, the separation distance between rounds was varied in accordance with standard quantal response techniques (2) to determine the propagation threshold. Separate tests were performed on inert loaded projectiles placed at separation distances at which the acceptor detonated. This permitted determination of the level of damage which would lead to violent reaction or detonation of the acceptor warheads. At the violent reaction threshold, each inert-loaded acceptor was severely deformed and failure of the warhead casing occurred. This provided an important clue with respect to the mechanism by which violent reaction occurs within the acceptor. All the data are consistent with a mechanism involving

. casing deformation
. compression of the explosive, generation of cracks within the explosive
. failure of the casing
. rapid extrusion of explosive through cracks in casing, causing ignition and rapid spread of reaction through the cracked explosive, with resultant catastrophic explosion.

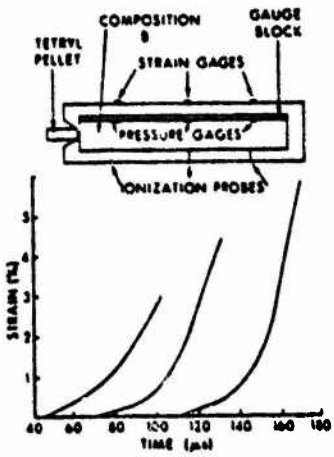

Figure 2. Schematic of apparatus used for mechanistic studies. Typical strain/time records at various gauge locations.

Additional experiments were conducted to explore some of the details of the initiation process. In one set of experiments, heavily confined composition B charges were fabricated, with internal manganin pressure gauges and externally mounted constantan strain gauges (see Figure 2). These charges were deliberately ignited, in order to permit observation of the development of violent reaction.

The detailed behavior of the charges was variable and strongly a function of geometry. Thus, for some experiments, a compression

wave propagated through the charge at a velocity of 2.0 - 2.5 mm/μsec. This wave was clearly not a shock, as the pressure gradient typically extended over a period of 10 - 30 μsec behind the wave front, to a peak pressure of 0.2 - 0.8 GPa. Generally speaking, strain records and stress records were similar. A plot of strain versus time at various gauge stations for such an experiment is shown in Figure 2. Ionization probes indicated reaction begins within a few microseconds of wave passage. Nonetheless, the pressures involved are too low to cause ignition by rapid compression of the explosive (3,4). (Note that, even with ignition, the reaction would not necessarily build up to violent reaction or detonation. In some instances, localized reaction occurs, and disrupts part of the charge without propagating to the rest.)

In other experiments, using larger diameter charges the pressure rose slowly but uniformly throughout the charge. After 200 - 600 μsec, a threshold was reached, at which point the pressure rose very rapidly and catastrophic reactions occurred. As in the previous experiments, the thresholds at various stations occurred sequentially and are associated with the arrival of a compression wave. In these latter experiments, the compression waves decayed as they propagated, and ionization probes responded erratically, indicating that low-level secondary ignition sources were developing at various locations. In both sets of experiments, large strains and strain rates were recorded coincident with the point at which the pressure transition points occurred.

At first we thought that charge deformation might be creating adiabatic shear bands which caused secondary ignition of the charge at points remote from the initial reaction. We analyzed the rate of temperature rise when two layers of explosive slip with respect to one another under pressure and with melting. The analysis indicates that sliding velocities of the order of $3X10^3$ cm/sec would be necessary for initiation at 0.1 GPa pressure. At lower sliding rates melting would suppress the temperature rise. In our experiments where the rate of shear deformation has been measured, such sliding velocities at shear bands could occur only if the shear bands were separated by distances of the order of a centimeter, which is unlikely. Therefore, it appears that the formation of shear bands does not explain the propagation of reaction in these experiments, although they could be responsible for the initiation of reaction in other circumstances.

An alternative explanation, consistent with the interround communication data and fragment impact data, is that homogeneous (on a macroscopic scale) deformation of the explosive does not cause secondary ignition, but that ignition results from casing failure and extrusion of the explosive into the cracks formed as the case opens.

An experiment was designed to test this hypothesis. It is shown schematically in Figure 3. Propellant was burned in the breech, thereby driving a plastic piston into the explosive, which was held in place by a deformable cylindrical container. The explosive was subjected to pressures and deformations similar to those of earlier experiments, but the deliberate ignition source was eliminated. In this experiment, ignition and violent reaction always occurred, but only after the metal case ruptured. We conclude that ignition and the development of violent reaction in confined charges is intimately connected with casing failure.

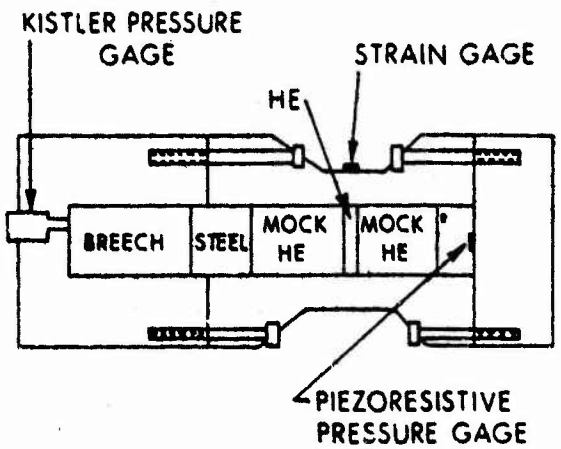

Figure 3. Apparatus used to show that ignition results from casing failure.

Huffington, in a parametric study of the response of thin shells to external blast loading, considered effects of geometry, loading, and material properties for fixed end cylinders subjected to a "frontal cosine" distribution of impulsive loading (3). The geometry is shown in Figure 4.

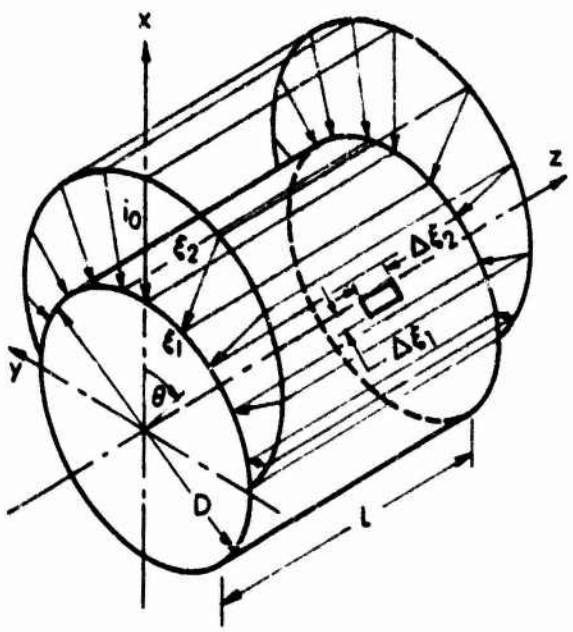

Figure 4. Frontal cosine impulsive loading for a fixed-ended cylinder (3).

The shells were considered to be thin (D/h <1) and Kirchhoff's hypothesis was applied (5). A mathematical formulation nonlinear in the equations of motion, the elasto-plastic stress strain relations, and the strain displacement relations was developed. The behavior of the solution was explored by varying non-dimensional ratios one

at a time, holding others constant. For complete details, the reader is referred to the original paper. Of special interest, however, is the fact that both maximum and residual deformation are strong functions of a scaled impulse density, $\frac{i\,C_o}{Eh}$, (where i is the impulse/area C_o the speed of sound in the casing, h the casing wall thickness, and E Young's modulus), and the fact that these functions depend only weakly on dimensionless ratios such as length/diameter, (L/D) and case thickness/diameter (h/D); (see Figure 5).

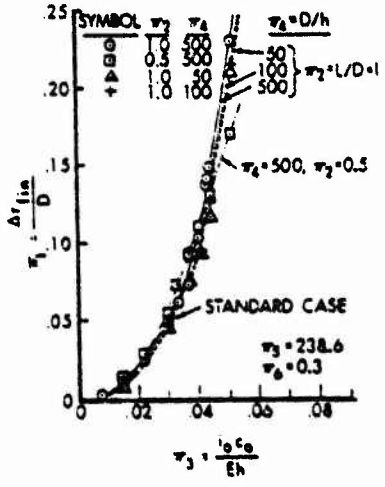

Figure 5. Casing response vs impulse intensity.

This is particularly important; it permits the identification of a critical deformation for casing failure with a unique value of the scaled impulse density delivered to the target, and the threshold inter-round communication distance can be obtained by equating the scaled impulse density to some critical value

$\pi_3 = \frac{i\,C_o}{Eh} = \pi_{crit}$. This critical value must be obtained from experiment. For fragmenting munitions contained within typical arrays such as tank ammunition compartments or pallets, the fireball of the donor munition envelopes the vicinal munitions.

Thus, both fragments and explosive products contribute to the impulse density delivered to the acceptors. We calculated values of the average areal fragment momentum according to the relation, applicable for cylindrical changes:

$$\frac{mV}{A} = \rho\,(r_o^2 - r_i^2)\,\frac{V}{2R}$$

where ρ is the donor casing material density

r_i is the donor casing inside radius

r_o is the donor casing external radius

v is the average fragment velocity, calculated using Gurney Formulae.

R is defined by Figure 1.

The total specific kinetic energy, E_{HE}, is given by

$$E_{HE} = \frac{\bar{V}_{HE}^2}{2}$$

where $\bar{V}$ is the average product speed. E_{HE} is proportional to the Gurney energy, E*, so

$$\bar{V} \propto \sqrt{2E^*}$$

and the scaled areal impulse ratio delivered by the explosive varies according to the relation

$$\frac{i\,C_o}{Eh} \propto \frac{r_i^2\sqrt{2E^*}}{RhE}$$

Thus, if the explosive products control the deformation, the critical deformation criterion implies that

$$\frac{R_o^2}{R}\,\frac{\sqrt{2E^*}}{h} = \text{constant, or } \frac{r_i^2\sqrt{2E^*}}{h} \text{ vs R be linear.}$$

(The parameters C_o, ρ, and E, which don't vary in our experiments are suppressed). The data are plotted in Figure 6 and pertinent calculated parameters are reported in Table 1. A regression analysis of R into each of the parameters in Table 1 was made and the correlation coefficients are shown in Table 2. Note that R correlates very well with i/h, but does not correlate significantly with any of the fragment parameters: in interround communication between fragmenting munitions, the development of violent reaction is independent of fragment parameters. That the fragments contribute to the initiation process can be seen by comparing the 50% separation distance for a 105mm HEP acceptor and a bare charge donor of the

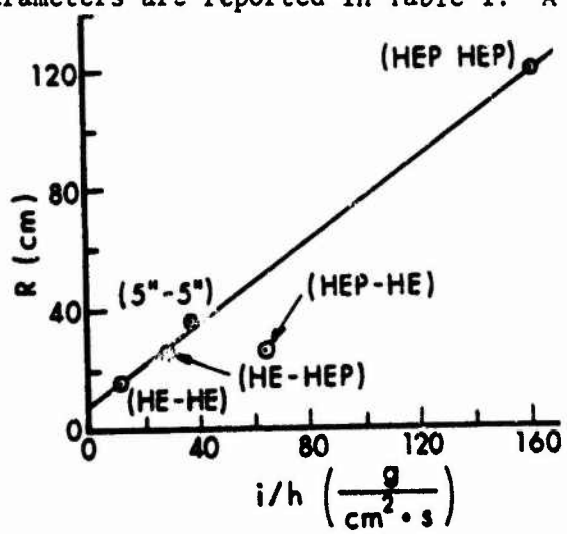

Figure 6. The dependence of R upon scaled impulse intensity.

Table 1. Measured and Calculated Results for Interround Communication

Donor	Acceptor	R (cm)	E_f (g/s^2)$\times 10^{10}$ Fragment Areal Kinetic Energy	P_f ($g/m \cdot s$)$\times 10^7$ Fragment Areal Momentum	i ($g/m \cdot s$)$\times 10^5$ Total Areal Momentum	h (cm) Acceptor Wall Thickness
M1 HE	Mi HE	17.8	5.6	3.6	11.3	1.02
M1 HE	M393A2	25 ± 5	5.6	3.6	11.3	0.4
M393A2	M1 HE	26	5.7	2.4	64.5	1.02
5" 54	5" 54	35.4	3.7	4.1	60.6	1.65
M393A2	M393A2	119.3	5.7	2.4	64.5	0.4

Table 11. Correlation Coefficients for Regression of R onto Various Parameters

	R	E_f	P_f	i	E_f/h	P_f/h	i/h
R	1	0.158	-0.548	0.524	0.557	0.227	0.960

same geometry and explosive content. The threshold for the HEP donor was 119.5 cm, that for the bare charge donor was 8.7 cm. The apparent ambiguity can be resolved by noting that the initiation of violent reaction requires casing failure and the explosive to be under compression when the casing fails. Casing failure is greatly facilitated by fragment impact, which induces high stresses in the casing, causing incipient spall. Compression of the explosive is determined by the deformation of the casing, however, and the deformation is proportional to the impulse, as shown earlier.

The Vulnerability of Cased Munitions to Impact by Single Fragments

The situation discussed above would change with increasing fragment mass and velocity; eventually an individual fragment would have sufficient areal impulse to reach the critical deformation to cause casing failure. Such is the case for threshold data from gun firings where there is no loading from explosive products and where the response of the target is to impact by single fragments. Reeves' data (6) covered fragment masses from 1.94 gm to 15.55 gm, impacting against composition B loaded 105mm HE warheads. We sponsored acquisition of additional data for identical targets, with fragments ranging from 75 gm to 300 gm. All fragments were steel, right circular cylinders, with L/D = 1. The response of the targets was inferred from post-firing examination of a 2.5 cm steel witness plate, and from recovery of target fragments. The criterion for a violent reaction was perforation of the witness plate. All data were obtained using

a standard quantal response technique (2). The data are plotted in Figure 7, together with Reeves' data. The fact that both sets of data fall upon the same curve is reassuring, and indicates that no experimental artifacts have been introduced because of different lots of munitions and different experimentors.

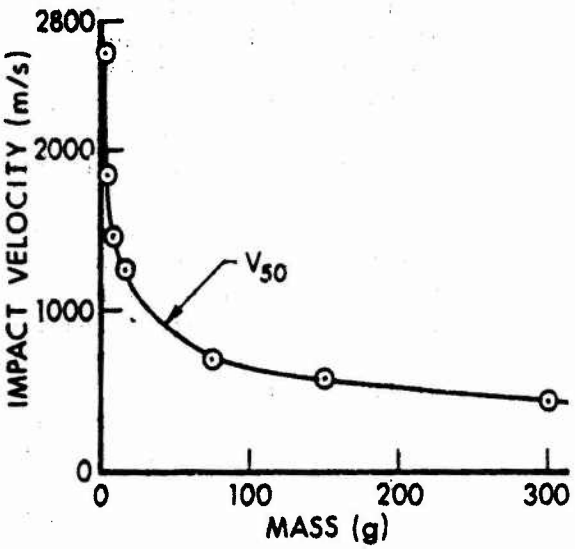

Figure 7. Threshold initiation (50%) for fragment impact of 105mm shell.

It is reasonable to expect that the fragment impact initiation of violent reaction in confined targets will obey the same mechanism as does interround communication. If so, the criterion for initiation of violent reaction is that a critical areal impulse/target casing thickness ratio be exceeded. Thus, we have for the 50% threshold locus of mass versus impact velocity, $\frac{mV}{Ah} = \text{constant} = \frac{\rho LV}{h}$ where m is the fragment mass, V its impact velocity, A its area, L its length, and h the target casing thickness. Geometric similarily requires that L be proportional to the fragment radius. In particular, for the L/D = 1 fragments used here,

$$\frac{mV}{Ah} = \frac{2\rho rV}{h}$$

Since

$$r = \left(\frac{m}{2\rho\pi}\right)^{1/3}$$

the criterion becomes

$$\frac{m^{1/3}V}{h} = \text{constant.}$$

The data of Figure 7 are replotted in Figure 8 (circles). The solid curve is a straight line with a slope of -3. Note that the fit is good over a three decade change in mass. This provides very strong support for a mechanism which leads to an areal impulse criterion for initiation of violent reaction.

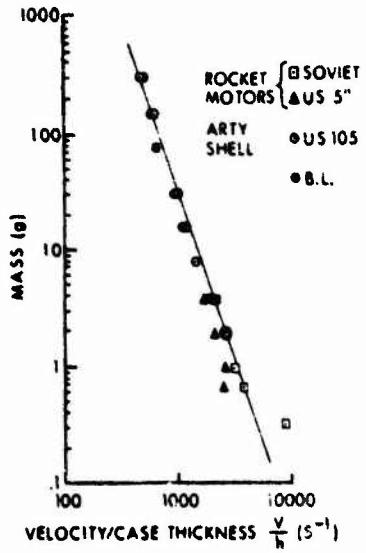

Figure 8. Comparison of initiation thresholds for rockets and shell, ballistic limit of shell.

Two corollaries follow from the above results: First, if the condition for initiation of violent reaction is that sufficient deformation of the casing occur to cause failure, i.e., crack generation, then the threshold for initiation should lie very close to the ballistic limit for the casing. To check this, firings against wax filled 105mm shell were conducted using 30 gm, 150 gm, and 300 gm L/D = 1 steel, cylindrical fragments. Some firings of fragments with masses of 3.87 g and 15.45g reported by Reeves (6) are included, also.

The data are shown in Figure 8, where the solid circles represent the average of the highest impact velocity at which no perforation of the casing was obtained and the lowest velocity at which perforation occurred. As can be seen, the conditions for initiation and the ballistic limit are nearly coincident.

The second corollary is that, if the condition for initiation is essentially that casing failure occur, then that condition would apply to different explosives systems, provided that the explosive is not very insensitive (a very insensitive explosive could cause the initiation to depend upon explosive parameters, rather than casing parameters). Some fragment impact data for the US 5" rocket motor and 122mm Soviet rocket motor from (7) are shown in Figure 8. Note that the data are concident with the 105mm M1 data, in spite of major differences in composition of the filler. The compositions of the rocket motor propellant and the explosive fill are shown in Table 3.

Table III. Chemical Composition

Munition	Composition	Principal Ingredients
105mm M1 HE	B	60% RDX, 40% TNT
105mm M393 HEP	A-3	91% RDX, 9% Wax
5" MK 10 Mod 7 Rocket	double base prop.	51.4% Nitrocellulose, 42.9% Nitroglycerine, 3% Diethylphthalate
122mm Soviet Rocket	double base	(Composition Classified)
Navy 5" 54	A-3	91% RDX, 9% Wax

It is apparent that, at least for those systems for which data exist, the initiation of violent reaction by fragment impact is independent of the filler and is determined by the response of the casing.

Remedial Techniques

An understanding of the mechanism of initiation permits development of techniques which prevent or reduce the frequency of violent reactions resulting from fragment impacts and the detonation of nearby warheads. For munitions in the inventory, protective shields can be developed which reduce the stress levels and stress gradients experienced by the target casings, thus reducing the probability of casing failure. Elementary considerations in shock physics indicate that the best shields are those composed of materials with low shock impedances. The presence of a low shock impedance material between the impacting fragments and the casing causes a more gradual buildup of pressure in the casing and allows more time for rarefactions to reduce the peak stress. Thus, materials such as polyvinyl chloride, foamed metal, etc. should make good shields.

Based on this reasoning, shields were designed to prevent interround communication between 105mm M 456 HEAT warheads contained in a tank ammunition compartment. The effectiveness of the shields relied upon prevention of direct impacts by fragments upon warhead casings and reduction of the shock wave strength experienced by casing and explosive. A series of tests involving two warheads and a single shield per test demonstrated that a 5cm x 5cm x 40cm polyvinyl chloride bar effectively prevented reaction of the acceptors. Thus, in fifteen tests, not a single acceptor warhead detonated, exploded, or showed any evidence of reaction. For these tests, the wall to wall warhead separation was 5 cm. Three further tests were conducted to assess the effectiveness of the shields in a simulated tank ammunition compartment. The compartment geometry, wall thicknesses, interround spacing, etc., closely replicated designs currently under consideration

for the XM1 tank. A schematic of the setup is shown in Figure 9.

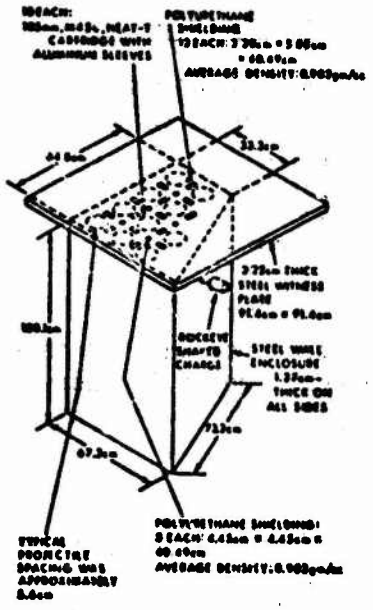

Figure 9. Mockup of tank compartment for confinement effects.

One warhead in each test was deliberately detonated by attacking it with Rockeye shaped charge. In each test, only the deliberately detonated warhead reacted. Results of tests and design information have been provided the project manager, for incorporation into the XM1 tank.

Another, complementary approach can be applied to new warheads entering the inventory. Ignition occurs when the casing fails, and is believed to be caused by the rapid extrusion of the explosive through casing cracks. If this is so, the ignition threshold could be raised by lining the warhead with a thin layer of a pliable polymeric material, which would act as a buffer between explosive and metal interface, during extrusion. (Experiments have shown that ignition occurs more readily as a result of metal- explosive friction than explosive-plastic or explosive-explosive interactions.) To test this hypothesis, 105mm M1 casings were lined with a 3mm coating of cellulose acetate butyrate. The coating thickness was chosen somewhat arbitarily and does not represent a minimum effective thickness. (Note, however, that 3mm is much too thin to provide significant shock attenuation - if shock ignition is the mechanism, the coating will be ineffectual.) Firings were conducted against the polymeric lined munitions with 8 gm steel fragments. The 50% threshold for such a fragment against an unprotected munition is 1470 m/s (4823 f/s). With the lined munitions, no evidence of reaction was obtained at impact velocities of 1740 m/s (5700 f/s), although this is well beyond the ballistic limit of the casing, and perforation occurred. Mild burning reactions were obtained at higher velocities. Even at impact velocities of nearly 2000 m/s (6500 f/s) the warheads did not react with sufficient violence to split open the casings.

SUMMARY AND CONCLUSIONS

Experiments are reported which were conducted to determine the interactions which occur between vicinal munitions. These experiments provided a data base we needed to address mass detonation issues and were designed to provide mechanistic information. Available theory and analysis provided a criterion for initiation, based upon an assumption about the mechanism. The initiation criterion permitted description of the threshold conditions for interround communication. In addition, it was found that, although the fragments participated in interround communication, the process was insensitive to donor fragment parameters, contrary to expectation.

Single fragment impact data was obtained against heavily confined targets. The data base was extended over that available in the literature so that the masses for impacting fragments ranged from 2 to 300 gms. The initiation criterion developed for interround communication was tested against single fragment impact initiation and shown to apply over three decades change in mass, the entire range for which data are available. Both the interround communication data and the single fragment impact data were shown to be consistent with a mechanism which involved deformation of the casing, compression of the explosive, failure of the casing, rapid extrusion of the explosive into cracks, causing ignition, and spread of reaction. Failure of the casing was found to be the critical step, and the initiation criterion was identified with the ballistic limit of the casing.

Since the rupture of the casing controlled the initiation process, the model should be applicable to other systems with similar geometries, but not necessarily similar chemical compositions. This hypothesis was tested against the US 5" MK 10 mod 7 rocket motor and the USSR 122mm rocket motor. Within the accuracy of the data, the initiation criterion applied equally well to these two systems as for the composition B targets for which it was developed.

Additional experiments were conducted to verify the hypothesis that initiation resulted from rupture of the casing and extrusion of the explosive into cracks. Constantan strain gauges and manganin pressure gauges were used to monitor the response of casing and explosive to various stimuli. It was found that catastrophic reaction resulted immediately after casing failure, given a deliberate ignition source. If the samples were not deliberately ignited, but were subjected to rapid deformation, ignition occurred when rupture occurred, with subsequent violent reaction

Understanding of the mechanism was used to develop remedial techniques. The use of low shock impedance materials to prevent casing fracture was explored and a technique which prevented any inter-round propagation in compartmentalized tank HEAT ammunition was developed. Design information was provided to the XM1 project manager, for incorporation into the new tank.

A technique was developed and tested applicable to munitions entering the inventroy. This technique isolates the explosive from the casing and greatly improves the response of the munition to fragment impact.

REFERENCES

1. Howe, P. et al, "Shock Initiation and the Critical Energy Concept" Sixth Symposium (Int.) on Detonation, San Diego (1976).

2. Dixon, W. J. and Massey, F. J. "Introduction to Statistical Analysis" McGraw-Hill, New York (1969).

3. Liddiard, T "The Initiation of Burning in High Explosives by Shock Waves" Fourth Symp. (Int.) in Detonation, Pasadena, (1965).

4. Taylor, B. BRL (Private communication).

5. Huffington, N. J., Journal of Engineering for Industry, Trans. ASME 1311 (Nov 1975).

6. Santiago, J., BRL R 1571 (1972).

7. Reeves, H., BRLMR 2031 (Mar 1970).

8. BRLCR #65, (Mar 72).

DESIGNING NUCLEAR PLANTS TO WITHSTAND PULSE AND IMPACT LOADS

by

Alexander L. Florence
SRI International, Menlo Park, California 94025

ABSTRACT

As a safety feature, nuclear reactors are enveloped in a reinforced concrete structure to prevent accidentally released radioactive material from escaping to the atmosphere. This containment structure should sustain only minor damage when subjected to missile impact. Potential missiles include those generated by tornados, such as steel rods, steel pipes, wooden poles, and automobiles. In certain locations, aircraft that are taking off or landing are potential missiles. Missiles may also be generated inside the nuclear power plant. They include steel pipes and fluid jets resulting from pipe breaks and portions of a fractured turbine hub. Reinforced concrete barrier walls are constructed to protect vulnerable parts of the power plant from internally generated missiles.

This paper concerns some of the elementary approaches to the design of reinforced concrete structures adopted by structural engineers working in the nuclear power industry. The approaches concentrate on local and overall response of reinforced concrete slabs to hard missile impact.

For local response, military empirical formulas are evaluated for use in nuclear industry safety analysis by comparing predicted penetration and scabbing thickness with the results of recent tests in which steel rods and pipes strike concrete slabs at velocities below 500 ft/sec. New empirical formulas are presented that are based on these tests.

For overall or structural response, standard resistance function methods are described for approximating elastic-plastic or rigid-plastic behavior. Suggestions are made for treating higher mode structural response.

Some design criteria are recommended.

1. Introduction

As a safety feature, nuclear reactors are enveloped in a reinforced concrete structure to prevent accidentally released radioactive material from escaping to the atmosphere. This containment structure should sustain only minor damage when subjected to missile impact. Potential missiles include those generated by tornadoes, such as steel rods, steel pipes, wooden poles, and automobiles. In certain locations, aircraft that are taking off or landing are potential missiles. Missiles may also be generated inside the nuclear power plant. They include steel pipes and fluid jets resulting from pipe breaks and portions of a fractured turbine hub. Reinforced concrete barrier walls are constructed to protect vulnerable parts of the power plant from internally generated missiles.

This paper concerns some of the elementary approaches to the design of reinforced concrete structures adopted by structural engineers working in the nuclear power industry. The approaches concentrate on local and overall response of reinforced concrete slabs to hard missile impact.[1,2]

To acquire predictive capabilities for local response, such as depth of missile penetration in a concrete slab, military empirical formulas derived for ballistic applications are being evaluated by comparing their predictions with the results of tests conducted by the nuclear power industry since 1973. In these tests, the missiles were steel rods or pipes and the impact velocities were below 500 ft/sec. Another approach being pursued is the formulation of new empirical formulas based on the recent test results.

A simple method, based on an approximation of the penetration behavior, is outlined for providing the loading required to determine the structural response. Methods are outlined for obtaining the loading when the target deforms structurally during impact and when the hard missile crushes slightly at the impact end.

For the approximate overall response of structures that suffer acceptable local damage, resistance function methods are applied to obtain elastic-plastic or rigid-plastic behavior. Suggestions are made for treating structural response when the missile impact stimulates high modes that change shape as deformation proceeds.

Some recommended design criteria are presented to show (1) the limits of slab deformation, in the form of ductility ratios and rotations at yield lines, and (2) slab reaction and missile punching shear.

Many of the problems of design against pulse and impact loads tackled by the nuclear power industry are not dealt with in this paper. These omissions include the topics of steel containment structures, soft missile impact, and blast or compartment pressurization effects.

2. Local Missile/Target Interaction

The design approaches depend on whether the missile is "hard" or "soft"; that is, whether the deformability is small or large relative to the deformability of the concrete target. Steel rods and pipes are examples of hard missiles, and wooden utility poles and aircraft are examples of soft missiles. Hard missile impact causes local wall damage and overall structural response, whereas soft missile impact causes only overall structural response.

To describe local damage from hard missiles, the following terms are defined according to usage in the nuclear industry.

Penetration:	missile displacement into the target
Perforation:	full penetration (target thickness for normal impact)
Perforation Thickness:	is the critical wall thickness $H = e$ at which perforation just occurs for a given missile and velocity
Scabbing:	peeling off of material from target back face (back face spall)
Scabbing Thickness:	is the critical wall thickness $H = S$ at which scabbing just occurs
Spalling:	ejection of material from target front face.

Figure 1 shows schematically the local interaction of a hard missile, such as a steel rod, and a reinforced concrete slab. Upon impact, a compressive stress wave is generated in both the rod and the concrete. The amplitude of the stress wave is governed by the material properties of the steel missile and the concrete target and by the impact velocity. The duration and shape of the stress wave is governed by the contact

area and the dimensions of the missile and target. Concrete compaction occurs at the edge of the contact area. This damage causes spalling from the front surface (Figure 1b).

The diverging stress wave propagating in the concrete is reflected from the back face as a diverging tensile stress wave, which can cause a tensile fracture plane that may result in scabbing, often to the depth of the back face reinforcing steel (Figure 1b). Occurrence of scabbing depends on slab thickness, missile configuration, and impact velocity. Increasing the slab thickness increases incident wave divergence and attenuation and consequently decreases the amplitude of the reflected tensile wave. Similarly, decreasing the contact area increases incident wave divergence and decreases wave amplitudes. A missile configuration change alone, such as a change from a steel rod to a steel pipe with the same contact area, will generally enhance divergence and decrease wave amplitudes.

Following the first few wave reflections, the stress distribution gradually changes to the bending and shear stress distribution for static plate loading. Concrete compaction ahead of the missile increases as the missile penetrates until an unloading wave arrives from the rear of the missile. Meanwhile, the initial shear cracking (punching shear) has been increasing. Because of the stress redistribution, this cracking develops into a spreading tensile crack (Figure 1c) to define a plug. At this time, the damage regions have been defined but cracking is still incipient because relative motions have not yet been great enough.

At a later time, the concrete plug may fully separate from the slab and bring the back face reinforcement into play. During this phase the missile reaches full penetration or it perforates. Figure 2 shows the main features resulting from missile/target interaction [3].

3. Local Missile Impact Formulas

Missile impact velocities in nuclear power safety analyses range from 100 to 500 ft/sec. Until 1975, empirical formulas for penetration, perforation, and scabbing were developed only for military applications

where the velocity range of interest is from 500 to 3000 ft/sec. The basis of these formulas are tests with nondeformable missiles in this high velocity range and parametric ranges limited to

$$H/d \geq 3,\ d \leq 16,\ 0.2 \leq W/d^3 \leq 0.8\ (lb/in^3)$$
$$500 \leq V \leq 3000\ (ft/sec),\ 3 \leq e/d \leq 18,\ 3 \leq s/d \leq 18$$

The nomenclature is listed in Appendix A. Because of the lack of test data in the low velocity range, the existing military formulas have been used.

Test data appropriate to the requirements of the nuclear power industry are now becoming available. The current approach to safety analysis is to compare test results with the predictions of the military formulas when used outside the range of test data from which they were developed to determine if any of the military formulas are applicable. Another current approach is to develop new empirical formulas based only on the new appropriate data.

The military formulas being evaluated with the new data are

- Modified Petry [4-7]
- Army Corps of Engineers (ACE) [6,8]
- Modified National Defense Research Committee (NDRC) [7,9,10]
- Amman and Whitney [11,12]
- Ballistics Research Laboratory (BRL) [6].

New formulas that have been developed with the new data are

- Bechtel [13,14]
- Stone and Webster [15]
- Kar modification of NDRC [16].

All the above formulas are presented in Appendix B. Much of the new data are presented in Section 4.

Figure 3 shows the penetration, perforation thickness, and scabbing thickness predicted by the military formulas for a typical missile for

impact velocities up to 500 ft/sec on a target made of concrete with a crush strength of 3000 psi. The example illustrates the wide range of predictions possible, which is not surprising since the formulas were developed for military applications. However, comparisons of penetration and scabbing thicknesses with the results of missile tests conducted for the nuclear reactor industry indicate that the modified NDRC formula provides useful predictions (Section 5). For pipe missiles, the formula requires a change in the definition of the symbol d (Appendix A), from the diameter of a circle with the same contact area to the pipe diameter, before an adequate fit of the data can be obtained.

Comparisons of the NDRC, Bechtel, and Kar predictions with test results are presented in Section 5.

4. Missile Tests

Data from missile tests conducted for the nuclear power industry are presented in Tables 1 through 4. The test programs are designated

- Bechtel (Table 1) [17]
- Bechtel/Calspan (Table 2) [13,18]
- EPRI/Sandia (Table 3) [19]
- EPRI/SRI (Table 4) [3]

The EPRI/SRI program was not conducted specifically to generate data but to investigate the more fundamental aspects of steel missile/concrete target interaction, including the applicability of small-scale testing.

An attempt has been made to include all the important data in each table. Details are to be found in the references cited above. All the penetrating missiles were made of steel and were axisymmetric, being either solid cylinders or pipes. All impacts were at normal incidence.

5. Comparison of Formula Predictions and Test Results

Penetration and scabbing thicknesses predicted by the NDRC, Bechtel, and Kar formulas are compared with test results of Tables 1, 2, 3, and 4 in Figures 4 through 8. Note that the NDRC and Kar formulas for penetration are the same for solid cylindrical missiles.

Figure 4 compares the NDRC predictions with the Bechtel rod test results of Table 1. The 1-inch-diameter rods weighed about 8 pounds and the average weight and concrete crush strength values used to generate the NDRC curves are shown. The letter P beside a data point indicates that perforation occurred in that test. Except for the one data point for a 3-inch-thick slab perforated by the rod, the penetration predictions are good. The difference occurs because the NDRC penetration formula was established for concrete that was thick enough to neglect rear surface effects (infinitely thick), whereas the slab thickness for this test was only three times the missile diameter. All the other points for 6-inch- and 9-inch-thick slabs are predicted very well.

It is harder to judge the quality of scabbing thickness predictions because of insufficient data. However, the predictions are at least consistent with the data. One test (labeled S in Figure 4) on a 6-inch-thick slab showed moderate scabbing damage at an impact velocity of 220 ft/sec, whereas the scabbing thickness prediction is about 5 inches. This comparison indicates that the NDRC predictions for scabbing thickness may be low.

Figure 5 compares the NDRC predictions with the Bechtel/Calspan steel slug test results of Table 2. Data points labeled P and S indicate perforation and scabbing. The 8-inch-diameter steel slug missile weighed about 214 pounds, and the slab thicknesses were 12, 18, and 24 inches. These dimensions do not provide slab thicknesses many times the missile diameter, so it is not surprising to see poor comparison of penetration predictions with the data. On the other hand, it is surprising to see such good agreement of the scabbing thickness predictions with the data.

Figure 6 compares the NDRC, Bechtel, and Kar predictions with the Bechtel/Calspan pipe test results in Table 2. The 8-inch-diameter steel pipe missile weighed about 206 pounds and the slab thicknesses were 12, 18, and 24 inches; the pipe missile weighs about the same as the slug missile. The NDRC and Kar penetration predictions are in good agreement with the pipe test results, unlike prediction comparison in Figure 5 for the slug. The main difference between the pipe and slug missiles is that

one dimension of the pipe contact area, the pipe thickness, is small relative to the slab thickness, which is more in keeping with the test conditions used to empirically establish the penetration formulas. The NDRC, Bechtel, and Kar scabbing thickness predictions agree well with the test results, especially those of Bechtel and Kar. The NDRC prediction is very conservative.

Figure 7 compares the NDRC, Bechtel, and Kar predictions with the EPRI/Sandia pipe test results in Table 3. The 12-inch-diameter pipe missile weighed 743 pounds and the slab thicknesses were 12, 18, and 24 inches. The NDRC and Kar penetration predictions are in good agreement with most of the pipe test results. The data point labeled P indicates that the pipe perforated the 12-inch-thick slab. This is the point farthest above the prediction curves because of departure from the condition that a massive block of concrete is required before the formulas can be expected to predict penetration. The point farthest below the prediction curves is from a test in which the impact velocity of 222 ft/sec led to considerable missile deformation (1.1 in), which accounts for the low penetration. The Bechtel and Kar scabbing thickness predictions compare well with the test results. The NDRC predictions, although safe, are excessively conservative.

Figure 8 compares the NDRC, Bechtel, and Kar predictions with the EPRI/SRI pipe test results in Table 4. The 2-inch-diameter pipe missile weighed 2.83 pounds and the slab thicknesses were about 1.9, 2.8, and 3.7 inches. The NDRC and Kar penetration predictions are in good agreement with most of the pipe test results. The two data points above the prediction curves are from tests with perforation and scabbing and represent a considerable departure from the massive concrete block required for application of the penetration formulas. The Bechtel and Kar scabbing thickness predictions compare well with the test results. The NDRC predictions, although safe, are again excessively conservative.

6. Hard Missile Structural Loading

A method of determining the force history on a reinforced concrete slab caused by hard missile impact is to use the contact pressure assumed

in the derivation of the NDRC penetration formula [9]. This empirical pressure relationship is

$$p = \begin{cases} cv^{0.2} \dfrac{x}{2d} & x < 2d \\ cv^{0.2} & x > 2d \end{cases} \tag{1}$$

where c is a constant and v and x are functions of time to be determined. Substituting (1) in the equation of motion for the missile

$$\frac{W}{g} \frac{d^2x}{dt^2} = -pA_c \tag{2}$$

provides an equation that can be solved for the missile penetration and velocity. The solutions are in the form $t = t(x)$ and $v = v(x)$ such that $p(t)$ is not obtained explicitly. However, a numerical determination of the pressure-time relationship is straightforward.

By making a comparison with the above derivation, Kennedy [1] has shown that, for many missile impact cases of interest, a satisfactory loading pulse is obtained by assuming that the resistive pressure is constant during penetration. The assumption is the same as assuming a constant missile deceleration or a missile velocity that decreases linearly with time. Thus, the constant force applied to the slab is

$$F = \frac{WV^2}{2gx} \tag{3}$$

where x is obtained from a penetration formula. The duration of the force is

$$t_d = \frac{2x}{V} \tag{4}$$

Equations (3) and (4) define a rectangular pulse.

Kennedy [1] also suggested how to account for target deformability and for a small amount of missile crushing. For target deformability only, let x_m, x_t and V_m, V_t be the missile and target displacements and velocities at time t, and let W_m and W_t be the missile weight

and target effective weight (effective weight is determined in Section 7.3). The empirical pressure relationship (1) becomes

$$p = \begin{cases} c(V_m - V_t)^{0.2} \, (x_m - x_t)/2d & x_m - x_t < 2d \\ c(V_m - V_t)^{0.2} & x_m - x_t > 2d \end{cases} \tag{5}$$

and the equations of motion for the missile and target, replacing (2), are

$$\frac{W_m}{g} \frac{d^2x_m}{dt^2} = -pA_c \qquad \frac{W_t}{g} \frac{d^2x_t}{dt^2} = pA_c \tag{6}$$

Setting $x = x_m - x_t$ and $v = v_m - v_t$ reduces equation (5) to equation (1) and reduces the difference between equations (6) to

$$\frac{1}{1 + (W_m/W_t)} \frac{W_m}{g} \frac{d^2x}{dt^2} = -pA_c \tag{7}$$

which is the same as equation (2) but with a smaller missile weight. The NDRC penetration, x, is therefore obtained by reducing the missile mass to $W_m/(1 + W_m/W_t)$. The rectangular pulse on the slab is then given approximately by (3) and (4) with this new value of x.

For a small amount of missile crushing at the impact end, Kennedy [1] has suggested using the empirical relationship for the contact pressure until the missile crush pressure is reached; the crush pressure may be approximated by the bilinear yield stress of the missile material. Keeping this crush pressure constant, the penetration and penetration [illegible] are still assumed to be related by (1); this relationship determines the penetration in the form $t = t(x)$. To describe how the missile stops, the equation of motion (2) is used with the constant crushing pressure. The difference between the distance travelled by the major undeformed part of the missile and the depth of penetration is

the missile crushup. Practical examples are presented in reference [1]. It is shown from these examples that the missile crush displacement must be over 40% of the nondeformable missile penetration depth before missile crush will have a significant influence on calculated scabbing thicknesses.

For the approximate slab loading when the end of the missile crushes, let F and x in (3) be interpreted as the missile crushing force and the stopping distance of the major undeformed portion of the missile. Substitution of x in (4) gives the pulse duration.

Methods for determining target loading from soft missile impact are not discussed here, but many papers are published on this topic in Nuclear Engineering and Design, an international journal devoted to the thermal, mechanical, and structural problems of nuclear energy (North Holland Publishing Company). A recommended approximate formula used in the nuclear power industry for preliminary calculations of the loading is contained in references [2] and [20].

7. Overall Structural Response

An approximate analysis for determining the structural response to missile impact uses the resistance function method [21] in which the structure is assumed to behave as an elastic-plastic or rigid-plastic single-degree-of-freedom system (SDFS).

7.1 Single-Degree-of-Freedom System

Figure 9a shows a SDFS having the bilinear elastic-plastic resistance function shown in Figure 9b. As discussed in the previous section, a reasonable approximation to the loading is the rectangular pulse shown in Figure 9c. In problems where the maximum deflection x_m is many times the elastic limit deflection x_e, the governing equations are

$$M\ddot{x} = \begin{cases} F_1 - kx & 0 < t < t_c \quad 0 < x < x_e \\ F_1 - R_m & t_c < t < t_d \quad x_e < x < x_d \\ -R_m & t_d < t < t_m \quad x_d < x < x_m \end{cases} \tag{8}$$

in which the nomenclaure of Figure 9 has been used. Solving (8), gives the maximum deflection as

$$x_m = x_d + \frac{M\dot{x}_d^2}{2R_m}$$

where

$$x_d = x_e + \dot{x}_c(t_d - t_e) + \frac{F_i - R_m}{2M}(t_d - t_e)^2$$

$$\dot{x}_d = \dot{x}_c + \frac{F_1 - R_m}{M}(t_d - t_e)$$

$$x_e = \frac{F_1}{k}(1 - \cos \omega t_e), \qquad \omega^2 = k/M, \qquad x_e = Rm/k$$

$$\dot{x}_c = \frac{F_1}{k} \sin \omega t_e$$

A measure of the deflection is the ratio of the final deflection to the maximum elastic deflection. This ratio is called the ductility ratio, μ, so

$$\mu = \frac{x_m}{x_e} \tag{9}$$

The loading and the structure are frequently characterized by the parameters

$$C_R = \frac{R_m}{F_1} \qquad C_T = \frac{t_d}{T} \tag{10}$$

where $T = 2\pi/\omega$ is the natural period of vibration of the SDFS. In terms of these parameters the ductility ratio is, from the solution of (8),

$$\mu = \frac{1}{2} + \frac{1}{C_R}\left[1 + \left(\frac{2}{C_R} - 1\right)\left\{2\pi C_T - \cos^{-1}\left(1 - C_R\right)\right\} + \frac{1}{2}\left(\frac{1}{C_R} - 1\right)\left\{2\pi C_T - \cos^{-1}\left(1 - C_R\right)\right\}^2\right] \tag{11}$$

One of the current safety criteria for structures is that the ductility factor should not exceed specified levels (Section 8). For different rectangular pulse loads and SDFS represented by C_R and C_T, the ductility ratio is determined by (11) provided the governing equations are those of (8). If equations (8) do not apply, as in the case of purely elastic response, formulas analogous to (11) are readily derivable. However, the ductility ratios for SDFS with elastic-plastic resistance functions subjected to rectangular pulse are available in the form of a chart. This chart is shown in Figure 10, which was taken from reference [22]; this chart is also contained in reference [21]. Similar charts for other simple pulse shapes are also available [21,22].

For deflections that are many times the elastic limit deflection, a rigid-plastic resistance function is adequate. Instead of (8), the governing equations are

$$M\ddot{x} = \begin{cases} F_1 - R_m & 0 < t < t_d \\ -R_m & t_d < t < t_m \end{cases} \tag{12}$$

and the solution is

$$x_m = \frac{F_1(F_1 - R_m)t_d^2}{2MR_m} \tag{13}$$

In terms of the ductility ratio (9) and the parameters (10), the result (13) is

$$\mu = 2\pi^2 \frac{C_T^2}{C_R}\left(\frac{1}{C_R} - 1\right) \tag{14}$$

Formula (14) provides a rapid initial assessment of a design for the structural resistance to hard missile impact.

7.2 Equivalent SDFS

Before the resistance function method can be used to determine the response of a structure, the structure must be idealized to an equivalent SDFS. The structure is then analyzed by solving the equations

$$M_e\ddot{X} + k_e X = F_e(t) \qquad 0 < X < X_E$$

$$M_e\ddot{X} + R_{me} = F_e(t) \qquad X < X_E \tag{15}$$

where

M_e = equivalent mass = $K_M M_t$

M_t = total mass of structure

k_e = equivalent stiffness = $K_R k$

k = stiffness of structure

F_e = equivalent load = $K_L F$

F = load on structure

R_{me} = equivalent maximum resistance = $K_R R$.

In these definitions, K_M, K_R, and K_L are the mass, stiffness, and load transformation factors. These factors are established by assuming a deflected shape or mode for the structure so that deflections are known once the amplitude has been determined. The assumed mode is usually taken as the shape caused by a static application of the dynamic loads. Because of the selection of a fixed mode, it is necessary to predict in advance whether response will be primarily elastic, elastic-plastic, or plastic.

The procedure for finding the transformation factors is described below by means of the example problem shown in Figure 11. In this problem a uniform clamped beam (Figure 11a) with an elastic-plastic resistance function (Figure 11c) is subjected to a rectangular pulse (Figure 11b) over a central length, and it is assumed that most of the response is plastic. The mode is therefore taken as the fundamental plastic mode (Figure 11d)

$$\phi(x) = 1 - \frac{2x}{L} \tag{16}$$

so that the deflection is

$$w(x,t) = X(t)\ \phi(x) \tag{17}$$

where X is the central deflection and the required amplitude of the mode.

The equivalent mass of the SDFS is derived by equating kinetic energy to that of the beam. Thus

$$\frac{1}{2} M_e \dot{X}^2 = 2 \int_0^{L/2} \frac{1}{2} m \dot{w}^2 dx \tag{18}$$

Substitution of (17) in (18) gives

$$M_e = 2 \int_0^{L/2} m[\phi(x)]^2 dx = \frac{1}{3} M_t$$

where the mode shape (16) has been introduced. Thus the mass transformation factor is

$$K_M = \frac{1}{3}$$

The equivalent load for the SDFS is derived by equating the work done by the load to that done on the beam. Thus

$$\int_0^t F_e dX = 2\int_0^{a/2}\int_0^t p(x,t)\,dw\,dx$$

which, for a uniformly distributed rectangular pulse and plastic mode shape (16), reduces to

$$F_e = F_1\left(1 - \frac{a}{2L}\right)$$

so that the load transformation factor is

$$K_L = 1 - \frac{a}{2L}$$

The equivalent stiffness of the SDFS is the same as the total static load (distributed in the same manner as the dynamic load) that produces the same unit deflection as the beam. For unit deflection

$$R_e = k_e \quad \text{(SDFS)} \qquad\qquad R = k \quad \text{(Beam)}$$

But $R_e = R(1 - a/2L)$ for the plastic deformation mode (16), so

$$k_e = R_e = K_L R = K_L k$$

The stiffness transformation factor K_R is the same as the load transformation factor K_L.

The equivalent maximum resistance of the SDFS is the same as the total static load (distributed in the same manner as the dynamic load) that causes collapse of the beam. Thus

$$R_{me} = k_e X_E \qquad \text{(SDFS)} \qquad\qquad R_m = kX_E \qquad \text{(Beam)}$$

giving

$$R_{me} = \frac{k_e}{k} R_m = K_L R_m$$

The static elastic central deflection of the clamped beam of span L subjected to a total load R uniformly distributed over a central length a is

$$X = \frac{RL^3}{192EI} f\left(\frac{a}{L}\right) = \frac{R}{k}$$

where EI is the flexural rigidity, and

$$f\left(\frac{a}{L}\right) = 1 + \left(\frac{a}{L}\right)^2 - \frac{1}{2}\left(\frac{a}{L}\right)^3$$

Hence the beam stiffness is

$$k = \frac{192EI}{L^3 f\left(\frac{a}{L}\right)}$$

The static collapse load, obtained from moment equilibrium when plastic hinges exist at the supports and center (Figure 11o) where the fully plastic moments are denoted by M_p, is

$$R_m = \frac{8M_p}{L\left(1 - \frac{a}{2L}\right)}$$

All the expressions have now been derived to proceed with the solution of the SDFS equations (15). The equations can be put in the form

$$\ddot{X} + \frac{K_L k}{K_M M_t} X = \frac{K_L}{K_M M_t} F$$

$$\ddot{X} + \frac{K_L}{K_M M_t} R_m = \frac{K_L}{K_M M_t} F \qquad (19)$$

for solution, according to the procedure in Section 7.1, to find the ductility ratio μ in terms of the parameters C_R and C_T. From (15) and (19) the natural period is

$$T = 2\pi\sqrt{\frac{M_e}{k_e}} = 2\pi\sqrt{\frac{K_M M_t}{K_L k}}$$

Transformation factors have been derived for common load and structural configurations [21]. In slabs, for example, where the plastic response dominates, the mode is obtained from yield line theory to determine transformation factors and static collapse loads.

7.3 Higher Mode Response

If the loading pressure is large enough, the structure will respond in a plastic mode that is higher than the static collapse mode and the mode shape will undergo considerable change during deformation. Consequently, the SDFS method of Section 7.2 is not applicable and another approximate method must be used.

The higher mode response is illustrated by the example of a clamped rigid-perfectly plastic beam subjected to a rectangular pulse over a short central segment, as shown in Figure 12a. If the pressure is low enough, the beam will deform in the same mode as the static plastic collapse mode with yield hinges at each support and at the center, as shown in Figure 12b. For higher pressures, the outer hinges will appear within the span instead of at the supports, as shown in Figure 12c. The outer hinge locations will depend on the pressure magnitude: the higher the pressure, the closer the hinges are to the center. According to the

rigid-plastic theory of beams, the hinges remain stationary under a constant pressure, and deformation proceeds in the higher mode of Figure 12d. When the pressure is removed, the outer hinges propagate to the supports, causing a changing mode of deforamtion, as shown in Figure 12e. After the hinges reach the supports, the remaining deformation occurs in the static collapse mode of Figure 12f.

A rigid-plastic circular plate subjected to a rectangular pulse over a small central circular area responds in a similar manner. The outer beam hinges are simply replaced by a hinge circle.

The above description of dynamic response to a central rectangular pulse shows that it is possible to determine the effective mass of the target during missile impact if the contact loading is approximated by a rectangular pulse, as suggested in Section 6. For deformation in the mode shown in Figure 12d, equation (18) with the half-span L/2 replaced by the hinge location X_1 leads to the effective mass

$$M_e = \frac{2}{3} mX_1 = \frac{2X_1}{3L} M_t$$

where rigid-plastic theory gives the hinge location X_1 in the form

$$\frac{2X_1}{3L} + \left(1 - \frac{a}{2L}\right) C_R + \frac{a}{2L}$$

No approximate method for analyzing higher mode response is in general use in the nuclear reactor industry, but methods under review are

- Available exact rigid-plastic solutions [23-25]
- Bound theorems for elastic-plastic deformations [26]
- Plastic mode approximations [27].

7.4 Computer Codes

Structural and continuum mechanics computer codes are used extensively in the nuclear power industry to obtain structural response of containment buildings to dynamic loads. For reinforced concrete structures, only responses in which the materials remain elastic can be treated, although introduction of tensile concrete cracking is far from straightforward. Treatment of elastic-plastic response is still in the research and development stage. Representative structural codes used in the nuclear power industry are listed in Table 5. Codes for analyzing the local missile/target interaction described in Section 2 are still research tools [3].

8. Design Criteria

Criteria governing design and analysis against impact loads include deformation limits and maximum reaction shear stresses for structural response and punching shear for local response.

Structural deformation limits are cast in the form of ductility ratios. The recommended ratios are based on tests [28-32]. For flexure of reinforced concrete beams and slabs these ratios are:

Beam flexure $$\mu < \frac{1}{10(\rho-\rho')} \leq 10$$

Slab flexure $$\mu < \frac{1}{10(\rho-\rho')} \leq 30$$

where

$\rho = \frac{A_s}{bd}$ = ratio of tensile reinforcement

$\rho' = \frac{A'_s}{bd}$ = ratio of compressive reinforcement

A_s = area of tensile reinforcement

A'_s = area of compressive reinforcement

b = width of beam or unit width of slab

d = distance of compression face to tensile reinforcement.

To ensure ductile behavior and attainment of the allowable concrete flexural ductility limits, the following limits on ammount of reinforcement are recommended [33,34]:

$$1.4\frac{\sqrt{f'_c}}{f_y}\cdot\left(\frac{H}{d}\right)^2 \leq \rho \qquad\qquad \rho - \rho' \leq \frac{f'_c}{4f_y}$$

where symbols additional to the above are

f'_c = concrete compressive strength (psi)

f_y = steel yield strength (psi)

H = beam depth or slab thickness.

The lower limit allows for transfer of bending stress where the concrete section cracks and is intended to preclude the possibility of brittle behavior in a grossly underreinforced section. The upper limit provides a margin against compressive failure of the concrete.

Structural deformation limits also include a recommended maximum rotation at plastic hinges and yield lines. A proposed criterion, based on tests [35,36] is

$$\theta < \theta_u = 0.0065\,\frac{d}{c} \leq 0.07 \text{ radians}$$

where

θ = plastic hinge or yield line rotation (radians)

θ_u = recommended maximum

c = distance from compression face to neutral axis for fully plastic moment.

The criterion is based on the results of tests on beam and slab depths ranging from 6 to 20 inches.

It is desirable to design structural elements subject to impact loads so that they provide sufficient shear capacity to promote deformation in the flexural mode. Missile impact can induce shear failure at the slab supports or near the periphery of the impact area; such failures are called reaction shear failure and punching shear failure.

The code provisions [37-39] for reaction shear for sections without shear reinforcement consider potential failure through diagonal tension cracking or shear compression failure in the compression zone. These considerations resulted in the allowable concrete shear stress

$$\tau = 1.9 \sqrt{f'_c} + 2500 \rho \frac{Vd}{M} \leq 3.5 \sqrt{f'_c}$$

where

V = shear force on the cross section

M = moment on the cross section.

Codes provide additional equations that permit an increase in concrete shear capacity in the presence of concurrent axial compression and require a decrease in capacity with axial tension.

Punching shear for hard missiles is implicit in the formulas for penetration, perforation, and scabbing. However, for large deformable or soft missiles, such as airplanes and automobiles, a punching shear criterion is applied.

The code provisions [37-39] for design against punching shear consider diagonal tension failure in the concrete adjacent to the load. The codes specify that the punching shear be

$$\tau < 4 \sqrt{f'_c}$$

on the section with a perimeter one-half the slab depth from the load. Work by Long [40] considered the beneficial effects of flexural stress and reinforcing strength and suggested the criterion

$$P = \frac{20(a + d)d(100\rho)^{\frac{1}{4}}}{(3/4 + 4a/L)} \sqrt{f'_c}$$

where

P = punching shear load (pound)

a = [loaded area]$^{\frac{1}{2}}$ (inch)

L = distance between local loads; for most impact cases $a/L \simeq 0$.

For most practical cases in nuclear power plant design, Long's formula results in the punching shear strength formula

$$\tau < 6 \sqrt{f'_c}$$

Missile impact tests [18] have demonstrated punching shear strengths greater than $10 \sqrt{f'_c}$ for thick walls within minimum reinforcement. It is believed that Long's formula is sufficiently conservative.

9. Summary

Elementary approaches have been outlined for designing reinforced concrete structures to withstand hard missile impact.

For local response, the modified NDRC, Bechtel, and Kar formulas provide adequate predictions for penetration and scabbing thickness for cases within the range of test data. Similar preliminary comparisons, not presented here, indicate that the Stone and Webster formula also provides adequate predictions. If nuclear safety analyses should require consideration of missile/slab impact cases that lie substantially outside existing test data, further testing would be required before the formulas could be used with confidence.

Computational techniques for investigating local impact require continued development with experiments to validate the complex modeling of dynamic material properties including fracture.

For structural response, the resistance function method conveniently provides an estimate of the deformation, provided modes higher than the fundamental mode are not stimulated. Techniques were suggested for treating the higher mode cases. A major shortcoming in the analyses where considerable plastic deformations occur is the neglect of membrane forces caused by support restraints or even plate action alone.

Computational techniques for analyzing structural response of reinforced concrete slabs to pulse loads that account for plastic deformation are still under development.

Design criteria were presented in the form of allowable ductility ratios, plastic hinge rotations, and reaction shear stresses for structural response to pulse loads, along with allowable punching shear stresses in slabs around the contact area of soft missiles.

Acknowledgements

The author is indebted to R. P. Kennedy of the Engineering Decision Analysis Company, Inc., for permission to make extensive use of his review paper [1], and to B. P. Bain for the computations required for Figures 3 through 8.

Appendix A

Nomenclature for Local Missile Impact Formulas

A_c = missile contact area (in^2)

D = missile diameter (in)

d = $[4A_c/\pi]^{\frac{1}{2}}$ = effective missile diameter (in). For noncircular cross sections, d is the diameter of an equivalent cylindrical shaped missile with the same contact area as that of the actual missile.*

e = perforation thickness (in), which is the maximum target thickness perforated by a missile with a given impact velocity. Theoretically, the missile exit velocity is zero. For concrete, the perforation thickness e is much greater than the penetration x because of scabbing.

f'_c = ultimate compressive strength of concrete (psi)

H = target thickness (in)

V = missile impact velocity (ft/sec)

v_i = missile velocity at time t_i during penetration

W = missile weight (lb)

x = penetration depth (in), that is, the depth that the missile will penetrate into an infinitely thick target. Thus, rear boundary effects are neglected, so target thickness must be great enough to prevent scabbing.

x_i = penetration at time t_i during penetration.

---

*Tests with pipe missiles show that d should be replaced by D in the modified National Defense Research Committee formula to achieve adequate predictions.

Appendix B

LOCAL MISSILE IMPACT FORMULAS

B.1 Modified Petry

The penetration depth for a missile impacting a massive target is

$$x = 12\, K_p A_p \log_{10}(1 + V^2/21500) \qquad \text{(B1)}$$

where

$$K_p = \begin{cases} 0.00799 & \text{massive concrete} \\ 0.00426 & \text{normal reinforced concrete} \\ 0.00284 & \text{specially reinforced concrete} \end{cases}$$

and A_p is the missile weight per unit projected area (lb/ft^3). Note that K_p has the shortcoming of not being dependent on concrete strength.

For specially reinforced cocnrete in which the front and back face steel is laced, Amirikian [5] has given the dependence of K_p on concrete strength shown in Figure B1. These values are sometimes used for normal reinforced concrete.

When the above tabulated numbers for K_p are used, the formula is referred to as the modified Petry 1. When Figure B1 is used for K_p, the formula is referred to as the modified Petry 2.

The perforation and scabbing thicknesses are usually taken to be

$$e = 2x \qquad \text{(B2)}$$

$$s = 2.2x \qquad \text{(B3)}$$

B.2 Modified National Defense Research Committee

The NDRC penetration formula is

$$x = \left[4KNWd\left(\frac{V}{1000d}\right)^{1.8}\right]^{0.5} \qquad \frac{x}{d} \leq 2 \qquad \text{(B4)}$$

$$x = KNW\left(\frac{V}{1000d}\right)^{1.8} + d \qquad \frac{x}{d} > 2 \qquad \text{(B5)}$$

The nose shape factor is

N = 0.72 flat
= 0.84 blunt
= 1.00 spherical
= 1.14 very sharp

The concrete penetrability factor is

$$K = \frac{180}{f'^{0.5}_c}$$

The perforation and scabbing thicknesses are given by the Army Corps of Engineers formulas

$$\frac{e}{d} = 1.32 + 1.24\frac{x}{d} \qquad 1.35 \leq \frac{x}{d} \leq 13.5 \qquad 3 \leq \frac{e}{d} \leq 18 \qquad \text{(B6)}$$

$$\frac{s}{d} = 2.12 + 1.36\frac{x}{d} \qquad 0.65 \leq \frac{x}{d} \leq 11.75 \qquad 4 \leq \frac{d}{d} \leq 18 \qquad \text{(B7)}$$

For ratios of slab thickness to projectile diameter of less than three ($h/d < 3$), Beth [41] has suggested the formulas

$$\frac{e}{d} = 3.19\frac{x}{d} - 0.718\left(\frac{x}{d}\right)^2 \qquad \frac{x}{d} \leq 1.35 \qquad \frac{e}{d} \leq 3 \qquad \text{(B8)}$$

$$\frac{s}{d} = 7.91\frac{x}{d} - 5.06\left(\frac{x}{d}\right)^2 \qquad \frac{x}{d} \leq 0.65 \qquad \frac{s}{d} \leq 3 \qquad \text{(B9)}$$

B.3 Army Corps of Engineers

The ACE penetration formula is

$$x = \frac{282W}{f_c'^{0.5} d^{2.8}} \left(\frac{V}{1000d}\right)^{1.5} \qquad \text{(B10)}$$

and the perforation and scabbing thicknesses are given by (B6) and (B7). It is suggested here that formulas (B8) and (B9) again be used for ratios of slab thickness to projectile diameter of less than three.

B.4 Ammann and Whitney

The Ammann and Whitney formula is intended to predict the penetration of small explosively generated fragments traveling over 100 ft/sec. According to this formula the penetration is

$$x = \frac{282NW}{f_c'^{0.5}} \left(\frac{V}{1000d}\right)^{1.8} \qquad \text{(B11)}$$

B.5 Ballistics Research Labortory

The BRL formula is the following direct prediction of perforation thickness

$$\frac{e}{d} = \frac{7.8W}{d^{1.67}} \left(\frac{V}{1000d}\right)^{1.33}$$

for an ultimate compressive stress of 3000 psi. By assuming that the perforation thickness is inversely proportional to $f_c'^{0.5}$ the BRL formula may be modified to

$$\frac{e}{d} = \frac{427W}{f_c'^{0.5} d^{1.67}} \left(\frac{V}{1000d}\right)^{1.33} \qquad \text{(B12)}$$

The scabbing formula recommended [42] is

$$s = 2e \tag{B13}$$

B.6 Bechtel

The results in Table 2 were used by the Bechtel Corporation to develop two empirical scabbing thickness formulas, one for a solid steel missile and the other for a steel pipe missile:

$$s = \frac{15.5W^{0.4}V^{0.5}}{f_c'^{0.5}D^{0.2}} \qquad \text{(solid steel missile)} \tag{B14}$$

$$s = \frac{5.42W^{0.4}V^{0.65}}{f_c'^{0.5}D^{0.2}} \qquad \text{(steel pipe missile)} \tag{B15}$$

where D is the missile diameter.

B.7 Stone and Webster

The results of an extensive series of quarter-scale tests were used by Stone and Webster to develop an empirical formula for predicting the scabbing thickness of concrete targets struck by steel missiles with velocities typical for nuclear plant applications. This formula directly accounts for the influence of (1) ratio of wall thickness h to outside diameter D and (2) missile deformability of steel pipe missiles. This formula is

$$s = \left(\frac{WV^2}{C}\right)^{1/3} \tag{B16}$$

where

$$3000 \leq f_c' \leq 4500 \text{ (psi)}$$

$$1.5 \leq H/D \leq 3.0$$

$$0.06 \leq \frac{2h}{D} \leq 1.0$$

$$75 \leq V \leq 250 \text{ (ft/sec)}$$

and the coefficient C is given by Figure B2.

B.8 Kar Modification of NDRC Formula

Penetration formulas (D4) and B5) are modified to become

$$x = \left[4KNWd\left(\frac{V}{1000d}\right)^{1.8}\frac{d}{D}\right]^{0.5} \qquad \frac{x}{d} \leq 2$$

$$x = KNW\left(\frac{V}{1000d}\right)^{1.8}\frac{d}{D} + d \qquad \frac{x}{d} > 2$$

where the nose shape factor is

$N = 0.72$ flat

$= 0.72 + 0.25\,(n - 0.25)^{0.5} \leq 1.17$

where n = nose radius/missile diameter

$= 0.72 + 0.36\,[(D/d)^2 - 1] \leq 1.17$

for pipes and irregular sections.

The diameter d is defined in Appendix A and the diameter

$D =$
- outside diameter for cylindrical solids and pipes
- d for rectangular cross sections
- diameter of circle inscribed in polygon joining vertices of cross sectional shape.

$D \geq d$

The concrete penetrability factor is modified to

$$K = \frac{180}{f'^{0.5}_c}\,\beta^{1.25}$$

where

$\beta = E_m/E_s$

E_m = modulus of elasticity of missile material (psi)

E_s = modulus of elasticity of steel = 29×10^6 psi

The perforation and scabbing thickness formulas are modified to

$$\frac{e}{d} = \begin{cases} \frac{a}{d} + 3.19\frac{x}{d} - 0.718\left(\frac{x}{d}\right)^2 & \frac{x}{d} \leq 1.35 \quad \text{(B17)} \\ \frac{a}{d} + 1.32 + 1.2\frac{x}{d} & 1.35 \leq \frac{x}{d} \leq 13.5 \quad \text{(B18)} \end{cases}$$

$$\frac{s}{d} = \begin{cases} \frac{a}{d} + \beta\left[7.91\frac{x}{d} - 5.06\left(\frac{x}{d}\right)^2\right] & \frac{x}{d} \leq 0.65 \quad \text{(B19)} \\ \frac{a}{d} + \beta\left[2.12 + 1.36\frac{x}{d}\right] & 0.65 \leq \frac{x}{d} \leq 11.75 \quad \text{(B20)} \end{cases}$$

where

a = maximum aggregate size (in).

REFERENCES

1. R. P. Kennedy, A Review of Procedures for the Analysis and Design of Concrete Structures to Resist Missile Impact Effects, Nuclear Engineering and Design, Vol. 37 (2) 1976.

2. Structural Analysis and Design of Nuclear Plant Facilities, Structural Division of ASCE, by editing board under chairmanship of J. D. Stevenson, task group chairmanship under R. Broman, Preliminary Draft, January 1976.

3. Y. M. Gupta and L. Seaman, Local Response of Reinforced Concrete to Missile Impacts SRI International Final Report RP393-1, to EPRI, October 1977.

4. F. J. Samuely and C. W. Hamann, Civil Protection (The Architectural Press, 1939).

5. A. Amirikian, Design of Protective Structures, Report NT-3726, Bureau of Yards and Docks, Department of the Navy, August 1950.

6. R. C. Gwaltney, Missile Generation and Protection in Light-Water-Cooled Power Reaction Plants, ORNL NSIC-22, Oak Ridge National Laboratory, Oak Ridge, Tennessee, for the USAEC, September 1968.

7. C. V. Chelapati, R. P. Kennedy, and I. B. Wall, Probablistic Assessment of Aircraft Hazard for Nuclear Power Plants, Nuclear Engineering and Design, Vol. 19 (2) 1972.

8. Fundamentals of Protective Design, Report AT1207821, Army Corps of Engineers, Office of the Chief of Engineers, 1946.

9. Effects of Impacts and Explosion, Summary Technical Report of Division 2, National Defense Research Committee, Vol. 1, Washington D.C.,1946.

10. R. P. Kennedy, Effects of an Aircraft Crash into a Concrete Reactor Containment Building, Holmes and Narver,Inc., Anaheim, California, July 1966.

11. Industrial Engineering Study to Establish Safety Design Criteria for Use in Engineering of Explosive Facilities and Operations Wall Response, Report submitted to Process Engineering Branch, APMED, Picatinny Arsenal, Dover, New Jersey, April 1963.

12. Structures to Resist the Effects of Accidental Explosions, Report TM 5-1300, Department of the Army, Washington, D.C., July 1965.

13. J. V. Rotz, Results of Missile Impact Tests on Reinforced Concrete Panels, Second ASCE Specialty Conference on Structural Design of Nuclear Plant Facilities, New Orleans, December 1975.

14. J. V. Rotz, Evaluation of Tornado Missile Impact Effects on Structures, Proceedings of a Symposium on Tornadoes, Assessment of Knowledge and Implications for Man, Texas Technical University, Lubbock, Texas, June 1976.

15. Z. D. Jankov, J. A. Shanahar, M. P. White, Missile Tests of Quarter Scale Reinforced Concrete Barriers, Presented at a Symposium on Tornadoes, Assessment of Knowledge and Implications for Man, Texas Technical University, Lubbock, Texas, June 1976.

16. A. K. Kar, Barrier Design for Tornado-Generated Missiles Transactions of the 4th International Conference on Structural Mechanics in Reactor Technology, Paper J10/3, August 1977.

17. R. B. Barber, Steel Rod/Concrete Slab Impact Test (Experimental Simulation), Bechtel Corporation, San Francisco, California, 1973.

18. F. A. Vassallo, Missile Impact Testing of Reinforced Concrete Panels, Report No. HC-5609-D-1, Calspan Corporation, Buffalo, New York, January 1975 (Prepared for Bechtel Corporation).

19. A. E. Stephenson, Full-Scale Tornado-Missile Impact Tests, Sandia Laboratories Final Report SAND 77-1166, July 1977, to EPRI (Project manager, G. E. Sliter), EPRI NP-440.

20. J. D. Riera, On the Stress Analysis of Structures Subjected to Aircraft Impact Forces, Nuclear Engineering and Design, North Holland Publishing Company, Amsterdam, Holland, Vol. 8, 1968, pp. 415-426.

21. J. M. Biggs, Introduction to Structural Dynamics (McGraw-Hill Book Co., New York, 1964).

22. Department of the Army Technical Manual, Design of Structures to Resist the Effects of Atomic Weapons, Principles of Dynamic Analysis and Design, TM 5-856-3, March 15, 1972.

23. A. L. Florence, Response of Circular Plates to Central Pulse Loading, International Journal of Solids and Structures, Vol. 13, pp. 1091-1102, 1977.

24. A. D. Cox and L. W. Morland, Dynamic Plastic Deformations of Simply Supported Square Plates, Journal of Mechanics and Physics of Solids, Vol. 7, pp. 229-241, 1959.

25. M. F. Conroy, The Plastic Deformation of Built-In Beams Due to Distributed Dynamic Loading, Journal of Applied Mechanics, Vol. 31, p. 507, 1964.

26. E. H. Lee and R. L. Mallett, Structural Analysis and Design for Energy Absorption in Impact, Department of Transportation Final Report, DOT-TST-44, December 1975.

27. J. B. Martin and P. S. Symonds, Mode Approximations for Impulsively Loaded Rigid-Plastic Structures, Journal of Engineering Mechanics Division, American Society of Civil Engineers, Vol. 92, No. EM5, pp.43-66, October 1966.

28. J. R. Gaston, C. P. Seiss, and N. M. Newmark, An Investigation of the Load-Deformation Characteristics of Reinforced Concrete Beams Up to the Point of Failure, University of Illinois Structural Research Service, No. 40, December 1952.

29. N. M. Newmark and J. D. Haltiwanger, Air Force Design Manual AFSWC-TDR-62-138, prepared by University of Illinois for Air Force Special Weapons Center, Kirtland Air Force Base, New Mexico, 1962.

30. C. H. Norris et al., Structural Design for Dynamic Loads (McGraw-Hill Book Company, Inc., New York 1959).

31. G. E. Albritton, Response of Deep Reinforced and Unreinforced Concrete Slabs to Static and Dynamic Loading, ASCE National Meeting on Structural Engineering, September 1968.

32. D. R. Denton, A Dynamic Ultimate Strength Study of Simply Supported Two-Way Reinforced Concrete Slabs, TR 1-789 U.S. Army Engineers, Waterways Experimental Station, Vicksburg, Mississippi, July 1967.

33. Response to AEC Request for Additional Information on Report BC-TOP-9, Revision 3, Bechtel Power Corporation, September 1974.

34. Design of Structures for Missile Impact, Topical Report BC-TOP-9-A, Bechtel Power Corporation, September 1974.

35. A. H. Mattock, "Rotational Capacity of Hinged Region in Reinforced Concrete Beams," Flexural Mechanics of Reinforced Concrete, ASCE 1965-50 (ACI SP-12), American Society of Civil Engineers, 1965.

36. Proposed Code Requirements for Nuclear Safety Related Concrete Structures, Draft of Section C.3.3.3, "Rotational Limits," American Concrete Institute, Committee 349, July 1975.

37. ASME Boiler and Pressure Vessel Code, Section III, Division 2, Code for Concrete Reactor Vessels and Containments, 1975 edition.

38. Building Code Requirements for Reinforced Concrete, American Concrete Institute, Standard 318-71, 1971.

39. Proposed Code Requirements for Nuclear Safety Related Concrete Structures, American Concrete Institute Report, Committee 349, 1975.

40. A. E. Long, A Two-Phase Approach to the Prediction of Punching Strengths of Slabs, American Concrete Institute Journal, February 1975.

41. R. A. Beth, Concrete Penetration, OSRD-4856, National Defense Research Committee Report A-319, March 1945.

42. R. B. Linderman, M. Fakhari, J. V. Rotz, et al., Design of Structures for Missile Impact, Topical Report BC-TOP-9, Revision 1, Bechtel Power Corporation, July 1973.

Table 1

BECHTEL MISSILE TESTS

Missile Type	Missile Weight (lb)	Missile Velocity (ft/sec)	Panel[1] Thickness (in)	Concrete Strength (in)	Penetration (in)	Scabbing Damage
Steel Rod 1-in dia	8.05	218	3	5910	____[2]	severe
	8.04	150	6	4810	1.23	light
	8.04	213	6	5910	1.60	light
	8.05	220	6	5940	1.98	moderate
	3.78	322	6	5940	1.68	moderate
	8.05	213	9	5760	1.71	none
	8.04	217	9[3]	4810	1.84	none
	8.01[4]	235[5]	9	5940	2.34	none

1. 4-foot-square panel, 3-foot, 10.5-inch free span.
2. Perforation. Residual velocity 180 ft/sec.
3. No reinforcement.
4. Round-nose missile.
5. May be high.

Table 2

BECHTEL/CALSPAN MISSILE TESTS

Missile Type	Missile Weight (lb)	Missile Velocity (ft/sec)	Panel[1] Thickness (in)	Reinforcement EWEF (%)	Concrete Strength (psi)	Missile Deformation (in)	Penetration (in)	Scabbing Damage	Scabbing Velocity (ft/sec)
Steel Slug 8-in dia	214	122	12	0.4	5770	0	0.4	moderate	25
	214	214	12	0.4	4550	0	—[2]	severe	105
	213	340	12	0.4	4550	0	—[3]	severe	172
	213	161	18	0.4	4500	0	0.5	none	0
	213	207	18	0.4	5100	0	3.0	incipient	15
	213	337	18	0.6	4900	0	9.0	severe	49
	213	295	24	0.6	4775	0	1.3	none	0
	215	377	24	0.6	4500	0	2.0	light	14
Steel Pipe 8-in dia Sch. 40[4]	202	135	12	0.6	5210	0	2.5	none	0
	202	209	12	0.6	5770	0	4.0	light	40
	205	210	18	0.4	5210	2.0	4.5	none	0
	209	319	18	0.4	5210	5.5	7.4	incipient	0
	209	370	24	0.4	4520	7.5	7.0	none	0
	208	470	24	0.4	4775	12.0	8.0	incipient	0
	210	470	24	0.6	4400	10.5	9.5	incipient	0
	132	370	18	0.6	4500	11.5	11.5	none	0
	132	455	18	0.6	5100	15.0	15.0	moderate	40
Wooden Pole 8-in dia	201	300	12	0.6	5770	24.0	0	none	0
	199	440	12	0.6	5770	48.0	0	none	0
	200	490	24	0.6	4400	51.0	0	none	0

1. 9-foot-square panel, 8-foot free span
2. 9-inch-diameter hole
3. Perforation
4. Outside diameter 8.625 in, wall 0.329 in

Table 3

EPRI/SANDIA MISSILE TESTS

Missile Type	Missile Weight (lb)	Missile Velocity (ft/sec)	Panel[1] Thickness (in)	Concrete Strength (psi)	Missile Deformation (in)	Penetration (in)	Backface Damage
Steel Pipe 12-in dia Sched. 40[2]	743	92	12	3545	0	3.9	flaking
	743	92	12	3350	0	3.5	flaking
	743	98	12	3595	0	4.5	scabbing
	743	143	12	3690	0	12.0	perforation
	743	143	18	4325	2.1	5.0	cracking
	743	152	18	4205	0.13	5.3	flaking
	743	157	18	4070	0.25	4.1	flaking
	743	198	18	3560	3.8	6.8	scabbing
	743	202	18	3350	3.8	7.0	scabbing
	743	203	18	4535	5.0	7.5	scabbing
	743	213	18	4420	2.5	9.1	scabbing
	743	222	18	3900	9.1	4.3	cracking
	743	202	24	3795	1.8	6.8	cracking
Steel Pipe 3-in dia[3]	78	212	12	3340	1.9	4.6	cracking
Steel Rod 1-in dia	8	435	12	3545	0	5.8	cracking
	8	303	18	3650	0	3.6	none
Wooden Pole[4] 13.5-in dia	1470	204	12	3620	69.4	0	cracking
	1500	205	18	3770	50.5	0	cracking

1. 15-foot-span square panel, reinforcement 0.3% EWEF.
2. Outside diameter 12.75 in, wall 0.406 in, length 165 in.
3. Schedule 40, outside diameter 3.5 in, wall 0.216 in, length 109 in.
4. Class 1, 35-foot utility pole.

Table 4

EPRI/SRI MISSILE TESTS

Missile Type	Missile Weight (lb)	Missile Velocity (ft/sec)	Panel[1] Thickness (in)	Concrete Strength (psi)	Penetration (in)	Backface Damage
Steel	2.83	101	1.875	5400	0.4	cracking
Pipe	2.83	117	1.875	5300	1.2	scabbing
	2.83	148	1.875	5300	1.9	perforation
2-in O.D.[2]	2.83	145	2.813	5950	0.6	cracking
	2.83	196	2.813	5050	1.0	cracking
	2.83	223	2.813	5000	1.1	cracking
	2.83	206	3.750	5900	0.9	cracking

1. 32-inch-square panel, reinforcement 0.27% EWEF.
2. Pipe inside diameter 1.875 in., wall 0.063 in.

Table 5

PROGRAM CAPABILITIES

Program Name	General Description	Method	Mesh Generation	Plots	Restart	Dynamic	Large Deflections	Nonlinear Material
MARC-CDC	3-D Structure	Finite Element	X	X	X	X	X	X
WILSON-GHOSH	Axisym. Solids (Fourier Loads)	Finite Element				X		
BOSOR	Axisym. Shells (Fourier Loads)	Finite Difference	X	X		X	X	
PISCES	2-D Contiuum	Finite Difference	X	X	X	X	X	X
SAP IV	3-D Structures	Finite Element		X	X	X		
STRUDL	3-D Structures	Finite Element	X	X	X	X	X	
NASTRAN	3-D Structures	Finite Element		X	X	X	X	X
ANSYS	3-D Structures	Finite Element	X	X	X	X	X	X
STAGS	3-D Shells	Finite Difference		X	X	X	X	
NONSAP	3-D Structures	Finite Element			X	X	X	X

FIGURE CAPTIONS

1. Local Interaction of Hard Missile and Reinforced Concrete Slab
2. Section of Reinforced Concrete Target Showing Damage Mechanisms
3. Predictions for a Steel Missile/Concrete Target
4. Comparison of NDRC Predictions and Bechtel Rod Test Results
5. Comparison of NDRC Predictions and Bechtel/Calspan Slug Test Results (Table 2)
6. Comparison of NDRC, Bechtel, Kar Predictions with Bechtel/Calspan Pipe Test Results (Table 2)
7. Comparison of NDRC, Bechtel, Kar Prediction with EPRI/Sandia Pipe Test Results (Table 3)
8. Comparison of NDRC, Bechtel, Kar Predictions and EPRI/SRI Pipe Test Results (Table 4)
9. Single-Degree-of-Freedom-System Problem
10. Ductility Ratio Curves for Elasto-Plastic System, Rectangular Load
11. Clamped Beam Problem for SDFS Analysis
12. Response of a Clamped Beam to Central Rectangular Pulse Loading (High Mode)

B1 Coefficient for Petry Formula

B2 Coefficient for Stone and Webster Formula

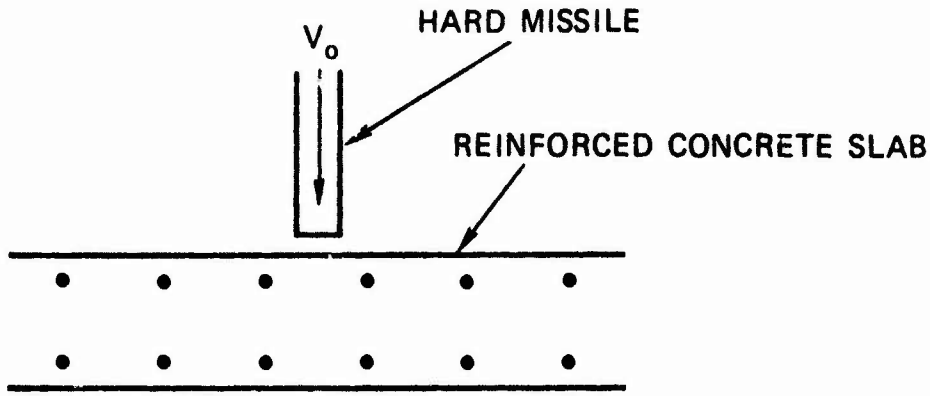

(a) Before Impact

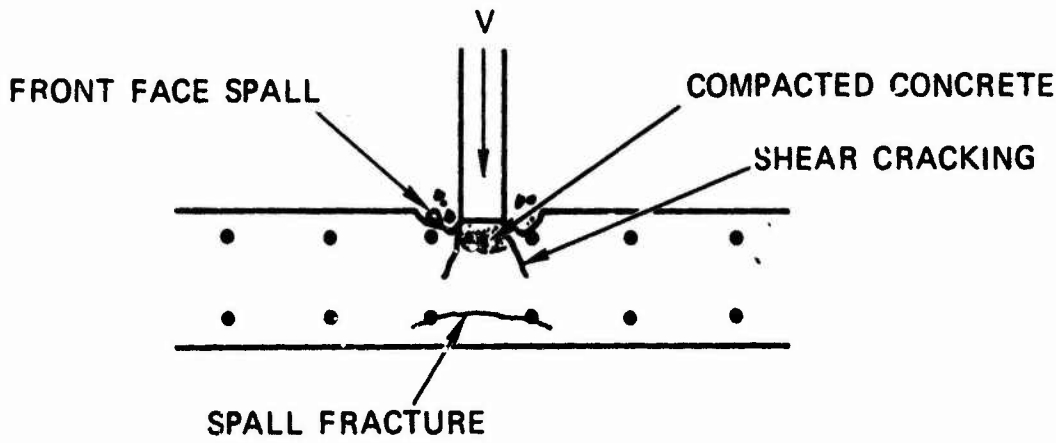

(b) Early Interaction

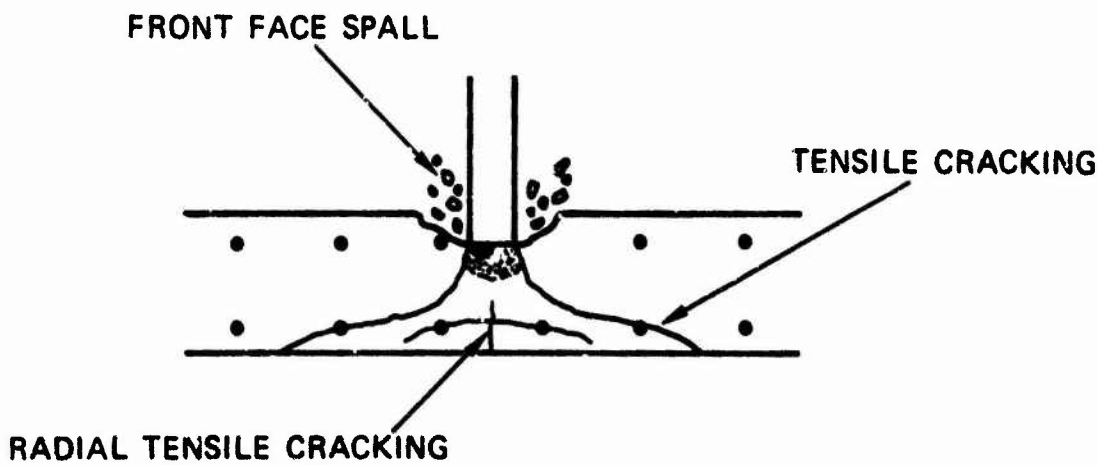

(c) Late Interaction

MA-317523-8

FIGURE 1

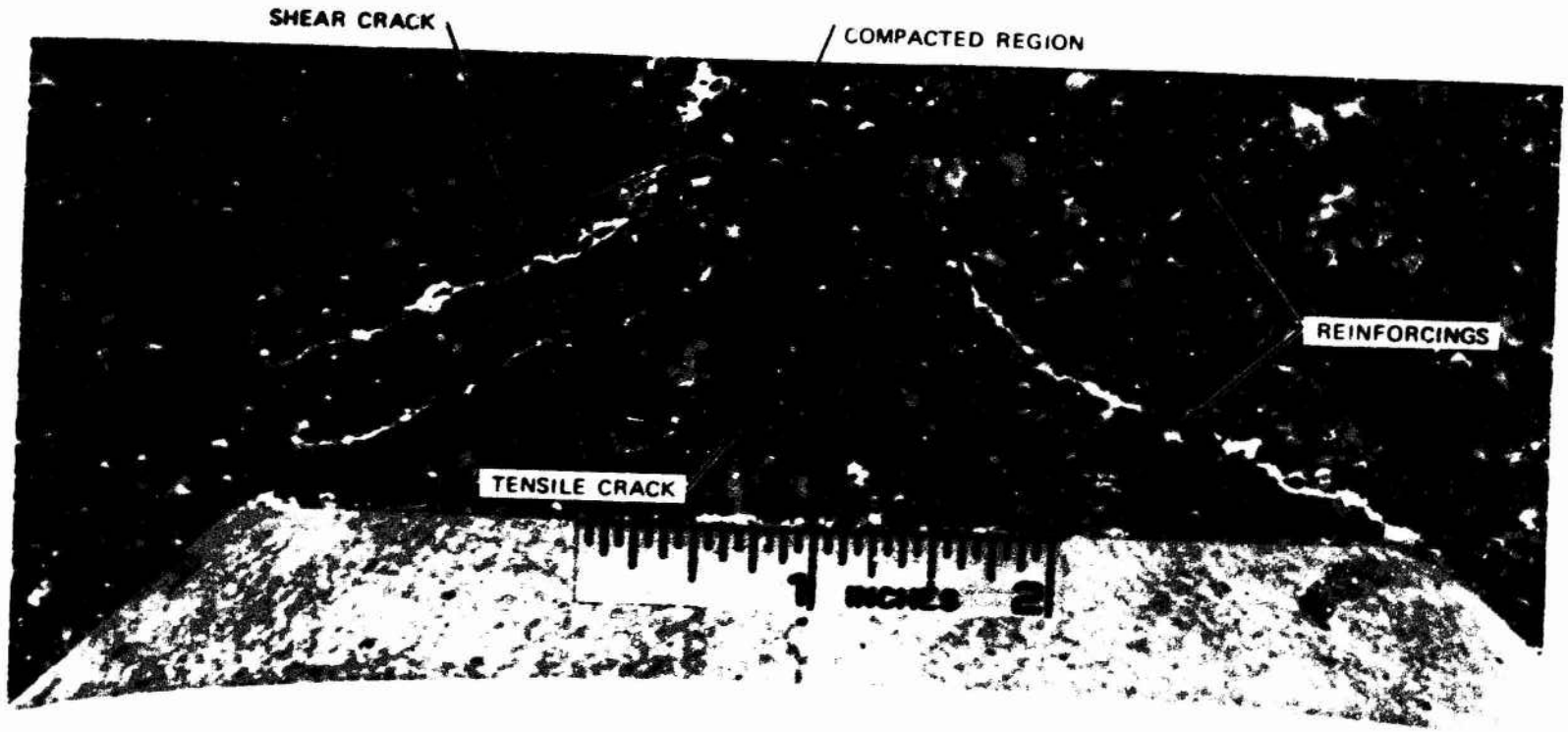

MP-4078-42

FIGURE 2

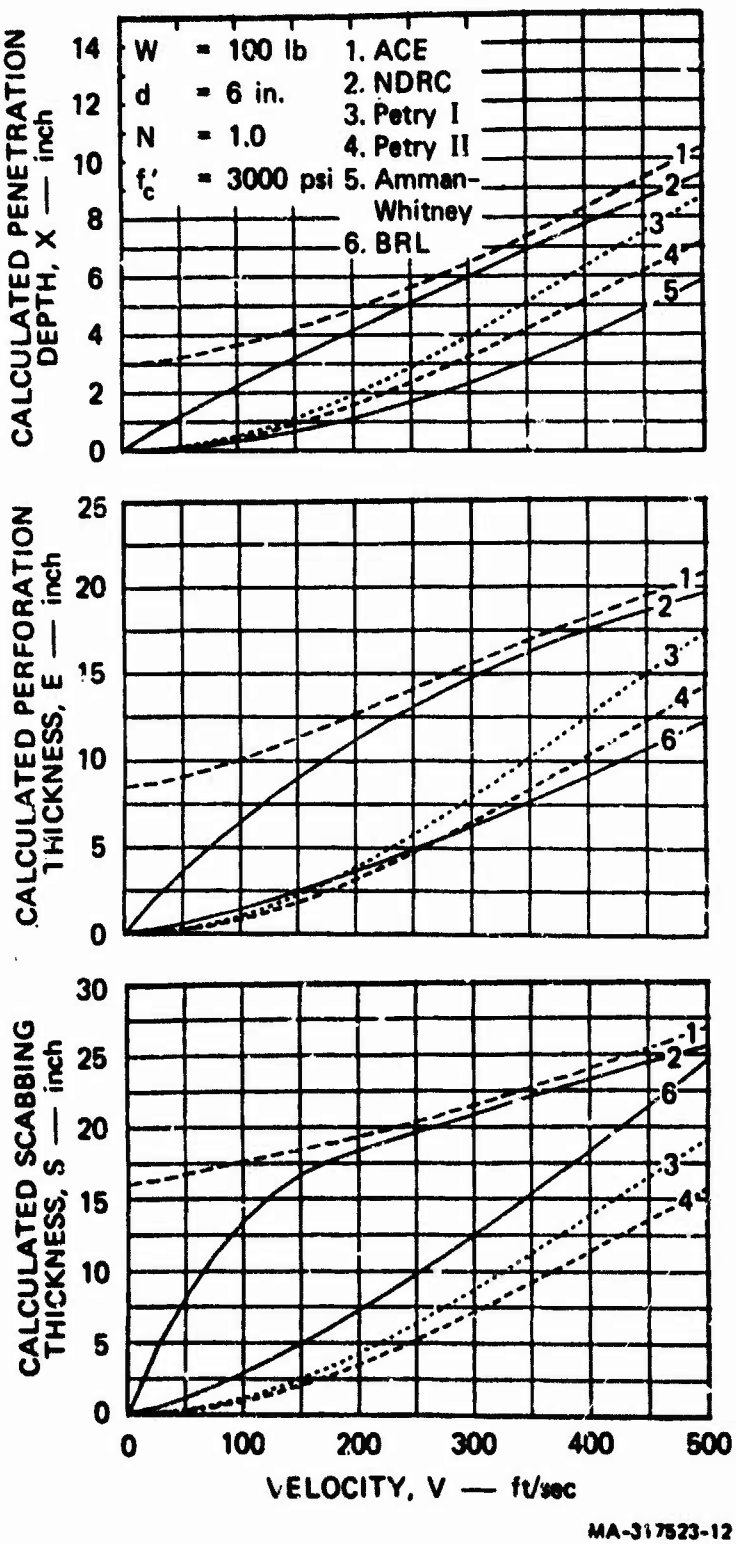
W = 100 lb
d = 6 in.
N = 1.0
f_c' = 3000 psi
1. ACE
2. NDRC
3. Petry I
4. Petry II
5. Amman-Whitney
6. BRL
CALCULATED PENETRATION DEPTH, X — inch
CALCULATED PERFORATION THICKNESS, E — inch
CALCULATED SCABBING THICKNESS, S — inch
VELOCITY, V — ft/sec
MA-317523-12

FIGURE 3

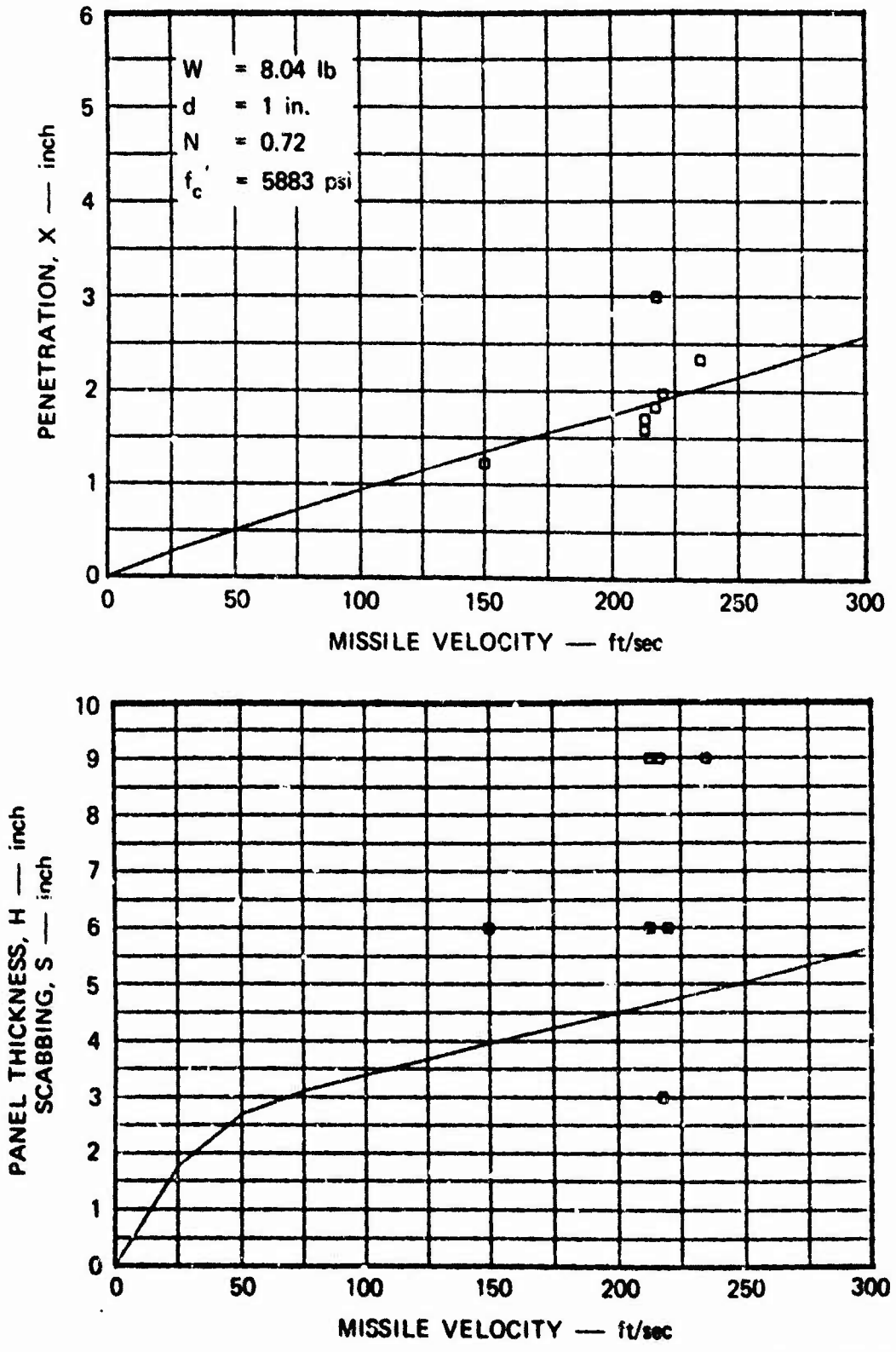
W = 8.04 lb
d = 1 in.
N = 0.72
f_c' = 5883 psi
PENETRATION, X — inch
MISSILE VELOCITY — ft/sec
PANEL THICKNESS, H — inch
SCABBING, S — inch
MISSILE VELOCITY — ft/sec
MA-317623-13

FIGURE 4

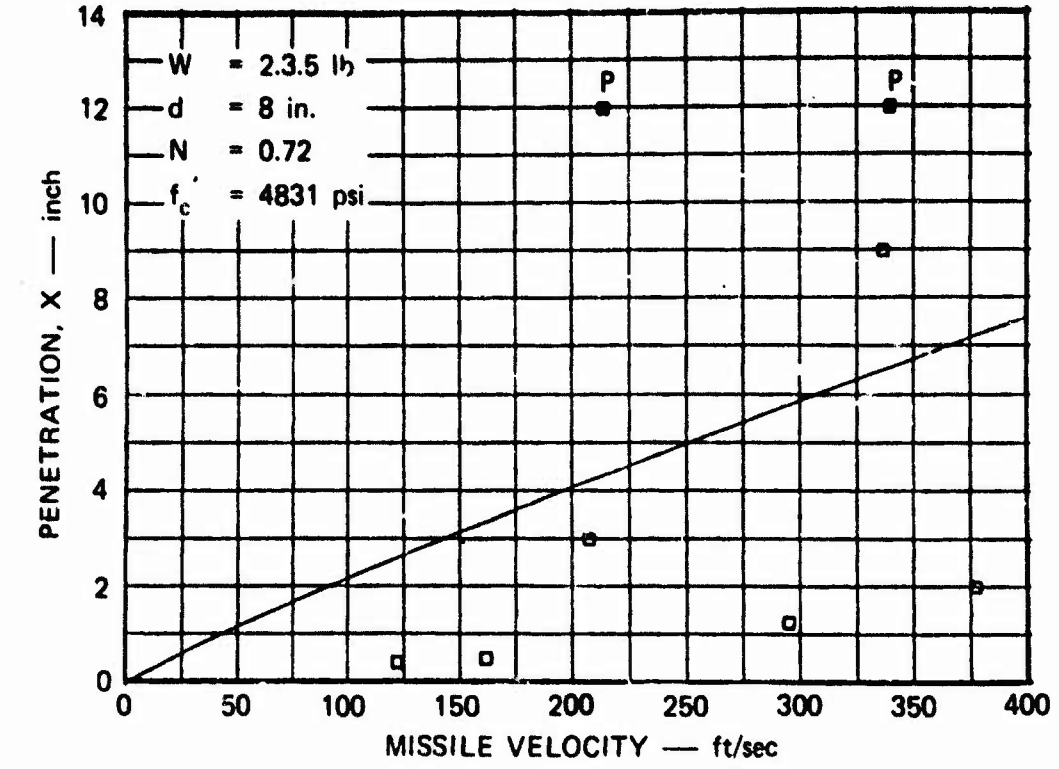

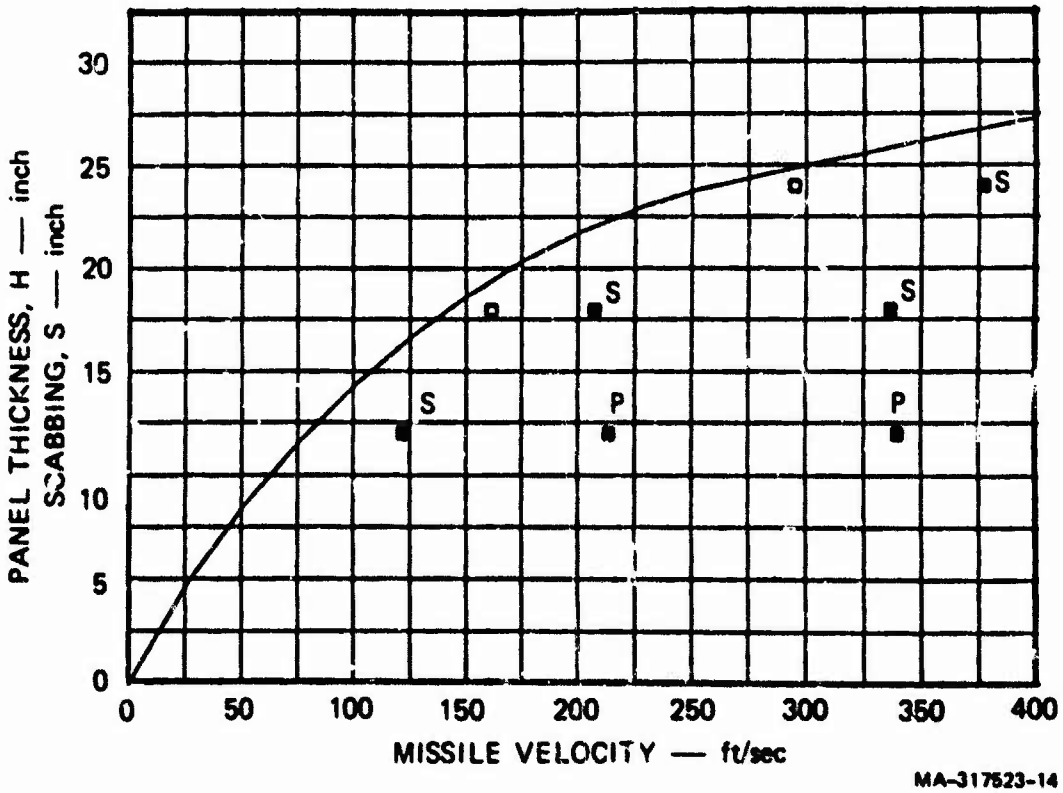

MA-317523-14

FIGURE 5

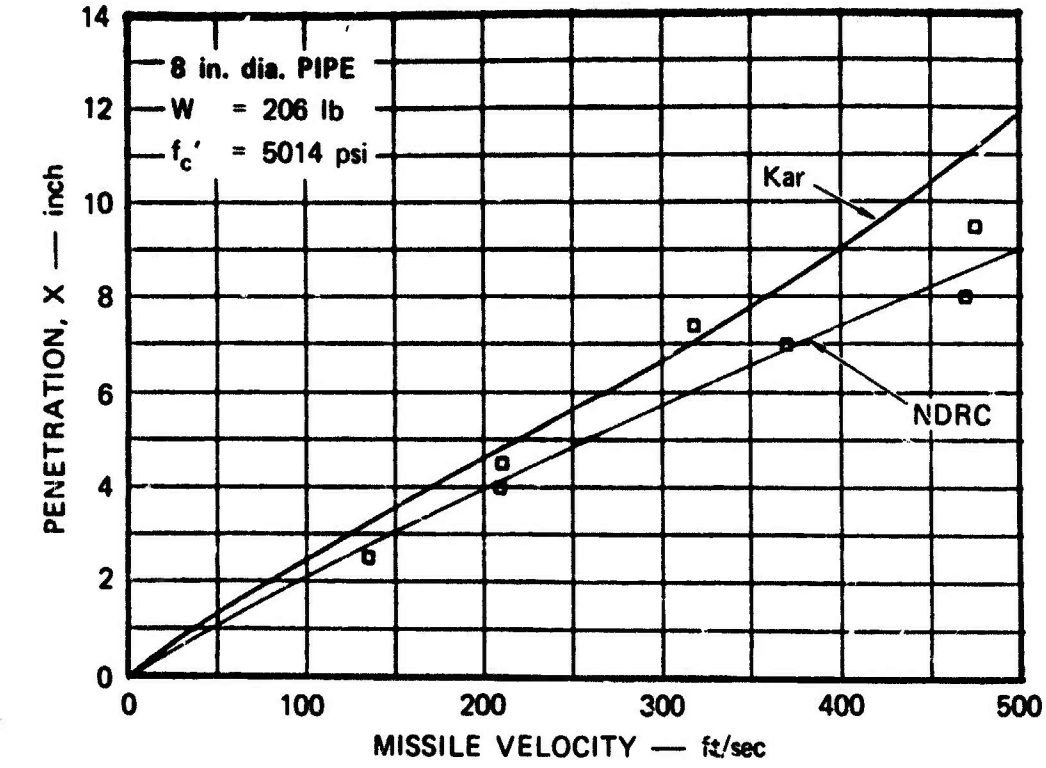

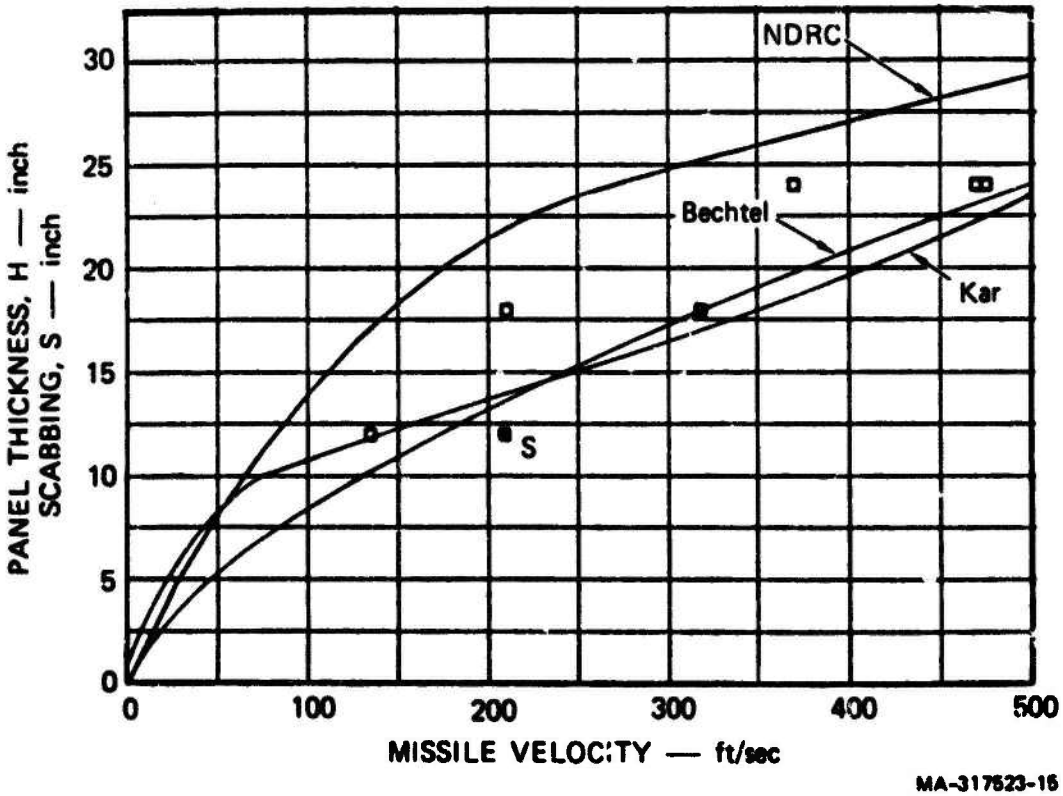

MA-317523-15

FIGURE 6

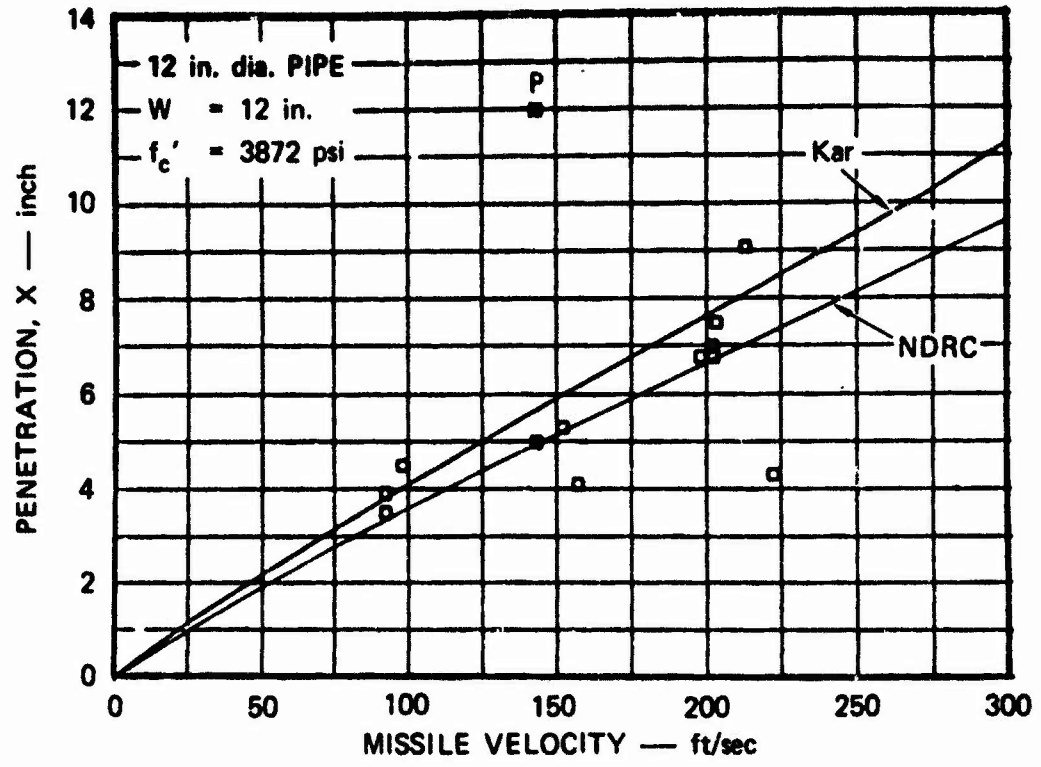

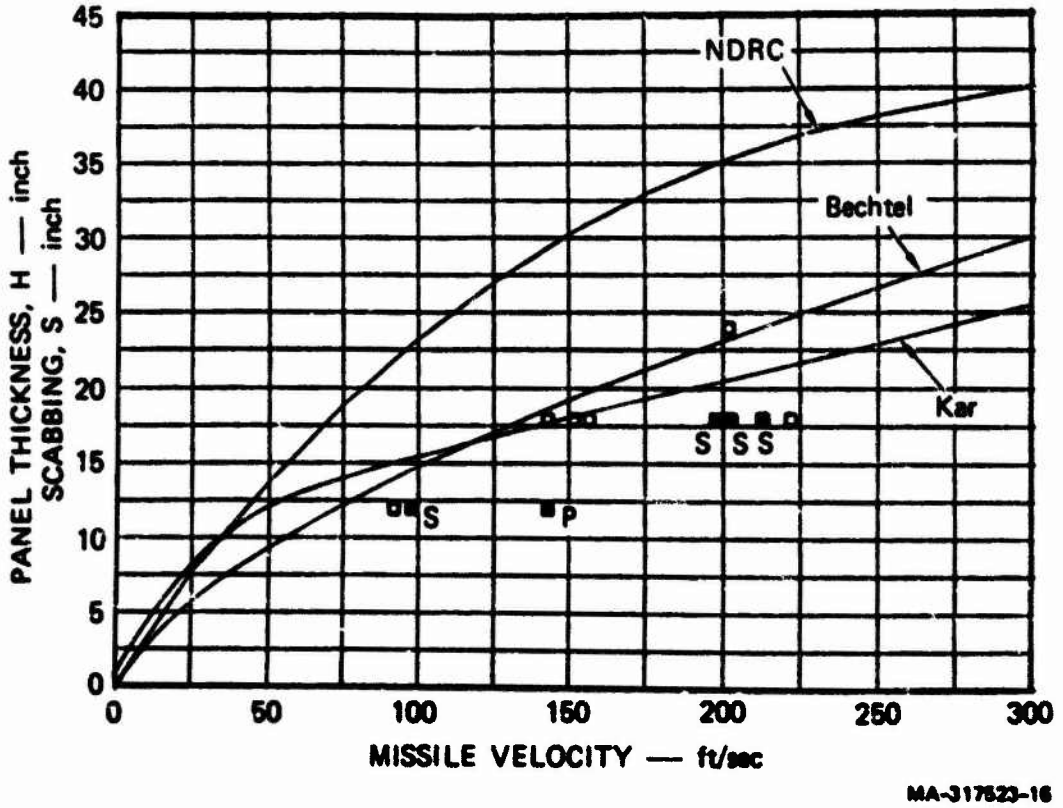

MA-317523-16

FIGURE 7

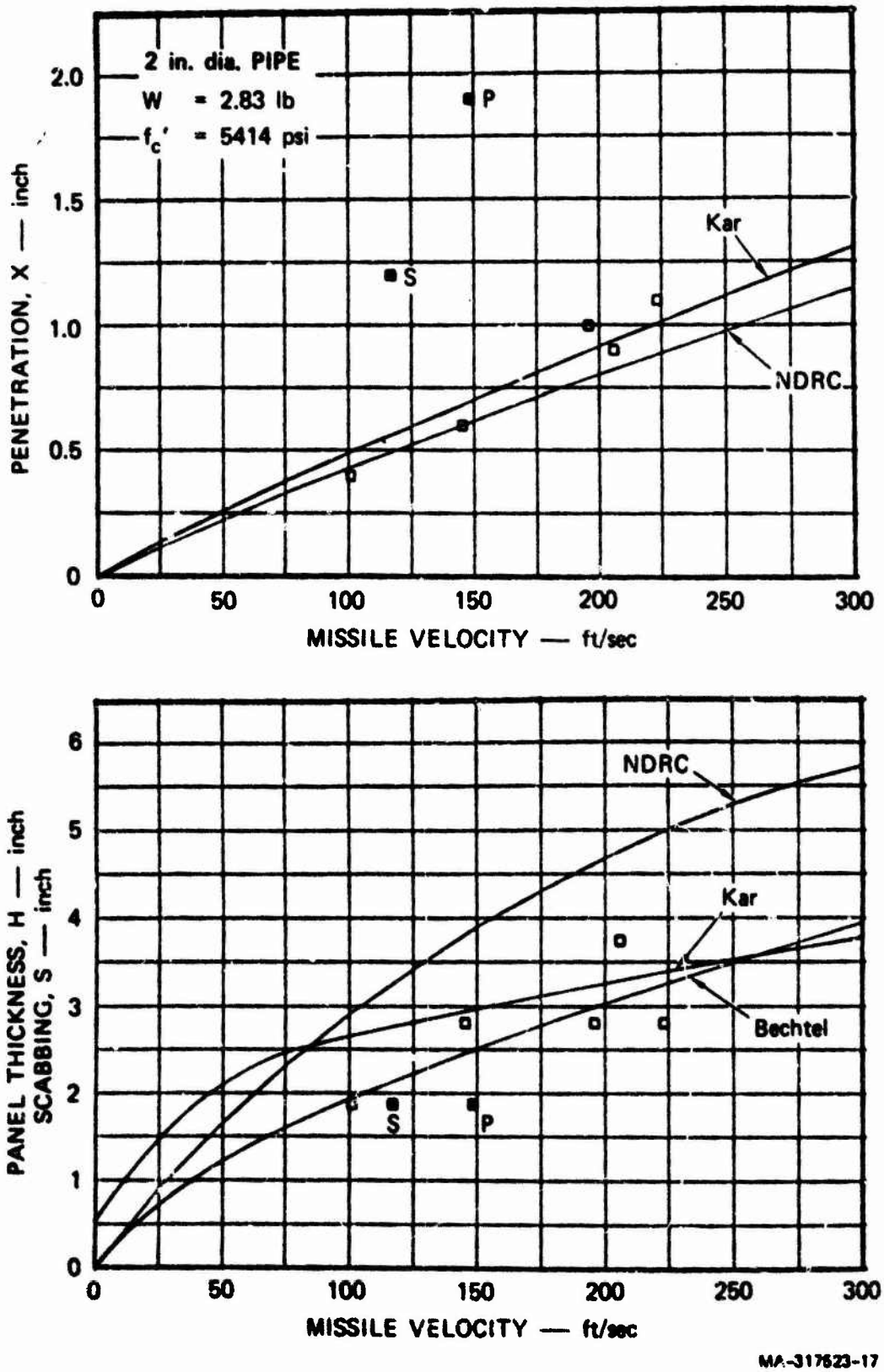
2 in. dia. PIPE
W = 2.83 lb
f_c' = 5414 psi
P
S
Kar
NDRC
PENETRATION, X — inch
MISSILE VELOCITY — ft/sec
NDRC
Kar
Bechtel
PANEL THICKNESS, H — inch
SCABBING, S — inch
MISSILE VELOCITY — ft/sec
MA-317623-17

FIGURE 8

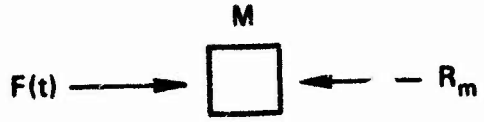

(a) Single-Degree-of-Freedom System

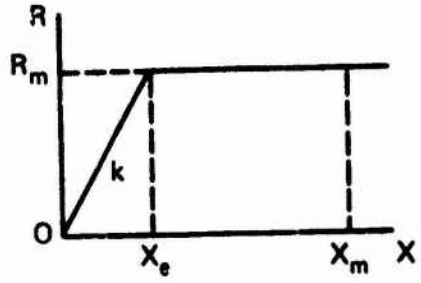

(b) Elastic-Plastic Resistance Function

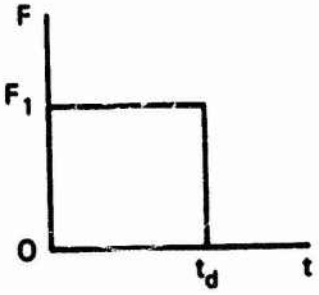

(c) Rectangular Pulse

MA-317523-9

FIGURE 9

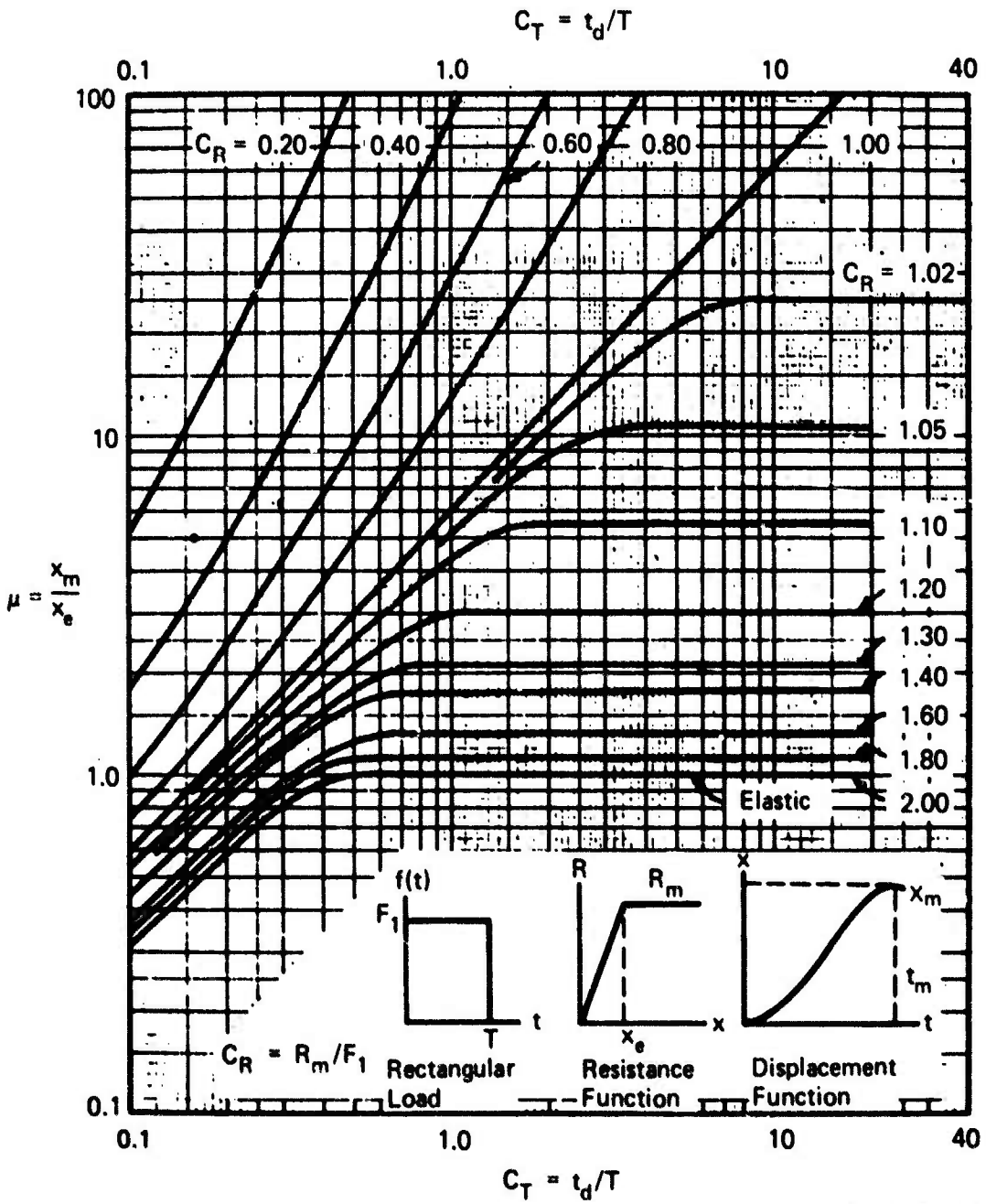

MA-317523-11

FIGURE 10

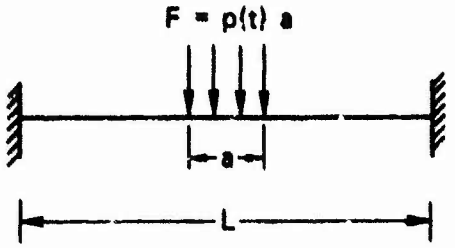

(a) Clamped Beam

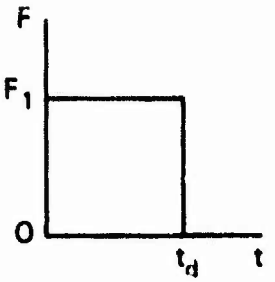

(b) Rectangular Pulse

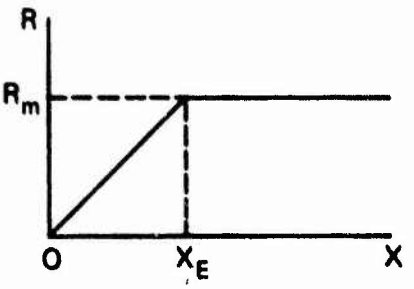

(c) Resistance Function

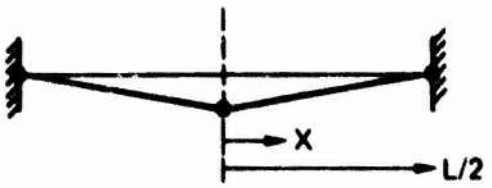

(d) Plastic Deflection Mode

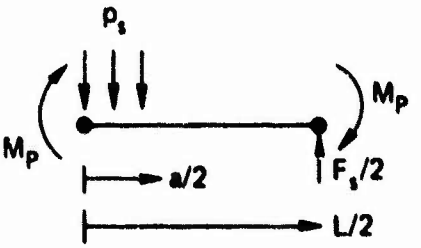

(e) Static Collapse

MA-317523-10

FIGURE 11

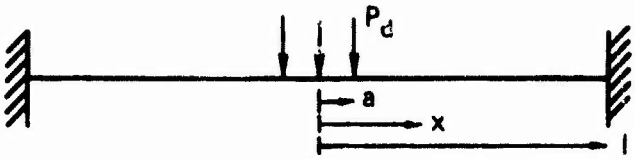

(a) Beam Problem

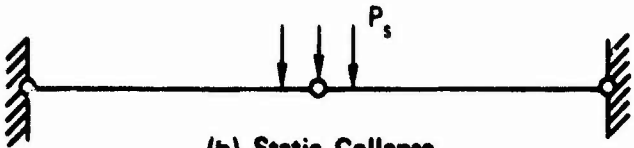

(b) Static Collapse

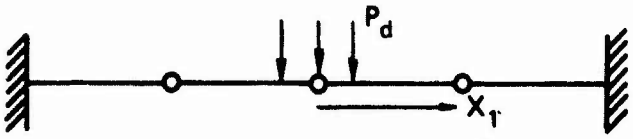

(c) Initial Mechanism

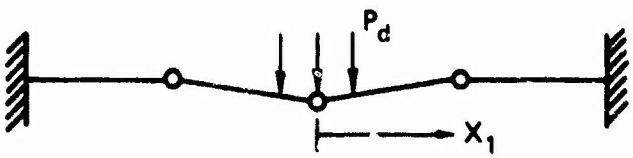

(d) Dynamic Collapse

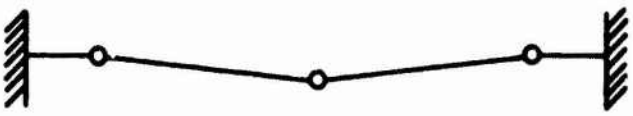

(e) Traveling Hinges



(f) Static Collapse Mode

MA-317523-18

FIGURE 12

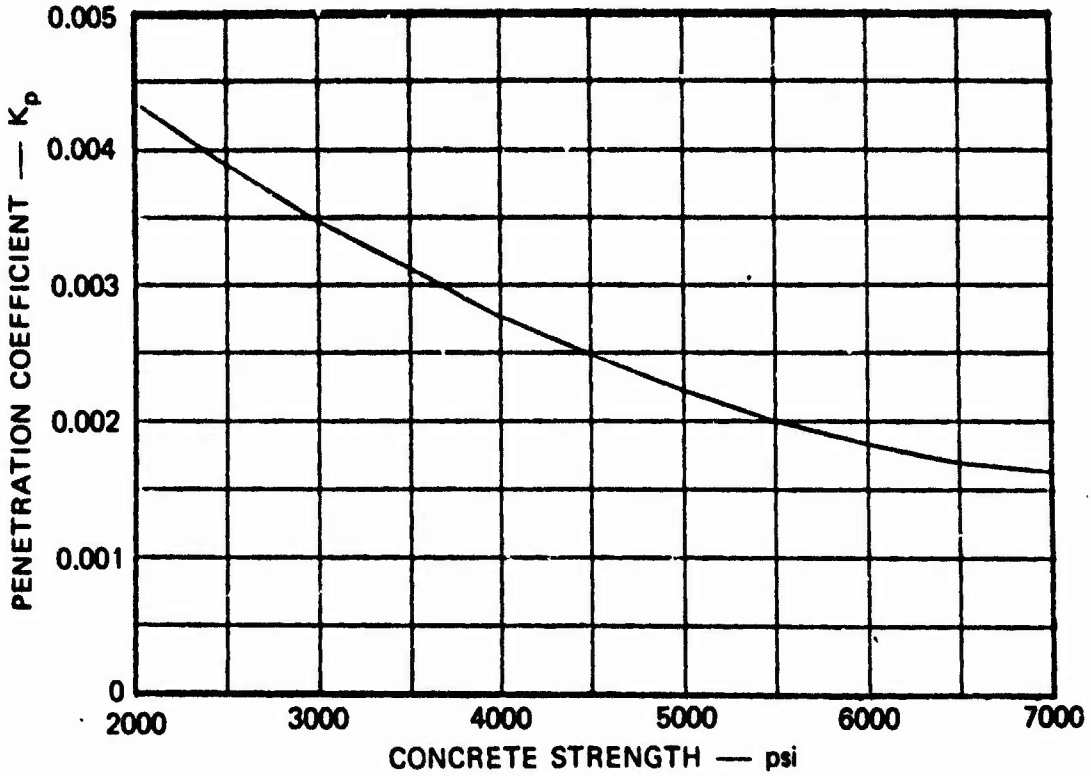

FIGURE B1

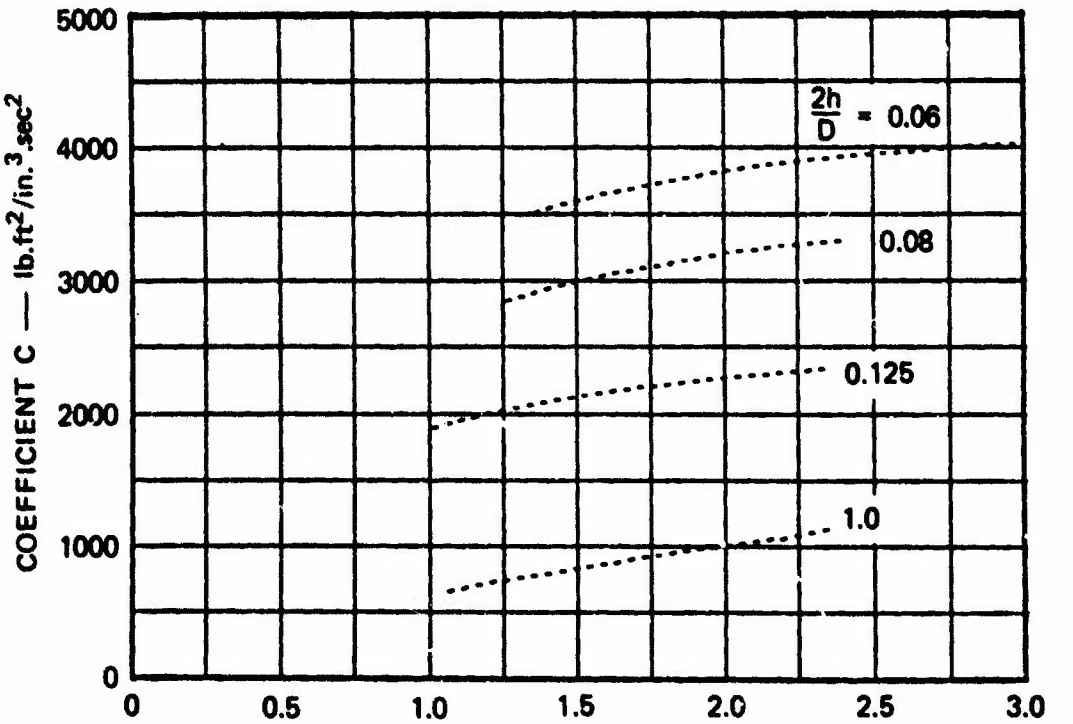

MA-317523-19

FIGURE B2

LIST OF ATTENDEES

ABRAHAMSSON, E. A.	FORTF:F, Stockholm, Sweden
ADAMS, A. E.	AFLC, Wright-Patterson AFB, OH
AIRY, R. D.	Rockwell International, Cedar Rapids, IA
ALLEVA, R. Q.	Catalytic Inc, Philadelphia, PA
AMLIE, June T.	NAVMATCOM, Washington, D. C.
ANDERSON, E. W.	NSWC White Oak, Silver Spring, MD
ANDERSON, R. W.	Agbabian Associates, El Segundo, CA
ANDREW, E. A.	Olin Corp, E. Alton, IL
ANDREWS, S. B., Jr.	NSWC Dahlgren, VA
ARANT, Richard	BEI Electronics, Inc, Camden, AR
ATKINS, J. R.	NASA, Kennedy Space Center, FL
BACHMAN, Georgia C.	DDESB, Washington, D. C.
BACHTELL, N. D.	Fairhope, AL
BAER, E. L.	Letterkenny Army Depot, Chambersburg, PA
BAKER, C. F.	UC Lawrence Livermore Lab, Livermore, CA
BAKER, W. E.	Southwest Research Institute, San Antonio, TX
BAILETS, Roy J.	AFFTC, Edwards AFB, CA
BAILEY, M. R.	DARCOM Field Safety Acty, Charlestown, IN
BALDWIN, Richard	Western Gear Corp, Jamestown, ND
BANNISTER, R. J.	Fort Shafter, Hawaii
BARKHOFF, J. W.	NWC China Lake, CA
BARRIOS, D. R.	MB Associates, San Ramon, CA
BEAUREGARD, R. L.	NAVSEASYSCOM, Washington, D. C.
BECKER, L. A.	David W Taylor Naval Ship R&D Ctr, Bethesda, MD
BENNETT, D. R.	Pacific Missile Test Center, Pt Mugu, CA
BERGMANN, E. P.	Southwest Research Institute, San Antonio, TX
BERKHOLTZ, N. E.	Honeywell, Inc, New Brighton, MN
BERRY, G. A.	Jet Propulsion Laboratory, Pasadena, CA
BIASUTTI, S.S.B.	Dr Ing Mario Biazzi Soc An, Vevey, Switzerland
BIBLE, W. B.	Martin Marietta Aluminum Sales, Milan AAP, TN
BLACKWELL, L. A.	Los Alamos Scientific Lab, Los Alamos, NM
BOBST, R. E.	172d Inf Bde, Fort Richardson, AK
BODDORFF, R. D.	Inst of Makers of Explosives, Wilmington, DE
BOTLEY, W. K.	Rockwell International, Columbus, OH
BOUCHARD, R. W.	Letterkenny Army Depot, Chambersburg, PA
BOUDREAU, A. E.	DCASR, Boston, MA
BOX, J. R.	Warner Robins ALC, Robins AFB, GA
BOYARS, Carl	Aerospace Corp, Washington, D. C.
BRADFORD, W. J.	Olin Corp, Stamford, CT
BRETTEL, E. G.	Day & Zimmermann Inc, Lone Star Div, Texarkana, TX
BRINKER, W. A.	Emerson Electric Co, St Louis, MO
BRINKMAN, E. J.	Olin Corp, East Alton, IL
BROCK, N. H., Jr.	Air Products & Chemicals Inc, Allentown, PA
BROCKWAY, W. R.	E I duPont, Martinsburg, WV
BROWN, H. O.	1606 ABW, Kirtland AFB, NM
BROWN, J. H.	Red River Army Depot, Texarkana, TX
BROWN, S. L.	DCASR, Philadelphia, PA

PRECEDING PAGE BLANK

BROWN, Sydney	Milan AAP, Milan, TN
BROWN, W. C.	Louisiana AAP, Shreveport, LA
BROWN, W. D.	Iowa AAP, Middletown, IA
BRUGMANN, H.D., LTC, GA	Bundesministerium der Verteidigung, FRGermany
BRYAN, K. M.	UN Command/US Forces Korea
BUCHANAN, H. G.	Ballistic Res Lab, Aberdeen Proving Ground, MD
BUCKNER, A. K.	Kansas AAP, Parsons, KS
BULMER, C. T.	Rockwell International, Cedar Rapids, IA
BURCH, C. A.	Dept of Energy, Albuquerque, NM
BURKE, E. F.	Olin Corp, St. Marks, FL
BURKE, R. H.	NavSeaSupCtr Pacific, San Diego, CA
BUTLER, S. L., LTC, USAF	HQ USAFE
BYRD, J. L., Jr	DARCOM Ammunition Ctr, Savanna, IL
CABBAGE, W. A.	Hercules Inc, Radford AAP, Radford, VA
CADOW, W. S., Jr, CDR, USN	Naval EOD Facility, Indian Head, MD
CALLAHAN, H. L.	Black & Veatch, Kansas City, MO
CAMPBELL, C. J.	Rock Island Arsenal, Rock Island, IL
CANADA, C. E.	Mason & Hanger-Silas Mason Co, Inc, Amarillo, TX
CANTOR, Issie	Ogden ALC, Hill AFB, UT
CAREW, D. L.	HQ ADCOM, Peterson AFB, CO
CARSON, R. C.	McDonnell Douglas Astronautics Co, St Louis, MO
CARPENTER, G. H.	NAVFACENGCOM, Bremerton, WA
CAVIN, D. L.	Hawthorne AAP, Hawthorne, NV
CHAN, S. K.	Canadian Industries Ltd, Quebec, Canada
CHAR, W. T.	US Army Engineer Div, Huntsville, AL
CHARTIER, H. A.	Commissariat A L'Energie Atomique, France
CHILES, J. R.	Canadian Industries Ltd, Quebec, Canada
CHURCHILL, Bill	Corps of Engineers, MRD, Omaha, NE
CHURCHILL, F. H.	SA-ALC, Kelly AFB, TX
CLARK, E. G.	Chemical Sys Lab, Aberdeen PG, MD
CLEAVELAND, Leroy	Day & Zimmermann Inc, Kansas AAP, Parsons, KS
COAKLEY, J. V.	Ofc Inspector General, DA, Washington, D. C.
COFFIN, J. P.	Thiokol Corp, Newtown, PA
CONGDON, J. W.	Bernard Johnson Inc, Houston, TX
CONLEY, J. H.	Aberdeen Proving Ground, MD
CONN, A. F.	Hydronautics Inc, Laurel, MD
CONNELLY, J. M.	Atlas Powder Co, Dallas, TX
CONNELLY, J. W.	Ofc, Chief of Naval Operations, Washington, D. C.
CONNOR, J. G., Jr	NSWC White Oak, Silver Spring, MD
COUCHMAN, J. F.	436 MAW, Dover AFB, DE
COURTRIGHT, W. C.	Los Alamos Scientific Lab, Los Alamos, NM
COWAN, G. H.	USA Armament Mat Readiness Com, Rock Island, IL
COWDRY, D F A, BRIGADIER, BA	Dir, Land Service Ammunition, United Kingdom
CRAIG, Edward	Fairfield, CA
CRIST, F. H.	Tooele Army Depot, Tooele, UT
CRANNEY, F. J.	NWS Concord, CA
CRATEN, J. D.	60th Ordnance Group, Germany
CRAWFORD, J. L.	ARRADCOM, Dover, NJ
CRUMPLEY, K. E.	Ogden ALC, Hill AFB, UT
CRUZ, I. T.	NWS Yorktown, VA
CULVER, J. M.	NPSRO, Magna, UT

CUNNINGHAM, R. B., CAPT, USN	DDESB, Washington, D. C.
CUTTING, R. T., COL, USA	DARCOM, Alexandria, VA
DAHN, J. C.	Safety Consulting Engineers Inc, Rosemont, IL
DALE, C. B.	NOS Indian Head, MD
DARLING, Art	Canadian Explosives Res Lab, Ottawa, Canada
DAVIS, C. F.	Hercules Inc, Magna, UT
DAVIS, J. O.	Lawrence Livermore Lab, Livermore, CA
DAVIS, J. L., LTC, USAF	Dir of Nuclear Safety, Kirtland AFB, NM
DEANS, H. L.	DDESB, Washington, D. C.
DEL REGNO, Lawrence	DCASR, Dallas, TX
DEMBERG, Edmund	ARRADCOM, Dover, NJ
DEMPSEY, R. D.	US Army Engineer Div, Huntsville, AL
DeSANDO, R. J.	Monsanto Research Corp, Miamisburg, OH
DES RIVIERES, J. T.	Energy Mines & Resources, Canada
DEVINE, J. P.	Aberdeen Proving Ground, MD
DEXTER, R. F.	BuAlcohol,Tobacco,Firearms, Washington, D. C.
DIETRICH, E. J.	Bernard Johnson Inc, Houston, TX
DITTMAN, H. A.	DCASR, Cleveland, OH
DOBBS, Norval	Ammann & Whitney, New York, NY
DODGEN, J. E.	Dodgen Engineering Co, Colorado Springs, CO
DOGGETT, C. J.	Defense Logistics Agency, Los Angeles, CA
DONAHUE, W. C.	Unidynamics/Phoenix Inc, Phoenix, AZ
DONALDSON, L. O.	22 AF, Travis AFB, CA
DONALDSON, P. A.	NWC China Lake, CA
DOW, Scott	Defense Logistics Agency, Marietta, GA
DOWDY, R. W.	Agbabian Associates, El Segundo, CA
DRAKE, J. T.	DDESB, Washington, D. C.
DRAKE, R. W.	Los Alamos Scientific Laboratory, Los Alamos, NM
DREYER, O. F.	Lockheed Missiles & Space Co, Inc, Sunnyvale, CA
DkUGMAND, J. R.	PM Mun Prod Base Mod & Exp, Dover, NJ
DUBIE, L. W.	Teledyne McCormick Selph, Hollister, CA
DUNN, M. L.	DDESB, Washington, D. C.
EACKER, O. L., 2LT, USAF	6515 Test Sup Sqdn, Edwards AFB, CA
EDDY, W. J.	NAVFACENGCOM, Alexandria, VA
EGLY, R. S.	International Minerals & Cmls, Terre Haute, IN
EHLERS, E. H.	DARCOM Ammunition Center, Savanna, IL
EHRINGER, A. G.	DARCOM Ammunition Center, Savanna, IL
EICHER, W. E., MAJ GEN, USA	CG, USA ArmMatReadiness Com, Rock Island, IL
ELIAS, Victor	Reinforced Earth Co, Washington, D. C.
ELSASSER, F. M.	60 MAW, Travis AFB, CA
ENG, Leslie	PMCDIR, Aberdeen Proving Ground, MD
ENGLE, J. J.	Thiokol Corp, Brigham City, UT
ESPARZA, E. E.	Southwest Research Institute, San Antonio, TX
EVERETT, L. A.	Defense Logistics Agency, Marietta, GA
EWING, H. M.	Sacramento Army Depot, Sacramento, CA
FAGAN, W. F., COL, USAF	3460 TTG, Lowry AFB, CO
FATZ, R. J.	Defense Logistics Agency, Syracuse, NY
FERGUSON, R. M.	Canadian Arsenals Ltd, Le Gardeur, Canada
FERRITTO, J. M.	Civil Engineering Lab, Port Hueneme, CA
FITZGERALD, J. A.	Honeywell Inc, Elk River, MN

FLIAKAS, P. J.	DepAsst Secretary of Defense (I&H), Washington, D.C.
FLOYD, T. G.	AFATL, Eglin AFB, FL
FORSTEN, Irving	ARRADCOM, Dover, NJ
FOWLER, W. T.	Radford AAP, Radford, VA
FOULK, D. W.	DARCOM, Alexandria, VA
FOW, L. F.	Werner & Pfleiderer Corp, Waldwick, NJ
FREIMANIS, Alvis	Lester B Knight & Assoc, Chicago, IL
FUGITTE, R. H.	Lexington-Blue Grass Depot Acty, Lexington, KY
FUNSTON, Ronald	Physics International Co, San Leandro, VA
GALLES, F. P.	NUWES Keyport, WA
GILMORE, A. E.	NAVSEASYSCOM, Crane, IN
GLENN, W. R.	Federal Cartridge Corp, Anoka, MN
GOEB, C. V.	Olin Corp, Badger AAP, Baraboo, WI
GOLDIE, R. H.	AFSC, Andrews AFB, MD
GOLIGER, Jean	Soc Nat des Poudres et Explosifs, France
GRACE, P. J., CPT, USAF	HQ PACAF, Hickam AFB, HI
GRIFFITHS, C. D.	NPBRO, Magna, UT
GROH, D. L.	NWSC Crane, IN
GROSCOST, K. R.	DARCOM Ammunition Ctr, Savanna, IL
GUARIENTI, R. P.	Lawrence Livermore Lab, Livermore, CA
GUERKE, G. H.	Ernst-Mach Institut, Fed Republic of Germany
HAHN, J. C.	Martin Marietta Aerospace, Orlando, FL
HALL, Clyde	Austin Powder Co, McArthur, OH
HALTER, D. I.	Red River Army Depot, Texarkana, TX
HAMBY, N. R.	Anniston Army Depot, Anniston, AL
HAMILTON-JONES, John, MGEN, BA	VP Ordnance Board, Ministry of Defence, United Kingdom
HANNA, R. J.	Boeing Aerospace Co, Seattle, WA
HANNAH, M. M.	63 MAW, Norton AFB, CA
HANSEN, G. L.	IRECO Chemicals, Salt Lake City, UT
HANSEN, S. G.	Pacific Missile Test Center, Pt Mugu, CA
HARPER, J. D.	Los Alamos Scientific Lab, Los Alamos, NM
HARRIS, C. F.	Martin Marietta Aerospace, Cocoa Beach, FL
HART, C. E.	NSWC Dahlgren, VA
HARTON, E. E.	Materials Transportation Bu, DOT, Washington, D. C.
HAWES, J. M.	DDESB, Washington, D. C.
HAWS, L. D.	Monsanto Research Corp. Miamisburg, OH
HEESEMAN, Al	Wyle Laboratories, Norco, CA
HEFLIN, K. R.	Lake City AAP, Independence, MO
HELBIG, Ralf, MAJ, GAF	TerrXdo S-H/DBrAFNORTH, Fed Republic of Germany
HELLE, C. F.	Cia. Brasileira de Cartuchos, Sao Paulo, Brazil
HERCHBERGER, C. K.	NWS Seal Beach, CA
HERMAN, R. C.	DDESB, Washington, D. C.
HESS, G. W., CMSGT, USAF	Fort Carson & 4th Inf Div, CO
HICKS, R. K.	DCASR, St Louis, MO
HIGGINS, J. M.	Mason & Hanger-Silas Mason Co, Cornhusker AAP, NE
HIGGS, W. M.	Holston AAP, Kingsport, TN
HILL, W. V.	Black & Veatch, Kansas City, MO
HILLARD, L. F.	DARCOM, Alexandria, VA
HOKANSON, J. C.	Southwest Research Institute, San Antonio, TX
HOLBROOK, D. L.	Aberdeen Proving Ground, MD
HOLLANDER, W. V.	Olin Corp, Winchester, CT

HOWE, P. M.	Ballistic Research Lab, Aberdeen Proving Ground, MD
HOWELL, E. D.	DDESB, Washington, D. C.
HRABE, D. W.	Pacific Missile Test Center, Pt Mugu, CA
HUANG, C. C.	Corps of Engineers, Huntsville, AL
HUDSON, M. C.	NOS Indian Head, MD
HUEHN, Wilfried, MAJ, GA	Wehrbereichskommando V, Fed Republic of Germany
IDE, H. R.	Savanna Army Depot Activity, Savanna, IL
INVERSO, Tony	Hill AFB, UT
IZOD, D. C.	British Embassy, Washington, D. C.
JANG, J. F.	DCAS, San Bruno, CA
JENSSEN, Arnfinn	Norwegian Defence Const Svc, Oslo, Norway
JERNIGAN, A. E.	Red River Army Depot, Texarkana, TX
JETER, J. G.	N L McCullough, Houston, TX
JOHNSON, R. E.	Olin Corp, Badger AAP, Baraboo, WI
JOHNSTON, W. B.	Dept of Energy, Albuquerque, NM
JONASZ, Fredric, CAPT, USN	Navy Member, DDESB, Washington, D. C.
JONES, C. P.	NAVSEASYSCOM, Washington, D. C.
JONES, F. M.	Aerojet Solid Propulsion Co, Sacramento, CA
JONES, F. A., COL, USA	EMCDIR, Aberdeen Proving Ground, MD
JUREK, R. C., MAJ, USAF	2701 EOD SQDN, Hill AFB, UT
KAO, A. M.	USA Const Engr Res Lab, Champaign, IL
KAPLAN, Ken	Management Science Assoc, Mountain View, CA
KARISNY, L. J.	Fort Polk, LA
KATSANIS, D. J.	Chemical Systems Lab, Aberdeen Proving Ground, MD
KEEFER, J. H.	Ballistic Research Lab, Aberdeen Proving Ground, MD
KEENAN, W. A.	Civil Engineering Lab, NCBC Port Hueneme, CA
KEETCH, A. K.	Dugway Proving Ground, MD
KELLEY, P. G., Jr, COL, USA	Chairman, DDESB, Washington, D. C.
KENDRICK, H. E.	Dept of Energy, Las Vegas, NV
KERKOWSKI, J. J.	ARRADCOM, Dover, NJ
KERNS, A. J.	Newton, NJ
KIM, B. C.	Battelle Columbus Laboratories, Columbus, OH
KING, C. Y.	Lawrence Livermore Lab, Livermore, CA
KING, D. P.	Science Applications Inc, Vandenberg AFB, CA
KINGERY, C. N.	Ballistic Research Lab, Aberdeen Proving Ground, MD
KINNISON, R. L.	DCASMA, Phoenix, AZ
KISH, Gustave	ARRADCOM, Dover, NJ
KOCHNIUK, D. L.	Atlantic Research Corp, Alexandria, VA
KONGEHL, H. F., MAJ, GA	Materialamt der Bundeswehr, Fed Republic of Germany
KRONICK, R. A., MAJ, USAF	ADTC, Eglin AFB, FL
LAIDLAW, B. G.	Defence Res Establishment, Suffield, Alberta, Canada
LAMB, H. C.	NAVFACENGCOM, Alexandria, VA
LARSEN, E. A.	Martin Marietta Corp, Denver, CO
LARSEN, Ted	Detector Electronics Corp, Minneapolis, MN
LARSON, A. E.	ARRADCOM, Dover, NJ
LATHAM, J. F.	NWS Earle, NJ
LAURENT, R. P.	General Electric Co, Burlington, VT
LAVERTU, R. R.	Defence Res Establishment Valcartier, Quebec, Canada
LAVALLEE, J. J.	DCASR, Boston, MA
LEANDER, R. C.	Thiokol/Longhorn Div, Marshall, TX

LEE, R. A.	Thiokol/LA Division, Shreveport, LA
LERWILL, R. J.	USA Test & Evaluation Com, Aberdeen PG, MD
LEVEY, D. V.	GOEX Inc, Cleburne, TX
LEWIS, H. L.	NavSeaSupCtr Pacific, San Diego, CA
LINDBERG, H. E.	SRI International, Menlo Park, CA
LINDELL, C. A.	KDI Precision Products, Inc, Cincinnati, OH
LINNENKOHL, H. C.	2750 ABW, Wright-Patterson AFB, OH
LOMINICK, R. T.	Boeing Aerospace Co, Seattle, WA
LONGO, Vito, COL, USAF	DDESB, Washington, D. C.
LOUSHINE, T. M.	Sunflower AAP, DeSoto, KS
LOVING, F. A.	E I duPont, Martinsburg, WV
LOWE, W. F.	AFAL, Eglin AFB, FL
LYMAN, O. R.	Ballistic Research Lab, Aberdeen Proving Ground, MD
McBRIDE, William	NWS Yorktown, VA
McCAY, W. C.	Longhorn AAP, Marshall, TX
McDONALD, J. B.	Brunswick Corp, Skokie, IL
McDONALD, J. L.	DCASR, Dallas, TX
McDONALD, J. P.	NWSC Crane, IN
McDOWELL, R. C.	19th Support Command, APO San Francisco
McGRAW, J. E.	David W Taylor Naval Ship R&D Ctr, Portsmouth, VA
McMULLAN, Frank, LTC, USA	Fld Com, DNA, Kirtland AFB, NM
McMULLEN, E. S.	Aberdeen Proving Ground, MD
McQUEEN, J. E., COL, USAF	AFISC, Norton AFB, CA
MAASCH, W. C., WO1, USA	7th DMMC, Fort Ord, CA
MacDONALD, J. C., LTC, CF	Canadian Defence Liaison Staff, Washington, D. C.
MARTIN, J. D., LTC, USAF	USAFE
MATHIS, T. R., CAPT, USN	NWS Seal Beach, CA
MARTINI, D. G.	Federal Hwy Admin, DOT, Fort Worth, TX
MARTIS, J. G.	Crane Army Ammunition Acty, Crane, IN
MAST, Beverly J.	DDESB, Washington, D. C.
MATTHIESEN, V. J.	Sierra Army Depot, Herlong, CA
MATSUGUMA, H. J.	ARRADCOM, Dover, NJ
MAY, R. E.	USAFORSCOM, Fort McPherson, GA
MEGAHAN, D. A., CPT, USA	USA Msl&MunCtr&School, Redstone Arsenal, AL
MELVIN, F. N.	Hawthorne AAP, Hawthorne, NV
METCALF, H. L.	Ofc, DASD(I&H), Washington, D. C.
MILLER, Henry	Uniroyal Inc, Joliet AAP, Joliet, IL
MILLER, R. W.	Strategic Wpns Facy Pacific, Bremerton, WA
MILLS, J. L.	MB Associates, East Camden, AR
MILNER, J. R.	Holston Defense Corp, Kingsport, TN
MIZE, H. J.	UC Lawrence Livermore Laboratory, Livermore, CA
MOODIE, W. J.	Monsanto Research Corp, Miamisburg, OH
MOORE, C. J.	AF Military Training Ctr, Lackland AFB, TX
MOORE, W. J.	Western Div, NAVFACENGCOM, San Bruno, CA
MORAN, E. P., Jr.	HQ US Army Europe & 7th Army
MOSELEY, T. K.	Southwest Research Institute, San Antonio, TX
MOSHER, P. R.	NOS Indian Head, MD
MULLINS, R. K.	UC Lawrence Livermore Lab, Livermore, CA
MUMMA, G. B.	Martin Marietta Corp, Denver, CO
MUNCY, C. R.	NAVSEA Safety School, NWSC Crane, IN

MURPHY, B.J., WING COMDR, RAAF	Embassy of Australia, Washington, D. C.
MURPHY, J. M.	Red River Army Depot, Texarkana, TX
MYERS, R. L.	Dir, DARCOM Fld Safety Acty, Charlestown, IN
NAPADENSKY, Hyla S.	IIT Research Institute, Chicago, IL
NATTA, M.C., Ing. General	Ministere de la Defense, St Cloud, France
NAYLOR, C.K., CAPT, USN	NAVSEASYSCOM, Washington, D. C.
NEUENSCHWANDER, C. W.	UC Lawrence Livermore Laboratory, Livermore, CA
NEWBERN, R. G.	AFSC, Andrews AFB, MD
NEWHOUSE, Alvin	NAVSEASYSCOM, Washington, D. C.
NEUHART, V. M.	DCASMA, San Diego, CA
NIGREVILLE, W. J.	5010 CSG, Eielson AFB, AK
NOLAN, W. J.	Ofc PM MunProdBaseMod&Exp, Dover, NJ
ODELL, W. J.	Mason & Hanger-Silas Mason Co Inc, Lexington, KY
O'HARA, J. R.	Boeing Aerospace Co, Seattle, WA
OLDHAM, B. L.	TRACOR Inc, Austin, TX
OLIVER, R. E.	David W Taylor Naval R&D Ctr, Portsmouth, VA
OLSEN, F. N.	Boeing Aerospace Co, Seattle, WA
OPEL, M. C.	ICI Americas Inc, Indiana AAP, Charlestown, IN
OPNELLAS, G. S.	NM Lualualei, HI
OSTREM, F. E.	GARD Inc, Niles, IL
OWEN, P. R.	BMDSCOM, Huntsville, AL
PADGETT, Bennie	USA Infantry Ctr, Fort Benning, GA
PALMER, R. E.	DCASR-Atlanta, Marietta, GA
PANTAGES, M. C.	Remington Arms Co, Inc, Bridgeport, CT
PAPAS, W. P.	Martin Marietta Corp, Denver, CO
PAPP, A. G.	Mason & Hanger-Silas Mason Co, Inc, Amarillo, TX
PARR, V. B.	Southwest Research Institute, San Antonio, TX
PARRISH, D. C., Jr.	N L McCullough, NL Industries, Inc, Houston, TX
PAYNE, D. G.	Umatilla AD, Hermiston, OR
PAYNE, L. H.	NWS Charleston, SC
PENA, A. O.	NOMTF, White Sands Missile Range, NM
PERKINS, R. G.	DDESB, Washington, D. C.
PETERS, J. A.	Hercules Inc, Radford AAP, Radford, VA
PETERSEN, A. H.	Detector Electronics Corp, Minneapolis, MN
PETES, Joseph	NSWC White Oak, Silver Spring, MD
PETINO, G. J.	Hazards Research Corp, Denville, NJ
PIETRZYKOWSKI, R. E.	DCASMA, Garden City, NJ
PITTMAN, J. F.	NSWC White Oak, Silver Spring, MD
PLATE, S. W.	Tri-State Motor Transit Co, Arlington, VA
PLOETZ, C. F., CPT, USAF	HQ USAFE, Ramstein, Germany
POJMANN, D. M.	TRADOC, Fort Monroe, VA
POOLE, C. R.	Mason & Hanger-Silas Mason Co, Inc.
PORZEL, F. B.	NSWC White Oak, Silver Spring, MD
POWELL, J. G.	NSWC Dahlgren, VA
PRADE, N. H.	NWSC Crane, IN
PRICE, Gilbert	Royal Ordnance Factories, London, UK
PRESCOTT, J. F.	NWC China Lake, CA
PREUITT, Russel	NOSC Point Loma, San Diego, CA
PRICE, P. D.	ARRADCOM, Dover, NJ
PRITCHARD, G. C.	Bureau of Mines, Washington, D. C.

PRITCHETT, T. C., COL, USAF	AFISC/SEW, Norton AFB, CA
QUEEN, W. G.	DARCOM, Alexandria, VA
QUINCHON, Jean	S.N.P.E., Paris, France
RACHEL, C. K.	Hughes Aircraft Co, Tucson, AZ
RANDALL, H. J.	DCASR, Los Angeles, CA
RANGER, P. T.	USA ADC, Fort Bliss, TX
RAUSIN, G. D.	Aerojet Ordnance & Mfg Co, Downey, CA
RECK, C. R., 2LT, USA	77th Ord Det (EOD), Yuma Proving Ground, AZ
REDDY, D. P.	Agbabian Associates, El Segundo, CA
REED, J. W.	Sandia Laboratories, Albuquerque, NM
REES, N. J.	Ministry of Defence, United Kingdom
REEVES, Harry	Ballistic Research Lab, Aberdeen Proving Ground, MD
REZETKA, W. L.	Pacific Missile Test Range, Point Mugu, CA
RHINEBECK, G. C.	NWS Concord, CA
RICE, E. W.	Naval EOD Facility, Indian Head, MD
RICHARDSON, J. W.	Vought Corp, Dallas, TX
RILEY, W. E.	Space & Missile Test Ctr, Vandenberg AFB, CA
RITTMAN, H. T., Jr.	E. I. duPont, Wilmington, DE
ROBERTS, Clayborn	DCASMA, Van Nuys, CA
ROBINSON, R. D.	AFWL, Kirtland AFB, NM
RODLAND, H. M.	ATC, Randolph AFB, TX
ROESLER, Helmut	Catalytic, Inc, Philadelphia, PA
ROGNHAUG, Harald	Norwegian Defence Construction Svc, Oslo, Norway
ROMO, R. H.	USARJapan
ROTH, E. R.	Hughes Aircraft Co, Canoga Park, CA
ROURE, J.F., Ing General	Ministere de la Defense, France
ROUSE, J. H.	USA Claims Svc, OTJAG, Fort Meade, MD
ROUSE, J. T., III	Strategic Weapons Facy Pacific, Bremerton, WA
ROWLEY, T.W., CPT, USAF	3460 TG, Lowry AFB, CO
RUDIN, I.A.G.	Nat Insp Explosives & Flammables, Solna, Sweden
RUDY, B. M.	MTMC Transportation Engr Agency, Newport News, VA
RUSSELL, J.W., COL, CF	Dir Gen Ammo, Canadian Defence HQ, Ontario, Canada
RUTLEDGE, P. J.	DARCOM, Alexandria, VA
SACKLEH, F. J.	AEDC, Arnold AFS, TN
SAFFIAN, L. W.	ARRADCOM, Dover, NJ
SAILER, R. G.	Hercules Aerospace Div, Salt Lake City, UT
SAINDON, B. W.	Rocky Mountain Arsenal, Commerce City, CO
SANCHEZ, F. B.	NSWC Dahlgren, VA
SANDS, C. A., COL, USA	DDESB, Washington, D. C.
SAUER, F. M.	Physics International Co, San Leandro, CA
SAVOLA, S. I.	Res Ctr of Natl Defense Forces, Lakiala, Finland
SAVOY, G. A.	Hercules Inc, Bacchus Works, Magna, UT
SAWYER, R. B.	DDESB, Washington, D. C.
SAYER, W. B.	Dept of Energy, Albuquerque, NM
SAYLORS, J. A.	Bernard Johnson Inc, Houston, TX
SHAFFER, M. B.	Science Applications Inc, Los Angeles, CA
SCHAICK, E.E.S., MAJ, GAF	LUFTWAFFENMUNITIONSDEPOT, Duren, FRGermany
SCHEER, J. M.	DCASR, Chicago, IL
SCHILLING, R. W.	Ministry of Defense, Bonn, FRGermany
SCHIPPERS, F.	Prins Maurits Lab, Aaryswyk, The Netherlands

SCHNEIDER, A. H.	NAVFACENGCOM, Alexandria, VA
SCHNEIDER, Thomas	Basler & Hofmann, Zurich, Switzerland
SCHULTZ, L. F.	NPRO, Sunnyvale, CA
SCOTT, J. B.	AF Comm Svc, Scott AFB, IL
SHANNAN, J. E.	Mason & Hanger-Silas Mason Co Inc, Iowa AAP, IA
SHOPHER, K. R.	Yucaipa, CA
SILER, A. K.	DCASR, Marietta, GA
SINGLETON, E. T., Jr.	NSWC Dahlgren, VA
SKOGMAN, D. P.	USAMRCOM, Rock Island, IL
SKOGMAN, M. W.	Indiana AAP, Charlestown, IN
SMALL, J. P.	Embassy of Australia, Washington, D. C.
SMITH, C. R.	General Dynamics, Pomona, CA
SMITH, L. E.	OPMCDIR, Aberdeen Proving Ground, MD
SMITH, R. L.	Vought Corp, Dallas, TX
SMITH, R. L.	Hercules Inc, Sunflower AAP, Lawrence, KS
SMITH, W. D.	NSWC Dahlgren, VA
SOLHEIM, Magne	Dyno Industrier, Lier, Norway
SONG, So-young	Agency for Defense Development, Korea
STEPHENS, L. D.	NWS Seal Beach, CA
STINSON, H. E.	Camp Stanley Stg Acty, San Antonio, TX
STOFFERS, F. W.	Jet Propulsion Lab; Pasadena, CA
STORCH, M., LTC	Infrastrukturslab der Bundeswehr, FRGermany
STOREY, R. B.	OO-ALC, Hill AFB, UT
SULIK, P.R., CPT, USAF	AAC, Elmendorf AFB, AK
SULLIVAN, T. J.	NSWC Indian Head, MD
SWISDAK, M. M., Jr.	NSWC White Oak Lab, Silver Spring, MD
TANCRETO, J. E.	Civil Engr Lab, Port Hueneme, CA
TAYLOR, G. S.	Aerojet Ord & Mfg Co, Chino, CA
TAYLOR, W. D.	McClellan AFB, CA
TAYLOR, W. J.	Atlas Powder Co, Dallas, TX
TEICHMANN, E. C.	TRADOC, Fort Monroe, VA
THOMAS, J.E., MAJ, USA	Fld Com, DNA, Kirtland AFB, NM
THORMAN, G. E.	UK MOD Rep, McDonnell Douglas, St Louis, MO
TIDMAN, J. P.	Canadian Industries Ltd, Quebec, Canada
TINKLER, W.S.N.	Ministry of Defence, London, United Kingdom
TOLLEY, Gilbert	DARCOM Intern Tr Ctr, Red River AD, Texarkana, TX
TOMLIN, Phil	MB Associates, San Ramon, CA
TREPOY, James	ADWC, Tyndall AFB, FL
TROTT, B. D.	Battelle Columbus Lab, Columbus, OH
TULL, J. D.	Lockheed Missiles & Space Co, Santa Cruz, CA
TURNBULL, B. C.	E I duPont, Wilmington, DE
TURNER, Dean	DA DCSLOG, Washington, D. C.
TURNER, H. R.	Etowah Mfg Co, Inc, Gadsden, AL
VANDERBILT, S. J.	31st ADA BDE, Homestead AFB, FL
VINSON, J. L.	Remington Arms Co, Inc, Lake City AAP, MO
WALSH, J. J.	NSWC Dahlgren, VA
WALTERSCHIED, R. A.	ARRADCOM, Dover, NJ
WANG, Shou-ling	David W Taylor Nav Ship R&D Ctr, Bethesda, MD
WARD, J. M.	NSWC White Oak, Silver Spring, MD
WARNECKE, C. H.	Dugway Proving Ground, UT

WATKINS, C. K.	HQ USAF, Washington, D. C.
WATSON, G. G., COL, USA	Army Member, DDESB, Washington, D. C.
WATSON, R. R.	Health & Safety Exec, London, United Kingdom
WATSON, R. W.	Bureau of Mines, Pittsburgh, PA
WATTS, Thurman, LTC, USA	Radford AAP, Radford, VA
WEALS, F. H.	NWC China Lake, CA
WEEDING, G. S.	Falcon R&D Co, Denver, CO
WENBORNE, A. S.	Naval Material Command, Washington, D. C.
WENZEL, A. B.	Southwest Research Institute, San Antonio, TX
WEST, F. L.	ADTC, Eglin AFB, FL
WESTINE, P. S.	Southwest Research Institute, San Antonio, TX
WHITACRE, C. G.	ARRADCOM, Aberdeen Proving Ground, MD
WHITE, G. A.	USA School, Fort Shafter, Hawaii
WIGHT, R. L.	Ofc, Chief of Engineers, DA, Washington, D. C.
WILD, R. W.	Bundesinstitut fuer chem. tech. Untersuchungen, FRG
WILKAITIS, N. J.	Olin Corp, Marion, IL
WILLIS, V. G.	Crane Army Ammo Acty, Crane, IN
WILSON, D. E.	NOS Indian Head, MD
WILTON, Chuck	Scientific Svc Inc, Redwood City, CA
WOEHLE, Richard	NOTU Cape Canaveral, FL
WU, Da-Lih	Catalytic Inc, Philadelphia, PA
VACCA, J. R., Jr.	DCASR, Reading, PA
VOSE, W. F.	Naval Safety Ctr, NAS Norfolk, VA
ZAKER, T. A.	DDESB, Washington, D. C.
ZAKRZEWSKI, P. H.	DCASR, St. Louis, MO
ZARRA, S. J.	ARRADCOM, Dover, NJ
ZEIDMAN, G. G.	Battelle Memorial Inst, Columbus, OH
ZOLLICKER, S. H.	Hercules Inc, Sunflower AAP, Lawrence, KS
ZUKE, W. G.	NAVAIRSYSCOM, Washington, D. C.